N° d'ordre : 4292

THÈSE

PRÉSENTÉE À

L'UNIVERSITÉ BORDEAUX 1

ECOLE DOCTORALE DES SCIENCES CHIMIQUES

Par Mme BOISSELIER MAILFAIT Élodie

POUR OBTENIR LE GRADE DE

DOCTEUR

SPECIALITÉ : CHIMIE ORGANIQUE ET INORGANIQUE

Titre : Synthèse et Optimisation de Dendrimères et de Nanoparticules d'Or en vue d'Applications Biomédicales.

Thèse dirigée par M. ASTRUC Didier

Soutenance le 4 décembre 2009

Devant la commission d'examen formée de :

M. Jean-Luc Pozzo, Professeur (Université de Bordeaux 1)	Président
Mme Claire-Marie Pradier, Professeur (Université Paris 6)	Rapporteur
M. Jacques Robert, Professeur (Université Victor Segalen de Bordeaux 2)	Rapporteur
Mme Maria Dalko-Csiba, Docteur (Centre de recherché de L'Oréal)	Examinateur
M. Yves Chauvin, Directeur de recherche émérite	Membre invité
M. Jaime Ruiz Aranzaes, Docteur (Université de Bordeaux 1)	Membre invité
M. Lionel Salmon, Docteur (Université de Toulouse 3)	Membre invité
M. Didier Astruc, Professeur (Université de Bordeaux 1)	Directeur de thèse

… REMERCIEMENTS …

Ce travail a été effectué dans le Groupe Nanosciences et Catalyse, ISM, Université de Bordeaux 1 (CNRS UMR 5255), sous la direction scientifique du Professeur Didier Astruc.

* * *

Je remercie M. le Professeur Didier Astruc pour m'avoir accueillie dans son équipe de recherche lors de mon stage de deuxième année de master et de m'avoir donné l'opportunité de réaliser ma thèse au sein de son équipe sur un sujet adapté à mes envies. Je le remercie pour son écoute quotidienne, ses conseils et sa patience avec lesquels il a dirigé cette thèse. Je le remercie également pour son enthousiasme et pour son désir permanent de valoriser le travail accompli.

* * *

J'adresse mes sincères remerciements à Mme Claire-Marie Pradier et à M. Jacques Robert pour avoir accepté d'être rapporteurs de ce manuscript.

* * *

J'exprime toute ma reconnaissance à Mme Maria Dalko-Csiba, M. Jean-Luc Pozzo et M. Yves Chauvin qui m'ont fait l'honneur de bien vouloir participer à mon jury.

* * *

Je remercie grandement M. Jaime Ruiz Aranzaes, ingénieur de recherche du CNRS, pour le temps passé à me faire découvrir et apprécier le savoir-faire du laboratoire, ainsi qu'à me faire profiter de son expérience. Je le remercie enfin pour son humanité, sa joie de vivre, ses précieux conseils qui m'ont permis de réaliser peu à peu mes objectifs et pour tout le soutien et l'écoute qu'il m'a apportés quotidiennement.

* * *

Au sein des différents laboratoires, je souhaite remercier les personnes qui ont participé, de près ou de loin, à ce travail de recherche : je remercie, entre autres, Mme Colette Belin pour sa patience lors des mesures AFM, sa gentillesse et son écoute; M. Eric Cloutet pour sa disponibilité pour les analyses SEC et de diffusion de lumière; M. Lionel Salmon pour son efficacité lors des analyses TEM; Mme Isabelle Pianet pour sa collaboration fructueuse concernant la RMN et M. Nöel Pinaud pour sa patience et ses conseils en RMN.

* * *

Je remercie chaleureusement chaque personne de l'ISM dans les différents étages que j'ai côtoyée pendant ma thèse, et qui ont apporté leurs contributions, tant au niveau professionnel que personnel.

* * *

J'adresse un salut amical à tous les étudiants de notre groupe, ceux qui sont présents et ceux qui l'ont été : Lily, Anett, Rodrigue, Vidya, Lauriane, Conny, Elodie, Milkard, Christophe, Tetsu, Badr, Sihem et tous les autres. Je leur souhaite à tous bon courage et beaucoup de réussite.

* * *

Je n'oublie pas non plus les étudiantes que j'ai encadrées avec beaucoup de bonheur et de rires : Emmanuelle, Marie-Angèle, Sophie et Alison, continuez ainsi et la vie vous sourira toujours.

* * *

Une pensée particulière va pour Catia et Jackson qui me manquent beaucoup. Merci à toi Catia pour tout ce qu'on a pu partager, que ce soit au sein des publications, notre bureau, nos joies, nos pleurs, … Merci pour ces vacances inoubliables partagées avec vous, et rendez-vous quelque part dans le monde pour continuer à rire ensemble.

* * *

Maintenant un merci spécial à mes amis, du labo et d'ailleurs qui m'ont permis de faire de mes trois années de thèse une des périodes les plus agréables de ma vie: Claire, Abdou, Adeline, Emilie, Tom, Jérémy, Aurélie, Daniel, Audrey, Pauline, Aurélie, Christophe, Martine, Sylvain, Julietta, merci à vous d'être comme vous êtes, je vous souhaite beaucoup de bonheur et de réussite car vous le méritez tous, et que la fête continue!

* * *

Le plus grand merci s'adresse à ma famille pour tout l'amour et le soutien qu'elle me donne, et pour tous les bonheurs partagés ensemble. Maman, Papa, Lily, Pascal, Fred, Stef, Véro, Yoyo, Sandie, Lolo, Kinou, Nico, Tom, Axel, Lenny, Swann, je vous porte au plus profond de mon cœur.

* * *

Enfin, le dernier merci, qui n'a pas d'équivalent, va à mon mari. Julien, merci à toi d'être l'homme doux, drôle et toujours amoureux que j'ai connu, merci pour tout l'amour et le soutien que tu m'apportes chaque jour, merci pour ton sourire réconfortant et merci de me faire vivre mon rêve éveillé en m'ayant demandé de devenir ta femme. Merci à ta famille, Florence, Philippe, Emeline, Ludo et Emma, pour leur soutien et leur joie de vivre. Que notre rêve dure toujours et que nos futures années soient riches en connaissances et en émotions. Le monde est tout petit lorsque l'amour est grand…

SYNTHESE ET FONCTIONNALISATION DE DENDRIMERES ET DE NANOPARTICULES D'OR EN VUE D'APPLICATIONS BIOMEDICALES.

INTRODUCTION GENERALE :

Diverses spécialités biologiques telles que la médecine, la pharmacie, la cosmétique ou encore les compléments alimentaires nécessitent une optimisation du conditionnement des produits actifs. L'objectif de ma thèse a été d'utiliser les différents domaines de la chimie pour synthétiser de nouveaux substrats aux multiples propriétés afin de créer ou d'améliorer le conditionnement et la délivrance de composés biologiquement actifs.

Parmi les nombreuses disciplines de la chimie, trois grands domaines: la chimie organique, organométallique et inorganique ont été exploités pour synthétiser de nouvelles molécules basées sur respectivement des dendrimères, des polymères et des nanoparticules d'or.

Ces substrats ont été synthétisés dans l'objectif d'encapsuler, de stabiliser ou d'améliorer plusieurs molécules biologiquement actives telles que des vitamines, des neurotransmetteurs ou des agents anti-cancéreux.

Le plan de ce mémoire de thèse se divise en deux parties principales: les applications biomédicales réalisables grâce aux dendrimères (A) et celles basées sur des nanoparticules d'or (B). Une revue a été écrite pour chaque partie afin de faire le point sur les bases ainsi que sur les dernières avancées scientifiques dans ces deux domaines. La revue portant sur les dendrimères décrit de manière très générale les diverses fonctions des dendrimères. Leurs propriétés physiques, photophysiques et supramoléculaires y sont détaillées ainsi que leurs applications dans les domaines de la reconnaissance, de la catalyse, de l'électronique moléculaire ainsi que de la nanomédecine. La revue portant sur les nanoparticules d'or seulement est ciblée sur leurs applications en nanomédecine, une revue générale ayant déjà été publiée par notre groupe en 2004. Les différentes techniques de préparations y sont explicitées ainsi que leurs utilisations en imagerie, diagnostic et thérapie. Le dernier paragraphe de cette revue traite de la toxicité *in vitro* et *in vivo* des nanoparticules d'or.

La première partie (A) concernant la synthèse, les caractérisations et les applications des dendrimères en nanomédecine se compose de quatre sujets indépendants visant à améliorer les propriétés de vitamines, de neurotransmetteurs ou encore de polymères utilisables pour la thérapie. En effet, un chapitre décrira l'encapsulation de vitamines (vitamines C, B3 et B6) dans différents dendrimères solubles dans l'eau. Un autre chapitre traitera de la synthèse de quatre générations de dendrimères solubles dans l'eau portant des terminaisons benzoates ainsi que des paires d'ions qu'ils forment avec des ammoniums d'intérêts biologiques (acétylcholine, benzyltriethylammonium et dopamine). La synthèse d'un nouveau polymère dendronisé ferrocénique sera abordé dans un troisième chapitre par deux méthodes : soit la dendronisation du polymère, soit la polymérisation du dendron. Le dernier chapitre concerne la métathèse d'oléfines en milieu aqueux sans co-solvant avec l'utilisation d'un dendrimère en tant que nanoréacteur.

La seconde partie (B) commence par une revue sur les nanoparticules d'or en nanomédecine et contient ensuite deux chapitres décrivant la synthèse et la fonctionnalisation de nanoparticules d'or dans le but de créer de nouveaux vecteurs thérapeutiques et d'optimiser des agents anti-cancéreux par exemple pour le traitement du cancer de la prostate. Le premier

chapitre (chapitre 2) décrit la synthèse et la stabilisation de nanoparticules d'or par des dendrimères en milieu aqueux permettant un contrôle du diamètre de ces nanoparticules dans une large gamme de taille. Le chapitre 3 traite de la fonctionnalisation propre des nanoparticules d'or avec des groupements polyethylènes glycols grâce à la chimie « click ».

Cette thèse s'articule sous la forme de mémoires en anglais publiés ou en cours de publication, et dont la liste suit. Chaque mémoire est précédé d'un résumé en Français. La conclusion générale en Français fera le bilan et situera les perspectives futures des applications biomédicales des dendrimères et des nanoparticules d'or.

--- PLAN ---

PARTIE B : LES APPLICATIONS BIOMEDICALES DES NANOPARTICULES D'OR

PARTIE A :

DENDRIMERES EN VUE D' APPLICATIONS BIOMEDICALES

Chapitre A-1

Revue sur les dendrimères et leurs applications

Un dendrimère est constitué d'un cœur avec des branches qui se divisent en 2 ou 3 à chaque génération. Il a donc une forme de chou-fleur. On le fonctionnalise avec des fonctions périphériques qui définissent grandement ses propriétés de solubilité et d'encapsulation. Un dendron est un arbuste qui possède aussi une fonction au tronc (point focal).

Avec plus de 500 publications par année depuis 2004, la chimie des dendrimères constitue un domaine d'avant-garde de la recherche. En effet, grâce à ses multiples propriétés, un dendrimère se trouve être une molécule très adaptable à un grand nombre d'applications, et aux propriétés bien souvent meilleures qu'un simple polymère grâce, entre autres, à sa précision moléculaire, sa sphéricité à partir d'une certaine génération, aux phénomènes de génération et d'effet dendritique.

Ce chapitre passe donc en revue de manière très générale toutes les fonctions et les applications des dendrimères résultant de leurs propriétés physiques et supramoléculaires. L'élaboration de cette revue s'étend sur trois années et repose sur un travail bibliographique réalisé par Melle Catia Ornelas, ancienne doctorante du Professeur Didier Astruc de 2002 à 2007 actuellement en post-doctorat à l'Université de New York, ainsi que par moi-même. Cette revue, comportant près de 1700 références, s'articule autour de cinq grands axes.

Le premier axe décrit les structures dendritiques et les propriétés photophysiques qui en découlent. Les résultats et l'intérêt des simulations des dendrimères sont abordés ainsi que les différents assemblages dendritiques existants. La visualisation de la forme et de l'organisation des dendrimères par des techniques de microscopie (TEM et AFM) ainsi que par des études de surface viennent compléter cette première partie. Ces propriétés sont importantes pour le diagnostic médical.

La seconde partie traite des propriétés physiques des dendrimères selon les groupements chimiques qui les composent avec, en autres, les dendrimères à coeur $[Ru(bpy)_3]^{2+}$, cyclam ou porphyrine, les dendrimères fullerènes ou polythiophènes et les dendrimères basés sur des nanotubes de carbone.

Les propriétés supramoléculaires des dendrimères sont ensuite abordées en passant en revue les différentes liaisons réalisables telles que les liaison hydrogène, électrostatique et de coordination. Une large partie concerne l'encapsulation de molécules, qu'ils s'agissent de molécules neutres, des nanoparticules ou encore de quantum dots. Enfin, des applications des dendrimères en tant que films ou membranes ou encore leurs utilisations pour l'impression moléculaire et la reconnaissance sont détaillées.

La partie suivante traite du rôle important des dendrimères en catalyse d'autant plus que différentes techniques de séparation et de recyclage sont réalisables permettant ainsi d'orienter la catalyse vers la chimie verte. Les nombreux complexes métallodendritiques sont détaillés (palladium, rhodium, ruthénium, …) ainsi que les organocatalyseurs et la catalyse avec des nanoparticules soit encapsulées soit stabilisées par des dendrimères.

Enfin la dernière partie porte sur les applications biomédicales des dendrimères avec leur rôle dans la délivrance de médicaments (de manière covalente ou non) et leurs utilisations dans différentes thérapies (antiangiogénique, génique, photodynamique, photothermique, …). Cette partie détaille également l'utilisation des dendrimères dans le but de réduire la toxicité des médicament et de réaliser un meilleur ciblage ou encore un meilleur diagnostic (techniques d'Imagerie par résonance magnétique, de fluorescence, …).

Cette revue est donc essentielle pour situer les capacités des dendrimères à s'adapter dans de nombreux domaines très variés grâce à leurs propriétés particulières et modulables à souhait. On retrouvera ces propriétés pour les nanoparticules d'or, celles-ci pouvant d'ailleurs avoir une structure dendritique.

Ce premier chapitre n'est composé que du plan de la revue. La revue complète, très volumineuse, est disponible en annexe (fascicule joint à la thèse).

Dendrimers Designed for Functions: From Physical, Photophysical and Supramolecular Properties to Applications in Sensing, Catalysis, Molecular Electronics, Photonics and Nanomedicine.

Didier Astruc,* Elodie Boisselier, Cátia Ornelas
ISM, UMR CNRS N°5255, Université Bordeaux 1, 33405 Talence Cedex France
E-mél: d.astruc@ism.u-bordeaux1.fr

Content

Chapitre A-2

Encapsulation de vitamines dans des dendrimères solubles dans l'eau

L'encapsulation de vitamines au sein de dendrimères solubles dans l'eau est le premier sujet qui m'a été confié lors de mon arrivée dans le groupe de recherche du Professeur Didier Astruc. Ce travail a consisté dans un premier temps à tester la capacité de dendrimères commerciaux à encapsuler des molécules de vitamine C (acide ascorbique) avant d'étendre la recherche à de nouveaux dendrimères synthétisés et fonctionnalisés au laboratoire ainsi qu'à d'autres vitamines.

Une des principales applications des dendrimères est la délivrance de médicaments par encapsulation ou par complexation vers des cibles spécifiques. Il s'agit ici plus précisément de transporter la vitamine C liée de manière supramoléculaire à des dendrimères solubles dans l'eau, fonctionnalisés à l'aide de groupements éthylènes glycols dans le but d'utiliser ces complexes dans le domaine cosmétique (peau, cheveux). En effet, la vitamine C, qui intervient dans les principales réactions d'oxydoréduction du métabolisme cellulaire, ne peut être synthétisée par l'organisme de l'homme, d'où la nécessité de lui en fournir selon un apport exogène. Les dendrimères semblent être des vecteurs appropriés pour le transport de molécules d'acide ascorbique grâce à leur multivalence contrôlée qui peut être utilisée à la fois pour attacher une ou plusieurs substances (médicaments, enzymes, agents de contraste pour l'imagerie médicale,.. ici la vitamine C) ainsi que des groupes ciblants et solubilisants à la périphérie. Les dendrimères utilisés réalisent effectivement des liaisons supramoléculaires avec les molécules d'acide ascorbique, ce qui permet leur maintien au coeur et la périphérie de ces macromolécules. De plus la fonctionnalisation de ces dendrimères avec différents groupements organiques contenant des chaînes polyéthylènes glycols assurent la solubilité dans l'eau de ces macromolécules qu'elles soient vides ou chargées de molécules d'acides ascorbiques, ainsi que leur biocompatibilité.

Dans un premier temps, l'encapsulation de la vitamine C a été étudiée par Résonance Magnétique Nucléaire (RMN) afin de quantifier le nombre de vitamines stabilisées par chaque génération dendritique. Ce travail a été breveté le 21 Janvier 2007 après une ré-écriture du texte sous forme juridique réalisée en collaboration avec la société BREDEMA . Ce brevet a gracieusement été financé par le Centre National de la Recherche Scientifique.

Par la suite, une étudiante de master 2, Melle Emmanuelle Favre, a continué à travailler, avec mon encadrement, sur la capacité de ces dendrimères à encapsuler des vitamines et a poursuivi ces études avec deux autres vitamines qui sont l'acide nicotinique (la vitamine B3) et la pyridoxine (la vitamine B6).

Les valeurs des constantes d'associations ont enfin été évaluées dans certains cas étudiés par RMN afin de comparer les différents systèmes dendritiques.

Le brevet étant aujourd'hui déposé depuis plus de dix-huit mois (brevet FR101305, n° 0850372, 01/21/07), une partie de ce travail a donc été récemment re-rédigé et soumis au New Journal of Chemistry. Cette publication suit.

Encapsulation of vitamins C, B_3 and B_6 by dendrimers in water

Elodie Boisselier, Jaime Ruiz and Didier Astruc*
Institut des Sciences Moléculaires, UMR CNRS N°5255, Université Bordeaux 1, 33405 Talence Cedex, France

Abstract
Titrations of commercial diaminobutane (DAB) and polyamidoamine (PAMAM) dendrimers by vitamins C (ascorbic acid, AA), B_3 (nicotinic acid) and B_6 (pyridoxine) was monitored by ^{1}H NMR using the chemical shifts of both dendrimer and vitamin protons and analyzed by comparison with the titration of propylamine by AA. Quaternarizations of the terminal primary amino groups and intradendritic tertiary amino groups, that are nearly quantitative with vitamins C and B_6, was characterized by more or less sharp variations $\Delta\delta$ of the ^{1}H chemical shift δ at the equivalent points. The peripheral primary amino groups of the DAB dendrimers were quaternarized first, but then not selectively, whereas a sharp chemical shift variation was recorded for the inner methylene protons near the tertiary amines, when all the dendritic amines were quaternarized. On the other hand, this selectivity was not observed with PAMAM dendrimers. All the amines were quaternarized even for high-generation DAB and PAMAM dendrimers. Analogous titration phenomena were observed for the titration of DAB dendrimers with vitamins B_3 and B_6 for which the carboxylic acid (B_3) and the phenol group (B_6) provided amine quaternarization and/or hydrogen bonding interactions. The special case of the titration of PAMAM dendrimer by vitamin B3 indicates only dominant supermolecular hydrogen-bonding interactions and no quaternarization. Although the titration graphs were most of the time dominated by these major amine protonation interactions, additional interactions were also weakly observed in particular after the equivalent points by comparison with the titration graph of propylamine.
Keywords: dendrimer, polyamine, vitamin C, nicotinic acid, pyridoxine

Introduction

Dendrimers[1] are known for their encapsulation properties[2] that are of very promising use *inter alia* for biomedical applications.[3] Indeed, Newkome's seminal article on arborols already pointed out the micellar character of these macromolecules,[4] then this aspect was also emphasized in Tomalia's early articles on dendrimers.[2a,5] In a review article entitled "*Unimolecular micelles: supramolecular use of dendritic constructs to create versatile molecular containers*", Moorefield and Newkome specifically surveyed host-guest encapsulation using dendrimers.[2c] Subsequent to the pioneering studies, this property of dendrimers has most strikingly been exemplified by Meijer's dendritic box[6] and Crooks' extensive catalytic studies using dendrimer-encapsulated nanoparticles.[7]
The path of fragile vitamins through biological membranes could also be facilitated by biodegradable molecular containers[8] of dendritic or nanoparticle type. Liposomes are classic drug vectors[9] that have also been used in food nanotechnology[10] and occasionally for vitamin C,[11] but host-guest disaggregation before reaching the targeted organ is a major obstacle to efficacy. Thus, engineered biocompatible dendrimers[3] should be better hosts for safe and efficient transport than liposomes. Recently, a peptide dendrimer model for vitamin B12 transport proteins was designed by Reymond et al.[12] A very important issue for cosmetic industry is the delivery of dermatological agent using suitable nanocarriers in formulations.

Given the fragility of vitamin C, protecting vectors such as dendrimers could be of high interest.[13] Vitamin C, the L-enantiomer of ascorbate, is not synthesized in the body, thus requires exogenous sources. It is well known as an anti-oxidant protecting the body against oxidative stress that is responsible for aging, and is an electron donor for eight different enzymes and a cofactor in several vital enzymatic reactions. It is involved in the synthesis of red blood cells, contributes to the immune system and to the defense against infections, favors the absorption of iron, is required for the synthesis of skin collagen (which explains the multiple cosmetic applications) and plays an essential role in the healing of wounds.[14] Vitamin B3 (niacin or nicotinic acid), is a water-soluble derivative of pyridine that is converted to nicotinamide and then to NAD and NADP *in vivo*. It is thus a precursor to NADH, NAD^+, $NADP^+$ and NADPH, which play essential metabolic roles in living cells and is involved in both DNA repair, and the production of steroid hormones in the adrenal gland.[15] Vitamin B6 (pyridoxine) is a water-soluble vitamin. It is an active form and cofactor in many reactions of amino-acid metabolism, including transamination, deamination, and decarboxylation. It is also necessary for the enzymatic reaction governing the release of glucose from glycogen and is involved in the synthesis of hemoglobin, neurotransmitters and histamin.[16]

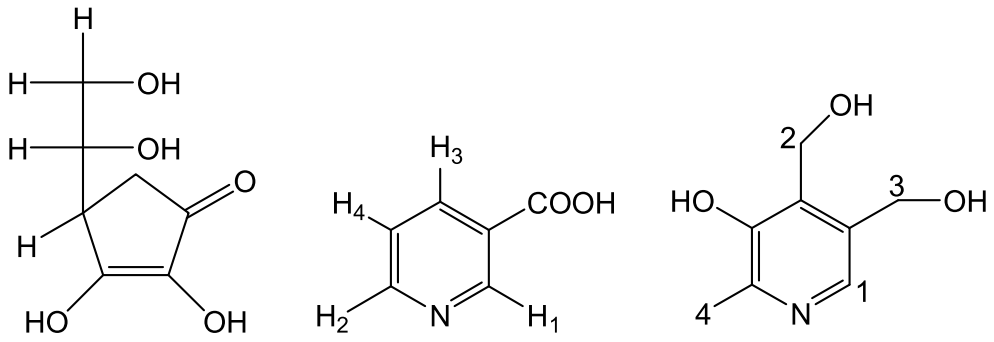

Vitamin C
ascorbic acid

Vitamin B3
nicotinic acid

Vitamin B6
pyridoxin

Chart 1. Molecular structures of the vitamins C, B_3 and B_6.

Therefore, the present study involves the investigation by ^{1}H NMR of the interaction in water of vitamins C, B_3 and B_6 (Chart 1) and their encapsulation in various water-soluble dendrimers terminated by amino groups. In previous studies with redox-active metallocenyl dendrimers[17] we have mostly used cyclic voltammetry[17-20] and ^{1}H NMR[17,18] for the recognition, sensing and titration of inorganic anions including ATP[19] and transition metal cations[20] or cations of biological interest such as acetylcholin. [18b,c]

Results and discussion

Dendrimers

Commercial, water-soluble polyamidoamine (PAMAM) and diaminobutane (DAB)-cored polypropylene-imine (PPI) dendrimers have been used. The DAB dendrimers used are those of generations 2, 3 and 5 (G2, G3 and G5), terminated by 8, 16 and 64 amino groups respectively, and the PAMAM dendrimers used are those of generations 1 and 4 (G1 and G4) terminated by 8 and 64 amino groups respectively (Chart 2). The use of these two well-known amino-terminated dendrimer families will allow comparing the behaviors of peripheral

primary amines with thoses of tertiary amines with and without amido groups in the dendrimer interiors.

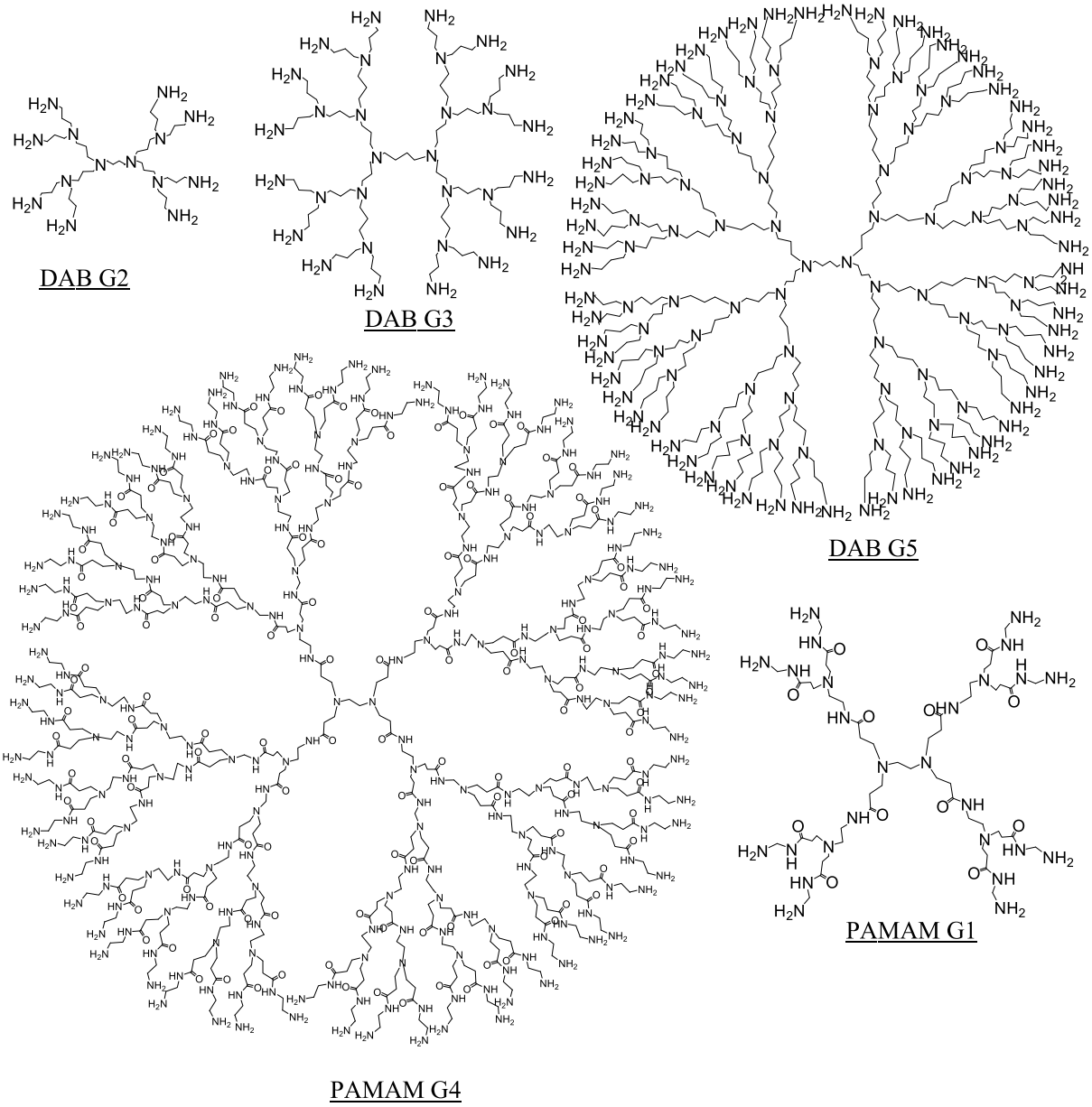

Chart 2. Molecular structures of the dendrimers.

^{1}H NMR study of the addition of vitamin C to propylamine

A titration has first been carried out using propylamine, a pre-model of the DAB dendrimers, with ascorbic acid, whereby both the variations of the propylamine protons ($H_2NC\mathit{H}_2$- and $H_2NCH_2C\mathit{H}_2$) and those of the ascorbic acid (AA) proton geminal to the side chain were monitored as a function of the number of equiv. AA added per dendrimer in D_2O (Fig. 1).

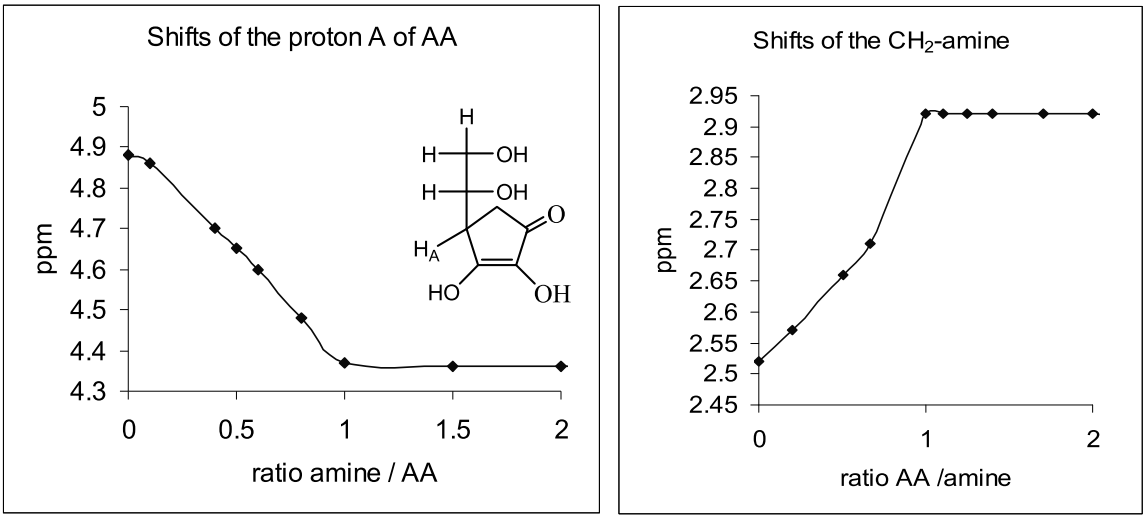

Figure 1. ^{1}H NMR titration of propylamine by vitamin C (AA) in D_2O: shift of the AA geminal proton H_A (left) and of the CH_2 amine protons (right)

It is observed on these graphs that the equiv. point is reached at the end of the variation of the chemical shift of the propylamine protons and at the beginning of the variation of the shift of the ascorbate geminal proton. The pK_a of AA and propylamine being respectively 4.1 and 10.59 in water, the titration reaction give propylammonium ascorbate quantitatively at the accuracy of ^{1}H NMR (the concentration of AA being around 10^{-7} M at the equiv. point). The second acidity of AA is too weak (p$K_{a\,2}$ = 11.8) for titration by amines.

^{1}H NMR study of the addition of vitamin C to G2 and G5 DAB dendrimers

The progressive addition of vitamin C to the DAB dendrimers in D_2O is followed by the ^{1}H NMR shifts of the DAB protons.

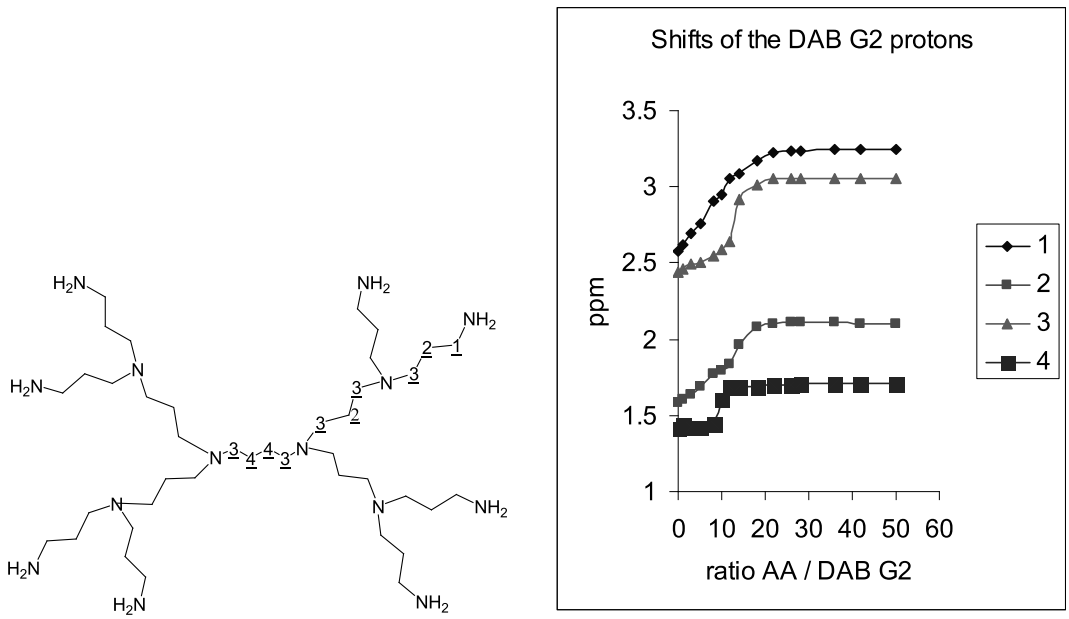

Figure 2. Titration of G2-DAB-8NH_2 by AA: shifts of the G2-DAB protons.

In the simplest case of G2-DAB-8NH_2, this titration (Fig. 2) clearly shows that the H_2NCH_2-protons near the peripheral amino groups are first perturbed, indicating that the peripheral primary ammonium ascorbates are first formed (Chart 3).

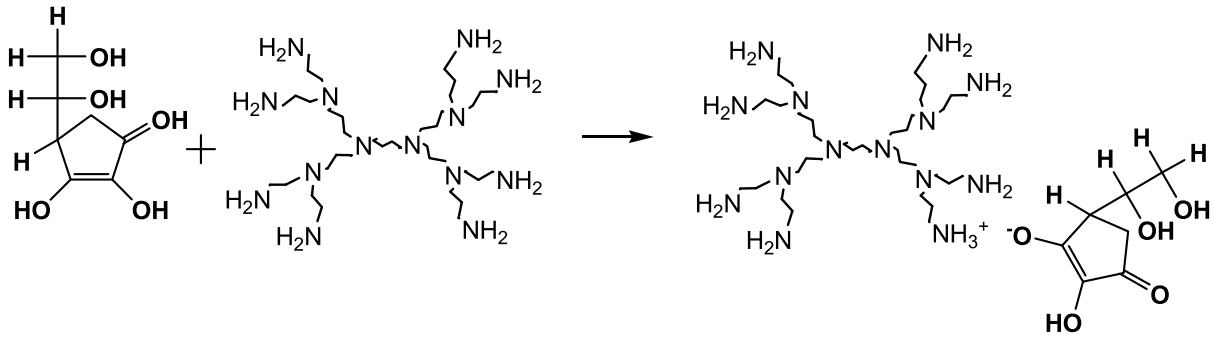

Chart 3.

But then, completion of the ammonium ascorbate formation at the periphery is very slow and progressive (mild slope) all along the addition of AA, without equiv. point, and thus competes with intradendritic tertiary ammonium ascorbate formation. The fact that one signal is observed confirms that the amino and ammonium groups exchange protons in a dynamic process that is faster than the ^{1}H NMR time scale. The quaternarization of the tertiary amines, on the contrary, is well followed by relatively sharp equiv. points located at 16 equiv. AA for the (tertNC*H*$_2$-) protons and at 12 equiv. for the core (NCH$_2$C*H*$_2$C*H*$_2$CH$_2$N) protons. This difference between the equiv. points at 16 AA and 12 AA shows that the core tertiary amines are quaternarized before the others as a result of the encapsulation effect. The core NC*H*$_2$CH$_2$CH$_2$C*H*$_2$N protons are not distinguishable from the other intradendritic protons; therefore this difference is not monitored for them, although they certainly undergo the same change as the other core protons. In theory, the equiv. point observed for the tertNC*H*$_2$ protons should be 14 equiv. AA instead of 16, and this difference is due to the experimental uncertainty.

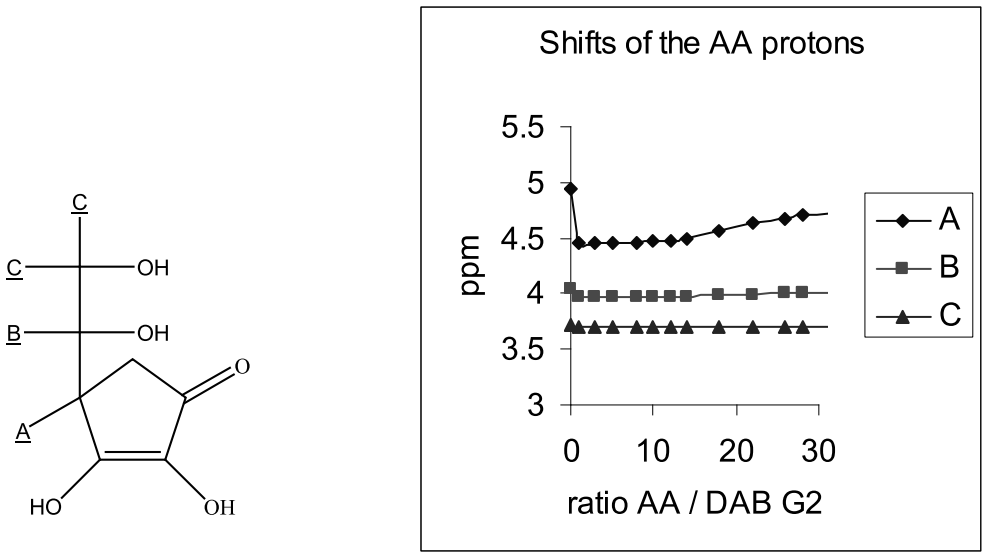

Figure 3. Titration of G2-DAB with AA: shifts of the AA protons.

Figure 3 shows the shift changes of the AA protons, and it is clearly observed that only the proton A geminal to the chain undergoes significant changes, but only after about 14 equiv. AA are added, i.e. the equiv. point corresponding to the end of the ascorbate formation. Afterwards, the graph very slowly changes, reflecting the progressive increase of the proportion of AA in addition to ascorbate. The fact that one signal is observed indicates a dynamic proton exchange equilibrium between AA and ascorbate at the ^{1}H NMR time scale.

For G5-DAB-NH_2-64 (Fig. 4), the terminal H_2NCH_2- protons near the peripheral amino groups are first perturbed, indicating that the peripheral primary ammonium ascorbates are first formed exactly as for G2-DAB-8NH2. The equiv. point is relatively well observed near approximately 120 to 130 equiv. AA, which corresponds to the theoretical number of 126 equiv. AA that are added to quaternarize the 126 amine groups of this dendrimer. The graph showing the variation of the chemical shift of the AA geminal proton shows a mild slope that does not allow to conclude on the equiv. point but that is consistent with an equiv. number of 126 AA.

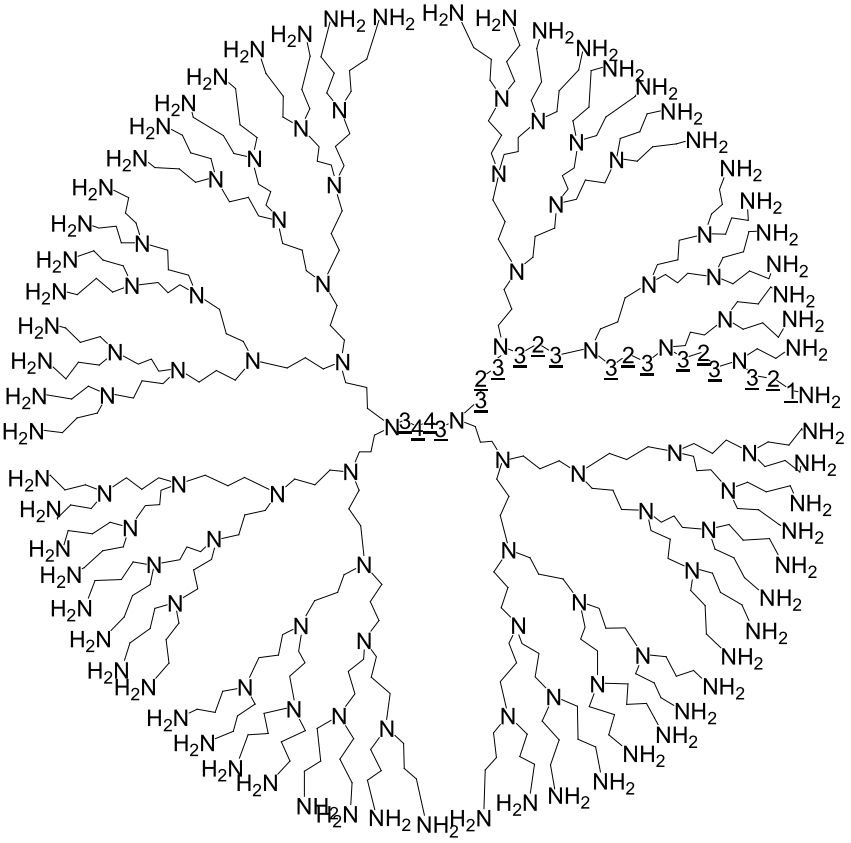

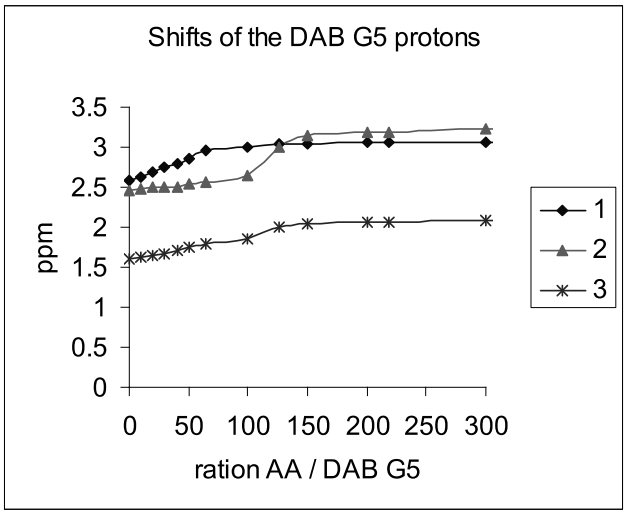

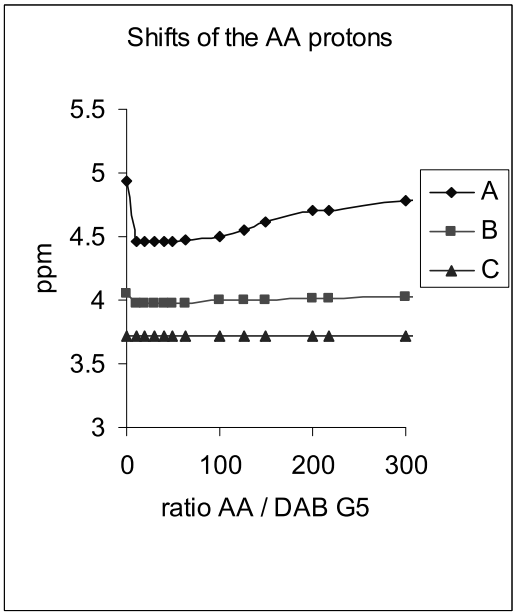

Figure 4. Titration of G5-DAB by AA.

^{1}H NMR study of the addition of vitamin C to G1 and G4-PAMAM dendrimers

The graphs (Fig. 5) of the dendrimer proton chemical shifts for the titration of the G1-PAMAM-8NH_2 dendrimer by AA shows a sharp equiv. point at 14 equiv. AA with the tertNCH_2- protons and a less sharp, but clear equiv. point also at 14 equiv. AA with the three groups of C$H_2$$NH_2$, C$H_2$$CH_2$$NH_2$ and NHCOCH_2 protons. All this corresponds well to the quaternarization of the 14 amine groups of this dendrimer. No selectivity is found on these graphs for the quaternarization of the peripheral primary amines before the intradendritic tertiary amines, contrary to what was found above with the DAB dendrimers. This is probably due to the synergy between quaternarization and supramolecular interactions with the amide groups inside the PAMAM dendrimer. The variations of the chemical shift of the geminal ascorbate proton only starts also after 14 equiv. AA, in agreement with the appearance of AA after this point and with the observation of the variation of the PAMAM protons above.

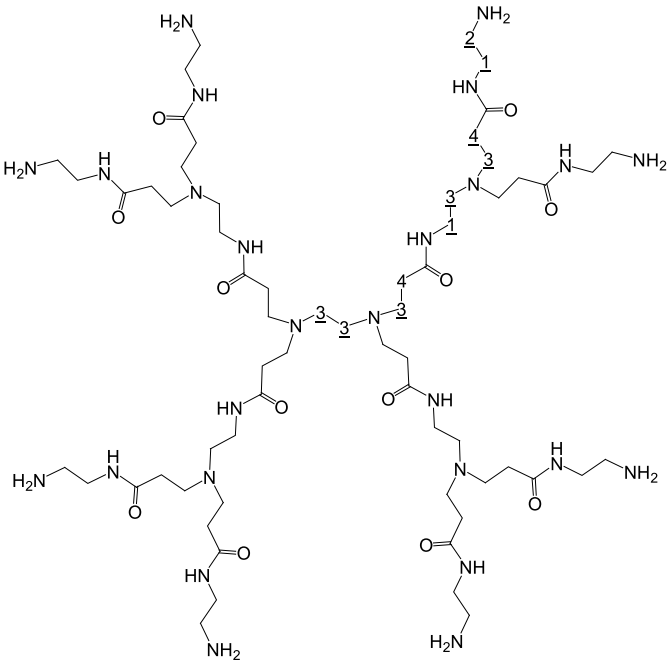

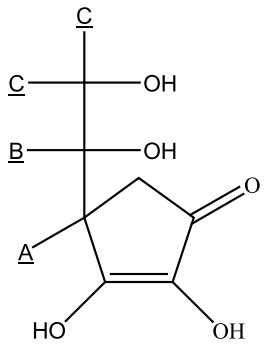

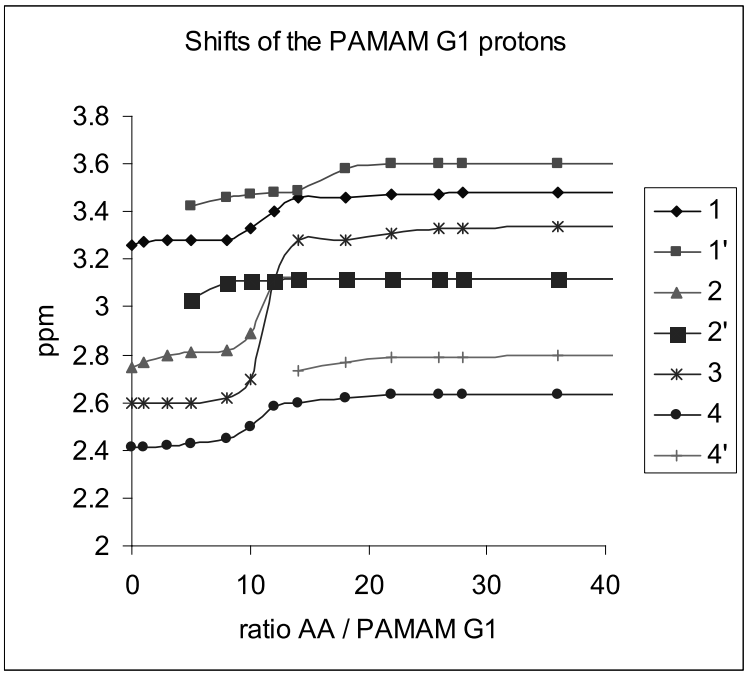

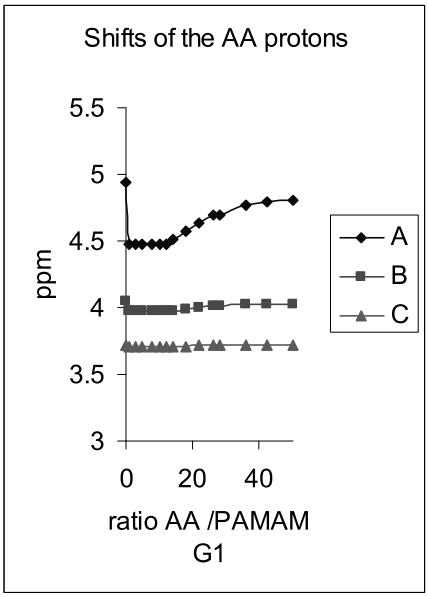

Figure 5. Titration of G1-PAMAM by AA.

With the G4-PAMAM-64NH_2 dendrimer, the AA titration graphs (Fig. 6) show sharp changes of proton chemical shifts, for both groups of intradendritic tertNCH_2- and NHCOCH_2 protons, at 150 equiv. AA, which is in 20% excess compared to the theoretical number of 126 amine groups of this dendrimer. This value in excess means that this commercial dendrimer contains some impurities due to incomplete branching or trapped solvent impurities. Interestingly, the change of chemical shift of the geminal ascorbate protons is observed around 65 AA per dendrimer, which could possibly mean that this chemical shift is not only influenced by the deprotonation of AA to ascorbate, but also by other supramolecular interactions inside the dendrimer, because there are 62 intradendritic ammonium ascorbate groups.

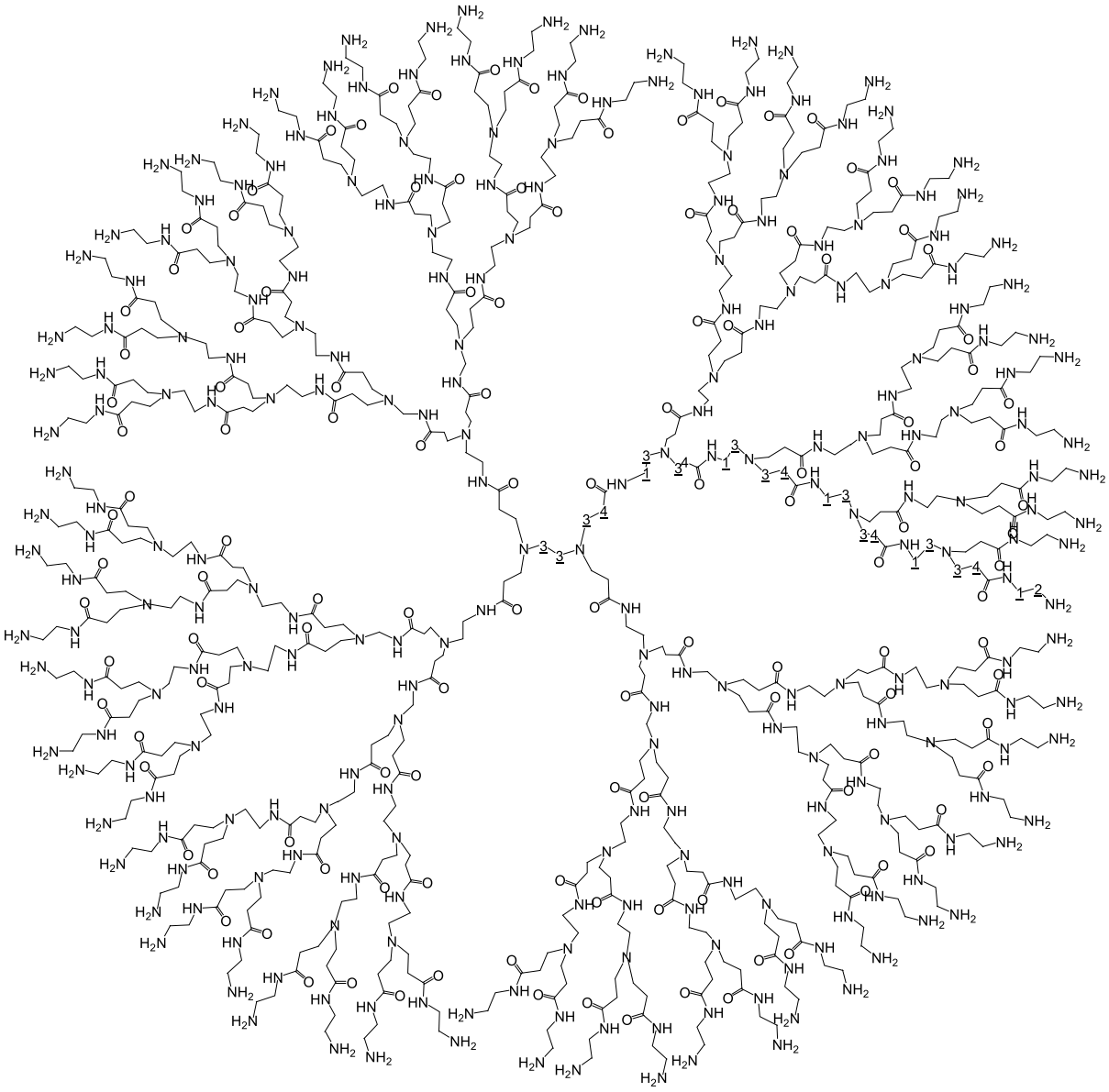

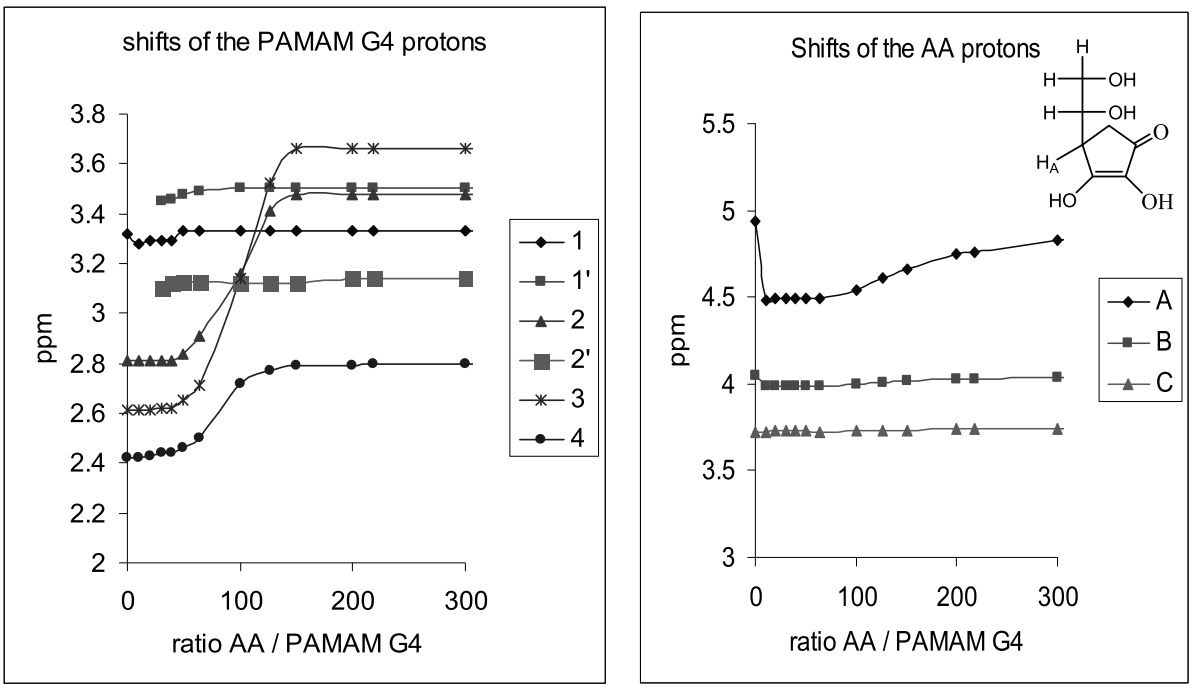

Figure 6. Titration of G4-PAMAM by AA.

^{1}H NMR study of the addition of vitamine B6 (pyridoxine) to G2-DAB and G1-PAMAM
Vitamine B6 contains a hydroxy group on its pyridyl ring, which corresponds to a pK_a value around 10, indicating that it can be partly deprotonated by amino groups (with hydrogen bonds between the amine nitrogen atom and the phenolic oxygen atom, Chart 4).

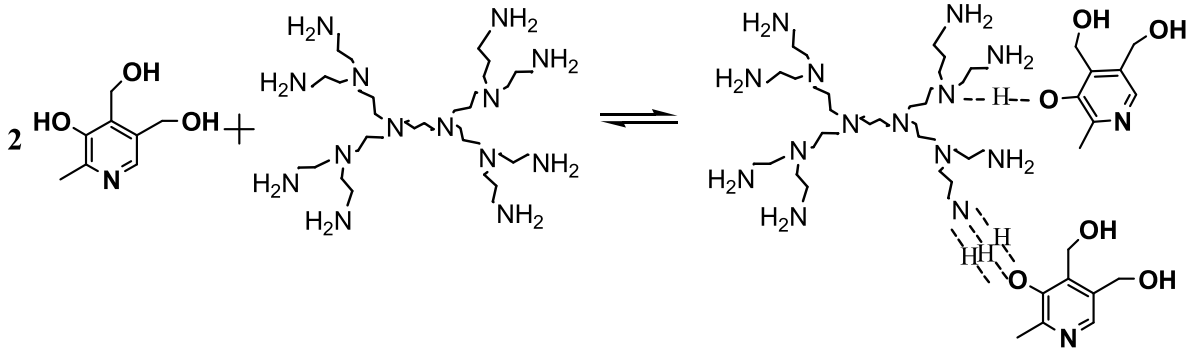

Chart 4.

The titration of the dendrimer G2-DAB-8NH_2 (Fig. 7) clearly shows that the 8 peripheral amino groups are first quaternarized with a sharp equiv. point at 8 equiv. pyridoxine per dendrimer. This corresponds to the formation of a triple-hydrogen bonding between the amino and phenol (or ammonium-phenolate). The core $NCH_2CH_2CH_2CH_2N$ protons figure an equiv. point at about 14 equiv. pyridoxine, which corresponds to the quaternarization of the 14 amine groups of this dendrimer. The shifts of the tertNC*H*$_2$- ad tertNCH2C*H*$_2$- protons show milder graph with equiv. points around 18 to 20 equiv. pyridoxine, which might indicate that additional supramolecular interactions occur inside the dendrimer with a few additional pyridoxine molecules. The shifts of the pyridyl ring protons is also very progressive until around 20 pyridoxine molecules, consistent with this latter observation.

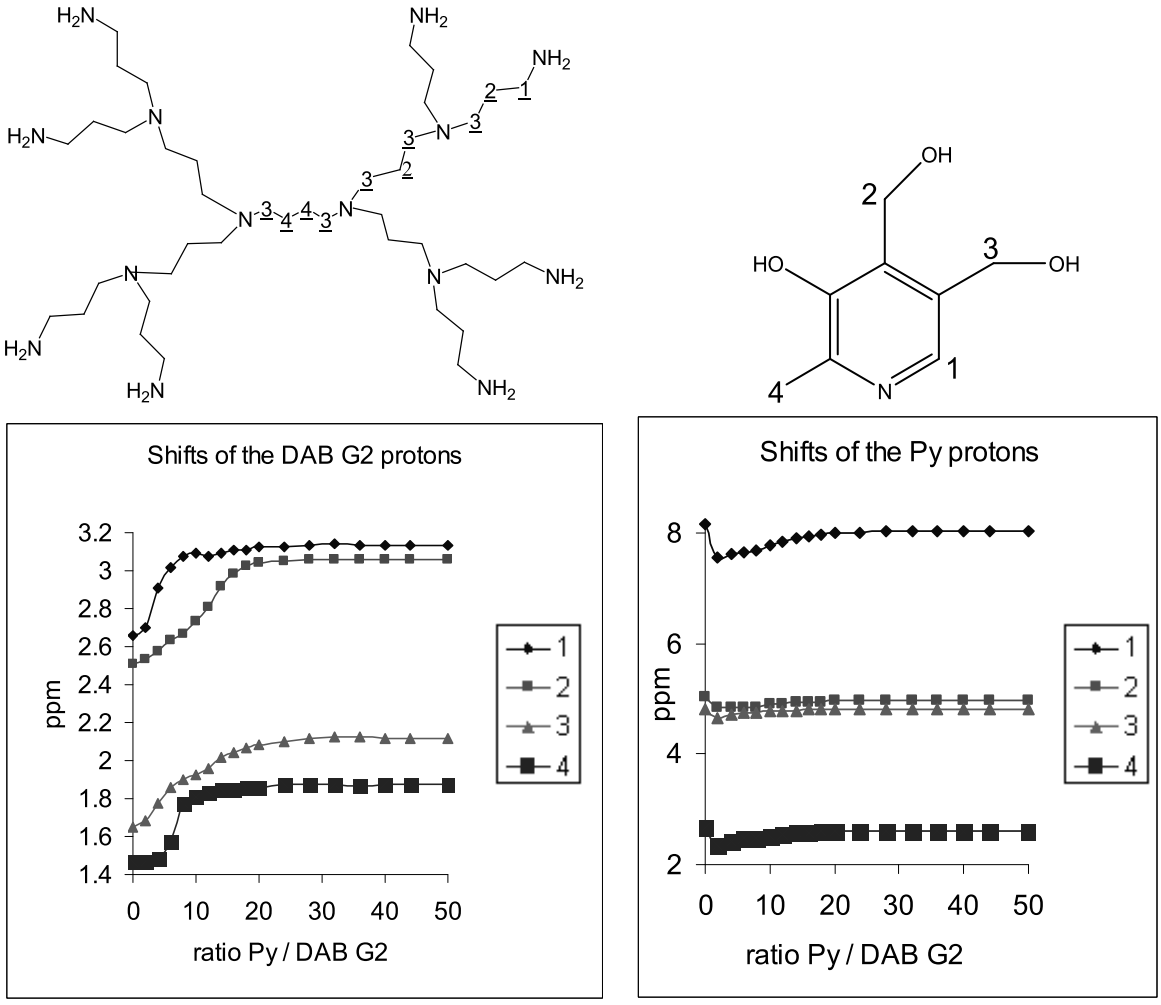

Figure 7. Titration of G2-DAB by pyridoxine (Py).

The ^{1}H NMR study of the addition of vitamin B6 to G1-PAMAM-8NH_2 (Fig.8) shows a progressive shift of the tertNCH_2 protons until around 14 to 20 equiv. pyridoxine without clear equiv. point consistent. A similar observation is made concerning the pyridyl proton in ortho position vs. the nitrogen atom. Curiously, the $CONHCH_2$ protons of the dendrimer undergo a sharp change at only 2 equiv. pyridoxine, which might signify dendritic encapsulation of each pyridoxine by 4 amido groups in addition to the interactions with the amines. Note that the chemical shift variations that are observed are much weaker than for all the other titrations (even much weaker than with the analogous DAB titration), showing that quaternarization does not proceed and that supramolecular hydrogen bonding interactions are dominant

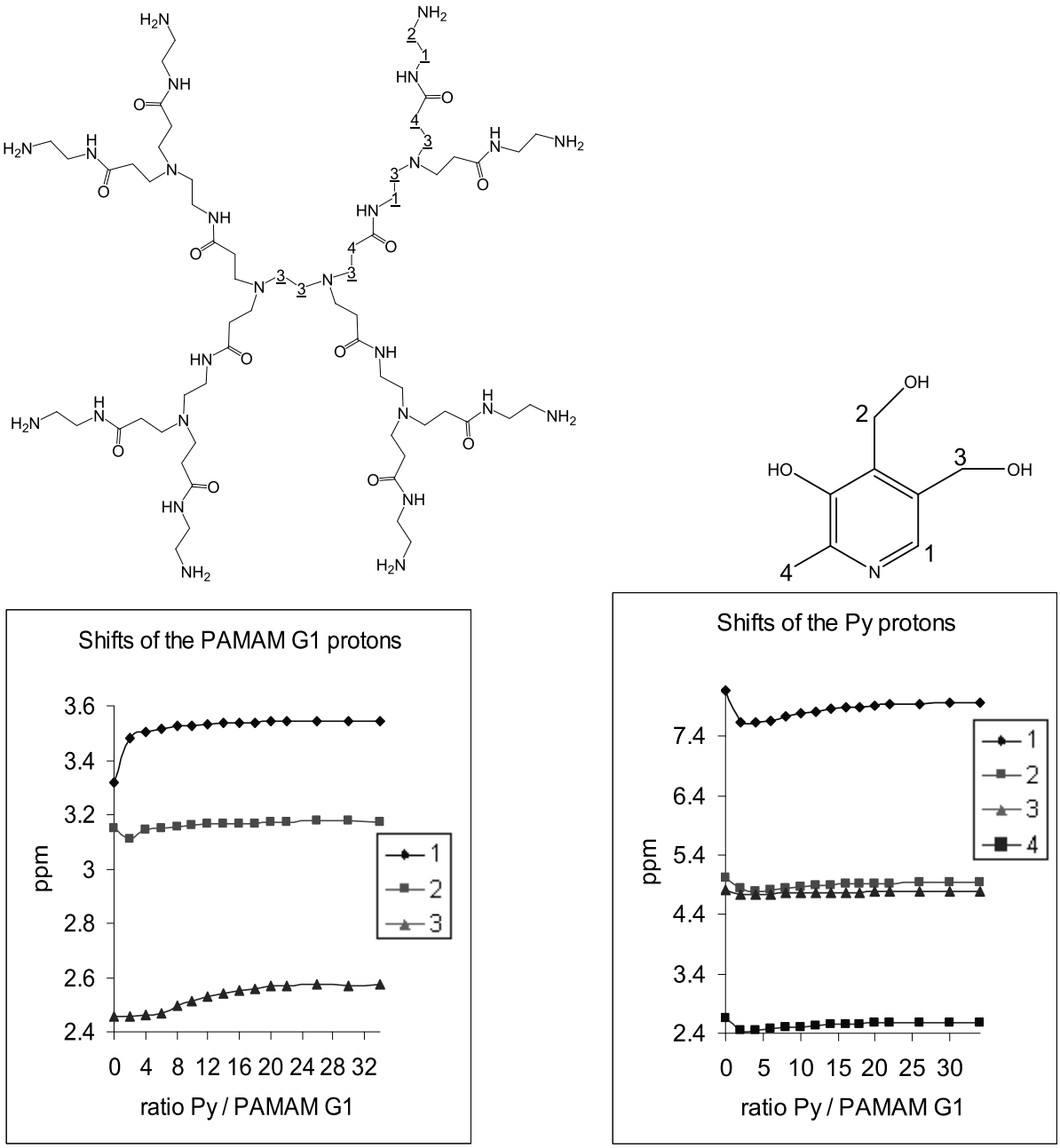

Figure 8. Titration of PAMAM G1 by pyridoxine (Py).

^{1}H NMR study of the addition of vitamin B3 (nicotinic acid) to G3-DAB and G4-PAMAM-64NH$_2$

The reaction of the carboxylic acid group of nicotinic acid (NA) and the dendritic amines quantitatively yields ammonium carboxylate (Chart 5).

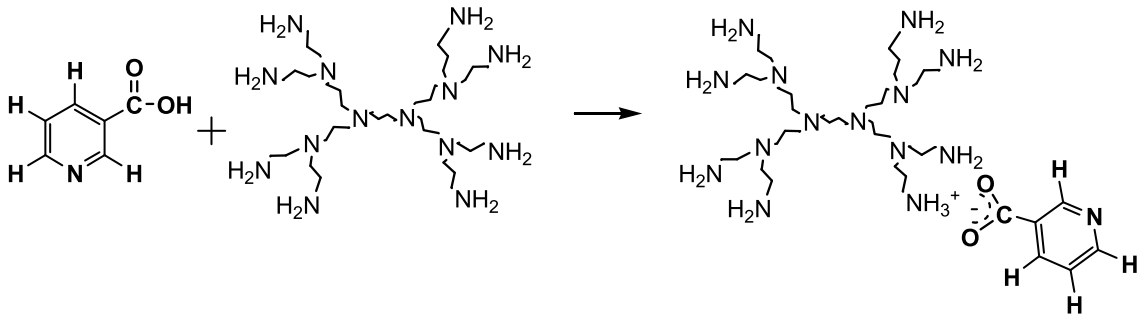

Chart 5.

With G3-DAB-16NH_2 that contains 30 amine groups, an equiv. point around 30 equiv. NA is indeed observed as expected for all the intradendritic protons (Fig. 9). On the other hand, with the periphery $CH_2N\mathit{H}_2$ protons, a clear equiv. point is observed at about 5 equiv. NA indicating formation of the peripheral primary ammonium carboxylates (with error or uncertainty on this number, however). The shifts of the four NA protons show important changes until very approximately 30 equiv. NA (for all 4 of them) consistent with the quaternarization of the 30 amine groups of the dendrimer.

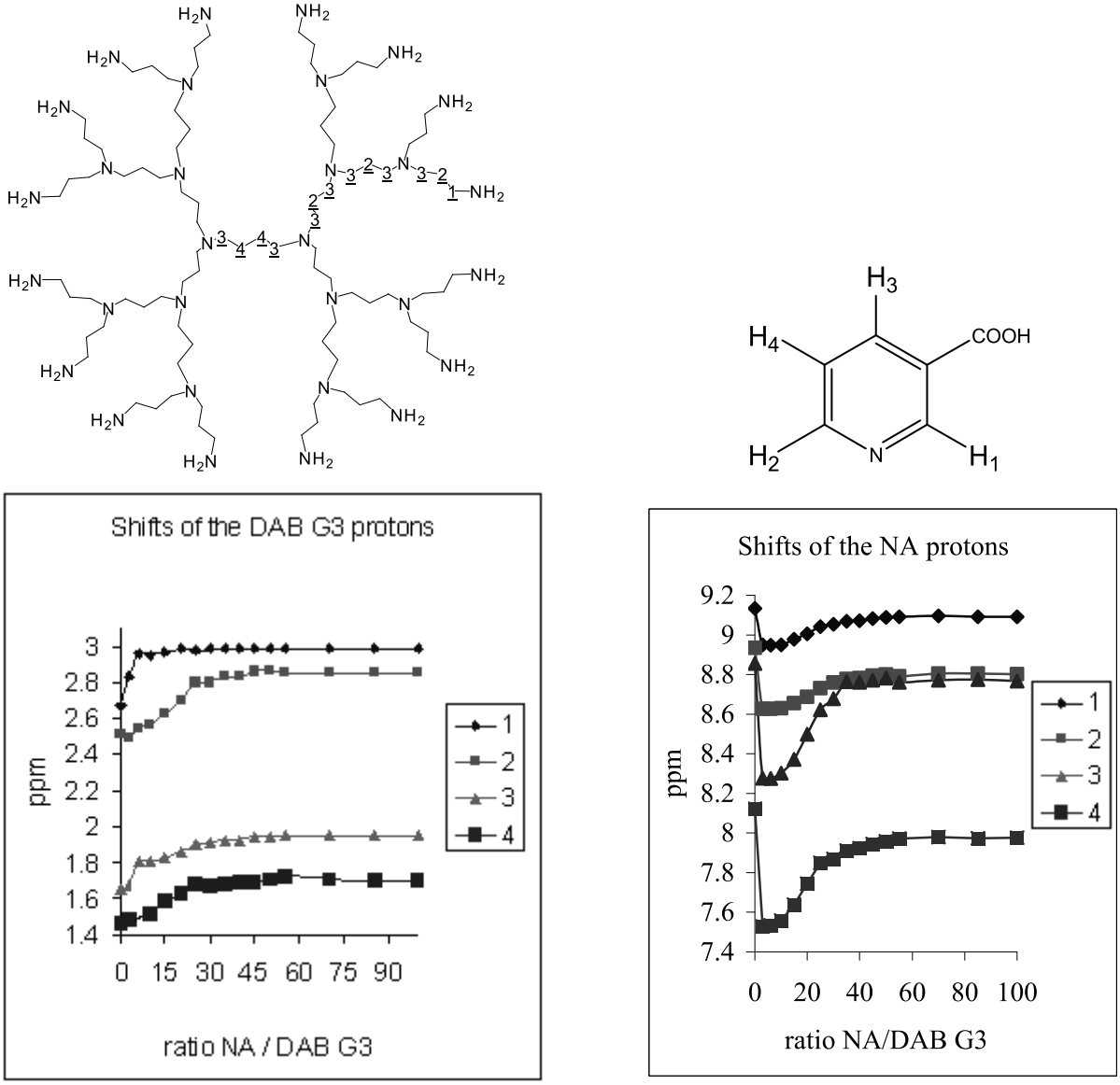

Figure 9. Titration of G1-PAMAM by nicotinic acid (NA).

The ^{1}H NMR study of the addition of vitamin B3 to G4-PAMAM-8NH_2 (Fig. 10) shows equiv. points around 55 to 65 NA for the four groups of dendritic protons C$H_2$$NH_2$, C$H_2$$CH_2$NH2, tertNC$H_2$ and NHCOCH2 that is in agreement of the complexation of 64 primary amine groups a the periphery. In addition, the inner protons tertNCH_2 and NHCOCH2 continue to be shifted until a broad zone corresponding to 120 to 200 equiv. NA consistent with a complexation of the additional 62 tertiary amine groups, but without clear equiv. points. The shift of pyridine ring proton located in para position versus the carboxylic group also undergoes a significant variation until very approximately 120 to 130 equiv. NA, which supports quaternarization of all the dendrimer amine groups. On the other hand, the proton located ortho vs. the carboxylic group does not undergo any variation all along the titration.

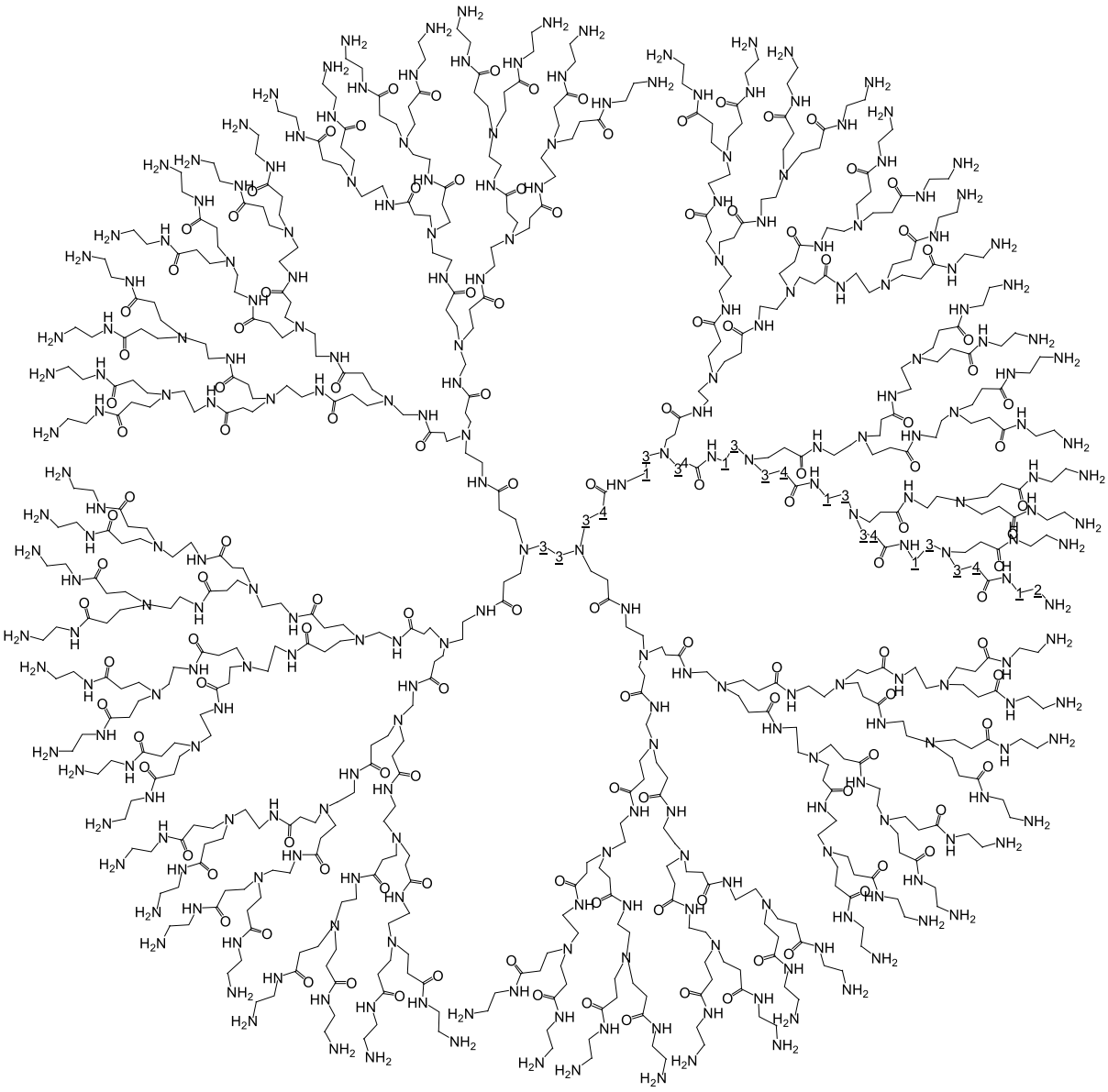

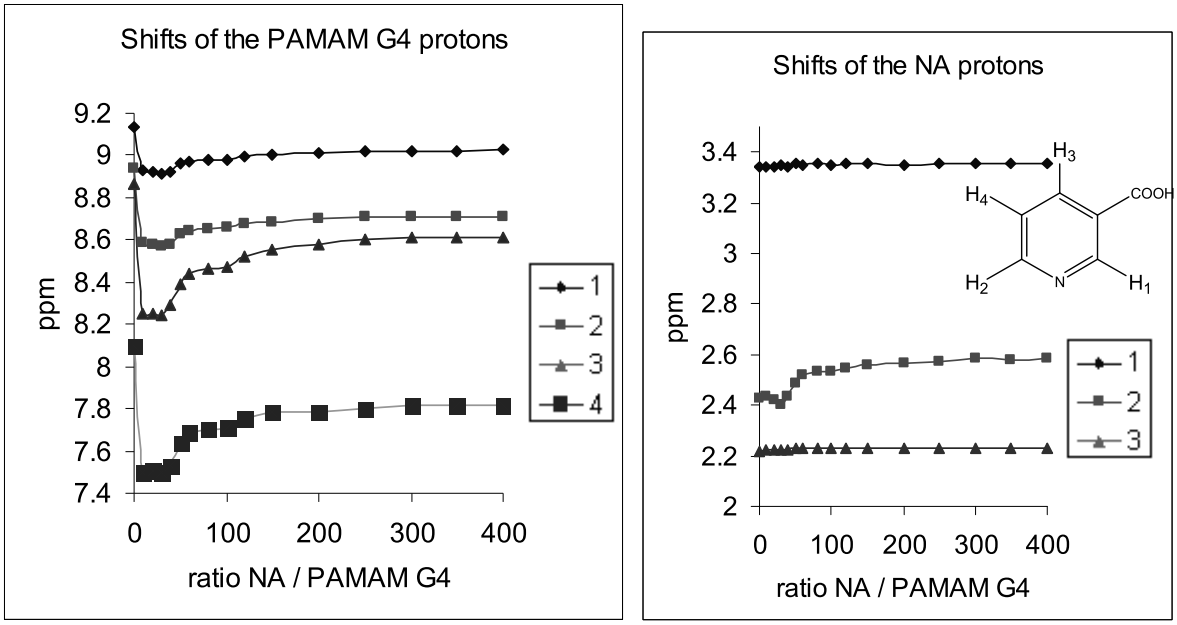

Figure 10. Titration of G4-PAMAM by nicotinic acid (NA).

Association constants between the polyamine dendrimers and vitamin C

The titrations of the DAB and PAMAM dendrimers by the acid vitamin C involve near-quantitative ammonium carboxylate ammonium formation. Thus these titrations are essentially clear-cut for most of them and allow determining association constants. The number of vitamin molecules bound to the dendrimer is determined as a function of the variation of the chemical shifts according to equation 1:[21]

$$\Delta\delta = \tfrac{1}{2}\,\Delta\delta_{max}\,[(1 + K_d / n[D_0] + [V] / n[D_0]) - \{(1 + K_d / n[D_0] + [V] / n[D_0])^2 - 4[V] / n[D_0]\}^{1/2}] \quad \text{(equation 1)}$$

n: number of AC molecules bound to the dendrimer; $[D_0]$: total concentration of dendrimer; [V]: total concentration of vitamin; K_d: dissociation constant.

This equation allows evaluating the association constants and dissociation constants of vitamin C (noted AA) and vitamin B3 (noted NA) with the DAB and PAMAM dendrimers (Table 1)

Supramolecular assembly	**$\Delta\delta_{max}$[a] (ppm)**	**χ_2[b]**	**n[c]**	***Kd*[d] (M)**	***Ka*[e] (M^{-1})**
DAB G2 + AA	0.48	0.0006	14	0.43	2.3
DAB G5 + AA	0.48	0.02	126	4	0.25
PAMAM G1 + AA	0.48	0.009	14	0.4	2.5
PAMAM G4 + AA	0.46	0.002	126	4	0.25

Table 1. Determination of the dissociation and association constants between the vitamins and the dendrimers; [a]$\Delta\delta_{max}$ is the maximum observed chemical shift variation; [b]χ_2 translated the difference between the experimental points and the numerical values extracted from a theoretical curve; [c]n is the number of vitamins as revealed by the first association constant; [d]K_d is the dissociation constant; [e]K_a is the association constant. The attenuated maximum error for all the values of this table is ±10%.

The values of the association constants characterizing the interactions between vitamin C and the dendrimers are between 0.25 M^{-1} to 2.5 M^{-1} and turn out to be relatively weak. They slightly decrease upon dendritic generation increase. Interdendritic interactionss might possibly cause this effect.

Concluding Remarks

The titrations of the DAB and PAMAM dendrimers by vitamin C, B_3 and B_6 show the excellent complexation and transport properties of these polyamine dendrimers with vitamins that are acidic. Polyammonium carboxylates are formed with both types of primary (peripheral) and tertiary (intradendritic) groups.
In the case of the DAB dendrimers, quaternarization clearly starts with peripheral primary amine groups, whereas with the PAMAM dendrimers, the encapsulation properties provided by the amido groups are presumably responsible for compensation of the steric peripheral preference, so that no or little selectivity is observed.
It is remarkable that all the internal tertiary amine groups are quaternarized despite the steric crowding inside the dendrimers in the high generations. More physical studies are called for, however, in order to examine whether the ion pairs formed remain in relatively short contact or are partly or totally dissociated inside and at the periphery of the dendrimers.
The titrations are largely dominated by the ion formations, and other supramolecular interactions are energetically much weaker. These additional supramolecular interactions are certainly present (and include those with the water solvent) but remain difficult to detect and ascertain by the rather sharp titration graphs. Nevertheless, the comparison between the titration of propylamine and those of the dendrimers shows that the end of the titrations is followed by a slight change of the chemical shifts of the dendrimer protons that is not observed in the case of propylamine. This is certainly a sign, albeit benign, of these additional supramolecular interactions leading to the transit of vitamin molecules in and out the dendrimer environment. Other studies of tetraethylene glycol terminated dendrimers give analogous titration results amplifying the observations of these supramolecular interactions but in addition bring about biocompatibility for biological applications.[22]

Experimental Section

General. All the reactions were carried out by Schlenk techniques or in a nitrogen- filled Vacuum Atmosphere drylab. The ^1H NMR spectra were recorded at 25°C with a Brucker AC 250 (250 MHz) spectrometer and the ^{13}C NMR spectra were obtained in pulsed FT mode at 62.0 MHz with a Brucker AC 250 spectrometer. All chemical shifts δ are reported in parts *per* million (ppm) relative to Me_4Si (TMS). Elemental analyses were performed by the Center of Microanalyses of the CNRS at Lyon Villeurbanne, France.
The dendrimers DAB G2, DAB G3, DAB G5, PAMAM G1 and PAMAM G4 are marketed by the Sigma-Aldrich company (Sigma-Aldrich Chemie S.a.r.l., L'Isle d' Abeau Chesnes, 38297 Saint-Quentin Fallavier, France), respectively under the references N° 679895, N° 469076, N° 469092, N° 597414 and N° 597856. The ascorbic acid used here is marketed with the reference N°255564 by the Sigma-Aldrich company (France).

Protocol of the titration of the dendrimer G2-DAB-8$NH_2$by vitamin C:
Fifteen samples E (numbered from 1 to 15) with increasing concentrations of ascorbic acid (AA) compared to DAB G2 dendrimer were prepared as follow:
- A solution S1 of ascorbic acid is obtained by dissolving 170.7 mg of ascorbic acid (AA) in 1.5 mL of D_2O.

- Each sample E was prepared by adding a volume V of solution S1 in a NMR tube containing 5 mg of the DAB G2 dendrimer in 300 µL of D_2O.
When the volume V is introduced, the ratio of the number of molecules of AA introduced *per* dendrimer and the mass of AA introduced into the NMR tube for each sample are detailed in the following table:

E	Volume V of the S1 solution (µL)	Mass of introduced AA (mg)	Ratio of the number of AA *per* DAB G2
1	0	0	0
2	10	1.138	1
3	30	3.414	3
4	50	5.690	5
5	80	9.104	8
6	100	11.380	10
7	120	13.656	12
8	140	15.932	14
9	180	20.484	18
10	220	25.036	22
11	260	29.588	26
12	280	31.864	28
13	360	40.968	36
14	420	47.796	42
15	500	56.900	50

The previous samples (from E1 to E15) were directly analyzed after the addition of the ascorbic acid solution without additional treatment or latency, because the encapsulation of vitamin C into the dendrimer is instantaneous. The data of the fifteen samples analyzed by NMR are detailed in the graphs shown in the results and discussion section.

Acknowledgement
Financial support from the Université Bordeaux 1, the CNRS and the ANR is gratefully acknowledged.

References

1. (a) G. R. Newkome, C. N. Moorefield and F. Vögtle, *Dendrimers and Dendrons. Concepts, Syntheses, Applications*, Wiley-VCH, Weinheim, 2001; (b) *Dendrimers and Other Dendritic Polymers*, D. A. Tomalia and J. M. J. Fréchet Eds, Wiley: Amsterdam, 2003; (c) *Dendrimers and Nanosciences*, D. Astruc Ed., *C. R. Chimie,* 2003, **6** (6-8), 709-1208, Elsevier, Paris (collection of Accounts); (d) F. Vögtle, G. Richardt and N. Werner, *Dendrimer Chemistry: Concepts, Syntheses, Properties, Applications,* Wiley: Weinheim, 2009.
2. (a) D. A. Tomalia, A. M. Naylor and W. Goddard III, *Angew. Chem., Int. Ed.,* 1990, **29**, 138-175; (b) G. R. Newkome, *Pure Appl. Chem.,* 1998, **70**, 2337-2343; (c) C. N. Moorefield and G. R. Newkome, *C. R. Chimie,* 2003, **6**, 715-724.
3. (a) R. Tekade, P. V. Kumar and N. K. Jain, *Chem. Rev.,* 2009, **109**, 49-87; (b) J. Grinstaff, *Polym. Sci.: Part A: Polym. Chem.,* 2008, **46**, 383-400; (c) S. Svenson and D. A. Tomalia, *Adv. Drug Deliv. Rev.,* 2005, **57**, 2106-2129; (d) E. R. Gillies and J. M. J. Fréchet, *Drug Discov. Today,* 2005, **10**, 35-43; (e) S. Svenson, *Eur. J. Pharm. Biopharm.,* 2009, **71**, 445-462; (f) U. Boas and P. M. H. Heegaard, *Chem. Soc. Rev.,*

2004, **33**, 43-63; (g) Y. Choi, T. Thomas, A. Kotlyar, M. T. Islam and J. R., Jr. Baker, *Chem. Biol.,* 2005, **12**, 35-43.
4. G. R. Newkome, Z. Yao, G. R. Baker and V. K. Gupta, *J. Org. Chem.,* 1985, **50**, 2003-2004.
5. D. A. Tomalia, V. Berry, M. Hall and D. M. Hedstrand, *Macromolecules*, 1987, **20**, 1164-1167.
6. (a) J. F. G. A. Jansen, E. M. M. de Brabander-van den Berg and E W. Meijer, *Science*, 1994, **266**, 1226-1229; (b) A. W. Bosman, H. M. Janssen and E. W. Meijer, *Chem. Rev.,* 1999, **99**, 1665-1688.
7. (a) R. M. Crooks, M. Zhao, L. Sun, V. Chechik and L. K. Yeung, *Acc. Chem. Res.,* 2001, **34**, 181-190; (b) R. W. J. Scott, O. M. Wilson and R. M. Crooks, *J. Phys. Chem B,* 2005, **109**, 692-704.
8. E. R. Gillies and J. M. J. Fréchet, *J. Am. Chem. Soc.,* 2002, **124**, 14137-14146.
9. (a) M. R. Mozafari and S. M. Mortazavi, *Nanoliposomes: From Fundamentals to Recent Developments*, Trafford Publishing Ltd, Oxford, 2005; (b) A. Gomez-Hens and J. M. Fernandez-Romero, *Trends Anal. Chem*., 2006, **25**, 167–178; (c) L. A. Meure, R. Knott, N. R. Foster and F. Dehghani, *Langmuir*, 2009, **25**, 326-337.
10. M. R. Mozafari, C. Johnson, S. Hatziantoniou and C. Demetzos, *J. Liposome Res*., 2008, **18**, 309-327.
11. C. J. Kirby, C. J. Whittle, N. Rigby, D. T. Coxon and B. A. Law, *Intern. J. Food Technol*., 1991, **26**, 437-449.
12. P. Sommer, N. A. Uhlich, J.-L. Reymond and T. Darbre, *ChemBioChem,* 2008, **9**, 689-693.
13. (a) T. D. McCarthy, P. Karellas, S. A. Henderson, M. Giannis, D. F. O'Keefe, G. Heery, J. R. A. Paull, B. R. Matthews and G. Holan, *Mol. Pharm.,* 2005, **2**, 312-318; (b) D. L. Patton, Y. T. C. Sweeney, T. D. McCarthy and S. L. Hillier, *Antimicrob. Agents Chemother.,* 2006, **50**, 1696-1700; (c) R. J. Mumper, M. A. Bell, D. R. Worthen, R. A. Cone, G. R. Lewis and J. R. A. Paull, *Drug Dev. Int. Pharm.,* 2009, **35**, 515-524.
14. S. Padayatty, A. Katz, Y. Wang, P. Eck, O. Kwon, J. Lee, S. Chen, C. Corpe, A. Dutta, S. Dutta and M. Levine, *J. Am. Coll. Nutr.*, 2003, **22**, 18–35.
15. M. Cox, A. L. Lehninger and D. R. Nelson, Principles of biochemistry. New York: Worth Publishers, 2000.
16. G. F. Combs, *The Vitamins: Fundamental Aspects in Nutrition and Health*, Elsevier, San Diego, Ca. 2008.
17. (a) C. Valério, J.-L.Fillaut, J. Ruiz, J. Guittard, J.-C. Blais and D. Astruc, *J. Am. Chem. Soc.,* 1997, **119**, 2588-2589; (b) E. Alonso, C. Valério, J. Ruiz and D. Astruc, *New J. Chem.,* 1997, **21**, 1139-1141; (c) D. Astruc, C. Ornelas and J. Ruiz, *Acc. Chem. Res*., 2008, **41**, 841-856; (d) D. Astruc, M.-C. Daniel and J. Ruiz, *Chem. Commun*, 2004, 2637-2649.
18. (a) C. Valério, E. Alonso, J. Ruiz, J.-C. Blais and D. Astruc, *Angew. Chem. Int. Ed. Engl.*, 1999, **38**, 1747-1751; (b) C. Ornelas, E. Boisselier, V. Martinez, I. Pianet, J. Ruiz and D. Astruc, *Chem. Commun.,* 2007, 5093-5095; (c) E. Boisselier, C. Ornelas, I. Pianet, J. Ruiz and D. Astruc, *Chem. Eur. J.,* 2008, **14**, 5577-5587.
19. (a) M.-C. Daniel, J. Ruiz and D. Astruc, *J. Am. Chem. Soc*., 2003, **125**, 1150-1151; (b) M.-C. Daniel, F. Ba, J. Ruiz and D. Astruc, *Inorg. Chem*., 2004, **43**, 8649-8657.
20. (a) C. Ornelas, J. Ruiz, E. Cloutet, S. Alves and D. Astruc, *Angew. Chem,. Int. Ed.*, 2007**,** **46**, 872-877; (b) C. Ornelas, L. Salmon, J. Ruiz and D. Astruc, *Chem. Eur. J*., 2008, **14**, 50-64.

21. (a) A. J. Charlton, N. J. Baxter, M. Davies and M. P. Williamson, *J. Agric. Food Chem.,* 2002, **50**, 1593-1601; (b) C. Simon, K. Barathieu, M. Laguerre, J. M. Schmitter, E. Fouquet, I. Pianet and E. J. Dufourc, *Biochemistry,* 2003, **42**, 10385-10395.
22. E. Boisselier, J. Ruiz and D. Astruc, French Patent FR101305 (n° 0850372, 01/21/07).

Chapitre A-3

Dendrimères à terminaison benzoate et reconnaissance de cations d'intérêts biologiques dans l'eau

Les dendrimères hydrosolubles présentent des applications potentielles en médecine comme transporteurs de médicaments, ce domaine étant l'un des plus prometteurs parmi les applications potentielles de la chimie dendritique. Cependant il est indispensable de conduire parallèlement des expériences de liaisons avec les substrats d'intérêt. Il semble bien établi jusqu'à présent que les dendrimères à terminaisons anioniques soient beaucoup moins toxiques et plus biocompatibles que les dendrimères à terminaisons cationiques. C'est pourquoi nous avons porté notre intérêt vers les dendrimères à terminaisons anioniques afin d'examiner leurs interactions avec les substrats anioniques d'intérêt biologique.

La synthèse du dendrimère à neuf terminaisons $ArCO_2H$ (generation 0) a été mise au point par Melle Catia Ornelas, ancienne doctorante du Pr. Astruc, puis appliquée par M. Victor Martinez, ancien doctorant du Professeur Didier Astruc, au dendrimère 81-CO_2H. J'ai donc renouvelé cette synthèse de dendrimères à terminaisons benzoates et réalisé l'étude RMN ^1H dans D_2O de l'interaction dendrimère-substrat. Cette étude a également été menée en collaboration avec Mme Isabelle Pianet du CESAMO (Centre d'Etude RMN de l'Université Bordeaux 1), en particulier en ce qui concerne le calcul des constantes d'équilibre d'association.

Un premier substrat comportant un ammonium est l'acétylcholine. L'acétylcholine est utilisée en tant que principe actif pour certains médicaments mais elle n'est pas très active lors d'une prise orale car elle est hydrolysée dans le tube digestif. C'est pourquoi l'utilisation de dendrimères pour l'encapsuler et la stabiliser devient utile. Cette étude est l'objet d'une communication préliminaire à *Chemical Communications* portant sur les liaisons ioniques des molécules d'acétylcholine avec des dendrimères comportant 81 branches à terminaisons benzoates.

Le mémoire suivant la note préliminaire compare les différentes générations à 9, 27, 81 et 243 branches de dendrimères à terminaisons benzoate solubles dans l'eau, dans leurs intéractions dans l'eau non seulement avec l'acétylcholine, mais également avec d'autres substrats ammoniums d'intérêt biologique ou médicinal tels que le chlorure de benzyltriethylammonium ou encore la dopamine. Le chlorure de benzyltriethylammonium appartient à une catégorie de composés contenant un ammonium quaternaire qui montrent une variété de propriétés physiques, chimiques et biologiques. Il peut par exemple interrompre certains processus cellulaires et est notamment utilisé en tant que biocide dans l'industrie pharmaceutique. La dopamine est, quant à elle, un neurotransmetteur présent dans certaines parties du système nerveux central et est prescrite pour un grand nombre de symptômes. Or, son temps de demi-vie dans le plasma est d'environ deux minutes lorsqu'elle est administré par intraveineuse. L'utilisation d'un complexe dendrimère-dopamine devrait allonger son temps de demi-vie et permettre ainsi une meilleure pénétration dans les systèmes visés.

Ce chapitre se compose donc de la note publiée à *Chemical Communications* en 2007 ainsi que du mémoire publié à *Chemistry, a European Journal* en 2008 ainsi que de leurs parties détaillant les informations complémentaires. Notre approche générale au cours de ce chapitre consiste à étudier les effets dendritiques (variations de propriétés observées en fonction de la variation du nombre de générations) pour affiner notre compréhension des processus et les optimiser.

New water-soluble polyanionic dendrimers and binding to acetylcholine in water by means of contact ion-pairing interactions†

Cátia Ornelas, Elodie Boisselier, Victor Martinez, Isabelle Pianet, Jaime Ruiz Aranzaes and Didier Astruc*

Received (in Cambridge, UK) 9th July 2007, Accepted 19th September 2007
First published as an Advance Article on the web 8th October 2007
DOI: 10.1039/b710391c

A new water-soluble polyanionic dendrimer containing 81 benzoate termini (diameter: 11 ± 1 nm from DOSY NMR spectroscopy) has been synthesized; it interacts with acetylcholine cations in water-soluble assemblies in which each carboxylate terminus reversibly forms contact ion pairs and aggregates at the tether termini, as shown by ^{1}H NMR spectroscopy.

The supramolecular facets of dendrimers[1] have been largely considered for uses as molecular boxes,[2] exoreceptors,[3] and sensors.[4] Indeed, applications of water-soluble dendrimers as drug vectors are most promising.[5,6] A possible drawback of polycationic dendrimers, however, is their toxicity. On the other hand, it has been recognized that polyanionic dendrimers usually display acceptable biocompatibility.[7,8] Therefore, we have investigated the route to polybenzoate-terminated dendrimers synthesized from polyiodomethylsilyl precursors, and their ability to transport cations of biomedical interest such as acetylcholine.

Acetylcholine (AC) chloride is produced naturally by the nervous system. It is also used as an active ingredient in some drugs, but it is not very active upon oral ingestion because of hydrolysis in the digestive tube. AC chloride has various pharmacological properties: it can be used as a parasympathomimetic,[9a] a peripheral vasodilator, an antihypertensive, a miotic or a coronarodilator.[9b] Its muscarinic parasympathomimetic action consists in contracting the smooth fibre in the digestive tube,[10b] the eye and the bronchi.[10a] It is used in a drug marketed as a parasympathomimetic preparation for intraocular use, although aqueous solutions are unstable and must thus be prepared just before use.[11]

We now report the assembly of polyanionic dendrimers and dendrimer–acetylcholine molecular architectures, including their water-solubility properties and ion-pair behavior in water.

For the dendritic construction, we used the 1 → 3 C connectivity, pioneered by Newkome *et al.*,[12] as shown in Scheme 1. It starts with the known nona-allylation of [FeCp(η^6-mesitylene][PF_6], **1**, that quantitatively yields the nona-allyl dendritic core 1,3,5-[$C(CH_2CH{=}CH_2)_3$]C_6H_3, **2**, on a large scale subsequent to visible-light photolysis that removes the metal moiety.[13] Hydrosilylation of the terminal olefinic bonds, a reaction pioneered in dendrimer synthesis by van Leeuwen *et al.*,[14] is carried out on **2**, using chloromethyldimethylsilane and Karsted catalyst, regioselectively giving the nona-chloromethyldimethylsilyl intermediate that, upon reaction with NaI, provides the nona-iodide **3**. The dendritic progression was achieved using the known phenoltriallyl dendron *p*-(HO)$C_4H_4C(CH_2CH{=}CH_2)_3$, obtained by one-pot reaction of [FeCp(η^6-*p*-chlorotoluene][PF_6] with allyl bromide and *t*-BuOK (Scheme 1).[13]

Williamson's reaction of the dendri-81-iodide, **6**, with methyl 4-hydroxybenzoate yielded the dendri-81-benzoate, **7**, that was characterized by its molecular peak at 29 471 (M^+) in the MALDI TOF mass spectrum (calcd for $C_{1611}H_{2352}O_{279}Si_{117}$: 29 469.75). The ^{1}H NMR spectrum of the dendrimer-81-acid, **8**, in MeOD shows all the signals of the molecule, including all the protons of the dendritic core, confirming the expected structure. When this dendrimer is solubilized in water upon addition of a stoichiometric amount of NaOH yielding **9**, the ^{1}H NMR spectrum in D_2O shows the proton signals of the periphery only.

The dendrimer **9**, containing 81 sodium carboxylate groups, reversibly reacts with AC chloride to form water-soluble assemblies whose structure can be examined by ^{1}H NMR spectroscopy.[15] The interaction between the dendrimer **9** and AC is characterized in the ^{1}H NMR spectrum by the large upfield shift of the four AC signals upon interaction with **9**. The dendrimer signals also move, but to a lesser extent, the average shift being 0.06 ppm in water for the peripheral protons numbered from 5 to 8. The titration of AC was achieved in order to tentatively quantify the number of AC that can be transported by **9**.‡

When the first 20 equivalents of AC are added, the AC signals are shifted from 4.56 ppm to 4.04 ppm for the CH_2–CH_2–N protons numbered 3, from 3.75 ppm to 3.18 ppm for the CH_2–N protons numbered 2, from 3.23 ppm to 2.78 ppm for the CH_3–N numbered 1, and from 2.16 ppm to 1.81 ppm for the CH_3–COO protons (see Fig. 1). These results correspond to an average displacement of 0.5 ppm. The four signals of AC are shifted during this titration because of the interactions of the whole molecule with **9**. Indeed, when AC interacts with **9**, the ammonium AC group should be located at the dendrimer periphery, reversibly forming contact ion pairs and aggregates with the carboxylate ion.

The number *n* of AC molecules bound to the dendrimer is determined as a function of the variation $\Delta\delta$ of chemical shifts according to eqn (1):[15]

$$\Delta\delta = \tfrac{1}{2}\Delta\delta_{max}[(1 + K_d/n[D_0] + [AC]/n[D_0]) - \{(1 + K_d/n[D_0] + [AC]/n[D_0])^2 - 4[AC]/n[D_0]\}^{1/2}] \quad (1)$$

n: number of AC molecules bound to **9**; $[D_0]$: total concentration of **9**; [AC]: total concentration of AC; K_d: dissociation constant.

Institut des Sciences Moléculaires, UMR CNRS N°5255, Université Bordeaux 1, 33405 Talence Cedex, France. E-mail: d.astruc@ism.u-bordeaux1.fr; Fax: +33 54040 6646

† Electronic supplementary information (ESI) available: Synthesis and detailed ^{1}H NMR data including DOSY and ROESY experiments. See DOI: 10.1039/b710391c

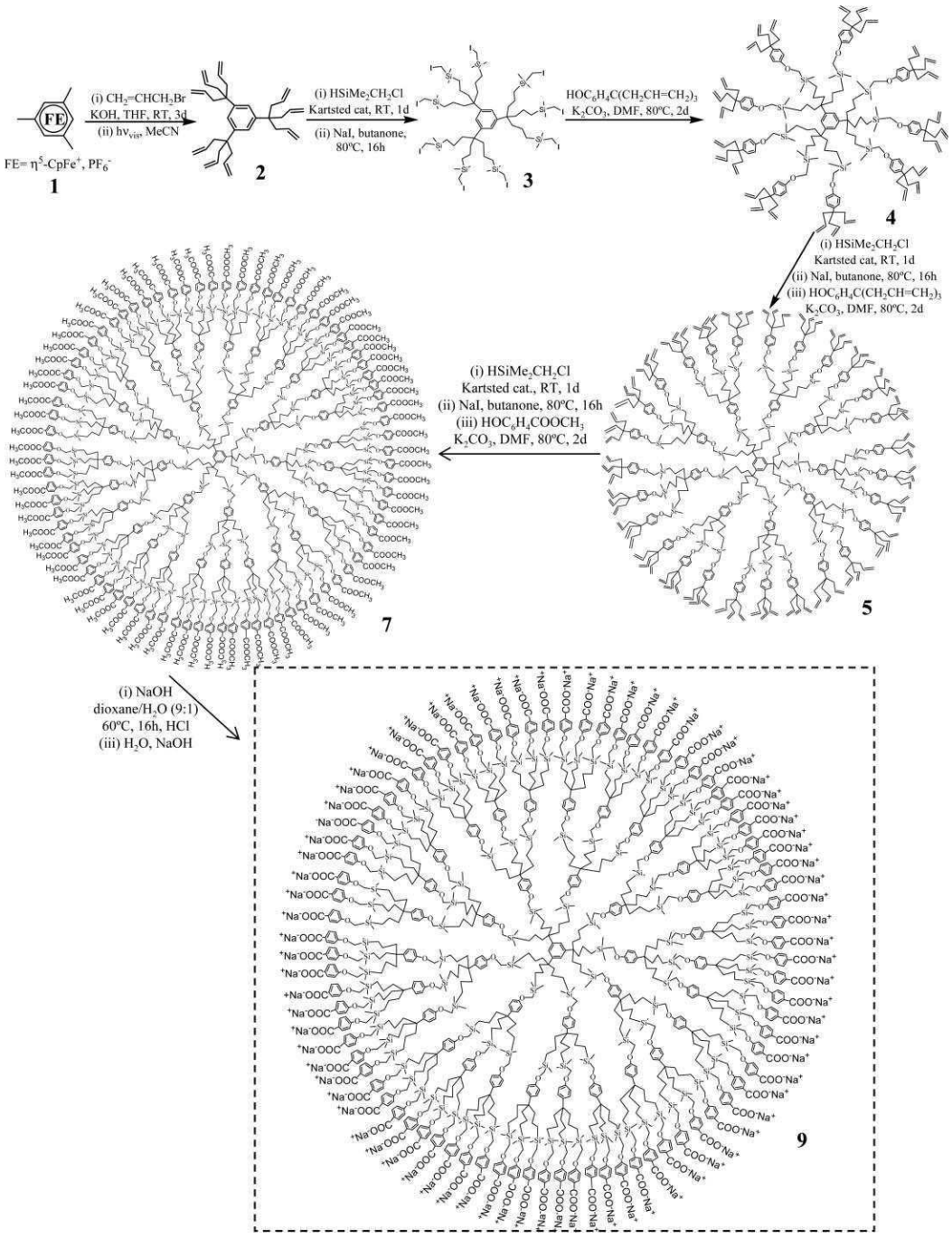

Scheme 1 Synthesis of the water soluble dendrimer-81-carboxylate G_2 (**9**).

The best fit is that for which dendrimer **9** interacts with 2 ($\pm$0.1) molecules of AC per dendritic branch. Indeed, the first AC molecule (per branch) interacts at the dendrimer periphery by electrostatic interaction with a dissociation constant K_{d1} of 17 ($\pm$2) $\times$ 10^{-3} M. Then, the other AC molecule (per branch) also interacts, with seemingly weaker interactions, with a dissociation constant K_{d2} of 230 ($\pm$20) $\times$ 10^{-3} M (eqn (2), R = dendrimer, R′ = AC).

$$\mathrm{RCO_2^-Na^+ + R'N^+Me_3Cl^- \overset{K_{d1}}{\rightleftharpoons} RCO_2^-R'N^+Me_3 \overset{K_{d2}}{\rightleftharpoons} RCO_2^-\left(R'N^+Me_3\right)_2} \quad (2)$$

$[Na(H_2O)_x]^+[Cl(H_2O)_y]^-$ is also formed in eqn (2).

DOSY experiments were carried out in order to follow the evolution of the diffusion coefficient of the dendrimer without AC and with an increasing concentration of AC. The dendrimer without AC in water has a diffusion coefficient of 4.4 $\times$ 10^{-11} m^2 s^{-1}, and a hydrodynamic diameter of 11 $\pm$ 1 nm; a molecule of AC has a diffusion coefficient of 5.9 $\times$ 10^{-10} m^2 s^{-1}, and a hydrodynamic diameter of 1.2 $\pm$ 0.1 nm (see the ESI†). The diffusion coefficient of **9** does not vary during the titration, meaning that the dendrimer has approximately the same size whether it is free or bound. This lack of dendrimer size increase upon AC binding, together with the upfield shift of the AC NMR

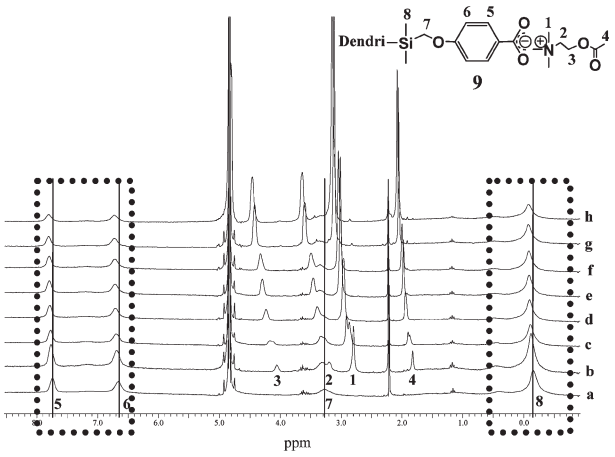

Fig. 1 ^{1}H NMR titration of AC with **9**: (a) **9** as its Na^+ salt; (b) **9** + 20 eq. of AC; (c) **9** + 40 eq. of AC; (d) **9** + 60 eq. of AC; (e) **9** + 80 eq. of AC; (f) **9** + 100 eq. of AC; (g) **9** + 200 eq. of AC; (h) **9** + 300 eq. of AC (similar to AC).

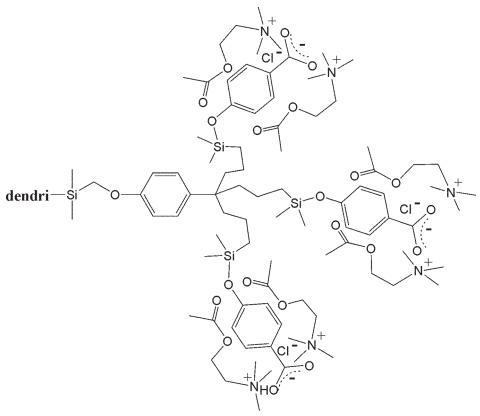

Fig. 2 Arbitrary representation of the ionic aggregates with 2 AC at the termini of **9**, taking into account the mutual influence of the AC and benzoate groups on the ^{1}H NMR shifts and lack of dendrimer size increase with AC (the AC molecules, whose ammonium parts form an aggregate with the carboxylate and chloride anions, are also folding back towards the hydrophobic dendritic interior).

signals upon dendrimer binding, suggest encapsulation of AC in the hydrophobic dendrimer interior (near the periphery, back folding of the dendrimer tethers being not excluded).

The diffusion coefficient of AC increases until a concentration matching approximately 162 ($\pm$5) AC per dendrimer, confirming the interaction of each carboxylate termini with two AC molecules, before stagnating at higher AC concentrations.

The observed behavior of the assembly **9** + AC is best taken into account by the reversible formation of ionic bonds between the dendrimer-81-carboxylate **9** and the AC cations as contact ion pairs.[16] The second stage most probably also involves agglomeration of additional charges of AC chloride to reversibly form an aggregate at each tether terminus. This should be due to the dual location of the anionic charge, delocalized onto both carboxylate oxygen atoms of the carboxylate group, that can form a five-component aggregate (one chloride anion in addition to the two oxygen atoms and the two AC cations, see Fig. 2). By comparison, $PhCO_2^-Na^+$ hardly shows any interaction with AC ($\Delta\delta < 0.1$ ppm), which demonstrates the positive dendritic effect.

Notes and references

‡ In an NMR tube, 5 mg of **9** were introduced in 0.5 mL D_2O, then AC was progressively added. The titration spans from 0 to 320 equivalents of AC *per* dendrimer **9** (Fig. 1, the shifts of the peripheral protons of **9** are framed). The shifts of the four signals of AC are represented and numbered from 1 to 4.

1 V. Percec, G. Johansson, G. Ungar and J. P. Zhou, *J. Am. Chem. Soc.*, 1996, **18**, 9855; F. Zeng and S. C. Zimmermann, *Chem. Rev.*, 1997, **97**, 1681; V. Balzani, S. Campana, G. Denti, A. Juris, S. Serroni and M. Venturi, *Acc. Chem. Res.*, 1998, **31**, 26; O. A. Matthews, A. N. Shipway and J. F. Stoddart, *Prog. Polym. Sci.*, 1998, **23**, 1; G. R. Newkome and C. N. Moorefield, *Chem. Rev.*, 1999, **99**, 1689; G. R. Newkome, C. N. Moorefield and F. Vögtle, Wiley-VCH, Weinheim, 2001.

2 J. F. G. A. Jansen, E. M. M. de Brabander-van den Berg and E. W. Meijer, *Science*, 1994, **266**, 1226; A. W. Bosman, E. W. Jensen and E. W. Meijer, *Chem. Rev.*, 1999, **99**, 1665.

3 C. Valério, J.-L. Fillaut, J. Ruiz, J. Guittard, J.-C. Blais and D. Astruc, *J. Am. Chem. Soc.*, 1997, **119**, 2588; D. Astruc, M.-C. Daniel and J. Ruiz, *Chem. Commun.*, 2004, 2637; M.-C. Daniel and D. Astruc, *Chem. Rev.*, 2004, **104**, 293.

4 M. Albrecht, N. J. Hovestad, J. Boersma and G. van Koten, *Chem.–Eur. J.*, 2001, **7**, 1289; A. W. Kleij, A. Ford, J. T. B. H. Jastrzebski and G. van Koten, in *Dendrimers and Other Dendritic Polymers*, ed. J. M. J. Fréchet and D. A. Tomalia, Wiley, New York, 2002, 185.

5 D. Astruc, *C. R. Acad. Sci., Ser. IIb: Mec., Phys., Chim., Astron.*, 1996, **322**, 757 (review); C. Kojima, K. Kono, K. Maruyama and T. Takagishi, *Bioconjugate Chem.*, 2000, **11**, 910; K. Sadler and J. P. Tam, *J. Biotechnol.*, 2002, **90**, 195; M. J. Cloninger, *Curr. Opin. Chem. Biol.*, 2002, **6**, 742; S. E. Stiriba, H. Frey and R. Haag, *Angew. Chem., Int. Ed.*, 2002, **41**, 1329; M. W. Grinstaff, *Chem.–Eur. J.*, 2002, **8**, 2838; U. Boas and P. M. H. Heegarard, *Chem. Soc. Rev.*, 2004, **33**, 43; C. C. Lee, J. A. Mac Kay, J. M. J. Fréchet and F. Szoka, *Nat. Biotechnol.*, 2005, **23**, 1517.

6 D. A. Tomalia, H. Baker, J. Dewald, M. Hall, G. Kallos, S. Martin, J. Roeck and P. Smith, *Macromolecules*, 1986, **19**, 2466; D. A. Tomalia, A. N. Naylor and N. A. Goddard, III, *Angew. Chem., Int. Ed. Engl.*, 1990, **102**, 119. For the first water-soluble dendrimers, see also ref. 12.

7 N. Malik, R. Wiwattanapatapee, R. Klopsch, K. Lorenz, H. Frey and J. W. Weener, *J. Controlled Release*, 2000, **65**, 133.

8 R. Jevprasesphant, J. Penny, R. Jalal, D. Attwood, N. B. McKown and A. D'Emmanuele, *Int. J. Pharm.*, 2003, **252**, 263.

9 (*a*) O. Voss, *Naunyn–Schmiedebergs Arch. Exp. Pathol. Pharmakol.*, 1926, **116**, 367; (*b*) E. A. Carmichael and F. R. Fraser, *Heart*, 1933, **16**, 263.

10 (*a*) B. A. Houssay and O. Orias, *C. R. Seances Soc. Biol. Ses Fil.*, 1934, **117**, 61; (*b*) M. Beauvallet, *C. R. Seances Soc. Biol. Ses Fil.*, 1938, **127**, 213.

11 D. M. Sletten, K. K. Nickander and P. A. Low, *J. Neurol. Sci.*, 2005, **234**, 1.

12 G. R. Newkome, Z. Yao, G. R. Baker and V. K. Gupta, *J. Org. Chem.*, 1985, **50**, 2003.

13 (*a*) V. Sartor, L. Djakovitch, J.-L. Fillaut, F. Moulines, F. Neveu, V. Marvaud, J. Guittard, J.-C. Blais and D. Astruc, *J. Am. Chem. Soc.*, 1999, **121**, 2929; (*b*) J. Ruiz, G. Lafuente, S. Marcen, C. Ornelas, S. Lazare, J.-C. Blais, E. Cloutet and D. Astruc, *J. Am. Chem. Soc.*, 2003, **125**, 7250; (*c*) C. Ornelas, D. Méry, J. Ruiz, J.-C. Blais, E. Cloutet and D. Astruc, *Angew. Chem., Int. Ed.*, 2005, **44**, 7399.

14 A. W. van der Made, P. W. N. M. van Leeuwen, J. C. de Wilde and R. A. C. Brandes, *Adv. Mater.*, 1993, **5**, 466.

15 (*a*) A. J. Charlton, N. J. Baxter, M. L. Khan, A. J. G. Moir, E. Haslam, A. P. Davies and M. P. Williamson, *J. Agric. Food Chem.*, 2002, **50**, 1593; (*b*) C. Simon, K. Barathieu, M. Laguerre, J. M. Schmitter, E. Fouquet, I. Pianet and E. J. Dufourc, *Biochemistry*, 2003, **42**, 10385.

16 (*a*) J. Smid, in *Ions and Ion Pairs in Organic Reactions*, ed. M. Schwarc, Wiley, New York, 1972, vol. 1, ch. 3; (*b*) *The Organic Chemistry of Electrolyte Solutions*, ed. J. E. Gordon, Wiley, New York, 1975; (*c*) J. D. Simon and K. S. Peters, *Acc. Chem. Res.*, 1984, **17**, 277; (*d*) A. Loupy, B. Tchoubar and D. Astruc, *Chem. Rev.*, 1992, **92**, 1141.

Supplementary Material (ESI) for Chemical Communications

New Water-soluble Polyanionic Dendrimers and Transport of Acetylcholin in Water By Means of Supramolecular Interactions

Cátia Ornelas, Elodie Boisselier, Victor Martinez, Isabelle Pianet, Jaime Ruiz Aranzaes, Didier Astruc*

Supplementary Information

Experimental section.

General data.

All reactions were carried out using Schlenk techniques or in a nitrogen-filled Vacuum Atmosphere drylab. ^{1}H NMR spectra were recorded at 25°C with a Brucker AC 300 (300 MHz) spectrometer. ^{13}C NMR spectra were obtained in the pulsed FT mode at 75.0 MHz with a Brucker AC 300 spectrometer and ^{29}Si NMR spectra were obtained in at 59.6 MHz with a Brucker AC 300 spectrometer. All chemical shifts are reported in parts per million (δ, ppm) with reference to Me_4Si (TMS). The MALDI TOF mass spectra were recorded with a PerSeptive Biosystems Voyager Elite (Framingham, MA) time-of-flight mass spectrometer. Elemental analyses were performed by the Center of Microanalyses of the CNRS at Lyon Villeurbanne, France. Diffusion measurements were performed at different AC concentrations using a ^{1}H NMR pulsed-gradient experiment:the simulated spin-echo sequence which leads to the measurement of the diffusion coefficient D, where D is the slope of the straight line obtained when ln(I) is displayed against the gradient-pulse power's square according to the following equation: $\ln(I) = -\gamma^2G^2D\delta^2(\Delta-\delta/3)$, where I is the relative intensity of a chosen resonance, γ is the proton gyromagnetic ratio, Δ is the intergradient delay (150 ms), δ is the gradient pulse duration (5 ms), and G is the gradient intensity. The diffusion constant of water (2.3×10^{-9} m²/s) was used to calibrate the instrument.

Synthesis of dendri-81-benzoate, 7:

Dendri-81-iodide **6** (0.30 g, 0.011 mmol), methyl 4-hydroxybenzoate (0.27 g, 1.78 mmol), K_2CO_3 (1.25 g, 8.91 mmol) and dry DMF (30 mL) were indroduced in a Schlenk flask. The reaction mixture was stirred at 80°C for 48 h. DMF was removed, the crude product was solved in 30 mL of dichloromethane and washed with water in order to remove the K_2CO_3. The organic layer was dried with Na_2SO_4, filtered, and the solvent was removed *in vacuo*. The product was washed with methanol and precipitated twice in CH_2Cl_2/methanol in order to remove the excess of methyl 4-hydroxybenzoate. The dendri-81-benzoate was obtained as a colourless waxy product (0.289 g, 89% yield).

^{1}H NMR ($CDCl_3$, 250MHz): 7.94 and 6.88 (d, 162H, *outer arom*), 7.10 and 6.80 (d, 72H, *inner arom*), 3.84 (s, 243H, COOCH_3), 3.51 (s, 234H, SiCH_2O), 1.60 (s, 234H, CH_2CH$_2$CH$_2$Si), 1.11 (s, 234H, CH$_2$CH_2CH$_2$Si), 0.55 (s, 234H, CH$_2$CH$_2$CH_2Si), 0.034 (s, 702H, Si(CH_3)$_2$). ^{13}C NMR ($CDCl_3$, 62 MHz): 167.2 (*C*OOCH$_3$), 164.2 (outer arom. *C*qO), 159.4 (*inner* arom. *C*qO), 131.8 and 114.2 (*C*H, arom.), 122.5 (arom. *C*qCOOCH$_3$), 61.1 (Si*C*H$_2$O), 52.2 (COO*C*H$_3$), 43.4 (*C*H$_2$CH$_2$CH$_2$Si), 42.3 (*C*qCH$_2$), 18.0 (CH$_2$*C*H$_2$CH$_2$), 14.9 (CH$_2$CH$_2$*C*H$_2$Si), -4.3 (SiMe$_2$). ^{29}Si NMR ($CDCl_3$, 59.62 MHz) δ ppm: 0.53 (*Si*CH$_2$O). MS (MALDI-TOF; m/z) Calcd. For $C_{1611}H_{2352}O_{279}Si_{117}$: 29 469.75; found: 29 471.00. Anal. Calc. for $C_{1611}H_{2352}O_{279}Si_{117}$: C 65.63, H 7.99; found: C 65.58, H 8.04. Infrared $\upsilon_{C=O}$: 1 719 cm^{-1}.

Synthesis of dendri-81-acid, 8:

Dendri-81-benzoate **7** (0.20 g, 0.0068 mmol), was dissolved in dioxane (50 mL), and 5 mL of an aqueous solution of NaOH (5.51 mmol, 10 equiv. *per* branch) was added. The reaction mixture was stired at 60°C for 48 h. Dioxane was removed under vacuum, and the aqueous solution was acidified with HCl. Dendri-81-acid precipitated as a white powder. The solution was filtrated, and the powder was washed twice with ether. The product was recovered from filter by dissolving in methanol. The methanol was removed *in vacuo,* and the product was obtained as a white powder in 67 % yield.

^{1}H NMR (MeOD, 250MHz): 7.90 and 6.83 (d, 162H, *outer arom*), 7.08 and 6.75 (d, 72H, *inner arom*), 3.43 (s, 234H, SiC*H*$_2$O), 1.58 (s, 234H, C*H*$_2$CH$_2$CH$_2$Si), 1.10 (s, 234H, CH$_2$C*H*$_2$CH$_2$Si), 0.49 (s, 234H, CH$_2$CH$_2$C*H*$_2$Si), -0.056 (s, 702H, Si(C*H*$_3$)$_2$). ^{13}C NMR (MeOD, 62 MHz): 169.9 (*C*OOH), 166.8 (*outer* arom. *C*qO), 160.5 (*inner* arom. *C*qO), 133.0 and 115.1 (*C*H, arom.), 123.8 (arom. *C*qCOOCH$_3$), 61.8 (Si*C*H$_2$O), 44.3 (*C*H$_2$CH$_2$CH$_2$Si), 43.4 (*C*qCH$_2$), 19.0 (CH$_2$*C*H$_2$CH$_2$), 15.8 (CH$_2$CH$_2$*C*H$_2$Si), -4.0 (SiMe$_2$). ^{29}Si NMR (MeOD, 59.62 MHz) δ ppm: 0.26 (*Si*CH$_2$O). Anal. Calc. for $C_{1530}H_{2190}O_{279}Si_{117}$: C 64.86, H 7.79; found: C 64.25, H 7.68. Infrared $\upsilon_{C=O}$: 1 686 cm^{-1}.

Chemical Shift Variations of the AC proton signals.

The number n of AC molecules bound to the dendrimer is a function of the variation $\Delta\delta$ of chemicals shift (equation 1):

$$\Delta\delta = ½\ \Delta\delta_{max}\ [(1 + K_d / n[D_0] + [AC] / n[D_0]) - \{(1 + K_d / n[D_0] + [AC] / n[D_0])^2 - 4[AC] / n[D_0]\}^{1/2}]$$

n: number of AC molecules bound to the dendrimer **9**; $[D_0]$: total concentration of the dendrimer **9**; [AC]: concentration of AC; K_d: dissociation constant; K_a: association constant; $\Delta\delta_{max}$: the highest chemical shift variation.

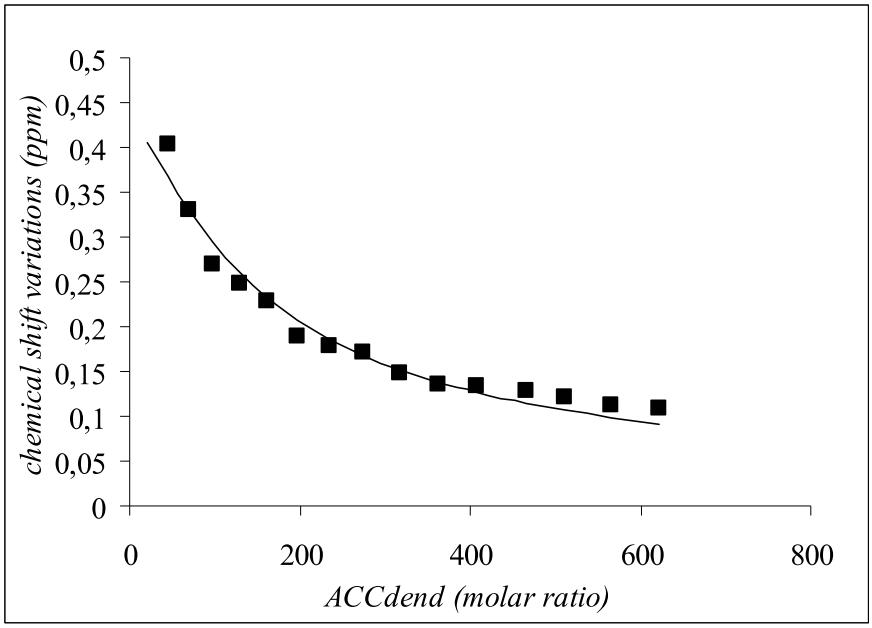

$\Delta\delta_{max} = 0,6$

$\chi_2 = 0,04$

For the first 81 molecules of AC bound to **9:** $Kd_1 = 17\ (\pm 2) \times 10^{-3}$ M

For the other 81 molecules of AC bound to **9:** $Kd_2 = 230\ (\pm 20) \times 10^{-3}$ M

Measurements of diffusion coefficient by ^{1}H NMR upon titration of acetylcholine (AC) with the dendrimer-81-benzoate 9.

The goal of this series of experiments is to measure the diffusion coefficient (noted D) by ^{1}H NMR. The studied molecules are the dendrimer-81-benzoate **9** and the acetylcholine (AC).

First, the measurement of D allows to calculate the hydrodynamic diameter of a molecule. Then the ^{1}H NMR experiment focuses on the diffusion that is mathematically treated according to a process DOSY (Diffusion Ordered SpectroscopY) in order to obtain the equivalent of a spectral chromatography. The objective is thus double: measure the size of the two free and bound molecules in solution by ^{1}H NMR, and obtain a DOSY spectrum that will account for the purity of the product.

The dendrimer **9** is considered as a spherical molecular object, and characterized by an apparent diffusion coefficient. The application of the Stokes-Einstein law gives an estimate of the diameter of the molecule.

Stokes-Einstein law:

$D = K_B T / 6\pi\eta r_H$

D: diffusion constant; K_B: Boltzman's constant; T: temperature (K); η: solvent viscosity; r_H: hydrodynamic radius of the species.

DOSY spectrum of the dendrimer-81- benzoate 9 in D_2O

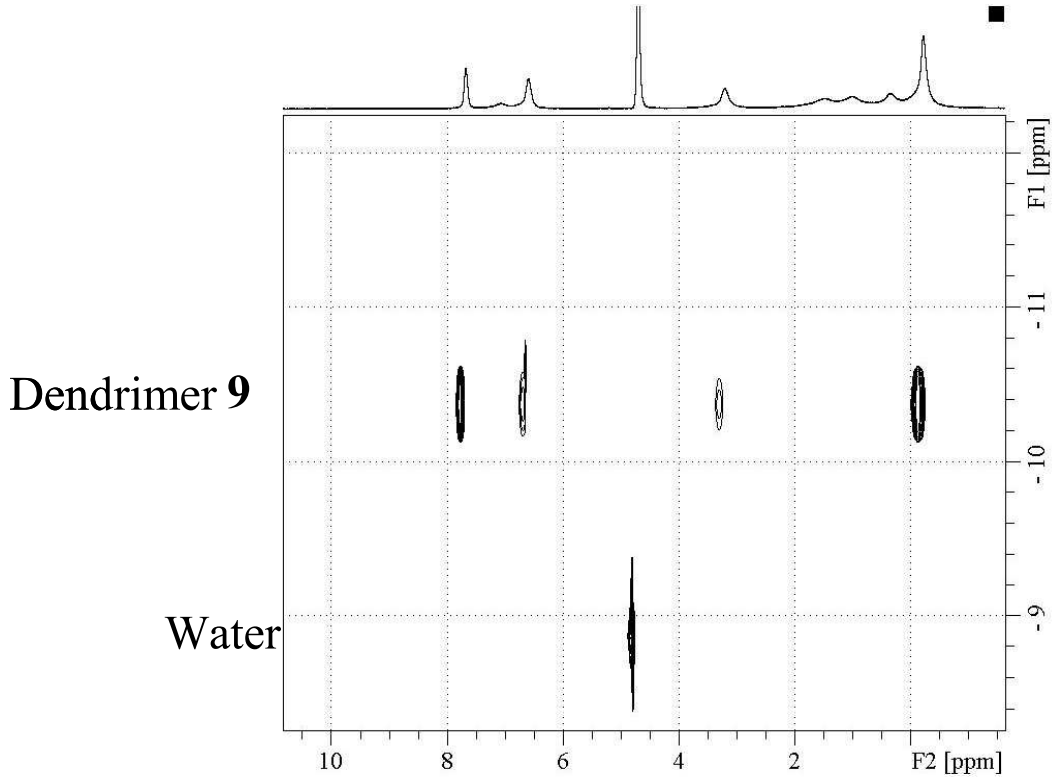

The four signals on the line (top) represent the log(D) of **9,** and the last signal below the line represents the log(D) of water.

$D_{\mathbf{9}} = 4.441 \times 10^{-11}$ m²/s (SD = 8.819×10^{-5})

$R_{H\,\mathbf{9}} = 5.517$ nm

$D_{\mathbf{9}}$: diffusion coefficient of the dendrimer **9**; $R_{H\,\mathbf{9}}$: hydrodynamic radius of the dendrimer **9**; SD: standard deviation.

DOSY spectrum of acetylcholine (AC) in D_2O

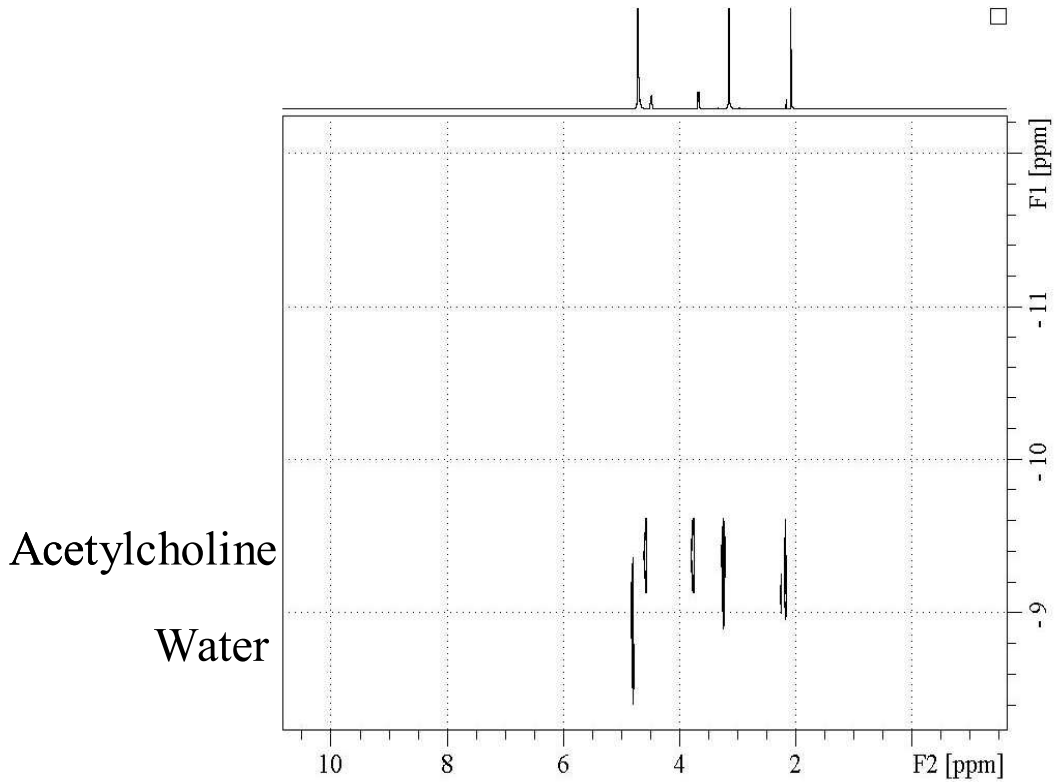

The four signals on the line (top) represent the log(D) of one molecule of acetylcholine (AC), and the last signal below the line represents the log(D) of water.

D_{AC} = 5.948 x 10^{-10} m^2/s (SD = 9.308 x 10^{-4})

$R_{H\,AC}$ = 0.594 nm

D_{AC}: diffusion coefficient of AC; $R_{H\,AC}$: hydrodynamic radius of AC; SD: standard deviation.

Superposition of the three DOSY spectra: free dendrimer 9, free acetylcholine (AC), and assembly 9 +AC in D_2O:

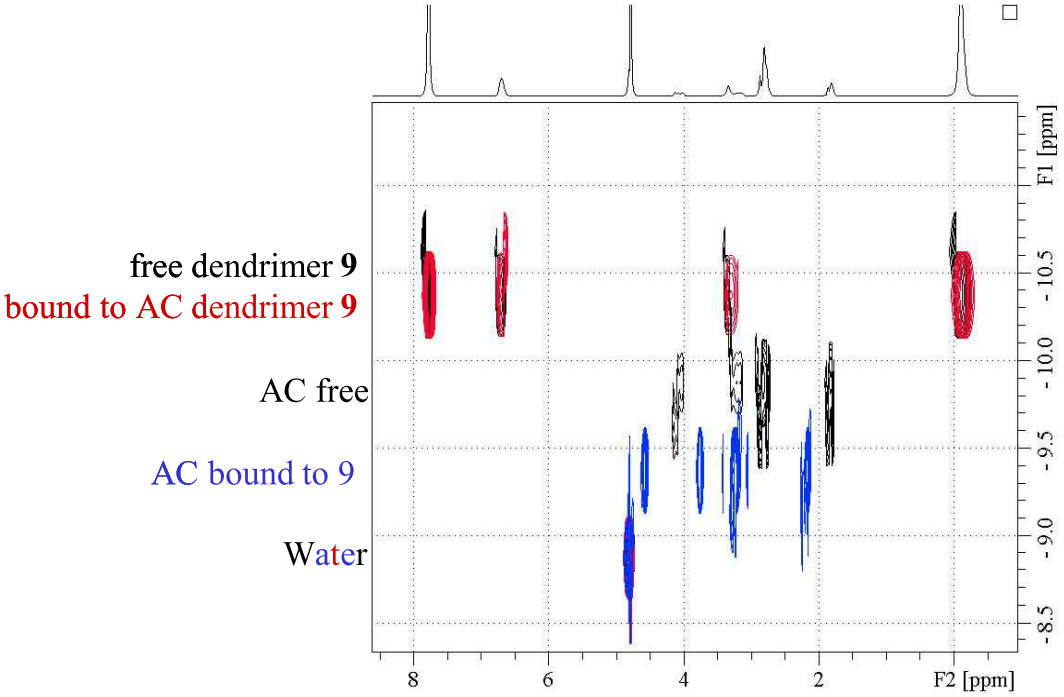

The four black signals on the line (top) represent the log(D) of the free dendrimer **9**; the four red signals on the line (top) represent the log(D) of the bound to AC dendrimer **9**; the four black signals on the medium line represent the log(D) of a free molecule of AC; the four blue signals (medium) represent the log(D) of a molecule of AC bound to the dendrimer. The last multicolor signal on the line below represents the log(D) of water.

$D_{\mathbf{9}} = 4.441 \times 10^{-11}$ m²/s (SD = 8.819×10^{-5})

$R_{H\,\mathbf{9}} = 5.517$ nm

$D_{\mathbf{9}}$: diffusion coefficient of the dendrimer **9**; $R_{H\,\mathbf{9}}$: hydrodynamic radius of the dendrimer **9**; SD: standard deviation.

Evolution of the diffusion coefficient of AC as a function of its concentration in water

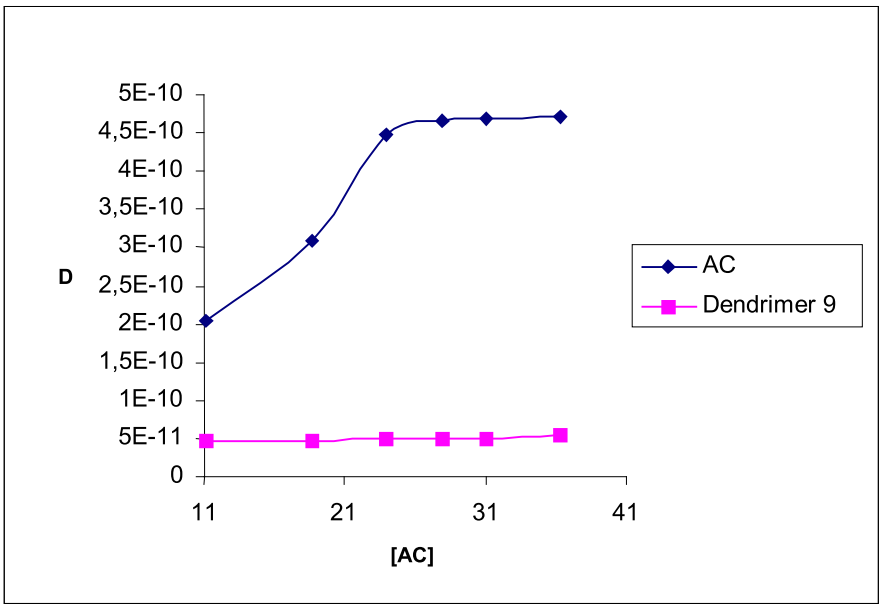

The diffusion coefficient of the dendrimer **9** does not vary the titration; this information means that the dendrimer has approximately the same size alone and in the complex.

The diffusion coefficient of AC very clearly increases until a concentration of 27.9 mM, that corresponds to 162 AC per dendrimer, before stagnating at higher concentrations. This means that there is a real interaction between the AC molecules and the dendrimer until a molar ratio of 162 AC per dendrimer. After this stage, the diffusion coefficient observed is an average between the free AC and the AC bound to the dendrimer, and its value slowly approaches that of free AC.

ROESY spectrum of acetylcholine (AC) in D_2O

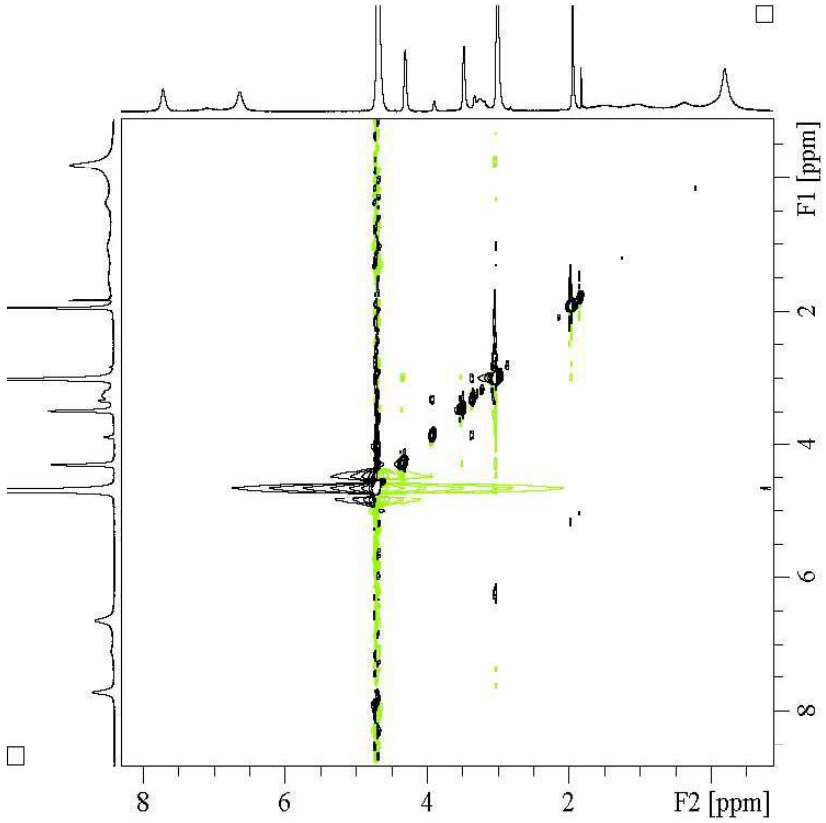

The ROESY spectrum shows that there is no dipolar interaction between the molecules of acetylcholine (AC) and the cavity of the dendrimer **9**; this confirms that the molecules of AC are bound to the dendrimer **9** at its periphery.

DOI: 10.1002/chem.200701607

Four Generations of Water-Soluble Dendrimers with 9 to 243 Benzoate Tethers: Synthesis and Dendritic Effects on Their Ion Pairing with Acetylcholine, Benzyltriethylammonium, and Dopamine in Water

Elodie Boisselier,[a] Cátia Ornelas,[a] Isabelle Pianet,[b] Jaime Ruiz Aranzaes,[a] and Didier Astruc*[a]

Abstract: Water-soluble benzoate-terminated dendrimers of four generations (from G_0 with 9 branches to G_3 with 243 branches) were synthesized and fully characterized. They form water-soluble assemblies by ion-pairing interactions with three cations of medicinal interest (acetylcoline, benzyltriethylammonium, and dopamine), which were characterized and investigated by ^{1}H NMR spectroscopy, whereas such interactions do not provoke any significant shift of ^{1}H NMR signals with the monomeric benzoate anion. The calculated association constants confirm that the dendritic carboxylate termini reversibly form ion pairs and aggregates. Diffusion coefficients and hydrodynamic diameters of the dendrimers, as well as changes thereof on interaction with the cations, were evaluated by DOSY experiments. The lack of increase of dendrimer size on addition of the cations and the upfield shifts of the ^{1}H NMR signals of the cation indicate encapsulation within the hydrophobic dendrimer interiors together with probable backfolding of the benzoate termini.

Keywords: aggregation · cations · dendrimers · ion pairs · supramolecular chemistry

Introduction

An attractive property of dendrimers is their supramolecular facet,[1] and they have indeed been used as unimolecular micelles,[2] molecular boxes,[3] exoreceptors,[4] and sensors.[5] Applications of water-soluble dendrimers as drug vectors are most promising.[6,7] Polycationic dendrimers are considered to be toxic, but polyanionic dendrimers usually exhibit acceptable biocompatibility.[8]

We have reported, in preliminary form, the ionic interaction of a single benzoate-terminated dendrimer (81 branches) with acetylcholine.[9] We have now extended this study to four generations of benzoate-terminated dendrimers (from G_0 with 9 branches to G_3 with 243 branches) and their supramolecular interactions with three cations of medicinal interest: acetylcholine (AC), benzyltriethylammonium (BTEA), and dopamine.

Acetylcholine chloride is produced naturally by the nervous system. It is also used as an active ingredient in some drugs, but it is not very active on oral ingestion because of hydrolysis in the digestive tract. Therefore, transport by dendrimers may be useful. Acetylcholine chloride has various pharmacological properties: it can be used as a parasympathomimetic,[10a] a peripheral vasodilator, an antihypertensive, a myotic, or a coronarodilator.[10b] Its muscarinic parasympathomimetic action consists of contracting the smooth fiber in the digestive tract,[10c] the eye, and the bronchi.[10d] It is used in a drug marketed as a parasympathomimetic preparation for an intraocular use, although aqueous solutions are unstable and must thus be prepared just before use.[11]

As a quaternary ammonium compound, benzyltriethylammonium chloride shows a variety of physical, chemical, and biological properties. It can disrupt the cell processes of microorganisms, and it is used as a phase-transfer catalyst, antimicrobial agent, emulsifying agent, and pigment disperser.

[a] E. Boisselier, C. Ornelas, Dr. J. R. Aranzaes, Prof. D. Astruc
Nanosciences and Catalysis Group
Institut des Sciences Moléculaires, UMR CNRS N° 5255
Université Bordeaux 1
351, Cours de la Libération, 33405 Talence Cedex (France)
Fax: (+33) 5-4000-6994
E-mail: d.astruc@ism.u-bordeaux1.fr

[b] I. Pianet
CESAMO
Université Bordeaux 1
351, Cours de la Libération, 33405 Talence Cedex (France)

Supporting information for this article is available on the WWW under http://www.chemistry.org or from the author.

Its interaction with dendrimers may allow it to be stabilized in various formulations.[12,13] Moreover, together with alkyldimethylbenzylammonium chloride, it belongs to a large category of chemical compounds whose surface-active and biocidal properties are widely used in the pharmaceutical industry.

Dopamine is a natural catecholamine formed by decarboxylation of 3,4-dihydroxyphenylalanine (DOPA). It is a precursor to norepinephrine in noradrenergic nerves and is also a neurotransmitter in certain areas of the central nervous system.[14] Dopamine produces positive chronotropic and inotropic effects on the myocardium, which result in increased heart rate and cardiac contractility.[15,16] Dopamine hydrochloride is indicated for the correction of hemodynamic imbalances present in the Shock syndrome.[17] The half-life of dopamine in plasma is about two minutes when it is intravenously administrated. Use of a dendrimer/dopamine assembly might lead to a longer half-life that would allow dopamine to better penetrate the target area. Supramolecular interactions of the new benzoate dendrimers with AC, BTEA, and dopamine in water were investigated by ^{1}H NMR spectroscopy, and the calculated association constants and dendritic effects, that is, comparison of the influence of benzoate monomer and dendrimers and that of the dendritic generation, are discussed.

Results and Discussion

Water-soluble polyanionic dendrimers with 3^{n+2} benzoate termini (generation number $n=0$–3) were synthesized as described below, and their assembly with AC, BTEA, and dopamine was investigated by ^{1}H NMR spectroscopy, as were their solubility properties and ion-pair behavior in water. Titration of the three compounds with each generation of dendrimers (i.e., twelve complexes is described and analyzed. Diffusion ordered spectroscopy (DOSY), dipolar correlation ROESY experiments, and a titration by ^{13}C NMR are provided for the interaction between 81-benzoate G_2 and AC.

Synthesis of benzoate-terminated dendrimers: For dendrimer construction, we used the 1→3 C connectivity pioneered by Newkome et al.[18] (Schemes 1 and 2). It starts with the known nonaallylation of [FeCp(η^6-mesitylene)][PF_6] (**1**), which quantitatively yields nonaallyl dendritic core 1,3,5-[$C(CH_2CH{=}CH_2)_3]_3C_6H_3$ (**2**) on a large scale after to visible-light photolysis to removes the metal moiety.[19] Hydrosilylation of terminal olefinic bonds, pioneered in dendrimer synthesis by van Leeuwen et al.,[20] was carried out on **2** by using chloromethyldimethylsilane and Karstedt catalyst to regioselectively give a nonakis(chloromethyldimethylsilyl) intermediate that reacts with NaI to form nonaiodide **3**.

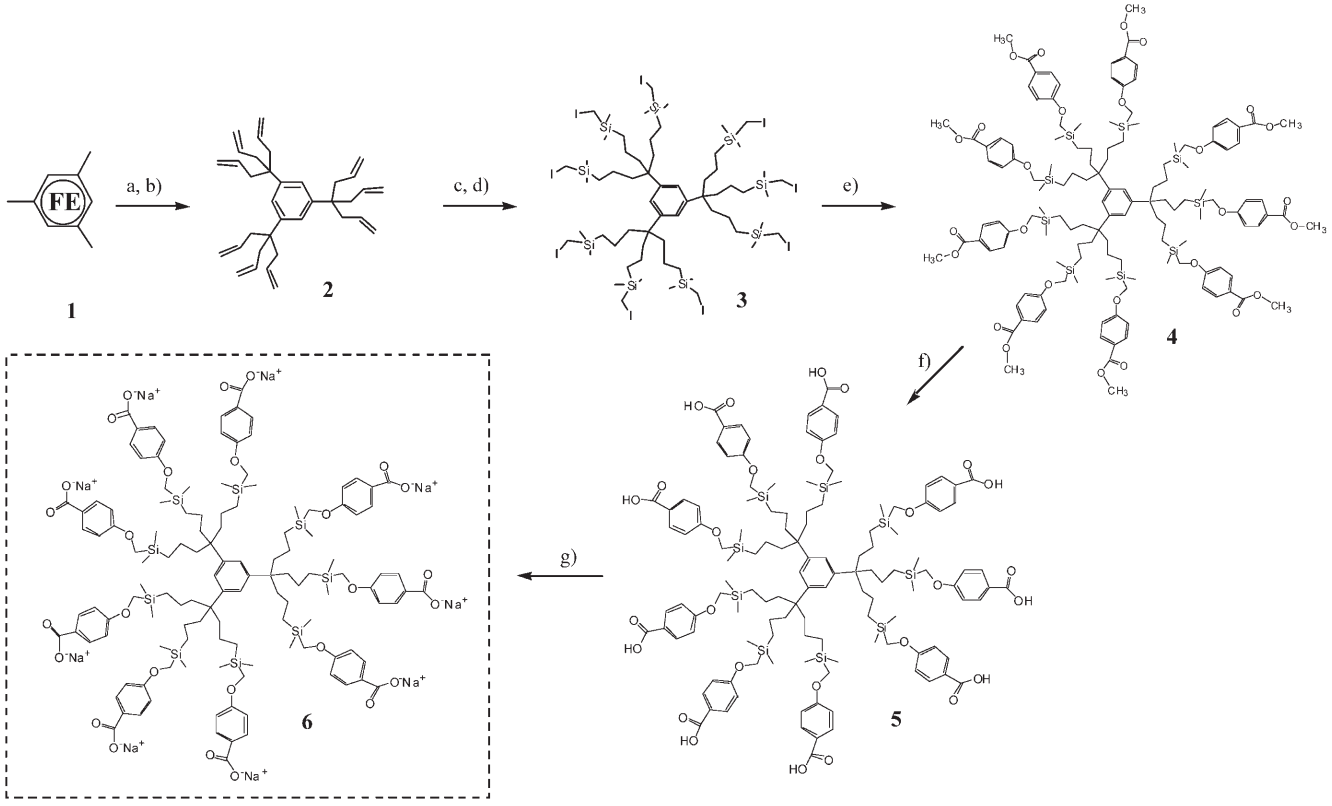

Scheme 1. Synthesis of water-soluble nonabenzoate G_0 dendrimer **6**. FE = $[\eta^5$-CpFe$]^+[PF_6]^-$. a) $CH_2{=}CHCH_2Br$, KOH, THF, RT, 3 days; b) $h\nu_{vis}$, MeCN; c) $HSiMe_2CH_2Cl$, Karsted cat., RT, 1 day; d) NaI, butanone, 80 °C, 16 h; e) $HOC_6H_4COOCH_3$, K_2CO_3, DMF, 80 °C, 2 days; f) NaOH, dioxane/water (9:1), 60 °C, 16 h, HCl; g) H_2O, NaOH.

We functionalized nine-branch G_0 dendrimer **3** with carboxylate termini to solubilize it in water. This was achieved in two steps: 1) Williamson reaction of dendri-9-iodide (dendrimer with 9 iodide termini) **3** with methyl 4-hydroxybenzoate yielded dendri-9-benzoate **4**, which was characterized by its molecular peak at 2520.21 $[M+Na]^+$ in the MALDI-TOF mass spectrum (calcd for $C_{135}H_{192}O_{27}Si_9Na$: 2522.71); 2) basic hydrolysis of dendri-9-benzoate **4** to form dendri-9-acid **5**, which was characterized by its molecular peak at 2394.44 $[M+Na]^+$ in the MALDI-TOF mass spectrum (calcd for $C_{126}H_{174}O_{27}Si_9Na$: 2396.47). Dendrimer **5** was easily solubilized in water as its sodium carboxylate form **6** in the presence of a stoichiometric amount of NaOH (Scheme 1).

Dendritic progression was achieved by using the known "phenoltriallyl" dendronic brick p-$HOC_4H_4C(CH_2CH=CH_2)_3$, obtained by one-pot reaction of [FeCp(η^6-p-chlorotoluene)]PF_6 with allyl bromide and tBuOK (Scheme 2).[19]

The same synthetic strategy was then applied to G_1 with 27 branches, G_2 with 81 branches, and G_3 with 243 branches. All new dendrimers were fully characterized by ^1H, ^{13}C, and ^{29}Si NMR spectroscopy, mass spectrometry (except G_3), and elemental analysis. The MALDI-TOF mass spectra show molecular peaks of the products (see Figure 1 and Supporting Information): dendri-27-$COOCH_3$ **7** (found: 9265.44 $[M]^+$; calcd for $C_{504}H_{732}O_{90}Si_{36}$: 9264.98), dendri-27-COOH **8** (found: 8886.4 $[M]^+$; calcd for $C_{477}H_{678}O_{90}Si_{36}$: 8886.3), and dendri-81-$COOCH_3$ **9** (found: 29 471 $[M]^+$; calcd for $C_{1611}H_{2352}O_{279}Si_{117}$: 29469.75). The ^1H NMR spectra of the benzoate dendrimers in MeOD show all the expected signals and thus confirm their structure. However, the ^1H NMR spectra of the higher generations in D_2O only show the peripheral proton signals. The synthesis of water-soluble 81-benzoate G_2 dendrimer **10** is shown in Scheme 2.

^1H NMR experiments and determination of association constants: Intermolecular interactions in solution play a key role in molecular recognition. NMR spectroscopy is a very useful technique to analyze them, because it allows the estimation of the association constants. It also gives information on the formation of aggregates, ion pairing, encapsulation, and size variations. This technique was used here to analyze three compounds that all contain ammonium moieties: AC, BTEA, and dopamine.

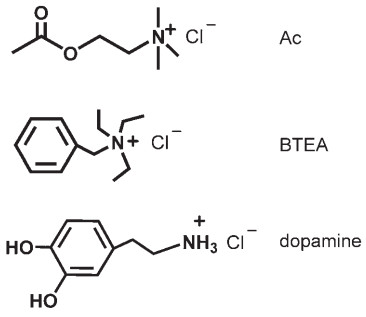

We investigated the supramolecular interactions of the three cations with the four generations of benzoate dendrimers to evaluate the role of dendrimer size and number of carboxylate groups at the periphery. The major advantage of these dendrimers is that they all become water-soluble on addition of a stoichiometric amount of NaOH relative to the number of acid groups. Thus, the supramolecular interactions can be tested at a pH close to neutrality, a condition for applications in biological systems (here pH 7.6 at $c = 10^{-3}$ M for all sodium carboxylate dendrimers).

The dendrimer with nine sodium carboxylate groups reversibly reacts with AC chloride to form water-soluble supramolecular assemblies whose structure can be examined by ^1H NMR spectroscopy.[21] The interaction between dendri-9-carboxylate and AC is characterized in the ^1H NMR spectrum by a large upfield shift of the four AC signals. The dendrimer signals also move, but to a lesser extent; the average shift is $\Delta\delta = 0.06$ ppm in water for peripheral protons H^5–H^8 (see Figure 2 for numbering scheme). Indeed, the protons at the periphery of the dendrimers that are detectable by ^1H NMR spectroscopy are too far away from the carboxylate groups, and this small shift is not representative of the interaction. The titration of AC was performed to quantify the number of AC molecules that can possibly be transported by dendri-9-carboxylate.

When the first equivalent of AC is added, the AC signals shift from $\delta = 4.56$ to 4.33 ppm for CH_2CH_2N proton H^3, from $\delta = 3.75$ to 3.30 ppm for CH_2N protons H^2, from $\delta = 3.23$ to 3.03 ppm for the CH_3N protons H^1, and from $\delta = 2.16$ to 2.00 ppm for the CH_3COO protons. These results correspond to an average displacement of $\Delta\delta = 0.26$ ppm. The four signals of AC shift during this titration because of interactions of the whole molecule with dendri-9-carboxylate. When AC interacts with this dendrimer, the ammonium AC group should be located at the dendrimer periphery, where it reversibly forms a contact ion pair and aggregates with the carboxylate ion (see Figure 2).

The number n of AC molecules bound to the dendrimer is determined as a function of the variation $\Delta\delta$ of chemical shifts according to Equation (1)[21]

$$\Delta\delta = {}^1/_2\Delta\delta_{max}\,[(1 + K_d/n[D_0] + [AC]/n[D_0]) - \{(1 + K_d/n[D_0] + [AC]/n[D_0])^2 - 4\,[AC]/n[D_0]\}^{1/2}] \quad (1)$$

where $[D_0]$ is the total concentration of dendrimer, [AC] the total concentration of acetylcholine, and K_d the dissociation constant.

The data fit best with dendri-9-carboxylate interacting on average (equilibrium) with 18 ± 2 molecules of AC. The first nine molecules interact electrostatically at the dendrimer periphery. The first dissociation constant K_{d1} of $(20 \pm 2) \times 10^{-3}$ M involves an equilibrium with nine AC molecules. A second weaker interaction in equilibrium with nine other AC molecule is obtained from the best fit, with a second dissociation constant K_{d2} of 1 ± 0.1 M [Eq. (2); R = dendrimer, R′ = Ac].

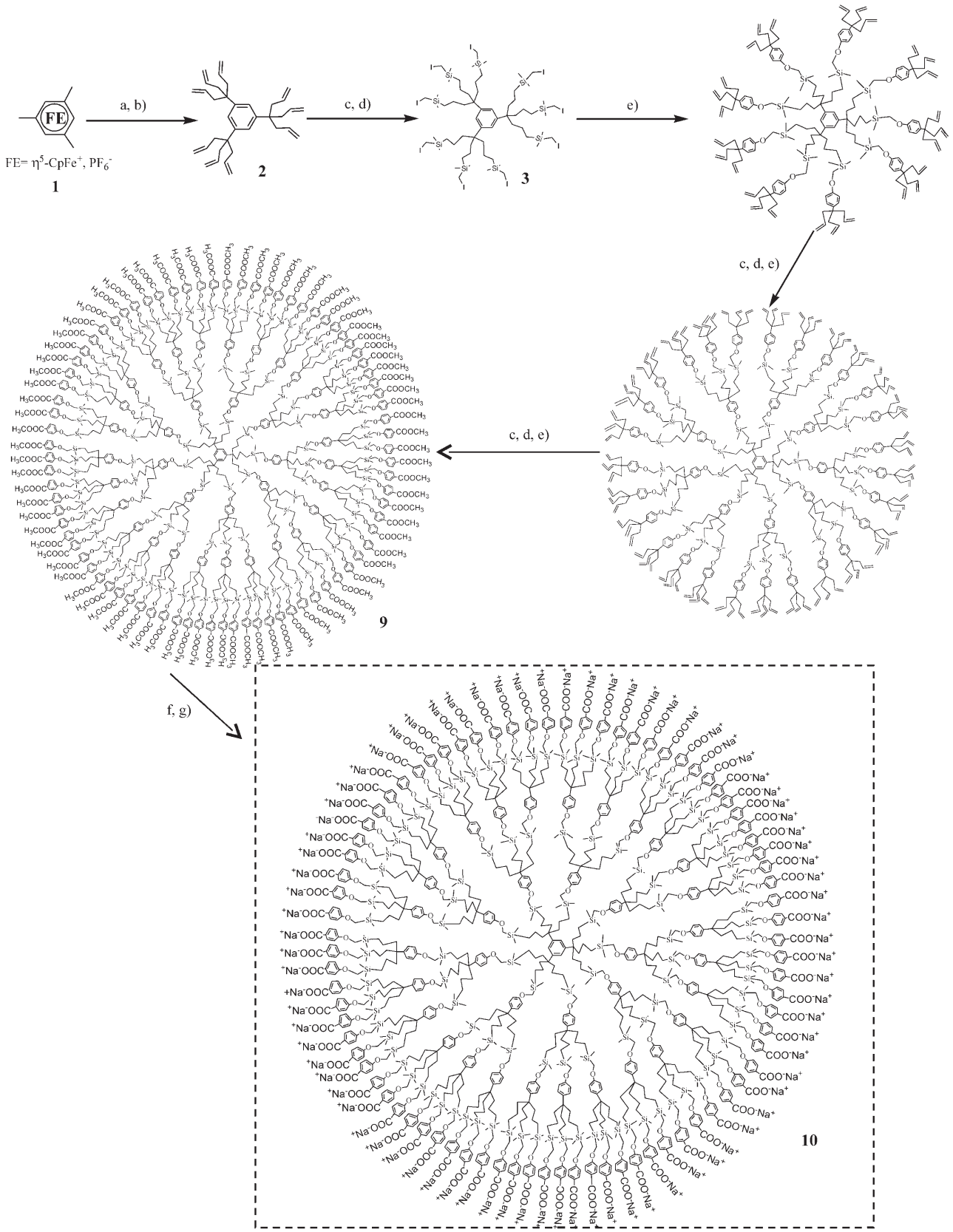

Scheme 2. Synthesis of the water-soluble G_2 dendri-81-benzoate **10**. FE = $[\eta^5\text{-CpFe}]^+[PF_6]^-$. a) $CH_2{=}CHCH_2Br$, KOH, THF, RT, 3 days; b) $h\nu_{vis}$, MeCN; c) $HSiMe_2CH_2Cl$, Karsted cat., RT, 1 day; d) NaI, butanone, 80 °C, 16 h; e) $HOC_6H_4C(CH_2CH{=}CH_2)_3$, K_2CO_3, DMF, 80 °C, 2 days; f) NaOH, dioxane/water (9:1), 60 °C, 16 h, HCl; g) H_2O, NaOH.

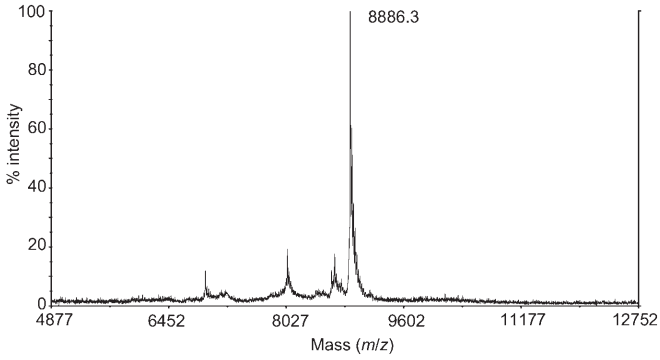

Figure 1. MALDI-TOF mass spectrum of G_1 dendri-27-benzoic acid **8**.

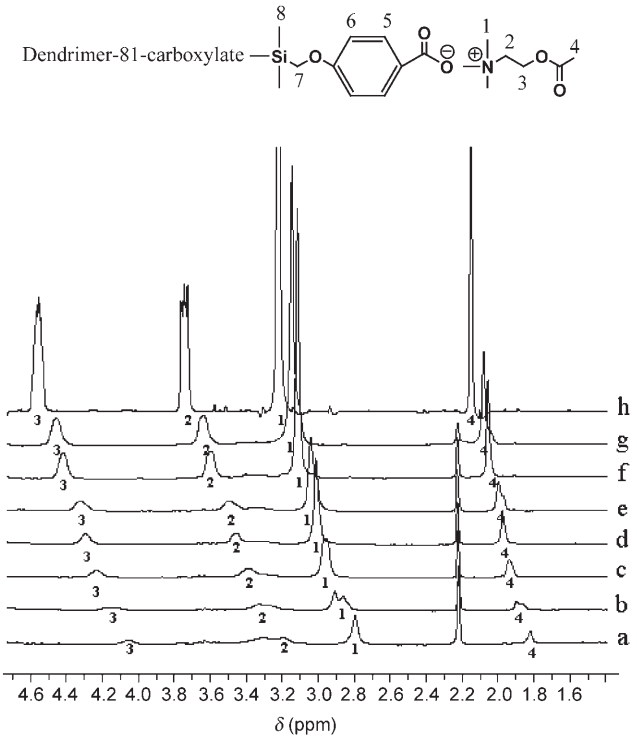

Figure 2. ^{1}H NMR titration of dendri-81-carboxylate with AC. AC proton signals: a) dendri-81-carboxylate + 20 equivalents of AC; b) dendri-81-carboxylate + 40 equivalents of AC; c) dendri-81-carboxylate + 60 equivalents of AC; d) dendri-81-carboxylate + 80 equivalents of AC; e) dendri-81-carboxylate + 100 equivalents of AC; f) dendri-81-carboxylate + 200 equivalents of AC; g) dendri-81-carboxylate + 300 equivalents of AC; h) AC alone.

$$[RCO_2^-Na^+] + [R'N^+Me_3Cl^-] \overset{K_{d1}}{\rightleftharpoons} [RCO_2^-R'N^+Me_3] + [Na(H_2O)_x^+Cl(H_2O)_y^-] \overset{K_{d2}}{\rightleftharpoons} [RCO_2^-(R'N^+Me_3)_2Cl^-] + [Na(H_2O)_x^+ Cl(H_2O)_y^-] \quad (2)$$

As AC is added to a D_2O solution of dendri-9-carboxylate, the ^{1}H NMR signals of the dendrimer benzoate termini progressively broaden, in confirmation of a reversible exchange interaction, and the signals of AC follow the same trend when the dendrimer is progressively added to a solution of AC (Figure 2).

The interactions of AC with dendrimers of higher generations are similar and were also analyzed, as were the interactions of all dendrimers with BTEA and dopamine (Table 1).

For the three cations, $\Delta\delta_{max}$ varies with dendrimer generation and has the largest value for dendri-81-carboxylate. The $\Delta\delta_{max}$ value is 0.6 for AC, 1.16 for BTEA, and 0.54 ppm for dopamine. These values show the large change in environment of each cation when it is in the presence of a dendrimer terminated by benzoate groups.

All AC proton signals are shielded upfield as the dendrimer concentration increases. This is best taken into account by incoming electron density near these AC protons due to the negatively charged carboxylate groups and by penetration of AC into the hydrophobic interior of the dendrimer, that is, AC is encapsulated in the dendrimer near its periphery.[22] A similar situation is found for the ammonium protons of the two other cations.

We can distinguish two different interactions, one for AC and BTEA (Figure 3a), and another for dopamine (Figure 3b). The evolution curves of the ^{1}H NMR signals have different shapes and thus reflect different interactions. In the cases of AC and BTEA, the cation interacts with the dendrimer in two steps, with a first association constant K_{a1} for a first number of molecules n_1 and a second association constant a_1 for a second number of molecules n_2 (Table 1).

The observed behavior of the dendrimer/cation assembly is best taken into account by reversible formation of ionic bonds between the dendrimers and the three cations located near the dendrimer periphery but inside the dendrimer.[23] The second stage most probably involves agglomeration of additional charges of chloride salt to reversibly form an aggregate at each tether terminus that is backfolded into the dendrimer interior.

This should be due to the dual location of the anionic charge delocalized on both carboxylate oxygen atoms of the carboxylate group, which can form a five-component aggregate (one chloride anion in addition to the two oxygen atoms and the two cations, see Figures 4 and 5).

This reasoning is also valid for AC and BTEA. The first association constant increases with increasing dendrimer generation, from 50 to 77 M^{-1} for AC, and from 125 to 200 M^{-1} for BTEA. The association constants are slightly smaller for AC than for BTEA, that is, the dendrimer/BTEA assembly is more strongly bound than the dendrimer/AC assembly. There is no significant difference between K_{a2} values of the two cations, which are both between 1 and 12 M^{-1}.

Dopamine has only one association constant that describes the interaction between a molecule of dopamine and a carboxylate group (Figure 6). Each dendrimer interacts with a number of dopamine molecules equal to the number of dendrimer carboxylate groups, and the association constant also increases from 2000 M^{-1} to 5000 M^{-1} with increasing dendrimer generation. This corresponds to a positive dendritic effect, which is observed in both cases.

The $\Delta\delta_{max}$ value observed in each case confirms the existence of the interaction, and the evolution of $\Delta\delta$ leads to an

Table 1. Results obtained from ^{1}H NMR titration of the three cations with the benzoate-terminated dendrimers.

Supramolecular assembly	$\Delta\delta_{max}$ [a] [ppm]	χ_2 [b]	n_1 [c]	K_{d1} [d] [M]	K_{a1} [e] [M^{-1}]	n_2 [f]	K_{d2} [g] [M]	K_{a2} [h] [M^{-1}]
Dendri-9-carboxylate + AC	0.32	0.06	9	20×10^{-3}	50	9	10×10^{-1}	1
Dendri-27-carboxylate + AC	0.35	0.02	27	18×10^{-3}	56	27	8	1
Dendri-81-carboxylate + AC	0.60	0.03	81	17×10^{-3}	59	81	23×10^{-2}	4
Dendri-243-carboxylate + AC	0.46	0.08	243	13×10^{-3}	77	243	8×10^{-2}	12
Dendri-9-carboxylate + BTEA	0.9	0.007	9	8×10^{-3}	125	9	3×10^{-1}	3
Dendri-27-carboxylate + BTEA	1.1	0.02	27	7×10^{-3}	143	27	3×10^{-1}	3
Dendri-81-carboxylate + BTEA	1.16	0.03	81	6×10^{-3}	167	81	3×10^{-1}	3
Dendri-243-carboxylate + BTEA	0.6	0.08	243	5×10^{-3}	200	243	3×10^{-1}	3
Dendri-9-carboxylate + dopamine	0.35	0.009	9	5×10^{-4}	2000	–	–	–
Dendri-27-carboxylate + dopamine	0.37	0.007	27	4×10^{-4}	2500	–	–	–
Dendri-81-carboxylate + dopamine	0.54	0.009	81	3×10^{-4}	3333	–	–	–
Dendri-243-carboxylate + dopamine	0.41	0.002	243	2×10^{-4}	5000	–	–	–

[a] $\Delta\delta_{max}$ is the maximum observed chemical shift variation. [b] χ_2 is the difference between the experimental points and the numerical values extracted from a theoretical curve. [c] n_1 is the number of cationic molecules revealed by the first association constant. [d] K_{d1} is the first dissociation constant. [e] K_{a1} is the first association constant. [f] n_2 is the number of cationic molecules involved with the second association constant. [g] K_{d2} is the second dissociation constant. [h] K_{a2} is the second association constant. The attenuated maximum error for all the values of this table is $\pm10\%$.

estimation of the association constants. By comparison, monomeric sodium benzoate hardly shows any interaction with the three cations ($\Delta\delta < 0.1$ ppm), which demonstrates a positive dendritic effect (i.e., comparison of the dendrimers with the monomer). Moreover, a study on a carboxylate dendrimer and the neutral amine benzylamine did not reveal any interaction that could be characterized by ^{1}H NMR spectroscopy.

In conclusion, in the studies on association constants, the data fits clearly show a plateau for dopamine, that is, the benzoate terminus interacts with a single dopamine molecule. Such a plateau is not found in titrations with AC and BTEA cations, for which the best fit is a sinusoidal curve involving two distinct association constants, the second of which very weak and thus only significant in its order of magnitude. These association constants are small, because water molecules also strongly interact with these ions. It is their order of magnitude that is informative, while their exact values have little meaning given that they are small. It is remarkable that dopamine behaves so differently from the two other cations given the similar structures of BTEA and dopamine. The association constant of the dendrimers with dopamine are indeed about 20 times larger that those with BTEA and 50 times larger than those with AC. In addition, the data only fit single 1:1 association between the benzoate

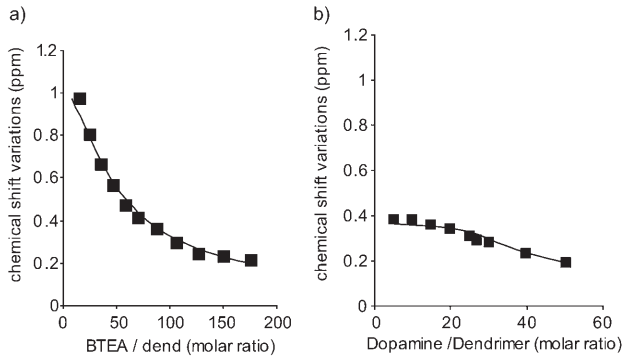

Figure 3. a) Titration of dendri-27-carboxylate with BTEA. b) Titration of dendri-27-carboxylate with dopamine.

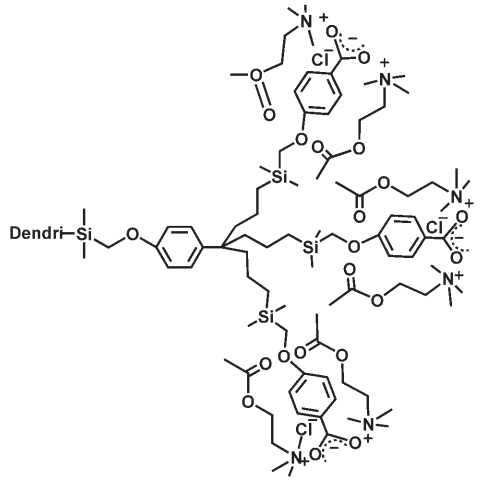

Figure 4. Representation of the ionic aggregates of carboxylate dendrimers with two AC molecules (close contacts between the whole AC groups and benzoate are omitted for clarity).

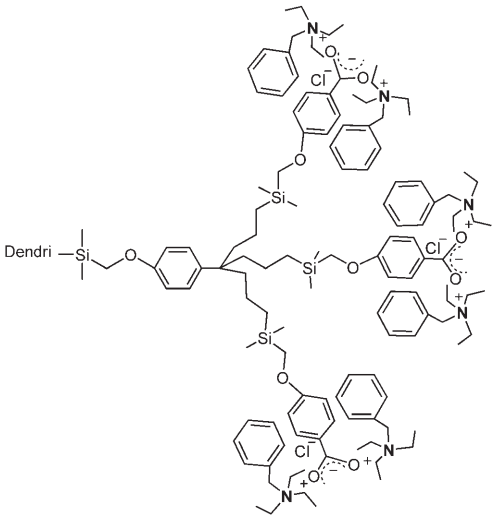

Figure 5. Representation of the ionic aggregates of carboxylate dendrimers with two BTEA molecules.

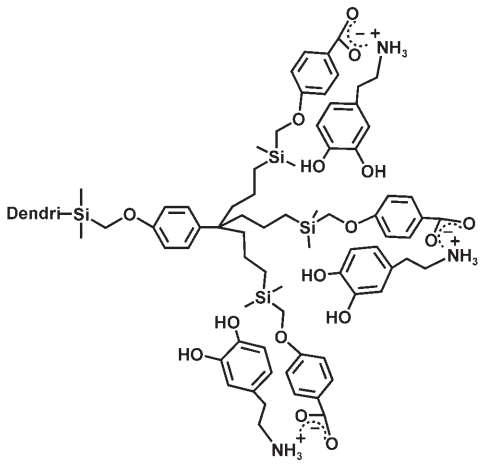

Figure 6. Representation of the ion pair between dopamine and carboxylate-terminated dendrimers.

termini and dopamine. Clearly, this completely specific behavior of dopamine is due to the fact that it is a primary ammonium compound, whereas the two other cations are quaternary ammonium compounds. Thus, dopamine has acidic hydrogen atoms on the ammonium center that can form hydrogen bonds with benzoate groups in synergy with the electrostatic attraction between the two oppositely charged ions. We know from recognition studies with ATP that synergistic interactions between two oppositely charged ions is considerably strengthened by such favorable hydrogen bonding.[4] Although the hydroxyl protons of the catechol moiety of dopamine are less acidic than the ammonium protons, they may also be involved in hydrogen bonding with one or two oxygen atoms of the bidentate carboxylate group. However, distinction between these two possible modes of hydrogen bonding is not feasible at this stage.

DOSY experiments to determine diffusion coefficients and ^{13}C NMR experiments: DOSY experiments were carried out for the dendrimer/cation assemblies involving dendri-81-carboxylate and the three cations in order to follow the evolution of the diffusion coefficient of the free dendrimer on addition of each cation. The main goal of these experiments was to measure the diffusion coefficient D by ^{1}H NMR spectroscopy. The D value allows the hydrodynamic diameter of a molecule to be calculated. In the ^{1}H NMR experiment diffusion is mathematically treated as a DOSY (diffusion-ordered spectroscopy) process in order to obtain the equivalent of "spectral" chromatography. The objective is thus double: measuring the size of the free and bound molecules in solution by ^{1}H NMR, and obtaining a DOSY spectrum that reflects the purity of the assembly.

Dendri-81-carboxylate is regarded as a spherical molecular object and characterized by an apparent diffusion coefficient. The Stokes–Einstein law [Eq. (3)] gives an estimate for the diameter of the molecule

$$D = k_B T/6\pi\eta r_H \quad (3)$$

where D is the diffusion coeficient, k_B the Boltzman constant, T the absolute temperature, η the solvent viscosity, and r_H the hydrodynamic radius of the species.

Figures 7–9 show the DOSY spectra of free dendri-81-carboxylate, free AC, and dendri-81-carboxylate/AC. Free dendri-81-carboxylate in water has a diffusion coefficient of $(4.4\pm0.2)\times10^{-11}\,m^2s^{-1}$ and a hydrodynamic diameter of 11 ± 1 nm. The AC, BTEA, and dopamine molecules have diffusion coefficients of $(5.9\pm0.03)\times10^{-10}$, $(5.0\pm0.04)\times10^{-10}$, and $(5.0\pm0.03)\times10^{-10}\,m^2s^{-1}$, and hydrodynamic diameters of 1.2 ± 0.1, 1.0 ± 0.1, and 1.0 ± 0.1 nm, respectively. When dendri-81-carboxylate is bound to 162 AC, 162 BTEA, or 81 dopamine molecules, it has diffusion coefficients of $(5.0\pm0.1)\times10^{-11}$, $(5.4\pm0.1)\times10^{-11}$, and $(7.0\pm0.1)\times10^{-11}\,m^2s^{-1}$, and its hydrodynamic diameter is to (9.8 ± 0.1), (9.0 ± 0.1), and (7.0 ± 0.1) nm, respectively. The diffusion co-

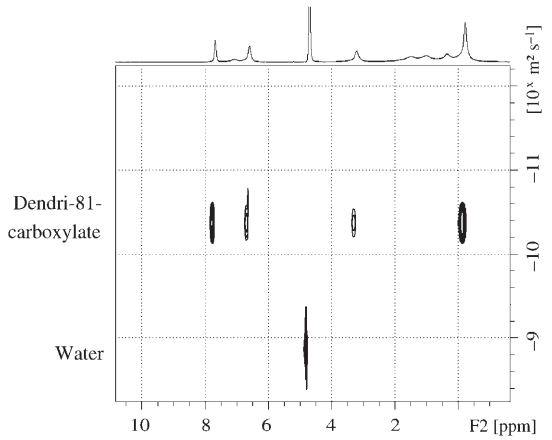

Figure 7. The four signals on the top line represent lg$D$ for the dendri-81-carboxylate, and the last signal below the line lg$D$ for water. $D_d=(4.4\pm0.1)\times10^{-11}\,m^2s^{-1}$ and $R_{H,d}=5.517$ nm, where D_d is the diffusion coefficient of the dendri-81-carboxylate, and $R_{H,d}$ its hydrodynamic radius.

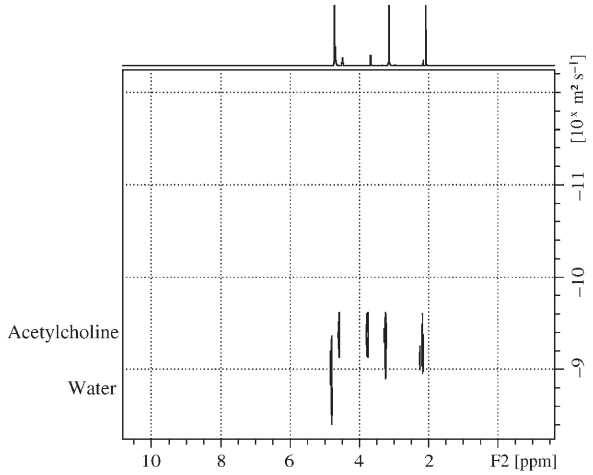

Figure 8. The four signals on the line (top) represent lg$D$ of one molecule of acetylcholine (AC), and the last signal below the line represents lg$D$ for water. $D_{AC}=(5.9\pm0.1)\times10^{-10}\,m^2s^{-1}$, $R_{H,AC}=0.59$ nm.

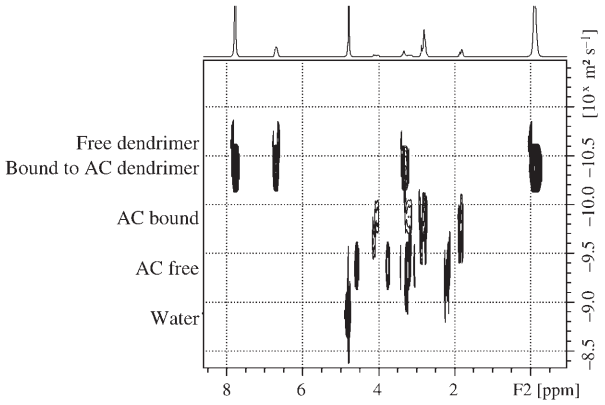

Figure 9. Four lines are identifiable from to bottom: the four signals on the first line (top) represent $\lg D$ for the free dendri-81-carboxylate; the four other signals on the same line (top) represent $\lg D$ for dendri-81-carboxylate bound to AC; the four signals on the second line represent $\lg D$ for an AC molecule bound to the dendrimer; the four signals on the third line represent $\lg D$ for a free molecule of AC. The last signal on the line below represents $\lg D$ for water. $D_d = (4.998 \pm 0.1) \times 10^{-11}\ m^2 s^{-1}$, $R_{H,d} = 4.902$ nm.

efficient of dendri-81-carboxylate increases on titration, that is, dendrimer size decreases in the dendrimer/guest assemblies. This is in accord with our above interpretation of $\Delta\delta$ in terms of encapsulation. For instance, although the diffusion coefficient of AC significantly increases on titration up to a concentration of 27.9 mM, which corresponds to 162 AC molecules per dendrimer, it stagnates at higher concentrations (plateau in Figure 10). This confirms interaction between the AC molecules and the dendrimer up to a molar ratio of 162 AC molecules per dendrimer. After this stage, the diffusion coefficient observed is an average between free AC and AC bound to the dendrimer, and its value slowly approaches that of free AC when the proportion of AC increases.

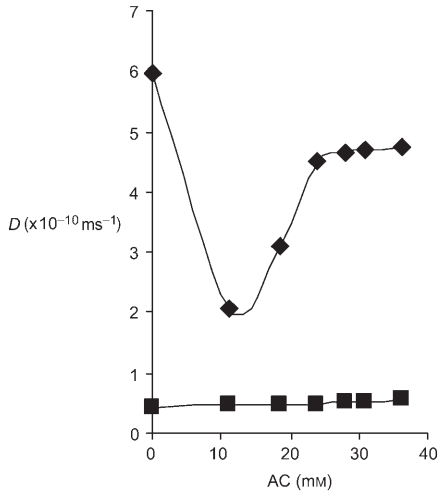

Figure 10. Evolution of the diffusion coefficients of AC (◆) and dendri-81-carboxylate **10** (■) as a function of their concentration in water.

The DOSY experiments show the evolution of the diffusion coefficients of each molecule and of the assembly. The dendrimer and the AC cation have their own diffusion coefficients in the free state that reflect their molecular weight. When a complex is formed with fast exchange on the NMR timescale, however, the observed diffusion coefficient is a weighted average of the diffusion coefficients for the free and bound species.

The diffusion coefficient of AC decreases at a a low concentration of AC, and then increases up to a concentration corresponding to 162 ± 5 AC molecules per dendrimer (i.e., [AC] = 28 mM), which shows the interaction between the two species, before stagnating at higher AC concentrations. In the beginning of AC addition to the dendrimer, the diffusion coefficient of AC becomes close to that of the dendrimer. Then, it becomes close to its initial value in the free state, as the amount of excess AC increases. The two other cations (BTEA and dopamine) follow approximately the same trend.

An increase in diffusion coefficient on titration is found for all three cations, but it is more pronounced for dopamine, which interacts more strongly with the dendrimers than the other two cations, as indicated by association constants that are one order of magnitude larger than those of AC and BTEA. These observations are in accord with the proposed encapsulation of the guest cations deduced from the shielding of their protons on interaction with the dendrimers. This encapsulation on ionic bonding forces the benzoate branch termini to be more strongly backfolded as the strength of this interaction increases. The free dendrimer is surrounded by a layer of hydrogen-bonded water molecules, and it appears that this layer is significant given the rather large hydrodynamic diameter of 11 nm. The decreased diameter of the dendrimers in the presence of cationic guests may not only signify backfolding of the dendrimer branch termini, but possibly also significant decrease of the water layer around the dendrimer, which is involved in the hydrodynamic diameter. This smaller surrounding water layer would itself be also due to the bakfolding of the ionic benzoate groups. Altogether, backfolding of the benzoate termini that is enforced by encapsulation of the ammonium guest most probably makes the dendrimers more compact.

Supramolecular interactions were investigated by ^{13}C NMR only for the single case of dendri-81-carboxylate and AC, because the ^{13}C NMR technique requires a considerably longer recording time than ^{1}H NMR and is thus impractical. In ^{1}H NMR spectra, the shifts of the dendrimer protons describing the effect of the dendrimer interaction are rather small ($\delta = 0.06$ ppm), because the closest protons are four bonds away from the carboxylate group that interacts with the AC molecules.

In the ^{13}C NMR experiment, when 81 equivalents of AC are added to dendri-81-carboxylate, the signal of the carbon atom of the carboxylate group shifts from $\delta = 174.4$ to 173.3 ppm, whereas the other carbon signals of the dendrimer do not move. Under the same conditions, the AC signals shift from $\delta = 60.9$ to 57.9 (CH_2CH_2N), from 67.2 to

64.2 (CH_2N), from 56.5 to 53.5 (CH_3N), from 23 to 20 (CH_3COO), and from 175.7 to 172.4 ppm (COO). These results correspond to an average shift of $\Delta\delta = 3$ ppm. The five signals of AC shift during titration because of interactions of the whole molecule with dendri-81-carboxylate, consistent with encapsulation of AC in the dendrimer.

When 81 additional equivalents are added, the AC signals always show an average shift of $\Delta\delta = 3$ ppm, and the signal of the carboxylate group of the dendri-81-carboxylate shifts from $\delta = 174.4$ to 172.0 ppm. These results confirm those obtained in the ^{1}H NMR experiments and the fact that the ammonium group of AC should be located at the dendrimer periphery. It forms an ion pair and aggregates with the carboxylate ion, which backfolds into the dendrimer interior so that the guest be encapsulated.

Conclusions

New water-soluble dendrimers were synthesized, characterized, and used as sensors of three cations of biological interest. The supramolecular interactions between the two entities were investigated by ^{1}H NMR spectroscopy.

The protons of dendritic benzoate tethers are deshielded (downfield shifts) on addition of any ammonium cation due to decreased electron density in ion-pairing interactions. Those of the ammonium cations are all shielded (upfield shift) due to encapsulation within the hydrophobic dendrimer interior.

The $\Delta\delta_{max}$ value observed in each case confirms the existence of the reversible interaction, and the evolution of $\Delta\delta$ led to an estimate of the association constants. By comparison, the monomeric sodium benzoate hardly shows any interaction with the three cations ($\Delta\delta < 0.1$ ppm), and this demonstrates a positive dendritic effect.

Two distinct cases were found: AC and BTEA on the one hand, and dopamine on the other. In the former case, the dendrimer acts in two steps: it first equilibrates with a stoichiometric number of cations by ionic association, and then form aggregates with the same number of cations with much weaker association. Dopamine has only one association constant characterizing the interaction between a dopamine molecule and a carboxylate group (i.e., 9 molecules of dopamine for the dendri-9-carboxylate, 27 for the dendri-27-carboxylate, 81 for the dendri-81-carboxylate, and 243 for the dendri-243-carboxylate). This interaction between dopamine and the dendrimers is much stronger than those between the dendrimers and AC and BTEA, as shown by the relative values of the association constants, because for dopamine hydrogen-bonding between the primary ammonium protons and the carboxylate termini acts in synergy with ion paring, which is not the case with the two other ammonium cations, which are quaternary.

For dendrimers of different generations, $\Delta\delta_{max}$ increases in all the cases with increasing generation number up to the dendri-81-carboxylate, then slightly decreases from the dendri-81-carboxylate to the dendri-243-carboxylate. For the association constants, the same trend is observed. Thus, the dendritic effect for the three ammonium cations is positive, that is, the $\Delta\delta_{max}$ and association constant increase as the dendrimer generation increases up to the dendri-81-carboxylate.

Experimental Section

General: All reactions were carried out by Schlenk techniques or in a nitrogen-filled Vacuum Atmosphere drylab. ^{1}H NMR spectra were recorded at 25 °C with a Brucker AC 250 (250 MHz) spectrometer. ^{13}C NMR spectra were obtained in pulsed FT mode at 62.0 MHz with a Brucker AC 250 spectrometer, and ^{29}Si NMR spectra were obtained at 59.6 MHz with a Brucker AC 300 spectrometer. All chemical shifts δ are reported in parts per million (ppm) relative to Me_4Si (TMS). The MALDI-TOF mass spectra were recorded with a PerSeptive Biosystems Voyager Elite (Framingham, MA) time-of-flight mass spectrometer. Elemental analyses were performed by the Center of Microanalyses of the CNRS at Lyon Villeurbanne, France. Syntheses of the precursor iodomethyltrimethylsilyl dendrimers were described previously.[19]

Synthesis of dendri-9-benzoate 4: Nonaiodide dendrimer **3** (1.1 g, 0.482 mmol), methyl 4-hydroxybenzoate (1.32 g, 8.68 mmol), K_2CO_3 (6.10 g, 43.4 mmol), and dry DMF (30 mL) were introduced into a Schlenk flask. The reaction mixture was stirred at 80 °C for 48 h. DMF was removed, and the crude product was dissolved in dichloromethane (30 mL) and washed with water to remove K_2CO_3. The organic layer was dried with Na_2SO_4, filtered, and the solvent was removed in vacuo. The product was washed with methanol and precipitated twice in CH_2Cl_2/methanol to remove excess methyl 4-hydroxybenzoate. Nonabenzoate dendrimer **4** was obtained as a colorless waxy material in 90% yield (1.089 g). ^{1}H NMR ($CDCl_3$, 250 MHz): $\delta = 7.93$ and 6.88 (d, 18H, arom.), 7.01 (s, 3H, arom. core), 3.86 (s, 27H, $COOCH_3$), 3.50 (s, 18H, $SiCH_2O$), 1.65 (s, 18H, $CH_2CH_2CH_2Si$), 1.13 (s, 18H, $CH_2CH_2CH_2Si$), 0.57 (s, 18H, $CH_2CH_2CH_2Si$), 0.040 ppm (s, 54H, $Si(CH_3)_2$); ^{13}C NMR ($CDCl_3$, 62 MHz): 165.8 ($COOCH_3$), 164.2 (arom. C_qO), 144.8 (CH, arom. core), 130.4 and 112.7 (CH, arom.), 121.2 (C_qCOOCH_3, arom.), 59.7 ($SiCH_2O$), 50.7 ($COOCH_3$), 42.9 ($CH_2CH_2CH_2Si$), 41.0 (C_qCH_2), 16.8 ($CH_2CH_2CH_2$), 13.6 ($CH_2CH_2CH_2Si$), −5.6 ppm ($Si(CH_3)_2$); ^{29}Si NMR ($CDCl_3$, 59.62 MHz): $\delta = 0.55$ ppm ($SiCH_2O$); MS (MALDI-TOF): m/z calcd for $C_{135}H_{192}O_{27}Si_9Na$: 2522.71; found: 2520.21 $[M+Na]^+$; elemental analysis (%) calcd for $C_{135}H_{192}O_{27}Si_9$: C 64.86, H 7.74; found: C 64.37, H 7.56; IR: $\tilde{\nu} = 1719$ ($\nu_{C=O}$) cm^{-1}.

Synthesis of dendri-9-benzoic acid 5: Dendri-9-benzoate **4** (0.50 g, 0.20 mmol) was dissolved in dioxane (40 mL), and an aqueous solution of NaOH (10 mL, 18 mmol, 10 equiv per branch) was added. The reaction mixture was stirred at 60 °C for 48 h. Dioxane was removed under vacuum, and the aqueous solution was acidified with HCl. The dendri-9-acid precipitated as a white powder. The solution was filtered, and the powder was washed twice with diethyl ether. The product was recovered from the filter by dissolving it with methanol. Methanol was removed in vacuo, and the product was obtained as a white powder in 72% yield. ^{1}H NMR (MeOD, 250 MHz): $\delta = 7.93$ and 6.91 (d, 18H, arom.), 7.06 (s, 3H, arom. core), 3.52 (s, 18H, $SiCH_2O$), 1.64 (s, 18H, $CH_2CH_2CH_2Si$), 1.16 (s, 18H, $CH_2CH_2CH_2Si$), 0.54 (s, 18H, $CH_2CH_2CH_2Si$), −0.003 ppm (s, 54H, $Si(CH_3)_2$); ^{13}C NMR (MeOD, 62 MHz): $\delta = 169.8$ ($COOH$), 166.7 (arom. C_qO), 147.2 (CH, arom. core), 132.9 and 115.0 (CH, arom.), 123.0 (arom. C_qCOOCH_3), 61.9 ($SiCH_2O$), 45.2 ($CH_2CH_2CH_2Si$), 43.3 (C_qCH_2), 19.3 ($CH_2CH_2CH_2$), 15.9 ($CH_2CH_2CH_2Si$), −4.1 ppm ($Si(CH_3)_2$); ^{29}Si NMR (MeOD, 59.62 MHz) $\delta = 0.36$ ppm ($SiCH_2O$); MS (MALDI-TOF): m/z calcd for $C_{126}H_{174}O_{27}Si_9Na$: 2 396.47; found: 2 394.44 $[M+Na]^+$; elemental analysis (%) calcd for $C_{126}H_{174}O_{27}Si_9$: C 63.76, H 7.39; found: C 62.71, H 7.22; IR: $\tilde{\nu} = 1686$ ($\nu_{C=O}$) cm^{-1}; ^{1}H NMR of **6** (D_2O + NaOH, 250 MHz): $\delta = 7.82$ and 6.79 (d, 18H, arom.), 7.08 (s, 3H, arom. core), 3.41 (s, 18H, $SiCH_2O$), 1.68 (s, 18H, $CH_2CH_2CH_2Si$), 1.16 (s, 18H, $CH_2CH_2CH_2Si$), 0.52 (s, 18H, $CH_2CH_2CH_2Si$), −0.045 ppm (s, 54H, $Si(CH_3)_2$).

Synthesis of dendri-27-benzoate 7: Dendri-27-iodide (0.1 g, 0.016 mmol), methyl 4-hydroxybenzoate (0.134 g, 0,882 mmol), K_2CO_3 (0.609 g, 4.40 mmol), and dry DMF (20 mL) were introduced into a Schlenk flask. The reaction mixture was stirred at 80 °C for 48 h, then DMF was removed, the crude product was dissolved in 30 mL of dichloromethane and washed with water to remove K_2CO_3. The organic layer was dried with Na_2SO_4, filtered, and the solvent removed in vacuo. The product was washed with methanol and precipitated twice in CH_2Cl_2/methanol to remove excess methyl 4-hydroxybenzoate. The dendri-27-benzoate was obtained as a colorless waxy material (0.140 g, 92% yield). ^{1}H NMR ($CDCl_3$, 250 MHz): $\delta = 7.94$ and 6.88 (d, 54 H, outer arom.), 7.10 and 6.80 (d, 18 H, inner arom.), 3.84 (s, 81 H, $COOCH_3$), 3.51 (s, 72 H, $SiCH_2O$), 1.60 (s, 72 H, $CH_2CH_2CH_2Si$), 1.11 (s, 72 H, $CH_2CH_2CH_2Si$), 0.55 (s, 72 H, $CH_2CH_2CH_2Si$), 0.025 (s, 216 H, $Si(CH_3)_2$). ^{13}C NMR ($CDCl_3$, 62 MHz): 165.8 ($COOCH_3$), 164.2 (outer arom. C_qO), 158.1 (inner arom. C_qO), 130.4 and 112.8 (CH, arom.), 121.1 (arom. C_qCOOCH_3), 59.7 ($SiCH_2O$), 50.7 ($COOCH_3$), 41.9 ($CH_2CH_2CH_2Si$), 41.9 (C_qCH_2), 16.6 ($CH_2CH_2CH_2$), 13.5 ($CH_2CH_2CH_2Si$), −5.5 ppm ($Si(CH_3)_2$); ^{29}Si NMR ($CDCl_3$, 59.62 MHz): $\delta = 0.53$ ppm ($SiCH_2O$); MS (MALDI-TOF): *m/z* calcd for $C_{504}H_{732}O_{90}Si_{36}$: 9264.9816; found: 9265.4374; IR: $\tilde{\nu} = 1719$ ($\nu_{C=O}$) cm^{-1}.

Synthesis of dendri-27-benzoic acid 8: Dendri-27-benzoate **7** (0.070 g, 0.007 mmol) was dissolved in dioxane (45 mL), and an aqueous solution of NaOH (5 mL, 2.5 mmol, 12 equiv per branch) was added. The reaction mixture was stirred at 60 °C for 48 h. Dioxane was removed under vacuum, and the aqueous solution was acidified with HCl. Dendri-81-acid precipitated as a white powder. The solution was filtered, and the powder was washed twice with diethyl ether. The product was recovered from the filter by dissolving in methanol. The methanol was removed in vacuo, and the product was obtained as a white powder in 67% yield. ^{1}H NMR (MeOD, 250 MHz): $\delta = 7.91$ and 6.86 (d, 54 H, outer arom.), 7.10 and 6.79 (d, 18 H, inner arom.), 3.48 (s, 81 H, $SiCH_2O$), 1.60 (s, 72 H, $CH_2CH_2CH_2Si$), 1.15 (s, 72 H, $CH_2CH_2CH_2Si$), 0.53 (s, 72 H, $CH_2CH_2CH_2Si$), −0.056 ppm (s, 216 H, $Si(CH_3)_2$); ^{13}C NMR (MeOD, 62 MHz): $\delta = 168.5$ (COOH), 165.4 (outer arom. C_qO), 159.1 (inner arom. C_qO), 131.5 and 113.6 (CH, arom.), 122.3 (arom. C_qCOOCH_3), 60.4 ($SiCH_2O$), 42.9 ($CH_2CH_2CH_2Si$), 41.8 (C_qCH_2), 17.6 ($CH_2CH_2CH_2$), 14.4 ($CH_2CH_2CH_2Si$), −4.9 ppm ($Si(CH_3)_2$); ^{29}Si NMR (MeOD, 59.62 MHz) $\delta = 1.57$ ppm ($SiCH_2O$); MS (MALDI-TOF): *m/z* calcd for $C_{477}H_{678}O_{90}Si_{36}$: 8886.3; found: 8886.4; IR: $\tilde{\nu} = 1686$ ($\nu_{C=O}$) cm^{-1}.

Synthesis of dendri-81-benzoate 9: Dendri-81-benzoate **9** was synthesized from dendri-81-iodide (0.30 g, 0.011 mmol) following the same procedure as for the synthesis of **4**, in 89% yield. ^{1}H NMR ($CDCl_3$, 250 MHz): $\delta =$ 7.94 and 6.88 (d, 162 H, exterior arom.), 7.10 and 6.80 (d, 72 H, interior arom.), 3.84 (s, 243 H, $COOCH_3$), 3.51 (s, 234 H, $SiCH_2O$), 1.60 (s, 234 H, $CH_2CH_2CH_2Si$), 1.11 (s, 234 H, $CH_2CH_2CH_2Si$), 0.55 (s, 234 H, $CH_2CH_2CH_2Si$), 0.034 ppm (s, 702 H, $Si(CH_3)_2$); ^{13}C NMR ($CDCl_3$, 62 MHz): $\delta = 167.2$ ($COOCH_3$), 164.2 (exterior arom. C_qO), 159.4 (interior arom. C_qO), 131.8 and 114.2 (CH, arom.), 122.5 (arom. C_qCOOCH_3), 61.1 ($SiCH_2O$), 52.2 ($COOCH_3$), 43.4 ($CH_2CH_2CH_2Si$), 42.3 (C_qCH_2), 18.0 ($CH_2CH_2CH_2$), 14.9 ($CH_2CH_2CH_2Si$), −4.3 ppm ($Si(CH_3)_2$); ^{29}Si NMR ($CDCl_3$, 59.62 MHz): $\delta = 0.53$ ppm ($SiCH_2O$); MS (MALDI-TOF): *m/z* calcd for $C_{1611}H_{2352}O_{279}Si_{117}$: 29 469.75; found: 29 471.00; elemental analysis (%) calcd for $C_{1611}H_{2352}O_{279}Si_{117}$: C 65.63, H 7.99; found: C 65.58, H 8.04; IR: $\tilde{\nu}_{C=O} = 1719$ cm^{-1}.

Synthesis of dendri-81-benzoate 10: Dendri-81-acid **10** was synthesized from dendri-81-benzoate **9** (0.20 g, 0.0068 mmol) by the same procedure as for the synthesis of **5**, in 67% yield. ^{1}H NMR (MeOD, 250 MHz): $\delta =$ 7.90 and 6.83 (d, 162 H, exterior arom.), 7.08 and 6.75 (d, 72 H, interior arom.), 3.43 (s, 234 H, $SiCH_2O$), 1.58 (s, 234 H, $CH_2CH_2CH_2Si$), 1.10 (s, 234 H, $CH_2CH_2CH_2Si$), 0.49 (s, 234 H, $CH_2CH_2CH_2Si$), −0.056 (s, 702 H, $Si(CH_3)_2$). ^{13}C NMR (MeOD, 62 MHz): 169.9 (COOH), 166.8 (exterior arom. C_qO), 160.5 (interior arom. C_qO), 133.0 and 115.1 (CH, arom.), 123.8 (arom. C_qCOOCH_3), 61.8 ($SiCH_2O$), 44.3 ($CH_2CH_2CH_2Si$), 43.4 (C_qCH_2), 19.0 ($CH_2CH_2CH_2$), 15.8 ($CH_2CH_2CH_2Si$), −4.0 ppm ($Si(CH_3)_2$); ^{29}Si NMR (MeOD, 59.62 MHz): $\delta = 0.26$ ppm ($SiCH_2O$); elemental analysis (%) calcd for $C_{1530}H_{2190}O_{279}Si_{117}$: C 64.86, H 7.79; found: C 64.25, H 7.68; IR: $\tilde{\nu} = 1686$ ($\nu_{C=O}$) cm^{-1}.

Synthesis of dendri-243-benzoate 11: Dendri-243-iodide (0.10 g, 0.001 mmol), methyl 4-hydroxybenzoate (0.088 g, 0.576 mmol), K_2CO_3 (0.398 g, 2.88 mmol), and dry DMF (20 mL) were introduced into a Schlenk flask. The reaction mixture was stirred at 80 °C for 48 h. DMF was removed, and the crude product dissolved in dichloromethane (30 mL) and washed with water to remove K_2CO_3. The organic layer was dried with Na_2SO_4, filtered, and the solvent was removed in vacuo. The product was washed with methanol and precipitated twice in CH_2Cl_2/methanol to remove excess methyl 4-hydroxybenzoate. Dendri-81-benzoate was obtained as a colorless waxy material (0.289 g, 89% yield). ^{1}H NMR ($CDCl_3$, 250 MHz): $\delta = 7.94$ and 6.88 (d, 486 H, outer arom.), 7.10 and 6.80 (d, 234 H, inner arom.), 3.79 (s, 729 H, $COOCH_3$), 3.47 (s, 720 H, $SiCH_2O$), 1.59 (s, 720 H, $CH_2CH_2CH_2Si$), 1.10(s, 720 H, $CH_2CH_2CH_2Si$), 0.53 (s, 720 H, $CH_2CH_2CH_2Si$), −0.012 ppm (s, 2160 H, $Si(CH_3)_2$); ^{13}C NMR ($CDCl_3$, 62 MHz): $\delta = 165.7$ ($COOCH_3$), 164.2 (outer arom. C_qO), 159.4 (inner arom. C_qO), 130.4 and 112.8 (CH, arom.), 121.1 (arom. C_qCOOCH_3), 59.6 ($SiCH_2O$), 50.7 ($COOCH_3$), 42.0 ($CH_2CH_2CH_2Si$), 40.9 (C_qCH_2), 16.6 ($CH_2CH_2CH_2$), 13.5 ($CH_2CH_2CH_2Si$), −5.7 ppm ($Si(CH_3)_2$); ^{29}Si NMR ($CDCl_3$, 59.62 MHz): $\delta = 0.47$ ppm ($SiCH_2O$); IR: $\tilde{\nu} = 1719$ ($\nu_{C=O}$) cm^{-1}.

Synthesis of dendri-243-benzoic acid 12: Dendri-243-benzoate (0.06 g, 0.0007 mmol) was dissolved in dioxane (45 mL), and an aqueous solution of NaOH (5 mL, 2.5 mmol, 15 equiv per branch) was added. The reaction mixture was stirred at 60 °C for 48 h. Dioxane was removed under vacuum, and the aqueous solution was acidified with HCl. Dendri-81-acid precipitated as a white powder. The solution was filtered, and the powder was washed twice with diethyl ether. The product was recovered from the filter by dissolving in methanol. The methanol was removed in vacuo, and the product was obtained as a white powder in 67% yield. ^{1}H NMR (MeOD, 250 MHz): $\delta = 7.94$ and 6.84 (d, 486 H, outer arom.), 7.08 and 6.75 (d, 234 H, inner arom.), 3.36 (s, 720 H, $SiCH_2O$), 1.62 (s, 720 H, $CH_2CH_2CH_2Si$), 1.10 (s, 720 H, $CH_2CH_2CH_2Si$), 0.54 (s, 720 H, $CH_2CH_2CH_2Si$), −0.020 ppm (s, 2160 H, $Si(CH_3)_2$); ^{13}C NMR (MeOD, 62 MHz): $\delta = 168.6$ (COOH), 165.3 (outer arom. C_qO), 160.5 (inner arom. C_qO), 131.6 and 113.6 (CH, arom.), 122.3 (arom. C_qCOOCH_3), 60.4 ($SiCH_2O$), 44.3 ($CH_2CH_2CH_2Si$), 43.4 (C_qCH_2), 19.0 ($CH_2CH_2CH_2$), 14.3 ($CH_2CH_2CH_2Si$), −5.3 ppm ($Si(CH_3)_2$); IR: $\tilde{\nu} = 1686$ ($\nu_{C=O}$) cm^{-1}.

General procedure for titration: In an NMR tube, carboxylate dendrimer (3 mg) was introduced into D_2O (0.4 mL), then one of the cations was progressively added. Titrations spanned from 0 to the $2x$ equivalents of the cation per dendrimer, where x is the number of carboxylate groups in each dendrimer.

Synthesis of all dendrimers and detailed ^{1}H NMR, ^{13}C NMR, DOESY, and ROESY spectra and data are available as Supporting Information.

Acknowledgements

We are grateful to the referees for helpful comments, to the Fundação para a Ciência e a Tecnologia (FCT), Portugal (Ph.D. grant to C.O.), the Institut Universitaire de France (IUF, DA), the CNRS, and the Université Bordeaux 1 for financial support.

[1] a) V. Percec, G. Johansson, G. Ungar, J. P. Zhou, *J. Am. Chem. Soc.* **1996**, *118*, 9855; F. Zeng, S. C. Zimmermann, *Chem. Rev.* **1997**, *97*, 1681; b) V. Balzani, S. Campana, G. Denti, A. Juris, S. Serroni, M. Venturi, *Acc. Chem. Res.* **1998**, *31*, 26; c) O. A. Mattews, A. N. Shipway, F. Stoddart, *Prog. Polym. Sci.* **1998**, 23; d) G. R. Newkome, C. N. Moorefield, *Chem. Rev.* **1999**, *99*, 1689; e) G. R. Newkome, C. N. Moorefield, F. Vögtle, *Dendritic Molecules*, Wiley-VCH, Weinheim, **2001**.

[2] a) G. R. Newkome, Z. Yao, G. R. Baker, V. K. Gupta, *J. Org. Chem.* **1985**, *50*, 2003; b) G. R. Newkome, *C. R. Chim.* **2003**, *6*, 715 (review).

[3] a) J. F. G. A. Jansen, E. M. M. de Brabander-van den Berg, E. W. Meijer, *Science* **1994**, *266*, 1226; b) A. W. Bosman, E. W. Jensen, E. W. Meijer, *Chem. Rev.* **1999**, *99*, 1665.
[4] a) C. Valério, J.-L. Fillaut, J. Ruiz, J. Guittard, J.-C. Blais, D. Astruc, *J. Am. Chem. Soc.* **1997**, *119*, 2588; b) S. Nlate, J. Ruiz, J.-C. Blais, D. Astruc, *Chem. Commun.* **2000**, 417; c) D. Astruc, M.-C. Daniel, J. Ruiz, *Chem. Commun.* **2004**, 2637; d) M-C. Daniel, D. Astruc, *Chem. Rev.* **2004**, *104*, 293.
[5] a) M. Albrecht, N. J. Hovestad, J. Boersma, G. van Koten, *Chem. Eur. J.* **2001**, *7*, 1289; b) A. W. Kleij, A. Ford, J. T. B. H. Jastrzebski, G. van Koten in *Dendrimers and Other Dendritic Polymers* (Eds.: J. M. J. Fréchet, D. A. Tomalia), Wiley, New York, **2002**, 185.
[6] a) D. Astruc, *C. R. Acad. Sci. Ser. IIb* **1996**, *322*, 757 (review); b) C. Kojima, K. Kono, K. Maruyama, T. Takagishi, *Bioconjugate Chem.* **2000**, *11*, 910; c) K. Sadler, J. P. Tam, *J. Biotechnol.* **2002**, *90*, 195; d) M. J. Cloninger, *Curr. Opin. Chem. Biol.* **2002**, *6*, 742; e) S. E. Stiriba, H. Frey, R. Haag, *Angew. Chem.* **2002**, *114*, 1385; *Angew. Chem. Int. Ed.* **2002**, *41*, 1329; f) M. W. Grinstaff, *Chem. Eur. J.* **2002**, *8*, 2838; g) U. Boas, P. M. H. Heegarard, *Chem. Soc. Rev.* **2004**, *33*, 43; h) C. C. Lee, J. A. Mac Kay, J. M. J. Fréchet, F. Szoka, *Nat. Biotechnol.* **2005**, *23*, 1517.
[7] For the first water-soluble dendrimers, see ref. [2a] and: a) D. A. Tomalia, H. Baker, J. Dewald, M. Hall, G. Kallos, S. Martin, J. Roeck, P. Smith, *Macromolecules* **1986**, *19*, 2466; b) D. A. Tomalia, A. N. Naylor, N. A. Goddard III, *Angew. Chem.* **1990**, *102*, 119; *Angew. Chem. Int. Ed. Engl.* **1990**, *29*, 138.
[8] a) N. Malik, R. Wiwattanapatapee, R. Klopsch, K. Lorenz, H. Frey J. W. Weener, *J. Controlled Release* **2000**, *65*, 133; b) R. Jevprasesphant, J. Penny, R. Jalal, D. Attwood, N. B. McKown, A. D'Emmanuele, *Int. J. Pharm.* **2003**, *252*, 263.
[9] C. Ornelas, E. Boisselier, V. Martinez, I. Pianet, J. Ruiz Aranzaes, D. Astruc, *Chem. Commun.* **2007**, 5093.
[10] a) O. Voss, *Archiv Experiment. Pathol. Pharmakol.* **1926**, *116*, 367–382; b) E. A. Carmichael, F. R. Fraser, *Heart* **1933**, *16*, 263; c) M. Beauvallet, *C. R. Seances Soc. Biol. Ses Fil.* **1938**, *127*, 213; d) B. A. Houssay, O. Orias, *C. R. Seances Soc. Biol. Ses Fil.* **1934**, *117*, 61.
[11] D. M. Sletten, K. K. Nickander, P. A. Low, *J. Neurol. Sci.* **2005**, *234*, 1.
[12] Y. Jia, H. Zhou, M. Wang, X. Huang, T. Dong, *Fudan Xuebao Ziran Kexueban* **1986**, *25*, 57.
[13] H. Koma, Y. Igarashi, H. Nobeshima, *Jpn. Kokai Tokkyo Koho* **2005**, 16.
[14] A. Bjoerklund, S. B. Dunnett, *Neuroscience* **2007**, *30*, 185.
[15] A. Dahan, D. S. Ward, *Adv. Exp. Med. Biol.* **1998**, *450*, 173.
[16] D. Horwitz, S. M. FoxIII, L. I. Goldberg, *Circ. Res.* **1962**, *10*, 237.
[17] A. Aronski, A. Kubler, M Sliwinski, A. Paszkowska, *Anaesthesist* **1978**, *27*, 183.
[18] G. R. Newkome, Z. Yao, G. R. Baker, V. K. Gupta, *J. Org. Chem.* **1985**, *50*, 2003.
[19] a) V. Sartor, L. Djakovitch, J.-L. Fillaut, F. Moulines, F. Neveu, V. Marvaud, J. Guittard, J.-C. Blais, D. Astruc, *J. Am. Chem. Soc.* **1999**, *121*, 2929; b) J. Ruiz, G. Lafuente, S. Marcen, C. Ornelas, S. Lazare, J.-C. Blais, E. Cloutet, D. Astruc, *J. Am. Chem. Soc.* **2003**, *125*, 7250; c) C. Ornelas, D. Méry, J. Ruiz, J.-C. Blais, E. Cloutet, D. Astruc, *Angew. Chem.* **2005**, *117*, 7565; *Angew. Chem. Int. Ed.* **2005**, *44*, 7399; C. Ornelas, L. Salmon, J. Ruiz Aranzaes, D. Astruc, *Chem. Eur. J.* **2007**, DOI: 10.1002/chem.200701410.
[20] A. W. van der Made, P. W. N. M. van Leeuwen, J. C. de Wilde, R. A. C. Brandes, *Adv. Mater.* **1993**, *5*, 466.
[21] a) A. J. Charlton, N. J. Baxter, M. L. Khan, A. J. G. Moir, E. Haslam, A. P. Davies, M. P. Williamson, *J. Agric. Food Chem.* **2002**, *50*, 1593; b) C. Simon, K. Barathieu, M. Laguerre, J. M. Schmitter, E. Fouquet, I. Pianet, E. J. Dufourc, *Biochemistry* **2003**, *42*, 10385.
[22] For seminal exemples of intradendritic encapsulation of guests, see refs. [3,7a] and G. R. Newkome, *Pure Appl. Chem.* **1998**, *70*, 2337.
[23] a) J. Smid in *Ions and Ion Pairs in Organic Reactions, Vol. 1* (Ed.: M. Schwarc), Wiley, New York, **1972**, Chap. 3; b) *The Organic Chemistry of Electrolyte Solutions* (Ed.: J. E. Gordon), Wiley, New York, **1975**; c) J. D. Simon, K. S. Peters, *Acc. Chem. Res.* **1984**, *17*, 277; d) A. Loupy, B. Tchoubar, D. Astruc, *Chem. Rev.* **1992**, *92*, 1141.

Received: October 11, 2007
Revised: January 31, 2008
Published online: April 2, 2008

Supplementary Information

Four Generations of Water Soluble Dendrimers with 9 to 243 Benzoate Tethers: Synthesis and Dendritic Effects on Their Ion Pairing with Acetylcholine, Benzyltriethylammonium and Dopamine in Water

Elodie Boisselier,[a] Cátia Ornelas,[a] Isabelle Pianet,[b] Jaime Ruiz Aranzaes,[a] Didier Astruc*[a]

[a] E. Boisselier, C. Ornelas, Dr. J. Ruiz Aranzaes, Pr. D. Astruc ; Nanosciences and Catalysis Group, Institut des Sciences Moléculaires, UMR CNRS N° 5255, Université Bordeaux 1, 351, Cours de la Libération, 33405 Talence Cedex, France ; Fax: (+033)5 40 00 69 94 ; E-mail: d.astruc@ism.u-bordeaux1.fr.

[b] I. Pianet ; CESAMO, Université Bordeaux 1, 351, Cours de la Libération, 33405 Talence Cedex, France

Summary

Experimental section.

General data.

All reactions were carried out using Schlenk techniques or in a nitrogen-filled Vacuum Atmosphere drylab. ^{1}H NMR spectra were recorded at 25°C with a Brucker AC 300 (300 MHz) spectrometer. ^{13}C NMR spectra were obtained in the pulsed FT mode at 75.0 MHz with a Brucker AC 300 spectrometer and ^{29}Si NMR spectra were obtained in at 59.6 MHz with a Brucker AC 300 spectrometer. All chemical shifts are reported in parts per million (δ, ppm) with reference to Me_4Si (TMS). The MALDI TOF mass spectra were recorded with a PerSeptive Biosystems Voyager Elite (Framingham, MA) time-of-flight mass spectrometer. Elemental analyses were performed by the Center of Microanalyses of the CNRS at Lyon Villeurbanne, France. Diffusion measurements were performed at different AC concentrations using a ^{1}H NMR pulsed-gradient experiment:the simulated spin-echo sequence which leads to the measurement of the diffusion coefficient D, where D is the slope of the straight line obtained when ln(I) is displayed against the gradient-pulse power's square according to the following equation: $\ln(I) = -\gamma^2G^2D\delta^2(\Delta-\delta/3)$, where I is the relative intensity of a chosen resonance, γ is the proton gyromagnetic ratio, Δ is the intergradient delay (150 ms), δ is the gradient pulse duration (5 ms), and G is the gradient intensity. The diffusion constant of water (2.3×10^{-9} m^2/s) was used to calibrate the instrument.

Synthesis of dendri-9-benzoate (4):

The dendrimer nonaiodide **3** (1.1 g, 0.482 mmol), the methyl 4-hydroxybenzoate (1.32 g, 8.68 mmol), K_2CO_3 (6.10 g, 43.4 mmol) and dry DMF (30 mL) were indroduced in a Schlenk flask. The reaction mixture was stirred at 80°C for 48 h. The DMF was removed, the crude product was solved in 30 mL of dichloromethane and washed with water in order to remove the K_2CO_3. The organic layer was dried with Na_2SO_4, filtered and the solvent was removed *in vacuo.* The product was washed with methanol and precipitated twice in CH_2Cl_2/methanol in order to remove the excess of methyl 4-hydroxybenzoate. The dendrimer-nona-benzoate de methyl was obtained as a colourless waxy product (1.089 g, 90% yield).

^{1}H NMR ($CDCl_3$, 250MHz): 7.93 and 6.88 (d, 18H, arom), 7.01 (s, 3H, arom. core), 3.86 (s, 27H, COOCH_3), 3.50 (s, 18H, SiCH_2O), 1.65 (s, 18H, CH_2CH$_2$CH$_2$Si), 1.13 (s, 18H, CH$_2$CH_2CH$_2$Si), 0.57 (s, 18H, CH$_2$CH$_2$CH_2Si), 0.040 (s, 54H, Si(CH_3)$_2$). ^{13}C NMR ($CDCl_3$, 62 MHz): 165.8 (*C*OOCH$_3$), 164.2 (arom. *C*qO), 144.8 (*C*H, arom. core), 130.4 and 112.7 (*C*H, arom), 121.2 (arom. *C*qCOOCH$_3$), 59.7 (Si*C*H$_2$O), 50.7 (COO*C*H$_3$), 42.9 (*C*H$_2$CH$_2$CH$_2$Si), 41.0 (*C*qCH$_2$), 16.8 (CH$_2$*C*H$_2$CH$_2$), 13.6 (CH$_2$CH$_2$*C*H$_2$Si), -5.6 (SiMe$_2$). ^{29}Si NMR ($CDCl_3$, 59.62 MHz): 0.55 (*Si*CH$_2$O). MS (MALDI-TOF; m/z) Calcd. for $C_{135}H_{192}O_{27}Si_9Na$: 2 522.71 ; found: 2 520.21 (MNa$^+$). Anal. Calc. for $C_{135}H_{192}O_{27}Si_9$: C 64.86, H 7.74; found: C 64.37, H 7.56. Infrared $\upsilon_{C=O}$: 1 719 cm^{-1}.

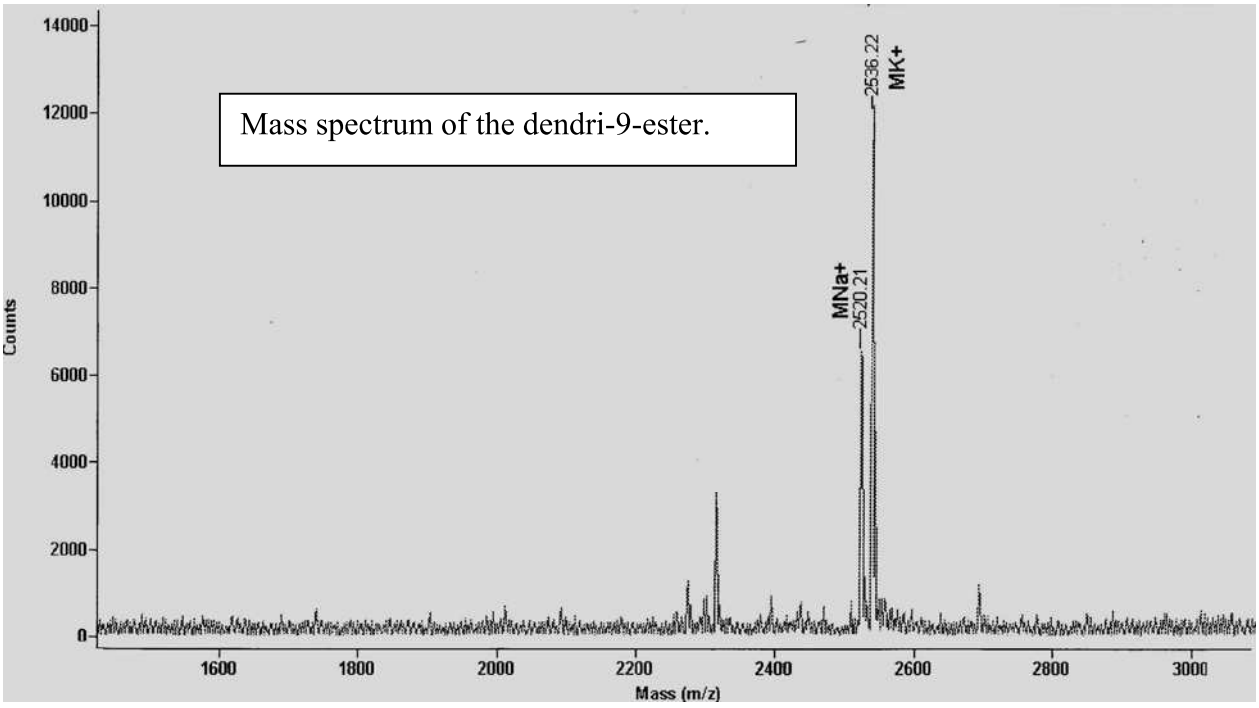

Synthesis of dendri-27-benzoate (7):

Dendri-27-iodide (0.1 g, 0.016 mmol), methyl 4-hydroxybenzoate (0.134 g, 0,882 mmol), K_2CO_3 (0.609 g, 4.40 mmol) and dry DMF (20 mL) were indroduced in a Schlenk flask. The reaction mixture was stirred at 80°C for 48 h. DMF was removed, the crude product was solved in 30 mL of dichloromethane and washed with water in order to remove the K_2CO_3. The organic layer was dried with Na_2SO_4, filtered, and the solvent was removed *in vacuo.* The product was washed with methanol and precipitated twice in CH_2Cl_2/methanol in order to remove the excess of methyl 4-hydroxybenzoate. The dendri-81-benzoate was obtained as a colourless waxy product (0.140 g, 92% yield).

^{1}H NMR ($CDCl_3$, 250MHz): 7.94 and 6.88 (d, 54H, *outer arom*), 7.10 and 6.80 (d, 18H, *inner arom*), 3.84 (s, 81H, $COOCH_3$), 3.51 (s, 72H, $SiCH_2O$), 1.60 (s, 72H, $CH_2CH_2CH_2Si$), 1.11 (s, 72H, $CH_2CH_2CH_2Si$), 0.55 (s, 72H, $CH_2CH_2CH_2Si$), 0.025 (s, 216H, $Si(CH_3)_2$). ^{13}C NMR ($CDCl_3$, 62 MHz): 165.8 ($COOCH_3$), 164.2 (outer arom. CqO), 158.1 (*inner* arom. CqO), 130.4 and 112.8 (CH, arom.), 121.1 (arom. $CqCOOCH_3$), 59.7 ($SiCH_2O$), 50.7 ($COOCH_3$), 41.9 ($CH_2CH_2CH_2Si$), 41.9 ($CqCH_2$), 16.6 ($CH_2CH_2CH_2$), 13.5 ($CH_2CH_2CH_2Si$), -5.5 ($SiMe_2$). ^{29}Si NMR ($CDCl_3$, 59.62 MHz) δ ppm: 0.53 ($SiCH_2O$). MS (MALDI-TOF; m/z) Calcd. For $C_{504}H_{732}O_{90}Si_{36}$: 9264.9816; found: 9265.4374. Infrared $\upsilon_{C=O}$: 1 719 cm^{-1}.

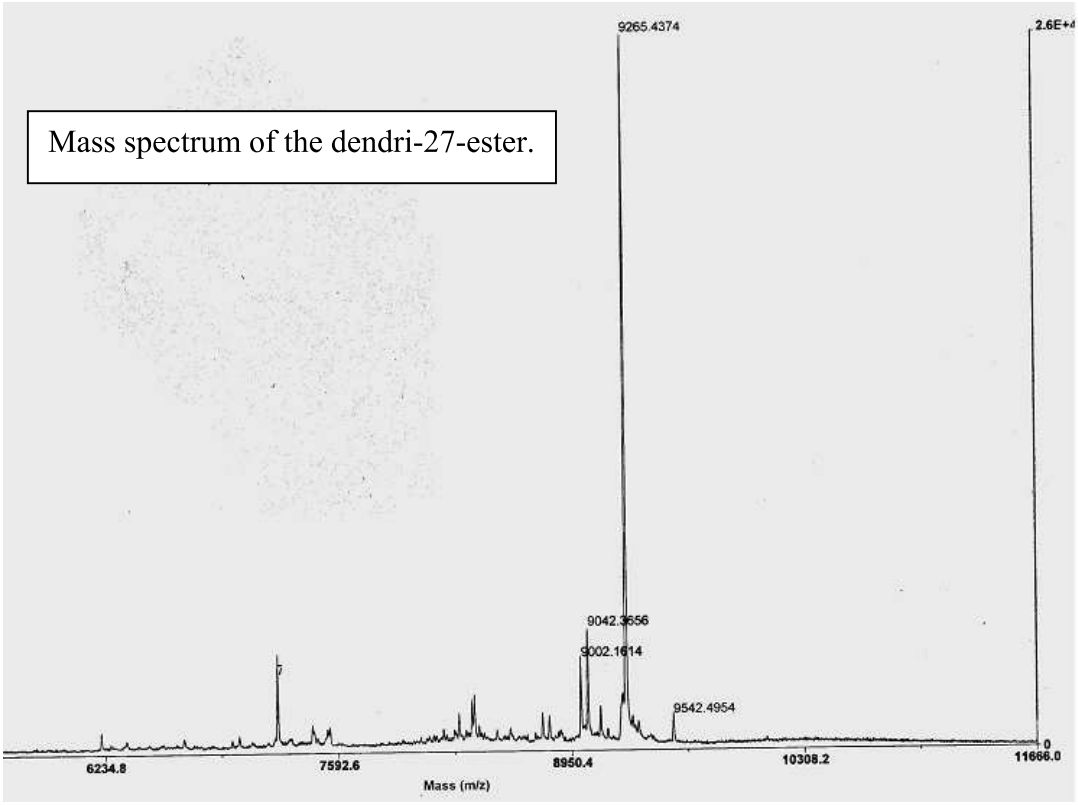

Mass spectrum of the dendri-27-ester.

Synthesis of dendri-81-benzoate (9):

Dendri-81-iodide **6** (0.30 g, 0.011 mmol), methyl 4-hydroxybenzoate (0.27 g, 1.78 mmol), K_2CO_3 (1.25 g, 8.91 mmol) and dry DMF (30 mL) were indroduced in a Schlenk flask. The reaction mixture was stirred at 80°C for 48 h. DMF was removed, the crude product was solved in 30 mL of dichloromethane and washed with water in order to remove the K_2CO_3. The organic layer was dried with Na_2SO_4, filtered, and the solvent was removed *in vacuo*. The product was washed with methanol and precipitated twice in CH_2Cl_2/methanol in order to remove the excess of methyl 4-hydroxybenzoate. The dendri-81-benzoate was obtained as a colourless waxy product (0.289 g, 89% yield).

^{1}H NMR ($CDCl_3$, 250MHz): 7.94 and 6.88 (d, 162H, *outer arom*), 7.10 and 6.80 (d, 72H, *inner arom*), 3.84 (s, 243H, $COOCH_3$), 3.51 (s, 234H, $SiCH_2O$), 1.60 (s, 234H, $CH_2CH_2CH_2Si$), 1.11 (s, 234H, $CH_2CH_2CH_2Si$), 0.55 (s, 234H, $CH_2CH_2CH_2Si$), 0.034 (s, 702H, $Si(CH_3)_2$). ^{13}C NMR ($CDCl_3$, 62 MHz): 167.2 ($COOCH_3$), 164.2 (outer arom. CqO), 159.4 (*inner* arom. CqO), 131.8 and 114.2 (CH, arom.), 122.5 (arom. $CqCOOCH_3$), 61.1 ($SiCH_2O$), 52.2 ($COOCH_3$), 43.4 ($CH_2CH_2CH_2Si$), 42.3 ($CqCH_2$), 18.0 ($CH_2CH_2CH_2$), 14.9 ($CH_2CH_2CH_2Si$), -4.3 ($SiMe_2$). ^{29}Si NMR ($CDCl_3$, 59.62 MHz) δ ppm: 0.53 ($SiCH_2O$). MS (MALDI-TOF; m/z) Calcd. For $C_{1611}H_{2352}O_{279}Si_{117}$: 29 469.75; found: 29 471.00. Anal. Calc. for $C_{1611}H_{2352}O_{279}Si_{117}$: C 65.63, H 7.99; found: C 65.58, H 8.04. Infrared $\upsilon_{C=O}$: 1 719 cm^{-1}.

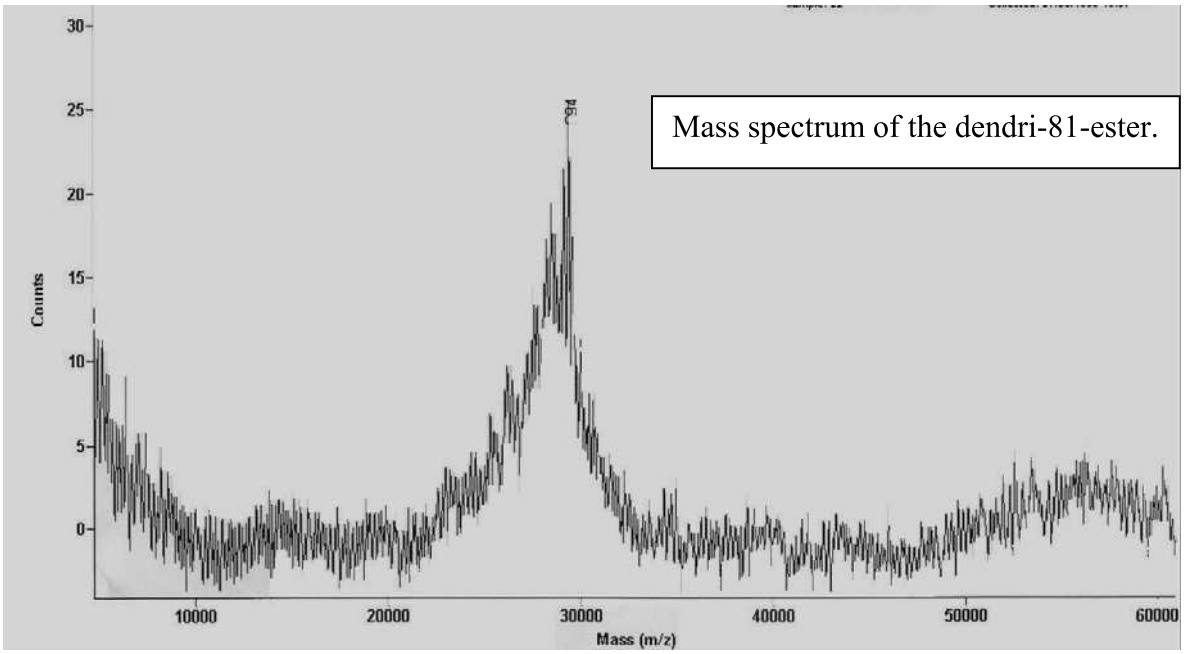

Mass spectrum of the dendri-81-ester.

Synthesis of dendri-243-benzoate (11):

Dendri-243-iodide **6** (0.10 g, 0.001 mmol), methyl 4-hydroxybenzoate (0.088 g, 0.576 mmol), K_2CO_3 (0.398 g, 2.88 mmol) and dry DMF (20 mL) were indroduced in a Schlenk flask. The reaction mixture was stirred at 80°C for 48 h. DMF was removed, the crude product was solved in 30 mL of dichloromethane and washed with water in order to remove the K_2CO_3. The organic layer was dried with Na_2SO_4, filtered, and the solvent was removed *in vacuo*. The product was washed with methanol and precipitated twice in CH_2Cl_2/methanol in order to remove the excess of methyl 4-hydroxybenzoate. The dendri-81-benzoate was obtained as a colourless waxy product (0.289 g, 89% yield).

^{1}H NMR ($CDCl_3$, 250MHz): 7.94 and 6.88 (d, 486H, *outer arom*), 7.10 and 6.80 (d, 234H, *inner arom*), 3.79 (s, 729H, COOCH_3), 3.47 (s, 720H, SiCH_2O), 1.59 (s, 720H, CH_2CH$_2$CH$_2$Si), 1.10(s, 720H, CH$_2$CH_2CH$_2$Si), 0.53 (s, 720H, CH$_2$CH$_2$CH_2Si), -0.012 (s, 2160H, Si(CH_3)$_2$). ^{13}C NMR ($CDCl_3$, 62 MHz): 165.7 (*C*OOCH$_3$), 164.2 (outer arom. *C*qO), 159.4 (*inner* arom. *C*qO), 130.4 and 112.8 (*C*H, arom.), 121.1 (arom. *C*qCOOCH$_3$), 59.6 (Si*C*H$_2$O), 50.7 (COO*C*H$_3$), 42.0 (*C*H$_2$CH$_2$CH$_2$Si), 40.9 (*C*qCH$_2$), 16.6 (CH$_2$*C*H$_2$CH$_2$), 13.5 (CH$_2$CH$_2$*C*H$_2$Si), -5.7 (SiMe$_2$). ^{29}Si NMR ($CDCl_3$, 59.62 MHz) δ ppm: 0.47 (*Si*CH$_2$O). Infrared $\upsilon_{C=O}$: 1 719 cm^{-1}.

Synthesis of dendri-9-benzoic (5):

The dendri-9-benzoate **6** (0.50 g, 0.20 mmol), was dissolved in dioxane (40 mL) and 10 mL of an aqueous solution of NaOH (18 mmol, 10 equiv. *per* branch) was added. The reaction mixture was stired at 60°C for 48 h. Dioxane was removed under vacuum and the aqueous solution was acidified with HCl. The dendri-9-acid precipitated as a white powder. The solution was filtrated and the powder was washed twice with ether. The product was recovered from filter by dissolving it with methanol. The methanol was removed *in vacuo* and the product was obtained as a white powder with 72% yield. ^{1}H NMR (MeOD, 250MHz): 7.93 and 6.91 (d, 18H, arom), 7.06 (s, 3H, arom-core), 3.52 (s, 18H, SiCH_2O), 1.64 (s, 18H, CH_2CH$_2$CH$_2$Si), 1.16 (s, 18H, CH$_2$CH_2CH$_2$Si), 0.54 (s, 18H, CH$_2$CH$_2$CH_2Si), -0.003 (s, 54H, Si(CH_3)$_2$). ^{13}C NMR (MeOD, 62 MHz): 169.8 (*C*OOH), 166.7 (arom. *C*qO), 147.2 (*C*H, arom. core), 132.9 and 115.0 (*C*H, arom), 123.0 (arom. *C*qCOOCH$_3$), 61.9 (Si*C*H$_2$O), 45.2 (*C*H$_2$CH$_2$CH$_2$Si), 43.3 (*C*qCH$_2$), 19.3 (CH$_2$*C*H$_2$CH$_2$), 15.9 (CH$_2$CH$_2$*C*H$_2$Si), -4.1 (SiMe$_2$). ^{29}Si NMR (MeOD, 59.62 MHz) δ ppm: 0.36 (*Si*CH$_2$O). MS (MALDI-TOF; m/z) Calcd. for $C_{126}H_{174}O_{27}Si_9Na$: 2 396.47; found: 2 394.44 (MNa^+). Anal. Calc. for $C_{126}H_{174}O_{27}Si_9$: C 63.76, H 7.39; found: C 62.71, H 7.22. Infrared $\upsilon_{C=O}$: 1 686 cm^{-1}.

^{1}H NMR of **7** (D$_2$O + NaOH, 250 MHz): 7.82 and 6.79 (d, 18H, arom), 7.08 (s, 3H, arom-core), 3.41 (s, 18H, SiCH_2O), 1.68 (s, 18H, CH_2CH$_2$CH$_2$Si), 1.16 (s, 18H, CH$_2$CH_2CH$_2$Si), 0.52 (s, 18H, CH$_2$CH$_2$CH_2Si), -0.045 (s, 54H, Si(CH_3)$_2$).

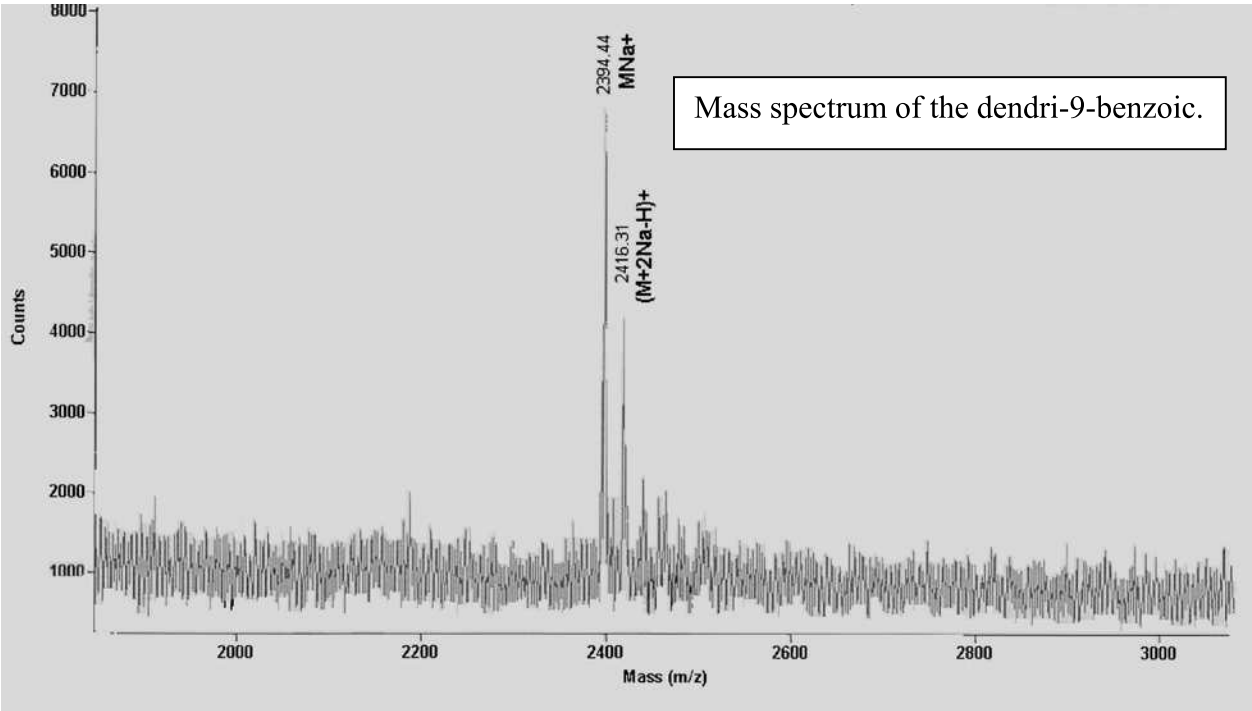

Mass spectrum of the dendri-9-benzoic.

Synthesis of dendri-27-benzoic (8):

Dendri-27-benzoate **7** (0.070 g, 0.007 mmol), was dissolved in dioxane (45 mL), and 5 mL of an aqueous solution of NaOH (2.5 mmol, 12 equiv. *per* branch) was added. The reaction mixture was stired at 60°C for 48 h. Dioxane was removed under vacuum, and the aqueous solution was acidified with HCl. Dendri-81-acid precipitated as a white powder. The solution was filtrated, and the powder was washed twice with ether. The product was recovered from filter by dissolving in methanol. The methanol was removed *in vacuo,* and the product was obtained as a white powder in 67 % yield.

^{1}H NMR (MeOD, 250MHz): 7.91 and 6.86 (d, 54H, *outer arom*), 7.10 and 6.79 (d, 18H, *inner arom*), 3.48 (s, 81H, SiCH_2O), 1.60 (s, 72H, CH_2CH$_2$CH$_2$Si), 1.15 (s, 72H, CH$_2$CH_2CH$_2$Si), 0.53 (s, 72H, CH$_2$CH$_2$CH_2Si), -0.056 (s, 216H, Si(CH_3)$_2$). ^{13}C NMR (MeOD, 62 MHz): 168.5 (*C*OOH), 165.4 (*outer* arom. *C*qO), 159.1 (*inner* arom. *C*qO), 131.5 and 113.6 (*C*H, arom.), 122.3 (arom. *C*qCOOCH$_3$), 60.4 (Si*C*H$_2$O), 42.9 (*C*H$_2$CH$_2$CH$_2$Si), 41.8 (*C*qCH$_2$), 17.6 (CH$_2$*C*H$_2$CH$_2$), 14.4 (CH$_2$CH$_2$*C*H$_2$Si), -4.9 (SiMe$_2$). ^{29}Si NMR (MeOD, 59.62 MHz) δ ppm: 1.57 (*Si*CH$_2$O). MS (MALDI-TOF; m/z) Calcd. For $C_{477}H_{678}O_{90}Si_{36}$: 8886.3; found: 8886.4. Infrared $\upsilon_{C=O}$: 1 686 cm^{-1}.

Mass spectrum of the dendri-27-benzoic.

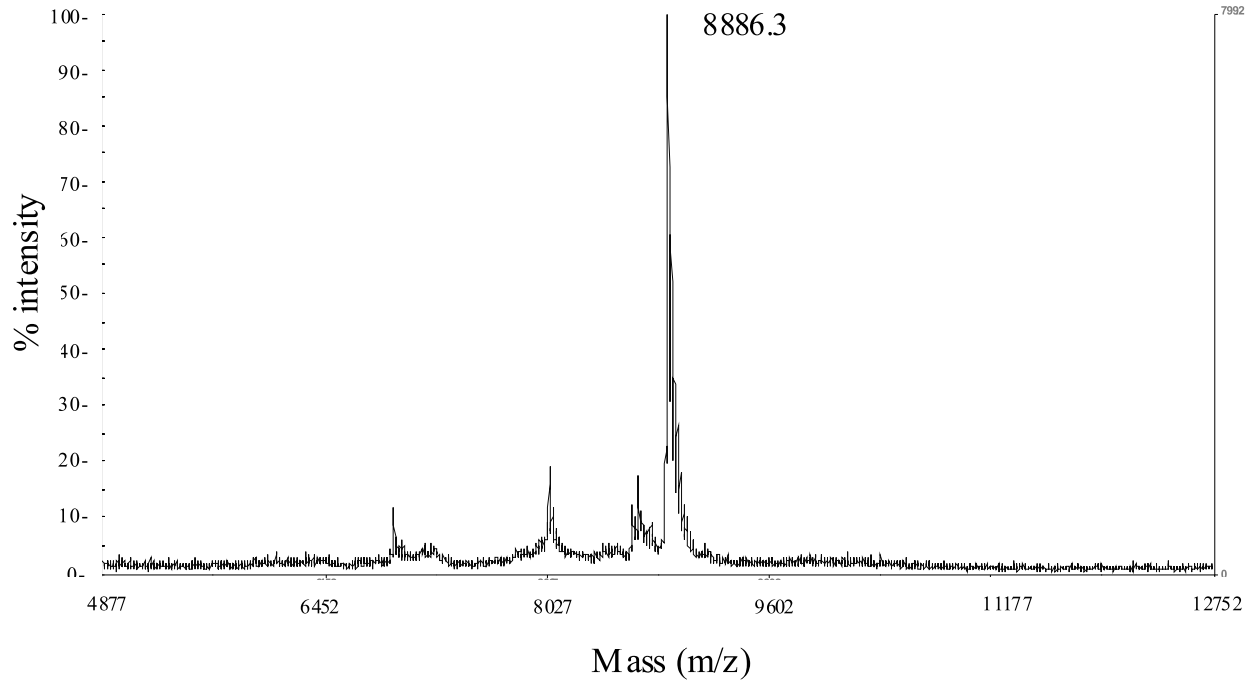

Synthesis of dendri-81-benzoic (10):

Dendri-81-benzoate **9** (0.20 g, 0.0068 mmol), was dissolved in dioxane (50 mL), and 5 mL of an aqueous solution of NaOH (5.51 mmol, 10 equiv. *per* branch) was added. The reaction mixture was stired at 60°C for 48 h. Dioxane was removed under vacuum, and the aqueous solution was acidified with HCl. Dendri-81-acid precipitated as a white powder. The solution was filtrated, and the powder was washed twice with ether. The product was recovered from filter by dissolving in methanol. The methanol was removed *in vacuo,* and the product was obtained as a white powder in 67 % yield.

^{1}H NMR (MeOD, 250MHz): 7.90 and 6.83 (d, 162H, *outer arom*), 7.08 and 6.75 (d, 72H, *inner arom*), 3.43 (s, 234H, SiCH_2O), 1.58 (s, 234H, CH_2CH$_2$CH$_2$Si), 1.10 (s, 234H, CH$_2$CH_2CH$_2$Si), 0.49 (s, 234H, CH$_2$CH$_2$CH_2Si), -0.056 (s, 702H, Si(CH_3)$_2$). ^{13}C NMR (MeOD, 62 MHz): 169.9 (*C*OOH), 166.8 (*outer* arom. *C*qO), 160.5 (*inner* arom. *C*qO), 133.0 and 115.1 (*C*H, arom.), 123.8 (arom. *C*qCOOCH$_3$), 61.8 (Si*C*H$_2$O), 44.3 (*C*H$_2$CH$_2$CH$_2$Si), 43.4 (*C*qCH$_2$), 19.0 (CH$_2$*C*H$_2$CH$_2$), 15.8 (CH$_2$CH$_2$*C*H$_2$Si), -4.0 (SiMe$_2$). ^{29}Si NMR (MeOD, 59.62 MHz) δ ppm: 0.26 (*Si*CH$_2$O). Anal. Calc. for $C_{1530}H_{2190}O_{279}Si_{117}$: C 64.86, H 7.79; found: C 64.25, H 7.68. Infrared $\upsilon_{C=O}$: 1 686 cm^{-1}.

Synthesis of dendri-243-benzoic (12):

Dendri-243-benzoate **7** (0.06 g, 0.0007 mmol), was dissolved in dioxane (45 mL), and 5 mL of an aqueous solution of NaOH (2.5 mmol, 15 equiv. *per* branch) was added. The reaction mixture was stired at 60°C for 48 h. Dioxane was removed under vacuum, and the aqueous solution was acidified with HCl. Dendri-81-acid precipitated as a white powder. The solution was filtrated, and the powder was washed twice with ether. The product was recovered from filter by dissolving in methanol. The methanol was removed *in vacuo,* and the product was obtained as a white powder in 67 % yield.

^{1}H NMR (MeOD, 250MHz): 7.94 and 6.84 (d, 486H, *outer arom*), 7.08 and 6.75 (d, 234H, *inner arom*), 3.36 (s, 720H, SiC*H*$_2$O), 1.62 (s, 720H, C*H*$_2$CH$_2$CH$_2$Si), 1.10 (s, 720H, CH$_2$C*H*$_2$CH$_2$Si), 0.54 (s, 720H, CH$_2$CH$_2$C*H*$_2$Si), -0.020 (s, 2160H, Si(C*H*$_3$)$_2$). ^{13}C NMR (MeOD, 62 MHz): 168.6 (*C*OOH), 165.3 (*outer* arom. *C*qO), 160.5 (*inner* arom. *C*qO), 131.6 and 113.6 (*C*H, arom.), 122.3 (arom. *C*qCOOCH$_3$), 60.4 (Si*C*H$_2$O), 44.3 (*C*H$_2$CH$_2$CH$_2$Si), 43.4 (*C*qCH$_2$), 19.0 (CH$_2$*C*H$_2$CH$_2$), 14.3 (CH$_2$CH$_2$*C*H$_2$Si), -5.3 (SiMe$_2$). Infrared $\upsilon_{C=O}$: 1 686 cm^{-1}.

Chemical Shift Variations of the AC proton signals with the dendri-9-carboxylate (5).

NMR titrations have been performed by titrating dendrimer solution with cation solutions.

The number n of AC molecules bound to the dendrimer is a function of the variation $\Delta\delta$ of chemicals shift (equation 1):

$\Delta\delta = ½\ \Delta\delta_{max}\ [(1 + K_d / n[D_0] + [AC] / n[D_0]) - \{(1 + K_d / n[D_0] + [AC] / n[D_0])^2 - 4[AC] / n[D_0]\}^{1/2}]$

n: number of AC molecules bound to the dendri-9-carboxylate; $[D_0]$: total concentration of the dendrimer ; [AC]: concentration of AC; K_d: dissociation constant; $\Delta\delta_{max}$: the highest chemical shift variation.

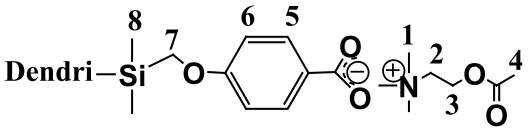

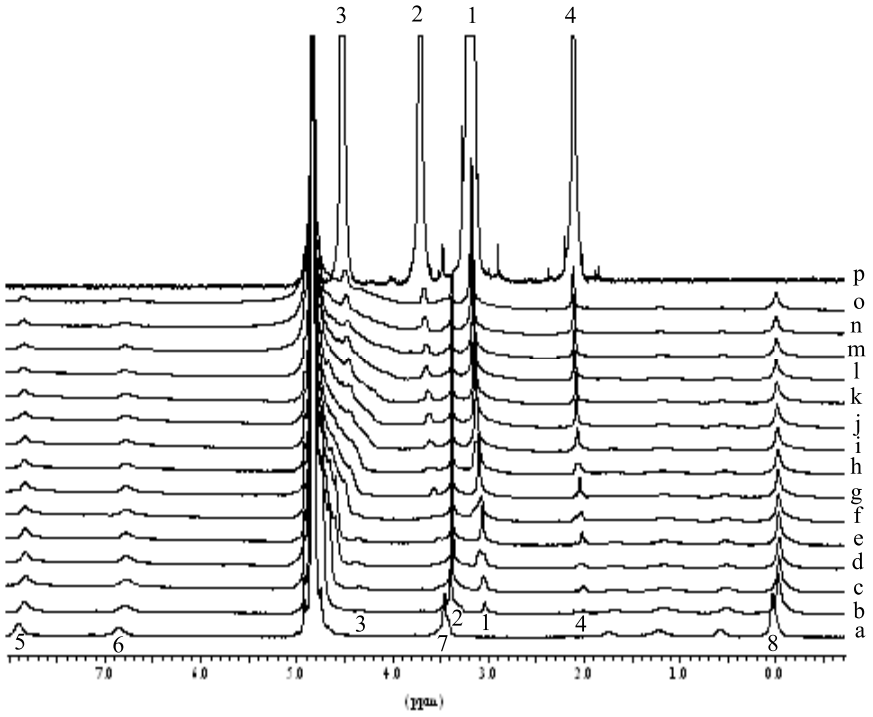

1H NMR titration of dendri-9-carboxylate solution with AC solution: a)dendri-9-carboxylate as its Na^+ salt; b) dendri-9-carboxylate + 1 eq. of AC; c) dendri-9-carboxylate + 2 eq. of AC; d) dendri-9-carboxylate + 3 eq. of AC; e) dendri-9-carboxylate + 4 eq. of AC; f) dendri-9-carboxylate + 5 eq. of AC; g) dendri-9-carboxylate + 6 eq. of AC; h) dendri-9-carboxylate + 7 eq. of AC; i) dendri-9-carboxylate + 8 eq. of AC; j) dendri-9-carboxylate + 9 eq. of AC; k) dendri-9-carboxylate + 10 eq. of AC; l) dendri-9-carboxylate + 12 eq. of AC; m) dendri-9-carboxylate + 14 eq. of AC; n) dendri-9-carboxylate + 16 eq. of AC; o) dendri-9-carboxylate + 20 eq. of AC; p) AC alone.

$\Delta\delta_{max} = 0.32$

$\chi_2 = 0.06$

For the first 9 molecules of AC bound to dendri-9-carboxylate**:** $Kd_1 = 20\ (\pm 2) \times 10^{-3}$ M

For the other 9 molecules of AC bound to dendri-9-carboxylate**:** $Kd_2 = 1\ (\pm 0.1)$ M

Chemical Shift Variations of the AC proton signals with the dendri-27-carboxylate (8).

NMR titrations have been performed by titrating dendrimer solution with cation solutions.

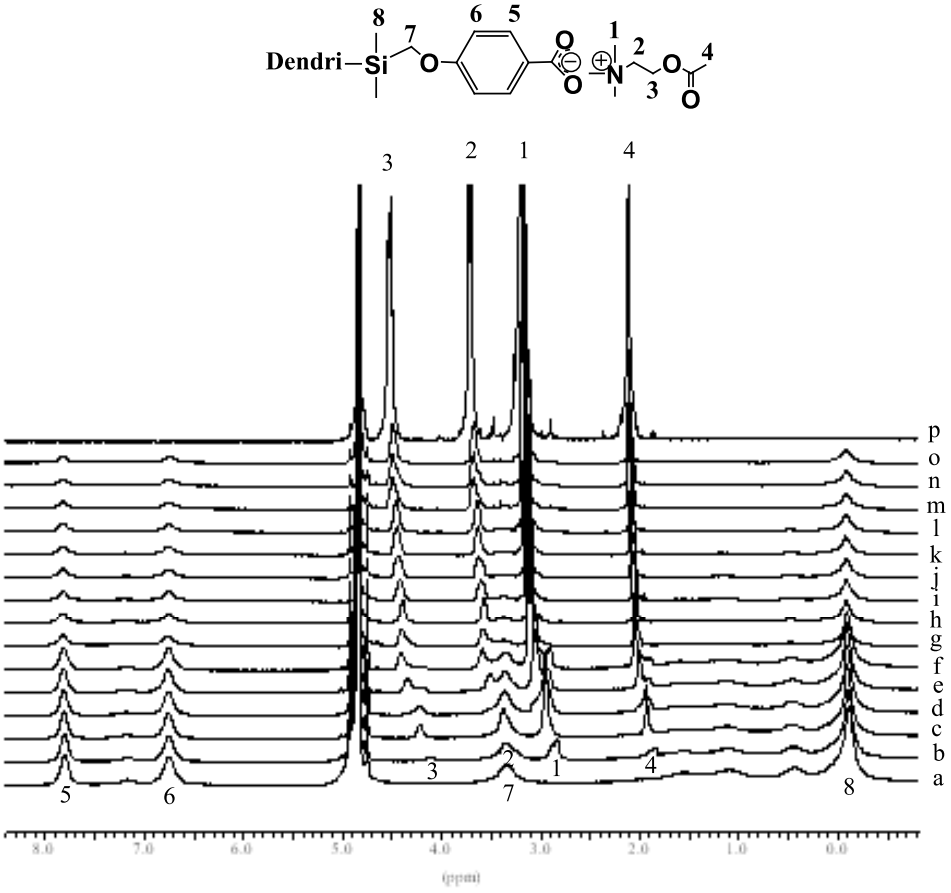

^{1}H NMR titration of dendri-27-carboxylate solution with AC solution: a)dendri-27-carboxylate as its Na^+ salt; b) dendri-27-carboxylate + 5 eq. of AC; c) dendri-27-carboxylate + 10 eq. of AC; d) dendri-27-carboxylate + 15 eq. of AC; e) dendri-27-carboxylate + 20 eq. of AC; f) dendri-27-carboxylate + 25 eq. of AC; g) dendri-27-carboxylate + 27 eq. of AC; h) dendri-27-carboxylate + 30 eq. of AC; i) dendri-27-carboxylate + 40 eq. of AC; j) dendri-27-carboxylate + 50 eq. of AC; k) dendri-27-carboxylate + 60 eq. of AC; l) dendri-27-carboxylate + 70 eq. of AC; m) dendri-27-carboxylate + 80 eq. of AC; n) dendri-27-carboxylate + 90 eq. of AC; o) dendri-27-carboxylate + 100 eq. of AC; p) AC alone.

$\Delta\delta_{max} = 0.35$

$\chi_2 = 0.02$

For the first 27 molecules of AC bound to dendri-27-carboxylate**:** $Kd_1 = 18\ (\pm 0.15) \times 10^{-3}$ M

For the other 27 molecules of AC bound to dendri-27-carboxylate**:** $Kd_2 = 8\ (\pm 0.8) \times 10^{-1}$ M

Chemical Shift Variations of the AC proton signals with the dendri-81-carboxylate (10).

NMR titrations have been performed by titrating dendrimer solution with cation solutions.

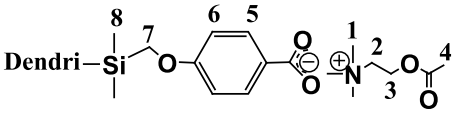

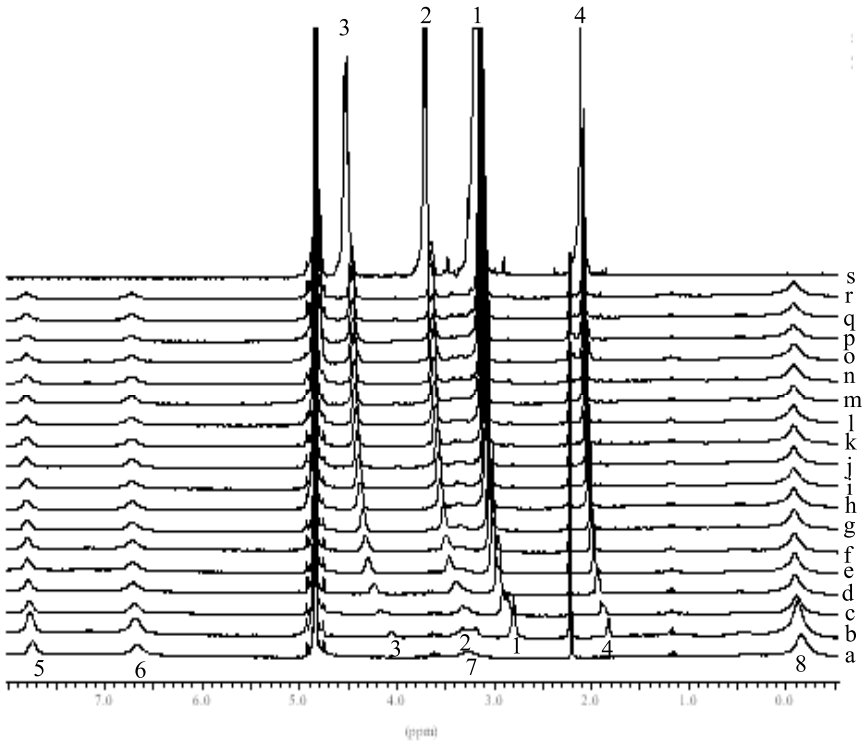

^{1}H NMR titration of dendri-81-carboxylate solution with AC solution: a)dendri-81-carboxylate as its Na^+ salt; b) dendri- 81 -carboxylate + 20 eq. of AC; c) dendri- 81 -carboxylate + 45 eq. of AC; d) dendri- 81 -carboxylate + 70 eq. of AC; e) dendri- 81 -carboxylate + 100 eq. of AC; f) dendri- 81 -carboxylate + 130 eq. of AC; g) dendri- 81 -carboxylate + 160 eq. of AC; h) dendri- 81 -carboxylate + 200 eq. of AC; i) dendri- 81 -carboxylate + 230 eq. of AC; j) dendri- 81 -carboxylate + 270 eq. of AC; k) dendri- 81 -carboxylate + 320 eq. of AC; l) dendri- 81 -carboxylate + 360 eq. of AC; m) dendri- 81 -carboxylate + 410 eq. of AC; n) dendri- 81 -carboxylate + 470 eq. of AC; o) dendri- 81 -carboxylate + 510 eq. of AC; p) dendri- 81 -carboxylate + 560 eq. of AC; q) dendri- 81 -carboxylate + 600 eq. of AC; r) dendri- 81 -carboxylate + 650 eq. of AC; s) AC alone.

$\Delta\delta_{max} = 0.6$

$\chi_2 = 0.04$

For the first 81 molecules of AC bound to dendri-81-carboxylate**:** $Kd_1 = 17 (\pm 2) \times 10^{-3}$ M

For the other 81 molecules of AC bound to dendri-81-carboxylate**:** $Kd_2 = 230 (\pm 20) \times 10^{-3}$ M

Chemical Shift Variations of the AC proton signals with the dendri-243-carboxylate (12).

NMR titrations have been performed by titrating dendrimer solution with cation solutions.

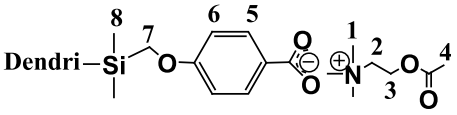

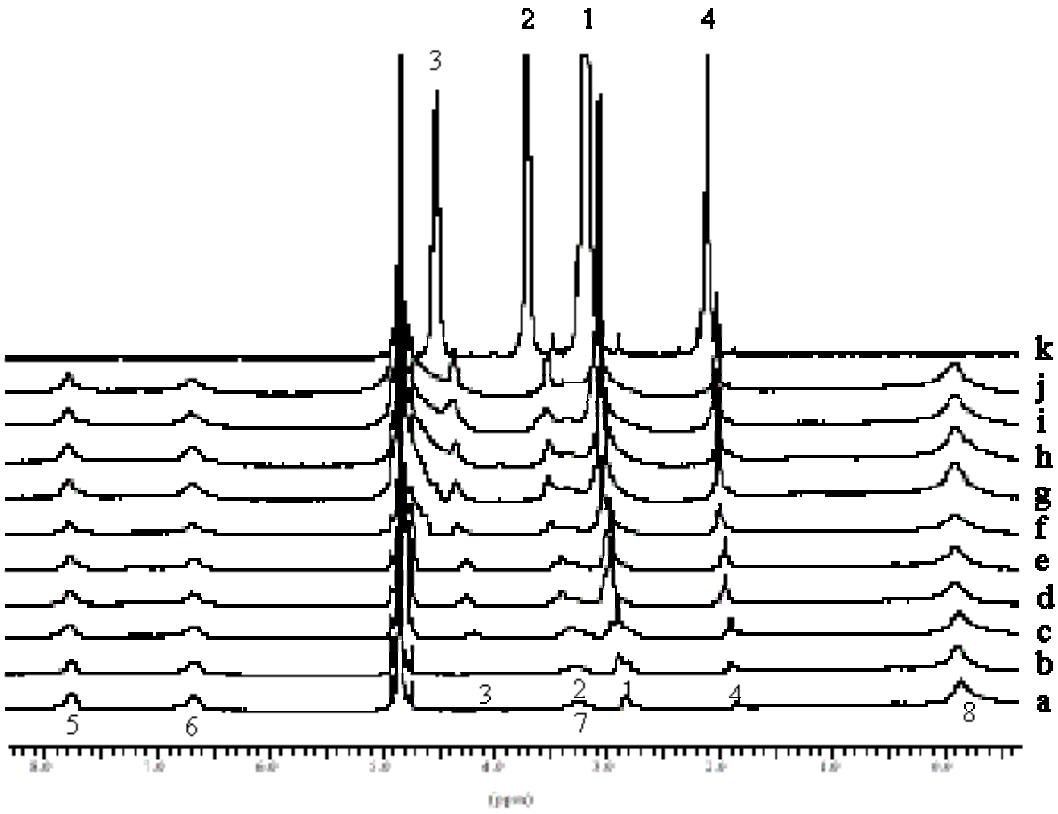

^{1}H NMR titration of dendri-243-carboxylate solution with AC solution: a)dendri-243 -carboxylate as its Na^+ salt; b) dendri- 243 -carboxylate + 40 eq. of AC; c) dendri- 243 -carboxylate + 80 eq. of AC; d) dendri- 243 -carboxylate + 120 eq. of AC; e) dendri- 243 -carboxylate + 160 eq. of AC; f) dendri- 243 -carboxylate + 200 eq. of AC; g) dendri- 243 -carboxylate + 240 eq. of AC; h) dendri- 243 -carboxylate + 280 eq. of AC; i) dendri- 243 -carboxylate + 320 eq. of AC; j) dendri- 243 -carboxylate + 360 eq. of AC; k) AC alone.

$\Delta\delta_{max} = 0.46$

$\chi_2 = 0.08$

For the first 243 molecules of AC bound to dendri-243-carboxylate**:** $Kd_1 = 13\ (\pm 1.3) \times 10^{-3}$ M

For the other 243 molecules of AC bound to dendri-243-carboxylate**:** $Kd_2 = 8\ (0.8) \times 10^{-2}$ M

Chemical Shift Variations of the BTEA proton signals with the dendri-9-carboxylate (5).

NMR titrations have been performed by titrating dendrimer solution with cation solutions.

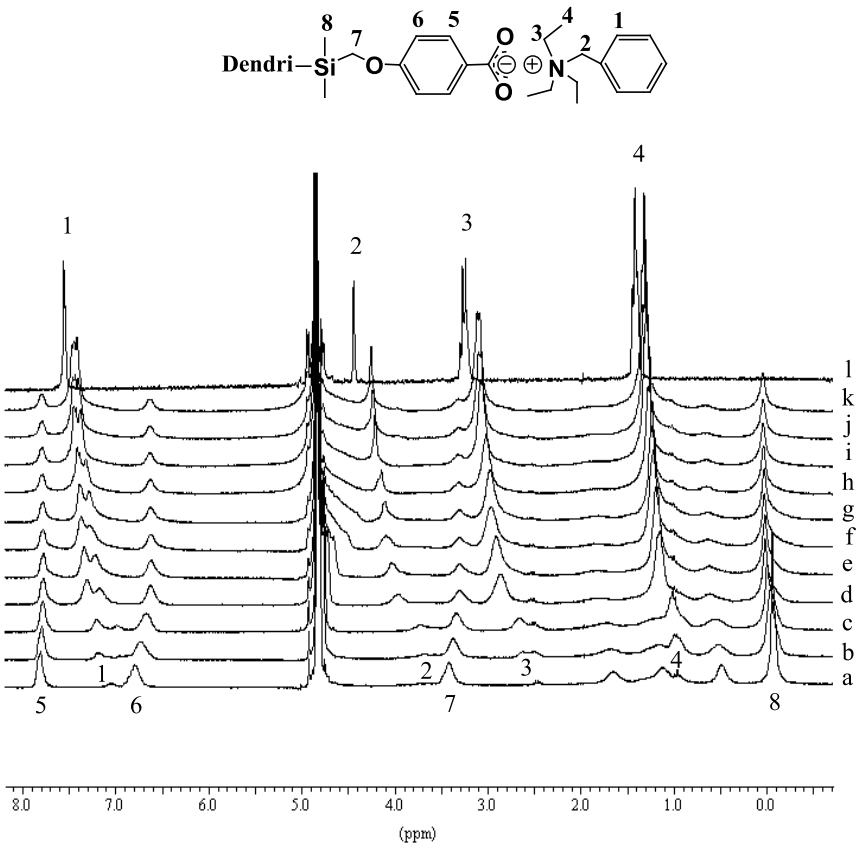

1H NMR titration of dendri-9-carboxylate solution with BTEA solution: a)dendri-9-carboxylate as its Na^+ salt; b) dendri-9-carboxylate + 2 eq. of BTEA; c) dendri-9-carboxylate + 4 eq. of BTEA; d) dendri-9-carboxylate + 6 eq. of BTEA; e) dendri-9-carboxylate + 8 eq. of BTEA; f) dendri-9-carboxylate + 9 eq. of BTEA; g) dendri-9-carboxylate + 10 eq. of BTEA; h) dendri-9-carboxylate + 12 eq. of BTEA; i) dendri-9-carboxylate + 14 eq. of BTEA; j) dendri-9-carboxylate + 15 eq. of BTEA; k) dendri-9-carboxylate + 18 eq. of BTEA; l) BTEA alone.

$\Delta\delta_{max} = 0.9$

$\chi_2 = 0.007$

For the first 9 molecules of BTEA bound to dendri-9-carboxylate**:** $Kd_1 = 8\ (\pm 0.8) \times 10^{-3}$ M

For the other 9 molecules of BTEA bound to dendri-9-carboxylate**:** $Kd_2 = 3\ (\pm 0.3) \times 10^{-1}$ M

Chemical Shift Variations of the BTEA proton signals with the dendri-27-carboxylate (8).

NMR titrations have been performed by titrating dendrimer solution with cation solutions.

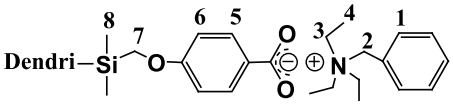

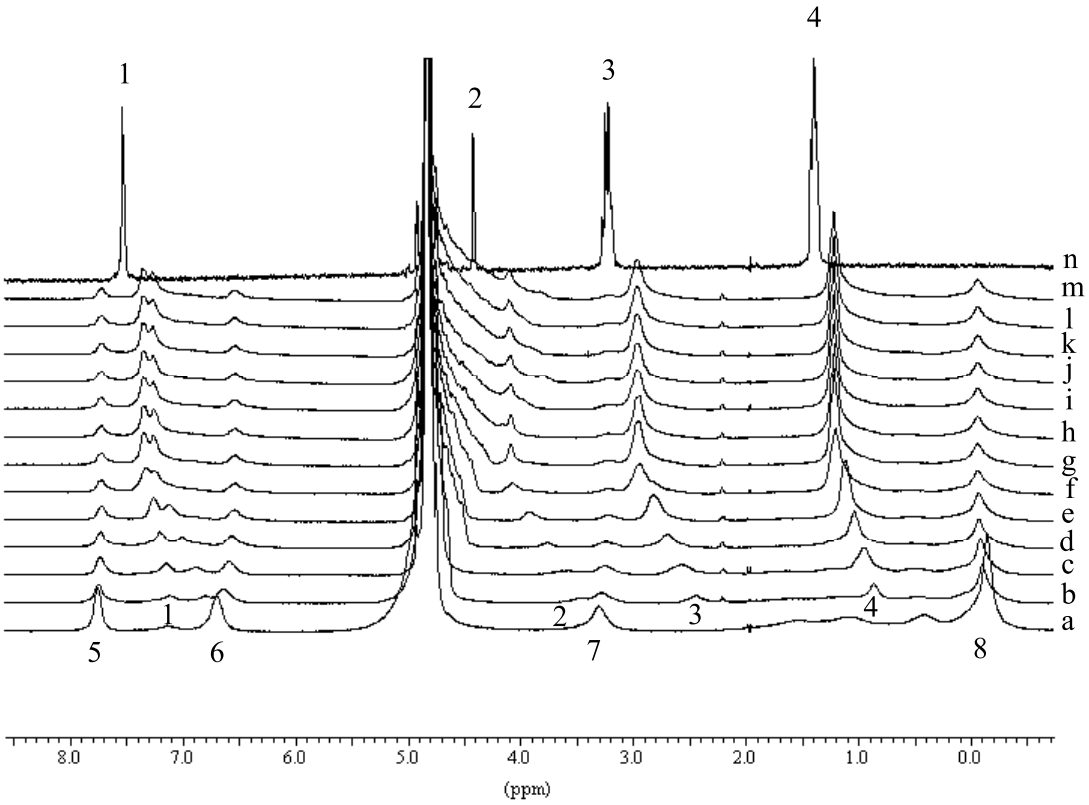

^{1}H NMR titration of dendri-27-carboxylate solution with BTEA solution: a)dendri-27-carboxylate as its Na^+ salt; b) dendri-27-carboxylate + 5 eq. of BTEA; c) dendri-27-carboxylate + 10 eq. of BTEA; d) dendri-27-carboxylate + 15 eq. of BTEA; e) dendri-27-carboxylate + 20 eq. of BTEA; f) dendri-27-carboxylate + 25 eq. of BTEA; g) dendri-27-carboxylate + 27 eq. of BTEA; h) dendri-27-carboxylate + 30 eq. of BTEA; i) dendri-27-carboxylate + 40 eq. of BTEA; j) dendri-27-carboxylate + 50 eq. of BTEA; k) dendri-27-carboxylate + 60 eq. of BTEA; l) dendri-27-carboxylate + 70 eq. of BTEA; m) dendri-27-carboxylate + 80 eq. of BTEA; n) BTEA alone.

$\Delta\delta_{max} = 1.1$

$\chi_2 = 0.02$

For the first 27 molecules of BTEA bound to dendri-27-carboxylate**:** $Kd_1 = 7\ (\pm 0.7) \times 10^{-3}$ M

For the other 27 molecules of BTEA bound to dendri-27-carboxylate**:** $Kd_2 = 3\ (\pm 0.3) \times 10^{-1}$ M

Chemical Shift Variations of the BTEA proton signals with the dendri-81-carboxylate (10).

NMR titrations have been performed by titrating dendrimer solution with cation solutions.

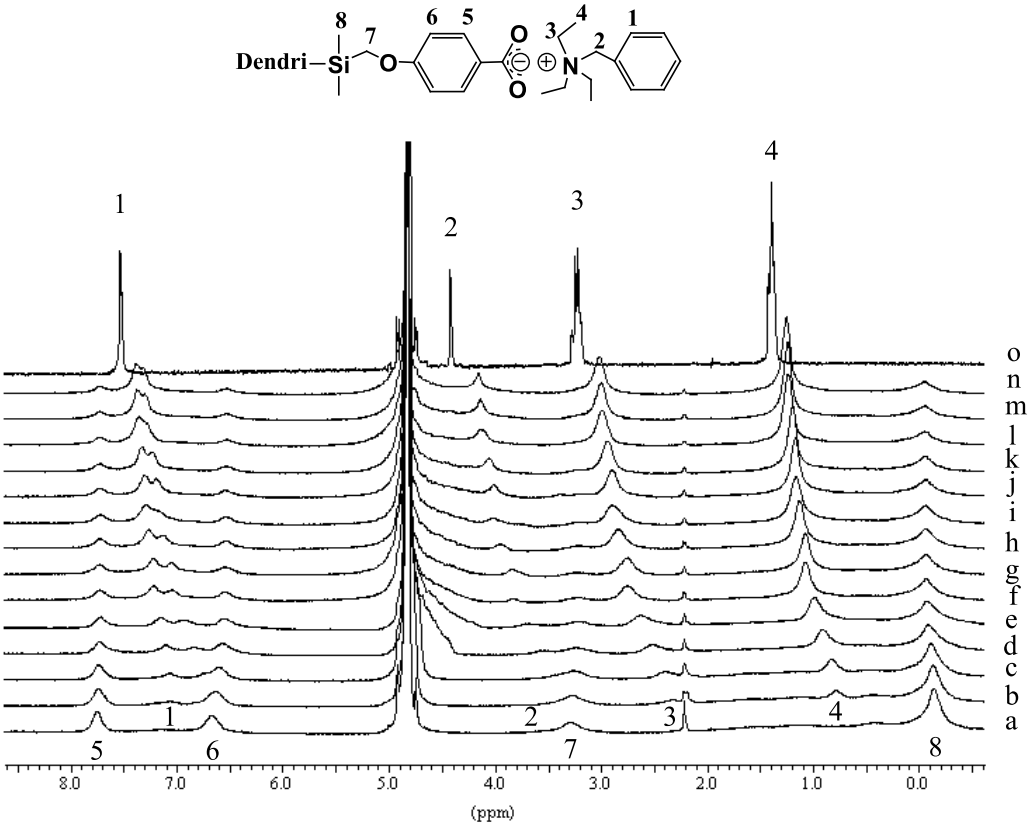

^{1}H NMR titration of dendri-81-carboxylate solution with BTEA solution: a)dendri-81-carboxylate as its Na^+ salt; b) dendri- 81 -carboxylate + 20 eq. of BTEA; c) dendri- 81 -carboxylate + 45 eq. of BTEA; d) dendri- 81 -carboxylate + 70 eq. of BTEA; e) dendri- 81 -carboxylate + 100 eq. of BTEA; f) dendri- 81 -carboxylate + 130 eq. of BTEA; g) dendri- 81 -carboxylate + 160 eq. of BTEA; h) dendri- 81 -carboxylate + 200 eq. of BTEA; i) dendri- 81 -carboxylate + 230 eq. of BTEA; j) dendri- 81 -carboxylate + 270 eq. of BTEA; k) dendri- 81 -carboxylate + 320 eq. of BTEA; l) dendri- 81 -carboxylate + 360 eq. of BTEA; m) dendri- 81 -carboxylate + 410 eq. of BTEA; n) dendri- 81 -carboxylate + 470 eq. of BTEA; o) dendri- 81 -carboxylate + 510 eq. of BTEA; p) dendri- 81 -carboxylate + 560 eq. of BTEA; q) dendri- 81 -carboxylate + 600 eq. of BTEA; r) dendri- 81 -carboxylate + 650 eq. of BTEA; s) BTEA alone.

$\Delta\delta_{max} = 1.16$

$\chi_2 = 0.03$

For the first 81 molecules of BTEA bound to dendri-81-carboxylate**:** $Kd_1 = 6\ (\pm 0.6) \times 10^{-3}$ M

For the other 81 molecules of BTEA bound to dendri-81-carboxylate**:** $Kd_2 = 3\ (\pm 0.3) \times 10^{-1}$ M

Chemical Shift Variations of the BTEA proton signals with the dendri-243-carboxylate (12).

NMR titrations have been performed by titrating dendrimer solution with cation solutions.

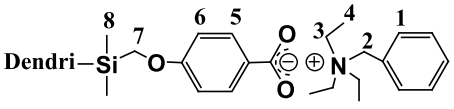

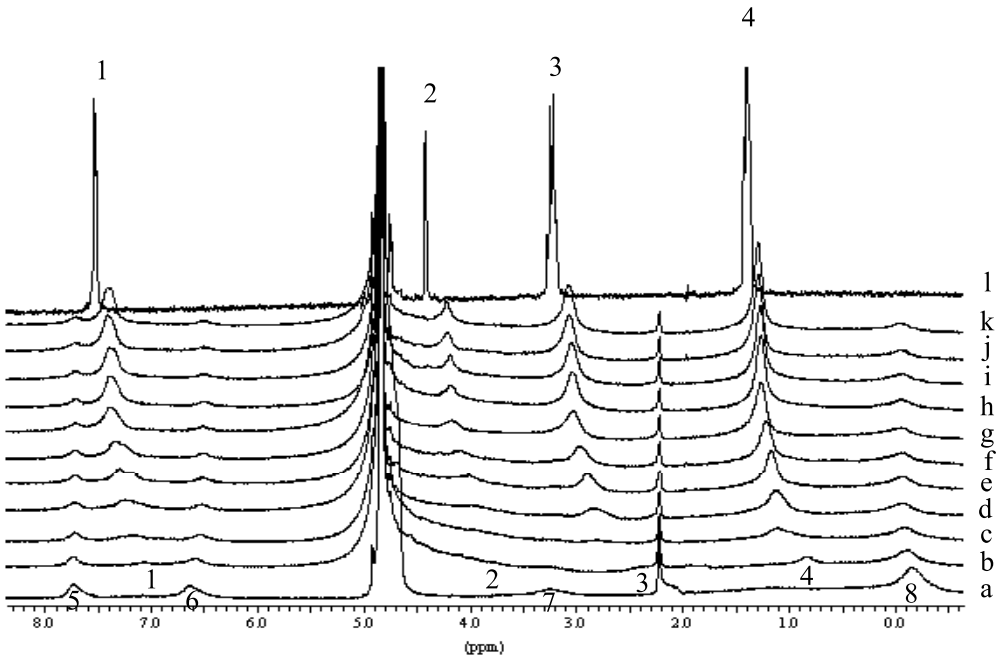

^{1}H NMR titration of dendri-243-carboxylate solution with BTEA solution: a)dendri- 243 -carboxylate as its Na^+ salt; b) dendri- 243 -carboxylate + 40 eq. of BTEA; c) dendri- 243 -carboxylate + 80 eq. of BTEA; d) dendri- 243 -carboxylate + 120 eq. of BTEA; e) dendri- 243 -carboxylate + 160 eq. of BTEA; f) dendri- 243 -carboxylate + 200 eq. of BTEA; g) dendri- 243 -carboxylate + 240 eq. of BTEA; h) dendri- 243 -carboxylate + 280 eq. of BTEA; i) dendri- 243 -carboxylate + 320 eq. of BTEA; j) dendri- 243 -carboxylate + 360 eq. of BTEA; k) BTEA alone.

$\Delta\delta_{max} = 0.6$

$\chi_2 = 0.08$

For the first 243 molecules of BTEA bound to dendri-243-carboxylate**:** $Kd_1 = 5\ (\pm 0.5) \times 10^{-3}$ M

For the other 243 molecules of BTEA bound to dendri-243-carboxylate**:** $Kd_2 = 3\ (\pm 0.3) \times 10^{-1}$ M

Chemical Shift Variations of the Dopamine proton signals with the dendri-9-carboxylate (5).

NMR titrations have been performed by titrating dendrimer solution with cation solutions.

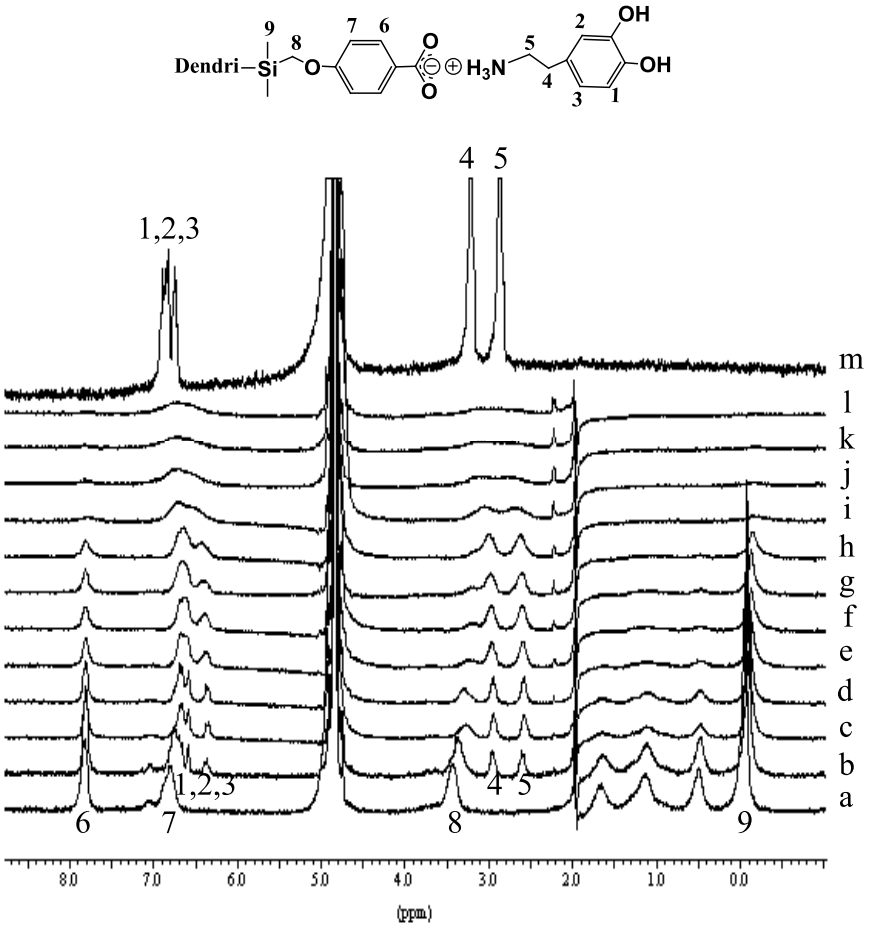

^{1}H NMR titration of dendri-9-carboxylate solution with Dopamine solution: a)dendri-9-carboxylate as its Na^+ salt; b) dendri-9-carboxylate + 2 eq. of Dopamine; c) dendri-9-carboxylate + 4 eq. of Dopamine; d) dendri-9-carboxylate + 6 eq. of Dopamine; e) dendri-9-carboxylate + 8 eq. of Dopamine; f) dendri-9-carboxylate + 9 eq. of Dopamine; g) dendri-9-carboxylate + 10 eq. of Dopamine; h) dendri-9-carboxylate + 12 eq. of Dopamine; i) dendri-9-carboxylate + 14 eq. of Dopamine; j) dendri-9-carboxylate + 15 eq. of Dopamine; k) dendri-9-carboxylate + 18 eq. of Dopamine; l) dendri-9-carboxylate + 20 eq. of Dopamine; m) Dopamine alone.

n = 9

$\Delta\delta_{max} = 0.35$

$\chi_2 = 0.009$

For the 9 molecules of Dopamine bound to dendri-9-carboxylate**:** $Kd_1 = 5\ (\pm 0.5) \times 10^{-4}$ M

Chemical Shift Variations of the Dopamine proton signals with the dendri-27-carboxylate (8).

NMR titrations have been performed by titrating dendrimer solution with cation solutions.

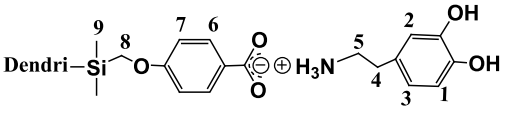

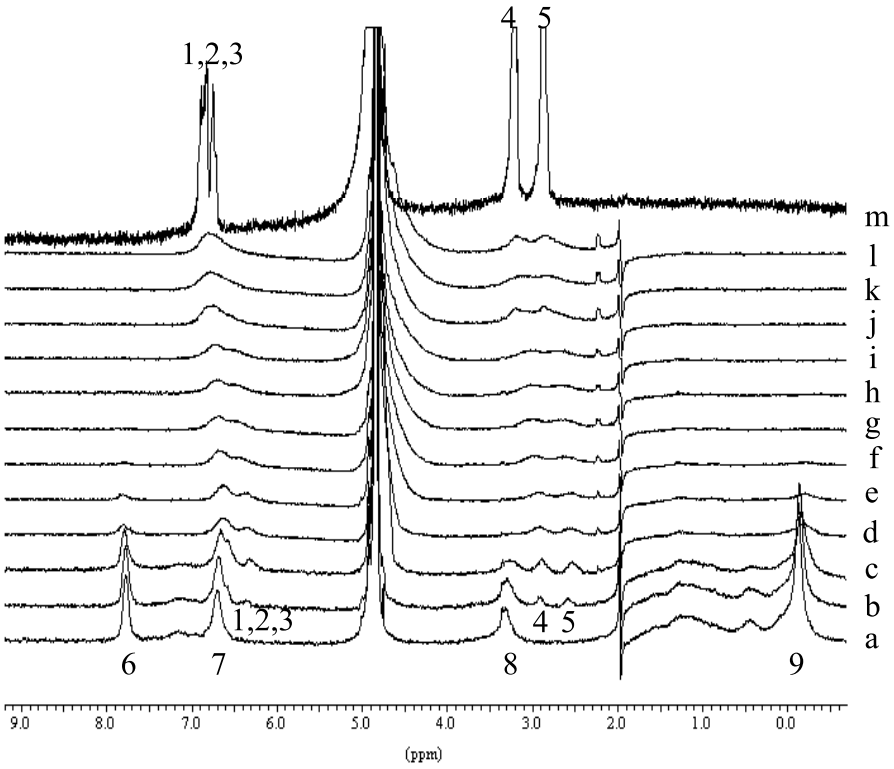

^{1}H NMR titration of dendri-27-carboxylate solution with Dopamine solution: a)dendri-27-carboxylate as its Na^+ salt; b) dendri-27-carboxylate + 5 eq. of Dopamine; c) dendri-27-carboxylate + 10 eq. of Dopamine; d) dendri-27-carboxylate + 15 eq. of Dopamine; e) dendri-27-carboxylate + 20 eq. of Dopamine; f) dendri-27-carboxylate + 25 eq. of Dopamine; g) dendri-27-carboxylate + 27 eq. of Dopamine; h) dendri-27-carboxylate + 30 eq. of Dopamine; i) dendri-27-carboxylate + 40 eq. of Dopamine; j) dendri-27-carboxylate + 50 eq. of Dopamine; k) dendri-27-carboxylate + 60 eq. of Dopamine; l) dendri-27-carboxylate + 70 eq. of Dopamine; m) Dopamine alone.

n = 27

$\Delta\delta_{max} = 0.37$

$\chi_2 = 0.007$

For the 27 molecules of Dopamine bound to dendri-27-carboxylate**:** $Kd_1 = 4\ (\pm 0.4) \times 10^{-4}$ M

Chemical Shift Variations of the Dopamine proton signals with the dendri-81-carboxylate (10).

NMR titrations have been performed by titrating dendrimer solution with cation solutions.

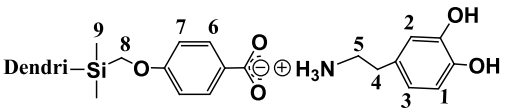

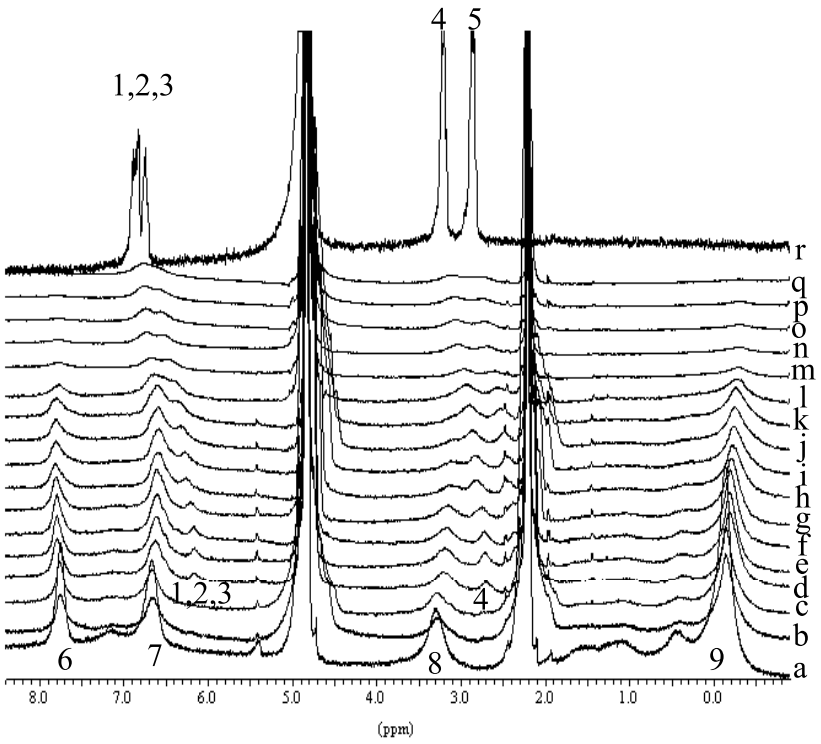

^{1}H NMR titration of dendri-81-carboxylate solution with Dopamine solution: a)dendri-81-carboxylate as its Na^+ salt; b) dendri- 81 -carboxylate + 10 eq. of Dopamine; c) dendri- 81 -carboxylate + 20 eq. of Dopamine; d) dendri- 81 -carboxylate + 30 eq. of Dopamine; e) dendri- 81 -carboxylate + 40 eq. of Dopamine; f) dendri- 81 -carboxylate + 50 eq. of Dopamine; g) dendri- 81 -carboxylate + 60 eq. of Dopamine; h) dendri- 81 -carboxylate + 70 eq. of Dopamine; i) dendri- 81 -carboxylate + 80 eq. of Dopamine; j) dendri- 81 -carboxylate + 90 eq. of Dopamine; k) dendri- 81 -carboxylate + 100 eq. of Dopamine; l) dendri- 81 -carboxylate + 120 eq. of Dopamine; m) dendri- 81 -carboxylate + 140 eq. of Dopamine; n) dendri- 81 -carboxylate + 160 eq. of Dopamine; o) dendri- 81 -carboxylate + 180 eq. of Dopamine; p) dendri- 81 -carboxylate + 200 eq. of Dopamine; q) dendri- 81 -carboxylate + 220 eq. of Dopamine; r) Dopamine alone.

$n = 81$

$\Delta\delta_{max} = 0.54$

$\chi_2 = 0.009$

For the 81 molecules of Dopamine bound to dendri-81-carboxylate**:** $Kd_1 = 3\ (\pm 0.3) \times 10^{-4}$ M

Chemical Shift Variations of the Dopamine proton signals with the dendri-243-carboxylate (12).

NMR titrations have been performed by titrating dendrimer solution with cation solutions.

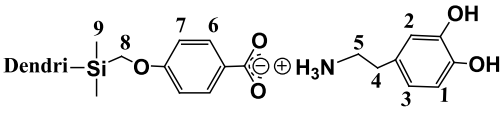

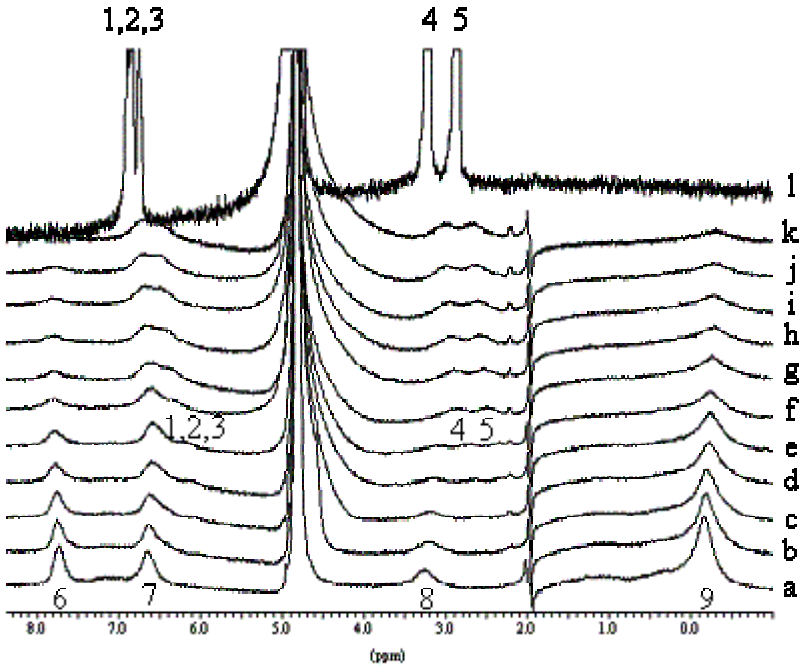

^{1}H NMR titration of dendri-243-carboxylate solution with Dopamine solution: a)dendri- 243 -carboxylate as its Na^+ salt; b) dendri- 243 -carboxylate + 40 eq. of Dopamine; c) dendri- 243 -carboxylate + 80 eq. of Dopamine; d) dendri- 243 -carboxylate + 120 eq. of Dopamine; e) dendri- 243 -carboxylate + 160 eq. of Dopamine; f) dendri- 243 -carboxylate + 200 eq. of Dopamine; g) dendri- 243 -carboxylate + 240 eq. of Dopamine; h) dendri- 243 -carboxylate + 280 eq. of Dopamine; i) dendri- 243 -carboxylate + 320 eq. of Dopamine; j) dendri- 243 -carboxylate + 400 eq. of Dopamine; k) dendri- 243 -carboxylate + 500 eq. of Dopamine; l) Dopamine alone.

n = 243

$\Delta\delta_{max} = 0.41$

$\chi_2 = 0.002$

For the 243 molecules of Dopamine bound to dendri-243-carboxylate**:** $Kd_1 = 2\ (\pm 0.2) \times 10^{-4}$ M

Supramolecular assembly	$\Delta\delta_{max}$ [a] (ppm)	χ_2 [b]	n_1 [c]	Kd_1 [d] (M)	Ka_1 [e] (M^{-1})	n_2 [f]	Kd_2 [g] (M)	Ka_2 [h] (M^{-1})
Dendri-9-carboxylate + AC	0.32	0.06	9	20×10^{-3}	50	9	1	1
Dendri-27-carboxylate + AC	0.35	0.02	27	18×10^{-3}	56	27	8×10^{-1}	1
Dendri-81-carboxylate + AC	0.6	0.04	81	17×10^{-3}	59	81	23×10^{-2}	4
Dendri-243-carboxylate + AC	0.46	0.08	243	13×10^{-3}	77	243	8×10^{-2}	12
Dendri-9-carboxylate + BTEA	0.9	0.007	9	8×10^{-3}	125	9	3×10^{-1}	3
Dendri-27-carboxylate + BTEA	1.1	0.02	27	7×10^{-3}	143	27	3×10^{-1}	3
Dendri-81-carboxylate + BTEA	1.16	0.03	81	6×10^{-3}	167	81	3×10^{-1}	3
Dendri-243-carboxylate + BTEA	0.6	0.08	243	5×10^{-3}	200	243	3×10^{-1}	3
Dendri-9-carboxylate + Dopamine	0.35	0.009	9	5×10^{-4}	2000	-	-	-
Dendri-27-carboxylate + Dopamine	0.37	0.007	27	4×10^{-4}	2500	-	-	-
Dendri-81-carboxylate + Dopamine	0.54	0.009	81	3×10^{-4}	3333	-	-	-
Dendri-243-carboxylate + Dopamine	0.41	0.002	243	2×10^{-4}	5000	-	-	-

Table of the Kd values: $\Delta\delta_{max}$ is the maximum of the observed chemical displacement ; χ_2 translated the difference between the experimental points and the numerical values extracted from a theoretical curve; n_1 is the number of cationic molecules fixed with the first association constant; Kd_1 is the first dissociation constant; Ka_1 is the first association constant; n_2 is the number of cationic molecules fixed with the second association constant; Kd_2 is
the second dissociation constant and Ka_2 is the second association constant.
The error of all the values of this table is 10%.

Measurements of diffusion coefficient by ^{1}H NMR upon titration of dendrimer-81-carboxylate (10) with cations (AC, BTEA and dopamine).

The goal of this series of experiments is to measure the diffusion coefficient (noted D) by ^{1}H NMR. The studied molecules are the dendrimer-81-carboxylate and the three cations (AC, BTEA and dopamine). The sample are those used during the titration by ^{1}H NMR.

First, the measurement of D allows to calculate the hydrodynamic diameter of a molecule. Then the ^{1}H NMR experiment focuses on the diffusion that is mathematically treated according to a process DOSY (Diffusion Ordered SpectroscopY) in order to obtain the equivalent of a spectral chromatography. The objective is thus double: measure the size of the two free and bound molecules in solution by ^{1}H NMR, and obtain a DOSY spectrum that will account for the purity of the product.

The dendri-81-carboxylate is considered as a spherical molecular object, and characterized by an apparent diffusion coefficient. The application of the Stokes-Einstein law gives an estimate of the diameter of the molecule.

Stokes-Einstein law:

$D = K_B T / 6\pi\eta r_H$

D: diffusion constant; K_B: Boltzman's constant; T: temperature (K); η: solvent viscosity; r_H: hydrodynamic radius of the species.

DOSY spectrum of dendrimer-81-carboxylate (10) in D_2O

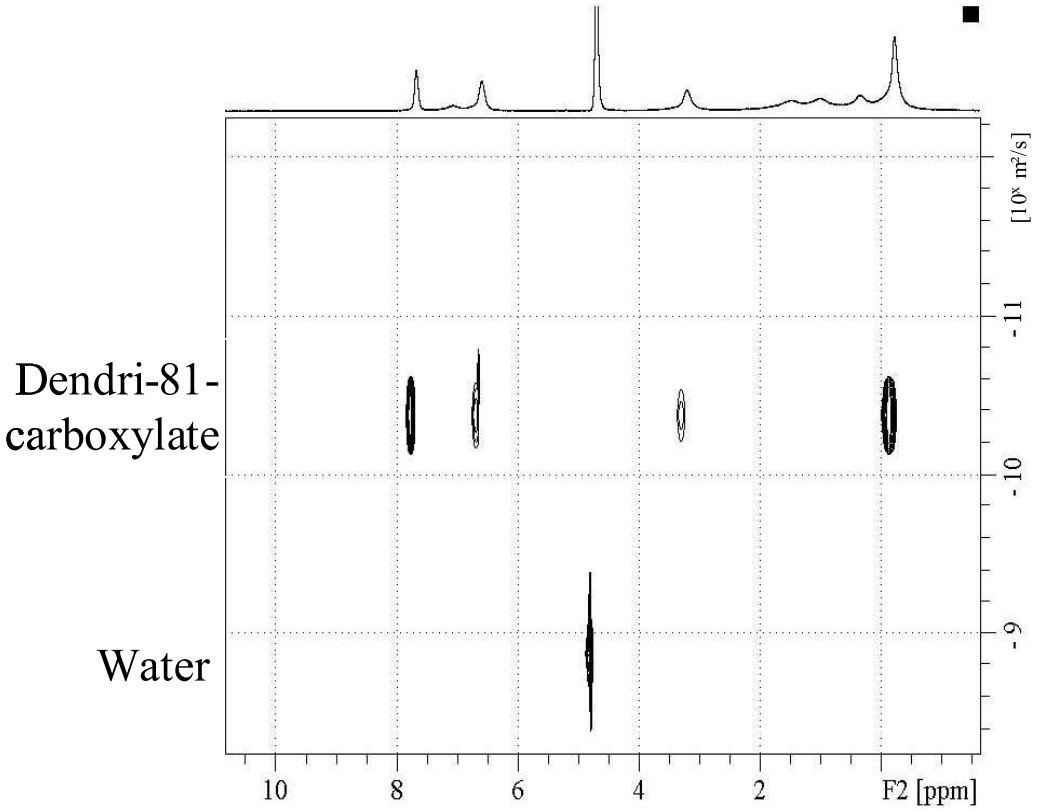

The four signals on the line (top) represent the log(D) of the dendri-81-carboxylate**,** and the last signal below the line represents the log(D) of water.

$D_{\mathbf{d}} = 4.441\ (\pm\ 0.1) \times 10^{-11}\ m^2/s$

$R_{H\,\mathbf{d}} = 5.517$ nm

$D_{\mathbf{d}}$: diffusion coefficient of the dendri-81-carboxylate; $R_{H\,\mathbf{d}}$: hydrodynamic radius of the dendri-18-carboxylate.

DOSY spectrum of acetylcholine (AC) in D_2O

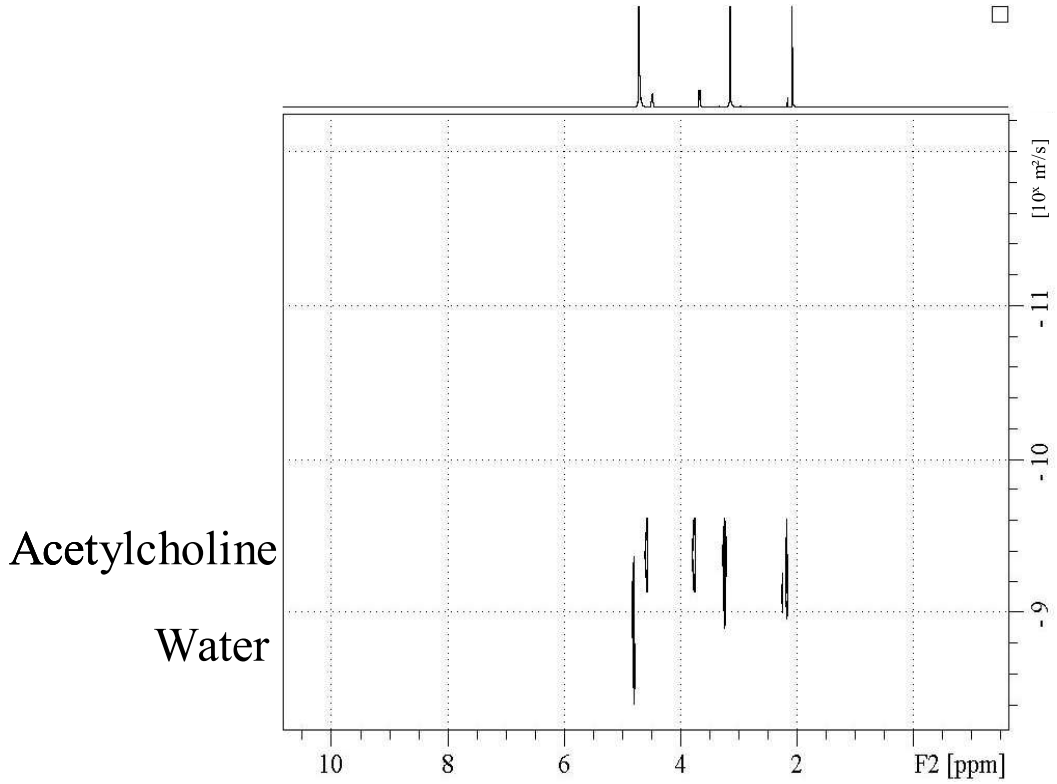

The four signals on the line (top) represent the log(D) of one molecule of acetylcholine (AC), and the last signal below the line represents the log(D) of water.

$D_{AC} = 5.948 (\pm 0.1) \times 10^{-10}$ m²/s

$R_{H\,AC} = 0.594$ nm

D_{AC}: diffusion coefficient of AC; $R_{H\,AC}$: hydrodynamic radius of AC.

Superposition of the three DOSY spectra: free dendrimer (10), free acetylcholine (AC), and assembly dendrimer +AC in D2O

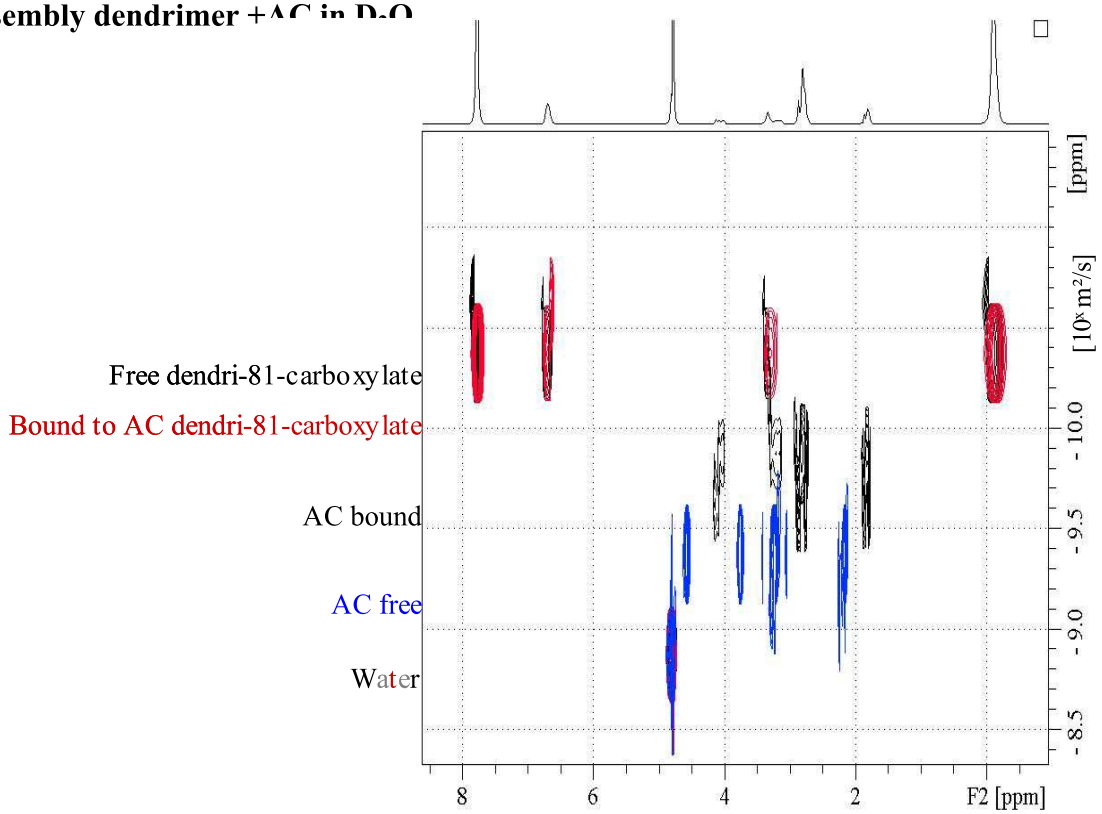

The four black signals on the line (top) represent the log(D) of the free dendrimer ; the four red signals on the line (top) represent the log(D) of the bound to AC dendrimer ; the four black signals on the medium line represent the log(D) of a molecule of AC bound to the dendrimer ; the four blue signals (medium) represent the log(D) of a free molecule of AC. The last multicolor signal on the line below represents the log(D) of water.

$D_d = 4.998\ (\pm\ 0.1) \times 10^{-11}\ m^2/s$

$R_{H\,d} = 4.902\ nm$

D_d: diffusion coefficient of the dendrimer ; $R_{H\,d}$: hydrodynamic radius of the dendrimer.

Evolution of diffusion coefficients of AC and dendrimer (10) as a function of the concentration of AC in water.

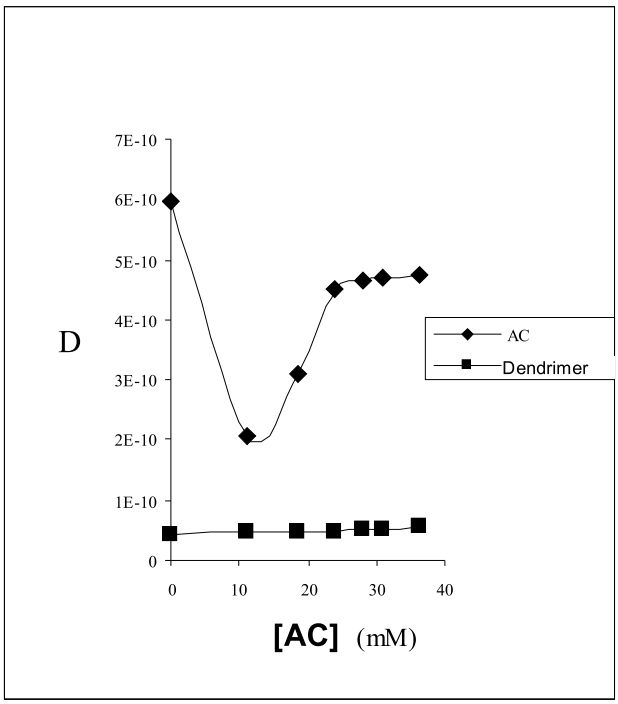

DOSY spectrum of assembly dendrimer (10) + BTEA in D_2O

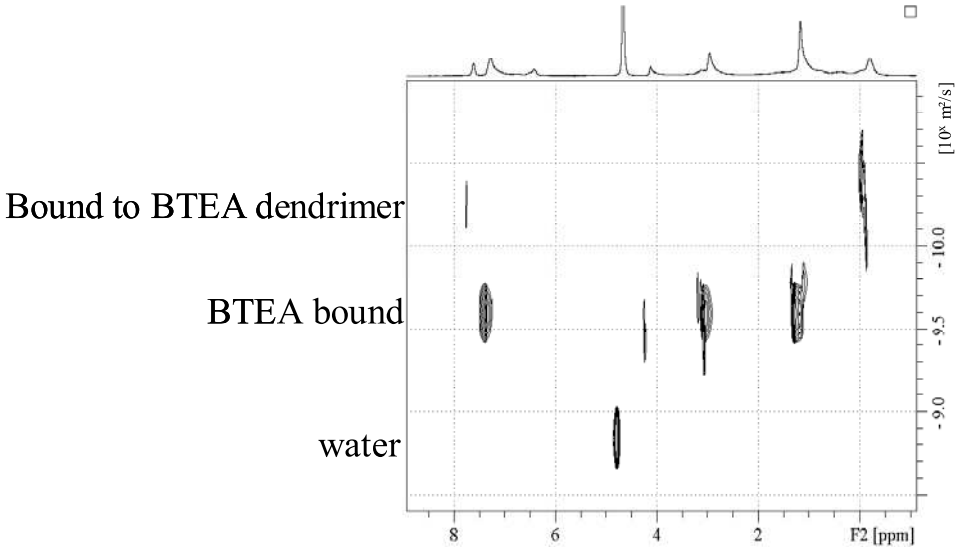

The two signals on the line (top) represent the log(D) of the bound to BTEA dendrimer ; the four black signals on the medium line represent the log(D) of a molecule of BTEA bound to the dendrimer ; the last signal on the line below represents the log(D) of water.

$D_{\mathbf{d}} = 5.4\ (\pm\ 0.1) \times 10^{-11}\ m^2/s$

$R_{H\,\mathbf{d}} = 4.537$ nm

$D_{\mathbf{d}}$: diffusion coefficient of the dendrimer ; $R_{H\,\mathbf{d}}$: hydrodynamic radius of the dendrimer.

DOSY spectrum of assembly dendrimer (10) + dopamine in D_2O

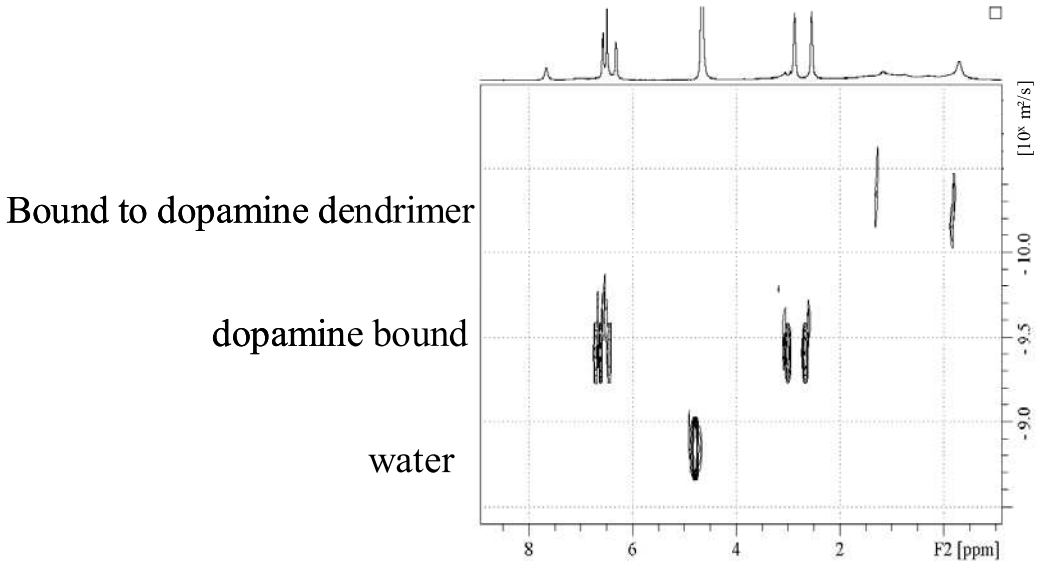

The two signals on the line (top) represent the log(D) of the bound to dopamine dendrimer ; the four black signals on the medium line represent the log(D) of a molecule of dopamine bound to the dendrimer ; the last signal on the line below represents the log(D) of water.

$D_{\mathbf{d}} = 7\ (\pm 1) \times 10^{-11}\ m^2/s$

$R_{H\,\mathbf{d}} = 3.5$ nm

$D_{\mathbf{d}}$: diffusion coefficient of the dendrimer ; $R_{H\,\mathbf{d}}$: hydrodynamic radius of the dendrimer.

ROESY spectrum of acetylcholine (AC) in D_2O

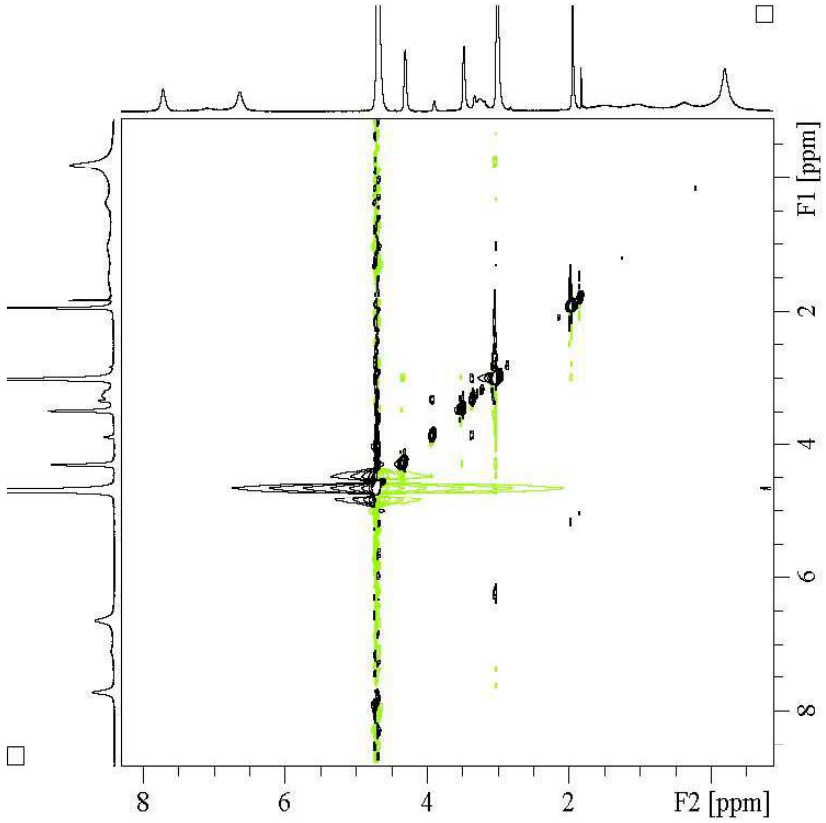

The ROESY spectrum shows that there is no dipolar interaction between the molecules of acetylcholine (AC) and the cavity of the dendrimer ; this confirms that the molecules of AC are bound to the dendrimer at its periphery.

Chemical shift variation of the AC proton signals with the dendri-81- carboxylate (10) by ^{13}C NMR

NMR titrations have been performed by titrating dendrimer solution with cation solutions.

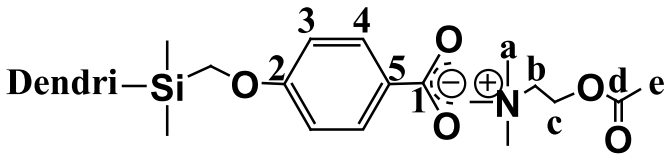

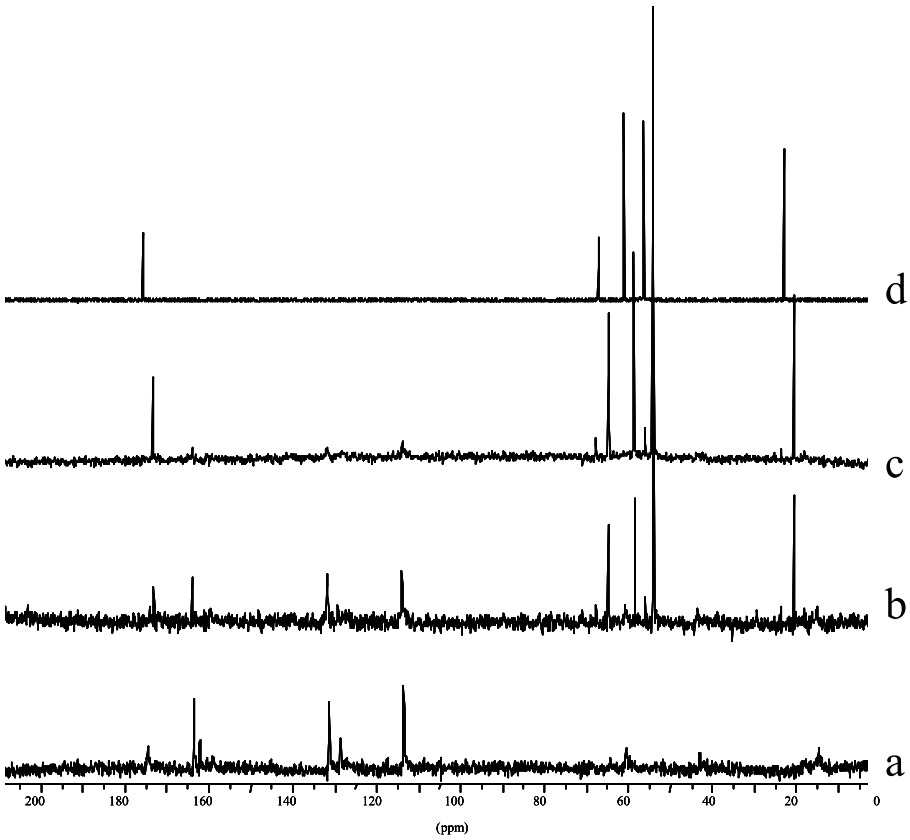

^{13}C NMR titration of dendri-81-carboxylate solution with AC solution: a)dendri-81-carboxylate as its Na^+ salt; b) dendri- 81 -carboxylate + 81 eq. of AC; c) dendri- 81 -carboxylate + 162 eq. of AC; d) AC alone.

Chapitre A-4

Synthèse de nouveaux polymères férrocéniques

Les polymères dendronisés sont des objets moléculaires relativement grands qui peuvent être synthétisés selon deux méthodes différentes, à savoir soit la dendronisation d'un polymère fonctionnel (méthode A), soit la polymérisation d'un dendron pré-formé (méthode B). Grâce à leur taille, leur forme et leur fonctionnalité particulières, ces polymères dendronisés possèdent un grand nombre d'applications potentielles spécifiques, notamment dans le domaine de la science des matériaux et en nanomédecine.

La publication qui compose ce chapitre, parue dans *New Journal of Chemistry* en 2009 dans un numéro spécial dédié au Docteur Jean-Pierre Sauvage, décrit les deux modes de synthèse possible sur un exemple de polymère composés de dendrons ferrocéniques à chaque branche (les ferrocènes étant des groupements chimiques utilisables pour certaines thérapies, notamment celle du cancer du sein).

La méthode B a été développé par M. Jaime Ruiz, l'ingénieur de recherche, avec une ancienne étudiante en Master 2 de notre groupe, Melle Anita Chan Kam Shun. Ils ont réalisés la synthèse ainsi que les différentes caractérisations du polymère obtenu. Nous avons ensuite, M. Jaime Ruiz et moi –même, mis au point la méthode A qui consiste à fonctionnaliser un polymère multichlorures en polymère multiazotures avant de réaliser la réaction « click » avec l'éthynylferrocène.

Les polymères obtenus sont soit sphérique soit cylindrique selon la taille des chaînes latérales dendroniques. La taille ainsi que la forme de ces polymères dendronisés peuvent être observées grâce à différentes techniques physico-chimiques. Etant donné leur grande taille, la visualisation de la forme de ces polymères dendronisés est réalisée par Microscopie de Force Atomique (AFM). Cette étude AFM a été menée en collaboration avec Mme Colette Belin, ingénieur de recherche d'un autre groupe de notre laboratoire. Il a ainsi été possible de visualiser la taille des polymères, leur comportement sur différentes surfaces ainsi que leur éventuelle aggrégation.

D'autres techniques ont permis de caractériser ces polymères : la Chromatographie d'Exclusion Stérique (CES) menée en collaboration avec M. Eric Cloutet, chercheur à l'Ecole Nationale Supérieure de Chimie et de Physique de Bordeaux, ENSCPB). Les résultats obtenus en CES ont permis d'évaluer les polydispersités des polymères qui sont parfaitement cohérentes avec leurs tailles. M. Eric Cloutet m'a également permis l'accès à l'appareil de diffusion dynamique de lumière présent à l'ENSCPB afin de confirmer ces tailles par cette méthode.

La voltammétrie cyclique de ces deux polymères, réalisée dans notre laboratoire, montre une vague ferrocénique réversible et permet de quantifier le nombre de groupements ferrocéniques présents par polymère.

L'objectif de ce travail a été de synthétiser des polymères organométalliques et d'adapter de nouvelles techniques de caractérisation à ces polymères dendronisés, molécules aux propriétés différentes de celle des dendrimères.

Ferrocenyl dendronized polymers†‡

Elodie Boisselier,[a] Anita Chan Kam Shun,[a] Jaime Ruiz,[a] Eric Cloutet,[b] Colette Belin[a] and Didier Astruc*[a]

Received (in Montpellier, France) 4th November 2008, Accepted 5th December 2008
First published as an Advance Article on the web 9th January 2009
DOI: 10.1039/b819604d

Styrenic dendrons functionalized with ferrocenyl and chloromethylsilyl termini were synthesized and polymerized by the AIBN-initiated radical polymerization procedure yielding a ferrocenyl dendronized polymer and a chloromethylsilyl dendronized polymer, respectively. The latter polymer was functionalized with ferrocenyl groups using "click" chemistry. The ferrocenyl dendronized polymers are soluble in common organic solvents such as tetrahydrofuran, dichloromethane, and chloroform. They show a reversible ferrocenyl wave in cyclic voltammetry (CV) and form derivatized Pt electrodes. Their sizes and shapes were examined by size exclusion chromatography (SEC), atomic force microscopy (AFM), dynamic light scattering (DLS) and DOSY ^{1}H NMR spectroscopy.

Introduction

Dendronized polymers[1] are large nano-objects that can be synthesized either by the dendronization of a functional polymer (Scheme 1, route A) or the macromonomer route involving polymerization of a pre-formed dendron (Scheme 1, route B).[1–5] Their size, shape and functionalities bring about specific potential applications, for instance in materials science[3,4] and nano-medicine.[5] It has been shown that dendronized polymers are either spherical or cylindrical depending on the size of the dendronic side chains.[4] Given their large size, the visualization of the shape of dendronized polymers can be carried out by microscopy techniques such as atomic force microscopy (AFM).

Metal-containing polymers are of great interest for their materials properties including catalysis, molecular electronics, sensors and semi-conductors.[6] Although ferrocene-containing polymers are well known for such applications,[6] only one example of dendronized polyferrocene is known: Manners and co-workers recently reported substitution of the chloro group in poly(ferrocenylchloromethylsilane),[7] with a Percec-type dendron[4] containing a benzylate focal point (*i.e.* Scheme 1, route A), as well as several physico-chemical studies including AFM observation of spherical cocoons for the single chains of the dendronized polymer and elongated single-chain structures.[3,8]

Continuing our interest in redox-robust systems in nano-objects,[9] we wished to investigate the synthesis of ferrocenyl dendronized polymers including their redox properties and functions.

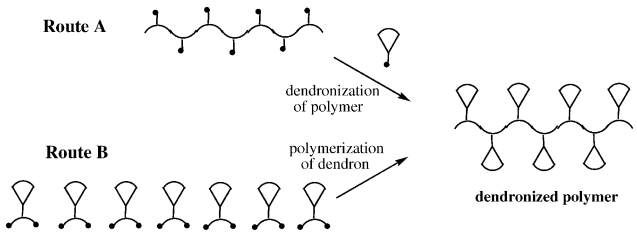

Scheme 1 Two routes to dendronized polymers.

In this paper, we report an alternative method to synthesize a ferrocene-containing dendronized polymer, *i.e.* the polymerization of new triferrocenylsilyl and tris-(chloromethylsilyl) dendrons containing a styrenyl group at the focal point (*i.e.* Scheme 1, route B). In recent work, we reported the attachment of triferrocenylsilyl dendrons containing other focal groups to the termini of dendrimers including gold nanoparticle (AuNP)-centered dendrimers as sensors for inorganic anions including ATP.[10] Thus, modification of this family of dendrons by the introduction of a styrenyl group now brings about the key entry to ferrocenyl dendronized polymers.

Experimental

1. General data

All operations were performed under a nitrogen atmosphere using standard Schlenk techniques. Prior to use, THF was dried over sodium benzophenone ketyl and freshly distilled under a nitrogen atmosphere. CH_2Cl_2 was dried over calcium hydride and freshly distilled under a nitrogen atmosphere. All other reagents were obtained from commercial sources and used without further purification. All glassware was previously dried in an oven and cooled under a nitrogen flow. Ferrocenyldimethylsilane was synthesized according to ref. 11.

2. Physical measurements

The ^{1}H NMR spectra were recorded at 25 °C on a Bruker AC 250 (250 MHz), a Bruker Advance 300 (300 MHz), and a Bruker

[a] *Institut des Sciences Moléculaires, UMR CNRS No. 5255, Université Bordeaux 1, 33405 Talence Cedex, France. E-mail: d.astruc@ism.u-bordeaux1.fr*
[b] *Laboratoire de Chimie des Polymères Organiques, UMR CNRS No. 5629, Université Bordeaux 1, 33607 Pessac Cedex, France*

† Electronic supplementary information (ESI) available: ^{1}H NMR, ^{13}C NMR and IR spectra, size exclusion chromatograms (SEC) and cyclic voltammograms (CV) of the ferrocenyl dendronized polymers. See DOI: 10.1039/b819604d

‡ This article is dedicated to our distinguished colleague Dr Jean-Pierre Sauvage, on the occasion of his 65th birthday.

DPX 400 (400 MHz) spectrometer. ^{13}C NMR spectra were recorded in the pulse FT mode on a Bruker AC 300 spectrometer at 75.50 MHz. ^{29}Si NMR spectra were recorded on a Bruker AC 300 spectrometer at 59.6 MHz. All chemical shifts are reported in parts per million (δ, ppm) with reference to $SiMe_4$ (TMS). Mass spectra were obtained at the CESAMO, Université Bordeaux 1, on a PerSeptive Biosystems Voyager Elite (Framingham, MA) time-of-flight mass spectrometer. This instrument was equipped with a nitrogen laser (337 nm), a delayed extraction, and a reflector. It was operated at an accelerating potential of 20 kV in both linear and reflection modes. The mass spectra shown represent an average over 256 consecutive laser shots (3 Hz repetition rate). Peptides were used to calibrate the mass scale using the two points calibration software 3.07.1 from PerSeptive Biosystems. Elemental analyses were performed at the Center of Microanalysis of the CNRS, Lyon Villeurbanne, France. All electrochemical measurements were recorded in degassed CH_2Cl_2 at 20 °C. Supporting electrolyte: [*n*-Bu_4N][PF_6] 0.1 M; working and counter electrodes: Pt, quasi-reference electrode: Ag; internal reference: $[Fe(\eta^5\text{-}C_5Me_5)_2]^{+/0}$;[15] scan rate: 0.200 V s^{-1}.

3. Synthesis and polymerization

Synthesis of the monomeric triferrocenyl dendron 3. The phenol triferrocenyl dendron **3** (0.562 g; 5.4 × 10^{-4} mol), *p*-iodomethylstyrene (0.152 g, 6.23 × 10^{-4} mol), and potassium carbonate (0.436 g; 3.15 × 10^{-4} mol) were successively introduced into a Schlenk tube. DMF (30 mL) was then added into the Schlenk tube in the dry lab. This reaction mixture was stirred for one day at ambient temperature. DMF was then evaporated under reduced pressure, and the crude residue was dissolved in dichloromethane, potassium carbonate was then filtered, and the concentrated solution was chromatographed over a silica gel column using dichloromethane as the eluant. Removal of dichloromethane under reduced pressure yielded 0.420 g of **3** as an orange–red solid (67%).

^{1}H NMR ($CDCl_3$, 300 MHz), δ_{ppm}: 0.6 (s, 6H, Si-C*H*$_3$); 0.6 (t, 2H, Si-C*H*$_2$); 1.12 (m, C*H*$_2$); 1.58 (t, 2H, Cq-C*H*$_2$); 4.11 (s, 2H, Cp, Si-C-C*H*); 4.15 (s, 5H, Cp); 4.36 (s, 2H, Si-C-CH-C*H*); 5.04 (s, 2H, C*H*$_2$O); 5.28 (m, 1H, vinyl); 5.76 (d, 1H, vinyl); 6.92 (q, 1H, vinyl); 7.16 (d, 2H, arom.); 7.19 (d, 2H, arom.); 7.19 (d, 2H, arom.); 7.42 (s, 4H, arom.).

^{13}C NMR ($CDCl_3$, 75.47 MHz), δ_{ppm}: 0.00 (Si-*C*H$_3$); 19.49 (*C*H$_2$); 20.06 (*C*H$_2$); 44.13 (*C*H$_2$); 45.26 (*C*q); 70.79–75.63 (Cp); 78.59 (*C*H$_2$-O); 116 (*C*H$_2$ vinyl); 128.39 and 129.73 (*C*H, arom.); 133.51 (*C*q arom.); 138.94 (*C*q arom.); 153.27 (*C*q arom.).

^{29}Si NMR ($CDCl_3$, 59.62 MHz), δ_{ppm}: −2.67 (s, Si).

Anal. calc. for $(C_{61}H_{76}Fe_3OSi_3)_n$: C 68.02, H 7.11; found: C 67.61, H 7.21.

MALDI TOF mass spectrum (*m*/*z*): calc.: 1077.05; found: 1044.34 $(M - CH_3)^+$; 1076.38 $(M)^+$.

Polymerization of the dendron 3. Radical polymerization was carried out using a 0.013 molar THF solution of AIBN[11] that was prepared by introducing 20 mg of AIBN in 10 μL of THF. The dendron **3** (0.146 g; 1.36 × 10^{-4} mol) was introduced into a Schlenk flask containing a side entry. The THF solution of AIBN (101 μL) was then added, the solution was degassed under vacuum, and the reaction mixture was stirred for 15 h in the closed Schlenk tube under a nitrogen atmosphere at 100 °C (pressure was kept with caution using the specially equipped Schlenk tube). The solvent was removed under vacuum, and the orange solid residue was partly dissolved in dichloromethane. The orange solid residue (37 mg) was insoluble in all solvents. The soluble fraction was concentrated to 2 mL and precipitated using 20 mL methanol, yielding an orange waxy product that was then reprecipitated twice from dichloromethane solutions with methanol, leaving a waxy orange product (44 mg, 30% yield).

^{1}H NMR ($CDCl_3$, 300 MHz), δ_{ppm} (broad signals): 0.5 (Si-CH_3); 0.6 (Si-CH_2); 1.13 (CH_2); 1.56 (Cq-CH_2); 3.99 (2H, Cp Si-C-CH); 4.05 (5H, Cp); 4.26 (2H, Cp, Si-C-CH); 5.3 (CH_2-O); 6.83 (H vinyl); 7.13 (H arom.).

^{13}C NMR ($CDCl_3$, 75.47 MHz), δ_{ppm}: −1.35 (Si-*C*H$_3$); 18.01 (*C*H$_2$); 18.51 (*C*H$_2$); 42.54 (*C*H$_2$); 43.63 (*C*q); 68.88–73.73 (Cp); 77.61 (*C*H$_2$-O); 127.87 and 128.18 (*C*H arom.); 156.94 (*C*q arom.).

^{29}Si NMR ($CDCl_3$, 59.62 MHz), δ_{ppm}: −2.658 (s, Si).

Size exclusion chromatography (SEC): M = 160 kDa; PDI = 1.9.

Synthesis of the tris(chloromethylsilyl) dendron 7. The triallyl phenol dendron **2** (100 mg, 0.18 mmol) and iodomethylstyrene (66 mg, 0.271 mmol) were introduced into a Schlenk flask, and dry DMF (20 mL), then K_2CO_3 (125 mg, 0.904 mmol) were added to the solution. The mixture was stirred for 3 days at ambient temperature. At the end of the reaction, DMF was removed, and the product was extracted with CH_2Cl_2, washed with water, and purified by chromatography (CH_2Cl_2 100%), which gave 86 mg of **7** as a yellow oil (70% yield).

^{1}H NMR spectrum of the dendron **7** ($CDCl_3$, 250 MHz): 7.43 (C*H* arom. core), 7.17 and 6.79 (C*H* arom. dendron), 6.73 (C*H*=CH_2), 5.74 and 5.24 (CH=C*H*$_2$), 5.06 (C*H*$_2$O), 2.74 (C*H*$_2$Cl), 1.63 (C*H*$_2$CH$_2$CH$_2$Si), 1.09 (CH$_2$C*H*$_2$CH$_2$Si), 0.59 (CH$_2$CH$_2$C*H*$_2$Si), 0.07 (Si(C*H*$_3$)$_2$).

^{13}C NMR ($CDCl_3$, 62 MHz): 153.35 (*C*q-O-CH$_2$), 139.96 (*C*q arom. and *C*H=CH$_2$), 127.86 (*C*H arom. dendron), 115.13 (*C*H arom. styrene), 70.26 (O-*C*H$_2$, arom.), 43.42 (*C*q arom. and *C*H$_2$CH$_2$CH$_2$Si), 30.85 (*C*H$_2$Cl), 17.95 (CH$_2$*C*H$_2$CH$_2$Si), 14.79 (CH$_2$CH$_2$*C*H$_2$Si), −4.10 (Si(*C*H$_3$)$_2$).

Polymerization of the tris(chloromethylsilyl) monomer 7. The monomeric dendron **7** (140 mg, 0.205 mmol) was dried in a Schlenk tube. A solution of azobisisobutyronitrile (AIBN) was prepared with 36 mg of AIBN in 10 mL of distilled THF. 100 μL of this solution (0.36 mg, 2.05 × 10^{-6} mol, 1% molar) were added to the monomer. The mixture was stirred for 15 h at 100 °C under a nitrogen atmosphere. At the end of the reaction, the product was extracted with CH_2Cl_2 and purified by precipitation with methanol. The precipitate was filtered and recovered with dichloromethane, and reprecipitated three times using methanol, yielding **8** as a yellow oil (70 mg, 50% yield).

^{1}H NMR of **8** ($CDCl_3$, 250 MHz): 7.17 and 6.89 (C*H* arom.), 4.87 (C*H*$_2$O), 2.71 (C*H*$_2$Cl), 1.93 (C*H*$_2$I), 1.62 (C*H*$_2$CH$_2$CH$_2$Si), 1.09 (CH$_2$C*H*$_2$CH$_2$Si), 0.58 (CH$_2$CH$_2$C*H*$_2$Si), 0.05 (Si(C*H*$_3$)$_2$).

^{13}C NMR of **8** ($CDCl_3$, 62 MHz): 157.00 (*C*q-O-CH_2), 139.93 (*C*q arom.), 134.61 (*C*HCH_2), 127.77 (*C*H arom.), 70.26 (O-H_2 arom.), 46.85 (*C*qCH_2), 42.28 (*C*$H_2CH_2CH_2Si$), 30.79 (*C*H_2Cl), 17.92 (CH_2*C*H_2CH_2Si), 13.93 (CH_2CH_2*C*H_2Si), −4.40 (Si(*C*H_3)$_2$). SEC: M = 33.6 kDa g mol^{-1}. Polydispersity: PDI = 1.58.

Functionalization of the polymer 8 and "click" reaction. The polymer **8** (0.06 g, 87.8 μmol) was dissolved in DMF (8 mL), and an excess of NaN_3 (0.068 mg, 1.05 mmol) was added. The reaction mixture was stirred at 60 °C for 12 h. DMF was removed, the crude product was dissolved in 10 mL of dichloromethane, and the salts were filtered. Dichloromethane was removed under vacuum, and the dendronized polymer **9** was obtained as a yellow oil in 85% yield.

^{1}H NMR ($CDCl_3$, 250 MHz): 7.16 and 6.89 (8H arom.), 6.50 (1H, C*H* arom.), 5.42 (2H, CH_2 CH arom.), 4.86 (2H, CH_2O), 2.7 (2H, CH_2N_3), 1.62 (2H, C$H_2CH_2CH_2Si$), 1.11 (2H, CH_2CH_2CH_2Si), 0.55 (2H, CH_2CH_2CH_2Si), 0.03 (6H, Si(CH_3)$_2$).

^{13}C NMR ($CDCl_3$, 62 MHz): 157.04 (*C*q-O-CH_2), 139.84 (*C*q arom.), 134.61 (*C*HCH_2), 127.68 (*C*H arom.), 70.31 (O-*C*H_2 arom.), 43.47 (*C*qCH_2), 42.27 (*C*$H_2CH_2CH_2Si$), 41.40 (*C*H_2N_3), 17.93 (CH_2*C*H_2CH_2Si), 15.26 (CH_2CH_2*C*H_2Si), −3.67 (Si(*C*H_3)$_2$). Infrared ν_{C-N3}: 2094 cm^{-1}. SEC: M = 34 600 g mol^{-1}.

The dendronized polymer **9** (0.028 g, 45.2 μmol, 1 eq.) and ethynylferrocene (0.019 g, 90.5 μmol, 2 eq. per branch) were dissolved in THF. $CuSO_4$ was added at 0 °C (4 eq. per branch, 1 M water solution), followed by dropwise addition of a freshly prepared solution of sodium ascorbate (8 eq. per branch, 1 M water solution) in order to obtain a ratio of solvent equal to 1 : 1 (THF–water). The solution was stirred for 12 h at 25 °C under nitrogen. After removing THF under vacuum, CH_2Cl_2 and an aqueous ammonia solution were added. The mixture was stirred for 10 min in order to remove all the Cu^I trapped inside the dendrimer as $Cu(NH_3)_6^+$. The organic phase was washed twice with water, dried with sodium sulfate and the solvent was removed under vacuum. The product was precipitated with CH_2Cl_2–pentane, and then with CH_2Cl_2–ether in order to remove excess ethynylferrocene (yield = 70%).

^{1}H NMR ($CDCl_3$, 250 MHz): 7.42 (C*H* triazole), 7.14 and 6.89 (C*H* arom.), 4.69 (C*H*, CH_2O), 4.69, 4.26, 4.04 (9H, Cp), 3.81 (2H, SiCH_2N), 1.58 (2H, C$H_2CH_2CH_2Si$), 1.11 (2H, CH_2CH_2CH_2Si), 0.58 (2H, CH_2CH_2CH_2Si), 0.06 (6H, Si(CH_3)$_2$).

^{13}C NMR ($CDCl_3$, 62 MHz): 157.0 (*C*qO), 146.1 (*C*q of triazole), 139.9 (*C*q arom.), 134.6 (*C*H arom.), 126.7 (*C*H_2CH arom.), 120.0 (*C*H of triazole), 114.5 (*C*H arom.), 73.4 (*C*q of Cp), 70.9 (*C*H_2O), 69.9, 68.9 and 66.9 (*C*H of Cp), 41.2 (*C*$H_2CH_2CH_2Si$), 40.8 (*C*H_2N), 15.2 (CH_2*C*H_2CH_2), 14.6 (CH_2CH_2*C*H_2Si), −3.5 ($SiMe_2$).

Infrared ν_{C-N3}: disappearance of the band at 2094 cm^{-1}.

DOSY ^{1}H NMR: D = 6.65 (±0.6) × 10^{-11} m^2 s^{-1}; r_h = 8.6 (±0.8) nm; (D: diffusion coefficient; r_h: hydrodynamic radius). Dynamic light scattering: r_h = 9.25 (±0.9) nm.

Derivatization of the Pt electrodes with the ferrocenyl dendronized polymers 5 and 10. A platinum electrode (Sodimel, Pt 30) was dipped into 10% aqueous HNO_3 for 3 h, then rinsed with distillated water, dried in air, and polished using cerium oxide powder (5 MU). The dendronized polymer **5** was electrodeposited onto the platinum-disk electrodes (A = 0.0078 cm^2) from degassed CH_2Cl_2 solutions (9.3 × 10^{-6} M) and [n-Bu_4N][PF_6] (0.1 M) by continuous scanning (0.20 V s^{-1}) up to 50 cycles between 0.0 and 0.9 V *vs.* [Fe(η^5-C_5Me_5)$_2$]$^{+/0}$. The coated electrode was washed with CH_2Cl_2 in order to remove the solution from material and dried in air. This modified electrode was characterized by cyclic voltammetry (CV) using freshly distilled CH_2Cl_2 as solvent containing only the supporting electrolyte. It showed a single symmetrical CV wave, and the linear relationship of the peak current with potential sweep rate was verified. The surface coverage Γ (mol cm^{-2}) by the ferrocenyl dendronized polymer **5** was determined from integrated charge of the CV wave. $\Gamma = Q/nFA$, where Q is the charge, n is the number of electrons transferred, F is the Faraday constant, and A is the area. Thus, the surface coverage for the electrode modified with **5** was 8.3 × 10^{-9} mol cm^{-2} (ferrocenyl sites), corresponding to 1.34 × 10^{-10} mol cm^{-2} of **5**. The dendronized polymer **10** was electrodeposited in the same way as **5**, and the surface coverage Γ for the electrode modified with **10** was 7. 4 × 10^{-10} mol cm^{-2} (ferrocenyl sites).

4. Dynamic light scattering measurements (DLS)

The DLS measurements were made using a Malvern Zetasizer 3000 HSA instrument at an angle of 90°, in dichloromethane solution at 25 °C. Measurements were carried out at different concentrations until the hydrodynamic diameter was found to be constant at three different concentrations (for high concentration, higher hydrodynamic diameter values were found, due to aggregation).

5. Atomic force microscopy (AFM) experiments

The AFM samples were prepared by spin coating of a suitable solution (1 mg mL^{-1}) (adjusted on a trial and error basis) of dendronized polymer in CH_2Cl_2. Before spin coating, the mica surface was cleaved with Scotch tape. The freshly cleaved highly oriented mica surface was covered with the solution and spinned at 1000 rpm with subsequent 10–15 second extra spinning at 3000 rpm for complete drying in air. The AFM apparatus is a Thermomicroscope CP Research capable of obtaining measurements in multiple modes, and the sample imaging is achieved in air immediately after spin coating. The tapping mode was used giving the weakest interaction with the surface and therefore the less chance of alteration. The cantilever–tip systems used were nanosensors (PPPNCL, spring constant = 40 N m^{-1}), with typical tip (silicon tip) radius of curvature of 6 nm. For each sample, the images of topography, amplitude and phase were obtained using the software Image Processing and Data Analysis 20.0. A sample was considered as good when a monolayer of ferrocenyl dendronized polymer was measured by AFM. In order to estimate the size of the polymers, it is necessary to consider the radius of curvature of the tip only if the measured nano-object is smaller than the tip. In the present case, the tip (6 nm) is much smaller than the measured object (22 nm), thus one does not need to eliminate the tip-shape induced impact by deconvolution.

6. Size exclusion chromatography

Size exclusion chromatography (SEC) or gel permeation chromatography (GPC) was performed using THF as eluant at 40 °C and a flow rate of 1 mL min^{-1} through 4 columns (TSK G5000HXL (9 μm), G4000HXL (6 μm), G3000HXL (6 μm), and G2000HXL (5 μm)) and connected to Varian refractometer and UV-visible spectrophotometer calibrated against linear polystyrene standards.

Results and discussion

Synthesis of the triferrocenyl dendron 4

The new triferrocenyl dendron **4** containing a styrenyl group was synthesized by Williamson reaction of the triferrocenyl dendron **3**[10b] with *p*-iodomethylstyrene, as shown in Scheme 2. The precursor triferrocenyl dendron **3** was synthesized according to a previously reported procedure by hydrosilylation of the triallylphenol dendron **2** using ferrocenyldimethylsilane[11] (Scheme 2). The substantial advantage of the catalyzed hydrosilylation reaction in the present chemistry is that it is compatible with the phenol group and thus does not require a tedious protection–deprotection procedure. Likewise, the ferrocenyl dendronic branch termini do not prevent the Williamson reaction to attach the styrenyl group, and this reaction proceeds smoothly in 67% yield.

Polymerization of the dendron 4 to the dendronized polymer 5

The best working procedure in our hands turned out to be the AIBN-initiated radical polymerization of the styrenyl derivative bearing the dendronic group as a *para* substituent.[12] A possible problem of the dendron polymerization is the bulk around the reactive focal point, as with any convergent molecular construction.[13] When the generation increases, the bulk becomes large around the focal point, which inhibits further coupling. Therefore, the structure of this dendron was designed to be located far enough from the bulky termini, and the number of ferrocenyl termini was kept low at the first generation although higher generations are known.[10] The radical polymerization, carried out using the standard procedure,[12] yielded an insoluble red powder (25% of the total mass that could be a high-molecular-weight polymer) and a polymer soluble in dichloromethane that was reprecipitated three times from dichloromethane solutions using methanol. This soluble polymer was analyzed using ^{1}H and ^{13}C NMR (see Experimental section) including DOSY NMR, dynamic light scattering (DLS), size exclusion chromatography (SEC) and AFM. The DOSY experiment was not successful, because the polymer was too large, and this technique does not work with very large nano-objects. DLS measurements reproducibly provided an apparent diameter size of 28 ± 2 nm. A large size was expected from the failure of the DOSY NMR experiment, but this latter value appears to be very large, presumably because of the solvent sphere around the polymer and the non-spherical shape of the polymer. Even larger values were observed for the other ferrocenyl dendronized polymers by Manners *et al.*[3] SEC provided a molecular weight of 160 kDa with a polydispersity index (PDI) of 1.9 (Fig. 1).

Synthesis and polymerization of a tris(chloromethylsilyl) dendron and "click" ferrocenylation

An alternative synthesis of a ferrocenyl dendronized polymer involves the synthesis of a tris(chloromethylsilyl) dendron that might be functionalized with ferrocenyl termini subsequent to polymerization. This strategy is a variant of the former one also starting with the polymerization of a dendron, but the latter method adds an additional series of two reactions after polymerization (Scheme 3).

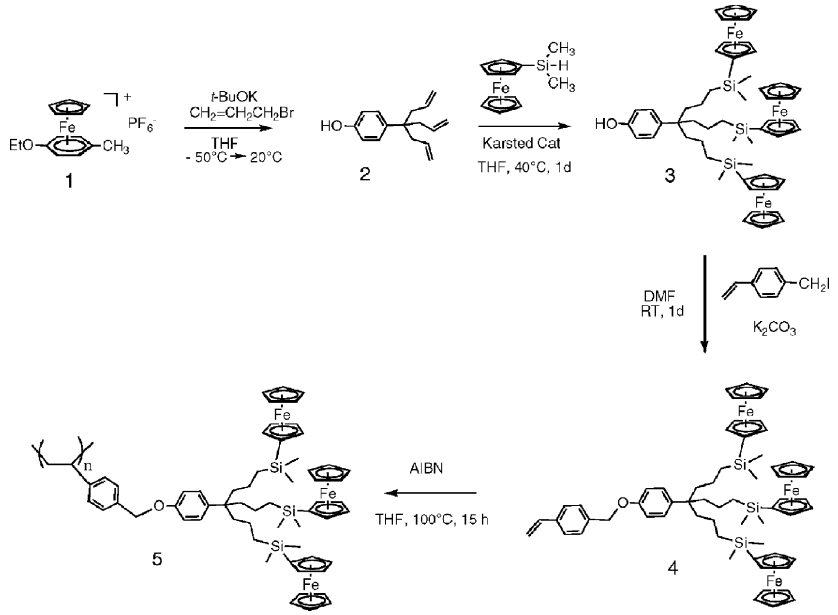

Scheme 2 Synthesis and AIBN-induced radical polymerization of the triferrocenyl styrenyl dendron **4**. The triallyl phenol dendron **2** and the triferrocenyl phenol dendron **3** were synthesized according to ref. 10*a*,*e* and 10*b*, respectively.

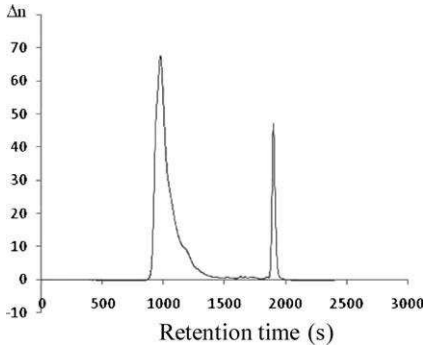

Fig. 1 Size exclusion chromatogram (SEC) of **5** (left) using polystyrene as the reference and 1,3,5-trichlorobenzene as a marker (shown on the right). The SEC was carried out using a refractometer. Δn is the variation of the refraction index as a function of time (seconds).

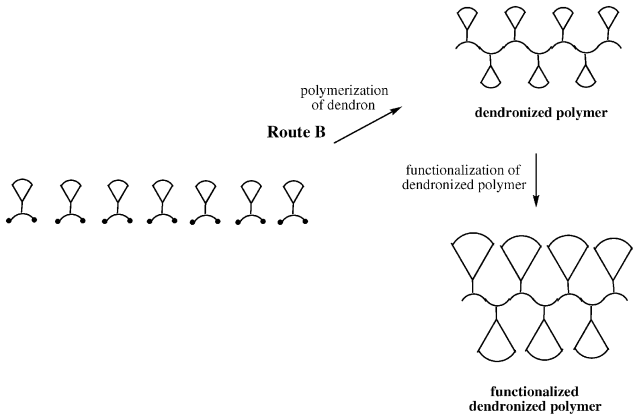

Scheme 3 Modification of route B (Scheme 1) with the functionalization of a dendronized polymer applied to the ferrocenylation reaction by "click" chemistry (Scheme 4).

These reactions are the substitution of the chloro group by the azido group followed by click reaction with ethynylferrocene. The initial polychloro polymer **8** was purified by reprecipitation from a dichloromethane solution using methanol, and this same type of purification was carried out for the "clicked" polyferrocenyl dendronized polymer. Using this method, a ferrocenyl dendronized polymer of dispersity PDI = 1.2 was obtained, which is satisfactory given the type of polymerization reaction that was used (Scheme 4). This good PDI value was obtained, because the polymer was purified by reprecipitation three times. The virtually quantitative conversion **8** → **9** → **10** (Scheme 4) is verified by ^{1}H NMR, because the CH_2Cl (and CH_2N_3) signal completely disappears upon "click" reaction of **9**.

The DOSY ^{1}H NMR experiments provided a mean diameter of 17.2 nm, whereas the dynamic light scattering (DLS) experiments yielded a diameter value of 18.5 nm, which is a reasonably good agreement consistent with the relatively low PDI value (Table 1).

Cyclic voltammetry shows the reversible behavior of the ferrocenyl oxidation wave in both **5** and **10** as with ferrocenyl-terminated dendrimers.[14] It is also a good means of determining the average number of ferrocenyl units in a polymer using the Bard–Anson equation.[15] This equation only applies in the absence of adsorption, however, because adsorption increases the peak intensity value, and the number of redox units would be provided in excess. In dichloromethane, the ferrocene oxidation wave of **10** at 0.69 V *vs.* decamethylferrocene–decamethylferrocenium[16] on a Pt anode indeed appears reversible without adsorption as indicated by a $E_{p,ox}-E_{p,red}$ value of 50 mV and a ratio between the anodic and cathodic peak current that is about unity (Fig. 2). The number of ferrocenyl units calculated for **10** with this equation yields an average value of 153 ferrocenyl units (51 triferrocenyl dendrons, corresponding to 67 kDa). This method could not be applied to the other ferrocenyl dendronized polymer **5**, because adsorption was too strong, even in dichloromethane. This is due to the larger size of ferrocenyl dendronized polymer **5** compared to **10**. Scanning around the ferrocenyl potential value easily led to the formation of fully derivatized Pt electrodes[17] for both **5** and **10** (Fig. 3 and S1, ESI†).

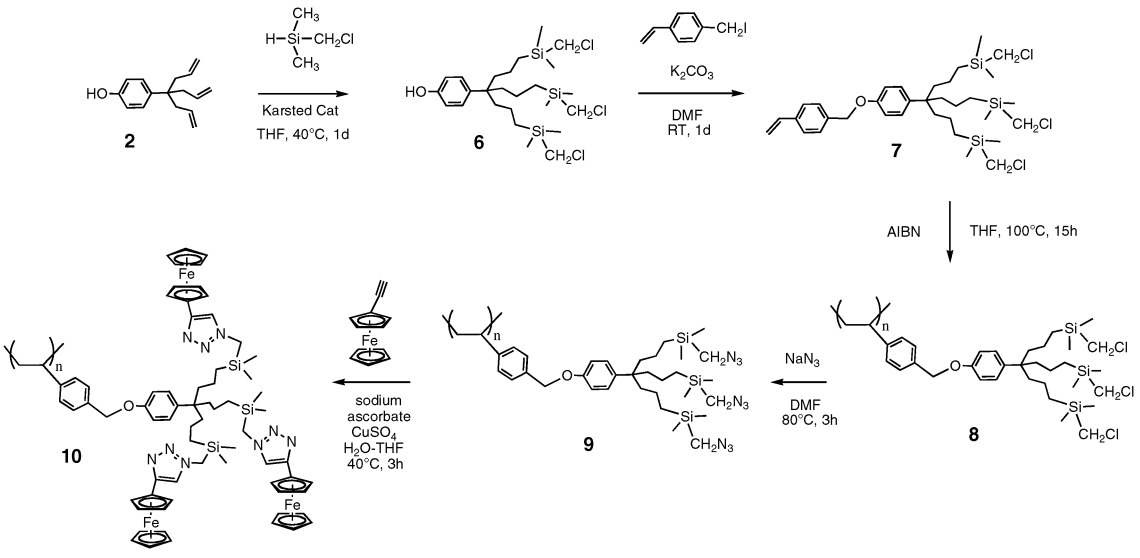

Scheme 4 Synthesis of a ferrocenyl dendronized polymer by functionalization of a poly(chloromethylsilyl) dendronized polymer.

Table 1 Compared physico-chemical data for the ferrocenyl dendronized polymers **5** and **10**

	SEC	DOSY ^{1}H NMR		DLS	AFM	
	PDI	Diffusion coefficient/m^2 s^{-1}	Diameter/nm	Diameter/nm	Height/nm	Width/nm
Fc-dendronized polymer **10**	1.2	6.65 (±0.6) × 10^{-11}	17.2 (±1.7)	18.5 (±1.8)	2.4 (±0.2)	22.5 (±2.2)
Fc-dendronized polymer **5**	1.9	Not applicable		28 (±2.8)	5 (±0.5)	100 (±10)

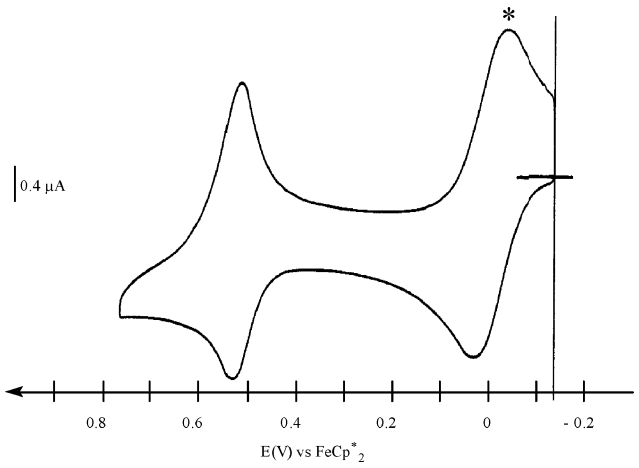

Fig. 2 Cyclic voltammetry of the ferrocenyl dendronized polymer **10** using decamethylferrocene as the internal reference (right wave). $E_{1/2}$ = 0.47 V. Solvent: CH_2Cl_2; temperature: 20 °C; supporting electrolyte: [*n*-Bu_4N][PF_6] 0.1 M; working and counter electrodes: Pt; reference electrode: Ag; scan rate: 0.400 V s^{-1}.

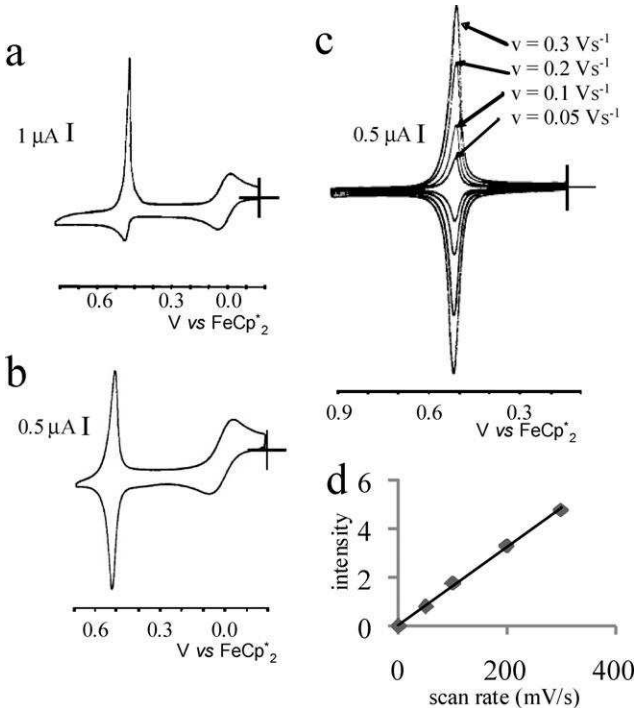

Fig. 3 Cyclic voltammograms of the ferrocenyl dendronized polymer **5** using decamethylferrocene as a reference (a and b): (a) in dichloromethane solution; (b) of an electrode modified with **5**; (c) of an electrode modified with **5** at various scan rates.

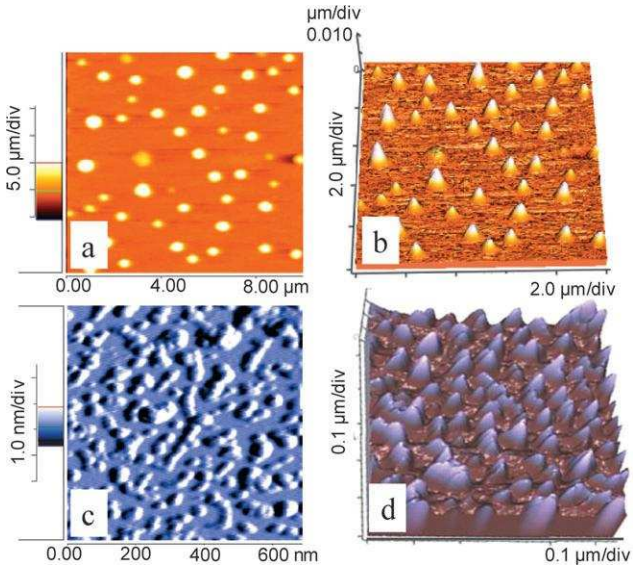

Fig. 4 AFM image of **5** and **10** on mica surface. (a) Topographic 2D AFM image of **5**. (b) Topographic 3D AFM image of **5**. (c) Amplitude mode 2D AFM image of **10**. (d) Topographic mode 3D AFM image of **10**.

AFM of the ferrocenyl dendronized polymers

Both ferrocenyl dendronized polymers **5** and **10** were examined by AFM on mica surfaces.[18] The largest dendronized polymer **5** gave pictures containing spots that were typically 5 nm high and 100 nm wide whereas pictures of **10** gave spots that were 22 nm wide and 2.5 nm high (Fig. 4). The spots of both dendronized polymers look globular as for classic polymers, *i.e.* like if polymers did not aggregate among one another. It does not appear that the dendronized polymer **10** agglomerates in its condensed state on the mica surface, because the width of 22 nm is close to the height measured by DOSY ^{1}H NMR and DLS (in deuterated chloroform and dichloromethane solution, respectively). On the other hand, the size of the spots obtained for **10** corresponds to clusters of aggregated dendronized polymers. One could observe by AFM that elongated shapes were not found, as expected with dendronized polymers in which the dendrons are not bulky. Elongated dendrimers are observed by AFM when dendrons of several generations are constructed, whereas no dendritic construction was elaborated in the present study. At some places in **10**, however, it can be seen that several polymeric units seem to stick together to form a chain fragment.

Concluding remarks

Two closely related routes to ferrocenyl dendronized polymers were conducted *via* AIBN-initiated radical polymerization of

functionalized styrenyl dendrons in this work: a direct polymerization of a triferrocenyl dendron and a ferrocenylation of a dendronized polymer using "click" chemistry.

The first route yielded a larger dendronized polymer than the former. A possible explanation is that the chlorine atoms located on the tris(chloromethylsilyl) dendrons could be responsible for radical reactions terminating the chains, thus shortening the polymer. The sizes and shapes of both materials have been analyzed using a variety of physico-chemical techniques.

The polydispersities (from SEC) were found to be larger for the directly polymerized ferrocenyl dendron (PDI = 1.9) than for the ferrocenylized dendronic polymer (PDI = 1.2), which is presumably due to their size difference.

DLS was an excellent technique to evaluate the size of these dendronized polymers (diameter: 28 nm for **5** *vs.* 18.5 nm for **10**), confirmed by DOSY ^{1}H NMR in the case of the smaller dendronized polymer **10**), whereas AFM shows that they are rather globular, *i.e.* the dendrons are not large enough to cause a sufficient rigidity of the materials.

AFM also shows the flattening of these materials on a mica surface in the condensed state[18] (height: 5 nm for **5** and 2.5 nm for **10**). The diameter found is not significantly different for **10** (22.5 nm) from that determined by DLS (18.5 nm), suggesting that the dendronic polymeric units of **10** do not aggregate on mica, whereas they do with the larger dendronized polymer **5** (100 nm width spots).

Both ferrocenyl dendronized polymers show a reversible ferrocene oxidation wave (which indicates that the ferrocenyl units are located at the periphery of the dendronized polymers)[19] and form stable derivatized Pt electrodes. The Bard–Anson equation can be used for **10** to determine the number of ferrocenyl groups (153) given the absence of adsorption in dichloromethane, but not for **5** due to adsorption.

Acknowledgements

Financial assistance from the Institut Universitaire de France (IUF), the Agence Nationale de la Recherche (ANR) (project no. ANR-06-NANO-026-02), the Université Bordeaux 1 and the Centre National de la Recherche Scientifique (CNRS) is gratefully acknowledged.

References

1 A. D. Schlüter, *Top. Curr. Chem.*, 1998, **197**, 165–191; A. D. Schlüter and J. P. Rabe, *Angew. Chem., Int. Ed.*, 2000, **39**, 865–883; A. D. Schlüter, *C. R. Chim.*, 2003, **6**, 843–851.

2 B. Karakaya, W. Claussen, K. Gessler, W. Saenger and A. D. Schlüter, *J. Am. Chem. Soc.*, 1997, **119**, 3296–3301; R. Yin, Y. Zhu, D. A. Tomalia and H. Ibuki, *J. Am. Chem. Soc.*, 1998, **120**, 2678–3301; H. Frey, *Angew. Chem., Int. Ed.*, 1998, **37**, 2193–2197; A. D. Schlüter and J. P. Rabe, *Angew. Chem., Int. Ed.*, 2000, **39**, 1200–1205; P. R. L. Malenfant and J. M. J. Fréchet, *Macromolecules*, 2000, **33**, 3634–3639; L. Shu, A. D. Schlüter, C. Ecker, N. Severin and J. P. Rabe, *Angew. Chem., Int. Ed.*, 2001, **40**, 4666–4669; Z. M. Fresco, I. Suez, S. A. Backer and J. M. J. Fréchet, *J. Am. Chem. Soc.*, 2004, **126**, 8374–3301; A. Zhang, L. Okrasa, T. Pakula and A. D. Schlüter, *J. Am. Chem. Soc.*, 2004, **126**, 6658–6666; A. Carlmark and E. E. Malmström, *Macromolecules*, 2004, **37**, 7491–7496; W. Li, A. Zhang and A. D. Schlüter, *Macromolecules*, 2008, **41**, 43–49.

3 K. T. Kim, J. Han, C. Y. Ryu, F. C. Sun, S. S. Sheiko, M. A. Winnik and I. Manners, *Macromolecules*, 2006, **39**, 7922–7930.

4 V. Percec, C.-H. Ahn, G. Ungar, D. J. P. Yeardley, M. Möller and S. S. Sheiko, *Nature*, 1998, **391**, 161–164; S. A. Prokhorova, S. S. Sheiko, M. Möller, C.-H. Ahn and V. Percec, *Macromol. Rapid Commun.*, 1998, **19**, 359–366; V. Percec, C.-H. Ahn, W. D. Cho, A. M. Jamieson, J. Kim, T. Leman, M. Schmidt, M. Grole, M. Möller, S. A. Prokhorova, S. S. Sheiko, S. Z. D. Cheng, A. Zhang, G. Ungar and D. J. P. Yearley, *J. Am. Chem. Soc.*, 1998, **120**, 8619–8631; V. Percec and M. N. Holcerca, *Biomacromolecules*, 2000, **1**, 6–16; V. Percec, J. G. Rudick, M. Peterca, M. Wagner, M. Obata, C. M. Mitchell, W.-D. Cho, V. S. Balagurusamy and P. A. Heiney, *J. Am. Chem. Soc.*, 2005, **127**, 15257–15264; V. Percec, C. B. Won, M. Petrarca and P. A. Heiney, *J. Am. Chem. Soc.*, 2007, **129**, 11265–11278.

5 J. L. Mynar, T. L. Choi, M. Yoshida, V. Kim, C. J. Hawker and J. M. J. Fréchet, *Chem. Commun.*, 2005, 5169–5171; C. C. Lee, M. Yoshida, J. M. J. Fréchet, E. E. Dy and F. C. Szoda, *Bioconjugate Chem.*, 2005, **16**, 535–541; D. Astruc, *C. R. Acad. Sci., Sér. IIb*, 1996, **322**, 757–766.

6 I. Manners, *Science*, 2001, **294**, 1664–1668; I. Manners, *Synthetic Metal-Containing Polymers*, Wiley-VCH, Weinheim, 2004; *Frontiers in Transition Metal-Containing Polymers*, ed. A. S. Abd-El-Aziz, I. Manners, Wiley Interscience, John Wiley and Sons Inc., New York, 2007.

7 D. A. Foucher, B.-Z. Tang and I. Manners, *J. Am. Chem. Soc.*, 1992, **114**, 6246–6248; M. Tanabe and I. Manners, *J. Am. Chem. Soc.*, 2004, **126**, 11434–11435; M. Tanabe, G. W. Vandermeulen, W. Y. Chan, P. W. Cyr, L. Vanderark, D. A. Rider and I. Manners, *Nat. Mater.*, 2006, **5**, 467–470.

8 For a linear-dendritic polyferrocenyl derivative, see: C. Tao, L. Wang, G. Jiang, J. Wang, X. Wang, J. Zhou and W. Wang, *Eur. Polym. J.*, 2006, **42**, 687–693.

9 M.-H. Desbois, D. Astruc, J. Guillin, F. Varret, A. X. Trautwein and G. Villeneuve, *J. Am. Chem. Soc.*, 1989, **111**, 5800–5809; D. Astruc, *Bull. Chem. Soc. Jpn.*, 2007, **80**, 1658–1671; D. Astruc, C. Ornelas and J. Ruiz, *Acc. Chem. Res.*, 2008, **41**, 841–856.

10 (*a*) V. Sartor, L. Djakovitch, J.-L. Fillaut, F. Moulines, F. Neveu, V. Marvaud, J. Guittard, J.-C. Blais and D. Astruc, *J. Am. Chem. Soc.*, 1999, **121**, 2929–2930; (*b*) S. Nlate, J. Ruiz, J.-C. Blais and D. Astruc, *Chem. Commun.*, 2000, 417–418; (*c*) J. Ruiz, G. Lafuente, S. Marcen, C. Ornelas, S. Lazare, E. Cloutet, J.-C. Blais and D. Astruc, *J. Am. Chem. Soc.*, 2003, **125**, 7250–7257; (*d*) M.-C. Daniel, J. Ruiz, J.-C. Blais, N. Daro and D. Astruc, *Chem.–Eur. J.*, 2003, **9**, 4371–4379; (*e*) D. Astruc, M.-C. Daniel and J. Ruiz, *Chem. Commun.*, 2004, 2637–2649; (*f*) C. Ornelas, J. Ruiz, E. Cloutet, S. Alves and D. Astruc, *Angew. Chem., Int. Ed.*, 2007, **46**, 872–877.

11 K. H. Pannel and H. Sharma, *Organometallics*, 1991, **10**, 954–958.

12 S. M. Grayson and J. M. J. Fréchet, *Chem. Rev.*, 2001, **101**, 3819–3868.

13 A. Kowlczuk-Bleja, B. Trzebicka, B. Voit and A. Dworak, *Polymer*, 2004, **45**, 595–608.

14 For a review of ferrocenyl dendrimers and their electrochemical properties, see: (*a*) C. M. Casado, I. Cuadrado, M. Moran, B. Alonso, B. Garcia, B. Gonzales and B. Losada, *J. Coord. Chem. Rev.*, 1999, **185–186**, 53–79; (*b*) for electrochemical studies of multi-ferrocenyl oligomers and polymers, see: R. Rulkens, A.-J. Lough, I. Manners, S. R. Lovelace, C. Grant and W. E. Geiger, *J. Am. Chem. Soc.*, 1996, **118**, 12683–12695; (*c*) N. Camine, U. T. Mueller-Westerhoff and W. E. Geiger, *J. Organomet. Chem.*, 2001, **637**, 823–826.

15 (*a*) J. B. Flanagan, S. Margel, A. J. Bard and F. C. Anson, *J. Am. Chem. Soc.*, 1978, **100**, 4248–4253; (*b*) A. J. Bard and R. L. Faulkner, *Electrochemical Methods*, Wiley, New York, 2nd edn, 2001.

16 J. Ruiz and D. Astruc, *C. R. Acad. Sci., Sér. IIc: Chim*, 1998, **t.1**, 21–27; J. Ruiz, M.-C. Daniel and D. Astruc, *Can. J. Chem.*, 2006, **84**, 288–299.

17 H. D. Abruña, in *Electroresponsive Molecular and Polymer Systems*, ed. T. A. Stotheim, Dekker, New York, 1988, vol. 1, p. 97; R. D. Murray, in *Molecular Design of Electrode Surfaces.*

Techniques of Chemistry XII, Wiley, New York, 1992, p. 1; M. Yamada, I. Quiros, J. Mizutani, K. Kubo and I. Nishihara, *Phys. Chem. Chem. Phys*., 2001, **3**, 3377–3383.
18 For the first AFM observation of the flattening of dendrimers on a surface, see: (*a*) A. Hierlemann, J. K. Campbell, L. A. Baker, R. M. Crooks and A. J. Rico, *J. Am. Chem. Soc*., 1998, **120**, 5323–5324, see also: (*b*) J. Li, L. T. Piehler, D. Qin, J. R. Baker, Jr and D. A. Tomalia, *Langmuir*, 2000, **16**, 5613–5617; (*c*) H. Zhang, P. C. M. Grim, T. Vosch, U.-M. Wiesler, A. J. Berresheim, K. Müllen and F. C. De Schryver, *Langmuir*, 2000, **16**, 9294–9298; (*d*) M. C. Coen, K. Lorenz, J. Kressler, H. Frey and R. Mulhaupt, *Macromolecules*, 2000, **29**, 8069–8079; (*e*) A. Mecke, I. Lee, J. R. Baker, Jr, M. M. B. Holl and B. G. Orr, *Eur. Phys. J. E*, 2004, **14**, 7–10.
19 J. Ruiz, C. D. Astruc, C. Ornelas and J. Ruiz, *Acc. Chem. Res*., 2008, **41**, 841–856.

Supplementary Material (ESI) for New Journal of Chemistry

Ferrocenyl Dendronized Polymers

Elodie Boisselier, Anita Chan Kam Shun, Jaime Ruiz, Eric Cloutet, Colette Belin, Didier Astruc

Supplementary Information

^{1}H NMR 300 MHz ($CDCl_3$) of 4

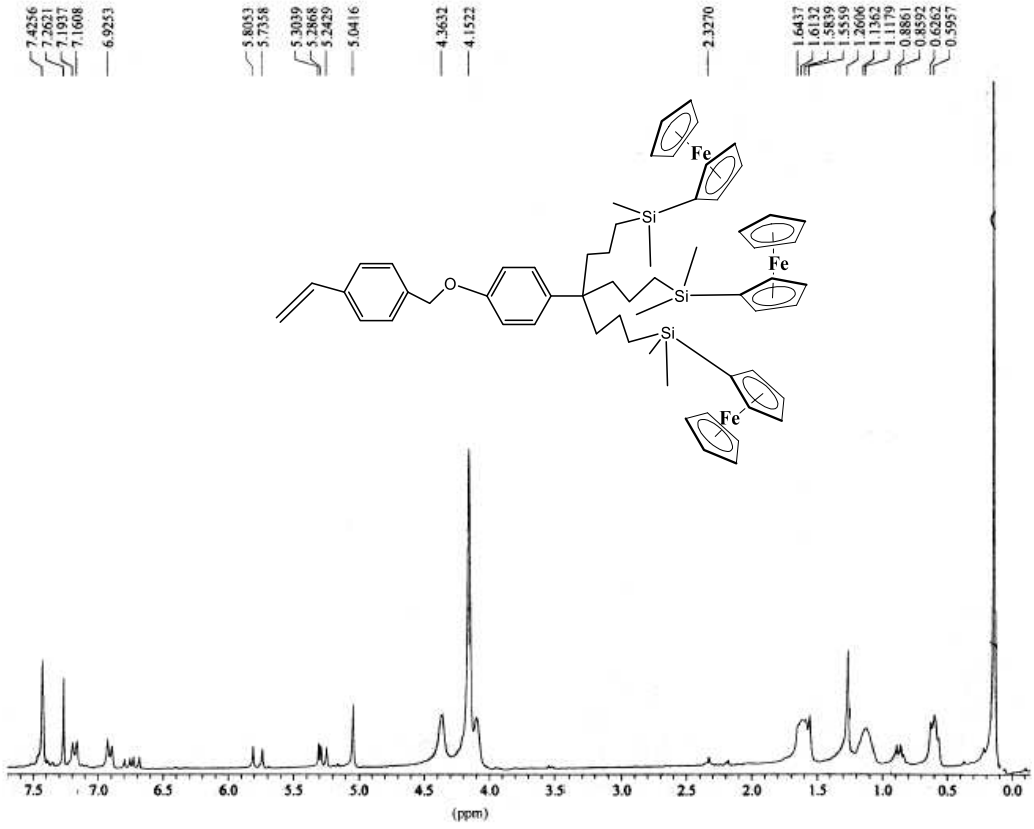

^{13}C NMR 75.47 MHz ($CDCl_3$) of 4

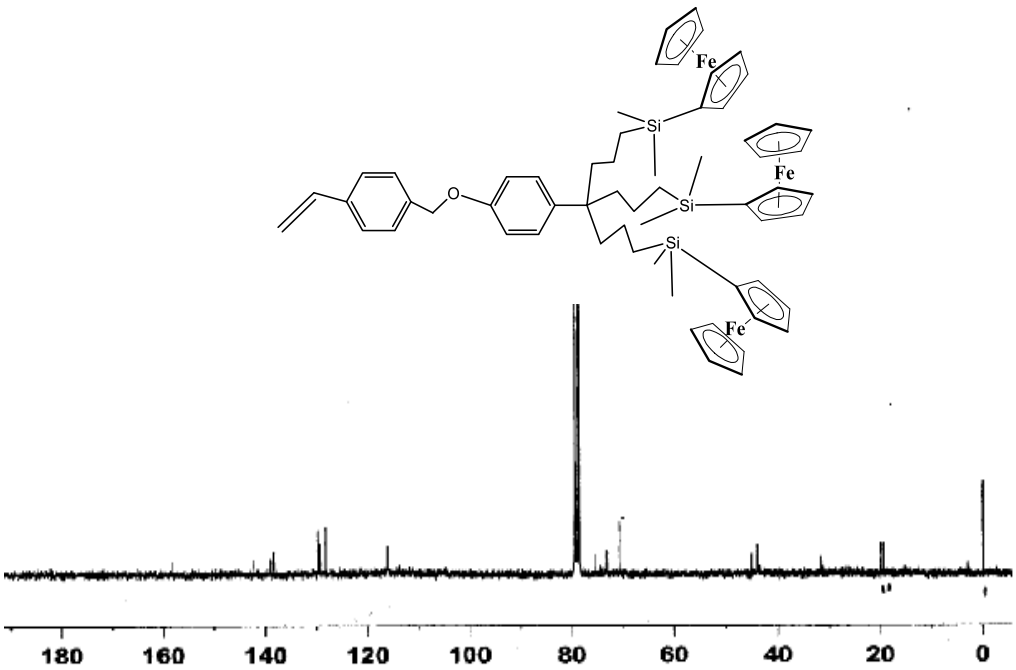

MALDI-TOF Mass Spectrometry of 4

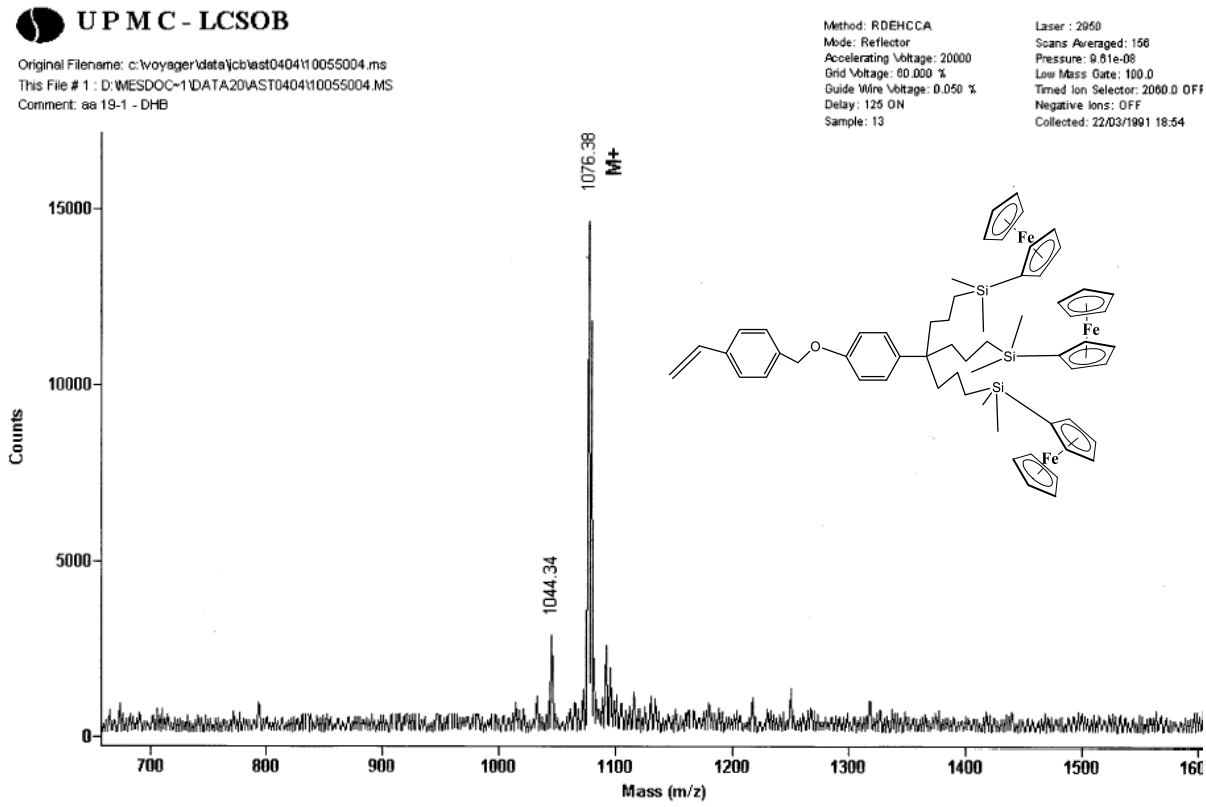

^{1}H NMR 300 MHz ($CDCl_3$) of 5

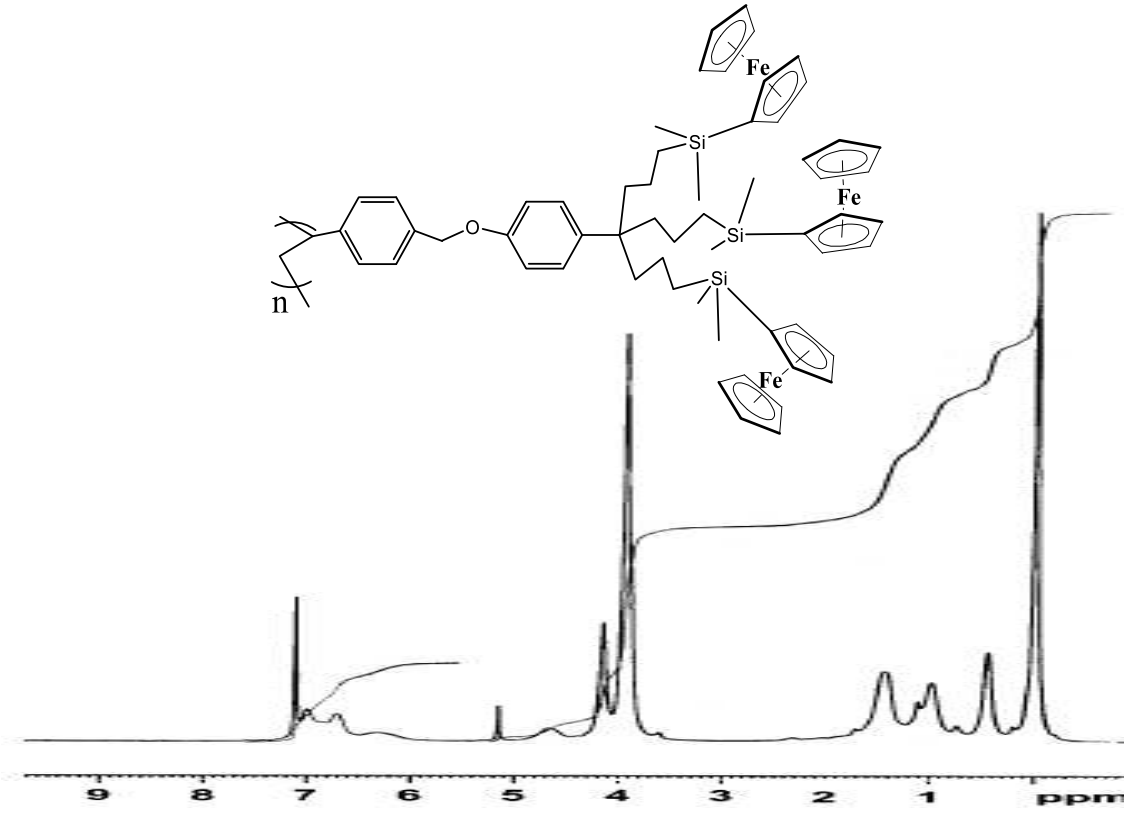

^{13}C NMR 75.47 MHz ($CDCl_3$) of 5

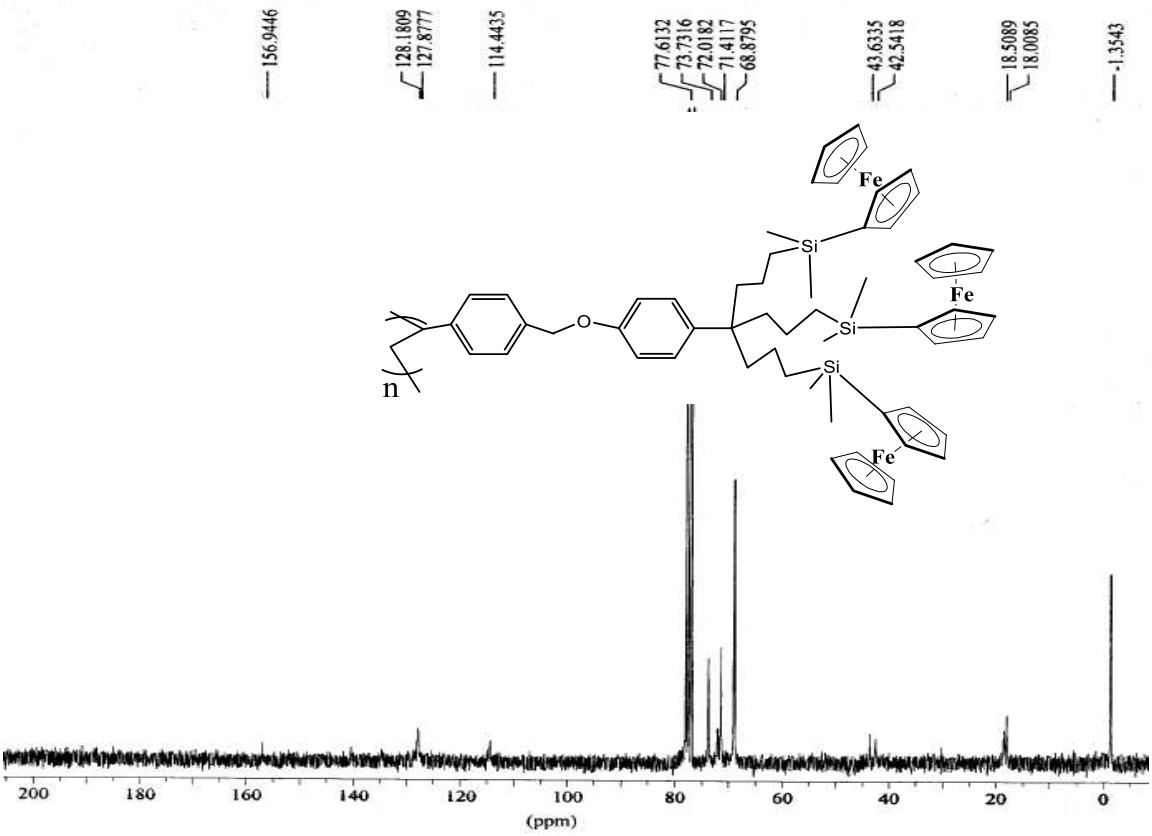

2D NMR COSY of 5: HC Correlation

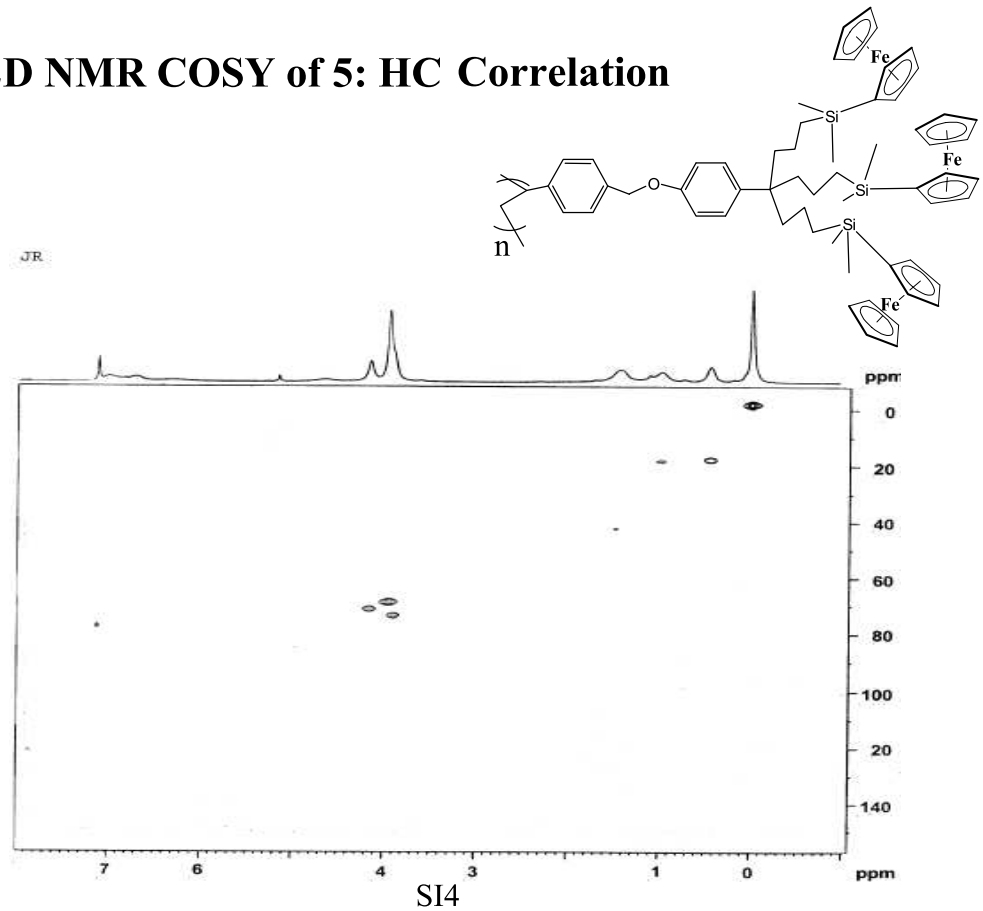

^{1}H NMR of 7

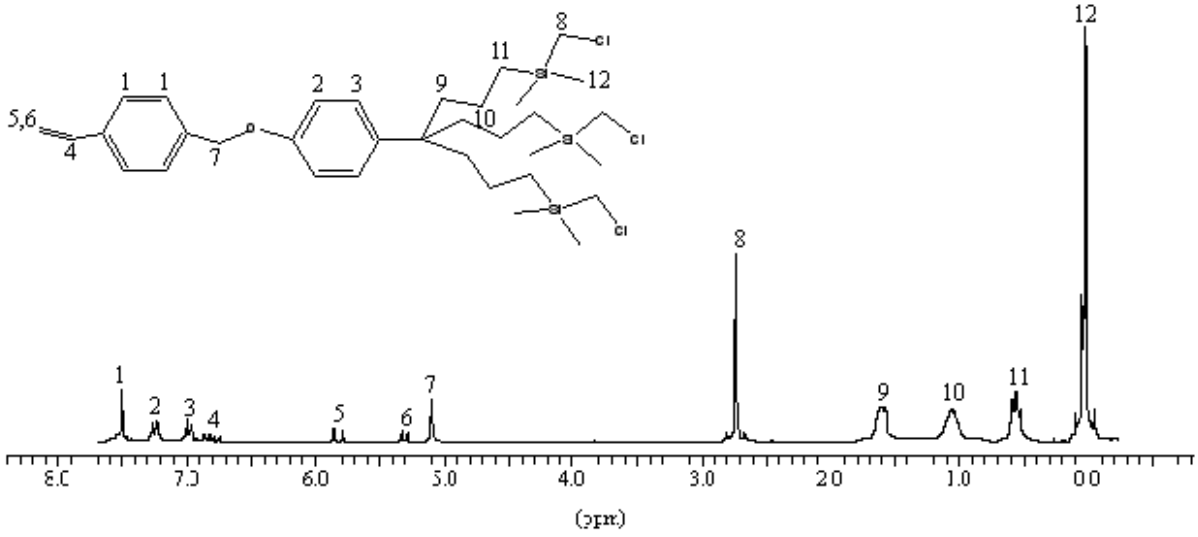

^{13}C NMR of 7

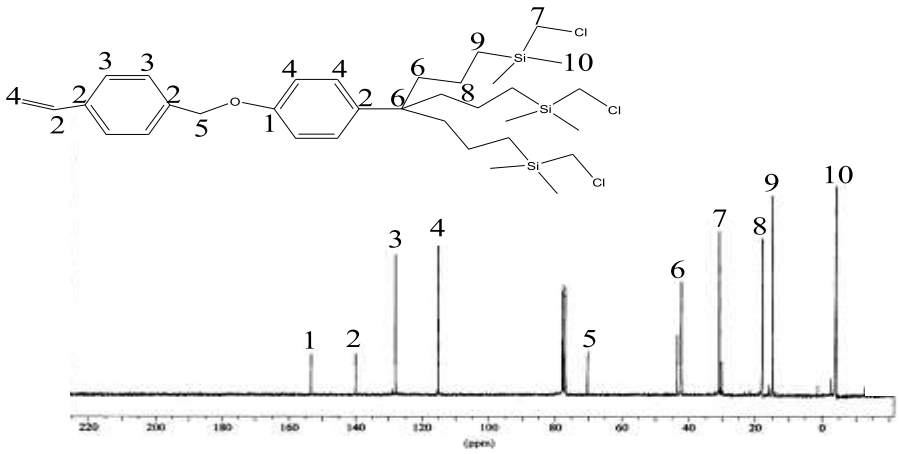

^{1}H NMR of 8

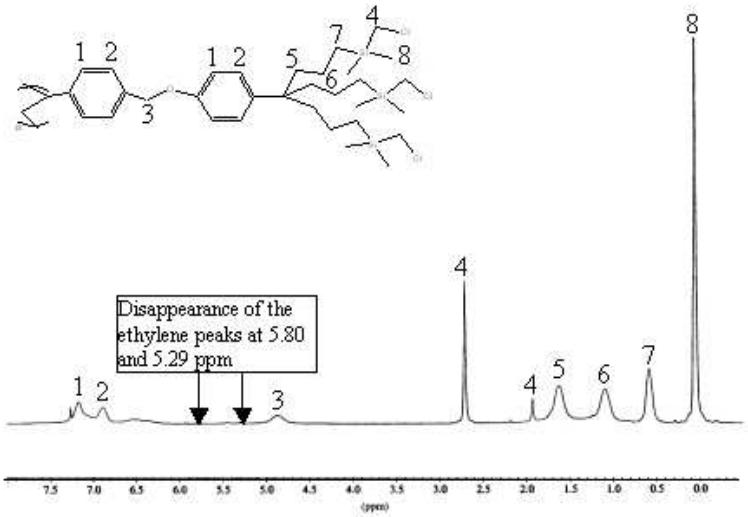

^{13}C NMR of 8

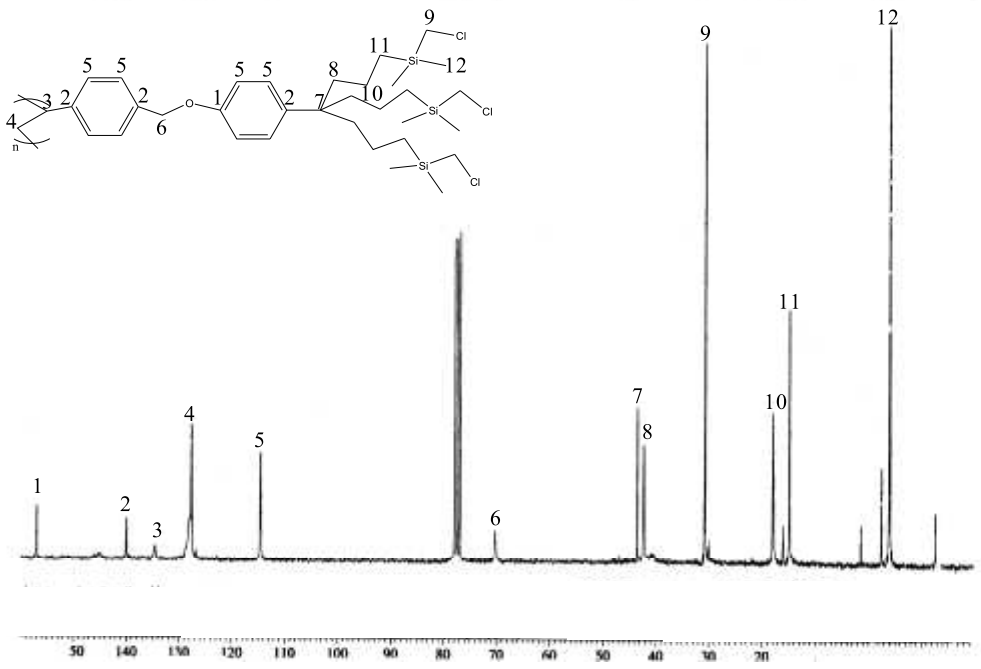

SEC of 8

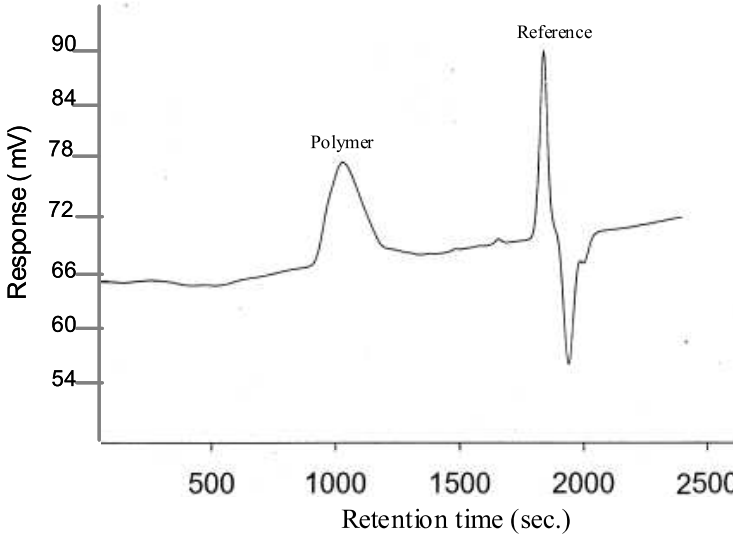

^{1}H NMR of 9

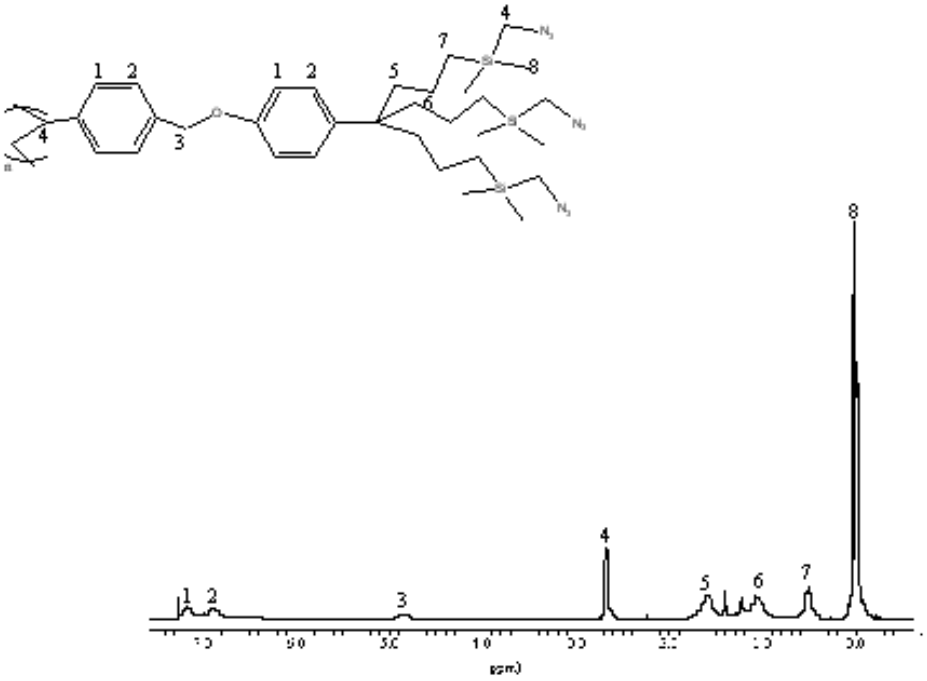

^{13}C NMR of 9

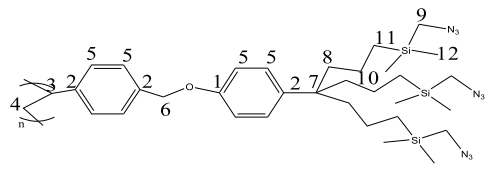

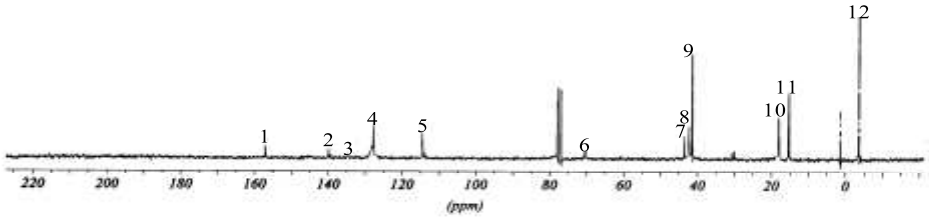

IR of 9

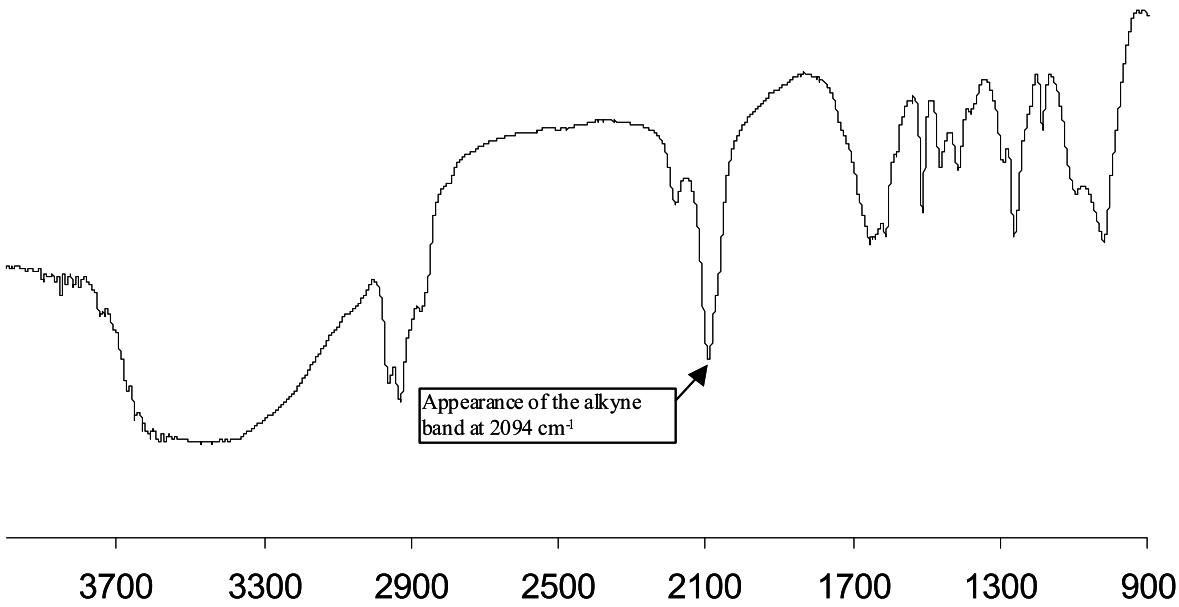

SEC of 9

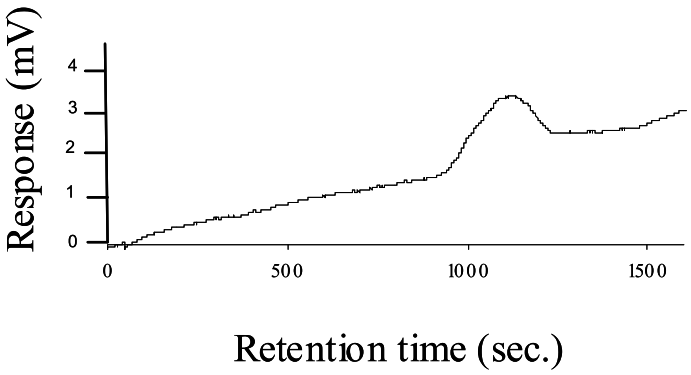

^{1}H NMR of 10

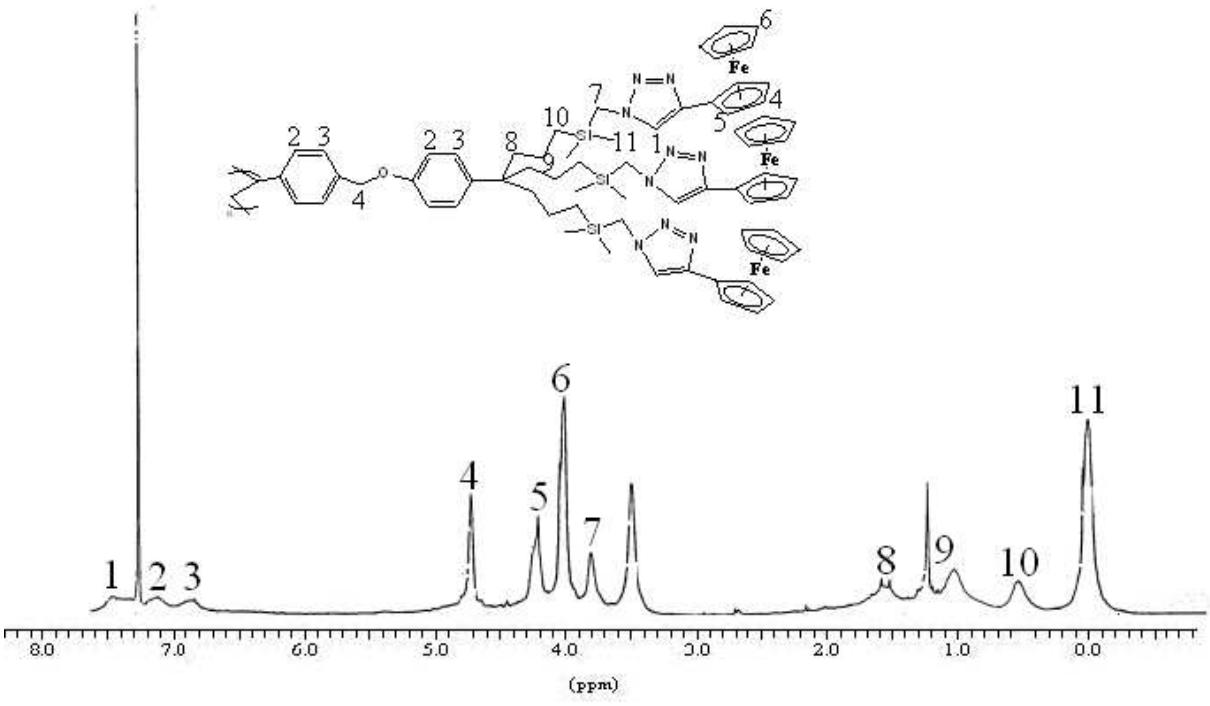

^{13}C NMR of 10

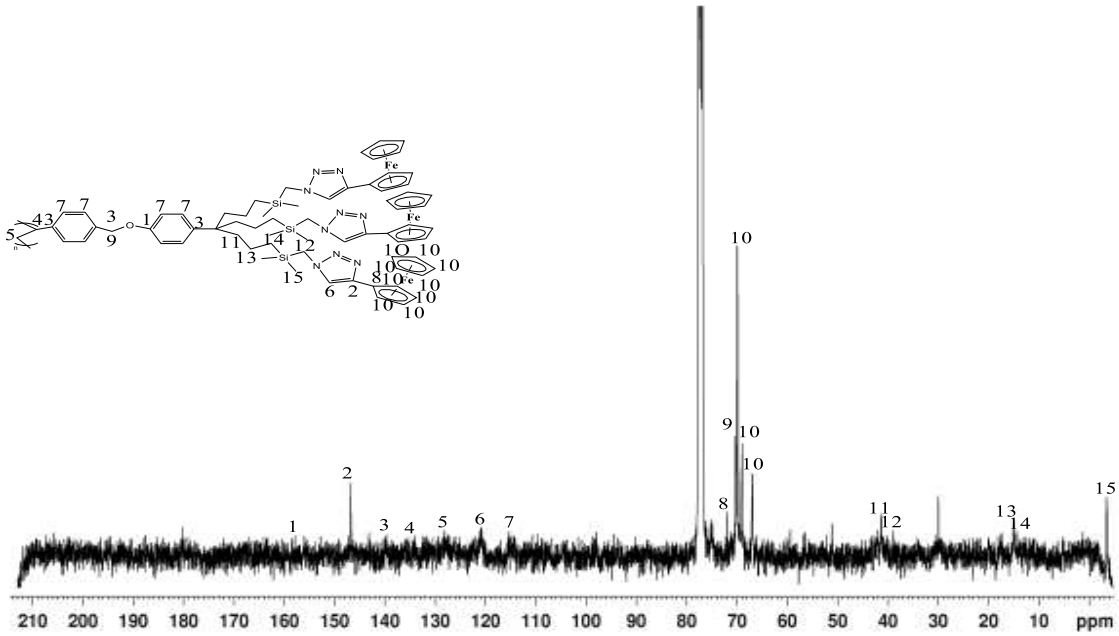

IR of 10

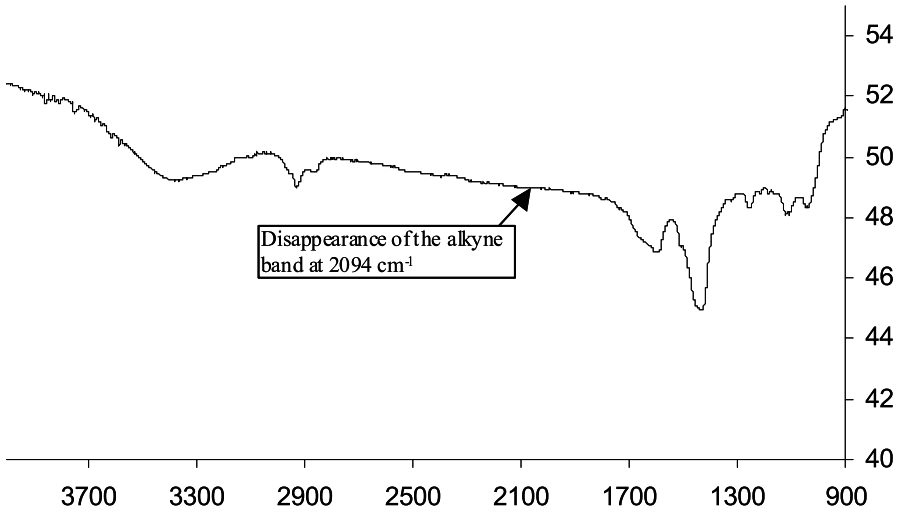

SEC of 10

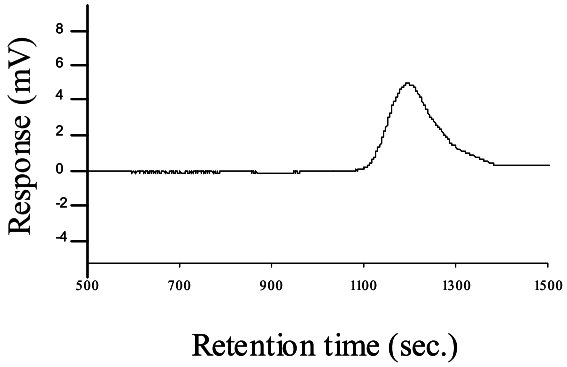

Calcul of the number of Fc per polymer 10 by cyclic voltammetry

i (poly)	1,2
i (Fc)	1,6
MM (poly)	67320
MM (Fc)	326
theoric number of dendrons *per* polymer	51
m (poly)	0,0015
m (Fc)	0,000336
n (poly)	2,22816E-08
n (Fc)	1,03067E-06
(Mp/MFc)^ 0.275	4,331165604
ip/np	53856000
if/cf	1552380,952
ratio of i	34,69251534
number of calculated Fc by cyclic voltammetry	150,2590291
theoric number of Fc *per* polymer	153

Stability of the Pt electrode with 10 for different scanning rate

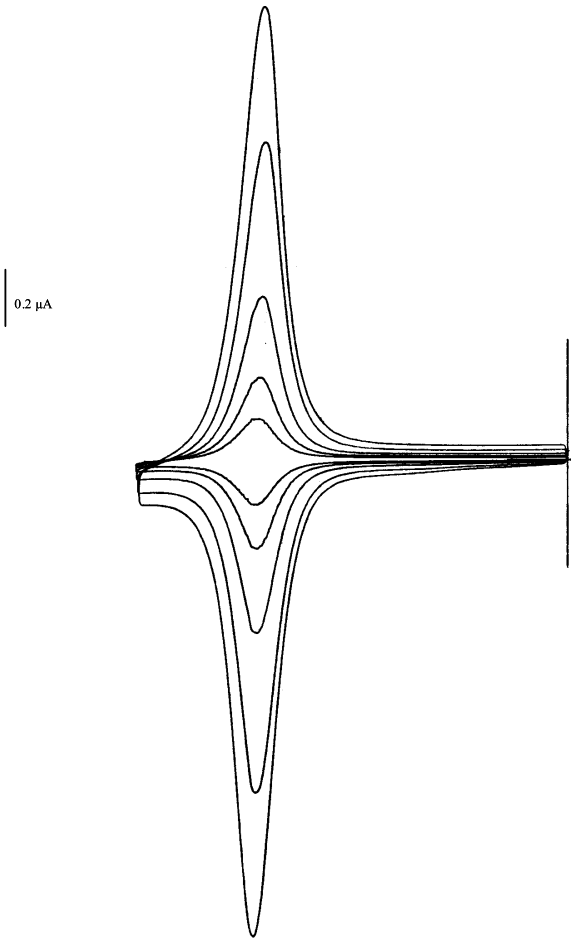

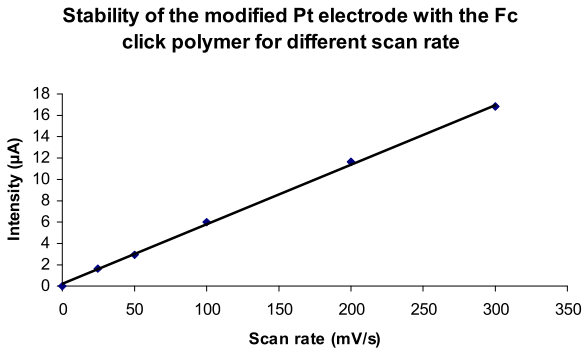

Different scanning rate from smaller to larger at 25 mV/s, 50 mV/s, 100 mV/s, 200 mV/s and 300 mV/s

Chapitre A-5

Métathèse d'oléfines en milieu aqueux sans co-solvant

Ce travail concerne un nouveau procédé de métathèse d'oléfines ou d'énynes dans l'eau sans ajout de co-solvant. En effet ces réactions de métathèse ont lieu dans des nanoréacteurs dendritiques solubles dans l'eau qui rendent la métathèse réalisable dans l'eau et dans des conditions bien meilleures que celles utilisées dans la littérature.

Ce travail a été breveté le 8 Octobre 2008. Les grandes lignes de ce projet réalisé au sein de notre laboratoire en collaboration avec M. Abdou K. Diallo, doctorant de notre groupe, sont les suivantes.

La réaction de métathèse des oléfines, dont l'importance a été soulignée par l'attribution en 2005 du prix Nobel à MM. Y. Chauvin, R. H. Grubbs, et R.R. Schrock, permet la transformation des hydrocarbures et dérivés organiques insaturés avec une haute valeur ajoutée. Ces réactions sont effectuées au moyen d'un catalyseur moléculaire contenant un métal, notamment le ruthénium. Cependant, ces catalyseurs présentent la plupart du temps l'inconvénient de n'être solubles que dans les solvants organiques, ce qui présente une certaine incompatibilité avec la notion de développement durable, limitant ainsi l'industrialisation de procédés les utilisant.

Le développement de procédés utilisant l'eau comme solvant représente donc un défi majeur, notamment pour l'environnement mais se heurte au manque de solubilité des catalyseurs et des substrats dans l'eau. En effet, les catalyseurs commerciaux et la majorité des oléfines utilisées généralement dans ces réactions sont insolubles dans l'eau.

Pour contourner ce problème de solubilité, des catalyseurs solubles dans l'eau ainsi que des méthodes utilisant les ultrasons ont été développés mais il reste toujours des problèmes de séparation, d'adaptation à l'échelle industrielle ou encore de quantité de catalyseur utilisée trop importante.

Les dendrimères, utilisés pour différentes applications, notamment comme micelles, boites moléculaires, exorécepteurs ou vecteur de médicament, pourront servir de nanoréacteurs afin de réaliser les réactions de métathèse dans l'eau selon un procédé compatible avec le développement durable. Ce procédé est applicable quel que soit le type de métathèse et peut aussi être réalisé à l'air ambiant.

Enfin, ces travaux ont prouvé qu'il est possible, dans ces conditions, d'utiliser les catalyseurs commerciaux au ruthénium les plus courants en quantité beaucoup plus faible que dans la littérature pour la métathèse de fermeture de cycle, que ce soit sous atmosphère inerte ou à l'air.

Ma contribution dans ce travail correspond à la synthèse des dendrimères utilisés dans ce projet. La partie catalyse a été réalisée par M. Abdou K. Diallo.

DOI: 10.1002/anie.200((will be filled in by the editorial staff))

Dendrimer-Induced Olefin Metathesis in Water and Air under Ambient Conditions Catalyzed by Low Amounts of Commercial Ruthenium-Benzylidene Catalysts

*Abdou K. Diallo, Elodie Boisselier, Jaime Ruiz, Didier Astruc**

Although olefin-metathesis reactions[1] have classically been carried out in the rigorous absence of air and moisture, ruthenium salts have long been known to catalyze ring-opening metathesis polymerization reactions in water.[2] More recently, ruthenium benzylidene catalysts that have been functionalized by ionic and other water-solubilizing groups have been shown to efficiently catalyze various types of homogeneous olefin-metathesis reactions in water.[3] Alternatively, metathesis also works well when the substrate is water soluble or if water-organic solvent mixtures are used, rendering the reaction mixture homogeneous.[4] Difficulties are encountered to carry out reactions in water however, when neither the catalyst nor the olefinic substrates are soluble in water, which is most often the case. Indeed, it would be desirable to eliminate organic co-solvent for sustainable reaction conditions.

Thus, the problem of catalyzing metathesis "in" or "on" water in the absence of a co-solvent using commercial ruthenium catalysts has very recently been addressed. Grela's group reported cross metathesis (CM), ring-closing metathesis (RCM) and enyne metathesis (EYM) in ultrasonicated water forming an emulsion at 40°C with 5 mol% of second-generation Grubbs catalyst (G2) and a related indenylidene ruthenium catalyst.[5] Sinou's group showed that the presence of surfactants such as sodium dodecylsulfonate (5%) and others favored the RCM diethyl(diallyl)malonate.[6] Lipshulz 's group used 0.8-2.5 mol % of a vitamin E-based amphiphile in water with 1 or 2 mol % of second-generation Grubbs catalyst to catalyze CM, ring-opening metathesis (ROM)-CM and RCM reactions in air.[7]

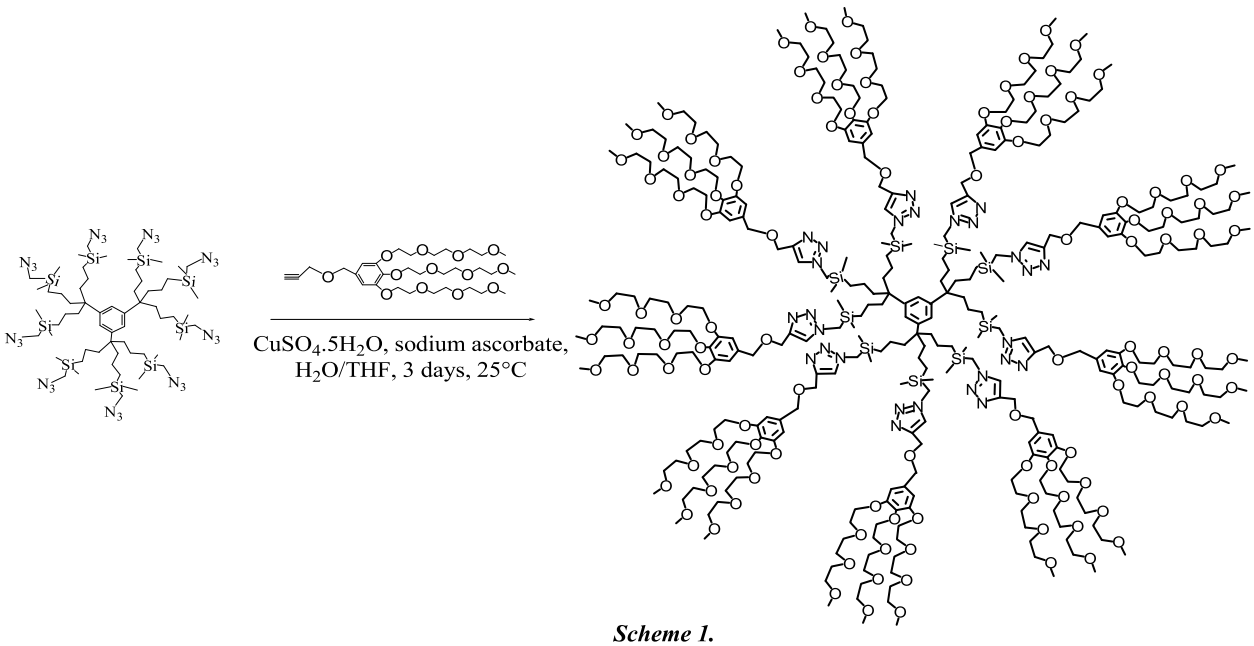

Scheme 1.

Dendrimers have been shown to be efficient in a variety of catalytic reactions. Indeed, their function as molecular micelles, pioneered by Newkome and Tomalia's groups[8,9] has been shown to be useful for the dendrimer encapsulation of guest substrates.[8-11] In the case of catalysis by palladium nanoparticles, Crooks also showed that dendrimer-encapsulation of such catalysts provides a remarkable selectivity.[11] Metallodendritic catalysis in which the metal complex is bound to the dendrimer at the core or periphery is a well-developed area.[12] A dendrimer can also provide a radial polarity gradient suitable for organocatalysis, and this principle was shown by Fréchet to accelerate the intradendritic dehydrohalogenation of 2-iodo-2-methylheptane proceeding with E_1 elimination mechanism and $^1O_2$-sensitized peroxidation reactions.[13] Catalysis by dendrimer-encapsulated molecular transition-metal catalysts is still unknown, however.

[*] Institut des Sciences Moléculaires, UMR CNRS N° 5255, Université Bordeaux 1, 33405 Talence Cedex, France, E-mail: d.astruc@ism.u-bordeaux1.fr http://www.ubordeaux1.fr/lcoo/members/eastruc.htm

[**] Financial support from the IUF, the Université Bordeaux 1, the CNRS and the ANR (project ANR-07-CPD-05-01) are gratefully acknowledged.

Supporting information for this article is available on the WWW under http://www.angewandte.org or from the author.

Along this line, we now report ring-closing metathesis (RCM), cross metathesis (CM) and enyne metathesis (EYM) in water and air in the absence of co-solvent using low amount of commercial benzylidene catalyst under ambient conditions (RCM and EYM) or 40°C (CM) in the presence of 0.028 mol% of the new recyclable water-soluble TEG dendrimer. This dendrimer was chosen to fulfill amphiphilic properties. It was synthesized by $CpFe^{+}$-induced nonallylation of mesitylene,[14] followed by photolytic removal of $CpFe^{+}$,[14b,c] hydrosylilation with chloromethyldimethylsilane,[15] chloride/azide substitution[16] and continuation of the 1→3 connectivity upon "click" reaction[17] with a Percec-type dendron[18] functionalized at the focal point with a propargyl group and on the periphery with tetraethyleneglycol tethers. (Scheme 1 and S.I.).

The first- and second-generation Grubbs catalysts (G1 and G2) and the first and second-generation Grubbs-Hoveyda catalysts (GH1 and GH2) all work at room temperature in various yields for RCM reactions in water and air using between 0.04% G2, the most successful catalyst under these conditions, and 0.2% for the other catalysts (see Table 2). CM with an electron-deficient olefin was found to be steroselective (eq. 1) but required heating to 40° with 2% G2 (66% yield). See the data in Tables 1-3.

We do not find very significant differences between reactions carried out under N_2 and those in air (for instance, with G2, 60% yield in air vs. 66% yield under N_2, using 0.06 mol% G2) despite a color change of the reaction mixture from off white to dark beige in air unlike for reactions carried out under N_2.

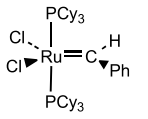

Grubbs' catalyst of 1rst generation (G1)

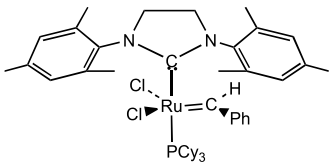

Grubbs' catalyst of 2nd generation (G2)

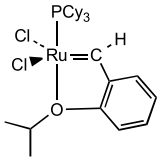

Grubbs-Hoveyda catalyst of 1rst generation (GH1)

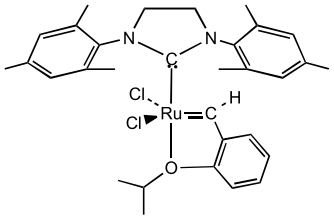

Grubbs-Hoveyda catalyst of 2nd generation (GH1)

The reactions do not yield any product in the absence of the dendrimer. A key feature of the present system also is that the aqueous solution of the water-soluble TEG dendrimer can be recycled, because it is insoluble in ether. Re-use can be carried out subsequent to filtration of the insoluble catalyst after the reaction and removal of the organic reaction product by decantation or extraction with ether. Alternatively, extraction of the organic product with ether at 0°C leaves the catalyst in suspension with the aqueous dendrimer solution, then both the dendrimer and the catalyst can be re-used if the initial catalyst loading is sufficient. For instance, when the initial amount of G2 is 2% at 25°C, the initial RCM reaction yields with **2** as a substrate is 98%, then the first recycling gives a yield of 91%, the second one 81%, and the third one 65%. This is an advantage over the use of surfactants that are not recycled, and it is a specific property of the dendrimer.

Table 1. Ring-closing metathesis reactions using 2 mol% Grubbs' 2nd generation catalyst and 0.028 mol % TEG dendrimer/H_2O at 25 °C.

Entry	Substrate	Product	Time(h)	Yield [%]
A	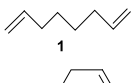 1	 8	3	96[a]
B	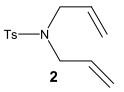 2	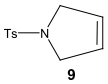 9	8	98[b]
C	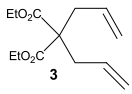 3	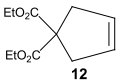 12	8	98[a]
D	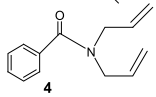 4	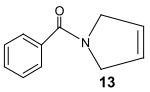 13	8	98[b]
E	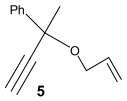 5	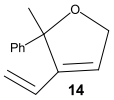 14	24	99[b]
F	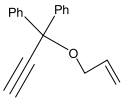 6	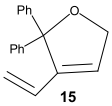 15	24	97[b]

[a] The reaction mixture with the catalyst was analyzed by ^1H NMR.
[b] The reaction mixture with the catalyst was analyzed by GC.

The dendrimer serves as a nanoreactor whereby the TEG termini solubilize it in water and in the same time are compatible with hydrophobic organic substrates and organometallic catalyst that are introduced inside the hydrophobic dendritic interior. The low generation of the dendrimer allows free exchange without much steric constraint between the hydrophobic dendritic interior and the hydrophilic outside via the TEG periphery that has intermediate properties allowing solubilization. This principle is consistent with the use of the dendrimer in low, catalytic, amount and retention in water, while the water-insoluble organic substrates are separated. This strategy could ideally be extended to other types of catalysis, and research along this line is ongoing in our laboratory.

Table 2. Influence of the nature of the catalyst on ring-closing metathesis reaction of **2** using 0.2 mol% catalyst and 0.028 mol% TEG dendrimer/H_2O at 25 °C during 6h.

Catalyst	Yield [%]
Gubbs 1 st generation	16
Gubbs 2 nd generation	80
Gubbs-Hoveyda 1 st generation	41
Gubbs-Hoveyda 2nd generation	35

Table 3. Influence of the amount of catalyst on the ring-closing metathesis of **2**[a]

% Grubbs 2nd generation catalyst	Yield [%]
0.2	96
0.1	90
0.06	66
0.04	62

[a] Conditions: 0.028 mol % TEG dendrimer/ H_2O (0.1 M), 25 °C, 24 h.

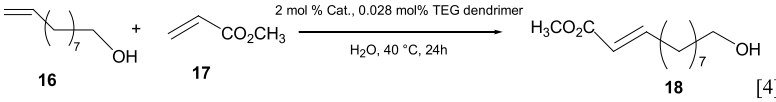

Equation 1.

In conclusion, it has been shown here that metathesis reactions (RCM, CM and EYM) can be carried out in water and air under ambient or mild conditions with remarkably low amounts of water-insoluble commercial ruthenium benzylidene catalysts (in particular Grubbs' second generation catalyst) and common water-insoluble olefinic substrates, if less than 0.03 mole % of a recyclable TEG-terminated dendrimer is used as a nanoreactor.

Experimental Section

Grubbs' second generation catalyst (between 0.4% and 2%, see Tables 1-3) was added to a Schlenk flask. An aliquot of 0.028 mol% TEG dendrimer/ H_2O (all metathesis reactions were conducted at 0.1 M) was added *via* syringe. The olefin or enyne was added, and the resulting solution was allowed to stir vigorously at room temperature. The homogeneous reaction mixture was filtered at 0.22 mm, and diethyl ether was used to extract the reaction product from the reaction mixture. The dendrimer, which is insoluble in diethyl ether, remained in the aqueous phase. The reactions were followed by ^{1}H RMN or GC. General data, full procedures, characterizations of the TEG dendrimer and products including GC and ^{1}H NMR spectra of reaction mixtures, and reaction kinetics, are described in the S.I.

Received: ((will be filled in by the editorial staff))
Published online on ((will be filled in by the editorial staff))

Keywords: dendrimer, metathesis, green chemistry, ruthenium

[1] *Handbook of Metathesis* (Ed.: R.H. Grubbs), Wiley, Weinheim, **2003**; A. Fürstner, *Angew. Chem., Int. Ed.* **2000**, *39*, 3012-3043; T. M. Trnka, R. H. Grubbs, *Acc. Chem. Res.* **2001**, *34*, 18-29 ; S. J. Connon, S. Blechert, *Angew. Chem., Int. Ed.* **2003**, *42*, 1900-1923; R. R. Schrock, A. H. Hoveyda, *Angew. Chem., Int. Ed.* **2003**, *115*, 4592-4633; D. Astruc, *New J. Chem.* **2005**, *29*, 42-56; H. Clavier, K. Grela, A. Kirsning, M. Mauduit, S. P. Nolan, *Angew. Chem., Int. Ed.* **2007**, *46*, 4786-6801 ; M. Bienek, A. Michrowska, D. M. L. Usanov, K. Grela, *Chem. Eur. J.* **2008**, *14*, 806-818.

[2] B. M. Novak, R. H. Grubbs, *J. Am. Chem. Soc.* **1988**, *110*, 960-961 ; B. M. Novak, R. H. Grubbs, *J. Am. Chem. Soc.* **1988**, *110*, 7542-7543; M. A. Hillmeyer, C. Lepetit, D. V. McGrath, B. M. Novak, R. H. Grubbs, *Macromolecules* **1992**, *25*, 3345-3350.

[3] D. M. Lynn, B. Mohr, R. H. Grubbs, *J. Am. Chem. Soc.* **1998**, *120*, 1627-1628 ; S. J. Connon, S. J. Blechert, *Biorg. Med. Chem. Lett.* **2002**, *12*, 1873-1876 ; T. Rölle, R. H. Grubbs, *Chem. Commun.* **2002**, 1070-1071; N. Jarroux, P. Keller, A. F. Mingotaud, C. Mingotaud, C. Sykes, *J. Am. Chem. Soc.* **2004**, *126*, 15958-15959 ; J. P. Gallivan, J. P. Jordan, R. H. Grubbs, *Tetrahedron Lett.* **2005**, *46*, 2577-2580 ; S. H. Hong, R. H. Grubbs, *J. Am. Chem. Soc.* **2006**, *128*, 3508-3509 ; D. Rix, H. Clavier, L. Gulajski, K. Grela, M. Mauduit, *J. Organomet. Chem.* **2006**, *691*, 5397-5405 ; L. Gulajski, A. Michrowska, R. Bujok, K. Grela, *J. Mol. Catal. A : Chem.* **2006**, *348*, 931-938 ; A. Michrowska, L. Gulajski, K. Grela, *Chem. Today* **2006**, *24*, 19-22 ; J. B. Binder, I. A. Guzei, R. T. Raines, *Adv. Catal.* **2007**, *349*, 395-404 ; D. Rix, F. Caijo, I. Lazurent, L. Gulajski, K. Grela, M. Mauduit, *Chem. Commun.* **2007**, 3771-3773 ; J. P. Jordan, R. H. Grubbs, *Angew. Chem., Int. Ed.* **2007**, *46*, 5152-5155 ; A. N. Robert, A. C. Cochran, D. A. Rankin, A. B. Lowe, H. J. Shantz, *Organometallics* **2007**, *26*, 6515-6518 ; L. Gulajski, A. Michrowska, J. Naroznik, Z. Kazmarska, L. Rupnicki, K. Grela, *ChemSusChem.* **2008**, *1*, 103-109; D. Samanta, K. Kratz, X. Zhang, T. Emrick, *Macromolecules* **2008**, *41*, 530-532.

[4] S. J. Connon, M. Rivard, M. Zaja, S. Blechert, *Adv. Synth. Catal.* **2003**, *345*, 572-575 ; A. Michrowska, L. Gulajski, Z. Kaczmarska, K. Mennecke, A. Kirschning, K. Grela, *Green Chem.* **2006**, *8*, 685-688 ; J. B. Binder, J. J. Blank, R. T. Raines, *Org. Lett.* **2007**, *9*, 4855-4888.

[5] L. Gulajski, P. Sledz, A. Lupa, K. Grela, *Green Chem.* **2008**, *10*, 279-282.

[6] K. J. Davis, D. Sinou, *J. Mol. Catal. A : Chem.* **2002**, *177*, 173-178.

[7] B. H. Lipschulz, G. T. Aguinaldo, S. Ghorai, K. Voigtritter, *Org. Lett.* **2008**, *10*, 1325-1328 ; B. H. Lipschutz, S. Ghorai, G. T. Aguinaldo, *Adv. Synth. Catal.* **2008**, *350*, 953-956.

[8] G. R. Newkome, Z. Yao, G. R. Baker, V. K. Gupta, *J. Org. Chem.* **1985**, *50*, 2003-2004; G. R. Newkome, C. N. Moorefield, G. R. Bakers, A. L. Johnson, R. K. Behera, *Angew. Chem., Int. Ed.* **1991**, *30*, 1176-1178; G. R. Newkome, C. N. Moorefield, G. R. Bakers, M. J. Saunders, S. H. Grossman, *Angew. Chem., Int. Ed.* **1991**, *30*, 1178-1180.

[9] D. A. Tomalia, H. Baker, J. Dewald, M. Hall, G. Kallos, S. Martin, J. Roeck, J . Ryder, P. Smith, *Polym. J.* (Tokyo) **1985**, *17*, 117-132; A. M. Naylor, W. A. Goddart III, G. E. Kiefer, D. A. Tomalia, *J. Am. Chem. Soc.* **1989**, *111*, 2339-2341; K. R. Gopidas, A. R. Leheny, G. Caminati, *J. Am. Chem. Soc.* **1991**, *113*, 7335-7342; G. Caminati, M. F. Ottaviani, K. Gopias, S. Jokusch, N. J. Turro, D. A. Dolia, *Polym. Mater. Sci. Eng.* **1995**, 73, 80-81.

[10] J. F. G. A. Jansen, E. M. M. de Brabander-van den Berg, E. W. Meijer, *Science* **1994**, *266*, 1226-1229 ; G. R. Newkome, *Pure Appl. Chem.* **1998**, *70*, 2337-2343 ; V. Balzani, P. Ceroni, S. Gestermann, M. Gorka, C. Kauffmann, F. Vögtle, *Tetrahedron* **2002**, *58*, 629-637 ; S. C. Zimmermann, F. W. Zeng, *Chem. Rev.* **1997**, *97*, 1681-1712 ; C. R. Moorefield, G. R. Newkome, *C. R. Chimie* **2003**, *6*, 715-724 .

[11] R. M. Crooks, M. Zhao, L. Sun, V. Chechik, L. K. Yeung, *Acc. Chem. Res.* **2001**, 34, 181-190; R. W. J. Scott, O. M. Wilson, R. M. Crooks, *J. Phys. Chem. B* **2005**, *109*, 692-704.

[12] G. E. Oosterom, J. N. H. Reek, P. C. J. Kamer, P. W. N. M. van Leeuwen, *Angew. Chem., Int. Ed.* **2001**, *40*, 1828-1849; D. Astruc, F. Chardac, *Chem. Rev.* **2001**, *101*, 2991-3023; R. Kreiter, A. W. Kleij, R. J. M. Klein Gebbink, G. van Koten, *Top. Curr. Chem.* **2001**, *217*, 163-199 ; R. van Heerbeek, P. C. J. Kamer, P. W. N. M. van Leeuwen, J. N. H. Reek, *Chem. Rev.* **2002**, *102*, 3717-3756; D. Méry, D. Astruc, *Coord. Chem. Rev.* **2006**, *250*, 1965-1979 ; R. Andrés, E. de Jesus, J. C. Flores, *New J. Chem.* **2007**, *31*, 1161-1191 ; E. de Jesús, J. C. Flores, *Ind. Eng. Chem. Res.* **2008**, *47*, 7968-7981.

[13] B. Helms, J. M. J. Fréchet, *Adv. Synth. Catal.* **2006**, *348*, 1125-1148.

[14] F. Moulines, L. Djakovitch, R. Boese, B. Gloaguen, W. Thiel, J.-L. Fillaut, M.-H. Delville, D. Astruc, *Angew. Chem. Int. Ed. Engl.* **1993**, *32*, 1075-1077 ; b) D. Catheline, D. Astruc, *J. Organomet. Chem.* **1983**, *248*, C9-C12; D. Catheline, D. Astruc, *J. Organomet. Chem.* **1984**, *272*, 417-426.

[15] a) V. Sartor, L. Djakovitch, J.-L. Fillaut, F. Moulines, F. Neveu, V. Marvaud, J. Guittard, J.-C. Blais, D. Astruc, *J. Am. Chem. Soc.* **1999**, *121*, 2929-2930 ; b) S. Nlate, J. Ruiz, J.-C. Blais, D. Astruc, *Chem. Commun* **2000**, 417-418 ; c) J. Ruiz, G. Lafuente, S. Marcen, C. Ornelas, S. Lazare, J.-C. Blais, E. Cloutet, D. Astruc, *J. Am. Chem. Soc*. **2003**, *125*, 7250-7257.

[16] C. Ornelas, J. Ruiz, C. Belin, D. Astruc, *J. Am. Chem. Soc*. **2009**, *131*, 590-601 ; J. Camponovo, J. Ruiz, E. Cloutet, D. Astruc, *Chem. Eur. J.* **2009,** *15*, 2990-3002.

[17] a) V. V. Rostovtsev, L. G. Green, V. V. Fokin, K. B. Sharpless, *Angew. Chem., Int. Ed.* **2002**, *41*, 2596-2599; b) V. D. Bock, H. Hiemstra, J. H. van Maarseveen, *Eur. J. Org. Chem.* **2006**, 51-68; c) P. Wu, M. Meldal, C. W. Tornoe, *Chem. Rev.* **2008**, *10*, 2952-3015.

[18] a) V. Percec, G. Johansson, G. Ungar, J. Zhou, *J. Am. Chem. Soc.* **1996**, 118, 9855-9866; b) V. S. K. Balagurusamy, G. Ungar, V. Percec, G. Johansson, *J. Am. Chem. Soc.* **1997**, *119*, 1539-1555; c) V. Percec, J. Smidrkal, M. Peterca, C. M. Mitchell, S. Nummelin, A. E. Dulcey, M. J. Sienkowska, P. A. Heiney, *Chem. Eur. J.* **2007**, *13*, 3989-4007; d) V. Percec, M. Peterca, A. E. Dulcey, M. R. Imam, S. D. Hudson, S. Nummelin, P. Adelman, P. A. Heiney, *J. Am. Chem. Soc.* **2008**, *130*, 13079-13094.

Dendrimer-Induced Olefin Metathesis in Water and Air under Ambient Conditions Catalyzed by Low Amounts of Commercial Ruthenium-Benzylidene Catalysts

Abdou K. Diallo, Elodie Boisselier, Jaime Ruiz, Didier Astruc*

Supporting Information

Materials. The ruthenium-benzylidene catalysts and the substrates **1**, **3**, **16** and **17** were purchased from Aldrich. All the dendrimer synthetic steps were carried out using standard Schlenk techniques under an atmosphere of N_2. The starting materials **2**,[S1] **4**,[S2] **5**,[S3] and **6**[S3] were synthesized according to literature procedures.

Characterization. The ^{1}H NMR spectra were recorded on a Bruker AC 300 using $CDCl_3$ as the solvent and internal standard.
Gas chromatograms were recorded on a Hewlett Packard 5890 Series II gas chromatograph, equipped with a Stabilwax® (Crossband® Carbowax®-PEG) column and a flame ionization detector. For all substrates, helium was used as the carrier gas. The injector and detector temperature were 240 °C.

Procedure for cross-metathesis catalysis. 2 mol % of Grubbs' second-generation catalyst was added to a Schlenk flask. A degassed aliquot of 0.028 mol% TEG dendrimer/ H_2O (0.1 M) was added *via* syringe. 9-den-1-ol **16** (0.20 ml, 1.12 mmol) and methylacrylate **17** (0.30 ml, 3.36 mmol) were added. The resulting solution was allowed to stir vigorously at 40 °C for 24h. The homogeneous reaction mixture was filtrated at 0.22 mm and ethyl acetate was used to extract the reagent and the product from reaction mixture. The volatiles were removed under vacuum to afford the crude material that was purified by chromatography on silica gel using a pentane-diethyl ether (90:10) mixture as the eluent. 0.158 g of **18** as a colorless oil was obtained (66 % yield).
^{1}H NMR of **18** ($CDCl_3$, 300 MHz) δ_{ppm}: 6.96 (m, 1H), 5.84 (dd, 1H), 3.72 (s,3H), 3.63 (t, 2H), 2.18 (q, 2H), 1.30 (m, 12H)

Procedure for the "click" synthesis of the TEG dendrimer.

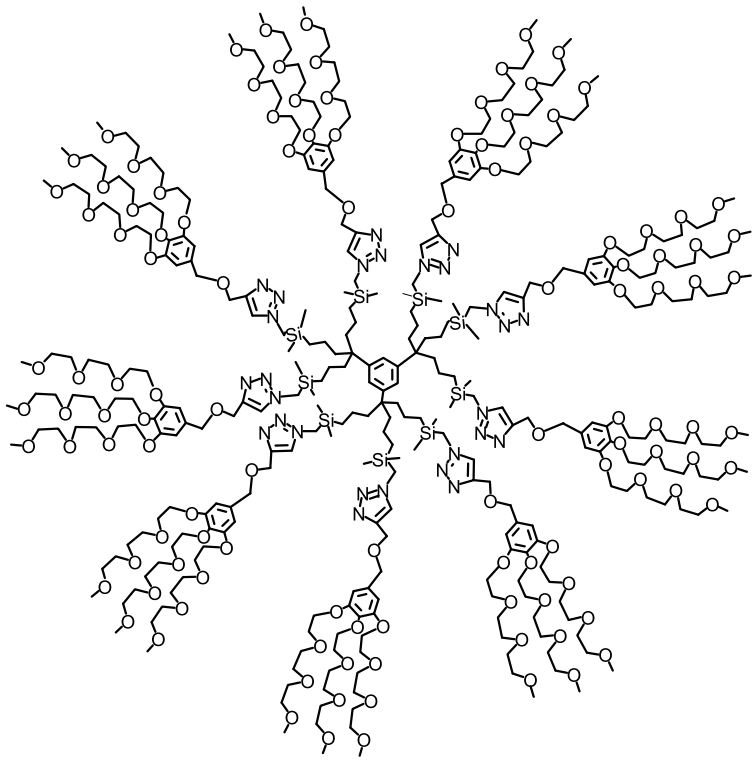

The nona-azide-dendrimer of Scheme 1 (1 *equiv*.) and the alcyne dendron (1.5 *equiv*. *per* branch) were dissolved in THF. At 0°C, $CuSO_4$ was added (2 *equiv*. per branch, 1M in water solution), followed by the dropwise addition of a freshly prepared solution of sodium ascorbate (4 *equiv*. per branch, 1M in water solution) in order to set a 1:1 THF/water ratio. The reaction mixture was stirred for 2 days at 25°C under N_2. After removing THF under vacuum, CH_2Cl_2 and an aqueous ammonia solution (2.0 M, 50 mL) were added. The mixture was allowed to stir for 10 min. in order to remove all the Cu^I trapped inside the dendrimer as $Cu(NH_3)_6^+$. The organic phase was washed twice with water, dried with sodium sulfate, and the solvent was removed under vacuum. The product was precipitated with MeOH/ diethyl ether in order to remove the excess of dendron.

^{1}H NMR ($CDCl_3$, 300 MHz) δ_{ppm}: 7.44 (9H, C*H*-triazole), 6.92 (36H, C*H*-arom. intern), 6.54 (18H, C*H*-arom. extern), 4.57 (18H, triazole-CH_2-0), 4.41 (18H, O-CH_2-arom. extern), 4.09 (72H, CH_2O-arom. extern and Si-CH_2-triazole), 3.61(270H, OCH_2CH_2O), 3.33 (27H, CH_3O), 1.59 (18H, CH_2CH$_2$CH$_2$Si), 1.06 (18H, CH$_2$CH_2CH$_2$Si), 0.60 (18H, CH$_2$CH$_2$CH_2Si), 0.008 (54H, Si(CH_3)$_2$).

^{13}C NMR ($CDCl_3$, 300 MHz) δ_{ppm}: 152.49 (*C*H, extern arom.), 144.48 (C_q of triazole), 137.67 (*C*q, arom. core), 132.28 (*C*q, arom. extern), 123.52 (*C*H of triazole and arom. core), 107.16 (C_qCH$_2$O), 70.39 (OCH_2CH_2O), 63.53 (triazole-CH_2-O), 58.91 (CH_3O), 53.38 (OCH$_2$

arom.extern), 43.77 ($CH_2CH_2CH_2Si$), 42.7 ($SiCH_2$-triazole), 40.93 (*C*q-arom.intern), 17.58 ($CH_2CH_2CH_2Si$), 15.18 ($CH_2CH_2CH_2Si$), -3.91 ($Si(CH_3)_2$).

SEC: retention time = 1348 seconds.

IR : disappearance of the alkyne and azide bands

Anal. calc. for $C_{414}H_{741}O_{153}N_{27}Si_9$: C 56.95, H 8.34; found: C 56.37, H 8.33.

Kinetic study of the ring-closing metathesis reaction of the substrate 2

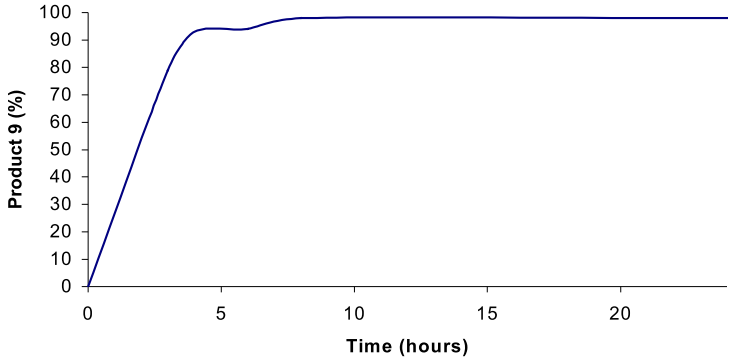

Fig. 1: Kinetics of the ring-closing metathesis reaction of substrate **2** at 25 °C using 2 mol% Grubbs 2nd generation catalyst and 0.028 mol% TEG dendrimer/ H_2O.

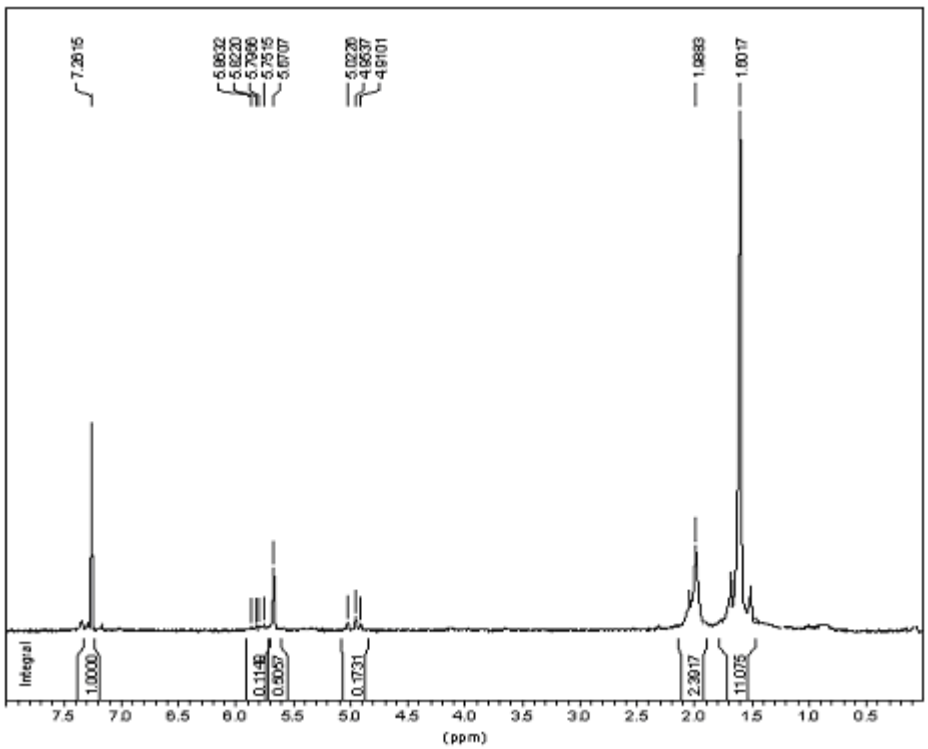

Fig. 2: ^1H NMR spectrum of entry **A** showing the ^1H RMN spectrum of **8** ($CDCl_3$, 300 MHz) δ_{ppm}: 5.67 (s, 2H), 1.99 (m, 4H), 1.60 (m, 4H)

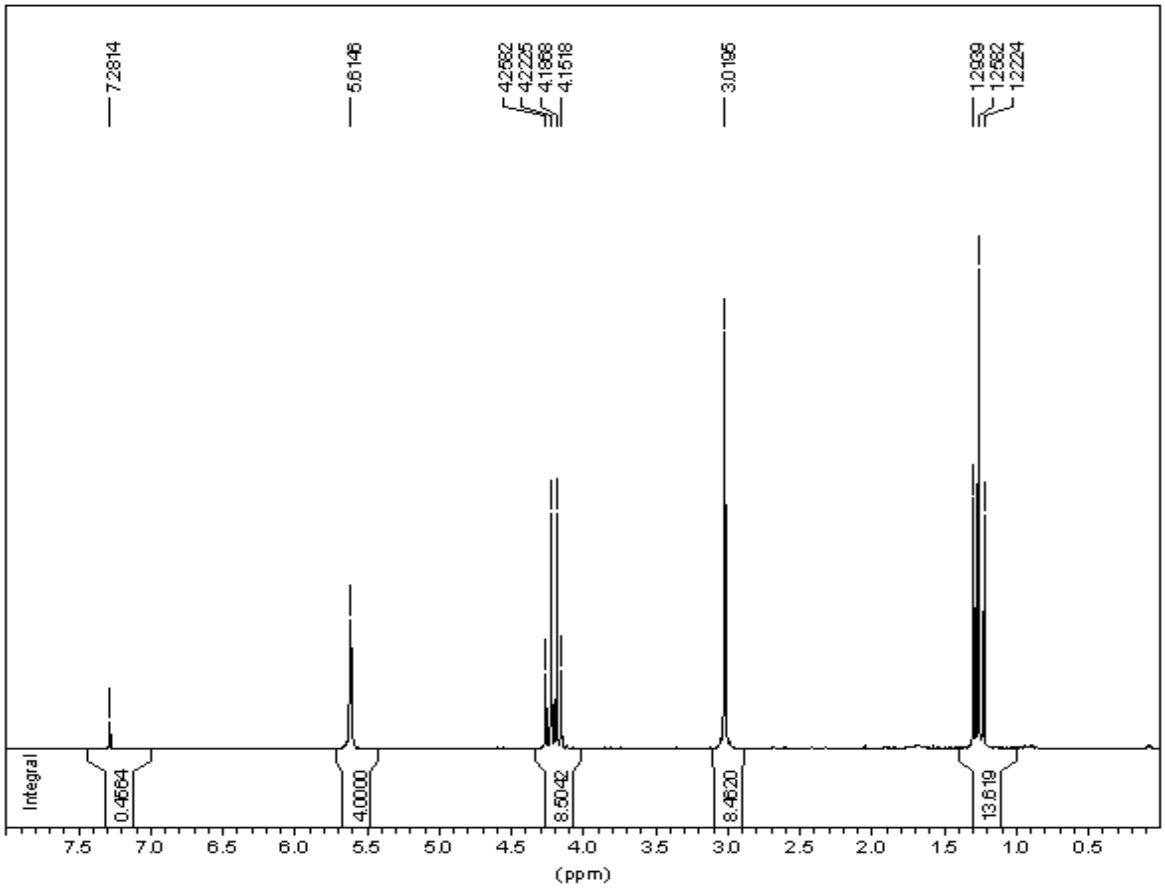

Fig. 3: ^{1}H NMR spectrum of entry **C** showing the ^{1}H RMN spectrum of **12** ($CDCl_3$, 300 MHz) δ_{ppm} : 5.61 (s, 2H), 4.26 (m, 4H), 3.02 (s, 4H), 1.29 (m, 6H)

Chromatographic data for the substrates and reaction products

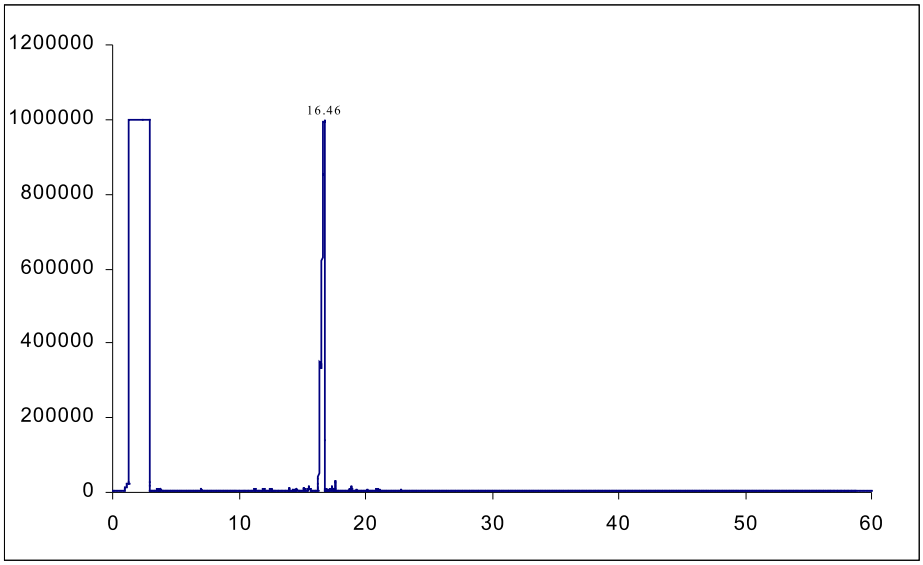

Fig. 4: GC of **2**

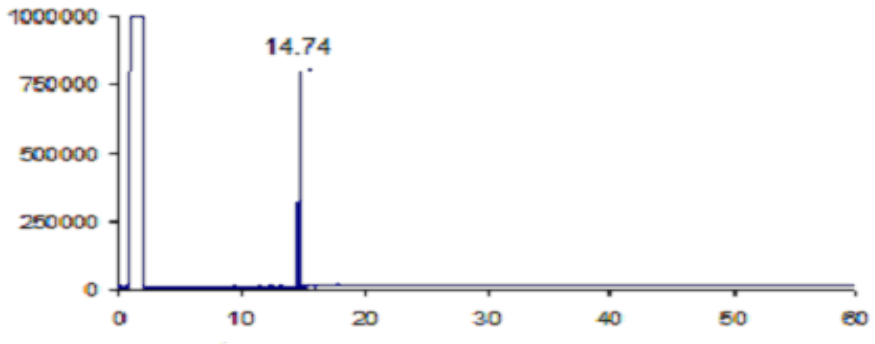

Fig. 5: GC of entry **B**

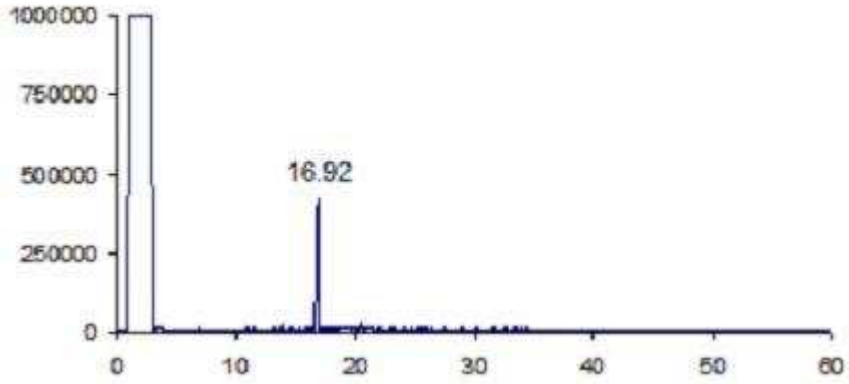

Fig. 6: GC of **5**

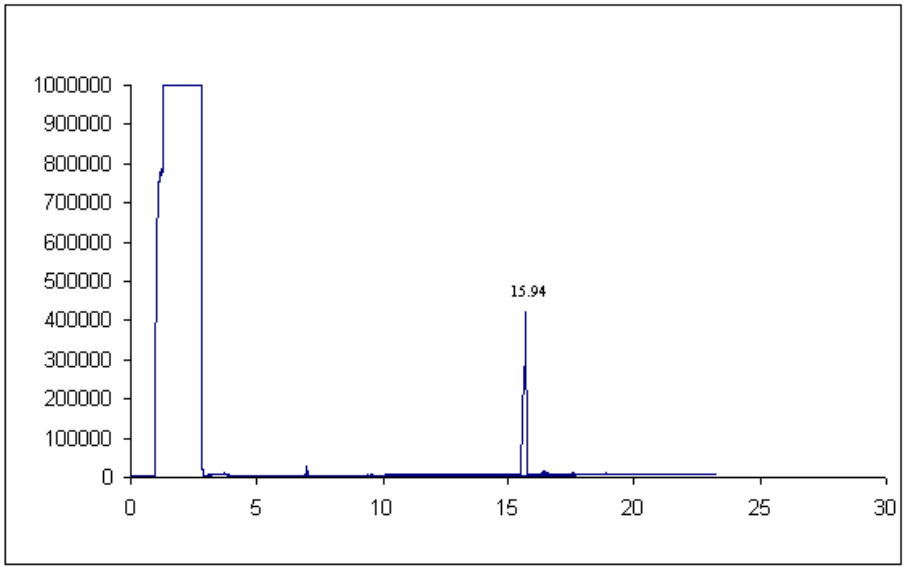

Fig. 7: GC of entry **E**

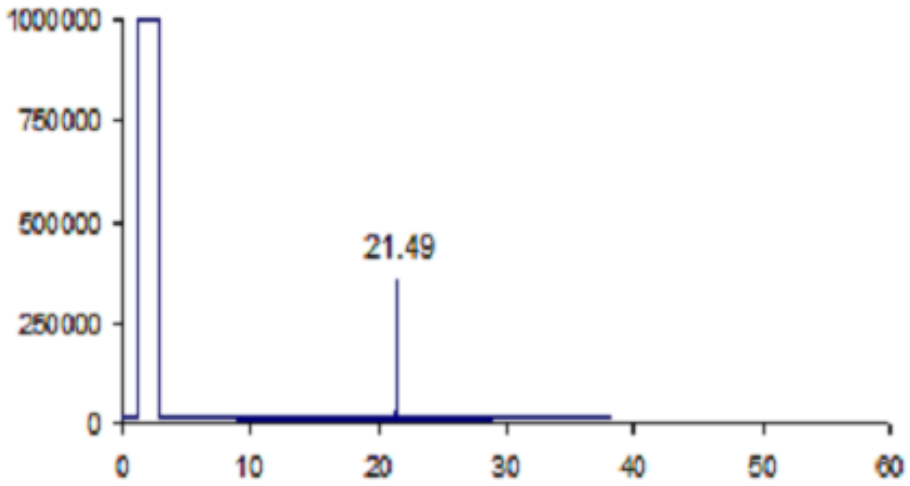

Fig. 8: GC spectrum of **6**

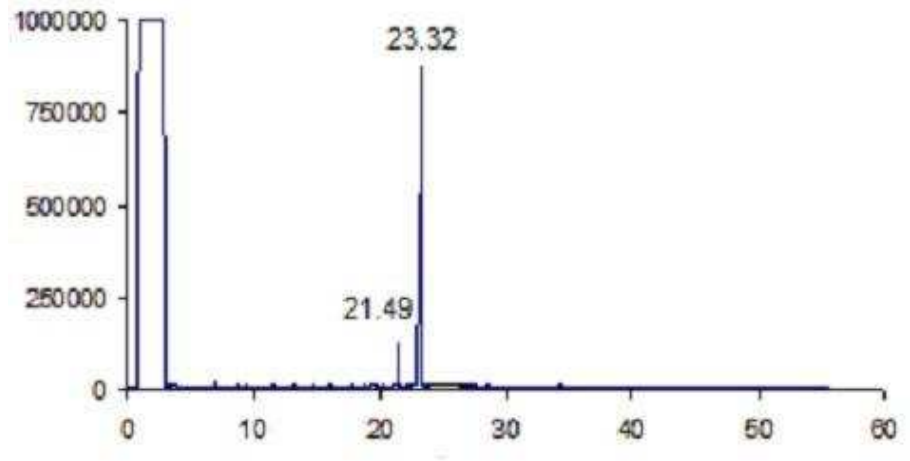

Fig. 9: GC spectrum of entry **F**

References (SI)

(S1) J. M. Berlin, K. Campbell, T. Ritter, T. W. Funk, A. Chlenov, R. H. Grubbs, *Org. Lett.* **2007**, *9*, 1339-1342.

(S2) J. D. Moore, R. J. Byrne, P. Vedantham, D. L. Flynn, P. R. Hanson, *Org. Lett.* **2003**, *5*, 4241-4244.

(S3) H. Clavier, S. P. Nolan, *Chem. Eur. J.* **2007**, *13*, 8029-8036.

PARTIE B :

LES APPLICATIONS BIOMEDICALES DES NANOPARTICULES D'OR

Chapitre B-1

Revue sur les nanoparticules d'or en nanomédecine

Cette revue a été écrite dans l'objectif de regrouper les dernières avancées scientifiques des nanoparticules d'or dans le domaine de la nanomédecine. Elle a été publiée cette année dans un numéro spécial du journal *Chemical Society Review* à l'occasion du 65ème anniversaire du Docteur Jean-Pierre Sauvage.

Grâce à leurs multiples propriétés, notamment celles dues à leur bande plasmon, les nanoparticules d'or possède aujourd'hui un rôle très prometteur dans les applications biomédicales.

Cette revue détaille les différentes synthèses et caractérisations des nanoparticules d'or ainsi que les différents assemblages et conjugaisons réalisés avec des ligands biologiques et biocompatibles. En effet, des nanoparticules d'or médicalement intéressantes peuvent être préparées et stabilisées avec un grand nombre de ligands selon les propriétés requises. Les meilleurs stabilisants de surface sont les thiolates qui permettent à ces nano-objets d'être stables dans un large laps de temps et dans différentes conditions biologiques ou non.

La bande plasmon de ces nanoparticules leur permet d'être utilisées pour le marquage, l'imagerie, la reconnaissance optique et électrochimique, le diagnostic et la thérapie.

Ces nouveaux vecteurs sont également utilisées dans de nombreuses études portant sur la délivrance de gènes et sur la vectorisation de médicaments agissant sur les cancers, la maladie d'Alzheimer, le virus HIV, la tuberculose, l'arthrite, les diabètes et d'autres maladies. La délivrance de médicaments (à la fois de médicaments d'origine chimique, naturelle et aussi de l'ADN) apparaît comme une des applications futures des nanoparticules d'or les plus prometteuses, comme le démontre grand nombre d'articles publiés sur ce sujet récemment.

Ces nanoparticules peuvent être analysées selon plusieurs techniques d'analyse modernes telles que l'imagerie par résonance magnétique, la diffusion Raman exaltée de surface ou encore par différentes techniques d'optique, de fluorescence et électrochimiques.

La partie thérapie est largement développée car il existe un grand nombre de traitements en étude avec ces nanoparticules d'or tels que la thérapie photothermique du cancer, de l'angiogénèse, de l'arthrite rhumatologique, anti-bactérienne et par vectorisation des médicaments. De plus, il est montré dans la partie traitant de la thérapie du cancer que l'irradiation photothermique des nanoparticules d'or dans le proche infra-rouge permet de combiner à la fois le diagnostic et la thérapie sélective, technique également applicable à d'autres maladies.

Une dernière partie porte sur la toxicité de ces nanoparticules avec le détail des dernières études réalisées *in vitro* et *in vivo,* et cette partie est assez encourageante quand aux applications futures en nanomédecine des nanoparticules d'or. En effet, ces nano-objets ont une toxicité relativement faible, voir nulle, car la plupart des tests de cytotoxicité rapportent des résultats cytotoxiques négatifs.

Cette revue a donc été essentielle pour visualiser l'impact des propriétés des nanoparticules d'or dans le domaine de la nanomédecine et nous a permis de mener des recherches appropriées en considérant à la fois les multiples propriétés de ces nanoparticules d'or, mais aussi les besoins de la médecine d'aujourd'hui.

Chem Soc Rev

This article was published as part of the

2009 Themed issue dedicated to
Professor Jean-Pierre Sauvage

Guest editor Professor Philip Gale

Please take a look at the issue 6 table of contents to access the other reviews.

Gold nanoparticles in nanomedicine: preparations, imaging, diagnostics, therapies and toxicity†

Elodie Boisselier and Didier Astruc*

Received 12th January 2009
First published as an Advance Article on the web 21st April 2009
DOI: 10.1039/b806051g

This *critical review* provides an overall survey of the basic concepts and up-to-date literature results concerning the very promising use of gold nanoparticles (AuNPs) for medicinal applications. It includes AuNP synthesis, assembly and conjugation with biological and biocompatible ligands, plasmon-based labeling and imaging, optical and electrochemical sensing, diagnostics, therapy (drug vectorization and DNA/gene delivery) for various diseases, in particular cancer (also Alzheimer, HIV, hepatitis, tuberculosis, arthritis, diabetes) and the essential *in vitro* and *in vivo* toxicity. It will interest the medicine, chemistry, spectroscopy, biochemistry, biophysics and nanoscience communities (211 references).

1. Introduction

Medicinal problems are a quest of all civilizations. Since nanoscience is one of the major areas of present scientific progress, it should shortly result in essential advancement for the benefit of human health. The biomedical applications of metal nanoparticles started in the 1970s with the use of nanobioconjugates after the discovery of immunogold labeling by Faulk and Taylor.[1] Traditional imaging techniques remain crucial in diagnostic, and AuNPs proves to be superior to classic chemicals. Subsequently, nanostructures have been introduced in a broad range of biological applications.[2–5] Supramolecular chemistry principles have also catalyzed major advances in this area including both imaging and sensors using biological host–guest recognition of biomolecules.[6] Presently, research is now also emphasizing drug vectorization[7–9] along with physical methods such as electron microscopy and spectroscopy.[10] Nanotechnology is bringing a key contribution, a crucial property being the plasmon absorption and scattering of AuNPs. It is involved particularly in both the photodiagnostics and photothermal therapy of cancers and other main diseases.[8] The goal of drug vectorization, promised to a bright future, is to diminish or suppress side effects due to toxicity, improve therapeutic efficiency and biodistribution, and overcome the problems of solubility, stability and pharmacokinetics of drugs.[9,10]

In this critical review, we will concentrate our attention on AuNPs, also including non-spherical AuNPs, in biochemistry and nanomedicine with emphasis on the above areas. This broad field presently involves a considerably increasing number of publications, thus we will focus on major ideas and most recent studies.

2. Gold nanoparticles (AuNPs) and bioconjugate chemistry

Gold was discovered in Bulgaria five thousand years ago, and the ancient colloidal gold must have first appeared in antiquity in China and Egypt for therapeutic and decorative purposes. A famous example is the Lycurgus cup, from the 4th century, visible at the British Museum in London. Gold colloids have

Institut des Sciences Moléculaires, UMR CNRS No. 5255, Université Bordeaux I, 33405, Talence Cedex, France. E-mail: d.astruc@ism.u-bordeaux1.fr

† Dedicated to our distinguished colleague Dr Jean-Pierre Sauvage at the occasion of his 65th birthday.

Elodie Boisselier

Elodie Boisselier obtained her bachelor of science degree in biochemistry from the Université Bordeaux II. She is presently studying for a PhD under the guidance of Professor Didier Astruc at the Université Bordeaux I in the area of Au nanoparticles. Her interests are in the synthesis and biomedical applications of Au nanoparticles.

Didier Astruc

Didier Astruc is Professor of Chemistry at the Université Bordeaux I and Member of the Institut Universitaire de France. He did his PhD in Rennes with R. Dabard and his postdoctoral work at MIT with R. R. Schrock. His present interests are in dendrimers and nanoparticles and their applications in catalysis, molecular materials science, and nanomedicine.

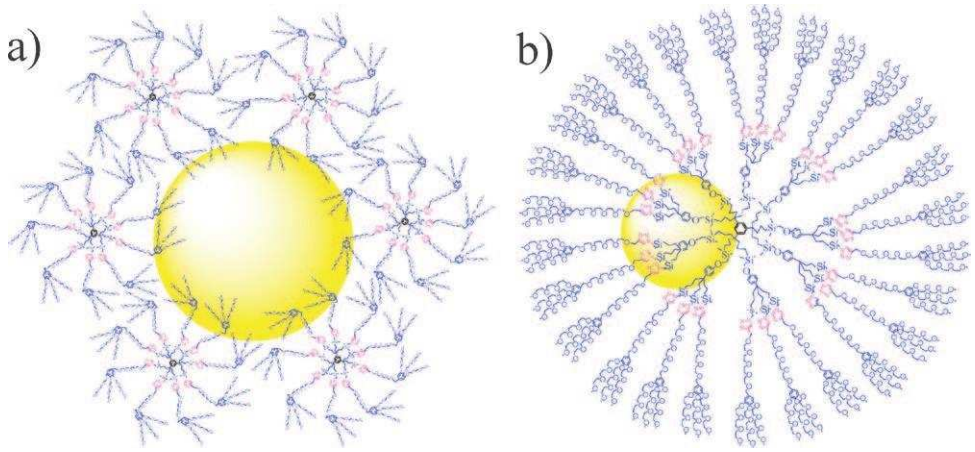

Fig. 1 (a) AuNPs stabilized by several G_0 dendrimers; (b) G_1-dendrimer-encapsulated AuNPs. Reprinted with permission of the Royal Society of Chemistry (ref. 24, Astruc's group).

been recommended for curing various diseases over the centuries and till recently, although the mechanisms of action are still poorly understood. In 1857, Faraday reported the first scientific article on AuNPs, attributing the red color to the colloidal nature of AuNPs,[11] and in 1908 Mie rationalized their visible absorption using Maxwell's electromagnetic equations.[12] AuNPs are available in the range from 1 to more than 120 nm, and their plasmon band visible absorption can be observed above 3 nm (*vide infra*). They disclose considerable applications in optics, catalysis, materials science and nanotechnology also including biology and nanomedicine.[13]

There are a large number of ways to synthesize AuNPs most of the time starting from commercial $HAu^{III}Cl_4$.[14] Citrate reduction of Au^{III} to Au^0 in water was introduced by Turkevitch *et al.* in 1951,[15] a method that is still used nowadays to subsequently replace the citrate ligand of these AuNPs by appropriate ligands of biological interest.[13] Recent modifications of the Turkevitch method have allowed better size distribution and size control within the 9–120 nm range.[16]

Although AuNPs can be stabilized by a large variety of stabilizers (ligands, surfactants, polymers, dendrimers, biomolecules, *etc.*),[13] the most robust AuNPs were disclosed by Giersig and Mulvaney to be stabilized by thiolates using the strong Au–S bond between the soft acid Au and the soft thiolate base.[17] Along this line, by far the most popular synthetic method using such sulfur coordination for AuNP stabilization is the Shiffrin–Brust biphasic synthesis using $HAuCl_4$, a thiol, tetraoctylammonium bromide and $NaBH_4$ in water–toluene yielding thiolate-AuNPs.[18] Functional thiolates can also be introduced using this method or upon subsequent bimolecular substitution of a thiolate ligand by such a functional thiol:[19]

$$(RS)_nAuNP + mR'SH \rightarrow (RS)_{n-m}(R'S)_mAuNP + mRSH$$

Oligonucleotides, peptides and PEGs are easily attached to AuNPs in this way. Since the solubility of these AuNPs is controlled by the solubilizing properties of the terminal group of the thiolate ligands, AuNPs can be transferred from an aqueous phase to an organic phase or *vice versa* by appropriate ligand exchange. Water-soluble AuNPs typically contain terminal carboxylate groups at their periphery. The carboxy group is used to attach the amino groups of biomolecules using 1-ethyl-3(3-dimethylaminopropyl)-carbodiimide-HCl abbreviated EDC (bioconjugate chemistry).[20]

Another useful protocol consists in using the famous "click" reaction linking a terminal alkyne and an azide.[21] The excellent efficiency of this method has recently been demonstrated.[22] A way to form AuNPs made of a precise number of metal atoms consists in using dendrimers containing a pre-organized number of internal ligands, which leads to dendrimer-encapsulated AuNPs (Fig. 1).[23,24] Super robust AuNPs, stable in the pH 1–14 range and under NaCl concentrations up to 5 M, were synthesized using PEG sorbitan fatty acid esters functionalized with lipoic acid. These scaffolds show both strong coordination through the chelating thiols and van der Waals interactions.[25]

Very interestingly, not only spherical AuNPs are synthesized, but also the shapes of the nanoparticles can be varied using appropriate techniques. In particular, Au nanorods (AuNRs) with controlled aspect ratio (*i.e.* the ratio of the length along the long axis to the short axis) in the range of 2–6 have been synthesized using the micelle-templated seed and feed technique developed by the groups of Murphy[26] (Fig. 2) and El Sayed,[27] and the Halas' group has developed the synthesis of Au nanoshells (AuNSs) composed of a silica core (100–200 nm in diameter) surrounded by a thin Au layer (5–20 nm).[28] Citrate-capped AuNPs and AuNSs as well as cetyl trimethylammonium bromide (CTAB)-capped AuNRs are not stable in the presence of a buffer solution, because salt ions have an aggregating effect, but these AuNPs are readily stabilized by thiol-functionalized PEG ligands.[29] The Murphy group has successfully engineered the surface chemistry of AuNRs. Thus, long AuNRs were obtained (500 nm long, 20 nm wide). The cationic surfactant used in the synthesis remains on the sides of the AuNR in the form of a bilayer resulting in a cationic charge to the AuNR, leaving the AuNR ends available for subsequent reaction. Bifunctional thiols such as biotin-disulfide can be bound to the Au(111) crystal face on the AuNR ends, whereas the CTAB bilayer is maintained on the AuNR sides. Addition of streptavidin further leads to end-to-end linkage of the AuNRs. Similarly,

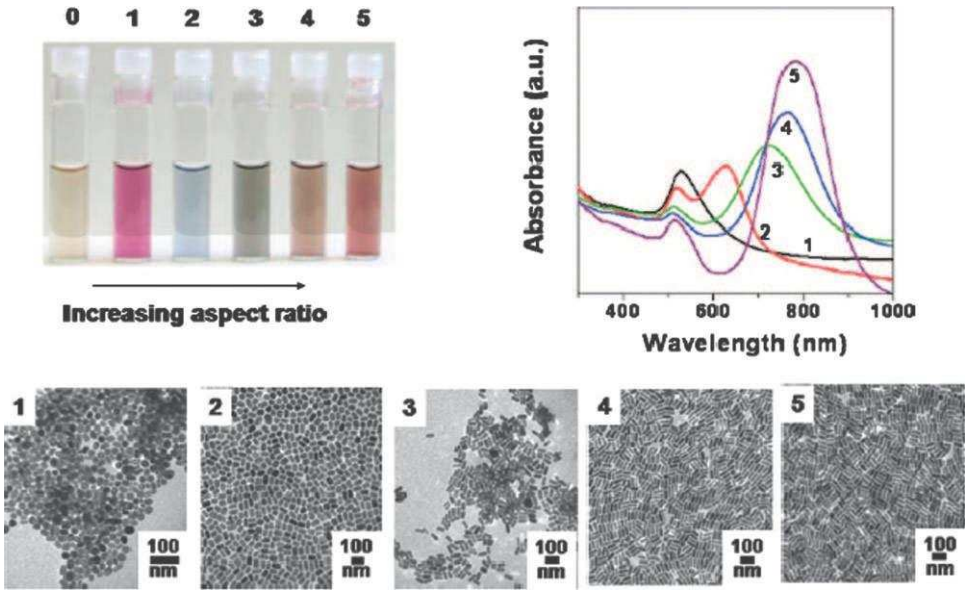

Fig. 2 The optical properties of gold and silver nanoparticles change drastically with nanoparticle shape. The photograph shows aqueous solutions of 4 nm gold nanospheres (vial 0) and progressively higher aspect ratio gold nanorods (1–5). The optical spectra and transmission electron micrographs for the particles in vials 1–5 are also shown. Scale bars in micrographs are all 100 nm. Reprinted with permission of the Royal Society of Chemistry (ref. 26, Murphy's group).

mercaptopropionic acid preferentially binds the AuNR ends leading to end-to-end bonded AuNRs linked by hydrogen bonds. Upon using Ag(I),[26] Guyot-Sionnest also grew AuNRs, because Ag(I) selectively slows down the growth of these AuNRs at faces that are less energetically favorable with "under-potential" Ag(0) deposition.[30]

In summary, the affinity of the surface of AuNPs having various sizes and shapes for thiols, disulfides, dithiocarbamates and amines allows facile bioconjugation with a variety of biomolecules. In particular, AuNPs conjugation with thiolated PEG masks them from the intravascular immune system and multifunctionalization for drug delivery is possible.[31] Since surfactants including CTAB have been found to be cytotoxic, other types of stabilization have been searched. For instance non-toxic liquid crystals have been used especially if the $NaBH_4$ reduction that leaves boride contamination can be avoided. Thus, liquid-chlorin photosensitizers based on purpurin-18 from green algae *Spirulina maxima* and choline hydroxide were recently used to synthesize AuNPs in the absence of surfactant and other reducing agent.[32]

3. The surface plasmon resonance (SPR) of AuNPs

According to the Mie theory,[12] an electromagnetic frequency induces a resonant coherent oscillation of the free electrons, called the surface plasmon resonance (SPR), at the surface of a spherical NP if it is much smaller than the light wavelength. This absorption lies in the visible region for Au, Ag and Cu. For metal nanoparticles, the localized surface plasmon resonance results in an enhanced electromagnetic field at the metal nanoparticle surface. The plasmon resonance of AuNPs[32] is observed down to 3 nm diameter, below which the AuNP can no longer be considered as a piece of metal with a conduction band but becomes a molecule depicted by molecular orbitals (then the term cluster should be used rather than nanoparticle). As a result, an enhanced electromagnetic field appears at the AuNP surface above this size allowing surface-enhanced optical properties revealed using spectroscopic techniques. Thus, the extinction coefficients of the SPR bands are extremely high, up to 10^{11} M^{-1} cm^{-1}, which is several orders of magnitude larger than those or all the organic dyes. AuNPs give rise to both absorption and scattering whose proportions depend on the AuNP size. AuNPs with a diameter smaller than 20 nm essentially show absorption, but size increase to 80 nm also increases the ratio of scattering to absorption. A high scattering cross section is indeed required for biological imaging based on light scattering.

For spherical AuNPs of 5 nm diameter, the surface plasmon band is located at 520 nm in ethanol, but it is very sensitive to the composition, size, shape, inter-particle distance and environment (dielectric properties) of the AuNPs. It is the high sensitivity to these factors that makes the basis of their use for biological labeling, detection, diagnostic and sensing. For instance, 5-nm AuNPs are orange-red, but they turn blue-purple upon aggregation (network formation) to larger AuNPs. Likewise, a change of refractive index of the solvent shifts the plasmon band. From the Mie theory, it follows that the frequency of the plasmon band varies from spherical to non-spherical nanoparticles of various shapes (rods, prisms, triangles, tetrapods, dogbones, cubes, shells). For instance, with AuNRs, two plasmon bands are observed, one corresponding to oscillations along the length of the AuNR (longitudinal plasmon band) and the other along the width of the AuNR (transverse plasmon band). The positions of these two bands vary with the AuNR aspect ratio. Thus AuNRs exhibit plasmon bands with maxima around 500 and

1600 nm. Since the ratio influences the position of the plasmon band absorption, the syntheses of AuNRs can be adjusted with suitable ratio so that they correspond to commercial lasers (*e.g.* 360 nm, 785 nm and 1064 nm). Moreover, the shift of the plasmon band to the near-IR region for AuNRs allows obtaining a penetration into living tissues that is much deeper than that of visible light and exciting less background fluorescence. In addition the multi-component plasmon absorption provides richer information than the single visible band of spherical AuNPs. Similarly, the plasmon band of AuNSs is shifted to the near-IR region and can be tuned by adjusting the ratio of the thickness of the AuNS to the diameter of the silica pore. The Halas group has shown that the smaller this ratio, the more redshifted is the plasmon absorption of the AuNS.[28]

4. Labeling and imaging

4.1 General: the techniques

Beside the most routine technique, transmission electron microscopy (TEM) that uses the high atomic weight of Au, several imaging techniques involve the surface plasmon band. Large AuNPs (>20 nm) can be imaged using an optical microscope in phase contrast or differential interference contrast mode. Detection with an optical microscope only involves scattered light in dark-field microcopy. Small AuNPs only absorb light, provoking heating of the environment that can be detected by photothermal imaging that record local variations of the refractive index by DIC microscopy or by photoacoustic imaging using heat-induced liquid expansion.

Other techniques are (i) fluorescence microcopy that allows detection at the single particle level, as the above plasmon-based techniques, (ii) photothermal coherence tomography (OCT) that is an optical analogue to ultrasound with relatively good penetration depth (1–2 mm) and resolution (1–10 μm),[33] (iii) multiphoton SPR microscopy (when illuminated by laser light in resonance with their plasmon frequency, these AuNPs generate an enhanced multiphoton signal measured in a laser scanning microscope),[34] (iv) X-ray scattering, involving better contrast AuNP agents than organic molecules with high signal-to-noise ratio with X-ray computer tomograpy, and (v) gamma radiation using neutron activation.[20]

The traditional application called immunostaining involves antibody-conjugated AuNPs that bind antigens of fixed, permeabilized cells thereby providing visualization by contrast using TEM. On the other hand, diluted AuNPs labeled with antibodies can label the outer cell surface without fixation and permeabilization, so that the inter-particle distance is larger than the optical resolution limit, which leads to single-particle imaging of cell movement. Receptor molecules that are bound to the membrane are observed in this way by time-resolved imaging within the cell membrane using the above optical techniques.[20] Magnetic Resonance Imaging (MRI) can be enhanced with or without gadolinium, and the main techniques are now discussed below.

In summary, facile bioconjugation and the variety of traditional and modern techniques including in particular the spectroscopic ones related to the plasmon resonance make AuNPs a remarkable up-to-date tool as imaging label and contrast agent (Fig. 3).

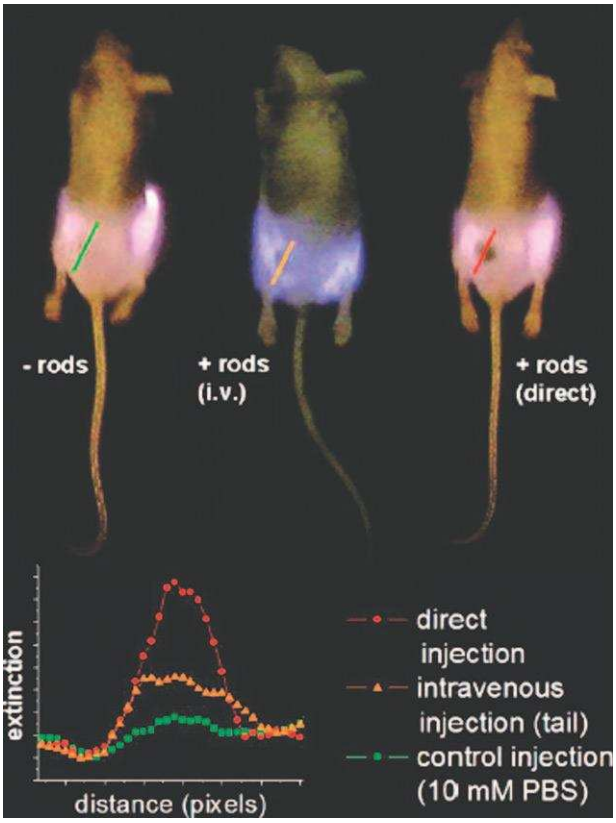

Fig. 3 NIR transmission images of mice *prior* to PPTT treatments. Inset shows intensity line-scans of NIR extinction at tumor sites for control (■), intravenous (▲), and direct (●) administration of pegylated gold nanorods. Control mice were interstitially injected with 15 μL 10 mM PBS alone, while directly administered mice received interstitial injections of 15 μL pegylated gold nanorods ($OD_{\lambda=800}$ = 40, 2 min accumulation), and intravenously administered mice received 100 μL pegylated gold nanorod ($OD_{\lambda=800}$ = 120, 24 h accumulation) injections. Reprinted with permission of Elsevier (ref. 37, El Sayed's group).

4.2 Enhancement of magnetic resonance imaging

The development of new contrast agents based on AuNPs for MRI is progressing fast. In addition to Gd chelates, several novel and highly efficient contrast agents were recently reported. The sensitivity of magnetic resonance imaging (MRI) can indeed be improved by using AuNPs as templating carriers of gadolinium chelates that are currently used for clinical diagnosis. Thus, the 2-nm-sized AuNPs carry about 150 ligands and exhibit a high relaxativity (r = 586 nM^{-1} s^{-1}) as compared to 3 nM^{-1} s^{-1} for the AuNP-free Gd chelate, which renders them very attractive as contrast agents for MRI (Fig. 4).[35]

The strong magnetism of magnetic NPs enhances MRI signals, and this property has recently been used. Iron oxide (Fe_3O_4) embedded in AuNP shells appears to be useful for this purpose, because the iron oxide provides magnetism, whereas the Au shell allows to use the optical properties of AuNPs.[36–38] In another study, Co@Pt-AuNPs with enhanced magnetism

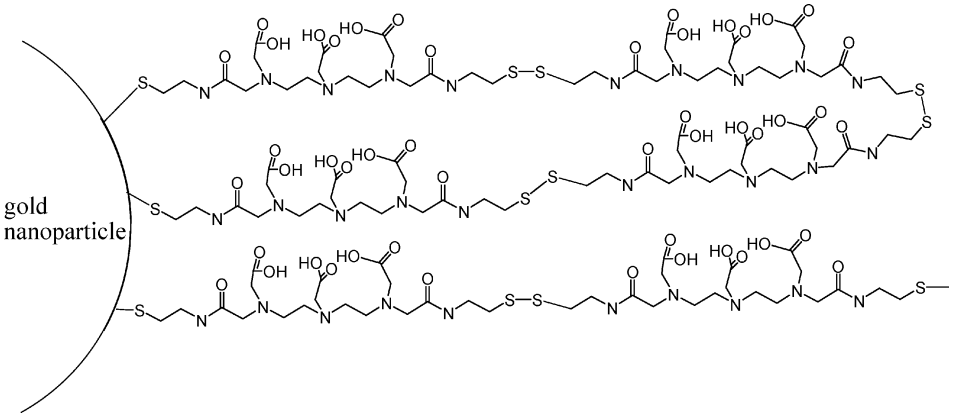

Fig. 4 Schematic illustration of the DTDTPA shell grafted onto gold nanoparticles (Au@DTDTPA). Reprinted with permission of Wiley InterScience (ref. 35, Roux's group).

and high stability were used. Binding to this AuNP surface is ensured using lipoic acid connected to neutravidin that shows strong interaction with biotin. These Co@Pt-AuNPs serve as MRI agents to monitor the structural evolution of Aß protofibrils, responsible for Alzheimer disease, in the early reversible stages. Magnetic NP-assisted MRI detection could also potentially be applied as sensitive probes of other proteins self-assemblies including prions, α-synuclein and Huntingtin.[39–41]

4.3 Surface-enhanced Raman scattering (SERS)

Molecules located on the AuNP surface are submitted to the large field caused by the plasmon resonance of the AuNP up to a distance of approximately 10 nm at most from the AuNP surface. Among the different spectroscopic techniques that characterize the electromagnetic field resulting from the plasmon resonance of AuNPs (surface-enhanced fluorescence, surface-enhanced Rayleigh scattering, surface-enhanced absorption and surface-enhanced Raman scattering, SERS), SERS is most attractive, because of the huge enhancement of the SERS signal, by a factor of *ca.* 10^{14}–10^{15}, which improves the detection limit from ensembles of molecules to the single-molecule level. The Raman effect in molecules that are not located at a metal nanoparticle surface is normally weak, because visible light that is not absorbed by this molecule is only weakly inelastically scattered off the molecular vibrations. The selection rule for Raman spectroscopy is the polarizibility change along the vibration, which usually provides only a weak Raman-active signal at usual concentration levels. Considerable enhancement occurs at the AuNP surface, however, because the intensity of the Raman signals depends on the fourth power of the local electric field that is very high at the AuNP surface due to the plasmon resonance. This enhancement also originates, in addition, from electronic coupling between adsorbed molecules and the AuNP surface resulting from charge transfer between the AuNP metal surface and adsorbed molecules. Since the selective enhancement of SERS is correlated with polarization-dependant resonance bands, amplified electromagnetic fields at AuNP junctions contribute to SERS. Thus, in addition to the *elastically* scattered visible light by the AuNPs themselves that can be imaged using a dark-field optical microscope, the AuNP surface provoke an *inelastic* SERS effect due to adsorbed molecules providing a Raman spectrum that leads to the identification of these molecules.[26] The two main strategies for SERS detection are (i) direct identification of Raman-active AuNP-adsorbed molecules and (ii) indirect detection of molecules incorporated into a biolabel. Interference from competing adsorbates can sometimes inhibit the

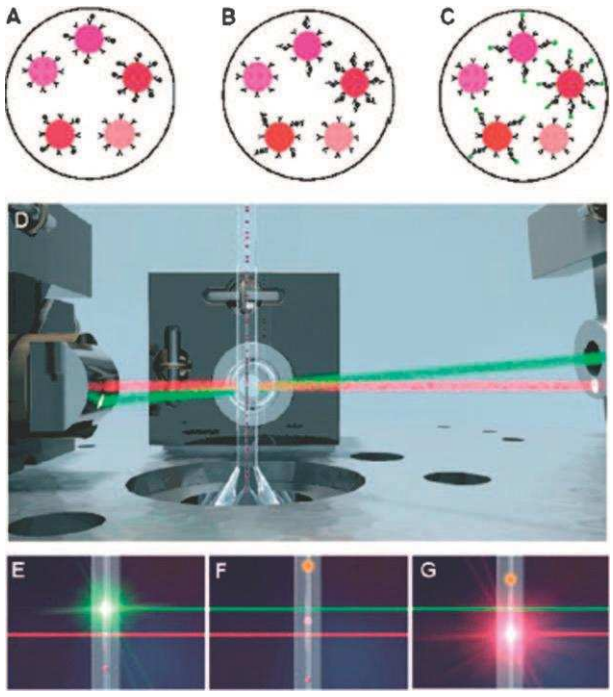

Fig. 5 This series of images show how multiplexed assays are carried out with a suspension array. (A) The suspension array, composed of encoded microspheres conjugated to capture antibodies, is mixed with a sample containing different cytokines. (B) The cytokines are sandwiched between the capture antibodies and the corresponding biotinylated detector antibodies. (C) Bound detector antibodies are labeled with fluorescent reporter molecules. (D) A stream of individual microspheres flows through the sensing points of a cytometer. (E–G) Images of a single encoded microsphere with bound reporter molecules as it flows past (E) a green laser that excites the reporters and (G) a red laser that excites the code. (Courtesy of Luminex Corp.) Reprinted with permission of Wiley InterScience (ref. 44, Wilson's group).

detection of molecules in complex solutions. The plasmon band can also be tuned from the visible region for spherical AuNPs to the NIR by changing the size (redshift with larger size), shape (AuNRs and AuNSs), aggregation (inter-AuNP distance lower than AuNP size) and medium (increase of the refractive index). A number of studies have optimized the SERS of small AuNP-adsorbed molecules with non-spherical AuNPs, and on the biological side El-Sayed *et al*. have recently shown that oral cancer cells can align AuNRs that have been conjugated with anti-epidermal growth factor receptor antibodies on the cell surface, leading to a SERS fingerprint specific of the cancer cells.[42] The Halas group has discriminated between acidic cancer cells and healthy cells by monitoring changes in the Raman spectrum induced by pH changes over a suitable range with carboxy groups of a mercaptobenzoic acid layer on AuNSs that were active in the NIR region where blood and tissues are less absorbing.[43]

The Wilson group has recently reported the use of this SERS method as signatures in multiplexed detection, based on the fact that each spectrum is unique and composed of multiple bands that are much narrower than those of fluorescent dyes or quantum dots (Fig. 5).[44] Wilson has reviewed this field,[45] and a number of companies have marketed Raman detectors, such as Oxonica (Oxford, UK), with biotags that detect up to three respiratory viruses in the same sample (Fig. 6).[46]

A few SERS applications of AuNPs follow. Mammalian cells surfaces were imaged using SERS with nitrile-functionalized AuNPs. SERS hot sites correlate well with small aggregated AuNPs oriented preferentially in the direction of incident laser polarization.[47] Spatially resolved probing and imaging of pH in live cells was demonstrated by SERS using 4-mercaptobenzoic acid-AuNP aggregates (Fig. 7).[48] AuNPs conjugated with heterofunctional PEG ligands allowed facile conjugation of ScFv antibody as a targeting ligand for SERS detection of small tumors (0.03 cm^3) at a penetration of 1–2 cm.[49] SERS imaging has been used for the targeting and highly sensitive imaging of specific cancer markers in live cells using core-shell Au-AgNPs conjugated with monoclonal antibodies (live HEK293 cells expressing PLCγ1) (Fig. 8).[50]

4.4 Optical biosensors

Parak indicated that, whereas labeling and imaging above use AuNPs in a passive way, sensing involves an active role of the AuNPs.[20] The AuNP-distance dependence of the analyte detection (antigens, nucleic acids, aptamers, enzymatic reactions) using the plasmon resonance as well as size and refractive-index dependence have recently been comprehensively reviewed by Wilson.[45] Thus, only some representative and new examples of plasmon-related sensors are illustrated below. The dramatic influence of the inter-AuNP distance on the plasmon resonance, when this distance is reduced to less than the AuNP diameter, is indeed the crucial factor in the sensor applications of AuNPs. Thus, linking AuNPs with a biological analyte results in color change that makes the basis of sensing, a principle pioneered by Leuvering,[51] for which sensitivity is now improved using hyper-Raleigh scattering (HRS), a differential light-scattering spectroscopy (DLSS).[52]

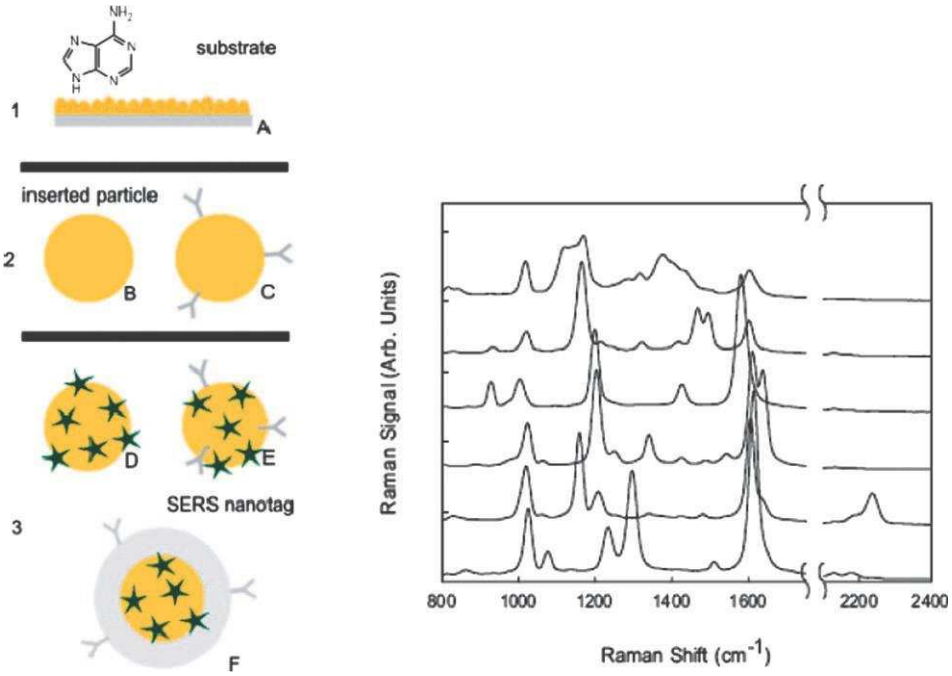

Fig. 6 Architectures used in SERS experiments. (A) 2D substrate with adenine on the surface. (B) Bare particle. (C) Antibody-targeted particle. (D) Reporter labeled particle. (E) Targeted and labeled particle. (F) Targeted particle with encapsulated Raman label. A Represents the substrate approach, B and C are examples of the inserted particle approach while D, E, and F can all be thought of as SERS nanotags/Raman spectra of six different Nanoplex biotags. From top to bottom, the label molecules used were 4-[4-hydroxyphenylazo]pyridine, 4,4′-azopyridine, d8-4,4′-dipyridyl, bis(4-pyridyl)ethylene, bis(4-pyridyl)acetylene, 4,4′-dipyridyl. Reprinted with permission of Wiley InterScience (ref. 46, Freeman's group).

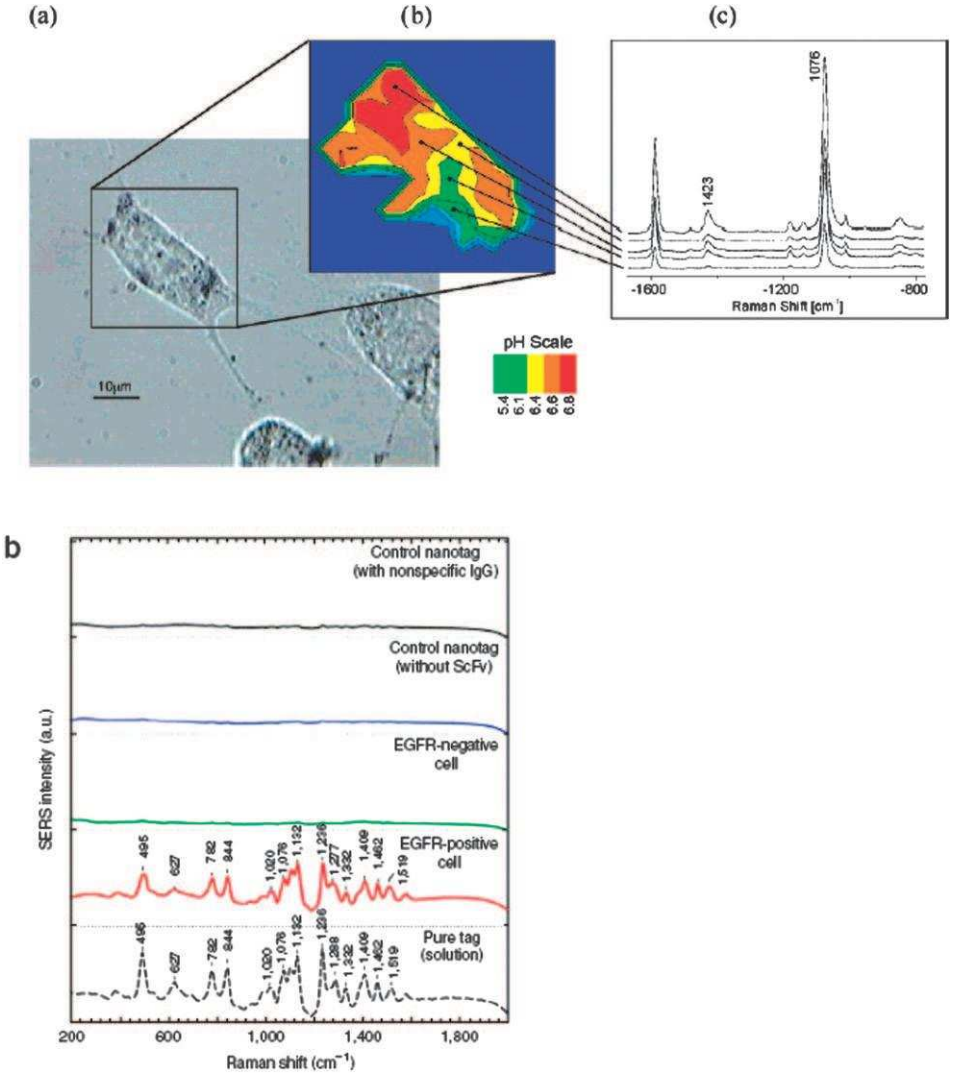

Fig. 7 Probing and imaging pH values in individual live cells using a SERS nanosensor. (a) Photomicrograph of an NIH/3T3 cell after 4.5 h incubation with the pMBA gold nanosensor. Numerous gold nanoparticles have accumulated in the cell, enabling pH probing in different endosomes over the entire cell based on the SERS signature of pMBA. Lysosomal accumulations can be observed as black spots at the resolution of the light microscope. (b) pH map of the cell displayed as false color plot of the ratios of the SERS lines at 1423 and 1076 cm^{-1}. The values given in the color scale bar determine the upper end value of each respective color. Scattering signals below a defined signal threshold (*i.e.*, where no SERS signals exist) appear in dark blue. (c) Typical SERS spectra collected in the endosomal compartments with different pH. The spectra were collected in 1 s each using 830 nm cw excitation (3 mW). Reprinted with permission of the American Chemical Society (ref. 48, Kneipp's group).

Mirkin and co-workers were the first to report colorimetric sensing of nucleic acids. Double-stranded DNA indeed link AuNPs with an inter-AuNP distance of only 0.34 nm causing a temperature-reversible red-to-purple color change. Each AuNP bears several oligonucleotides resulting in the formation of a network (aggregation) leading to the color change of the AuNPs to blue-violet, because of the reduced inter-AuNP distance.[53] Removing aliquots for spotting onto a C18 reverse-phase thin-layer chromatography plate as the temperature is increased results in a visual record of the color change that is known as the "*Northwestern spot test*", the most well-known example of AuNP-based sensor. The addition of complementary target oligonucleotide strand by hybridization can be colorimetrically detected also leading to specific melting-temperature test for mismatched DNA.[55–58] Indeed, even single DNA sequence mismatch results in a different disaggregation (melting) temperature provoking a color change.[59]

Studies of AuNP-DNA interactions have subsequently been pursued by several groups,[60–63] and quantitative detection of DNA sequences at very low concentration including detection of genetic mutations is now achievable using such a principle.[59] The Mirkin group has recently extended this method from specific detection of DNA sequences to a real-time screening assay for endonuclease activity.[60]

The Franco group has developed a non-cross-linking hybridization method also based on color changes, in which AuNP aggregation is induced by an increasing salt concentration. This method was used to detect eukaryotic gene expression (RNA) without need for retro-transcription

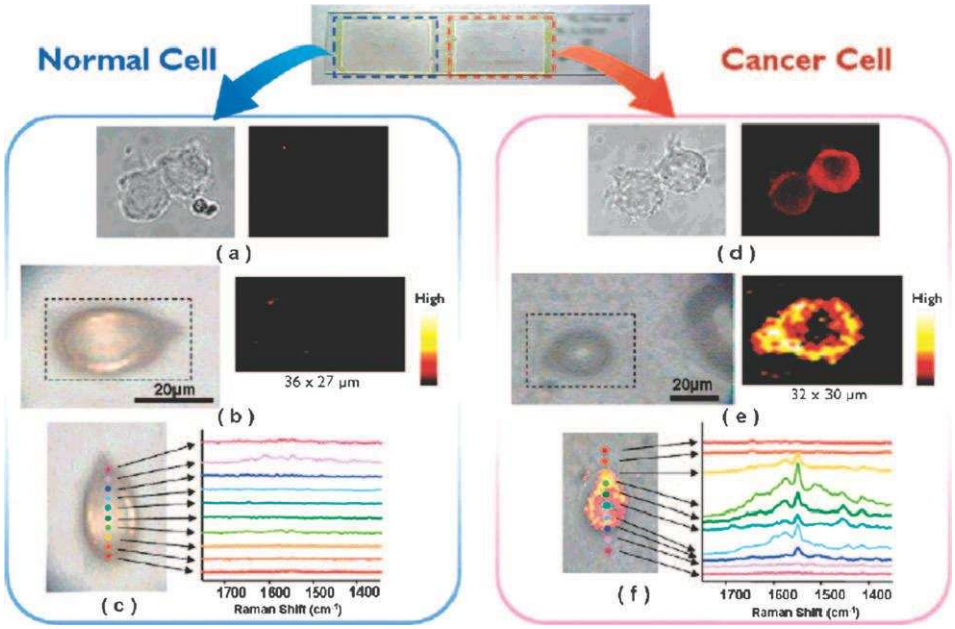

Fig. 8 Fluorescence and SERS images of normal HEK293 cells and PLCζ1-expressing HEK293 cells. (a) QD-labeled fluorescence images of normal cells: (left) brightfield image, (right) fluorescence image. (b) SERS images of single normal cell: (left) brightfield image, (right) Raman mapping image of single normal cell based on the 1650 cm^{-1} R6G peak. The cell area was scanned with an interval of 1 μm. Intensities are scaled to the highest value in each area. (c) Overlay image of brightfield and Raman mapping for single normal cell. Colorful spots indicate the laser spots across the middle of the cell along the *y* axis. (d) QD-labeled fluorescence images of cancer cells: (left) brightfield image, (right) fluorescence image. (e) SERS images of single cancer cell: (left) brightfield image, (right) Raman mapping image of single cancer cell based on the 1650 cm^{-1} R6G peak. The cell area was scanned with an interval of 1 μm. Intensities are scaled to the highest value in each area. (f) Overlay image of brightfield and Raman mapping for single cancer cell. Colorful spots indicate the laser spots across the middle of the cell along the *y* axis. Reprinted with permission of the American Chemical Society (ref. 50, Choo's group).

or PCR amplification. It was possible to detect mRNA from 0.3 μg of unamplified total RNA.[61] The detection of proteins and antibodies (anti-protein A, biotin and streptavidin and lectin) as well as molecules (adenosine, glucose) and metal ions (Pb, Hg, Cd, Li) has also been achieved using AuNPs in this way (Fig. 9).[26,62]

Although spherical AuNPs work well, non-spherical ones have also been used, the advantage being that the plasmon frequency can be finely adjusted with AuNRs and AuNSs. For instance, the Halas group has synthesized AuNSs with a 96-nm diameter and a 22-nm shell thickness to carry out distance-dependent immunoassays in dilute serum,[63,64] and the Murphy group has used biotin-avidin as a model system for optical detection of aggregated AuNRs (*i.e.* biotinylated AuNR aggregation upon addition of the protein streptavidin).[26,65] Other 3-D assemblies of AuNRs and AuN wires using DNA

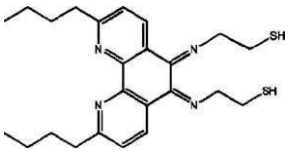

Fig. 9 Chemical structure of the modified 1,10-phenanthroline ligand that binds to gold nanoparticles through the thiols, and to lithium ion through the chelating phenanthroline nitrogens. Two ligands are required to bind to one lithium ion in a tetrahedral fashion. Reprinted with permission of the Royal Society of Chemistry (ref. 26, Murphy's group).

are known.[66–68] Transducers have been set up to detect streptavidin concentration through the specific recognition with biotin-conjugated AuNPs. Polyelectrolyte functionalization provides a simple way to conjugate AuNPs with charged molecules such as biotin.[69] Chilkoti *et al.* have tracked scattering changes at 780 nm from a single AuNR to sense streptavidin in nanomolar concentration, using a dark-field microscope (Fig. 10 and 11).[70]

Willner and co-workers reported the first example of AuNP combination with thiolated aptamers (*i.e.* DNA-, RNA- or peptide-based sequences) thereby showing how thrombin could be detected upon aptamer-conjugated-AuNP linking.[71] PEG-15-nm-AuNPs covalently bound to F19 monoclonal antibodies *via* terminal PEG carboxylate group were used to label stroma tumor in resected pancreatic adenocarcinoma, and the tissues were imaged by darkfield microscopy at 560 nm.[72] Wilson has summarized the methods of detection that involve separation steps including microsphere assays and planar support.[45] Detection methods based on separation, must be used to improve sensitivity when naked eye detection is insufficient. Deposition of Ag onto the AuNPs upon Ag(I) reduction, called Ag enhancement was pioneered by Mirkin's group.[73] It allows imaging with unaided eye as the spot size after enhancement reaches 200 nm (a technique improved upon replacing Ag by Au).[45] Unamplified DNA and RNA target sequences can be detected in the presence of genomic DNA in this way, and CCD cameras and CD players have been used for recording such biosensing events.[74] The easiest

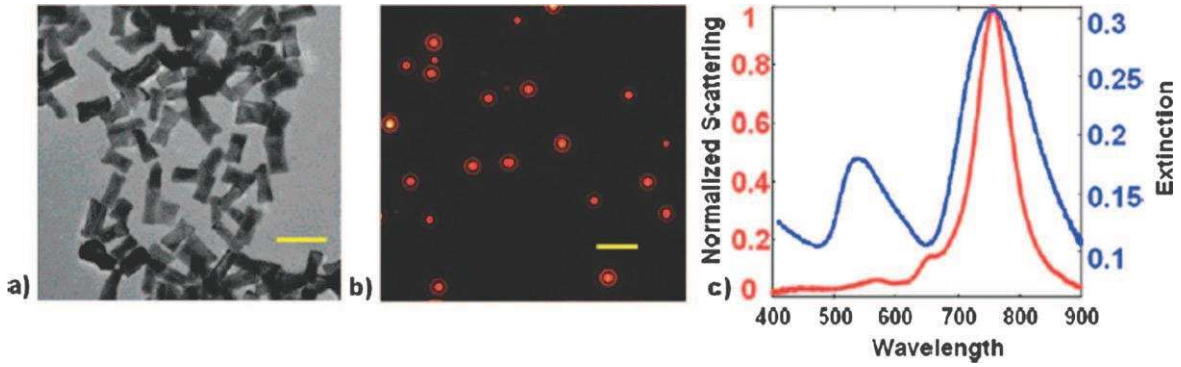

Fig. 10 (a) TEM of gold nanorods used for biodetection experiments and (b) dark-field micrograph of gold nanorods immobilized on a glass substrate. (c) Scattering spectra of a single gold nanorod on a glass substrate (red) and the extinction spectrum of an ensemble of gold nanorods suspended in water (blue). Scale bar is 100 nm in (a) and 5 μm in (b). Reprinted with permission of the American Chemical Society (ref. 70, Chilkoti's group).

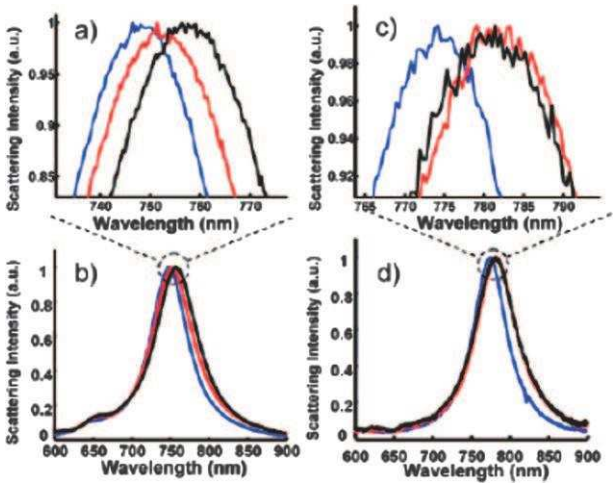

Fig. 11 (a and b) Scattering spectra of a single gold nanorod after sequential incubation in EG3SH/MHA (blue), biotin (red), and 10 nM streptavidin (black). (c and d) Scattering spectra of a single gold nanorod in EG3SH/MHA (blue), biotin (red), and 100 nM streptavidin presaturated with free biotin (black). Reprinted with permission of the American Chemical Society (ref. 70, Chilkoti's group).

AuNP supports are 0.5-μ-polystyrene microspheres, but assays also use planar supports (glass, nitrocellulose, nylon[45] and thin films[75]). Magnetic microspheres that facilitate separation of bound AuNPs have also been reported.[76] Other separation methods involve lateral flow devices for immunoassays, nucleic acid flow devices, flow-through devices, blots and arrays, silver-enhanced arrays, "biobarcode" (marker) assays, electrical detection, SERS and fingerprint detection.[45]

4.5 Fluorescence

Fluorescence of AuNPs includes fluorescence spectrometry, fluorescence correlation spectroscopy (FCS) and fluorescence microscopy. Especially, the fluorescence of AuNPs possesses the excellent behavior of antiphotobleaching under strong light illumination. Despite low quantum yields, AuNPs exhibit strong native fluorescence under relatively high excitation power. The fluorescence of AuNPs could be characterized by fluorescence imaging and FCS at the single-particle level. A new fluorescence method for cell imaging involves, after cells stained with AuNPs are illuminated with strong light, the fluorescence of AuNPs on cell membrane or inside cells that can be collected for cell imaging.[77]

Fluorescence Resonance Energy Transfer (FRET) is a spectroscopic technique whereby the excitation energy of the donor is transferred to the acceptor *via* an induced-dipole,

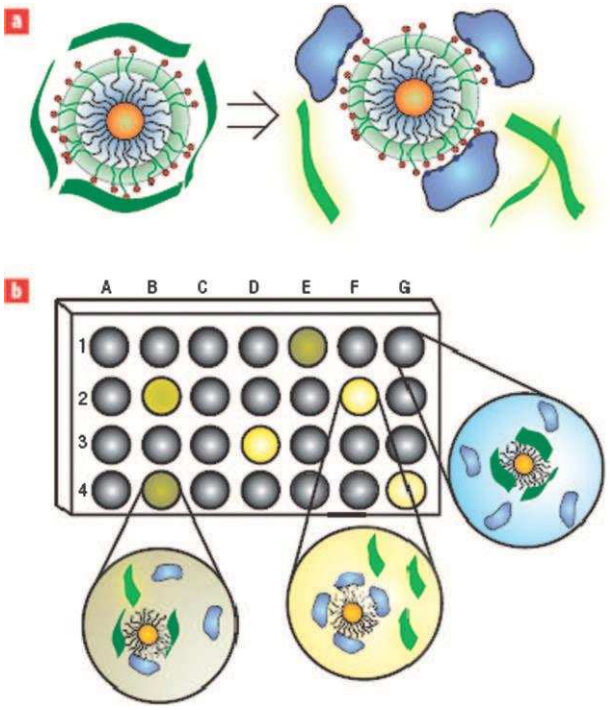

Fig. 12 Fluorophore displacement protein sensor array. (a) Displacement of quenched fluorescent polymer (dark green strips, fluorescence off; light green strips, fluorescence on) by protein analyte (in blue) with concomitant restoration of fluorescence. The particle monolayers feature a hydrophobic core for stability, an oligo(ethylene glycol) layer for biocompatibility, and surface charged residues for interaction with proteins. (b) Fluorescence pattern generation through differential release of fluorescent polymers from gold nanoparticles. The wells on the microplate contain different nanoparticle-polymer conjugates, and the addition of protein analytes produces a fingerprint for a given protein. Reprinted with permission of the Nature Publishing Group (ref. 80, Rotello's group).

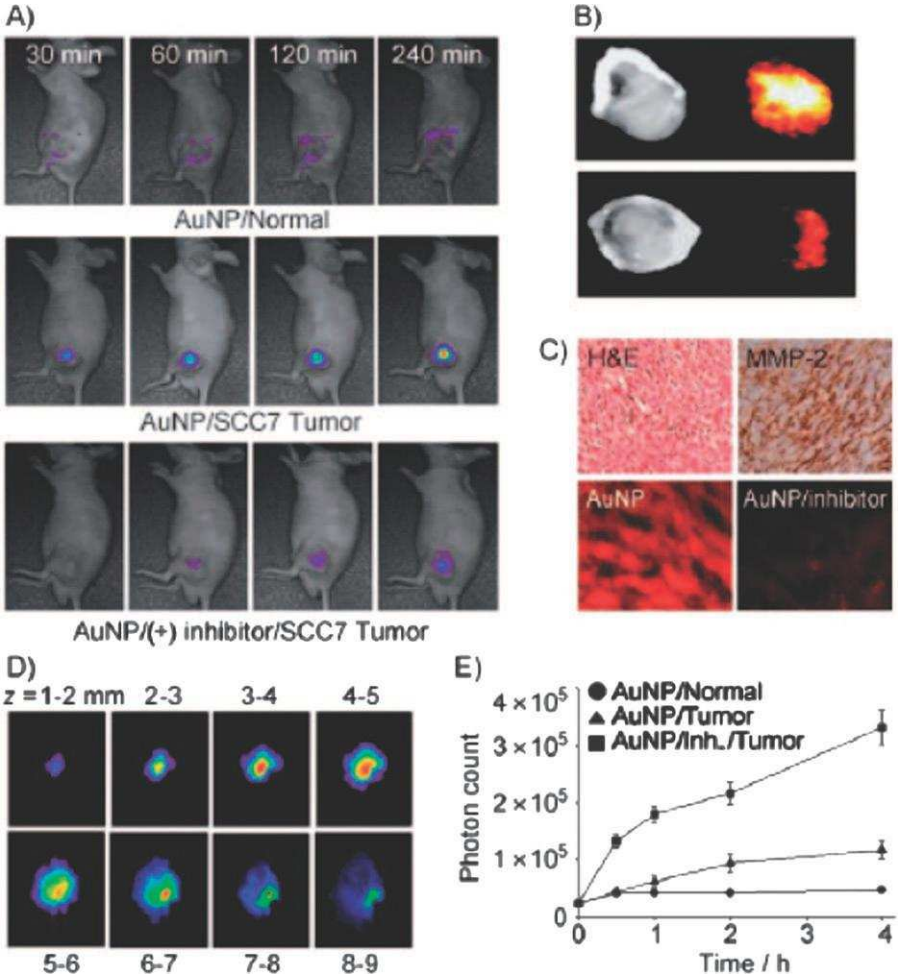

Fig. 13 (A) NIRF tomographic images of normal and subcutaneous-SCC7-tumor-bearing mice after injection of the AuNP probe with and without inhibitor (blue: low intensity, red: high intensity). (B) NIRF images of excised AuNP-probe-treated SCC7 tumors with and without MMP-2 inhibitor. (C) Immunohistology results for SCC7 tumors with MMP-2. H&E = Hematoxylin/eosin stain; lower row: NIRF microscopy of SCC7 tumors containing AuNP probes without and with inhibitor. (D) 2D slices of the image from (A) reconstructed in the *z* direction (blue: low concentration, red: high concentration). (E) Quantitative image analysis performed by counting the total number of photons in the tumors as a function of time. Reprinted with permission of Wiley InterScience (ref. 81, Ahn's group).

induced dipole interaction. The efficiency of energy transfer E is given by $1/1[1 + (R/R_0)^6]$ where R is the distance between the donor and the acceptor and R_0 is the distance at which 50% of the energy is transferred; thus small distance changes result in sizeable change in E. With AuNPs, at small distance (<1 nm), radiative rate enhancement is observed; at 2–3 nm, energy transfer dominates, and at large distances (>50 nm), fluorescence oscillations take precedence. AuNP-based FRET monitors DNA hybridization and DNA cleavage by nucleobases. For instance, after hybridization, by varying the DNA length, the separation distance between AuNP and Cy3 dye was systematically varied between 3 and 100 nm, and 50% quenching efficiency was observed even at 25 nm separation.[78] Fluorescent dyes and quantum dots are quenched by close proximity of AuNPs, even at distances larger than 2 nm. Quenching effects have even been shown to operate over much larger distances than the Förster resonance quenching transfer distance between dyes.[79] Therefore, increase of fluorescence is observed upon hybridization to a complementary nucleic acid sequence, because the fluorescent dye or quantum dot and the quencher are forced apart. In this way, large molecules such as proteins can be sensed, and Rotello *et al.* have applied this principle using a fluorescent polymer to decode the response produced by nanomolar concentrations of proteins in unknown samples based on selective AuNP-protein affinities (Fig. 12).[80] For instance, 20-nm AuNPs stabilized by Cy5.5-Gly-Po-Leu-Gly-Val-Arg-Gly-Cys-(amide) showing selectivity for a matrix metalloprotease served as fluorescent imaging probe for *in vivo* drug screening and protease activity (Fig. 13).[81]

4.6 Electrochemical biosensors

AuNPs are useful in electrochemical bioassays, in particular to connect enzymes to electrode surfaces, mediate electrochemical reactions as redox catalysts and amplify recognition signals for biological processes.[82] Their first use as labels for immunosensors was reported by the group of Degrand and Limoges,[83] which was followed by hundred of electrochemical bioassay articles including excellent reviews.[84–86] The two

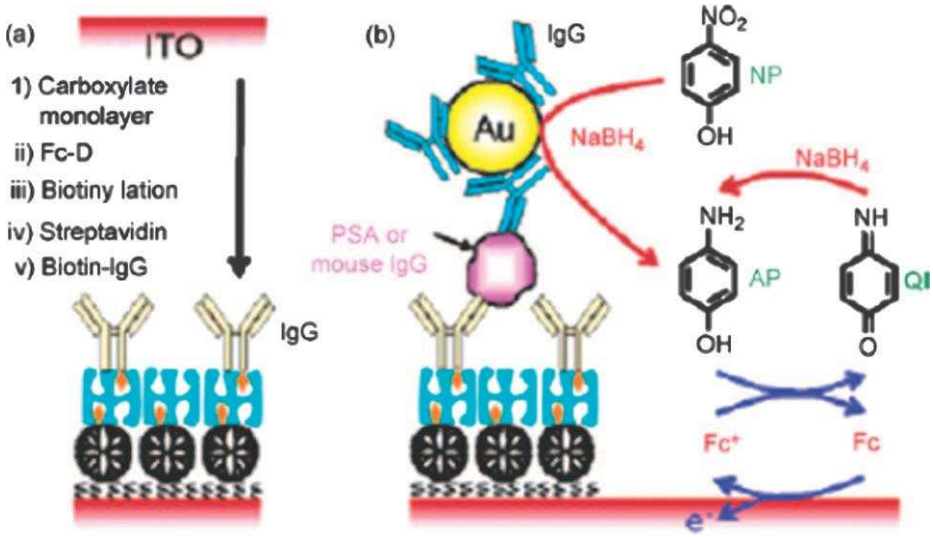

Fig. 14 (a) Schematic representation of the preparation of an immunosensing layer. (b) Schematic view of electrochemical detection of mouse IgG or prostate specific antigen. Reprinted with permission of the American Chemical Society (ref. 85, Wang's group).

main research areas are AuNP nanoelectrodes for bioassays and AuNPs as biomolecular tracers, and in both of them applications are found in enzymatic biosensing, genosensing and immunosensing.

As a representative example, AuNPs are used as wires connecting electrode surfaces to the redox center of enzymes. Fixation of the AuNPs onto the electrode surface provides a microenvironment comparable to that of redox proteins and more protein freedom for orientation. In this way, the insulation by the protein shell is reduced, and electron transfer can occur through the conducting tunnels of the AuNPs (Fig. 14).[85] Thus, AuNPs attached to enzymes such as, typically, glucose oxidase (GO), serve as nanoelectrodes so that the turnover rate of electrons transferred *via* AuNPs to the electrode surface reaches about 5000 which is seven times higher than the turnover rate of electrons from the active site of GO to O_2.[87–89] As an amperometric and potentiometric immunosensor example, multilayer films of negatively charged AuNPs/positively charged tris(2,2′-bipyridyl)cobalt(III) were assembled on a Pt electrode surface covered with a layer of plasma-polymerized Nafion film for hepatitis B surface antigen determination.[90–92]

For genosensor applications (DNA electrochemical sensing), AuNPs modified with thiol-functionalized oligonucleotides were submitted to hybridization of the target DNA sequence. This type of assay relies on the release of AuNPs by oxidative metal dissolution and indirect determination of the HBr solubilized Au(III) ions by anodic stripping voltammetry.[93,94] Subsequently, methods based on the direct electrochemical detection of the AuNP tag were developed in order to avoid the high toxicity of the HBr/Br_2 oxidant.[95,96] A signal amplification strategy consists in attaching ferrocenylhexanethiol or electrogenerated chemiluminescence (ECL) indicator to the AuNP label. AuNP-streptavidin conjugate to which 6-ferrocenylhexanethiol was bound were attached onto a biotinylated DNA detection probe of a sandwich DNA complex. A detection limit of 5×10^{-12} mol L^{-1} for target DNA was reached.[97] The use of AuNPs for "fingerprint" detection involves immersion of a substrate in AuNPs at low pH provoking electrostatic binding to the print that is enhanced by catalytic deposition of Ag or better, Au.[98]

AuNPs bearing alkylthiolate ligands terminated with redox centers[99,100] proved to be useful for the redox recognition, sensing and titration of ATP^{2-},[101,102] an electrochemical method based on the shift of redox potential of the redox system attached to the ATP recognition site (ferrocenylsilyl or amido-Fe_4 cluster).[103] AuNP-centered dendrimers are most useful for this type of sensing, because the positive dendritic effect (increase of potential shift as the dendrimer generation increases) facilitates sensing.[104] Large dendritic AuNPs adsorb so strongly on Pt electrodes for sensing using the AuNP-dendrimer-modified electrode that the modified electrodes are robust enough to be washed for further re-use.[104]

5. Clinical diagnostics

5.1 General

AuNPs have been used as radioactive labels *in vivo* since the 1950s, and immuno-AuNPs conjugated to antibodies have been used since the 1980s for biological staining in electron microscopy. They present several advantages in biodiagnostic over quantum dots and organic dyes: (i) much reduced or no toxicity (*vide infra*), (ii) much better contrast agents for imaging (compare with organic dyes that suffer from rapid photobleaching), (iii) surface-enhanced and distance- and refractive index-dependent spectroscopic properties. In their excellent micro-review article, Baptista *et al.* distinguish three approaches for biodiagnostics based on AuNPs: (i) inter-AuNP distance dependent colorimetric sensing for specific DNA hybridization for the detection of specific nucleic acid sequences in biological samples (the most developed approach), (ii) surface-functionalized AuNPs providing highly selective nanoprobes, and (iii) electrochemical-based methods for signal enhancement.[61] The bases of these methods are detailed in the preceding sections. Here, we are essentially emphasizing clinical diagnosis applications.

Among the clinical diagnosis methods involving AuNPs immunoassays, promising applications are found in signal enhancement of the standard enzyme-linked immunosorbent assays (ELISAs) such as immunochromatographic test strips where both the primary and secondary antibodies are conjugated with the AuNPs.[105] The detection of the chorionic gonadotropin hormone reaches 1 pg mL^{-1} using this set-up. Other sensors are based on AuNP-functionalized fiber-optic evanescent wave[106] or AuNP-functionalized Cy5-antibody as the fluorescence probe which could replace the standard ELISA assay, because they do not require a secondary antibody and offer increased sensitivity.[107]

Chemiluminescent analysis of antibodies, such as anti-IgG to determine IgG content in human plasma, is optimized with irregular-shaped AuNPs that are more active than spherical AuNPs.[108] Hirsch *et al.* have reported a rapid whole-blood immunoassay using AuNSs capable of detecting sub-nanogram-per-mililiter quantities of various analytes upon aggregation of antibody-AuNS conjugates including successful detection of immunoglobulins in saline serum and whole blood. The simplicity of this assay also makes it superior to conventional ELISAs, because it requires less technical proficiency than ELISAs.[109]

The use of AuNPs is very promising in the field of immunosensors based on metal-enhanced fluorescence.[110] As recent examples of the use of electrochemical approaches based on the derivatization of electrodes with AuNPs, let us mention the label-free detection of the carcinoembryonic antigen (CEA).[111,112] A sensitivity-enhanced immunosensor based on the SPR was developed for the detection of by AuNR-antibody complex.[113] The pathogen Escherichia coli O157:H7 was rapidly detected on a piezoelectric oligonucleotide-AuNP-based biosensor.[114] Below, we summarize AuNP diagnostic for main diseases.

5.2 Cancer

Cancer diagnosis/detection based on the imaging of micro-anatomical features of diseased tissues uses OCT and RCM methods (*vide supra*). Cancer biomarkers and optical contrast agents provide excellent signal sources from cancer tissues. The intense scattering of large AuNPs makes them promising probes for cancer detection based on imaging. Immunotargeting of antibody-AuNPs label cancer cells by conjugating them with antigens overexpressed in cancer cells. For instance, cervical epithelial cancer cells (SiHa cells) that overexpress the transmembrane glycoprotein, epithelial growth factor receptor (EGFR), were imaged by immunotargeted AuNPs. AuNP scattering was strong enough to allow the use of even a red laser pointer, a resource-poor setting, instead of a scanning laser to image the cancer cells.[115]

Besides antibodies and some viruses, some biomolecules such as in particular folate are avidly taken up by cancer cells, which allows their selective targeting (Fig. 15).[116] El-Sayed *et al.* demonstrated the use of dark-field microscopy, an extremely simple and inexpensive technique, for the successful selective detection of cancerous cells. Thus, 35-nm AuNPs conjugated with anti-EGFR antibodies immunotargeted to two malignant epithelial cell lines were selected for optimal intense surface plasmon scattering using a white-light source from a conventional microscope resulting in a colored AuNP image with dark background.[117] Extension to other optical imaging techniques such as photo-acoustic tomography, multiphoton plasmon resonance microscopy, optical coherence microscopy and third-harmonic microscopy for cancer imaging is promising.[118]

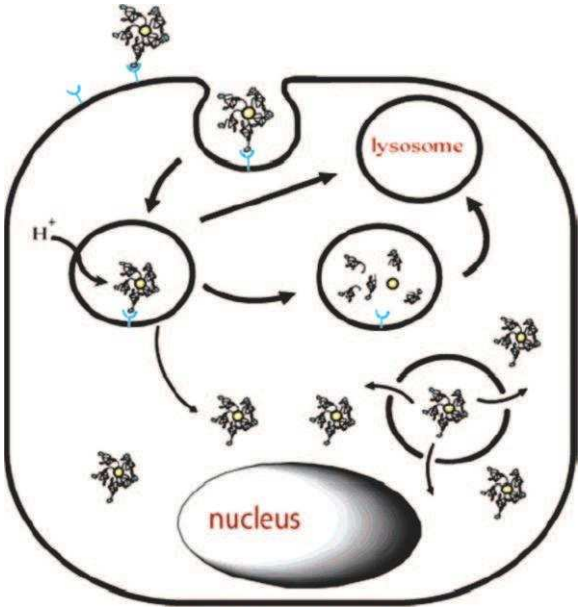

Fig. 15 Conceptual diagram of folate receptor-mediated binding, internalization, endosomal acidification, intracellular trafficking, and endosomal escape of F-PEG1500-T:AuNP by folate receptor-positive cells. Reprinted with permission of the American Chemical Society (ref. 116, Andres's group).

The nanoprobe method has been used by the Franco group to detect single nucleotide polymorphisms (SNPs) and mutations due to diseases such as cancer.[119,120] Recently, a colorimetric assay was reported for the direct detection of cancer cells by using aptamer-conjugated AuNPs. It was shown that the AuNP-aptamers could be assembled on a cell membrane surface for spectral changes, providing a direct visualization of cancer cells. The assay was also demonstrated on two different cell types that had cell-SELEX aptamers selected for them, indicating possible extension for any cell type. This could include colorimetric assays for various cancers or other diseases. The cell-SELEX aptamers have been generated for leukemia and lymphoma, lung cancer and liver cancer, suggesting that the assays could work out for the detection of these diseases.[121] Purine-9-β-D-ribofuranoside were found to substantially enhance the anti-proliferative effect against K-562 leukemia cells, due to enhanced intracellular transport followed by the subsequent release in lysosomes (Fig. 16).[122] AuNPs covalently conjugated with PEG and monoclonal antibody Herceptin, that enables recognition of breast cancer cells expressing specific tumor associated antigens, were shown to be stable and active *in vitro* in the presence of blood and *in vivo* in nude mice model for breast cancer.[123]

Many articles deal with both diagnostic and therapy, especially those dealing with the SPB-based photothermal effects, thus the reader is also referred to the other sections of this review concerning cancer.

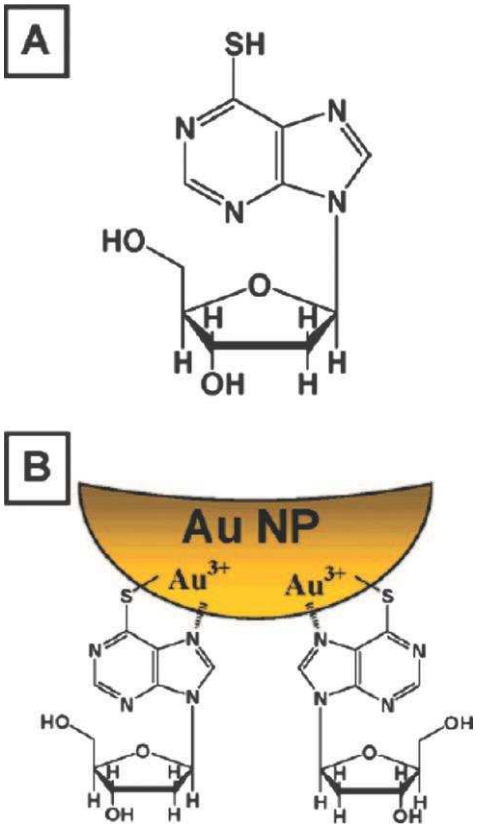

Fig. 16 Gold nanoparticles stabilized with 6-mercaptopurine-9-ß-D-ribofuranoside. (A) Chemical formula of 6-MPR. (B) Schematic of 6-MPR stabilization of AuNPs. Simple geometrical calculations based on the available surface atoms and/or geometry of the (6-MPR) moiety indicates that there might be 100–350 molecules of 6-MPR on the surfaces of the AuNPs. Reprinted with permission of the American Chemical Society (ref. 122, Kotov's group).

5.3 Alzheimer

Pioneering work toward an assay of Alzheimer diseases using AuNPs has been firstly reported by Van Duyne's group where a nanoscale optical biosensor based on LSPR spectroscopy has been described to monitor the interaction between the antigen, amyloid derived diffusible ligands (ADDLs), and specific anti-ADDL antibodies.[124,125] The Mirkin traditional method consisting in AuNP-nanoprobe cross-linking known for protein detection in attomolar sensitivity was successfully used for measuring the concentration of amyloid-β-derived diffusible ligands, a potential Alzheimer disease marker present at extremely low concentration (<1 pmol L^{-1}) in the cerebrospinal fluid of affected individuals.[126]

5.4 HIV

Multivalent AuNPs were found to inhibit HIV fusion. Therefore, 2-nm AuNP-mercaptobenzoic acid were conjugated to SDC-1721, a derivative of TAK-779, a known CCR5 antagonist that serves as the main entry co-receptor for most commonly transmitted strained of HIV-1. In this way, TAK-779 inhibited HIV-1 replication with an IC_{50} of 10 nM (Fig. 17).[127] A highly sensitive screening assay based on electrochemical impedance spectroscopy (EIS) has been

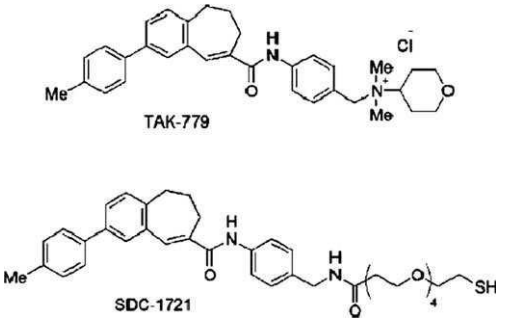

Fig. 17 TAK-779 and SDC-1721. Reprinted with permission of the American Chemical Society (ref. 127, Feldheim's group).

developed for the detection of HIV-1 protease using a thiol-terminated ferrocenyl-pepstatin conjugate was therefore attached to a single-wall carbon nanotube-AuNP modified electrode.[128]

5.5 Hepatitis B

Successfully prepared AuNPs-Hepatitis B virus (HBV) DNA gene probes could be used to detect HBV DNA directly. The detection-visualized fluorescence-based method is highly sensitive, simple, low cost and could potentially apply to multi-gene detection chips.[129]

5.6 Tuberculosis

A successful application of the AuNP-nanoprobe colorimetric method to clinical diagnosis reported by Baptista *et al.* was the sensitive detection in clinical samples of *Mycobacterium tuberculosis*, the human tuberculosis etiologic agent.[130] A specific oligonucleotide [5′-thiol-GGACGTGGAGGC-GATC-3′] derived from the *M. tuberculosis* RNA polymerase β-sub-unit gene sequence, suitable for mycobacteria identification, was used. At high NaCl concentration, nanoprobe aggregation in the absence of a complementary DNA sequence turns the solution purple. In the event of specific probe hybridization to a complementary sequence (*i.e.* DNA from *M. tuberculosis*), no nanoprobe aggregation occurs, and the solution remains red.[130]

5.7 Diabetes

Diabetes was characterized as a multifactorial disease using the AuNP-nanoprobe method mentioned above and involving the capture of the analyte with a magnetic particle featuring recognition elements followed by binding of a AuNP with a second recognition agent and marker DNA strands for cancer detection.[130]

6. Therapy

6.1 Photothermal cancer therapy

Conventional treatments of most cancers are surgical removal that is limited to large, accessible tumors, chemotherapy that suffers from dramatic side effects, and radiotherapy that is also invasive to healthy tissues along the radiation path. On the other hand, laser hyperthermia (photothermal therapy) that uses optical heating for tumor ablation is a mild solution that

avoids all these drawbacks. Organic photoabsorbers such as *Indocyanine green* and inorganic ones such as iron oxide have been used for photothermal tumor ablation but suffer respectively from small cross section requiring high irradiation energy and the need of iron oxide in high quantities (up to 10% weight) that is more or less toxic. The advantages of AuNPs are that they have high absorption cross sections requiring only minimal irradiation energy and are considered as non-toxic (*vide infra*). Irradiation of the SPR of AuNPs is followed by fast conversion of light into heat (about 1 ps).[131–135] Relatively small AuNPs (*e.g.* 10–30 nm) are delivered more easily to cancer cells using various methods (physiological transportation, conjugation with antibodies, *etc.*) than larger AuNPs.[136] After delivery, these AuNPs are self-assembled into larger clusters of closely located AuNPs directly within cells, resulting in laser-induced bubble formation that are more effective for cell killing and SPR shift from the visible region to the 700–1000 nm NIR region.[137]

AuNPs of various shapes absorb light in a broad spectrum range from near UV to NIR, but the NIR region is especially crucial in order to penetrate inside living tissues unlike visible light. The depth of light penetration can reach a few centimetres in the "biological window" (650–900 nm), a region ideal for the SPR absorption of AuNSs, AuNRs and Au nanocages. Thus, localized photothermal destruction of SK-BR-3 cancer cells was demonstrated by the Halas group *in vitro* and *in vivo* using thiolated-PEG-passivated AuNSs (passivation avoids aggregation in saline solution) with a 110 nm-diameter core and a 10 nm-thick shell resulting in a peak absorbance at 820 nm designed to match the emission wavelength of the diode laser. *In vitro*, silver staining revealed that the protein-adsorbent AuNS surface promoted binding to the AuNS surface. *In vivo*, the temperature increase upon AuNS NIR irradiation was of 37.4 ± 6.6 °C at a depth of 2.5 mm beneath the dermal surface on 5 min exposure, which is well above the temperature at which irreversible tissue damage occurs (40 °C) with laser dosage 10 to 25 times less than those used with *Indocyanine green* dye. Maximal depth of treatment was 6 mm, but could reach 1 cm or even more in related studies.[131] In order to explain these very positive therapy results, it appears that thiolated PEG ligands, that are biocompatible, mask the AuNPs from the immune system and inhibit aggregation. These PEG ligands also facilitate accumulation of the AuNSs at the tumor site due to the highly permeable vascular network in neoplastic tumors, referred to as the so-called "enhanced permeability and retention (EPR) effect".[138] Indeed, PEGs are currently used as carriers of anticancer drugs, and the efficiency of this means must be related to this EPR effect. In addition, selectively targeting of AuNPs to biomarkers on cancer cells appears as a very promising technique of cancer therapy.[139,140] Thus, using AuNSs conjugated with antibodies to HER2, a protein overexpressed in breast cancer cells, the Halas group photodamaged breast cancer cells *in vitro* using NIR laser phototherapy.[133]

The El-Sayed group used immunotargeted 40-nm AuNPs with two oral squamous cancer cell lines, HOC and HSC, that overexpress EGFR proteins. For this purpose, they used the 514-nm excitation of a common laser with the spherical AuNPs whose plasmon band had its maximum at 530 nm. These cancerous cells underwent photodamage *in vitro* within 4 min at laser energies of 19- and 25 W cm^{-2} unlike AuNP-free

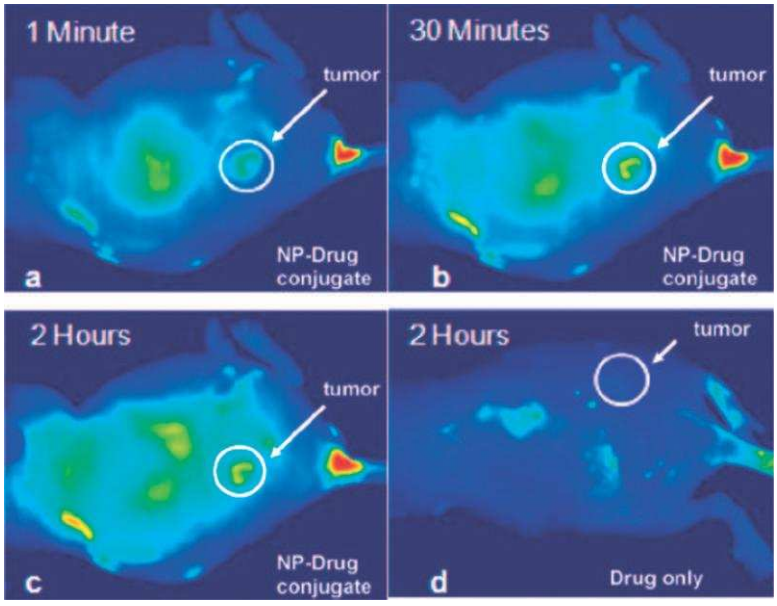

Fig. 18 Fluorescence images of a tumor-bearing mouse after being injected with AuNP-Pc4 conjugates in normal saline (0.9% NaCl, pH 7.2), (a) 1 min, (b) 30 min, and (c) 120 min after intravenous tail injection. Any bright signal is due to Pc4 fluorescence, without which no fluorescence signals were detected from the mouse. (To reduce autofluorescence, the animal was fed a special diet for more than 2 weeks before the experiment.) Unprecedented delivery efficiency and accumulation rate of the drug in the tumor are monitored *via* the fluorescence increase in the tumor area (white circle). For comparison, a mouse that got only a Pc4 formulation without the AuNP vector injected is shown in panel (d). No circulation of the drug in the body or into the tumor was detectable 2 h after injection without the AuNP as drug vector. Reprinted with permission of the American Chemical Society (ref. 149, Burda's group).

cells. AuNRs with a strong longitudinal absorption in the NIR region around 800 nm were used to observe malignant HOC and HSC cells labeled with the AuNR bioconjugate, upon AuNR red scattering in dark-field optical microscopy. The over expression of EGFR on the cell cytoplasmic membrane for various tumors was used for the selective delivery of anti-EGFR biconjugates in high concentrations to cancer cells for phototherapy.[141] Excitation of AuNRs passivated by phosphatidylcholine using a pulsed Nd-YAG laser provoked cell death,[142] and excitation of AuNRs conjugated to folate using a CW Ti:saphire laser was used for hyperthermia of KB oral cancer.[143]

Prospects for AuNRs in diagnostic and therapeutic applications have been reviewed.[144] AuNSs were also efficiently used *in vivo* with a subcutaneous prostate cancer (PC-3 cells) model whereby histological analysis of the tumor following direct tumor injection of AuNPs revealed even distribution throughout the tumor.[145] AuNSs conjugated to dextran afforded both photonic-based imaging and therapy of macrophage cells *in vitro*, which should prove useful for diseases such as arthrosclerosis and in-stent restenosis.[146]

Hollow dendrite-shaped $Au_{0.3}Ag_{0.7}$ NPs were used as NIR photothermal absorbers for destroying A549 lung cancer cells with laser powers required for cell damage significantly reduced relative to those used for AuNRs (Fig. 18).[147] 110-nm AuNSs with 10-nm shell thickness were used for prostate cancer ablation (PC-3 cells) using a 810-nm NIR laser with a 200-nm laser fiber and an energy setting of 4 W cm^{-2}, and resulted in 98% tumor necrosis.[148]

Phototherapies that do not use the AuNP SPB have also been reported. Photodynamic therapy using a PEG-5-nm-AuNP-Si-phthalocyanine conjugate generates singlet oxygen, very efficiently inducing apoptosis or necrosis directly in tumor-bearing mice as shown by fluorescence images. In this case, a crucial point is that the Au-PEG vector preferentially accumulates in tumor sites through the leaky tumor vasculature (''enhanced permeability and retention'', EPR effect).[149]

6.2 Radiofrequency therapy

Radiofrequency (RF) current, with a frequency between 10 kHz and 900 MHz has been applied for medical purposes for nearly a century with limited use due to thermal injury, but has been proposed in the 1990s as effective for destroying liver tumors. Limitations, however, included the requirement for invasive needle placement, accuracy of image guidance, tumor size, and collateral damage to non-tumorous liver parenchyma and adjacent structures, the occurrence of learning curves and relatively high local tumor recurrence. Thus a non-invasive technique has very recently been reported for tumor ablation using a variable power (0–2 kW) RF signal (13.56 MHz) by direct injection of citrate-AuNPs into the tumor to focus the radiowave for selective heating both *in vitro* and *in vivo* (rat exposure at 35 W).[150] Human cell lines were also exposed to a 13.56 MHz RF field, and the resulting induced heat was lethal to these cancer cells bearing AuNPs *in vitro*.[151]

6.3 Angiogenesis therapy

Angiogenesis is the formation of new blood vessels from existing ones, and ''abnormal'' angiogenesis was shown to play an important role in the growth and spread of cancer, due to the feed of cancer cells by the new blood vessels with oxygen and nutrients. Mukherjee *et al*. discovered than AuNPs inhibit angiogenesis and recently published a review article on this subject.[152] The authors showed that addition of AuNPs profoundly inhibited phosphorylation of the proteins responsible for angiogenesis in a dose-dependent manner, almost complete inhibition being observed at concentrations of 335–670 nM. It was suggested that the responsible inhibition mechanism involves AuNPs direct binding to heparin-binding growth factors presumably through cysteine residues of the heparin-binding domain (Fig. 19).[152]

6.4 Rheumatoid arthritis therapy

AuNPs have been used in the treatment of rheumatoid arthritis for a very long time, and medical treatment dates

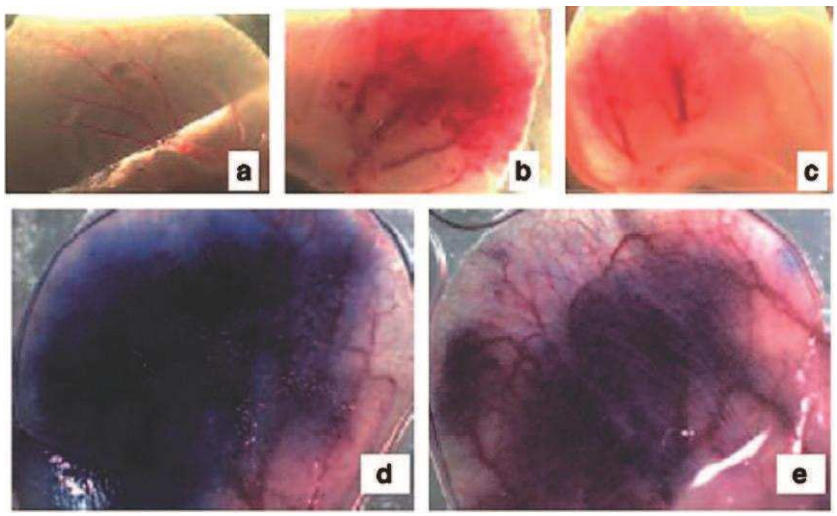

Fig. 19 Effect of nanogold on angiogenesis *in vivo* in the ears of nude mice. Gross appearance of angiogenesis 7 days after injection of nanogold only (a), Ad-VEGF only (b), nanogold and Ad-VEGF (c). Effect of nanogold on permeability, Ad-VEGF only (d), nanogold and Ad-VEGF (e). Reprinted with permission of the American Association for Cancer Research (ref. 152, Mukherjee's group).

from the 1920s. Recently, it was shown that 13-nm AuNPs prepared by the citrate reduction method inhibited proliferation and migration of the protein responsible for angiogenesis. Angiogenesis plays a key role in the formation and maintenance of rheumatoid arthritis. Furthermore, animal testing by intradermal injection of these AuNPs for 7 and 10 days resulted in a significant reduction of joint inflammation, and immunohistochemical staining revealed a significant decrease in macrophage infiltration into the synovium of rats. This is important, because rheumatoid arthritis is still currently essentially incurable. Photoacoustic tomography of joints aided by an Etanercept-conjugated AuNR contrast agent was shown to visualize the AuNR-drug conjugate down to 1 pM in phantoms or 10 pM in biological tissues.[153]

6.5 Anti-bacterial therapy

Strong laser-induced overheating effects accompanied by the bubble-formation phenomena around clustered AuNPs cause bacterial damage, and this nanotechnology was used for selective killing of the Gram-positive Staphylococcus aureus by targeting bacteria surface using 10-, 20- and 40-nm AuNPs conjugated with anti-protein A antibodies.[154]

6.6 Drug vectorization

Therapeutic vectors carry drugs, genes and imaging agents into living cells and tissues.[155–157] The drugs vectors should also be stable in the circulatory system, yet become labile under appropriate conditions when the targeted organ is reached. The drug vectors carry the drug by encapsulation or more or less strong binding (covalent, coordination or supramolecular bond). The potential vectors include micelles, liposomes, steroids, folate, peptides, hyaluronic acid, fatty acids, antigens, polymers, dendrimers, nanotubes, and nanoparticles.[9,10] AuNPs have recently been considered as excellent drug-delivery systems due to their biocompatibility, optical properties and excellent abilities to bind (bioconjugation) biological ligands, DNA and small interfering RNA (siRNA) (noncovalent interaction) and drugs through AuNP surface bonding.[158,159] Specific applications can be classified in targeted drug delivery and mediated gene delivery. Targeted drug delivery has been achieved by endocytosis through a transmembrane receptor. For this purpose, AuNPs are conjugated to a ligand that specifically recognizes the receptor.

The protein transferin has been conjugated to AuNPs, because many tumors cells overexpress transferin receptors, and uptake of AuNP-transferin by tumor cells has been characterized by AFM and confocal scanning laser microscopy.[160] PEG chains were anchored by thiotic acid and folic acid on opposite ends and conjugated to 10-nm AuNPs that proved to be stable in the pH 2–12 range and NaCl concentrations up to 0.5 M and could be taken up by folate-receptor-positive tumor cells. Cellular uptake was demonstrated by TEM of KB cells that actively express folate receptors on their membrane.[161] In a rare example of *in vivo* study, 26-nm AuNPs conjugated with the tumor-necrosis factor (TNF) were injected into tumor-bearing mice. They preferentially accumulated in the tumor and diminished the tumor mass more effectively than free TNF.[162] Enhanced efficacy of such AuNPs with a thiolated paclitaxel was also shown.[163]

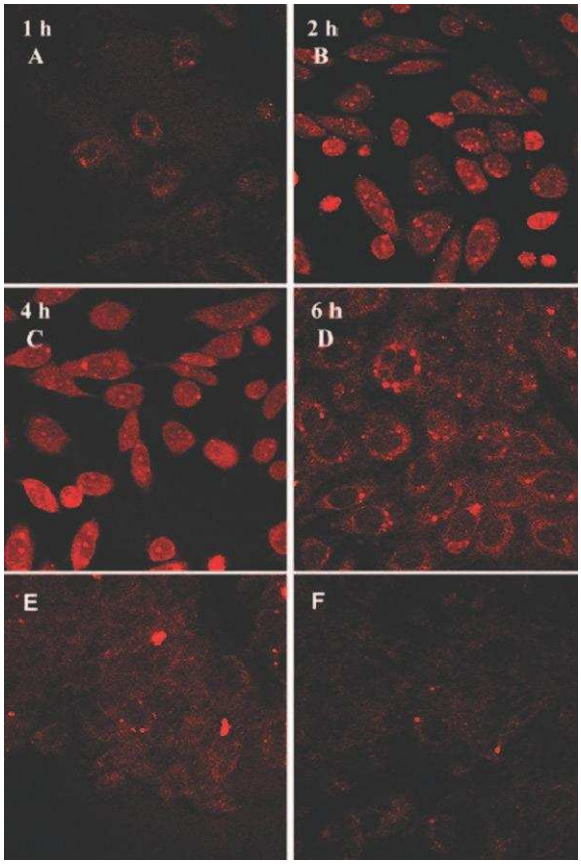

Fig. 20 Cellular uptake and distribution of liposome entrapped gold nanoparticles in CHO cells. Images were taken after 1, 2, 4 and 6 h (A to D) incubation with liposome entrapped gold nanoparticles. Images E and F were taken after 1 and 2 h incubation when plain gold nanoparticles were used. Reprinted with permission of Elsevier (ref. 165, Devi's group).

A TEM study of 16-nm AuNPs conjugated with human fibroblast cells shows control of the uptake mechanism either *via* delivery of AuNPs by liposomes or by surface modification of the AuNPs with cell-penetrating peptides.[164] Liposome-entrapped AuNPs showed enhanced uptake by Chinese Hamster Ovary cells compared to liposome-free AuNPs (Fig. 20).[165] AuNPs were conjugated with transferrin molecules for imaging and therapy of breast cancer cells (Hs578T, ATCC). The transferrin/transferrin-receptor mediated cellular uptake of the AuNPs was six times of that in the absence of this interaction. The cellular uptake was only one fourth of that by the cancerous cells.[166] Tumor necrosis factor-α is a potent cytokine with anticancer efficacy, but it is systemically toxic, thereby needing selective delivery. Thus, the Paciotti group reported that PEG-33-nm AuNPs with incorporated TNF-α payload (several hundred TNF-α *per* AuNP) maximize tumor damage and minimize exposure to TNF-α.[167,168] Gene delivery is very promising, but common viral vectors raise cytotoxicity and immune response problems. Thus AuNP-based DNA-delivery vectors have been developed by Rotello's group first using cationic ligands, then with amphiphilic ligands that were more efficient on transfection.[169,170]

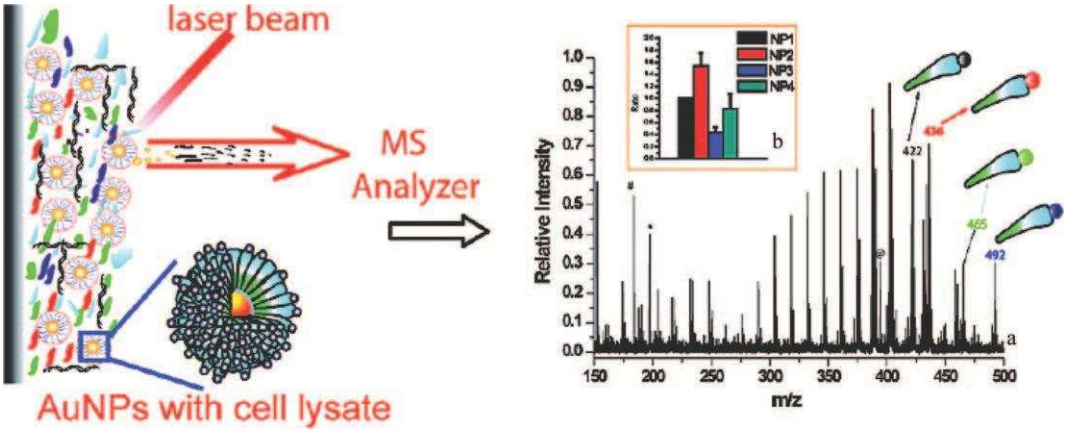

Fig. 21 Schematic illustration of the analysis of the AuNPs in cell lysates by LDI-MS; (a) Multiplexed LDI mass spectrum of COS-1 cell lysate with the four cationic AuNPs **1–4**. m/z 422, m/z 436, m/z 492, and m/z 465 correspond to AuNP **1**, AuNP **2**, AuNP **3**, and AuNP **4**, respectively. The symbol key is the same as in Fig. 3. (b) Relative amounts of AuNPs **1–4** obtained from LDI-MS. The AuNP amounts are normalized to that of AuNP **1**. Reprinted with permission of Elsevier (ref. 174, Rotello's group).

Klibanov's group also reported the transfection efficiency of AuNP-PEI conjugates into kidney (Cos-7) cells.[171] Mirkin *et al.* showed the use of AuNPs conjugated to negatively-charged oligodeoxynucleotide for gene therapy,[156] and Rotello's group showed that intracellular concentrations of glutathione can trigger the restoration of DNA from cationic AuNP-NDA conjugate with potential applications in the creation of transfection vectors and gene-regulation systems.[172] Rotello *et al.* also reported photolabile AuNPs that provide light-regulated control over DNA-AuNP interactions, which is evidenced by a high level of DNA-transcription recovery *in vitro* and significant nuclear localization of DNA in cells.[173] The techniques that are available to characterize cell uptake by AuNPs carriers and intracellular probes are essentially luminescent imaging (including barcoding), AFM and TEM. Multiplexed screening of cellular uptake has been demonstrated with laser-ionization mass spectrometry[174] (Fig. 21) and time-of-flight secondary ion mass spectrometry (TOF-SIMS).[175]

Adding polyelectrolyte-coated AuNRs to three-dimensional constructs composed of collagen and cardiac fibroblasts reduced contraction and altered the expression of mRNA encoding γ-actin, α-smooth muscle actin and collagen type 1. These data show that AuNRs can modulate cell-mediated matrix remodeling and suggest that the targeted delivery of AuNRs can be applied for antifibrotic therapies.[176] Polyelectrolyte-AuNP-sensors are also based on refractive-index change.[177] "Gellan gum", widely used in food as a thickening and gelling agent, has been used in the reductive synthesis and stabilization of AuNPs that were applied to load anthracyclin

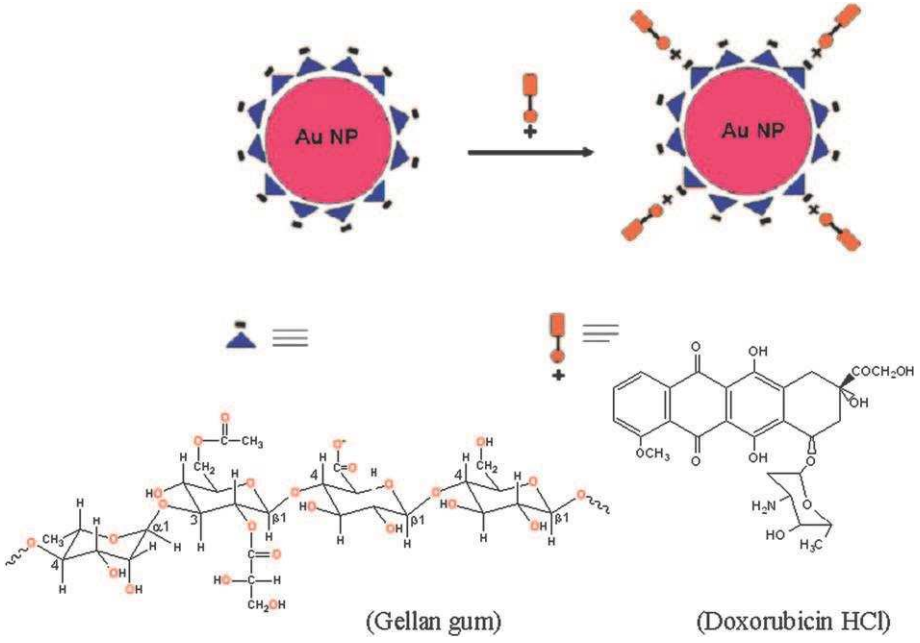

Fig. 22 Schematic diagram showing anionic gellan gum gold nanoparticles and subsequent loading of cationic doxorubicin HCl on gellan gum capped gold nanoparticles. Reprinted with permission of Wiley InterScience (ref. 178, Prasad's group).

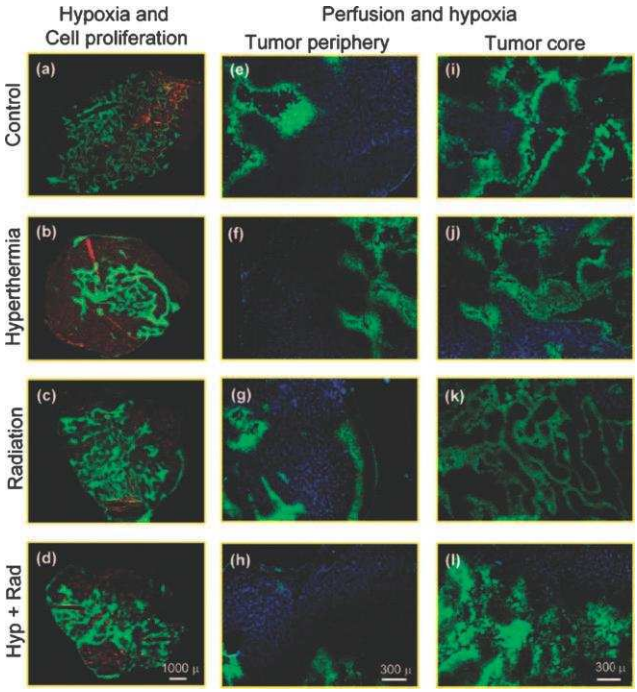

Fig. 23 Immunofluorescence staining of control, hyperthermia, radiation, and thermoradiotherapy treated tumors showing hypoxia, cell proliferation (a–d), and hypoxia, perfusion in tumor periphery (e–h), and tumor core (i–l), respectively. Red, blue, and green fluorescence represents cell proliferation, perfusion, and hypoxic regions in tumors. Patchy hypoxic region seen in (l) is attributed to the vascular disruption effect induced by gold nanoshell-mediated thermoradiotherapy. Scale bars are represented in the bottom image of each column. Reprinted with permission of the American Chemical Society (ref. 182, Krishnan's group).

ring antibiotic doxorubicin hydrochloride. Such drug loading showed enhanced cytotoxic effects on human glioma cell lines LN-18 and LN-229 (Fig. 22).[178]

The Paciotti group has reported cryosurgery. The cytokine adjuvant TNF-α can be used to achieve complete cancer destruction at the periphery of an iceball (0 to −40 °C). Although both surgery alone or TNF treatment alone caused only a minimal damage to the tumor tissues, the combination of TNF and cryosurgery produced a significant damage to the tumor tissues.[179,180] The surfactant dodecylcysteine hydrochloride was reported to improve the antitumor activity of AuNPs in a cell line of the Ehrlich ascites carcinoma.[181] Hyperthermia of cancer cells using AuNPs appears essential to fight against intratumoral hypoxia that is a key mediator of the resistance of tumor cells to radiation therapy. Thus, an integrated antihypoxic and localized vascular disrupting therapeutic strategy was developed using tumor-vasculature-focused effects mediated by perivascularly sequestered AuNSs (Fig. 23).[182] Carbonic anhydrase inhibitors coated AuNPs were shown to selectively inhibit the tumor-associated isoform IX over the cytosolic isozymes I and II (Fig. 24).[183]

7. Cytotoxicity

The long history of (almost legendary) gold colloid use for therapeutic purposes suggests that AuNPs should be biocompatible. The considerable potential use of AuNPs in nanomedicine, especially for imaging, diagnostic and therapy requires, however, their toxicity to be thoroughly examined with maximum care and accuracy. The cytotoxicity of AuNPs, *i.e.* their cellular toxicity, has indeed been examined by several research groups and reviewed.[184,185] Since everything is toxic at high dose, the important question is whether AuNPs are toxic at the concentration at which they will be used, believed to be in the range of 1–100 AuNPs *per* cell.

7.1 Cytotoxicity *in vitro*

Some AuNPs can transfect cells. Rotello has shown that cationically functionalized alkylthiolate-AuNPs containing trimethylammonium ligand termini mediate DNA translocation across cell membranes in mammalian cells at a high level. Toxicity of these AuNPs was observed at concentrations only 2-fold higher than that found for maximal transfection activity. In fact, it is essential to distinguish between the toxicity of the AuNP core and that due to the ligands of the AuNP. In this case, it was shown that, whereas these cationic AuNPs are moderately toxic, the same alkylthiolate-AuNPs containing carboxylate termini are quite non-toxic. Accordingly, concentration-dependent lysis mediated by electrostatic binding was observed in dye release studies using lipid vesicles, suggesting the operating mechanism for the

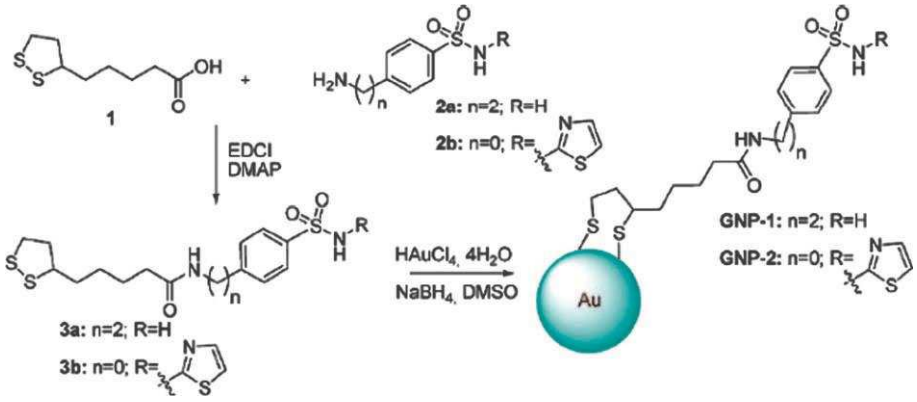

Fig. 24 Synthesis of AuNPs coated with sulfonamide CAI, of type **GNP-1** and **GNP-2**. Reprinted with permission of the American Chemical Society (ref. 183, Supuran's group).

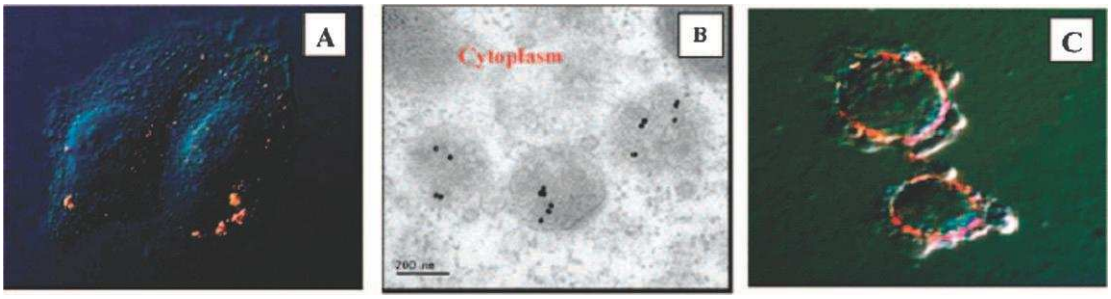

Fig. 25 M1 nanoparticles incubated with HeLa cells. After 1 h, nanoparticles were observed by video-enhanced color differential interference contrast microscopy (A) and transmission electron microscopy (B) clustered in compartments inside the cytoplasm. After 2 h, nanoparticles were found accumulated around the nuclear membrane (C). Reprinted with permission of the American Chemical Society (ref. 188, Feldheim's group).

observed toxicity of these cationic AuNPs.[186] In another evidence of the key role of AuNP ligands, large AuNPs conjugated with biotin, cysteine, citrate, and glucose did not appear to be toxic in human leukemia (K562) cells at concentrations up to 250 mM in contrast to $HAuCl_4$ solutions were was found to be 90% toxic.[187]

AuNP cytotoxicity may also eventually more or less depend on the cell lines, although this point is somewhat controversial, because differences observed might perhaps be due to variation of ligands (Fig. 25).[188] No physiological complication were found either in mice with AuNSs in another study.[29] Dose-dependent cytotoxicity was found with Au–Cu–NSs with 100% viability at low dose in mice, but 67% viability at high dose.[189] With AuNRs, strong cytotoxicity was associated with a low concentration of CTAB-stabilized AuNRs, and free CTAB was proposed to cause the toxicity.[190,191] Phosphatidylcholine was reported to reduce the cytotoxicity of CTAB-coated AuNRs.[192] It was pointed out that non-cytotoxic AuNPs can eventually cause cell damage, and abnormal filaments formation was produced by such 13-nm citrate-AuNPs.[193] AuNRs coated with layer-by-layer polyelectrolytes such as the common poly(diallyldimethylammonium chloride)-poly(4-styrenylsulfonic acid) showed low toxicity and were considered as well suited for therapeutic applications.[194] The cytotoxicity of AuNPs conjugated with PEGylated biotin-PEG-poly(ε-caprolactone) copolymers towards Caco-2 cells in culture was shown to be negligible.[195]

7.2 Cytotoxicity *in vivo*

The full potential of innovations in terms of AuNP medical use can only be achieved with the concomitant realization of *in vivo* profiles for pharmacological intervention.[196] Different routes of administration can result in various effects on the biodistribution of drug carriers.[197] Subcutaneous, intramuscular or topical administration of colloidal drug carriers generally results in retention of the drug carrier for longer time than free drug, and these drug carriers are mainly retained by local lymph nodes.[198,199] *In vivo* distribution subsequent to administration largely depends on NP size, surface charge and surface hydrophobicity.[200,201] The influence of these factors on the uptake of NPs by the mononuclear phagocyte system has been described.[201] The presence of biocompatible amphiphilic chains on NP surface decreases phagocytosis of the NPs by the non-parenchymal cells of the liver, allowing longer circulation time in blood.[202] Permeation of small AuNPs through skin and intestine was found to be size dependent.[203] The biological distribution of various sizes (15, 50, 100 and 200 nm) of AuNPs on intravenous administration in mice was investigated and revealed that AuNPs of all sizes were mainly accumulated in liver, lung and spleen, whereas accumulation in various tissues depended on AuNP size. High amounts of 15-nm AuNPs were found in all tissues including blood, liver, lung, spleen, kidney, and stomach and were able to pass the blood-brain barrier, as 50-nm AuNPs also did. On the other hand, only minute amount of 200-nm AuNPs were found in blood, brain, stomach and pancreas.[204] Accordingly, in another study, rats intravenously injected with AuNPs of 10-, 50-, 100- and 250-nm diameters were shown to contain the 10-nm AuNPs in the various organs, whereas larger AuNPs were only detected in blood, liver and spleen.[205] The Paciotti group reported that the tumor-necrosis factor (TNF)-conjugated AuNPs show similar antitumor effects to TNF alone, but with less systeic toxicity in mice.[206] Studies of biodistribution of 1.4-nm and 1.8-nm AuNPs that were administrated by intravenous injection or intratracheal instillation in rats indicated that the 1.4-nm AuNPs can be translocated through the air/blood barrier of the respiratory tract in significant amounts, whereas the 1.8-nm AuNPs are almost completely trapped in the lungs. Additionally, there is evidence that the AuNPs are modified during the translocation process.[207] In a study of pharmacokinetics and biodistribution in nude mice of PEG-coated AuNPs, AuNPs coated with thioctic acid-anchored PEG exhibited higher colloidal stability in phosphate-buffered saline in the presence of dithiothreitol than did AuNPs coated with monothiol-anchored PEG. AuNPs coated with 5000-Da PEG were more stable than those coated with 2000-Da PEG. Of the 20-nm, 40-nm, and 80-nm AuNPs coated with thioctic acid-terminated 5000-Da PEG, the 20-nm AuNPs exhibited the lowest uptake by retinoendothelial cells and the lowest clearance by the body, and showed significantly higher tumor uptake and extravasation from the tumor blood vessels than did the 40- and 80-nm AuNPs.[208]

Although all these studies show the AuNP size distribution, it would also be of interest in the future to obtain information on the influence of other AuNP characteristics such as morphology, crystallinity, surface defects, charge and reactivity.

7.3 Conclusion on toxicity studies

In conclusion to the toxicity survey, it appears that AuNPs usually show rather little toxicity, if any, because many cytotoxicity studies report negative cytotoxicity finding results. The cationic ligands of AuNPs, however, clearly cause moderate toxicity, and some toxicity may also be specific to other types of ligands. A systematic toxicity study must be carried out for each specific case under precise conditions, before imaging, diagnosis and therapeutic applications of AuNPs can be carried out in human. Also, *in vivo* conditions are different from *in vitro* results, and in particular more *in vivo* studies are called for. Thus, no general conclusion can be drawn at present. It has been suggested, however, that it could be applicable to use AuNPs as reference nanoparticles for low toxicity in the set-up of a nanoparticle toxicity scale, given the higher toxicity of carbon nanotubes and quantum dots compared to non-cationic AuNPs. Finally, AuNPs are redox active and therefore reduce the production of reactive oxygen- and nitrite species.[209] The non-cytotoxicity, non-immunogenicity and biocompatibility of many AuNPs make us relatively optimistic concerning their future essential applications in nanomedicine.

8. Conclusion and outlook

Medically useful AuNPs can be prepared and stabilized (conjugated) with a large variety of stabilizers (citrate, various ligands, polymers, dendrimers, surfactants) including biomolecules such as oligonucleotides and DNA. The best stabilizers are thiolates (for instance oligonucleotides modified with a thiolate group). New practical stabilizers such as "gellan gum" exemplify this variety.[178] Thiolated PEGs are especially useful because they masks AuNPs from the intravascular immune system and help targeting cancer cells due to the EPR effect.

The surface plasmon absorption of AuNPs provides outstanding optical properties that can be used with a variety of techniques for labeling, imaging, sensing leading to both diagnostics and therapies. This SPB is extremely dependent on the surface, AuNP shape, inter-AuNP distance, medium (refractive index) and ligands, which makes the basis for molecular recognition, imaging and sensing sensitivity. The most famous example of sensor is Mirkin's "*Northwestern spot test*", a visual record of the inter-AuNP distance-dependent color change and temperature-dependent disaggregation (melting) that can detect mismatched DNA.[54]

Modern spectroscopic techniques, such as SERS that provides a huge enhancement of the Raman signal, by a factor of *ca.* 10^{14}–10^{15}, allowing detection at the single molecule level,[210] considerably facilitates the diagnostic of cancer and other diseases (SERS combines *elastically* scattered visible light from the AuNP themselves that can be imaged using a dark-field optical microscope with *inelastic* SERS effect due to adsorbed molecules providing a Raman spectrum leading to the identification of biomolecules). For instance, antibody-modified AuNPs displayed a million-fold higher sensitivity than conventional ELISA-based assay in the detection of prostate specific antigen (PSA).[211]

A number of other useful optical and electrochemical techniques including fluorescence, Ag staining and electrocatalytic biosensors have been discussed here. These biosensing techniques allow clinical diagnosis of cancer, Alzheimer, HIV, hepatitis B, tuberculosis, diabetes and arthritis.

In the cancer therapy section, it was shown how photothermal AuNP NIR irradiation of cancer cells combines both diagnosis (imaging) and selective therapy, a technique also applicable to other diseases. In addition, the discovery that the SPB can be shifted from the visible region for spherical AuNPs to the NIR region for AuNRs and AuNSs led the groups of Halas,[28] Murphy[26] and El-Sayed[140] to introduce a breakthrough with the extension of the efficient use of the SPB for cancer therapy, a non-invasive method with efficient tumor ablation in the NIR region were blood and tissues are less absorbing ("biological window": 650–900 nm).[29]

Techniques that do not use the SPB, however, such as RF heating of AuNPs and AuP-targeting with singlet oxygen therapy are also known. Indeed, the use of AuNPs as vectors is very general, because it can be directly applied in a non-invasive way for various therapies including angiogenesis, anti-bacterial treatments, *etc.*

Drug delivery (both drugs and DNA) appears as one of the most promising future applications of AuNPs, as exemplified by a number of recent reports that were reviewed here. For instance AuNP-based DNA-delivery vectors have been developed by Rotello who showed that intracellular concentrations of glutathione can trigger the restoration of DNA with potential applications in the creation of transfection vectors.[172] Mirkin showed the use of AuNPs conjugated to oligodeoxynucleotide for gene therapy.[156] The Paciotti group reported cryosurgery, indicating that the combination of TNF-α and cryosurgery produced a significant damage to the tumor tissues.[179,180]

Finally, a very important problem in potential therapy for human is that of toxicity that must be carefully and precisely studied. Many groups have reported the non-toxicity of AuNPs. One must distinguish between the toxicity of the AuNP core and that of ligands. Cationic ligands including CTAB appear moderately toxic, and some other ligands also may be toxic. Many biocompatible ligands including thiolated PEGs are non-toxic, however. AuNPs appear much less toxic than other types of nanoparticles, and one should be reasonably optimistic concerning potential applications. In conclusion, AuNPs are biocompatible, easily bio-conjugable and very promising for imaging, diagnostics and therapy biomedical applications for cancer and a number of other diseases for human.[7]

List of abbreviations

AFM	Atomic force microscopy
ATP	Adenosine triphosphate
AuNPs	Gold nanoparticles
AuNRs	Gold nanorods
AuNSs	Gold nanoshells
CCD	Charge-coupled device
CCR5	Chemokine CC motif receptor 5
CD	Compact disc

CEA	Carcinoembryonic antigen
CTAB	Cetyl trimethylammonium bromide
Cy	Cyanine
DIC	Differential interference contrast
DLSS	Differential light-scattering spectroscopy
DNA	Deoxyribonucleic acid
ECL	Electrogenerated chemiluminescence
EDC	1-Ethyl-3(3-dimethylaminopropyl)-carbodiimide-HCl
EGFR	Epithelial growth factor receptor
EIS	Electrochemical impedance spectroscopy
ELISA	Enzyme-linked immunosorbent assay
FCS	Fluorescence correlation spectroscopy
FRET	Fluorescence resonance energy transfer
GO	Glucose oxidase
HBV	Hepatitis B virus
HEK	Human embryonic kidney
HER2	Human epidermal growth factor receptor 2
HIV	Human immunodeficiency virus
HOC	Human ovarian cancer
HRS	Hyper-Raleigh scattering
HSC	Hematopoetic stem cells
IC_{50}	Half maximal inhibitory concentration
IgG	Immunoglobulin G
IR	Infrared
MRI	Magnetic resonance imaging
mRNA	Messenger ribonucleic acid
Nd-YAG	Neodymium-doped yttrium aluminium garnet
NIR	Near infrared
PCT	Photothermal coherence tomography
PCR	Polymerase chain reaction
PEG	Polyethylene glycol
PEI	Polyethylene imine
PLC	Phospholipase C
PSA	Prostate specific antigen
RCM	Reflection contrast microscopy
RF	Radiofrequency
RNA	Ribonucleic acid
ScFv	Single-chain variable-fragment
SDC	Shielded dynamic complex-gate
SELEX	Systematic evolution of ligands by exponential enrichment
SERS	Surface-enhanced Raman scattering
siRNA	Small interfering ribonucleic acid
SNPs	Single nucleotide polymorphisms
SPB	Surface plasmon band
SPR	Surface plasmon resonance
TEM	Transmission electron microscopy
TNF	Tumor-necrosis factor
TOF-SIMS	Time-of-flight secondary mass spectrometry
UV	Ultraviolet

Acknowledgements

We are grateful to the Université Bordeaux I, the Centre National de la Recherche Scientifique (CNRS), the Institut Universitaire de France (IUF, DA) and the Agence Nationale de la Recherche (ANR) for financial support.

References

1 W. P. Faulk and G. M. Taylor, *Immunochemistry*, 1971, **8**, 1081–1083.
2 G. M. Whitesides, *Nat. Biotechnol.*, 2003, **21**, 1161–1165.
3 E. Katz and I. Willner, *Angew. Chem., Int. Ed.*, 2004, **43**, 6042–6108.
4 N. L. Rosi and C. A. Mirkin, *Chem. Rev.*, 2005, **105**, 1547.
5 D. Astruc, *C. R. Acad. Sci.*, 1996, **322**(Série II b), 757–766.
6 U. Dreshler, B. Erdogan and V. M. Rotello, *Chem.–Eur. J.*, 2004, **10**, 5570–5579.
7 R. Langer and D. A. Tirrell, *Nature*, 2004, **428**(6982), 487–492.
8 M. Ferrari, *Nat. Rev. Cancer*, 2005, **5**, 161–171.
9 T. Ganesh, *Bioorg. Med. Chem.*, 2007, **15**(1), 3597–3623.
10 P. K. Jain, X. Huang, I. H. El-Sayed and M. A. El-Sayed, *Plasmonics*, 2007, **2**, 107–118.
11 M. Faraday, *Philos. Trans. R. Soc. London*, 1857, **147**, 145–181.
12 G. Mie, *Ann. Phys.*, 1908, **25**, 377–445.
13 M.-C. Daniel and D. Astruc, *Chem. Rev.*, 2004, **104**, 293–346 and refs. cited therein.
14 M. Tréguer-Delapierre, J. Majimel, S. Mornet and S. Ravaine, *Gold Bull.*, 2008, **41**(2), 195–207.
15 J. Turkevitch, P. C. Stevenson and J. Hillier, *Discuss. Faraday Soc.*, 1951, **11**, 55–75.
16 J. Kimling, M. Maier, B. Okenve, V. Kotaidis, H. Ballot and A. Plech, *J. Phys. Chem. B*, 2006, **110**, 5700–5707.
17 M. Giersig and P. Mulvaney, *Langmuir*, 1993, **9**, 3408–3413 and refs. cited therein.
18 M. Brust, M. Walker, D. Bethell, D. J. Schiffrin and R. J. Whyman, *J. Chem. Soc., Chem. Commun.*, 1994, 801–802.
19 A. C. Templeton, W. P. Wuelfing and R. W. Murray, *Acc. Chem. Res.*, 2001, **33**, 27–36.
20 R. A. Sperling, P. Rivera Gil, F. Zhang, M. Zanella and W. J. Parak, *Chem. Soc. Rev.*, 2008, **37**, 1896–1908 and refs. cited therein.
21 H. C. Kolb, M. G. Finn and K. B. Sharpless, *Angew. Chem., Int. Ed.*, 2001, **40**, 2004–2021.
22 E. Boisselier, L. Salmon, J. Ruiz and D. Astruc, *Chem. Commun.*, 2008, 5788–5790.
23 R. W. J. Scott, O. M. Wilson and R. M. Crooks, *J. Phys. Chem. B*, 2005, **109**, 692–704 and refs. cited therein.
24 E. Boisselier, A. K. Diallo, L. Salmon, J. Ruiz and D. Astruc, *Chem. Commun.*, 2008, 4819–4821.
25 H. Wu, H. Zhu, J. Zhang, S. Yang, C. Liu and Y. C. Cao, *Angew. Chem., Int. Ed.*, 2008, **47**, 3730–3734.
26 C. J. Murphy, A. M. Gole, S. E. Hunyadi, J. W. Stone, P. N. Sisco, A. Alkilany, B. E. Kinard and P. Hankins, *Chem. Commun.*, 2008, 544–557 and refs. cited therein.
27 X. H. Huang, P. K. Jain, I. H. El-Sayed and M. El-Sayed, *Laser Med. Sci.*, 2008, **23**, 217–228 and refs. cited therein.
28 S. L. Lal, S. E. Clare and N. J. Halas, *Acc. Chem. Res.*, 2008, **41**(12), 1842–1851 and refs. cited therein.
29 T. Niidome, M. Yagamata, Y. Okamoto, Y. Akiyama, H. Takahashi, T. Kawano, Y. Katayama and Y. Niidome, *J. Controlled Release*, 2006, **114**(3), 343–347.
30 M. Z. Liu and P. Guyot-Sionnest, *J. Phys. Chem. B*, 2005, **109**, 22192–22200.
31 G. F. Paciotti, D. G. I. Kinston and L. Tamarkin, *Drug Dev. Res.*, 2006, **5**, 2255–2262 and refs. cited therein.
32 L. M. Liz Marzan, *Langmuir*, 2006, **22**, 32–41 and ref. cited therein.
33 M. C. Skala, M. J. Crow, A. Wax and J. A. Izatt, *Nano Lett.*, 2008, **8**(10), 3461–3467.
34 D. Yelin, D. Oron, S. Thiberge, E. Moses and Y. Silberberg, *Opt. Express*, 2003, **11**(12), 1385–1391.
35 P.-J. Debouttière, S. Roux, F. Vocanson, C. Billotey, O. Bæuf, A. Favre-Réguillon, Y. Lin, S. Pellet-rostaing, R. Lamartine, P. Perriat and O. Tillement, *Adv. Funct. Mater.*, 2006, **16**, 2330–2339.
36 Y. T. Lim, M. Y. Cho, J. K. Kim, S. Hwangbo and B. H. Chung, *ChemBioChem*, 2007, **8**, 2204–2209.
37 T. A. Larson, J. Bankson, J. Aaron and K. Sokolov, *Nanotechnology*, 2007, **18**, 325101.
38 X. Ji, R. Shao, A. M. Elliott, R. J. Stafford, E. Esparza-Coss, J. A. Bankson, G. Liang, Z.-P. Luo, K. Park, J. T. Markert and C. Li, *J. Phys. Chem. C*, 2007, **111**, 6245–6251.

39 J.-s. Choi, H. J. Choi, D. C. Jung, J.-H. Lee and J. Cheon, *Chem. Commun.*, 2008, 2197–2199.
40 J. Aaron, N. Nitin, K. Travis, S. Kumar, T. Collier, S. Y. Park, M. Jose-Yacaman, L. Coghlan, M. Follen, R. Richards-Kortum and K. Sokolov, *J. Biomed. Opt.*, 2007, **12**(3), 034007.
41 X. H. Huang, P. K. Jain, I. H. El-Sayed and M. A. El-Sayed, *Lasers Med. Sci.*, 2008, **23**, 217–228.
42 X. H. Huang, I. H. El-Sayed, W. Qian and M. A. El-Sayed, *Nano Lett.*, 2007, **7**(6), 1591–1597.
43 S. W. Bishnoi, C. J. Rozell, C. S. Levin, M. K. Gheith, B. R. Johnson, D. H. Johnson and N. J. Halas, *Nano Lett.*, 2006, **6**, 1687–1692.
44 R. Wilson, A. R. Cossins and D. G. Spiller, *Angew. Chem., Int. Ed.*, 2006, **45**, 6104.
45 R. Wilson, *Chem. Soc. Rev.*, 2008, **37**, 2028–2045.
46 W. E. Doering, M. E. Piotti, M. J. Natan and R. G. Freeman, *Adv. Mater.*, 2007, **19**, 3100–3108.
47 Q. Hu, L.-L. Tay, M. Noestheden and J. P. Pezacki, *J. Am. Chem. Soc.*, 2007, **129**, 14–15.
48 J. Kneipp, H. Kneipp, B. Wittig and K. Kneipp, *Nano Lett.*, 2007, **7**, 2819–2823.
49 X. Qian, X.-H. Peng, D. O. Ansari, Q. Yin-Goen, G. Z. Chen, Dong M. Shin, L. Yang, A. N. Young, M. D. Wang and S. Nie, *Nat. Biotechnol.*, 2008, **26**, 83–90.
50 S. Lee, S. Kim, J. Choo, S. Y. Shin, Y. H. Lee, H. Y. Choi, S. Ha, K. Kang and C. H. Oh, *Anal. Chem.*, 2007, **79**, 916–922.
51 J. H. W. Leuvering, P. J. H. M. Thal, M. van der Waart and A. H. W. M. Schuurs, *Fresenius Z. Anal. Chem.*, 1980, **301**, 132–132.
52 C. X. Zhang, Y. Zhang, X. Wang, Z. M. Tang and Z. H. Lu, *Anal. Biochem.*, 2003, **320**, 136–140.
53 C. A. Mirkin, R. L. Letsinger, R. C. Mucic and J. J. Storhoff, *Nature*, 1996, **382**, 607–609.
54 R. Elghanian, J. J. Storhoff, R. C. Mucic, R. L. Letsinger and C. A. Mirkin, *Science*, 1997, **75**, 1078–1081.
55 D. Murphy and G. Redmond, *Anal. Bioanal. Chem.*, 2005, **381**, 1122–1129.
56 J. H. Li, X. Chu, Y. L. Liu, J. H. Jiang, Z. He, Z. Zhang, G. J. Chen and R. Q. Yu, *Nucleic Acids Res.*, 2005, **33**, E168.
57 B. M. Reinhard, M. Siu, H. Agarwal, A. P. Alivisatos and J. Liphardt, *Nano Lett.*, 2005, **5**, 2246–2252.
58 J. Stehr, C. Hrelescu, R. A. Sperling, G. Raschke, M. Wunderlich, A. Nichtl, D. Heindl, K. Krzinger, W. J. Parak, T. A. Klar and J. Felmann, *Nano Lett.*, 2008, **8**, 619–622.
59 J. N. Nam, S. I. Steva and C. A. Mirkin, *J. Am. Chem. Soc.*, 2004, **126**, 5932–5933.
60 X. Y. Xu, M. S. Han and C. A. Mirkin, *Angew. Chem., Int. Ed.*, 2007, **46**, 3468–3470.
61 P. Batista, E. Pereira, P. Eaton, G. Doria, A. Miranda, I. Gomes, P. Quaresma and R. Franco, *Anal. Bioanal. Chem.*, 2008, **391**, 943–950.
62 J. W. Liu and Y. Lu, *Org. Biomol. Chem.*, 2006, **4**, 3435–3441.
63 L. R. Hirsch, J. B. Jackson, A. Lee, N. J. Halas and J. West, *Anal. Chem.*, 2003, **75**, 2377–2381.
64 L. R. Hirsch, A. M. Gobin, A. R. Lowery, F. Tam, R. A. Drezek, N. J. Halas and J. L. West, *Ann. Biomed. Eng.*, 2006, **34**, 15–22 and refs. cited therein.
65 A. Gole and C. J. Murphy, *Langmuir*, 2005, **21**(23), 10756–10762.
66 E. Dujardin, L.-B. Hsin, C. R. C. Wang and S. Mann, *Chem. Commun.*, 2001, 1264–1265.
67 J. K. N. Mbindyo, B. D. Reiss, B. R. Martin, C. D. Keating, M. J. Natan and T. E. Mallouk, *Adv. Mater.*, 2001, **13**(4), 249–254.
68 C. Y. Chang, H. Wu, H. Chen, Y.-C. Ling and W. Tan, *Chem. Commun.*, 2005, **8**, 1092–1093.
69 X. Li, L. Jiang, Q. Zhan, J. Qian and S. He, *Colloids Surf., A*, 2009, **332**, 172–179.
70 G. J. Nusz, S. M. Marinakos, A. C. Curry, A. Dahlin, F. Hok, A. Wax and A. Chilkoti, *Anal. Chem.*, 2008, **80**, 984–989.
71 V. Pavlov, Y. Xiao, B. Shlyahovsky and I. Wilner, *J. Am. Chem. Soc.*, 2004, **126**, 11768–11769.
72 W. Eck, G. Craig, A. Sigdel, G. Ritter, L. J. Old, L. Tang, M. F. Brennan, P. J. Alle and M. D. Mason, *ACS Nano*, 2008, **2**, 2263–2272.
73 T. A. Taton, C. A. Mirkin and R. L. Letsinger, *Science*, 2000, **289**, 1157–1160.
74 S. A. Lange, G. Roth, S. Wittermann, T. Lacoste, A. Vetter, J. Grassle, S. Kopta, M. Kolleck, B. Breitinger, M. Wick, J. K. H. Horber, S. Dubel and A. Bernard, *Angew. Chem., Int. Ed.*, 2006, **45**, 270–273.
75 R. Martins, P. Batista, L. Silva, L. Raniero, G. Doria, R. Franc and E. Fortunato, *J. Non-Cryst. Solids*, 2008, **354**, 2580–2584.
76 R. Wilson, *Chem. Commun.*, 2003, 108–109.
77 H. He, C. Xie and J. Ren, *Anal. Chem.*, 2008, **80**, 5951–5957.
78 P. C. Ray, G. K. Darbha, A. Ray, J. Walker and W. Hardy, *Plasmonics*, 2007, **2**, 173–183.
79 T. Pons, I. L. Medintz, K. E. Sapsford, S. Higashiya, A. F. Grimes, D. S. English and H. Mattoussi, *Nano Lett.*, 2007, **7**, 3157–3164.
80 C. C. You, O. R. Miranda, B. Gider, P. S. Ghosh, I. B. Kim, B. Erdogan, S. A. Krovi, U. H. F. Bunz and V. M. Rotello, *Nat. Nanotechnol.*, 2007, **2**, 318–323.
81 S. Lee, E.-J. Cha, K. Park, S.-Y. Lee, J. K. Hong, I.-C. Sun, S. Y. Kim, K. Choi, I. C. Kwon, K. Kim and C.-H. Ahn, *Angew. Chem., Int. Ed.*, 2008, **47**, 2804–2807.
82 D. Astruc, *Electron Transfer and Radical Processes in Transition Metal Chemistry*, VCH, New Yok, 1995, ch. 4 and 7.
83 M. Dequaire, C. Degrand and B. Limoges, *Anal. Chem.*, 2000, **72**, 5521–5528.
84 M. Pumera, S. Sanchez, I. Ichinose and J. Tang, *Sens. Actuators*, 2007, **123**, 1195–1205 and refs. therein.
85 S. Guo and E. Wang, *Anal. Chim. Acta*, 2007, **598**, 181–192 and refs. cited therein.
86 M. T. Castaneda, S. Alegret and A. Merkoçi, *Electroanalysis*, 2007, **19**, 743–753.
87 Y. Xiao, F. Patolsky, E. Katz, J. F. Hainfeld and I. Willner, *Science*, 2003, **299**, 1877–1881.
88 P. Scodeller, V. Flexer, R. Szamocki, E. J. Calvo, N. Tognalli, H. Troiani and A. Fainstein, *J. Am. Chem. Soc.*, 2008, **130**, 12690–12697.
89 Y. Wang, W. Wei, X. Liu and X. Zeng, *Mater. Sci. Eng., C*, 2009, **29**, 50–54.
90 D. Tang, R. Yuan, Y. Chai, Y. Fu, J. Dai, Y. Liu and X. Zhong, *Biosens. Biochem.*, 2005, **21**, 539–548.
91 J. Manso, N. M. L. Mena, P. Yánez-Sedeño and J. M. Pingarrón, *Anal. Biochem.*, 2008, **375**, 345–353.
92 J. Lin, C. He, L. Zhang and S. Zhang, *Anal. Biochem.*, 2009, **384**, 130–135.
93 L. Authier, C. Grossiord, P. Grossier and B. Limoges, *Anal. Chem.*, 2001, **73**, 4450–4456.
94 J. Wang, A. Xu and R. Polsky, *J. Am. Chem. Soc.*, 2002, **124**, 4208–4209 and refs. cited therein.
95 K. Idegami, M. Chikae, K. Kerman, N. Nagatami, T. Yuki, T. Endo and E. Tamiya, *Electroanalysis*, 2008, **20**, 14–21.
96 K. Hu, D. Lan, X. Li and S. Zhang, *Anal. Chem.*, 2008, **80**, 9124–9130.
97 H. Wang, C. X. Zhang, Y. Li and H. L. Qi, *Anal. Chem.*, 2006, **575**, 205–211.
98 A. Becue, C. Champod and P. Margot, *Forensic Sci. Int.*, 2007, **168**, 169.
99 M. Yamada and H. Nishihara, *C. R. Chim.*, 2003, **6**(8–10), 919–934 and refs. cited therein.
100 A. Labande, J. Ruiz and D. Astruc, *J. Am. Chem. Soc.*, 2002, **124**, 1782–1789.
101 M.-C. Daniel, J. Ruiz and D. Astruc, *J. Am. Chem. Soc.*, 2003, **125**, 1150–1151.
102 M.-C. Daniel, J. Ruiz, S. Nlate, J.-C. Blais and D. Astruc, *J. Am. Chem. Soc.*, 2003, **125**, 2617–2628.
103 D. Astruc, C. Ornelas and J. Ruiz, *Acc. Chem. Res.*, 2008, **41**, 841–856.
104 C. Valerio, J.-L. Fillaut and J. Ruiz, *J. Am. Chem. Soc.*, 1997, **119**, 2588–2589.
105 R. Tanaka, T. Yuhi, N. Nagatani, T. Endo, K. Kerman, Y. Takamura and E. Tamiya, *Anal. Bioanal. Chem.*, 2006, **385**, 1414–1420.
106 N. S. Lai, C. C. Wang, H. L. Chiang and L. K. Chau, *Anal. Bioanal. Chem.*, 2007, **388**, 901–907.
107 B. Y. Hsieh, Y. F. Chang, M. Y. Ng, W. C. Liu, C. H. Lin, H. T. Wu and C. Chou, *Anal. Chem.*, 2007, **79**, 3487–3493.

108 Z. P. Wang, J. Q. Hu, Y. Jin, X. Jiao and J. H. Li, *Clin. Chem.*, 2006, **52**, 1958–1961.
109 L. R. Hirsch, J. B. Jackson, A. Lee, N. J. Halas and J. L. West, *Anal. Chem.*, 2003, **75**, 2377–2381.
110 C. P. Chan, Y. C. Cheung, R. Renneberg and M. Seydack, *Adv. Biochem. Eng. Biotechnol.*, Springer, Heidelberg, 2007.
111 C. Ou, R. Yuan, Y. Chai and X. He, *Anal. Chim. Acta*, 2007, **603**, 205–213.
112 J. Lin, W. Qu and S. Zhang, *Anal. Sci.*, 2007, **23**, 1059–1063.
113 C. Yu and J. Irudayara, *Anal. Chem.*, 2007, **79**, 572–579.
114 S.-H. Chen, V. C. H. Wu, Y.-C. Chuang and C.-S. Lin, *J. Microbiol. Methods*, 2008, **73**, 7–17.
115 K. Sokolov M. Follen, J. Aaron, I. Pavlova, A. Malpica, R. Lotan and R. Richards-Kortum, *Cancer Res.*, 2003, **63**, 1999–2004.
116 V. Dixit, J. van der Bossche, D. M. Sherman, D. H. Thompson and R. P. Andres, *Bioconjugate Chem.*, 2006, **17**, 603–609.
117 I. H. El-Sayed, X. H. Huang and M. A. El-Sayed, *Nano Lett.*, 2005, **5**, 829–834.
118 X. H. Huang, P. K. Jain, I. H. El Sayed and M. A. El-Sayed, *Future Nanomed.*, 2007, **2**, 681–693.
119 G. Doria, R. Franco and P. Batista, *IET Nanobiotechnol.*, 2007, **1**, 53–57.
120 L. G. Carascosa, M. Moreno, M. Alvarez and L. M. Lechuga, *Trends Anal. Chem.*, 2006, **25**, 196–206.
121 C. M. Medley, J. E. Smith, Z. Tang, Y. Wu, S. Bamrungsap and W. Tan, *Anal. Chem.*, 2008, **80**, 1067–1072.
122 P. Podsiadlo, V. A. Sinani, J. H. Bahng, N. W. S. Kam, J. Lee and N. A. Kotov, *Langmuir*, 2008, **24**, 568–574.
123 M. Eghtedari, A. V. Liopo, J. A. Copland, A. A. Oraevsky and M. Motamedi, *Nano Lett.*, 2009, **9**, 287–291.
124 A. J. Haes, W. P. Hall, L. Chang, W. L. Klein and R. P Van Duyne, *Nano Lett.*, 2004, **4**, 1029–1034.
125 A. J. Haes, L. Chang, W. L. Klein and R. P Van Duyne, *J. Am. Chem. Soc.*, 2005, **127**, 2264–2271.
126 D. G. Georganopoulos, L. Chang, J. M. Nam, C. S. Taxton, E. J. Mufson, W. L. Klein and C. A. Mirkin, *Proc. Natl. Acad. Sci. U. S. A.*, 2005, **102**, 2273–2276.
127 M.-C. Bowman, T. E. Ballard, C. J. Ackerson, D. L. Feldheim, D. M. Margolis and C. Melander, *J. Am. Chem. Soc.*, 2008, **130**, 6896–6897.
128 K. A. Mahmoud and J. H. T. Luong, *Anal. Chem.*, 2008, **80**, 7056–7062.
129 D. Xi, X. Luo, Q. Ning, Q. Lu, K. Yao and Z. Liu, *J. Nanjing Med. Univ.*, 2007, **21**(4), 207–212.
130 P. V. Baptista, M. Koziol-Montewka, J. Paluch-Oles, G. Doria and R. Franco, *Clin. Chem.*, 2006, **52**, 1433–1434.
131 L. R. Hirsch, R. J. Stafford, J. A. Bankson, S. R. Sershen, B. Rivera, R. E. Price, J. D. Hazle and N. J. Halas, *Proc. Natl. Acad. Sci. U. S. A.*, 2003, **100**, 13549–13554.
132 D. P. O'Neal, L. R. Hirsch, N. J. Halas, J. D. Payne and J. L. West, *Cancer Lett.*, 2004, **209**, 171–176.
133 C. Loo, A. Lowery, N. J. Halas, J. West and R. Drezeck, *Nano Lett.*, 2005, **5**, 709–711.
134 I. H. El Sayed, X. H. Huang and M. A. El-Sayed, *Cancer Lett.*, 2006, **239**, 129–135.
135 X. H. Huang, P. K. Jain, I. H. El-Sayed and M. A. El-Sayed, *Photochem. Photobiol.*, 2006, **82**, 412–417.
136 I. Brigger, C. Dubernet and P. Couvreur, *Adv. Drug Delivery Rev.*, 2002, **54**, 631–651.
137 V. P. Zharov, E. N. Galitovskaya, C. Johnson and T. Kelly, *Lasers Surg. Med.*, 2005, **37**, 219–226.
138 H. Maeda, *Adv. Enzyme Regul.*, 2001, **41**, 187–207.
139 P. Jain, I.-H. El-Sayed and M. A. El-Sayed, *Nanotoday*, 2007, **2**, 18–29.
140 X. H. Huang, P. K. Jain, I. H. El-Sayed and M. El Sayed, *Nanomedicine*, 2007, **2**, 681–693.
141 X. H. Huang, I. H. El-Sayed, W. Qian and M. A. El-Sayed, *J. Am. Chem. Soc.*, 2006, **128**, 2115–2120.
142 H. Takahashi, T. Niidome, A. Nariai, Y. Niidome and S. Yamada, *Chem. Lett.*, 2006, **35**, 500–501.
143 T. B. Huff, L. Tong, Y. Zhao, M. N. Hansen, J. X. Cheng and A. Wei, *Nanomedicine*, 2007, **2**, 125–132.
144 D. Pissuwan, S. M. Valenzuela and M. B. Cortie, *Biotechnol. Gen. Eng. Rev.*, 2008, **25**, 93–112.
145 J. M. Stern and J. A. Cadeddu, *Urol. Oncol.*, 2008, **26**, 93–96.
146 Y. T. Lim, M. Y. Cho, B. S. Choi, Y.-W. Noh and B. H. Chung, *Nanotechnology*, 2008, **19**, 375105.
147 K. W. Hu, C.-C. Huang, J.-R. Hwu, D.-B. Shieh and C.-S. Yeh, *Chem.–Eur. J.*, 2008, **14**, 2956–2964.
148 J. M. Stern, J. Stanfield, W. Kabbani, J.-T. Hsieh and J. A. Caddedu, *J. Urol.*, 2008, **179**, 748–753.
149 Y. Cheng, A. C. Samia, J. D. Meyers, I. Panagopoulos, B. Fei and C. Burda, *J. Am. Chem. Soc.*, 2008, **130**, 10643–10647.
150 J. Cardinal, J. R. Klune, E. Chory, G. Jeyabalan, J. S. Kanzius, M. Nalesnik and D. A. Geller, *Surgery*, 2008, **144**, 125–132.
151 C. J. Gannon, C. R. Patra, R. Bhattacharya, P. Mukherjee and S. A. Curley, *J. Nanobiotechnol.*, 2008, **6**, 2, DOI: 10.1186/1477-3155-6-2.
152 R. Bhattacharya and P. Mukherjee, *Adv. Drug Delivery Rev.*, 2008, **60**, 1289–1306.
153 D. L. Chamberland, A. Agarwal, N. Kotov, J. B. Fowlkes, P. L. Carson and X. Wang, *Nanotechnology*, 2008, **19**, 095101.
154 V. P. Zharov, K. E. Mercer, E. N. Galitovskaya and M. Smeltzer, *Biophys. J.*, 2006, **90**, 619–627.
155 D. Peer, J. M. Karp, S. Hong, O. C. Frarokhzad, R. Margalit and R. Langer, *Nat. Nanotechnol.*, 2007, **2**, 751–760.
156 N. L. Rosi, D. A. Giljohann, C. S. Thaxon, A. K. R. Lytton-Jean, M. S. Han and C. A. Mirkin, *Science*, 2006, **312**, 1027–1030.
157 P. Ghosh, G. Han, M. De, C. H. Kim and V. M. Rotello, *Adv. Drug Delivery Rev.*, 2008, **60**, 1307–1315.
158 G. Han, P. Ghosh and V. M. Rotello, *Nanomedicine*, 2007, **2**(1), 113–123.
159 G. Han, P. Ghosh and V. M. Rotello, in *Advanced Experimental Medicine and Biology: Bio-Applications of Nanoparticles*, ed. W. C. W. Chan, Springer, Heidelberg, 2007, vol. 620, ch. 4, pp. 48–56.
160 P. H. Yang, X. S. Sun, J. F. Siu, H. Z. Sun and Q. Y. He, *Bioconjugate Chem.*, 2005, **16**, 494–496.
161 R. J. Lee and P. S. Law, *Biochim. Biophys. Acta*, 1995, **1233**, 134–144.
162 G. F. Paciotti, L. Myer and D. Weinreich, *Drug Delivery*, 2004, **11**, 169–183.
163 G. F. Paciotti, D. G. I. Kingston and L. Tamarkin, *Drug Dev. Res.*, 2006, **67**, 47–54.
164 P. Nativo, I. A. Prior and M. Brust, *ACS Nano*, 2008, **2**, 1639–1644.
165 A. Pal, S. Shah, V. Kulkarni, R. S. R. Murthy and S. Devi, *Mater. Chem. Phys.*, 2009, **113**, 276–282.
166 J. L. Li, L. Wang, X.-Y. Liu, Z.-P. Zhang, H.-C. Guo, W.-M. Liu and S.-H. Tang, *Cancer Lett.*, 2009, **274**, 319–326.
167 R. K. Visaria, R. J. Griffin, B. W. Williams, E. S. Ebbini, G. F. Paciotti, C. W. Song and J. C. Biscof, *Mol. Cancer Ther.*, 2006, **5**, 1014–1020.
168 G. F. Paciotti, D. G. I. Kingston and L. Tamarkin, *Drug Dev. Res.*, 2006, **67**, 47–54.
169 G. Han, C. T. Martin and V. M. Rotello, *Chem. Biol. Drug Des.*, 2006, **67**, 78–82.
170 K. K. Sanhu, M. M. McIntosh, J. M. Smard, S. W. Smith and V. M. Rotello, *Bioconjugate Chem.*, 2002, **13**, 3–6.
171 M. Thomas and A. M. Klibanov, *Proc. Natl. Acad. Sci. U. S. A.*, 2003, **100**, 9138–9143.
172 G. Han, N. S. Chari, A. Verma, R. Hong, C. T. Martin and V. M. Rotello, *Bioconjugate Chem.*, 2005, **16**, 1356–1359.
173 G. Han, C.-C. You, B.-J. Kim, R. S. Turingan, N. S. Forbes C. T. Martin and V. M. Rotello, *Angew. Chem., Int. Ed.*, 2006, **45**, 3165–3169.
174 Z.-J. Zhu, P. S. Ghosh, O. S. Miranda, R. W. Vachet and V. M. Rotello, *J. Am. Chem. Soc.*, 2008, **130**, 14139–14243.
175 Y.-P. Kim, E. Oh, H. K. Shon, D. W. Moon, T. G. Lee and H.-S. Kim, *Appl. Surf. Sci.*, 2008, **255**, 1064–1067.
176 P. N. Sisco, C. G. Wilson, E. Mironova, S. C. Baxter, C. J. Murphy and E. C. Goldsmith, *Nano Lett.*, 2008, **8**, 3409–3412.
177 X. Li, L. Jiang, Q. Zhan, J. Qian and S. He, *Colloids Surf., A*, 2009, **332**, 172–179.
178 S. Dhar, E. M. Reddy, A. Shiras, V. Pokharkar and B. L. V. Prasad, *Chem.–Eur. J.*, 2008, **14**, 10244–10250.
179 R. Goel, D. Swanlund, J. Coad, G. F. Paciotti and J. C. Bischof, *Mol. Cancer Ther.*, 2007, **6**, 2039–2047.

180 R. Goel, G. F. Paciotti and G. F. Bischof, *Prog. Biomed. Optics Imag. Proceeding of SPIE*, 2008, 68420R.
181 E. M. S. Azzam and S. M. I. Morsy, *J. Surf. Deterg.*, 2008, **11**, 195–199.
182 P. Diagaradjane, A. Shetty, J. C. Wang, A. M. Elliot, J. Schwartz, S. Shentu, H. C. Park, A. Deorukhar, R. J. Stafford, S. H. Cho, J. W. Tunnell, J. D. Hazle and S. Krishnan, *Nano Lett.*, 2008, **8**, 1492–1500.
183 M. Stiti, A. Cecchi, M. Rami, M. Abdaoui, V. Baragan-Montero, A. Scozzafava, Y. Guari, J.-Y. Winum and C. T. Supuran, *J. Am. Chem. Soc.*, 2008, **130**, 16130–16131.
184 N. Lewinsky, V. Colvin and R. Drezek, *Small*, 2008, **4**, 26–49.
185 C. J. Murphy, A. M. Gole, J. W. Stone, P. N. Sisco, A. M. Alkilany, E. C. Goldsmith and S. C. Baxter, *Acc. Chem. Res.*, 2008, **41**, 1721–1730.
186 C. M. Goldman, C. D. McCusker, T. Yilmaz and V. M. Rotello, *Bioconjugate Chem.*, 2004, **15**, 897–900.
187 E. Connor, J. Mwamuka, A. Gole, C. J. Murphy and M. Whyatt, *Small*, 2005, **21**, 325–327.
188 A. Tkatchenko, H. Xie, Y. Liu, D. Coleman, J. Ryan, W. Glomm, M. Shipton, S. Franzen and D. Feldheim, *Bioconjugate Chem.*, 2004, **15**, 482–490.
189 C. H. Hu, H. S. Sheu, C. Y. Pu, J. C. Wang, D. B. Shieh, Y. H. Chen and C. S. Yeh, *J. Am. Chem. Soc.*, 2007, **129**, 2139–2146.
190 H. Takahashi, Y. Niidome, T. Niidome, K. Kaneko, H. Kawasaki and S. Yamada, *Langmuir*, 2006, **22**, 2–5.
191 T. Niidome, M. Yamagaa, Y. Okamoto, Y. Akiyama, H. Takahashi, T. Kawano, Y. Katayama and Y. Niidome, *J. Controlled Release*, 2006, **114**, 343–347.
192 M. Hu, J. Chen, Z.-Y. Li, L. Au, G. V. Hartland, X. Li, M. Marquez and Y. Xia, *Chem. Soc. Rev.*, 2006, **35**, 1084–1094.
193 N. Pernodet, X. Fang, Y. Sun, A. Bakhtina, A. Ramakrishnan, J. Sokolov, A. Ulman and M. Radfailovitch, *Small*, 2006, **6**, 766–773.
194 T. S. Hauck, A. A. Ghazani and W. C. W. Chan, *Small*, 2008, **4**, 153–159.
195 R. Gref, P. Couvreur, G. Barratt and E. Mysiakine, *Biomaterials*, 2003, **24**, 4529–4537.
196 N. Hillyer and R. Albrecht, *J. Pharm. Sci.*, 2001, **90**, 1927–1937.
197 A. E. Hawley, S. Davis and L. Illum, *Adv. Drug Delivery*, 1995, **17**, 129–148.
198 P. Maincent, P. Thouvenot, C. Amicabile, M. Hoffman, J. Kreuter, P. Couvreur and J. Devissaguet, *Pharm. Res.*, 1992, **9**, 1534–1539.
199 A. Florence, *Pharm. Res.*, 1997, **14**, 259–266.
200 G. Zhang, Z. Yang, W. Lu, R. Zhang, Q. Huang, M. Tian, L. Li, D. Liang and C. Li, *Biomaterials*, 2009, **30**, 1928–1936.
201 S. Douglas, S. Davies and L. Illum, *CRC Crit. Rev. Ther. Drug Carrier Syst.*, 1986, **3**, 233–261.
202 S. Stolnik, L. Illum and S. Davis, *Adv. Drug Delivery Rev.*, 1995, **16**, 195–214.
203 G. Sonavane, K. Tomoda, A. Sano, H. Ohshima, H. Terada and K. Makino, *Colloids Surf., B*, 2008, **65**, 1–10.
204 G. Sonavane, K. Tomoda and K. Makino, *Colloids Surf., B*, 2008, **66**, 274–280.
205 W. H. de Jong, W. I. Hagens, P. Krystek, M. C. Burger, A. J. A. M. Sips and R. E. Geertsma, *Biomaterials*, 2008, **29**, 1912–1919.
206 J. M. Farma, M. Puhlmann, P. A. Soriano, D. Cox, G. F. Paciotti, L. Tamarkin and H. R. Alexander, *Int. J. Cancer*, 2007, **120**, 2474–2480.
207 E. A. Gratton, P. Polhaus, J. Lee, J. Guo, M. Cho and J. DeSimone, *J. Controlled Release*, 2007, **121**, 10–18.
208 M. Semmler-Behnke, W. G. Kreyling, J. Lipka, S. Fertsch, A. Wenk, S. Takenaka, G. Schmid and W. Brandau, *Small*, 2008, **12**, 2108–2111.
209 R. Shukla, V. Bansal, M. Chaudhary, A. Basu, R. B. Bhonde and M. Satry, *Langmuir*, 2005, **21**, 10644–10654.
210 C. Sönnischen, B. M. Reinhard, J. Liphardt and A. P. Alivisatos, *Nat. Biotechnol.*, 2005, **23**, 741–745.
211 J. M. Nam, C. S. Thaxton and C. A. Mirkin, *Science*, 2003, **301**, 1884–1886.

Chapitre B-2

Synthèse et stabilisation de nanoparticules d'or dans des dendrimères en milieu aqueux

Une nouvelle méthode de réduction des nanoparticules d'or en milieu aqueux est détaillée dans ce chapitre, réduction réalisée au sein de dendrimères fonctionnalisés à leurs périphérie avec des groupements polyethylène glycol (PEG).

Ce chapitre se compose tout d'abord d'une note préliminaire publiée en 2008 à *Chemical Communications* portant sur la synthèse d'une nouvelle série de dendrimères, composée de trois générations et fonctionnalisée par la réaction « click ». Ces dendrimères, rendus solubles et biocompatibles grâce aux PEGs ajoutés en périphérie, sont capables de stabiliser des nanoparticules d'or de manière intra- ou inter-dendritique selon la génération utilisée. Ma contribution à cette note s'arrête à la synthèse dendritique, et M. Abdou K. Diallo, doctorant du groupe, a réalisé la réduction des nanoparticules d'or au sein des dendrimères. Toutes les images de MET (microscopie électronique par transmission) sont réalisées par M. Lionel Salmon, chargé de recherche CNRS membre de l'équipe du Professeur Azzedine Bousseksou, au LCC (Laboratoire de Chimie de Coordination) de Toulouse.

Le travail a ensuite été poursuivi par mes soins afin de déterminer exactement les conditions de stabilisation des nanoparticules d'or par ces dendrimères. Différentes séries de dendrimères (« click » et « non-click », avec et sans PEG) ont été synthétisées et largement caractérisées par IR (Infra-Rouge), RMN ^{1}H (Résonance Magnétique Nucléaire), RMN ^{13}C, chromatographie d'exclusion stérique, analyse élémentaire, MALDI-TOF (Matrix-Assisted Laser Desorption/Ionisation-time-of-flight mass spectrometry), RMN DOSY (Diffusion-Ordered SpectroscopY) et diffusion de lumière.

La stabilisation des nanoparticules d'or est ensuite réalisée soit dans le méthanol avec l'utilisation d'un réducteur ($NaBH_4$, ferrocène, …), soit dans l'eau sans ajout de réducteur supplémentaire selon les séries dendritiques utilisées. Les cinétiques de réaction sont étudiées pour mieux comprendre la fixation des atomes d'or au départ et le mécanisme réactionnel de réduction. Ce travail montre en effet que l'interaction entre les ions Au^{III} et les atomes d'azote des triazoles résultant de la réaction « click » ralentit le phénomène de réduction dans l'eau.

Une autre étude de variation du nombre d'équivalents d'atomes d'or par dendrimère est également menée et une augmentation du diamètre des nanoparticules d'or est observée. Ceci nous mène à l'obtention d'une large gamme de taille de nanoparticules d'or dont le diamètre évolue progressivement de 2 à plus de 40 nm.

La réduction de l'or est suivie par différentes techniques telles que la spectroscopie UV-vis avec l'apparition d'une bande plasmon entre 530 et 570 nm, ou la MET (microscopie électronique de transmission) afin d'estimer les tailles des nanoparticules d'or lorsque leur croissance est finie.

Plusieurs tests non concluants sont réalisés avec différentes dendrons PEG, des polymères contenant ou non des PEG et des dendrimères sans PEG, et ces travaux prouvent que la réduction des nanoparticules d'or dans l'eau n'est réalisable qu'à la condition que le vecteur soit dendritique et qu'il possède des groupements PEG en périphérie.

Ce chapitre se compose de la note préliminaire publiée à *Chemical Communications* ainsi que de ces derniers résultats qui viennent d'être rédigés sous forme de mémoire et soumis au *Journal of the American Chemical Society*.

Gold nanoparticles synthesis and stabilization *via* new "clicked" polyethyleneglycol dendrimers†

Elodie Boisselier,[a] Abdou K. Diallo,[a] Lionel Salmon,[b] Jaime Ruiz[a] and Didier Astruc*[a]

Received (in Cambridge, UK) 28th May 2008, Accepted 27th June 2008
First published as an Advance Article on the web 21st August 2008
DOI: 10.1039/b808987f

Gold nanoparticles (AuNPs) are synthesized and stabilized by new "clicked" dendrimers of generations zero to two (G_0–G_2) containing tri- and tetra-ethyleneglycol tethers; they are either encapsulated by G_1 (81 tethers) and G_2 (243 tethers) or stabilized without encapsulation by G_0 (27 tethers).

The synthesis and stabilization of transition metal nanoparticles (NPs) inside dendrimers have created a timely entry to their application in catalysis and nanosciences.[1–3] In particular, nanometer-sized gold nanoparticles (AuNPs) have been synthesized in this way.[2] Small AuNPs[3,4] are important nanomaterials for catalysis,[5] nanomedicine[6] (*e.g.* cancer cell diagnosis[6a] and treatment[6b]), optics[7] and materials science.[8] So far, however, AuNPs stabilization by dendrimers has only been carried out using PAMAM dendrimers.[9] We recently reported the stabilization of PdNPs by "click" dendrimers and their high catalytic efficiency.[10] We now find that these dendrimers do not stabilize AuNPs, but also that "click" functionalization of the arene-cored polyazido dendrimers with polyethyleneglycol (PEG) tethers provides stabilization of nano-sized AuNPs. Indeed, the "click" reaction[11] has already been largely exploited in dendrimer synthesis.[12]

The synthesis of three generations of dendrimers from G_0 PEG to G_2 PEG dendrimers is shown on Scheme 1. It starts with the known $CpFe^+$-induced nanoallylation of mesitylene under ambient conditions in the presence of KOH and allyl bromide[13a,b] followed by visible-light photolysis in MeCN in the presence of PPh_3 to remove the $CpFe^+$ group and hydrosilylation with $HSiMe_2CH_2Cl$ and Karsted catalyst,[13c,d] then reaction with NaN_3 yields the nona-azide core. The Newkome-type 1 → 3 connectivity[14] is insured by Williamson reaction between the nonachloromethyl core and a Percec-type dendron[15] made of modified gallic acid core functionalized at the focal point by a tetraethylene glycol (TAEG) linker, then by a propargyl group and on the peripheral tethers by triethylene glycol (TEG) termini. Finally, the dendrons are linked to the core using the Cu^I-catalyzed click reaction between the terminal alkyne tail and the azido-terminated dendritic core.[13] We are using stoichiometric amounts of Cu^I, (generated using $CuSO_4$ and ascorbic acid), because dendritic metal encapsulation considerably slows down the reaction or inhibits it,[10b] especially with large dendrimers. The dendrimers of generation 0 (27 TEG termini) to 2 (243 TEG termini) were synthesized in this way and characterized by IR, ^1H and ^{13}C NMR, size exclusion chromatography (G_1, G_2 and G_3), correct elemental analysis (G_0), MALDI TOF (G_0, major peak at M^+: calc. 8820.91; found: 8821.24). DOSY and light scattering gave consistent data for both G_0 and G_1, both methods giving a diameter values of 9 ± 1 nm for G_0 and 18 ± 2 nm for G_1. For G_2, light scattering yielded a diameter value of 20 ± 2 nm (ESI).

The AuNPs were synthesized by reaction between the triazole-containing dendrimers and a stoichiometric amount of $HAuCl_4$ *vs.* the dendrimer triazolyl groups, followed by $NaBH_4$ reduction in methanol. The UV-Vis spectrum shows a plasmon band[4] at 540 nm for the G_0-27-TEG dendrimer-stabilized AuNPs, but this band is absent in the AuNPs stabilized by the higher-generation dendrimers (G_1 and G_2) (Fig. 1). The transmission electron microscopy (TEM) data confirm this trend (Fig. 2) showing that the G_0-dendrimer-stabilized AuNPs are large (4.1 ± 0.5 nm) and cannot be encapsulated in such a small dendrimer that contain only 27 tethers. Thus, several dendrimers are surrounding each AuNP (Fig. 3). On the other hand, the dendrimers of next generations G_1 and G_2 containing, respectively 81 and 243 TEG tethers encapsulate AuNPs of small size (1.9 ± 0.4 nm). The two arguments in favor of dendrimer-encapsulated AuNPs with G_1 and G_2 *vs.* dendrimer-stabilized (but not encapsulated) AuNPs with G_0 are (i) the small size of the AuNPs obtained with G_1 and G_2 *vs.* the their large size with G_0, (ii) the fact that with click-dendrimer-stabilized PdNPs, the same trend was previously shown.[10b] It is noteworthy that the presence of PEG tethers in these dendrimer is required for the formation of AuNPs. Indeed, if either the PEG tethers or the triazole ligands are absent in the dendrimer structure (see ESI†), the AuNPs do not form or are not stable longer than one hour. In conclusion, three generations of "click" dendrimer with PEG tethers has been synthesized and characterized. These dendrimers stabilized AuNPs either by surrounding the AuNP if the dendrimer is small (G_0) or by encapsulating the AuNP if it is large (G_1 and G_2). This stabilization is possible only by the combined action of the 1,2,3-triazolyl and PEG ligands. Other reported non-PEG "click" dendrimers that stabilize PdNPs do not stabilize such AuNPs. Given the optimized biocompatibility of PEG dendrimers and AuNPs,[16] the present PEG dendrimer-stabilized AuNPs might be useful as drug vectors.

[a] *Institut des Sciences Moléculaires, UMR CNRS N°5255, Université Bordeaux 1, 33405 Talence Cedex, France. E-mail: d.astruc@ism.u-bordeaux1.fr; Fax: 33 54040 6646*
[b] *Laboratoire de Chimie de Coordination, UPR CNRS N° 8241, 205 Route de Narbonne, 31077 Toulouse Cedex 04, France*

† Electronic supplementary information (ESI) available: Synthesis, data and spectra for G0–G2 and AuNPs (27 pp.). See DOI: 10.1039/b808987f

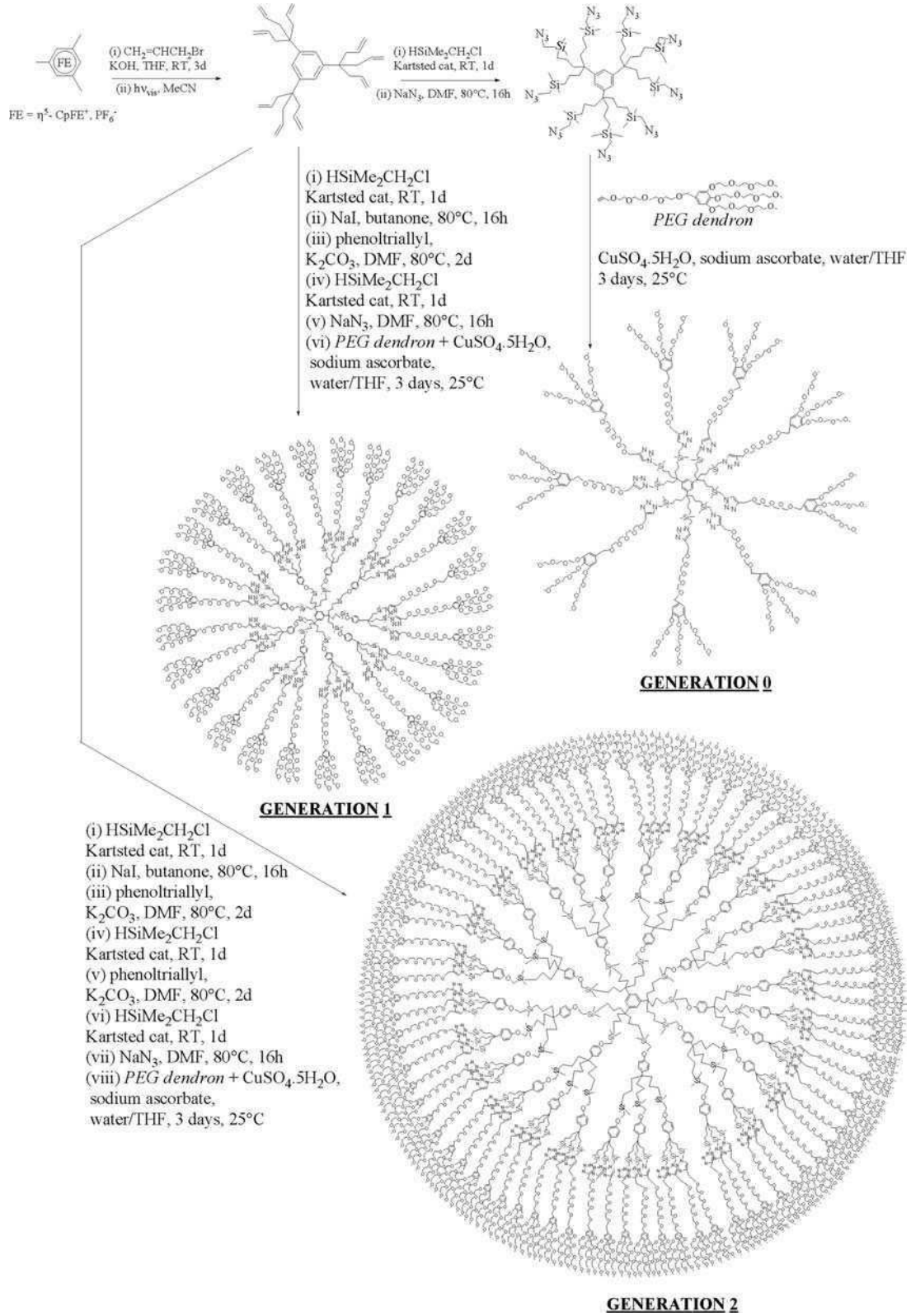

Scheme 1 Synthesis of the three generations of dendrimers from G_0-27-TEG to G_2-243-TEG.

Notes and references

1 M. Zhao, L. Sun and R. M. Crooks, *J. Am. Chem. Soc.*, 1998, **120**, 4877; L. Balogh and D. A. Tomalia, *J. Am. Chem. Soc.*, 1998, **120**, 7355; K. Esumi, A. Suzuki, N. Aihara, K. Usui and K. Torigoe, *Langmuir*, 1998, **14**, 3157.

2 (*a*) R. M. Crooks, M. Zhao, L. Sun, V. Chechik and L. K. Yeung, *Acc. Chem. Res.*, 2001, **34**, 181; (*b*) R. W. J. Scott, O. M. Wilson and R. M. Crooks, *J. Phys. Chem. B*, 2005, **109**, 692.

3 M. Brust, M. Walker, D. Bethell, D. J. Schiffrin and R. Whyman, *J. Chem. Soc., Chem. Commun.*, 1994, 801; J. L. Brennan, N. S. Hatzakis, T. R. Tshikhudo, N. Dirvianskyte, V. Rasumas, S.

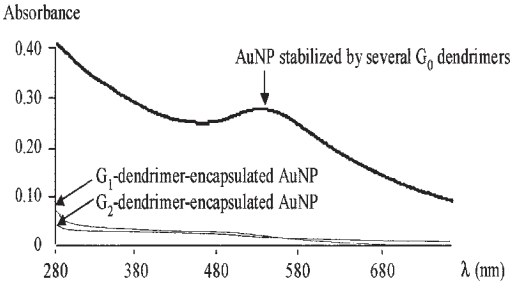

Fig. 1 UV-Vis spectra of AuNP stabilized by several G_0 dendrimers and encapsulated by G_1- and G_2 dendrimers.

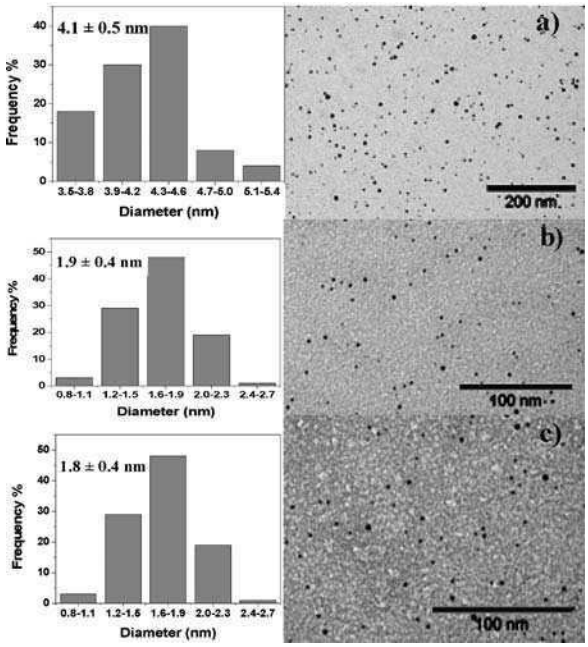

Fig. 2 (a) Dendrimer G_0-27-TEG/AuNPs: TEM image and size distribution; (b) dendrimer G_1-81-TEG/AuNPs: TEM image and size distribution; (c) dendrimer G_2-243-TEG/AuNPs: TEM image and size distribution.

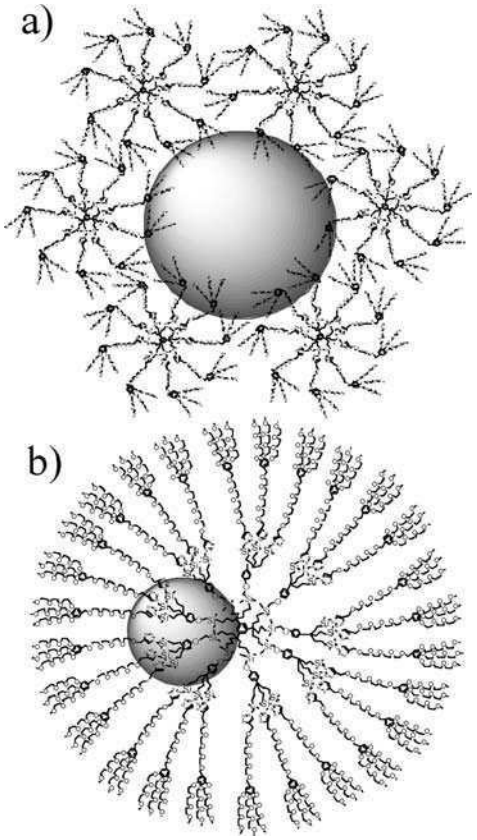

Fig. 3 (a) AuNPs stabilized by several G_0 dendrimers; (b) G_1 dendrimer-encapsulated AuNPs.

Patkar, J. Vind, A. Svendsen, R. J. M. Nolte, A. E. Rowan and M. Brust, *Bioconjugate Chem.*, 2006, **17**, 1373.

4 M.-C. Daniel and D. Astruc, *Chem. Rev.*, 2004, **104**, 293.

5 (*a*) M. Haruta, *Cattech*, 2002, **6**, 102; S. Biela and M. Rossi, *Chem. Commun.*, 2003, 378; A. Abad, H. Corma and H. Garcia, *Chem.–Eur. J.*, 2008, **14**, 212.

6 (*a*) C. A. Mirkin, *Science*, 1997, **277**, 1078; (*b*) V. P. Zharov, E. N. Galitovskaya, C. Johnson and T. Kelly, *Lasers Surg. Med.*, 2005, **37**, 219; (*c*) C. L. Johson, E. Snoeck and M. Ezcurdia, *Nat. Mater.*, 2008, **7**, 120; (*d*) D. Astruc, *C. R. Seances Acad. Sci. Sér. IIb*, 1996, **322**, 757.

7 M. Faraday, *Philos. Trans. R. Soc. London*, 1857, **147**, 145; *Optical Properties of Metal Clusters*, ed. U. Freibig and M. Vollmer, Springer Verlag, New York, 1995.

8 A. Corma, P. Atienzar, H. Garcia and J.-Y. Chan-Ching, *Nat. Mater.*, 2004, **3**, 394.

9 D. A. Tomalia, A. M. Naylor and W. A. Goddard, *Angew. Chem., Int. Ed. Engl.*, 1990, **29**, 138.

10 (*a*) C. Ornelas, J. Ruiz, E. Cloutet, S. Alves and D. Astruc, *Angew. Chem., Int. Ed.*, 2007, **46**, 872; (*b*) C. Ornelas, L. Salmon, J. Ruiz and D. Astruc, *Chem.–Eur. J.*, 2007, **14**, 50; (*c*) C. Ornelas, L. Salmon, J. Ruiz and D. Astruc, *Chem. Commun.*, 2007, 4946; (*d*) A. K. Diallo, C. Ornelas, L. Salmon, J. Ruiz and D. Astruc, *Angew. Chem., Int. Ed.*, 2007, **46**, 8644; (*e*) N. Candelon, D. Lastécouères, A. K. Diallo, J. Ruiz, D. Astruc and J.-M. Vincent, *Chem. Commun.*, 2008, 741; (*f*) C. Ornelas, J. Ruiz, L. Salmon and D. Astruc, *Adv. Synth. Catal.*, 2008, **350**, 837.

11 V. V. Rostovtsev, L. G. Green, V. V. Fokin and K. B. Sharpless, *Angew. Chem., Int. Ed.*, 2002, **41**, 2596; C. W. Tonoe, C. C. Christensen and M. Meldal, *J. Org. Chem.*, 2002, **67**, 3057; V. D. Bock, H. Hiemstra and J. H. van Maarseveen, *Eur. J. Org. Chem.*, 2006, 51.

12 P. Wu, A. K. Felman, A. K. Nugent, C. J. Hawker, A. Scheel, B. Voit, J. Pyun, J. M. J. Fréchet, K. B. Sharpless and V. V. Fokin, *Angew. Chem., Int. Ed.*, 2004, **43**, 3928; M. J. Joralemon, R. K. O'Reilly, J. B. Matson, A. K. Nugent, C. J. Hawker and K. L. Wooley, *Macromolecules*, 2005, **13**, 5436.

13 (*a*) F. Moulines, L. Djakovitch, R. Boese, B. Gloaguen, W. Thiel, J.-L. Fillaut, M.-H. Delville and D. Astruc, *Angew. Chem., Int. Ed. Engl.*, 1993, **32**, 1075; (*b*) V. Sartor, L. Djakovitch, J.-L. Fillaut, F. Moulines, F. Neveu, V. Marvaud, J. Guittard, J.-C. Blais and D. Astruc, *J. Am. Chem. Soc.*, 1999, **121**, 2929; (*c*) J. Ruiz, G. Lafuente, S. Marcen, C. Ornelas, S. Lazare, E. Cloutet, J.-C. Blais and D. Astruc, *J. Am. Chem. Soc.*, 2003, **125**, 7250.

14 (*a*) G. R. Newkome, Z. Yao, G. R. Baker and V. K. Gupta, *J. Org. Chem.*, 1985, **50**, 2003; (*b*) G. R. Newkome, *Pure Appl. Chem.*, 1998, **70**, 2337; G. R. Newkome, C. N. Moorefield and F. Vögtle, *Dendrimers and Dendrons. Concepts, Syntheses, Applications*, Wiley-VCH, Weinheim, 2001.

15 (*a*) V. Percec, G. Johansson, G. Ungar and J. Zhou, *J. Am. Chem. Soc.*, 1996, **118**, 9855; (*b*) V. S. K. Balagurusamy, G. Ungar, V. Percec and G. Johansson, *J. Am. Chem. Soc.*, 1997, **119**, 1539.

16 K. Kono, *Bioconjugate Chem.*, 1999, **10**, 1115; N. Malik, *Anticancer Drugs*, 1999, **10**, 767; N. Malik, *J. Controlled Release*, 2000, **65**, 133; S. H. Battah, *Bioconjugate Chem.*, 2001, **12**, 980; F. Aulenta, W. Hayes and S. Rannard, *Eur. Polym. J.*, 2003, **39**, 1741; E. R. Gillies and J. M. J. Fréchet, *Rev. DDT*, 2005, **10**, 1; S.-Y. Shim, D.-K. Lim and J.-M. Nam, *Nanomedicine*, 2008, **3**, 215; K. K. Jain, *Med. Princ. Pract.*, 2008, **17**, 89.

Supplementary Material (ESI) for Chemical Communications

Gold Nanoparticles Synthesis and Stabilization via New "Clicked" Polyethyleneglycol Dendrimers

Elodie Boisselier, Abdou Khadri Diallo, Lionel Salmon, Jaime Ruiz, Didier Astruc*

ELECTRONIC SUPPLEMENTARY INFORMATION

General procedure for the synthesis of the new "clicked" PEG dendrimers:

The azido-terminated dendrimer (1 eq.) and the alkyne dendron (1.5 eq. *per* branch) were dissolved in THF. At 0°C, $CuSO_4$ was added (2 eq. *per* branch, 1M water solution), followed by the dropwise addition of a freshly prepared solution of sodium ascorbate (4 eq. *per* branch, 1M water solution) in order to set a 1:1 (THF/water) ratio. The solution was allowed to stir for 12h at 25°C under N_2. After removing THF under vacuum, CH_2Cl_2 and an aqueous ammonia solution were added. The mixture was allowed to stir for 10 min. in order to remove all the Cu^{II} trapped inside the dendrimer as $[Cu(NH_3)_6]^{2+}$. The organic phase was washed twice with water, dried with sodium sulfate, and the solvent was removed under vacuum. The product was precipitated with MeOH/ether in order to remove the excess dendron.

Equation for the measurement of the diffusion coefficients by ^1H NMR

The goal of this series of experiments is to measure the diffusion coefficients (noted D) of G_0-27-TEG, G_1-81-TEG and G_2-243-TEG by ^{1}H NMR.

First, the measurement of D allows to calculate the hydrodynamic diameter of a molecule. Then, the ^{1}H NMR experiment focuses on the diffusion that is mathematically treated according to a DOSY process (Diffusion Ordered SpectroscopY) in order to obtain the equivalent of a spectral chromatography. The objective is to measure the size of the molecules in solution by ^{1}H NMR.

The dendrimers are considered as spherical molecular objects, and characterized by an apparent diffusion coefficient. The application of the Stokes-Einstein law gives an estimate of the diameter of the molecule.

Stokes-Einstein law:

$D = K_B T / 6\pi\eta r_H$

D: diffusion constant; K_B: Boltzman's constant; T: temperature (K); η: solvent viscosity; r_H: hydrodynamic radius of the species.

Synthesis and characterization of the alkyne dendron

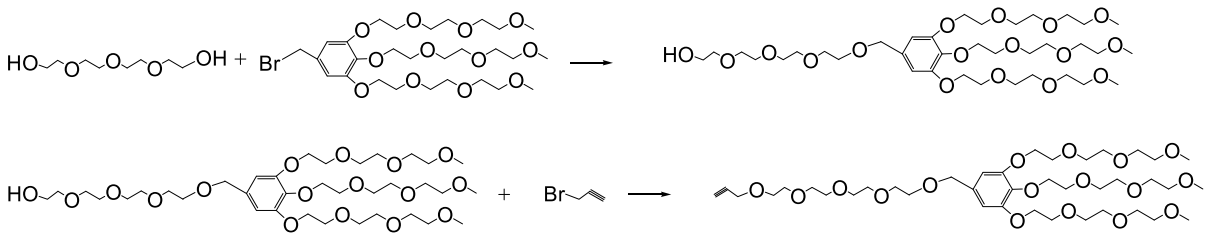

The tris-triethylene glycol dendron (1 g, 1.57 mmol) and the tetraethylene glycol (2.95 g, 15.7 mmol) were introduced in a Schlenck, and dry THF (50 mL) was added. NaH (108 mg, 2.7 mmol) was added to the solution. The mixture was stirred for 12 hours at 50°C. At the end of the reaction, water was added, then THF was removed. The product was extracted with CH_2Cl_2 and purified by chromatography (MeOH). 1g of a yellow oil was obtained (83% yield).

The tris-triethylene glycol tetraethylene glycol dendron (600 mg, 0.65 mmol) and dry THF (50 mL) were introduced in a Schlenck, and NaH (47 mg, 1.95 mmol) was added at 0°C. Propargyl bromide (155 mg, 1.3 mmol) was added to the solution. The mixture was stirred for 2 hours at 0°C, then 2 hours at 25°C. At the end of the reaction, water was added, then THF and excess propargyl bromide were removed under vacuum. The product was extracted with CH_2Cl_2 yielding 600 mg of a yellow oil (95% yield).

^{1}H NMR ($CDCl_3$, 250MHz): 6.39 (2H, C*H*-arom. extern), 4.26 (2H, O-CH_2-arom. extern), 3.98 (4H, CH_2O-arom. extern and CH_2-alkyne), 3.46 (30H, OCH_2CH_2O), 3.17 (9H, CH_3O), 2.36 (1H, C-C*H* alkyne) **(see the spectrum page 4)**

^{13}C NMR ($CDCl_3$, 62 MHz): 152.41 (*C*q-O arom.), 137.50 (*C*q-CH_2 arom.), 133.63 (Cq-*C*H2-O), 106.87 (*C*H arom.), 79.54 (*C*q alkyne), 74.75 (*C*H alkyne), 70.46 (O-*C*H_2), 58.74(O-*C*H_3), 58.13 (*C*H_2-alkyne) **(see the spectrum page 5)**

Infrared υ_{alkyne}: 2100 cm^{-1} **(see the spectrum page 6)**

Maldi TOF : Calc. for $C_{39}H_{68}O_{17}$: 808; found: 831 (MNa^+) **(see the spectrum page 6)**

^{1}H NMR spectrum of the alkyne dendron

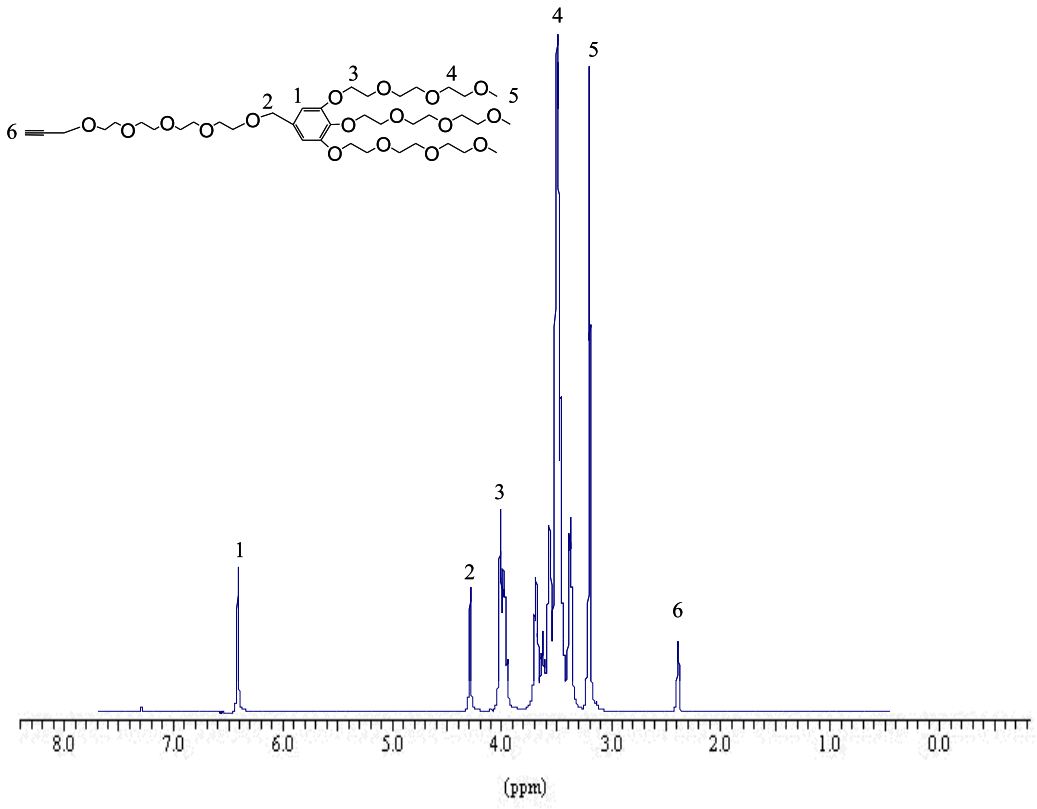

^{1}H NMR ($CDCl_3$, 250MHz): 6.39 (2H, C*H*-arom. extern), 4.26 (2H, O-CH_2-arom. extern), 3.98 (4H, CH_2O-arom. extern and CH_2-alkyne), 3.46 (30H, OCH_2CH_2O), 3.17 (9H, CH_3O), 2.36 (1H, C-C*H* alkyne).

^{13}C NMR spectrum of the alkyne dendron

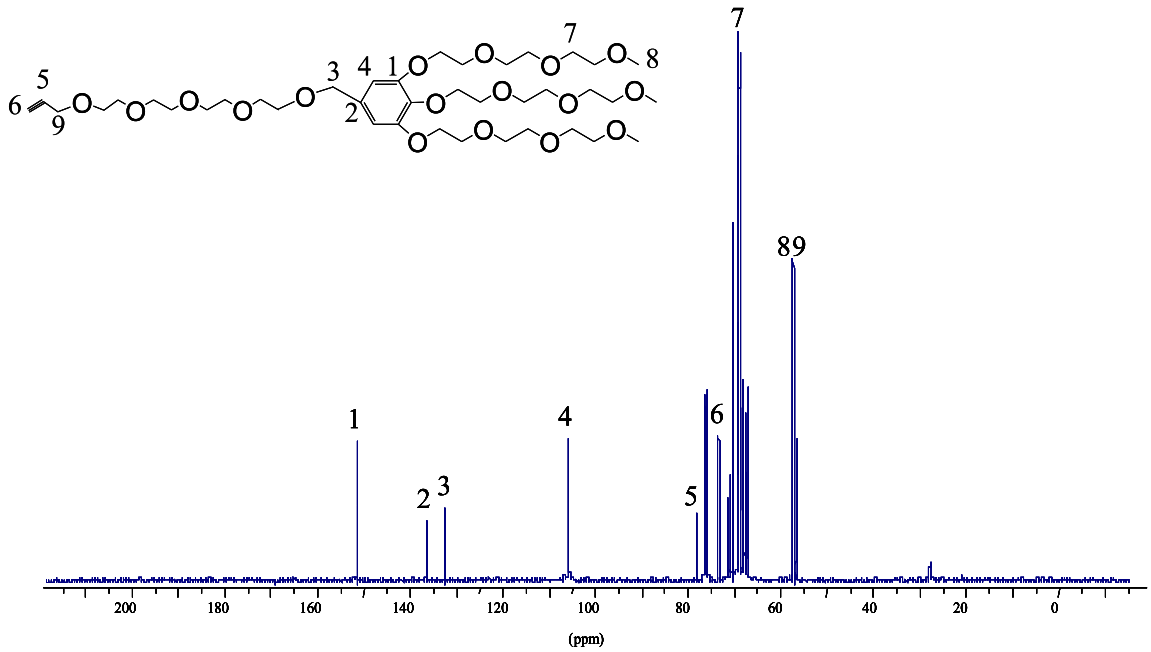

^{13}C NMR ($CDCl_3$, 62 MHz): 152.41 (*C*q-O arom.), 137.50 (*C*q-CH_2 arom.), 133.63 (Cq-*C*H2-O), 106.87 (*C*H arom.), 79.54 (*C*q alkyne), 74.75 (*C*H alkyne), 70.46 (O-*C*H_2), 58.74(O-*C*H_3), 58.13 (*C*H_2-alkyne).

IR spectrum of the alkyne dendron

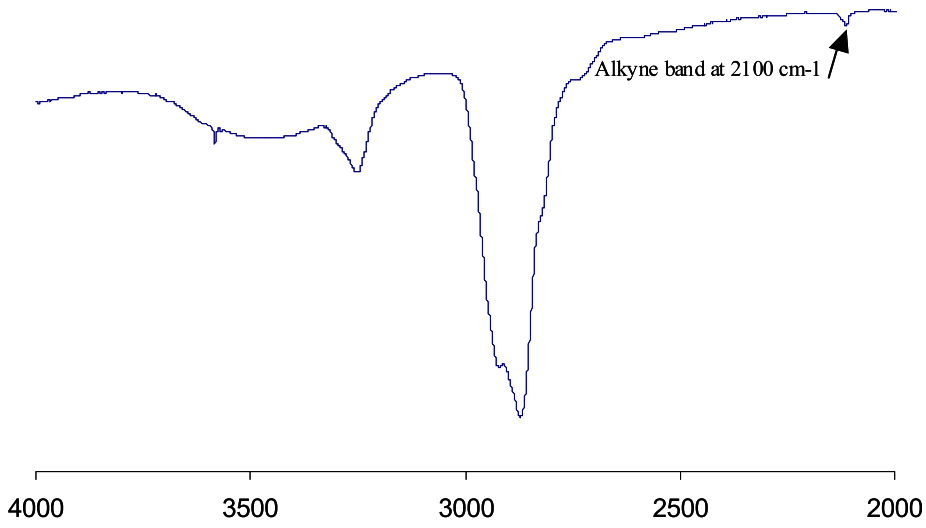

Infrared υ_{alkyne}: 2100 cm^{-1}.

Mass spectrum of the alkyne dendron

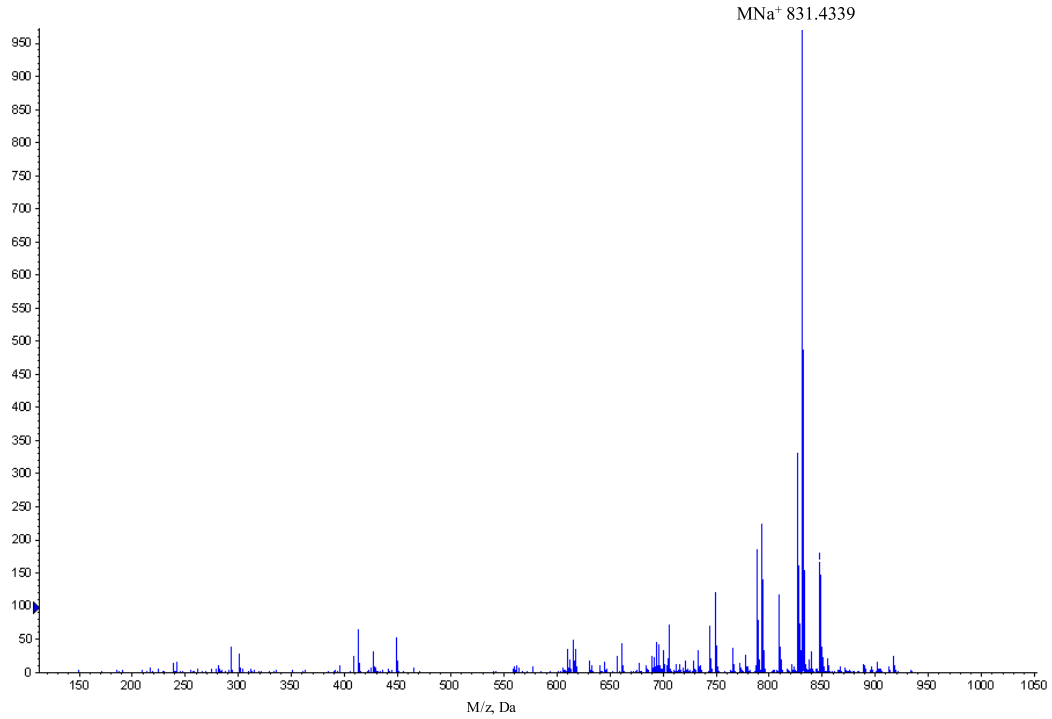

Maldi TOF : Calc. for $C_{39}H_{68}O_{17}$: 808; found: 831 (MNa^+).

G_0-27-PEG

Mw = 8 787 $g.mol^{-1}$

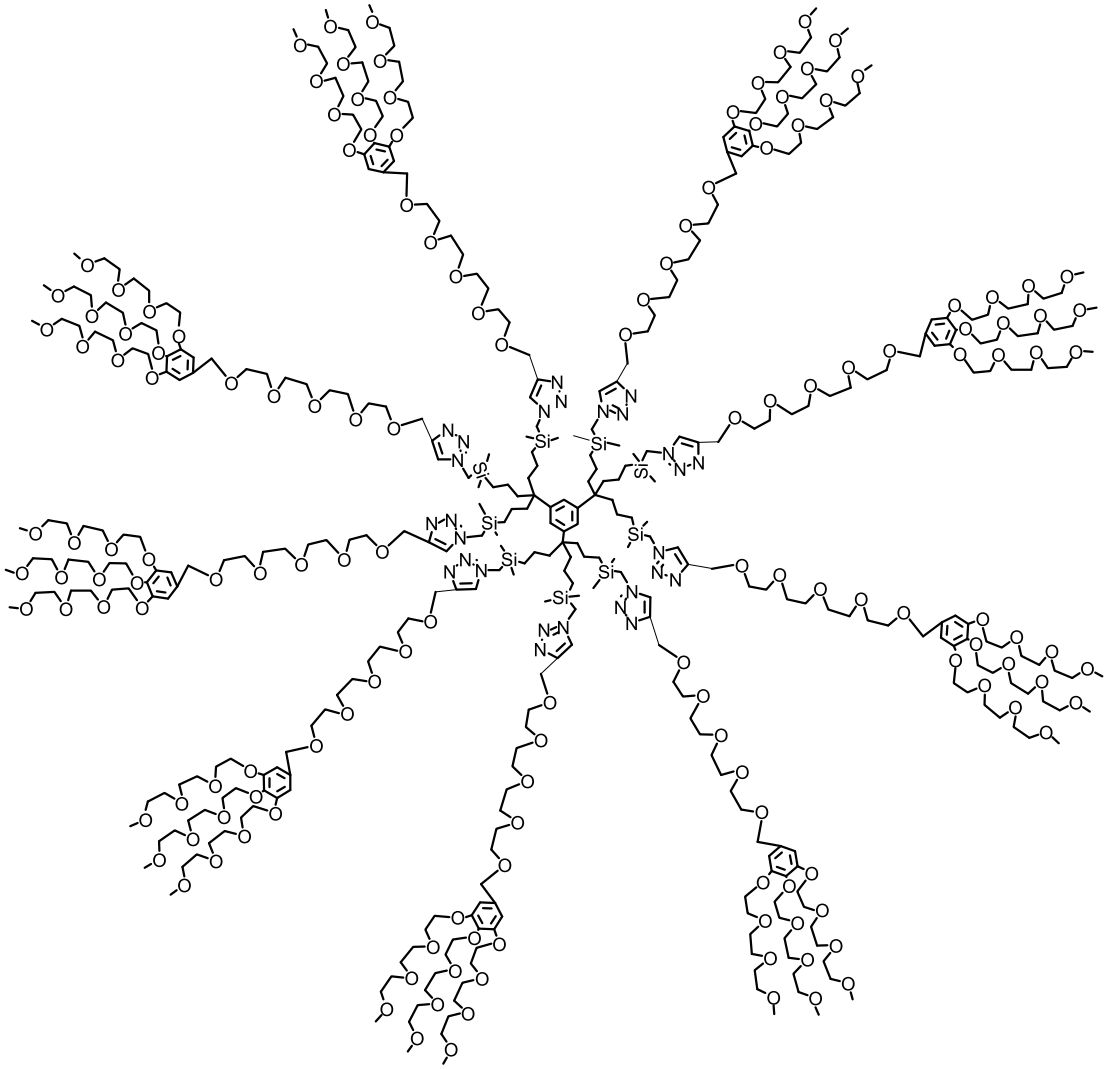

Characterization of G_0-27-TEG

^{1}H NMR ($CDCl_3$, 250MHz): 7.45 (9H, C*H*-triazole), 6.93 (36H, C*H*-arom. intern), 6.56 (18H, C*H*-arom. extern), 4.62 (18H, triazole-CH_2-0), 4.43 (18H, O-CH_2-arom. extern), 4.11 (72H, CH_2O-arom. extern and Si-CH_2-triazole), 3.64 (414H, OCH_2CH_2O), 3.37 (27H, CH_3O), 1.59 (18H, CH_2CH$_2$CH$_2$Si), 1.07 (18H, CH$_2$CH_2CH$_2$Si), 0.60 (18H, CH$_2$CH$_2$CH_2Si), 0.006 (54H, Si(CH_3)$_2$). **(see the spectrum page 9)**

^{13}C NMR ($CDCl_3$, 62 MHz): 151.62 (*C*H, extern arom.), 144.48 (C_q of triazole), 136.83 (*C*q, arom. core), 132.75 (*C*q, arom. extern), 123.52 (*C*H of triazole and arom. core), 106.23 (C_qCH$_2$O), 69.54 (OCH_2CH_2O), 63.53 (triazole-CH_2-O), 58.00 (CH_3O), 53.38 (OCH2-arom.extern), 43.77 (CH_2CH$_2$CH$_2$Si), 42.7 (SiCH_2-triazole), 40.93 (*C*q-arom.intern), 17.82 (CH$_2$CH_2CH$_2$Si), 14.90 (CH$_2$CH$_2$CH_2Si), -4.84 (Si(CH_3)$_2$). **(see the spectrum page 10)**

DOSY : D = 1.16 (± 0.1) x 10^{-10} m²/s
Rh = 4.9 (± 0.1) nm
(D: diffusion coefficient; Rh : hydrodynamic radius) **(see DOSY spectrum page 11)**

IR: no alkyne and azide bands **(see the spectrum page 12)**

SEC : **(see the spectrum page 23)**

MALDI-TOF mass spectrum: Calc. for $C_{414}H_{741}O_{153}N_{27}Si_9$: 8798; found: 8824 ($MNa^+$). **(see the spectrum page 12)**

Elemental Analysis: Anal. Calc. for $C_{414}H_{741}O_{153}N_{27}Si_9$: C 56.52, H 8.49; found: C 56.31, H 8.49

Light scattering : Rh = 4.5 (± 0.4) nm

^{1}H NMR spectrum of G_0-27-PEG

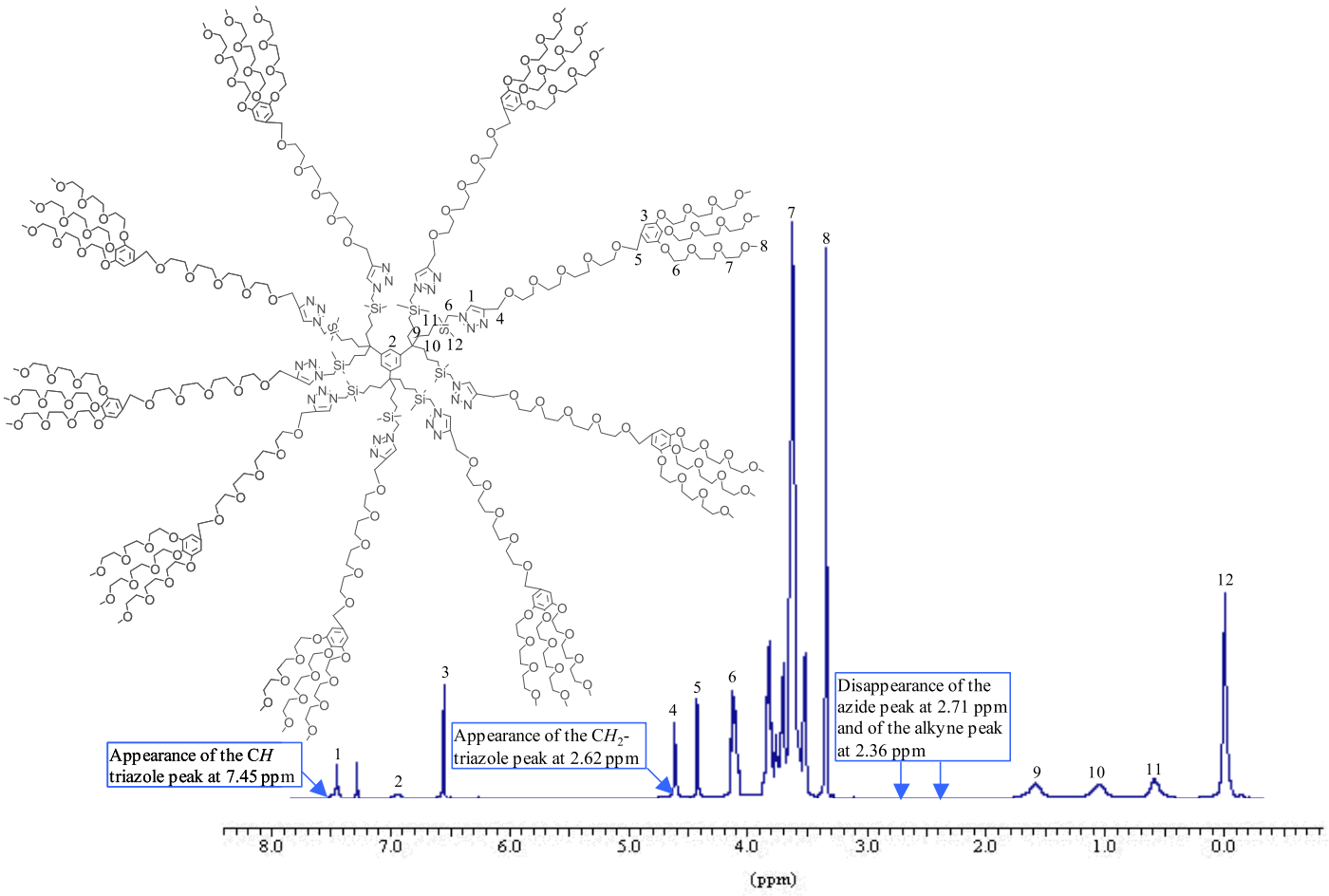

^{1}H NMR ($CDCl_3$, 250MHz): 7.45 (9H, C*H*-triazole), 6.93 (36H, C*H*-arom. intern), 6.56 (18H, C*H*-arom. extern), 4.62 (18H, triazole-CH_2-0), 4.43 (18H, O-CH_2-arom. extern), 4.11 (72H, CH_2O-arom. extern and Si-CH_2-triazole), 3.64 (414H, OCH_2CH_2O), 3.37 (27H, CH_3O), 1.59 (18H, CH_2CH$_2$CH$_2$Si), 1.07 (18H, CH$_2$CH_2CH$_2$Si), 0.60 (18H, CH$_2$CH$_2$CH_2Si), 0.006 (54H, Si(CH_3)$_2$).

^{13}C NMR spectrum of G_0-27-PEG

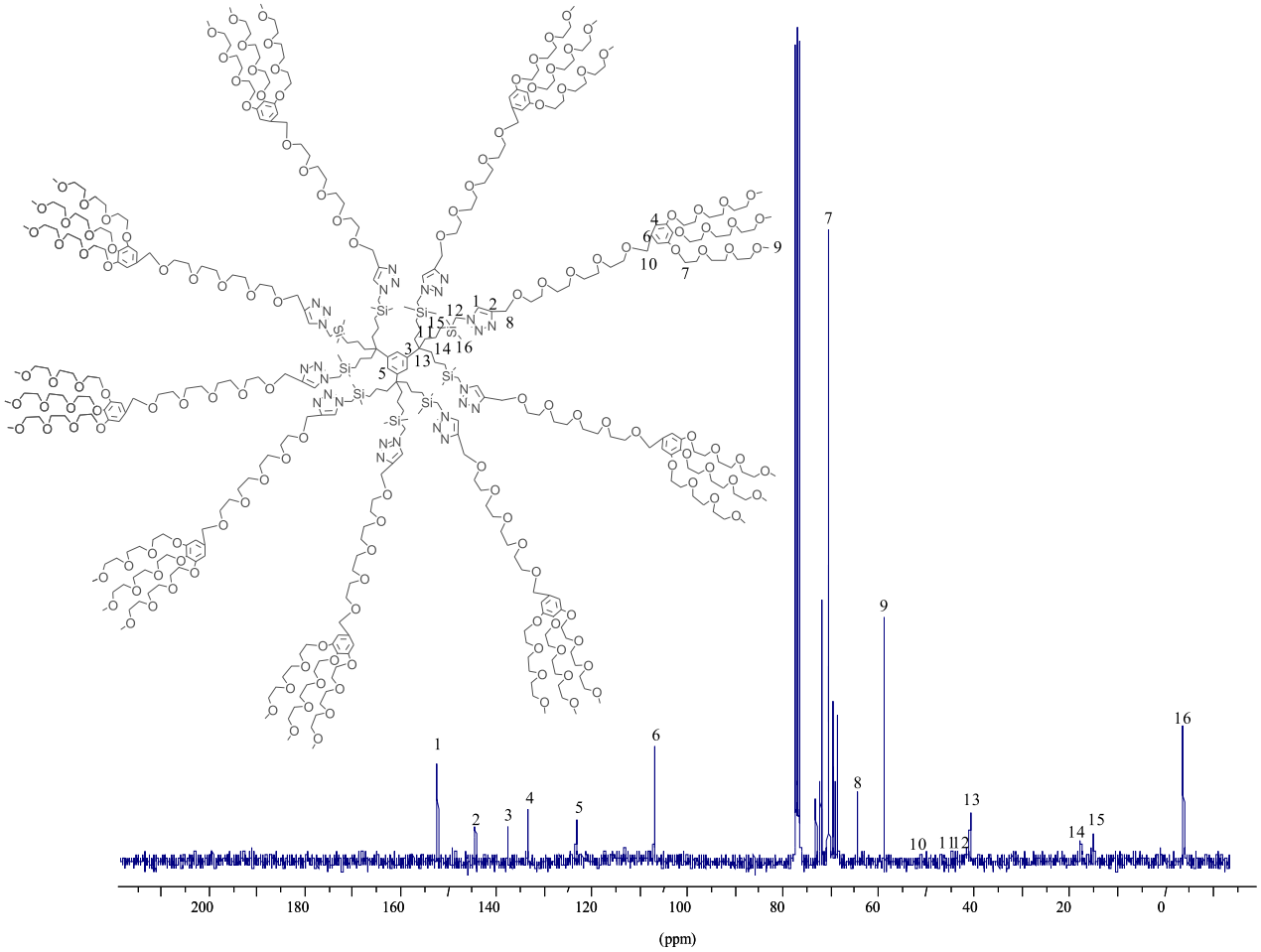

^{13}C NMR ($CDCl_3$, 62 MHz): 151.62 (*C*H, extern arom.), 144.48 (C_q of triazole), 136.83 (*C*q, arom. core), 132.75 (*C*q, arom. extern), 123.52 (*C*H of triazole and arom. core), 106.23 (C_qCH_2O), 69.54 (OCH_2CH_2O), 63.53 (triazole-CH_2-O), 58.00 (CH_3O), 53.38 (OCH2-arom.extern), 43.77 ($CH_2CH_2CH_2Si$), 42.7 ($SiCH_2$-triazole), 40.93 (*C*q-arom.intern), 17.82 ($CH_2CH_2CH_2Si$), 14.90 ($CH_2CH_2CH_2Si$), -4.84 ($Si(CH_3)_2$).

DOSY spectrum of G_0-27-PEG

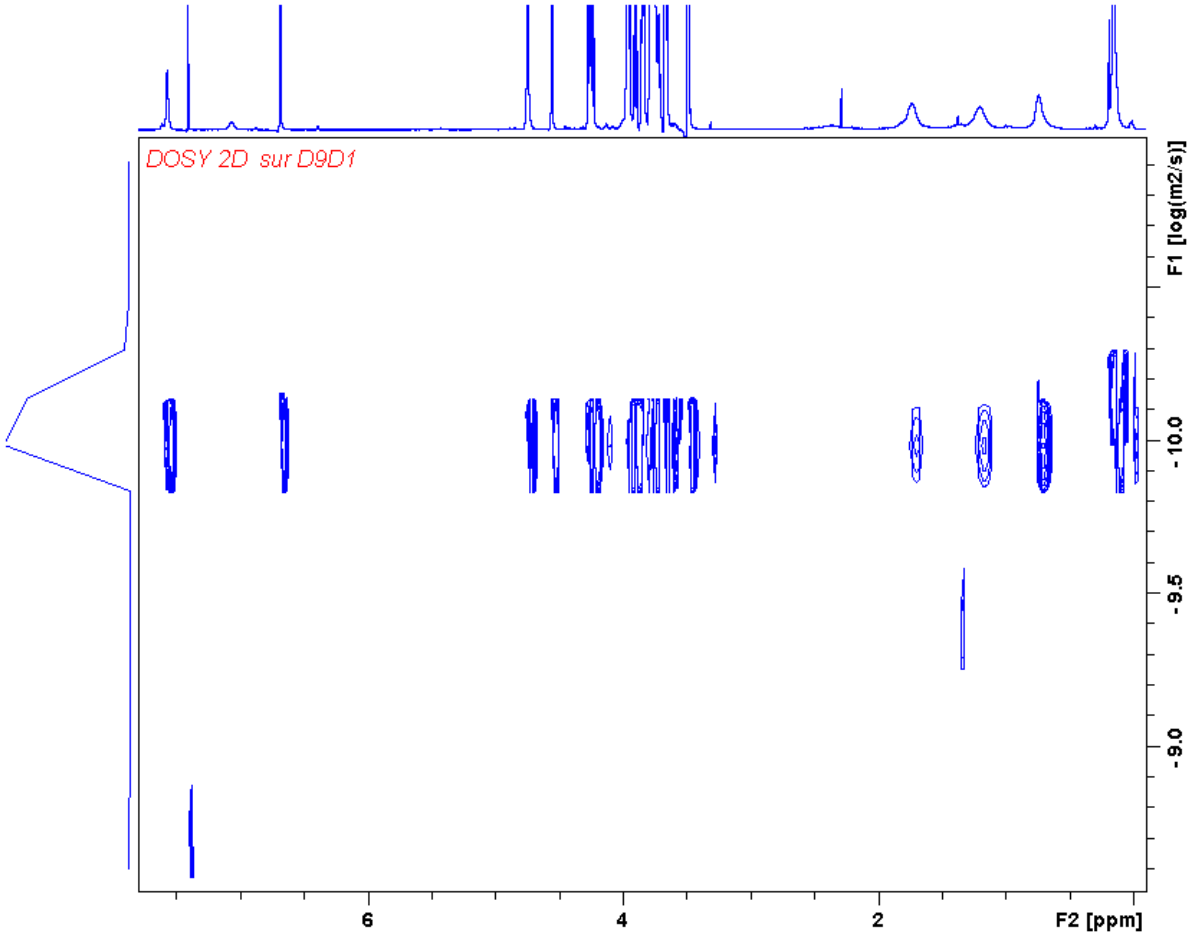

DOSY : D = 1.16 (± 0.1) x 10^{-10} m^2/s
Rh = 4.9 (± 0.1) nm
(D: diffusion coefficient; Rh : hydrodynamic radius) .

IR spectrum of G_0-27-PEG

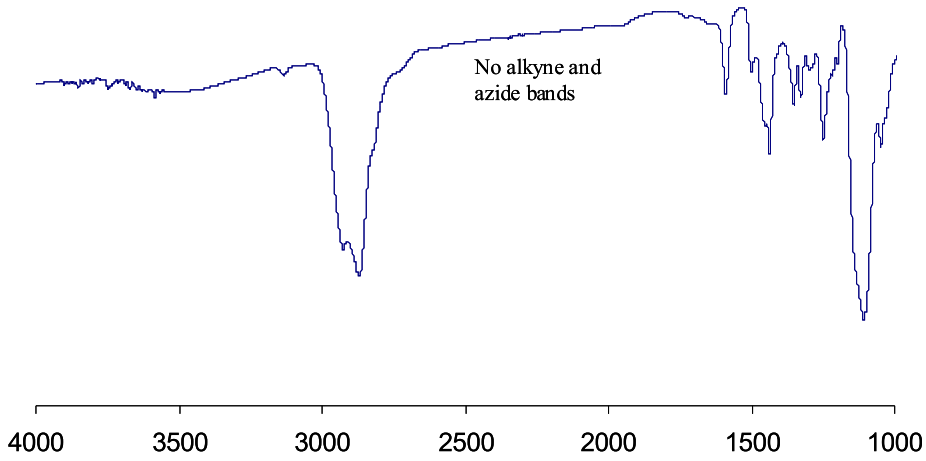

MALDI-TOF mass spectrum of G_0-27-PEG

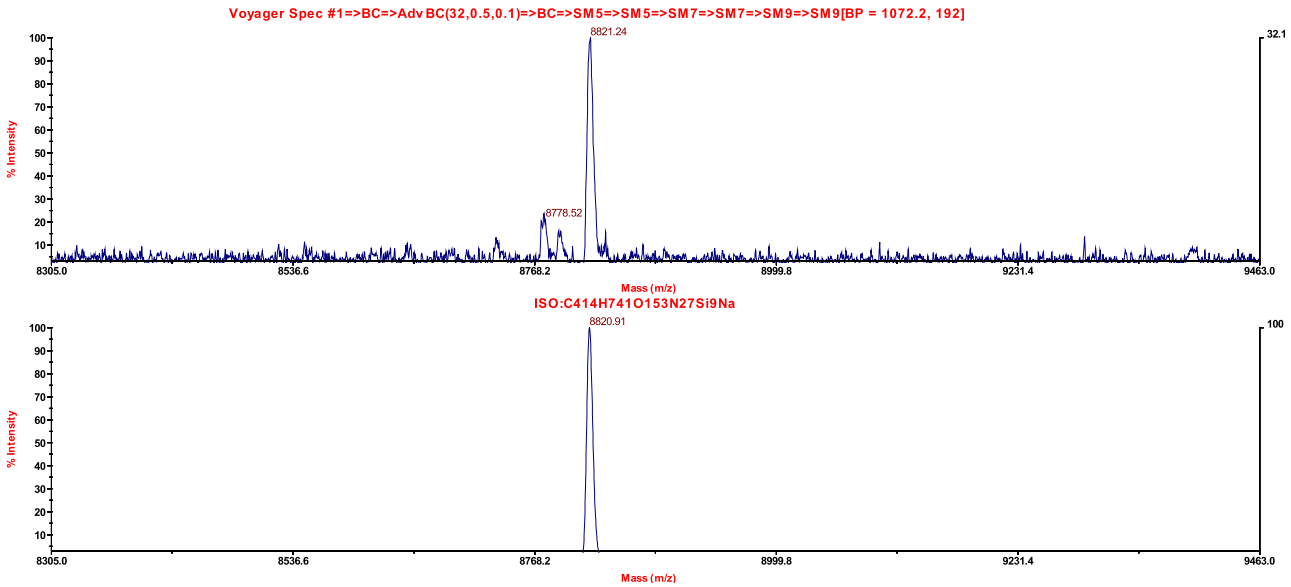

MALDI-TOF: Calc. for $C_{414}H_{741}O_{153}N_{27}Si_9$: 8798; found: 8821.25 ($MNa^+$).

G_1-81-PEG

Mw = 28 462 $g.mol^{-1}$

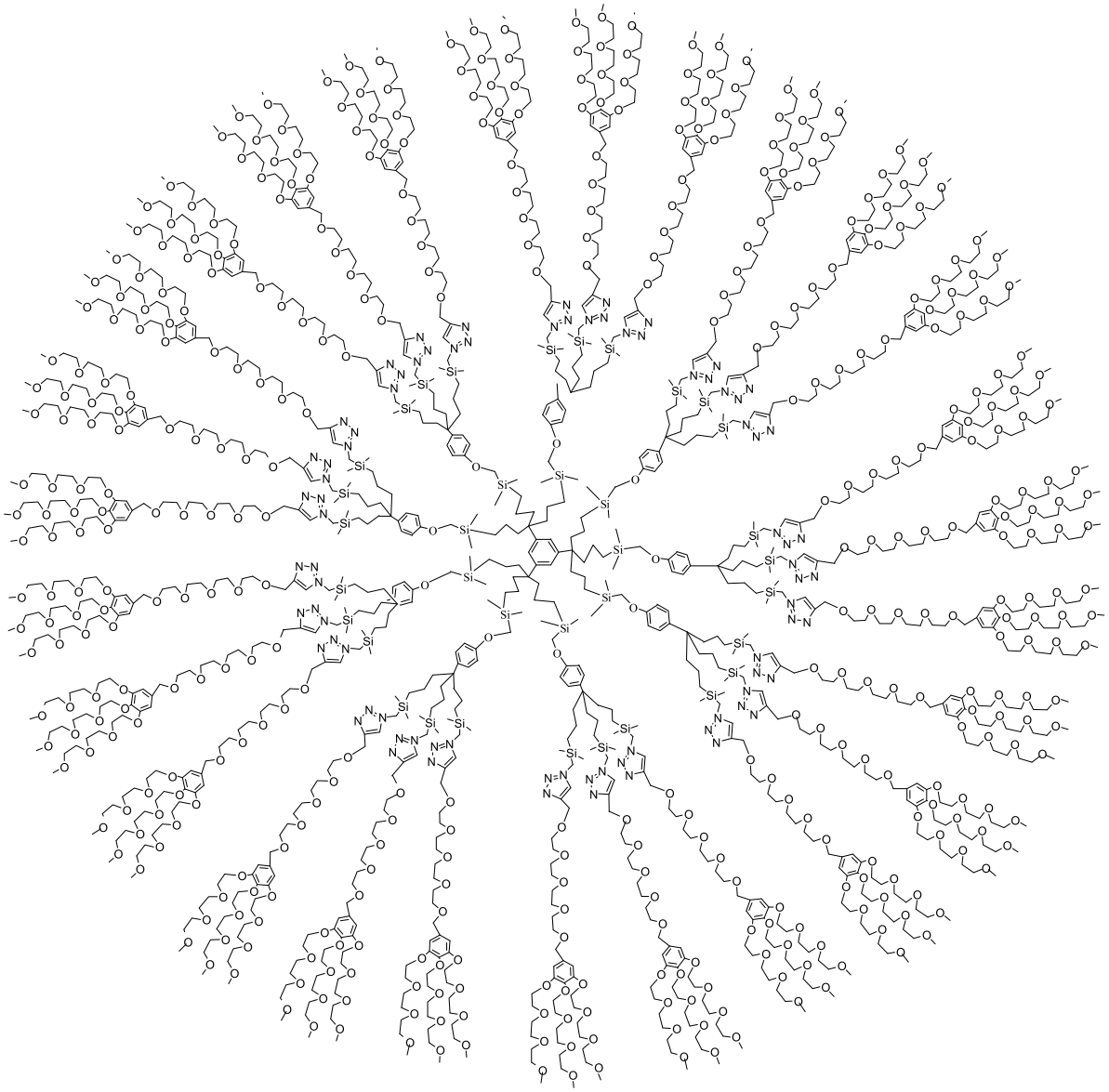

Characterization of G_1-81-TEG

^{1}H NMR ($CDCl_3$, 250MHz): 7.41 (27H, C*H*-triazole), 6.97 (144H, C*H*-arom. intern), 6.56 (54H, C*H*-arom. extern), 4.62 (54H, triazole-CH_2-0), 4.43 (54H, O-CH_2-arom. extern), 4.13 (126H, CH_2O-arom. extern and Si-CH_2-triazole), 3.64 (1242H, OCH_2CH_2O), 3.37 (81H, CH_3O), 1.59 (54H, CH_2CH$_2$CH$_2$Si), 1.09 (54H, CH$_2$CH_2CH$_2$Si), 0.57 (54H, CH$_2$CH$_2$CH_2Si), 0.06 (216H, Si(CH_3)$_2$) **(see the spectrum page 15)**

^{13}C NMR ($CDCl_3$, 62 MHz): 152.60 (*C*H, extern arom.), 144.48 (C_q of triazole), 137.79 (*C*q, arom. core), 133.75 (*C*q, arom. extern), 126.12 and 113.9 (*C*H-arom. Intern), 123.52 (*C*H of triazole and arom. core), 107.23 (C_qCH$_2$O), 70.66 (OCH_2CH_2O), 69.11 (Si-CH_2-O), 63.53 (triazole-CH_2-O), 58.99 (CH_3O), 53.38 (OCH_2-arom.extern), 43.77 (CH_2CH$_2$CH$_2$Si), 42.7 (SiCH_2-triazole), 40.93 (*C*q-arom.intern), 17.82 (CH$_2$CH_2CH$_2$Si), 14.90 (CH$_2$CH$_2$CH_2Si), -4.84 (Si(CH_3)$_2$) **(see the spectrum page 16)**

DOSY : D = 5.94 (± 0.1) x 10^{-11} m²/s
Rh = 9.7 (± 0.7) nm
(D: diffusion coefficient; Rh : hydrodynamic radius)**(see the DOSY spectrum page 17)**

IR: no alkyne and azide bands **(see the spectrum page 17)**

SEC : **(see the spectrum page 23)**

Light scattering : Rh = 9.1 (± 0.6) nm

^{1}H NMR spectrum of G_1-81-PEG

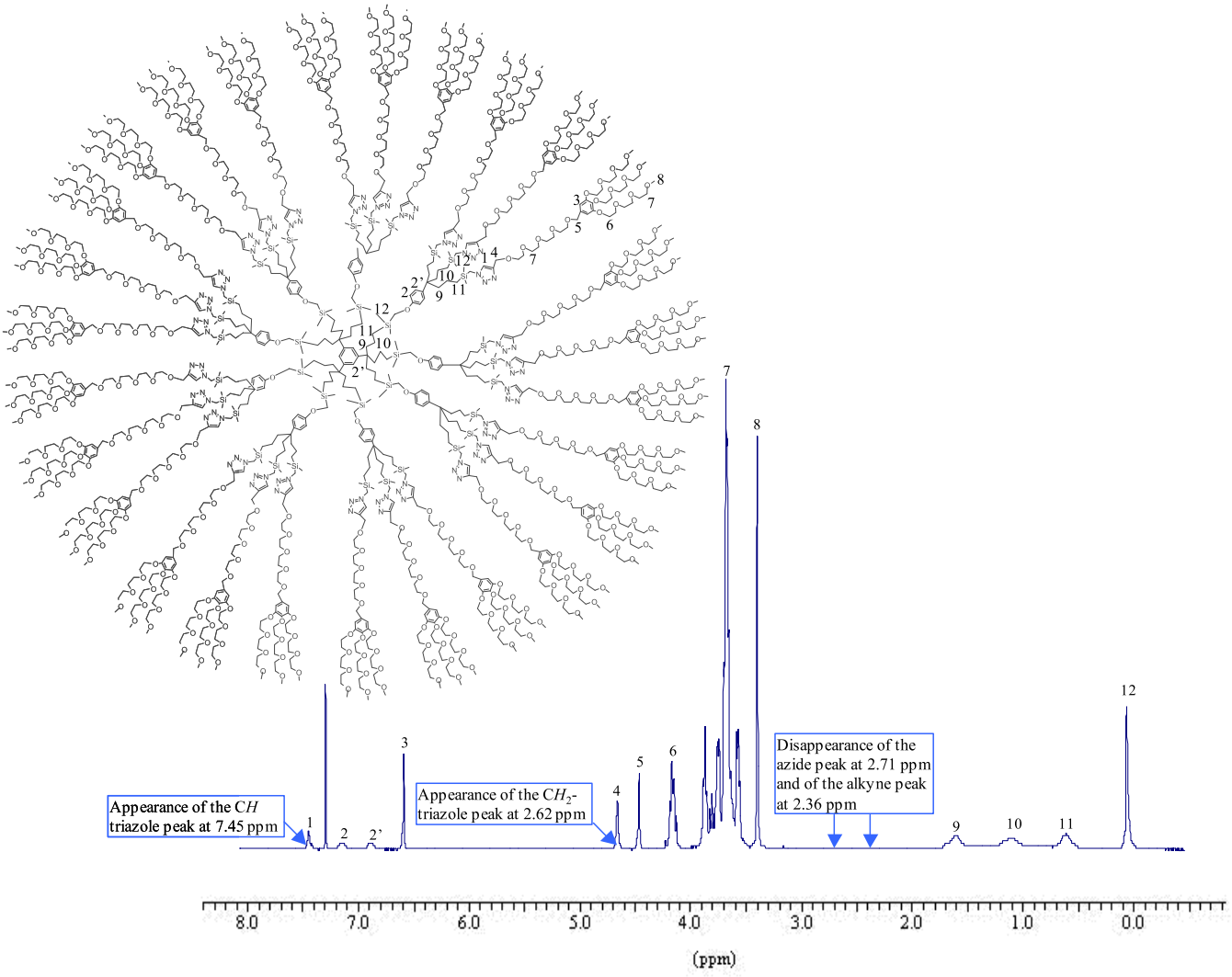

^{1}H NMR ($CDCl_3$, 250MHz): 7.41 (27H, C*H*-triazole), 6.97 (144H, C*H*-arom. intern), 6.56 (54H, C*H*-arom. extern), 4.62 (54H, triazole-CH_2-0), 4.43 (54H, O-CH_2-arom. extern), 4.13 (126H, CH_2O-arom. extern and Si-CH_2-triazole), 3.64 (1242H, OCH_2CH_2O), 3.37 (81H, CH_3O), 1.59 (54H, CH_2CH$_2$CH$_2$Si), 1.09 (54H, CH$_2$CH_2CH$_2$Si), 0.57 (54H, CH$_2$CH$_2$CH_2Si), 0.06 (216H, Si(CH_3)$_2$).

^{13} C NMR spectrum of G_1-81-PEG

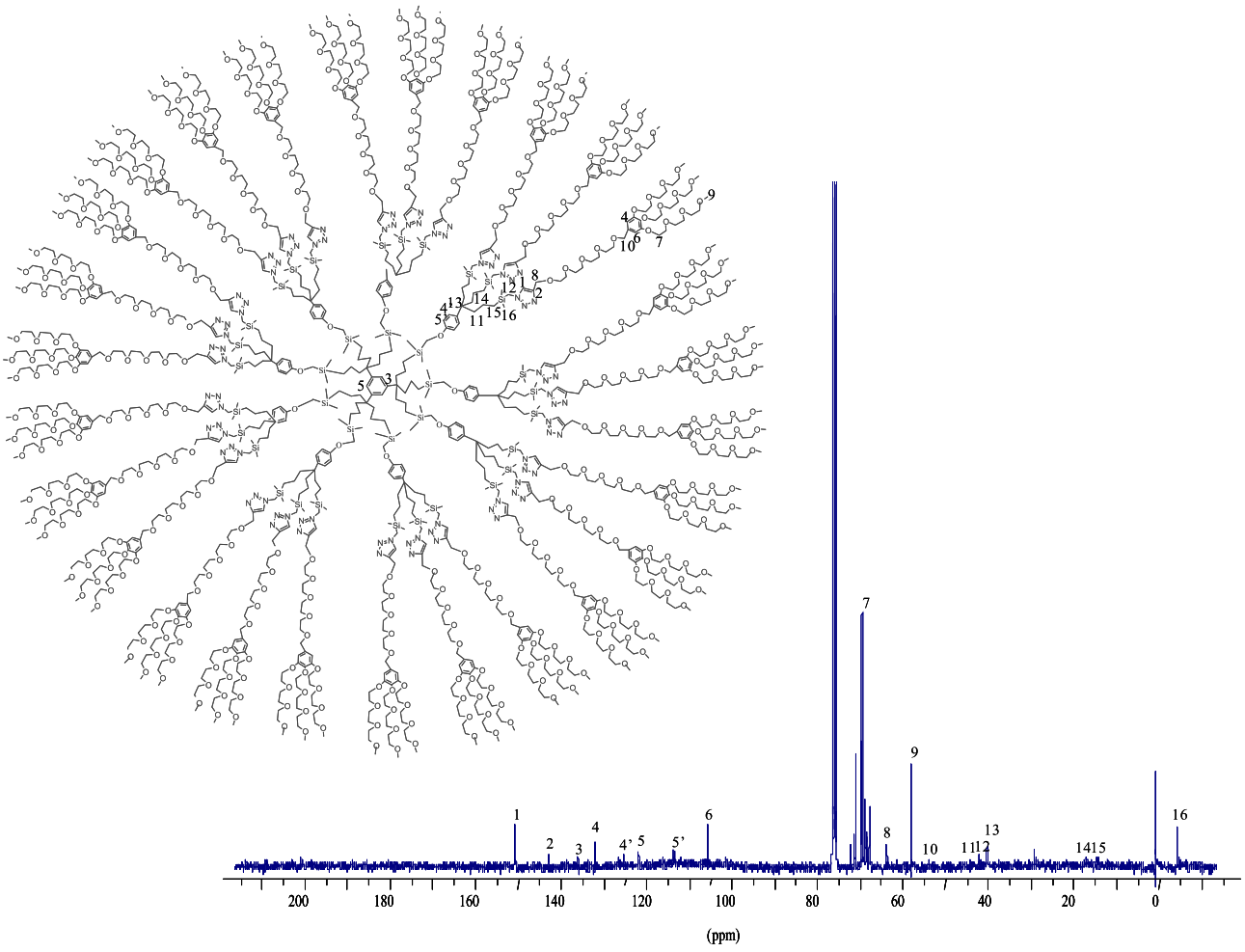

^{13}C NMR ($CDCl_3$, 62 MHz): 152.60 (*C*H, extern arom.), 144.48 (C_q of triazole), 137.79 (*C*q, arom. core), 133.75 (*C*q, arom. extern), 126.12 and 113.9 (*C*H-arom. Intern), 123.52 (*C*H of triazole and arom. core), 107.23 (C_qCH_2O), 70.66 (OCH_2CH_2O), 69.11 (Si-CH_2-O), 63.53 (triazole-CH_2-O), 58.99 (CH_3O), 53.38 (OCH_2-arom.extern), 43.77 ($CH_2CH_2CH_2Si$), 42.7 ($SiCH_2$-triazole), 40.93 (*C*q-arom.intern), 17.82 ($CH_2CH_2CH_2Si$), 14.90 ($CH_2CH_2CH_2Si$), -4.84 ($Si(CH_3)_2$).

DOSY spectrum of G_1-81-PEG

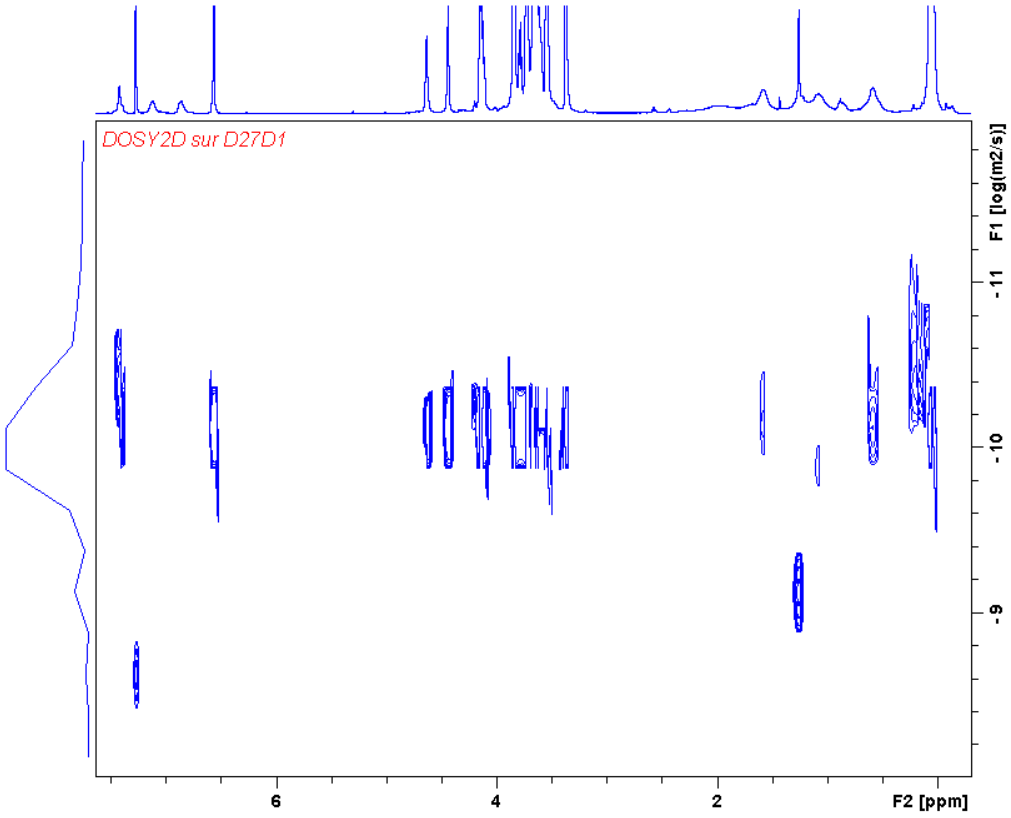

DOSY : $D = 5.94 (\pm 0.1) \times 10^{-11}$ m²/s
Rh = 9.7 (± 0.7) nm
(D: diffusion coefficient; Rh : hydrodynamic radius)

IR spectrum of G_1-81-PEG

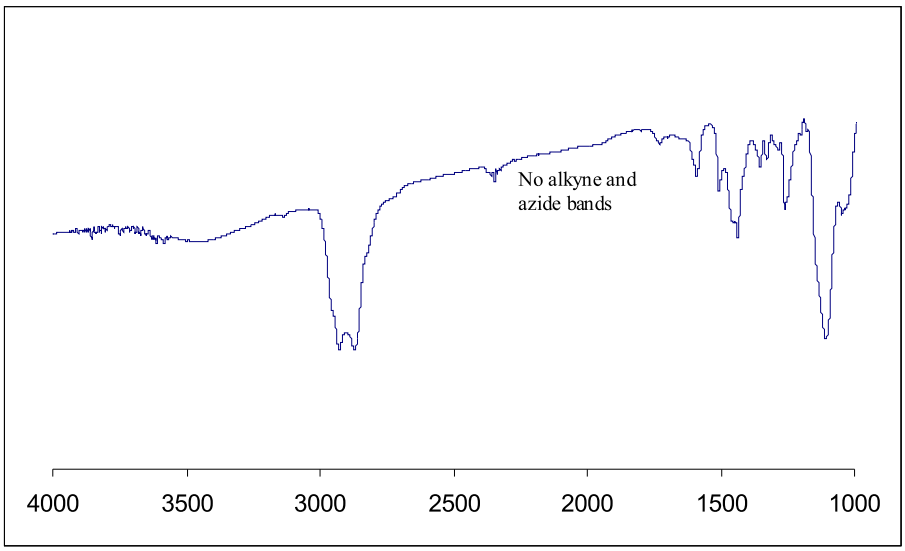

G_2-243-PEG

Mw = 80 319 $g.mol^{-1}$

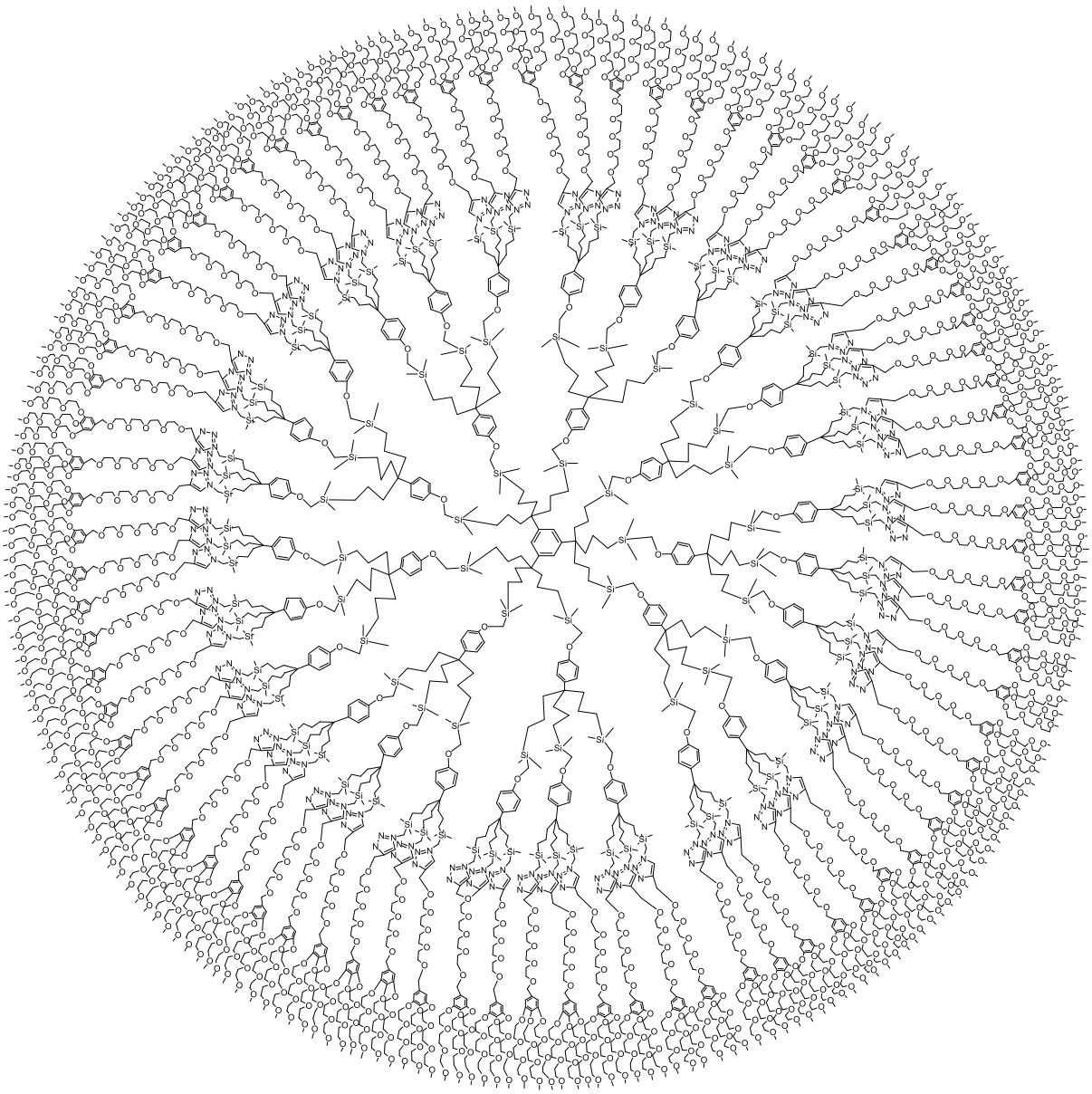

Characterization of G_2-243-TEG

^{1}H NMR ($CDCl_3$, 250MHz): 7.41 (81H, C*H*-triazole), 7.09 (117H, C*H*-arom. intern), 6.56 (234H, C*H*-arom. extern), 4.61 (162H, triazole-CH_2-0), 4.44 (234H, O-CH_2-arom. extern), 4.11 (396H, CH_2O-arom. extern and Si-CH_2-triazole), 3.64 (3726H, OCH_2CH_2O), 3.37 (243H, CH_3O), 1.59 (234H, CH_2CH$_2$CH$_2$Si), 1.09 (234H, CH$_2$CH_2CH$_2$Si), 0.54 (234H, CH$_2$CH$_2$CH_2Si), 0.06 (702H, Si(CH_3)$_2$) **(see the spectrum page 20)**

^{13}C NMR ($CDCl_3$, 62 MHz): 151.60 (*C*H, extern arom.), 144.48 (C_q of triazole), 136.80 (*C*q, arom. core), 132.78 (*C*q, arom. extern), 126.12 and 113.94 (*C*H-arom. intern) 123.52 (*C*H of triazole and arom. core), 106.23 (C_qCH$_2$O), 69.13 (Si-*C*H$_2$-O), 68.73 (OCH_2*C*H$_2$O), 63.53 (triazole-*C*H$_2$-O), 57.39 (*C*H$_3$O), 53.38 (OCH$_2$-arom.extern), 43.77 (*C*H$_2$CH$_2$CH$_2$Si), 42.7 (SiCH_2-triazole), 40.93 (*C*q-arom.intern), 17.82 (CH$_2$*C*H$_2$CH$_2$Si), 14.90 (CH$_2$CH$_2$*C*H$_2$Si), -4.84 (Si(*C*H$_3$)$_2$) **(see the spectrum page 21)**

IR: no alkyne and azide bands **(see the spectrum page 22)**

SEC : **(see the spectrum page 23)**

Light scattering : Rh = 10 (±1) nm

^{1}H NMR spectrum of G_2-243-PEG

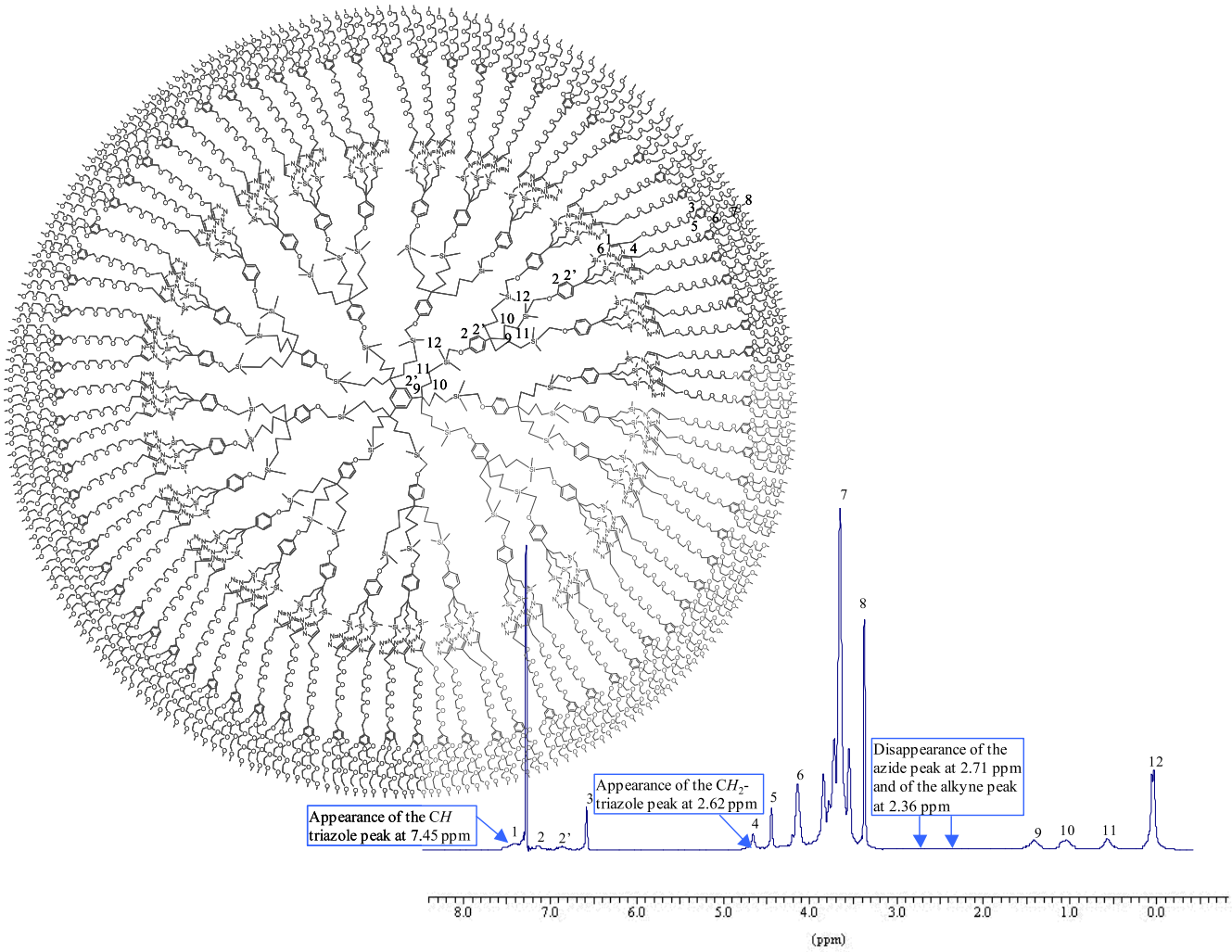

^{1}H NMR ($CDCl_3$, 250MHz): 7.41 (81H, C*H*-triazole), 7.09 (117H, C*H*-arom. intern), 6.56 (234H, C*H*-arom. extern), 4.61 (162H, triazole-CH_2-0), 4.44 (234H, O-CH_2-arom. extern), 4.11 (396H, CH_2O-arom. extern and Si-CH_2-triazole), 3.64 (3726H, OCH_2CH_2O), 3.37 (243H, CH_3O), 1.59 (234H, CH_2CH$_2$CH$_2$Si), 1.09 (234H, CH$_2$CH_2CH$_2$Si), 0.54 (234H, CH$_2$CH$_2$CH_2Si), 0.06 (702H, Si(CH_3)$_2$).

^{13}C NMR spectrum of G_2-243-PEG

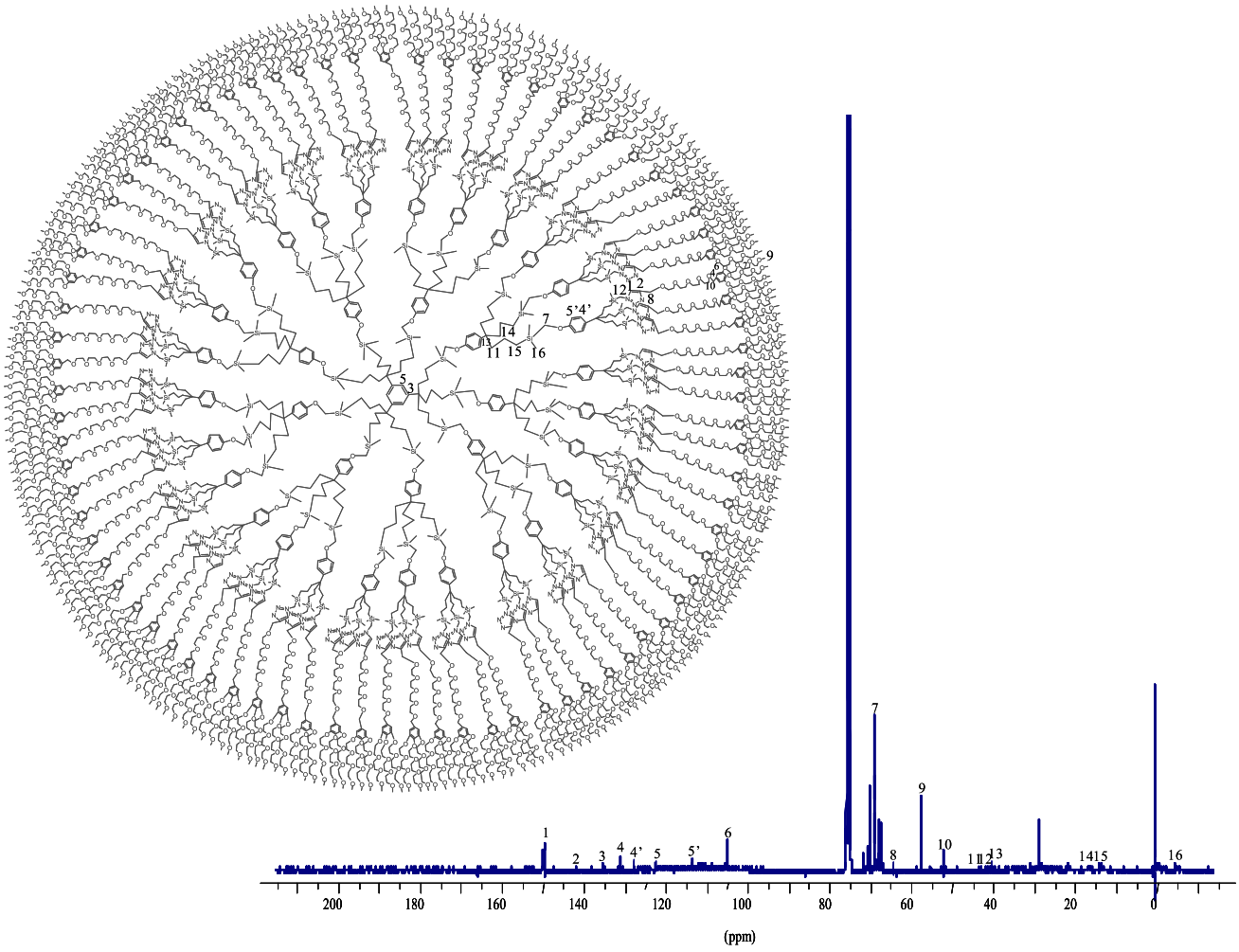

^{13}C NMR ($CDCl_3$, 62 MHz): 151.60 (*C*H, extern arom.), 144.48 (C_q of triazole), 136.80 (*C*q, arom. core), 132.78 (*C*q, arom. extern), 126.12 and 113.94 (*C*H-arom. intern) 123.52 (*C*H of triazole and arom. core), 106.23 (C_qCH_2O), 69.13 (Si-*C*H_2-O), 68.73 (O*C*H_2*C*H_2O), 63.53 (triazole-*C*H_2-O), 57.39 (*C*H_3O), 53.38 (O*C*H_2-arom.extern), 43.77 (*C*H_2CH$_2$CH$_2$Si), 42.7 (SiC*H*$_2$-triazole), 40.93 (*C*q-arom.intern), 17.82 (CH$_2$*C*H$_2$CH$_2$Si), 14.90 (CH$_2$CH$_2$*C*H$_2$Si), -4.84 (Si(*C*H$_3$)$_2$).

IR spectrum of G_2-243-PEG

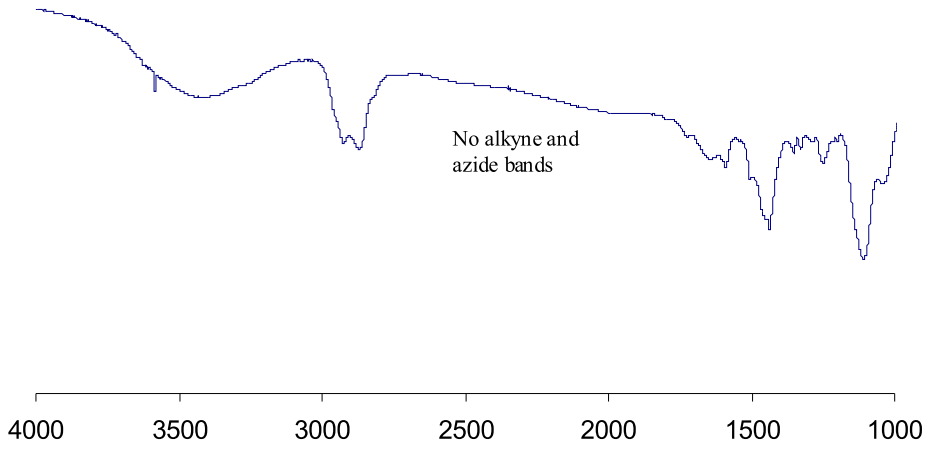

Size Exclusion Chromatography (SEC) of the three generations of "click" dendrimers containing polyethyleneglycol tethers

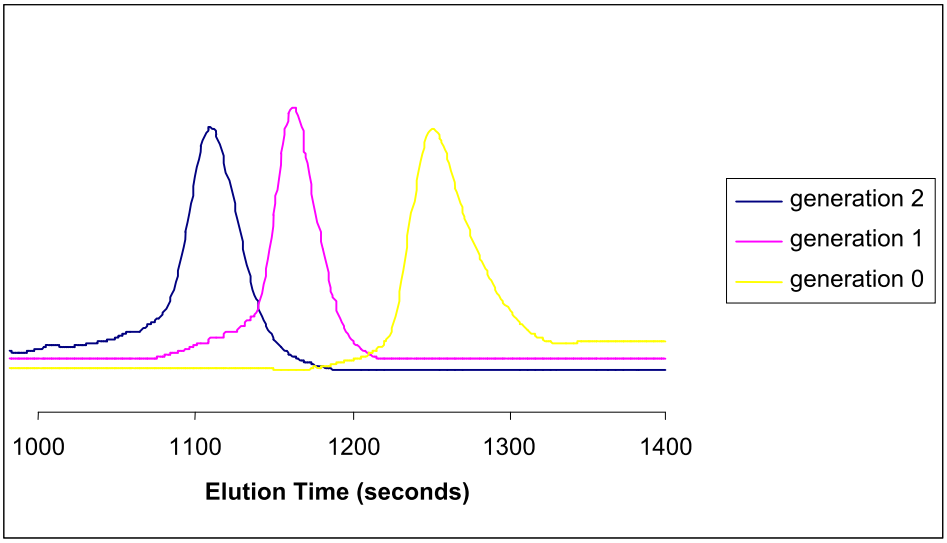

Transmission Electron Microscopy (TEM)

The samples were prepared by placing a drop of 1.6 10^{-4} M solution (MeOH) of gold nanoparticles (concentration in mol Au) on a holey-carbon-coated Cu TEM grid.

General procedure for the preparation of AuNPs (these procedures are described using preparation of D-27-polyethylene glycol): 1 mL of a $1.14x10^{-4}$ M solution of dendrimer (1mg, $1.14x10^{-4}$ mmol) in MeOH was placed in a Schlenk flask under nitrogen.0.349 mL of a $2.94x10^{-3}$ M solution of $HAuCl_4$ (0.349 mg, $1.03x\ 10^{-3}$ mmol, 1 equiv. *per* triazole). 4.65 mL of MeOH was added to obtain a solution $2.21x10^{-4}$ M (in Au)
The solution was stirred for 1h and $NaBH_4$ wad added (0.39 mg, $1.03x10^{-2}$ mmol, 10 equiv. *per* Au), the yellow solution turned to golden brown indicating the nanoparticule formation.

Attempts to stabilize AuNPs by "click" dendrimers that do not contain PEG ligands

The stabilization of AuNPs was attempted using five others dendrimers. Four of them only contain triazolyl groups and do not contain any PEG, and the last one only contains PEG but no triazolyl groups.

"Click" dendrimers with 9, 27 and 81 allyl tethers and a "click" dendrimer with 27 phenyl tethers were used. All the syntheses and structures of these dendrimers are described in the following publication: "Click" Dendrimers: Synthesis, Redox Sensing of $Pd(OAc)_2$, and Remarkable Catalytic Hydrogenation Activity of Precise Pd Nanoparticles Stabilized by 1,2,3-Triazole-Containing Dendrimers by Catia Ornelas, Jaime Ruiz Aranzaes, Lionel Salmon, and Didier Astruc, and published in *Chem. Eur. J.* **2007**, *14*, 50.
The procedure used for the addition and reduction of $HAuCl_4$ in these dendrimers is the same one as that described page 24 of this ESI using a stoichiometric amount of $HAuCl_4$ vs. the dendrimer triazolyl groups. When $NaBH_4$ in methanol is added, the gold nanoparticles are formed but they precipitate after a few minutes.

A dendrimer containing 81 PEG tethers, but no triazolyl ligand (whose synthesis will be described latter) is used for comparison. The procedure used for the addition and reduction of $HAuCl_4$ in this dendrimer is the same as that described page 24 of this ESI with 81 equiv. Au *per* dendrimer. The result is similar to that obtained with the above dendrimers containing only triazolyl groups (this page), i.e. AuNPs immediately precipitate when $NaBH_4$ in methanol is added.

These five experiments support the fact that the presence of both the PEG and triazolyl groups in these dendrimers are essential for the stabilization of AuNPs.

Encapsulation and Stabilization of Gold Nanoparticles with "Click" Polyethyleneglycol Dendrimers

Elodie Boisselier,[1] Abdou K. Diallo,[1] Lionel Salmon,[2] Jaime Ruiz Aranzaes ,[1] Didier Astruc [1*]

1. Institut des Sciences Moléculaires, UMR CNRS N°5255, Université Bordeaux 1, 33405 Talence Cedex, France.
2. Laboratoire de Chimie de Coordination, UPR CNRS N° 8241, 205 Route de Narbonne, 31077 Toulouse Cedex 04, France
E mail : d.astruc@ism.u-bordeaux1.fr

Abstract

Dendrimer-encapsulated gold-nanoparticles (DEAuNPs) are well known for polyamidoamine (PAMAM) and polypropyleneimine (PPI) dendrimers, and are of high interest *inter alia* for catalytic purpose. Here we examine the formation of DEAuNPs and dendrimer-stabilized AuNPs (DSAuNPs) with polyethyleneglycol (PEG) termini because of the high interest of PEGylated dendrimers and AuNPs in nanomedicine. Arene-cored "clicked" and non-"clicked" dendrimers terminated by 27, 81 and 243 tetraethyleneglycol (TEG) tethers (G1, G2, and G3) have indeed been synthesized (and characterized by IR, ^{1}H NMR, ^{13} NMR, size-exclusion chromatography, elemental analysis, MALDI TOF, DOSY NMR and light scattering) in order to stabilize AuNPs using a variety of reduction modes, including $NaBH_4$ in methanol, various single-electron metallocene-type reductants and even in the absence of additional reductants. The important role of the "clicked" triazole rings, dendrimer generation, stoichiometry of Au precursor, nature of the reductant and of the solvent are delineated, leading to DEAuNPs and DSAuNPs in the size range 1.9 to 38 nm that are characterized by Transmission Electron Microscopy (TEM) or High Resolution TEM (HRTEM) and UV-vis spectroscopy.[9]

Keywords: dendrimer, gold nanoparticle, redox, polyethylene glycol, click, biocompatible

Introduction

Substrate encapsulation by dendrimers[1] is a major property of dendrimer chemistry that has potential applications in catalysis,[2] photophysics,[3] materials science[4] and nanomedicine.[5] One of the most remarkable examples of dendritic encapsulation is that of transition-metal nanoparticles (NPs) that was disclosed more than a decade ago using polyamidoamine PAMAM dendrimers,[6] then polypropyleneimine (PPI) dendrimers.[7] Crooks and his group,[8] among others,[7-9] have demonstrated the enormous potential of this concept in catalysis under various "green" conditions and shown that the dendrimer plays the role of a nanoreactor and nanofilter.[8] In particular, NP encapsulation has been applied to many transition metals including with the use of a redox reaction between a NP and other metal cations.[2] However, the studies of dendrimer-encapsulated NPs (DENs) have exclusively concerned the PAMAM and PPI dendrimer families that are commercial, with the exception of Yamamoto's phenylazomethine dendrimers whose rigidity brings about new specific features for properties of phenylazomethine-DENs in materials science.

It has recently been shown that dendrimers assembled by click chemistry[10] can coordinate and electrochemically recognize various transition-metal cations,[11] and that such palladodendritic complexes can be reduced to DEPdNPs that have remarkable catalytic properties.[12] Such a strategy does not work in the same way for an approach to arene-cored DEAuNPs,[13] and the investigation towards a rationalization of the molecular engineering towards this goal is presented and generalized here. Besides encapsulation, exo-dendrimer stabilization is also well-known,[14] and this alternative has also been searched with arene-cored dendrimers[15] constructed using a Newkome-type 1 → 3 connectivity.[16] Moreover, our goal was to stabilize or encapsulate AuNPs using polyethyleneglycol-terminated dendrimers,[17] because of their biocompatibility[17] and the applications of AuNPs in nanomedicine.[18]

A major finding in this work is that not only Percec-type tetraethyleneglycol (TEG) tethers[19] are tolerated for the synthesis of DEAuNPs and DSAuNPs, but they are even required for this purpose in this new arene-cored dendrimer series, and under certain circonstances they allow the AuNP formation in the absence of the nitrogen ligands of the intradendritic 1,2,3-triazole rings formed by click reaction.

Results

The synthesis of two series of arene-cored, PEG terminated dendrimers of three generations has been carried out. For both series, the dendrimer syntheses start by $CpFe^{+}$-induced nanoallylation of mesitylene[15] followed by photolytic decomplexation[20] and Newkome-type 1→3 connectivity.[16] The first series of dendrimers was synthesized using "click" chemistry (dendrimers **4**, **5** and **6**), and the other one using the Williamson reaction (dendrimers **10**, **11** and **12**) in order to graft PEG dendrons at the periphery of the dendrimers. The AuNPs are stabilized by these PEGylated dendrimers, synthesized by "click" chemistry (**4**, **5** and **6**), in methanol using $NaBH_4$ as the reductant. The PEG-terminated (dendronized) dendrimers (**4-6** and **10-12**) also allowed the reduction of Au^{III} to Au^0 in water without the presence of an additional reductant. The shape and the size of the AuNPs have been studied by U.V.-vis. spectroscopy and Transmission Electron Microscopy (TEM) and the kinetics of formation and size variations of the AuNPs have been examined when the number of equiv. of added equiv. $HAuCl_4$ *per* dendrimer was increased. The influence of the nature of the reductant used in methanol, i.e. $NaBH_4$ or an electron-reservoir organometallic sandwich complex, was also studied, and the role of the standard redox potential of the reductant on the AuNP formation was finally scrutinized. Overall, the molecular engineering of the AuNP synthesis stabilized or encapsulated by PEGylated dendrimers is detailed.

1. Synthesis and characterizations of dendrimers 4, 5 and 6 synthesized by "click" chemistry

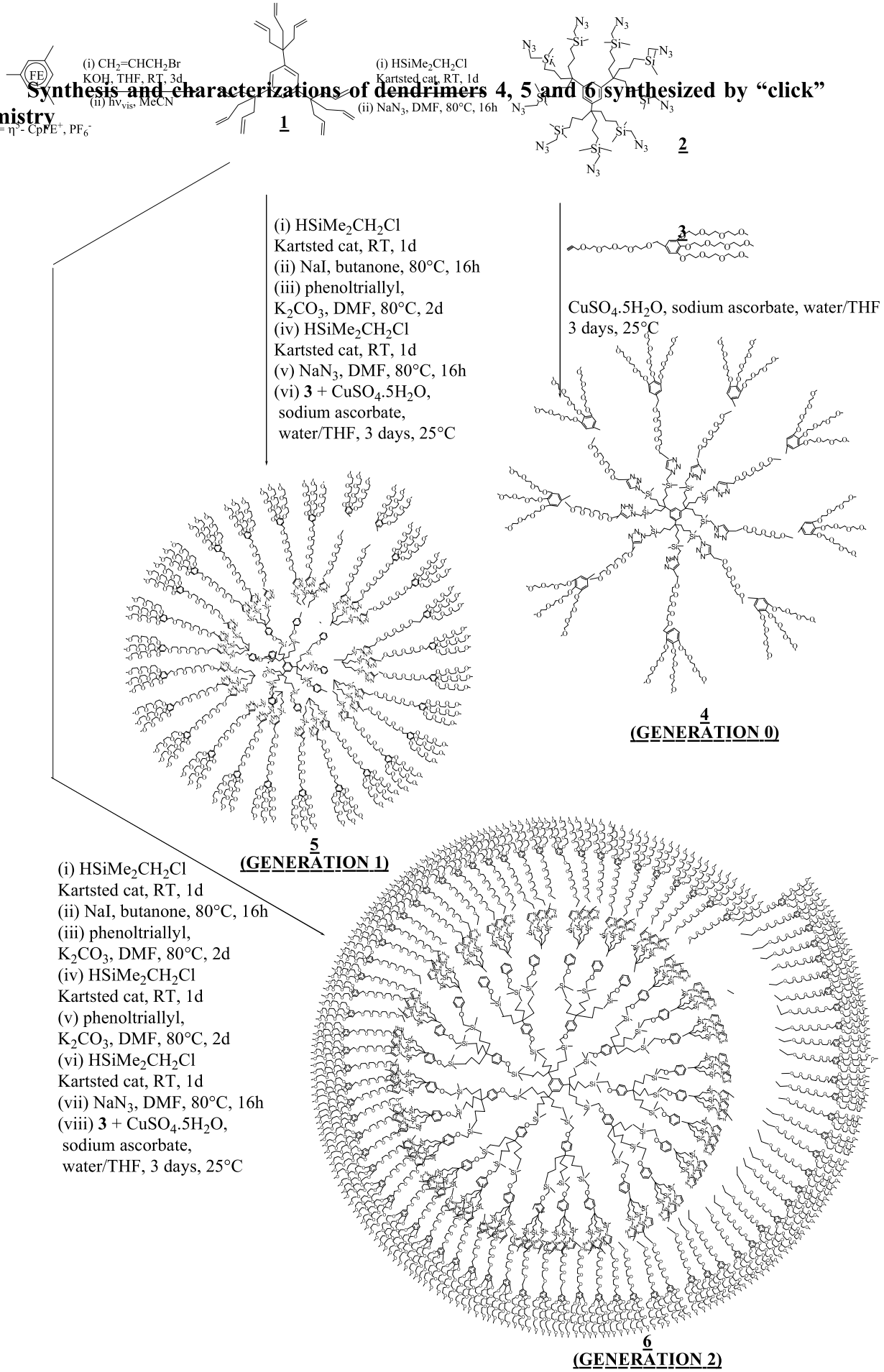

Scheme 1. Synthesis of the three generations of "click" dendrimers **4**, **5** and **6**.

The synthesis of three generations of arene-cored dendrimers with 1→3 connectivity (**4**, **5** and **6**) terminated with 27 to 243 PEG tethers (G_0 to G_2) is shown on Scheme 1. The dendritic precursors with 27 chloromethyl and azido groups were reported earlier.[15] The Newkome-type 1→3 connectivity[16] was continued by Williamson reaction between the nonachloromethyl core and a Percec-type dendron.[19] This dendron was synthesized from modified gallic acid core functionalized at the focal point by a tetraethyleneglycol (TAEG) linker, then by a propargyl group and on the peripheral tethers by triethylene glycol (TEG) termini (**3**). Finally, the dendrons were linked to the core using the Cu^I-catalyzed "click" reaction between the terminal alkyne tail and the azido-terminated dendritic core.[20] A stoichiometric amounts of Cu^I, (generated using $CuSO_4$ and ascorbic acid) has been used, because dendritic metal encapsulation considerably slows down the click reaction or inhibits it,[11,21] especially with large dendrimers. The dendrimers of generation 0 (**4**, 27 TEG termini) to 2 (**6**, 243 TEG termini) were synthesized in this way and characterized by IR, ^1H and ^{13}C NMR, size exclusion chromatography (**4**, **5** and **6**, Figure 1), correct elemental analysis (**4**), MALDI TOF (**4**, major peak at M^+: calc. 8820.91; found: 8821.24, Figure 2). DOSY and light scattering give consistent data for dendrimers **4** and **5**, both methods giving a diameter values of 9 ± 1 nm for **4** and 18 ± 2 nm for **5**. For the dendrimer **6**, light scattering yields a diameter value of 20 ± 2 nm (Figure 3, also see ESI).

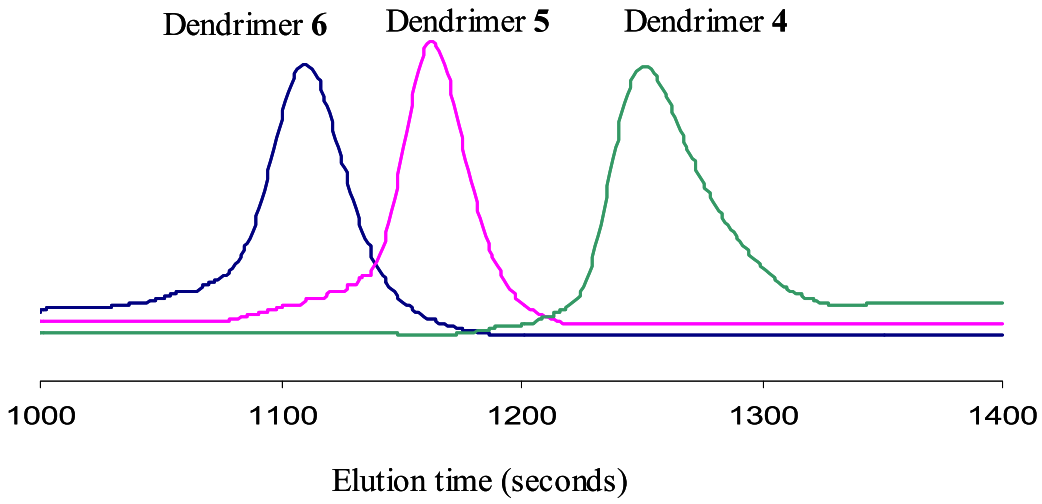

Figure 1. Size Exclusion Chromatography of the three generations of "click" dendrimers containing polyethyleneglycol tethers.

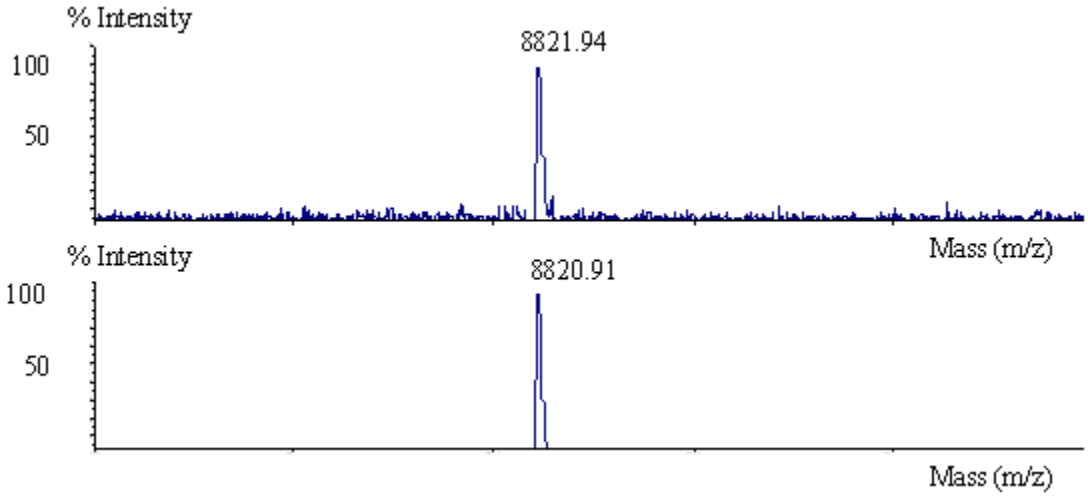

Figure 2. MALDI-TOF mass spectrum of the dendrimer **4**. Calc. for $C_{414}H_{741}O_{153}N_{27}Si_9$: 8798; found: 8821.25 (MNa).

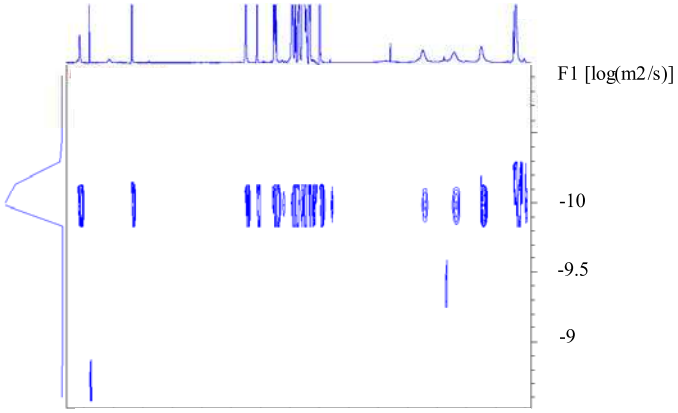

Figure 3. DOSY spectrum of the dendrimer **4**. D = 1.16 (± 0.1) x 10^{-10} m²/s, Rh = 4.9 (± 0.1) nm; (D: diffusion coefficient; Rh: hydrodynamic radius).

2. Synthesis and characterizations of dendrimers 9, 10 and 11 synthesized by Williamson reaction

The synthesis of three generations of the arene-cored, TEG-terminated dendrimers **9**, **10** and **11** with 27 to 243 TEG dendrimers (G_0 to G_2) is shown on Scheme 2. The synthesis starts with the same steps as dendrimers **4**, **5** and **6** (see Scheme 1) until the hydrosilylation step. Then reaction with NaI yields the nona-iodide core (**7**). The Percec-type dendron is functionalized at the focal point by a hydroquinone linker in order to introduce a phenol terminus (**8**). Finally, the dendrons are linked to the core using a Williamson reaction between the terminal phenol tail and the iodo-terminated dendritic core. The dendrimers **9**, **10** and **11** of generation 0 (**9**, 27 TEG termini) to 2 (**11**, 243 TEG termini) were synthesized in this way and characterized by IR, ^{1}H and ^{13}C NMR, size exclusion chromatography (**9**, **10** and **11**), MALDI TOF (**9**, major peak at M^+: calc. 7311.54; found: 7334.47 (MNa^+). DOSY ^{1}H NMR and light scattering give consistent data for the dendrimers **10** and **11**, both methods giving a diameter values of 13 ± 1.2 nm for **10** and 15 ± 1.5 nm for **11**. For the dendrimer **9**, DOSY ^{1}H NMR yielded a diameter value of 8 ± 0.6 nm (see ESI).

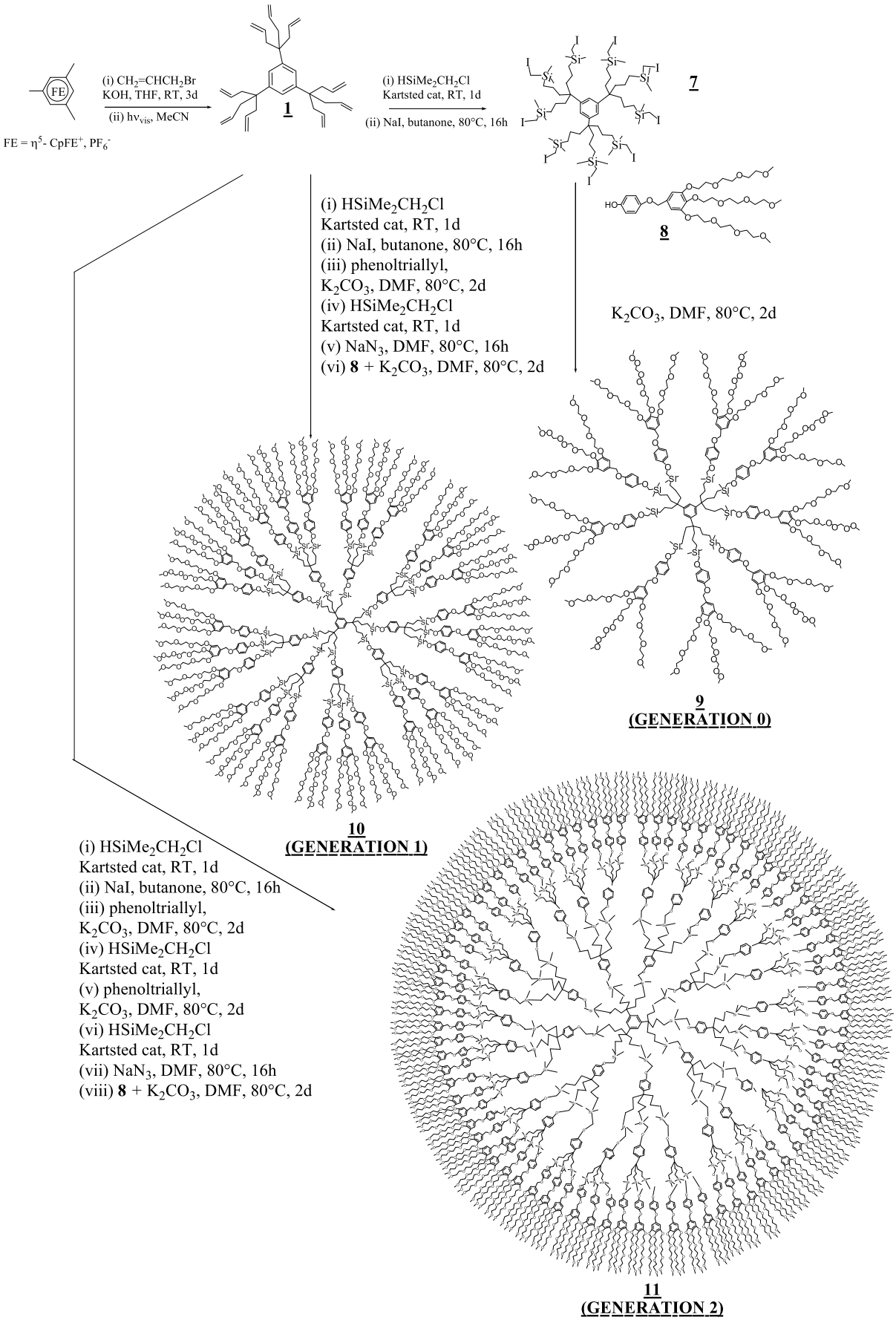

Scheme 2. Synthesis of the three generations of dendrimers **9**, **10** and **11** by Williamson reaction.

3. AuNPs synthesized using $NaBH_4$ and stabilization in methanol by the click dendrimers 4, 5 and 6

The AuNPs are synthesized by reaction between the "click" dendrimers **4**, **5** and **6,** and a stoichiometric amount of $HAuCl_4$ vs. the dendrimer triazolyl groups, followed by $NaBH_4$ reduction in methanol. The U.V.-vis. spectrum shows a plasmon band at 540 nm for the dendrimer **4**-stabilized AuNPs, but this band is absent in the spectrum of the AuNPs stabilized by the higher-generation dendrimers **5** and **6** (Figure 4). The transmission electron microscopy (TEM) data confirm this trend (Figure 5) showing that the dendrimer **4**-stabilized AuNPs are larger than the dendrimer (4.1 ± 0.5 nm) and cannot be encapsulated in a small dendrimer that contains only 27 tethers. Thus, several dendrimers **4** are surrounding each AuNP (Figure 6). On the other hand, the dendrimers of the following generations **5** and **6** containing respectively 81 and 243 TEG tethers encapsulate AuNPs of small size (1.9 ± 0.4 nm).

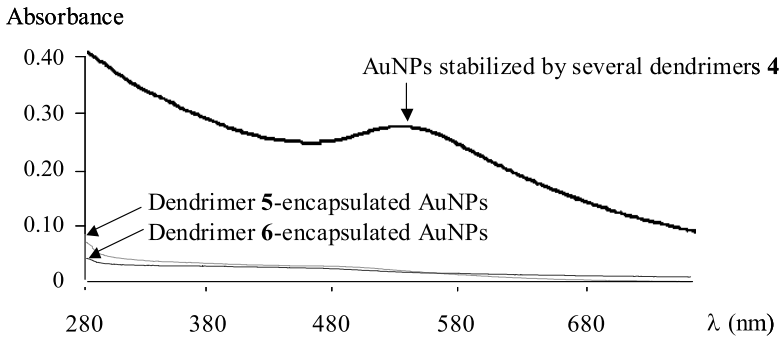

Figure 4. U.V.-vis. spectra of AuNPs stabilized by several dendrimers **4** and encapsulated by dendrimers **5** and **6**.

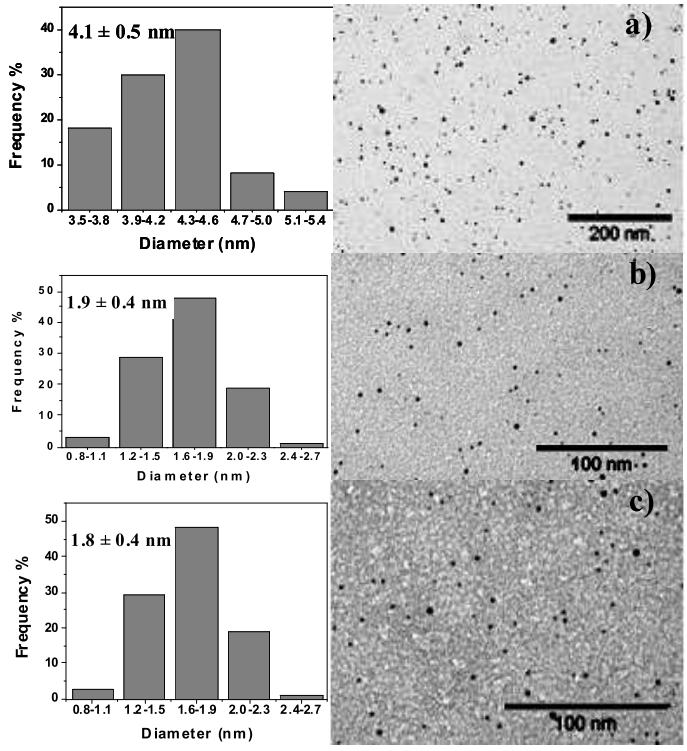

Figure 5. a) Dendrimer **4** / AuNPs: TEM image and size distribution; b) dendrimer **5** / AuNPs: TEM image and size distribution; c) dendrimer **6** / AuNPs: TEM image and size distribution.

4. Attempts to stabilize AuNPs in methanol by others dendrimers

The stabilization of AuNPs in the same conditions as previously was attempted using six others dendrimers. Three of them only contain triazolyl groups and do not contain any PEG (**12**, **13** and **14**), and the three others only contain PEG but no triazolyl groups (**9**, **10** and **11**).[15b] "Click" dendrimers with 27 and 81 allyl tethers (**13** and **14)** and a "click" dendrimer with 27 phenyl tethers (**12**) were used (Scheme 3). All the syntheses and structures of these dendrimers were reported earlier.[12a]

The procedure used for the addition and reduction of $HAuCl_4$ in these dendrimers was the same one as that previously described using a stoichiometric amount of $HAuCl_4$ vs. the dendrimer triazolyl groups. When $NaBH_4$ in methanol was added, the AuNPs were formed, but they precipitated after a few minutes, and AuNPs could never be obtained (although PdNP could form[19]).

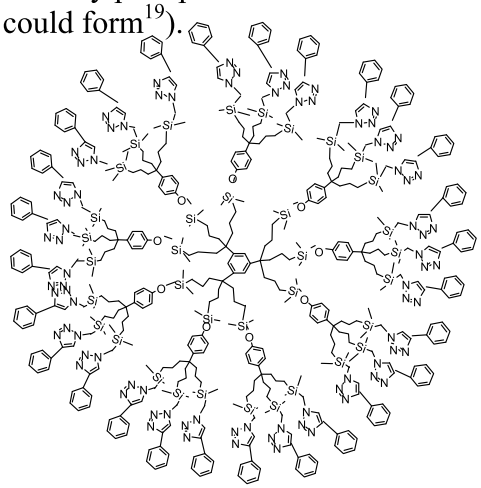

13

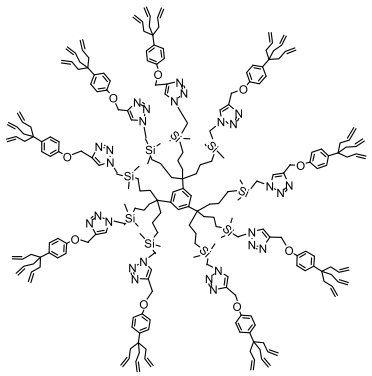

14

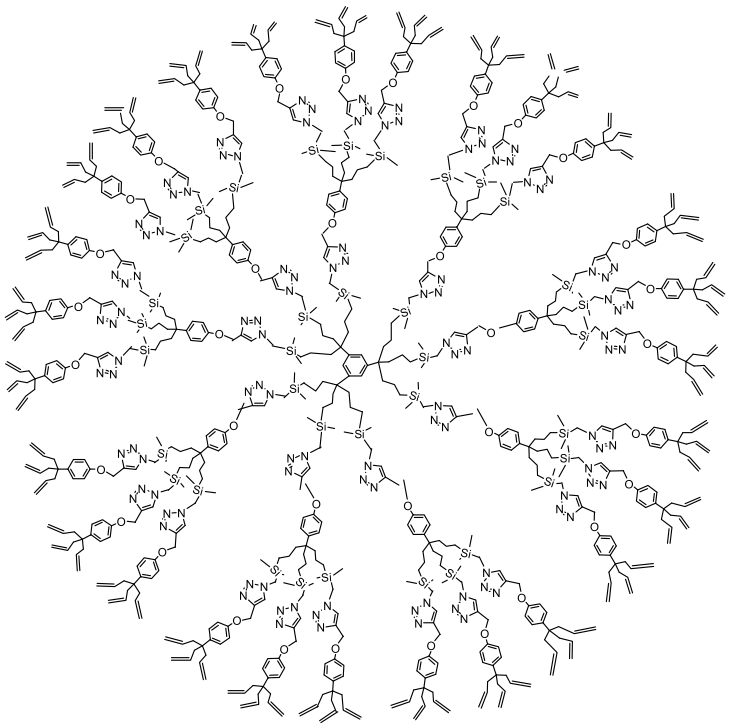

15

Scheme 3. **12**: 27-phenyl "click" dendrimer; **13**: 27-allyl "click" dendrimer; **14**: 81-allyl "click" dendrimer.

The dendrimers **9**, **10** and **11** containing respectively 27, 81 and 243 PEG tethers but no triazolyl ligand were used for comparison (Scheme 2). The procedure used for the addition and reduction of $HAuCl_4$ in this dendrimer was the same as previously described with 27, 81 and 243 equiv. Au *per* dendrimer. The result was similar to that obtained with the above dendrimers containing only triazolyl groups, i.e. AuNPs immediately precipitated when $NaBH_4$ in methanol was added, and no AuNP could be obtained.

These six experiments support the fact that the presence of both the PEG and triazolyl groups in the dendrimers **4**, **5** and **6** are essential for the stabilization of AuNPs in methanol when $NaBH_4$ is used as reductant.

5. AuNP size variation

The size variation of the AuNPs synthesized using $NaBH_4$ in methanol was observed in the case of AuNP stabilization with the dendrimer **5**. TEM images have been recorded (Figure 6) for an increase of the equiv. number of added gold atoms from 1 to 20 atoms *per* intra-dendritic triazole ligand. All the AuNPs obtained are spherical, and their size is very homogenous. Moreover, a high resolution TEM was recorded for 7 equiv. gold atoms *per* triazole in order to observe the crystalline structure of the AuNP (Figure 6, *G*). The increase of the number of equiv. $HAuCl_4$ *per* triazole leads to a variation of the diameter of the AuNPs from 1.9 ± 0.2 nm (1 equiv. *per* triazole) to 11.3 ± 1 nm (20 equiv. *per* triazole). From one to ten equiv. *per* triazole, the AuNP size varies linearly with the number of $NaBH_4$ equiv. added before reaching a plateau at approximately 11 nm (Figure 7). This maximum size is expected, because the AuNPs are stabilized with the dendrimer **5** in an intra-dendritic way (see paragraph 2), and the diameter of this dendrimer is confirmed by both DOSY NMR and light scattering (18 ± 2 nm). When the number of equiv. $HAuCl_4$ *per* triazole is larger than 10, excess Au^0 immediately precipitate.

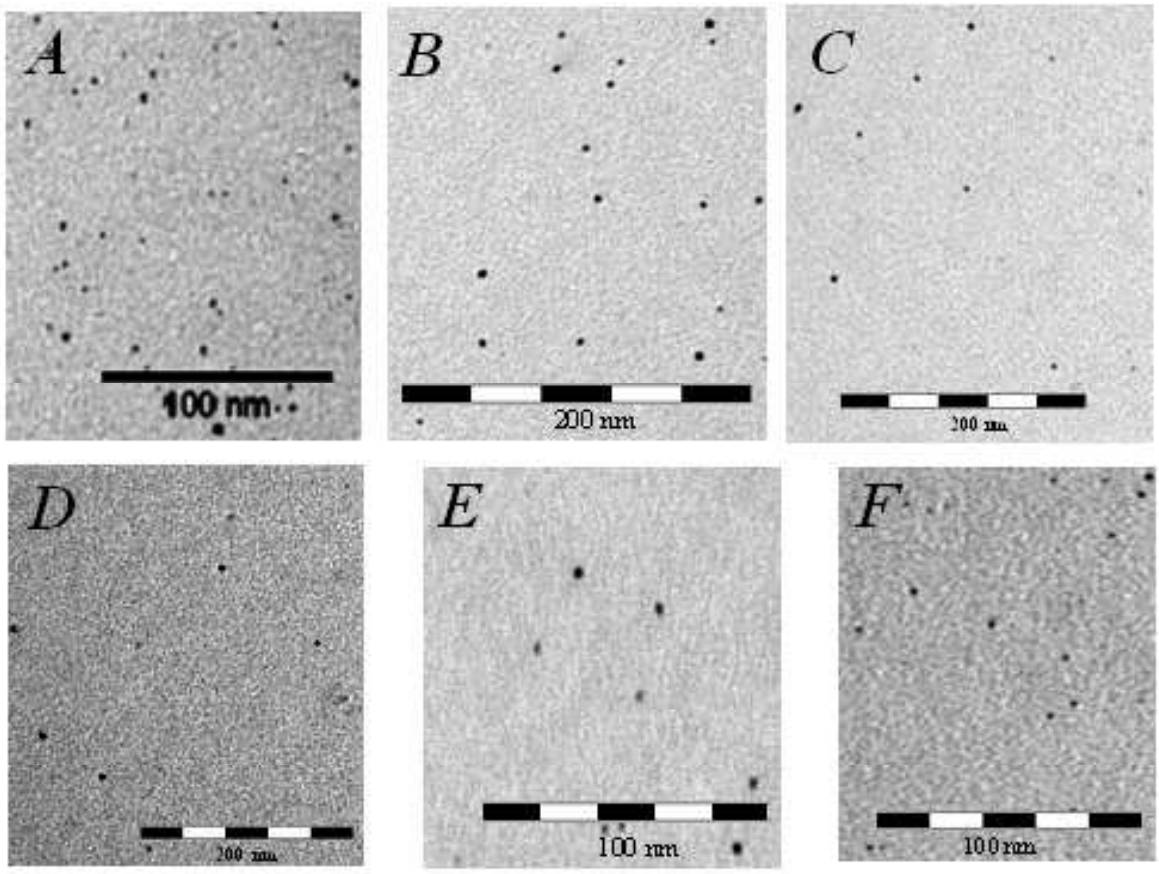

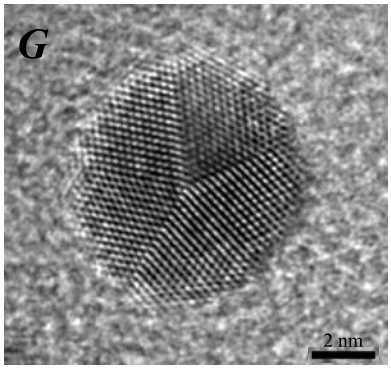

Figure 6. a) Dendrimer **5** + 1 equiv. $HAuCl_4$ *per* triazole, diameter = 1.9 (± 0.2) nm; b) dendrimer **5** + 3 equiv. $HAuCl_4$ *per* triazole, diameter = 3.8 (± 0.4) nm; c) dendrimer **5** + 5 equiv. $HAuCl_4$ *per* triazole, diameter = 5.3 (± 0.5) nm; d) dendrimer **5** + 7 equiv. $HAuCl_4$ *per* triazole, diameter = 6.8 (± 0.7) nm; e) dendrimer **5** + 10 equiv. $HAuCl_4$ *per* triazole, diameter = 11.0 (± 1) nm; f) dendrimer **2** + 20 equiv. $HAuCl_4$ *per* triazole, diameter = 11.3 (± 1) nm; g) HRTEM of dendrimer **5** + 7 equiv. $HAuCl_4$ *per* triazole.

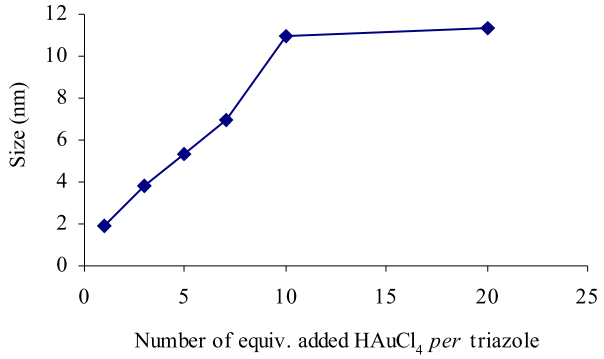

equiv. number of $HAu^{III}Cl_4$ per triazole	AuNP diameter (nm)
1	1.9 (± 0.2)
3	3.8 (± 0.4)
5	5.3 (± 0.5)
7	6.8 (± 0.7)
10	11.0 (± 1)
20	11.3 (± 1)

Figure 7. Size variation of AuNPs stabilized by the "click" dendrimer **6** G1-81-PEG in methanol upon reduction using $NaBH_4$ in methanol.

6. AuNP synthesis and stabilization by TEGylated dendrimers in water

AuNPs are synthesized according to a new protocol, without reductant and in aqueous dendrimer solution at room temperature. The AuNP are formed by reaction between the TEGylated dendrimers and a stoichiometric amount of $HAuCl_4$ *per* PEG dendron in water (i.e. 9 equiv. $HAuCl_4$ *per* dendrimers **4** and **9**, 27 *per* dendrimers **5** and **10** and 81 *per* dendrimers **6** and **11**). The solution becomes red after a few minutes of stirring. The synthesis of the AuNPs in the presence of dendrimers **9**, **10** and **11** is faster than for the AuNPs

obtained with "click" dendrimers **4**, **5** and **6**. This reduction is followed by the evolution of the AuNP plasmon band in U.V.-vis. spectroscopy. For example, the synthesis of the AuNPs with the dendrimer **9** is completed in 3.5h, whereas that with the dendrimer **5** is completed in one day in order to achieve the reduction (Figure 8).

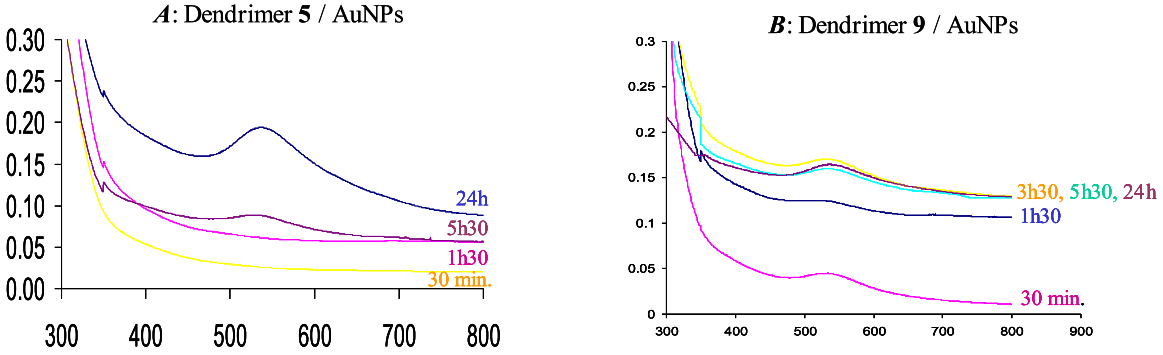

Figure 8. UV-vis spectra of AuNPs formed and stabilized by the dendrimers **5** and **9** at different times.

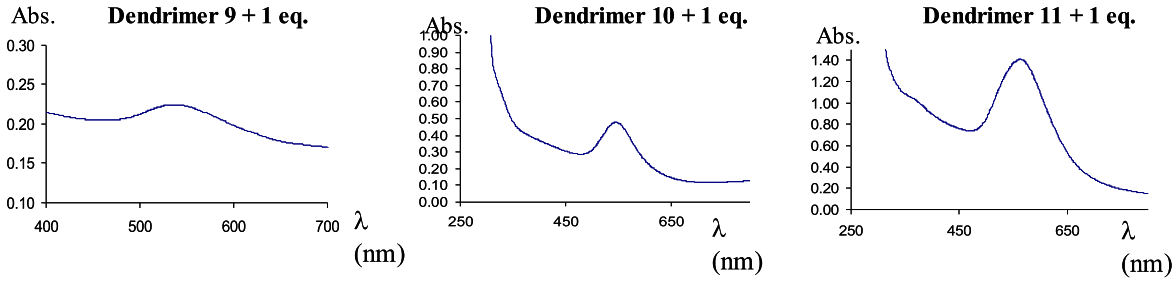

Figure 9. UV-vis spectra of AuNPs formed and stabilized by the dendrimers **9**, **10** and **11**.

For all the experiments, the U.V.-vis. spectrum shows a plasmon band between 530 nm and 570 nm depending on the cases (see the examples with the dendrimers **9**, **10** and **11** on Figure 9). This means that all the observed AuNPs have a diameter larger than 3 nm. The transmission electron microscopy (TEM) data confirm this trend (see ESI), showing that the dendrimer **9**-stabilized AuNPs have a diameter of 23 ± 0.5 nm, the dendrimer **10**-stabilized AuNPs have a diameter of 34 ± 1 nm and the dendrimer **11**-stabilized AuNPs have a diameter of 36 ± 0.5 nm.

The various generations of "click" dendrimers **4**, **5** and **6** give the same AuNP diameters as dendrimers **9**, **10** and **11**. Indeed, the dendrimer **4**-stabilized AuNPs have a diameter of 22 ± 0.5 nm, the dendrimer **5**-stabilized AuNPs have a diameter of 33 ± 0.5 nm and the dendrimer **3**-stabilized AuNPs have a diameter of 36 ± 1 nm (see ESI). This leads to a characteristic size for each generation of dendrimers containing or not triazole groups, and in these synthesis, only the reaction time changes.

The sizes of these AuNPs are much larger than that observed with the first protocol with $NaBH_4$ in methanol. The presence of PEG tethers in these dendrimers is required for the reduction and the stabilization of AuNPs in water.

Several tests were performed with the PEG polymer **17** (mass molar: 5000 $g.mol^{-1}$) and with the two PEG dendrons **15** and **16** used to functionalize the dendrimers, and none of these structures allows the reduction of $HAuCl_4$ nor the formation and the stabilization of AuNPs (Scheme 4).

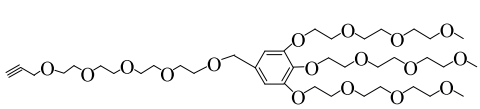

15

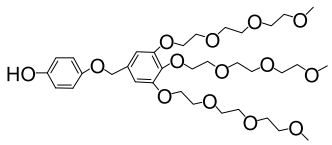

16

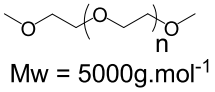

17

Scheme 4. **11**: 27-phenyl dendrimer; **12**: 27-allyl dendrimer; **13**: 81-allyl dendrimer.

7. AuNPs size variation

The AuNP size variation when $HAuCl_4$ is reduced and the AuNPs stabilized by dendrimers **9**, **10** and **11** in water is observed when the number of equiv. of added $HAuCl_4$ is multiplied by two and by five (i.e. 18 and 45 equiv. Au for **9**, 54 and 135 equiv. Au for **10,** and 162 and 405 equiv. Au for **11**). The TEM images have been recorded (see ESI), and the diameters of the AuNPs obtained were estimated (table 1). The diameter of dendrimer **9**-stabilized AuNPs varies from 23 ± 0.5 nm to 32 ± 1 nm, from 34 ± 1 nm to 38 ± 1 nm for dendrimer **10**-stabilized AuNPs and from 36 ± 0.5 nm to 42 ± 1 nm for dendrimer **11**-stabilized AuNPs.

Dendrimer + number of equiv. Au *per* dendron	AuNP diameter (nm)
Dendrimer **9** + 1 equiv.	23 ± 0.5
Dendrimer **9** + 2 equiv.	26 ± 1.0
Dendrimer **9** + 5 equiv.	32 ± 1.0
Dendrimer **10** + 1 equiv.	34 ± 1.0
Dendrimer **10** + 2 equiv.	36 ± 0.5
Dendrimer **10** + 5 equiv.	38 ± 1.0
Dendrimer **11** + 1 equiv.	36 ± 0.5
Dendrimer **11** + 2 equiv.	38 ± 1.0
Dendrimer **11** + 5 equiv.	42 ± 1.0

Table 1. Size evolution of AuNPs stabilized by dendrimers **9**, **10** or **11** in water.

8. AuNPs reduction by organometallic compounds

The AuNP precursor $HAuCl_4$ were also reduced to AuNPs by the organometallic electron-reservoir sandwich complexes, $[Fe^{I}Cp(\eta^6\text{-}C_6Me_6)]$,[23] ferrocene, ethynylferrocene and decamethylferrocene that are single-electron reductants with various redox potentials. In these cases, the AuNPs were synthesized by reaction between the "click" dendrimer **5** and a stoichiometric amount of $HAuCl_4$ *per* dendrimer triazolyl group, followed by reduction in methanol using the organometallic compound. The TEM data (see ESI) show that the dendrimer **5**-stabilized AuNPs obtained using the organometallic compounds are much larger than the AuNPs obtained by reduction using $NaBH_4$ (1.9 ± 0.4 nm). Indeed, the AuNP diameter synthesized using ferrocene is 38 ± 3 nm, with ethynylferrocene it is 30 ± 3 nm, with decamethylferrocene it is 23 ± 2 nm, and with $[Fe^{I}Cp(\eta^6\text{-}C_6Me_6)]$ it is 7 ± 1 nm. The high resolution TEM (Figure 10, B) shows the cubic crystalline structure of the AuNPs obtained AuNP under these conditions using $[Fe^{I}Cp(\eta^6\text{-}C_6Me_6)]$ as the reductant.

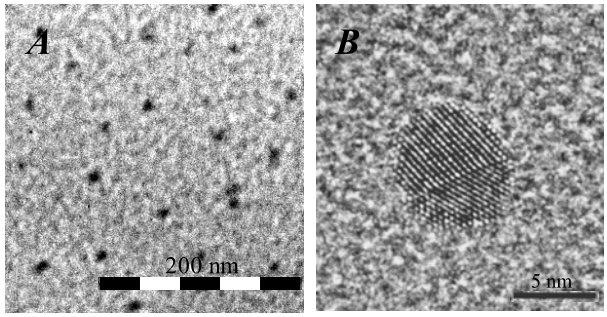

Figure 10. a) TEM of the dendrimer **5** + 1 equiv. of $HAuCl_4$ reduced by $[Fe^{I}Cp(\eta^6\text{-}C_6Me_6)]$; b) HRTEM of the dendrimer **5** + 1 equiv. of $HAuCl_4$ reduced by $[Fe^{I}Cp(\eta^6\text{-}C_6Me_6)]$.

Discussion

Click TEG-terminated dendrimer-stabilized AuNPs formed by $NaBH_4$ reduction in methanol, but the generation dependence logically influenced the AuNP size. DSAuNPs are formed with G_0-27TEG, and they are larger (4.1 nm) than the dendrimer and thus surrounded by several dendrimers (Figure 11). On the other hand, DEAuNPs are formed from the large G_1-81TEG and G_2-243 TEG dendrimers. These findings were obtained using a 1:1 $HAuCl_4$/triazole stoichiometry, but the AuNP size was steadily increased when this stoichiometry was increased until a plateau was reached at a 10:1 stoichiometry with G_1-81TEG, indicating that the AuNPs have become so large that they could no longer be encapsulated. This shows the progressive transition between DEAuNPs and DSAuNPs as well as the maximum size of AuNPs that can be reached by this method.

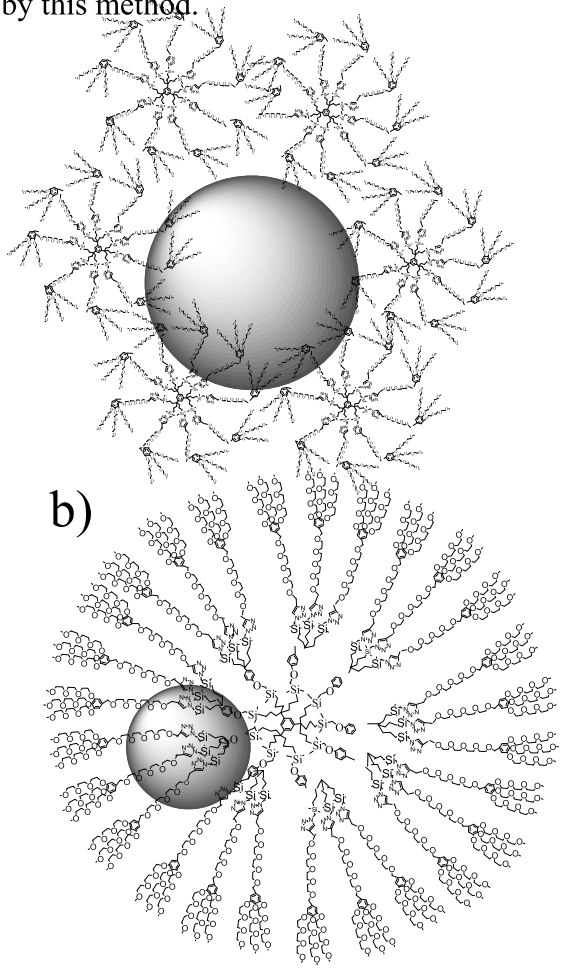

Figure 11. a) AuNPs stabilized by several dendrimers **4**; b) dendrimer **5**-encapsulated AuNPs.

Whereas AuNPs were easily formed from PAMAM and PIP dendrimers by the pioneers in the area,[6] it is surprising that AuNPs could not be formed by $NaBH_4$ reduction in methanol of Au^{III} complexes of arene-cored "clicked" dendrimers in the absence of TEG termini. This is all the more striking as our previous studies had shown that, using these same dendrimers, PdNPs were formed and were shown to be very active in the catalysis of alkene hydrogenation and C-C forming reactions. This contrast might be due to the difference of aggregation mechanism and rate between these two metals.

Also remarkable is the success to form these AuNPs when the TEG termini were introduced as structural complement for all the dendrimers studied here. It is thus likely that this outstanding property of PEG termini could be extended to many other dendrimers. Another interesting distinction is the impossibility to form the dendrimer-stabilized AuNPs by $NaBH_4$ reduction of $HAuCl_4$ in methanol when the arene-cored TEG-terminated dendrimers do not contain the 1,2,3-triazole ring whatever the generation (non-click dendrimer series **9** , **10** and **11**). This demonstrates the essential role of the Au^{III} coordination to the nitrogen ligand of the triazole ring. Such coordination and its precise mode have been shown by crystallography in the case of Pd.[24a]

$NaBH_4$ is currently believed to be a convenient reductant of Au^{III} to form AuNPs (despite the undesired formation of borides at the AuNP surface),[24b] but this study demonstrates this it does not always work, probably because in this precise case the reduction is too fast to be compatible with stabilization of the AuNPs. Even if $NaBH_4$ fails to lead to the formation of AuNPs with TEG-terminated dendrimers, the presence of TEG termini is sufficient to allow the formation of the AuNPs in water in the absence of reductant. The dendritic effect is required for this property, as it was shown that non-dendritic linear PEGs and even tripodal dendronic PEGs do not have this property. Au^{III} is a rather strong oxidant,[25] but oxidation of non-dendritic PEG is endergonic and not sufficiently entropy-driven. On the other hand, Au^{III} encapsulation achieved upon multiple coordination by the oxygen atoms of the TEG pseudo-cavities is facilitated by the dendritic inter-tether constriction, which brings about the favorable entropy conditions for reduction. Yet, the AuNP formation is very slow, but protected within the dendritic frame. This slow rate could be monitored by the progressive appearance, then stagnation of the plasmon band.[18] The large size of the AuNPs formed by this process is due to this very slow kinetics. This means that the AuNPs start growing inside the dendrimers and that these germs continue growing outside the dendrimers owing to their large size by trapping the Au atoms formed in the TEG pseudo-cavities near the dendrimer periphery near. It is likely that, once the large AuNPs grow, the native Au atoms do not form small stable DEAuNPs inside the dendrimer, because the latter are not observed by TEM.

Note that the AuNPs obtained by this method have the same size whether or not their contain triazole ligands, confirming that it is the TEG oxygen pseudo-cavities that play the main role in the AuNP formation in this case rather that the triazole ring. Yet, the kinetics study shows that the triazole ring slows down the AuNP formation. This means that coordination of the triazoles to the Au^{III} ions is not responsible for Au^{III} reduction but on the contrary partly inhibits it by removing the Au^{III} ions from the TEG pseudo-cavities. The size of the DSAuNPs formed in this way is much larger than that formed by $NaBH_4$ reduction, because the driving force is considerably larger with $NaBH_4$ than with the TEG pseudo-cavities.

It is surprising that, owing to the undesired boride impurities formed at the AuNP surface of AuNPs synthesized using $NaBH_4$,[18d] no monoelectronic oxidant has even been probed to form clean AuNPs. For biomedical applications, the AuNPs are usually synthesized with the Turkevich method,[25] because most (although not all) of the temporary citrate stabilizers can be removed to introduce the biomedical probe or target and the large AuNPs formed by this method allow monitoring a large plasmon band. Also, whereas small AuNPs (< 5 nm) are of

great interest for efficient catalysis,[26] large AuNPs are important in nanomedicine, because the plasmon band (AuNP > 3 nm) is an indispensable tool in this later area.[18]
In the present study, the use of single-electron reductants successfully leads to the formation of AuNPs that are much larger than those formed using the $NaBH_4$ reduction modes. This is due to the fact that the mechanism of $NaBH_4$ reduction follows inner-sphere electron transfer involving chloride elimination from $AuCl_4^-$, whereas the mechanism of the single-electron reductants involves outer-sphere electron transfer. As shown by the seminal work of Henry Taube, inner-sphere mechanisms are considerably superior to outer-sphere electron-transfer mechanisms in terms of reaction kinetics.[27] Again, slow reduction is well known to result in a prolonged aggregation process leading to large NPs.[25] Reetz has shown a linear correlation between the driving force of carboxylate reductants and the PdNP size, i.e. the PdNPs are all the larger as the driving force is weaker.[28] This is also exactly what is found here with the series of monoelectronic reductants, as the DSAuNPs formed are all the larger as the standard oxidation potential of the reductant is more positive (or less negative). Since the reactions of electron-reservoir complexes are clean because, by definition, both the oxidized and reduced forms are stable,[23] it is possible to define the size of the DSAuNPs between 7 nm (strong Fe^I monoelectronic reductant) and 38 nm (weakest Fe^{II} monoelectronic reductant). The standard potentials of these electron-reservoir complexes are perfectly defined and can be easily tuned even with small variations by change of the nature and number of ring substituents of the transition-metal sandwich complex.[29] This flexibility allows to finely tune the AuNPs size without inhibiting the AuNP surface upon ligand coordination.

Concluding Remarks

1- This study reports the synthesis and characterization of three generations of arene-cored "click" and non-"click" dendrimers with 1→ 3 connectivity up to 243 tethers, with the aim to stabilize AuPs with new dendrimers.
2- The introduction of Percec-type tripodal TEG tethers at the termini of all the dendrimers allows the formation of DEAuNPs and DSAuNPs even if AuNPs cannot be formed in the same dendrimers in the absence of these tripodal TEG tethers. The DEAuNP vs. DSAuNP nature and size (between 1.9 and 42 nm) depends on the dendrimer generation, medium, reduction mode and $HAuCl_4$ /dendrimer stoichiometry.
3- These AuNPs are only weakly stabilized and thus should be very useful for catalytic (small size) and biomedical applications (large size).
4- With the classic $NaBH_4$ reduction in methanol, DEAuNPs and DSAuNPs are formed from click TEG-terminated dendrimers with size variation from 1.9 nm to 11.3 nm depending on the dendrimer generation and $HAuCl_4$ /triazole stoichiometry.
5- Remarkably, DSAuNPs are formed with all the dendrimers from $HAuCl_4$ in the absence of additional reductant (23 to 42 nm-size depending on the generation but not on the nature, click or non-click). Reduction Au^{III} → Au^0 is due to the multiple coordination of the oxygen atoms of the pseudo-cavity of the TEG and to a constraining dendritic effect, non-dendritic PEG or TEG tripods being inefficient, and the presence of triazole ligands that compete with the TEG coordination slowing down the reduction.
6- Monoelectronic reductants have been used for the first time for the reduction of Au^{III} to AuNPs. Their outer-sphere reduction mechanism implies a much slower reduction than the inner-sphere reductant $NaBH_4$, and the size of the DSAuNP formed (between 7 and 38 nm) is directly related to the standard oxidation potentials of the Fe^I and Fe^{II} reductants. This provides the possibility to finely tune the DSAuNP size.

Experimental section

1. Synthesis and characterization of the alkyne dendron **3** (see ESI)
A Percec-type dendron[22] containing a tris-triethylene glycol group (1 g, 1.57 mmol) and tetraethylene glycol (2.95 g, 15.7 mmol) were introduced into a Schlenck flask, and dry THF (50 mL) was added. NaH (108 mg, 2.7 mmol) was added to the solution. The mixture was stirred for 12 hours at 50°C. At the end of the reaction, water was added, and then THF was removed under vacuum. The product was extracted with CH_2Cl_2 and purified by chromatography (MeOH) giving 1g of yellow oil (83% yield).
The tris-triethylene glycol tetraethylene glycol dendron (600 mg, 0.65 mmol) and dry THF (50 mL) were introduced into a Schlenck flask, and NaH (47 mg, 1.95 mmol) was added at 0°C. Propargyl bromide (155 mg, 1.3 mmol) was added to the solution, and the mixture was stirred for 2 hours at 0°C, then 2 hours at 25°C. At the end of the reaction, water was added, then THF and excess propargyl bromide were removed under vacuum. The product was extracted with CH_2Cl_2, yielding 600 mg of yellow oil (95% yield).
^{1}H NMR ($CDCl_3$, 250MHz): 6.39 (2H, C*H*-arom. extern), 4.26 (2H, O-CH_2-arom. extern), 3.98 (4H, CH_2O-arom. extern and CH_2-alkyne), 3.46 (30H, OCH_2CH_2O), 3.17 (9H, CH_3O), 2.36 (1H, C-C*H* alkyne); ^{13}C NMR ($CDCl_3$, 62 MHz): 152.41 (*C*q-O arom.), 137.50 (*C*q-CH_2 arom.), 133.63 (Cq-*C*H2-O), 106.87 (*C*H arom.), 79.54 (*C*q alkyne), 74.75 (*C*H alkyne), 70.46 (O-*C*H_2), 58.74(O-*C*H_3), 58.13 (*C*H_2-alkyne). Infrared υ_{alkyne}: 2100 cm^{-1}; MALDI TOF : Calc. for $C_{39}H_{68}O_{17}$: 808; found: 831 (MNa^+)

2. General procedure for the synthesis of the "clicked" PEG dendrimers **4**, **5** and **6**
The azido-terminated dendrimer (**2** for the synthesis of the dendrimer **5**, 1 equiv.) and the alkyne dendron **3**(1.5 equiv. *per* branch) were dissolved in THF. At 0°C, $CuSO_4$ was added (2 equiv. *per* branch, 1M water solution), followed by the dropwise addition of a freshly prepared solution of sodium ascorbate (4 equiv. *per* branch, 1M water solution) in order to set a 1:1 (THF/water) ratio. The solution was allowed to stir for 12h at 25°C under N_2. After removing THF under vacuum, CH_2Cl_2 and an aqueous ammonia solution were added. The mixture was allowed to stir for 10 min. in order to remove all the Cu^{II} trapped inside the dendrimer as $[Cu(NH_3)_6]^{2+}$. The organic phase was washed twice with water, dried with sodium sulfate, and the solvent was removed under vacuum. The product was precipitated with MeOH/ether in order to remove the excess dendron.[19]
Characterization of **1**: ^{1}H NMR ($CDCl_3$, 250MHz): 7.45 (9H, C*H*-triazole), 6.93 (36H, C*H*-arom. intern), 6.56 (18H, C*H*-arom. extern), 4.62 (18H, triazole-CH_2-0), 4.43 (18H, O-CH_2-arom. extern), 4.11 (72H, CH_2O-arom. extern and Si-CH_2-triazole), 3.64 (414H, OCH_2CH_2O), 3.37 (27H, CH_3O), 1.59 (18H, CH_2CH_2CH_2Si), 1.07 (18H, CH_2CH_2CH_2Si), 0.60 (18H, CH_2CH_2CH_2Si), 0.006 (54H, Si(CH_3)$_2$); ^{13}C NMR ($CDCl_3$, 62 MHz): 151.62 (*C*H, extern arom.), 144.48 (C_q of triazole), 136.83 (*C*q, arom. core), 132.75 (*C*q, arom. extern), 123.52 (*C*H of triazole and arom. core), 106.23 (C_qCH_2O), 69.54 (OCH_2CH_2O), 63.53 (triazole-CH_2-O), 58.00 (CH_3O), 53.38 (OCH2-arom.extern), 43.77 (CH_2CH_2CH_2Si), 42.7 (SiCH_2-triazole), 40.93 (*C*q-arom.intern), 17.82 (CH_2CH_2CH_2Si), 14.90 (CH_2CH_2CH_2Si), -4.84 (Si(CH_3)$_2$); DOSY : D = 1.16 (± 0.1) x 10^{-10} m²/s, Rh = 4.9 (± 0.1) nm (D: diffusion coefficient; Rh : hydrodynamic radius); IR: no alkyne and azide bands; MALDI-TOF mass spectrum: Calc. for $C_{414}H_{741}O_{153}N_{27}Si_9$: 8798; found: 8824 ($MNa^+$); Anal. Calc. for $C_{414}H_{741}O_{153}N_{27}Si_9$: C 56.52, H 8.49; found: C 56.31, H 8.49; light scattering : diameter = 9(± 0.8) nm.

3. Synthesis and characterization of the phenol dendron **8** (see ESI)
The tris-triethylene glycol dendron (300 mg, 0.46 mmol) and hydroquinone (251 mg, 2.28 mmol) were introduced into a Schlenck flask, and dry DMF (30 mL) was added. K_2CO_3 (315 mg, 2.28 mmol) was added to the solution. The mixture was stirred for 18 hours at 80°C under reflux. At the end of the reaction, DMF was removed. The product was extracted with CH_2Cl_2, washed with water, and purified by chromatography (CH_2Cl_2:MeOH, (97:3). 205 mg of a yellow oil was obtained (65% yield).
^{1}H RMN ($CDCl_3$, 250MHz) : 3,35 (C*H*$_3$O); 3,63 (C*H*$_2$O); 4,11 (C*H*$_2$Oarom.); 4,83 (OC*H*$_2$arom.); 6,59 (C*H* arom.); 6,87 (C*H* arom.-OH); ^{13}C NMR ($CDCl_3$, 62 MHz): 152.82 (*C*q-O-CH_2), 152.19 ((Cq-OH),150.56 (*C*q extern.-CH_2-O), 137.87 (*C*q middle-CH_2-O), 132.83 (*C*H_2-Cq), 116.17 (*C*H arom.-Cq-O), 107.19 (*C*H arom.-Cq-CH_2), 71.93 (0-CH_2-arom), 70.71 (O-*C*H_2), 59.06 (O-*C*H_3); MALDI TOF: Calc. For $C_{34}H_{54}O_{14}$: 686.35; found: 709.34 (MNa^+); Anal. Calc. for $C_{54}H_{54}O_{14}$: C 59.46, H 7.92, found: C 59.21, H 8.18.

4. General procedure for the synthesis of the dendrimers **9**, **10** and **11** by Williamson reaction
The iodo-dendrimer[20d] **7** (5.46 x 10^{-6} mol) and the phenol dendron **8** (10 equiv. for the G_0, 30 equiv. for the G_1 and 90 equiv. for the G_2) were introduced into a Schlenck flask, and dry DMF (30 mL) was added, then K_2CO_3 (2 equiv. *per* dendron) was added to the solution. The mixture was stirred for 2 days at 80°C under reflux. At the end of the reaction, DMF was removed. The product was extracted with CH_2Cl_2 and washed with water. G_0 and G_1 were purified by chromatography (CH_2Cl_2:MeOH, (97:3) in order to remove the excess dendron and then (90:10) to extract the dendrimer). G_2dHQ was precipitated with MeOH/ether in order to remove the excess dendron. The yields were 80% for the G_0, 78% for the G_1 and 85% for the G_2.
Characterization of the dendrimer **9**: ^{1}H NMR ($CDCl_3$, 250MHz): 6.92 (C*H*-arom.core), 6.87 (C*H*-arom. intern), 6.65 (C*H*-arom. extern), 4.85 (0- C*H*$_2$-arom. extern), 4.16 (C*H*$_2$O-arom. extern), 3.65 (OC*H*$_2$C*H*$_2$O and Si-C*H*$_2$O), 3.38 (C*H*$_3$O), 1.69 (C*H*$_2$CH$_2$CH$_2$Si), 1.12 (CH$_2$C*H*$_2$CH$_2$Si), 0.62 (CH$_2$CH$_2$C*H*$_2$Si), 0.06 (Si(C*H*$_3$)$_2$); ^{13}C NMR ($CDCl_3$, 62 MHz): 156.09 (O-*C*q intern), 152.61 (*C*q intern), 144.71 (*C*q arom. Core), 137.97 (*C*q-Cq intern), 130.95 (*C*H arom. extern), 118.55 (*C*H arom. Core), 115.61 (*C*H-arom intern), 114.79 (*C*H arom extern), 107.07 (*C*H arom intern), 72.3 (O*C*H$_2$CH$_2$), 70.80 (O*C*H$_2$ arom extern), 68.85 (Si*C*H$_2$O), 59.05 (*C*H$_3$O), 43.77 (*C*H$_2$CH$_2$CH$_2$Si), 17.82 (CH$_2$*C*H$_2$CH$_2$Si), 14.49 (CH$_2$CH$_2$*C*H$_2$Si), -4.58 (Si(*C*H$_3$)$_2$)**;** Maldi TOF : Calc. for $C_{369}H_{606}O_{126}Si_9$: 7311.54; found: 7334.47 (MNa^+); DOSY : D = 1.47 (± 0.1) x 10^{-10} m²/s, Rh = 3.9 (± 0.3) nm (D: diffusion coefficient; Rh : hydrodynamic radius); SEC : retention time = 1221 seconds (polydispersity = 1.05). Anal. calc. for $C_{369}H_{606}O_{126}Si_9$: C 60.62, H 8.35, found: C 59.64, H 8.57.

5. General procedure for AuNPs reduction in methanol with the dendrimers **4**, **5** and **6**.
The following procedure is described using the preparation of the dendrimer **4**: 1 mL of a 1.14x10^{-4} M solution of dendrimer (1mg, 1.14x10^{-4} mmol) in MeOH was introduced into a Schlenk flask under nitrogen, then 0.349 mL of a 2.94x10^{-3} M solution of $HAuCl_4$ (0.349 mg, 1.03x 10^{-3} mmol, 1 equiv. *per* triazole) and 4.65 mL of MeOH was added in order to obtain a solution 2.21x10^{-4} M (in Au). The solution was stirred for 1h, the reductant [$NaBH_4$ (0.39 mg), [Fe^{I}Cp(η^6-C_6Me_6)] (4.4 mg), ferrocene (1.92 mg), ethynylferrocene (2.16 mg) or decamethylferrocene (3.36 mg)] was added (1.03x10^{-2} mmol, 10 equiv. *per* Au), and the yellow solution turned to golden brown indicating the formation of the AuNPs.

6. General procedure for the preparation of AuNPs in water without reductant.
The following procedure is described using the preparation of the dendrimer **9**:1 mL of a 1.37 x 10^{-4} M solution of dendrimer (1mg, 1.37x10^{-4} mmol) in H_2O was placed into a Schlenk

flask under ambient condition, then 0.416 mL of a 1.23 $x10^{-3}$ M solution of $HAuCl_4$ (0.416 mg, 1.23x 10^{-3} mmol, 1 equiv. *per* tether). 1.584 mL of H_2O was added in order to obtain a final volume of 3 mL. The solution was stirred, and the yellow solution turned to pink then red, indicating the formation of the AuNPs.

7. Transmission Electron Microscopy (TEM and HRTEM)
The samples were prepared by placing a drop of 1.6 10^{-4} M solution of AuNPs (concentration in mol Au) on a holey-carbon-coated Cu TEM grid and they were then analysed with a JEOL JEM 1011 machine

Acknowledgements

Financial support from the IUF, the Université Bordeaux 1, the ANR and CNRS are gratefully acknowledged.

References

1. a) Newkome, G. R.; Moorefield, C. N.; Vögtle, F. *Dendrimers and Dendrons. Concepts, Syntheses, Applications*, Wiley-VCH, Weinheim, 2001; b) *Dendrimers and Other Dendritic Polymers*, Tomalia, D. A.; Fréchet; J. M. J. Eds; Wiley: Amsterdam, 2003; c) *Dendrimers and Nanosciences*, D. Astruc Ed., *C. R. Chimie* 2003*, 6,* Elsevier, Paris*;* d) Vögtle, F.; Richardt, G.; Werner, N. *Dendrimer Chemistry: Concepts, Syntheses, Properties, Applications,* Wiley: Weinheim, 2009.
2. a) Crooks, R. M.; Zhao, M.; Sun, L.; Chechik, V.; Yeung, L. K. *Acc. Chem. Res.* **2001**, *34*, 181-190; b) Scott, R. W. J.; Wilson, O. M.; Crooks, R. M. *J. Phys. Chem B* **2005**, *109*, 692-704; c) Helms, B.; Fréchet, J. M. J. *Adv. Syn. Catal.* **2006**, *348*, 1125-1148; d) Chandler, B. D.; Gilbertson, J. D. *Top. Organomet.* **2006**, *20*, 97-120.
3. a) Juris, A.; Balzani, V.; Barrigelletti, F.; Campagna, S.; Denti, G.; Juris, A.; Serroni, S.; Venturi, M. *Acc. Chem. Res.* **1998**, *31*, 26-34; b) Andronov, A.; Fréchet, J. M. J. *Chem. Commun.* **2000**, 1701-1710 ; c) Hecht, S.; Fréchet, J. M. J. *Angew. Chem., Int. Ed.* **2001**, *40*, 74-91; d) Ceroni, P.; Bergamini, G.; Marchioni, F.; Balzani, V. *Prog. Polym. Sci.* **2005**, *30*, 453-473.
4. a) Newkome, G. R.; Yao, Z.; Baker, G. R.; Gupta, V. K. *J. Org. Chem.* **1985**, *50*, 2003-2004; b) Jansen, J. F. G. A., de Brabander-van den Berg, E. M. M.; Meijer, E W. *Science*, **1994**, *266*, 1226-1229; c) Moorefield, C. N.; Newkome, G. R. *C. R. Chimie* **2003**, *6*, 715-724; d) Schenning, A. P. H.; Meijer, E. W. *Chem. Commun.* **2005**, 3245-3258; e) Hahn, U.; Cardinali, F.; Nierengarten, J.-F. *New J. Chem.* **2007**, *31*, 1128-1138; f) Hwang, S.-H.; Shreiner, C. D.; Moorefield, C. N.; Newkome, C. N. *New J. Chem.* **2007**, *31*, 1192-1217; g) Knecht, M. R.; Crooks, R. M. *New J. Chem*. **2007**, *31*, 1349-1353.
5. a) Liu, M.; Kono, K.; Fréchet, J. M. J. *Controlled Release* **2000**, *85*, 85-90; b) Boas, U.; Heegaard, P. M. H. *Chem. Soc. Rev.* **2004**, *33*, 43-63; c) Svenson, S.; Tomalia, D. A. *Adv. Drug Deliv. Rev.* **2005**, *57*, 2106-2129; d) Patri, A. K.; Kukowska-Latallo, J. F.; Baker, J. R., Jr. *Adv. Drug. Deliv. Rev.* **2005**, *57*, 2203-2214; e) Duncan, R.; Izzo, L. *Adv. Drug. Deliv. Rev.* **2005**, *57*, 2215-2237; f) D'Emanuele, A.; Attwood, D. *Adv. Drug Deliv. Rev.* **2005**, *57*, 2147-2162; g) Grinstaff J. *Polym. Sci.: Part A: Polym. Chem.* **2008**, *46*, 383-400; h) *Dendrimer based nanomedicine.* Majoros, I. J.; Baker, J. R., Jr. Eds., Pan Stanford Publishing: Stanford, 2008; i) Fox, M. E.; Szoka, F. C.; Tekade, R.; Kumar, P. V.; Jain, N. K. *Chem. Rev.* **2009**, *109*, 49-87; j) Fréchet, J. M. J. *Acc. Chem. Res*. **2009**, *42*, 1141-1151.

6. a) Zhao, M.; Sun, L.; Crooks, R. M. *J. Am. Chem. Soc.* **1998**, *120*, 4877-4878; b) Balogh, L.; Tomalia, D. A. *J. Am. Chem. Soc.* **1998**, *120*, 7355-7356.
7. a) Yeung, L. K.; Crooks, R. M. *Nano Lett.* **2001**, *1*, 14-17; b) Rahim, E. H.; Kamounah, F. S.; Frederiksen, J.; Christensen, J. B. *Nano Lett.* **2001**, *1*, 499-503; c) Li, Y.; El Sayed, M. A. *J. Chem. Phys. B* **2001**, 105, 8938-8946; d) Oee, M.; Murata, M.; Mizugaki, T.; Ebitani, K. Kaneda, K. *Nano Lett.* **2002**, *2*, 999-1002; e) Pittelkow, M.; Moth-Poulsen, K.; Boas, U.; Christensen, J. B. *Langmuir* **2003**, *19*, 7682; f) Chung, Y.; Rhee, H. K. *J. Mol. Catal. A* **2003**, *206*, 291-298; g) Ooe, M.; Murata, M.; Mizugaki, T.; Ebitani, K. *J. Am. Chem. Soc.* **2004**, *126*, 1604-1608; h) Lemo, J.; Heuze, K.; Astruc, D. *Inorg. Chim. Acta* **2006**, *359*, 4909-4911.
8. a) Zhao, M.; Crooks, R. M. *Angew. Chem., Int. Ed.* **1999**, *38*, 364-366; Sun, L.; Crooks, R. M. *Langmuir* **2002**, *18*, 8231-8236; b) Scottt, R. W. J.; Datye, A. K.; Crooks, R. M. *J. Am. Chem. Soc*. **2003**, *125*, 3708-3709; c) Scott, R. W.; Wilson, O. M.; Oh, S.-K.; Kenik, E. A.; Crooks, R. M. *J. Am. Chem. Soc.* **2004**, *126*, 15583-15591; d) Wilson, O. M.; Scott, R. W. J.; Garcia-Martinez, J. C.; Crooks, R. M. *J. Am. Chem. Soc.* **2005**, *127*, 1015-1024; e) Scott, R. W. J.; Sivadiranarayana, C.; Wilson, O. M.; Yan, Z.; Goodman, D. W.; Crooks, R. M. *J. Am. Chem. Soc.* **2005**, *127*, 1380-1381; f) Gomez, M. V.; Guerra, J.; Velders, A. H.; Crooks, R. M. *J. Am. Chem. Soc.* **2008**, *131*, 341-350.; g) Feng, Z. V.; Lyon, J. L.; Croley, J. S.; Crooks, R. M.; Vanden Bout, D. A.; Stevenson, K. J. *J. Chem. Ed.* **2009**, 86, 368-372.
9. a) Higushi, M.; Shiki, S.; Ariga, S.; Yamamoto, K. *J. Am. Chem. Soc.* **2001**, *123*, 4414-4420; b) Yamamoto, K.; Higushi, M.; Shiki, S.; Tsuruta, M.; Chiba, H. *Nature* **2002**, *415*, 509-511; c) Satoh, N.; Cho, J. S.; Higushi, M.; Yamamoto, K. *J. Am. Chem. Soc.* **2003**, *125*, 8104-8105; d) Higushi, M.; Shiki, S.; Yamamoto, K. *Org. Lett.* **2000**, *2*, 3079-3082; e) Cho, J.-S.; Takanashi, K.; Higushi, M.; Yamamoto, M. *Syn. Metals* **2005**, *150*, 79-82; f) Nakashjima, T.; Satoh, N.; Albrecht, K.; Yamamoto, K. *Chem. Mater.* **2008**, *20*, 2538-2543; g) Satoh N.; Nakashima T.; Kamikura K.; Yamamoto, K. *Nature Nanotechnol.* **2008**, *3*, 106-111; h) Yamamoto, K.; Takanashi, K. *Polymer* **2008**, *49*, 4033-4041.
10. a) Rostovtsev, V. V. ; Green, L. G. ; Fokin, V. V. ; Sharpless, K. B. *Angew. Chem., Int. Ed.* **2002**, *41*, 2596-2599 ; b) Tornoe, C. X. W. ; Christensen, C. ; Meldal , M. *J. Org. Chem*. **2002**, *67*, 3057-3064 ; c) Feldman, A. K. ; Nugent, A. K. ; Hawker, C. J. ; Scheel, A.; Voit, B. ; Pyun, J. ; Fréchet, J. M. J. ; Sharpless, K. B. *Angew. Chem., Int. Ed*. **2004**, *43*, 3928-3932 ; d) Reviews: Kolb, H. C.; Finn, M. G.; Sharpless, K. B.; *Angew. Chem., Int. Ed.* **2001**, *40*, 2004-2021; e) Bock, V. D.; Hiemstra, H.; van Maarseveen, J. H.; *Eur. J. Org. Chem.* **2006**, 51-68 ; f) Wu, P. ; Meldal, M; Tornoe, C. W. *Chem. Rev.* **2008**, *10*, 2952-3015.
11. a) Ornelas, C.; Ruiz, J.; Cloutet, E.; Alves, S.; Astruc, D. *Angew. Chem., Int. Ed.* **2007,** *46*, 872-877; b) Camponovo, J.; Ruiz, J.; Cloutet, E.; Astruc, D. *Chem., Eur. J.* **2009,** *15*, 2990-3002; c) Astruc, D.; Daniel, M.-C.; Ruiz, J. *Chem. Commun*. **2004**, 2637-2649.
12. a) Ornelas, C.; Salmon, L.; Ruiz, J.; Astruc, D. *Chem. Eur. J.* **2008**, *14*, 50-64; b) Ornelas, C.; Salmon, L.; Ruiz, J.; Astruc, D. *Chem. Commun*. **2007**, 4946-4948; c) Diallo, A. K.; Ornelas, C.; Salmon, L.; Ruiz, J.; Astruc, D. *Angew. Chem., Int. Ed.* **2007**, *46*, 8644-8648; d) Ornelas, C.; Ruiz , J.; Salmon, L.; Astruc, D. *Adv. Syn. Catal*. **2008**, *350*, 837-845.
13. Boisselier, E. ; Diallo, A. K.; Salmon, L.; Ruiz, J. ; Astruc, D. *Chem. Commun*. **2008**, 4819-4821.
14. a) Esumi, K.; Suzuki, A. ; Aihara, N.; Usui, K.; Torigoe, K. *Langmuir* **1998**, 14, 3157-3159; b) Yoshimura, T.; Fukai, J.; Mizutani, H.; Esumi, K. J. *Colloid Interf. Sci.* **2002**,

255, 428-431; c) Esumi, K.; Akiyama, S.; Yoshimura, T. *Langmuir* **2003**, *19*, 7679-7681.

15. a) Sartor, V.; Djakovitch, L.; Fillaut, J.-L.; Moulines, F.; Neveu, F.; Marvaud V.; Guittard, J.; Blais, J.-C.; Astruc, D. *J. Am. Chem. Soc.*, **1999**, *121*, 2929-2930; b) Ruiz, J. ; Lafuente, G.; Marcen, S.; Ornelas, C.; Lazare, S.; Blais, J.-C.; Cloutet, E.; Astruc, D. *J. Am. Chem. Soc*. **2003**, *125*, 7250-7257; c) Ornelas, C.; Ruiz, J.; Belin, C.; Astruc, D. *J. Am. Chem. Soc*., **2009**, *131*, 590-601.
16. a) Newkome, G. R.; Moorefield, C. N. *Aldrichim. Acta*, **1992**, *25*, 31-38; b) Newkome, G. R. *Pure Appl. Chem.* **1998**, *70*, 2337-2343; c) Moulines, F.; Djakovitch, L.; Boese, R.; Gloaguen, B.; Thiel, W.; Fillaut, J.-L.; Delville, M.-H.; Astruc, D. *Angew. Chem. Int. Ed. Engl.*, **1993**, *32*, 1075-1077; d) Nlate, S.; Ruiz, J.; Blais, J.-C.; Astruc, D. *Chem. Commun.* **2000**, 417-418.
17. a) Liu, M.; Kono, K.; Fréchet, J. M. J. *Polym. Sci. A* **1999**, *37*, 3492-3503; b) Liu, M.; Kono, K.; Fréchet, J. M. J. *Controlled Release* **2000**, *65*, 121-131; c) Duncan, R. *Nat. Rev. Drug. Discovery* **2003**, *2*, 347-360.
18. a) Katz, E.; Willner, I. *Angew. Chem., Int. Ed.* **2004**, *43*, 6042-6108; b) Dreshler, U.; Erdogan, B.; Rotello, V. M. *Chem. Eur. J.* **2004**, *10*, 5570-5579; c) Paciotti, G. F.; Myer, L.; Weinreich, D. *Drug Deliv*. **2004**, 11, 169-183; d) Daniel, M-C.; Astruc, D. *Chem. Rev*. **2004**, *104*, 293-346; e) Jain, P.; El-Sayed, I.-H.; El-Sayed, M. A. *Nanotoday* **2007**, *2*, 18-29 ; f) Murphy, C. J.; Gole, A. M.; Hunyadi, S. E.; Stone, J. W.; Sisco, P. N.; Alkilany, A.; Kinard, B. E.; Hankins, P. *Chem. Commun* (feature article) **2008**, 544-557; g) Lal, S. L.; Clare, S. E.; Halas, N. J. *Acc. Chem. Res*. **2008**, *41*, 1842-1851; h) Boisselier, E.; Astruc, D. *Chem. Soc. Rev*. **2009**, *38*, 1759–1782.
19. a) Percec, V.; Johansson, G.; Ungar, G.; Zhou, J. *J. Am. Chem. Soc.*, **1996**, 118, 9855-9866; b) Balagurusamy, V. S. K.; Ungar, G.; Percec, V.; Johansson, G. *J. Am. Chem. Soc.*, **1997**, *119*, 1539-1555; c) Percec, V.; Smidrkal, J.;Peterca, M.; Mitchell, C. M.; Nummelin, S.; Dulcey, A. E.; Sienkowska, M. J.; Heiney, P. A. *Chemistry* **2007**, *13*, 3989-4007; d) Percec, V.; Peterca, M.; Dulcey, A. E.; Imam, M. R.; Hudson, S. D.; Nummelin, S.; Adelman, P.; Heiney P. A. *J. Am. Chem. Soc.* **2008**, *130*, 13079-13094.
20. a) Catheline, D.; Astruc, D. J. *Organomet. Chem.* **1983**, *248*, C9-C12; b) Catheline, D.; Astruc, D. J. *Organomet. Chem.* **1984**, *272*, 417-426.
21. Candelon, N.; Lastécouères, D.; Diallo, A. K.; Ruiz, J.; Astruc, D. ; Vincent, J.-M. *Chem. Commun.*, **2008**, 741-743.
22. a) Liu, K. J. *Macromolecules* **1968**, *1*, 308-311; b) Yanagida, S.; Takahashi, K.; Okahara, M. *Bull. Chem. Soc. Jpn.* **1977**, *50*, 1386-1390; c) Warshawsky, A.; Kalir, R.; Deshe, A.; Berkovitz, H.; Patchornik, A. *J. Am. Chem. Soc*. **1979**, *101*, 4249-4256; d) Elliott, B. J.; Scranton, A. B.; Cameron, J. H.; Bowman, C.N. *Chem. Mater.* **2000**, *12*, 633-642; e) Adams, M. D.; Wade, P. W.; Hancock, R. D. *Talanta* **1990**, *37*, 875-883; f) Mathur, A. M.; Scranton, A. B. *Sep. Sci. Technol.* **1995,** *30*, 1071-1086; g) Sanai, Y.; Ono, K.; Hidaka, T.; Takagi, M.; Cattrall, R. W. *Bull. Chem. Soc. Jpn.* **2000**, *73*, 1165-1169; h) Yokota, K.; Matsumura, M.; Yamaguchi, K.; Takada Y. *Makromol. Chem. Rapid Commun.* **1983**, *4*, 721-724.
23. a) Hamon, J.-R.; Astruc, D.; Michaud, P. *J. Am. Chem. Soc*. **1981**, *103*, 758-766; b) Green, J. C.; Kelly, M. R.; Payne, M. P.; Seddon, E. A.; Astruc, D.; Hamon, J.-R; Michaud, P. *Organometallics* **1983**, *2*, 211-218; c) Desbois, M.-H.; Astruc, D.; Guillin, J.; Varret, F.; Trautwein, A. X.; Villeneuve, G. *J. Am. Chem. Soc.* **1989**, *111*, 5800-5809.
24. a) Badèche, S.; Daran, J.-C.; Ruiz, J.; Astruc, D. *Inorg. Chem* **2008**, *47*, 4903-4908; b) *Nanoparticles and Catalysis*, Astruc, D. Ed. Wiley-VCH: Weinheim, 2007.

25. Cotton, F. A.; Wilkinson, G.; Murillo, C. A.; Bochmann, M. *Advanced Inorganic Chemistry*, 6th ed., John Wiley, New York, pp. 1084-1086.
26. a) Turkevitch, J.; Stevenson, P. C.; Hillier, J. *Disc. Faraday Soc*. **1951**, *11*, 55-75; b) Turkevitch, J.; Kim, G. *Science* **1970**, *169*, 873-879; c) Watson, K. J.; Ngyuen, S. B. T.; Mirkin, C. A. *J. Am. Chem. Soc*. **1999**, *121*, 462-463.
27. a) Haruta, M.; Kobayashi, T.; Sano, H.; Yamada, N. *Chem. Lett*. **1987**, 405-410; b) Haruta, M; Tsuboda, S.; Kobayashi, T.; Kagehiama, H.; Genet, M. J.; Demon, B. *J. Catal*. **1993**, 144, 175-180; c) Haruta, M. *CATTECH* **2002**, *6*, 102-107.
28. a) Taube, H.; Myers, H.; Rich, R. L. *J. Am. Chem. Soc*. **1953**, *75*, 4118-4123; b) Taube, H. *Angew. Chem., Int. Ed*. **1984**, *23*, 329-340; c) Taube, H. *Electron-Transfer Reactions of Complex Ions in Solution*. Academic Press: New York, 1970.
29. a) Reetz, M. T.; Maase, M. *Adv. Mater.* **1999**, *11*, 773-777; b) for an insightful discussion, see Reetz, M. T. in ref. 24, Chap. 8.
30. a) Connelly, N. G.; Geiger, W. E. *Chem. Rev*. **1996**, *96*, 877-910; b) Geiger, W. E. *Organometallics* **2007**, *26*, 5738-5765; c) Astruc, D. *Bull. Soc. Chim. Jpn*. **2007**, *80*, 1658-1671; d) Astruc, D. *New J. Chem*. **2009**, *33*, 1191–1206.

Encapsulation and Stabilization of Gold Nanoparticles with "Click" Polyethyleneglycol Dendrimers

Elodie Boisselier, Abdou K. Diallo, Lionel Salmon, Jaime Ruiz Aranzaes , Didier Astruc *

SUPPLEMENTARY INFORMATION

Synthesis and characterization of the alkyne dendron ***3***

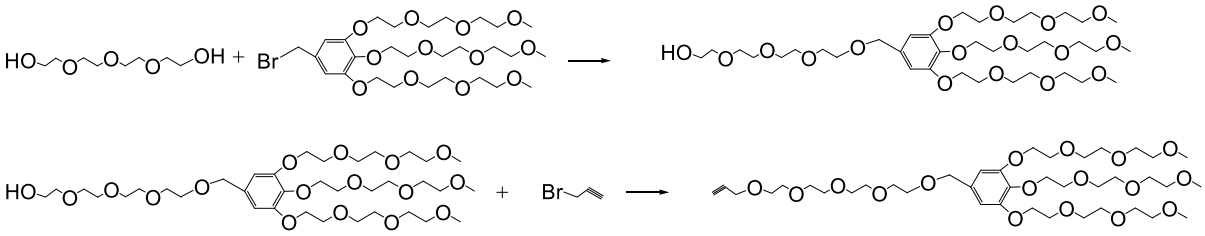

The tris-triethylene glycol dendron (1 g, 1.57 mmol) and the tetraethylene glycol (2.95 g, 15.7 mmol) were introduced in a Schlenck, and dry THF (50 mL) was added. NaH (108 mg, 2.7 mmol) was added to the solution. The mixture was stirred for 12 hours at 50°C. At the end of the reaction, water was added, then THF was removed. The product was extracted with CH_2Cl_2 and purified by chromatography (MeOH). 1g of a yellow oil was obtained (83% yield).

The tris-triethylene glycol tetraethylene glycol dendron (600 mg, 0.65 mmol) and dry THF (50 mL) were introduced in a Schlenck, and NaH (47 mg, 1.95 mmol) was added at 0°C. Propargyl bromide (155 mg, 1.3 mmol) was added to the solution. The mixture was stirred for 2 hours at 0°C, then 2 hours at 25°C. At the end of the reaction, water was added, then THF and excess propargyl bromide were removed under vacuum. The product was extracted with CH_2Cl_2 yielding 600 mg of a yellow oil (95% yield).

^{1}H NMR ($CDCl_3$, 250MHz): 6.39 (2H, C*H*-arom. extern), 4.26 (2H, O-CH_2-arom. extern), 3.98 (4H, CH_2O-arom. extern and CH_2-alkyne), 3.46 (30H, OCH_2CH_2O), 3.17 (9H, CH_3O), 2.36 (1H, C-C*H* alkyne) **(see the spectrum page 2)**

^{13}C NMR ($CDCl_3$, 62 MHz): 152.41 (*C*q-O arom.), 137.50 (*C*q-CH_2 arom.), 133.63 (Cq-*C*H2-O), 106.87 (*C*H arom.), 79.54 (*C*q alkyne), 74.75 (*C*H alkyne), 70.46 (O-*C*H_2), 58.74(O-*C*H_3), 58.13 (*C*H_2-alkyne) **(see the spectrum page 3)**

Infrared υ_{alkyne}: 2100 cm^{-1} **(see the spectrum page 4)**

Maldi TOF : Calc. for $C_{39}H_{68}O_{17}$: 808; found: 831 (MNa^+) **(see the spectrum page 4)**

*^{1}H NMR spectrum of the alkyne dendron **3***

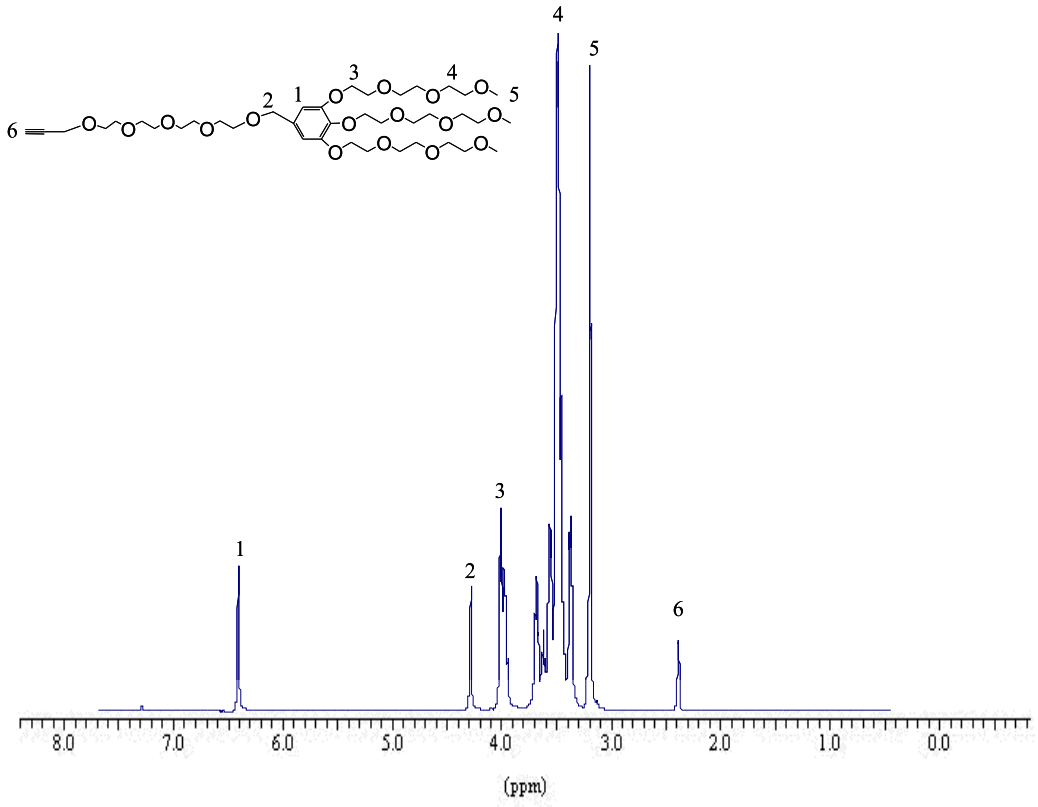

^{1}H NMR ($CDCl_3$, 250MHz): 6.39 (2H, C*H*-arom. extern), 4.26 (2H, O-CH_2-arom. extern), 3.98 (4H, CH_2O-arom. extern and CH_2-alkyne), 3.46 (30H, OCH_2CH_2O), 3.17 (9H, CH_3O), 2.36 (1H, C-C*H* alkyne).

*^{13}C NMR spectrum of the alkyne dendron **3***

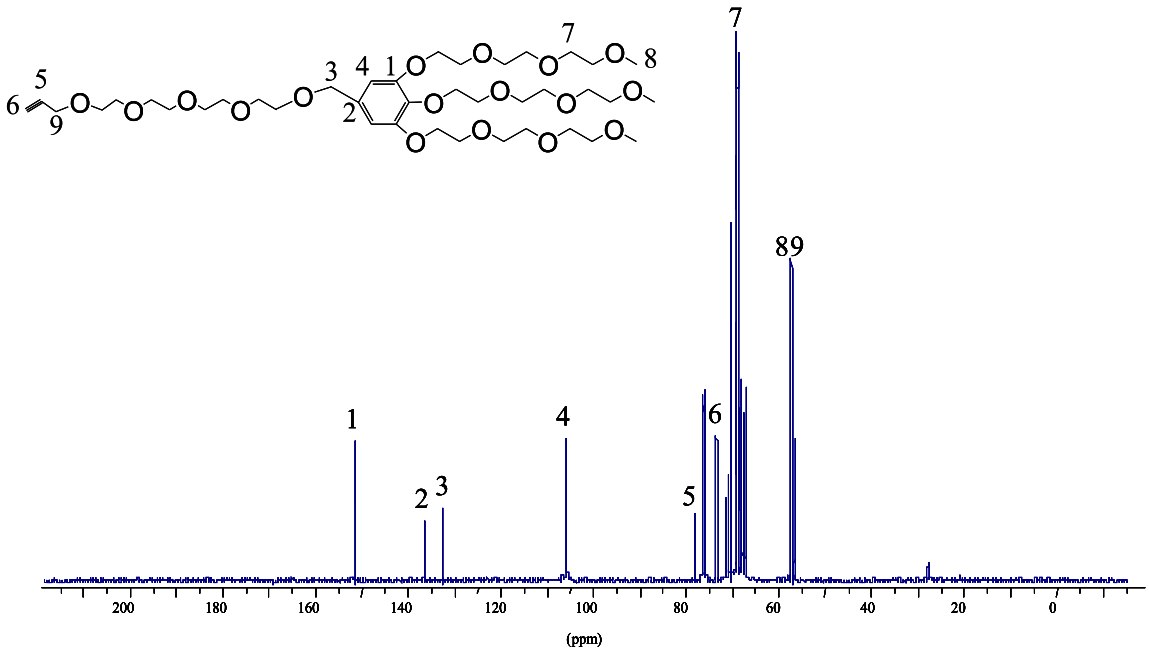

^{13}C NMR ($CDCl_3$, 62 MHz): 152.41 (*C*q-O arom.), 137.50 (*C*q-CH_2 arom.), 133.63 (Cq-*C*H2-O), 106.87 (*C*H arom.), 79.54 (*C*q alkyne), 74.75 (*C*H alkyne), 70.46 (O-*C*H_2), 58.74(O-*C*H_3), 58.13 (*C*H_2-alkyne).

*IR spectrum of the alkyne dendron **3***

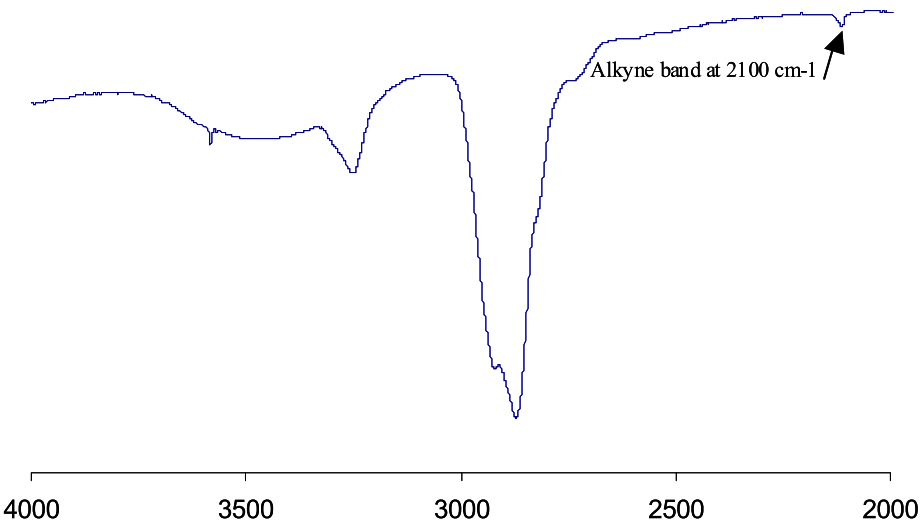

Infrared υ_{alkyne}: 2100 cm^{-1}.

*Mass spectrum of the alkyne dendron **3***

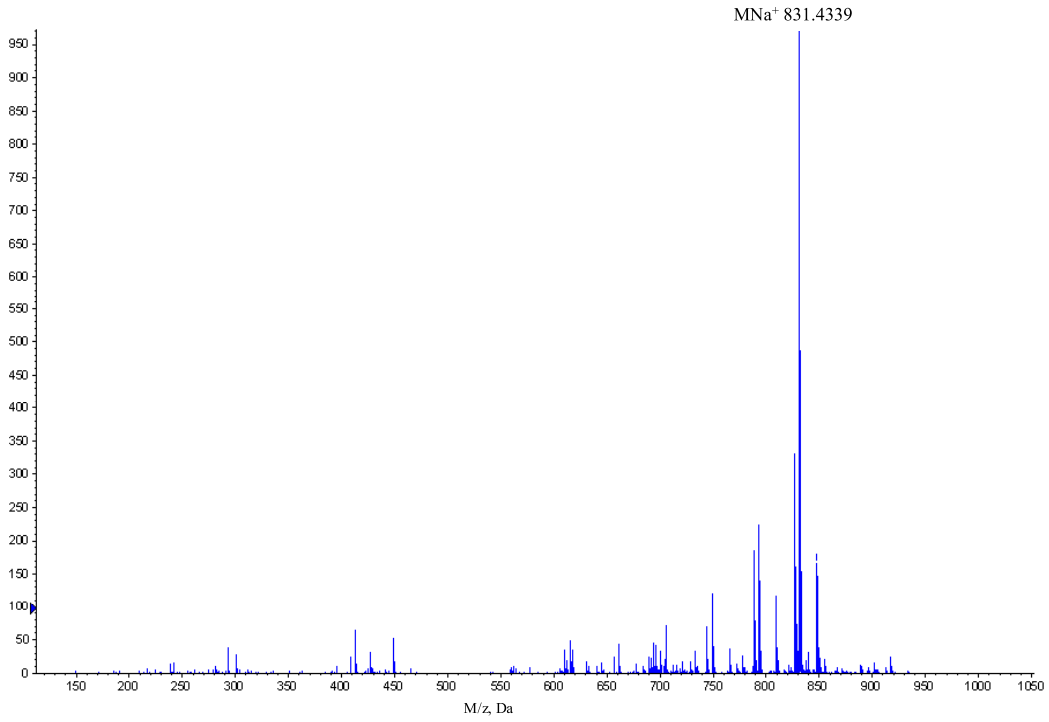

Maldi TOF : Calc. for $C_{39}H_{68}O_{17}$: 808; found: 831 (MNa^+).

Dendrimer **4**

Mw = 8 787 g.mol^{-1}

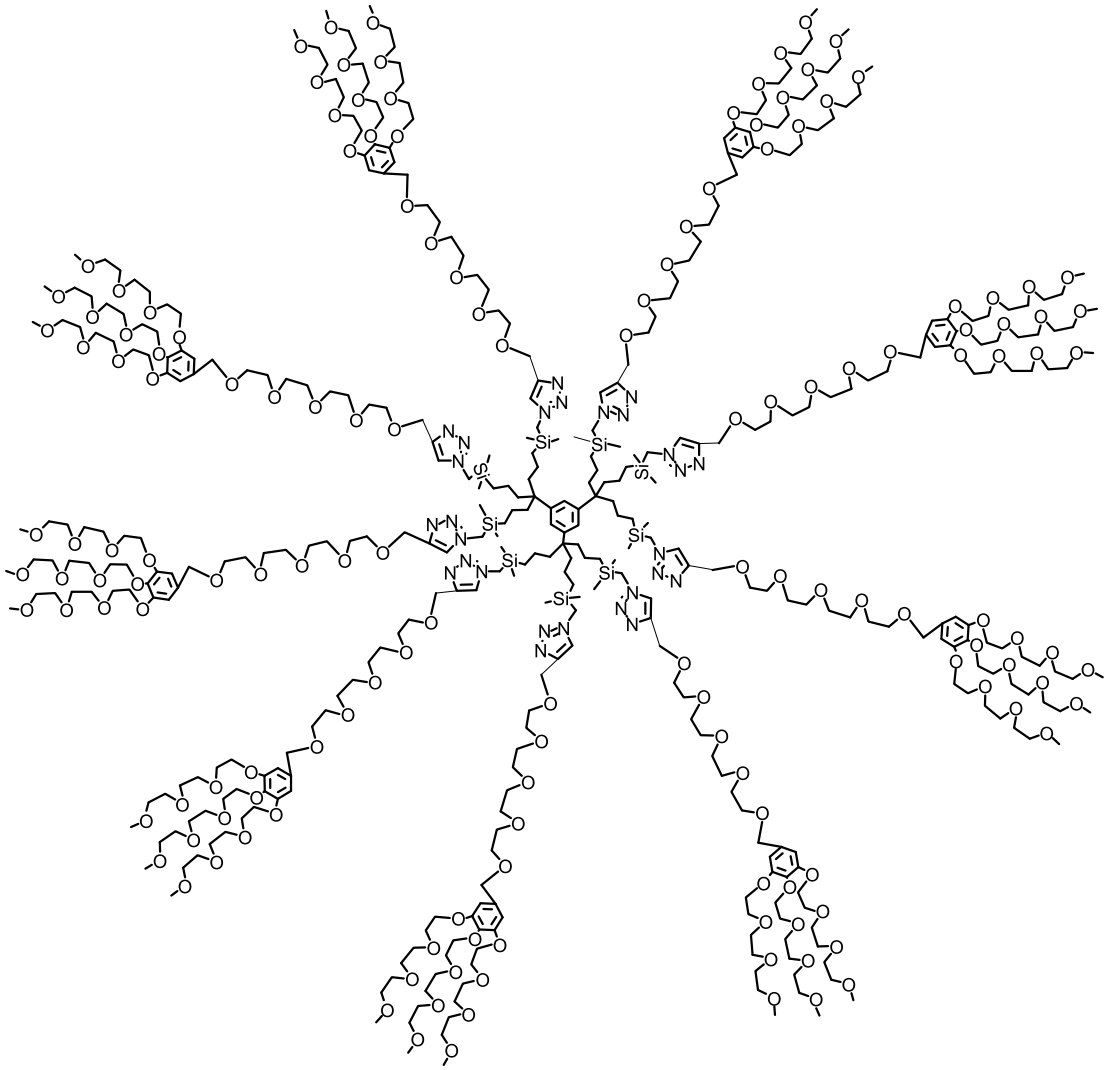

^{1}H NMR ($CDCl_3$, 250MHz): 7.45 (9H, C*H*-triazole), 6.93 (36H, C*H*-arom. intern), 6.56 (18H, C*H*-arom. extern), 4.62 (18H, triazole-CH_2-0), 4.43 (18H, O-CH_2-arom. extern), 4.11 (72H, CH_2O-arom. extern and Si-CH_2-triazole), 3.64 (414H, OCH_2CH_2O), 3.37 (27H, CH_3O), 1.59 (18H, CH_2CH$_2$CH$_2$Si), 1.07 (18H, CH$_2$CH_2CH$_2$Si), 0.60 (18H, CH$_2$CH$_2$CH_2Si), 0.006 (54H, Si(CH_3)$_2$). **(see the spectrum page 7)**

^{13}C NMR ($CDCl_3$, 62 MHz): 151.62 (*C*H, extern arom.), 144.48 (C_q of triazole), 136.83 (*C*q, arom. core), 132.75 (*C*q, arom. extern), 123.52 (*C*H of triazole and arom. core), 106.23 (C_qCH$_2$O), 69.54 (OCH$_2$CH$_2$O), 63.53 (triazole-*C*H$_2$-O), 58.00 (*C*H$_3$O), 53.38 (OCH2-arom.extern), 43.77 (*C*H$_2$CH$_2$CH$_2$Si), 42.7 (SiCH_2-triazole), 40.93 (*C*q-arom.intern), 17.82 (CH$_2$*C*H$_2$CH$_2$Si), 14.90 (CH$_2$CH$_2$*C*H$_2$Si), -4.84 (Si(*C*H$_3$)$_2$). **(see the spectrum page 8)**

DOSY : D = 1.16 (± 0.1) x 10^{-10} m²/s
Rh = 4.9 (± 0.1) nm
(D: diffusion coefficient; Rh : hydrodynamic radius) **(see DOSY spectrum page 9)**

IR: no alkyne and azide bands **(see the spectrum page 10)**

SEC : **(see the spectrum page 21)**

MALDI-TOF mass spectrum: Calc. for $C_{414}H_{741}O_{153}N_{27}Si_9$: 8798; found: 8824 ($MNa^+$). **(see the spectrum page 10)**

Elemental Analysis: Anal. Calc. for $C_{414}H_{741}O_{153}N_{27}Si_9$: C 56.52, H 8.49; found: C 56.31, H 8.49

Light scattering : Rh = 4.5 (± 0.4) nm

*^{1}H NMR spectrum of dendrimer **4***

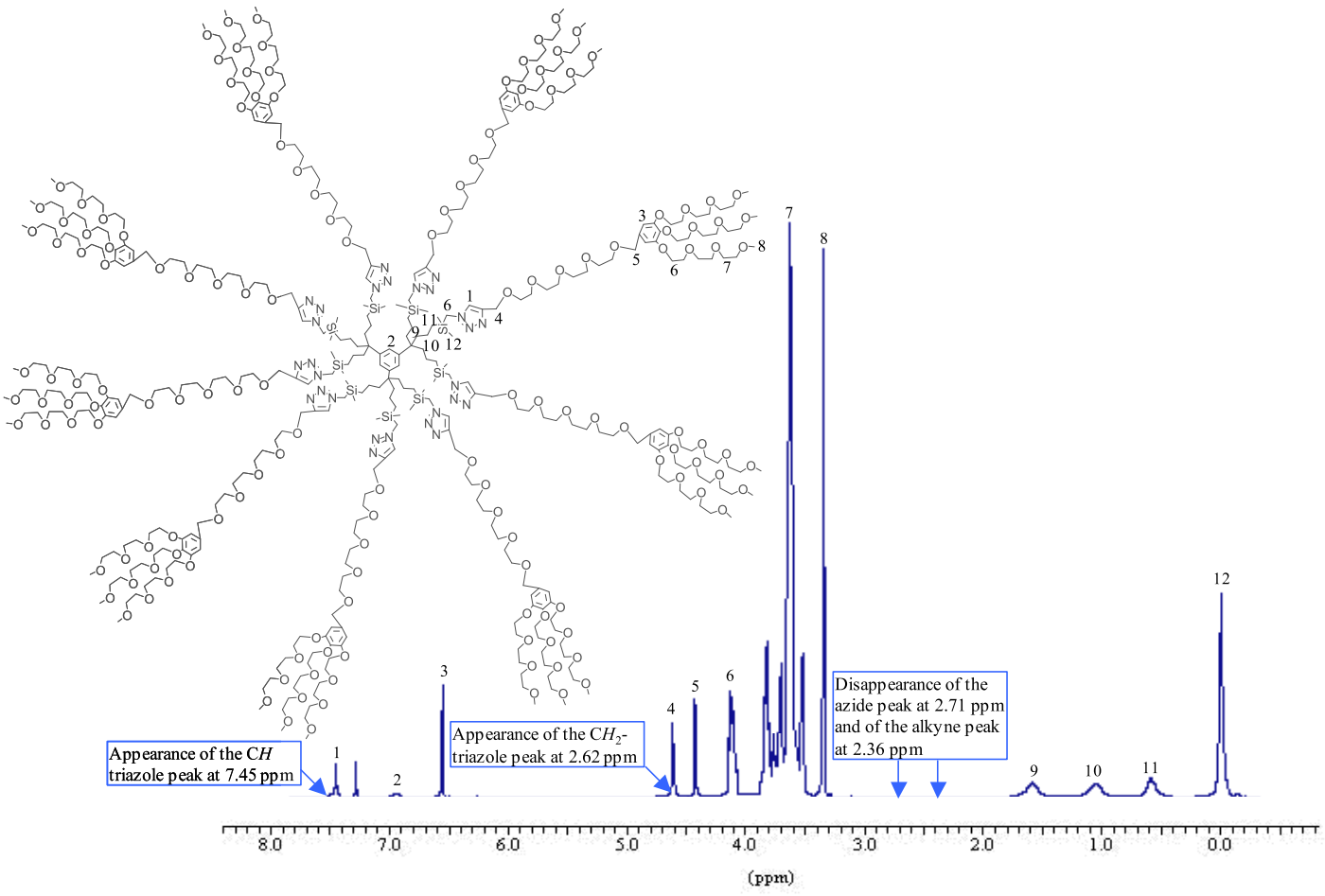

^{1}H NMR ($CDCl_3$, 250MHz): 7.45 (9H, C*H*-triazole), 6.93 (36H, C*H*-arom. intern), 6.56 (18H, C*H*-arom. extern), 4.62 (18H, triazole-CH_2-0), 4.43 (18H, O-CH_2-arom. extern), 4.11 (72H, CH_2O-arom. extern and Si-CH_2-triazole), 3.64 (414H, OCH_2CH_2O), 3.37 (27H, CH_3O), 1.59 (18H, CH_2CH$_2$CH$_2$Si), 1.07 (18H, CH$_2$CH_2CH$_2$Si), 0.60 (18H, CH$_2$CH$_2$CH_2Si), 0.006 (54H, Si(CH_3)$_2$).

*^{13}C NMR spectrum of dendrimer **4***

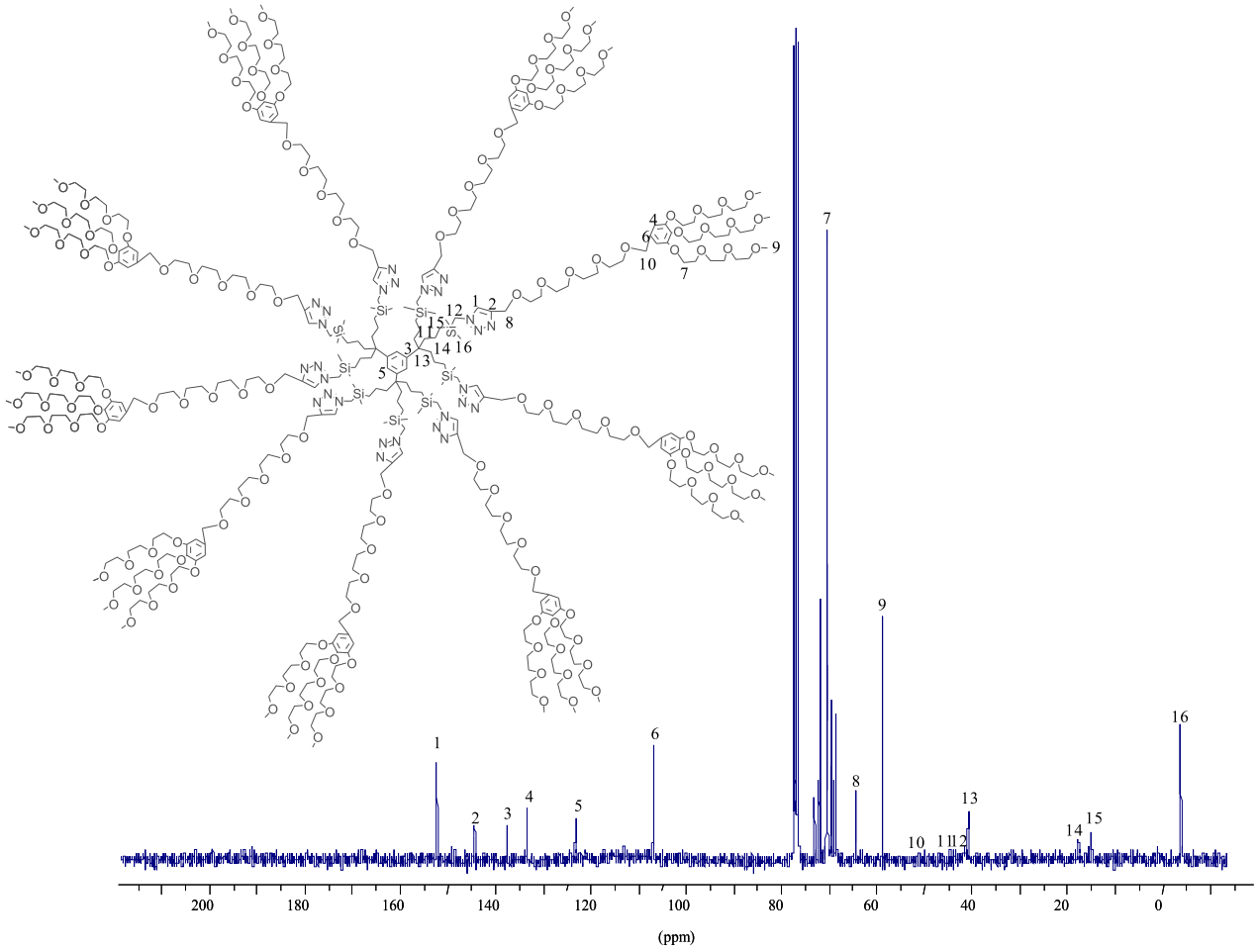

^{13}C NMR ($CDCl_3$, 62 MHz): 151.62 (*C*H, extern arom.), 144.48 (C_q of triazole), 136.83 (*C*q, arom. core), 132.75 (*C*q, arom. extern), 123.52 (*C*H of triazole and arom. core), 106.23 (C_qCH_2O), 69.54 (OCH_2CH_2O), 63.53 (triazole-CH_2-O), 58.00 (CH_3O), 53.38 (OCH2-arom.extern), 43.77 ($CH_2CH_2CH_2Si$), 42.7 ($SiCH_2$-triazole), 40.93 (*C*q-arom.intern), 17.82 ($CH_2CH_2CH_2Si$), 14.90 ($CH_2CH_2CH_2Si$), -4.84 ($Si(CH_3)_2$).

*DOSY spectrum of dendrimer **4***

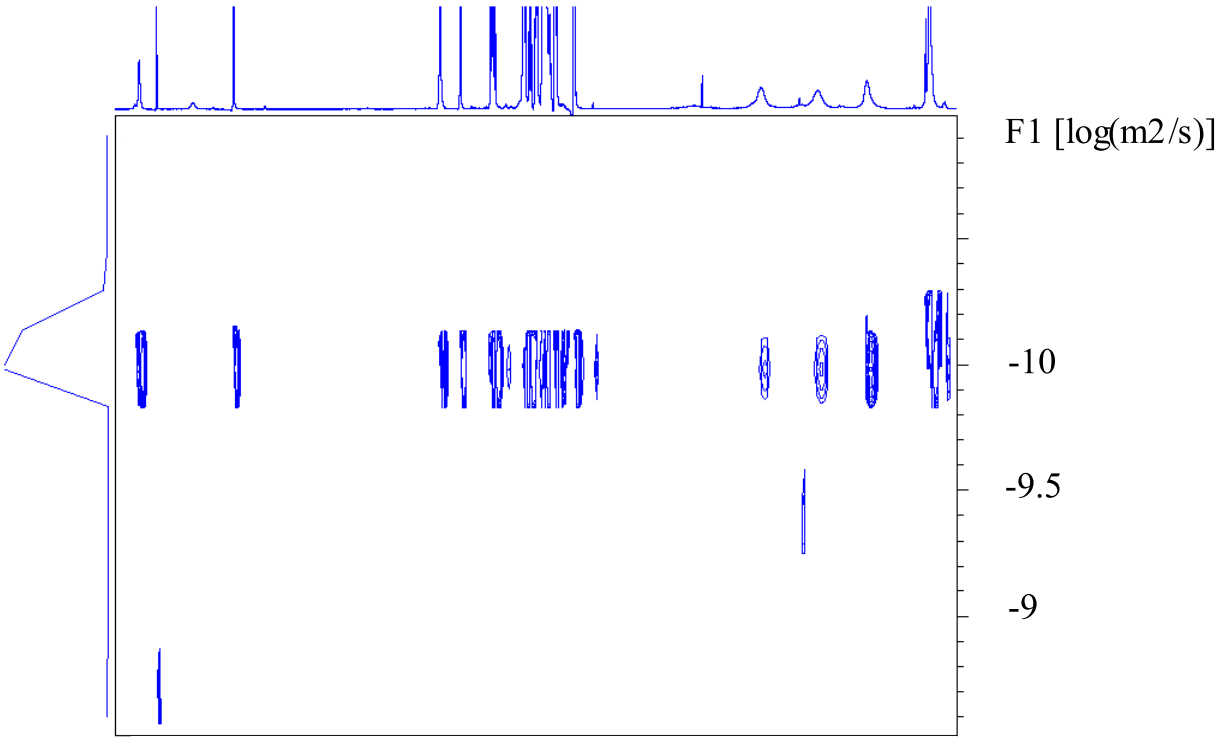

DOSY : D = 1.16 (± 0.1) x 10^{-10} m²/s
Rh = 4.9 (± 0.1) nm
(D: diffusion coefficient; Rh : hydrodynamic radius) .

IR spectrum of dendrimer ***4***

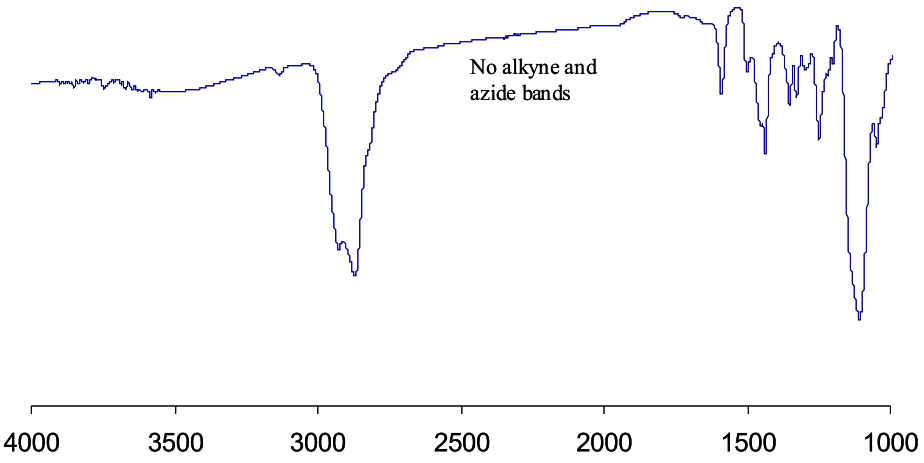

MALDI-TOF mass spectrum of dendrimer ***4***

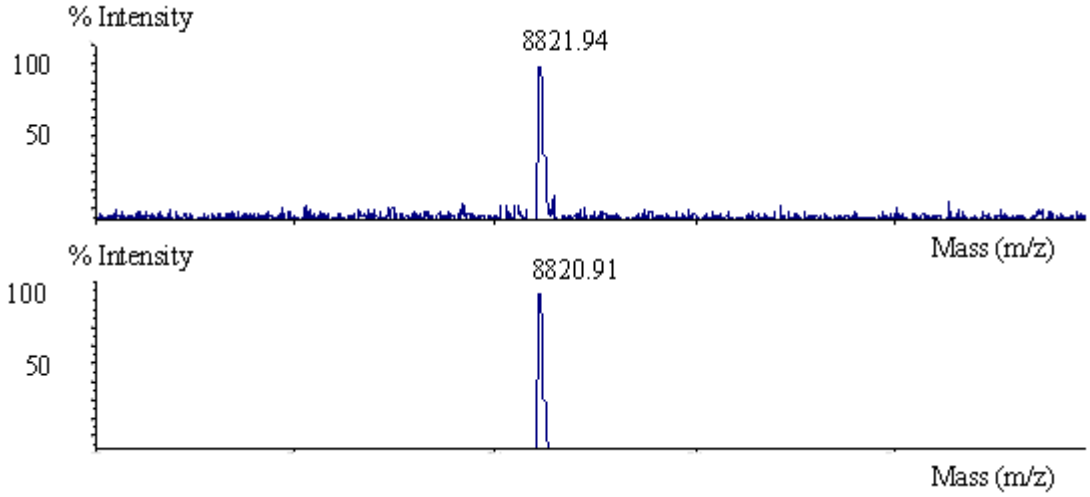

MALDI-TOF: Calc. for $C_{414}H_{741}O_{153}N_{27}Si_9$: 8798; found: 8821.25 ($MNa^+$).

Dendrimer **5**

Mw = 28 462 g.mol^{-1}

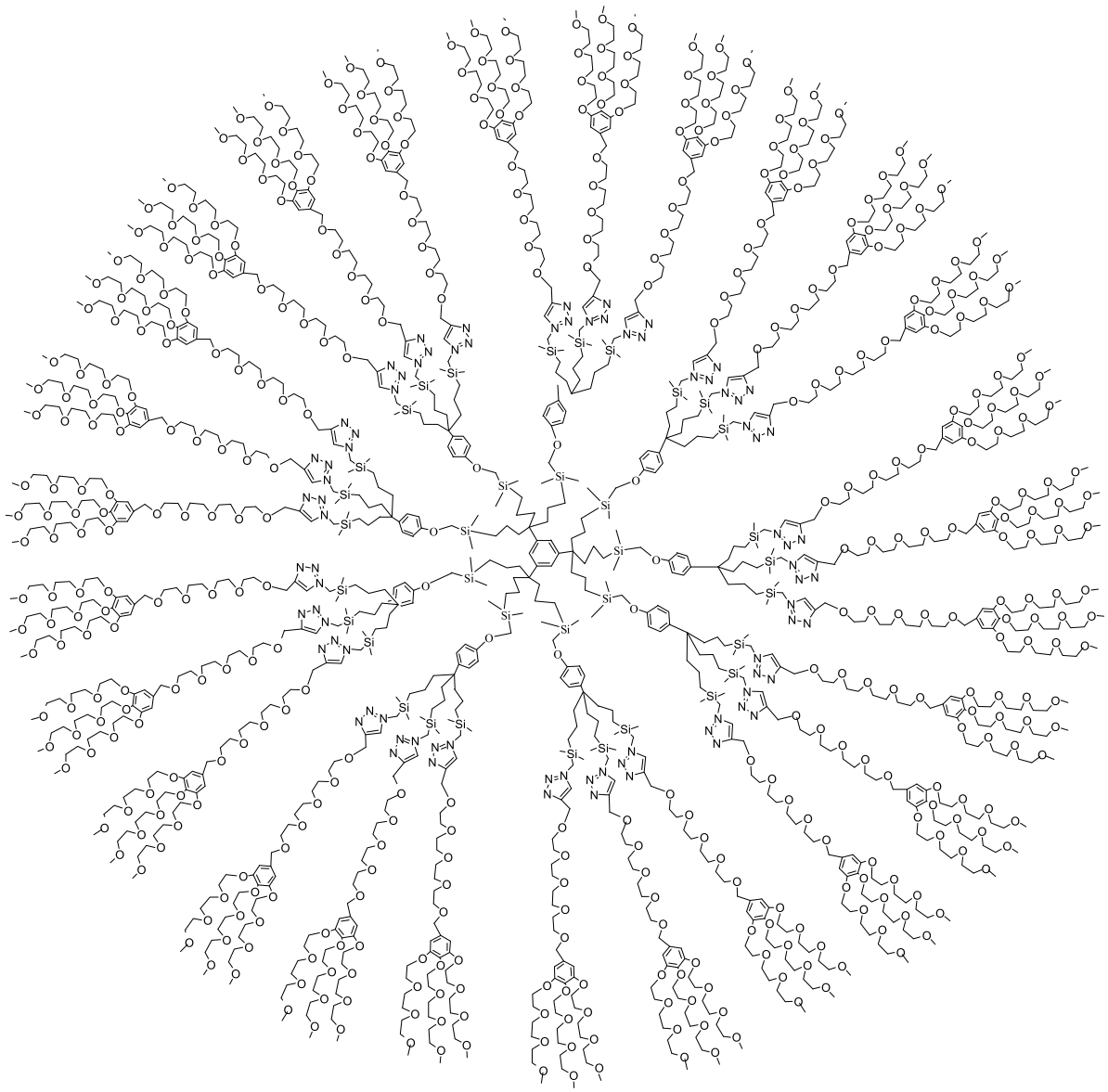

^{1}H NMR ($CDCl_3$, 250MHz): 7.41 (27H, C*H*-triazole), 6.97 (144H, C*H*-arom. intern), 6.56 (54H, C*H*-arom. extern), 4.62 (54H, triazole-CH_2-0), 4.43 (54H, O-CH_2-arom. extern), 4.13 (126H, CH_2O-arom. extern and Si-CH_2-triazole), 3.64 (1242H, OCH_2CH_2O), 3.37 (81H, CH_3O), 1.59 (54H, CH_2CH$_2$CH$_2$Si), 1.09 (54H, CH$_2$CH_2CH$_2$Si), 0.57 (54H, CH$_2$CH$_2$CH_2Si), 0.06 (216H, Si(CH_3)$_2$) **(see the spectrum page 13)**

^{13}C NMR ($CDCl_3$, 62 MHz): 152.60 (*C*H, extern arom.), 144.48 (C_q of triazole), 137.79 (*C*q, arom. core), 133.75 (*C*q, arom. extern), 126.12 and 113.9 (*C*H-arom. Intern), 123.52 (*C*H of triazole and arom. core), 107.23 (C_qCH$_2$O), 70.66 (OCH_2CH_2O), 69.11 (Si-CH_2-O), 63.53 (triazole-CH_2-O), 58.99 (CH_3O), 53.38 (OCH_2-arom.extern), 43.77 (CH_2CH$_2$CH$_2$Si), 42.7 (SiCH_2-triazole), 40.93 (*C*q-arom.intern), 17.82 (CH$_2$CH_2CH$_2$Si), 14.90 (CH$_2$CH$_2$CH_2Si), -4.84 (Si(CH_3)$_2$) **(see the spectrum page 14)**

DOSY : D = 5.94 (± 0.1) x 10^{-11} m²/s
Rh = 9.7 (± 0.7) nm
(D: diffusion coefficient; Rh : hydrodynamic radius)**(see the DOSY spectrum page 15)**

IR: no alkyne and azide bands **(see the spectrum page 15)**

SEC : **(see the spectrum page 21)**

Light scattering : Rh = 9.1 (± 0.6) nm

*^{1}H NMR spectrum of dendrimer **5***

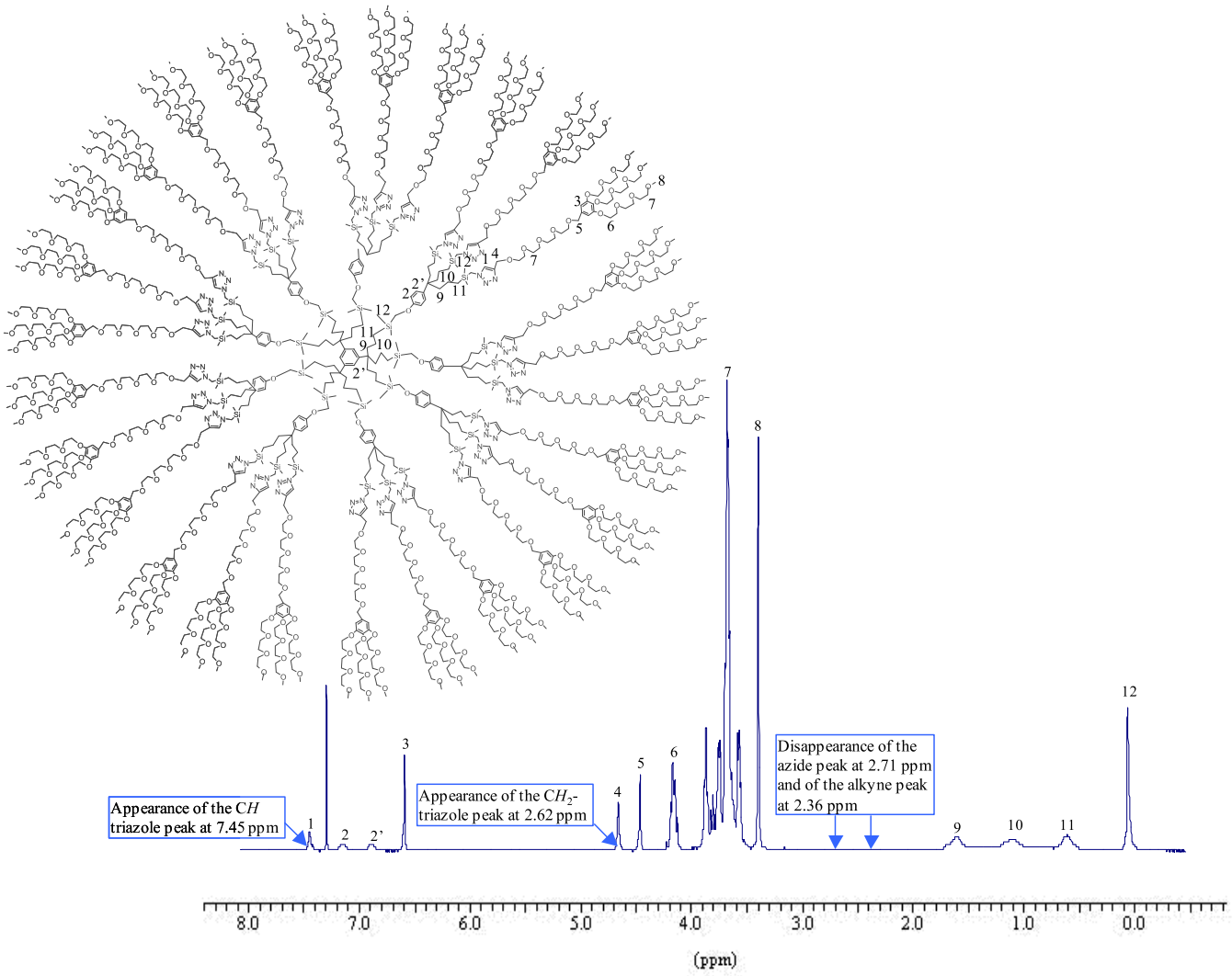

^{1}H NMR ($CDCl_3$, 250MHz): 7.41 (27H, C*H*-triazole), 6.97 (144H, C*H*-arom. intern), 6.56 (54H, C*H*-arom. extern), 4.62 (54H, triazole-CH_2-0), 4.43 (54H, O-CH_2-arom. extern), 4.13 (126H, CH_2O-arom. extern and Si-CH_2-triazole), 3.64 (1242H, OCH_2CH_2O), 3.37 (81H, CH_3O), 1.59 (54H, CH_2CH$_2$CH$_2$Si), 1.09 (54H, CH$_2$CH_2CH$_2$Si), 0.57 (54H, CH$_2$CH$_2$CH_2Si), 0.06 (216H, Si(CH_3)$_2$).

*^{13} C NMR spectrum of dendrimer **5***

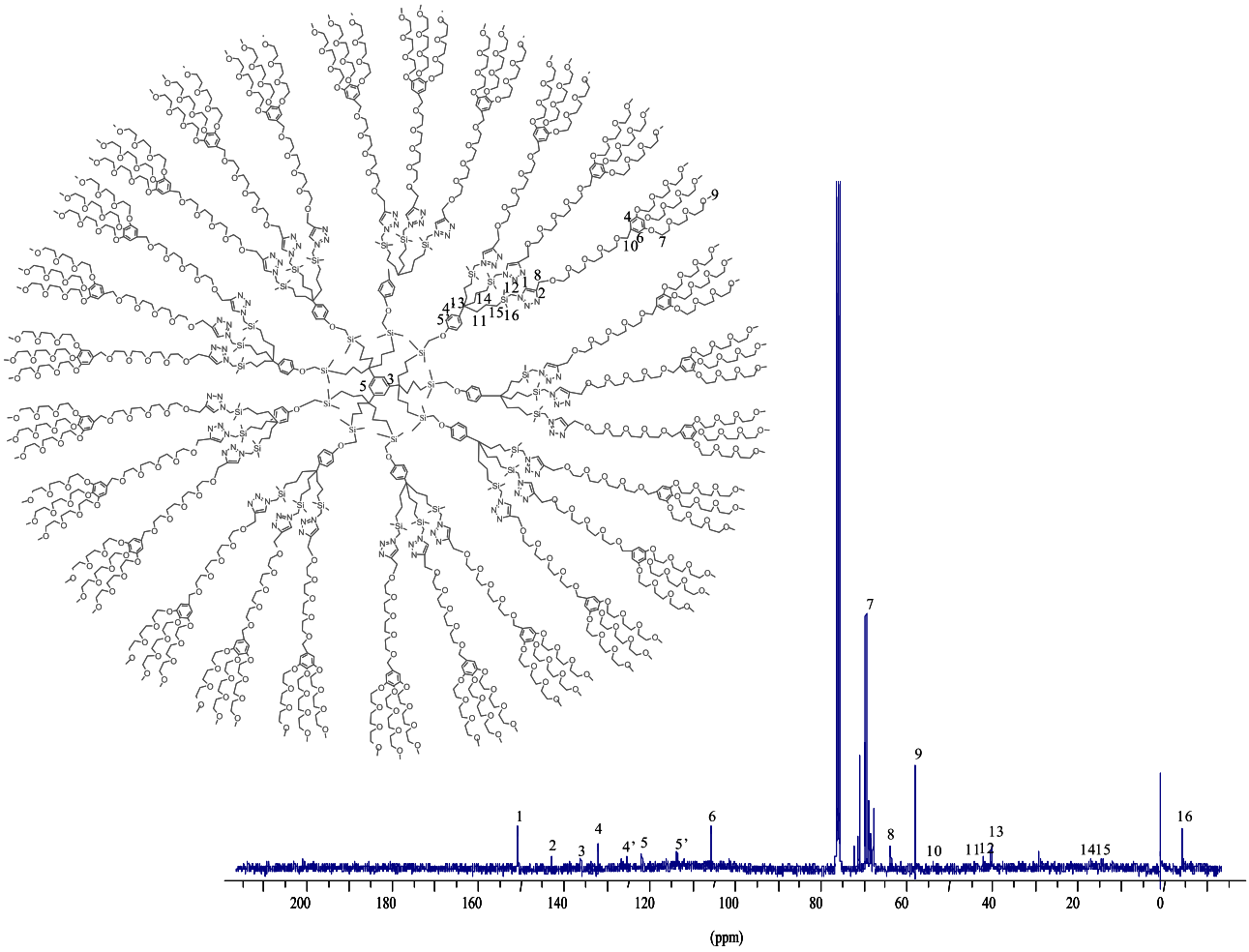

^{13}C NMR ($CDCl_3$, 62 MHz): 152.60 (*C*H, extern arom.), 144.48 (C_q of triazole), 137.79 (*C*q, arom. core), 133.75 (*C*q, arom. extern), 126.12 and 113.9 (*C*H-arom. Intern), 123.52 (*C*H of triazole and arom. core), 107.23 (C_qCH_2O), 70.66 (OCH_2CH_2O), 69.11 (Si-CH_2-O), 63.53 (triazole-CH_2-O), 58.99 (CH_3O), 53.38 (OCH_2-arom.extern), 43.77 ($CH_2CH_2CH_2Si$), 42.7 ($SiCH_2$-triazole), 40.93 (*C*q-arom.intern), 17.82 ($CH_2CH_2CH_2Si$), 14.90 ($CH_2CH_2CH_2Si$), -4.84 ($Si(CH_3)_2$).

DOSY spectrum of dendrimer ***5***

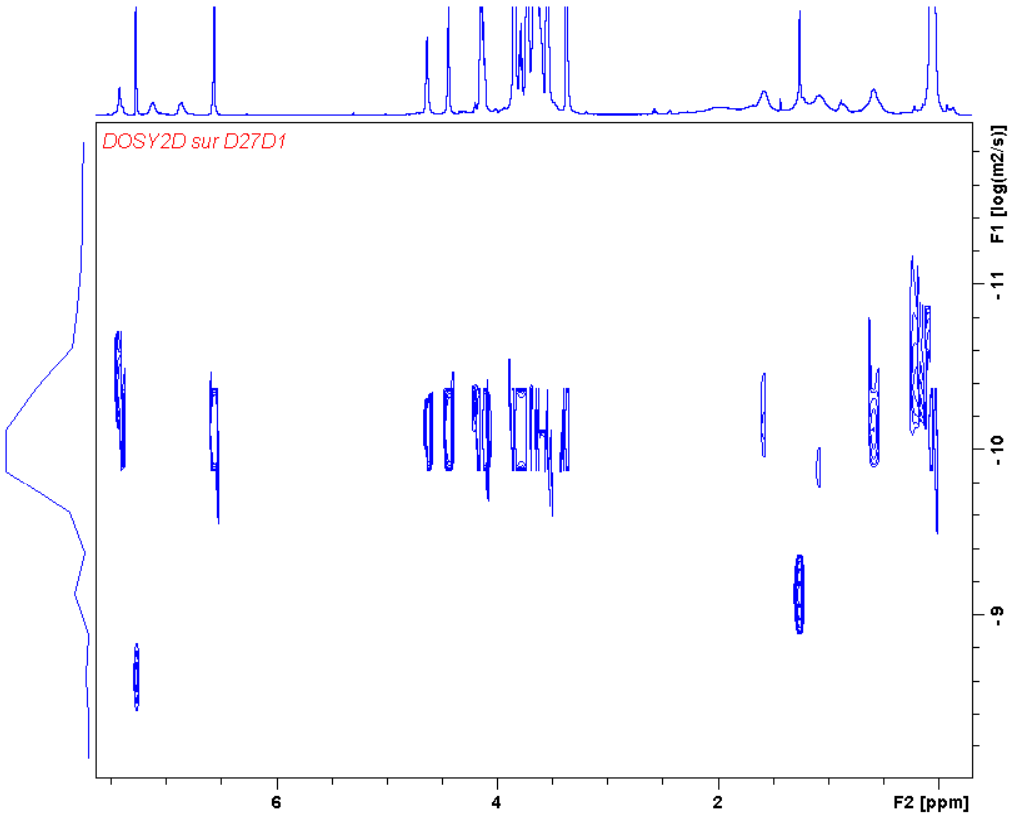

DOSY : D = 5.94 (± 0.1) x 10^{-11} m²/s
Rh = 9.7 (± 0.7) nm
(D: diffusion coefficient; Rh : hydrodynamic radius)

IR spectrum of dendrimer ***5***

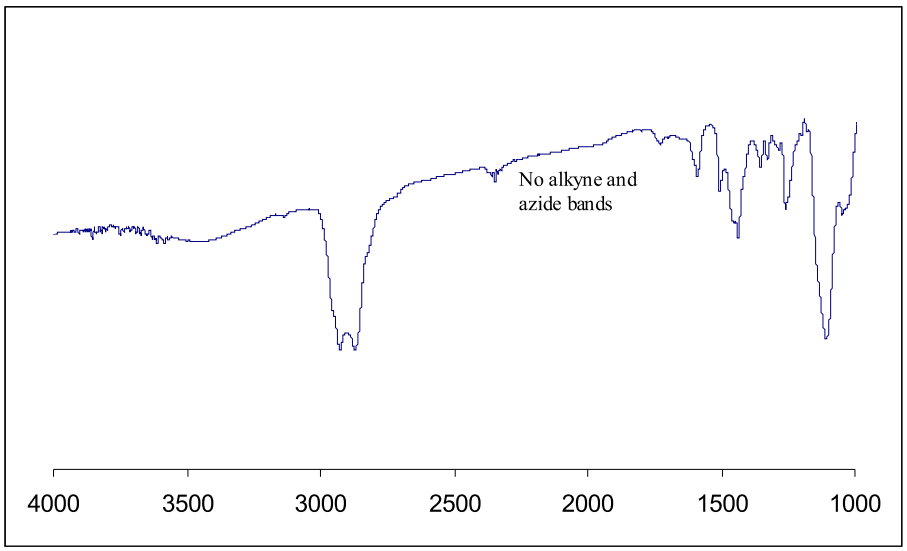

Dendrimer **6**

Mw = 80 319 g.mol^{-1}

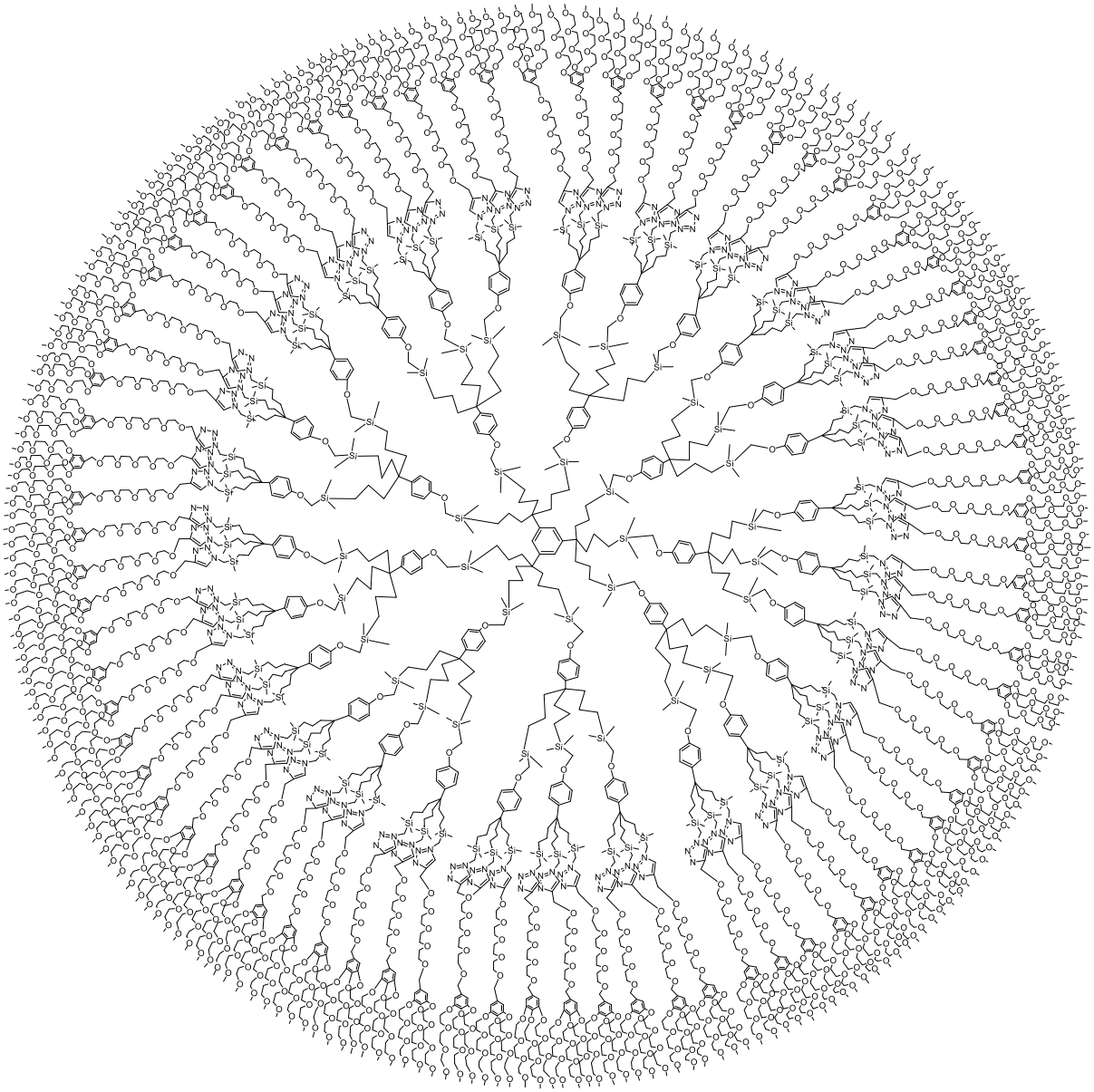

^{1}H NMR ($CDCl_3$, 250MHz): 7.41 (81H, C*H*-triazole), 7.09 (117H, C*H*-arom. intern), 6.56 (234H, C*H*-arom. extern), 4.61 (162H, triazole-CH_2-0), 4.44 (234H, O-CH_2-arom. extern), 4.11 (396H, CH_2O-arom. extern and Si-CH_2-triazole), 3.64 (3726H, OCH_2CH_2O), 3.37 (243H, CH_3O), 1.59 (234H, CH_2CH$_2$CH$_2$Si), 1.09 (234H, CH$_2$CH_2CH$_2$Si), 0.54 (234H, CH$_2$CH$_2$CH_2Si), 0.06 (702H, Si(CH_3)$_2$) **(see the spectrum page 18)**

^{13}C NMR ($CDCl_3$, 62 MHz): 151.60 (*C*H, extern arom.), 144.48 (C_q of triazole), 136.80 (*C*q, arom. core), 132.78 (*C*q, arom. extern), 126.12 and 113.94 (*C*H-arom. intern) 123.52 (*C*H of triazole and arom. core), 106.23 (C_qCH$_2$O), 69.13 (Si-*C*H$_2$-O), 68.73 (OCH$_2$*C*H$_2$O), 63.53 (triazole-*C*H$_2$-O), 57.39 (*C*H$_3$O), 53.38 (O*C*H$_2$-arom.extern), 43.77 (*C*H$_2$CH$_2$CH$_2$Si), 42.7 (SiCH_2-triazole), 40.93 (*C*q-arom.intern), 17.82 (CH$_2$*C*H$_2$CH$_2$Si), 14.90 (CH$_2$CH$_2$*C*H$_2$Si), -4.84 (Si(*C*H$_3$)$_2$) **(see the spectrum page 19)**

IR: no alkyne and azide bands **(see the spectrum page 20)**

SEC : **(see the spectrum page 21)**

Light scattering : Rh = 10 (±1) nm

^{1}H NMR spectrum of dendrimer ***6***

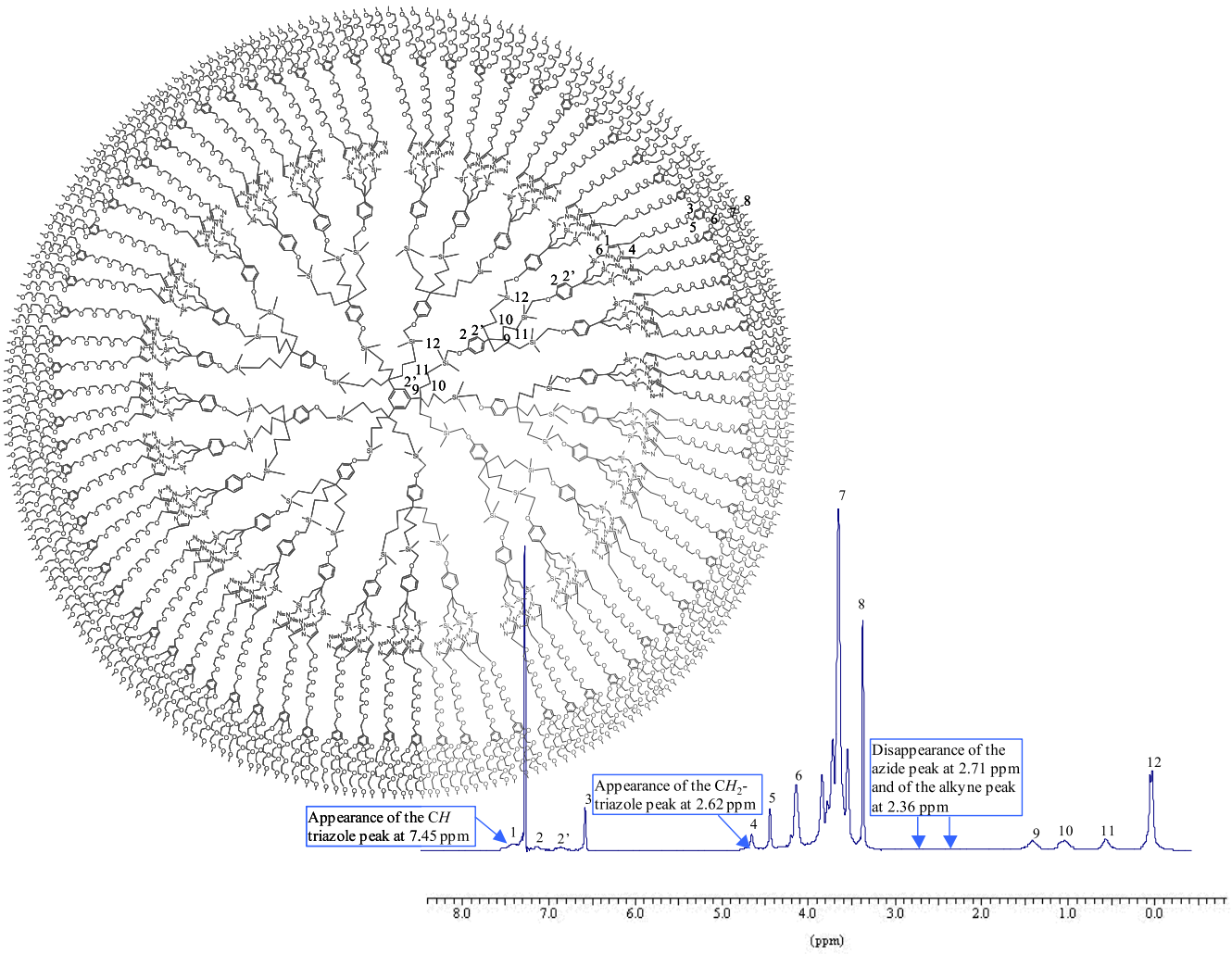

^{1}H NMR ($CDCl_3$, 250MHz): 7.41 (81H, C*H*-triazole), 7.09 (117H, C*H*-arom. intern), 6.56 (234H, C*H*-arom. extern), 4.61 (162H, triazole-CH_2-0), 4.44 (234H, O-CH_2-arom. extern), 4.11 (396H, CH_2O-arom. extern and Si-CH_2-triazole), 3.64 (3726H, OCH_2CH_2O), 3.37 (243H, CH_3O), 1.59 (234H, CH_2CH$_2$CH$_2$Si), 1.09 (234H, CH$_2$CH_2CH$_2$Si), 0.54 (234H, CH$_2$CH$_2$CH_2Si), 0.06 (702H, Si(CH_3)$_2$).

*^{13}C NMR spectrum of dendrimer **6***

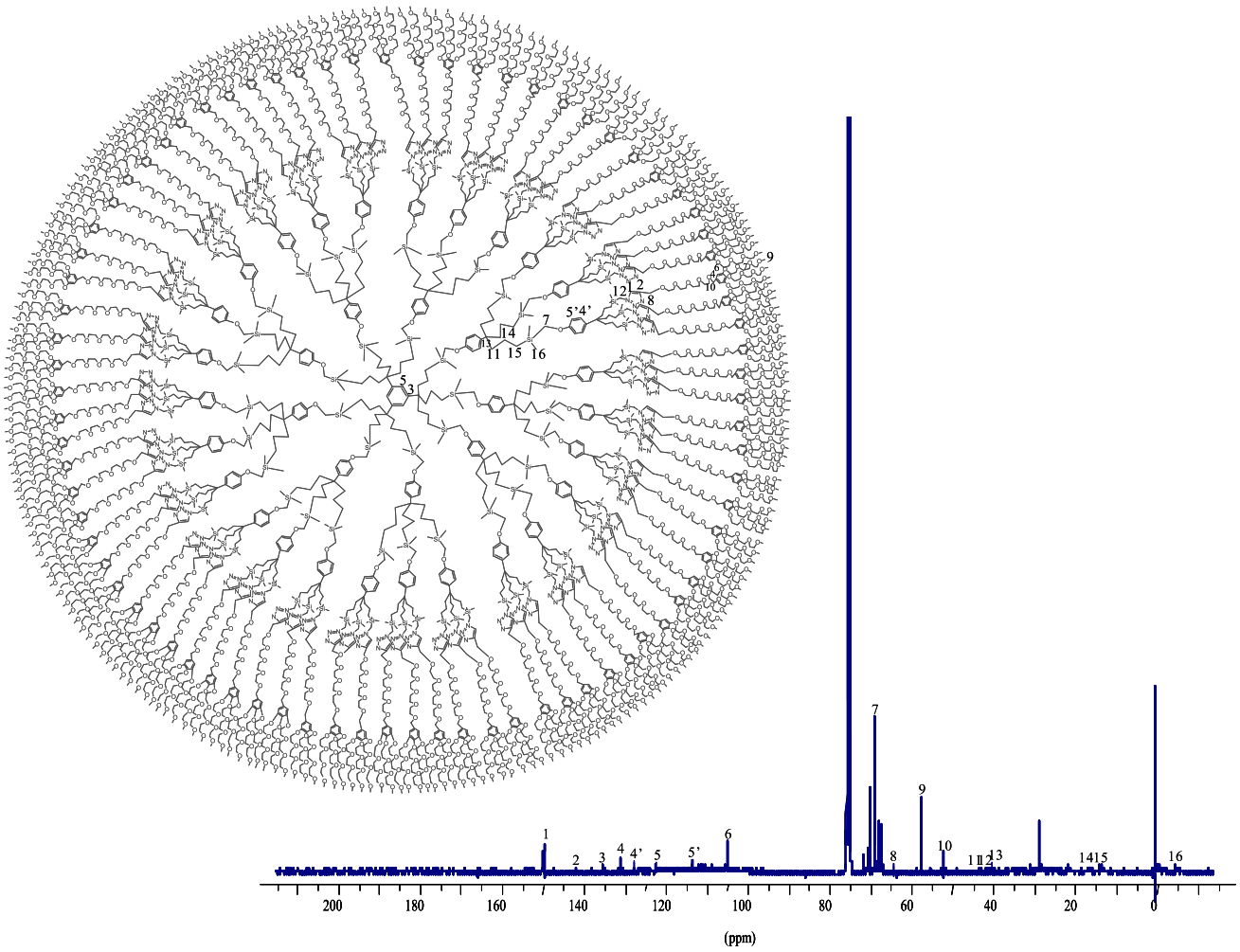

^{13}C NMR ($CDCl_3$, 62 MHz): 151.60 (*C*H, extern arom.), 144.48 (C_q of triazole), 136.80 (*C*q, arom. core), 132.78 (*C*q, arom. extern), 126.12 and 113.94 (*C*H-arom. intern) 123.52 (*C*H of triazole and arom. core), 106.23 (C_qCH_2O), 69.13 (Si-*C*H_2-O), 68.73 (O*C*H_2*C*H_2O), 63.53 (triazole-*C*H_2-O), 57.39 (*C*H_3O), 53.38 (O*C*H_2-arom.extern), 43.77 (*C*H_2CH_2CH_2Si), 42.7 (SiC*H*$_2$-triazole), 40.93 (*C*q-arom.intern), 17.82 (CH$_2$*C*H$_2$CH$_2$Si), 14.90 (CH$_2$CH$_2$*C*H$_2$Si), -4.84 (Si(*C*H$_3$)$_2$).

IR spectrum of dendrimer ***6***

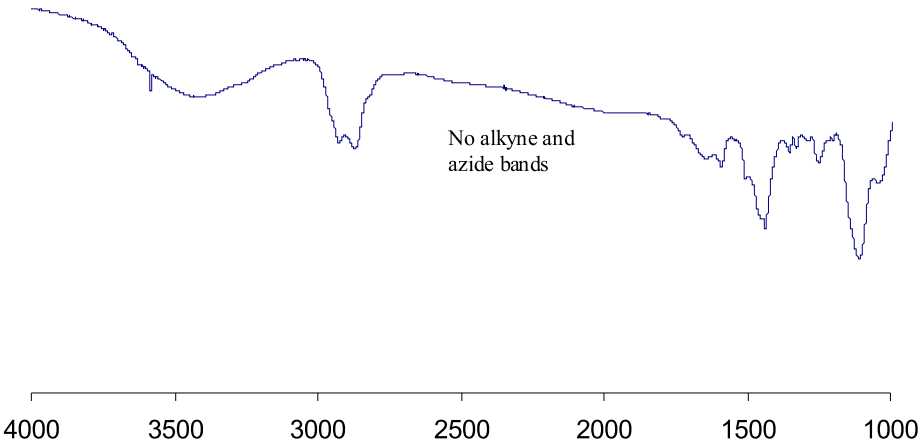

*Size Exclusion Chromatography (SEC) of the three generations of "click" dendrimers containing polyethyleneglycol tethers **4**, **5** and **6***

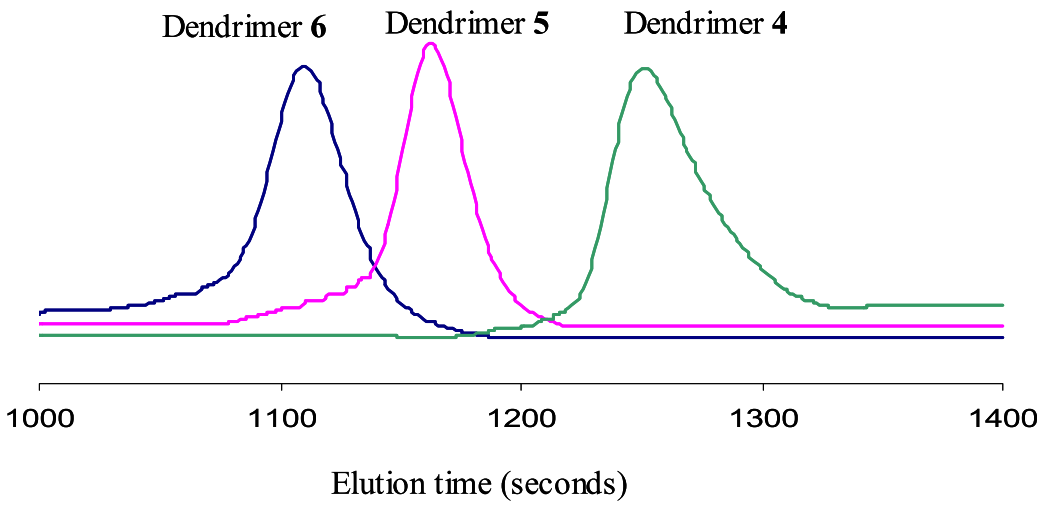

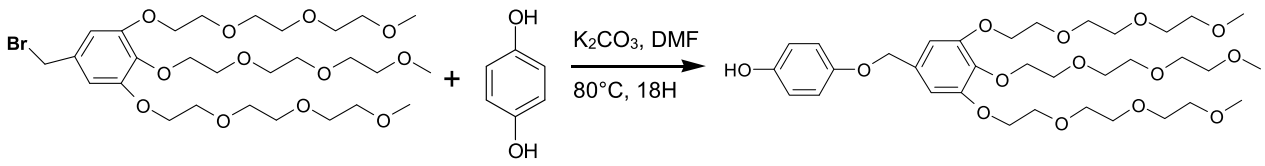

Mw : 686 $g.mol^{-1}$

The tris-triethylene glycol dendron (300 mg, 0.46 mmol) and the hydroquinone (251 mg, 2.28 mmol) were introduced in a Schlenck, and dry DMF (30 mL) was added. K_2CO_3 (315 mg, 2.28 mmol) was added to the solution. The mixture was stirred for 18 hours at 80°C under reflux. At the end of the reaction, DMF was removed. The product was extracted with CH_2Cl_2, washed with water, and purified by chromatography (CH2Cl2:MeOH, (97:3)). 205 mg of a yellow oil was obtained (65% yield).

^{1}H RMN ($CDCl_3$, 250MHz) : 3,35 (C*H*$_3$O); 3,63 (C*H*$_2$O); 4,11 (C*H*$_2$Oarom.); 4,83 (OC*H*$_2$arom.); 6,59 (C*H* arom.); 6,87 (C*H* arom.-OH) **(see the spectrum page 23)**.

^{13}C NMR ($CDCl_3$, 62 MHz): 152.82 (*C*q-O-CH_2), 152.19 ((Cq-OH),150.56 (*C*q extern.-CH_2-O), 137.87 (*C*q middle-CH_2-O), 132.83 (*C*H_2-Cq), 116.17 (*C*H arom.-Cq-O), 107.19 (*C*H arom.-Cq-CH_2), 71.93 (0-CH_2-arom), 70.71 (O-*C*H_2), 59.06 (O-*C*H_3) **(see the spectrum page 24)**.

Maldi TOF : Calc. For $C_{34}H_{54}O_{14}$: 686.35; found: 709.34 (MNa^+)**(see the spectrum page 25)**.

Elemental Analysis: Anal. Calc. for $C_{54}H_{54}O_{14}$: C 59.46, H 7.92, found: C 59.21, H 8.18.

*^{1}H NMR spectrum of the dHQ dendron **8***

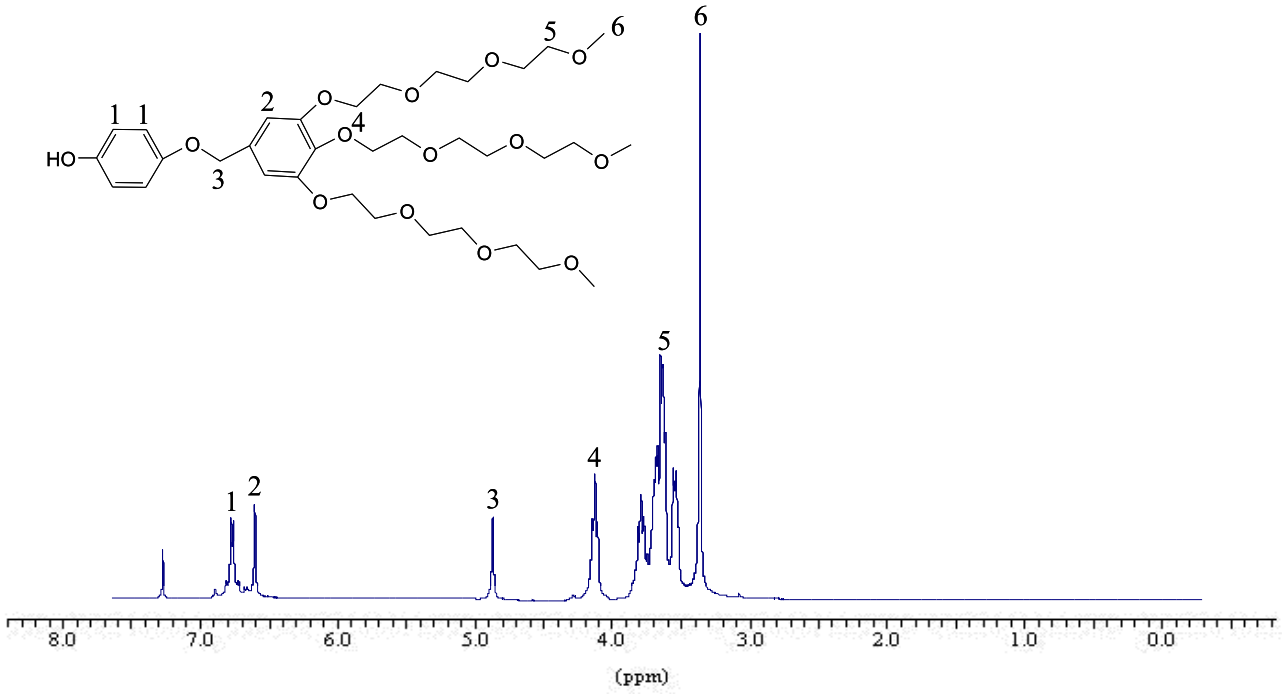

^{1}H RMN spectrum of the dHQ dendron ($CDCl_3$, 250MHz) : 3,35 (CH_3O); 3,63 (CH_2O); 4,11 (CH_2Oarom.); 4,83 (OCH_2arom.); 6,59 (*CH* arom.); 6,87 (*CH* arom.-OH).

^{13}C NMR spectrum of the dHQ dendron ***8***

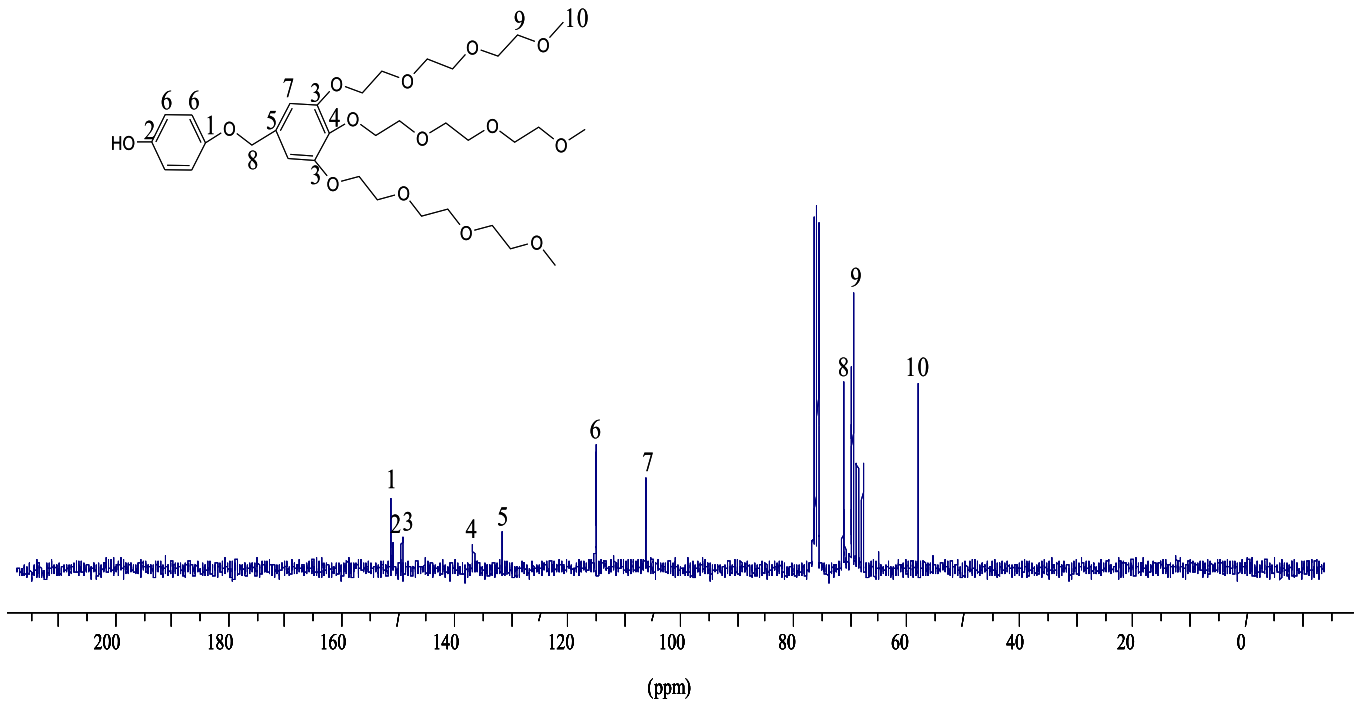

^{13}C NMR spectrum of the dHQ dendron ($CDCl_3$, 62 MHz): 152.82 (*C*q-O-CH_2), 152.19 ((Cq-OH),150.56 (*C*q extern.-CH_2-O), 137.87 (*C*q middle-CH_2-O), 132.83 (*C*H_2-Cq), 116.17 (*C*H arom.-Cq-O), 107.19 (*C*H arom.-Cq-CH_2), 71.93 (O-CH_2-arom), 70.71 (O-*C*H_2), 59.06 (O-*C*H_3).

Masse spectrum of the dHQ dendron ***8***

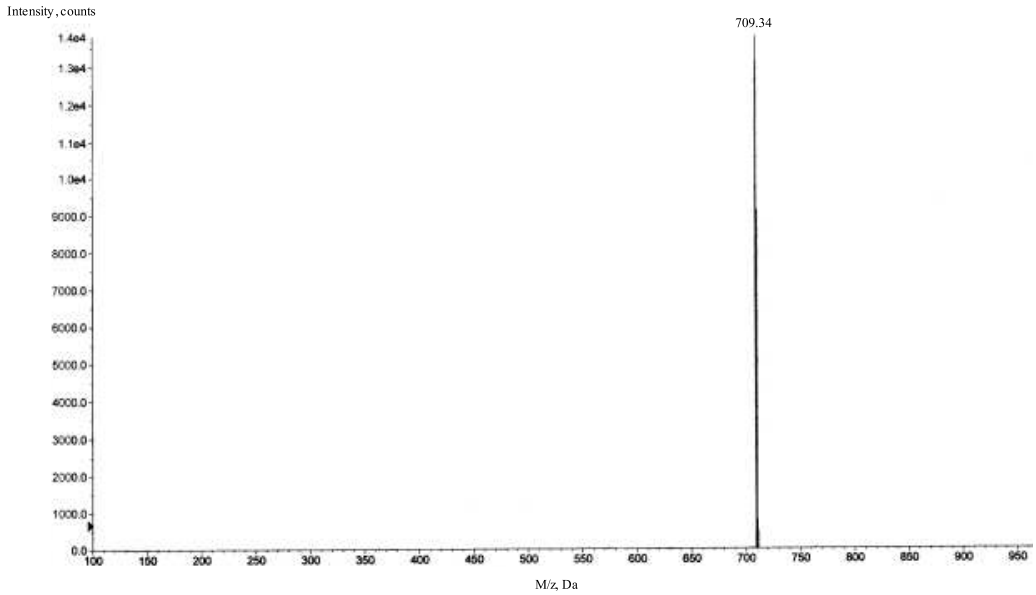

Maldi TOF : Calc. For $C_{34}H_{54}O_{14}$: 686.35; found: 709.34 (MNa^+).

Dendrimer **9**
Mw = 7 312 g.mol^{-1}

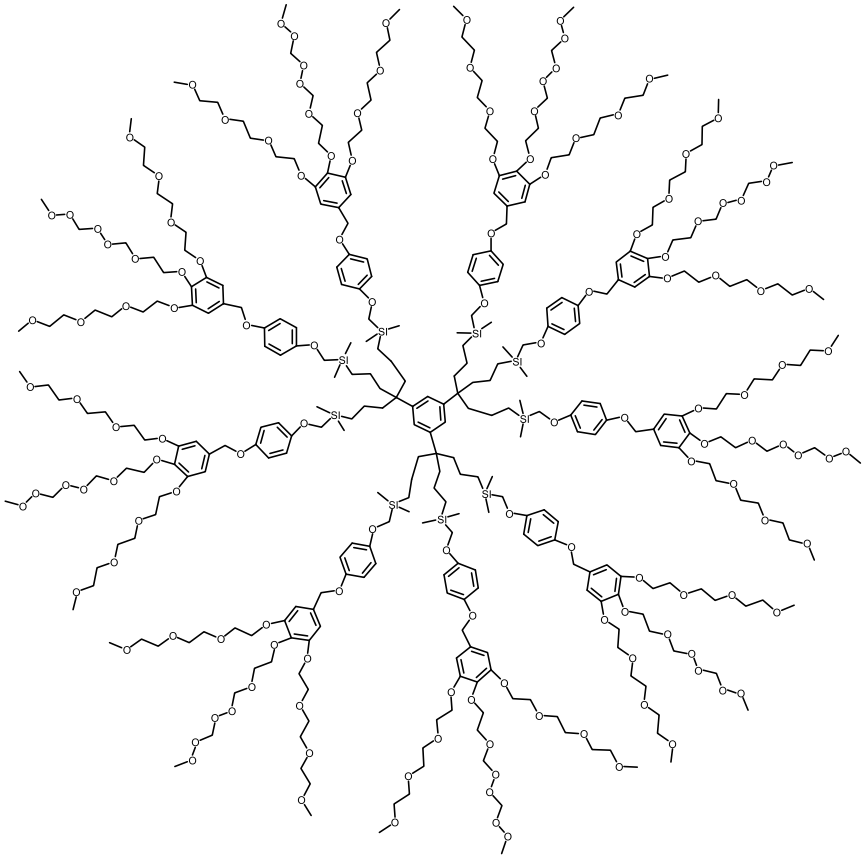

^{1}H NMR ($CDCl_3$, 250MHz):6.92 (C*H*-arom.core), 6.87 (C*H*-arom. intern), 6.65 (C*H*-arom. extern), 4.85 (0- CH_2-arom. extern), 4.16 (CH_2O-arom. extern), 3.65 (OCH_2CH_2O and Si-CH_2O), 3.38 (CH_3O), 1.69 (CH_2CH_2CH_2Si), 1.12 (CH_2CH_2CH_2Si), 0.62 (CH_2CH_2CH_2Si), 0.06 (Si(CH_3)$_2$) **(see the spectrum page 28)**.

^{13}C NMR ($CDCl_3$, 62 MHz): 156.09 (O-*C*q intern), 152.61 (*C*q intern), 144.71 (*C*q arom. Core), 137.97 (*C*q-Cq intern), 130.95 (*C*H arom. extern), 118.55 (*C*H arom. Core), 115.61 (*C*H-arom intern), 114.79 (*C*H arom extern), 107.07 (*C*H arom intern), 72.3 (O*C*H_2CH_2), 70.80 (O*C*H_2 arom extern), 68.85 (Si*C*H_2O), 59.05 (*C*H_3O), 43.77 (*C*H_2CH_2CH_2Si), 17.82 (CH_2*C*H_2CH_2Si), 14.49 (CH_2CH_2*C*H_2Si), -4.58 (Si(*C*H_3)$_2$) **(see the spectrum page 29)**.

Maldi TOF : Calc. For $C_{369}H_{606}O_{126}Si_9$: 7311.54; found: 7334.47 (MNa^+) **(see the spectrum page 30)**.

DOSY : D = 1.47 (± 0.1) x 10^{-10} m²/s
Rh = 3.9 (± 0.3) nm
(D: diffusion coefficient; Rh : hydrodynamic radius) **(see the spectrum page 31)**.

SEC : retention time = 1221 seconds (Polydispersity = 1.05) **(see the spectrum page 42)**

Elemental Analysis: Anal. Calc. for $C_{369}H_{606}O_{126}Si_9$: C 60.62, H 8.35, found: C 59.64, H 8.57.

*^{1}H NMR spectrum of dendrimer **9***

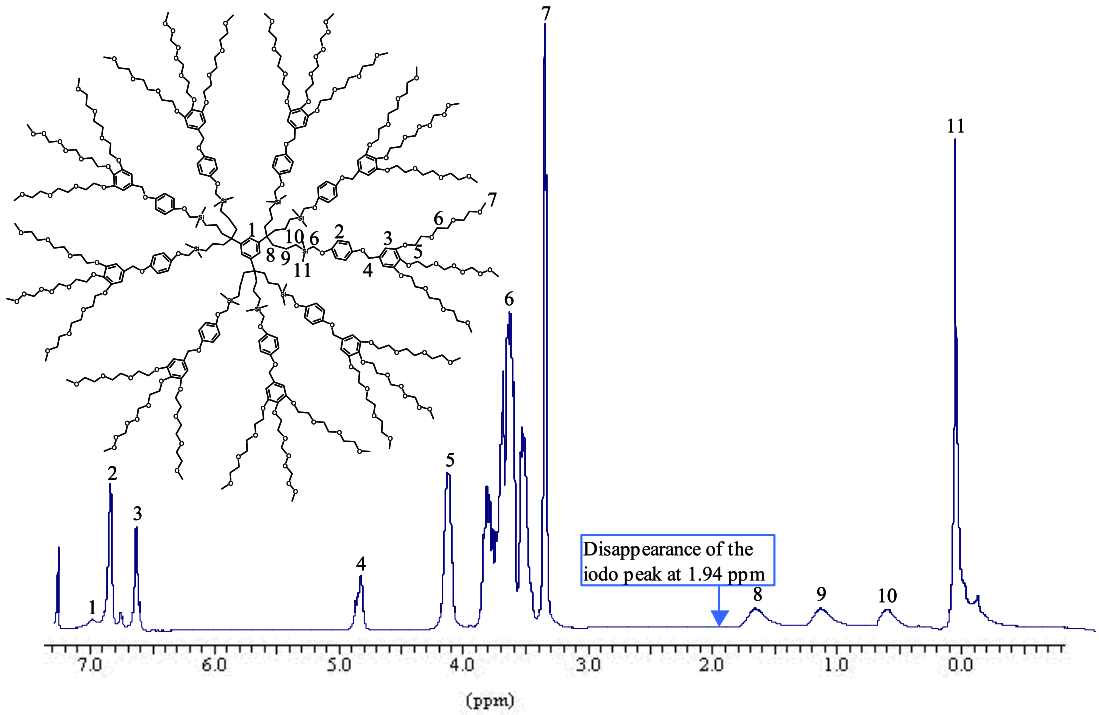

^{1}H NMR spectrum of G_0dHQ ($CDCl_3$, 250MHz):6.92 (C*H*-arom.core), 6.87 (C*H*-arom. intern), 6.65 (C*H*-arom. extern), 4.85 (0- CH_2-arom. extern), 4.16 (CH_2O-arom. extern), 3.65 (OCH_2CH_2O and Si-CH_2O), 3.38 (CH_3O), 1.69 (CH_2CH$_2$CH$_2$Si), 1.12 (CH$_2$CH_2CH$_2$Si), 0.62 (CH$_2$CH$_2$CH_2Si), 0.06 (Si(CH_3)$_2$).

*^{13}C NMR spectrum of dendrimer **9***

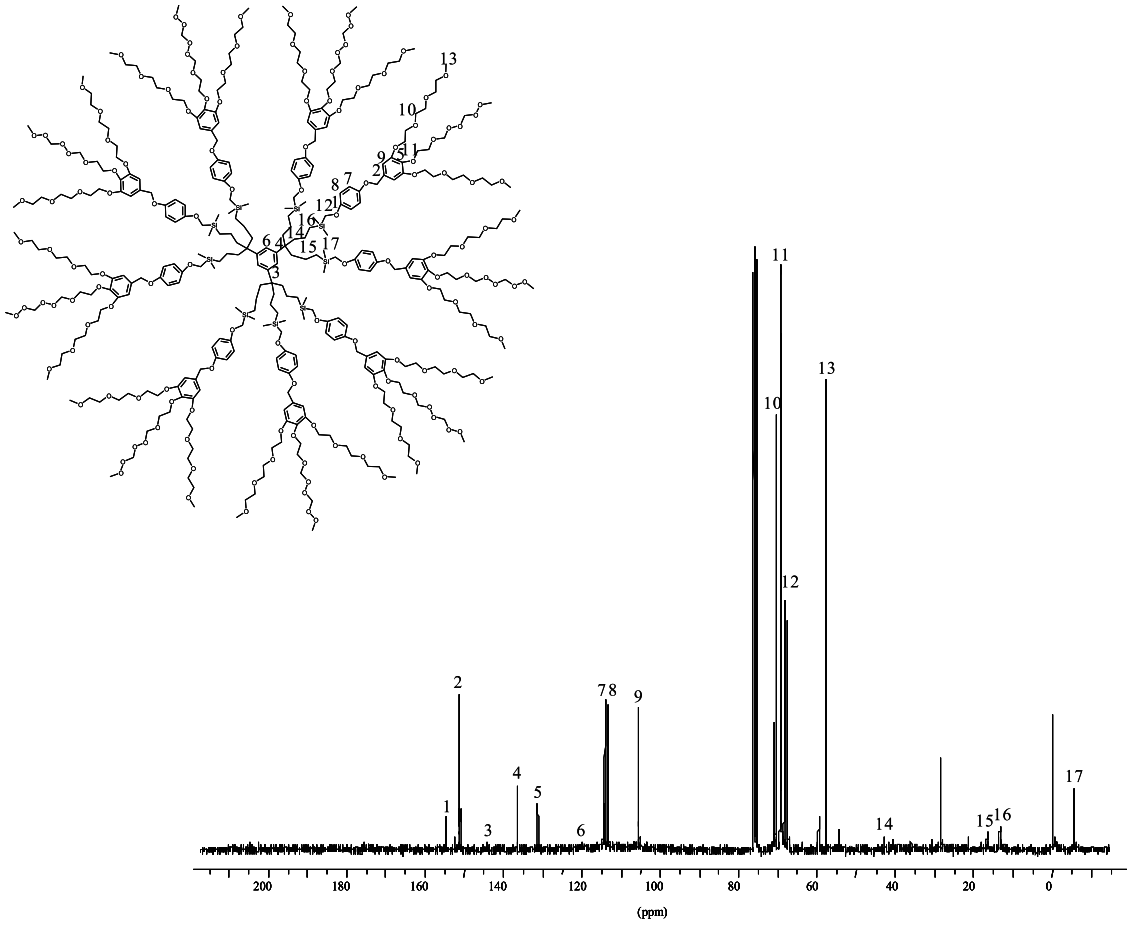

^{13}C NMR spectrum of G_0dHQ($CDCl_3$, 62 MHz): 156.09 (O-*C*q intern), 152.61 (*C*q intern), 144.71 (*C*q arom. Core), 137.97 (*C*q-Cq intern), 130.95 (*C*H arom. extern), 118.55 (*C*H arom. Core), 115.61 (*C*H-arom intern), 114.79 (*C*H arom extern), 107.07 (*C*H arom intern), 72.3 (OCH_2CH_2), 70.80 (OCH_2 arom extern), 68.85 ($SiCH_2O$), 59.05 (CH_3O), 43.77 ($CH_2CH_2CH_2Si$), 17.82 ($CH_2CH_2CH_2Si$), 14.49 ($CH_2CH_2CH_2Si$), -4.58 ($Si(CH_3)_2$).

Masse spectrum of dendrimer ***9***

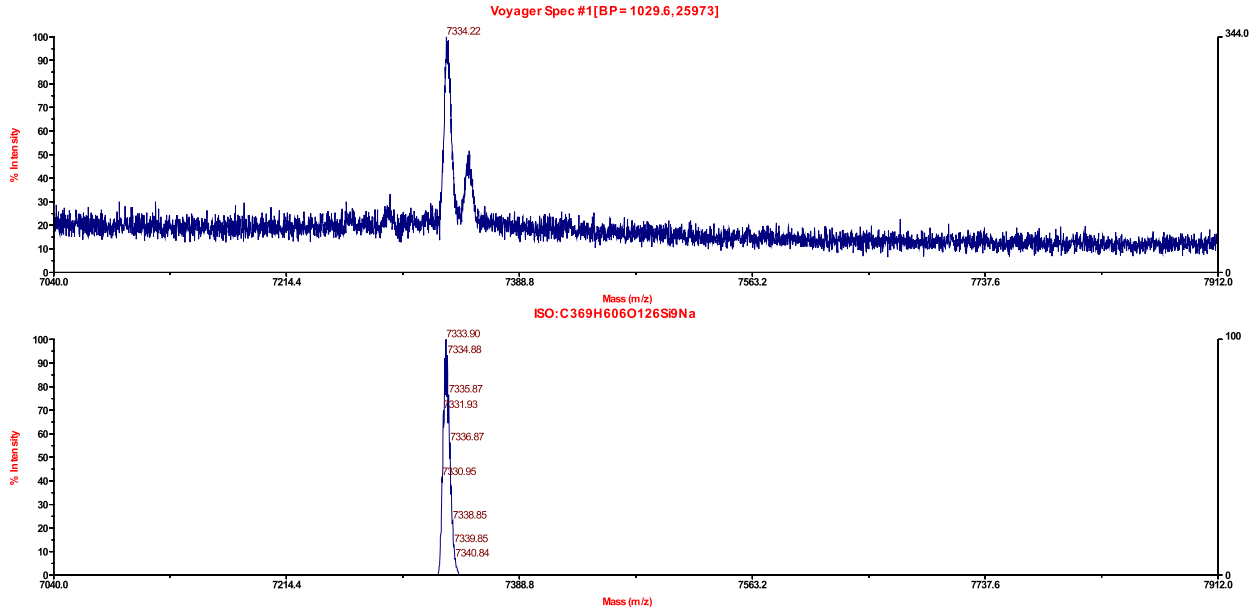

Maldi TOF : Calc. For $C_{369}H_{606}O_{126}Si_9$: 7311.54; found: 7334.47 (MNa^+).

DOSY spectrum of dendrimer ***9***

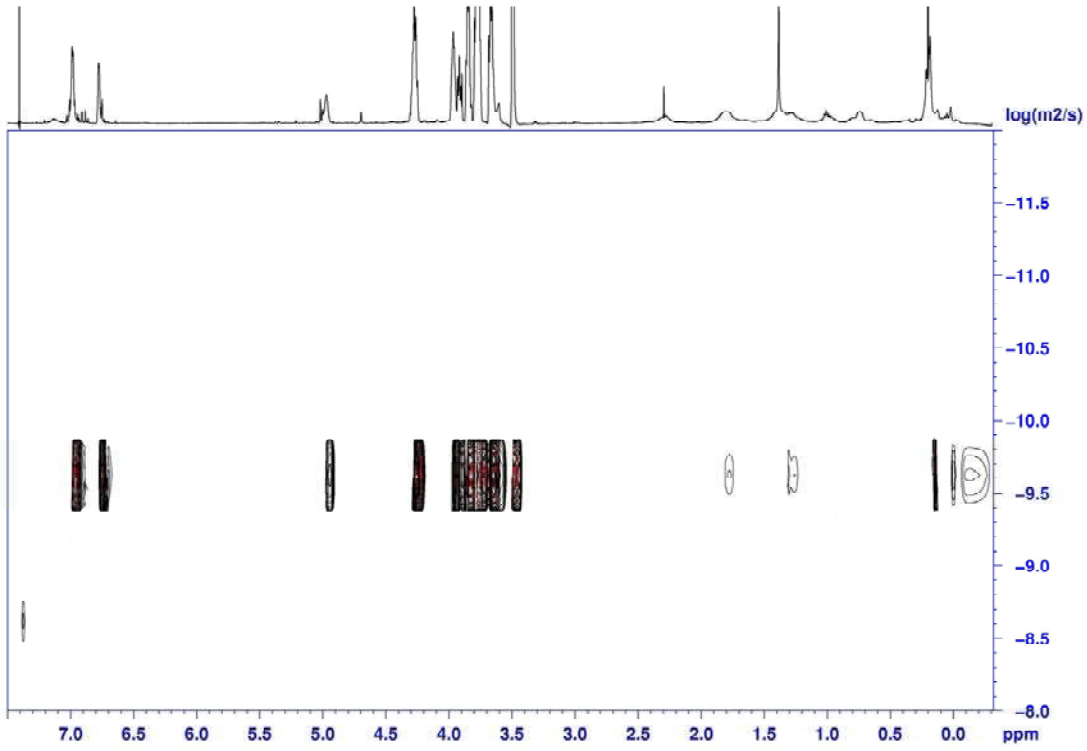

DOSY : $D = 1.73 (\pm 0.1) \times 10^{-10}$ m²/s

Rh = 3.9 (± 0.3) nm

(D: diffusion coefficient; Rh : hydrodynamic radius)

Dendrimer **10**
Mw : 23 656 g.mol^{-1}

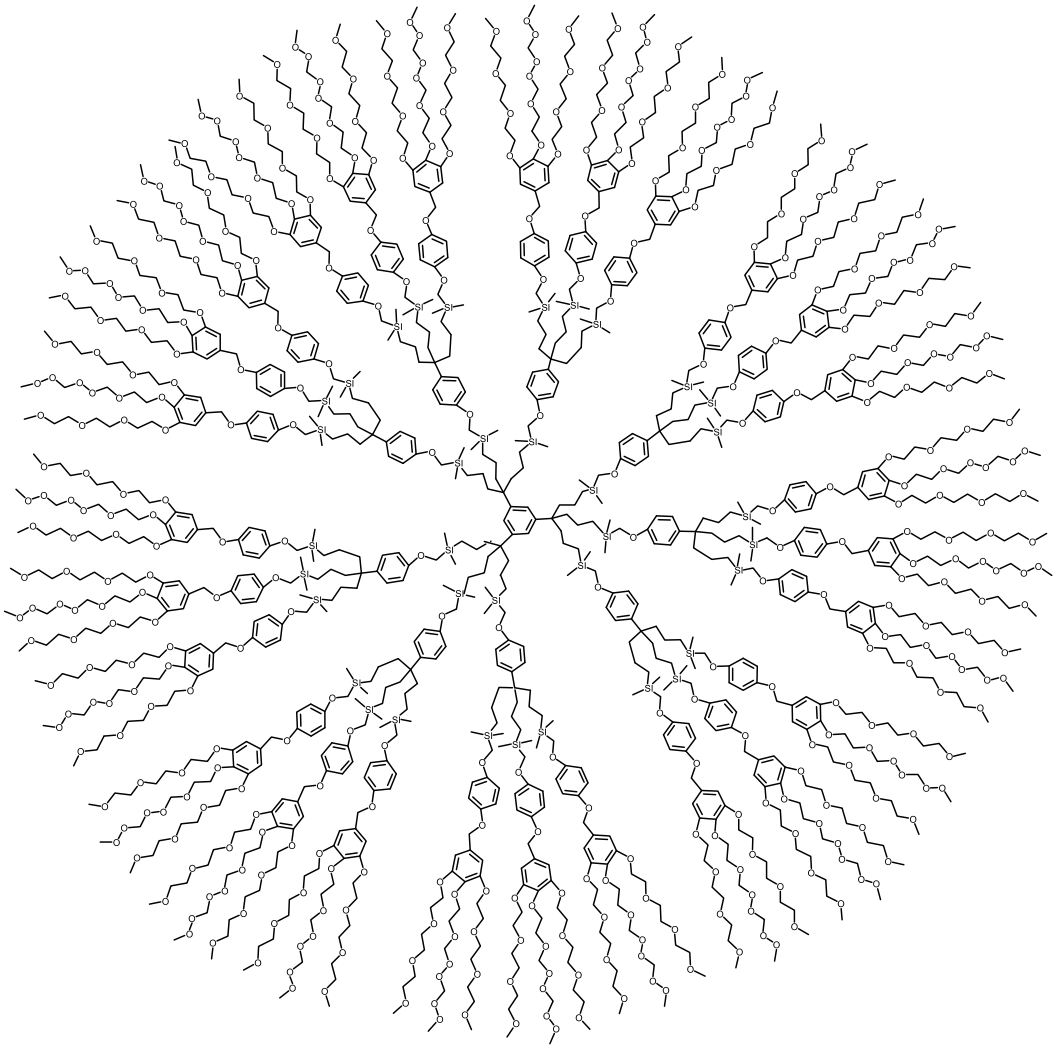

^{1}H NMR spectrum of G_1dHQ ($CDCl_3$, 250MHz): 7.14 (C*H* arom. core), 6.83 (C*H*-arom. intern), 6.63 (C*H*-arom. extern), 4.83 (0- CH_2-arom. extern), 4.13 (CH_2O-arom. extern), 3.63 (OCH_2CH_2O and Si-C$H_2$0), 3.34 (CH_3O), 1.619 (CH_2CH$_2$CH$_2$Si), 1.13 (CH$_2$CH_2CH$_2$Si), 0.57 (CH$_2$CH$_2$CH_2Si), 0.06 (Si(CH_3)$_2$) **(see the spectrum page 34)**.

^{13}C NMR ($CDCl_3$, 62 MHz): 156.09 (O-*C*q intern), 152.61 (*C*q intern), 145.71 (*C*q arom. Core), 137.97 (*C*q-Cq intern), 130.95 (*Cq* arom. extern), 118.87 (*C*H arom. Core), 115.61 (*C*H-arom intern), 114.79 (*C*H arom extern), 107.07 (*C*H arom intern), 72.3 (O*C*H$_2$CH$_2$), 70.80 (O*C*H$_2$ arom extern), 68.85 (Si*C*H$_2$O), 59.05 (*C*H$_3$O), 42.92 (*C*H$_2$CH$_2$CH$_2$Si), 17.82 (CH$_2$*C*H$_2$CH$_2$Si), 14.49 (CH$_2$CH$_2$*C*H$_2$Si), -4.58 (Si(*C*H$_3$)$_2$) **(see the spectrum page 35)**.

DOSY : D = 9.08 (± 0.9) x 10^{-11} m²/s
Rh = 6.3 (± 0.6) nm
(D: diffusion coefficient; Rh : hydrodynamic radius)**(see the spectrum page 36**).

Light scattering : Rh = 6.4 (± 0.6) nm

SEC : retention time = 1121 seconds (Polydispersity = 1.02) **(see the spectrum page 42)**

*^{1}H NMR spectrum of dendrimer **10***

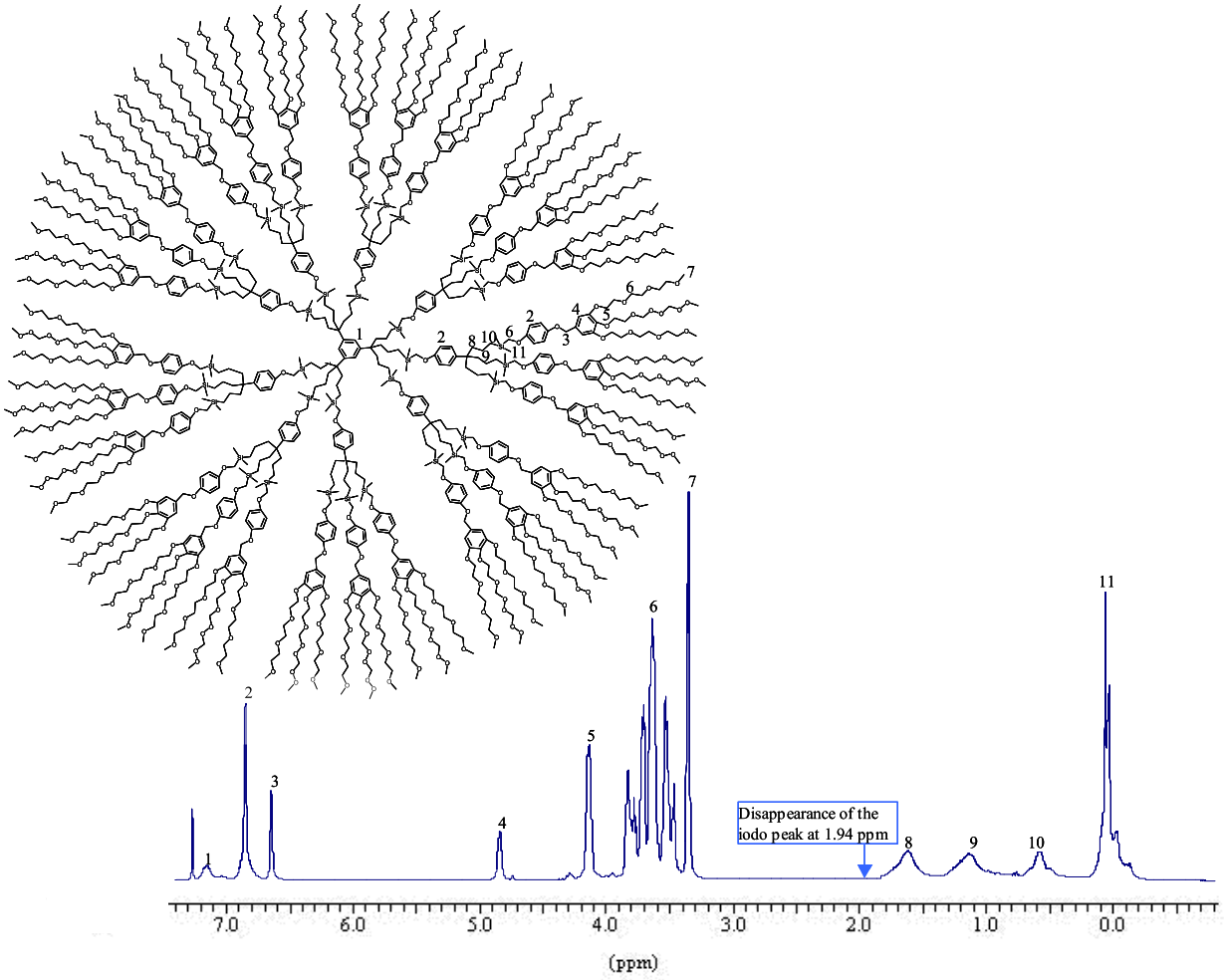

^{1}H NMR spectrum of G_1dHQ ($CDCl_3$, 250MHz): 7.14 (C*H* arom. core), 6.83 (C*H*-arom. intern), 6.63 (C*H*-arom. extern), 4.83 (0- CH_2-arom. extern), 4.13 (CH_2O-arom. extern), 3.63 (OCH_2CH_2O and Si-CH_2O), 3.34 (CH_3O), 1.619 (CH_2CH_2CH_2Si), 1.13 (CH_2CH_2CH_2Si), 0.57 (CH_2CH_2CH_2Si), 0.06 (Si(CH_3)$_2$).

*^{13}C NMR spectrum of dendrimer **10***

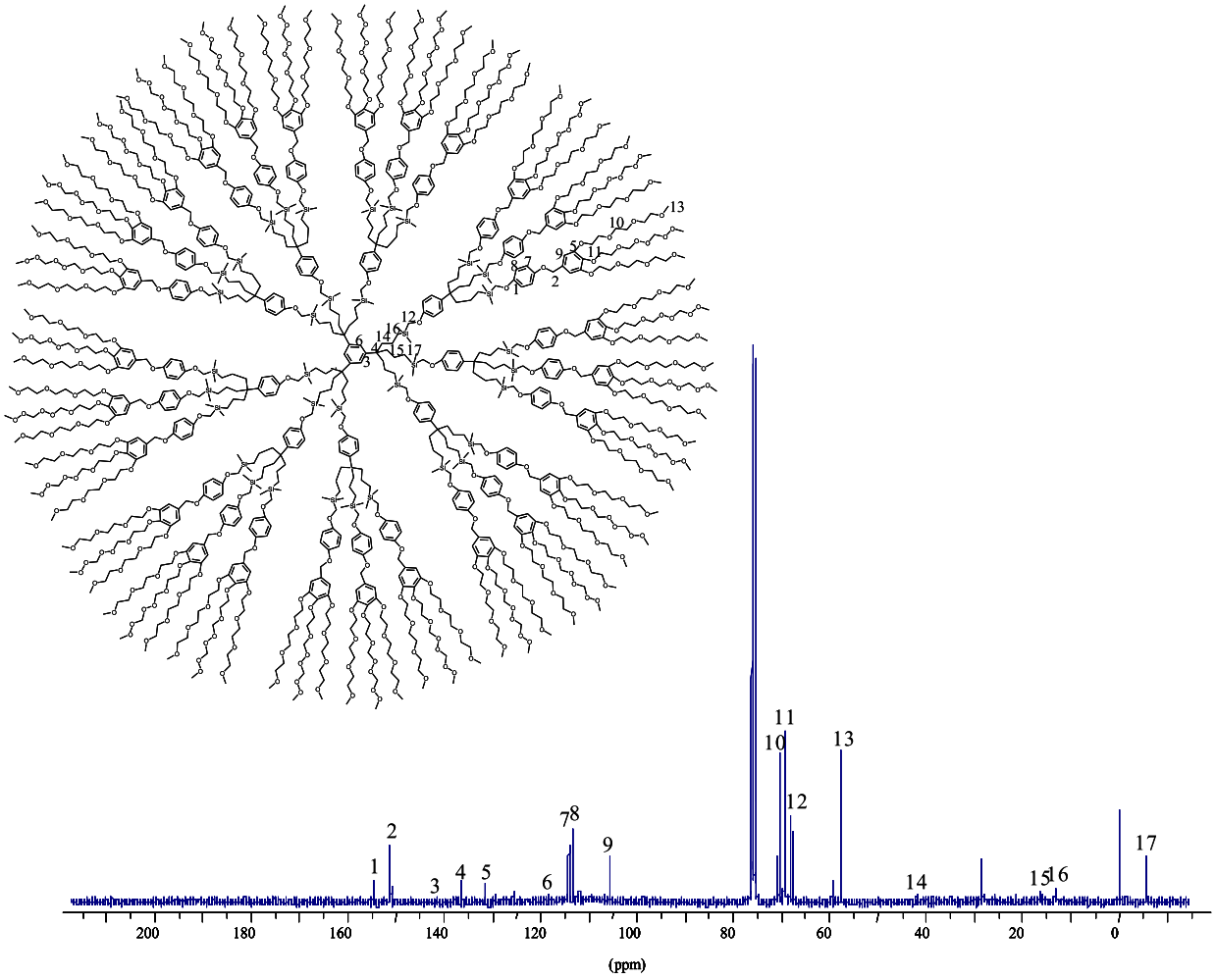

^{13}C NMR spectrum of G_1dHQ ($CDCl_3$, 62 MHz):156.09 (O-*C*q intern), 152.61 (*C*q intern), 145.71 (*C*q arom. Core), 137.97 (*C*q-Cq intern), 130.95 (*C*q arom. extern), 118.87 (*C*H arom. Core), 115.61 (*C*H-arom intern), 114.79 (*C*H arom extern), 107.07 (*C*H arom intern), 72.3 (OCH_2CH_2), 70.80 (OCH_2 arom extern), 68.85 ($SiCH_2O$), 59.05 (CH_3O), 42.92 ($CH_2CH_2CH_2Si$), 17.82 ($CH_2CH_2CH_2Si$), 14.49 ($CH_2CH_2CH_2Si$), -4.58 ($Si(CH_3)_2$).

DOSY spectrum of dendrimer ***10***

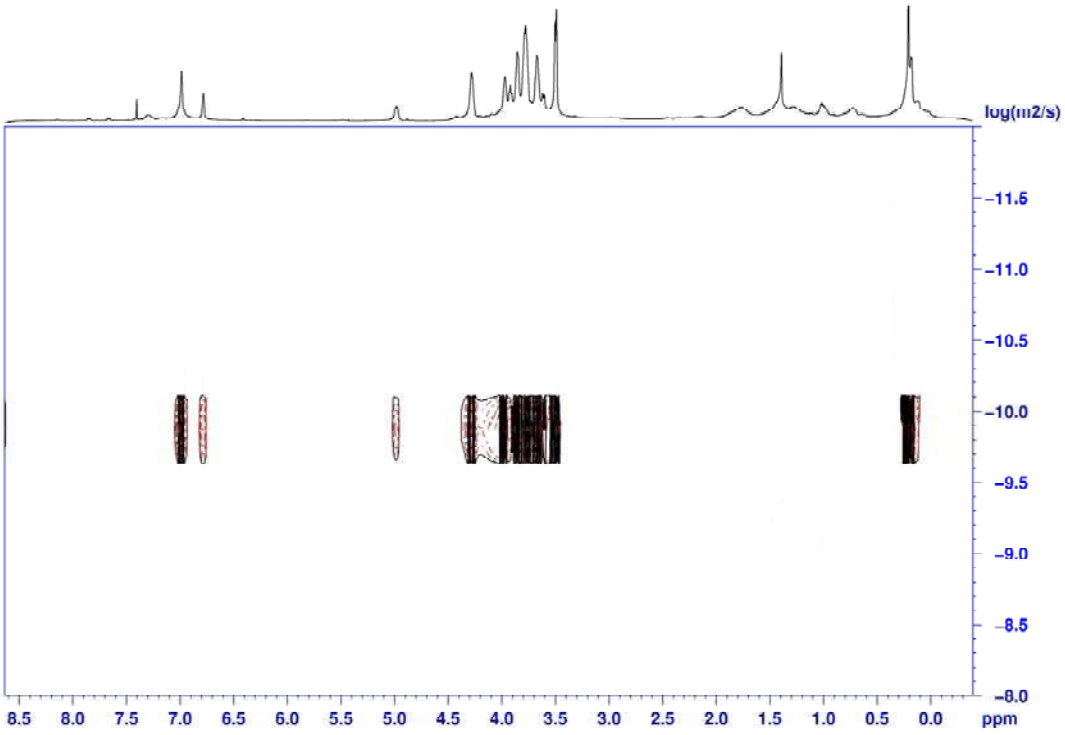

DOSY : $D = 9.08 (\pm 0.9) \times 10^{-11}$ m²/s
Rh = 6.3 (± 0.6) nm
(D: diffusion coefficient; Rh : hydrodynamic radius) .

Dendrimer **11**
Mw = 72 540 g.mol^{-1}

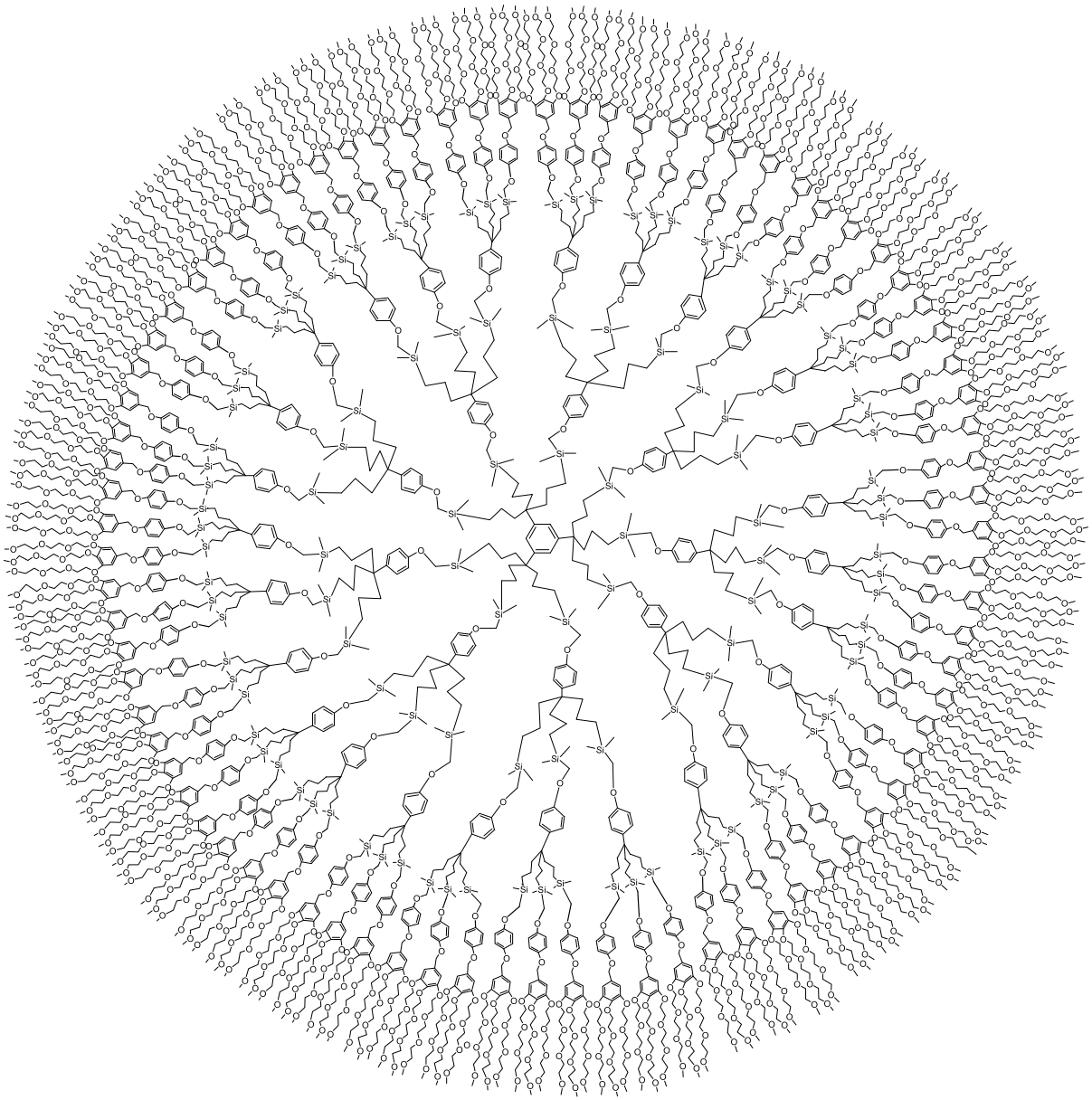

^{1}H NMR ($CDCl_3$, 250MHz): ^{1}H NMR spectrum of G_2dHQ ($CDCl_3$, 250MHz): 7.13 et 6.82 (C*H*-arom. intern), 6.61 (C*H*-arom. extern), 4.85 (0- CH_2-arom. extern), 4.11 (CH_2O-arom. extern), 3.62 (OCH_2CH_2O and Si-CH_2O), 3.35 (CH_3O), 1.59 (CH_2CH$_2$CH$_2$Si), 1.11 (CH$_2$CH_2CH$_2$Si), 0.56 (CH$_2$CH$_2$CH_2Si), 0.05 (Si(CH_3)$_2$) **(see the spectrum page 39)**.

^{13}C NMR ($CDCl_3$, 62 MHz): 156.08 (O-*C*q intern), 152.56 (*C*q intern), 145.69 (*C*q arom. Core), 137.62 (*C*q-Cq intern), 132.93 (*C*q arom. extern), 118.86 (*C*H arom. Core), 115.62 (*C*H-arom intern), 114.78 (*C*H arom extern), 106.96 (*C*H arom intern), 72.23 (O*C*H$_2$CH$_2$), 70.61 (O*C*H$_2$ arom extern), 68.72 (Si*C*H$_2$O), 59.04 (*C*H$_3$O), 43.05 (*C*H$_2$CH$_2$CH$_2$Si), 17.65 (CH$_2$*C*H$_2$CH$_2$Si), 14.54 (CH$_2$CH$_2$*C*H$_2$Si), -4.55 (Si(*C*H$_3$)$_2$) **(see the spectrum page 40)**.

DOSY : D = 7.70 (± 0.7) x 10^{-11} m²/s
Rh = 7.5 (± 0.7) nm
(D: diffusion coefficient; Rh : hydrodynamic radius) **(see the spectrum page 41)**

Light scattering : Rh = 7.7 (± 0.7) nm

SEC : retention time = 1060 seconds (Polydispersity = 1.05) **(see the spectrum page 42).**

*^{1}H NMR spectrum of dendrimer **11***

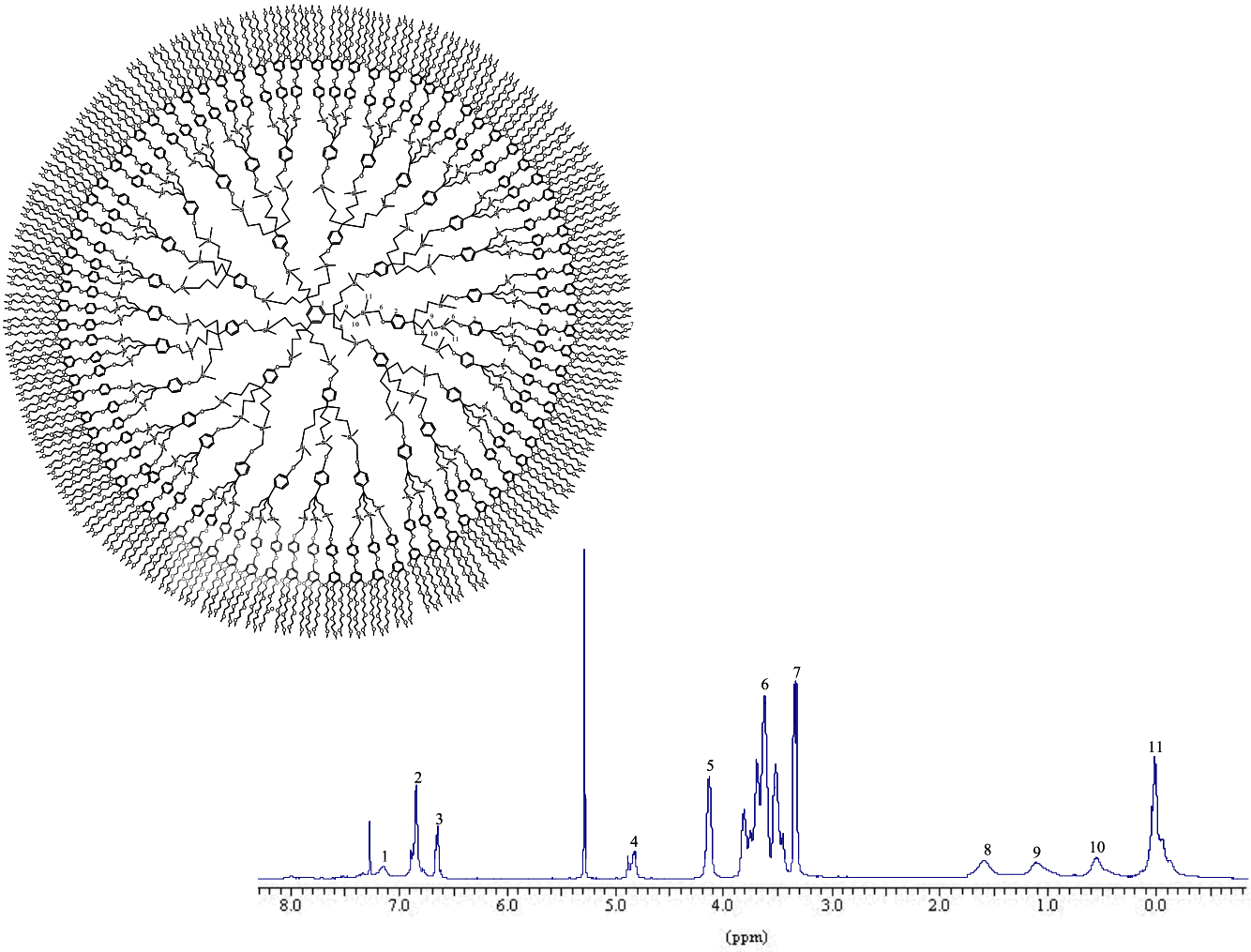

^{1}H NMR spectrum of G_2dHQ ($CDCl_3$, 250MHz): 7.13 et 6.82 (C*H*-arom. intern), 6.61 (C*H*-arom. extern), 4.85 (0- CH_2-arom. extern), 4.11 (CH_2O-arom. extern), 3.62 (OCH_2CH_2O and Si-CH_2O), 3.35 (CH_3O), 1.59 (CH_2CH_2CH_2Si), 1.11 (CH_2CH_2CH_2Si), 0.56 (CH_2CH_2CH_2Si), 0.05 (Si(CH_3)$_2$).

*^{13}C NMR spectrum of dendrimer **11***

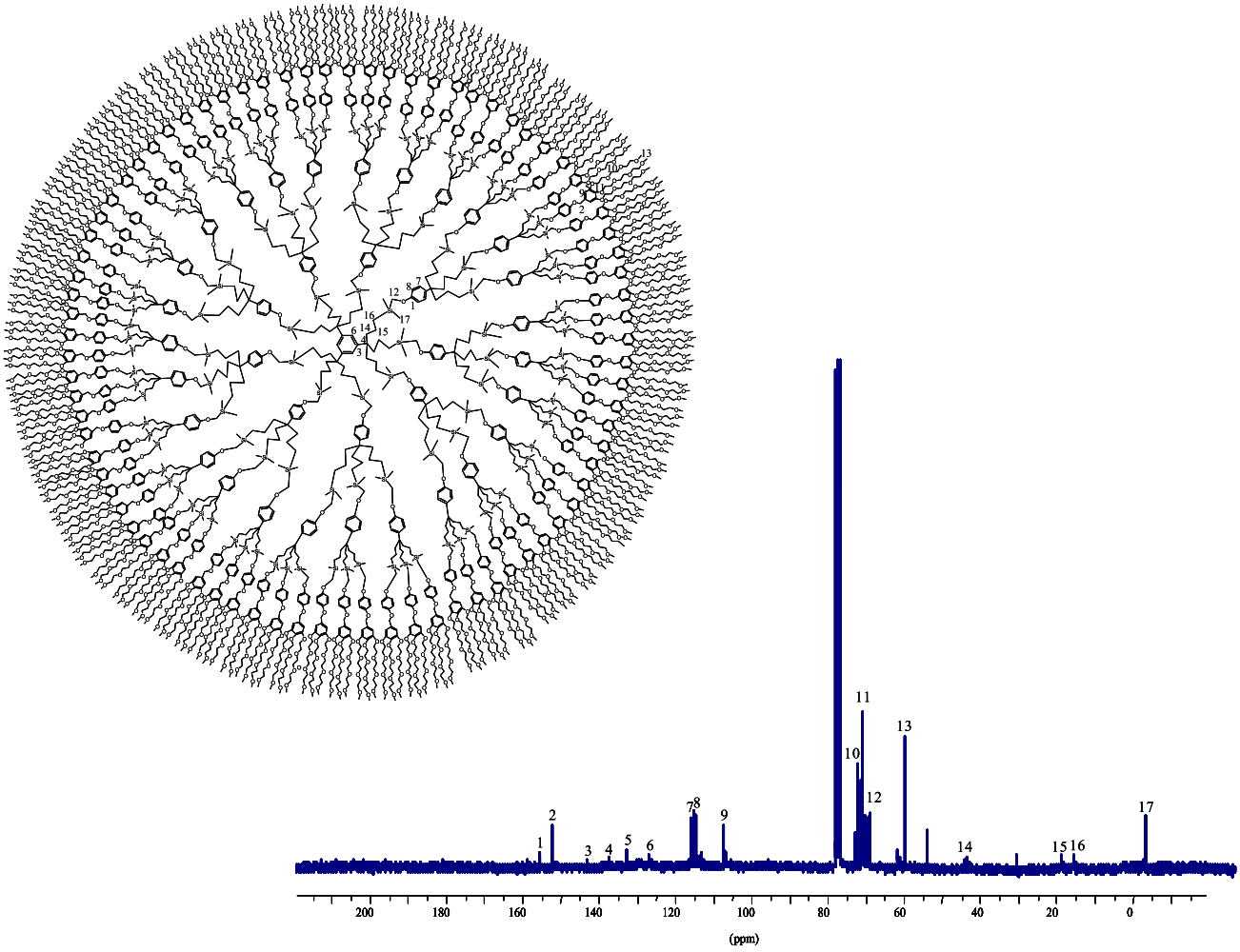

^{13}C NMR spectrum of G_2dHQ ($CDCl_3$, 62 MHz): 156.08 (O-*C*q intern), 152.56 (*C*q intern), 145.69 (*C*q arom. Core), 137.62 (*C*q-Cq intern), 132.93 (*C*q arom. extern), 118.86 (*C*H arom. Core), 115.62 (*C*H-arom intern), 114.78 (*C*H arom extern), 106.96 (*C*H arom intern), 72.23 (OCH_2CH_2), 70.61 (OCH_2 arom extern), 68.72 ($SiCH_2O$), 59.04 (CH_3O), 43.05 ($CH_2CH_2CH_2Si$), 17.65 ($CH_2CH_2CH_2Si$), 14.54 ($CH_2CH_2CH_2Si$), -4.55 ($Si(CH_3)_2$).

*DOSY spectrum of dendrimer **11***

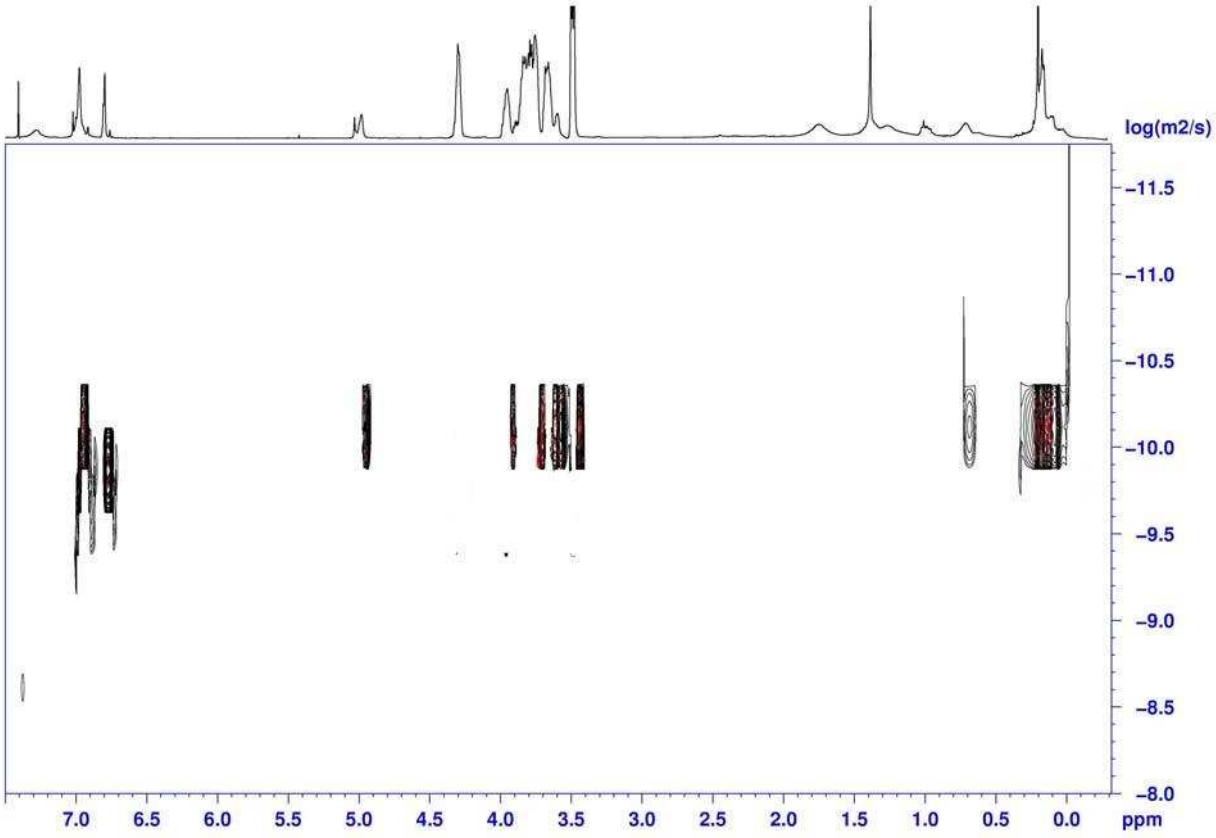

DOSY : $D = 7.70 (\pm 0.7) \times 10^{-11}$ m²/s

Rh = 7.5 (± 0.7) nm

(D: diffusion coefficient; Rh : hydrodynamic radius)

*Size Exclusion Chromatography (SEC) of the three generations of dendrimers synthesized by Williamson reaction **9**, **10** and **11***

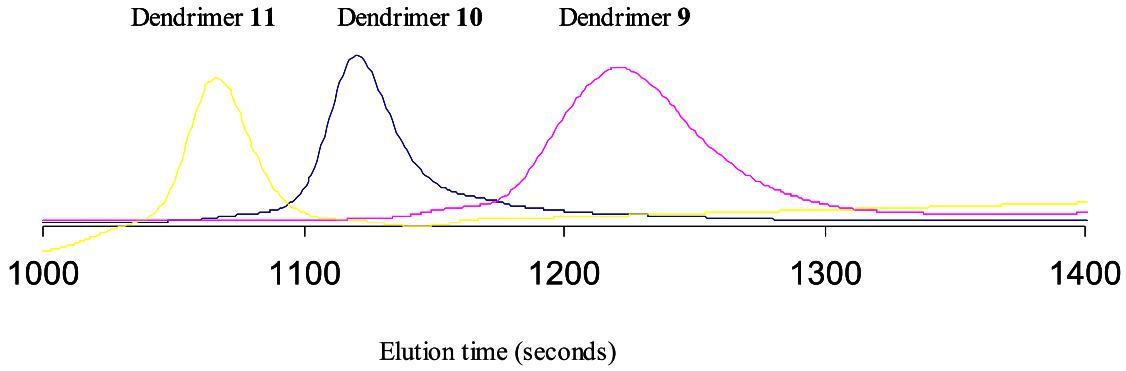

Retention time for dendrimer **4** = 1221 seconds (Polydispersity =1.05)
dendrimer **5** = 1121 seconds (Polydispersity =1.02)
dendrimer **6**= 1060 seconds (Polydispersity =1.05)

Dendrimers **9**, **10** and **11** + 1 equiv. of $HAuCl_4$ *per* dendron:

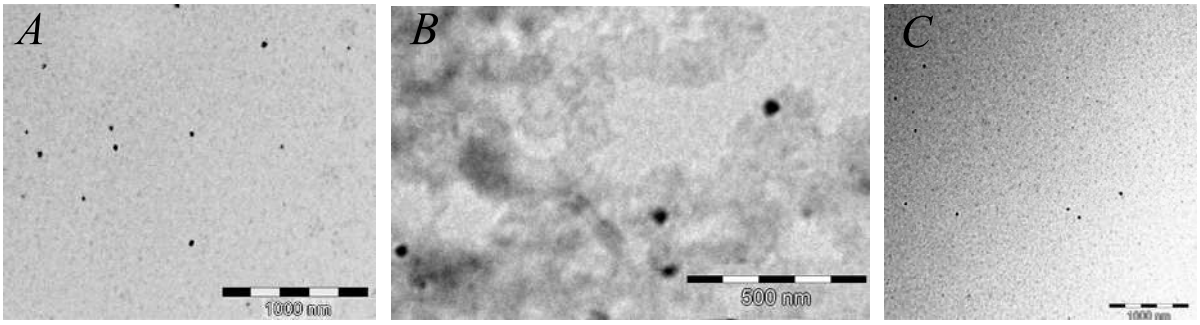

a) Dendrimer **9** + 1 equiv. of $HAuCl_4$ *per* dendron, diameter = 23 (± 0.5) nm; b) dendrimer **10** + 1 equiv. of $HAuCl_4$ *per* dendron, diameter = 34 (± 1) nm; c) dendrimer **11** + 1 equiv. of $HAuCl_4$ *per* dendron, diameter = 36 (± 0.5) nm.

Dendrimers **4**, **5** and **6** + 1 equiv. of $HAuCl_4$ *per* dendron:

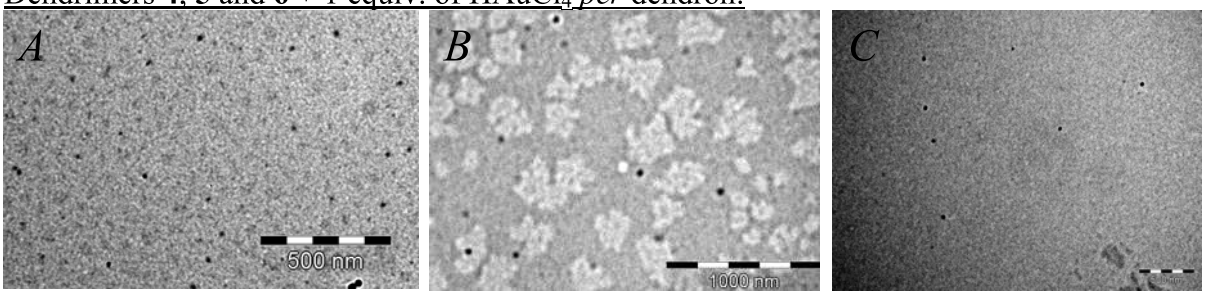

a) Dendrimer **4** + 1 equiv. of $HAuCl_4$ *per* dendron, diameter = 22 (± 0.5) nm; b) dendrimer **5** + 1 equiv. of $HAuCl_4$ *per* dendron, diameter = 33 (± 0.5) nm; c) dendrimer **6** + 1 equiv. of $HAuCl_4$ *per* dendron, diameter = 36 (± 1) nm.

Dendrimers **9, 10** and **11** + 2 or 5 equiv. of $HAuCl_4$ *per* dendron:

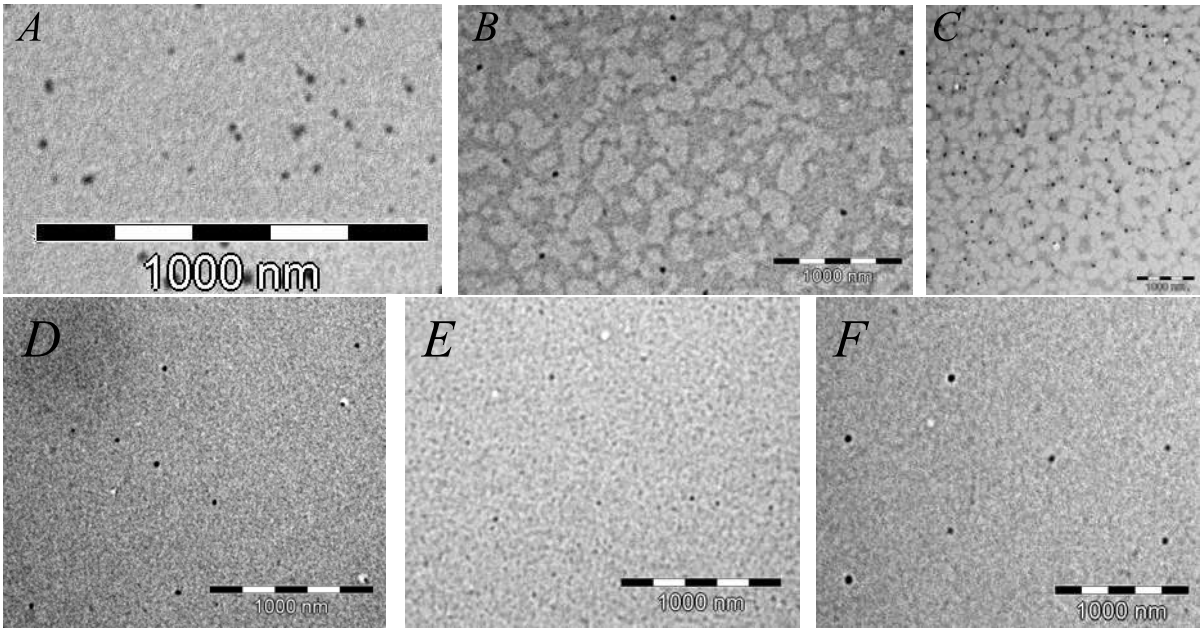

a) Dendrimer **9** + 2 equiv. of $HAuCl_4$ *per* dendron, diameter = 26 (± 1) nm; b) dendrimer **10** + 2 equiv. of $HAuCl_4$ *per* dendron, diameter = 36 (± 0.5) nm; c) dendrimer **11** + 2 equiv. of $HAuCl_4$ *per* dendron, diameter = 38 (± 0.5) nm; d) dendrimer **9** + 5 equiv. of $HAuCl_4$ *per* dendron, diameter = 32 (± 1) nm; e) dendrimer **10** + 5 equiv. of $HAuCl_4$ *per* dendron,

diameter = 38 (± 1) nm; f) dendrimer **11** + 5 equiv. of $HAuCl_4$ *per* dendron, diameter = 42 (± 1) nm.

Dendrimers **5** + 1 equiv. of $HAuCl_4$ *per* dendron with different organometallic reductants:

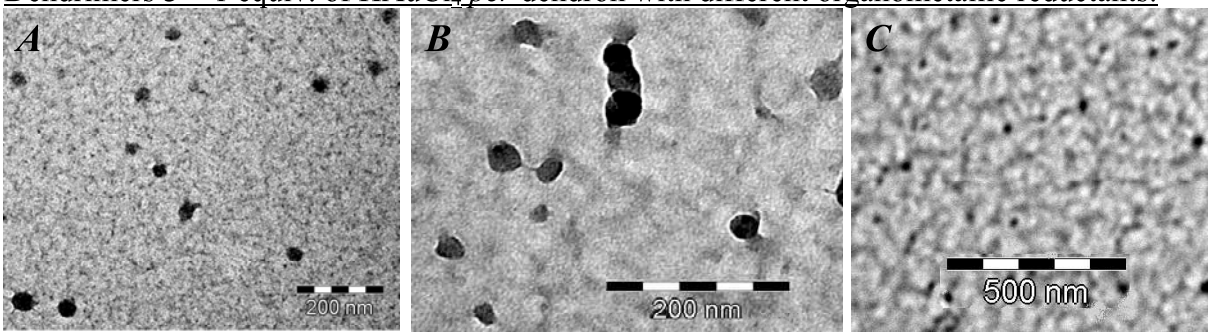

a) TEM of the dendrimer **5** + 1 equiv. of $HAuCl_4$ reduced by ferrocene; b) TEM of the dendrimer **5** + 1 equiv. of $HAuCl_4$ reduced by ethynylferrocene; c) TEM of the dendrimer **5** + 1 equiv. of $HAuCl_4$ reduced by decamethylferrocene.

Equation for the measurement of the diffusion coefficients by ^1H NMR

First, the measurement of D allows calculating the hydrodynamic diameter of a molecule*. Then, the ^1H NMR experiment focuses on the diffusion that is mathematically treated according to a DOSY process (Diffusion Ordered SpectroscopY) in order to obtain the equiv. of a spectral chromatography. The objective is to measure the size of the molecules in solution by ^1H NMR.

The dendrimers are considered as spherical molecular objects, and characterized by an apparent diffusion coefficient. The application of the Stokes-Einstein law gives an estimate of the diameter of the molecule.

Stokes-Einstein law:

$D = K_B T / 6\pi\eta r_H$

D: diffusion constant; K_B: Boltzman's constant; T: temperature (K); η: solvent viscosity; r_H: hydrodynamic radius of the species.

Example for the dendrimer 4:

DOSY : $D = 1.16 (\pm 0.1) \times 10^{-10}$ m²/s
$K_B = 1.38 \times 10^{-23}$ $m^2.kg.s^{-2}.K^{-1}$
T = 298 K
η (CH_2Cl_2)= 0.38×10^{-3} Pa.s

$\rightarrow r_H = K_B T / 6\pi\eta D =$ 4.9 (± 0.1) nm

*Reference : Diaz, M. D.; Berger, S. *Carbohydr. Res.* **2000,** *329*, 1-5.

Chapitre B-3

Fonctionnalisation efficace de nanoparticules d'or biocompatibles

Afin d'utiliser des nanoparticules d'or dans les domaines de la biologie, de la nanomédecine, de l'optique et de la catalyse, il est essentiel de maîtriser leurs synthèses ainsi que leurs différents modes de fonctionnalisation dans l'objectif de les « décorer » avec les ligands nécessaires pour chaque cas.

Or nous avons récemment effectué la bibliographie sur les différentes fonctionnalisations des nanoparticules d'or par la réaction « click » et il s'est avéré qu'un grand nombre de problèmes avaient été rencontrés. Les diverses conditions utilisées ne permettaient donc pas à ces nano-objets d'être fonctionnalisés de manière efficace. En effet trois articles récents exposent ces difficultés avec des rendements de réaction compris entre 0,3% et 22% (54% de rendement étant obtenu seulement pour un cas). Ceci diverge radicalement des résultats obtenus régulièrement avec la chimie « click » en synthèse organique qui est très efficace dans des conditions très douces, d'où son essor actuelle en synthèse.

Nous avons réfléchi aux éventuelles conditions qui gêneraient cette fonctionnalisation et aux éventuelles modifications qui nous permettraient d'améliorer les rendements de ces fonctionnalisations. Les trois principaux problèmes se sont avérés être des problèmes de solubilité des différents réactifs mis en jeu et des problèmes de décomposition ou d'agrégation du catalyseur de cuivre qui entraînaient ce manque de réactivité.

Le solvant de cette réaction a donc été modifié afin qu'il soit à la fois capable de réaliser la réaction « click » entre les deux produits (polaires ou apolaires) de départ mais aussi capable de solubiliser le catalyseur polaire $CuSO_4$. Nous avons donc choisi un milieu réactionnel homogène composé d'eau et de THF (tétrahydrofurane) afin de solubiliser le tout.

La quantité de catalyseur a également été modifiée, ainsi que celle d'ascorbate de sodium utilisé pour réduire *in situ* le Cu^{II} en Cu^{I}. En effet, ces quantités ont été augmentées afin de surmonter l'éventuel problème d'agrégation du Cu^{I}. Une autre précaution est également prise, celle de travailler dans des conditions d'atmosphère inerte afin de limiter la ré-oxydation du Cu^{I}.

Grâce à ces nouvelles conditions, nous avons réalisé la fonctionnalisation de nanoparticules d'or contenant des groupements azoture en périphérie avec différents alcynes terminaux dont des alcynes organiques, dendroniques, polyéthylene glycol (PEG), … Malgré les différences de taille et d'hydrophilie, toutes les réactions ont pu être réalisées dans les conditions précédentes avec un rendement proche de 100%.

Toute la partie synthèse de ce travail, qui a fait l'objet d'une note publiée en 2008 dans le journal *Chemical Communications*, a été réalisée au sein de notre laboratoire. Les analyses MET (Microscopie Electronique par Transmission) ont été réalisées par M. Lionel Salmon, chargé de recherche CNRS, membre de l'équipe du Professeur Azzedine Bousseksou, au LCC (Laboratoire de Chimie de Coordination) de Toulouse. Ces nouvelles conditions réactionnelles pour la réaction « click » sur ces nanoparticules d'or peuvent également s'adapter à d'autres types de support pour surmonter d'éventuels problèmes de rendements. Il est également à noter que certaines des nanoparticules PEG synthétisées par cette méthode ont ensuite servi pour la vectorisation de médicaments anti-cancéreux et montrent un caractère non-cytotoxique et actif contre le cancer.

How to very efficiently functionalize gold nanoparticles by "click" chemistry†

Elodie Boisselier,[a] Lionel Salmon,[b] Jaime Ruiz[a] and Didier Astruc*[a]

Received (in Cambridge, UK) 17th July 2008, Accepted 9th September 2008
First published as an Advance Article on the web 1st October 2008
DOI: 10.1039/b812249k

Difficulties previously encountered in the very useful "click" functionalization of gold nanoparticles (AuNPs) resulting in low yields are now overcome by using specific conditions: 1 : 1 water–THF medium, stoichiometric $CuSO_4$ and sodium ascorbate, inert atmosphere at 20 °C that provide quantitative "click" reactions between azidoalkylthiolate-AuNPs with various hydrophilic (PEG-containing) and hydrophobic (organic and organometallic) alkynes.

Functionalization of gold nanoparticles (AuNPs)[1] is a key challenge given the broad range of applications of AuNPs in biology,[2] nanomedicine,[3] optics[4] and catalysis.[5] Since the seminal reports by Brust and Schiffrin[6] of the stable alkylthiolate AuNPs, considerable interest has arisen in their chemistry and physics. A large variety of functional AuNPs are now known,[1–7] but many families of AuNPs are still resistant to direct synthesis,[6] ligand exchange reactions[7] or functionalization using high-temperature or other incompatible processes.[1] Thus, in view of these multiple applications, it was essential to reconsider here the problem of the efficiency of AuNP functionalization.

The recently improved Huisgen 1,3-dipolar cycloaddition of azide with alkynes, called "click" chemistry, has opened new avenues in organic synthesis under mild conditions.[8] Thus, this strategy is potentially very useful to functionalize AuNPs and is the subject of the present report. Three recent papers reported attempts to carry out such "click" reactions on AuNPs containing thiolate ligands.[4] Brust's group introduced 2500 azide-functionalized thiolate ligands onto AuNPs of 12 nm diameter and 7 lipase groups by "click chemistry" using excess lipase, which corresponds to 0.3% of clicked azido groups.[9] Williams' group substituted 52% of the alkylthiolate ligands by reaction with bromoundecane thiols, and the substitution of the bromide by azide was achieved in 92% yield. The subsequent "click" reactions with several terminal alkynes (in excess) that were activated by a carbonyl linkage produced triazole rings with conversions mostly between 1 and 22% yields of 1,2,3-triazole formation in various solvents (54% was obtained in one specific case).[10] Simon's group assembled AuNPs on DNA templates *via* click chemistry using a 1000-fold excess of AuNPs.[11] These repeated low yields showed that difficulties are encountered in the application of "click" chemistry to the functionalization of AuNPs. They were attributed to the lack of reactivity due to solubility problems and to decomposition or aggregation of the Cu^I catalysts,[10] but they dramatically contrast with the exceedingly easy "click" reactions that are well known in organic synthesis to proceed under very mild conditions and that made these "click" reactions so popular.[8]

In addressing this problem, we reasoned that, on one hand, solubility must be an important constraint that needs to be carefully ensured for the click reaction, and that, on the other hand, a polar co-solvent such as water must be used to solubilize $CuSO_4$. We know that alkanethiol-coated AuNPs are soluble in organic solvents, not in water, which is a probable source of difficulty.[12] Thus, we investigated the possibility of using a homogeneous water–THF reaction medium obtained by adding the AuNPs in THF to the aqueous solution of a water-soluble alkyne or a THF–water solution of a purely organic alkyne. We also increased the amount of Cu^I catalyst obtained from $CuSO_4$ and sodium ascorbate in order to overcome the potential problem of aggregation of Cu^I, which was invoked as a reason for systematic low-yielding reactions. Finally, we found that it is essential to carry out the "click" reactions with AuNPs under an inert atmosphere, which inhibits re-oxidation of Cu^I, rather than the aerobic "click" reaction conditions generally used in organic synthesis.

If any of the above conditions is not fulfilled, we found that the "click" reaction proceeds in very low yields with thiolate-AuNPs, fully confirming the literature reports. If these precise conditions are fulfilled, however, we now find that the "click" reactions are virtually quantitative at room temperature in THF–water under an inert atmosphere between alkylthiolate-AuNPs terminated by azido groups and linear or dendronic alkynes, which leads to various functional AuNPs containing the 1,2,3-triazolyl groups, even including AuNP-cored dendrimers.[12,13] A variety of terminal alkynes including organic, organometallic, dendronic, polyethylene glycol (PEG), and long-chain dendronic, PEG-containg alkynes **1–6** were chosen (Chart 1) and always provided very satisfactory results despite the variety of size and hydrophilicity.

Undecanethiolate-AuNPs of 2.5 nm (by TEM) diameter containing 480 gold atoms and 230 dodecanethiolate ligands (from elemental analysis) were synthesized by the Schiffrin–Brust method,[6] then submitted to alkylthiolate ligand substitution by 1-bromoundecanethiolate using a 10-fold excess of 1-bromoundecanethiol in dichloromethane.‡ This led to AuNPs in which 72 ± 3% (*i.e.* 166 ± 6) of the

[a] *Institut des Sciences Moléculaires, UMR CNRS No. 5255, Université Bordeaux 1, 33405 Talence Cedex, France. E-mail: d.astruc@ism.u-bordeaux1.fr; http://www.u-bordeaux1.fr/lcoo/members/eastruc.htm; Fax: +33 540 00 66 46; Tel: +33 540 00 62 71*
[b] *Laboratoire de Chimie de Coordination, UPR CNRS No. 5255 205, Route de Narbonne, 31077 Toulouse Cedex 04, France*

† Electronic supplementary information (ESI) available: Syntheses, TEM images, ^1H NMR, UV-Vis, IR, and cyclic voltammetry spectra. See DOI: 10.1039/b812249k

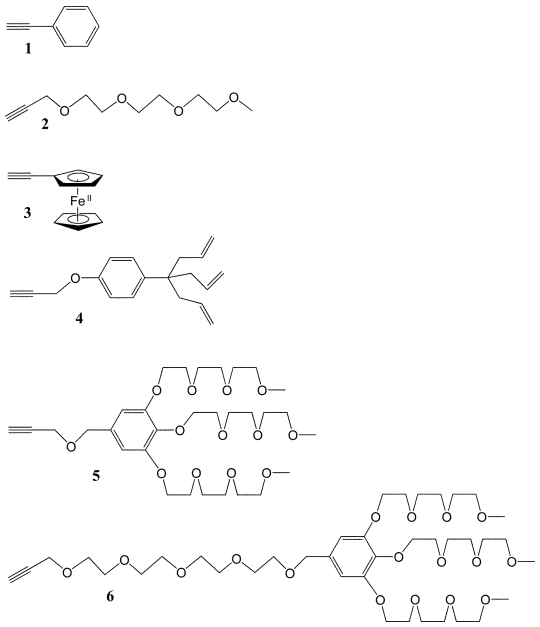

Chart 1

undecanethiolate ligands have been substituted as shown by ^{1}H NMR in $CDCl_3$ upon replacement of the terminal methyl and methylene signal at δ = 0.83 ppm and δ 1.22 ppm, respectively by the CH_2Br signal at δ = 3.40 ppm. After purification by reprecipitation upon addition of ether, quantitative nucleophilic substitution of bromide by azide was achieved upon reaction with a 20-fold excess NaN_3 in a dichloromethane–DMSO 1 : 1 mixture at ambient temperature (20 °C) for two days as shown, after purification upon reprecipitation using ether, by the complete replacement of the CH_2Br signal at δ = 3.40 ppm by the CH_2N_3 signal at δ = 3.25 ppm in the ^{1}H NMR spectra. The "click" reactions were carried out with the six terminal alkynes **1–6** (Chart 1) at room temperature under N_2 in water–THF for two days using a stoichiometric amount of $CuSO_4$ and sodium ascorbate. Then, extraction with dichloromethane and purification by precipitation was carried out using ether for the reactions with **1** and **3**, and using methanol for **4**, and from methanol solutions with ether for the polyethylene glycol-containing compounds **2**, **5** and **6**. (AuNPs functionalized with **1**, **3** and **4** are soluble in dichloromethane and chloroform, and the AuNPs functionalized with **2**, **5** and **6** are also water soluble.) Subsequent washing with a 15 N

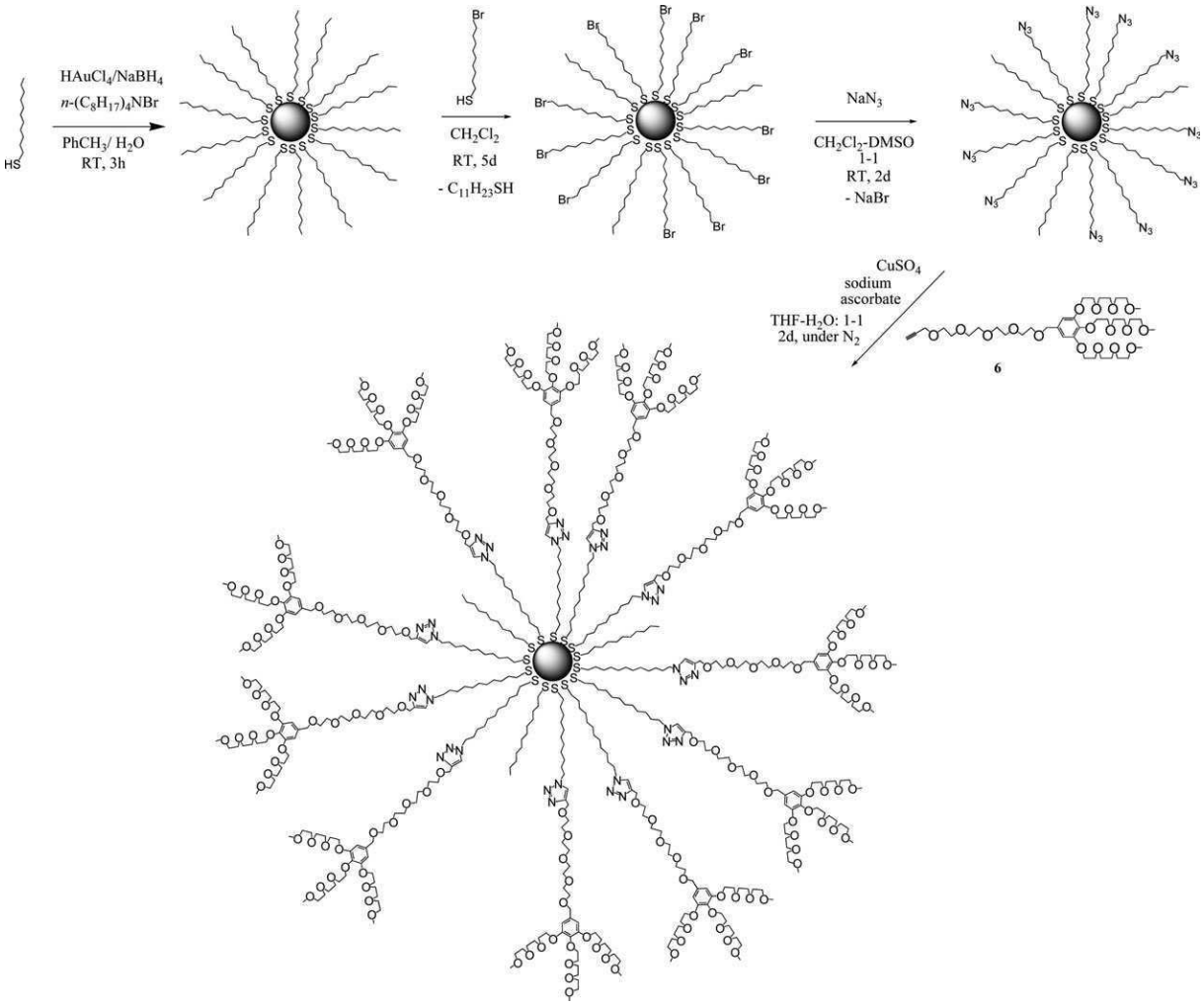

Scheme 1 Overall synthetic scheme for the efficient functionalization of AuNPs under ambient conditions using the "click" reaction with the dendronic alkyne **6**.

aerobic aqueous ammonia solution removed the Cu^{II} cations from all the functionalized AuNPs. All these "click" reactions where found to be virtually quantitative under these optimized conditions, as shown by the disappearance of the CH_2N_3 signal at $\delta = 3.25$ ppm in the ^1H NMR spectra and N_3 absorption band at $\nu = 2094\ cm^{-1}$ and alkyne band at $\nu = 2160\ cm^{-1}$ in the IR spectra. Note that all the reactions of Scheme 1 proceed at room temperature, which is also the case for all the "click" reactions of **1–6**. The AuNPs can be dissolved and reprecipitated (*vide supra*) without change in the spectra, the plasmon band at 520 nm in the UV-Vis spectrum remaining constant along the reactions, and the TEM data showed that there was no change in the AuNP core size along the reactions of Scheme 1.

In conclusion, we have investigated the reasons causing the repeated low-yield "click" reactions with AuNPs, discovered the experimental solutions to overcome these difficulties, optimized the new "click" reactions with a variety of organic, organometallic, polyethylene glycol, and dendronic (including organic and PEG-containing) terminal alkynes and found a general procedure exemplified in Scheme 1 that works ideally in all the investigated examples. It is in particular noteworthy that PEG-containing AuNPs are biocompatible[14] and should be very useful in nanomedicine, an area that we are presently investigating.[15]

Financial support from the CNRS, the University Bordeaux 1 and the Institut Universitaire de France (IUF, DA) is gratefully acknowledged.

Notes and references

‡ Experimental procedure: *Synthesis of the azidoundecenylthiolate AuNPs*: Undecanethiolate-AuNPs of 2.5 nm diameter (by TEM, see ESI†) were obtained by following the Schiffrin–Brust procedure using 0.9 mmol of $C_{11}H_{23}SH$, 0.9 mmol of hydrogen tetrachloroaurate (30 mL, aqueous solution) and 10 mmol of $NaBH_4$, after washing with ethanol and acetone followed by precipitation from ethanol. ^1H NMR ($CDCl_3$, 250 MHz): 1.22 (22H, CH_2), 0.83 (3H, CH_3). UV-Vis: plasmon band at 520 nm. TEM: diameter = 3 ± 0.4 nm. Undecanethiolate-AuNPs (130 mg) were dissolved in distilled CH_2Cl_2, and bromoundecanethiol (500 mg) was added to the solution that was further stirred for 5 d under N_2 at room temperature (RT). The solvent was then removed under vacuum, the resulting mixed AuNPs were precipitated with acetone and ethanol in order to remove the excess thiol. ^1H NMR ($CDCl_3$, 250 MHz): 3.40 (2H, CH_2-Br), 1.22 (22H, CH_2), 0.83 (3H, CH_3). UV-Vis: plasmon band at 520 nm. TEM: diameter = 3 ± 0.4 nm.
These mixed AuNPs (10 mg mL^{-1}, 150 mg) were dissolved in 15 mL CH_2Cl_2 and added to an equal volume of 0.25 M NaN_3 (244 mg) in DMSO. The solution was stirred for 48 h under N_2 at RT, water was added, and the black organic layer was isolated. This organic layer was dried over sodium sulfate and filtered, the solvent was evaporated, and the AuNPs containing the azidoundecenylthiolate ligands were washed with ethanol and dried. ^1H NMR ($CDCl_3$, 250 MHz): 3.26 (2H, CH_2-Br), 1.22 (22H, CH_2), 0.83 (3H, CH_3). UV-Vis: plasmon band at 520 nm. TEM: diameter = 3 ± 0.4 nm.
General procedure for the "click" reactions. The azidoundecenylthiolate-AuNPs (50 mg) and the alkyne substrate (0.1 mmol) were dissolved in THF. At 0 °C, $CuSO_4$ was added (2 equiv. *per* alkyne substrate, 1 M water solution), followed by the dropwise addition of a freshly prepared solution of sodium ascorbate (4 equiv. *per* branch, 1 M water solution) adjusted for a 1 : 1 THF : water ratio. The solution was allowed to stir for 2 d at 30 °C under N_2. After removing THF under vacuum, CH_2Cl_2 and an aqueous ammonia solution were added. The mixture was allowed to stir for 10 min in order to remove all the Cu^{II} trapped inside the AuNPs as $Cu(NH_3)_6^{2+}$. The organic phase was washed twice with water, dried with sodium sulfate, and the solvent was removed under vacuum. In order to remove the excess alkyne substrate, the product was precipitated with MeOH–ether for the PEG ligand, with CH_2Cl_2–MeOH for the triallyl aryl dendron, and with CH_2Cl_2–ether for the phenylacetylene and ferrocenylacetylene substrates.[14]
Example of the "click" reaction with **5**: ^1H NMR ($CDCl_3$, 250 MHz): 7.53 (1H, C*H*-triazole), 6.58 (2H, C*H*-arom.), 4.60 (2H, triazole-CH_2-0), 4.49 (2H, CH_2-CH_2-triazole), 4.14 (8H, OCH_2_arom. and arom-OC-H_2CH_2), 3.66 (30H, OCH_2CH_2O), 3.37 (9H, CH_3O), 2.47 (2H, CH_2S), 1.25 (18H, CH_2CH_2CH_2), 0.87 (3H, CH_2CH_3). Elemental analysis: S (1.47%); Au (18.86%). ^{13}C NMR ($CDCl_3$, 62 MHz): 126.1 (*C*H of triazole and arom. core), 107.16 (C_qCH_2O), 70.39 (OCH_2CH_2O), 65.90 (triazole-CH_2-O), 58.91 (CH_3O). IR: disappearance of the ν_{N3}band at 2094 cm^{-1}. UV-Vis: plasmon band of the AuNPs: 520 nm in CH_2Cl_2. TEM: diameter = 2.5 nm (±0.3 nm).

1 M.-C. Daniel and D. Astruc, *Chem. Rev.*, 2004, **104**, 293–346.
2 Biology: R. Elghanian, J. J. Storhoff, R. C. Mucic and C. A. Mirkin, *Science*, 1997, **277**, 1078–1081; J. J. Storhoff and C. A. Mirkin, *Chem. Rev.*, 1999, **99**, 1849–1862.
3 D. Astruc, *C. R. Acad. Sci., Sér. IIb*, 1996, **322**, 757–766; H. Liao, C. L. Nehl and J. H. Hafner, *Future Med.*, 2006, **1**, 201–208; G. R. Souza, D. R. Christianson, F. I. Staquicini, M. G. Ozawa, E. Y. Snyder, R. L. Sniman, J. H. Miller, W. Arap and R. Pascalini, *Proc. Natl. Acad. Sci. USA*, 2006, **103**, 1215–1220; J. Kim, S. Park and J. E. Lee, *Angew. Chem., Int. Ed.*, 2006, **45**, 7754–7758; G. An, P. Gosh and V. M. Rotello, *Nanomedicine*, 2007, **2**, 113–123; S. J. Son, X. Bai and S. B. Lee, *Drug Discovery Today*, 2007, **12**, 657–663; S. E. Skrabalak, L. Au, X. L. Lu, X. D. Li and Y. N. Xia, *Nanomedicine*, 2007, **2**, 657–668; S.-Y. Shim, D.-K. Lim and J.-M. Nam, *Nanomedicine*, 2008, **3**, 215–232; K. K. Jain, *Med. Princ. Pract.*, 2008, **17**, 89–101; C. L. Johson, E. Snoeck and M. Ezcurdia, *Nat. Mater.*, 2008, **7**, 120–124.
4 Optics: P. Mulvaney, *Langmuir*, 1996, **12**, 788–800; Y. Yamanoi and N. Nishihara, *Chem. Commun.*, 2007, 3983–3989.
5 Catalysis: M. Haruta and M. Date, *Appl. Catal., A*, 2001, **222**, 427–437; R. M. Crooks, M. Zhao, L. Sun, V. Chechik and L. K. Yeung, *Acc. Chem. Res.*, 2001, **34**, 181; S. Biela and M. Rossi, *Chem. Commun.*, 2003, 1359–1360; R. W. J. Scott, O. M. Wilson and R. M. Crooks, *J. Phys. Chem. B*, 2005, **109**, 692; A. Abad, A. Corma and H. Garcia, *Chem.–Eur. J.*, 2008, **14**, 212–222.
6 M. Brust, M. Walker, D. Bethell, D. J. Schiffrin and R. Whyman, *J. Chem. Soc., Chem. Commun.*, 1994, 801–802.
7 A. C. Templeton, W. P. Wuelfing and R. W. Murray, *Acc. Chem. Res.*, 2000, **33**, 27–36.
8 (*a*) H. C. Kolb, M. G. Finn and K. B. Sharpless, *Angew. Chem., Int. Ed.*, 2001, **40**, 2004; (*b*) V. D. Bock, H. Hiemstra and J. H. van Maarseveen, *Eur. J. Org. Chem.*, 2006, 51; (*c*) J. E. Moses and A. D. Moorhouse, *Chem. Soc. Rev.*, 2007, **36**, 1249–1262.
9 J. L. Brennan, N. S. Hatzakis, T. R. Tsikhudo, N. Dirvianskyte, V. Razumas, S. Patkar, J. Vind, A. Svendsen, R. J. M. Nolte, A. E. Rowan and M. Brust, *Bioconjugate Chem.*, 2006, **17**, 1373–1375.
10 (*a*) D. A. Fleming, C. J. Thode and M. E. Williams, *Chem. Mater.*, 2006, **18**, 2327–2334; (*b*) C. J. Thode and M. E. Williams, *J. Coll. Interface Sci.*, 2008, **320**, 346–352.
11 M. Fischler, A. Sologubenko, J. Mayer, G. Clever, G. Burley, J. Gierlich, T. Carell and U. Simon, *Chem. Commun.*, 2008, 169–171.
12 M.-C. Daniel, J. Ruiz, S. Nlate, J. Palumbo, J.-C. Blais and D. Astruc, *Chem. Commun.*, 2001, 2000–2001; M.-C. Daniel, J. Ruiz, S. Nlate, J.-C. Blais and D. Astruc, *J. Am. Chem. Soc.*, 2003, **125**, 2617–2628.
13 For metallodendrimers (including also ferrocenyl- and AuNP-containing dendrimers), see: C. M. Casado, I. Cuadrado, M. Moran, B. Alonso, B. Garcia, B. Gonzalez and J. Losada, *Coord. Chem. Rev.*, 1999, **185–6**, 53–79; G. R. Newkome, E. He and C. N. Moorefield, *Chem. Rev.*, 1999, **99**, 1689–1746; S. H. Hwag, V. Balzani, P. Ceroni, A. Juris, M. Venturi, S. Campagna, F. Puntoriero and S. Serroni, *Coord. Chem. Rev.*, 2001, **219**, 545–572; Y. Niu and R. M. Crooks, *C. R. Chim.*, 2003, **6**, 1049–1060; C. D. Shreiner, C. N. Moorefield and G. R. Newkome, *New J. Chem.*, 2007, **31**, 1192–1217.
14 R. Shukla, V. Bansal, M. Chaudhari, A. Basu, R. R. Bhonde and M. Sastry, *Langmuir*, 2005, **21**, 10644–10654.
15 See the spectroscopic, cyclic voltammetry and analytical data in the ESI† (14 pp) for all AuNPs.

How to Very Efficiently Functionalize Gold Nanoparticles by "Click" Chemistry

*Elodie Boisselier, Lionel Salmon, Jaime Ruiz, Didier Astruc**

SUPPLEMENTARY INFORMATION

1. Synthesis of dodecanethiolate-AuNPs

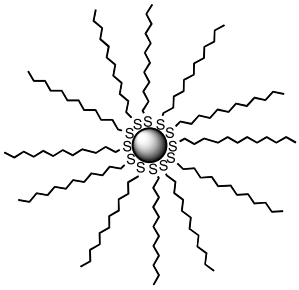

An aqueous solution of hydrogen tetrachloroaurate (30 mL, 30 mmol dm^{-3}, 0.9 mmol) was mixed with a toluene solution of tetraoctylammoniumbromide (80 mL, 50 mmol dm^{-3}, 4 mmol). The two-phase mixture was vigorously stirred until all the hydrogen tetrachloroaurate was transferred into the organic layer, and dodecanethiol ($C_{12}H_{25}SH$, 0.9 mmol) was then added to the organic phase. A freshly prepared solution of sodium borohydride (25 mL, 0.4 mol dm^{-3}, 10 mmol) was slowly added with vigorous stirring. After further stirring for 3 h, the organic phase was separated, evaporated to 10 mL in a rotary evaporator and mixed with 400 mL ethanol to remove excess thiol. The mixture was kept for 4 h at –18°C, and the dark brown precipitate was filtered off and washed with ethanol and acetone. The crude product was dissolved in 10 mL toluene and again precipitated with 400 mL ethanol.

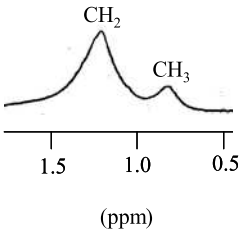

Fig. S1: ^{1}H NMR spectrum of dodecanethiolate-AuNPs in $CDCl_3$ (δ ppm)

^{1}H NMR ($CDCl_3$, 250MHz): 1.22 (22H, C*H*$_2$), 0.83 (3H, C*H*$_3$)

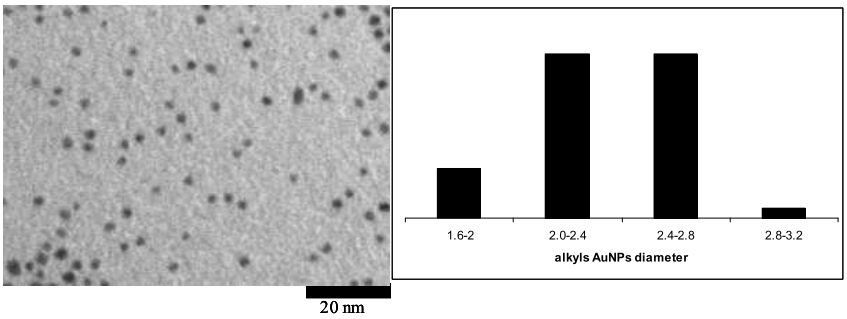

Fig. S2: TEM image of dodecanethiolate-AuNPs

diameter = 2.5 nm (± 0.3 nm)

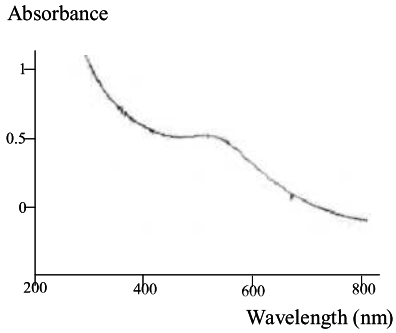

Fig. S3: UV-vis. Spectrum of dodecanethiolate-AuNPs in CH_2Cl_2

Plasmon band of the AuNPs at 520 nm

2. Ligand exchange with bromoundecanethiol

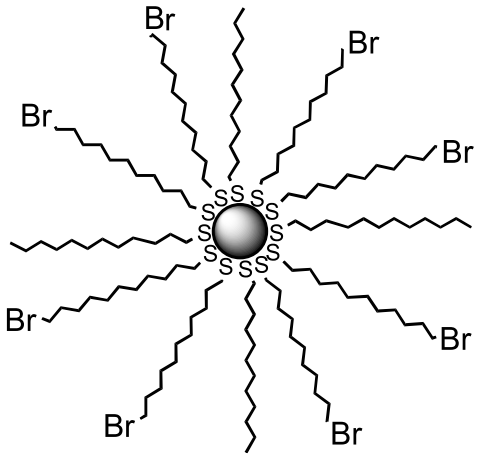

Dodecanethiolate-AuNPs (130 mg) were dissolved in distilled CH_2Cl_2 and bromoundecanethiol (500 mg) was added to the solution. After stirring for 5 days under N_2 at room temperature, AuNPs was evaporated and precipitated with acetone and ethanol to remove the excess thiol (m = 130 mg, yield = 94%).

Fig. S4: ^{1}H NMR spectrum of mixed dodecanethiolate-1-bromoundecanethiolate AuNPs in $CDCl_3$ (δ ppm)

^{1}H NMR ($CDCl_3$, 250MHz): 3.40 (2H, CH_2-Br), 1.22 (22H, CH_2), 0.83 (3H, CH_3)

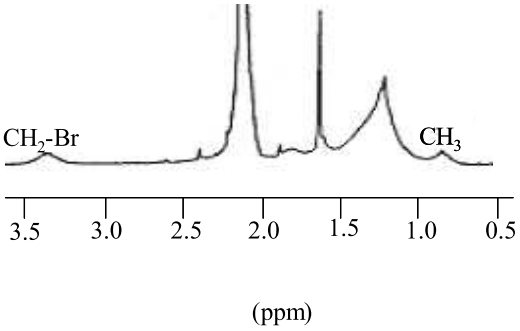

Fig. S5: UV-vis. Spectrum of mixed dodecanethiolate-1-bromoundecanethiolate

Plasmon band of mixed AuNPs at 520 nm

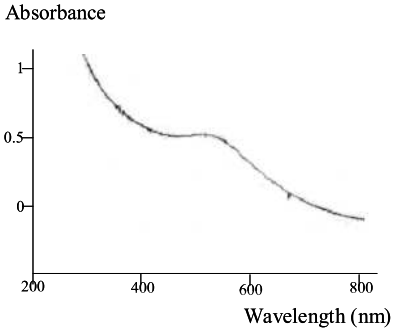

3. Azidation of the AuNPs

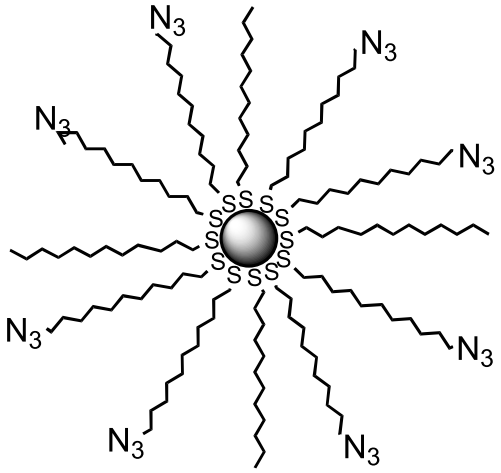

The mixed AuNPs (10 mg/mL, 150 mg) were dissolved in CH_2Cl_2 (15 mL) and added to an equal volume of 0.25 M NaN_3 (244 mg) in DMSO. The solution was stirred for 48 h under N_2 at rt, water was added, and the black organic layer was isolated. The organic layer was dried over sodium sulfate, the solvent was evaporated, and the AuNPs were washed with ethanol and dried (m = 140mg, yield = 98%).

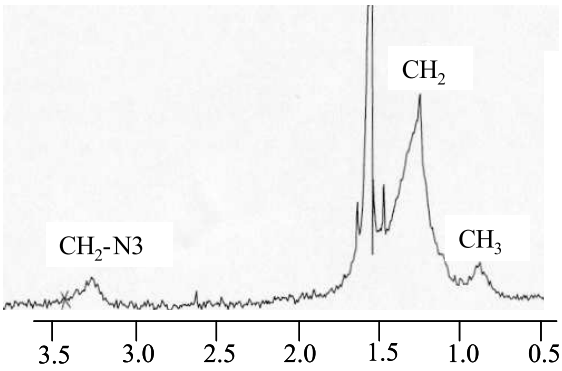

Fig. S6: ^{1}H NMR spectrum of mixed dodecanethiolate-1-azidoundecanethiolate AuNPs in $CDCl_3$ (δ ppm)

^{1}H NMR ($CDCl_3$, 250MHz): 3.26 (2H, C*H*$_2$-Br), 1.22 (22H, C*H*$_2$), 0.83 (3H, C*H*$_3$)

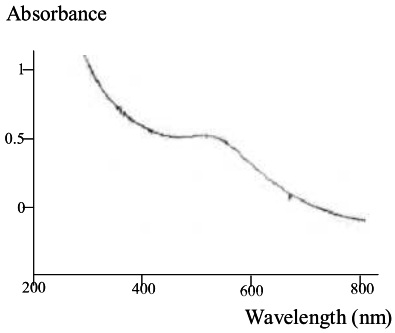

Fig. S7: UV-vis. spectrum of mixed dodecanethiolate-1-azidoundecanethiolate AuNPs in CH_2Cl_2

Plasmon band of mixed AuNPs at 520 nm

4. General procedure for "click" reactions

The azidoalkylthiolate-AuNPs (50 mg) and the alkyne (0.1 mmol) were dissolved in THF. At 0°C, $CuSO_4$ was added (2 eq. *per* alkyne, 1M water solution), followed by dropwise addition of a freshly prepared solution of sodium ascorbate (4 eq. *per* branch, 1M water solution) in order to set a 1:1 (THF/water) ratio. The solution was allowed to stir for 2 days at rt under N_2. After removing THF under vacuum, CH_2Cl_2 and water solution of ammonia were added. The mixture was allowed to stir for 10 min. in order to remove all the Cu^{II} trapped inside the AuNPs as $Cu(NH_3)_6$. The organic phase was washed twice with water, dried with sodium sulfate, and the solvent was removed under vacuum. In order to remove the excess alkyne, the product was precipitated with MeOH/ether for the PEG ligand, with CH_2Cl_2/MeOH for the triallyl dendron, and with CH_2Cl_2/ether for the ferrocenyl and phenyl derivatives.

5. Click chemistry with phenylacetylene

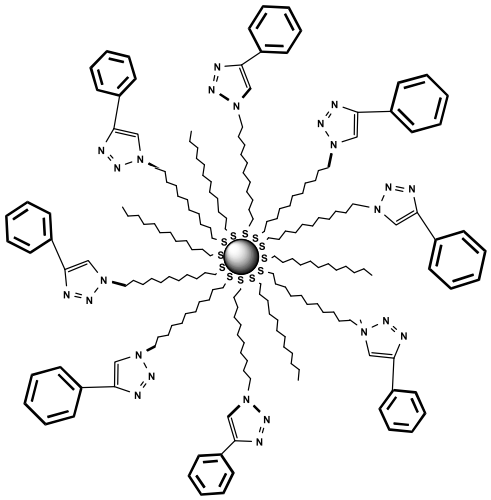

yield = 81%

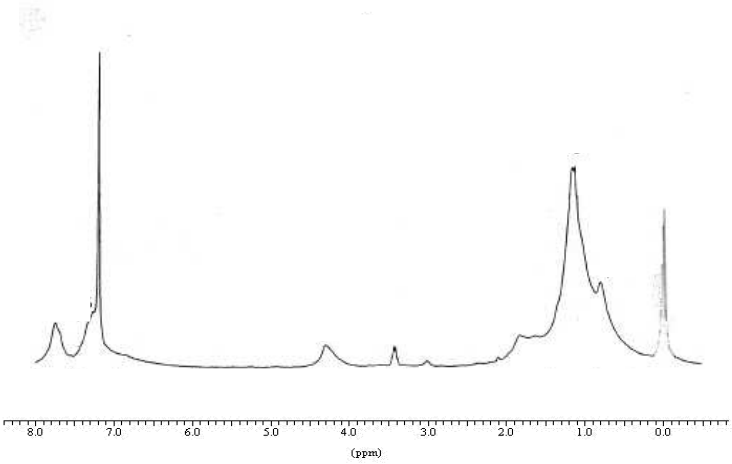

Fig. S8: ^{1}H NMR spectrum of phenyltriazolylakanethiolate AuNPs in $CDCl_3$ (δ ppm)

^{1}H NMR ($CDCl_3$, 250MHz):7.74 (2H, C-C*H*-phenyl) 7.60 (1H, C*H*-triazole), 7.33 (3H, C*H*-CH-C), 4.36 (2H, triazole-CH_2), 1.25 (18H, $CH_2CH_2CH_2$), 0.87 (3H, CH_2CH_3)

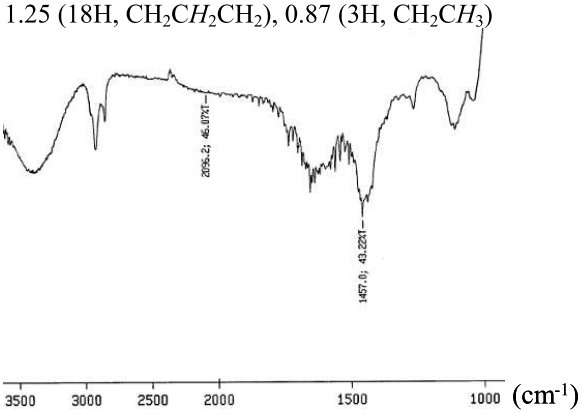

Fig. S9: IR spectrum of phenyltriazolylakanethiolate AuNPs

Disappearance of the ν_{N_3} band at 2094 cm^{-1}

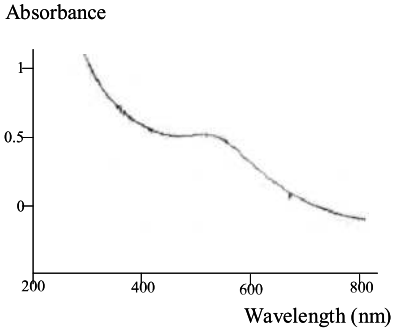

Fig S10: UV-vis. spectrum of phenyltriazolylakanethiolate AuNPs in CH_2Cl_2

Plasmon band of the AuNPs at 520 nm

6. Click chemistry with ferrocenylacetylene

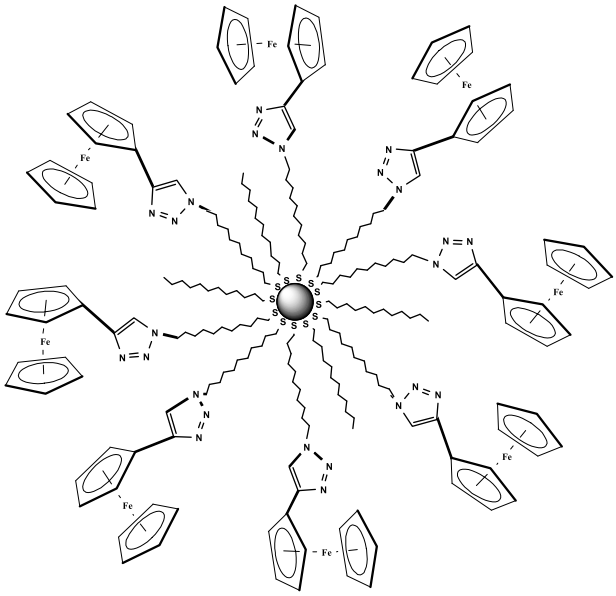

yield = 80%

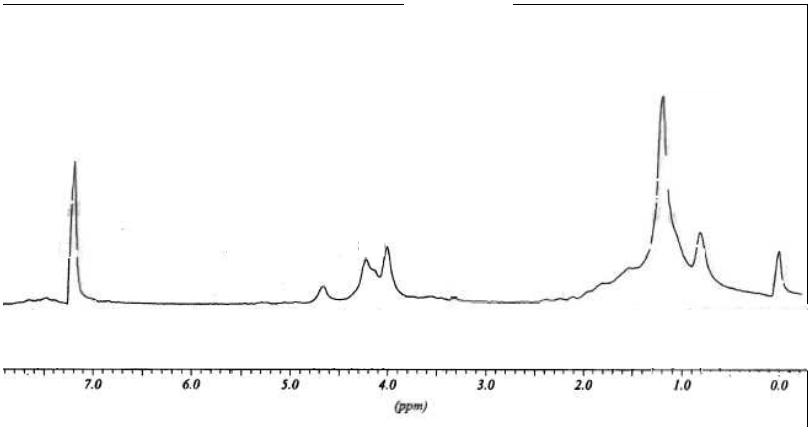

Fig. S11: ^{1}H NMR spectrum of ferrocenyltriazolylakanethiolate AuNPs in $CDCl_3$ (δ ppm)

^{1}H NMR ($CDCl_3$, 250MHz): 7.54 (1H, C*H*-triazole), 7.33 (3H, C*H*-CH-C), 4.73, 4.28, 4.07 (9H, Cp), 4.19 (2H, triazole-CH_2), 1.25 (18H, $CH_2CH_2CH_2$), 0.87 (3H, CH_2CH_3)

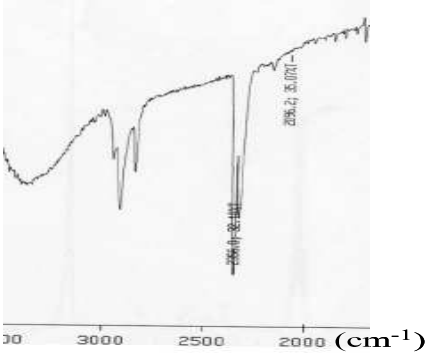

Fig. S12: IR spectrum of ferrocenyltriazolylakanethiolate AuNPs

Disappearance of the ν_{N_3} band at 2094 cm^{-1}

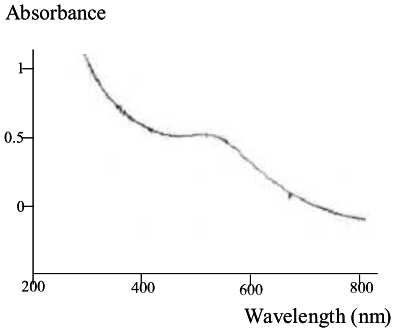

Fig. S13: UV-vis. spectrum of ferrocenyltriazolylakanethiolate AuNPs in CH_2Cl_2

Plasmon band of the AuNPs at 520 nm

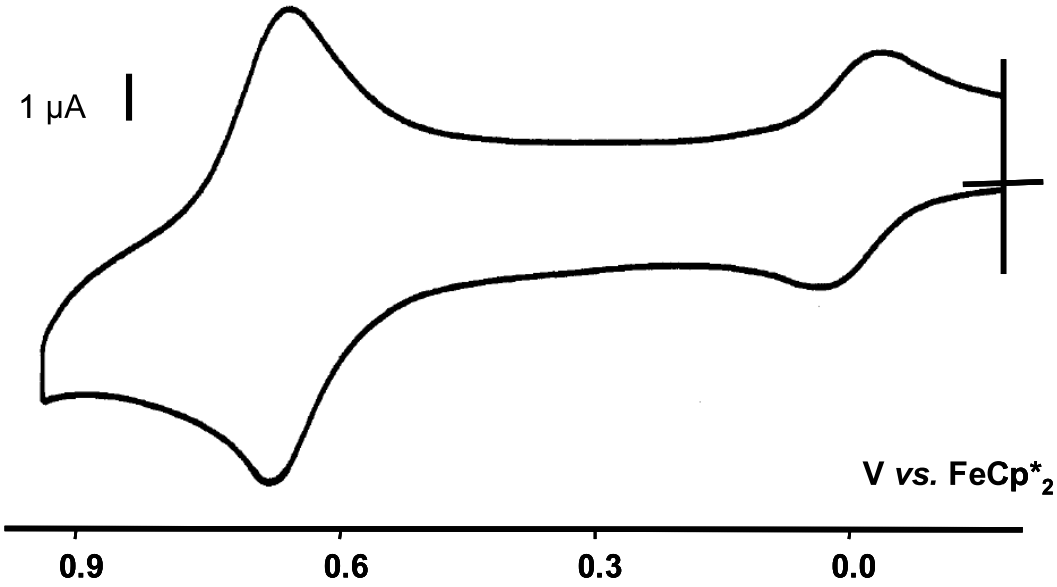

Fig. S14: Cyclic voltammetry of AuNPs with ferrocenyl termini obtained by "click" chemistry

$E_{1/2}$ 0.67 V. Solvent :CH_2Cl_2; temperature: 20ºC; supporting electrolyte: [nBu$_4$N][PF_6] 0.1M; working and counter electrodes: Pt; reference electrode: Ag; scan rate: 0.200 V.s^{-1} ; internal reference: decamethylferrocene.

7. Click chemistry with the tetraethyleneglycol derivative

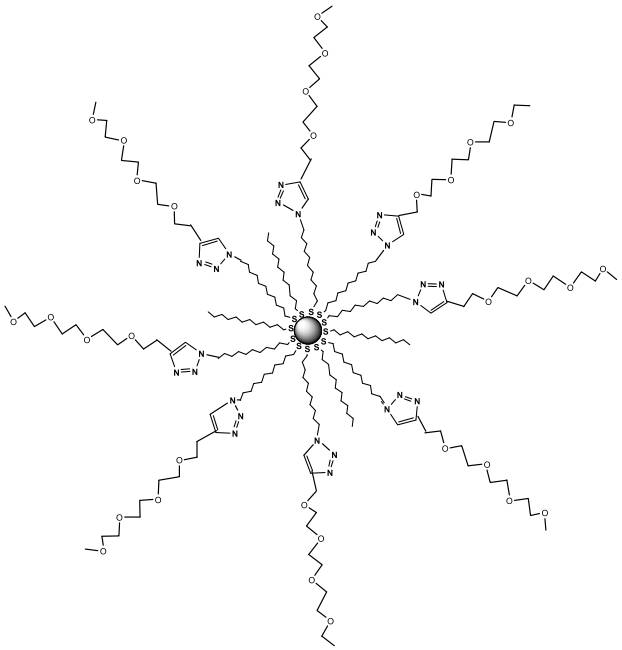

yield = 82%

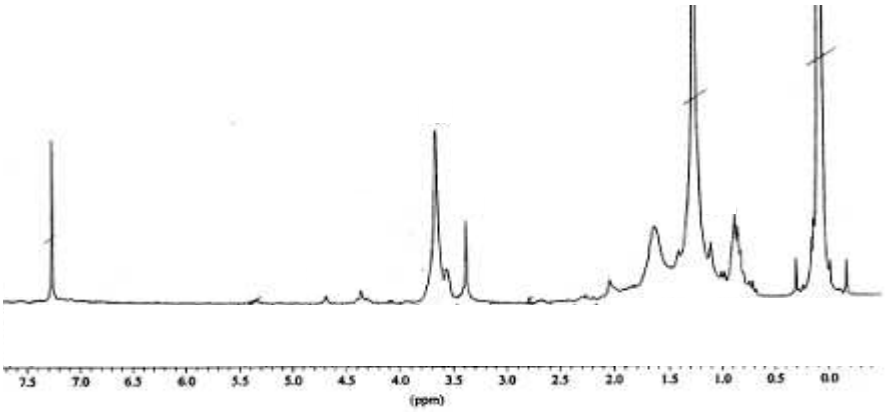

Fig. S15: ^{1}H NMR spectrum of AuNPs with tetraethyleneglycol termini in $CDCl_3$ (δ ppm)

^{1}H NMR ($CDCl_3$, 250MHz): 7.53 (1H, C*H*-triazole), 4.69 (2H, triazole-CH_2-0), 4.35 (2H, CH_2-CH_2-triazole), 3.66 (12H, OCH_2CH_2O), 3.37 (3H, CH_3O), 2.66 (2H, CH_2S), 1.25 (18H, CH_2CH_2CH_2), 0.87 (3H, CH_2CH_3).

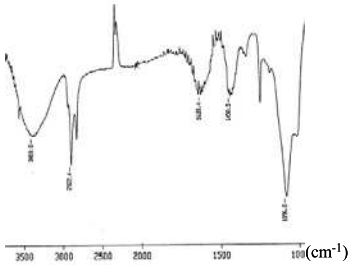

Fig. S16: IR spectrum of AuNPs with tetraethyleneglycol termini

Disappearance of the ν_{N_3}band at 2094 cm^{-1}

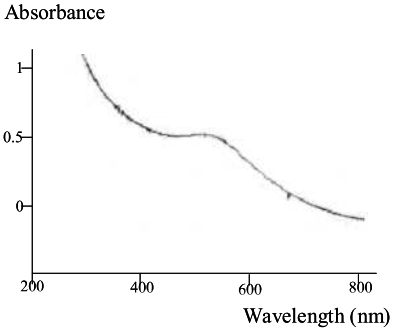

Fig. S17: UV-vis. spectrum of AuNPs with tetraethyleneglycol termini in CH_2Cl_2

Plasmon band of the AuNPs at 520 nm

8. Click chemistry with the triallyl aryl dendron

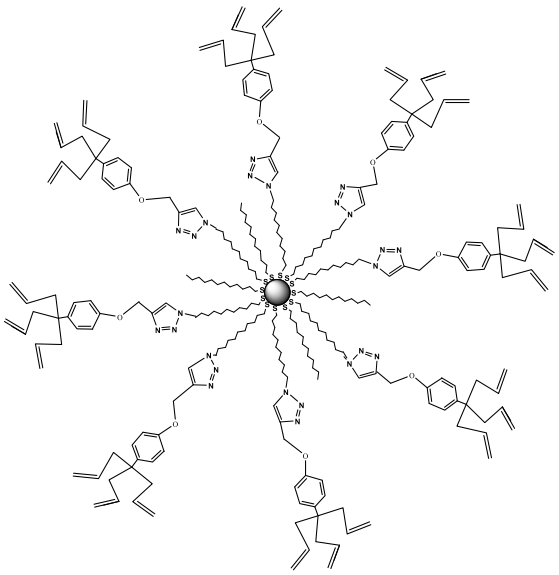

yield = 81%

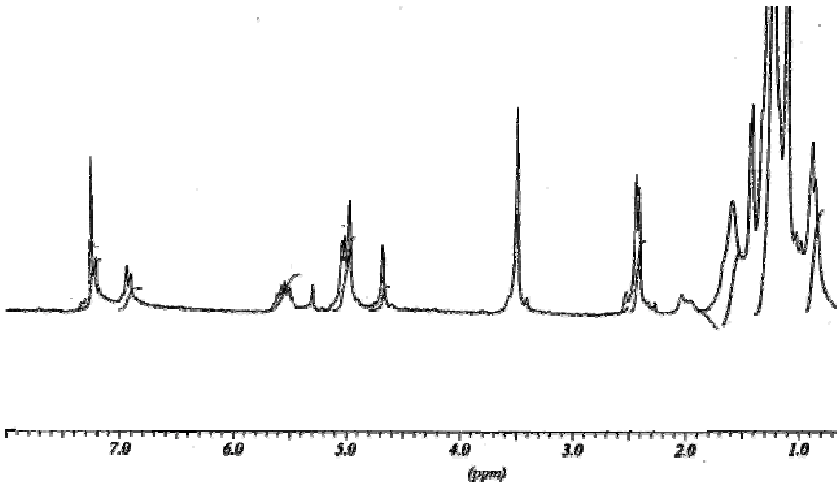

Fig. S18: ^{1}H NMR spectrum of AuNPs with triallyl aryl dendron termini in $CDCl_3$ (δ ppm)

^{1}H NMR ($CDCl_3$, 250MHz): 7.53 (1H, C*H*-triazole), 7.21 and 6.94 (4H, C*H* aromatic), 5.54 (3H, C*H* allyl), 5.01 (6H, CH-CH_2-allyl), 4.69 (2H, triazole-CH_2-0), 2.44 (2H, CH_2 allyl), 1.25 (18H, $CH_2CH_2CH_2$), 0.87 (3H, CH_2CH_3)

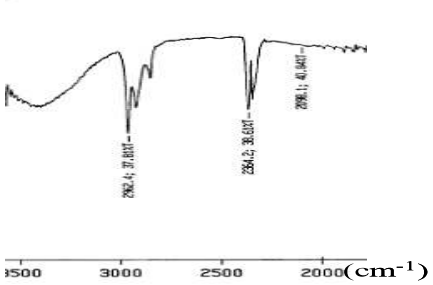

Fig. S19: IR spectrum of AuNPs with triallyl aryl dendron termini

Disappearance of the ν_{N_3}band at 2094 cm^{-1}

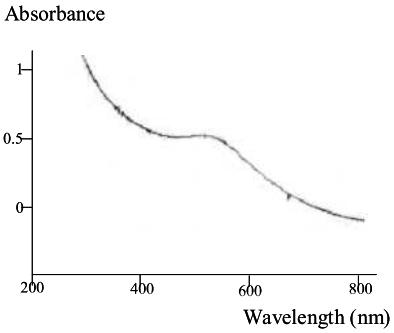

Fig. S20: UV-vis. spectrum of AuNPs with triallyl aryl dendron termini in CH_2Cl_2

Plasmon band of the AuNPs at 520 nm

9. Click chemistry with the short polyethyleneglycol (PEG) containing dendron

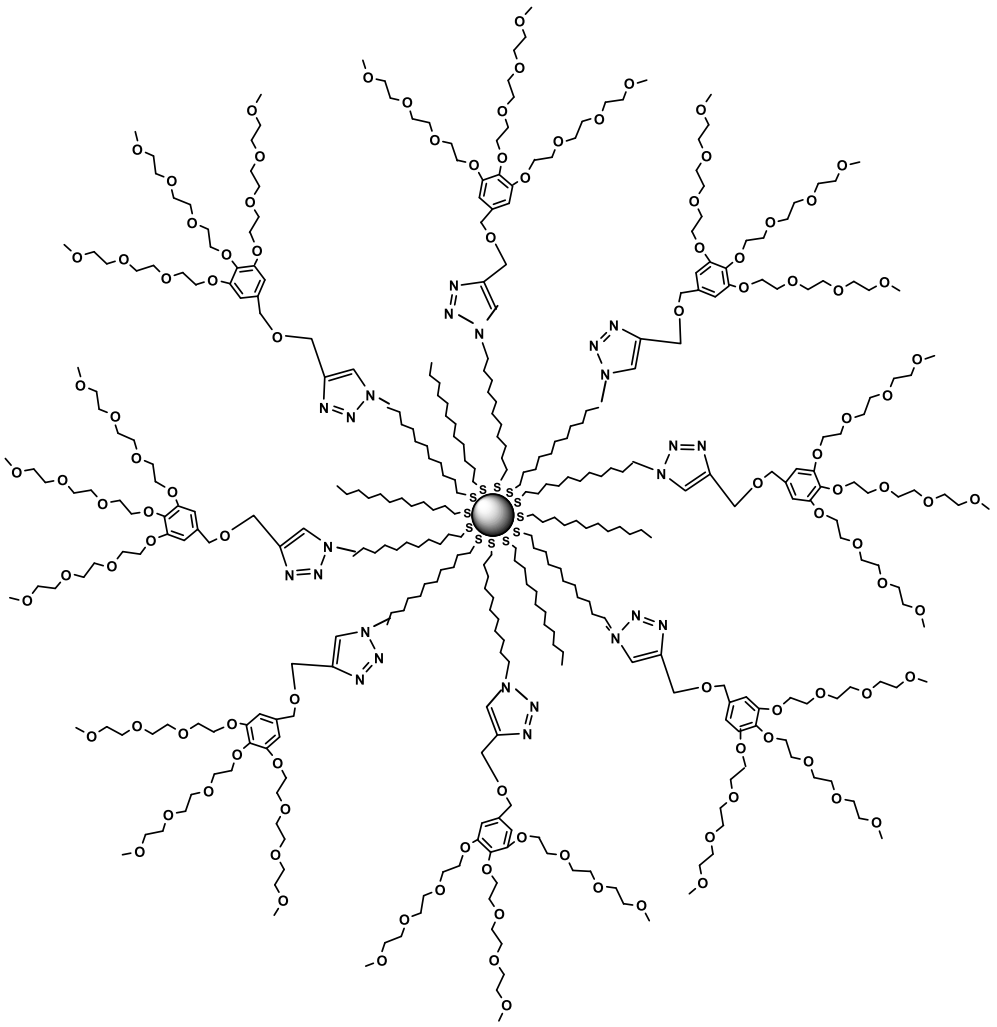

yield = 85%

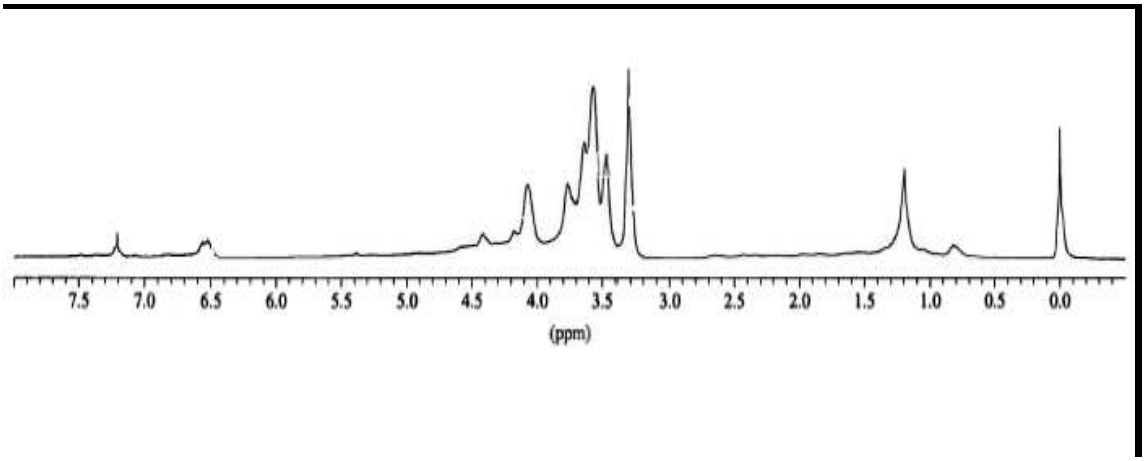

Fig. S21: ^{1}H NMR spectrum of AuNPs with short dendronic PEG termini in $CDCl_3$ (δ ppm)

^{1}H NMR ($CDCl_3$, 250MHz): 7.53 (1H, C*H*-triazole), 6.58 (2H, C*H*-arom.), 4.60 (2H, triazole-CH_2-0), 4.49 (2H, CH_2-CH_2-triazole), 4.14 (8H, OCH_2-arom. and arom-OCH_2CH_2), 3.66 (30H, OCH_2CH_2O), 3.37 (9H, CH_3O), 2.47 (2H, CH_2S), 1.25 (18H, CH_2CH_2CH_2), 0.87 (3H, CH_2CH_3).

Microanalysis: S (1.47%) ; Au (18.86%)

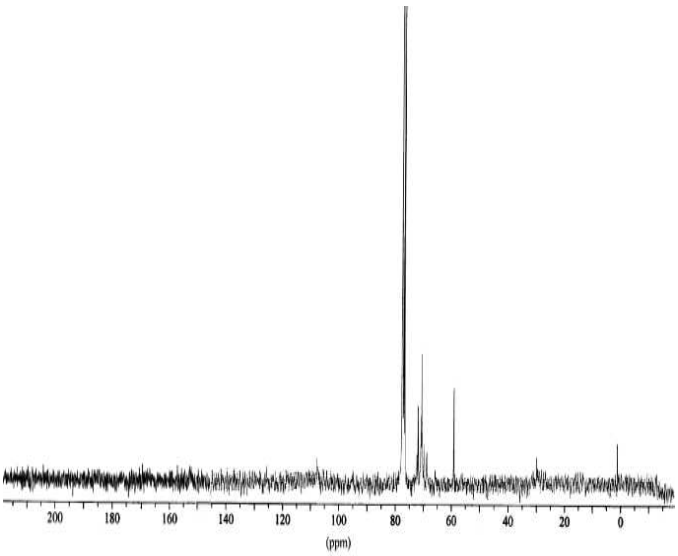

Fig. S22: ^{13}C NMR spectrum of AuNPs with short dendronic PEG termini in $CDCl_3$ (δ ppm)

^{13}C NMR ($CDCl_3$, 62 MHz):126.1 (*C*H of triazole and arom. core), 107.16 (C_qCH_2O), 70.39 (OCH_2CH_2O), 65.90 (triazole-CH_2-O), 58.91 (CH_3O)

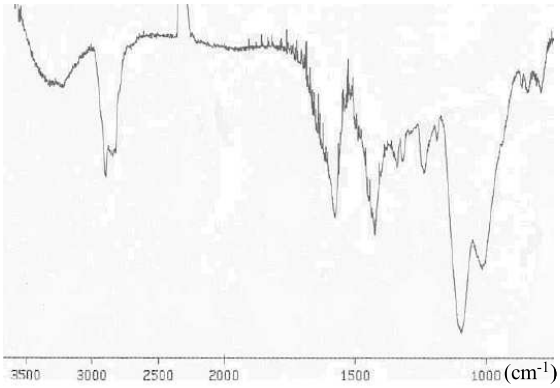

Fig. S23: IR spectrum of AuNPs with short dendronic PEG termini

Disappearance of the ν_{N_3}band at 2094 cm^{-1}

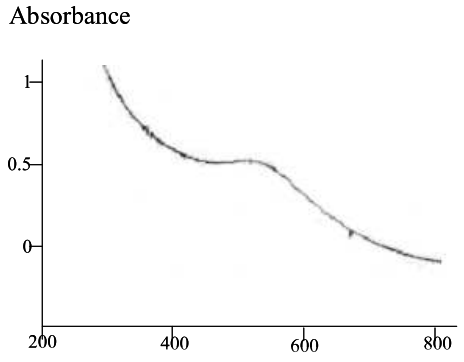

Fig. S24: UV-vis. spectrum of AuNPs with short dendronic PEG termini in CH_2Cl_2

Plasmon band of the AuNPs at 520 nm

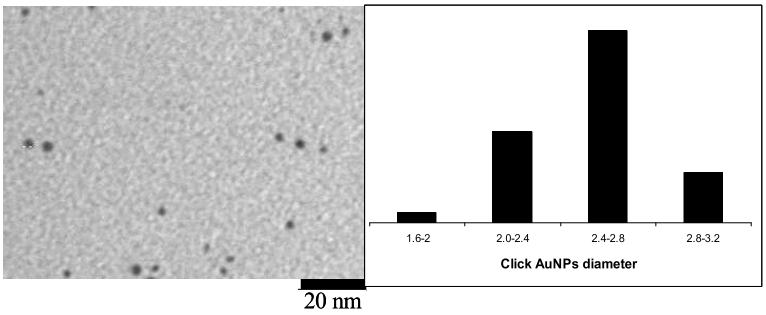

Fig. S25: TEM image of AuNPs with short dendronic PEG termini

diameter = 2.5 nm (± 0.3 nm)

10. Click chemistry with the long PEG-containing dendron

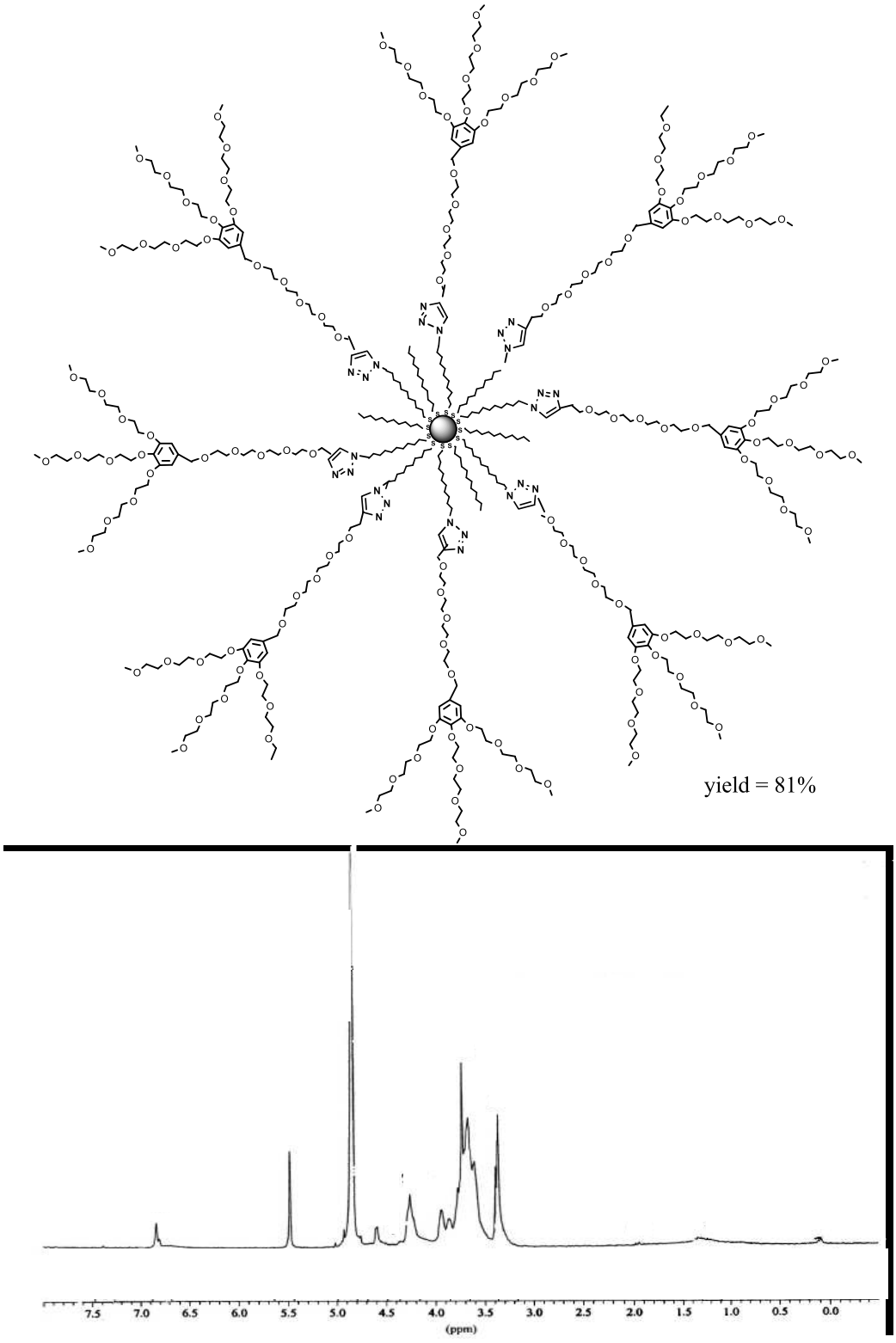

Fig. S26: ^{1}H NMR spectrum of AuNPs with long dendronic PEG termini in $CDCl_3$ (δ ppm)

^{1}H NMR ($CDCl_3$, 250MHz): 7.53 (1H, C*H*-triazole), 6.58 (2H, C*H*-arom.), 4.60 (2H, triazole-CH_2-0), 4.49 (2H, CH_2-CH_2-triazole), 4.14 (8H, OCH_2-arom. and arom-OC$H_2$$CH_2$), 3.66 (48H, OC$H_2CH_2$O), 3.37 (9H, C$H_3$O), 2.47 (2H, C$H_2$S), 1.25 (18H, CH_2C$H_2$$CH_2$), 0.87 (3H, CH_2CH_3)

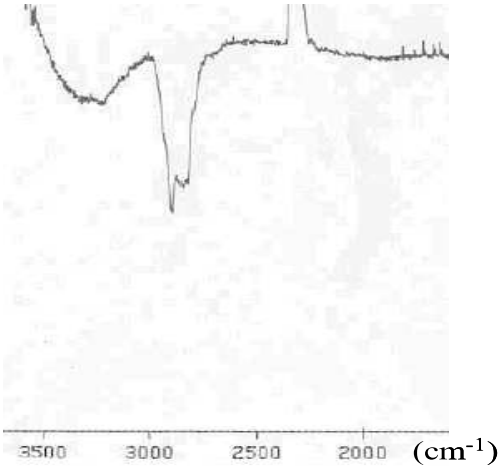

Fig. S27: IR spectrum of AuNPs with long dendronic PEG termini

Disappearance of the ν_{N_3}band at 2094 cm^{-1}

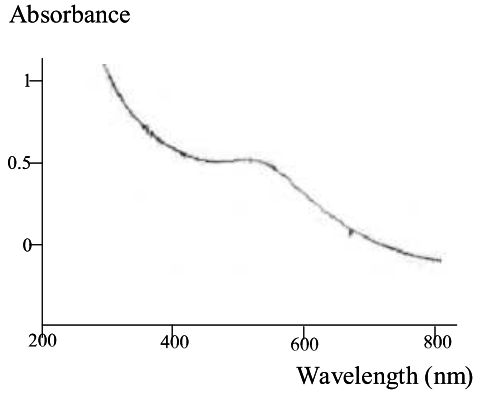

Fig. S28: UV-vis. spectrum of AuNPs with long dendronic PEG termini in CH_2Cl_2

Plasmon band of the AuNPs at 520 nm

11. Calculations of the diameters and molar masses of AuNPs

Diameter of AuNPs obtained by TEM before and after AuNP transformations: 2.5 nm (±0.3)

Number of gold atoms: $N(Au) = \frac{4\pi \times 12.5^3}{3 \times 17} =$ 481 gold atoms *per* AuNP

Elemental analysis : Au (18.86%); S (1.47%).

This leads to 230 S atoms *per* AuNP.

Each AuNP contains 72% (±3) of functionnalized ligand and 28% (±3) of alkyl thiolate ligands, i.e. 166±6 functionnal ligands (% obtained by peak integrations in the ^{1}H NMR spectrum); the molar mass (MM) of each AuNP is calculated using the following formula:

MM(AuNP) = MM(functionnalized ligand) x (230 x 0.72) + MM (alkyl ligand) x (230 x 0.28) + MM(Au) x N(Au)

	Dodecane-thiolate	Bromoundecane-thiolate	Azidoalkyl thiolate	Phenyltriazolyl derivative	Ferrocenyltriazolyl derivative	TEG derivative	Triallyl dendronic derivative	Short PEG-containing dendron	Long PEG-containing dendron
MM (thiolate ligand) (g.mol^{-1})	201	266	228	330	438	444	494	860	1036
MM (functionnalized AuNP) (g.mol^{-1})	140000	150000	145000	160000	180000	180000	190000	250000	280000

Using these results, equivalent numbers used for the synthesis of the AuNPs are calculated: approximately 2000 bromoundecanethiol *per* AuNP were used for the ligand exchange, and approximately 20 NaN_3 molecules *per* bromoundecanethiol were used for the azidation of the AuNPs.

CONCLUSION GENERALE :

L'utilisation des multiples ressources de la chimie au profit de la biologie est aujourd'hui d'un intérêt majeur au vue de la progression scientifique dans le domaine biomédical. En effet, il est nécessaire de trouver de nouvelles molécules biocompatibles capables de soigner des patients, d'imager des symptômes caractéristiques ou encore de vectoriser des médicaments afin d'optimiser leur effet thérapeutique.
C'est dans cet objectif que nous avons décidé d'étudier deux types particuliers de molécules organiques et inorganiques qui sont respectivement les dendrimères et les nanoparticules d'or. Ces deux familles de nano-objets sont très modulables grâce à un contrôle de la taille, de la solubilité et des fonctions périphériques qui permettent de créer des vecteurs remarquablement bien adaptés aux besoins.

Notre groupe de recherche développe la synthèse de nouveaux dendrimères ainsi que l'utilisation de ces nouvelles architectures moléculaires dans un plusieurs domaines (les capteurs, les batteries moléculaires, la reconnaissance moléculaire, les catalyseurs recyclables, …) y compris le domaine biomédical (complexes avec des plasmides ADN, transport de molécules à visée thérapeutique, …).
La plupart des travaux réalisés se situe essentiellement à l'intersection de deux applications potentielles des dendrimères développées dans notre laboratoire, à savoir les dendrimères solubles en milieu aqueux et la vectorisation spécifique de médicaments.
Différents types de molécules d'intérêt biologique ont été étudiés tels que les vitamines, les neurotransmetteurs ou encore des agents anti-cancéreux.

Les nanoparticules d'or sont, quant à elles, de plus en plus utilisées dans le domaine biomédical grâce à leurs propriétés particulières, notamment apportées par leur bande plasmon, ce qui les rend utilisables dans les domaines de l'imagerie, du diagnostic ainsi que de la thérapie. Plusieurs travaux portant sur leur synthèse, leur stabilisation, leur fonctionnalisation et le contrôle de leur taille ont été menés ce qui conduit aujourd'hui à la possibilité d'étudier l'efficacité, c'est-à-dire la cytotoxicité de ces nanoparticules. En effet, des tests de cytotoxicité de ces nanoparticules sont en cours et nous permettent d'être optimistes sur leur éventuelle utilisation dans le domaine biomédical. Ces études préliminaires d'encapsulation d'un agent anti-cancéreux prouvent non seulement la faible toxicité des nanoparticules d'or chargées envers les cellules saines et l'efficacité du médicament dans le "complexe".

Les perspectives de ce travail sont multiples et concernent essentiellement les domaines de la synthèse organique, inorganique ainsi que le domaine biochimique avec les études de toxicité pour déceler l'efficacité de nouveaux vecteurs que sont les dendrimres et nanoparticules d'or dont l'ingéniérie moléculaire aura été optimisée. De plus la chimie verte constitue l'un des objectifs principaux de notre groupe de recherche, ce qui caractérise bien ces vecteurs conçus pour être solubles dans l'eau. L'objectif de notre groupe est donc d'engager de nouveaux projets portant sur le transport de différentes molécules bioactives à l'aide de dendrimères et de nanoparticules d'or biocompatibles et efficace au plan thérapeutique.

Titre : Synthèse et fonctionnalisation de dendrimères et de nanoparticules d'or en vue d'applications biomédicales.

Résumé :

Plusieurs substrats issus de la chimie organique, inorganique et organométallique ont été synthétisés et fonctionnalisés avec différents groupes chimiques, notamment des polyethylene glycol qui leur permet d'améliorer leur solubilité dans l'eau et de les rendre biocompatible pour une éventuelle application dans le milieu biomédical. Ces substrats sont des dendrimères synthétisés sur plusieurs générations, des polymères obtenus soit par polymérisation d'un dendron soit par dendronisation d'un polymère, ou encore des nanoparticules d'or qui peuvent être stabilisées par des ligands thiolates ou bien par des dendrimères de manière intra- ou inter-dendritique. Ces nano-objets ont été designés dans l'objectif d'encapsuler, de stabiliser ou d'améliorer différentes molécules biologiques telles que des vitamines (vitamine C, B3 et B6) ou des neurotransmetteurs (acétylcholine et dopamine).

Mots clés : Dendrimères, Nanoparticules d'or, Polymères, Polyéthylene glycol, Synthèse, Fonctionnalisation, Encapsulation, Reconnaissance, Vectorisation, Biocompatibilité, Click, Métathèse, Vitamines, Neurotransmetteurs.

Title : Synthesis and functionnalization of dendrimers and gold nanoparticles for biomedical applications.

Abstract :

Several substrates resulting from the organic, inorganic and organometallic chemistry were synthesized and functionalized with various chemical groups, including polyethylene glycol which enables them to improve their water solubility and to make them biocompatible for a possible application in the biomedical field. These substrates are dendrimers synthesized for several generations, polymers obtained either by polymerization of a dendron or by dendronization of a polymer, or gold nanoparticules which can be stabilized by thiolate ligands or by dendrimers in an intra- or inter-dendritic way. These nano-objects were designed with the aim of encapsulating, stabilizing or improving various biological molecules such as vitamins (vitamin C, B3 and B6)or neurotransmitters (acetylcholine and dopamine).

Key words : Dendrimers, Gold nanoparticles, Polymers, Polyethylene glycol, Synthesis, Functionalization, Encapsulation, Sensing, Vectorization, Biocompatibility, Click, Metathesis, Vitamins, Neurotransmitters.

THÈSE

N° d'ordre : 4292

PRÉSENTÉE À

L'UNIVERSITÉ BORDEAUX 1

ECOLE DOCTORALE DES SCIENCES CHIMIQUES

Par Mme BOISSELIER MAILFAIT Élodie

POUR OBTENIR LE GRADE DE

DOCTEUR

SPECIALITÉ : CHIMIE ORGANIQUE ET INORGANIQUE

Titre : Synthèse et Optimisation de Dendrimères et de Nanoparticules d'Or en vue d'Applications Biomédicales.

ANNEXE

Chapitre A-1 : Revue sur les dendrimères et leurs applications

Dendrimers Designed for Functions : From Physical, Photophysical and Supramolecular Properties to Applications in Sensing, Catalysis, Molecular Electronics and Nanomedicine, *Chem. Rev.*, **2009**, soumis le 30 septembre 2009.

Dendrimers Designed for Functions: From Physical, Photophysical and Supramolecular Properties to Applications in Sensing, Catalysis, Molecular Electronics, Photonics and Nanomedicine.

Didier Astruc,* Elodie Boisselier, Cátia Ornelas
ISM, UMR CNRS N°5255, Université Bordeaux 1, 33405 Talence Cedex France
E-mél: d.astruc@ism.u-bordeaux1.fr

Content

4.10. Dendrimer- encapsulation and/ or stabilization of metal nanoparticles and quantum dots
4.11. Interactions of dendrimers on surfaces: self-assembled monolayers and surface patterning
4.12. Application of dendrimer films, membranes and surface interactions to gas sensors
4.13. Molecular imprinting inside dendrimers
4.14. Electron-transfer processes in dendrimers

5. Dendritic Catalysts: Dendritic Effects, Efficiency and Recycling
5.1. Introduction: basic concepts and seminal studies
5.2. Methods of separation/recycling
5.2.1. The classic laboratory method: precipitation
5.2.2. Solid supports
5.2.3 Biphasic catalysis
5.2.4. Membrane nanofiltration
5.3. Catalysis with metallodendritic complexes
5.3.1.1. Palladium complexes
5.3.1.1. Pd-catalysed carbon-carbon bond formation: Heck, Suzuki, Sonogashira and Stille coupling
5.3.1.2. Hydrogenation, hydrovinylation, polymerization and copolymerization of olefins
5.3.1.3. Allylic substitution
5.3.1.4. Other Pd^{II}-catalysed reactions
5.3.2. Rhodium complexes
5.3.3. Ruthenium catalysts
5.3.3.1. Olefin metathesis catalysts
5.3.3.2. Hydrogenation catalysts
5.3.3.3. Electron-transfer-chain catalysis
5.3.4. Other transition-metal catalysts
5.4. Organocatalysis
5.5. Catalysis with dendrimer-encapsulated and dendrimer-stabilized nanoparticles
5.5.1. Single-metal based nanoparticles in homogeneous catalysis
5.5.1.1. Selective hydrogenation
5.5.1.2. Nitroarene reduction
5.5.1.3. Pd-catalyzed heterocoupling
5.5.2. Heterobimetallic nanoparticles in homogeneous catalysis
5.5.2.1. Characterization of heterobimetallic nanoparticles
5.5.2.2. Selective hydrogenation
5.5.2.2.1.Alloys
5.5.2.2.2.Core-shell
5.5.3. Dendrimer-encapsulated nanoparticles in heterogeneous catalysis
5.5.3.1. Methods of DEN immobilization and dendrimer removal
5.5.3.2. Electrocatalytic O_2 reduction
5.5.3.3. CO oxidation
5.5.3.4. Ethylene hydrogenation
5.5.3.5. Nitrile hydrogenation
5.5.3.6. Ethane hydrogenolysis
5.5.3.7. Photocatalysis with TiO_2 NPs

6. Biomedical Applications
6.1. Drug delivery
6.2.1. Drug solubilization by encapsulation: drug-dendrimer "complexes"
6.2.2. Covalent drug binding to dendrimer termini: drug-dendrimer "conjugates"
6.2.3. PEGylated dendrimers as biocomptabible drug nanocarriers
6.2.4. Folate : a major tumor recognition group in drug-dendrimer conjugates
6.2.5. Glyco- and glycopeptide dendrimers : anti-bacterial anti-cancer and anti-viral agents using the "cluster effect" and antigen-antibody interactions
6.2.6. Peptide dendrimers for antiangiogenic therapy

1. Introduction, Scope and Organization of the Text

Dendrimer chemistry[1-2] is largely relying on supramolecular properties.[3] Since the pioneering work on iterative reaction sequences[4,5] and dendrimer syntheses,[6-8] the supramolecular dendritic aspects[8-10] have been extended to the macromolecular nanoscale.[9] In this review, we focus on the functions and applications of dendrimers resulting from supramolecular and physical properties. We will not address the synthetic aspects that have been the subject of many reviews.[9-46] During the early days, the properties of dendrimers were first examined with PAMAM dendrimers [7,9,17] and arborols (molecular micelles),[8,14-16] then with polypropylelene imine (PPI dendrimers)[10,12,13,22] that are, as the PAMAM dendrimers, commercial, and with polyether dendrimers.[23-26] The spectrum of dendrimer families is now very broad,[10-27] so that there are large possibilities of molecular engineering in order to obtain a desired function (Chart 1). Books on dendrimers have been published,[1,2,11-13] and the dendrimer literature is huge.[9-46] Thus, since topics of synthetic interest have already been addressed early on, we will concentrate our attention on the most powerfull concepts of dendrimer chemistry in terms of functions and potential applications. We will especially emphasize dendritic effects whenever they are known. We will quote the seminal reports, the review articles and will review essentially the most recent work even if the major concepts will be recalled. Dendrons bonded to polymers were called dendronized polymers[47] and disclose properties relevant to those of dendrimers and will be discussed whenever a specific function or application is involved. Dendritic polymers, pioneered by Flory,[48] are useful alternatives to dendrimers that are commercially of great interest and can sometimes show closely related properties for functions. They are not included here unless they fall in the dendrimer context, but reviews are available.[48-49] Most application of the physical and photophysical properties (§ 3) of dendrimers are in catalysis (§ 5), nanomedicine (§ 6) and sensing (§ 3.16, 4.12, 6.9), but optoelectronic applications also appear throughout § 3.

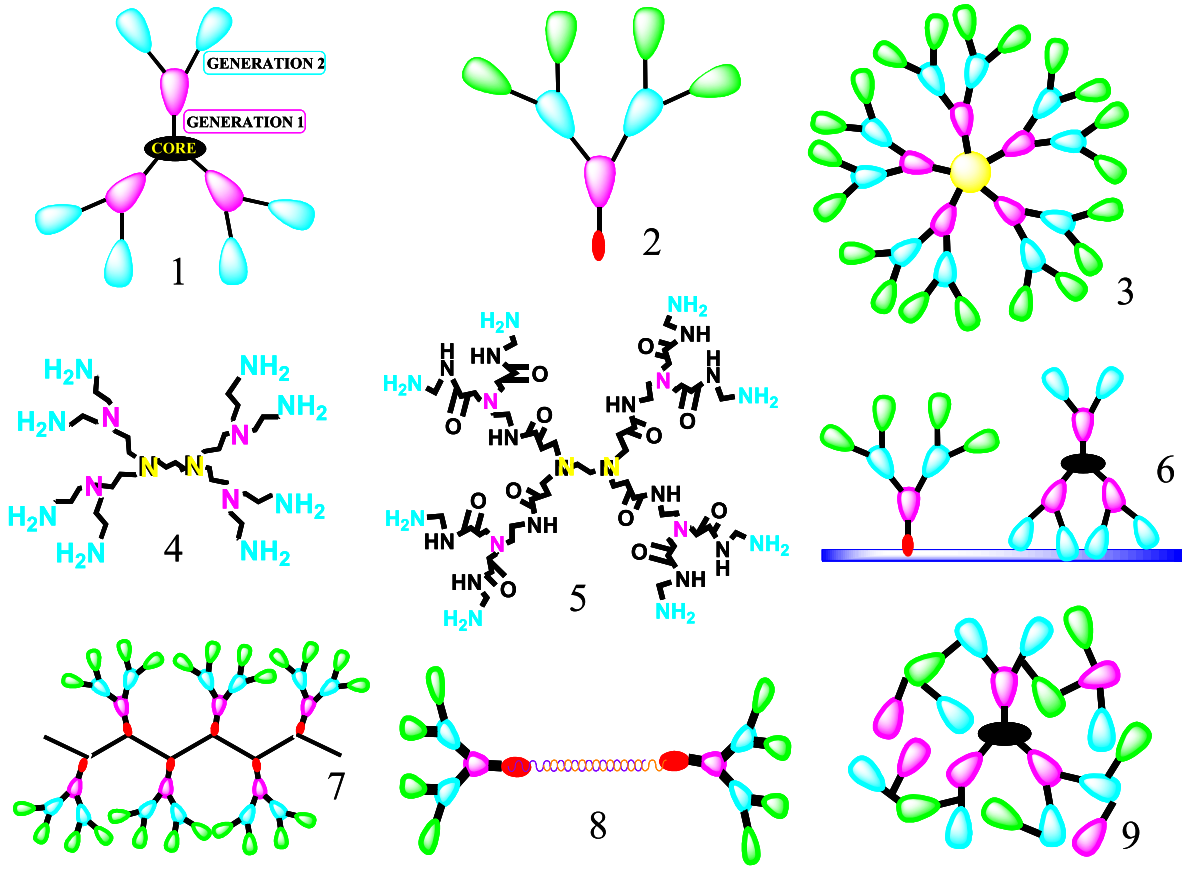

Chart 1. Schematic representations of dendritic structures:1: dendrimer; 2: dendron; 3: dendritic nanoparticle; 4: DAB dendrimer; 5: PAMAM dendrimer; 6: dendronic and dendritic surface; 7: dendritic polymer; 8: dendriplexe; 9: dendrigraft.

2. Dendritic Structures and Physical Properties

2.1 Simulation *vs.* experiment: localization of the terminal groups

The well-known de Gennes dense-packing model has dominated the attention for about two decades. It predicted that surface congestion occurs at the periphery of a dendrimer after a certain generation. The surface area A_Z is given by equation 1 in which Z is the number of terminal groups, A_D the total surface of the dendrimer, N_Z the number of surface groups *per* generation, r the radius of the dendrimer, N_C the number of core branches, N_b the number of branches at each generation, and G the number of generations.

$$A_Z = A_D N_Z (r^2/N_C.N_b.G) \quad (1)$$

This means that A_Z decreases as the number of generations increases. The dense-packed generation G_l is reached when A_Z reaches the cross-sectional area corresponding to the van der Waals radii. A simple equation was provided for PAMAM dendrimers having a branch-cell segment P.:

$$G_l = 2.88(\ln P + 1.5) \quad (2)$$

According to this equation, the dense packed generation is reached between 10 and 11.[50] Other theoretical studies have concluded differently. For instance, it has been suggested that the most probable conformation has its maximum density in the center of the dendrimer.[51] Indeed, the "dense-core" approach appeared since 1990.[52] Such an overall structure is an average of a large number of possible conformers. Such theoretical calculations are in agreement with the fact that flexible dendrimers would be characterized by a surface and internal holes. A survey of a large number of theoretical studies has recently appeared, converging towards this latter analysis.[53] This implies that the end groups of dendrimers backfold towards the center. For PAMAM dendrimers, such backfolding has been considered

despite the interchain H-bonded termini that contribute to minimizing this back bonding. ^{13}C NMR relaxation studies (G_0 to G_{10}) suggest that the chain termini are not densely packed at the surface of G_{10} bearing a theoretical number of 3072 terminal branches. Examination of CPK models[10] shows a maximum radius of 71Å whereas the SEC experiments indicate an actual radius of 62Å. At full extension, each terminal group needs a surface area of 21Å, but only 16Å is available, which suggests some backfolding.[44] The dynamics of PAMAM dendrimers was recently made available by the use of dielectric relaxation spectroscopy (DSR) showing different relaxation behavior below and above the glass transition temperature T_g that is around -30°C.[45] Untill recently, the syntheses of dendrimers did not overtake the de Gennes dense packing limit, however. Syntheses of dendrimers far beyond the de Gennes "dense packing" limit has been reported in 2004 till the 9th generation[54] with a theoretical number of 3^{11} = 177 147 allyl branch termini using a Newkome-type 1→ 3 connectivity (Figure 1).[7,10] At the ^1H NMR accuracy (i. e. approx. 97%), all the reactions appeared to be completed whereas the de Gennes dense-packing limit was below generation 6 (3^8 = 6561 termini). AFM and TEM experiments for the highest generations showed a steady growth with increase of the generation number. Since these giant dendrimers have small methylene termini, severe backfolding is necessary, so that the limit of construction is dictated by the dendritic volume rather than by the surface of the de Gennes model.

Computer-assisted molecular modeling initially showed that the PAMAM dendrimers are spherical above generation 4, but have hemispherical domes below this generation. The surface congestion was confirmed by viscosity and refractive index experiments that reflected the reduced interaction between the surface groups and the solvent above generation 4.[8] The only experimental tools available to analyze the spatial structure of dendrimers in solution are scattering methods such as small-angle neutron scattering and small-angle X-ray scattering,[55] but the information obtained is limited.[56-59] Combining scattering and theoretical simulation methods converged to satisfying conclusion, however.[56-61] A common feature of all generations is the strong backfolding of the terminal groups, a tendency that grows with increasing the generation number. As noted early on,[8] most of the surface of high-generation dendrimers lies inside the dendrimer, and construction beyond the dense-packing limit proceeds in the dendritic interior, which is confirmed by slow kinetics.[54] The size of the end groups plays a key role in termini back-folding, the ability to backfold being all the more reduced as the termini are larger.[64] Charged dendrimers expend with maximum size occupancy compared to uncharged ones,[8,65] although this trend has also been controversed (Figure 1).[62,63,66,67]

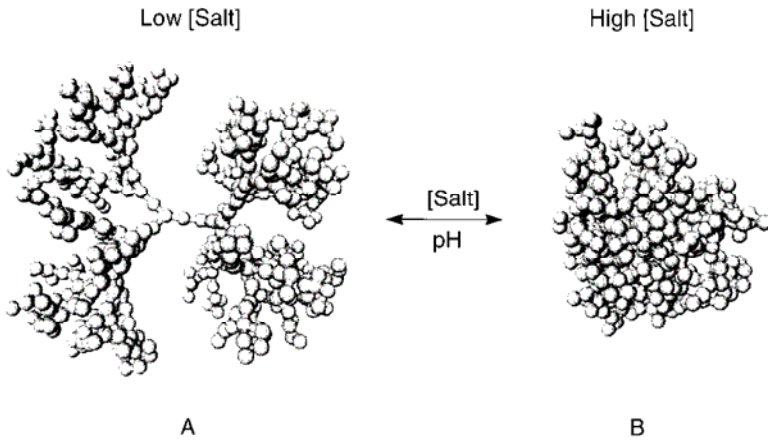

Figure 1. (A) Hollow core, "dense shell" picture. (B) "Dense core" picture. These are representative snapshots from the statistical ensembles generated in this study for the sixth generation with two springs between branch points. Reprinted with permission of the American Chemical Society (ref. 65, Muthukumar's group).

For instance, SANS studies of the counterion effects on the molecular conformation and structure of charged G_4-PAMAM dendrimers in aqueous solutions show that strong repulsion is introduced by protonation of the amino groups deeply modifying the internal dendrimer structure, although the gyration radius R_G only changes by about 4% when the *pD* value varies from 10.25 to 4.97.[60] The solvents also influence R_G; for instance with $D(CD_2)_mOD$, R_D of G_8-PAMAM is reduced by 10% changing the solvent from m = 0 to m = 4.[60,61] With Newkome-type dendrimers containing carboxylate termini, SANS studies showed that addition of a salt suppressed the inter-dendrimer interactions, and that accumulation of tetramethylammonium counterions occurs around the surface with a counterion thickness between 4 and 6Å.[62] Capillary electrophoresis studies showed that the effect of an electric field increased the mobility of these dendrimers.[63]

Local dendrimer dynamics including local motion has been compared to supercooled liquids and linear polymers,[68] including glass transition aspects.[69] A hybrid approach involving both a single-chain Monte Carlo simulation and DFT calculation of the Helmholtz energy allowed to investigate the microscopic dendrimer properties.[70] The shape of dendrimers was related to the shear viscosity using nonequilibrium molecular-dynamics simulations.[71] Atomistic molecular dynamics simulations were applied to negatively charged PAMAM dendrimers with sodium counteractions, indicating that the charge effect on conformations is more pronounced for low generations than for large ones.[72]

A Brownian dynamic study indicates how the adsorption of charged dendrimers can be tailored by changing various parameters.[73] The rigid polyphenylene dendrimers do not present the possibility of backfolding terminal groups contrary to the flexible dendrimers (Figure 2).[35]

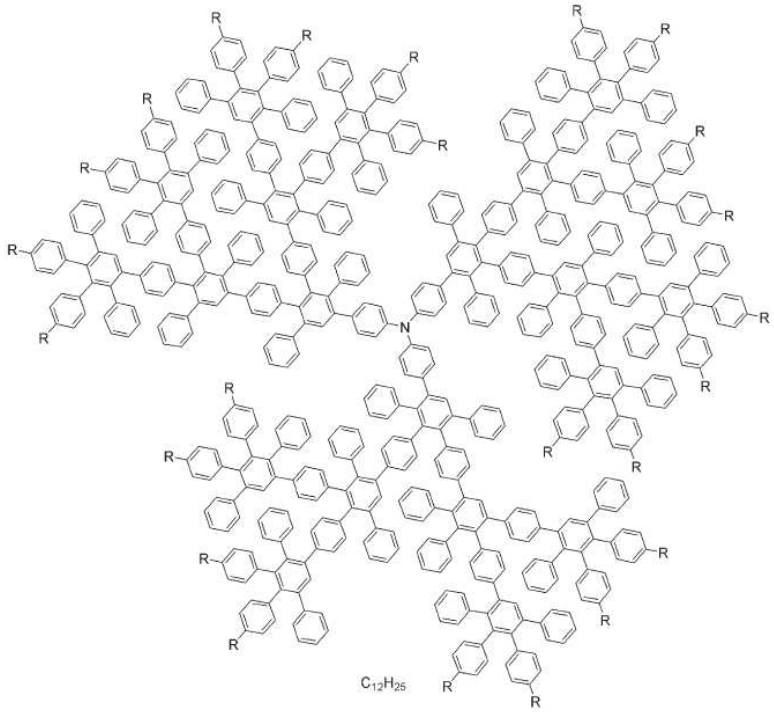

Figure 2. Third-generation dendrimer with a triphenylamine core. Reprinted with permission of the American Chemical Society (ref. 411, Müllen's group).

This remarkable family has been the subject of recent simulations using atomistic molecular dynamics,[74] molecular modeling,[75] and polymer reference interaction site model integration theory.[76] The effect of repeat dendrimer unit flexibility on conformation was studied by atomic molecular dynamic simulations, which showed that all dendrimers are radially distributed throughout their interiors due to backfolding for flexible dendrimers or to branching angle effects for stiff-chain polyphenylene ones.[77]

In azobenzene-terminated dendrimers, UV irradiation causes changes in the shape and size of the dendrimers due to the chromophore units that reversibly photoisomerize E → Z.[12,13] In ferrocenylazobenzene-terminated dendrimers, this reversible photo-isomerization provokes a generation-dependent size change that could be monitored by cyclic voltammetry, because the diffusion-coefficient dependent intensity increases upon E → Z irradiation due to dendrimer size decrease. This effect is all the more marked as the generation is higher.[78]
A strong correlation was established between the solvent polarity and the mean radius of gyration.[79] For instance, simulations with dendritic polyelectrolytes indicate a dramatic contraction upon increasing the ionic strength of the solvent,[80] and a similar effect was demonstrated with PPI dendrimers upon addition of a salt.[22]
Experimentally, backfolding of the dendritic tethers was initially shown in the flexible Fréchet-type polyarylether dendrimers using SEC coupled with differential viscosimetry (viscosity reaches a maximum as a function of generations),[81] rotational-echo-double-resonance NMR (REDOR),[82,83] spin relaxation (T_1) with a paramagnetic core,[84] and fluorescence depolarization using rubicene cores.[85]
On the other hand, Percec-type dendrimers containing perfluorinated[86] or perhydrogenated[87,88] tethers were shown by X-ray diffraction to present solid-state assemblies precluding backfolding (Figure 3).[89]

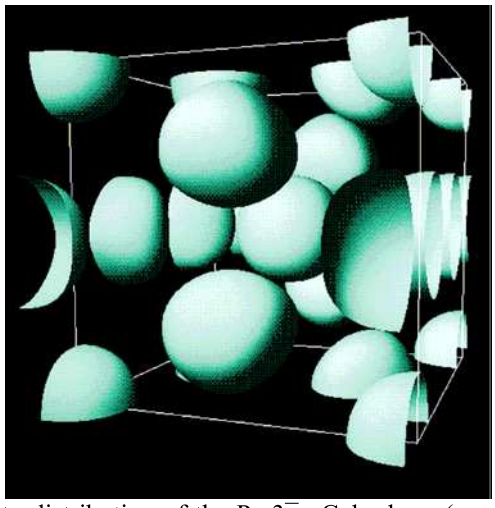

Figure 3. The 3D electron density distribution of the $Pm3^{-}n$ Cub phase (a = 79.2 Å at 80°C) of the spherical supramolecular dendrimers self-assembled from 16 monodendrons. These isoelectron surfaces were generated from XRD by Fourier synthesis with the structure factor phases determined by TEM. Reprinted with permission of the American Association for the Advancement of Science (ref. 89, Hudson's group).

Many studies carried out with PAMAM dendrimers (SEC, viscosity, ^{13}C NMR relaxation, ^{2}H NMR, SAXS, SANS, photophysical and ESR), reviewed elsewhere,[8,19] have shown that the interbranch terminal H-bonded groups preclude backbonding (confirming the validity of the de Gennes model in this case) to a certain extent, the conclusions being variable among the studies.[90-93] Likewise, the degree of inter-branch H-bonding in PPI dendrimers was shown to grow with increasing the generation numbers, and these studies (IR and NIR)[94] have been reviewed.[22]
PPI dendrimers terminated with CN and palmitoyl groups were studied by translational diffusion and viscosimetry. Their volumes was shown to increase proportionally with the number of end groups, meaning that these end groups were predominently located at the dendrimer periphery (due to H-bonding between CN and NH groups and possible repulsion between the palmitoyl groups and the core).[95] The translational diffusion coefficient D is a hydrodynamic characteristic sensitive to the dendrimer size, with a linear correlation :

$M[\eta] \sim D^{-3}$, $[\eta]$ being the intrinsic viscosity, and the hydrodynamic radii R can be calculated from D according to the Stokes-Einstein equation :

$R_D = kT/6\pi\eta_0 D$

or from vicosimetric data and molecular weight according to the equation :[96]

$R_\eta = (3/10\pi N_A)^{1/3} (M[\eta])^{1/3}$

The comparison between the physical properties of dendrimers and polymers shows the specific structure and behavior of large dendrimers, with trends clearly demonstrated in the pioneering work by Hawker.[81,97-101] For instance, large dendrimers are most often globular (except specifically designed Percec dendrimers), and the influence of terminal groups is crucial on the physical properties, whereas this influence decreases with increasing molecular weight for linear polymers. Thus, contrary to linear polymers, the intrinsic viscosity of large dendrimers is very dependent on the nature of the end groups and is not increasing with molecular mass, but has been reported for the main dendrimer classes to reach a maximum at a certain generation.[8,22,81] Polyester dendrimers were shown to be soluble in a large variety of organic solvents contrary to linear polymers. The reactivity of end groups is higher with large dendrimers, because they are more numerous and not so shielded as in linear polymers , and because dendrimers are more soluble than polymers. The hydrodynamic volume of large dendrimers is smaller than that of linear analogues, because dendrimers are more compact (with backfolding of termini) than polymers (Figure 4).[97-101]

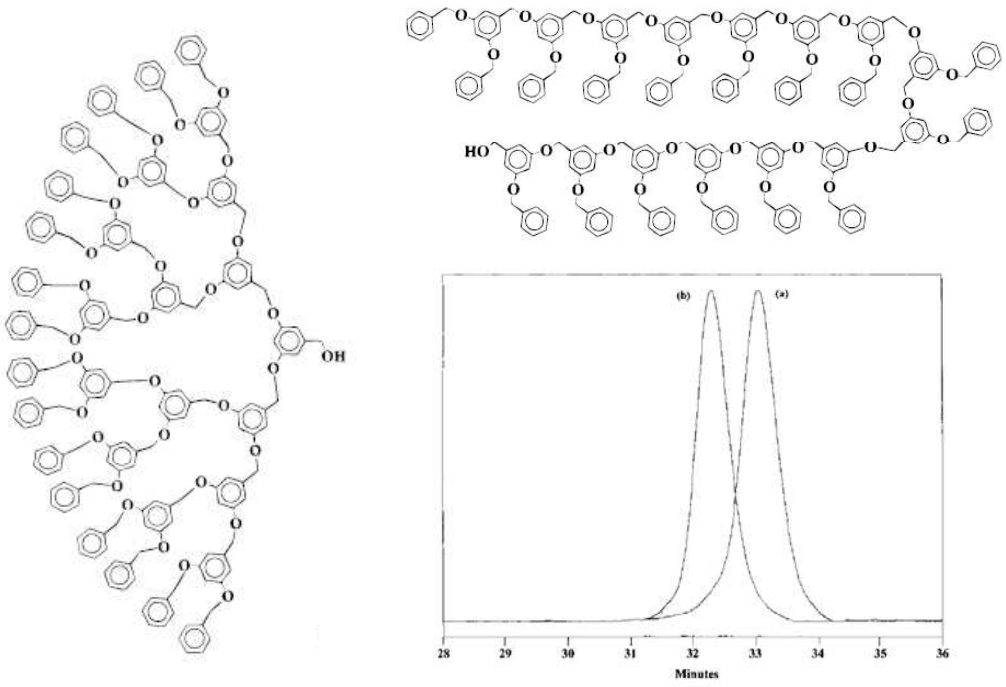

Figure 4. Comparative structures of the fourth-generation dendritic alcohol and its exact linear analogue; GPC traces for the (a) fifth generation dendritic alcohol, and (b) the corresponding exact linear analogue. Reprinted with permission of the American Chemical Society (ref. 97, Hawker's group).

Self-folding of charged dendronized polymers was shown for G_2- and G_3-polyamide-polyether dendronized polymers with aminopropoxybenzoic methacrylate cores and neutral and negatively charged peripheral groups.[99,100]

In conclusion, the specificity of dendrimers compared to linear polymers appears at high generation, with severe property change above a certain generation.[8,22,97] This trend also clearly appears from photophysical studies that are the subject of the forthcoming section. Molecular dynamic and mean field theory studies also indicate that, in polyelectrolyte dendrimers, electrostatic interactions are strongly screened, the dendrimer core being filled,

with very weak conformation dependence on ionic strength.[98] Conformational changes in dendrimers were shown by bare Coulomb interactions to be induced by charges. The presence of charges leads to an increase in the dendrimer size due to the combined effect of electrostatic repulsion and the presence of counterions within the dendrimer. Accordingly, the bond lengths near the dendrimer center increase to facilitate a more effective usage of space in the region of the dendrimer periphery.[99,100] G_3 and G_4-poly(aryl ether) dendrimers containing a naphthyl group as the core were shown by fluorescence measurements in dichloromethane-acetonitrile to form an intramolecular exciplex between the naphthyl core and benzyloxy backbone units (resulting from photo-electron transfer) that validate exciplex formation enhancement by backfolding conformation of the dendrimers.[101]

2.2. Gelation of dendrimers

From the initial publication, Newkome-type arborols were designed as water-soluble dendritic micelles with hydrophobic interiors and water-solubilizing alcohol termini.[7,102] Such or closely related structures are susceptible to gelation as shown with the [9]-10-[9] dendrimer for which negative staining TEM revealed the presence of fibers.[103,104] In these dendritic structures, the core is a polymethylene chain of variable length. The gel is dried, then coated with phosphotungstic acid solution prior to TEM visualisation. Static and dynamic light scattering and viscosimetry were also used to study gelation of these dendrimers.[105] Gelation usually requires 5-10 min. and can be reversed by heating. Differential scanning calorimetry shows the transition point, and freeze-fracture TEM of the arborols shows the fiber-like texture.[106] A variety of gelating dendritic structures were subsequently synthesized based on Newkome's concept of linear chain (that sometimes is a polyethylene glycol chain, or a molecular wire[107]) separating two covalently bound dendronic units, sometimes called "two-component" dendritic gels (Figure 5).[108]

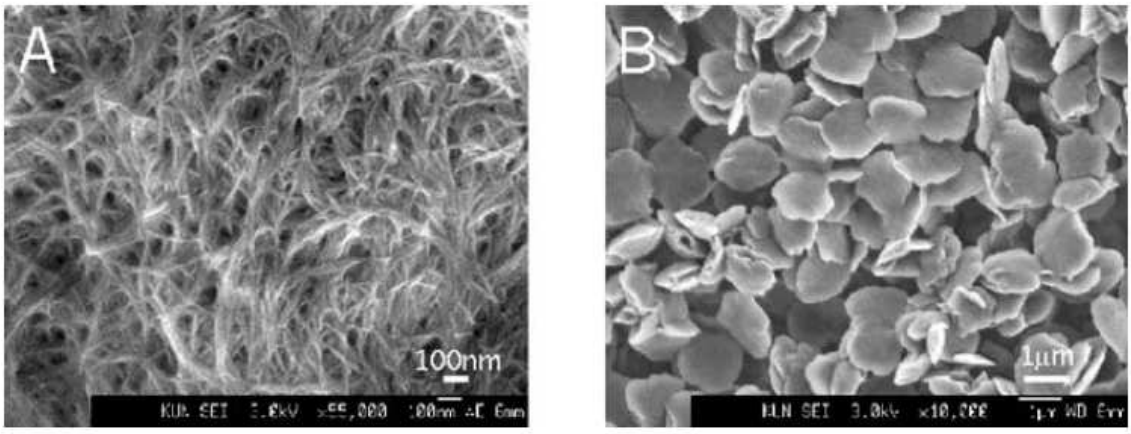

Figure 5. The nanoscale morphology observed using SEM for the two-component gelation system. a = 2 : 1 dendron:diamine ratio. b = 1 : 4.5 dendron:diamine ratio. Reprinted with permission of the American Chemical Society (ref.108, Smith's group).

On the other hand, other denditic gels with a polymeric and dipeptide component bound to a dendron were reported by Stupp's group[109] and Aida's group[110] respectively. In the latter case, dipeptide rather than monopeptide, ester functionalities on the dendron surface, and higher-generation dendrons favored gelation. In a recent study, glycine and L-glutamic acid have been used as cores to form dendritic gels, with gelation properties increasing from the first to the third generation. Hydrogen bonding and π-π stacking were the main driving forces to form the fibrous networks at low concentrations (0.5%), as shown by TEM, AFM, fluorescence, IR, CD, ^{1}H NMR, small-angle X-ray statterring (SAXS) and wide-angle X-ray diffraction.[111] Alltogether, dendritic gels benefit from strong fibrous assemblies resulting from multiple dendronic branch interactions, steric role in the formation of one-dimentional

assemblies, and multiple-site crosslinking units for crosslinked dendronized polymer gels.[108] Butyl-terminated poly(amidoamine) dendrons with either a Boc group or a carbonyl group at the focal point formed dendronic gelators with lamellar structures of 30-100-nm size as shown by TEM, WAXD, SAXS, NMR and FTIR spectroscopy. The nature of the focal group impacted greatly on the gelation ability, and dendron generation increase favored gelation. Hydrogen-bonding and hydrophobic forces were shown to be the main driving forces for the fibrous assembly.[112,113] Dumbbell-shaped dendrimers with a *p*-terphenylene core with bulky dendronic wedges self-assembled, forming gels with elastically interpenetrating 1-dimensional nanostructures in several organic solvents through cooperative π-π stacking, hydrogen bonding and van der Waals forces.[114]

2.3 Dendrimer-polymer blends and aggregates

Promising possibilities of coupling the physical properties of polymers and dendrimers led to studies of blended materials such as dendrimer-hyperbranch polymers,[115,116] polystyrene-polyphenylene hyperbranched structures,[117] aryl ester dendrimer-bis-phenol polycarbonate[118] and 12-*tert*-butyl ester dendrimer-poly(methyl methacrylate) (PMMA).[119] Glass transition temperatures (T_g) are found between those of the components. The methods used for these sudies are viscosity, refractometry, UV-vis and FTIR spectroscopies, DSC and DEA.[119] Copolymers based on polyether dendrimers and polyethylene glycol (PEG) form micelles in methanol/water.[120] Polystyrene-PPI dendrimers are amphiphilic and aggregate in water, forming vesicles, micellar rods or spherical micelles depending on the dendritic generation.[121] Block co-polymers assembled from polyether dendrimers and thermoresponsive polar poly(N-isopropylacrylamide) self-assemble in aqueous solution into bilayer spherical aggregates.[122,123] Dendrimer-rod-coil incorporating a dendritic block at the end of a rod segment formed self-supporting gels in dichloromethane at concentrations down to 0.2 wt %, observed by TEM and AFM. They self-assemble into flat or helical ribbons and can incorporate electronically conductive groups and can be mineralized with inorganic semiconductors (Figure 6).[124-127]

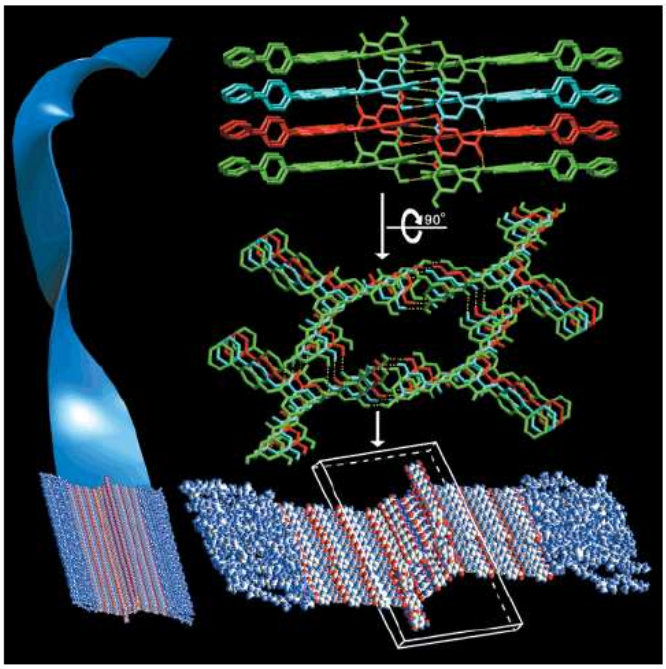

Figure 6. Side view of the ribbonlike structure taken directly from the crystal structure of a dendrimer shows color-coded hydrogen-bonded tetramers (upper right) stacked on top of each other along the direction of the crystal (top view is shown in the middle right). Schematic (left and bottom right) representation of the proposed structure for a DRC nanoribbon. Reprinted with permission of the American Chemical Society (ref. 124, Stupp's group).

2.4 TEM, AFM and studies on surfaces

The behavior of dendrimers on surfaces and in amphiphilic materials has been reviewed in 1999.[22] PAMAM (most frequently),[8] Newkome-type,[128] phosphorus,[129] carbosiloxane[130] and polyphenylacetylene[131,132] dendrimers have been examined by TEM or cryo-TEM with the observation of aggregation when intermolecular H-bonding occurs (carboxylic acid or hydroxy end groups).[10,14-16,22] Spherical shapes were observed for large dendrimers as expected. Sodium phostungstate was used for amine terminated large PAMAM dendrimers (15 nm radii for G_{10}).[133] Gold phosphine-terminated dendrimers with up to a theoretical number of 3072 end groups were recorded with up to 15 nm diameter.[129] Monolayers are usually observed on surfaces, but multilayer films of oppositely charged PAMAM ($-NH_3^+$ and CO_2^- termini) were also shown.[134] Wetting of mica surface was observed when hydroxyl groups preferentially adsorb on the surface. Flexible dendrimers such as PAMAM ones flatten on surfaces (Figure 7).[135] AFM observation of the PPI dendrimer G_2-DAB hydrophobically modified with dodecanoyl end groups deposited on mica by adsorption from solution shows that, after 20 s, the dendrimer formed a sub-monolayer thin film that contained many fractal aggregates that were larger than 1 μm and 0.8 nm thick. After longer time, the initial fractal aggregate transformed into disks and other less branched shapes with average heights of the domains of 0.6 nm and 0.4 nm respectively.[136]

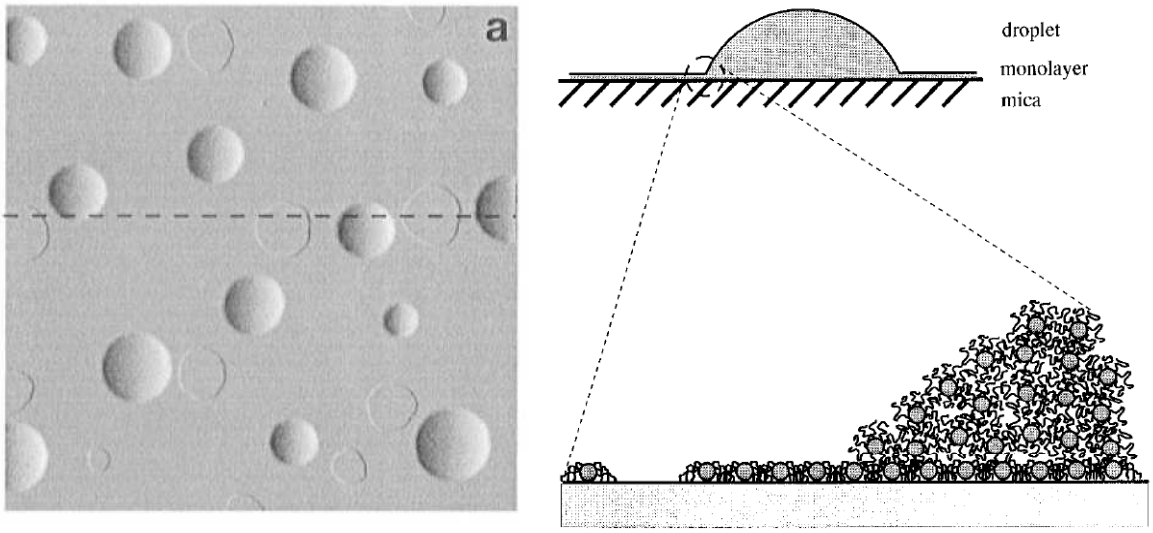

Figure 7. Amplitude (a) micrograph demonstrating autophobic wetting of the mica surface by the carbosilane dendrimer with hydroxyl end groups. Fluid droplets with a contact angle of about 8.7° were observed.
Two-dimensional sketch of the autophobic spreading of the carbosilane dendrimer on mica. Due to the preferential adsorption of the end OH-groups on the surface of mica, the hydrocarbon core gets exposed to air. The picture is consistent with scanning force microscopy studies and molecular dynamic simulation of the dendrimer on mica. Reprinted with permission of the American Chemical Society (ref. 135, Sheiko's group).

Fréchet-type polyether,[137,138] PAMAM,[139] PPI[140] and dendrimers functionalized with various groups have been examined at the air-water and Langmuir-Blodgett interfaces resulting in deformation of the dendrimers at the interfaces. With mesogenic functionalities, liquid cristalline (nematic or smectic) were obtained with sheetlike conformations.[141,142]
Polyallyl dendrimers of 4th generation with a theoretical terminal olefin branch number of 729 were fonctionnalized to glycolate metallocycles by vaporization of OsO_4 under a well-ventilated hood, which showed individual dendrimers by HRTEM with about 5 nm diameter , and the 9th generation with a theoretical terminal branch number of 177 047 were functionalized by hydrosilylation using $HSiMe_2CH_2Cl$. The corresponding iodomethylsilyl-terminated dendrimers were observed by HRTEM on a graphite support, showing the globular

shape with a diameter of 13 nm.[54] Atomic force microscopy (AFM) also is a useful analytical tool, because it provides high-resolution imaging and measurement of surface topology.[143-145] The layer-by-layer deposition technique has been monitored herewith,[146] surface morphologies of high-generation PAMAM dendrimers has been studied,[147] and assembled films of dendrimers in monolayers or multilayers have been investigated.[134] The series of polylallyl-terminated dendrimers with 3^{n+2} end allyl groups (n = generation number) were also observed by AFM on highly oriented pyrolytic graphite (HOPG) support from the 1^{rst} to the 9th generation, which showed a steady size increase of the heigh of the flatenned dendrimers up to 25 nm, probably resulting from double or multilayers in the highest generations.[54] PAMAM dendrimers were imaged by AFM, and the molecular weights and volumes calculated therefrom for G_5-G_8 were in agreement with theoretical values. G_5-G_{10} PAMAM dendrimers could be imaged by taping-mode AFM, although single G_4 dendrimers could not be imaged.[148]

Adhesion forces could be quantified, and dendrimer distorsions have been revealed upon physisorbtion.[148-151] Increasing charge on the PAMAM dendrimers at low *pH* resulted in volume expansion[149,150] and delocalized stack formation.[151] High-generation PAMAM dendrimers have also been characterized at the interface between an aqueous solution and a hydrophobic or hydrophilic substrate, and for instance G_5 gives large aggregates on the HOPG surface when water is used as a solvent.[152] Müllen's rigid polyphenylene dendrimers were also examined on various surfaces by noncontact AFM (NCAFM) and pulse force mode AFM (PFM-AFM), which showed either individual dendrimers or agregates, globular clusters and monolayers with long nanofibers.[153,154] Monolayers of dendritic polymers were prepared by covalent attachment to a silicon wafer surface, and these ultrathin dendrimer films served as effective resists for high-resolution lithography using a scanning probe microscope.[155,156]

PPI dendrimers labeled with rhodamine B and attached to glass substrates via imine bonds were able to move on the surface by hydrolysis and reformation of these imine bonds as shown on confocal microscopy images. In the presence of a gradient, it was suggested that the dendrimers move in one direction with the gradient (Figure 8).[157]

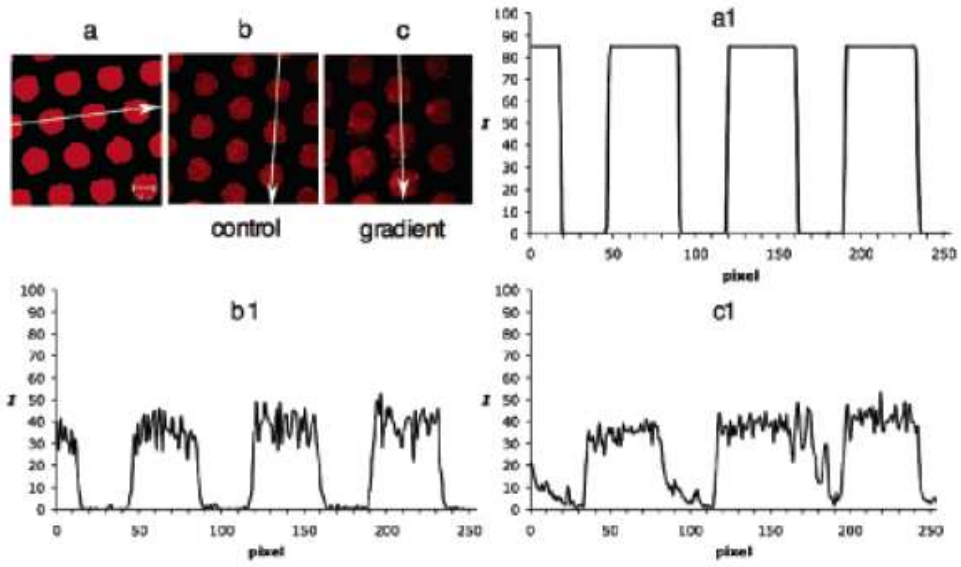

Figure 8. Averaged fluorescence profiles and their corresponding confocal microscope images of dendrimers (a) before immersion and (b) control and (c) gradient substrates, after 16h of immersion. Reprinted with permission of the American Chemical Society (ref. 157, Reinhoudt's group).

The morphology of immobilized first-generation PPI-salicylaldiamine dendritic ligands was examined by AFM and related to the electrochemical behavior of surface-confined films.[158]

Brownian dynamic simulations were used to study the structure and transport properties of dendrimers in dilute solutions, the diffusity and the zero-shear-rate intrinsic viscosity. Incorporation of hydrodynamic interactions was sufficient to reproduce the maximum in the intrinsic viscosity vs. molecular weight observed experimentally.[159]

3. Photophysical Studies: Light-Harvesting and Light-Driven Processes

3.1. Concepts and pioneering studies

This aspect probably is the most presently studied field of dendrimer science together with nanomedicine, because solar light harvesting is an essential way to capture the energy necessary for living organisms including both the biosphere[160] and human activities.[161] Biosphere activities have produced, over million years on earth, fuel that is being consumed overall in only a few decades, thus future generation will need return to solar light to capture energy for human activities. Many photosynthetic organisms in the biosphere, the most important of which are purple bacteria, are models for the design of artificial light-harvesting devices. The photosynthetic unit shows that the reaction center is surrounded by light-harvesting complexes such as a ring-shaped assembly of chlorophyll and carotenoid forming an antenna in which collected photons are transferred to the reaction center with a remarkable unit eficiency.[160] Mimicking Nature is relevant to supramolecular photochemistry.[1,2,162-168] It is obvious that molecular trees, i.e. dendrons (rather than dendrimers) are topologically framed to potentially model natural photosynthetic centers. Indeed, once the photons are collected by the photon absorbers located at the periphery of the dendronic device, they must reach the reaction center at the dendron focal point that need be connected to the reaction center (the root of the tree).[10,11,39]

Beside light harvesting, photophysical studies of dendrimers are also important from both a fundamental viewpoint (theoretical studies on energy transfer processes,[164] studies of fluorescence anisotropy giving information on the dendrimer structure, motion, and aggregation, [165-166] fluorescence at the single-molecule level[167]) and an applied one changing the color of light, sensing with signal amplification, quenching and sensitization processes).

There are two mechanisms that allow the photoexcited state of a chromophore D (donor) to transfer energy to another chromophore A (acceptor) in its ground state located at the focal point near the reaction center. The first one is the short-range (<10Å) through-bond (Dexter) mechanism involving simultaneous electron exchange between the S_1 states of D and A and between the S_0 states of D and A, thus requiring strong D-A orbital overlap with an interaction that exponentially decreases with the D-A distance (rigidity and conjugation between the D and A chromophores are key parameters). The second one is the relatively long-range (10-100Å) through-space (Förster) mechanism that only involves dipole-dipole interactions (the intrinsic properties of the D and A chromophores: transition dipole moments and spectral overlap of D emission with A absorption are the key parameters).[169] The first approach to light-harvesting using a photoactive dendritic antenna that undergoes intramolecular energy transfer was reported by Balzani's group in 1991 with a series of polypyridyl Os-Ru complexes as ligands that allowed the construction of luminescent dendrimers containing up to 22 metal-based units with 1090 atoms with an estimated size of 5 nm. Ligand-dependent bandgap energies were controlled by the location of Ru and Os atoms at the different sites of the dendrimers.[170-173] In the heterobimetallic Ru-Os complexes, Dexter-type energy migration occurs from Ru to Os [174-177] (either from the dendritic core to the periphery or the opposite depending on the respective locations of Ru and Os atoms). This work has been the subject of several reviews.[180-185] Xu and Moore designed rigid polyacelylene dendrons linked to an energy-sink perylene at the focal point. The conjugated phenylacetylene units that act as peripheral energy donors show a strong absorption around 250-300 nm whose intensity doubles for each additional dendritic generation. Excitation of

the periphery at 312 nm yielded only perylene core emission with almost complete quenching of the dendron emission.[130,187-189] Further analogous dendronic synthesis using phenylacetylene linkers induced the formation of an energy gradient that increased the energy-transfer rate by two orders of magnitude.[190] Theoretical work confirmed that such directional multi-step process is more productive than the random walk.[191,192] Fréchet's group designed dendrimers based on a lanthanide ion core (Er^{3+} or Tb^{3+}) surrounded by three benzoate Fréchet-type dendrons (polybenzyl ethers) in order to inhibit the self-quenching of these ions when they were clustered in the solid state diminishing their effectiveness as signal amplifiers for optical fiber communication. Irradiation of the dendrimer dendrons near 280-290 nm resulted in strong luminescence from the lanthanide ion core. The postulated Förster mechanism was more efficient for Tb^{3+} than for Er^{3+} due to better overlap of dendrimer emission with Tb^{3+} absorption.[193-197] Several groups also observed similar antenna effect with energy transfer from Fréchet-type dendrons or 1,3,5-phenylene-based dendrons to a porphyrin core.[198-202] Jiang and Aida reported acceleration of *cis-trans* isomerization of azobenzene-cored G_4 and G_5 poly(benzylether) dendrimer under the influence of either IR (2500 or 1155 cm^{-1}) or UV (280 nm) light. Both isolation of the chromophore from energy dissipation (similar to Fréchet's lanthanide-cored dendrimer) and harvesting antenna effects were invoked to rationalize the observations. The later effect was justified by the fact that the energy corresponding to 4.9 IR photons was required for the rate acceleration.[199] Fréchet's group also designed dendrimer-independent energy transfer involving through-space (Förster) interaction between chromophores located at the core and periphery using coumarin-type and oligothiophene chromophores. Large spectral overlap between donor emission and acceptor absorption is required for efficient energy transfer as shown by time-resolved experiments at sub-picoscond timescales. This through-space energy transfer has also been experimented with dendrimers containing peripheral naproxen units as donors and a naphtalene acceptor.[202] Dendrimer-based light-emitting diodes (LED) were also designed using such coumarin and oligothiophene chromophores. The principle consists in isolating the chromophores in a dendronic structure in order to inhibit energy transfer in mixtures in single-layer LEDs.[195-197] Thin films based on rigid dendrimers exhibited modest electroluminescence due to solid-state aggregation.[203] NLO properties of DAB dendrimers functionalized up to the fifth generation with the typical NLO chromophores 4-dimethylaminophenylcarboxamide as end groups were investigated using the hyper-Rayleigh technique providing sensitivity to molecular symmetry, and the measurements showed that the dendrimers in solution form globular structures with the 32- and 64-armed DAB dendrimers.[204] Forward (singlet-singlet) and backward (triplet-triplet) energy transfer have been demonstrated in a dendrimer containing peripheral naphthalene units and a benzophenone core (Figure 9).[205]

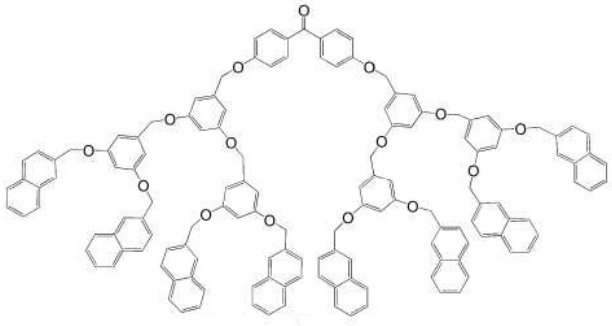

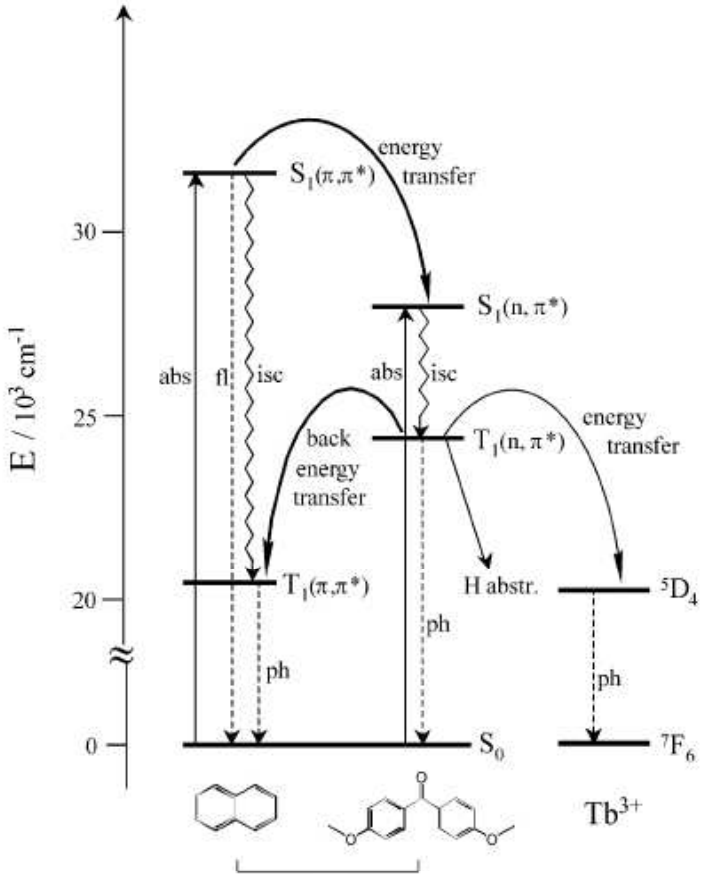

Figure 9. Energy level diagram showing the excited states involved in the photochemical and photophysical processes of the dendrimer. Reprinted with permission of the Royal Society of Chemistry (ref. 205, Vögtle's group).

The photochemical and photophysical properties are broad and varied, and specific studies are often connected to specific dendrimer families as shown below.

3.2. Dendrimers with $[Ru(bpy)_3]^{2+}$ core

Luminescent dendrimers have largely been used as ligands for transition-metal and lanthanide ions. The resulting properties are (i) shielded excited states from quenching processes, (ii) light harvesting, (iii) conversion of incident UV light into visible or infrared emission and (iv) metal ion sensing with signal amplification.[178-183] The Balzani group studied the photophysics of dendrimers that exhibit interactions of luminescent units within dendrimers, quench dendrimer luminescence by external species, sensitize luminescent metal ions and sensitive and quench dye luminescence. Examples of such photoactive dendrimers include dendrimers based on a metal-complex core, dendrimers with metal complexes at the branching centers and dendrimers containing fluorescent organic units. A series of dendrimers whose photophysical studies were carried out by the Balzani group have a $[Ru(bpy)_3]^{2+}$ core (bpy = 2,2'-bipyridine) that exhibited photophysical (luminescence) and redox properties (Figure 10).[179-184,206-212]

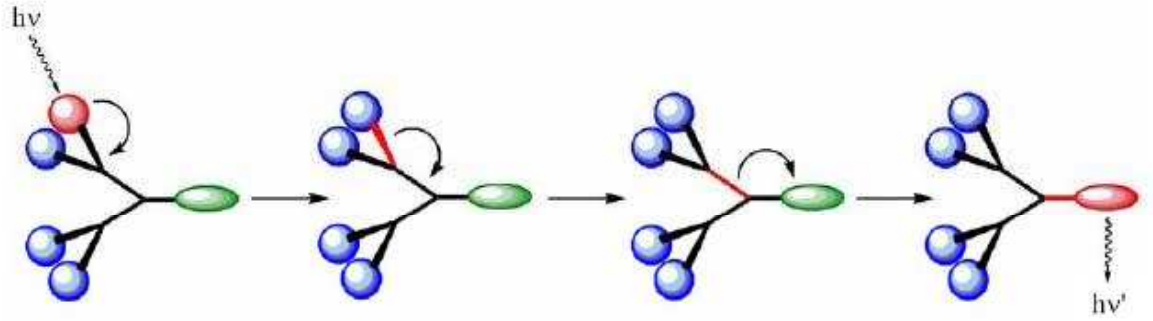

Figure 10. Schematic illustration of a dendrimer as an antenna. The excitation energy hν (shown in red) migrates along the dendrimeric framework until it reaches the core where the energy is used for some purpose such as a chemical reaction. Reprinted with permission of Elsevier (ref. 210, Flomembom's group).

It was shown that the rate of quenching reactions by nearby acceptor systems such as dioxygen, tetrathiafulvalene (TTF) and methylviologen (MV^{2+}) was slower when the $[Ru(bpy)_3]^{2+}$ complex was burried in the dendrimer core than in the free (non-dendritic) complex. *A contrario*, such dendrimers can also be supramolecular hosts for quenching reactions due to guest molecules. The Stern-Volmer equation gives the rate constant k_q of a quenching process taking place by a diffusional mechanism, and luminescence studies showed that the quenching process obeys this equation:

$$\tau°/\tau = \phi°/\phi \quad 1 + k_q\tau°[Q] \qquad (3)$$

In $[Ru(bpy)_3]^{2+}$-cored dendrimers containing dimethoxybenzene- and naphthyl-type units on the branches, antenna effects were observed, i.e. very efficient (90%) energy tranfer takes place from the fluorescence of these units to the orange core whose phosphoresecence is sensitized (λ_{max} = 610 nm). As a result, these dendrimers exhibit a strong emission in the visible region upon UV excitation of the branch groups.[179-184,211] An unusual lanthanide complex, exploiting a dendrimer and a $[Ru(bpy)_2(CN)_2]$ moiety as ligand, exhibits luminescence in the near-IR region. In the absence of the ruthenium component, the dendrimer is unable to transfer energy to the Nd^{III} ion, despite direct coordination.[212]

3.3. Ionic dendrimers electrostatically bound to $[Ru(bpy)_3]^{2+}$ on their surface

In early studies, Tomalia and Turro investigated the quenching of $[Ru(bpy)_3]^{2+}$ by PAMAM dendrimers terminated by carboxylate groups that were not covalently bound to the photoactive probe, but only electrostatically connected with interactions that depended on the dendrimer generation. It was concluded that efficient quenching was mostly due to interactions at the dendrimer surface, and this study also confirmed that the PAMAM dendrimer structure undergoes change at about $G_{3.5}$.[213] Later, in a careful although less conclusive study, it was shown that, at high generations, the dendritic backbone acted as the solvent.[214] Similarities of dendrimer and micelles structures were also revealed based on the dynamics of electron-transfer quenching of photoexcited $[Ru(bpy)_3]^{2+}$ by methyl viologen that was investigated using the luminescence decay of the metal-based chromophore.[215] Quenching studies of $[Ru(bpy)_3]^{2+}$ electrostatically bound to the carboxylate PAMAM dendrimer surface by $[Co(phen)_3]^{2+}$ showed that the quenching process was intradendritic.[216]

3.4. Poly(propylene)imine (PPI)- and polyamide dendrimers with dansyl chromophores attached to the periphery

The photophysical studies of PPI dendrimers of generations G_1 to G_5 containing 2^{n+1} terminal dansyl groups show that these groups behave independently from one another. They exhibit intense absorption that is characteristic of the dansyl chromophores (λ_{max} = 252 and 339 nm; ε = 12 000 resp. 3 900 mol^{-1} cm^{-1} for each dansyl unit in acetonitrile: dichloromethane 1:1v/v

solution) and a strong fluorescence band in the visible region (λ_{max} = 500 nm). If a Co^{2+} salt is added, fluorescence quenching takes place due to coordiation of the Co^{2+} ion in the dendrimer interior, and this quenching is all the more pronounced as the generation number is higher. The coordination is also shown to be fully reversible. The fluorescence of all the dansyl groups of the periphery is quenched when a single Co^{2+} ion enters the dendrimer,[217-219] whereas in polyamide-cored dendrimers only fewer dansyl units are quenched.[220] Ultrafast energy transfer between dansylated PPI dendrimers and eosin was monitored by femtosecond transient absorption spectroscopy, and the time constants (1 ps and 6 ps) were found to be independent of the dendrimer generation. Relaxation processes in eosin were faster with these dendrimers than in solution due to both eosin-dendrimer and intradendritic eosin-eosin interactions (Figure 11). [221,222]

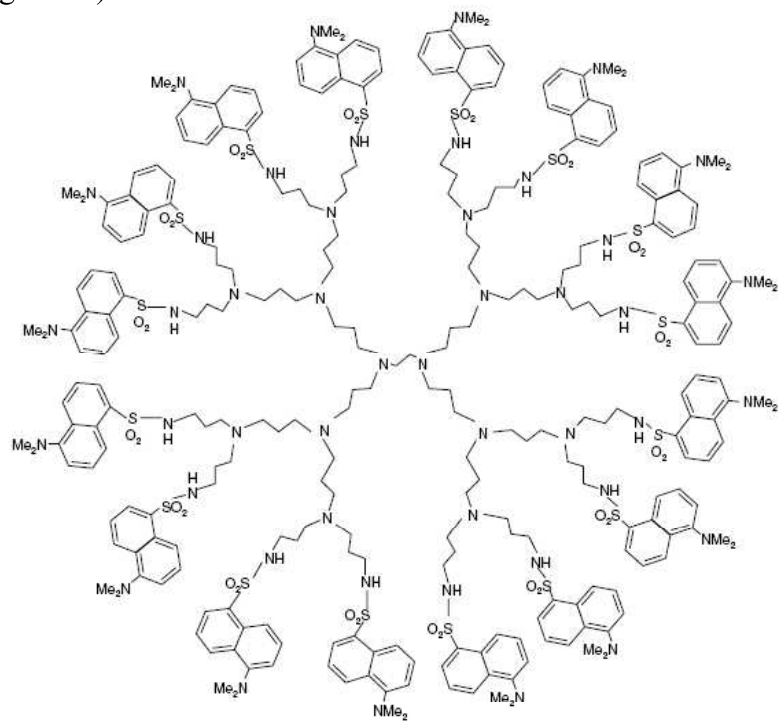

Figure 11. Structural formula of third generation dansylated POPAM dendrimer (G3). Reprinted with permission of Elsevier (ref. 221, Aumanen's group).

With polylysine cores instead of PPI cores, the lanthanide ions (Nd^{3+}, Eu^{3+}, Gd^{3+}, Tb^{3+}, Er^{3+}, Yb^{3+}) quenched the dansyl fluorescence, and with Nd^{3+}, Er^{3+} and Yb^{3+}, a sensitized near-infrared emission of the lanthanide ion was observed.[223]

Highly efficient photoinduced energy transfer was observed for adducts between G_1, G_3 and G_4-dansylated PPI dendriers and anthracene clips. The coordination properties of Zn^{II} therein have been exploited in the self-assembly of complex structures in which Zn^{II} mediates the dansyl-anthracene interactions.[224]

3.5. Dendrimers with cyclam cores

Dendrimers with a 1,4,8,11-tetraazacyclodecane (cyclam) core with dimethoxybenzene branches and naphthyl termini exhibit emission bands of the naphthyl excited states (λ_{max} = 337 nm), naphthyl excimers (λ_{max} ca. 390 nm), and naphthyl-amine exciplexes (λ_{max} = 480 nm).[225-226] The two successive protonations using trifluoacetic acid prevent exciplex formation and cause rearrangements affecting excimer formation between the peripheral naphthyl units. Coordination of the cyclam core with Zn^{2+} forms bis-cyclam complexes $[Zn(dendrimer)_2]^{2+}$, which also prevents exciplex formation, with a resulting increase of the naphthyl

fluorescence. The photophysical studies also provides information on the relative conformation of the dendrimers.[227-228] Similar photophysics results were obtained with complexes of lanthanide ions (Nd^{3+}, Eu^{3+}, Gd^{3+}, Tb^{3+}, Dy^{3+}), but emission data were best fitted with 1:3 and 1:2 complexes.[229] Dendrimers containing two covalently linked cyclams as a core exhibited photophysical data suggesting that the two cyclams did not behave independently upon protonation, but formed a sandwich structure. Upon titration with $[Zn(CF_3SO_3)]$ or $[Cu(CF_3SO_3)]$, the emission spectral changes showed evidence for the formation of a 1:1 complex, then replaced by a 2:1 complex, although the results were different both in absorption and emission spectra for these two metal ions.[230] An adduct between $[Ru(bpy)(CN)_6]^{2-}$ and a dendrimer metal-cyclam core was shown to form when the dendrimer was appended with 12 dimethoxybenzene units and 16 naphthyl termini. The photophysical data show that this dendrimer plays the role of a light-harvesting second coordination sphere that transfers the collected energy to $[Ru(bpy)(CN)_6]^{2-}$. Moreover, the adduct can be disrupted by addition of either acid or base exhibiting two distincts optical outputs according to an XOR and an XNOR logic respectively (Figure 12).[231-234] In europium-cyclen-cored dendrimers formed by "click" reaction between a teravalent cyclen core alkyne containing four alkyne groups and dendrons containing an azido group at the focal point, the photophysical results showed that the proximate triazoles acted as sensitizers, transferring their singlet-singlet excitation in the UV region (270-290 nm) to the partially filled luminescent lanthanide 4f shell. An increase of luminescence decay time from the lanthanide $5d^0 \rightarrow 7f^2$ emission was observed with increasing dendrimer size, indicating that the shielding effect of the dendron wedges is important for the relaxation of the photo-excitation and energy transfer.[235]

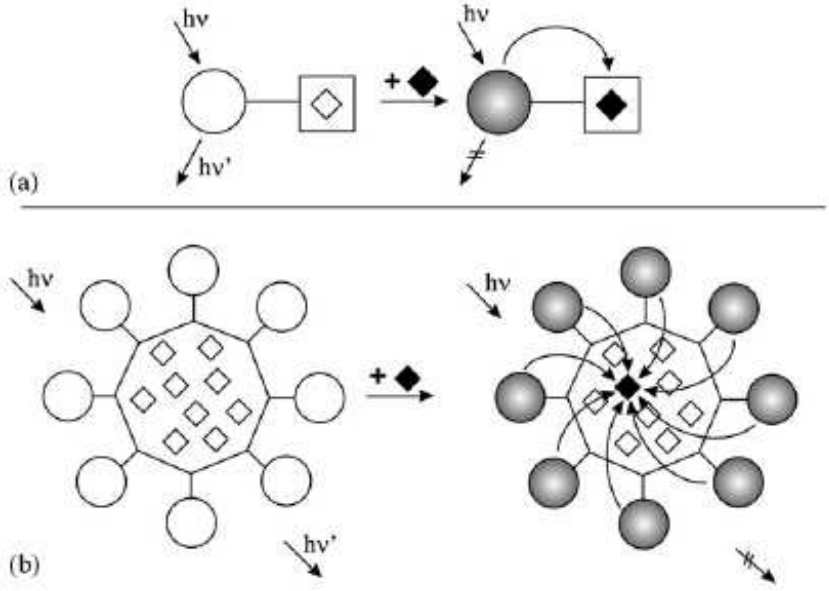

Figure 12. Schematic representation of (a) a conventional fluorescent sensor and (b) a fluorescent sensor with signal amplification. Open rhombi indicate coordination sites and black rhombi indicate metal ions. The curved arrows represent quenching processes. In the case of a dendrimer, the absorbed photon excites a single fluorophore component, that is quenched by the metal ion, regardless of its position. Reprinted with permission of the Royal Society of Chemistry (ref. 232, Balzani's group).

3.6. Porphyrin dendrimers

Since the first example with Fréchet-type dendron units,[236] Aida has investigated the photoactivity of bioinspired porphyrin-cored and other porphyrin dendrimers as artificial hemoproteins[236-239] such as cytochrome C mimics[240,241] and for photodynamic cancer therapy.[242-245] Another porphyrin- centered dendrimer with PAMAM units mimicking

hemoproteins was reported by Diederich, Collman and co-workers.[245] Vectorial excitation energy transfer was achieved using porphyrin-cored dendrimers,[246-249] and such a process was efficiently achieved using a multiporphyrin array with energy donating zinc-porphyrin dendrimer units to a metal-free porphyrin dendrimer core yielding enhanced core emission.[250,251] In a dendronic analogue having a metal-free porphyrin acceptor at the focal point, energy transfer from peripheral Zn-porphyrin units appeared to be less efficient.[252,253] Stern-Volmer analysis was used to investigate the access of benzylviologen to the porphyrin core in several generations of dendrimers containing Fréchet-type dendrons. No fluorescence quenching inhibition was found for generations 1-3, but only a slight rate enhancement for G_4. The study also suggested that the periphery does not interfere with the photophysics of the porphyrin core.[244] The dynamics of electronic energy transfer was investigated for porphyrin-terminated poly(propylene imine) dendrimers using time-resolved fluorescence anisotropy in a glass environment. Depolarization of fluorescence was observed for all the generations studied compared to monoporphyrin model compounds.[245] With porphyrin-cored dendrimers containing carbazole chromophores on the branches, the fluorescence observed indicated that the light collected by the peripheral chromophores was quantitatively transferred to the core.[246] Snowflake-shaped dendrimers containing a Zn porphyrin core and anthraquinonyl peripheral groups provided highly efficient (100%) intramolecular singlet energy transfer. Electron transfer in this system was more efficient than with linear analogues showing that covering of the conjugated chain enhanced electron transfer partly due to charge-transfer interaction.[249]
In phthalocyanine dendrimers, fast carrier movement is dominated by polaron hopping and tunneling charge transfer mechanisms.[254]

3.7. Two-photon absorption (TPA) using porphyrin-cored dendrimers

"Two-photon absorption" (TPA) involves the simultaneous absorption of two photons by the same molecule, and non-linear dependence on light intensity leads to various optical and imaging applications.[255,256] The efficient section of the absorber is a key parameter that must be optimized, because it is related to the probability of absorption of two photons. Branched or dendritic molecules are useful in this respect.[257-266] The groups of Fréchet and Prasad examined the generation of cytotoxic singlet oxygen for photodynamic therapy to subcutaneous tumors by fluorescence resonance energy transfer (FRET) using porphyrin sensitizers as dendritic cores of dendrimers containing two-photon donor chromophores such as the complex polyaromatic AF-343 at the periphery.[267-269] Whereas much work is involved in decreasing the band-gap energy to shift the porphyrin absorbance to the near infrared,[270,271] the advantage of two-photon chromophores (TPA) is that they absorb 750-1000 nm light (near infrared) where tissues are more transparent, which allows deeper light penetration with reduced risk.[272-274] TPI of dendrimers containing a stilbene core and benzyl ether dendrons showed that the quantum yield of stilbene core radical cation during the 308-nm TPI was independent of dendrimer generation, whereas the 266-nm TPI disclosed generation dependence. Since both the stilbene core and benzyl ether dendrons were ionized, it was suggested that the dendrons acted as hole-harvesting antennae.[275] TPA was also studied with two-photon chromophores located at the periphery of non-porphyrinic dendrimers (Figure 13).[276-278]

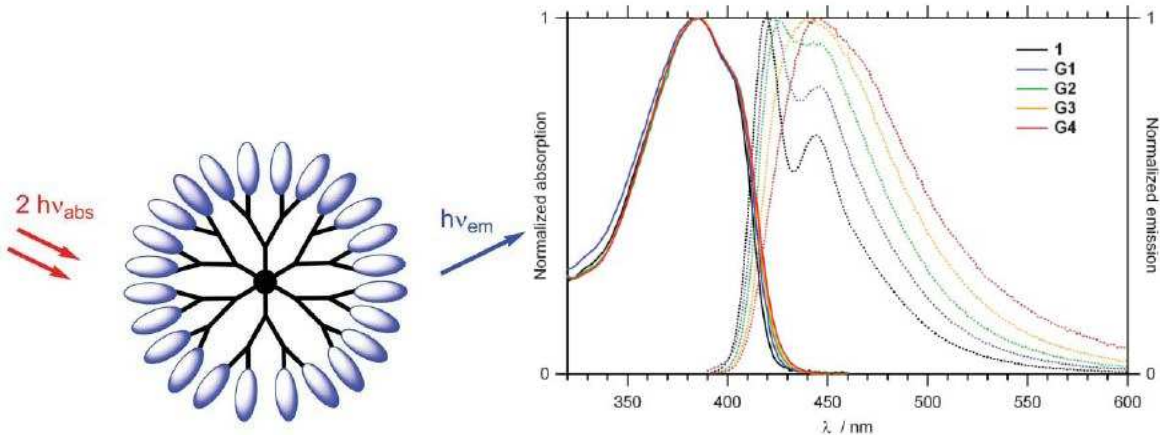

Figure 13. Schematic representation of dendrimeric two-photon absorbing fluorescent organic ''nanodots''. Normalized absorption and emission spectra in toluene of dendrimers G_1–G_4 and model chromophore noted 1. Reprinted with permission of the Royal Society of Chemistry (ref. 276, Blanchard-Desce's group).

In another TPI study with porphyrin-cored dendrimers, Fréchet's group showed that TPA also displays quadratic dependence on laser intensity providing better spatial resolution of treatment. Tetraethylene glycol termini provided water solubility of some of these dendrimers, allowing generation of singlet oxygen in water using this strategy.[268] Some systems involving both porphyrin and fullerene chromophore units have been reported and are detailed in the following fullerene dendrimer section.

3.8. Fullerene dendrimers

Fullerenes (C_{60}) were introduced at the termini of star-shape[279,280] and dendritic[281,282] structures for electrochemical and photophysical purposes. The alternative strategy consists in the introduction of the fullerene at the dendrimer core (Figure 14).[283-290]

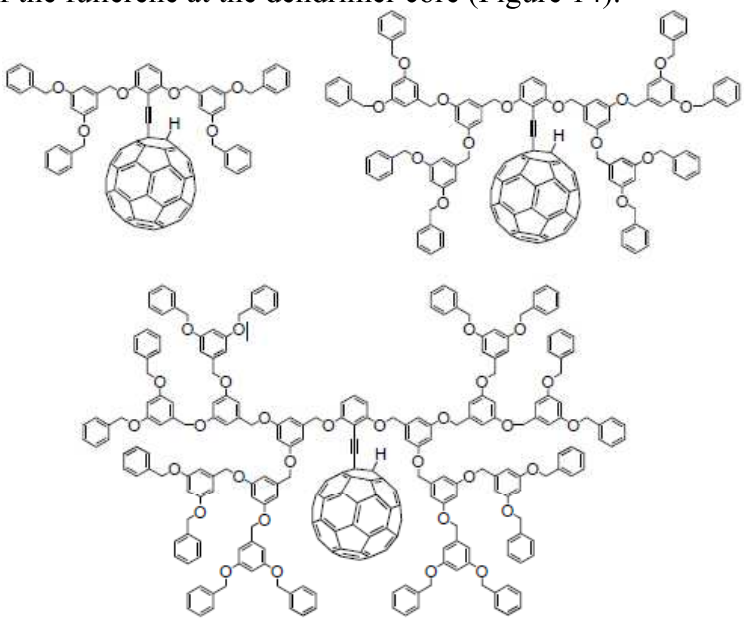

Figure 14. Fullerodendrimers. Reprinted with permission of Wiley Interscience (ref. 288, Nierengarten's group).

It was indeed shown that the lifetime of the first triplet excited state of such fullerodendrimers is very sensitive to the solvent, which could be used to evaluate the degree of isolation of the fullerene core.[283-293]. Electrooptical properties, such as Kerr constants determined in the pulsed electric field, which depend on the polarity and anisotropy of optical polarisibility determined for several fullerodendrimer families were shown to be generation dependent.[294]

Whereas photophysical studies of chromophore-containing dendrimers mostly focused on energy transfer from a donor to an acceptor (light-harvesting with antenna effect and phototherapy), photophysical studies on fullerodendrimers often involve photo-induced electron transfer from a donor chromophore to the C_{60} fragment that also is an electron acceptor, because the reduction potential of C_{60} and its derivatives to $C_{60}^{\cdot-}$ is low, only about -0.9 V vs. the ferrocene/ferrocenium redox couple that is most usually used as the reference.[295-298] Thus, covalently linked porphyrin-C_{60} dyads integrated in a dendritic frame are photo-induced electron-transfer units involving charge separation ($P^{\cdot+}$-$C_{60}^{\cdot-}$ state) from the porphyrin P to C_{60}. Dendrons containing Zn-porphyrin units (P_{Zn}) on the branches and C_{60} at the focal point exhibit a Soret band that becomes broader from $1P_{Zn}$-C_{60} and 3PPZn-C_{60} to $7P_{Zn}$- C_{60} (difference in the full-width at half-maximum of +54 cm^{-1}), i.e. as the generation increases, suggesting electronic interaction among the P_{Zn} moieties in $7P_{Zn}$-C_{60}. Fluorescence quenching was found to arise from the P_{Zn} unit to the focal half point, formation of the ion pair $P_{Zn}^{\cdot+}$-$C_{60}^{\cdot-}$ being confirmed by means of picosecond time-resolved spectroscopy. The back-electron-transfer process was also shown to be retarded.[299] Fullerodendrimers with peripheral ferrocenyl units disclose steady-state emission intensities that were quenched relative to the *N*-methylfulleropyrrolidine model, nanosecond transient absorption revealing efficient charge separation in both systems with longer lifetimes of the (ferrocenyldendron$^{\cdot+}$-$C_{60}^{\cdot-}$) state.[300] Dendrimers with fullerene units at the periphery have been assembled either by electrostatic[219] or covalent binding[290,300-302] and some of them disclose unique luminescence properties.[287,290,300,302] Multiple porphyrin-C_{60} dyads have been successfully constructed at a dendrimer surface,[303,304] and a remarkable dendrimer containing a Zn-tetraphenylporphyrin core rigidly linked and conjugated to four C_{60} peripheral units was reported to show a dendrimer effect on the singlet energy transfer.[305] Dendrimers containing up to 16 fullerene peripheral units designed by the Nierengarten and Vögtle groups showed enhanced absorption in the region between 360 and 500 nm by increasing the generation number and disclosed a size-dependent trend in decreasing singlet lifetime and fluorescence quantum yields.[306]

3.9. Carbon nanotube-based dendrimers

Very few nanotube-dendrimer composites are known.[307-310] Single-wall carbon nanotubes, functionalized by 1,3-dipolar cycloaddition of $HO_2CCH_2NHCH_2OCH_2CH_2OCH_2CH_2NHBoc$ and *para*-formaldehyde at 120°C in DMF followed by solid-phase PAMAM dendrimer synthesis and tetraphenylporphyrin linking, were studied by steady-state and time-resolved spectroscopy. The fluorescence kinetics provided evidence for a very short-lived transient decay (0.04 ± 0.01 ns) and a long-lived one (8.6 ± 1.3 ns), indicating that the porphyrin presumably does not interact with the nanotube.[310]

3.10. Rigid dendrimers with conjugated poly(arylene) units

Moore elegantly pioneered the area of rigid dendrimers that contained poly(phenyleneethynylene) backbones with photophysical properties (*vide supra*).[131,132] Another remarkable family including giant dendrimers were reported by Müllen's group with polyarylene scaffolds.[311-318] First-generation dendrimers containing a triarylamine core parasubstituted with three Müllen-type dendrons one of which was covalently attached to a peryleneimide chromophore at the rim were investigated by steady-state and time-resolved spectroscopic techniques in different solvents of medium and low polarity. Single-photon counting experiments revealed a fast charge separation and a thermally activated back reaction from the charge-separated state to the locally excited state. A through-space electron transfer mechanism was suggested. At 77K, the recombination luminescence is long-lived.[315] Multichromophoric dendrimers containing peripheral perylenecarboximide units were studied by far-field fluorescence microscopy which underlined the dynamic character of the

interactions among the chromophores.[311,312] Intramolecular Förster-type excitation energy transfer (FRET) was investigated in polyphenylene dendrimers with peripheral peryleneimide chromophores.[318] Poly-*p*-phenylene macromolecules (PPP) have large HOMO-LUMO energy gap giving rise to blue emission that has been the subject of intense research to make full color organic displays. Since it is necessary to solubilize these materials without hampering conjugation and to prevent aggregate formation, Fréchet-type[319] and Müllen-type[320-322] dendrons have been successfully used to endcap polyfluorene materials. An OLED using such a polyfluorene containing 9,9-diaryl substituents produced blue emission with onset voltages below 4V.[320-322] A polyphenylene dendrimer carrying three perylenemonoimide dyes and one biotin group exhibited stability in the presence of serum proteins, and specific binding to the protein streptavidin was demonstrated using a magnetic bead assay.[323] A rigid 1,3,6,8-tetraethynylpyrenyl-cored dendrimer with a polyphenylene shell could encapsulate pyrene, this material presenting high quantum efficiency and good film-forming properties for applications in electronic devices.[324] Terphenyl-cored dendrimers containing oligosulfonimide dendrons exhibited high steady-state anisotropy. In these dendrimers, energy transfer from the dendronic chromophores to the terphenyl core does not occur, and the terphenyl core shows a very high fluorescence quantum yield (c.a. 75%) and a short emission lifetime (0.8 ns) allowing investigation of the fluorescence depolarization caused by the rotation of the dendrimers.[325] Polyphenylene dendrimers are promising OLEDs, especially because they can reach up to 28 nm at 271.6 kD.[326-329]

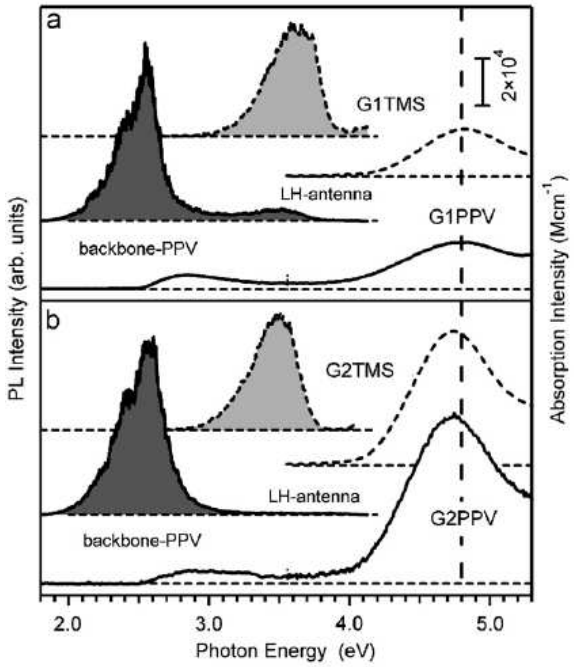

Figure 15. Absorption and PL spectra of G_nPPVs (G_nPPV: n^{th} generation dendrimer with poly-(phenylenevinylene) backbone; n = 1, 2) and G_nTMSs (G_nPPV: n^{th} generation dendrimer with trimethylsilyl group backbone; n = 1, 2) in solutions. PL spectra are displayed with grayish shadow. Vertical broken line marks the energy of the excitation. Reprinted with permission of Elsevier (ref. 328, Akai's group).

Energy transfer in wire-type dendrimers having oligophenylene peripheries as light-harvesting antennae proceed from these peripheries to the backbone polymers, and in solid dendrimer films, red shifts of this backbone photoluminescence bands were observed (Figure 15).[328] Polytriphenylene dendrimers were designed for blue-light-emitting materials with high photoluminescent quantum yields, stiff dendritic backbones preventing intermolecular fluorescence quenching (Figure 16).[329]

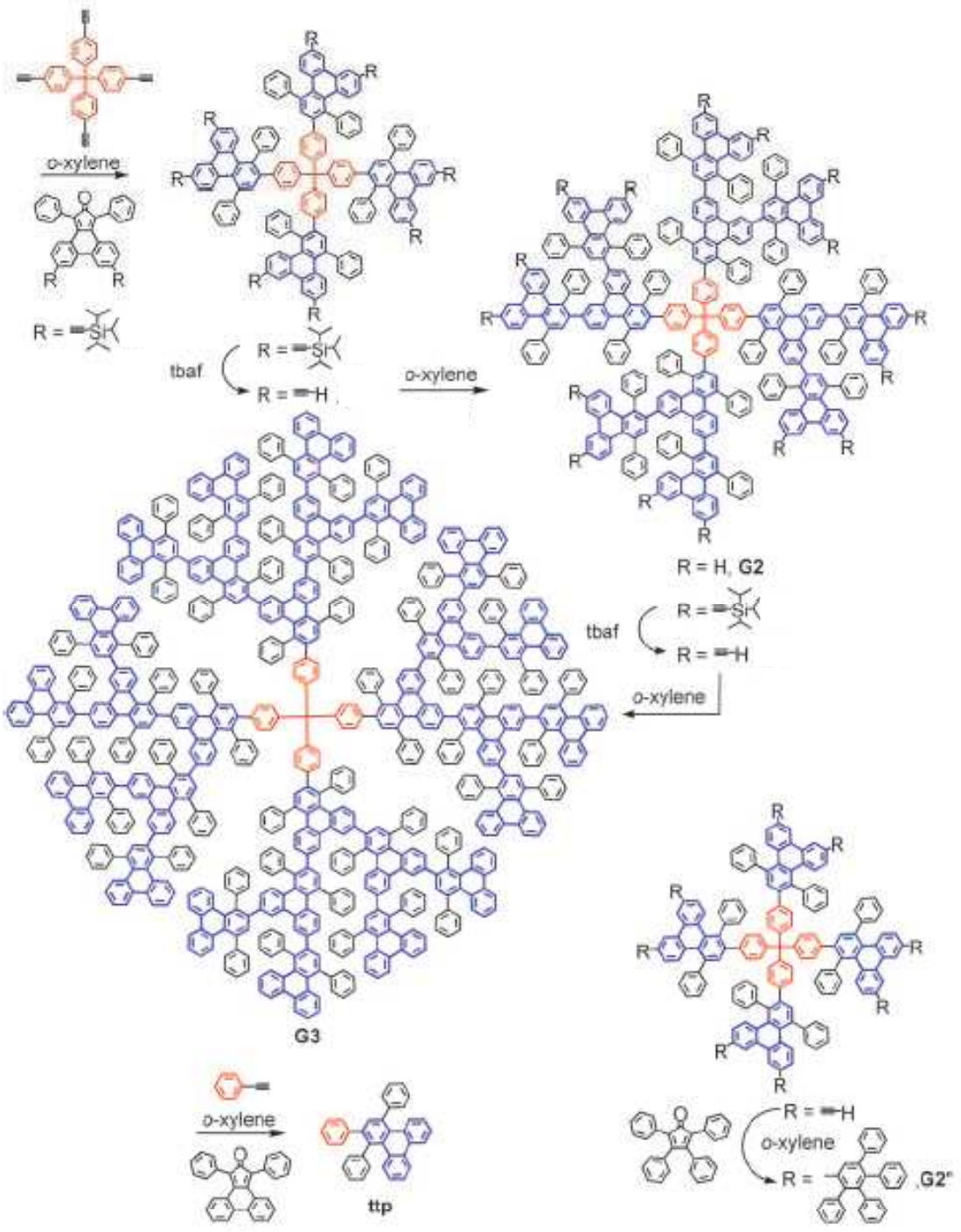

Figure 16. Synthesis of polytriphenylene dendrimer G_2, G_3, G_2', and the model compound 1,2,4-triphenyltriphenylene (ttp). Reprinted with permission of Wiley Interscience (ref. 329, Müllen's group).

3.11. Azobenzene and azomethine dendrimers

Azobenzene derivatives undergo an efficient and fully reversible photoisomerization, and it is a photochrome system that has been used in photoswitchable devices.[162,330] Thus, azobenzene-terminated (polypropyleneimine) dendrimers have been studied[331-342] and used as photoswitchable dendritic hosts. For instance, with eosin, the quenching is most likely due to an electron-transfer reaction between the singlet excited state of eosin and the tertiary amine unit, and quenching from the Z form is more efficient than quenching by the E form. The E→ Z and Z → E photoisomerization reactions of the azobenzene units are sensitized by eosin via

a triplet-triplet energy-transfer mechanism.[331-333] Transmission microcopy and confocal fluorescence microscopy images have shown that azobenzene-terminated (polypropyleneimine) dendrimers assemble (by H-bonding at $pH < 8$ and π-π stacking) to form giant vesicles in aqueous dispersions.[339] Yamamoto's group has designed remarkable phenylazomethine dendrimers,[343-347] and the electroluminescence of these dendrimers as double-layer organic light-emitting diodes (OLED) has been demonstrated using tris-(8-hydroxyquinoline) aluminum as an emitter.[348-350] Moreover, upon complexation of the dendrimer nitrogen ligands by $SnCl_2$, the properties of the hole-transporting layer were improved, and the luminance and EL efficiency was drastically increased by comparison with the dendrimers alone. Dendritic effects were also observed, G_3 being the opimal generation among the G_1-G_5 phenylazomethine dendrimer series.[348-350] Quantum size effect were observed in TiO_2 nanoparticles prepared by finely controlled metal assembly on such phenylazomethine dendrimer templates (Figure 17).[349]

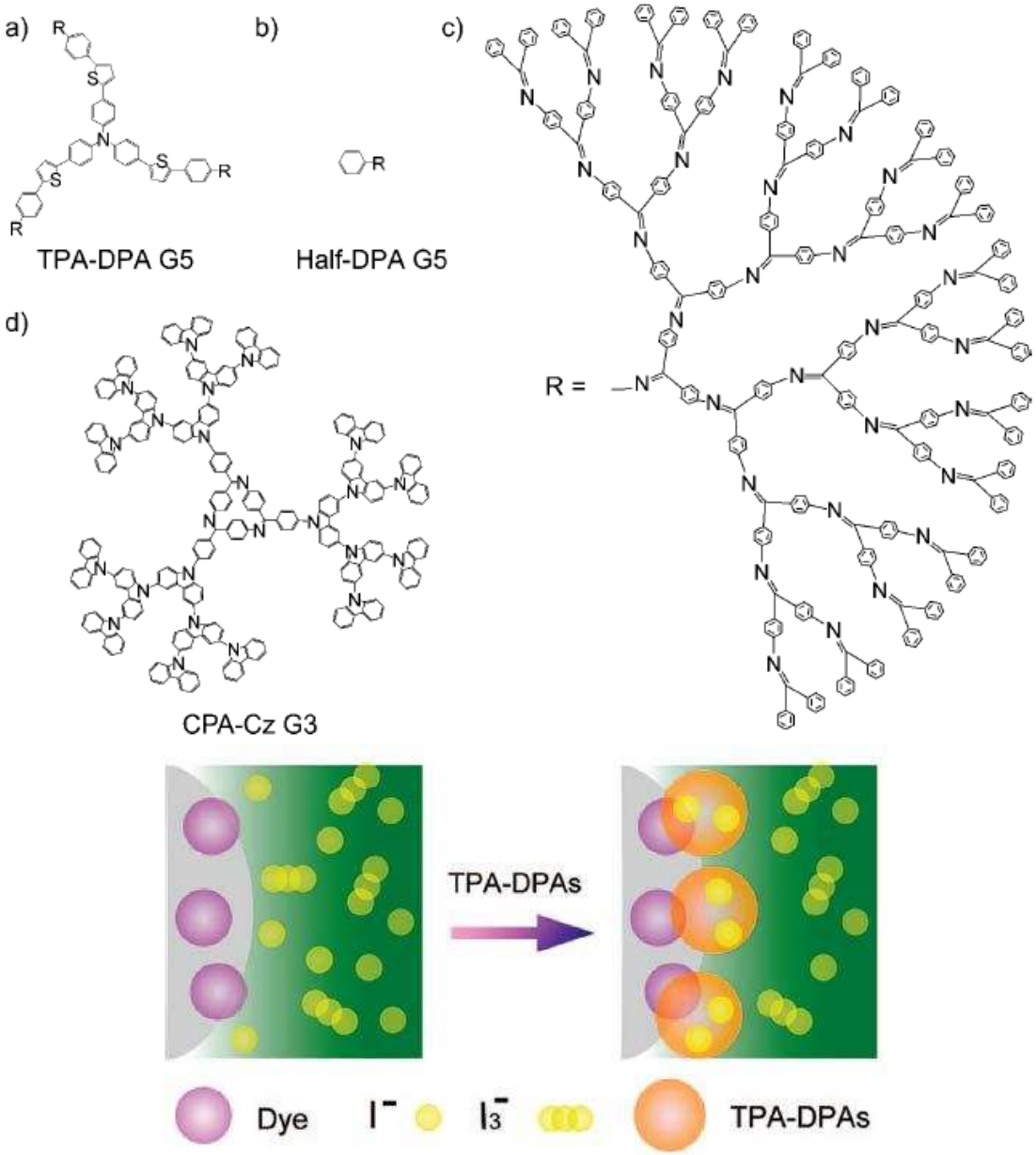

Figure 17. Structure of the dendrimers. (a) Triphenylamine core (TPA-DPA G_5). (b) Half-dendric phenylazomethine core (Half-DPA G_5). (c) Generation 5 of DPA dendron units. (d) Carbazole dendrimer containing cyclic phenylazomethine of generation 3 (CPA-Cz G_3); interface modification by dendrimers on TiO_2 electrode. Reprinted with permission of the American Chemical Society (ref. 349, Yamamoto's group).

3.12. Polythiophene dendrimers

Oligo- and polythiophene derivatives have been extensively investigated and used as organic light-emitting diodes (OLEDs), organic field-effect transistors (OFETs) and photovoltaic (PV) applications. These organic materials exhibiting large electro-optic response have potential for use in telecommunications, digital signal processing, phased-array radar, THz generation and other photonic devices.[351-356] For OLEDs, light is emitted upon application of a few volts to a thin layer of these materials. Red, green and blue colors can be obtained, and such colored components may be assembled to provide vivid color displays. Organic compounds are cheap, easy to process and integrate in devices, and they have low dielectric contants and high bandwith. For instance, solar power conversion efficiencies of up to 4.8% have been certified at the National Renewable Energy Laboratory for devices based on blended polymer-fullerene assemblies.[357] High-quality films formed by π-conjugated dendrimers make this dendritic approach a priviledged one, because self-order and crystalline ordering on several nanometer-length scales are essential to success.[358] Dendrimers offer the possibility of introducing multichromophores in EO materials for the control of interchromophore electrostatic interactions, and thiophene-containing dendritic EO chromophores were found to exhibit more stable EO properties as compared to the corresponding isolated chromophores.[359,360] Oligo-and polythiophenes are the most commun units that take part in these devices, but other units discussed in the following sections such as poly(phenylenevinylene), carbazole, triarylamines are aso used (*vide infra*).

Phenyl-cored polythiophene dendrimers have been blended with [6,6]-phenyl C_{60} butyric acid methyl ester (PCBM) for the fabrication of bulk heterojunction PV devices.[361] A significant increase of fluorescence quantum yield in dendrimers with an increasing number of bithiophenesilanes was obtained compared to linear analogues.[362] Encapsulating individual chromophores inside a dendritic structure greatly enhances their optical properties due to reduced self-quenching. For instance, electroluminescence studies in OLED devices confirmed that color tuning could be achieved by mixing both encapsulated dyes (pentathiophene and coumarin 343 interacting via Forster energy transfer) in a single layer, even if selective trapping by one of the dyes dramatically modifies the efficiency of the others.[363] OLEDS involving dendrimers as both hole transporting and electron transporting components as well as emitters have been designed,[363-373] but the requirement of site isolation in relatively large dendrimers is crucial.[363] There are only few reports on the applications of dendrimers in organic solar cells.[374-377] With oligothiophene-centered dendrimers containing bis-triarylamine substituted carbazole tethers, the absorption and fluorescence emission peaks red-shifted with increasing the oligothiophene core length. Thus, the conversion efficiencies of the solar cells using the composite of this dendrimer and PCBM also increased with increasing the oligothiophene core length from 0.04% with a dithiophene core to 0.13% with a pentathiophene core under AM 1.5 simulated solar illumination at an irradiation of 100 mW/cm^2. [377] In addition, rigid, terthiophene-terminated Müllen dendrimers were found to be good conductors due to the hopping process in the 3D network as a result of the small distances between the planarized wings of different cores.[378] Ultrafast energy transfer (200-300 fs) to the longest dendrimer branch, and super-linear increase of 2-photon absorption section due to increased excitation delocalization were disclosed in thiophene dendrimers (Figure 18).[379]

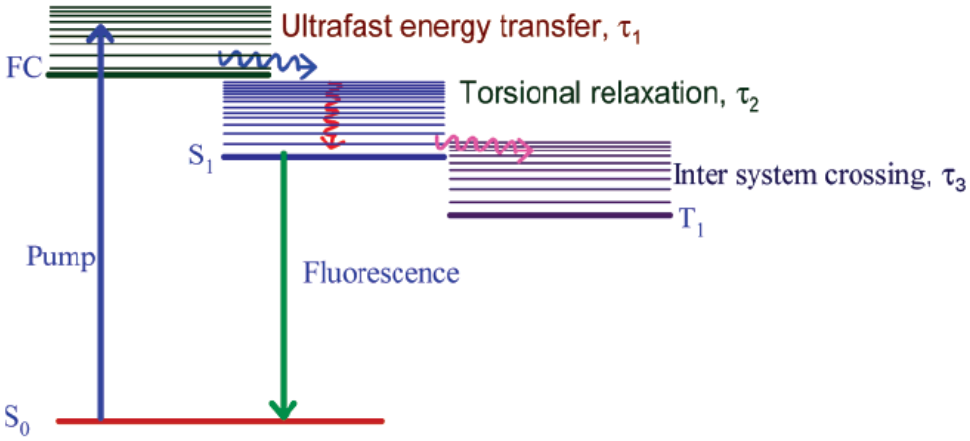

Figure 18. Mechanism of excited state deactivation of higher generation thiophene dendrimers. Reprinted with permission of the American Chemical Society (ref. 379, Goodson III's group).

In such oligothiophene dendrimers, the excitation is delocalzed over a large number of thiophene units in the dendrimer, and there is ultra-fast energy transfer (200-300 fs) to the longest dendrimer branch. A super-linear increase of 2-photon absorption was observed with an increase in thiophene dendrimer generation.[380] Thiophene dendrimers with aryl cores and thiophene termini were modified by introduction of ethynyl spacers, with a decrease of bangap for the four-arm dendrimer due to the reduction of interactions between the arms and the congested 1,2,4,5-arrangement around the core.[381] Dendritic oligothiophene (DOT)-perylene bisimide hybrids showed optoelectronic properties indicating that the perylene core and dendritic oligothiophene units were electronically decoupled. Photoinduced electron transfer was facilitated with increasing DOT generation and donor strength, and electropolymerization led to cross-linked donor-acceptor conducting films.[382]

3.13. Poly(phenylenevinylene) dendrimers

Distyrylbenzene is fluoresecent blue in solution, but in the solid state the fluorescence is suppressed due to aggregation. A dendrimer protection of a distyrylbenzene core could form processable films for a working device. Excimer formation causes the presence of a red tail that is all the more reduced as the dendrimer generation is higher.[383,384] A distyrylbenzene core was used to obtain blue emission, a distyrylanthracene core gave green, and a *meso*-tetraarylporphyrin core provided the red, yielding OLED materials for these colors consisting in a single dendrimer layer between ITO and calcium contacts. Non-dendritic units with these structures are inefficient, however, because strong interchromophoric interactions quench the luminescence.[385] Likewise, in tris(distyrylbenzyl) amine-cored dendrimers, aggregate-excimer emission responsible for a red tail in the zeroth generation progressively disappears as the generation increases.[386] Quantum chemical calculations were helpful in providing an accurate description of the measured absorption data and understanding the observed fluorescence dynamics.[387] Another important factor in an OLED is the charge-transport properties. In triarylamine-centered dendrimers, charge mobility due to the amine photoxidation decreases as the generation increases, and determination of mobility using gel-permeation chromatography showed that the mobility was proportional to $D^2 \exp(-D/D_0)$, where D is the molecular diameter and D_0 a characteristic hopping parameter. The results showed that the conjugated dendrons did not participate in charge mobility that entirely proceeded from core to core.[388] Low mobility enhances charge capture and quantum efficiency, but it should not be too low or power efficiency would decrease. Thus, a number of oligo(*p*-phenylenevinylene) dendrimers have been reported as candidates for OLED mterials,[389-391] including crystalline phases and copolymers (Figure 19).[392-397]

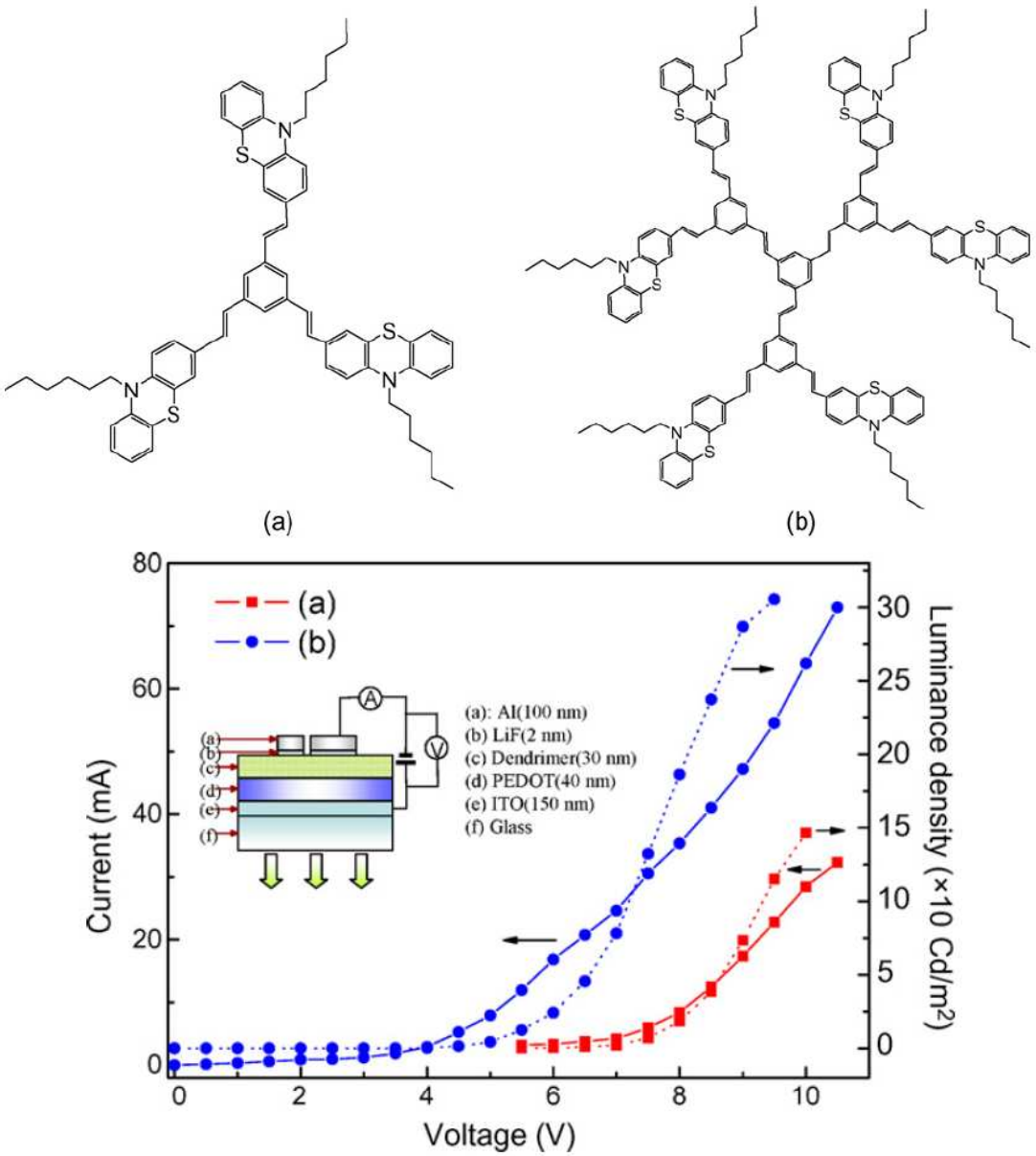

Figure 19. Current–voltage–luminance curves for two LEDs made of dendrimers. Reprinted with permission of Elsevier (ref. 397, Choi's group).

Oligo(*p*-phenylenevinylene)-decorated PPI dendrimers were synthesized, extensively studied and coated on films by the Meijer group.[398] Dendron-containing copolymers with high molecular weights show that both quantum efficiency and hole injection are significantly enhanced by increasing the dendron generation. Double-layer light emitting devices including these copolymers were fabricated whose performances benefited from dendron generation increase.[399,400] Prolonged irradiation of PPI dendrimers functionalized with stilbene or 1,4-distyrylbenzene chromophores led to the destruction of the chromophores upon oligomerization (crosslinking).[400] With the dendrimers, the efficiency remains low (up to 0.1%), however. Indeed, this efficiency is proportional to the numbers of excitons formed by charge recombination, the fraction of excitons generating light (PL quantum yield), the fraction of singlet excitons (fluorescence: 0.25 due to spin statistics), and the fraction of light that escapes from the device (usually 0.2). In poly(phenylenevinylene) dendrimers, these factors are not optimized, although the increase in dendrimer generation is favorable in phenothiazine-terminated dendrimers containing phenylene-vinylene cores and dendrons.

Highly efficient dendritic OLED optimizing all these factors involved phosphorescent dendrimers (thus utilizing both the singlet and triplet formed in the devices) with polyphenylene, carbazole, triarylamine and/or oligothiophene units (rather than poly(phenylenevinylene) ones), and a *fac*-tri(2-phenylpyridyl)iridium (III) core (*vide infra*).

3.14. Highly efficient dendritic OLEDS with a *fac*-tri(2-phenylpyridyl)iridium (III) core and polyphenylene, carbazole, triarylamine and/or oligothiophene units

The Burns and Samuels groups have developed green phosphorescent dendrimers providing highly efficient OLEDs with high PL quantum yields of up to 70% in dilute solution (with the highest generation) using the *fac*-tri(2-phenylpyridyl)iridium (III) core.[401,402] This core provides a fast radiative decay rate (or shorter excitation lifetime). Charge is injected into this Ir^{III}-centered core as shown by electrochemical data.[403] PL quantum yields were lower in the solid state, and the dendritic effect was positive, i.e. the first dendrimer generation gave a higher PL quantum yield than a non-dendritic film, and a lower PL quantum yield than the second dendrimer generation. Another crucial parameter for these highly efficient dendritic OLEDs was the use of biphenyl units and 2-ethyl-hexyloxy surface groups.[404,405] Blending these dendrimers with 4,4'-bis(*N*-carbazolyl)biphenyl that spaces the dendrimers was highly efficient. For instance, a 20:80 wt% dendrimer 4,4'-bis(N-carbazolyl)biphenyl blend film showed a PL quantum yield of 78%.[401,402] Small structural variations in the Ir^{III} ligand substituents and linkers also provided red[406,407] and blue[408] phosphorescent dendritic OLEDs. The peripheral groups have an important influence, and solubilizing alkyl groups located at the periphery of Ir^{III}-centred dendrimers provided good device efficiencies in bilayer devices upon blending with 4,4'-bis(*N*-carbazolyl)biphenyl.[409,410] Peripheral groups such as Müllen-type units yielded good results for arylthiophene OLEDs.[411,412] A strategy involving charge-transporting groups such as oxadiazole or carbazole units used in conjonction with perylenes led to the preparation of devices. An example with eight carbazole units had a quantum efficiency of 0.1% at a brightness of ca. 6 cd m^{-2}. Another one included oxadiazole or triarylamine charge-transporting peripheral units, leading to three-layer devices that gave red emission with quantum yield of 1.5-1.9% and power efficiencies of 1.0-2.1 lm W^{-1}.[413,414] Fully conjugated systems also gave blue emissions for bilayer devices.[415,416] *fac*-tri(2-phenylpyridyl)iridium (III)-cored dendrimer containing carbazole groups gave very good devices, especially upon blending with 2-(4-biphenyl)5-(4-*t*-butylphenyl)-1,3,4-oxadiazole.[415-418] An europium-centered dendritic OLED with carbazole groups at the periphery is also known with white emission (resulting from several emissions).[419] The advantage of dendrimer devices (containing only a dendrimer/host blend, a light-emitting layer and an electron-transport layer) is that they lead to a simplification of the device compared to other OLEDs having five or six components in four or five layers. Such simple dendritic device structures are highly efficient, because (i) the light-emitting processes from solution leads to possible variation of colors and (ii) the exciton diffusion length in the dendrimer is much smaller in the dendrimer film than in devices containing small molecules.[410-426] Highly efficient light-harvesting systems based on a blue Ir^{III}-centered phosphorescent dendritic acceptor coupled with dendronic carbazole-based donors via singlet-singlet (efficiency greater than 90%) and triplet-triplet (efficiency greater than 90%) energy transfer were recently reported.[427] PPI dendrimers decorated with *E*-stilbene termini have been subjected to photoisomerization and fluorescence studies; comparison with the monomer shows a decrease of the fluorescence quantum yield in the dendrimer.[430,431] Photoluminescence and triplet-triplet exciton annihilation in a neat film of a *fac*-tris(2-phenylpyridyl)iridium(III)-cored dendrimer and its blend with a 4,4'-bis(*N*-carbazolyl)biphenyl host were recently observed in the temperature range 77-300K.[428] Triplet-exciton hopping was shown to be controlled by electron-exchange interactions and

could be over 600 times faster than phosphorescence quenching in films of Ir^{III}-centered phosphorescent dendrimers.[429] A double-layer dendrimer with carbazole as the outer layer and phenylazomethine as the inner layer of the dendrons was shown by Yamamoto and his Keio group to be an excellent hole transporter in an OLED device, with performances increasing with generation increase.[432]
Newkome's group has delineated the general concepts, design criteria, and physical parameters such as component placement and electroluminescence, that relate to the construction of OLED devices, and illustrated and discussed these key electroluminescent elements with dendritic examples, calling for more research effords in this attractive field of dendrimer design.[433]

3.15. Miscellaneous photophysical studies

Triarylamine dendrimers are excellent energy donor cores (compare with triaryl amines as electron donor cores upon photoexcitation[315]), and energy migration was shown to be due to a coherent excitonic mechanism for which the exciton was delocalized in multichromophoric branched systems.[434] On the other hand, trialkylamines, that are much better reductants than triaryl amines, could be used to quench, by electron-transfer, the excited state of the anthracene chromophore that was located at the core of dendrimers of various generations. These trialkylamines including several diamine and triamine quenchers gave lower Stern-Volmer bimolecular quenching rate constants with increasing dendrimer generations, consistent with greater site isolation with increased dendrimer generations. Shape selectivity was observed as well, rigid amines being shown to approach the anthracene core more easily than flexible ones.[435] The fluorimetric titration technique could be successfully used for quantitative analysis of binding cationic PAMAM dendrimers with anionic fluorescent probes.[436] Fluorescence anisotropy was revealed to be a very useful tool to investigate dendrimer structures and energy migration processes as recently illustrated with four distinct luminophores: terphenyl, dansyl, stilbenyl and eosin that showed distinct fluorescence depolarization mechanisms in PPI dendrimers.[437] Electro-optics effects were analyzed in multichromophore dendrimers from joint theory and experimental viewpoints, and a reasonably linear relationship between chromophore number density and electro-optic activity was disclosed.[438] The photoluminnescence of poly(methyl methacrylate) was doped with fluoresceine and carbosilane dendrimers, and lasing effect was obtained herewith from a simple photonic band gap resonance cavity.[439]
Dendrimer-based multilayer films that incorporate redox and/or photoactive sites have been shown to exhibit photocurrent flow from the dendrimer to an electrode.[440-446] Stepwise assembly of dendrimers containing covalently bound $[Ru(bpy)_3]^{2+}$ termini and tris-viologen core on ITO surface using the layer-by-layer approach led to the disclosure of dendrimer generation effect by UV-vis., AFM and electrochemistry. Anodic and cathodic photocurrents were observed upon visible irradiation and were attributed to light-harvesting properties.[446]
PAMAM dendrimers of generations 2.5, 3.5 and 4.5 have been shown to drastically accelerate the crystallization of fluorescent dyes upon reprecipitation in water, a process whose kinetics was monitored by UV/vis absorption spectroscopy.[447,448] Non-conjugated dendrimers including diarylaminopyrene energy and electron-donor termini and a benzyl ether-based backbone with a benzthiadiazole moiety were subjected to electron-transfer quenching of the photoexcited state or a prevalent sequencial energy-transfer + electron-transfer pathway.[449]
Theoretical methods have been developed to test and evaluate the electronic structures and physical properties of polyacenes, polypyrroles, polyfurans, polyphenylenes, vinylene and PAMAM dendrimers (Figure 20).[450]

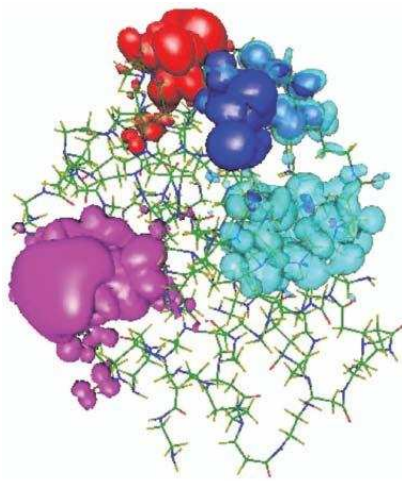

Figure 20. The probability density of the HOMO-1 (light blue), HOMO (dark blue), LUMO (red), and LUMO+1 (pink) orbitals of the generation 3 PAMAM dendrimer. The isosurfaces corresponds to the probability of finding an electron inside the surface of 90%. Reprinted with permission of the American Institute of Physics (ref. 450, Vukmirović's group).

A strong charge transfer interaction between an electron-accepting guest, diazapyrenium dication and a third-generation electron-donating amine-containing dendrimer was shown with 1:1 stoichiometry and monitored by strong changes in the absorption and emission spectra.[451] Static fluorescence of a series of ten perylene-cored dendrimers with anthracene termini revealed that excitation of the anthracene groups led to the core emission, indicating efficient energy transfer.[452] Cyclic phosphazene-cored dendrimers with amino-pyrene groups are processable blue fluorescent systems used as emissive layers in OLEDs that reach current efficiencies of 3.9 cd/Â at brightness levels near 1000 cd/m^2. Depending on the bridge between the core and fluorescent dendrons, the emissive wavelength varies between 470 and 545 nm due the stacking of the aminopyrene units.[453] The green fluorescence intensity of first-generation PPI dendrimers containing 1,8-naphthalimide fluorophores increases in the presence of protons and a variety of transition-metal cations (Figure 21).[454]

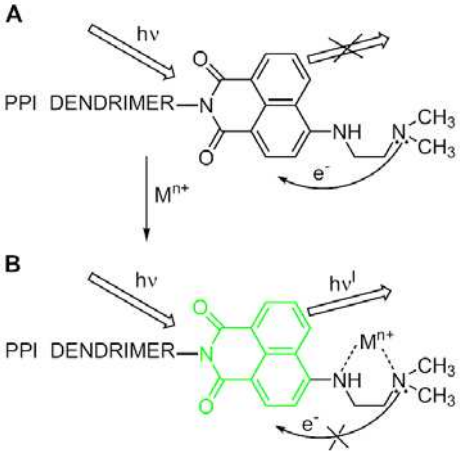

Figure 21. Proposed mechanism of fluorescence enhancement of 4-*N,N*-dimethylaminoethylamino-1,8-naphthalimide labeled PPI dendrimer. Reprinted with permission of Elsevier (ref. 454, Grabchev's group).

Hydroxy-terminated poly(propyl ether imine) dendrimers of generations one to five were reported to absorb in the region of 330 nm, in methanol and aqueous solutions, which led to an emission near 390 nm whose intensity increased under acidic *pH* and in more viscous solvents.[455]

The photochemistry of organic guests included within water-soluble dendrimers terminated by carboxylate groups were conducted with 4-methyl dibenzyl ketone, benzoin ethyl ether

and acenaphtylene photodimerization, and the cage effect was involved. Other prototypical reactions were photo-Fries reactions of 1-naphthylbenzoate and 1-naphthyl phenyl ether. It was found that the dendritic environment restricts the mobility of the radical intermediates and strongly inhibits leaking of substrate, intermediate and products outside the dendrimers.[456,457] Rapid energy transfer was reported in a stilbenoid phthalocyanine dendrimer having π-conjugated light-harvesting antennae.[458] The dendrimer generation-dependent fluorescence properties of poly(ester-amine) dendrimers with focal 4-amino-*N*-benzylphthalimide were used for switchable proton sensing.[459] Excellent energy funneling ability (over 95%) was disclosed by time-resolved fluorescence spectroscopy for π-conjugated dendrimers with 5,5,10,10,15,15-hexahexyltruxene as the node and oligo(thienylethynylene)s with various lengths as the branching units.[460] Dendrimers consisting of a *p*-pentaphenylene core branched to two G_2- or G_4 sulfonimide dendrons and two *n*-octyl chains showed pentaphenylene fluorescence (λ_{max} = 410 and 420 nm in fluid solution resp. solid state) without enegy transfer from the chromophoric groups of the dendrimer branches.[461] Ir^{III} organometallic supramolecular core-shell dendrimers were characterized as phosphorescent emitters, and these host-guest materials were applied as luminophores in OLED devices. [462]

3.16. Dendritic fluorescent sensors

The majority, if not all, the studies carried out with fluorescent dendritic materials reviewed in this § 3 can involve or can be directly applied to sensing, especially if they are or can be integrated in an adequate device. As an example from the St Andrew group, sensing of 1,4-dinitrobenzene, a model of the explosive substance 2,4,6-trinitrotoluene (TNT), used bisfluorene dendrimer-distributed feedback lasers. Indeed, fluorescence quenching of a G_1-dendrimer conjugated with 2,2'-bis(9,9-di-*n*-hexylfluorene) core was obtained with much greater sensitivity by using the material as such a surface emitting distributed feedback laser. The slope efficiency of the laser is very convenient to detect the analyte, as it decreased by 50-fold in its presence.[463] Immunosensing is an alternative for trace TNT detection (Figure 22).[464]

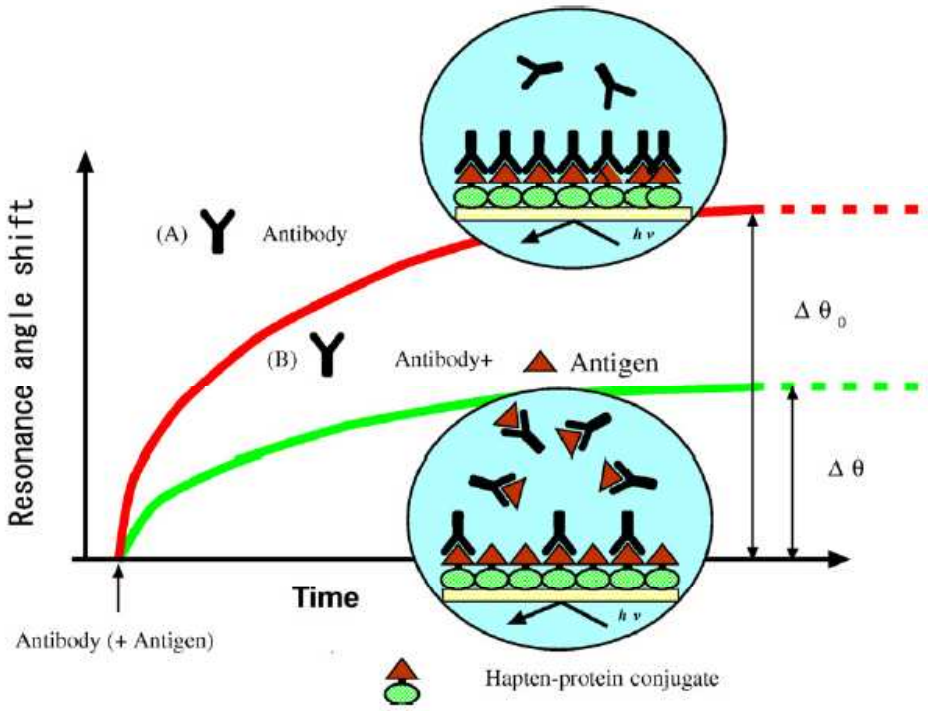

Figure 22. Principle of competitive inhibition assay on SPR immunosensor. Reprinted with permission of Elsevier (ref. 464, Singh's group).

The $G_{4.5}$-PAMAM-CO_2Na dendrimer was found to be a fluoride sensor in methanol, based on the intensely decreased fluorescence (blue : λ_{max} = 445 nm) with fluoride ion, but not with the other halides.[465]

3.17. Nonlinear optical properties

With three-branched dendritic nonlinear optical (NLO) chromophores, it was shown that the NLO activity can overtake the sum of the three noninteracting single-stand subunits, when the dendrimers show nearly parallel or helical alignments of the single-stranded subunits. Because of this conformational situation, the NLO activity can be enhanced up to nine times the value of the "independent chromophores".[466]

Cubic NLO properties were determined for phenyl and ferrocenyl-terminated resorcinarene-cored dendrimers in which these end groups were joined to the core by vinyl moieties with *trans* configuration. The $\chi(3)$ values estimated from the THG Maker-fringe technique for these dendrimers dispersed in thin solid films are of the order of 10-13 esu.[467] Dispersion of the NLO properties was observed for triphenylamine-cored alkynylruthenium dendrimers. The NLO performances of these inorganic dendrimers is an order of magnitude greater than that of similar organic dendrimers, demonstrating the key role of the incorporation of metal centers at appropriate positions and with adequate bridging ligands in the molecular architecture.[468] Increasing the generations of thiophene dendrimers increased the cross-section for both entangled and random two-photon absorption cross-sections, suggesting that the thiophene groups within the dendrimer nonlinearly absorb in a cooperative manner.[469]

4. Supramolecular Properties

4.1. Concepts and pioneering studies

Supramolecular chemistry, defined by Lehn as "Chemistry beyond the Molecule"[3] is strongly involved in dendritic structures. Dendrimers can encapsulate guest substrates in their interior and interact through supramolecular interactions (H bonding, ionic bonding, coordination) of their many branch termini with substrates at the dendrimer periphery. This most important supramolecular property[1,2] of dendrimers, their ability to encapsulate guest molecules or ions, was underlined at the very beginning of dendrimer chemistry by the pionners when Newkome coined the term "molecular micelle" in 1985[7] and Tomalia reported the encapsulation of several molecular guests at the end of the 1980's.[8] Subsequently, a variety of supramolecular interactions in- and with dendrimers were shown to contribute, eventually in synergy, to guest encapsulation by dendrimers and inter-dendritic (or dendronic) interactions for the formation of more complex dendritic nano-assemblies. Newkome promoted the concept of "Molecular Micelles" with his dendritic arborols encapsulating *inter alia* phenol blue as shown by dynamic light scattering, fluorimetry, fluorescence microscopy and UV-vis spectroscopy.[122]

The study of the encapsulation of acetylsalicylic acid in PAMAM dendrimers was carried out by Goddart and Tomalia using spin-lattice relaxation times.[470]

Supramolecular interactions with guests inside the dendrimers included hydrophobic dendrimer cavities, hydrogen bonding, metal-ligand coordination and physical encapsulation (such as Meijer's dendritic box encapsulating Rose Bengal),[9] whereas supramolecular interactions at the periphery involved electrostatic or H-bonding interactions, peptide-protein interactions for the production of peptide antibodies and synthetic vaccines[471] and carbohydrate-protein interactions[472] for cell recognition and infection.[473,474]

Newkome also pioneered the bolaamphililes that have two hydrophilic, water-soluble polyol dendrons linked by a variety of hydrophobic chains at the dendrimer interior and form gels.[475] Large dendritic micelles and vesicles were subsequently synthesized.[476-478] Self-organization of dendrimers led Percec to prepare spectacular liquid crystalline phases with sharp transition peaks and low degrees of supercooling. Enantiotropic nematic mesophases and a smectic

mesophase were formed with increasing phase transition temperatures as the generation number increased.[479,480] Carbosilane-based liquid crystalline dendrimers were also synthesized.[481] Stoddart assembled dendrimers using the π-π interaction between a π-donor and a π-acceptor, including rotaxanes with stoppers that could eventually also be dendritic.[482-486]

Finally, various ligands were installed at the periphery of dendrimers to form classic coordination complexes including dendritic transition metal catalysts that will be dealt with in § 5. The supramolecular properties of dendrimers were systematically reviewed, besides Tomalia's early reviews,[8,17,18] in other early reviews on dendrimers,[7-22] and in the excellent reviews that appeared in the late 1990's including the reviews by Newkome's group,[10,15,16] Zeng and Zimmermann[473] and Meijer's group.[22] Thus we will now focus on more recent supramolecular properties of dendrimers that were reported during this decade. Obviously, this section largely overlaps with the photophysical section for the characterization of the supramolecular properties, with the catalytic section for the approach of the coordination sites of the metals and with the biomedical section, because biological and drug-biological-substrate interaction are essentially supramolecular.

4.2. H-bonding

H-bonding is common in Nature with the two complementary strands of DNA and with proteins. Thus H-bonding in dendrimers may be more or less biomimetic, because dendrimers can be of sizes close to those of biomolecules. A typical biomimetic example is the supramolecular interaction between avidin and biotin on dendrimers, for instance on surfaces and SAMs that was quantified by time-of-flight secondary ion mass spectrometry (Figure 23).[474]

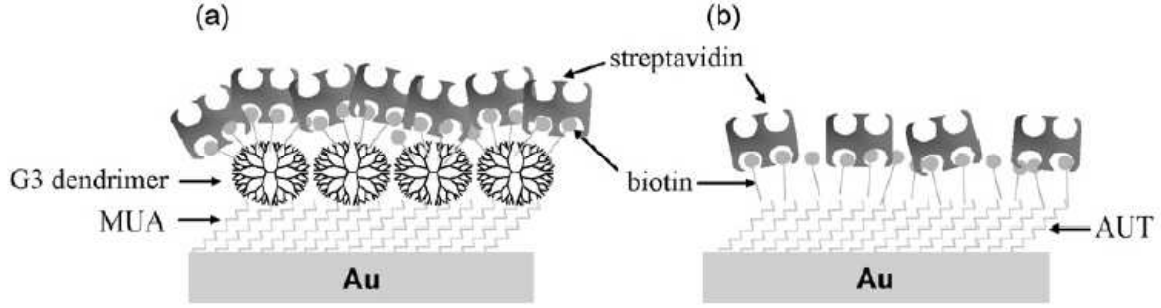

Figure 23. Schematic of streptavidin immobilized on a (a) G_3 PAMAM dendrimer monolayer and (b) self-assembled monolayer of 11-amino-1-undecanethiol (AUT) onto gold. Reprinted with permission of Elsevier (ref. 474, Lee's group).

The best known example of H-bonding in dendrimer chemistry is Zimmermann self-assembly of dendrons that has been reviewed.[473,474] Supramolecular assemblies based on H bonding between diaminobutane (DAB)-cored dendrimers with dendronic phenol were shown by ^{1}H NMR and cyclic voltammetry to reversibly form. The dendritic framework was sufficient on the electrochemical time scale (0.1 s) to recognize the $H_2PO_4^-$ anion whose sensing requires such a dendritic exoreceptor structure. Moreover, titration of the anion occured with a sudden intensity drop at the equivalent point. This was taken into account by a drop of the diffusion coefficient due to the supramolecular formation of a larger framework incorporating the $H_2PO_4^-$ anion bridging amidoferrocenyl groups.[487-491] Dendrons with other functional groups such as the redox-active 4,4'-bipyridinium showed that the redox potential can be influenced by the dendron size.[490] Self-assembled dendrimers have been reported since 2002. In particular, Zimmerman's supramolecular dendrimers involved complementary H-bonding motifs in the core.[492-493] Other self-assembled supramolecular dendrimers involved other types of H-bonded arrangements.[494-495] More recently, whole dendritic assemblies were built

up, shell by shell, in a self-assembly process. Such assemblies are based on a single complementary pair of H-bonding motifs A and B forming an AB assembly. Self-assembly dendrimers are formed by mixing a tripodal core A_3 with a branched linker BA_2 and a capping unit B in the required ratio.[496] Uniform self-assembled dendritic architectures were subsequently reported using tri- and tetra-urea derived calixarenes including ^{1}H DOSY NMR studies (Figure 24).[497]

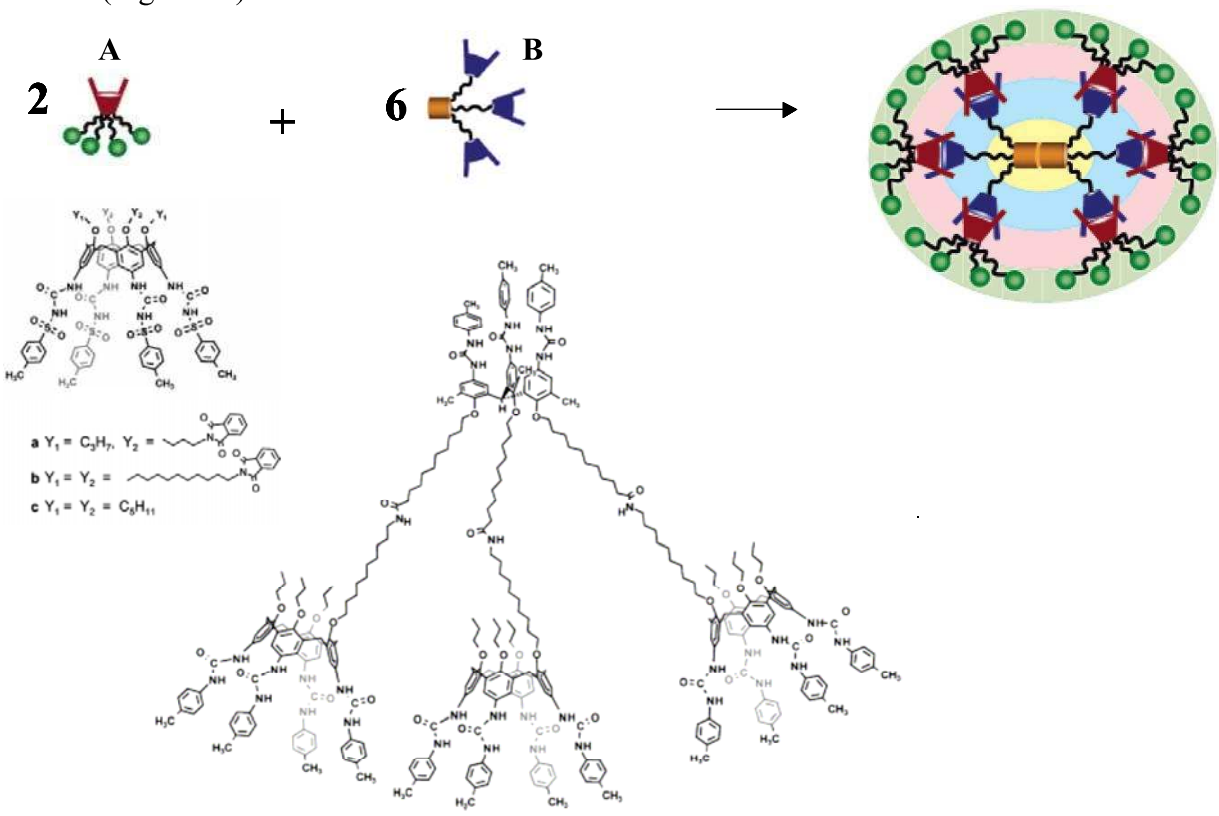

Figure 24. Schematic representation of a dendrimer self-assembled of two molecules of A and six molecules of B. Reprinted with permission of the American Chemical Society (ref. 497, Böhmer's group).

Meijer introduced transient supramolecular dendritic networks based on H-bonding of termini with guest substrates. The dynamic supramolecular interaction was studied by dynamic light scattering showing concentration-dependent assiciation.[498] Porous networks were formed by attaching multiple hydrogen-bonding sites to dendritic cores based on pentaerythrityl tertraphenyl ether. This concept creates links between crystal engineering involving tectons and dendrimers whose cores are not too flexible.[499] DAB dendritic tectons have been used in crystal engineering upon halogen bonding between DAB-$(NHC_6F_4)_{22}$ and (E)-1,2-bis(4-pyridyl)ethylene in a 1:2 supramolecular adduct.[500]

4.3. Electrostatic binding

Classic examples are dendrimers whose tethers are terminated by ionic groups such as carboxylate groups that are well-known in Newkome,[10,14-16] Tomalia[9,17,18] and Fréchet's dendrimers.[26-30] These ionic interactions play a key role in the binding between such dendrimers with cationic termini and DNA or oligonucleotides (see § 6.2.3 and 6.9). When a dendron is functionalized at the focal point with a 4,4'-bipyridinium (viologen) residue, non-covalent complexation with a crown ether (that encircles the viologen unit) can be followed by the variations of the stability constant that is very sensitive to the dendron generation. Indeed, it decreases as the size of Newkome-type dendrons increases because of steric hindrance. For Fréchet-type dendrons that are quite rigid, such an effect is not observed. The

electrochemistry of these dendrons shows electrochemical reversibility, i.e. fast electron transfer between the redox site and the electrode.[501-505] Note, on the other hand, that in dendrimers burried redox centers disclose irreversibility (slow electron transfer) that increases as the dendrimer generation increases, because the distance between these redox centers and the electrode increases as the generation increases.[506,507] The focal point of a dendron can more easily reach the electrode surface within a small distance, because it is more exposed to the outside, and the cationic charge of viologen is electrostatically attracted by the negatively charged electrode. In connection with these electrochemical studies, the diffusion coefficients were determined using the NMR technique of pulse-gradient stimulated echo (PGSE)[508,509] and compared with the cyclic voltammetry peak currents that are proportional to the square root of the diffusion coefficient.[501-504,509-510] Interactions of this kind with ferrocenyl and other redox dendrimers containing β-cyclodextrin[356] and cucurbit[7]uril[511] hosts were also reported. Electrochemistry is a current method to generate charges, and measure of electrochemial redox potentials gives indications on the stabilization of these charges by the medium.[512] Specially interesting types of ionic dendrimers are those that include their ion pairing deeply burried inside the dendrimer interior, because such ion pairs are shielded by the peripheral group and can even be solubilized in hexane, when the terminal groups are apolar. For instance, dendrimers with polyammonium cores solubilize the dye methyl orange in organic solvents (Figure 25).[513,514]

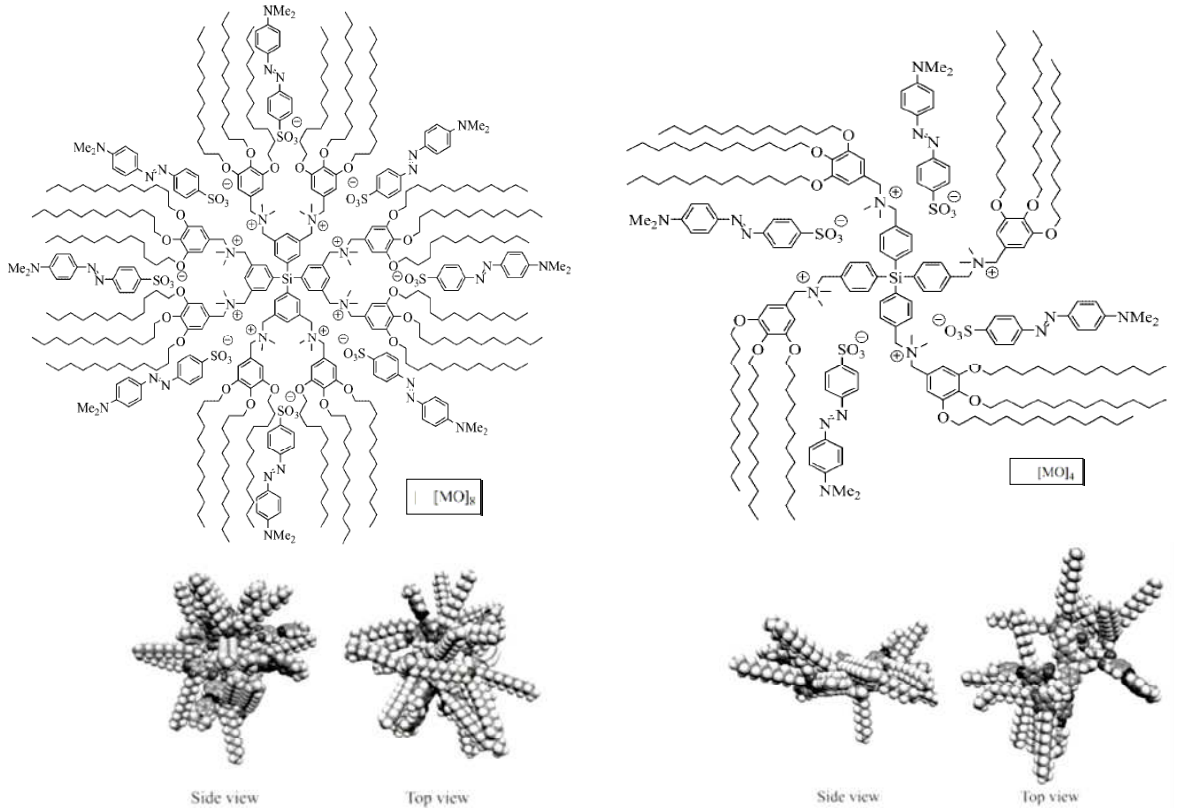

Figure 25. Space filling models of the calculated molecular structures of dendritic MO assemblies $[MO]_8$ and $[MO]_4$ (side and top view). Reprinted with permission of Wiley-VCH (ref. 513, Koten's group).

It was shown that fluorescent dyes such as eosin, fluorescein and rose bengal are extracted from water solutions as their neutral aryl carboxylic acid forms by dichloromethane solutions of dansyl-decorated DAB dendrimers, forming ammonium-carboxylate bonds in the dendritic framework upon protonation of the DAB amino groups.[515] Likewise, cationic dendrimers containing viologen units form ionic bonds with eosin, completely quenching the eosin fluorescence, but these ionic bonds can be destroyed by the addition of chloride, then re-

established upon chloride precipitation with Ag^+.[516] With cationic poly-Lysine dendrimers, ionic interactions were probed with the fluorescent anion 8-aniline-1-naphthalene sulfonate (ANS), but the interaction was also shown by ANS fluorescence studies to rely on additional aromatic-aromatic interactions between the dendritic host and the ANS guest.[517] In these cases, the polarity is opposite to that used in a seminal study for PAMAM dendrimers functionalized with terminal carboxylate groups, these later dendrimers being able to host cationic dyes such as methylene blue, acridine orange, pyronine G and phenosafranine.[518] Applications of G_5-DAB have appeared for *pH*-dependent rapid perchlorate water depollution.[519] The ionic bond can also be that of the guest rather than that of the dendrimer. For instance, Shriver studied ion transport of $Li[CF_3SO_2)_2N]$, a well-known electrolyte for batteries in DAB and PAMAM dendrimers. It was shown that G_5-DAB-64 forms more-conducting electrolytes with this salt than PAMAM-64 dendrimers. At low salt doping, the ionic conductivity and glass transition of DAB-64 are more favorable than those of the standard branched polymer, which was attributed to the reduced motion of the dendrimer upon coordination of the lithium cation to the nitrogen atoms at the DAB-dendrimer periphery.[520] Electrostatic interactions with guests such as 5-aminosalicyclic acid, pyridine, mefenamic acid and diclofenac within citric-acid terminated PEG dendrimers have been proposed to be responsible for solubility enhancement.[521,522] Other assemblies of two dendrons through focal point interactions around ammonium units also leeds to dendrtic assemblies.[523]

Atomistic molecular dynamics simulations of a G_4-PAMAM-NH_2 dendrimer carried out in aqueous solutions with explicit water molecules and counterions predicted that the gyration radius changes little between *pH*10 and *pH*5 (126 protons), agreeing with small-angle neutron-scattering experiments. Dramatic conformational change was found, however, ion pairing at low *pH* leading to a locally compact dense shell, contrasting with a dense core at high *pH*, a useful information in view of guest encapsulation and release using the *pH* trigger (Figure 26).[524]

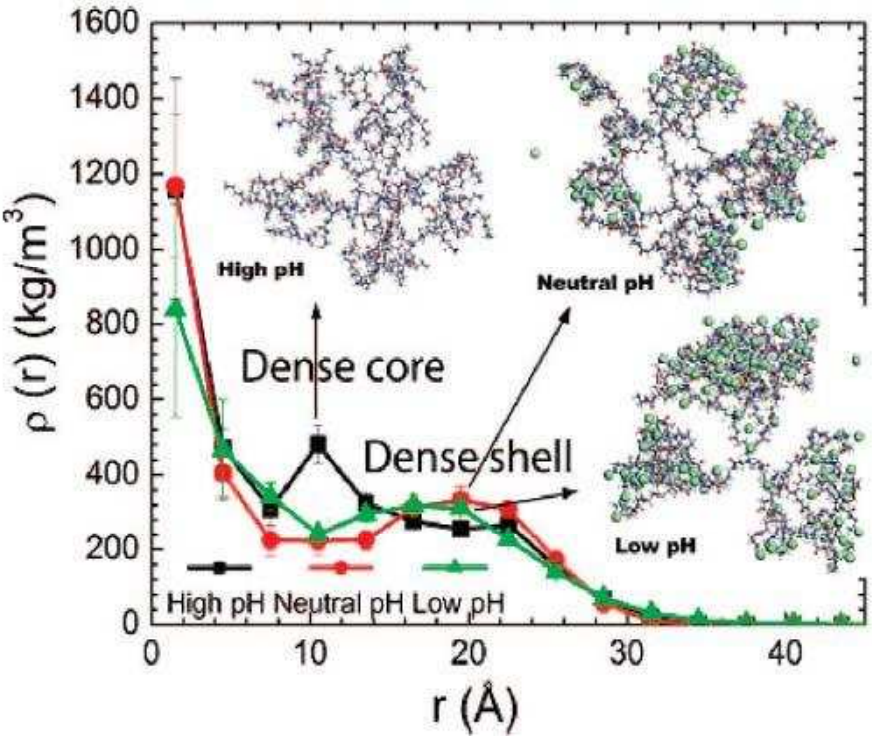

Figure 26. Radial density distribution of G_4-NH_2 PAMAM dendrimer at various *pH* values (using the center of mass of the dendrimer as the reference and averaged over 200 ps). Snapshots from MD simulations are shown in the insert. Reprinted with permission of the American Chemical Society (ref. 524, Goddart III's group).

The Newkome group has reported dendrimer-metallomacrocycle composites that form nanofiber by multi-ion pairing. Ion-promoted, automorphogenic, and stoichiometric self-assembly of a hexameric, Ru-based macrocycle and a dodecacarboxylate-terminated dendrimer produced a stable nanofiber. These polyanionic dense-packed counterions led to ion-pair superstructures in which the randomness of single-charged counterions has been eliminated.[525]

4.4. Combined H-bonding/ionic bonding

Polycationic dendrimers terminated by redox-active groups that are bonded to an amido group providing H-bonding with anions of environmental or biological interest give rather strong binding with these anionic guest that can be monitored by cyclic voltametry. These redox active dendrimers such as polycobaltocenium[526-528] or polyferrocene-ferrocenium dendrimers[487-490,529,530] are thus excellent sensors, especially because electrode derivatization is easy and strong, which make possible to wash and re-use the electrochemical sensors (Figure 27).[529,530]

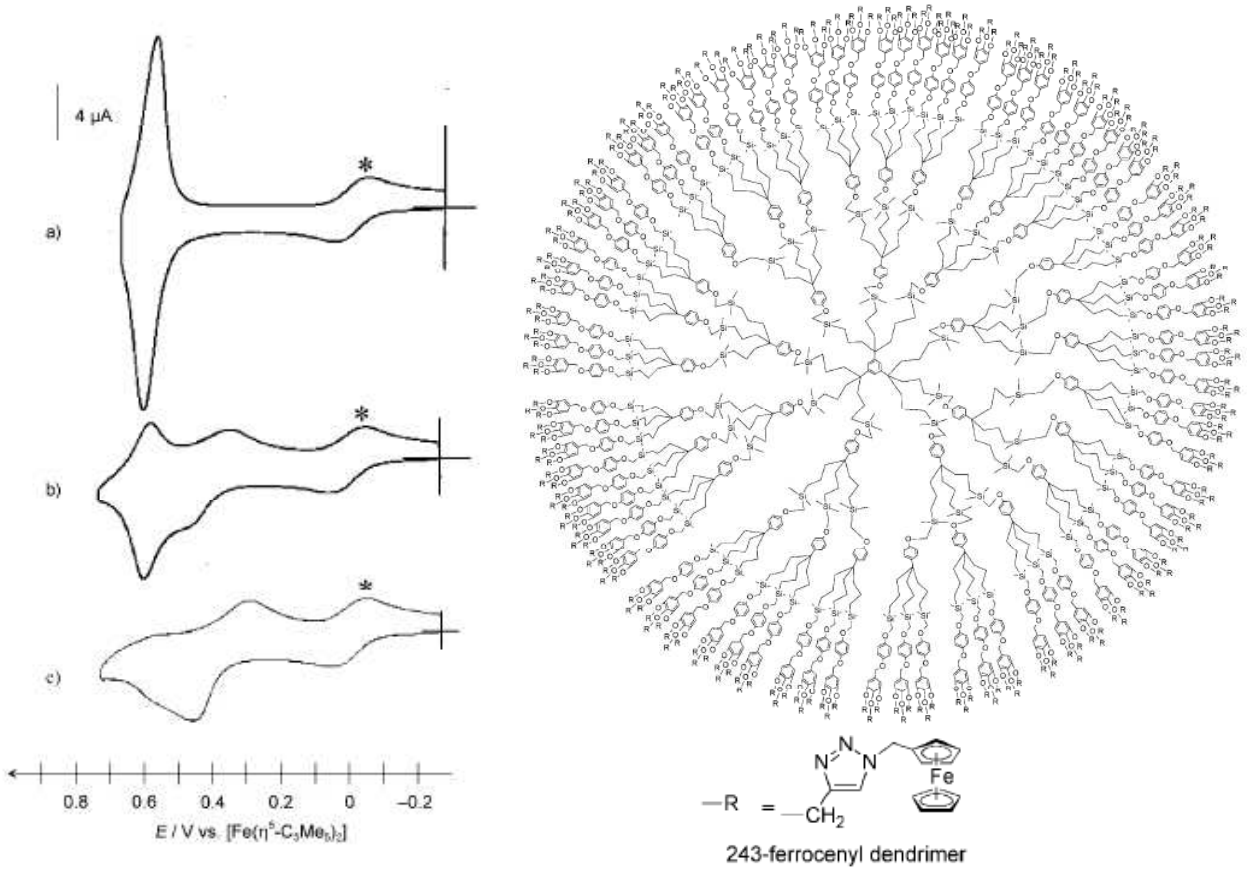

Figure 27. Cyclic voltammograms for the titration of [*n*-$Bu_4N]_2$[ATP] by the modified Pt electrode with adsorbed 243-ferrocenyl dendrimer in CH_2Cl_2 at 20°C: a) before addition of [*n*$Bu_4N]_2$[ATP], b) during titration of [*n*$Bu_4N]_2$[ATP], and c) after addition of excess [*n*$Bu_4N]_2$[ATP]; * internal reference: [Fe(η^5-$C_5Me_5)_2$]. Reprinted with permission of Wiley Interscience (ref. 530, Astruc's group).

Meijer and his group have designed PPI dendrimers whose tethers are terminated by ureid groups and whose internal tertiary ammonium groups are electrostatically bound to anionic guests also containing an ureido group or a peptide. In this way, the ureid groups of two dendritic branches provide H-bonding with the ureid or peptide group of the anion. Protonation of the internal tertiary amines of the dendrimer was best achieved using phosphonic or sulfonic acid groups. Binding constants, that are high, were determined by using fluorescence titrations, and optimized by fitting the appropriate length of the anionic

ureido guest. The stability of these dendritic host-guest assemblies was confirmed by collision-induced dissociation mass spectrometry (CID-MS), ^{1}H, ^{13}C and ^{31}P NMR, nuclear Overhauser enhancement NMR, T_1-relaxation, IR and dynamic light scattering.[531-534] The interaction of various ammonium cations with benzoate-terminated dendrimers containing 9, 27, 81 or 243 tethers in water was studied by ^{1}H and ^{13}C NMR in D_2O including DOSY experiments that allowed access to the diffusion coefficients. The lack of significant size change upon cation binding indicated intra-dendritic encapsulation of the cationic guest and backfolding of the host terminal carboxylates, and deshielding of the benzoate proton signals showed the intimate guest-host contacts. In the case of dopamine as a guest, combined ionic/H-bonding induced a much stronger bonding (characterized by the association constants) than with the guests that only involved ionic bonding. Positive dendritic effects upon cation binding by the poly-anionic dendrimers were observed as the generation increases from 0 to 2, and non-dendritic benzoates provided almost no ^{1}H NMR perturbation upon association in D_2O (Figure 28).[535,536]

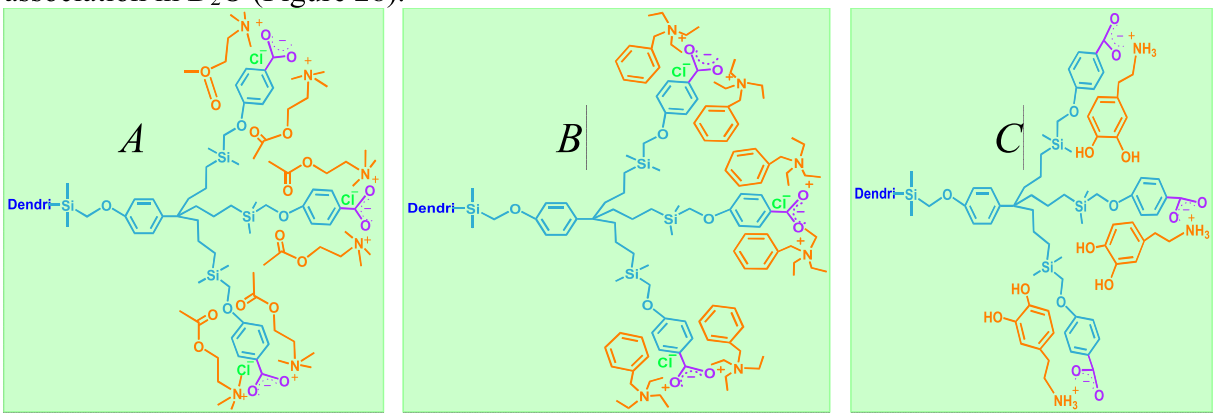

Figure 28. Representation of the ionic aggregates of carboxylate dendrimers with two actetylcholine, two benzyltriethylammonium and one dopamine. Reprinted with permission of the Royal Society of Chemistry (ref. 536, Astruc's group).

4.5. Coordination of metal ions

The incorporations of metal ions in dendritic architectures involves an essential part of dendritic chemistry and has been the subject of numerous reviews[10-22] including recent ones.[537-542] The metal ions are found at the dendritic core, dendronic focal point, tether termini, branching points and sometimes on other places of the tethers. Pionnier work in inorganic dendrimers is found in Balzani's ruthenium polypyridine complexes,[170-186] whereas the first organometallic dendrimers were those of iron sandwich complexes.[4,19] Applications are found with the luminescent and other photophysical properties of the ruthenium polypyridine and metalloporphyrin complexes (see § 3), catalysis with V, Fe, Co, Ni, Cu, Ru, Co, Rh and W-based complexes (see § 5), PAMAM gadolinium complexes as NMR contrast agents (see § 6), sensors and molecular electronics materials (see § 3). The supramolecular aspects are involved in all these domains of metallodendrimer chemistry and physics and are discussed in the appropriate sections. Here, we just recall that metal-dendritic ligands interactions are intimate parts of supramolecular chemistry whereby the supramolecular aspects are more or less involved from dendrimer assembling (for instance Fréchet's Europium-cored dendrimers[195] and Newkome's terpy-metal-ion building blocks[544], Figures 29 and 30) to various functions and applications indicated above. Applications are also found in electrochemical sensors (see § 4.4 and 6.9).[543]

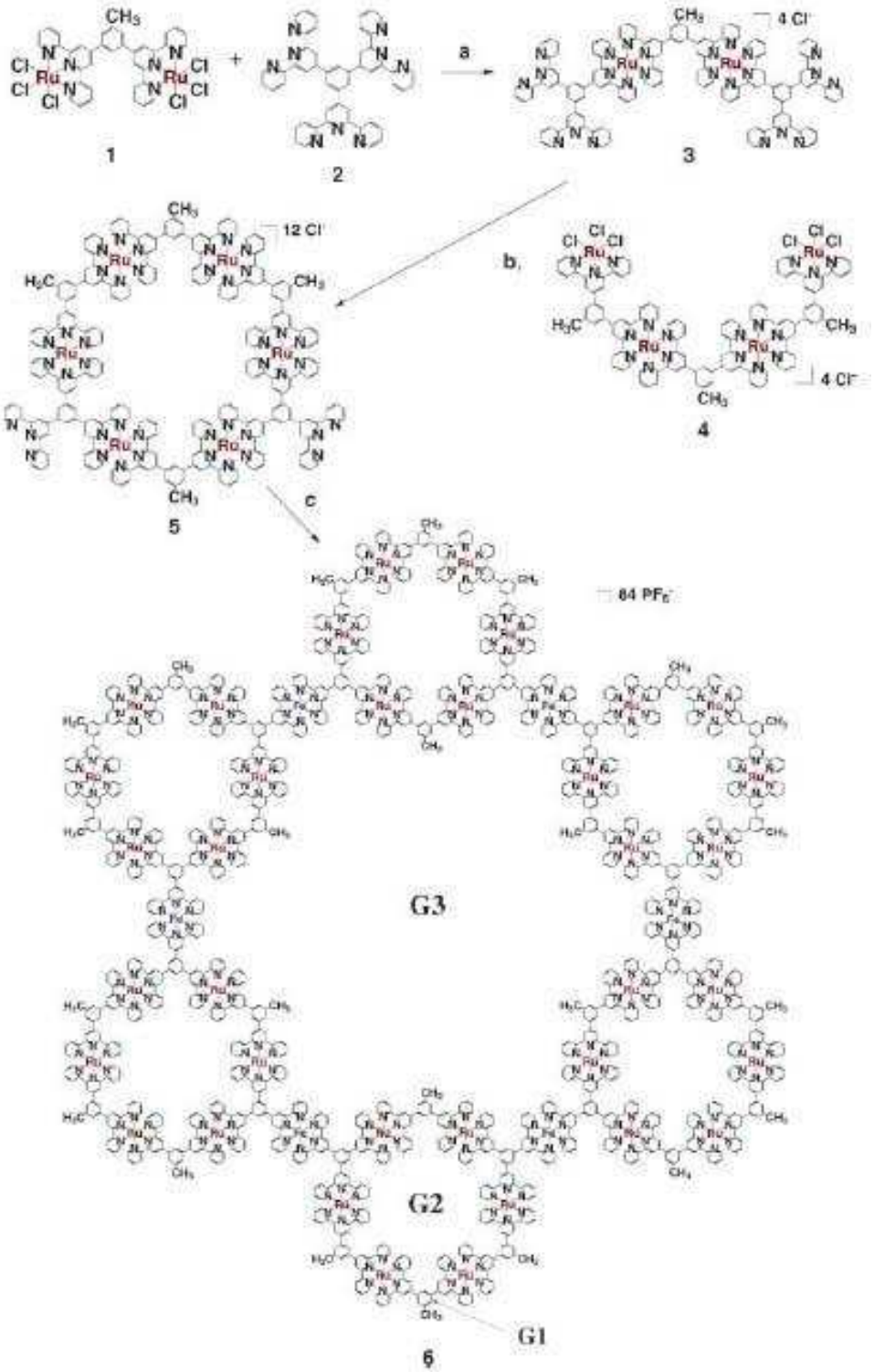

Figure 29. Reaction scheme for the synthesis of trimer 3, hexamer 5, and the fractal gasket 6. Reaction conditions were as follows: (a) 1 and 2 were mixed with N-ethylmorpholine in refluxing $CH_3OH/CHCl_3$ (2:1 v/v), for 20 hours. (b) 3 and 4 were stirred in refluxing CH_3OH with added N-ethylmorpholine for 12 hours. (c) First, hexamer 5 was refluxed in CH_3OH in the presence of 1 equiv. of $FeCl_2.6H_2O$ for 20 hours. Then, to a CH_3OH solution of $5(Cl^-)_m(NO_3^-)_n$ was added a solution of NH_4PF_6 to obtain the desired gasket 6 as a precipitate. G_1 to G_3 indicate generations 1 to 3 that can be envisioned for this fractal-based construct. Reprinted with permission of the American Association for the Advancement of Science (ref. 544, Newkome's group).

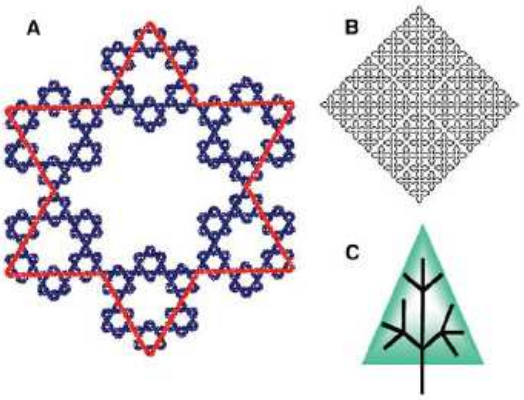

Figure 30. Sierpinski's hexagonal gasket (A) incorporating the Star of David and the Koch snowflake motifs. Images of the snakelike ''kolam'' pattern (B) and (C) the 1→3 branching pattern of a tree. Reprinted with permission of the American Association for the Advancement of Science (ref. 544, Newkome's group).

4.6. Intra-dendritic π-π Interactions

A well-known case of intra-dendritic π-π interaction is found in Stoddart's rotaxanes with dendronic stoppers, the so-called "threading" approach, in which the thread based on electron-poor bipyridinium dications is terminated by Fréchet-type dendrons and encircled by the electron-rich aromatics of the bis(tetra-ethyleneglycol-phenylene) ring (Figure 31).[20,545]

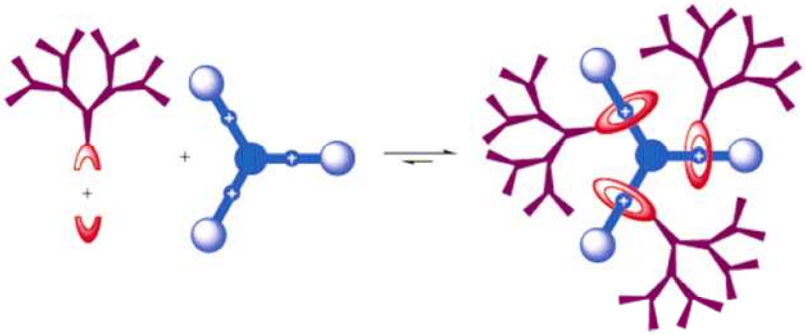

Figure 31. Graphical representation of the template-directed synthesis of mechanically interlocked dendrimers. Reprinted with permission of the American Chemical Society (ref. 545, Stoddart's group).

Another remarkable example is the π-π interaction between dendritic cycloveratrylenes for which Nierengarten showed that the binding association constant with C_{60} increased together with the increase of the dendrimer generation, reaching 340 M^{-1} for G_4 in CH_2Cl_2.[293, 546-548] In Fréchet'seminal polyarylether dendrimers functionalized with water-solubilizing carboxylate groups, the unimolecular micelle behavior was demonstrated by pyrene solubilization, but possible π-π interaction was invoked, because twice more of the electron-deficient 2,3,6,7-tetranitrofluorenone was solubilized as pyrene. It is likely that many cases of less clear-cut examples may involve *inter alia* such interactions in dendritic encapsulation of guests containing aromatic residues in dendrimers. In a recent review of weak aromatic interactions, yet containing a dendrimer section, the paucity of other reported studies of intradendritic interaction appears in spite of the frequent occurrence of these interactions,[549] in contrast with studies of inter-dendritic assemblies.

4.7. Encapsulation of neutral guest molecules

Since the seminal proposal of dendrimers as molecular micelles by Newkome in 1985,[8] guest encapsulation by dendrimers has appeared as one of the major dendritic properties, because of the potential applications for drugs.[550] A well-known example is Meijer's dendritic box, a PPI dendrimer for which the dendrimer-guest complex is capped by reaction of the terminal

amino groups with Boc- or Fmoc-protected amino-acids for permanent guest encapsulation or subsequent release upon deprotection using formic acid.[477] Studies by various authors of neutral guest encapsulation have involved simple molecules such as iodine, pyridine or benzoic acid,[551] 2,6-dibromo-4-nitrophenol,[551] dyes (Reichart's dye,[552] Bengal Rose,[553] orange OT,[554] 4,5,6,7-tetrachloro-fluorescein[553]), other molecules of photophysical interest (anthracene,[555] pyrene[550,556-558]) and many drugs[559] (see § 6.2.1). A large majority of studies have concerned PAMAM dendrimers, because they are commercial, water soluble, can be functionalized with terminal groups and work very well for a variety of encapsulations. Most often, the PAMAM dendrimers were used with further functionalization by means of their terminal NH_2 groups, but sometimes the PAMAM hosts were terminated by OH or PEG groups, and occasionally by other groups such as esters, citric acid or lauroyl.[559] Many other dendrimers have also been used such as PPI, polyether- and PEG dendrimers. Following Newkome's concept,[8] dendrimers with hydrophobic core and hydrophilic periphery exhibited micelle-type behavior and showed the marked property to act as molecular containers. The guest-encapsulating property of dendrimers goes together with their solubilizing properties. The water-insoluble molecules can be encapsulated by water-soluble dendrimers (owing this property to water-solubilizing termini) that have hydrophobic interiors. The property of guest solubilization by encapsulation increases as the dendrimer generation increases. This has been shown by all the precise studies with various guests and dendrimers (Figure 32).[521-525,557,560,561] G_4-PAMAM dendrimers functionalized with phenylalanine or γ-benzylglutamate moieties were terminated with PEG_{2000}, which enhanced their nanocontainer properties, for instance with Rose Bengal and indicated their potential capacities for drug delivery (cf. § 6.2).[562] Up to 50 Rose Bengal molecules could be encapsulated in PEGylated PEI dendrimers. The encapsulation capacities were dependent linearly with the degree of the PEG shell, either as PEG length or degree of functionality, confirming that the PEG chains play a predominant role in the encapsulation process.[563] As an example, PAMAM dendrimers having both PEG and β-cyclodextrin termini could solubilize 2μM C_{60} in water.[564]

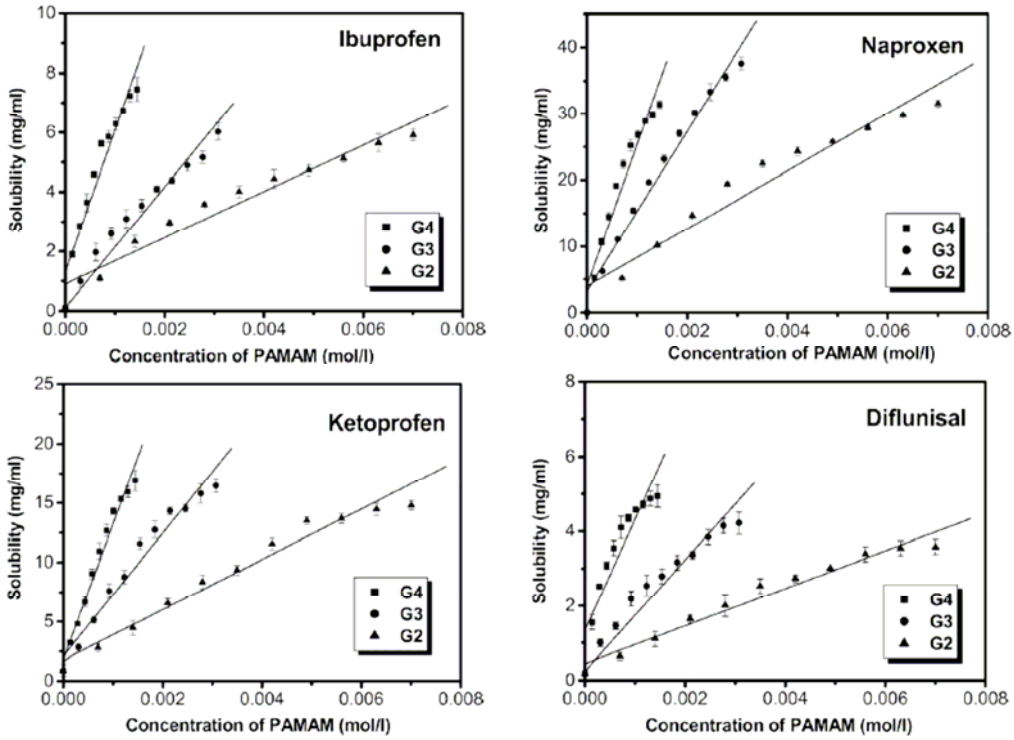

Figure 32. Solubility of Ibuprofen, Naproxen, Ketoprofen and Diflunisal in the presence of increasing concentration of PAMAM dendrimers. Reprinted with permission of Elsevier (ref. 561, Yiyun's group).

The dendrimers have open shapes for low generations, and the dendrimer shapes progressively become globular as the generation number increases, which has been related to the concomitant increase of guest solubilization. It has also been shown that small guests are more easily encapsulated and solubilized than larger ones.[521-525] Amphiphilic dendrimers, first reported by Fréchet's group, produce emulsions in dichloromethane/water.[555] Recently, it was shown that amphiphilic dendrimers having both hydrophilic (carboxylic acid) and hydrophobic (decyl) groups in the dendrimer repeat unit and 3,5-dihydroxybenzyl alcohol termini solubilize both hydrophobic and hydrophilic guest molecules.[558] Another variation is hydraamphiphiles, so-called when the dendrimer contains hydrophilic, hydrophobic and central polar groups. The solubility of the dye Orange OT increased linearly with the concentration of such a dendrimer that could be useful as well in the solubilization of both polar and hydrophobic substrates.[554] Dendrimers can be used as surfactants.[565] In a seminal example, PPI dendrimers functionalized with a fluorous-group-containing CO_2-philic shell extracted the hydrophilic methyl orange, a CO_2-insoluble dye from an aqueous CO_2 solution.[566] Dendrimers consisting of PPI core and PAMAM dendrons encapsulated pyrene all the more as the *pH* and generation number were higher, solubilized pyrene being located in the hydrophobic PPI cavities of the core (Figure 33).[567]

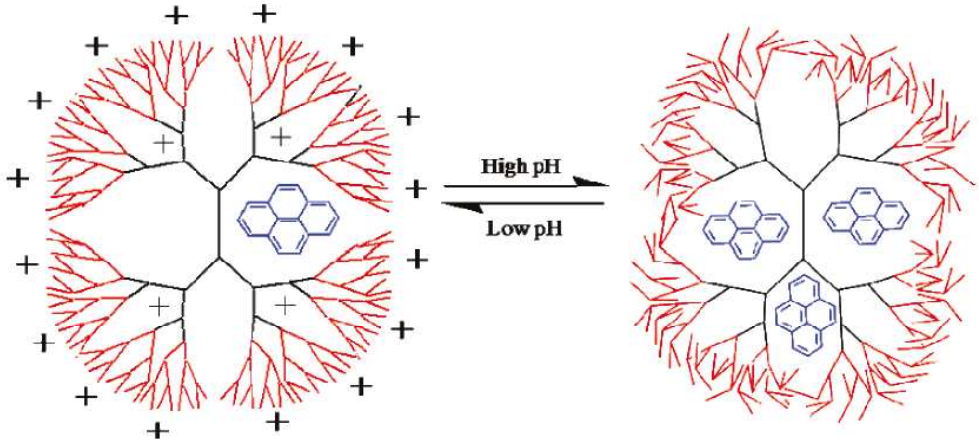

Figure 33. Schematic representation of pyrene encapsulation in PPI-core:PAMAM-shell dendrimers at acidic and basic *pH*. Reprinted with permission of the American Chemical Society (ref. 567, Imae's group).

4.8. Inter-dendritic supramolecular associations

4.8.1. Liquid crystals

In the preceding sections, we discussed inter-dendronic supramolecular associations involving the dendron focal point by coordination around a central template that can be a metal ion or an organic or inorganic core by H-bonding and/or electrostatic interactions. Inter-dendronic supramolecular interactions reach a higher level of organizational sophistication with Percec's work in which the termini are three or four C_{12} to C_{14} alkoxy chains on gallic-acid-based aryl groups, and the dendronic focal point is carefully designed to supramolecularly direct shape-specific assemblies that have liquid crystalline properties ("dendromesogens"). Globular dendrimers self-assemble from conical or other conformers that represent a fragment of a sphere,[568,569] and chiral assemblies from conical dendrons were reported to form hollow globular assemblies (Figure 34).[570]

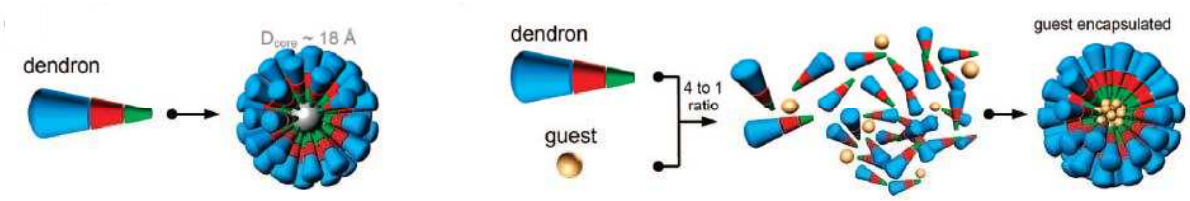

Figure 34. Schematic representation of encapsulation of LiOTf and RbOTf guests in the hollow core of the supramolecular sphere assembled from the dendron. Reprinted with permission of the American Chemical Society (ref. 570, Percec's group).

Columnar thermotropic supramolecular assemblies formed from conical dendrons.[571] Hydrophobic interactions are responsible for the formation of librairies of such dendrons.[572] Dendrimers centered on cycloveratrylene cores self assemble into helical pyramidal columns, and cubic and tetragonal lattices.[573,574] Percec's group[568-581] and Jain's group[582-583] have recently reported a number of examples of such dendrimers that self-assemble into supramolecular lattices or ensembles. In particular, the cylindrical phases of supramolecular dendrimers have attracted attention because of their potential applications as optoelectronic materials,[584-586] selective membranes[569,587] and nanopaterning templates.[588,589] The degree of control and selectivity in the orientation of fan-shaped supramoleclar cyclinders has been dramatically improved by applying magnetic fields to perfluorinated dendrimers.[590] As pointed out by Tomalia, "fluorine makes the difference", as fluorination of a self-assembling dendrimer enhanced the ability of Percec's dendrimer to self-assemble compared to its non-fluorinated analogue,[591] despite some counter-examples.[584]

The area of dendritic liquid crystals is indeed broad and rich and has recently been the subject of an excellent review by the Donnio-Guillon group.[592] Classic dendrimers such as PAMAM, PPI[593-596] and carbosilane dendrimers[597-601] have been decorated with side chain liquid crystalline groups. An example is known with H-bonding with G_1 to G_4 pyridine-terminated PPI dendrimers to which 3-cholesteryloxycarbonyl propanoic acid was added. These liquid crystals form birefringent glasses at room temperature and viscous smectic A phases at higher temperatures.[602] Amphiphilic polyether dendrons containing a polyethylene oxide chain connected to the focal point form crystalline lamellar, micellar cubic, continuous cubic phases upon increasing the length of the polyethylene oxide chain and the temperature. In this case, the microphase separation between the hydrophobic dendron and the hydrophilic chain is responsible for mesomorphism.[582,583] Amphiphilic polester dendrimers terminated with chiral mesogenic calamitic groups form ferroelectric liquid crystals exhibiting smectic C and smectic A phases. The liquid-crystal design was also introduced as a main chain such as in wilow-like dendrons and dendrimers based on terphenylene units forming enantiotropic N and smectic phases.[479] The Donnio-Guillon group reported octopus-shape dendrimers terminated with aliphatic chains adopting a prolate conformation and exhibiting remarkable smectic A and B phases resulting from parallel disposition of the mesogenic groups on both sides of the core.[604,605] Subsequently, a wide range of mesogenic structures were elaborated with homolytic and heterolytic dendrimers based on octopus cores.[601-606] Ferrocenyl- and C_{60}-terminated dendrimers and other fullerene-containing dendrimers were also shown to fom smectic A phases,[286,607-613] but only very few other metallomesogens are known, with nitrogen ligand-metal complexes (Figure 35).[614-615]

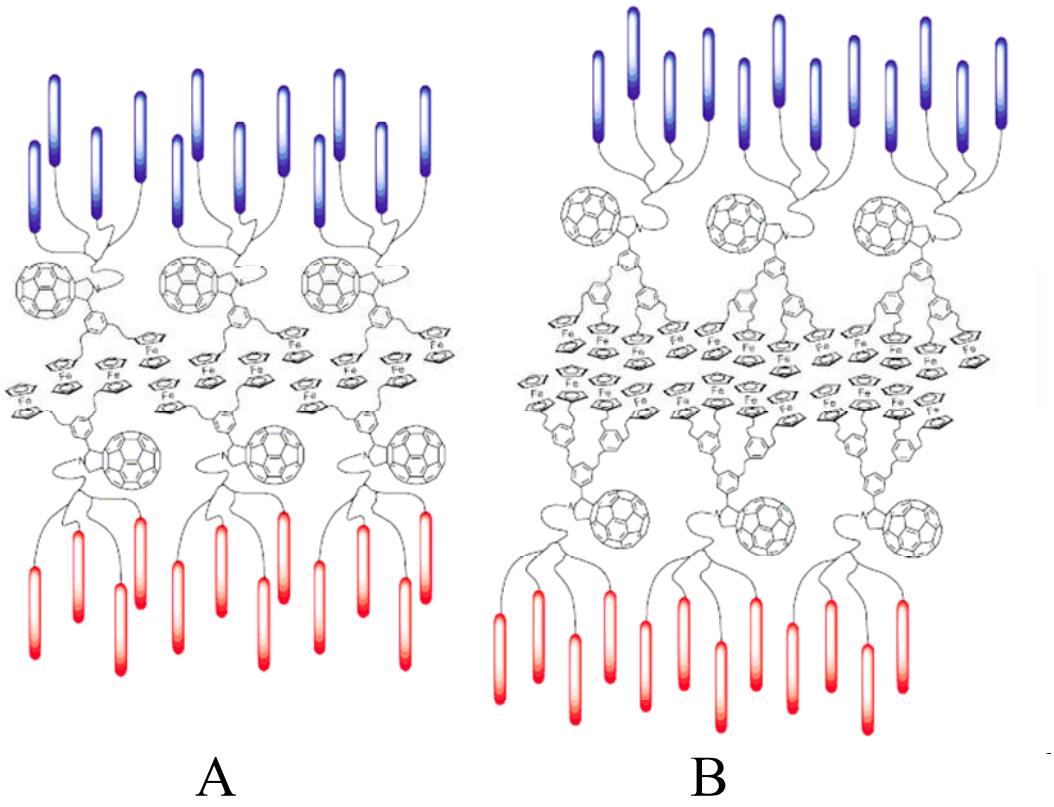

Figure 35. Postulated supramolecular organization of A (left) and B (right) within the smectic A phase. Reprinted with permission of Elsevier (ref. 610, Deschenaux's group).

On the other hand, Moore's rigid-cored dendrimers[130] terminated with oligo(ethylene oxide) chains formed columnar discotic liquid crystals with clearing-point temperatures that were dramatically generation dependent.[616] Photosensitive ionic nematic liquid crystalline complexes were designed based on dendrimer and hyperbranched polymers and a cyanobenzene carboxylic acid. High and stable values of the in-plane order parameter up to 0.67 have been reached.[617] PAMAM and PPI dendrimers modified by decanoic, 4-octylbenzoic, and 1,3,5-trioctyloxybenzoic acid termini generated dendritic liquid crystals of smectic and columnar phases that were luminescent with blue emission at 370 nm, which shows that PAMAM and PPI based mesogenic structures exhibit intrinsic emission in the visible region without additional chromophores.[618]

4.8.2 Other dendritic self-assemblies

The self-assembly mechanism and molecular dynamics for poly-L-lysine-terminated polyphenylene dendrimers were examined using X-ray, solid-state NMR, calorimetry and dielectric spectroscopy by Florence et al. Poly-L-lysine length dependence, packing restriction and glass transitions related to the rigid polyphenylene cores were shown. Monolayers at the solid/air, solid/water or air/water interface represent interacting structures,[619,620] and these dendrimers self-associate in aqueous media to form micellar aggregates.[621] The self-assembly pattern takes the form of micelles and turns to vesicles called "dendrisomes" upon increasing the lipophilicity of dendrons.[622] Incorporation of cholesterol affected the morphology, size and thermal transition of these dendrisomes.[622,623] Dendrimer terminated with hydrophobic groups spontaneously aggregate in aqueous media and form nanoparticles whose size and stability depend on the packing characteristics of the dendrimers (Figure 36).[624]

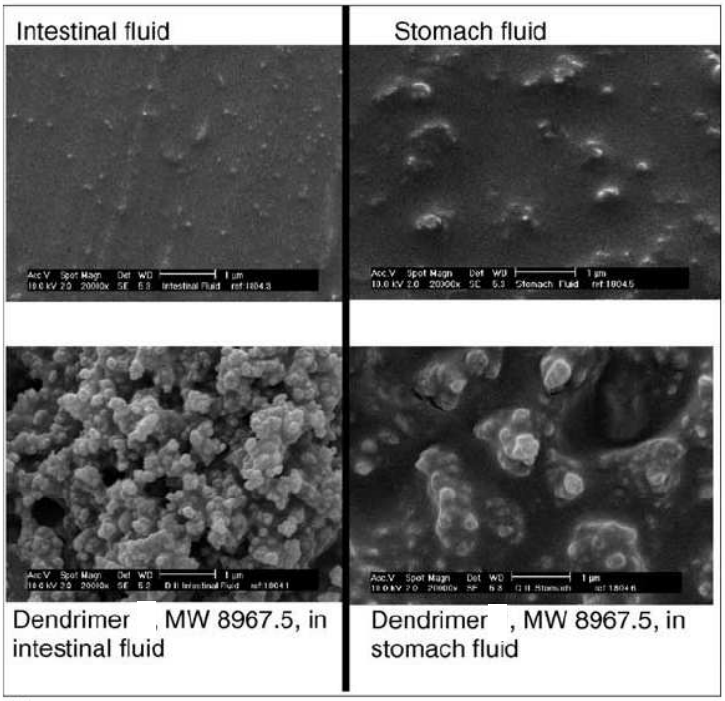

Figure 36. SEM pictures of purified intestinal and stomach fluid with and without dendrimer (1.71 mg/ml) after 3-h incubation. Reprinted with permission of Elsevier (ref. 624, Florence's group).

Müllen and his group have shown how to self-assemble a second-generation polyphenylene dendrimer into nanofibers. 1H,1H,2H,2H-perfluorodecyltrichlorosilane was grafted in the gas phase onto a silicon substrate in order to guide the formation of the dendrimer fibers into well-defined patterns.[625] The self-assembly of amphiphilic dendrons with homopolymer polystyrene at the focal point and polyacrylic acid periphery produced micelles of uniform size (14-18 nm) with 43 dendrons per micelle.[626] Designed dendronized supramolecular nanocapsules are *pH* independent with water-soluble, deep-cavity cavitands that assemble via the hydrophobic effect around a range of molecular guests.[627] Helical supramolecular dendrimers were generated by Percec's group from self-assembling dendrons and dendrimers and from self-organizable dendronized polymers, as indicated by the X-ray diffraction pattern of their oriented fibers. Hundreds of samples were screened until a library containing 14 supramolecular dendrimers and dendronized polymers provided a sufficient number of helical structures.[628] Amphiphilic dendrimers, that contain both hydrophobic and hydrophilic groups in every repeat unit, exhibit environment-dependent assemblies both in a hydrophilic solvent, water, and in a lipophilic solvent, toluene. In a mixture of immiscible solvents, these dendrimers were kinetically trapped in the solvent in which they are kinetically assembled. This property has been exploited to extract peptides from aqueous solution into an organic phase, where the peptides bind to the interior functionalities of the dendritic inverse micelles.[629] Large π-extended dendrimers self-assemble in the gas phase, in solution and on a mica surface (from DLS, AFM and SEM experiments), and encapsulate C_{60}.[630] G_5-PAMAM-OH dendrimers were hydrophobically modified with varying amounts of dodecyl moieties or cholesteryl moieties which caused aggregation and molecular interactions between dendrimers that are absent in unmodified G_5-PAMAM-OH dendrimers. The chlolesteryl moiety being a rigid lipid found in abondance in biological system did not cause toxicity increase of these dendrimers (cf. § 6.6).[631]

4.9 Supramolecular assemblies between dendrimers and surfactants and polymers

Such assemblies tranform the physical and solubility properties of dendrimers.[619,620] They were pioneered by Tomalia's studies of the interaction between PAMAM and dodecylammonium bromide leading to generation-dependent surfactant aggregates.[632] Surface activity and hydrophobicity of the surfactants are enhanced upon interaction with PAMAM dendrimers, and the apparent dendrimer diameter considerably increases with such interactions. Largely improved capacity of hydrophobic guest solubilization, such as pyrene, results.[633-635] The techniques used to study these assembies are fluorescence correlation spectroscopy and dyamic light scattering.[619,620] The non-ionic surfactants polysorbate 20 and polysorbate 60 exhibit dendrimer solubilizing properties, which was taken into account by the flexibility of the hydrophobic tail of the surfactant that penetrates into the hydrophobic dendrimer interior.[636] Assembly properties were also reported for phosphorous dendrimers with galactosylceramide analogs.[637] Electrostatic interactions were used to create a template-assisted supramolecular assembly consisting of a polymeric dendrimer at the core and amphiphilic substrates on the periphery. The positioning of guest molecules within the supramolecular complex could be modulated with dendrimer generation, surfactant chain length, and dendrimer: surfactant concentration ratio.[638] Competitive interactions in ternary systems including a slightly crosslinked polyanionic hydrogel, a protonated PPI dendrimer and an ionic surfactant indicated that the direction of the substitution reactions in systems containing cationic surfactants depended on the length of the aliphatic radical in the surfactant molecule as well as on the dendrimer generation number.[639]
Emulsions can also be stabilized by dendrimers. Emulsion polymerization of styrene was carried out using dendrimer DAB-dendr-$(NH_2)_{64}$ as seed, and the nanosized dendrimer/polystyrene polymer emulsion particles obtained were monodisperse in the range of 26 to 64 nm in diameter. The size and size distribution of emulsion particles were influenced by the contents of dendrimer, emulsifier and initiator, as well as the *pH* value.[640,641] With dodecylsulfate, latexes are formed,[642] and comparable results were obtained with PPI dendrimers.[643-645] The geometry and surface chemistry of PPI dendrimer assemblies can be varied through the addition of surfactants, and these dendrimer/surfactant aggregates can be tuned to template the formation of the different phases of calcium carbonate.[646] Catanionic surfactants were prepared with dendrimers using unprotected lactose or lactobionic acid, and these amphiphilic dendrimers bearing sugar polar heads are of interest for their biological applications as mimics of natural ligands of proteins.[647]
The effect of ionic binding on the self-diffusion of anionic dendrimers and hydrophilic polymers in aqueous systems has been studied by pulsed gradient NMR techniques and was shown to have most significant effect on dendrimer diffusion.[648]
Covalent dendrimer-polymer assemblies are dealt with in section 2.3 and dendrimer-biomolecule interactions, in particular with DNA, are discussed in § 6.

4.10. Dendrimer- encapsulation and/ or stabilization of metal nanoparticles and quantum dots

Metal nanoparticles (MNPs) can be stabilized either by encapsulation[649,650] within dendrimers or by inter-dendrimer stabilization.[651] Crooks demonstrated that PAMAM dendrimer that have protonated amine termini or terminated by OH groups can complex metal ions such as Cu^{2+}, Pd^{2+}, Pt^{2+}, Ni^{2+}, Fe^{2+}, Mn^{2+}, Au^{3+}, and Ru^{3+} inside the dendrimers. Subsequent reduction by $NaBH_4$ of various PAMAM dendrimers complexed by Cu^{2+} and Pt^{2+} leads to dendrimer-encapsulated MNPs.[649,652,653] For several ions for which the complexation was not strong enough such as Ag^+, it was possible to form dendrimer-encapsulated MNPs by redox reaction from CuNP-encapsulated PAMAM dendrimers:
$Cu + 2\ Ag^+ \rightarrow Cu^{2+} + 2\ Ag$

The redox displacement method also works to form dendrimer-encapsulated MNPs with Au^{3+}, Pt^{2+} and Pd^{2+}, because the standard reduction potentials ($E°$) of these ions are more positive than that of Cu^{2+}/ Cu. This method can also be extended to the synthesis of heterobimetallic metal NPs if a sub-stoichiometric amount of such oxidizing ion Pd^{2+}, Pt^{2+}, Au^{3+} or Ag^{+} is used with G_6-OH (Cu_n) PAMAM dendrimer yielding dendrimer-encapsulated PdCuNPs, PtCuNPs AuCuNPs or AgCuNP respectively. Dendrimer-encapsulated heterobimetallic NPs can also be prepared by simultaneous co-complexation followed by a single reduction step. It is also possible to form dendrimer-encapsulated metal NPs such as G_6-PAMAM-OH-PtPdNPs sequentially, because after the formation of a monometallic MNP, the complexation sites are free for the complexation of another metal. It has been pointed out that one disadvantage of PAMAM dendrimers is their thermal instability above 100°C due to retro-Michael reactions. PPI dendrimers are stable up to 470°C, however, allowing PPI dendrimer-encapsulated MNPs to be used for applications at high temperature.[655,656] Monodisperse MNPs have applications in catalysis, optoelectronics, magnetism, and chemical sensing, and the MNPs synthesized by dendrimer encapsulation are relatively monodisperse as observed by the various TEM and HRTEM histograms reported. Their sizes range from 1 to 4 nm depending on the dendrimer type, dendrimer generation and dendrimer/metal ion ratio. The terminal dendrimer groups allow to solubilize them in a variety of solvents, and the dendrimer periphery serves as nanofilter whose filtration power depends on the dendrimer generation.[654] Evidence of encapsulation is provided by compared NMR spectra in the presence and absence of PdNP showing more perturbation of the intra-dendritic methylene group signals.[657] "Click" metallodendrimers have been designed to coordinate metal ions in their interior at each 1,2,3-triazolyl layer.[530,658,661] Such dendrimers can electrochemically sense both anions such as ATP^{2-} and metal cations such as Cu^{+} Cu^{2+}, Pd^{2+} and Pt^{2+}, using the ferrocenyl termini that is directly bonded to a terminal triazolyl recognition site. Further reduction for instance of Pd^{II}-click-dendrimer complexes yields dendrimer-encapsulated (G_1 and G_2) or dendrimer-stabilized PdNPs (G_0), the latter being obtained when the dendrimer is too small.[657,658] Using PEG-modified "click" metallodendrimers, dendrimer-encapsulated- and dendrimer-stabilized AuNPs could also been obtained upon reduction of their 1,2,3-triazolyl $-Au^{III}$ intra-dendritic complexes, yielding various AuNP sizes depending on the Au^{III} loading (Figure 37).[663]

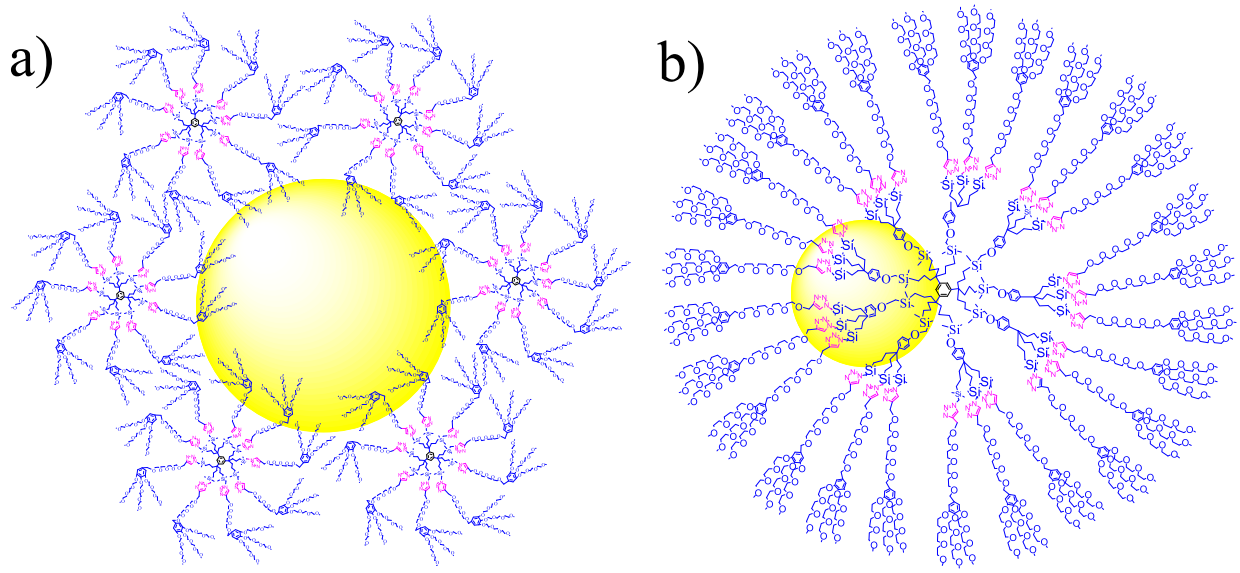

Figure 37. (a) AuNPs stabilized by several G_0 dendrimers; (b) G_1 dendrimer-encapsulated AuNPs. Reprinted with permission of the Royal Society of Chemistry (ref. 663, Astruc's group).

Various syntheses and studies of other dendrimer-encapsulated AuNPs and AgNPs have recently expanded the interest in this area.[664-674] Ag-CuNPs having various shapes were

prepared by co-complexation in the presence of PAMAM dendrimers. Small and evenly sized spherical Ag-CuNPs were obtained with N_2H_4. H_2O as reductant, whereas long, rod-shape bimetallic NPs were prepared using $NaBH_4$ as the reductant.[674] The synthesis of heterobimetallic NPs (such as AuPdNPs) encapsulated in dendrimers has been achieved for catalytic applications (cf. § 5.5.2). The Yamamoto group designed rigid azomethine (imine) dendrimers incorporting Sn^{II} and Ti^{IV} ions that could be reduced to dendrimer-encapsulated SnNPs and oxidized to dendrimer-encapsulated TiO_2NPs respectively.[675] These dendrimer–encapsulated nanomaterials served as catalysts, high-intensity light-emitting devices, efficient organic solar cells and metal delivery systems.[675] AuPs covered with thiolate ligands terminated by carboxylic acid groups were supramolecularly bound to PAMAM dendrimers of generation 1 to 4 via their terminal amino groups, leading to mixed thiolate-AuNP-PAMAM dendrimer assemblies that precipitated all the more slowly as the generation was higher. SAXS was used to quantify the interparticle spacing that ranged from 0.6 nm for G_0 to 1.9 nm for G_4 (edge-to-edge), indicating dendrimer constriction upon assembly (compare G_4: 4.5 nm). The interparticle spacing increase observed upon increasing dendrimer generation shifted the AuNP plasmon absorption in these assemblies from 592 nm for G_0 to 538 nm for G_4.[676] Quasi-alloy PdAu G_6-PAMAM DENs rearrange upon oxidation in air to yield core-shell configurations.[677,678] Polymer-cored DAB-dendrimer-shelled NPs in 15-20-nm size range could trap more than 900 Cu^{2+} ions *per* NP-DAB16, and external amine groups could be covalently linked to up to 1000-1500 azobenzene chromophores per NP through aza-Michael addition in aqueous suspension.[679] CoNPs were stabilized by G_5-PAMAM-NH_2 dendrimers (approx. 38 Co atoms per dendrimer), and investigation of the magnetic properties indicated superpamagnetism with a blocking temperature of 50K.[680]
Similarly, various dendrimers have been used for the stabilization of other NPs, in particular CdS and CdSe, the best characterized semi-conductors that are of great interest for the fabrication of nanoelectronic devices.[681-685] Finally, dendrimers, such as PPI dendrimers modified with long alkyl chains, can serve as templates to direct the formation of biominerals such as calcium carbonate, the main constituant of mollusk shells. It was found that Ca^{2+}-induced assemblies of dendrimer/surfactant aggregate into giant spherical particles.[685] On the other hand, PAMAM dendrimers ($G_{5.5}$) with surface carboxylate groups inhibited the crystal formation of hydroxyapathite nanorods and affected the crystal morphology and particle size during the preparation.[686,687] AgNP dispersions were obtained via a dendrimer-polymer template approach, which allowed their use as antibacterial surface treatment.[688]

4.11. Interactions of dendrimers on surfaces: self-assembled monolayers (SAMs) and surface patterning

Self-assembled monolayers (SAMs) are an essential part of nanoscience.[689,690] Reinhoudt's group has shown that ferrocenyl-terminated dendrimers[691-693] and biferrocenyl-terminated dendrimers[694,695] bind cyclodextrin[501-504] attached to gold or silicon oxide surfaces ("molecular printboard") and are removed upon oxidation to ferricinium.[689-694] For high-generation dendrimers, only a determined fraction of the ferrocenyl groups are bound.[693] A coarse-grained molecular-dynamics model was developed to study the multivalent or multisite binding of small functionalized dendrimers to β-cyclodextrin SAMs, the molecular printboard.[695] Dendrimers that encapsulate MNPs can be immobilized on surfaces,[696] and polycationic PPI or PAMAM dendrimers encapsulating MNPs can also be immobilized on surfaces using the well-known layer-by-layer technique[697] by alternating their deposition with that of polystyrenesulfonate anion.[698] Alternatively, the negatively charged layers can consist in hydroxy-PAMAM dendrimers encapsulating AgNPs.[699,700] Microshells can also be coated in this way by dendrimer-encapsulated AuNPs.[701] Layer-by-layer assembled thin films composed of PAMAM-CO_2H dendrimers could be used as a *pH*-sensitive nanodevice.[702]

AuNP-centered dendrimer terminated by silylferrocenyl termini strongly adsorb on Pt electrodes, which allows ATP^{2-} anion sensing using the modified electrodes, and washing the ATP^{2-} substrate allows re-use of these AuNP-dendrimer-modified electrodes.[487-490,529]
Soft-lithography patterning has been applied to dendrimers using the ink-jet printing technique,[703-706] and PAMAM-dendrimer-absorbed Pd^{2+} ions can be microcontact printed (μCP), then guide Co or Pd metal plating by electroless deposition.[707,708] Adamantyl- and ferrocenyl-terminated dendrimers have also been used for such microcontact printing.[709-711]
Application of surface adsorbed dendrimer-metal ion has been used to form Fe_2O_3 NPs and catalyzed the growth of carbon nanotubes using the plasma-enhanced chemical-vapor-deposition technique.[712] PPI dendrimers with ferrocenyl termini were used with cyclodextrin-coated surfaces to contact two gold electrodes with supramolecular junction by metal transfer printing.[713] A combined surface plasmon resonance spectroscopy and electrochemical set up was used to monitor the *in situ* adsorption and desorption of ferrocenyl dendrimers and β-CD-functionalized AuNPs (approx. 2.8 nm) onto and from the molecular printboard. Wih larger silica NPs (approx. 60 nm), ultrasonification was used to reduce the desorption time (Figure 38).[714]

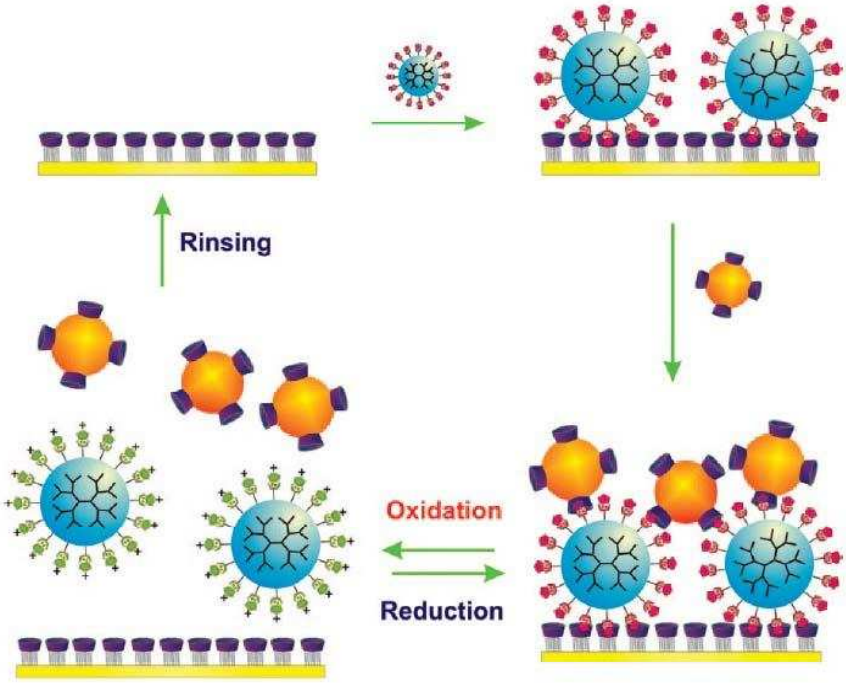

Figure 38. Illustration of the adsorption and desorption of ß-CD-functionalized NPs onto and from ß-CD SAMs with Fc dendrimers as a reversible supramolecular glue. Reprinted with permission of the American Chemical Society (ref. 714, Huskens's group).

In conclusion, nanofabrication using surface supramolecular coating of ferrocenyl-, biferrocenyl and adamantyl-terminated dendrimers as well as dendrimer-encapsulated metal nanoparticles is a productive and promising area as shown in particular by the Reinhoudt group.[715] Recent dendrimer-mediated transfer printing of DNA and RNA microarrays also gives a biomedical direction (cf. § 6.9.1, Figure 39).[716]
The work function of indium-tin-oxide (ITO) anodes has been modified by adsorption of cationic PAMAM dendrimers. Kelvin probe characterization of these PAMAM-functionalized ITO films and electroadsorption measurements on polymer LEDs incorporating poly(9,9-dioctylfluorene) active layers revealed an abrupt lowering (0.55 eV) of the effective work function upon addition of the adsorbed layer and a weak dependence on PAMAM generation.[717]

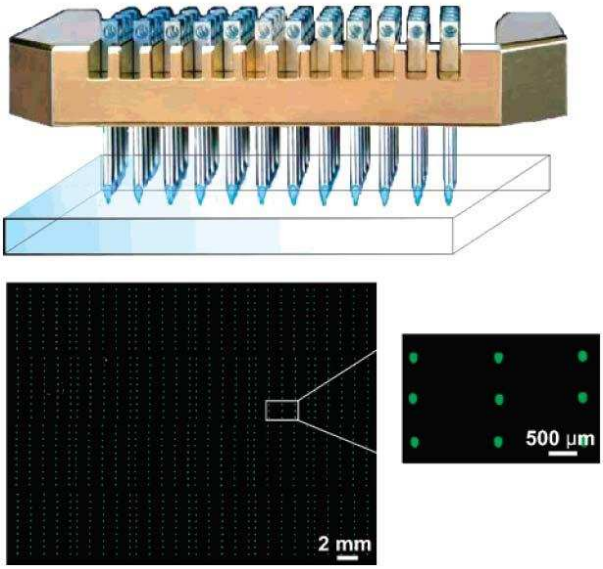

Figure 39. Robotic contact printing of DNA onto a flat dendri-stamp. Fragment of a fluorescence image of an aldehyde-terminated glass slide with an array of 400 spots of oligonucleotide labeled with fluorescein printed using a dendri-stamp. Reprinted with permission of the American Chemical Society (ref. 716, Reinhoudt's group).

The TiO_2 electrode interface was modified by Yamamoto and his Keio group using various dendrimers including G_3-phenylazomethine dendrimers with a triarylamine core in dye-sensitized solar cells.[718]

4.12. Application of dendrimer films, membranes and surface interactions to gas sensors

Most dendritic sensors are biosensors, an area reviewed in § 6.9. Sensors are based on photophysics[230,719-724] or electrochemistry[725-731] for which the reader is also refered to the photophysical and electrostatic sections respectively. Here we mention gas sensors using composite dendrimer films and membranes. Thin films of dendrimer-containing AuNPs were fabricated by layer-by-layer assembly, and they were efficiently used as resistors with conductivity measurements (relative resistance change $\Delta R/R$) for sensing vapors of toluene, 1-propanol and water.[732] Membranes based on PAMAM dendrimers were used for CO_2 separation with high CO_2/N_2 selectivity.[733,734] Arrays of carbon black-dendrimer composites could detect volatile organic amines and carboxylic acids.[735] Hyaluronic acid in a chitosan gutter layer was added to PAMAM dendrimer composite membrane to improve its CO_2 separation performance, because it improved the swelling degree of the membrane.[736] A siloxane dendrimer-AuNP composite served as CO sensor, with CO concentration proportional to the current.[737] G_0-G_8 PAMAM dendrimer films were found to sense volatile organic compounds with different functional groups by sequentially dosing dendrimer-modified surface acoustic wave (SAW) mass balance. It was found that G_4 was the optimal generation, which was tentatively attributed to the fact that it is the smallest spheroid generation with accessible interior. CO_2 adsorbents based on melanine-terminated dendrimers were designed by functionalizing SBA-15.[738]

4.13. Molecular imprinting inside dendrimers

Zimmerman designed an inprinting strategy based on the synthesis of cored dendrimers, attachment of dendrons, then removal of the core for selective binding of the remaining hollow macromolecular host to specific guest substrates.[739,740] This molecular imprinting methodology involved porphyrin cores whose large sizes were appropriate for large guest substrates. Peptide-type coupling was carried out between *meta*-di-hydroxy-phenyl porphyrin

meso substituents and butenoxy-terminated Fréchet-type dendrons bearing a carboxylic acid group at the focal point. Thus 1-butenoxy-terminated dendrimers were synthesized, and olefin metathesis using Grubbs-1 catalyst yielded only intramolecular ring closing metathesis producing dendritic spheres[739,740] despite the tendency of olefin–terminated dendrimers to cross metathesize (Figure 40).[745-749]

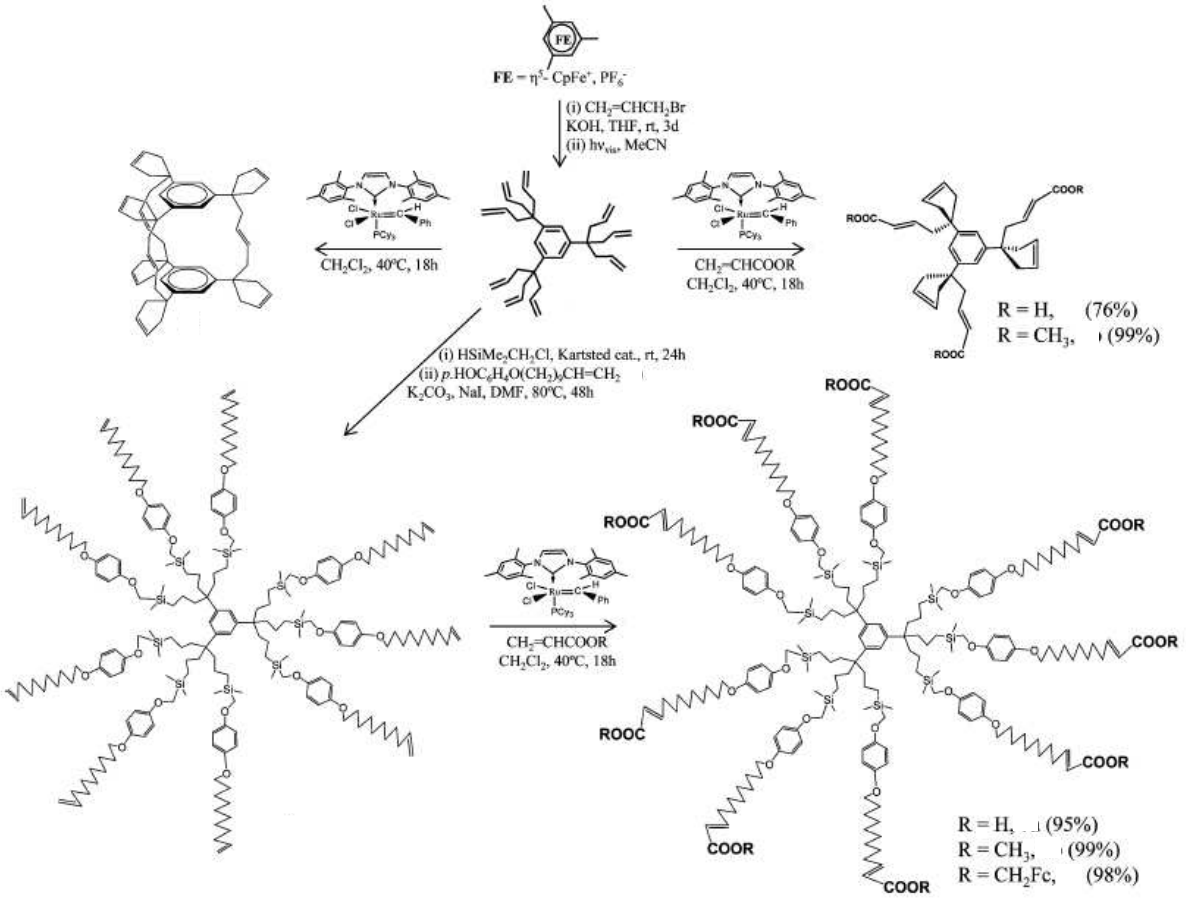

Figure 40. Bifunctionalization of the nonallyl core, lenthening of the dendrimer tethers, and efficient monofunctionalization by cross metathesis for the dendrimer solubilization in water. Reprinted with permission of the American Chemical Society (ref. 745, Astruc's group).

It appears that this process is entropically controlled and forms the single thermodynamic product following the primary formation of many kinetic products that slowly rearrange by metathesis.[744-747] Hollow dendritic architectures were then formed upon ester hydrolysis. The cleaved porphyrin groups could be replaced by pyridyl derivatives as guest substrates that were hydrogen-bonded to the carboxylic acid groups of the hollow cavities.[739-743] The concept was further extended to (trifluoroacetyl)azobenzene as a chromogenic reporter for amines and diamines.[751] Other new applications of this dendrimer coring/hollowing research were the formation of organic nanotubes[752-754] and organic nanoparticles.[755] In a related strategy, Peng's group covered CdSe particles with olefin-terminated dendrimers with [dendr-$CH(allyl)_2$] branches. Olefin metathesis using Grubbs catalyst produced a dendritic box by cross metathesis between the olefin termini of the dendrons in spite of the very favorable ring-closing-metathesis producing cyclopentenyl rings in a few minutes under ambient conditions with such branches.[746,747] The CdSeNP core was removed from dendrimer boxes using concentrated HCl producing a dendritic hollow sphere whose mass spectrum showed Gaussian mass dispersities between 10 000 and 12 000 Da.[756-759]

4.14. Electron-transfer processes in dendrimers

With dendrimers, this topic is involved *inter alia* in the photophysical aspects, § 3, redox sensing,[50-60] redox catalysis (glucose sensors, § 6.9.3, oxygen electroreduction, § 5.5.3.2 and other redox catalyzed processes, § 5.3.4), and electron-transfer-chain catalysis, § 5.3.4.[760] Gorman's group has extensively studied iron-cluster-cored dendrimers as metalloprotein mimics,[761] and the Diederich and Gross groups have reported electron-transfer studies in metalloporphyrin-centered dendrimers as hemoprotein models.[762] In both cases, the dendron shielding modifies the redox-potential values, and considerably slown dow electron-transfer processes.

Our group has long been interested in redox-system-terminated stars and dendrimers with ferrocenyl and other transition-metal sandwich units with various redox-potential regions whereby the redox systems are chemically and electrochemically reversible.[763] The interest of these latter systems is that only one reversible cyclic voltammetry (CV) wave is observed, which is of interest for redox sensing, modified electrodes, electrocatalysis, electron-transfer-chain catalysis, and molecular batteries. The fact that only one wave is observed does not mean that all the redox systems, which are equivalent, are active at exactly the same standard potential, although all the potentials are almost the same and look identical. In fact, all these standard redox potentials are statistically distributed around a mean value according to a binomial law as indicated in a seminal article by Bard and Anson.[764] Dendrimers with 9 and 21 viologen groups were reported by the Balzani and Stoddart groups, in which only the peripheral redox viologen sites are active, not the inner ones.[765] A very interesting aspect is that this CV wave is electrochemically reversible, indicating that electron transfers are fast between all the redox systems and the electrode, even for metallodendrimers containing up to 14 000 ferrocenyl or cobaltocenyl groups at the dendrimer periphery.[766,767]

Two mechanisms have been proposed to take this phenomenun into account: (i) electron hoping among the flexible redox termini[768,769] and (ii) fast rotation of the dendrimer,[770] although the later cannot proceed if the dendrimer is attached to a modified electrode. Inter-dendrimer electron-tranfer processes are also fast, and their kinetics has been determined.[771,772] Finally the molecular-battery concept has been raised for these systems that include an enormous amount of charging capacity in a minuscule volume (for instance 14 000 electrons for a G_7-dendrimer that has a volume of $27x10^3$ nm^3).[766,767,773]

5. Dendritic Catalysts: dendritic effects, efficiency and recycling

5.1 Introduction: basic concepts and seminal studies

The most important problems in catalysis are the cost related to the catalyst efficiency (turnover number of the catalyst: TON, and turnover frequency: TOF) and the removal of the catalyst from the reaction mixtures for both economical (catalyst recycling) and ecological reasons (prevent pollution of the reaction product by the catalyst). Selectivity is another important aspect concerned with efficiency: chemoselectivity, regioselectivity, stereoselectivity, enantioselectivity and diastereoselectivity, and these selectivity factors are always optimum with homogeneous catalysts. Most often, however, these catalysts cannot be removed from reaction media, because separation is too difficult due to their small sizes. Supported, biphasic and heterogeneous catalysts have brough possible solutions for catalyst separation, but these solutions are somewhat limited by lack of selectivity, metal leaching and poisoning respectively.[774,775] Dendrimer catalysis has appeared since the early 1990's as an interesting possibility to explore, because homogeneous catalysts could be bound to the periphery or interior of dendrimers, providing homogeneous catalysts for a tailored, well-controlled definition of the molecular environment of the catalytic site and solubility. Moreover, such metallodendritic catalysts are nano-objects that can be easily separated, as macromolecules, from the reaction products by precipitation or ultra-filtration, and

industrially using membranes. The extreme variety of dendritic definition for a catalyst environment in metallodendrimers renders the outcome intellectually challenging, and indeed a large body of data is now available after two decades of dendritic catalysis research.

Initial results were obtained at Shell by van Leeuwen who patented in 1992 catalysis of CO/alkene polymerization upon comparing mononuclear and star-shaped hexaphosphine-palladium catalysts. The star-shaped catalyst gave 3% fouling whereas the mono-palladium catalyst gave 50% fouling, which was already a dendritic effect.[776] In 1993-1994, five research groups reported catalysis by metallodendrimers, those of Brunner (dendrisymes for Cu^{I}-catalyzed enantioselective styrene cyclopropanation and Rh^{I}-catalyzed acetamidocinnamic acid hydrogenation, the latter reaction with a positive dendritic effect),[777-780] Du Bois (palladodendrimer for electrocatalytic reduction of CO_2 to CO),[781] Ford (catalysis by ammonium-terminated dendrimers of decarboxylation and phosphonate hydrolysis),[782] and van Koten together with van Leeuwen (Ni^{II}-catalyzed anti-Markovnikov Kharash addition of CCl_4 to methacrylate).[783]

An important conceptual advance in dendrimer catalysis was the metallodendrimer recycling that was pioneered by Reetz in 1997 with PPI dendrimers terminated by $N(CH_2PR_2)_2$ groups whose Pd complexes catalyzed the Heck reaction between bromobenzene and styrene. More than 98% of the catalyst with 16 peripheral Pd groups was recovered by precipitation, and the recovered catalyst (with an uncertain structure) displayed comparable activity and selectivity. This catalyst had a TON three times higher than the monometallic catalyst, showing a positive dendritic effect.[784] We now know, however, that PdNPs form in the Heck reactions of bromobenzene, because they require high temperatures, leading to catalytically active PdNPs.[785-787] Thus, we believe that the higher reactivity of the metallodendrimer in this case was due to the fact that such PdNPs formed were stabilized by the dendrimer (*vide infra*) which could not occur when the monometallic catalyst was used in the absence of dendrimer (Pd black formation).

Another vey important tehnological improvement was that involving nanofiltration with membranes. Membrane nanofiltration was pioneered by the groups of group Kragl and Reetz when they described in 1999 the retention of Meijer's diaminopropyl-type dendrimers modified with palladium phosphine termini by such ultra- or nanofiltration membranes. These groups used the dendritic catalysts for the allylic substitution in a continuously operating chemical membrane reactor. Retention rates were higher than 99.9 % resulting in a six-fold increase of the total turnover number for the dendritic Pd catalyst of generation 3 bearing 16 diphophine-Pd groups at the periphery.[788]

The heterogenization of metallodendritic catalysts, for which the seminal work by Alper's group appeared in 1999 and was steadily continued later, is a concept involving dendritic catalysis with both advantages of molecular design on support and easy removal of the catalyst by simple filtration. Thus, inititially Alper et al reported hydroformylation with Rh^{I} catalysts supported on PAMAM-dendronized silica gel support, i.e. the dendron was constructed on the silica support in a divergent way and terminated by catalyst binding.[789]

A breakthrough in dendrimer catalysis was the use of dendrimer-encapsulated PdNPs in catalysis by Crooks' group with PAMAM dendrimers that was reported in 1999 and successfully continued further on. This approach was previously carried out with other polymers, ligands or surfactants in order to control the size and prevent agglomeration. Dendrimers have a better-defined shape than ordinary polymers or surfactants, however, and were choosen because they were hoped by Crooks to function as "nanoreactors" and nanoporous stabilizers. The catalytic reactions were carried out in organic solvents, water, supercritical CO_2 (sc CO_2), or fluorous/organic biphasic solvents, exploiting the large flexibility of dendrimer solubilization provided by the nature of the branch termini.[790]

A rather general trend in catalyst-terminated dendrimers that are the majority of reported metallodendritic catalysts is the bulk provided at the periphery upon increasing the dendrimer generation restricting access of the substrate to the catalylic metal center. Thus, the Astruc group reported in 1997 that star metallodendrimers do not suffer from such steric constraints. Metallostars with electron-reservoir iron-sandwich termini were shown to be redox catalysts for nitrate and nitrite reduction to ammonia in water without kinetic loss compared to monometallic catalysts, whereas similar bulky monometallic iron-sandwich catalysts are kinetically limited by the bulk.[791-797]

Localization of the catalyst at the dendrimer core is a powerful concept, because it recalls enzymatic catalysis. The catalytically active metal center can in this way be fully protected by the surrounding dendrimer. Kinetic restrictions are an obvious drawback in this situation, but the stability and protection of the metal center can be decisive and dominant factors as shown in various exemples of dendrimer catalysis reports. The first examples where those reported in 1996 by Suslick's group with manganese-porphyrin-centered dendritic catalysts provided enhanced selectivity[794] followed in 1999 by van Leeuwen group's report of 1,1'-diphenylphosphinoferrocene-centered dendrimers providing enhanced stability of Pd catalysts.[795] Dendrimer-encapsulated catalysis was also encountered with Crooks' PAMAM dendrimer-encapsulated PdNPs[545] and in organic catalysis as shown first by Fréchet's group in 2003 with 4-(diakylamino)pyridine-containing dendronized polymers that catalyzed acylation reactions using sterically demanding tertiary alcohol substrates. In these catalysts, the nanoenvironment played the dominant role in determining the catalytic activity.[796]

Altogether, various locations have been reported for catalytically active centers in dendritic architectures: dendritic and supported dendronic branch termini, core, branch intersection and between the branches (NPs).

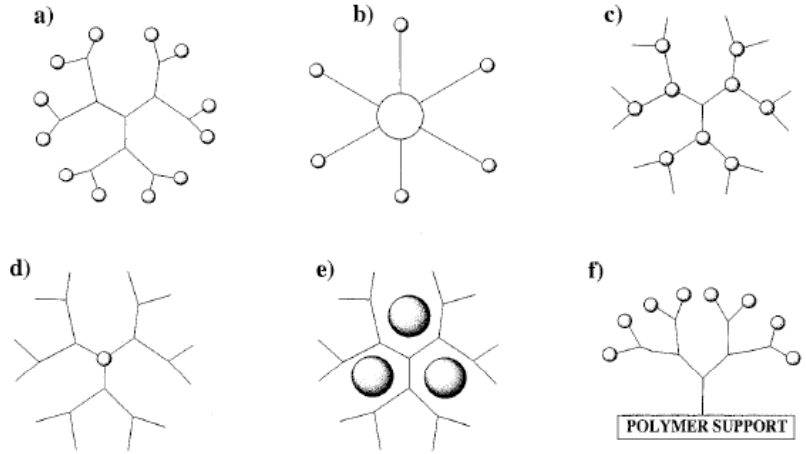

Figure 41 Various metallodendritic assemblies efficient for metallodendritic catalysis: a) Reetz: Heck reaction 1rst recycle in 1997; b) Redox catalysts kinetics shows no steric congestion; c) Kakkar's phosphine-Rh at focal points; d)Van Leeuwen ferrocenyldiphos Pd-centered; e) Crooks: PAMAM inserted Pd nanoparticles; f) Alper's Pd-phosphine dendrons anchored on polystyrene. Reprinted with permission of the American Chemical Society (ref. 799, Astruc's group).

The first general reviews on dendritic catalysis were published in 2001 by the groups of van Leeuwen[798] and Astruc (Figure 41).[799] Since then, a large number of specialized reviews have appeared on the various aspects of this field that has become very large.[800-819] The most important problems that are presently addressed are those of the dendrimer recovery/recycling[801,819] and the dendritic effects. We will thus focus our attention in this review essentially on these efficiency aspects and the results that were reported during the second half of this decade.

5.2. Methods of separation/recycling

5.2.1. The classic laboratory method: precipitation

This method is the most widely used one, as it already was in Reetz' seminal examples.[784] It takes advantage of the macromolecular nature of metallodendrimers. As biomolecules and polymers, the nanoscopic size allows separation. The desired solubility of a dendrimer being easily adjusted by the choice of the terminal groups, systems can be designed for separation between the metallodendrimer and products after the catalytic reaction. For instance, Fréchet-type dendrons with a Ir-BINAP species at the focal point up to G_4 catalyzed the hydrogenation of quinolines under H_2 atm in THF with TON of 43 000 at 0.0002 mol% catalyst, whereas a non-dendronic diphoshine complex was much less active, and with higher ee (90% vs. 74%). Interestingly, the activity increased from 43% conversion for G_0 to > 95% for G_4, also with higher TOF for the latter (3 450 h^{-1}). The G_3 catalyst was reprecipitated from hexane and re-used six times with similar ee's, but with relatively lower activities.[820]

In another study, chiral dendronized-diamine-Ru^{II} and Rh^{III} complexes catalyzed asymmetric transfer hydrogenation of ketones and activated olefns using HCO_2H or HCO_2Na as the hydrogen source with about the same efficiency as the non-dendronized catalyst. The catalytic activity droped, however, for high-generation metallodendritic catalysts, which was attributed to site wrapping by dendron tethers. Recovery of the G_2 catalyst was carried out by reprecipitation using methanol, and 10% catalyst was lost due to leaching after each run, but the ee remained high (97%).[821] Aqueous conditions were used with high efficiency (99% conversion and 96% ee) for the G_1-to-G_3 Rh-diamine-dendron-catalyzed reduction of acetophenone. In water, down to 0.01 mol % catalyst loading yielded 61% conversion and 95% ee for G_2. Upon precipitation with hexane, the recovered dendronic Rh catalyst worked similarly for six runs.[822]

After a seminal example by Newkome and Hill of tetra-branched POM-catalyzed tetrahydrothiophene oxidation,[823] it was shown in our group that cationic dendrimer- or dendron-protected polyoxometallate (POM) catalysts active for olefin epoxidation, sulfide oxidation to sulfones and secondary alcohols to ketones in biphasic $CDCl_3$/aqueous mixtures using H_2O_2 as the oxidant were recyclable by precipitation upon addition of ether, as shown by ^{31}P NMR (Figure 42).

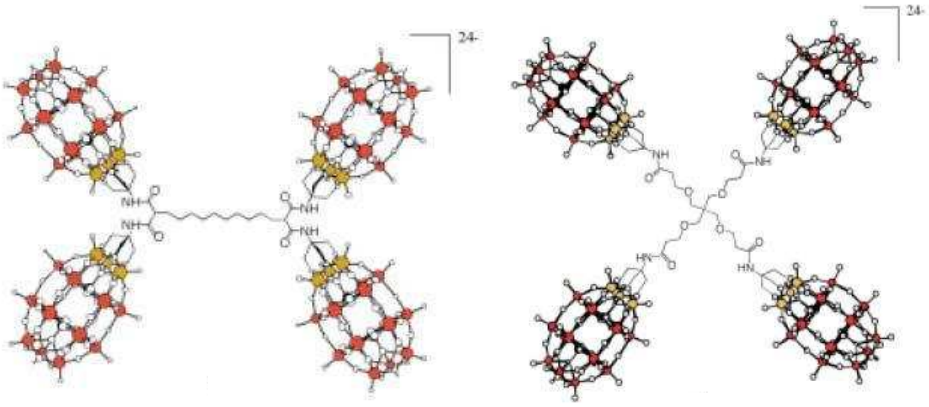

Figure 42. Representative structures of two dendritic tetra(POM) molecules. Each has a charge of 24^- countered by 24 cations that are not shown for clarity. The V, W, P, and O atoms are colored orange-yellow, red, black and white (open circles), respectively. Reprinted with permission of Wiley-VCH (ref. 823, Hill's group).

This contrasted with non-dendritic tetraalkyl ammonium salts that were not recyclable due to decomposition. The dendron-protected POM catalysts were slightly more air stable than the dendrimer-protected catalysts, although both could be used several times without loss of activity, but the activity of the dendron-protected catalyst decreased upon increasing the dendron generation and bulk.[824-828]

The $Pd(OAc)_2$ complexes of PPI dendrimers terminated with 4, 8 and 16 $N(CH_2PR_2)_2$ chelating ligands were shown in our group to be efficient for the Suzuki coupling of unactivated chloroarenes (best medium: $NaOH/THF/H_2O$, R = Cy, 65°C)[829] and the copper-free Sonogashira coupling of halogenoarenes including activated chloroarenes (NEt_3, 80°C for bromo- and chloroarenes, -20° to 20°C for iodoarenes, R = *t*-Bu).[830-833]
The cyclohexyl phosphine dendrimers were more active than the *ter*-butyl phosphine dendrimers for the Susuki reactions, but the opposite was found for the Sonogashira reactions, showing the change of the steroelectronic balance for the Pd complexes from one reaction to the other. The dendritic effect was negative for both reactions, i.e the G_3 catalysts were less active than G_1 and G_2 (the kinetics decreased upon increasing generation number). The dendritic catalysts were precipitated with pentane for recovery with R = Cy (but not with R = *t*-Bu, because they were too soluble). The best efficiency after recovery was G_2 for which practically no loss of efficiency was observed contrary to G_1 and G_3. By comparison, the monopalladium complex gave palladium black under the reaction conditions, which prevented recycling. With star complexes containing six Pd-Buchwald-type phosphine termini, chloroarene with one or two ortho methyl substituents could couple to arylboronic acids containing one or two ortho methyl groups in yields higher than 90% under Suzuki conditions, an efficiency equal to that of the monomer, and the catalyst could be recycled five times with progressively decreasing yields.[834]
Asymmetric allylic alkylation of racemic *trans*-1,3-diphenyl-2-propenyl acetate with pivalate was catalyzed by iminophosphorane-terminated Majoral-type dendrimers combined with $[Pd(allyl)Cl]_2$ with similar activity to that of the non-dendritic complex, but the enantioselectiviy was improved with the dendrimer (90% ee) compared to the non-dendritic complex (80% ee).[835] The dendritic catalyst was recovered by precipitation using ether and re-used with practically the same efficiency. Azabis(oxazoline)-terminated phoshorus dendrimers bound to Cu^{II} catalyzed asymmetric benzoylation of diols in good yields and excellent enantioselectivities (up to 99%). The catalyst was recovered by precipitation from CH_2Cl_2 with hexane and re-used three more times with quite the same efficiency.[836]
Fréchet-type dendrons-functionalized 2,2'-bipyridine-$Cu(OTf)_2$ complexes catalysed the Mannich condensation of aldehydes, *o*-anisidine and a silyl enolate or triethyl phosphite nucleophile in CH_2CH_2, a solvent in which the catalyst was recyclable, and in water. The catalyst was poorly soluble in water but gave a 3-fold better yield than in CH_2Cl_2. The yield increased with increasing catalytic generation, which was taken into account by a favorable hydrophobic environment provided by the dendrons for the catalyst.[837]

5.2.2. Solid supports

After his seminal work on silica gel-supported metallodendronic catalysis of olefin hydroformylation with Rh^I,[789] Alper's group developed this field with polystyrene supports and hydrogenation, hydroesterication, cabonylation, oxidation and carbon-carbon coupling reactions.[838-844] Further works in the area was carried out by the Portnoy group, in particular for carbon-carbon coupling reactions with studies of the influence of the generati[847-850] on effects and influence of the backbone structure.[812,845,846] The influence of silica pore size andcoordinative ability of the dendrimer backbone were investigated.[845] Organocatalysis of the aldol reaction with proline dendronic endings has also been carried out on polystyrene-supported dendron, and the first and second generation catalysts showed yields and selectivities that were comparable or better than in solution.[851] Magnetic separation of NPs is a well-developped field in supported catalysis that has been extended to supported dendrons. Silica-supported magnetic NPs were indeed dendronized with PAMAM and bound to Rh^I for catalysis of styrene hydrogenation with good recycling properties.[852]

Subsequent to the design of dendrimer-encapsulated NP catalysts by Crooks,[652-654] supported metal-NP-containing dendrimers were shown to be active and recyclable catalysts, and this field has been reviewed by Chandler et al. who brought an important contribution (*vide infra*).[853-856]

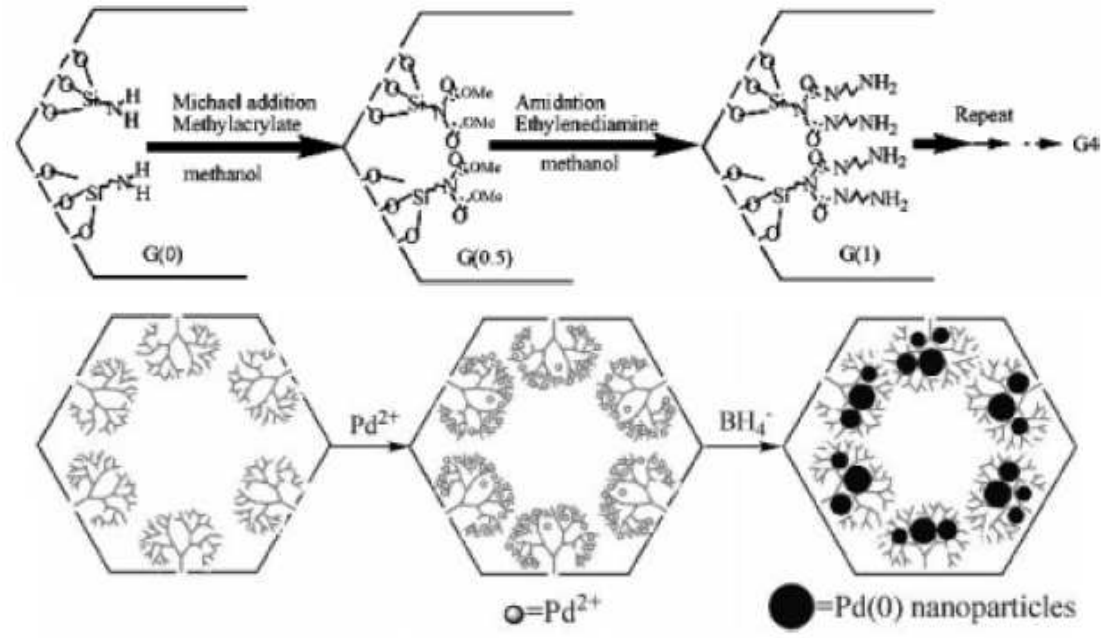

Figure 43. Preparation of SBA-15 supported dendrimers; formation of nanoparticles. Reprinted with permission of the American Chemical Society (ref. 858, Gao's group).

Two approaches were used. In the first one, metal NPs were generated in SBA-15-supported dendrons,[857,858] whereas in the other one, the dendrimer containing the NPs were deposited onto a solid support followed by thermal removal of the dendrimer (Figures 43 and 44).[853-856,859-863]

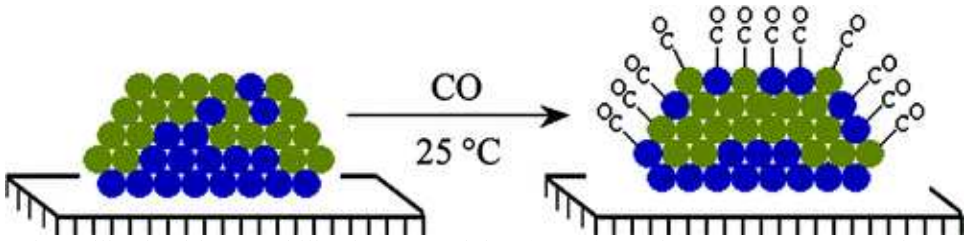

Figure 44. Bimetallic dendrimer-stabilized nanoparticles (DSNs) used to prepare supported Pt−Au catalysts within the bulk miscibility gap for a binary system. Reprinted with permission of the American Chemical Society (ref. 861, Chandler's group).

Finally, in another approach, cross-linking of scandium-based dendrimers yielded insoluble catalysts that were active in various reactions.[864]

5.2.3 Biphasic catalysis

Dendrimers are easily amenable to biphasic catalysis, because the solubility can be designed by an appropriate choice of terminal endings (tails). In particular, this property has been astutely used with dendrimer-encapsulated NPs that have been solubilized in water[652-654,865,866] and in fluorous solvents[867,868] for fluorous/organic biphasic catalysis.[652-654] Thermotropic mixtures of two solvents, such as dimethylformamide and heptane, are homogeneous at relatively high temperatures, whereas they form two phases at lower temperatures, which allows both homogeneous reaction conditions and the possibilities of separation upon cooling. This principle has been applied to dendritic catalysis by Kaneda's group. The dendritic

catalyst in the DMF phase can be recycled, because the organic products remain in heptane. The terminal amino group of PPI dendrimers was functionalized with decanoyl chloride, providing the possibility for the Pd catalyst to bind the nitrogen atoms inside the dendrimer. Such systems are active for the Heck and allylic amination reactions.[869] A positive dendritic effect was observed for the Heck coupling between iodobenzene and *n*-butyl acrylate in which the polyammonium dendrimer cores obtained by protonation of DAB dendrimers terminated by long alkyl chains bind the Pd catalyst *via* a triarylphosphine bearing a *para*-carboxylated phenyl substituent. Indeed, the reaction rate increased with increasing the dendrimer generation, whereas the nondendritic catalyst was unreactive. In the same reaction with 1,4-diiodobenzene, the dendritic catalyst selectively yielded the mono substitution whereas the analogous non-dendritic catalyst was little selective (*mono:di* = 45:55). On the other hand, the dendritic effect was negative for the allylic amination with these dendritic catalysts, athough the dendrimer nanoenvironment improved the linear:branch selectivity.[869] Further reactions that were carried out using the thermotropic property of this solvent mixture included amination of cinnamylmethyl carbonate with piperidine, then the hydrogenation of dienes by dendrimer-encapsulated PdPtNPs.[870] A metal-free dendritic pyridine has been used with recovery and re-used in a thermotropic DMF/cyclohexane mixture (homogeneous at 60°C) in the catalysis of the Baylis-Hillman coupling reaction of unsaturated ketones and aromatic aldehydes.[871]

With non-thermotropic solvent mixtures such as hexane/ethanol or hexane/butanol/acetonitrile that are miscible, the addition of water after the catalytic reaction provokes phase separation, which allows separation of the catalyst and recycling. For instance, a dendritic OsO_4-glycolate complex with alkyl termini was soluble in non-polar solvents. It was used for olefin dihydroxylation reactions yielding polar diol products that were retained in the polar phase after addition of water, whereas the hexane-soluble catalyst was successfully recovered (99%) in hexane and re-used ten times.[872]

5.2.4. Membrane nanofiltration

Membrane technology, based on size-exclusion filtration, is a fast growing area, and solvent resistant commercial membranes allow a cut-off of molecular weights between 200 and 1000 Da (Figure 45).[873]

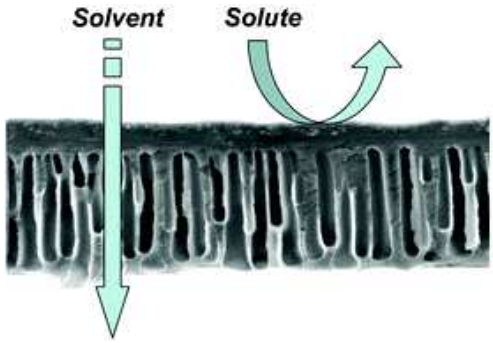

Figure 45. Solvent-resistant nanofiltration: separating on a molecular level. Reprinted with permission of the Royal Society of Chemistry (ref. 873, Vankelekom's group).

Continuous-flow membranes reactors (CFMRs) were already efficiently used by Kragl and Reetz in their seminal study of the dendrimer separation of catalyst-terminated with third- and fourth-generation PPI dendrimers. Following studies involved Ni^{II}-catalyst-terminated dendrimers for atom-transfer radical addition reaction.[874] These dendrimer-Ni^{II} and Pt^{II} complexes of NCN-pincer ligands have been used extensively with membrane filtration in the early 2000's, and this work has been reviewed.[46,514,800,803,875] van Leeuwen's Pd complexes 1,1'-bis(diphenylphosphino)ferrocenyl-centered dendrimers were found to be much more

stable in a CFMR than when the Pd^{II} groups are located on the dendrimer periphery.[804] A fifth-generation dendrimer in which the peripheral part containing the Pd^{II} catalyst is strongly bound to the PPI core by combined ionic bonding and multiple hydrogen bonding (cf section 4.4) showed retention rates of 99.4-99.9% in a CFMR.[876] Star-shape dodecanuclear NCN pincer Lewis-acid catalysts for double Michael addition of ethyl cyanoacetate to methyl vinyl ketone were found to be retained with very high efficiency (> 99.9 %) in a CFMR under continuous reactions conditions, very small yield decrease occurring with time. The rigidity was also considered to be a favorable factor.[877] This indicated that high-generation dendrimers are not necessary for efficient recovery, and confirmed that star-shaped catalysts may work better than sterically congested catalyst-terminated dendrimers.[74]

5.3. Catalysis with metallodendritic complexes

5.3.1. Palladium complexes

The role of palladium complexes in catalysis is of considerable importance, because it deals with the key carbon-carbon bond formation and oxidation reactions.[878-886] Thus it is not surprising to observe that among dendritic organometallic catalysts, palladium complexes have been the first ones studied,[776] are by far the most numerous, and have been the subject of excellent reviews.[539-542,819]

5.3.1.1: Pd-catalyzed carbon-carbon bond formation: Heck, Suzuki, Sonogashira and Stille coupling

The Heck reaction being one of the very most essential C-C coupling reactions has been searched with dendritic catalysts since the pioneering time.[784,798-819,869] Heck reactions between iodobenzene and various alkenes using diphosphine that were supported by poly(ether imine) dendrimers selectively yielded the *trans* compounds.[887] Recycling was observed to proceed with a decrease of activity. With iminophosphorane G_4 dendrimers, Pd black formed extensively,[888] but with pyridylimine ligands, higer rates, conversions and stability were found.[889] Tris- and hexanuclear (star-shape) *N*-heterocyclic carbene complexes[886] have been shown to catalyze Heck coupling between iodobenzene or activated bromobenzes with acrylates, although truely dendritic complexes are not known[890,891] Heck reactions between iodobenzene and methyl acrylates, that were not productive with $[PdCl_2(PPh_3)_2]$ as the catalyst in $scCO_2$, became possible with 40% conversion when $(CH_2)_3SiMe_2Et$ tails were introduced in *para* position of the phenyl rings of the ligands (Figure 46).[892] Negative dendritic effects upon increasing dendron generation in catalysis of bidentate phosphine-Pd-dendronized support for the Heck reaction have been reported.[893]

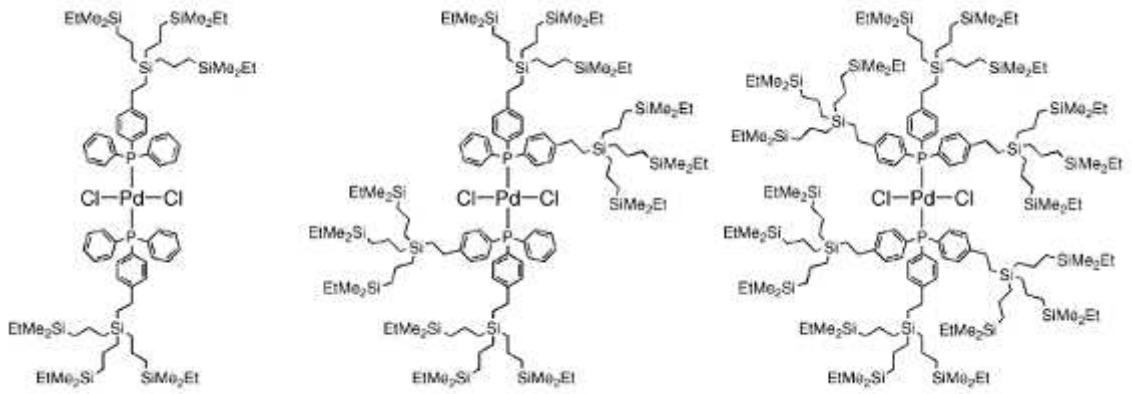

Figure 46. Palladium complexes. Reprinted with permission of the American Chemical Society (ref. 892, De Jesus's group).

Suzuki coupling has become recently very important, because boron reagents are now widely available and expected to be mostly non-toxic, whereas analogous Stille coupling uses toxic tin derivatives. In addition, Suzuki coupling can be catalyzed by palladium complexes under relatively mild conditions, for instance at temperature much lower than the Heck reactions.[879-886] Suzuki reactions catalyzed by recyclable palladium-catalyst-terminated dendrimers have been discussed in section 5.2.1. Recently, palladium complexes have been heterogenized by crosslinking homogeneous star-shape catalysts with oxime palladacycles, and good activity and recyclability were observed.[894-896] Suzuki reactions between aryl bromides and aryl boronic acids were carried out at 80°C with high frequencies (2586 h^{-1}) and TONs (59 000) using *N*-heterocyclic carbene palladium complexes branched on water-soluble polyglycerol containing 65 peripheral metal centers that were recycled five times without loss of activity.[895] Triarylphosphanes with dendritically arranged tetraethylene glycol moieties at the dendrimer periphery were efficient ligands for the Pd-catalyzed Suzuki-Miyaura coupling reaction of aryl chlorides (Figure 47).[896]

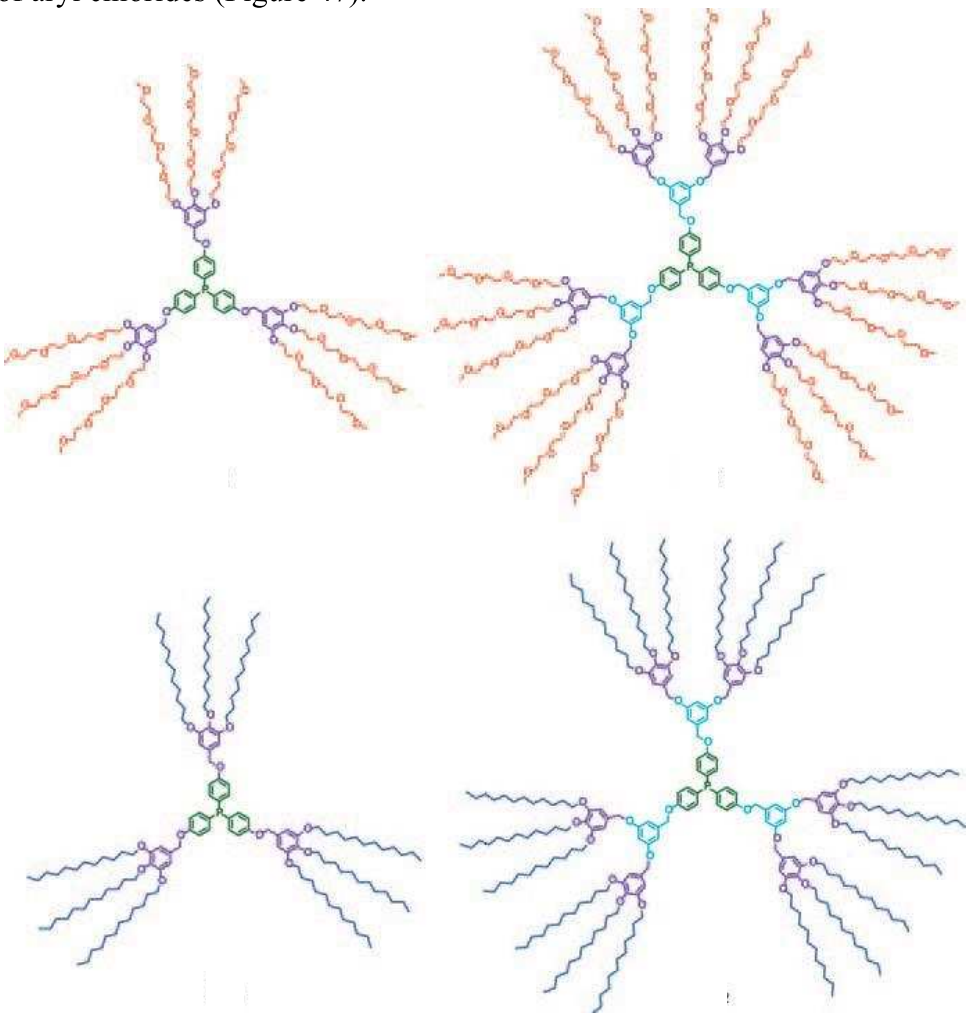

Figure 47. Novel phosphane ligands bearing tetraethylene glycol or *n*-C_{12} moieties. Reprinted with permission of Wiley-VCH (ref. 896, Tsuji's group).

The Sonogashira reaction is of high interest, because it avoids synthesizing organometallic *trans*-alkynylating complexes by direct use of a mixture of palladium and copper catalysts, or sometimes even with the palladium catalyst alone.[886] Copper-free Sonogashira coupling using dendritic catalysts, showed, as for Suzuki reactions, that the rates and conversions to reaction products decreased upon increasing the generation number of Pd-diphosphine-terminated PPI dendrimers (i. e. with negative dendritic effect). With the most active low-generation bis(*tert*-

butylphosphine) ligands, reactions with iodoarenes could even be carried out under ambient conditions in the absence of copper.[829,831] With phosphorus dendrimers containing bis(diphenylphosphinomethyl)amino ligand termini, the conversion increased with the generation number,[832] contrary to other studies.[813,829]
No report has appeared on Stille coupling subsequent to publications on cross coupling of aryl iodides with thienyl or vinyl organostannanes catalyzed by bis(diphenylphosphanylmethyl)amine or imnophosphane palladium-terminated dendrimers that could be recycled for three runs with only slightly decreased reactivity.[897] Pd PAMAM DENs were compared to $PdAc_2$ as pre-catalysts for the Stille coupling reaction between $SnCl_3Ph$ and PhI in water, and a similar reactivity was observed, but the DEN suppressed the formation of homocoupling products and allowed catalytic recycling. The leaching mechanism seems to operate, with the PdNP remaining bound to the dendrimer.[898]

5.3.1.2. Hydrogenation, hydrovinylation, polymerization and copolymerization of olefins
Carbosilane-cored aminopropyl palladium-terminated dendrimers catalyzed the reduction of C=C and C=O bonds, and these palladodendrimers were shown to be recyclable.[899] Palladocatalysts prepared *in situ* from hemilabile P,O-ligand-terminated carbosilane dendrimers catalyzed the styrene-ethylene coupling to 3-phenyl-2-butene (styrene hydrovinylation) in a CFMR with high regioselectivity (no formation of oligomers) and minimization of the subsequent isomerization reaction at low conversion. Deactivation with formation of Pd black was observed after 10 hours, however, which limited the catalyst efficient and practical use. The dendrimer was less stable than the monomer under batch conditions, which could be taken into account by the flexibility of the dendrimer tethers.[900] Similar results were obtained with diphenyl-[901] or phenyl(aryl)phosphines-terminated carbosilane dendrimers,[902] the dendrimers being less active than the monomer, although these catalysts were more active than those with the P,O ligands above. Interestingly, with a P-stereogenic phosphine, the cationic catalyst, as a BF_4^- salt, produced an excess of the (S)-3-phenyl-1-butene enantiomer (ee: 63-68%) at 35% conversion. The activity, chemoselectivity and enantioselectivity of the cationic catalyst were even improved for G_1 with the BARF counter anion. Even better esults (73% to 82% ee) were obtained with the P-stereogenic phophine (S)-MePPh(2-biphenylyl) located at the focal point of carbosilane dendrimers.[903]
The Pd-initiated polymerization has been recently examined with dendrimers. A MAO-activated tetrabranched alkylpyridyliminepalladium complex catalyzed ethylene polymerization. Remarkably, this tetranuclear initiator was more active than the mono- and binuclear analogues and yielded high molecular-weight linear polyethylene.[904] Cationic arylpyridylimine-palladium dendrimer catalyzed the alternating copolymerization of CO and 4-*tert*-butylstyrene with an activity that increased with increasing the dendrimer generation, although the half-lives were similar for the monomer and dendrimers. Generation increase also resulted in lower and broader distributions of molecular weights and in a constant decrease of the steroregularity of the syndiotactic polyketones polymers. These results were taken into account by steric enhancement of chain-transfer processes that inhibited the polymer chain-end control and lengthening (Figure 48).[905]

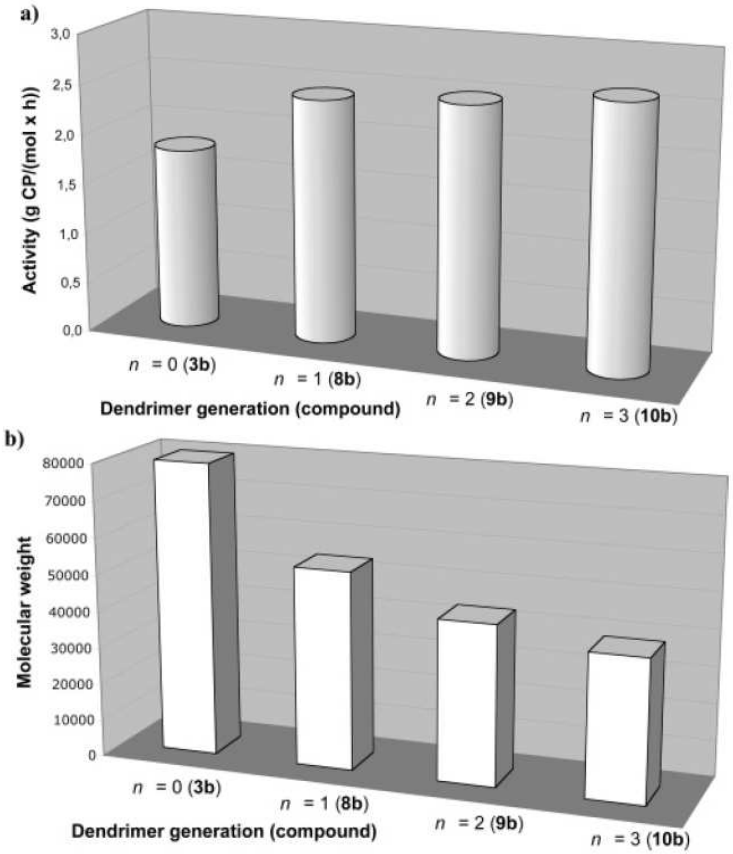

Figure 48. (a) Activities for G_n-ONNMe$_2$[Pd(MeCN)Me$^+$] and (b) copolymer Mw values obtained using neat TBS as a solvent. Reprinted with permission of the American Chemical Society (ref. 905, Flores's group).

5.3.1.3. Allylic substitution

Following Kragl and Retz who pioneered the CFMR technology with palladodendrimer-catalyzed allylic substitution,[788] further work was carried out in CFMR with phosphine-terminated carbosilane dendrimers with a reactivity that was rather analogous to that of monomeric Pd catalysts. Allylic amination of crotyl acetate and piperidine yielded mixtures of branched and linear *trans* products, and dendritic tether lengthening by addition of a methylene spacer improved the yields and catalyst stabilities.[906] The amination of *trans*-cinnamyl acetate with morpholine was catalyzed by PPI dendrimers terminated by diphosphino-palladium groups, and the linear *vs.* branch selectivity (90:10) was unchanged from monomer to dendrimers. In sharp contrast, the reaction of *cis*-3-acetoxy-5-carbomethoxycyclohex-1-ene proceeded with a *cis* product selectivity, whereas this stereselectivity increased up to 94% with the G_5 catalyst. This strong dendritic effect was attributed to steric shielding of the π-allyl-Pd spieces from *endo* attack.[907] The seminal introduction by Togni's group of the asymmetric version with the reaction between racemic *trans*-1,3-diphenyl-2-propenyl acetate and dimethyl malonate resulted in 89-91% ee using a dendrimer terminated by chiral ferrocenyl phosphines, which was slightly less than using the parent mononuclear ligand-complex (93 % ee).[908] Recently, Majoral-type phosphorus dendrimers produced a higher ee (90%) than the mononuclear analogue (ee: 80%), and the dendrimer showed good stability and recovery/reuse with an efficieny that was almost completely preserved. Optimized conditions yielded an ee of 95%.[909] The dendritic effect was spectacular on the enantioselectivity of the allylic amination of *trans*-1,3-diphenyl-2-propenyl acetate with morpholine reported by Gade's group. The ee was only 9 % for the monomer and regularly increased with generation increase up to 40% for G_5 pyrphos-terminated PPI dendrimer and up to 69% for G_5 pyrphos-terminated PAMAM dendrimers. These results were

taken into account by a conformational change of the aryl substituents of the phosphine ligands upon steric increase at the dendrimer periphery concomitant with increasing generations.[805,806,910]

5.3.1.4. Other Pd^{II}-catalyzed reactions

The catalysis by a variety of dendritic Pd^{II}-cyanometallated CN and pincer-NCN complexes of aldol-type condensation beetwen benzaldehyde and ethyl isocyanoacetate yielding an oxazoline has been extensively reported and reviewed by van Koten et al.[46,800,803,809,875,911-914]
In short, the reaction rates of monomers and dendrimers were comparable but were diminished when the dendritic tethers bearing the catalyst suffered from bulk at the periphery. Interestingly, a first example of hyperbranched polymer instead of a dendrimer was reported in collaboration with Frey's group, showing the same diastereoselectivity (*trans*/*cis* = 2) and only slightly decreased activity compared to the monomer.[914]
The Michael addition between ethyl cyanoacetate and methyl vinyl ketone was the subject of several reports by van Koten et al using pincer-Pd complexes that gave comparable yields for mononuclear catalysts and dendrimers (except when lower solubility resulted in poorer yields).[915] In this context, it was surprising to observe the case of a star-shaped dodecanucear complex providing a 3-fold increase in activity that was taken into account by a positive cooperation between the peripheral metal centers.[916] This complex was very efficient in a CFMR (Figure 49).[917]

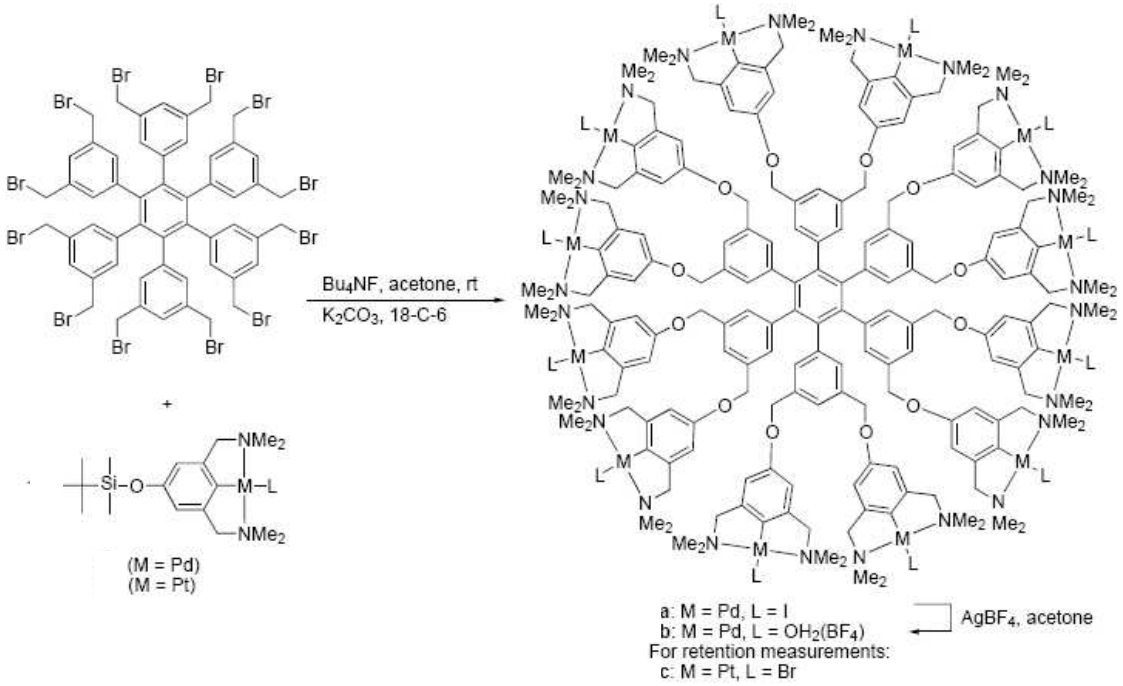

Figure 49. Modular approach for the synthesis of multi(pincer-metal) complexes. Reprinted with permission of Wiley-VCH (ref. 917, Van Koten's group).

5.3.2. Rhodium complexes

Rhodium (I) catalysts are mostly studied for hydroformylation (linear vs. branch regioselectivity), asymetric hydrogenation and (more rarely) hydrosilylation reactions,[918,919] at least in their metallodendritic versions. Following the seminal work by Reetz et al with Rh^{I}-diphosphine-terminated PPI dendrimers[784] including the first CFMR in collaboration with Kragl,[788] and by Alper et al. with Rh^{I} catalysts immobilized on silica or polystyrene supports (cf section 5.2.2), the area was developed in the 1990's by Cole-Hamilton et al.[920] using silesquioxane-cored dendrimers terminated by phosphine groups and by van Leeuwen et

al.[798,801] and has been reviewed.[539,798,799,801] For instance, the phosphine-terminated silesquioxane-cored G_1 dendrimer loaded with [Rh(acac)$(CO)_2$] or [Rh$(OAc)_4$] catalyzed the hydroformylation of propen-1-ol followed by reduction of the aldehyde to butane-1,4-diol and 2-methylpropan-1-ol, and the mechanism was proposed to proceed via a rhodium-hydroxycarbene intermediate.[920] G_1 to G_5 PPI dendrimers terminated with alkoxycyclopentadienyl rhodium complexes were shown to be active olefin hydroformylation catalysts.[921] Wilkinson's catalyst supported on dendrimer-SBA shows minimized leaching.[922] Some rhodium(I)-phosphine dendrimers were also used for simple olefin hydrogenation reactions, with results comparable to those of mono-rhodium catalysts and slight turnover decrease for large dendrimers.[923-925] Asymmetric hydrogenation of 2-acetylacetamidocinnamate using bicarbazolediol chiral phosphoramidite-rhodium dendrimers gave an excellent enantioselectivity (93% ee at full conversion), confirming that phosphoramidite are superb ligands for asymmetric olefin hydrogenation.[926,927] G_1-G_4 pyrphos-Rh^I-terminated dendrimers (pyrphos = 3,4-bis(diphenylphosphino)pyrrolidine) catalyzed asymmetric hydrogenation of α-acetamidocinnamic acid with dendritic effects assigned to dendrimer shape change from G_3 to G_4.[928] Monodentate phosphoramidite-Rh^I-terminated Fréchet-type dendrons catalyzed the asymmetric hydrogenation of α-dehydroamino acid esters and itaconate with up to 97.9 % ee and high catalytic activities, athough G_3 showed a slightly decreased activity. The positive dendritic effect in these reactions disclosed from the monomer to the low-generation dendrimers was assigned to the catalyst shielding by the dendrons against hydrolysis of the complex.[929]
Rhodium catalysts with imidazolium salts attached to Fréchet-type dendrons catalyze the hydrosilylation of acetophenone with dendritic effects, yield decrease with time being observed for G_1, not for G_2-G_4.[930]

5.3.3. Olefin metathesis catalysts

Early work of ruthenium-branched compounds were dealing with metathesis catalysts. Hoveyda's group synthesized two tetra-branched Ru-based complexes in which the branches were $–(CH_2)_3SiMe_2(CH_2)_3OC(O)(CH_2)_2–$ units that were connected to the styrenyl ether ligand. This complex catalyzed ring-closing, ring-opening and cross metathesis. The yield of ring closing metathesis of $TsN(CH_2CH{=}CH_2)_2$ using 5% mol Ru of the dendritic catalyst was 99%. The catalyst was recovered with 13% vacant styrenyl ligand (*i.e.* 13% Ru loss). It was suggested that the catalytically active Ru species was released from the dendrimer into the reaction mixture and could be trapped again by a styrenyl ether ligand arm of the dendrimer.[931] Another analogous 4-branch metallodendritic catalyst containing the *N*-heterocyclic carbene promoted the formation of trisubstituted allylic alcohol and was recovered with only 8% Ru loss. It also catalyzed tandem ROM/RCM, and was easily separable from reaction mixtures because of its polarity and high molecular weight. RCM reactions of diethyldiallylmalonate to the favored 5-membered cyclopentene ring using chelating dendritic ligands coordinated to Ru was also reported by the van Koten group.[932] Thus, dendrimers containing four or twelve branches, i. e. $Si[(CH_2)_3SiMe_2\textit{p}.C_6H_4CHOH(CH_3)py]_4$ and $Si\{(CH_2)_3Si[(CH_2)_3SiMe_2\textit{p}.C_6H_4CHOH(CH_3)py]_3\}_4$ reacted with [Ru(=CHPh)$Cl_2(PR_3)_2$] (R = *i*-Pr or *c*-Hex) to give 5-coordinate dendritic Ru complexes in which the O,N-chelating ligands were attached to Ru with the alkoxy ligand in equatorial- and the pyridyl ligand in axial postions. The RMC reactions were quantitative after 30 min at 80°C with 1 mol% (based on ruthenium) of either catalyst, as with the monometallic catalyst. In CFMR, conversion did not increase above 20%. Extensive decomposition occurred as a black precipitate formed in the vessel containing the catalyst, presumably because the catalyst was deactivated by the membrane surface.

The Ru-benzylidene dichloro complexes of G_1-G_3 PPI dendrimers terminated by chelating amino-di(phosphinomethyl) ligands were metathesis catalysts for the ROMP of norbornene under ambient conditions, forming metallodendritic stars in which each branch has incorporated for instance 100 norbornene units.[824] The G_1 metallodendrimer containing 4 ruthenium centers was more active than the monoruthenium catalyst, which was taken into account by more tether-flexibility induced facile phosphine decoordination (rate limiting step providing the active 14-electron catalytically active Ru centers) in this dendrimer than in the monomeric model catalyst. The metathesis polymerization rate decreased with increasing dendrimer generation, however, due to increasing steric congestion at the dendrimer periphery inhibiting the olefin approach to the Ru centers (Figure 50).[933-935] Norbornene polymerization was also catalyzed by G_1- and G_2-nickel catalyst-terminated PPI dendrimers using methylaluminoxane as the co-catalyst, whereby the catalytic activity was influenced by the dendrimer generation.[935]

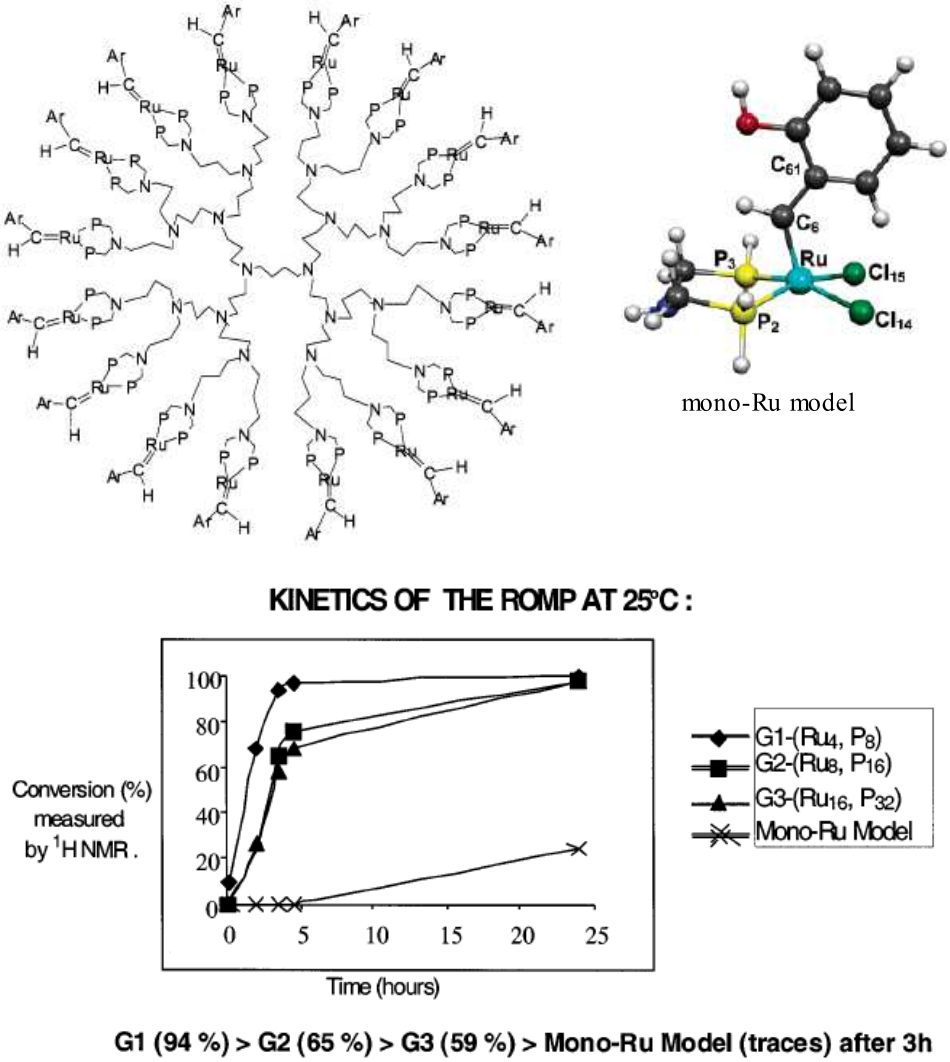

Figure 50. Comparison of norbornene ROMP rates for the mono-Ru model and the dendrimers. Reprinted with permission of the American Chemical Society (ref. 934, Astruc's group).

5.3.3.2. Hydrogenation catalysts

The asymmetric hydrogenation of β-ketoesters was catalyzed by dendritic chiral phosphine ruhenium complexes with good activity and remarkable dendritic effects on the ee, the stereoselectiviy being strongly influenced by the dihedral angle of the diphosphine that is related on the generation-dependent dendritic wedge.[936] A tetrabranched phosphoranyl-

terminated carbosilane derivative coordinated to four [Ru(*p*.cymene)Cl bipyRu(*p*.cymene) Cl_2] units catalyzed hydrogen-transfer hydrogenation of cyclohexanone, the stoichiometric hydrogen donor being cyclohexadiene or formic acid. This G_1 dendrimer was very active, but less so than the mononuclear species, and the dendritic effect was also negative up to G_3 that was less active than G_1.[937]

5.3.3.3. Other types of catalysis

5.3.3.3.1. Electron-transfer-chain catalysis

G_3 and G_4 Reetz' dendritic phosphines (PPI terminated with with $N(CH_2PPh_2)_2$) were loaded with the cluster $[Ru_3(CO)_{11}]$ on each of the 32 or 64 phosphines by Fe^I-catalzed substitution of one CO ligand of $[Ru_3(CO)_{12}]$ by a phosphine branch.[938,939] The reaction was very clean, as shown by ^{31}P NMR, upon electron-transfer-chain catalysis under ambient conditions with 1% of the standard electron-reservoir complex $[Fe^I(\eta^5\text{-}C_5H_5)(\eta^6\text{-}C_6Me_6]$.[940-942] The Knoevenagel condensation of malononitrile and cyclohexanone was catalyzed by a G_3 dendrimer terminated by 24 Ru-diphosphine species. The catalytic activity was often higher than that of the monomeric complex, and the dendritic catalyst was recycled without significant loss of activity.[943] An hexa-branch compound terminated with $[Ru(\eta^5\text{-}C_5H_5)(CO)_2(alkyl)]$ termini was supported on silica. This material was compared to Ru/SiO_2 in the CO hydrogenation catalysis, but did not produce Fischer-Tropsch products, indicating that a single Ru site was insufficient for Fischer-Tropsch catalysis.[944]

5.3.4. Other transition-metal catalysts

G_2 and G_3 alkoxysilyl-terminated Ti-containing carbosilane dendrimers catalyzed the epoxidation of cyclohexene with better yields and initial rates than the Shell catalyst based on the reaction of silica with $Ti(O\text{-}i\text{-}Pr)_4$. These catalysts were generated by acid-catalyzed hydrolysis of the carbosilane dendrimers in benzene giving monolithic gels followed by reaction with $Ti(O\text{-}i\text{-}Pr)_4$. A positive dendritic effect was disclosed on the gel surface area.[945] Fréchet-type dendrons having styrenyl end groups and bearing $Ti(OCHMe_2)_2$ species coordinated by TADDOL (α,α,α', α'- tetraaryl-1,3-dioxolane-4,5-dimethanol) were cross-linked into a polystyrene support, and this material catalyzed asymmetric addition of dithylzinc to benzaldehyde with 98% ee in 20 sequential applications. Non-dendritic supported catalysts had slightly lower ee's. The catalyst efficiency decreased with increasing the spacer length between TADDOL and the polymer backbone.[946] Rigid dendrimers based on 4,4',6,6'-tetrabromo-1,1'-bi-2-naphthol coordinated to $Ti(O\text{-}i\text{-}Pr)_4$ catalyzed the addition of diethylzinc to 1-naphthaldehyde with 90% ee and 100% conversion and were easily separated by precipitation using methanol.[947] Ti and Zr cyclopentadienyl (β-diketiminato) complexes surrounded by dendritic wedges catalyzed ethylene polymerization with higher activity than $[Ti(\eta^5\text{-}C_5H_5)Cl_3]$, $[Zr(\eta^5\text{-}C_5H_5)Cl_3]$, and the monometallic β-diketiminato complexes.[948-950] The zirconocene-type α-olefin polymerization precatalyst ($[Zr(Ind)_2Me_2]$ showed enhanced activity even in aliphatic solvents when the perfluorophenylborane Lewis acid was covalently attached to the periphery of a carbosilane dendrimer (4, 12 or 36 tethers, but no effect of tether number was found).[951] Steric crowding of the anion resulting from the dendrimer frame can be compared to that in methylaluminoxane (MAO). Bis(imino)pyridyl iron (II) catalyst precursors of ethylene polymerization attached to similar G_1 and G_2 dendrimers provided positive dendritic effects (compared to the parent iron catalyst) on the activity, molecular weight and melting temperature only at relatively low MAO/Fe ratio (< 1000).[952] With Ni(II) pyridylimine catalyst decorating the periphery of G_0 to G_3 carbosilane dendrimers, strong generation dependence was found concering the molecular weight and topology of polyethylene products, increasing generations leading to preferred oligomerization (chain transfer) over polymerization (Figure 51).[953]

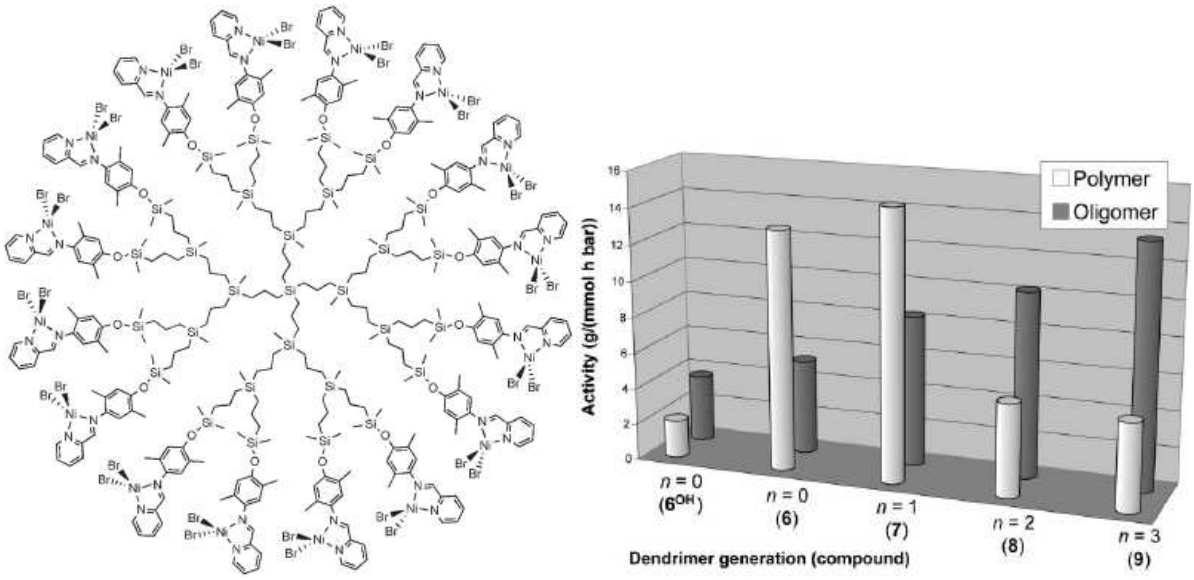

Figure 51. Metallodendrimer G_3–$[(ONNMe_2)NiBr_2]_{16}$; Activities by precursors 6OH and G_n–$[(ONNMe_2)NiBr_2]_m$. Reprinted with permission of the Royal Society of Chemistry (ref. 953, Flores's group).

Dendritic G_1- and G_2-DAB-salicyldimine-Ni complexes catalyzed ethylene oligomerization in the presence of $EtAlCl_2$ as an activator, the octabranched G_2 dendrimer showing higher activity than the tetrabranched G_1 catalyst.[954] A few copper and cobalt catalysts were reported in the 1990's.[539] More recently, dendronized supports linked to 2- and 4-(diphenylphosphino)benzoic acid groups that were coordinated to cobalt by reaction with $[Co_2(CO)_8]$ catalyzed the Pauson-Khand [2 + 2 +1] cycloadditions[886] with increased activity and selectivity compared to non-dendronized supports.[955]

After Suslick's seminal reports on dendritic Mn-porphyrin-catalyzed epoxidation,[794] Mn^{II} salen complexes immobilized on ultrafine silica in PAMAMs catalyzed olefin epoxidation with an activity that improved with generation increase.[956]

The catalytic properties of PPI-bound carbo-BINAP ligands in Cu-catalyzed hydrosilylation of acetophenone displayed a strong dependence of the enantioselectivity and activity on the dendrimer generation, and immobilized BINAL ligands were recycled several times without loss of enantioselectivity.[957]

The dendritic polyoxometallate oxidation catalysts and various other transition-metal-based dendritic catalysts are discussed in section 5.2. Although selenium is not a transition metal, it behaves as such in catalysis upon accepting an oxo ligand from hydrogen peroxide as cytochrome P450 as its models do, despite mechanistic variations. Thus, positive dendritic effects were found in the dendritic organoselenide-catalyzed bromination of cyclohexene using hydrogen peroxide and sodium bromide and attributed to autocatalytic formation of Br^+ at the selenide dendrimer surface (Figure 52).[957-959]

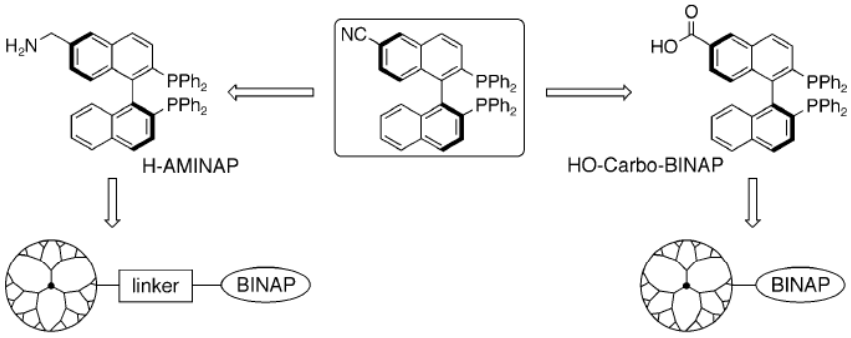

Figure 52. Attachment of the BINAP ligand on dendrimers with (left) and without (right) an additional linking unit. Reprinted with permission of Wiley-VCH (ref. 957, Gade's group).

5.4. Organocatalysis

Organic reactions in dendrimers can be either accelerated or slowed down by the dendritic framework, i. e. the dendritic effect can be positive or negative. As an example of precise study of negative dendritic effect, a dendrimer-encapsulated tertiary amine catalyzed the nitroaldol (Henry) reaction between benzaldehyde and 2-nitroethanol with pseudo-first-order rate constants that decreased with increasing the dendrimer generation (12.11, 1.89 and 1.03 x 10^{-4} s^{-1} for generation 1, 2 and 3 respectively).[960] The authors provided a quantitative treatment of the dendritic crowding by molecular dynamics simulations involving the "reagent accessible surface" of the dendrimer. Indeed, such negative dendritic effect due to increased crowding upon generation increase has been frequently observed experimentally.[656,813,816,831,832,933-936,961-966]

On the other hand, examples of dendrimer-encapsulated metal complexes have been reported for which dendritic pyridine,[967] phosphine,[968] *N*-heterocyclic carbene[969] or P,O (*o*-phenylphosphinophenol)[970] ligands increase the stability of the complex or protect it against deactivation when the generation increases. Sometimes, the environment of dendritic interior pockets provides optimized binding and reactivity as in enzymes,[971] and such a situation indeed led to positive dendritic effects in glutathione peroxidase activity for hydrogen peroxide reduction by benzenethiol in diselenide-cored Fréchet-type dendrimers.[972]

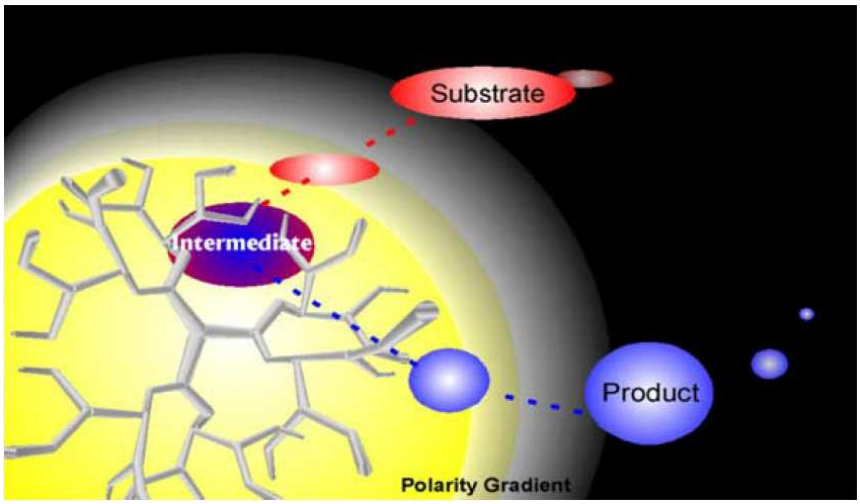

Figure 53. Illustration of substrate migration into the dendrimer interior. The nanoenvironment is greatly influenced by the branching units and creates a gradient of polarity with respect to the distinct interior and exterior solvent. These favorable conditions encourage substrate concentration and transition state stabilization. The resulting product is released from the nanoreactor into the solvent. Reprinted with permission of Elsevier (ref. 971, Fréchet's group).

Another example of dendritic nanoenvironment is that using the dielectric effect[973] inducing a radial polarity gradient. For this purpose, dendrimers were designed with long alkyl tethers at the periphery and polar ester or alcohol *functionalities* in the interior for the catalysis of reactions that develop a positive charge in the transition state. The unimolecular dehydrohalogenation of 2-iodo-2-methylheptane procceding with E_1 elimination mechanism matches these criteria, and it was achieved with a positive dendritic effect, i.e. improved with G_4. In the higher generation G_4, the interior cavities were larger thereby allowing a higher substrate concentration around polar alcohol groups, whereas the non-polar olefin product escaped towards the non-polar periphery to favor turnover and the so-called free-energy driven catalytic pump[974] The Fréchet group extended this concept to the $^1O_2$-sensitizing benzophenone denditic core incorporated in amphiphilic dendrimers with hydrophobic peripheries. Oxidation of hydrophobic cyclopentadiene with O_2 herewith was favored in the

hydrophobic dendrimer core, and the *endo*-peroxide cycloadduct was reduced *in situ* with thiourea to hydrophilic *cis*-cyclopentene-1,4-diol in order to favor rapid conversion even with only 0.1 mol% of catalyst (despite some photobleaching). The dendritic effect was again positive, i.e. increasing the dendrimer generation from G_1 to G_3 gave the diol in 15%, 35% and 50% yield respectively, in contrast with the 10% yield obtained with a non-dendritic model compound.[975]

The reverse polarity (hydrophilic dendritic polyammonium interior and hydrophobic periphery) was designed by Kaneda's group to use iodide anion for Lewis-base catalysis of the Mukayama aldol reaction of 1-methoxy-2-methyl-1-(trimethylsilyloxy) propene with aldehydes whereby these dendritic polyiodide polyammonium-cored dendritic catalysts were more efficient than tetrahexylammonium iodide salts. The anionic reaction intermediate is better stabilized by the polar polyammonium environment as well as by a more polar solvent, DMF providing better results than toluene.[976] The nanoenvironment effect was also similarly shown in acylation reactions of tertiary alcohols yielding linalol pivalate catalyzed by various amphiphilic dendritic and dendronized polymeric 4-(dialkylamino)pyridines, and non-dendritic model compounds such as DMAP were only marginally efficient. Related positive nanoenvironment dendritic effects were observed in Ford'seminal and subsequent decarboxylation studies[782,640-645] (sections 4.9 and § 5.1) and in metallodendritic catalyzed reactions (section 5.3).[793-797,869,977,978]

Several generations (G_1 to G_6) of PAMAM dendrimers containing pyridoxamine and pyridoxal at their cores were used by Breslow's group as biomimics of transaminases and amino acid racemases. Positive dendritic effects were disclosed in the transamination of pyruvic acid and phenylpyruvic acid in aqueous buffer by PAMAM-pyridoxamine dendrimers, as indicated by Michaelis-Menten kinetics and higher efficiency than simple pyridoxamine. Thus, the more globular G_6 generation was shown to exhibit enzyme-like conformation with highest reaction rates resulting from acid-base catalysis due to the large number of tertiary amines at the dendrimer periphery.[979]

Combinatorial librairies of diaminoacid units for dendritic branching with catalysts at the denrimer periphery were constructed with the aim to mimic lipases.[980-983] Knovenagel condensations have been heterogeneously catalyzed with 100% selectivity by polystyrene-G_1 to G_3-PAMAM dendrimers, and these catalysts could be recycled 10 times.[984] The esterolytic activity therein was selective and higher than that of the model catalyst 4-methylimidazole.[981]

Along this line, a series of G_1 to G_4 dendrimers with His-Ser dipeptide repeat units as catalysts were shown to undergo a positive dendritic effect attributed to enhanced substrate binding and more important contribution of the proximal His residue to the catalysis rate in G_4.[982]

Dendritic chiral phosphine Lewis bases catalyzed asymmetric aza-Morita-Baylis-Hillman reactions of *N*-sulfonated imines with activated olefins in excellent yields with up to 97% ee and could be recovered and reused.[983-985]

5.5. Catalysis with dendrimer-encapsulated and dendrimer-stabilized nanoparticles

5.5.1. Single-metal based nanoparticles in homogeneous catalysis

In section 4.8, the stabilization of various metal- or metal oxide NPs by dendrimers has been reviewed. Such mono- and heterobimetallic MNPs have been efficiently used in catalysis. The advantages of dendrimer-encapsulated NP (DEN) catalysis disclosed by Crooks' seminal work (see § 5.1) are (i) the control of the chemical composition of the catalyst and the solubility, (ii) the lack of passivation of the NP surface in the absence of anionic ligands such as thiolates that usually stabilize transition-metal NPs and (iii) the possibility to heterogenize the catalyst by fixation on a solid support.[652-657,696,790,860]

5.5.1.1. Selective hydrogenation

From Crooks' concept of dendritic nanofilter using PAMAM dendrimers, size selectivity resulted in catalytic hydrogenation reactions carried out using Pd DENs in various media such as water,[652,986] fluorous phase,[652,655] biphasic media.[652,655] and supercritical CO_2.[654,987] Similarly, selectivity was also observed with Pd DENs prepared using PPI dendrimers; for instance the rate of hydrogenation decreased with increasing the size of the cyclic dienes.[988] The influence of bulk at the periphery of dendrimers on the catalytic efficiency of resulting DENs was studied to confirm the validity of the nanofilter concept. Using α-amino alcohol-terminated G_4-PAMAM dendrimers used as templates for the preparation of Pd_{40} NPs, it was shown that DENs functionalized with bulkier peripheral groups were poorer catalysts than those with less steric bulk on their surface.[654,989] The effect of generation and peripheral groups on PdNP size and selective hydrogenation activity of cyclic dienes and internal alkynes to monoenes was determined (Figure 54).[990]

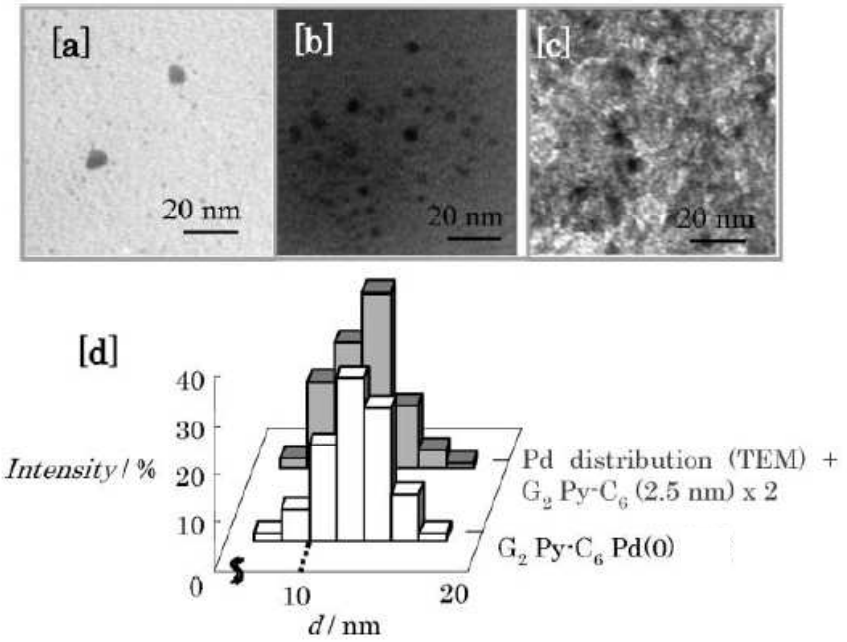

Figure 54. TEM images of Pd nanoparticles encapsulated within the G_2 dendrons; (a) G_2 Py–CO_2Me Pd(0), (b) G_2 Py–C_6 Pd(0), (c) G_2 Py–C_{12} Pd(0) and (d) the size distributions of G_2 Py–C_6 Pd(0). Reprinted with permission of the Royal Society of Chemistry (ref. 990, Kaneda's group).

Poly(amidoamine) hyperbranched polymer-stabilized PtNPs (1.8 nm) were also shown to be effective and robust hydrogenation catalysts in water.[991]

5.5.1.2. Nitroarene reduction

3,5-dihydroxybenzyl-terminated dendrimer-stabilized AgNPs were found to be highly active catalysts for the selective reduction of chloronitrobenzenes to chloroanilines.[992] Nitrophenol reduction by $NaBH_4$ catalysed by PAMAM Pd DENs was shown to depend on the nature of the terminal dendrimer group with rate constants in the order: amine > carboxylate > sugar > methyl ester.[993] Heterobimetallic Au-Pt, Au-Pd and Pt-Pd DENs as alloys were also prepared for this reaction in water, based on G_3, $G_{3.5}$ and $G_{5.5}$ PAMAM dendrimers. The Au-Pd and Pt-Pd DENs exhibited higher activities than monometallic DENs, but the Au-Pt DENs showed activity that was comparable that of monometallic Pt DENs, and the rate decreased compared to that found with Au DENs, because Pt poisoned catalysis. The catalytic activity was also dependent on the nature of the terminal group of the PAMAM dendrimer.[994]

G_4-phenylazomethine dendrimers and G_4-OH-PAMAM dendrimers were loaded with $RhCl_3$, and 1.2-nm Rh DENs formed upon reduction by $NaBH_4$ and containing 64 Rh atoms (assuming face-centered cubic, fcc, closed-packed structure) were active catalysts for the hydrogenation of various olefins and nitroarenes in methanol under 1 atm H_2 at room temperature.[995]
G_4-phenylazomethine- and G_4-PAMAM-OH Rh DENs catalyzed olefin and nitroarene hydrogenation very effectively, affording high TOFs (up to 17 520 h^{-1}). It was shown that the substrates could pass though the branches of the dendrimers without releasing the RhNPs (Figure 55).[996]

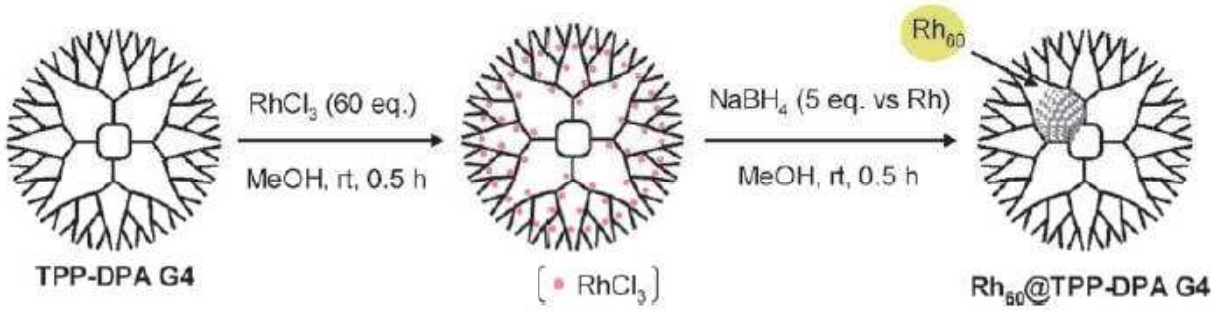

Figure 55. Synthetic procedure of Rh_{60}@TPP-DPA G_4. Reprinted with permission of the Royal Society of Chemistry (ref. 996, Nishihara's and Yamamoto's groups).

The Crooks group reported the synthesis and catalytic evaluation of Cu DENs as an undergraduate experiment to explore catalytic nanomaterials. The model reaction was the $NaBH_4$ reduction of *p*-nitrophenol to *p*-aminophenol. The rate constant for the catalytic activity was estimated by measuring the pseudo-first-order reaction kinetics obtained by monitoring the absorbance variatios of *p*-nitrophenol reduction by UV-vis spectroscopy.[997]

5.5.1.3. Pd-catalyzed heterocoupling

DENs also show enhanced efficiency and selectivity of heterocoupling such as Heck reactions.[655,987-992,998-1000] For instance, the coupling of *n*-butyl acrylate with aryl halides in biphasic organic solvents catalyzed by PPI Pd DENs was shown to proceed at 90°C instead of temperatures higher than 120°C used for other PdNPs. The reaction was also 100% selective for the *trans*-isomer of *n*-butyl formylcinnamate.[655] The comparison of the catalytic efficiency of PdNPs stabilized by polymers such as poly(vinylpyrrololidone) (PVP) and dendrimers (DENs) for the Suzuki-Miyaura reaction by El Sayed's group showed that the dendrimers provide higher stability but lower activity than PVP. The lowest activity was disclosed for the highest dendrimer generations as a result of highest resistance to mass transfer and/or passivation of catalyst surface by functional groups.[998,999] Pd NP catalysis of the Suzuki-Miyaura reaction by DENs has been studied by several research groups.[865,988,998,999]
The well-known "click" reaction has been used by the Astruc group to stabilize transition-metal ions including Pd^{II} by the 1,2,3-triazole ligand[658-661] and to form "click"-dendrimer-protected Pd nanoparticles by reduction of the Pd^{II} species to PdNP either as DENs or dendrimer-stabilized PdNPs (DSNs) when the dendrimers are too small (G_0). Such PdNPs are very active catalysts for selective hydrogenation[536,1001] and Suzuki-Miyaura cross coupling reactions.[1002] This latter reaction was efficient under ambient conditions for the coupling of phenyl iodide with down to 1 ppm catalysts, and the TON of this catalyst was all the higher as the catalyst amount was decreased. This "homeopathic" behavior was taken into account by a leaching mechanism of extremely reactive ligandless Pd atoms from the PdNPs subsequent to oxidative addition of phenyl iodide and less efficient quenching of these Pd atoms by PdNPs at the catalyst concentration is decreased. Such a mechanism was proposed for the high-

temperature Heck reaction with catalysts such as $PdAc_2$ that decompose to PdNPs,[785] but in the present case, it is proposed to be operating at room temperature with non-liganded PdNPs (Figures 56 and 57).[1002]

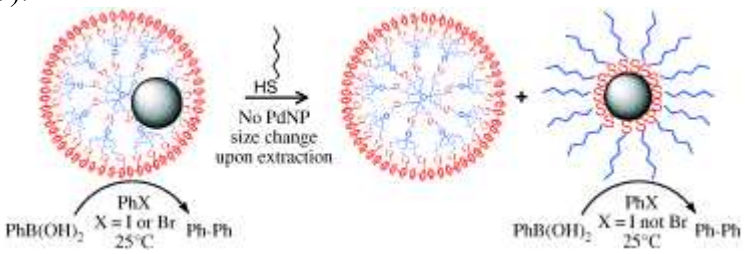

Figure 56. Extraction of PdNPs from DSNs or DENs with hexanethiol without any change in the size of the PdNPs to produce air- and water-stable, catalytically active hexanethiolate PdNPs. Reprinted with permission of Wiley-VCH (ref. 1002, Astruc's group).

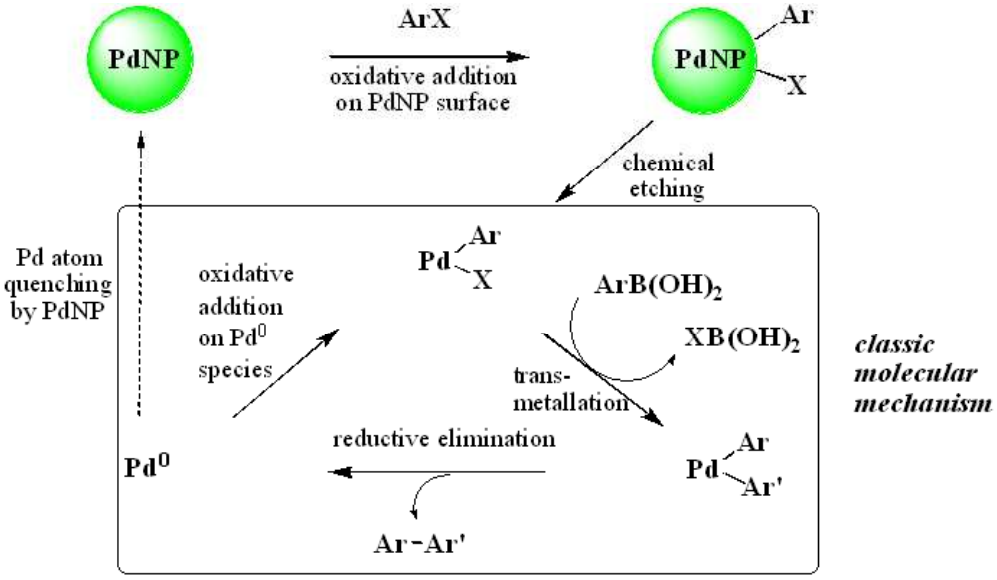

Figure 57. Proposed mechanism for the Suzuki reaction at RT by dendrimer-encapsulated Pd nanoparticles resembling that suggested by de Vries for the Heck reaction at 130°C. Reprinted with permission of Wiley-VCH (ref. 1002, Astruc's group).

Moreover, the "click"-dendrimer-stabilized PdNPs can be solubilized in water by using propargyl sulfonate for the "click" reaction, leading to sulfonate-terminated "click" dendrimers. The PdNPs were then formed by $NaBH_4$ reduction of the Pd^{II}-sulfonate-triazole dendritic complexes and were equally efficient catalysts at room temperarture for styrene hydrogenation and Suzuki-Miyaura cross-coupling reaction of phenyl iodide in an aqueous medium.[1003,1004] Air-stable dendritic phosphine oxide-stabilized PdNPs were demonstrated to be efficient catalysts for Suzuki and Stille coupling reactions and for hydrogenation.[1005]

5.5.2. Heterobimetallic nanoparticles in homogeneous catalysis

5.5.2.1. Characterization of heterobimetallic nanoparticles

Heterobimetallic nanoparticles can be alloys, obtained by co-reduction of two metal salts, or of "core-shell" structure obtained by successive reduction of each metal salt. A variety of techniques is being used for their analysis:[1006] TEM, including HRTEM, allows to examine their size and morphology (Figure 58);[986,1007-1009] AFM provides a vertical heigh measurement complementing the lateral dimensional TEM measurement;[1006,1012] UV-vis explores the results of various synthetic routes but cannot quantitatively analyze the composition;[1006,1008,1010] infrared spectroscopy analyzes the metallic surface composition for the distinction of different structures and approximately evaluates the surface

composition;[1006,1013] Single-particle energy-dispersed X-ray spectroscopy (EDS) examines the variations in composition (but with large standart deviation when the NPs are smaller than 1.5 nm);[986,1006-1016] XPS provides information about the surface electronic state and elemental composition; EXAFS estimates the possible structure via calculation of the number of surrounding atoms of each absorbing metal element (although it may be difficult to get a precise set of absolute values of coordination numbers);[1017] chemical extraction allows to analyze the chemical composition.[1010]

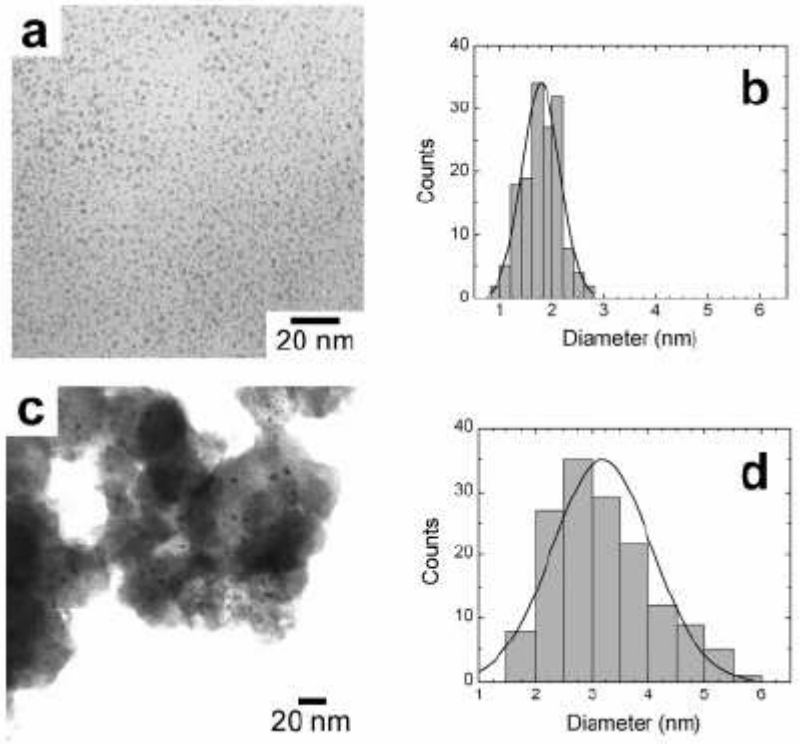

Figure 58. Bright-field TEM images and particle-size distributions for G_4- $NH_2(Pd_{27.5}Au_{27.5})$ DENs prepared by co-complexation of the corresponding metal salts followed by reduction. (a), (b) As synthesized. (c), (d) After incorporation into the titania matrix and subsequent calcination at 500 °C under O_2 and H_2. Reprinted with permission of the American Chemical Society (ref. 1011, Crooks's group).

5.5.2.2. Selective hydrogenation

5.5.2.2.1. Alloys

Heterobimetallic nanoparticle catalysts find their origin in the late 1980's,[1018] and were developed in Toshima's group for 1-3 nm AuPdNPs stabilized using poly(N-vinyl-2-pyrrolidone). These NPs exhibited enhanced efficiency for the partial hydrogenation of 1,3-cyclooctadiene compared to mixtures of single-metal NPs.[1017,1019,1020] More recently, Crooks pioneered the use of heterobimetallic DEN nanoparticles in selective catalysis including under "green" conditions.[652-654] Heterobimetallic water-soluble alloy DENs were prepared by co-complexation of G_4-PAMAM-OH dendrimers with mixtures of K_2PdCl_4 and K_2PtCl_4 followed by $NaBH_4$ reduction. The resulting metal ratio in the DENs is controlled by the initial loading and verified by single-particle EDS. These PdPtNPs gave significantly higher TONs for the hydrogenation of allylic alcohol than single-metal analogues.[986] Related enhancements were also observed for the partial hydrogenation of cyclohexene[1021] and 1,3-cyclo-octadiene.[1015] Toshima had, in the early 1990's, taken such enhancements by 1-2 nm PdPtNPs (alloy) stabilized by polymers into account by synergistic electronic effects involving the ligands.[1019,1020]

5.5.2.2.2. Core-shell

Core-shell heterobimetallic NPs were first synthesized by Schmid's group, the core-shell structure being demonstrated by HRTEM and EDS microanalyses.[1022] Crooks' group showed that some core-shell heterobimetallic NPs such as [Au]PdNPs ([Au] indicates the AuNP core) are also superior catalysts to PdNPs. For instance selective reduction of $PdCl_4^{2-}$ onto G_6-$Q_{116}(Au_{55})$ seeds using H_2 yielded [Au]PdNPs with shells of 95 and 455 Pd atoms with sizes of 1.8 and 2.3 nm respectively that had significantly enhanced catalytic activity for the hydrogenation of allylic alcohol in water.[1009] Peng et al found that dendrimer-derived PtXNPs and PtPdNPs showed kinetics trends indicating enhanced catalytic behavior for selective 3,4-epoxy-1-butene hydrogenation compared to traditional catalysts prepared by wet impregnation of metal salts.[1006] These authors also reported that G_5-$Q(Ru_5Rh_5)$ DENs catalyze the regioselective reaction of poly(methylhydro)siloxane with 1-hexene to poly(methylhexyl)siloxane with high efficiency.[1006,1023]

5.5.3. Dendrimer-encapsulated nanoparticles in heterogeneous catalysis

In heterogeneous catalysis, nanoparticles stabilized by encapsulation in PAMAM dendrimers (PAMAM DENs) are immobilized on solid supports such as gold, silica, alumina, titania or a polymer matrix, most frequently using the terminal-NH_2 and -OH groups of the dendrimers. The advantage of using dendrimers is that the NP size, composition and dispersity are well defined and controlled. Although such systems are catalytically active when a solvent is present,[655] this is no longer the case, however, in the absence of solvent. For instance the gas-phase reactant CO cannot bind the DEN surface, because the dendrimer collapses around the NP and poisons the NP surface, rendering it inactive.[859] The difficulty then resides in the removal of the dendrimer without transforming or perturbing the NP.[853,854,863] Indeed, dendrimer removal may lead to increase in both particle size and distribution. This is illustrated by FT-infrared studies of PAMAM dendrimer removal leading to the formation of surface carboxylates and the need to use high temperature for decomposition.[1024]

5.5.3.1. Methods of DEN immobilization and dendrimer removal

DENs terminated with amine and partially quaternized amines covalently linked to mercaptoundecanoic acid formed self-assembled monolayers (SAMs) bound the Au surface via their thiol groups.[1025-1027] DENs terminated by alcohols were linked to glassy carbon electrodes by cycling the potentials three times between 0 and 1 V vs. Ag/AgCl, 3M NaC.[1029] Thiophene-terminated PAMAM Pt DENs were co-electropolymerized with poly(3-methylthiophene).[654,1028] Dendrimers have also been calcinated on support when they were loaded with unreduced metal ions.[1029-1031] Pd DENs supported on mica or highly oriented pyrolytic graphite (HOPG) were calcinated at 630°C, forming large aggregates from the PdNPs.[696] Chandler reported the first successful dendrimer removal upon calcination using G_5-PAMAM-OH Pt_{50} DENs and G_5-PAMAM-OH Pt_{100} DENs at 300°C in a O_2/He flow which resulted in PtNPs that largely retained their original size (for instance from 1.9 nm to 2.2 nm).[1024] Dendrimer removal was indeed accelerated by PdNP catalysis. Calcination using these conditions of Pd DENS and Au DENs required around 500°C to remove the PAMAM dendrimers accompanied by considerable NP size increase, for instance from 1.7 nm to 7.2 nm for G_4-$Q_{32}Au_{55}$,[654] although lower temperatures yielded better results.[1032] Incorporation of Pd DENs and Au DENs into sol-gel matrixes minimize NP growth due to isolation within the sol-gel framework, for instance from 2.0 nm to 2.7 nm for Au_{55} DENs upon calcination at 500°C.[1033,1034] Extension of this procedure to the heterobimetallic nanoparticles PdAu DENs for G_4-$NH_2(Pd_{27.5}Au_{27.5})$ increased the NP size from 1.8 nm to 3.2 nm upon calcination.[1011]

5.5.3.2. Electrocatalytic O_2 reduction

Electrocatalytic O_2 reduction using Pt DENs was initially shown subsequent to immobilzation of OH-terminated PAMAM dendrimers onto Au surfaces, but these DENs were easily displaced from the electrode.[1011] Subsequently, G_4-PAMAM-OH Pt_{40} DENS electrodeposited on glassy carbon electrodes as stable films upon anodic oxidation (*vide supra*) yielded electrocatalytic O_2 reduction at 0.22V, with a gain of 0.6 V compared to the non-catalytic reduction.[1033-1035] G_6-PAMAM-OH PtPd DENs electrodeposited onto such electrodes in an aqueous 0.1 M $LiClO_4$ electrolyte solution catalyzed the 4-electron O_2 electroreduction as characterized by cyclic and rotating voltammetry with relative mass activity enhancement of a factor up to 2.4 compared to monometallic Pt DENs (Figure 59).[1036,1037]

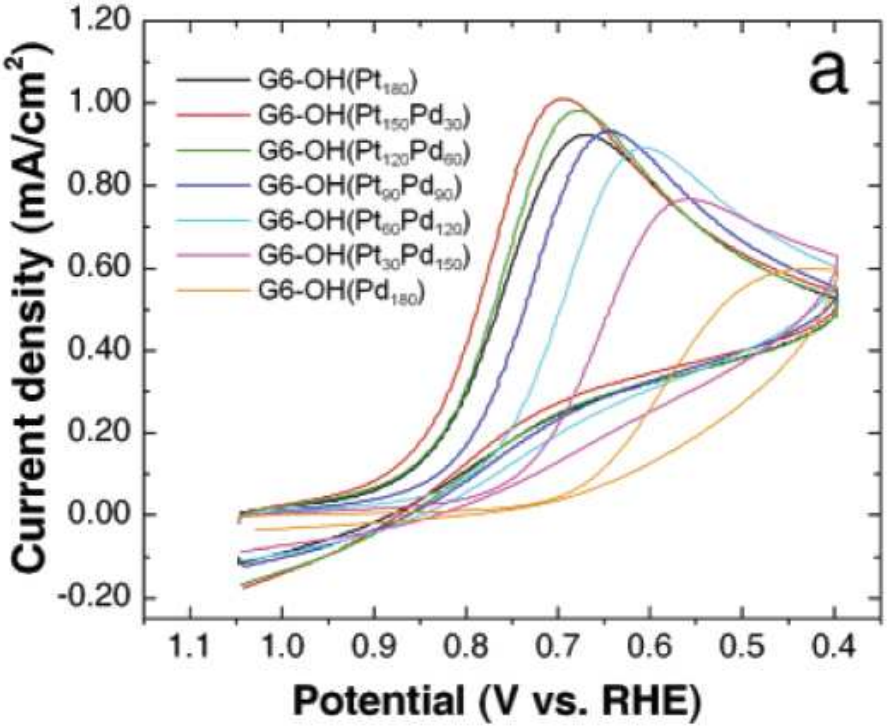

Figure 59. Cyclic voltammograms of G_6-OH(Pt_nPd_{180-n})(n =180, 150, 120, 90, 60, 30, and 0). Reprinted with permission of the American Chemical Society (ref. 1036, Crooks's group).

G_4-PAMAM-NH_2 AuPt DENs electrodeposition in a 0.5 M H_2SO_4 supporting electrolyte solution onto an indium tin oxide (ITO) surface yielded nanoflowers of bimetallic NPs that also exhibited a good electrocatalytic activity for O_2 reduction.[1038]

5.5.3.3. CO oxidation

The seminal work by Haruta on CO oxidation demonstrated the need of small (< 5 nm) AuNPs deposited on oxides for facile CO oxidation by O_2 as well as many other AuNP-oxide catalyzed oxidation and reduction reactions.[1039-1041] These very important systems still require improved mechanistic understanding, however, concerning the AuNP-oxide interaction for the precise substrate activation mode(s).[1041-1045] CO oxidation by Pt DENs on TiO_2 has also been probed.[1042] The dendrimer encapsulation of AuNPs and heterobimetallic NPs, that provides a unique way to control the exact definition in terms of size and composition, should thus introduce enlightning data. Thus, Chandler's group reported the catalytic CO oxidation with SiO_2-supported PtAuNPs prepared from G_5-PAMAM-OH $Pt_{16}Au_{16}$. At 30°C-80°C, Pt_{32} NPs disclosed little activity, but the rate (2.0-2.6 mol CO/mol pt/min) for $Pt_{16}Au_{16}$ NPs catalysis was substancial. At 100°C, $Pt_{16}Au_{16}$ NPs catalyzed the reaction at a rate 8.5 times higher than that of a mixture of Pt_{16} NPs and Au_{16} NPs. At 120°C, the rates of Pt_{32} NPs and $Pt_{16}Au_{16}$ were similar and Au_{32} showed an activity of only 0.5 mol CO/mol Au/min. It

appeared that Pt atoms, that are less active in PtNPs alone, play a favorable synergistic role in AuPt NPs, possibly by re-locating O_2 activation at Au-atom sites of the AuPt NPs.[861] The catalytic activity for CO oxidation of TiO_2-supported G_4-PAMAM-NH_2 $Pd_{27.25}Au_{27.25}$ NPs was compared to those of monometallic Pd_{55}NPs and Au_{55}NPs. At 150°C, the PdAuNPs started to react with 1% CO conversion whereas the PdNPs and AuNPs were unreactive, and complete CO conversion was obtained at 250°C for the PdAuNPs and only at 285°C for PdNPs, in agreement with the above results.[853-856,859-863,1011]

5.5.3.4. Ethylene hydrogenation

G_4-PAMAM dendrimer-templated small RhNPs and PtNPs supported on a high-surface-area SBA-15 mesoporous support catalyzed ethylene hydrogenation under mild conditions with or without removing the dendrimer capping. The activity was highest after hydrogenation at 423K. Pyrrole was also hydrogenated using this catalyst (Figure 60).[1043,1044]

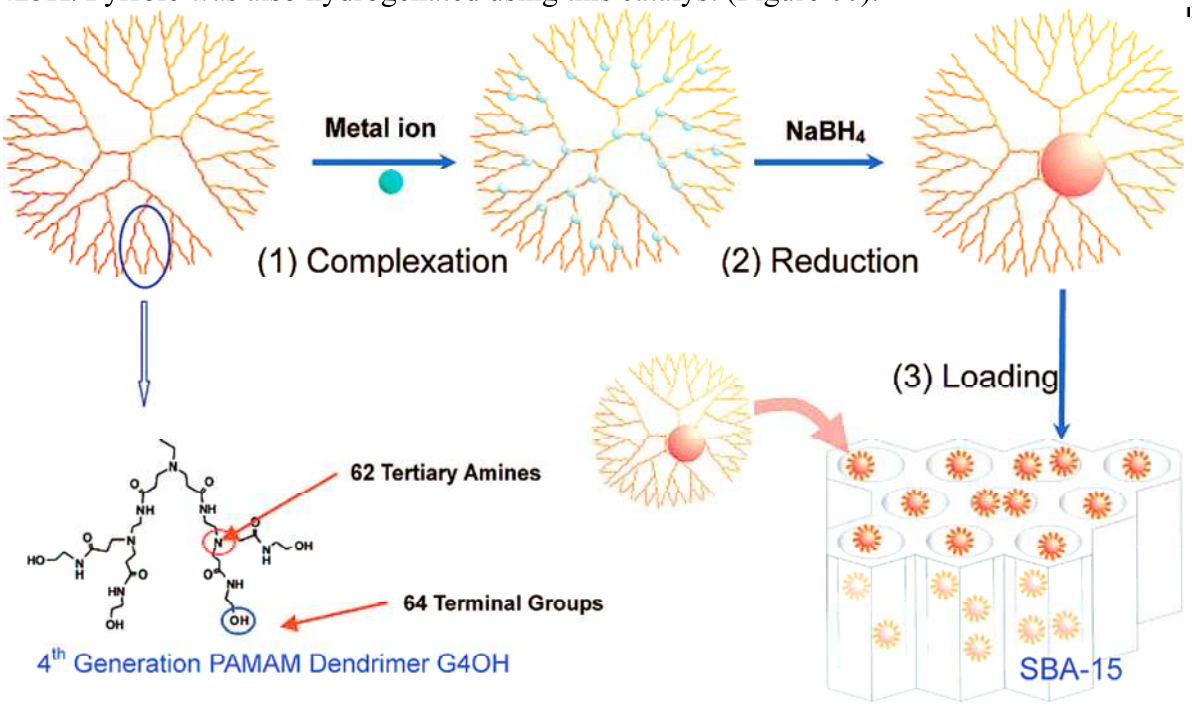

Figure 60. Synthesis of dendrimer encapsulated metal nanoparticles and the subsequent immobilization of the nanoparticle on mesoporous SBA-15 support. Reprinted with permission of the American Chemical Society (ref. 1043, Somorjai's group).

5.5.3.5. Nitrile hydrogenation

Dendrimer-derived supported IrNP catalysts were active in benzonitrile hydrogenation and showed an increase in TOF with increasing dispersion, and selectivity towards dibenzylamine was affected by the catalyst preparation method, with the oxidation-reduction treatment resulting in lower selectivity.[1045]

5.5.3.6. Ethane hydrogenolysis

Heterogeneous RhNP/ZrO_2 catalysts have been prepared for ethane hydrogenation. [$RhCl_3(H_2O)_3$] was loaded in aqueous solution into G_4-PAMAM-OH dendrimers and reduced by $NaBH_4$, and the Rh_{20}-G_4-PAMAM-OH samples formed were impregated with ZrO_2, followed by oxidation under O_2 at 400°C for 1h, then reduction with H_2 at 200°C for 1h. The diameters of the resulting RhNPs were estimated by TEM to be 0.7 nm and 0.8 nm corresponding to Rh_{10}NP and Rh_{20}NPs respectively. In contrast, conventional preparation by wetness impregnation and identically treated exhibited a 1.6 nm size corresponding to approximately 150 Rh atoms. Ethane hydrogenolysis at 200°C is a classic structure-sensitive

probe utilized to examine the catalytic properties of various Rh/ZrO_2 catalysts, and this study showed that the optimum RhNP size is 1.6 nm. The increase of activity when the RhNP size decreases from 6 nm to 1.6 nm is well-known and corresponds to an increase in the ratio of highly energetic low-coordination sites (corners and edges) required for C-C cleavage adjacent to high planar coordination sites required for hydrogen adsorption. Interestingly, this study showed a drastic decrease of activity when the RhNP size decreased from 1.6 nm to 0.7 nm, which was attributed to the absence of large planes on the surface of subnanometer RhNPs that restricted the ethane dehydrogenation step.[1046-1048]

5.5.3.7. Photocatalysis with TiO_2 NPs

Sub-nanometre size control of both anatase and rutile forms of TiO_2 particles with phenylazomethine dendrimers led to samples with very narrow size distributions. Quantum-size effects were observed in the NPs, and the energy gap between the conduction and valence bands exhibited a crystal-form-dependent blueshift with decreasing NP size (Figure 61).[350]

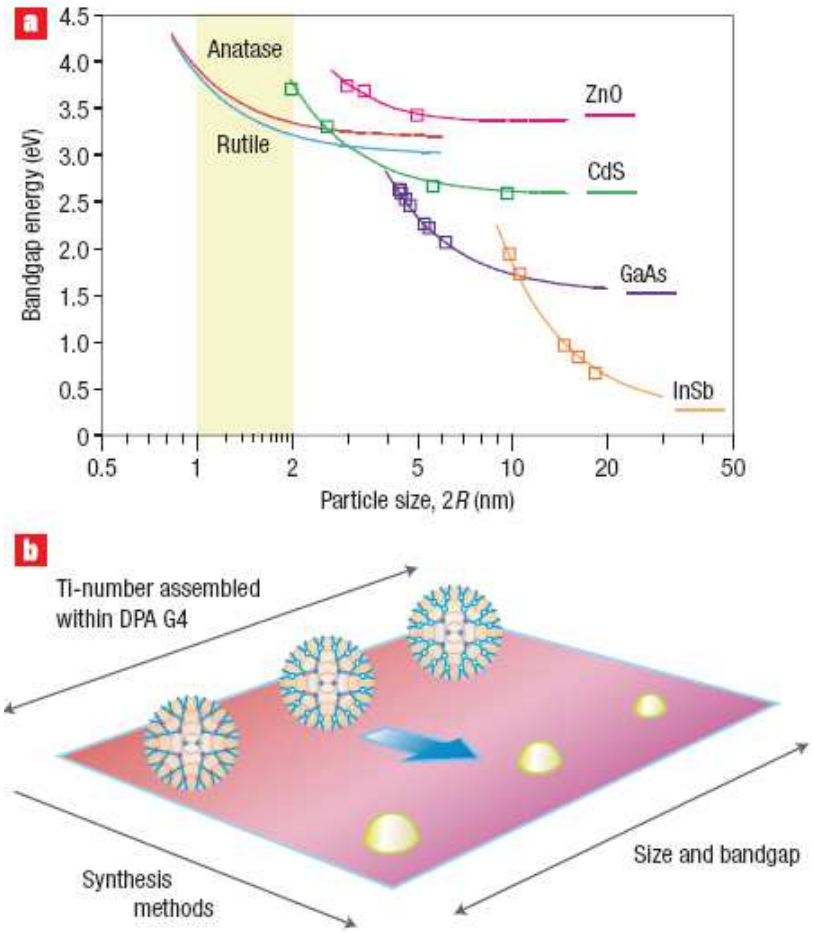

Figure 61. Sub-nanometer size control and synthetic strategy for Q-size TiO_2 using the DPA G_4 template. A) Calculated size dependence of the TiO_2 bandgap energy. Unlike previously reported Q-size effects for other semiconductors (experimental data shown by squares), the estimated bandgap energy for TiO_2 dramatically increases as particle size decreases from 2 nm to 1 nm. In other words, in this range, a sub-nanometre difference in size critically affects the bandgap energy of TiO_2. b) Scheme for size-controlled TiO_2 particle formation using the DPA G_4 template. The number of metal ions assembled within the DPA G_4 can be controlled, offering the means to construct size-controlled particles of ≈1 nm in dimension. Different methods of synthesis are well known to produce different crystal forms, that is, the anatase or rutile forms, under certain conditions. Reprinted with permission of the Nature Publishing Group (ref. 350, Yamamoto's group).

5.5.3.6. Hydrodechlorination of 1,2-dichloroethane

Dendrimer-metal nanocomposites were used as precursors to prepare SiO_2-supported monometallic Pt, Cu, and bimetallic Pt-Cu catalysts with PtCu at 1:1 and 1:3 ratio for heterogeneous hydrodechlorination of 1,2-dichloroethane. These MNPs in SiO_2 on SiO_2 support were smaller and had narrower size distribution than those in conventional catalysts prepared using metal salts via the wet-impregation method. The overall activity decreased with increasing CuNP loading in the catalyst. The process allowed for effective treatment of chlorinated hydrocarbon waste streams with recovery of useful chemical feedstocks.[1049]

6.Biomedical Applications

6.1 Introduction

The biomedical future of dendrimers was apparent since their discovery with Denkewalter's polylysine dendrimers,[6] Tomalia's multi-generation PAMAM dendrimers[7] and Newkome micellar arborols[8] in the early 1980's. This aspect was delineated through comparison with biological systems and encapsulation properties for instance in Tomalia' seminal review in 1990.[9] The biomimetism of dendrimers appeared from their sizes and globular shapes that match those of bioassemblies such as DNA duplexes (2.4 nm), insulin (4 nm), hemoglobin (5.5 nm) and lipid bilayer membranes (5.5 nm).[800,801] Meijer's molecular box was a striking example along this line.[10] In another review, Fréchet referred to dendrimers as artificial proteins in which the dendritic encapsulation of function applies Nature site isolation principle.[28] Dendrimers self-assemble by supramolecular interactions (see § 4) as do molecular-level organized biological structures; they are site-selective catalysts as shown with metalloporphyrin-cored systems mimicking hemoglobin;[245] they are also enzyme mimics as shown by Fréchet upon designing dendritic nanoreactors with polarity gradient that stabilize polar transition states.[816,817] Rigid dendrimers could mimic bacteriophilic units that are light-harvesting antennae[189] (§ 3.1) and natural proteins including redox-active enzymes with iron-sulfur cores.[507]

Medicinal engineering using dendrimers started in the early 1990's by mimicking antibodies for immunological applications and sensor functionalities to selectively recognize DNA branches and to detect and quantify AIDS virus, and were reviewed in the mid' 1990s.[39] Since then, biomedical applications became more and more promising, and reviews are available.[1050-1076] Thus, we will focus here on the major concepts and most recent developments.

Dendrimers belong to a group of nanocarriers designed to improve the water solubility, pharmacodynamics and pharmacokinetics (circulation time, organ uptake and tumor accumulation) and bioavailability of drugs *in vivo*.[1077-1082] These nanocarriers started with liposomes.[1083] They more recently developed with macrolecules including polymeric micro- and nanoparticles,[1084,1085] dendrimers, polymeric micelles (nanostructures formed by self-assembly of amphiphiles in water)[1086] and polymersomes (polymeric vesicles made of amphiphilic block copolymers that self-assemble in aqueous medium).[1087,1088]

The leading principles for the use of dendrimers as delivery vehicles involve (i) the charge of the terminal groups that must be neutral or negative in order to avoid or minimize toxicity (or largely masked if cationic), (ii) the design of the molecular architecture to optimize the pharmacokinetics, (iii) the PEGylation for water solubility and biodistribution, (iv) the choice between dendritic encapsulation and covalent attachment to the branches and (v) the use of cancer-cell-targeting groups (folic acid, peptides, monoclonal antibodies and glycosides) with overexpressed receptor targets (Figure 62).

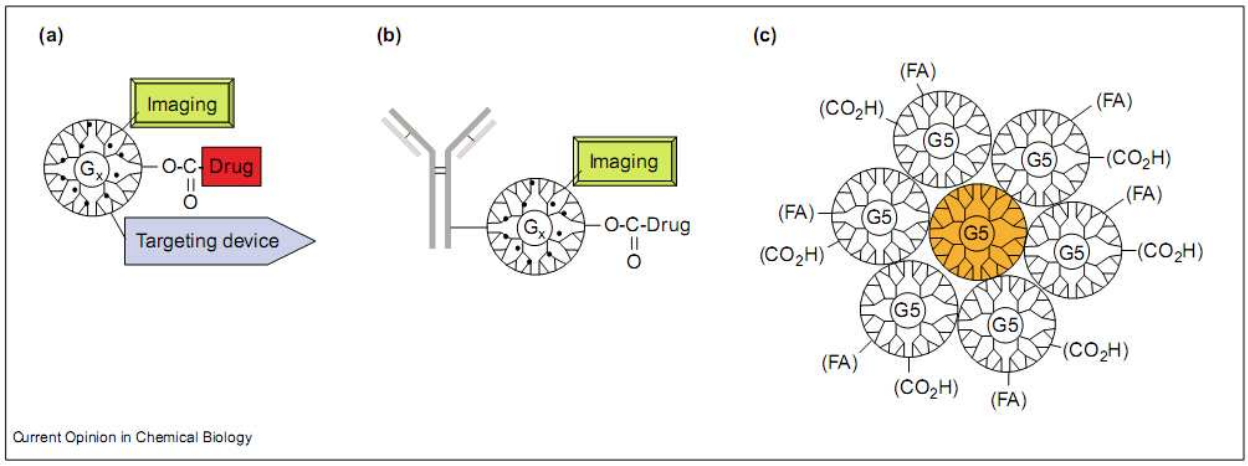

Figure 62. Dendritic nanodevices for therapeutic applications. (a) Surface-modified PAMAM dendrimer for targeting, imaging and drug delivery. (b) Antibody–dendrimer conjugate. (c) Tecto(dendrimer). FA, folate. Reprinted with permission of Elsevier (ref. 1088, Baker Jr.'s group).

Dendrimers are also used as non-viral gene carriers. The dendrimers probed for this purpose are terminated by cationic groups to form electrostatic complexes with negatively charged DNA for gene transfection. Toxicity and efficiency issues are important in this field, however, and need be discussed (see § 6.2.7).

Among biologically relevant dendrimers, peptide dendrimers are an important class that consists in assemblies of amino-acids linked by amido bonds and containing both α-peptides and ε-peptides. The majority of peptide dendrimers currently in use are based on the multiple antigen peptide system and have been reviewed by Tam's group[1089] who pioneered the field, and by Crespo et al.[1090] Their multiple applications are in immunoassays and serodiagnosis, as inhibitors, mimetics, artificial proteins and in intracellular delivery and medical diagnosis (MRI, magnetic resonance angiography, fluorogenic imaging and serodiagnosis). They play key roles as anticancer, antimicrobial and antiviral agents,[1091] in the central nervous system, analgesia, asthma, allergy and calcium metabolism, and some peptide dendrimers are useful in antiangiogenic therapy (cf. § 6.2.6).[1089-1091] Glycopeptide dendrimers are a broad class of peptide dendrimers involved in targeting with antigen-antibody interactions (cf. § 6.2.5). In turn, classic dendrimers interact with peptides and proteins in a specific way, the interactions being of electrostatic and hydrophobic nature. A dramatic example was the remarkable discovery by Prusiner (2004 Nobel Laureate in medicine) and his group in 1999 that 14 cationic PAMAM, PEI and PPI dendrimers were effective in removing prion molecules in the infectious state (Pr^{PSc}) from both ScN2a cells (Pr^{PSc}-infected neuroblastoma cells) and from Pr^{PSc}-containing brain homogenates.[1092,1093] This field of protein-dendrimer interactions is promising[1094-1098]and has recently been reviewed.[1094]

In addition to their function of drug and gene delivery nanovectors, dendrimers are used for their intrinsic drug properties (for instance to remove prions), as scaffolds for tissue repair, photodynamic and photothermal therapy based on photosensitizing agents, photothermal therapy based on gold and iron oxide nanoparticles, boron neutron capture therapy based on lethal $^{10}B(n,\alpha)$ capture reactions, antimicrobiol therapy, anti-viral therapy and immunogens and vaccines. Besides therapy, dendrimers are used in diagnostics as sensors (molecular probes) and for imaging techniques (cf. § 6.8) based on magnetic resonance (MRI) with gadolinium paramagnetic contrast agents and computed tomography (X-ray contrast agents) especially with iodinated contrast agents (Figures 63 to 65).[1069-1071]

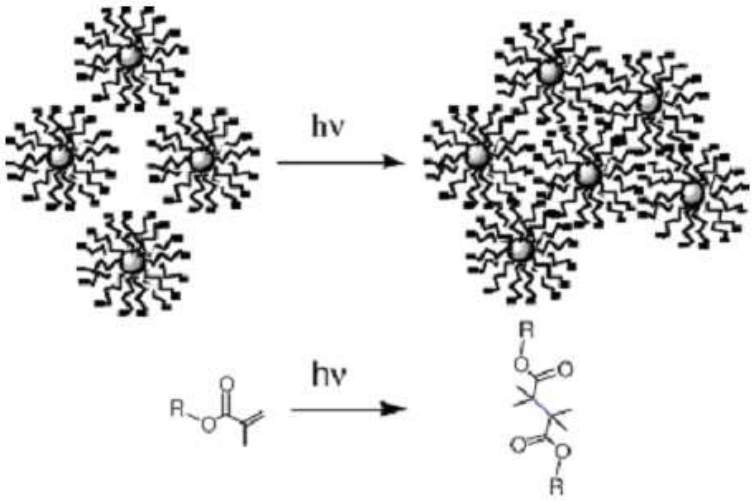

Figure 63. Photochemical crosslinking reaction to form the hydrogels. Reprinted with permission of Wiley Interscience (ref. 1069, Grinstaff's group).

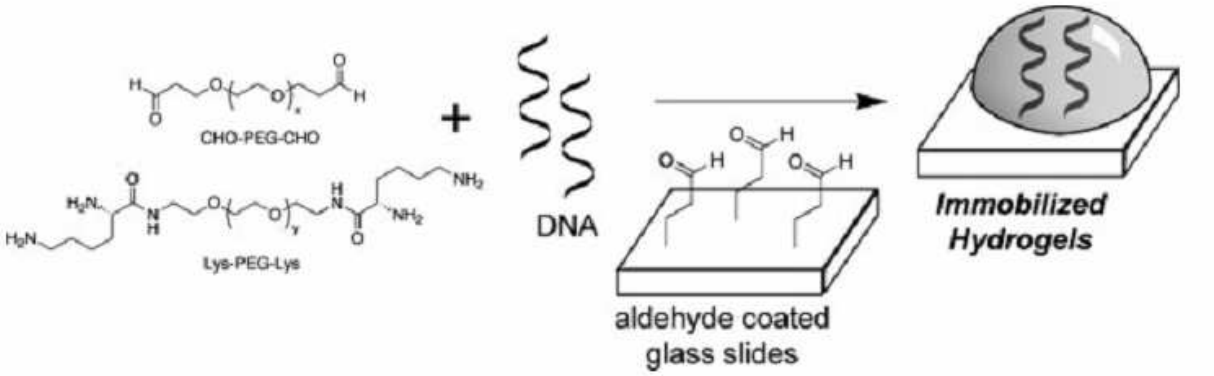

Figure 64. Construction of IgG immobilized hydrogels on aldehyde coated slides using $(CHO)_2$-PEG and $(Lys\text{-}NH_2)_2$-PEG. Reprinted with permission of Wiley Interscience (ref. 1069, Grinstaff's group).

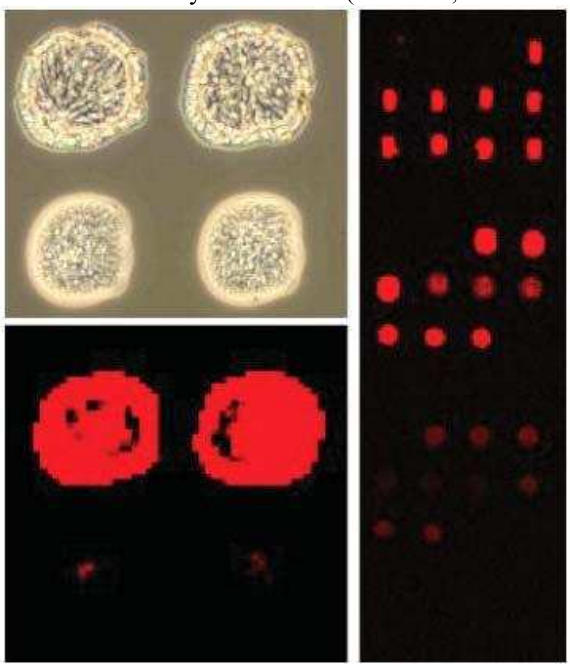

Figure 65. (left-top) optical and fluorescent (left-bottom) image of two hydrogel reaction chambers containing aRNA (250–5000 nt) (top row) and controls (without aRNA) (bottom row) after probing with Cy5-aRNA (60–200 nt). (right) Example of a screening experiment performed with an array of reaction chambers. Reprinted with permission of Wiley Interscience (ref. 1069, Grinstaff's group).

6.2. Drug delivery

Drug delivery using nanomaterials has revolutionized medicine by largely improving the efficiency and reducing the side effects of drugs, creating a new branch, nanomedicine. Although polymers have been used for several decades for this purpose, better defined macromolecules such as dendrimers, dendronized polymers and hyperbranched polymers are becoming more attractive because of their low dispersity, specific morphology, branching tethers, multi-valency, high density of functional groups, globular or other well-defined shapes and controlled molecular weights. In addition, high penetration abilities through the cell membrane results in increased level of cellular drug uptake. Such enhanced penetration and retention (EPR) can be designed by the functionnalization of dendrimers with polyethylene glycol (PEG) tethers, folate, etc (Figures 66 and 67).

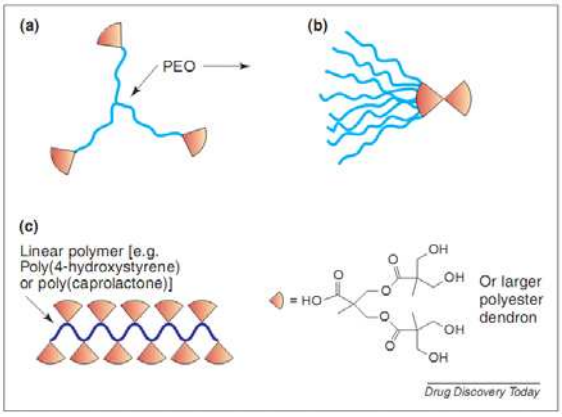

Figure 66. Polyester dendrimer-linear polymer hybrids. (a) Hybrid of polyester dendrons and a PEO star in which the multivalent dendron can carry several copies of drug and the linear PEO provides solubility. (b) 'Bow-tie' hybrid of polyester dendrimers and PEO. (c) Polyester dendronized linear polymer. Reprinted with permission of Elsevier (ref. 1169, Fréchet's group).

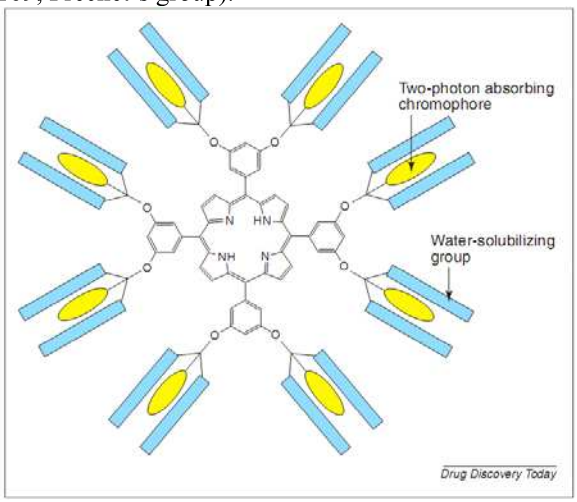

Figure 67. A water-soluble dendrimer porphyrin incorporating two-photon absorbing chromophores for photodynamic therapy. Reprinted with permission of Elsevier (ref. 1169, Fréchet's group).

Very often, the lack of immunogenicity makes dendrimers safer than synthesized peptides and natural proteins. Finally, the pharmacodynamic (PD) and pharmacokinetic (PK) behaviors of dendrimer-drug assemblies can be monitored in a reproducible manner and thus optimized upon dendrimer design. The targeted properties of improvements brought by dendrimers or their derivatives are the water solubility, biodistribution, circulation time in blood and therapeutic efficiency of formulations involving these nanocarriers. The drugs that are involved are mainly (i) potent anti-cancer drugs, (ii) non-steroidal anti-inflammatory drugs and (iii) anti-microbial and anti-viral drugs, but many other drugs have been probed with dendrimers. Two distinct strategies are being used: (i) drug "*complexation*" to dendrimers by

encapsulation inside dendrimers or electrostatic binding by ionic groups at the dendrimer periphery and (ii) drug "*conjugation*" by covalent attachment to the dendritic tethers (Figure 68).[1056-1062,1069-1073,1099-1116] These principles also apply to the design of antibacterial agents.[1117]

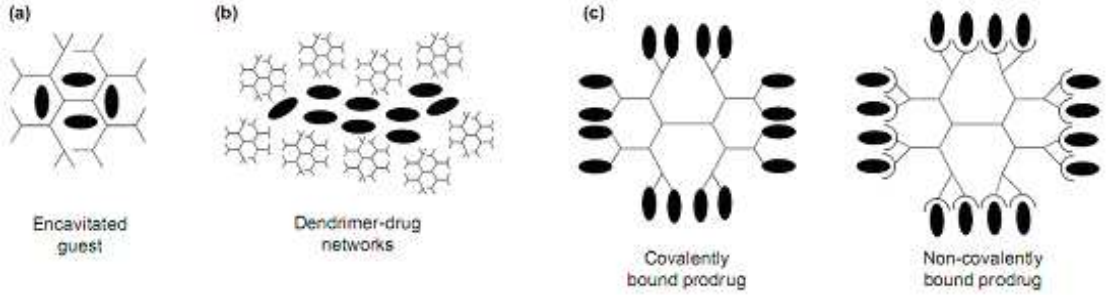

Figure 68. Schematic representations of dendrimer drug-delivery systems. The darkened oval represents an active substance. Reprinted with permission of Elsevier (ref. 1105, Cloninger's group).

6.2.1. Drug solubilization by encapsulation : drug-dendrimer "complexes"

The major problem of most drugs is their lack of water solubility. The solubility of dendrimers is essentially dictated by the solubility of their terminal groups. Thus, dendrimers have been designed with water-soluble termini and hydrophobic interiors in such a way that they be able to encapsulate hydrophobic drugs (Figure 69).[1056,1057,1062,1107-1127] Alternatively, positively or negatively charged dendrimer termini can electrostatically bind drugs bearing opposite charges.[1106,1109,1128,1129] With the term "complex", the community of dendrimer scientists means drugs that are bound to the dendrimers by non-covalent bonds, i.e. supramolecular bonds: ionic, hydrogen bonding, van der Waals interactions, π bonding, hydrophobic solvatation. Small drug molecules are most of the time encapsulated in the dendrimer interior, whereas large molecules preferably adsorb near the surface (even if some back-folding can still occur[536]).

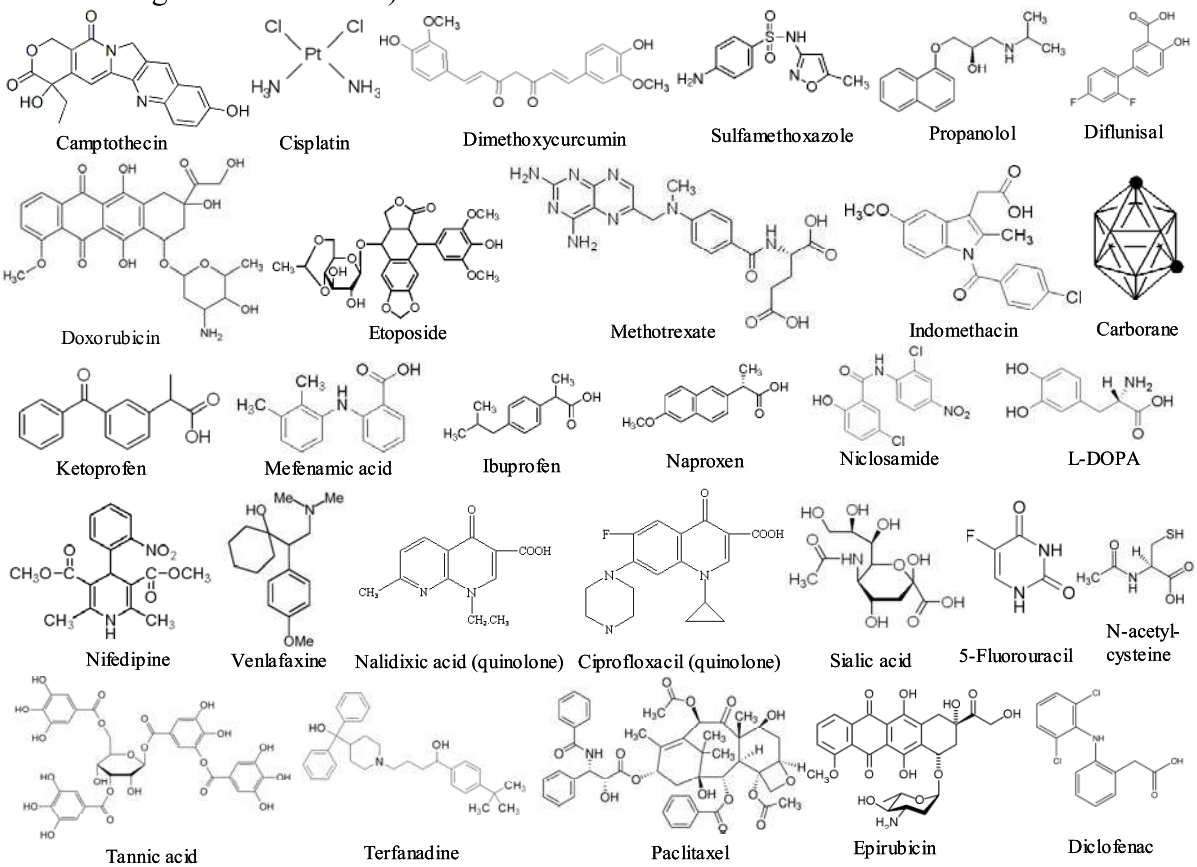

Figure 69. Molecular structures of the drugs encapsulated or stabilized by dendrimers.

A classic example is the anti-inflammatory drug ibuprofen for which 78 molecules were found to complex G_4-PAMAM dendrimer at the amine dendrimer groups through electrostatic interactions with the carboxy groups of the drug. *In vitro* release was shown to be slow compared to the free drug. The drug-dendrimer complex was found to enter A549 cells much more rapidly than free ibuprofen, suggesting efficient drug carrying inside the cell.[1130,1131]
The water-insoluble anti-cancer drugs camptothecins were encapsulated in $G_{4.5}$ carboxylate-terminated polyester dendrimer.[1125,1126,1132] Poly(glycerol succinic acid) dendrimers (PGLSA dendrimers) were also investigated for their capacity to encapsulate camptothecins. G_4-PGLSA-CO_2Na (unlike G_4-PGLSA-OH) was successfully used in the case of 10-hydroxycamptothecin, and exposure to MCF-7 human breast cancer cells led to significant toxicity increase with less than 5% of viable cells at a concentration of 20 μM.[1133]
Solubilization of the dendrimer-drug complex depends on the dendrimer generation. For instance, the solubilization of the hydrophobic drug nifedipine, a calcium channel-blocking agent, was improved upon increasing the PAMAM dendrimer generation.[1134,1135] PAMAM dendritic drug solubilization increased the flux of indomethacin in transdermal delivery *in vitro* and *in vivo*.[1136] PAMAM-dendrimer encapsulation of pilocarpine nitrate and tropicamide resulted in significantly enhanced miotic and mydriatic activities on rabbit eyes compared to that of free drug. Greatly enhanced penetration of the drugs through the cornea and drug release are favored by the bioadhesive properties of the dendrimers.[1137]
All these examples indicate that drug complexation in water-soluble dendrimers enhanced drug activities, but it has been pointed out that this rule is not universal. For instance, G_4-G_6 amine-terminated dendrimer-camptothecin complexes showed lower anti-cancer activities than the free drug despite significantly enhanced drug solubilization using these dendrimers (Figure 70).

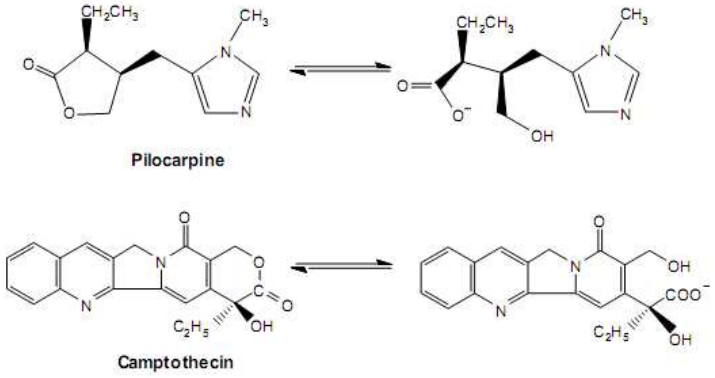

Figure 70. Hydrolysis of camptothecin and pilocarpine from lactone forms to carboxylate forms. Reprinted with permission of Elsevier (ref. 1107, Xu's group).

This was taken into account by accelerated hydrolysis of camptothecins from an active lactone form to an inactive carboxylate form upon dendrimer complexation.[1106]
Thus, the *pH* of the medium plays an important role. In another such example, a 3400 molecular-weight PEG core was introduced into G_4-PGLSA providing $(G_4\text{-PGLSA-OH})_2$-PEG_{3400}, and this complex with 10-hydroxycamptothecin showed 20-fold water solubility increase but only similar cytotoxicity to the free drug towards HT-29 human colon cancer cells.[1132]
Biodistribution of the PAMAM dendrimers has been considered to be a problem, because they mostly accumulate in the liver and for instance only 1% of intravenously injected dendrimer was still in the blood after one hour.[1138] PEGylated dendrimers, however, exhibit a considerably longer circulation time in the blood (*vide infra*).[1139]

The non-steroidal anti-inflammatory drugs (NSAIDs) are intensively studied as amino-terminated dendrimer complexes (PAMAM or PPI), especially because most of them contain a carboxy group that can electrostatically bind these dendrimers yielding ammonium carboxylate complexes. Thus, successful results were obtained with aspirin, indomethacin, flurbiprofen, ketoprofen, ibuprofen, naproxen, diflunisal, diclofenac, aceclofenac and proicam.[559,1106-1119,1140,1141] Inflammatory inhibition, mean residence time in blood and bioavailability are generally superior with these dendrimer-drug complexes compared to the corresponding free drug. Thus the pharmacodynamic (PD) and pharmacokinetics (PK) are usually improved with these complexes, and when this is not the case, the problem can be resolved by local administration of the complex or using targeting groups such as PEG, folate or galactose in dendrimer conjugates (*vide infra*).[1106-1118,1136,1142-1146]
A drawback of drug-dendrimer complexes is the possible primary removal of the drug from the complex before it reaches the cancer cells. Indeed dendrimer-drug complexes have been shown to be unstable in plasma and buffers (Figure 71).[1130,1131,1147,1148]

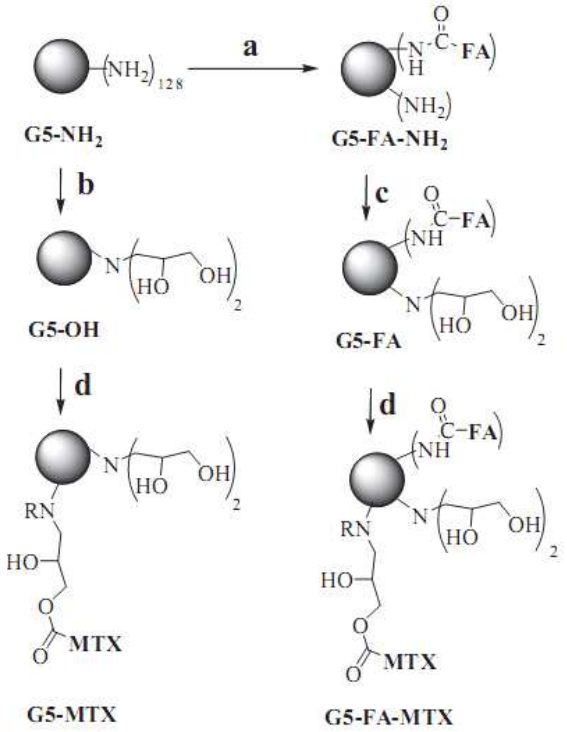

Figure 71. Synthesis of dendrimer conjugates. a) Folic acid, EDC, DMSO; b) Glycidol, DMSO; c) Glycidol, DMSO/PBS; d) Methotrexate, EDC, DMSO. Reprinted with permission of Elsevier (ref. 1147, Baker Jr.'s group).

Therefore the drug-dendrimer conjugate strategy has also been used (*vide infra*). The advantage of non-covalent drug-dendrimer interactions, however, is a higher solubility of otherwise water-insoluble drugs than with conjugates. On the other hand, conjugation allows a higher drug payload.[1149-1154]

Table1. Alphabetical list of drugs solubilized in dendrimer-drug "complexes"[1052]

Drug	Disease	Dendrimer	Reference
Artemer	malaria	poly(L-lysyne)-PEG	1218
Camptothecin	cancer	polyester, polyether	1052,1125-1127
Cisplatin	cancer	PAMAM	1165

Diclofenac	inflammation	citric acid-PEG_{600}	521
Diflunisal	inflammation	G_2-G_4-PAMAM	1128,1146
Dimethoxycurcumin	cancer	$G_{3.5}$-G_4-PAMAM	1149
Doxorubicin	cancer	G_3-G_4-PAMAM-PEG_{2000}	1059,1050,1192-1195
Etoposide	cancer	G_2-PAMAM-OH-PEG_{5000}	1151
5-Fluorouracil	cancer	G_4-PAMAM-PEG	1216,1217
Ibufrofen	inflammation	G_4-PAMAM	1128,1130,1131
Indomethacin	inflammation	$G_{3.5}$-PAMAM-CO_2^-, PEG	1100,1143,1469
Ketoprofen	inflammation	G_2-G_5-PAMAM	1109,1110,1144
Mefenamic acid	inflammation	citric acid-PEG_{600}	521
Methotrexate	cancer	G_3-G_4-PAMAM-PEG_{2000}	1147,1148,1150,1152,1206-1208
Naproxen	inflammation	G_4-PAMAM	1128
Niclosamide	tapeworm infection	PAMAM	1135
Nifedipine	inflammation	G_0-G_3-PAMAM	1134
Paclitaxel	cancer	polyglycerol	1202,1203
Quinolones	infections	G_3-G_5-MAMAM	1107,1108
Sialic acid	Alzheimer	PAMAM	1209
Silver salts	Gram-positive bacteria	G_4-PAMAM	664
Sulfamethoxazole	infections	G_2-G_4-PAMAM	1111,1112

6.2.2. Covalent drug binding to dendrimer termini: drug-dendrimer "conjugates"

Dendrimer-drug conjugates appear superior to drug-dendrimer complexes, because the latter can be released before reaching the targeted cell. They are superior to the free drugs, because the drug can be specifically targeted to the cancer cell, then the multiple drug molecules are released from a single dendrimer-drug conjugate by *pH* change at the cancer cell. They decrease non-specific toxicity, optimize biodistribution and increase circulation time in blood. Plasma half-life is increased as well as drug resistance.[1073] Dendrimer-drug conjugates rapidly penetrate into the cells and cytoplasm.[1155-1159] For instance, when PAMAM dendrimers were conjugated with ibuprofen via an ester linkage, hydrolysis in the cells produced prostaglandin expression in 30 min instead of 1 h for the free ibuprofen.[1158]

In another example, methotrexate delivery to CCRF-CEM human acute lymphoblastoid leukemia and CHO Chinese hamster ovary cell lines was achieved by PAMAM-methotrexane conjugates. It was more efficient when the $G_{2.5}$-PAMAM dendrimer was functionalized with CO_2H termini (3- and 8-fold more potent than free methotrexate) than with amine G_3-PAMAM, the latter showing no sensitivity increase compared to the free drug. The decrease of lyposomal residence time of the cationic PAMAM subsequent to drug cleavage was taken as responsible for reduced drug release.[1162]

When paclitaxel was conjugated to PAMAM dendrimers via a succinic acid linker, the release profile and cell penetration were as good as those of PEG-paclitaxel conjugates, but the dendrimer-paclitaxel conjugate exhibited much higher anti-cancer activity than free paclitaxel (10-fold) and than the PEG-paclitaxel conjugate (250-fold).[1163] 5-Fluorouracil (5-FU), an anti-cancer drug with very toxic side effects, was conjugated with dendritic polymers centered on 1,4,7,10-tetraazacyclodecane, and these water-soluble conjugates release free 5-FU at a slow rate with concomitant reduction of toxicity upon incubation with phosphate-buffered saline.[1164] In an early study, it was shown that $G_{3.5}$-PAMAM-*cis*-platin conjugates were active against intraperitineal B16F10 melanoma, whereas *cis*-platin alone was not; 50-fold increase toxicity was found against solid tumor tissues, and toxicity was 3 to 15 fold smaller than that of the free drug.[1165] PPI dendrimer-*cis*-platin conjugates were obtained by reactions of the free amine dendrimers with potassium tetrachloroplatinate.[1166] The anti-cancer drug

doxorubicin conjugated to a dendritic polyester was used to deliver the drug using a *pH*-sensitive linkage. Whereas this linkage is stable at the physiological *pH* of 7.4, it is cleaved at the lower *pH* value of the cancer cell,[1167] which then allows liberation of doxorubicin (Figure 72).[1168-1170]

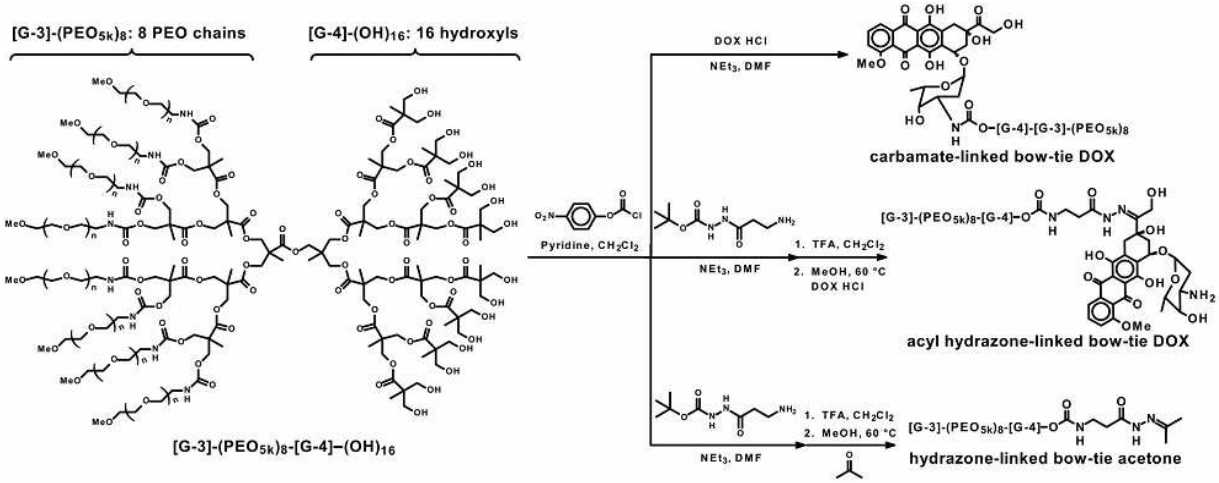

Figure 72. Functionalization of the $[G_3]$-$(PEO_{5000})_8$-$[G_4]$-(OH) bow-tie dendrimers for therapeutic studies. DOX is linked to the bow tie by means of a carbamate (top) or acyl hydrazone (middle) linkage. In the bottom route, hydrazide groups of the bow tie are blocked upon reaction with acetone. The top and bottom bow ties represent control treatments. Reprinted with permission of the National Academy of Sciences of the USA (ref. 1169, Szoka's ans Fréchet's groups).

The linkage is the acid-labile hydrazone group, allowing the drug to be released and successfully taken up by several cancer lines.[1139,1168-1170] G_4-PAMAM was conjugated to 12 molecules of a glutaric acid derivative of methylprednisolone, a model contruct in A549 human lung epithelial carcinoma cells and further to fluorescein isothiocyanate. Evaluation of the dynamics of cellular entry on A549 human lung epithelial carcinoma cells by fluorescence and confocal microscopy showed localization in the cytosol, and the pharmacological activity was comparable to that of free methylprednisolone.[1171]

N-acetyl cysteine, an anti-inflammatory agent with significant potential for clinical use in the treatment of neuroinflammation, stroke and cerebral palsy, was conjugated to PAMAM dendrimers via a disulfide linkage for intracellular delivery of this drug to enhance its efficacy, reduce dosage and prevent it from binding plasma proteins. Evaluation of the conjugates for its release kinetics in the presence of glutathione, cysteine and bovine serum albumin at both physiological and lysosomal *pH* indicated that the conjugate can deliver 60% of its *N*-acetyl cysteine payload within 1h at intracellular GSH concentrations at physiological *pH*.[1172]

Streptokinase, a 47-kDa single-chain protein used as intravenous thrombolitic agent especially in myocardial ischemia and stroke since the 1980s, was conjugated to $G_{3.5}$-PAMAM dendrimers using the active ester method under mild aqueous conditions, and the conjugates exhibited high enzymatic activity retention (up to 80%) and quick *in vitro* clot lysis (comparable to that of free streptokinase).[1173]

In conclusion, non-covalent and covalent drug-dendrimer assemblies usually increase drug efficiency compared to the free drug, and several drug-dendrimer complexes or conjugates are in early clinical trials.[1174] Remaining problems include hemolytic toxicity of NH_2-terminated dendrimers,[1073,1175-1178] therefore biocompatible dendrimers containing PEG tethers, i.e. PEGylated dendrimers, have been more recently actively investigated as drug-delivery nanocarriers.

Table 2. Examples of drug-dendrimer "conjugates"

Drug	dendrimer	linker	reference
Methotrexate (cancer)	G_3-PAMAM	amide	1162
Propanolol (cardiac)	G_3-PAMAM	amide	1156,1159
Terfenadine (allergy)	G_1-PAMAM	succinic acid	1156
		succinyl-diethylene glycol	1156
L-DOPA (Parkinson)	L-DOPA	diester	1178
Doxorubicin (cancer)	polyester	carbamate	1169,1170
Epirubicin (cancer)	adipic- or β-glutamic acid	PEG	1132
Methotrexate (cancer)	G_5-PAMAM	ester	1249-1254,1158
Naproxen (inflammation)	G_0-PAMAM	amide	1155
N-acetylcysteine	PAMAM-CO_2H	amide	1214
(neuroinflammation)		ester (L-lactic acid, DET)	1152,1157
Paclitaxel (cancer)	G_4-G_5-PAMAM-OH	ester (succinic acid)	1163,1250
Carborane (NCBT, cancer)	G_5-PAMAM	ester	1154,1242-1244
Sialic acid (Alzheimer)	G_4-PAMAM	amide or ether (anomeric)	1210
Hydroxypyridinone (haemochromatosis)		polyamide dendrimers	1211
Streptokinase (thrombosis)	polyglycerol	ether	1212
Venlafaxine (depression)	$G_{2.5}$-PAMAM-PEG	ester	1213
Tannic acid (aneurysm)	tannic acid mimicking dendrimers		1215

6.2.3. PEGylated dendrimers as biocomptabible drug nanocarriers

The advantages of drug biostability in polymeric nanocarriers has been initially illustrated by Ringsdorf in 1975.[1179,1180] Subsequently, many water-soluble polymers were tested for drug delivery. Among a variety of water-solubilizing groups,[1180] PEG has appeared as one of the most promising component of polymers[1180,1182-1186] and dendrimers[1175,1176,1187,1188] or so-called dendrimeric micelles[1189] in drug-delivery systems, in particular because of its biocompatibility (Figure 73).[1190]

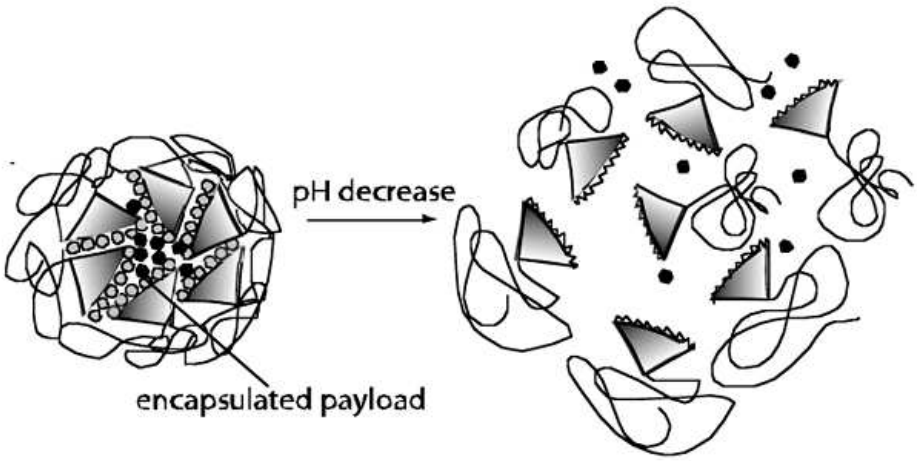

Figure 75. Schematic representation of release of guest molecules from a *pH* sensitive micelle of linear-dendritic copolymer. Reprinted with permission of the National Institutes of Health (ref. 1189, Thayumanavan's group).

The advantages of attaching PEG tethers to the dendrimer termini are (i) solubilization of the dendrimers in water, (ii) solubilization of the hydrophobic drugs in water by encapsulating the drug inside the water-soluble dendrimer, (iii) increase drug loading inside the dendrimer

compared to the non-PEGylated dendrimers, (iv) eliminate hemolytic toxicity, (v) considerably increase the circulation time in blood of the drug-dendrimer assemblies, (v) decrease dendrimer uptake by the organs, (vi) considerably increase the bioavailability of the drug, (vii) improve the dendrimer kinetic stability, (viii) decrease undesired toxicity, (ix) reduce immunogenicity and antigenicity by shielding the dendrimers against destructive mechanisms in the body and (x) improve targeting to the active site by EPR effect.

Fréchet's group, who pioneered the design and use of PEGylated dendrimers,[1175,1176] also combined PEGylation with biodegradable polyester dendrimers for therapeutic applications of drug delivery in cancer treatment with studies of accumulation in solid tumors. These "bow-tie" shaped dendrimers consisted of two covalently attached polyester dendrons, where one dendron provided multiple functional handles for the attachment of therapeutically active moieties, while the other was used for attachment of PEG tethers. Drug loading could be controlled by varying the generation of the dendrons and the mass of the PEG tethers.[1191]

Since PAMAM dendrimers are by far the most frequently probed dendrimers towards biomedical applications, early studies involved the decoration of G_3 and G_4-PAMAM generations with PEG tethers, and the water-insoluble anti-cancer drugs MTX and adriamycin were encapsulated into these PAMAM-PEG dendrimers. The encapsulation ability increased with increasing the PAMAM generation and length of the PEG chains, the highest results being obtained with G_4-PAMAM-PEG_{2000} that could retain 26 MTX molecules or 6.6 adriamycin molecules *per* dendrimer.[1192-1195]

Melanine dendrimers are an interesting family of dendrimers synthesized by Simanek's group, and functionalization of these dendrimers using various water-solubilizing surface groups (amine, guanidine, carboxylate, sulfonate, phosphonate and PEG) was followed by evaluation for hemolytic potential and cytotoxicity *in vivo* in mices. In particular, PEGylated dendrimers showed no toxicity, lethality or abnormalities in blood.[1196-1198]

G_3, G_4 and G_5 polyglycerol dendrimers increased the water solubility of the anti-cancer drug paclitaxel by 270-, 370- and 434-fold respectively. With a similar molecular weight of 2000, the water solubility of paclitaxel was 11-fold increased with G_3 dendrimer compared to non-dendritic PEG_{2000}. The paclitaxel solubility in water is commonly increased using PEG_{400} as a co-solvent or hydrotropic agent, but the solubility increase using these dendrimers is considerably higher.[1201-1203]

PEGylation of PAMAM dendrimers with higher generation (G_4) and longer PEG strand (2000 Da) gave better drug encapsulation.[1192-1200] The solubility of guest molecules is not always enhanced by increasing the length of the PEG tethers, however. For instance, G_3-PAMAM-PEG_{2000} solubilized more pyrene in water than either G_3-PAMAM-PEG_{750} or G_2-PAMAM-PEG_{2000}, which was explained by interpenetration from adjacent dendrimers.[1204,1205]

Heterofunctionalization of PEG for instance with di-*tert*-butylpyrocarbonate can be used to covalently link the drug to the PAMAM dendrimer.[1160,1161,1202,1203] A study of the influence of the degree of PEG substitution on the methotrexate encapsulation efficiency and release profile of PEGylated G_3-PAMAM dendrimer indicated only a small effect. This was taken as an indication that the drug was enclosed in the dendrimer interior and not on the surrounding chains of the PEG. Effect of PEG chain substitution on the release profile was not significant (Figures 74 and 75).[1206-1215]

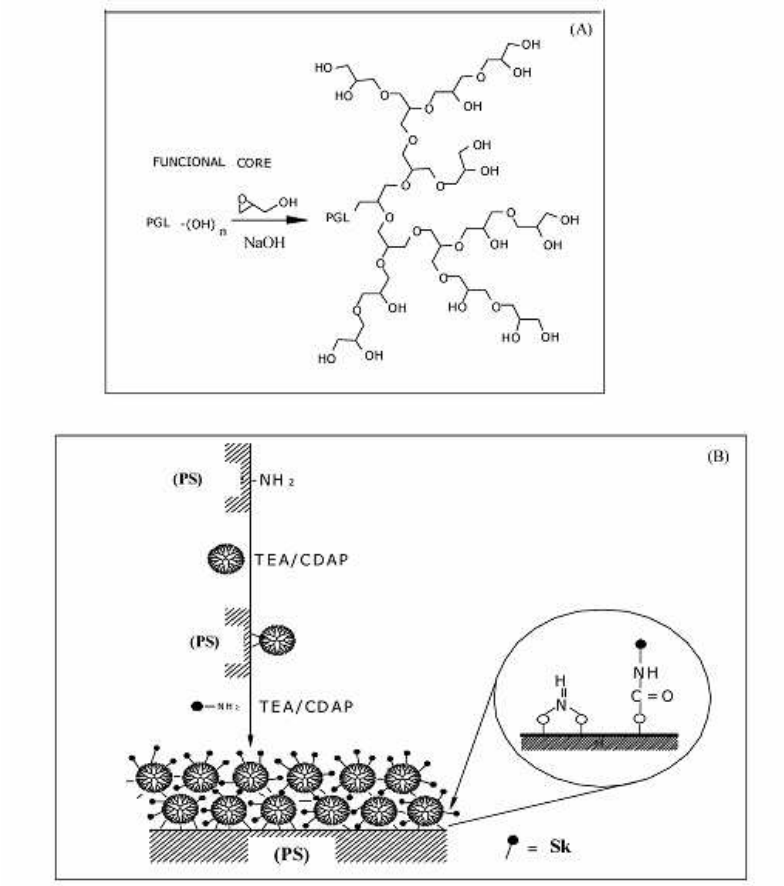

Figure 74. (A) Schematic diagram of the PGLD synthesis and (B) immobilization of the bioconjugate PGLD-Sk onto wells of ELISA (PS) plates. The epifluorescence microscopy results indicate that PGLD-Sk coating showed an improved antithrombogenic character relative to the uncoated ELISA plates. Reprinted with permission of Springer Science (ref. 1212, Roman's group).

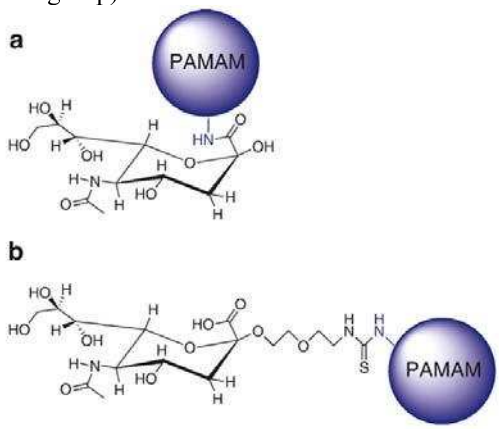

Figure 75. Two different attachments of the sialic acid moiety on the dendrimers: (a) non-physiological attachment of sialic acid to dendrimeric termini via carboxylic acid and (b) physiological attachment of sialic acid to dendrimeric termini via anomeric hydroxyl group. Sialic acid functionalized dendrimeric polymers can act asmimics of cell surface sialic acid clusters and attenuate the neurotoxicity of β-Amyloid (Aβ), the primary protein component of senile plaques in Alzheimer's disease. Reprinted with permission of Elsevier (ref. 1209, Good's group).

PEGylation of G_4-PAMAM dendrimer with PEG_{5000} increased 12-fold the entrapment of 5-fluorouracil, which was taken into account by sealing of the dendritic structure at the dendrimer periphery by PEG coating that prevented drug release. This PEGylated dendrimer showed a drug-release profile rate that was one-sixth of that of the non-PEGylated dendrimer, and release of 5-fluorouracil was observed for up to 6 days across the dialysis membrane.

PEGylation of the dendrimers also resulted in decreased hemolysis of red blood cells to less than 5% of the level recorded with the non-PEGylated dendrimers, and similar results were obtained in related studies with other drugs and PEGylated dendrimers.[1216,1217] Although the toxicity of PAMAM dendrimers is controversal and seems to be concentration and dose dependent, an interesting observation is that PEGylation or lauroylation resulted in a significant decrease in the toxicity of cationic PAMAM dendrimers, due to a shielding of the positive charges.[1218,1219] For instance, the IC_{50} values of PEGylated PAMAM dendrimers were 12-105 fold higher than those of parent PAMAM dendrimers. PEGylation of PAMAM dendrimers indeed reduced PAMAM-induced cell apoptosis by attenuating the reactive oxygen species production and inhibiting PAMAM-induced mitochondrial membrane potential collapse. PAMAM dendrimers with low molecular-weight PEG or with little PEG did not significantly change the endocytic properties, and PAMAM dendrimers with high molecular weight were much less cytotoxic.[1220] Similarly, other chemical groups are also efficient in toxicity reduction.[1221-1225] PEGylation of G_6-lysine dendrimers resulted in blood retention, lower accumulation in organs depending on the degree of PEGylation and effective accumulation in mice tumor due to the EPR effect.[1126,1227]

For dendrimer conjugates, the introduction of the PEG chain can be carried out either in a bow-tie dendrimer without PEG functionalization[1191] or by linking the dendrimer core to the drug via a PEG tether. In the latter case, a functionalization of the PEG is necessary. For instance, the functionalization of PEG with a bicarboxylic amino acid was achieved.[1228,1229] In complement, the *pH*-driven hydrolysis of the drug-dendrimer linker at the lower *pH* value of the cancer cells is an elegant solution pioneered by the Fréchet group (acetal,[1230] hydrazone[1139,1168-1170]).

The Paleos group achieved mono- and polyfunctionalization of G_5-PPI dendrimer using PEGylation with methoxy PEG isocyanate (MW = 5kDa) leading to 4 or 8 PEG chains out of the 64 amino termini. The water-insoluble betamethanosone valerate and betamethanosone dipronionate were solubilized in water, the loading being 13 and 7 wt % respectively for G_5-PPI-8PEG and 6 and 4 wt % respectively for G_5-PPI-4PEG.[1231] Further functionalization of the latter dendrimer was achieved with guanidinium moieties for targeting by interaction with carboxylate and phosphate receptors towards gene therapy (*vide infra* § 6.2.6). The introduction of eight guanidine moieties almost doubled the water solubility of betamethanosone valerate.[1232] Hyperbranched polyglycerol exhibiting low toxicity and biocompatibility was also functionalized by PEGylation and folate-PEGylation, providing a multifunctional drug delivery sytem.[1233] PEGylation was also carried out with PAMAM dendrimers such as G_5, which decreased toxicity and allowed gene transfection.[1234] Bifunctional PEG was linked to the dendrimer on one side and to brain-targeting transferrin or lactoferrin on the other side, and the DNA dendriplex was shown to cross the blood-brain barrier of mice subsequent to intravenous injection for transfection to the brain.[1235,1236] PEGylated poly (L-lysine) dendrimers coated with chondroitin sulfate A (CSA) were used to encapsulate the drug by the dialysis method, which increased drug-loading capacity, controlled and sustained the release of a blood schizonticide, chloroquine phosphate.[1237] The proportion of branch PEGylation was optimized in the more biocompatible low-generation $G_{2.5}$ to G_4-PAMAM dendrimers in order to efficiently utilize as many remaining branches as possible for drug loading, while maintaining the drug carrier cytocompatibility. 3PEG-G_3 and 10PEG-G_4 were considered initially optimized stealth dendrimers that would be further modified to deliver drugs of interest.[1238] A G_5-PPI dendrimer was PEGylated using dicarboxylic acid PEG_{2000} and was loaded with famotidine. PEGylation improved the dendrimer drug loading capacity, reduced haemolytic toxicity and demonstrated suitability for prolonged drug delivery *in vitro* and *in vivo* level and tissue distribution in albino rats (Figure 76).[1239]

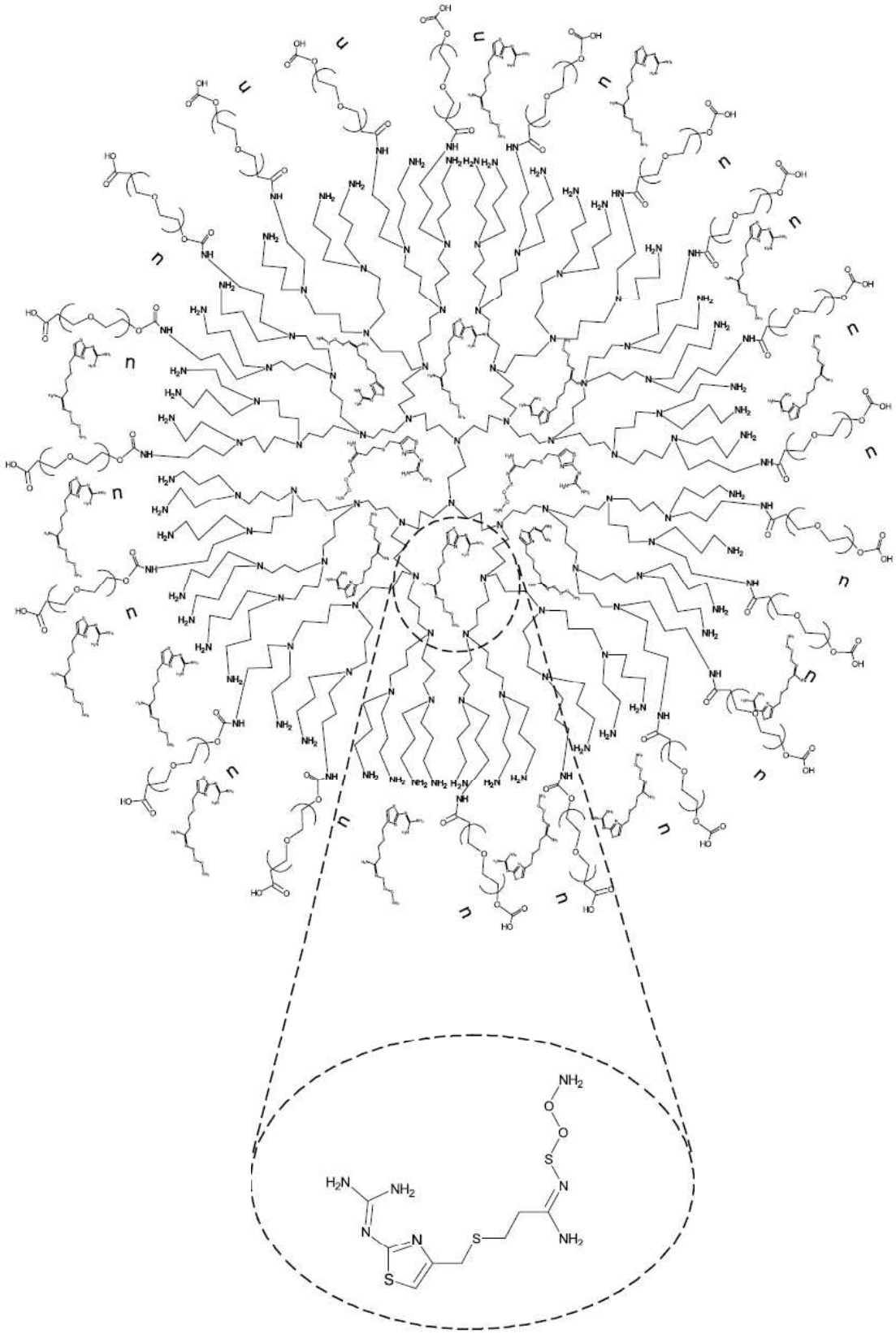

Figure 76. Famotidine loaded PEGylated PPI $G_{5.0}$ dendrimer (n ¼ PEG $_{2000}$). Reprinted with permission of Elsevier (ref. 1239, Jain's group).

6.2.4. Folate : a major tumor recognition group in drug-dendrimer conjugates

Tumor cells overexpress folate, specific gylosides (*vide infra*, § 6.2.5) and some other receptors such as specific peptide sequences (*vide infra*, § 6.2.6) that can be used as targets

when they are conjugated to dendrimers or other nanocarriers[1240-1244] that are also conjugated to anti-cancer drugs. This strategy of vectorization considerably reduces the drug distribution to normal cells and reduces side effects in the same time as it improves the drug efficiency.
Cancer inhibition by folic acid has been known since 1944.[1245] The folate receptor is overexpressed by ovarian, lung, colon, kidney, choriocarcinoma, choroid plexas (brain) and childhood ependynomas tumors and various diseased tissues.[1073,1246] Therefore folate has been conjugated to various delivery devices (polymers, polymeric micelles, liposomes, nanoparticles, proteins, protein toxins),[1073,1247] and especially to dendrimers first by the groups of Fréchet[1248] and Tomalia.[1053] The former used polyether dendrimers conjugated to an average of 12.6 folate residues and to an average of 4.7 molecules of the antineoplastic drug MTX via hydrazide linkers, whereas the latter used G_5-PAMAM-folate conjugate dendrimers with complexation to MTX. In a recent study, G_5-PAMAM dendrimers, conjugated to folate, MTX and fluorescein through thiourea, ester and amide linkages respectively, inhibited cell growth in KB cells more efficiently than non-targeted dendrimers. Slow hydrolysis of the dendrimer-MTX linkage, however, caused reduced antiproliferative activity compared to free MTX. This was attributed to the function of the β-carboxyl group as a linker inhibiting physiological polyglutamation of MTX[1249-1254] that proceeded with this β-carboxyl group in free MTX (Figure 77).[1255]

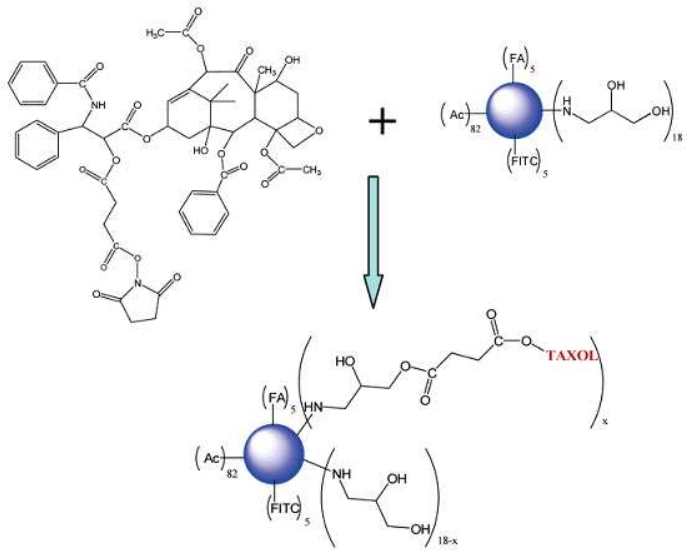

Figure 77. Conjugation of taxol to the carrier G_5-Ac^3-FITC-FA-OH, forming the trifunctional dendrimer conjugates G_5-Ac^3-FITC-FA-OH-Taxol. Reprinted with permission of the American Chemical Society (ref. 1250, Majoros's group).

PAMAM dendrimers conjugated to folic acid and MTX or tritium were 10 times more efficient than the free drug in delaying human tumor growth in immunodeficient mice bearing KB tumors, and they could also extend the life of these mice's. In addition, these dendrimers were also conjugated to fluorescein or 6-carboxytetramethyl rhodamine for detection. Folate conjugation provoked the concentration in the tumor tissue during 4 days, and confocal microscopy confirmed internalization into tumor cells.[1256] HPLC, size exclusion chromatography, and capillary electrophoresis have been used to analyze the purity of G_5-PAMAM-folate-MTX dendrimer conjugates.[1257,1258]
Finally, G_5-PAMAM dendrimer-folate conjugates that also contain oligonucleotides such as 5'-phosphate-modified 34-base long oligonucleotides were specifically bound to KB cells that express folate receptor, internalization being shown by confocal microscopy.[1259] This approach also using cDNA is promising for imaging and gene transfection (*vide infra*).[1260-1261]

The delivery of dendritic folate-bound MRI contrast agents and fluorescent probes to tumor cells that overexpress folate is a powerful diagnostic strategy.[1262] For this purpose, 2-(4-isothiocyanatobenzyl)-6-methyldiethylene triaminepentaacetic acid (TU-DTPA), a chelating ligand of Gd for MRI, and fluorescein isothiocyanate for fluorescence were bound to G_4-PAMAM-folate conjugates and disclosed largely enhanced signals monitoring rapid cell surface fixation followed by slow internalization.[1263] In the same way, overian tumor xenografts resulted in large MRI contrast enhancements,[1264-1266] and biodistribution studies indicated low level of agents in blood and high level in kidneys.[1266,1267] A water-soluble PAMAM-folate-poly(L-glutamic acid) dendrimer conjugated to the near-infrared dye indocyanine green was bound to tumor cells using human nasopharyngeal epidermal carcinoma cell line KB with similar results (Figure 78).[1073,1268]

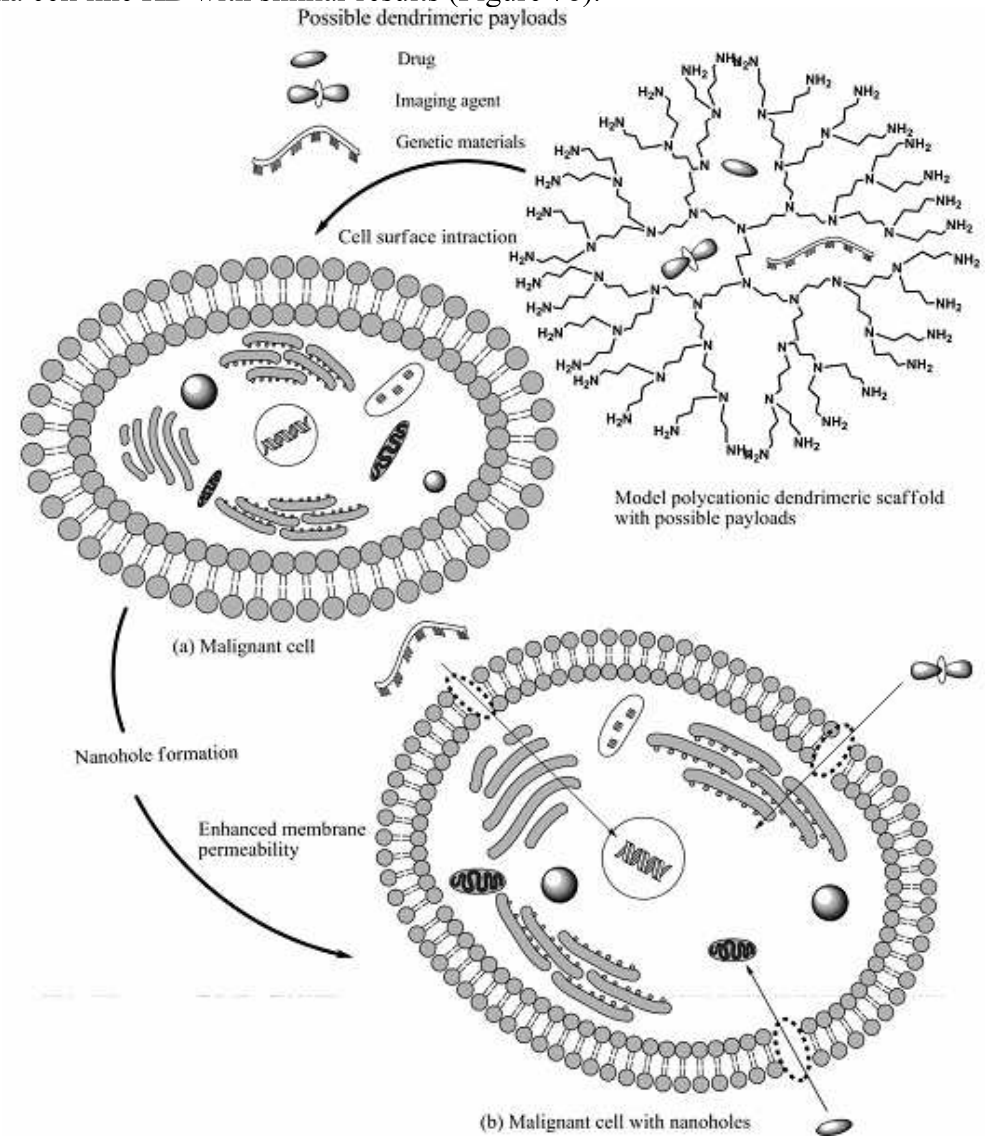

Figure 78. Schematic showing interaction of polycationic dendrimers with cells: nanoscale hole formation and enhanced membrane permeability. (a) malignant cell in usual state; (b) malignant cell with nanoholes, which possibly mediate enhanced cellular uptake. Reprinted with permission of the American Chemical Society (ref. 1073, Jain's group).

In addition to overexpression of folates, tumor cells also express some peptides (*vide infra*) and surface antigens. Thus, specific interactions between antigens and antibodies (150 kDalton glycopeptides) mediate targeting.

6.2.5. Glyco- and glycopeptide dendrimers: anti-bacterial, anti-cancer and anti-viral agents using the "cluster effect" and antigen-antibody interactions

Glycodendrimers (a term introduced by Roy)[1269-1273] now feature a broad branch of dendrimer chemistry that is devoted to promising biomedical applications, as least for dendrimers terminated by the carbohydrate groups, due to their lack of immunogenicity.[1274-1283] Glycodendrimers incorporate sugar moieties such as glucose, galactose, mannose and disaccharides in their structures. Glycopeptide dendrimers are sometimes referred to as glycoclusters in which the multivalency resulting from the multiple carbohydrate groups at the dendrimer periphery allows useful affinities between these carbohydrate groups and their protein receptors. The so-called "cluster effect" (in this context) results in significant amplification of the biological activity by a factor that is several orders of magnitude higher than the sum of the individual contributions. Indeed, although isolated carbohydrate-protein interactions are very weak (with association constants of the order of 10^{-6} to 10^{-3} M), cooperative binding by cluster (multivalent) effect results from supramolecular-type interactions[1284,1285] yielding affinity that increase exponentially with the glucoside number up to the optimal limit number of carbohydrate units that is usually small.[1271-1273,1276,1280] Tetra-valent glycoside often give the best results, although cases with larger numbers are known.[1271-1273,1276,1278-1280,1286-1291] This "cluster effect" is typically observed in the increase of lectin-binding affinity.[1292-1301] As a typical example, a cysteine-cored dendrimer terminated by eight 2,3-diaminopropionic acid-branched glycoside groups was not as anti-proliferative as the drug cholicine alone, but was 20-100 times more effective at inhibiting proliferation of HeLa cells than non-transformed mouse embryonic fibroblasts (non-glycosylated dendrimers showed a selectivity of less than 10-fold for HeLa cells).[1296]

The cores of glycodendrimers are mostly based on classic ones (most frequently PAMAM,[1270-1273,1280-1281,1288,1302] but also PPI,[1271-1273,1279-1280,1296-1300] polypropylamine,[1271-1273,1280,1295] carbosilane,[1297] silsesquioxane,[1298] polyphenylene,[1299] etc.[1280]), cyclic ones (carbohydrates,[1279-1282,1296-1300] cyclodextrins,[1303-1305] cycloveratrylene,[1306] calixarene,[1291,1303-1310] calix (4) resorcarene,[1311-1313] carbopeptides[1276,1314,1315]) porphyrin,[1316] fullerene,[1317] transition metal (Cu^{2+}) bipyridyl[1318-1321] and cyclic decapeptide template (Figure 79).[1319-1321]

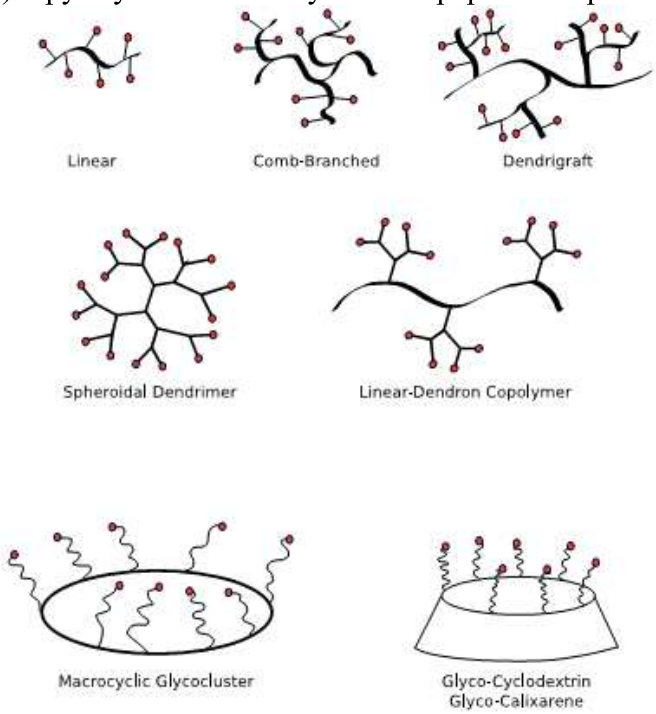

Figure 79. Multivalent carbohydrate-functionalized macromolecular architectures. Reprinted with permission of Wiley Interscience (ref. 1281, Jezek's group).

Glycopeptide dendrimers contain polypeptides branches including *inter alia* lysine (in most cases)[1281,1305,1322] and also ornithine,[1323] proline[1324] and α,α-disubstituted β-alanine.[1325] Other less frequently found glycodendrimer types are also known (i.e. self-immolative).[1269-1273,1280-1283] In particular, non-symmetrical dendrimers such as dendronized oligopeptide polymers (for instance based on "chitosan",[1282,1326] "brush"[1282,1327,1328] and "comb"[1329]) have been designed. Linker groups are usually amide, thiourea, thiether, and current coupling reactions are also glycosylation, photoaddition to allyl ethers and reductive amination.[1281]
Multiple antigen glycopeptide (MAG) are now of common use for glycopeptide dendrimers, since this term (MAG) was first coined by Cantacuzene et al., when they prepared tetra-branched glycopeptides containing four T_N antigens bound to peptide T groups. Note that the word dendrimer is not necessary at this point, and is really overdue for tetra-branched compounds.[1301] Glycopeptide dendrimers have biomedical applications as (i) anti-bacterial agents, (ii) anti-cancer agents (immunotherapy and anti-angiogienic) and (iii) antiviral (including anti-HIV and anti-influenza) agents.[1269-1283] Glycopeptide dendrimers that contain tumor-associated carbohydrate antigens (T_N, TF, sialyl-T_N, sialyl-TF, sialyl-Le^x, sialyl-Le^a, etc.) have been used in cancer diagnosis and therapy. These dendrimers with T-cell glucosides have been used as antitumor vaccines, especially with multiantigenic vaccines containing five or six different tumor-associated antigens.[1282] Therefore, both the peptide and the carbohydrate groups of the glycoprotein contribute to change immunological behavior in comparison with healthy tissues. Thus tumor-associated carbohydrate antigens play a key role in cancer diagnosis and synthesis of anti-cancer vaccines.[1330-1337] For instance, a single dose of glycodendrimer could be a substitute for multiple injections of neoglycolipid-coated liposomes.[1338] Anti-cancer vaccines have to fulfill several criteria for success: (i) antigen highly expressed on tumor cells; (ii) high Ab reduction dependence on clustering of the antigen and adequate choice of carrier and adjuvant, (iii) specific high T-cell response against tumor antigens; (iv) expression of the same antigen in normal epithelial tissues must not be a problem. There are important obstacles, however, and the mechanisms of carbohydrate antigen processing and presentation in the context of major histocompatibility complex class in molecules are not yet fully understood. Tumor-associated carbohydrate antigens that are overexpressed in clusters at the cancer cell surface represent targets for epithelial cancer immunotherapy, but their immunogenicity is a limiting factor for the design of efficient synthetic anticancer vaccines. A new generation of multiple antigens glycopeptides based on dendritic lysine scaffold is promising as nonimmunogenic carriers for B-cell antigens and T-cell helpers peptides, however.[1283,1330] Dendritic glycodendrimer antitumor reagents have been reviewed.[1283,1330,1336-1345] For instance, Reymond's group showed that colchicine, located at the core of glycosylated peptide dendrimers, is cytotoxic to cancer cell lines such as HeLa and is more selective towards these cancer cells than noncancerous cells compared to colchicine itself (Figure 80).[1296,1340,1341]

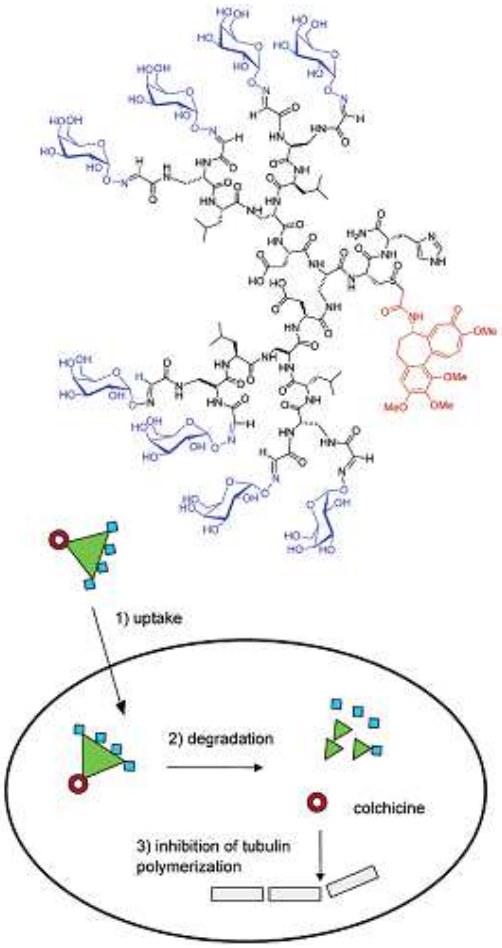

Figure 80. Glycopeptide dendrimer drug conjugates deliver colchicine selectively to cancer cells. Reprinted with permission of the American Chemical Society (ref. 1340, Reymond's group).

Glycoprotein antibodies can fight against tumors in various ways: (i) they specifically combine with antigens on malignant cell surfaces and make them susceptible to destruction by immune host cells or direct them to self-destruction, (ii) they attack blood vessels or stoma that supports the tumor.[1346-1350] Difficulties are involved in modifications of antibodies such as changes of biological activity and solubility however, thus alternatives such a immuno-liposomes and other immuno-conjugates that can be loaded with cancer drugs are used.[1073,1348] The number of conjugates on the dendrimer, not the dendrimer size, determines the immunoreactivity.[1349]

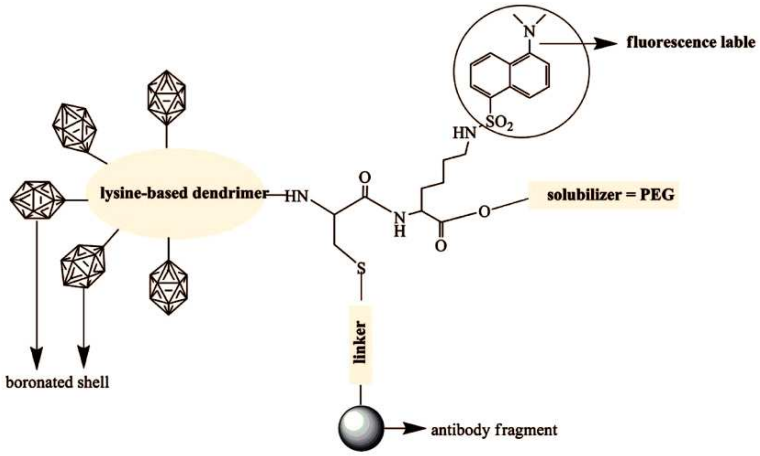

Figure 81. Example of PEG-antibody conjugated boronated lysine dendrimers. Reprinted with permission of the American Chemical Society (issue of ref. 1073, Moroder's group).

For instance, a prostate specific membrane antigen (PSMA), J591, was conjugated to G_5-PAMAM dendrimers, and it was found that PSMA is overexpressed in all prostate cancers, non-prostatic tumor neovasculature, and vascular endothelium in most solid sarcoma and carcinoma tumors.[1350]

Dendrimer-based anti-HIV vaccines have to induce both humoral and cellular immunity. The identification of glucosides is the most difficult task in HIV vaccine design for inducing broadly neutralizing Abs. Major HIV defense mechanisms are (i) frequent mutation of neutralizing glucosides, (ii) conformational masking of receptor binding sites, (iii) extensive glycosylation to evade immune recognition of the underlying protein domain and (iv) formation of envelope of glycoproteins to occlude conserved glycosides.[1283,1346-1355] Sulfatation of oligosaccharides resulted in an increase of their anti-tumor and anti-viral activities.[1356] Glyocopeptide antigens as HIV vaccines have been reviewed.[1283,1342,1344,1345]

Concerning influenza, the binding of HA, a viral carbohydrate-binding membrane protein to SA-containing oligosaccharides on the host cell surfaces, plays an important role in infectivity. Therefore, glycopeptide dendrimers with high affinity to HA are candidates for blocking this virus.[1283,1357-1359]

Multiple Ag peptides (MAPs) containing eight proteolipid proteins arranged around a dendritic branched lysine core were used to influence the expression and development of relapsing allergic encephalomyelitis in SJL mice. The PLP 139-151 MAPs were very efficient agents in preventing the development of clinical desease when administrated after immunization with the PLP 139-151 monomeric encephalitogenic peptide. Glycopeptide dendrimer biofilm inhibitors were synthesized combinatorially and optimized for binding to the fucose-specific lectin LecB that has high fucose affinity. These dendrimers are potential antibacterial agents against Pseudomonas aeruginosa, an antibiotic–resistant human pathogen.[1360,1361] A collagen model peptide-attached dendrimer was designed as a potential functional collagen material. The peptides that clustered at the dendrimer surface formed a thermally reversible functional collagen material. This dendrimer worked as a drug carrier with thermoresponsive capabilities and produced a hydrogel at low temperature (Figure 82).[1362]

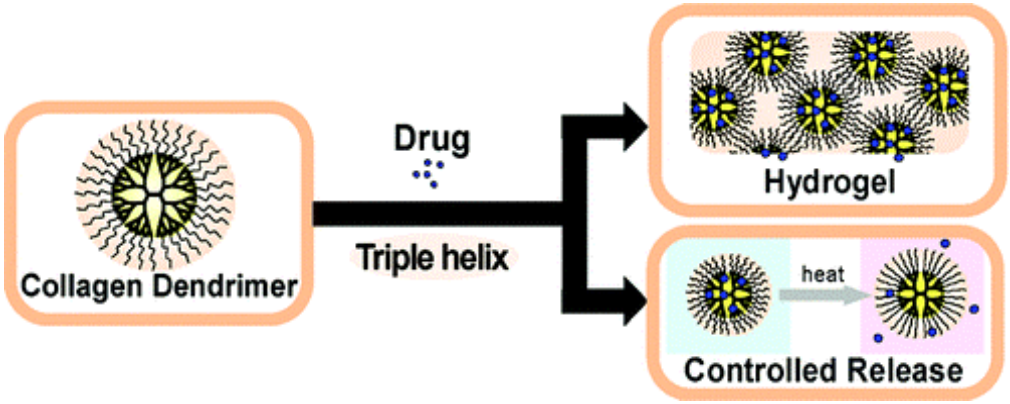

Figure 82. Mechanism of the collagen model peptide-attached dendrimer. Reprinted with permission of the American Chemical Society (ref. 1362 Kono's group).

6.2.6. Peptide dendrimers for antiangiogenic therapy

Angiogenesis consists in the formation of new blood vessels from existing ones. "Abnormal angiogenesis" plays a key role in the growth and spread of cancer, because cancer cells are fed with oxygen and nutrients by the new blood vessels. Angiogenic therapy involves the prevention of this neovascularization by inhibiting proliferation, migration and differentiation of endothelial cells. Tumor-induced angiogenesis results from ligation of extracellular matrix proteins to the $\alpha_V\beta_3$ integrin that is one of the most exclusive markers highly expressed on

many tumor cells and found on the luminal surface of the endothelial cells only during angiogenesis.[1346,1347] Peptides and peptidomimetics that contain the common amino-acid sequence arginine-glycine-aspartic acid (RGD) are antagonists of the $\alpha_V\beta_3$ integrin that is inhibited in order to block angiogenesis. Alexa Flu 488 fluorescent-labeled, partly acetylated G_5-PAMAM dendrimer was conjugated to the multiple $\alpha_V\beta_3$ selective doubly cyclized RGD (RGD-4C) peptide sequence to target the tumor neovasculature. Binding studies were performed on several cell lines with varying levels of integrin receptor expression. The free RGD-4C bound much more rapidly than the RGD-4C-dendrimer conjugates, but the dendrimers dissociated approximatively 522 times more slowly, which suggested a synergistic effect of multiple peptide conjugation on binding avidity.[1363-1365] RGD-4C has also been bound to DOTA-conjugated mono-, bis-, and tetravalent alkyne-terminated dendrimers to target $\alpha_V\beta_3$ integrin. Biodistribution studies *in vitro* and *in vivo* in mice with human SK-RC -52 tumors showed that the tetrameric RGD-4C-dendrimer showed the highest level of tumor targeting.[1366]

6.2.7 Dendritic DNA carriers for gene therapy

Gene therapy involves the transfer (transfection) of DNA into cells to correct genetic defects.[1367-1369] The vector should be cell specific, efficient, biodegradable, non toxic and non immunogenic.[1370] Viruses,[1371] cationic lipids and cationic peptides,[1372] cationic polymers[1373] such as the successful polyethylene imine (PEI),[1374] and chitosan[1375] have been used. Viruses and chitosan have been discarded due to severe toxicity problems.[1371,1375] Then, the difficulty is that some non-viral synthetic vectors are insufficiently efficient to transfer genes into the interior of the nucleus.[1372,1376,1377] Also, the carrier must be released from the endosome following endocytosis.[1377] Dendrimers are much more stable than liposomes and present the advantage of precise design of the size, monodispersity, generation and nature of termini. Early work on dendrimers as transfecting agents has been reviewed.[1378-1380]

Electrostatic interactions between the anionic phosphate groups of the DNA backbone and the positively-charged protonated (under physiological conditions) primary amine-terminated dendrimer results in the formation of dendrimer-DNA association called dendriplex,[1381] and has been reviewed.[1382] The dendriplex binds the cell membrane, again by electrostatic interaction between its positive charges and the phosphate and carboxylate membrane groups, and is internalized into the cytoplasm upon endosomal uptake. The mechanism of follow-up introduction into the nucleus is unclear.[1383]

The unmodified amino-terminated dendrimers PAMAM, by far the most frequent dendrimer family used for gene transfection, enhance the transfection of DNA into the cell nucleus. PAMAM dendrimers are now a well-established, commercial class of gene-transfer agents that has been reviewed.[1056,1057,1380]Partially degradated, non-spherical PAMAM dendrimers (commercialized as “Superfect”) are about 50 times more efficient for gene delivery than intact ones, fragmentation by hydrolytic amide bond cleavage enhancing transfection. Non-spherical PAMAM dendrimers, such as those obtained upon fragmentation, seem to be more flexible to form a more compact complex with DNA as desired for gene delivery through endocytosis.[1056,1057,1385] A cholesterol-dependent mechanism has been proposed for transfection with “Superfect”.[1386] Polycationic dendrimers also induce nanoscale hole formation enhancing molecular exchange across cell membranes.[1387] Dynamic interaction between PAMAM dendrimers and cellular lipid membranes can indeed stimulate such membrane hole formation and expansion, as with some natural proteins (MSI-78 [pexiganan] and Trans-Activator of Transcription protein, Figure 83).[1388,1389]

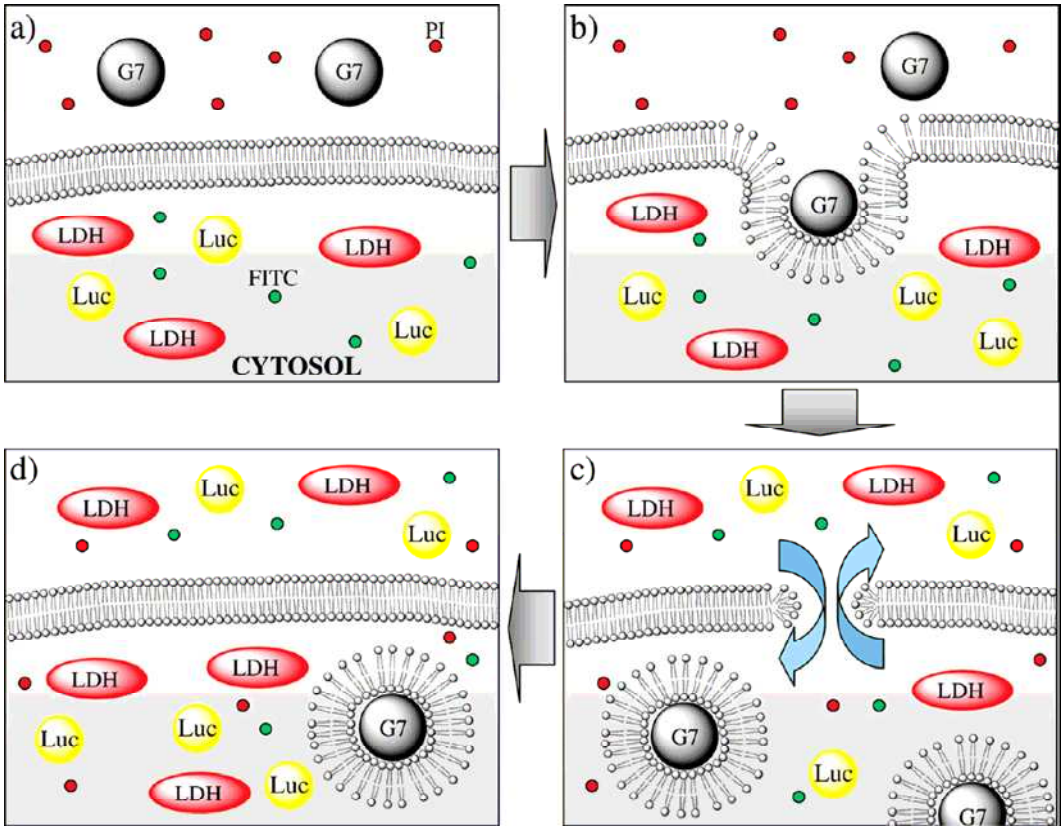

Figure 83. Schematic diagram of the proposed nanoscale hole formation mechanism induced by positively charged PAMAM dendrimers. Reprinted with permission of the American Chemical Society (ref. 1389, Banaszak Holl's group).

Low-generation PAMAM and PPI dendrimers are less cytotoxic, thus more appropriate for effective gene transfection than high generations.[1396] Gene transfer has been carried out *in vivo* using these dendrimers to cure mice tumors.[1390,1391] Phosphorus dendrimers[1390,1391] and carbosilane dendrimers,[1392] both series also terminated by various amino groups, were efficient tranfecting agents, as well as various Janus-type dendrimers with long alkyl chains on one side and amine-terminated tethers on the other side.[1393-1395]

PAMAM dendrimers terminated by OH groups (PAMAM-OH) appeared less toxic but also inefficient due to the lack of positive surface charge. Internally quaternized PAMAM-OH dendrimers with various quaternized proportions of the tertiary amino groups preserve both the lack of toxicity by rendering the dendrimer surface neutral and (partly) the transfection efficiency with positive charges to bind DNA electrostatically. The transfection efficiency of these dendrimers is one order of magnitude lower than with parent PAMAM dendrimers, however.[1397] PAMAM dendron were used for gene delivery to mammalian cells, and functionalization at the focal point with PEG increased their efficiency while decreasing toxicity.[1398] Attachment of PAMAM dendron focal point to magnetic iron oxide nanoparticles allowed dendriplexes to enter into tumor cells and inhibit their growth. The magnetic nanoparticles therein are useful for imaging and hyperthermal cancer treatment.[1399,1400] A significant improvement to transfection efficiency appeared with arginine-rich peptides,[1401-1403] because they are terminated by guanidinium moieties that form, with DNA phosphate groups as well as cell carboxylate and phosphate groups, hydrogen bonds coupled to electrostatic interactions.[1404,1405] PAMAM-Arg, i. e. PAMAM dendrimers terminated by arginine groups, are easily prepared and effect more efficient gene delivery than parent PAMAM dendrimers. This efficiency is comparable to that of PEI for HepG2 and primary rat vascular smooth muscle and is higher than that of PEI and lipofectamine with Neuro 2A cells.

Thus it is outstanding, with relatively low cytotoxicity.[1405] G_4-partially functionalized PPI dendrimers with guanidinium termini and containing residual amino termini were reacted with propylene oxide to give hydroxylated derivatives in order to avoid the toxicity of these residual amino groups. Study with HEK 293 and COS-7 cells and of the serum effect in HEK 293 cells showed that the transfection efficiency increased with increasing the number of guanidinium groups introduced with a maximum for the fully functionalized dendrimer, whereas the lowest toxicity was exhibited with 12 guanidinium groups. The introduction of terminal hydroxy groups was proposed to contribute to lowering cytotoxicity.[1406] Likewise, PAMAM-arginine dendrimers self-assembled electrostatically with plasmid DNA to form dendriplexes (dendrimer-DNA complexes) that were shown to be 200-nm large based on dynamic light-scattering measurements and increased gene delivery compared to parent PAMAM dendrimer and PAMAM-lysine dendrimers.[1407,1408] L-phenylalanine and leucine moieties have been introduced at the termini of a G_4-PAMAM dendrimer, and its transfection efficiency for CV1 cells, an African green monkey kidney cell line, increased concomitantly with the increase of the number of phenylalanine termini up to 46 phenylalanine moieties, but was not improved with leucine moieties (probably due to the lower hydrophobicity of this latter amino-acid), compared to the parent G_4-PAMAM dendrimer. With 64 phenylalanine termini, the dendrimer had poor water solubility and hardly form a dendriplex with DNA at neutral *pH*, but in weakly acidic conditions, the dendriplex formed, achieving highly efficient transcription. These phenylalanine-terminated PAMAM dendrimers exhibited low toxicity and were efficient, promising gene carriers.[1409] A dendrimer-peptide conjugate based on G_5-PAMAM platform and LH-releasing hormone peptide as a targeting moiety was found to be stable after 72 h incubation in phosphate-buffered saline buffer (*pH* 7.4) and may find applications in gene delivery.[1410,1411] Electrostatic shielding and steric blocking by histones participate in the control of the local rates of transcription of chromatin. How the degree of DNA condensation affects enzyme accessibility and gene expression has been determined with a simple model disclosing the G_5-PAMAM dendrimer-DNA self-assembly.[1412] Charge-charge interactions are prevalent, and the shape of the polymer helps direct the packaging of the nucleic acid.[1413] Interactions between posititively charged G_4-PAMAM and DNA of 2000 base pairs and 4331 base pairs have also been modelized (Figure 84).[1414]

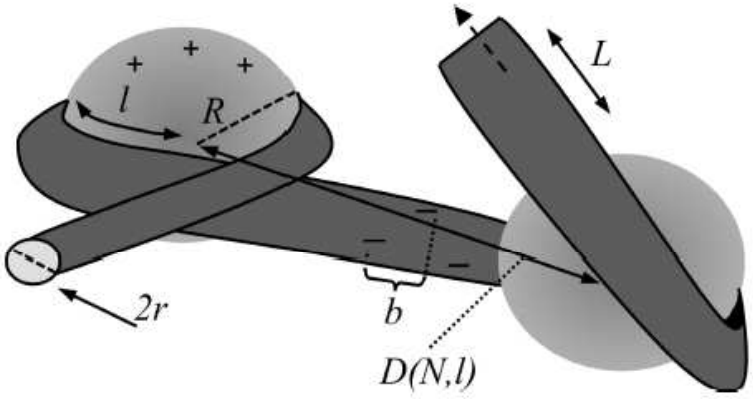

Figure 84. Proposed binding model between DNA of contour length L, radius r, and distance between negative charges b and G_4 PAMAM dendrimers modeled as hard spheres of radius R. The DNA is shown to wrap around the dendrimer with the length of the wrapping part equal to l, and a distance between the centers of two neighboring dendrimers, D(N,l). Reprinted with permission of the American Chemical Society (ref. 1414, Qamhieh's group).

The use of PPI dendrimers for delivering a triplex-forming oligonucleotide in breast, prostate and ovarian cancer cell lines using 32P-labelled antisense oligonucleotides enhanced oligonucleotide uptake by 14-fold in MDA-MB breast cancer cells, with G_4-dendrimer having the maximum efficacy.[1415] G_2- and G_3-PPI dendrimers grafted via 1,6-hexanedioldiacrylate

with branched oligoethyleneimine (88 D) or G_2-PPI dendrimers were able to efficiently compact DNA to nanosized polyplexes (100-200 nm) and exhibited an increased colloidal stability and *in vitro* much higher transfection levels as compared to unmodified counterparts. The incorporation of linear or branched polyethyleneimine was demonstrated to be the key factor to this boosted transfection efficiency. No polymer-induced erythrocyte aggregation resulted, and tumor gene expression levels in tumor-bearing mice significantly increased with the higher dendrimer core generation.[1416]

Protection of the peripheral amino groups was also combined with targeting properties using folate termini. This was achieved by the synthesis of a PEI-PEG-folate dendrimer, the folate moiety being bound to the termini of PEG tethers. This nanocarrier (MW = 25 000) transfected plasmid DNA to the folate receptor-overexpressing GFP-KB cells that produce the exogenous green fluorescent protein, more efficiently than the comparable folate-free carrier. This confirms that the folate receptor-mediate endocytosis is a major pathway for cellular uptake.[1417] Lipidic dendrimers were used for protein transduction into cultured cells and intracellular protein delivery, and these dendrimers could also be used for gene and drug delivery.[1418-1420] PAMAM-coated multi-wall carbon nanotubes conjugated with antisense c-myc oligonucleotides have been designed and successfully tested for application in gene delivery systems.[1421] α-Cyclodextrin conjugates could enhance gene transfer activity (Figure 85).[1422-1424]

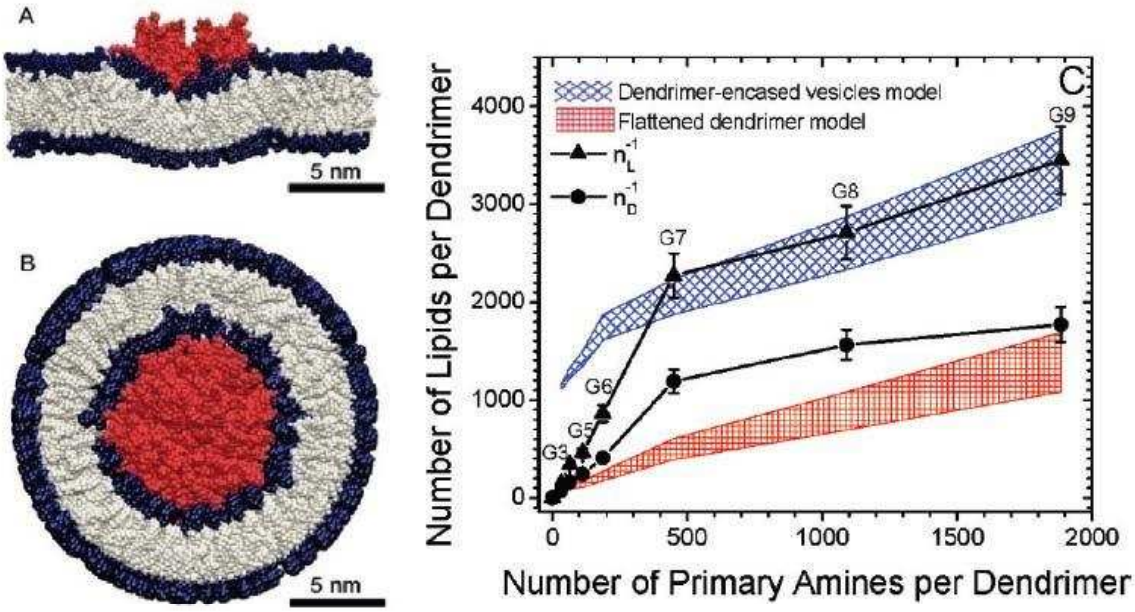

Figure 85. Chemical structures of dendrimer (G_3) (A), α-CDE conjugate (G_3) (B) and Man-α-CDE conjugate (G_3) (C). Reprinted with permission of Elsevier (ref. 1422, Uekama's group).

Dendrimer-DNA complexes were encapsulated in the functional water-soluble biodegradable polymer poly α, α, β-[*N*-(2-hydroxyethyl)-(L)-aspartamide] for substrate-mediated gene delivery.[1425] Even though all dendrimers are taken up by fluid-phase endocytosis upon transfection, significant differences in uptake mechanisms exist. Anionic dendrimers appear to be mainly taken up by caveole-mediated endocytosis in A549 lung epithelial cells, while cationic and neutral dendrimers appear to be taken in by a non-clathrin, non-caveolae mediated mechanism that may involve electrostatic interactions or other non-specific fluid-phase endocytosis.[1426] DAB-8 dendrimer conjugated to β-cyclodextrin had low toxicity and high transfection efficiency *in vitro*.[1427] In conclusion, it is likely that the first class of synthetic gene delivery agent that will completes the clinical development journey may be a cationic dendrimer with targeting ability.

Non-toxic phototriggered gene transfection by G_4-PAMAM-dendrimer conjugate was developed as an innovative strategy in cytosolic release providing the possibility of light-induced gene delivery systems.[1424-1434] Synergistic effects in gene delivery were disclosed on combining chlolesterol units with spermine-functionalized dendrons. Enhanced transfection ability resulted from mixing aspects of both main classes of synthetic vectors, i. e. cationic polymers or dendrimers and lipids.[1429]

Cell-penetrating peptides (CPP) are promising delivery vectors for nucleic acids, and their potentials have been evaluated using a functional splicing redirection assay. CPP oligomerization greatly improves cellular delivery and increases transfection of plasmid DNA; CPP-peptide nucleic acids incorporating dendrimer-like tetrameric (p53t) forms of the p53 tetramerization domain containing peptides enhance the splice-redirecting activity of DNA conjugates in cells.[1430]

Interactions and recognition between dendrimers and double-helical DNA have been modeled, allowing reproduction of the observed binding effects. These modeling studies indicate that ligand flexibility and framework rigidity are not always beneficial for multivalent recognition; ligand sacrifice and binding site screening combine to enable high-affinity binding, which brings about a new paradigm in multivalency.[1431] The supramolecular structures of DNA duplex-G_2- and G_3-PAMAM dendrimer complexes were characterized in pure water by small-angle X-ray scattering as a function of dendrimer charge (degree of amine protonation) and molar ratio dendrimer amine group/DNA phosphate group. The DNA chains were found to self-organize into two-dimensional hexagonal (G_2) or square lattice (G_3)(Figure 86).[1432]

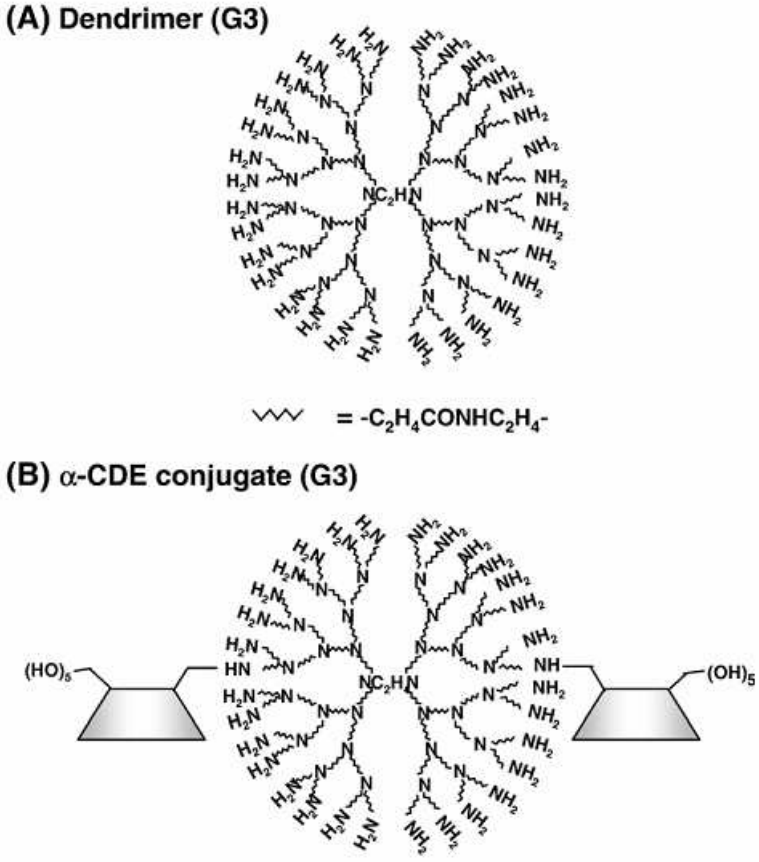

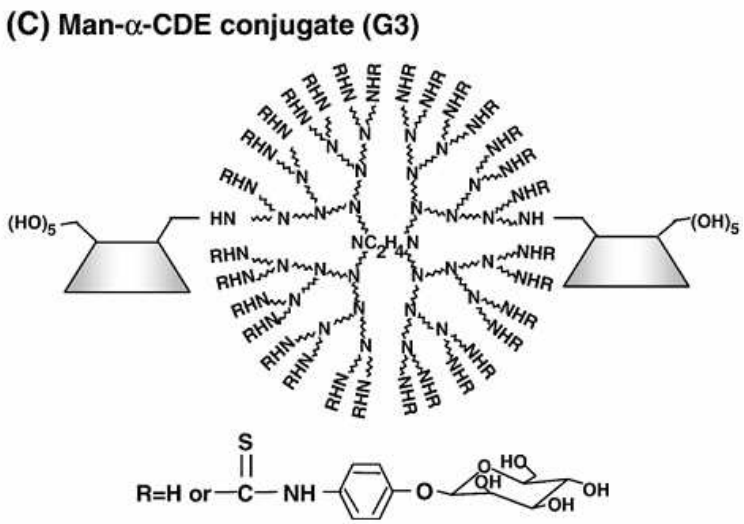

Figure 86. Schematic illustrations of the organization of dendrimer molecules in the 3-fold interstitial tunnels of the hexagonal lattice formed by DNA: (a) the top view; (b) the side view. D_{cc} represents the center-to-center distance between dendrimer molecules along the DNA long axis (i.e., z axis). Reprinted with permission of the American Chemical Society (ref. 1432, Ivanov's group).

Using various generations of PAMAM dendrimers for transfection studies and a β-galactosidase reporter gene system, the Madeira group showed that even a low transfection level could be sufficient to induce *in vitro* differentiation of mesenchymal stem cells to the osteoblast phenotype.[1433] Phosphorus dendrimers with pyrrolidine, morpholine, methylpiperzine or phenylpiperazine terminal groups disclosed low cytotoxicity towards cell strains, and electrophoresis study of DNA interaction indicated the formation of dendriplexes, with pyrrolidinium-terminated dendrimers yielding the best transfection results.[1434]
Short, doubled stranded RNAs, known as interfering RNA (siRNA), can be used to specifically down-regulate expression of the targeted gene in the RNA interference (RNAi) process. One of the primary limitations of siRNA as a technique for gene regulation, however, is effective siRNA delivery into the target cells. PAMAM dendrimers self-assemble with siRNA into nanoscale particles that are efficient for siRNA delivery and induce potent endogenous gene silencing.[1435,1436] Amino-terminated carbosilane dendrimers were used to protect and transport siRNA, and siRNA was found to be resistant to degradation by RNase. Cytotoxicity assays of these dendriplexes with peripheral blood mononuclear cells (PBMC) and the lymphocytic cell line SupT1 revealed a maximum safe dendrimer concentration of 25 μg/mL, lymphocyte were successfully transfected by fluorochrome-labeled siRNA, and the dendriplexes silenced GADPH expression and reduced HIV replication in SupT1 and PBMC.[1437] A bis-(guanidinium)-tetrakis-(β-cyclodextrin) tetrapod formed molecular association with siRNA and DNA whose affinity was evaluated using capillary electrophoresis, an efficient transfection of siRNA into human embryonic lung fibroblasts was observed by fluorescence microscopy.[1438] Increased efficiency for siRNA delivery was disclosed with internally cationic PAMAM dendrimers, modification of surface amine groups to amides also reducing cytotoxicity.[1439,1440]

6.2.8. Dendrimer-liposome assemblies

Liposomes, artificial vesicles formed by concentric amphiphilic phosholipid bilayers containing aqueous compartments, are more and more used as intravenous drug nanovectors, because they can carry hydrophilic as well as hydrophobic drugs, protect them against enzymatic degradation or elimination by the immune system, limit side effect and allow also carrying imaging agents. Their drawbacks, however, is their lack of cell specificity, the

oxidation and instability of phospholipids and drug leaking out of the liposome after dilution or application.[1441] Liposome formulations of doxorubicin, amphotericin B and cytarabine are on the market, however, and various others are in clinical phase. It has appeared that dendrimers can largely improve the efficacy of liposomes, and dendrimer-liposome associations (dendrisomes) are now actively studied as nanocarriers.

The Florence group examined the nature of the interactions between dendrimers and lipids, which paved the way for applications in drug delivery.[619-631,1381,1442] The Baker group investigated the stoichiometry and structure of PAMAM dendrimer-lipid complexes as a function of generations. Large dendrimers demonstrated a decreased number of bonds and heat release *per* primary amine, possibly due to steric restriction of dendrimer deformation by the lipid layer. The G_7-PAMAM dendrimer and larger ones bound to lipids with an average stoichiometry that was consistent with each dendrimer having been wrapped by a bilayer of lipids, whereas smaller dendrimers did not (Figure 87).[1443]

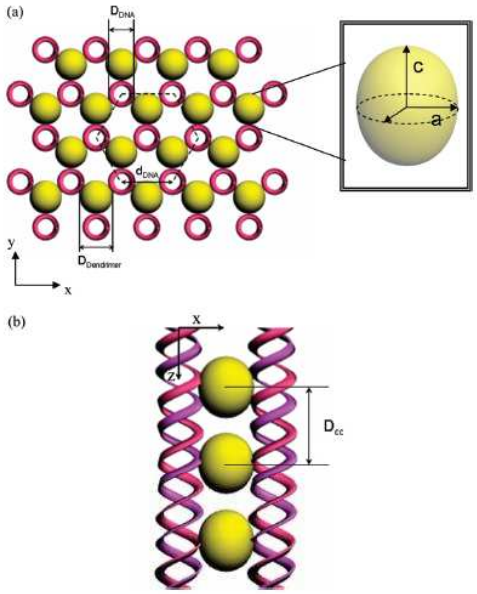

Figure 87. (A) Flattened dendrimer model and (B) dendrimer-encased vesicle model of dendrime lipid complexes. These models depict the interaction of a single dendrimer with a lipid bilayer and suggest a fundamental structure of local dendrimer-lipid interaction. Aggregation of the flattened dendrimers may induce sufficient curvature to create a separated vesicle, and separated vesicles may readily aggregate. (C) ITC-determined binding stoichiometries for the dendrime-lipid complexes compared with the expected stoichiometry of these models. Small and medium dendrimers ($<G_6$) flatten over the membrane and induce slight membrane curvature and/or flocculation of vesicles. Larger dendrimers ($>G_6$) become encased by a lipid vesicle. (A) G_5 and (B) G_7 are colored red. The hydrophilic headgroups are colored blue, and the hydrophobic tails are colored gray. Reprinted with permission of the American Chemical Society (ref. 1443, Banaszak Holl's group).

It was shown that dendrimers, having the size corresponding to that of the thickness of the aqueous space between two liposomal bilayers, could be encapsulated in this aqueous liposome phase to form a dendrosome stabilized by electrostatic interactions. This type of interaction also favors accumulation of positively charged dendrosomes on negatively charged cancer cell surfaces.[1444,1445] Indeed, encapsulation of MTX molecules in liposomes increased in the presence of dendrimer (best generation: G_4). A liposome formulation incorporating a doxorubicin-PAMAM complex ensured controlled drug release, avoiding fast release of cytotoxic drug observed with conventional liposomes.[1446] G_4-PAMAM dendrimer-poly(styrene sulfonate) microcapsule deposited using a layer-by-layer method around a removable melanine formaldehyde colloidal core provided an even better stability than the dendrisome.[1447,1448] Altogether, this dendrisome transfection approach looks very promising.[1073]

Liposomes are considered the closest analogs of cells. Thus, the interactions of guanidinium-terminated DAB dendrimers with multilamellar liposomes consisting in phosphatidylcholine, cholesterol and guanidinium-complementary dihexadecylphophate (19 :9.5 :1) dispersed in aqueous or phosphate buffer solutions was investigated, in order to model drug delivery efficiency. Such DAB-guanidinium dendrimers were loaded with a corticosteroid drug betamethasone valerate or betametasone dipropionate to investigate its transfer to liposomes. The liposomes are molecularly recognized by these dendrimers behaving as glues adhering liposomes together, which forms large aggregates at dendrimer: dihexadecyl phosphate molar ratios higher than 1: 30, as observed by phase contrast optical microscopy. The liposome membrane remains almost intact during this molecular recognition, a reversible process as shown by redispersion upon addition of concentrated phosphate buffer. The amount of drug in the precipitate increases from 25% in the absence of guanidinium termini to 80% with 12 guanidinium termini on the DAB dendrimer, showing that the functionalization with guanidinium results in an effective adhesion to the multilayer liposomes[1449] (see also Paleos' excellent review[1377]). PEG chains mediate the steric stabilization of complexes formed between negatively charged liposomes and folate-conjugated PAMAM dendrimers in water; thus they play an important role in the dispersion stability of these supramolecular complexes preventing them from aggregating.[1450]

6.3 Boron neutron capture therapy

Boron neutron capture therapy (BNCT) relies on lethal $^{10}B(n,\alpha)^{7}Li$ capture reaction occurring when a substrate containing ^{10}B atoms is irradiated with low-energy thermal neutrons that produces high-energy α-particles and ^{7}Li nuclei.[1449,1450] ^{10}B atoms must be internalized in the targeted cells, because these α-particles have a path in tissues that is limited to less than 10 μm.[1451] It is necessary to locate a minimum of 10-30 mg/g to the tumor (10^{9} atoms/cell) for effective therapy. Consequently, tumor targeting of the ^{10}B-containing substance is crucial, which has been a severe limit to this technique for some time. Therefore conjugated boron-containing substances to receptor-targeting reagents are called for (Figure 88).[1451-1454]

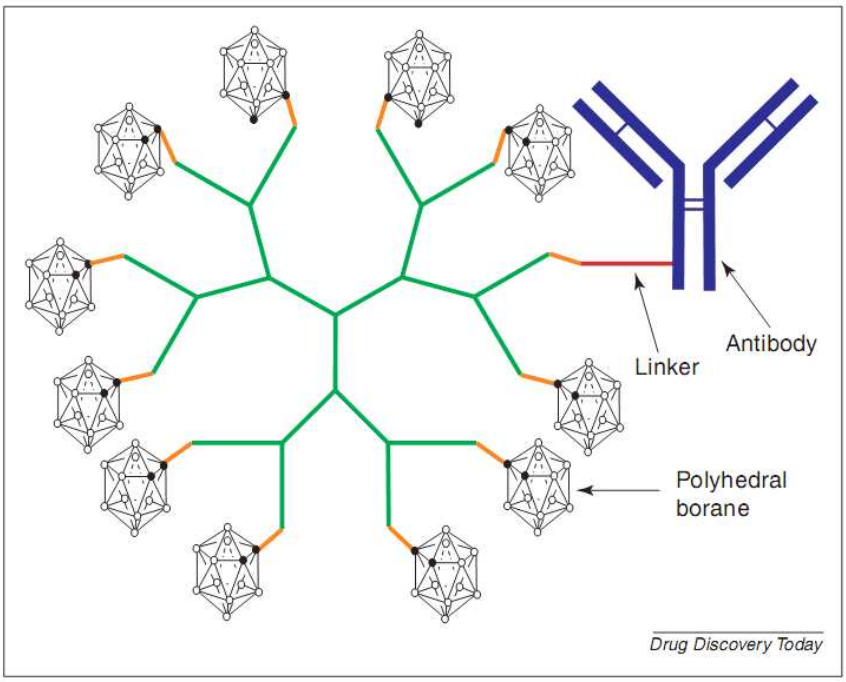

Figure 88. An antibody-targeted dendritic boron carrier for boron neutron capture therapy. Reprinted with permission of Elsevier (ref. 1169, Fréchet's group).

Dendrimers are adequate molecular tools, because they can contain many branches with boron-containing moieties at their periphery, and target-type engineering is well advanced. The PAMAM dendrimers have been the most used dendrimers for this purpose and reviewed.[1069-1071,1073,1452-1456]

A review of recent reports follows. Intratumoral injection of a G_5-PAMAM dendrimers conjugated with cetuximab, an EGF receptor-specific monoclonal antibody and containing 1100 B atoms, increased by 13.8 times the tumor B content compared to free boronated G_5-PAMAM dendrimer.[1457,1458] The same dendrimer-cetuximab conjugate delivered for the treatment of $F98_{EGFR}$ glioma followed by BNCT on animals approximately doubled animal survival compared to dendrimer-free treatment, demonstrating the therapeutic value of this conjugate. This treatment was best delivered via convection-enhanced delivery, a positive-pressure method facilitating transport across the blood-brain barrier, which resulted in 50% more accumulation than using intratumoral treatment. In addition, survival time still increased by 30 to 50% when this treatment was carried out together with borophenylalanine or sodium borocaptate, two drugs currently used for BNCT.[1459] A similar study for the treatment of L8A4, a monoclonal antibody targeting a mutant isoform of EGFR, EGFRvIII exclusively expressed in tumors (EGFR is also located in healthy liver and spleen) resulted in a mean survival time of 85.5 days with 20% long-term survival, compared to 30.3 days when the dendrimer was not used.[1460] Treatment by G_5-PAMAM dendrimer conjugated with vascular endothelial growth factor (VEGF, overexpressed in tumor vasculature) and near-infrared Cy5 dye allowed to confirm by near-infrared imaging that VEGF-dendrimer-Cy5 accumulates in 4T1 mouse breast carcinoma with increased concentration at the tumor periphery where tumor neovascularization was most active.[1461,1462] Gadolinium neutron capture therapy has been proposed but rarely used due to difficulty in achieving therapeutic doses intravenously. Simultananeous imaging (*vide infra*) and neutron therapy treatment to sentinel lymp node was optimized for G_6-PAMAM dendrimers.[1463]

6.4. Photodynamic and photothermal therapies

6.4.1. Photodynamic therapy

Photodynamic therapy (PDT) was discovered by Friedrich Meyer–Betz with porphyrins in humans in 1913. It consists in irradiating with visible or infrared light a sensitizer, such as protoporphyrin IX that subsequently transfers its excited-state energy to dioxygen by intersystem crossing to form singlet oxygen (Figure 89).

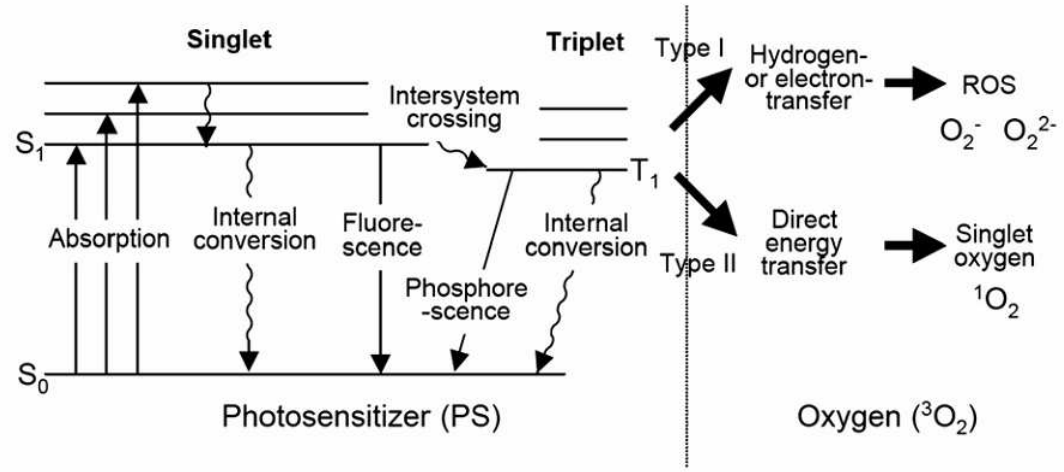

Figure 89. Jablonski diagram showing the energy transfer from photosensitizers (PSs) to molecular oxygen. Reprinted with permission of Elsevier (ref. 1487, Kataoka's group).

The latter is a very aggressive species that then destroys the cell through apoptosis or necrosis (Figure 90).[1464]

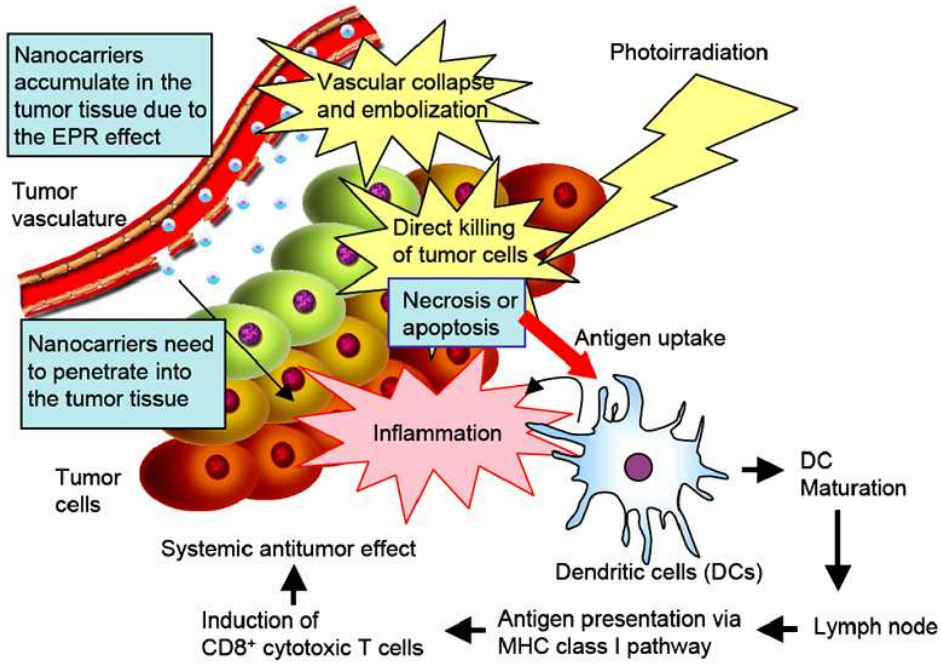

Figure 90. *In vivo* mechanisms of PDT(PhotoDynamic Therapy). The nanocarrier-encapsulated PSs accumulate in the tumor tissue by the enhanced permeability and retention (EPR) effect. Upon photoirradiation, reactive oxygen species (ROS) generated from PSs can directly kill tumor cells. PDT can also cause vascular collapse and embolization, leading to tumor destruction through a lack of oxygen and nutrients. Furthermore, PDT induces acute inflammation, attracting leukocytes such as dendritic cells (DCs). PDT might provide a tumor environment that facilitates antigen uptake by DCs and antigen presentation via the MHC class I pathway. As a result, PDT can induce CD8+ cytotoxic T cells, thereby achieving a systemic antitumor effect. Reprinted with permission of Elsevier (ref. 1487, Kataoka's group).

A precursor, 5-aminolevulinic acid (ALA) is a classic photosensitizer that produces protoporphyrin IX in cells via the haeme-biosynthesis pathway,[1465] and various other sensitizers are authorized or under clinical evaluation.[1466] Skin cancer is the main focus of PDT. The porphyrin sensitizers are selective for tumor cells because of their leaky vasculature and collagen and lipid content. Dendrimers, however, can largely improve the selectivity and pharmacokinetics, leading to efficient killing of cells after illumination. A major limitation of ALA and some ALA-containing dendrimers is their hydrophilicity that inhibits penetration through the skin and cell membranes. Indeed, dendrimers with improved *in vitro* and *in vivo* transdermal fluxes have been designed and probed by the Jain group[1020] and others.[1069-1071,1073,1467,1468]

Compared with the lipophilic hexyl ester derivative of ALA that has been much investigated, tris-ALA dendrons led to higher porphyrin accumulation *in vivo*.[1470] The phototoxicity, in cell culture, of these dendrons containing amino, aminobenzyloxycarbonyl or nitro groups at the focal point was shown the be likely related to lipophilicity and esterase accessibility, the nitro dendron being the most lipophilic with 10-times higher phorphyrin accumulation than free ALA. The aminobenzyloxycarbonyl dendron was also able to generate high porphyrin fluorescence when applied to expanded rat skin and was especially most effective at high concentration at which the nitro dendron precipitates.[1471] With larger tripodent aromatic-cored dendrimers terminated by 18 ALA moieties, polyamidoamine linkers to the core resulted in higher efficiency than acetamido linkers, because the former allowed greater esterase accessibility for the cleavage of the ALA groups. At lower concentrations, these large dendrimers were superior to free ALA for porphyrin production even after one day of incubation, which showed that cleavage of the polyamido bridges was gradual over time.[1472] G_3-zinc-porphyrin-cored poly(benzylether) dendrimers terminated by carboxylate groups were found to be 280 times more phototoxic against Lewis lung cells *in vitro* when they were

surrounded by positively charged PEG-lysine block copolymers than alone. This micellar dendritic assembly was found to target the neovascular regions due to the EPR effect. On the other hand, the dendrimer alone exhibited decreased uptake due to the negatively charged carboxylate termini, and lack of steric protection in the absence of micelle caused porphyrin aggregation resulting in fluorescence quenching.[1473,1474]

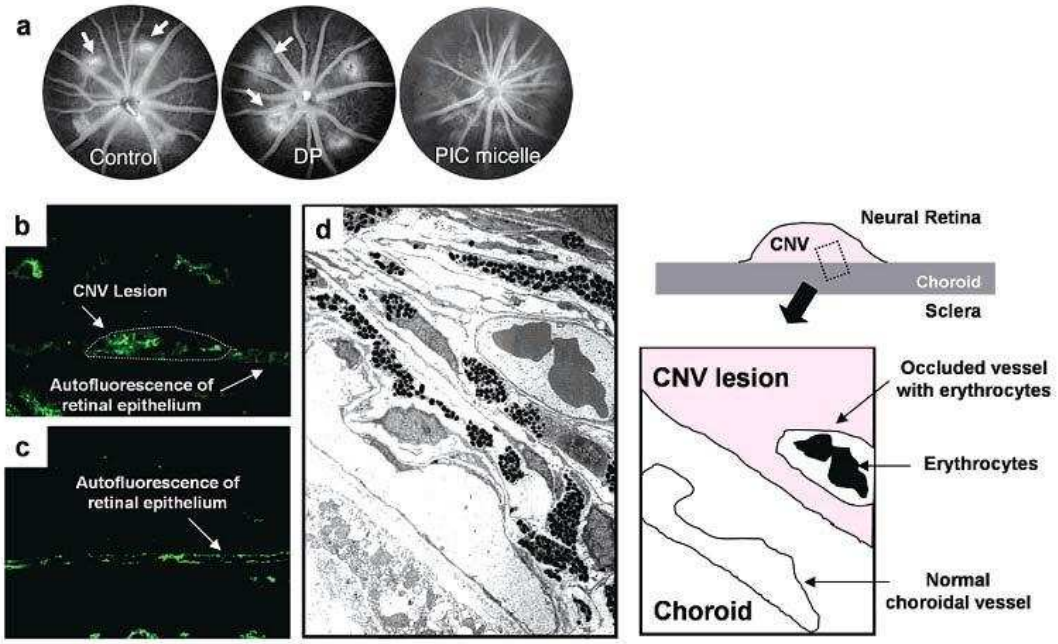

Figure 91. Efficacy of PDT laser after administration of the DP(Dendrimer Porphyrin)-loaded micelle. (a) Representative images of fluorescein angiograms in control, PDT-laser-irradiated eye after free DP was administered (DP), and PDT-laser-irradiated eye after the DP-loaded micelle was administered (PIC micelle). Note that the enhanced accumulation of DP-loaded micelles in CNV(Choroidal NeoVascularization) lesions resulted in a significantly pronounced photodynamic effect, whereas almost all of the CNV lesions showed a strong hyperfluorescence (marked with arrows), and the CNV endothelial cells appeared normal when free DP was administered. (b) Immunostaining of the endothelial cells with factor VIII antibody. Strong fluorescence from the CNV lesion is observable. (c) Immunostaining of the endothelial cells with factor VIII antibody after PDT treatment with DP-loaded micelle. Note that CNV lesion is occluded, and only autofluorescence from retinal pigment epithelium is observable. (d) Transmission electron microscopy of the CNV lesion of the PDT laser-irradiated eye after the DP-loaded micelle was administered. The neovascular blood vessel in CNV lesion is occluded by erythrocytes, whereas the normal choroidal vessel is not destroyed. Reprinted with permission of the American Chemical Society (ref. 1490, Kataoka's group).

The *pH*-value was found to play an important role in these[1474] and electrostatically connected PAMAM-porphyrin dendrimers, because of the aggregate structure that wee involved.[1475] Iron chelators were also shown to improve the efficiency of ALA.[1476] Photobleaching rates were temperature[1477] and solvent-polarity dependent,[1478] and photofrin was shown to strongly activate PDT.[1479] Micellar-formulation optimization[1480] and immunoconjugates[1481-1483] can improve circulation time and accumulation.[1480] PEGylated tetraarylphorphirin have been incorporated in vesicular carriers for improved efficacy.[1484] PEGylated PAMAM and PEGylated PPI dendrimers are also promising vehicles for PDT.[1485] Two-photon excitation with ultrafast pulses of near-infrared light (see § 3.7) is a less tissue-damaging technique than the standard single-photon PDT that causes damages to healthy tissues, because the low-energy two-photon beam is localized in three dimension, allowing treatment volumes of a few femtoliters.[1486] The Kataoka group revealed that dendrimer photosensitizer-loaded micelles showed a higher antitumor effect than clinically used photofrin without any sign of phototoxicity to the normal tissues even at high dose (Figures 91 to 93).[1487-1490] A photosensitizer formulation with dendrimer phthalocyanine-encapsulated polymeric micelle

induced efficient rapid cell death and cell membrane blebbing upon irradiation. In addition, treated mice did not show skin phototoxicity, suggesting usefulness in clinical PDT.[1491]

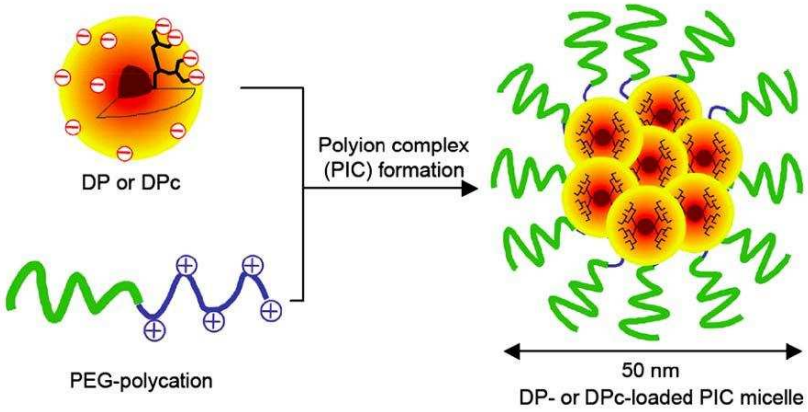

Figure 92. Formation of DP(Dendrimer Porphyrin)- or DPc-loaded polyion complex (PIC) micelles through the electrostatic interaction between anionic dendrimers and PEG-polycations. The DP or DPc-loaded micelle is assumed to induce an effective photochemical reaction because the dendritic wedges can sterically prevent or weaken aggregation of the center dye molecules in the micellar core. Reprinted with permission of Elsevier (ref. 1487, Kataoka's group).

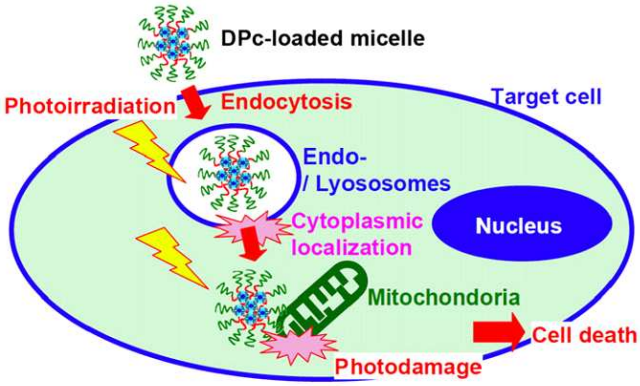

Figure 93. Hypothetical mechanisms of the light-induced cell death by the DP(Dendrimer Porphyrin) c-loaded micelle. The DPc-loaded micelle is internalized through endocytosis. Upon photo- irradiation, the DPc-loaded micelle might escape from the endo-/lysosomes to the cytoplasm by photodamaging the endo-/lysosomalmembranes. Finally, the DPc-loaded micelle might induce photodamage to the mitochondria, leading to the oncosis-like cell death. Reprinted with permission of Elsevier (ref. 1487, Kataoka's group).

6.4.2. Photothermal therapy

Besides PDT, another recently emerging phototherapy technique is photothermal therapy. It is based on irradiation in the visible or infrared region of the plasmon band of silver and gold nanoparticles AgNPs resp. AuNPs (for review, see ref.1247) that are encapsulated in targeted dendrimers (see § 4.10).[663,1492-1496] The principle consists in irradiating the AuNPs that convert absorbed light to thermal energy that is transferred to the nearby cells resulting in hyperthermia treatment by cell destruction. Appropriate targeting is required to be specific for cancer cells. G_5-PAMAM-folid acid-fluorescein dendrimers containing AuNPs were shown to be specifically delivered to KB cells *in vitro* and were internalized into lyposomes within 2h.[1493] G_4-PAMAM-PEG dendrimers,[1494] and "click" dendrimers[663] incorporating AuNPs were also probed and found to be superior to PEG-free dendrimers in terms of thermal stability. Acetylation of amine terminated G_5-PAMAM-encapsulated AuNPs and AgNPs decreases the surface charge towards neutral with an increasing degree of acetylation, transfers Ag DENs to dendrimer-stabilized AgNPs, and is expected to decrease the toxicity of DENs.[1495] These dendrimer-stabilized AuNPs can specifically target to cancer cells expressing high-affinity folic acid receptors *in vitro*.[1496]

6.5. Drug delivery to specific organs and for specific diseases

Colonic delivery of 5-aminosalicilic acid was efficiently carried out using PAMAM dendrimers, the drug being bound to the dendrimers using two spacers containing azo bonds.[1497] PAMAM dendrimers demonstrated physicochemical characteristics (*pH*, osmolality, viscosity) that are compatible with ocular dosage formulations. In addition to size and molecular weight, charge and molecular geometry of bioadhesive dendrimers also influenced the residence time; $G_{1.5}$ and G_4-PAMAM-OH and PAMAM-CO_2H showed the best bioavailability for drugs.[1498] Antiarrhythmic quinidine was covalently attached to anionic $G_{2.5}$ and cationic G_3-PAMAM-PEG (stealth) dendrimers via a glycine spacer, and *in vitro* hydrolysis was carried out in *pH*-7.4 buffer at 37°C to confirm the bioavailability of the conjugated quinine.[1499] Ionic binding was shown between the amino groups of cationic PAMAM dendrimers and sulfate groups of enoxaparin, a low-molecular weight heparin, and the resulting drug-dendrimer complex was effective in preventing deep vein thrombosis after pulmony administration. Positively charged dendrimers increased enoxaparin bioavailability by 40%, whereas negatively charged dendrimers had no effect.[1500] The binding between glitazones, PPARg agonistic insulin sensitizers clinically used for the treatment of type-2 diabetes, via free hydrogen bonds with dendrimers was shown using *ab initio* calculations and molecular electrostatic potentials.[1501]

Tissue integration between a tissue-engineered corneal equivalent and the host eye is of critical importance in ensuring long-term implant success. Therefore collagen matrices were cross-linked with heparin-modified G_2-PPI octaamine dendrimer for the delivery of basic fibroblast growth factor (FGF-2).[1502] Mimicking key aspects of the multivalent architecture of the phage on an AB_5 dendritic wedge enhanced the affinity of a phage-display derived collagen-binding peptide 100-fold, which allows direct visualization of collagen architecture in native tissue (Figure 94).[1503]

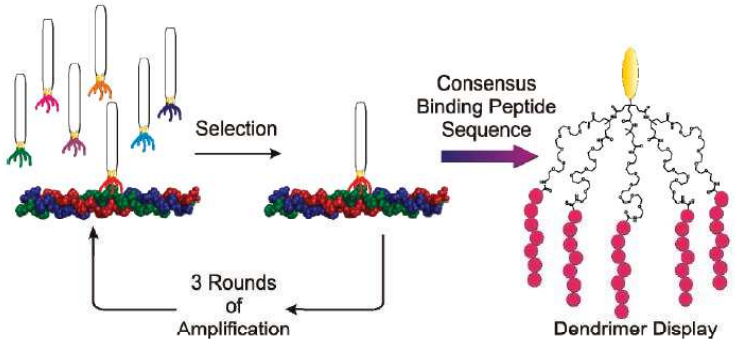

Figure 94. From phage display to dendrimer display: phage display to collagen reveals a consensus binding sequence that is translated into a high affinity, versatile synthetic collagen-specific probe by mimicking the original pentavalent phage architecture on a dendritic wedge. Reprinted with permission of the American Chemical Society (ref. 1503, Meijer's group).

Dual drug delivery was explored as a treatment against leukemia under optimized *pH* conditions and dialysis time. One molecule of PAMAM dendrimer could entrap 27 molecules of methotrexate and 8 molecules of all-*trans* retinoic acid. The release kinetics was governed by the degree of dendrimer protonation, with more sustained and controlled behavior at *pH* 7.4.[1504] G_3- to G_5-PAMAM dendrimers were shown to be potential efficient agents against fibrillation of α-synuclein, a Parkinson's disease-related protein.[1505] The release kinetics of PAMAM dendrimers, conjugated with the anti-inflammatory drug *N*-acetyl cystein containing disulfide linkages, was determined in the presence of glutathione, cysteine and bovine serum albumin, in activated microglial cells, using the reactive oxygen species. The conjugates showed an order of magnitude increase in antioxidant activity compared to the free drug.[1506,1507]

6.6. Drug biocompatiblity and toxicity

Toxicity has been defined as "a measure of non-specific, unwanted arm the drug may elicit towards cells, organs or the patient as a multi-organ system" (Figure 95).[1066,1067] The toxicity is assessed by:

- *In vitro* testing (i) the cytotoxicity on a panel of cell lines, haematocompatibility (red blood cells, RBC), lysis (Hb release) and complement activation, (ii) ability to induce cytokine release and biodegradation of the dendrimer (cytotoxicity of the degradation products), (iii) intracellular fate (endocytic pathway and fate of the dendrimer, degradation) and (iv) pharmacological activity of the construct.
- *In vivo testing* (i) the body distribution (short term fate, 1h, and long term fate, 1 month, (ii) definition of organ specific toxicity (liver, kidney, etc.), immunogenicity (IgG and IgM induction and cytotoxine induction) and metabolic fate.
- Preclinical testing (teratogenenicity, therapeutic index, single dose and multiple-dose toxicity, metabolic fate).
- Testing on the patient.

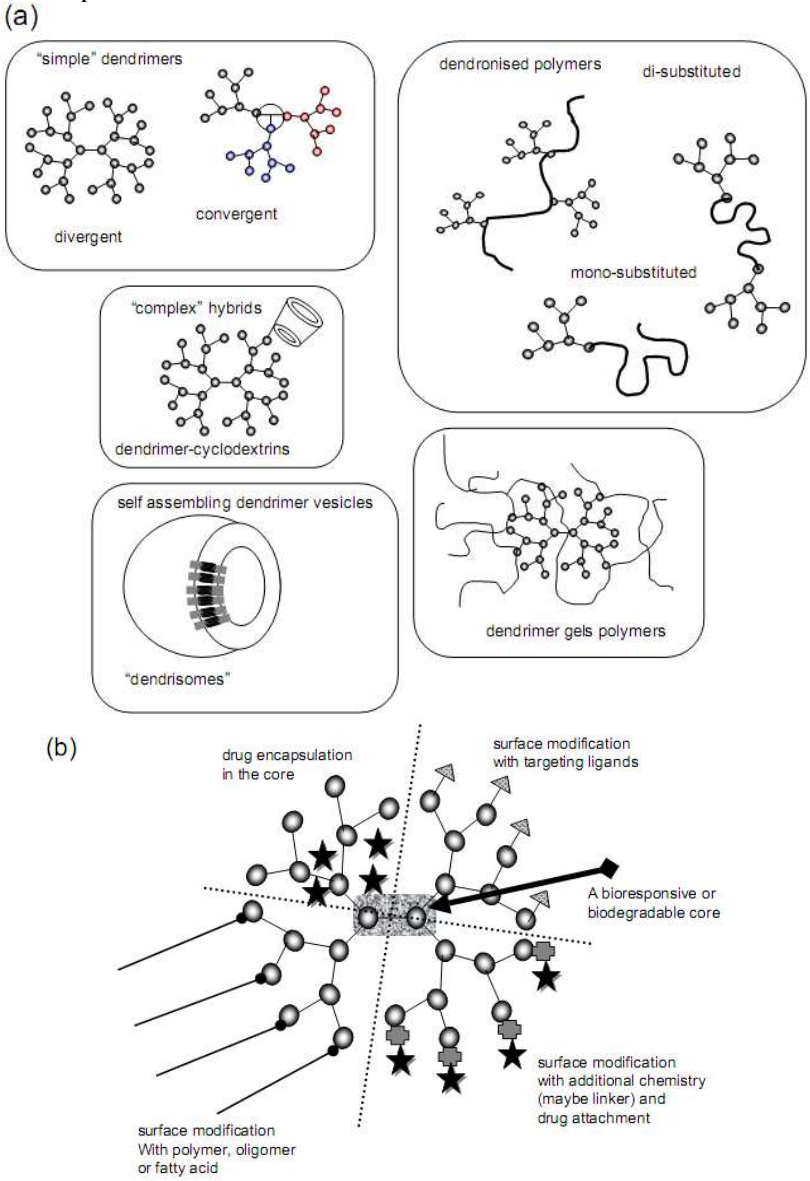

Figure 95. Diagram showing schematically (a) dendritic architectures under development for biomedical and (b) approaches for design of therapeutics and drug delivery systems. Reprinted with permission of Elsevier (ref. 1066, Duncan's group).

Biocompatibility was defined as "the ability of a material to perform with an appropriate host response in a specific application".[1508] These definitions must be intended to a precise use.[1066] A dendrimeric carrier to be suitable for parental application should be non-toxic, non immunogenic and preferably biodegradable. *In vitro* and *in vivo* tests were developed by Duncan and have been routinely used as a pre-screen of polymers and dendrimers under consideration as potential drug delivery systems.[1509]Overall, dendrimers show promising biocompatibility. The cytotoxicity of dendrimers with cationic amino surface groups is similar to that found for liposomes, which have found medical applications (e.g., Doxil, the liposomal formulation of doxorubicin).[1052] The toxicity of a dendrimer is connected to the pharmacodynamics and biodistribution that depend on the dendrimer molecular weight, charge and hydrophobicity and must be screened at the early stage as well as antigenicity (IgG and IgM induction) and cellular immunogenicity (cytokine and chemokine induction). Cytotoxicity studies require appropriate incubation time and concentration to define the inhibitory concentration diminishing viability (IC_{50} value). Toxicity to vital organs such as the lungs, liver or kidneys may result if the dendrimer accumulates in these organs.

The toxicities of the main families of dendrimers, i.e. PAMAM and DAB, has been reviewed.[1510-1513] For PAMAM dendrimers, cytotoxicity is generation dependent. Cationic G_4-PAMAM and G_4-DAB dendrimers were found cytotoxic with IC_{50} values of 50-300 μg/mL, but cytotoxicity strongly depended on the nature and charge of the surface groups.[1066,1067,1220,1225] Atomic force microscopy and fluorescence microscopy were used to visualize membrane damage. The addition of two PEG_{2000} chains had no effect on G_4-PAMAM dendrimers, but 4 PEG_{2000} chains resulted in sixfold decrease in toxicity, showing that sufficient shielding of the terminal amino group is necessary for toxicity reduction.[1221,1222] PEG stars with polyester dendrons had IC_{50} of 40 mg/mL towards B16F10 cells during a 2-day incubation, indicating real potential for further development in drug delivery applications.[1139,1509]

Haemolytic activity is defined by the measure of haemoglobin (RBC) release (haemolysis), and is a simple method to study dendrimer-membrane interactions. Cationic PAMAM and polyethyleneimine (PEI)-based DAB dendrimers show generation dependent haemolysis above concentrations of 1 mg/mL, but PEG dendrimers were not haemolytic. Anionic $G_{1.5-3.5}$-PAMAM dendrimers showed no haemolysis up to 2 mg/mL after 1h, but anionic $G_{7.5-9.5}$-PAMAM dendrimers were haemolytic at doses 2 mg/mL and above, confirming the previously observed general toxicity likely to be due to increase in molecular weight.[1514,1515] PAMAM dendrimers and some other high-molecular-weight dendrimers were found complement activators. Toxicity studies have also been reported for dendrimers of the PEI, carbosilane, polyether and melamine families.[1066,1067,1510-1513] The intracellular responses such as the content of reactive oxygen species (ROS, superoxide radical anion and hydrogen peroxide), mitochondria membrane potential, cell size and cell cycles profiles in U-937 human macrophages treated with PPI dendrimers (G_2-DAB and G_3-DAB) showed that ROS responses in macrophages were strongly influenced by the nature of the dendrimer surface and the generation.[1516] Other recent studies on PPI dendrimers show decreased toxicity when the terminal amino groups are protected or masked.[1517,1518] Intravenous injection of poly(lysine) dendrimers resulted in rapid removal from plasma, and highly charged cationic dendrimers rapidly bind to endothelial cell surfaces immediately after injection and are subsequently hydrolyzed to produce free lysine.[1519]

Dendrimers, like other macromolecules, are transported into and across cells by endocytosis, although the mechanisms are not well known.[1066,1067] On the other hand, the biodistribution of dendrimers has been widely studied especially with dendrimer-conjugated imaging agents and for their use in BNCT. A detailed haemocompatibility testing *in vitro* of high-molecular

weight (M_n up to 700, 000) polyglycerol dendrimers for effects on coagulation, prothrombic time, activated partial thromboplastin time, plasma recalcification time, thrombelastograph parameters, complement activation, platelet activation, RBC aggregation and cytotoxicity showed that they are highly biocompatible and potential candidates for various applications in nanomedicine (Figure 96).[1521-1522]

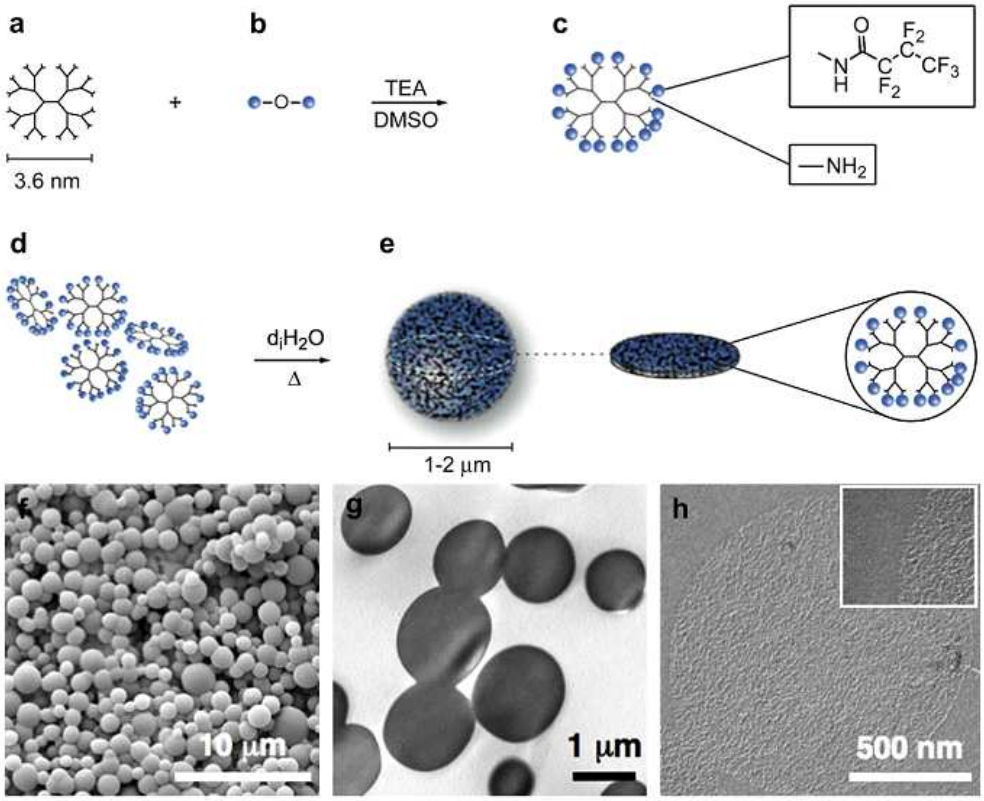

Figure 96. Self-assembly model of fluorinated, PAMAM(G_3) dendrimer-based particulates. Fifteen primary amines on the surface of (a) PAMAM(G_3) starburst dendrimers were functionalized through reaction with (b) HFAA (heptafluorobutyric acid anhydride) to yield (c) heptafluoroacylated PAMAM(G_3) terminal branches. The blue sphere and the branch terminus represent the heptafluoroacyl substituent and the terminal primary amine, respectively. The (d) randomized mixture of partially fluorinated dendrimers aggregated in aqueous environment and formed (e) self-assembled particulates with the addition of sufficient thermal energy (100°C for 1 h). The cross-sectional diameter of the particulate in (e) illustrates the densely packed internal network of partially fluorinated dendrimers. (f) Scanning electron micrograph of the fluorinated PAMAM(G_3) dendrimer-based particulates formulated with 5 mg/mL initial concentration of PAMAM(G_3) dendrimers and 25 molar equivalents of HFAA. Scale bar is 10 μm. (g) Transmission electron micrograph of 80-nm-thick cross-section of the particulates in (f) treated with 1.0% OsO_4, embedded in Embed-812 epoxy, and stained with uranyl acetate and lead citrate. Scale bar is 1 mm. (h) Transmission electron micrograph of a freeze fracture replica of the particulates in (f) depicting a dense matrix-like internal structure upon cross-fracture. Scale bar is 500 nm.). Reprinted with permission of Elsevier (ref. 1521, Fahmy's group).

There are rather few studies *in vivo* concerning the general toxicity of dendrimers,[1056,1057,1066,1067,1196-1198,1241] and, although little general toxicity is reported in these studies, no definitive conclusion can be formulated. Unwanted immunogenicity (antigenicity) of dendrimers could prohibit clinical development, but few report of studies have appeared, and no evidence of immunogenicity has been found.[1066,1067]

Interestingly, naked, unmodified G_4- and $G_{4.5}$-PAMAM dendrimers bearing simple surface groups (-NH_2, -OH, CO_2H) showed anti-inflammatory properties with three independently recognized *in vivo* anti-inflammatory assay methods. For instance, G_4-PAMAM-NH_2 showed higher activity compared to naked indomethacin.[1523]

D'Emanuele's Manchester group showed the influence of G_3-PAMAM dendrimer surface modification on the mechanism of cellular internalization into HT-29 cells using confocal

laser scanning microscopy and flow cytometry using dendrimers that were labeled with fluorescein isothiocyanate at an average molar ratio of 1:1 and modified with lauroyl and propanolol chains. The subcellular colocalization data showed that all these G_3-PAMAM dendrimers were internalized and trafficked to endosomes and lysosomes.[1524] G_5-PAMAM dendrimer-biotin-fluorescein isothiocyanate conjugates were shown not to exhibit much higher cellular uptake into HeLa cancer cells than the conjugate without biotin, thus the dendrimer-biotin conjugates might be a promising nanoplatform for cancer diagnosis and therapy.[1525]

6.7. Oral drug delivery and other delivery means

A major challenge for drugs is the possibility of oral delivery, but an obstacle is the limited drug transport across the intestitinal epithelium due to their large size relative to the tight epithelial barrier of the gastrointestinal (GI) tract. Duncan's group showed that only macromolecules with diameters up to 3 nm could penetrate through the rat's intestinal membranes via the transcelllular or paracellular pathway, which allows $G_{2.5}$-$G_{3.5}$-PAMAM dendrimers to transport across the intestine.[1515,1526] In addition, the acidic environment of the stomach and GI-tract enzymes can affect the drug and nanocarrier. Nonspecific interactions with food proteins must also be reduced. D'Emanuele et al. also investigated the transport route of a G_3-PAMAM- propanolol dendrimer conjugate across Caco-2 cell monolayers. They suggested that the route of propanalol transport was primarily transcellular, while the conjugate was able to bypass the P-gp efflux transporter, and they arrived as the same conclusion as above concerning the penetration pathway of intestinal membrane.[1159] The PAMAM-phospholipid dendrimer conjugate with the anti-cancer drug 5-FU was found by the Jain group to be significantly more effective upon oral delivery to albino rats than the free drug.[1527] The Cheng and Xu group, who recently reviewed the field,[1526] found that a PAMAM dendrimer complex of the anti-inflammatory drug ketoprofen sustained anti-noninceptive activity (inhibit rate > 50%) until 8 h of oral administration to Kunming mice, whereas this activity was absent with the free drug after 3 h.[1110] G_4-PAMAM complexation brings about a tenfold increase in permeability and more than hundredfold increase in cellular uptake with respect to free 7-ethyl-10-hydroxy-camphtothecin, suggesting that this complex has the potential to improve the oral bioavailability of this drug.[1528] Permeability studies of 4-PAMAM-arginine and ornithine conjugates across IPEC-J2 cell monolayers, a new intestinal cell line model for drug absorption studies, suggested that these dendrimer-polyamine conjugates are potential carriers for antigen/drug delivery through the oral mucosa.[1529]

Transdermal drug delivery (TDD) is a noninvasive, safe method of penetrating drugs through the skin that has revolutionalized the pharmaceutical industry, because skin is the most easily accessible organ in the body, and TDD provides a steady drug concentration in the blood, thus simplifies dosing and minimizes pain.[1530,1531] Dendrimers can act as effective transdermal penetration enhancers that are required to overcome the barrier function of the skin involving closely-packed dead cells that impose tortuosity on the diffusion path across the membrane. PAMAM dendrimers including cationic ones were found to be efficient, in particular to solubilize hydrophobic drugs.[1146] This technique appears as an emerging choice for various skin diseases in clinical trials.[1526]

In ocular drug delivery, the main challenge is to increase the drug bioavailability and prolong the residence time on the cornea, conjunctival and cornal epithelia. Dendrimers might dissolve hydrophobic drugs and accomplish retention and sustained, controlled drug release.[1137] Various PAMAM-NH_2, PAMAM-OH and PAMAM-CO_2^- dendrimer complexes, and some PPI, PAMAM and lipid-lysyne dendrimer conjugates significantly improved the bioavailability of drugs.[1526,1532-1538] Recent studies indicated that some lipid-lysine dendrimers, for which *in vivo* studies showed lack of toxicity, might be used as biocompatible

ocular gene carriers to prevent ocular neovascularization that can be a main cause of blindness, when it is not controlled.[1537,1538] Dendrimers are being increasingly proposed in various other delivery routes including rectal, vaginal and nasal routes due to their tissue penetration abilities. For instance, the poly (L-lysyne)-dendrimer based microbiocide Vivagel^{TM} (Starpharma) has been clinically tested for topical administration in the vagina against HIV and other sexually transmitted infections such as herpes.[1351,1539,1540] An advanced local, non-invasive and effective technique, iontophoresis, consists in inducing the penetration of ionic nanomaterials such as highly charged drug-dendrimer complexes or conjugates into tissues using a weak electric field; it is widely used in transdermal and ocular delivery.[1532]
Transepithelial transport of PEGylated anionic $G_{3.5}$- and $G_{4.5}$-PAMAM-CO_2H dendrimers with 1, 2 and 4 PEG per dendrimer was examined concerning the cytotoxicity, uptake and transport across Cacao-2 cells in view of oral drug delivery. Dendrimer PEGylation reduced the opening tight junctions; modulation of the tight junctional complex correlated well with changes in PEGylated dendrimer transport and suggested that anionic PEGylated PAMAM dendrimers are transported primarily through the paracellular route and show promise in oral delivery.[1541]

6.8. Medical diagnostics: imaging

Pretargeting of receptors is a useful approach in molecular imaging and therapy to reduce background noise or toxicity and enhanced selectivity. Such an approach was carried out using a biotinylated antibody, avidin/streptavidin, and a biotinylated imaging with a G_4-PAMAM-MRI T1 DTPA-Gd-biotin dendrimer.[1533]

6.8.1. Magnetic resonance imaging

Magnetic resonance imaging (MRI) is now currently used in medical diagnostics to visualize organs and blood vessels. It consists in improving the quality of visualization by enhancing the longitudinal (T_1) relaxation rate of protons of H_2O molecules by coordination to paramagnetic contrast agent that are Gd^{III} chelates complexes such as widely used [Gd^{III}(DTPA)] (DTPA = diethylenetriamine pentacetic acid) commercially known as Magnevist (Schering AG) and [Gd^{III}(DOTA)] (DOTA = tetracarboxymethyl-1,4,7,10-tetraazacyclododecane). In these complexes, the relaxativity (relaxation rates of H_2O protons *per* mmol of Gd^{III} ion as a function of the magnetic field strength) is high enough. The key properties required for Gd^{III} MRI contrast agents are the good biocompatibility (low toxicity), the use at a low dose, a good excretion from the system and a high thermodynamic and kinetic stability (Figure 97).[1542-1550] Gd^{III}-containing PAMAM dendrimers were loaded with paramagnetic probes, which allowed determining the relative locations and concentrations of Gd^{III} by ESR.[1550]

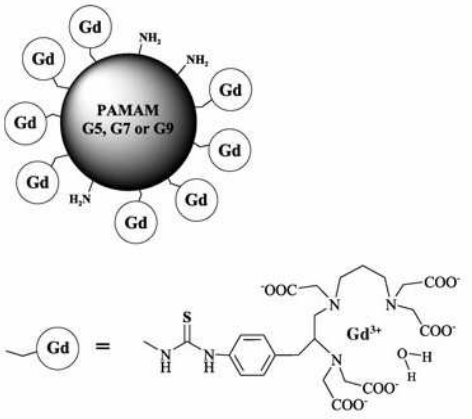

Figure 97. PAMAM dendrimers functionnalized with gadolinium. Reprinted with permission of Wiley Interscience (ref. 1545, Merbach's group).

Major problems of these low molecular-weight complexes are short circulation times within the body and lack of discrimination between diseased and normal tissues. Subsequently, macromolecular derivatives were designed by combination with polylysine, PEG, polysaccharides and proteins, but their slow secretion rate and resulting accumulation in the liver and toxicity risk related to Gd^{III} release during metabolism limited their clinical applications.[1050-1052,1055]

The development and commercialization of PAMAM dendrimers was decisive in bringing a breakthrough in the MRI field when, in 1994, the groups of Lauterbur (2003 Nobel Prize in medicine) and Tomalia reported G_2- and G_6-PAMAM dendrimer-based Gd^{III} chelates conjugated to the chelate [Gd^{III}(dtpa)] {dtpa = 2-(4-isothiocyanatobenzyl)-6-methyldiethylenetriaminepentacetic acid} via a thiourea linkage. Excellent MRI images of blood vessels and long blood circulation times (> 100 min.) were obtained with G_6-PAMAM-[Gd^{III}(dtpa)] upon intravenous injection on rabbits.[1551-1554] The relaxativity increasing linearly with the molecular weight, the best results were obtained later with G_9- and G_{10}-PAMAM dendrimers. The incorporation of PEG units was successful in considerably lowering liver retention after seven days (from 40% without PEG) to 1-8%, and conjugation to monoclonal antibodies or avidin provided tumor-specific MRI agents. Commercial applications of these concepts followed with Gadomer 17, a 24-Gd^{III}-DTPA dendrimer containing trimesic acid core connected to G_2-polylysine dendrons bearing 24 DTPA and 24 DOTA peripheral chelating-Gd^{III} groups respectively.[800] PPI-Gd^{III}(dtpa) dendrimers were used as well.[1555,1556]

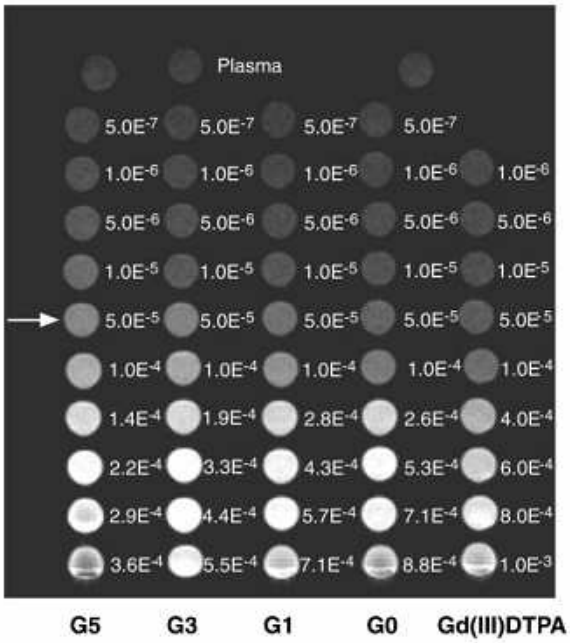

Figure 98. *In vitro* T1-weighted MR measurements of different concentrations of Gd^{III} (M) of Gd^{III}DTPA, reference Gd^{III}DTPA complex (G_0) and the dendritic contrast agents in mouse plasma illustrates that at a concentration of, for example, $5.0x10^{-5}$M (row indicated by arrow) the signal increases on going to higher generations of the dendritic contrast agent, which corresponds with the findings in Table 2. The higher Gd^{III} concentrations illustrate (i) a shift towards lower concentrations for the maximum signal enhancement with higher generations and (ii) that concentrations at which T_2* susceptibility effects are observed for the higher generations (G_3 and G_5) are well below the concentrations of maximum signal enhancement for the lower generations of the dendrimer and Gd^{III}DTPA. Reprinted with permission of Wiley Interscience (ref. 1561, Backes's group).

Dendrimer-Gd^{III} complexes for MRI have been reviewed.[1050-1052] More recently, a G_8-PAMAM-Gd dendrimer conjugate allowed to visualize changes in tumor permeability after a single dose of radiation.[1557] *In vivo* imaging in mice of a G_4-PAMAM-dendrimer-Gd^{III}-DTPA

conjugate showed a reasonnably fast clearance ($t_{1/2}$ = 24 min), suggesting that it is a viable agent for use in clinical applications.[1558] Micromagnetic resonance lymphangiography, a new method relying on temporarily enhanced permeability of tumor vasculature to drugs, was probed in mice bearing hematomas to improve the contrast between intralymphatic and extralymphatic imaging.[1159,1560] Beside PAMAM and lysyne dendrimers, PPI and DAB dendrimers conjugates have been used as macromolecular MRI agents (Figure 98).[1561] With the same number of termini, DAB-based reagents cleared more rapidly from the body than PAMAM-based agents.[1562] High generations such as G_5 showed more gradual diffusion than lower ones.[1563] Imaging of oncogene mRNA in tumor cells by hybridization of complementary oligonucleotides was achieved with polyamidopropionate-peptide nucleic acid-Gd^{III} conjugates.[1564] The groups of Fréchet and Prasad examined the generation of cytotoxic singlet oxygen for PDT to subcutaneous tumors by fluorescence resonance energy transfer (FRET) using porphyrin sensitizers as dendritic cores of dendrimers containing two-photon donor chromophores such as the complex polyaromatic AF-343 at the periphery (see § 3.7).[267-269] ^{19}F NMR has been used as an MRI technique utilizing *pH*-responsive fluorinated dendrimers.[1565] MRI lymphangiograhy using dendrimer-based contrast agents has been compared at 1.5T and 3T.[1566] A dual CT-MRI dendrimer contrast agent was used as a surrogate marker for convection-enhanced delivery of intracerebral macromolecular therapeutic agents.[1565]

Superparamagnetic iron oxide NPs are effective contrast agents for labeling cells to provide high sensitivity in MRI, but this sensitivity depends on the ability to label cells with sufficient quantities of SPIO, which is challenging for nonphagocytic cells such as cancer cells. Therefore cell-penetrating polyester dendron with peripheral guanidines was conjugated to the SPIO surface. In GL261 mouse glyoma cells, the dendritic guanidine exhibited similar cell-penetrating capabilities to the HIV-Tat47-57 peptide for the transport of fluorescein, and when conjugated to SPIO, it provided enhanced uptake in comparison with NPs having no dendron or dendrons with hydroxyl or amine peripheries. Greater toxicity than with hydroxylated or aminated dendrons was disclosed, however, although the NPs were relatively nontoxic at the concentrations required for labeling (Figure 99).[1566]

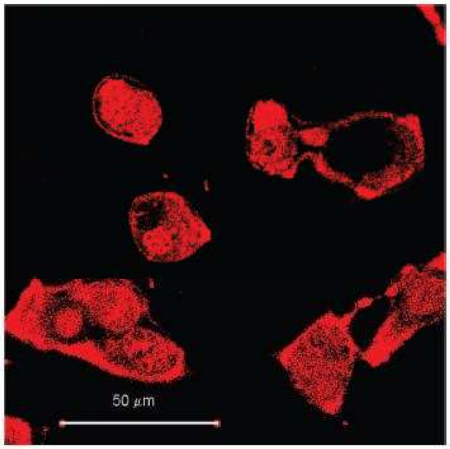

Figure 99. Confocal laser scanning microscopy image of GL261 cells following a 2h incubation with the dendritic nanoparticle at a concentration of 25 μg of Fe/mL. Reprinted with permission of the American Chemical Society (ref. 1566, Gillies's group).

Multicolor imaging of lymphatic function was advantageously carried out with two probes: dendrimer-based optical agents and quantum dot-labeled cancer cells, because the lymphatics, critical conduits of metasases, are difficult to study using only one method given their size and location.[1567]

6.8.2. Computed tomography, a radiolabeling and imaging method

Computed tomography (CT) is a medical imaging method used to generate a three-dimensional image of the inside of an object from a large series of two-dimensional X-ray images taken around a single axis of rotation. It is an important tool in medical imaging used in the diagnosis of various disease entities, and has recently begun to also be used for preventive medicine or screening for disease. CT usually utilizes mostly iodinated agents and is regarded as a moderate-to-high radiation diagnostic technique. Targeted delivery is a key issue, as for other imaging methods; therefore dendrimer conjugation is most useful. Iodinated contrast agents based on iobitridol-G_3-G_5 poly (lysine) dendrimers containing PEG cores have been used for tumor microvasculature CT imaging and produced strong visualization of normal rat vasculature. The large molecular weight of the dendrimer conjugate was responsible for good retention, half time in blood being 35 min, compared to typical exhaustion time of 5 min recorded for small-molecule CT contrast agents.[1568]

Metallation of G_5 to G_7-dendrimers terminated with tridentate bis(pyridyl)amine by another radioactive element, 99mTc(I) provided dendrimer radiolabeling, and distribution in healthy adult Copenhagen rat using dynamic small-animal single photon emission computed tomography indicated that the labeled dendrimers were rapidly eliminated from the bloodstream via the kidneys.[1569]

Positron-emitting tomography (PET) allows a tri-dimensional view, and the Fréchet group designed a biodegradable dendritic radiohalogen-based (^{125}I and ^{76}Br) PET nanoprobe targeted at $\alpha_V\beta_3$ integrin, a biogical marker for the modulation of angiogenesis (cf § 6.2.6). The radioactive halogens were located at the dendrimer core in order to prevent *in vivo* dehalogenation that is frequently encountered in imaging. Targeting peptides of arginine-glycine-aspartic acid (RGD) motifs were located at the termini of the PEG chains to favor their accessibility to the $\alpha_V\beta_3$ integrin receptors. This dendritic engineering enabled a 50-fold increase of the binding affinity to $\alpha_V\beta_3$ integrin receptors compared to the monovalent RGD alone. *In vivo* biodistribution studies of ^{76}Br-labeled dendritic nanoprobes showed excellent bioavailability. *In vivo* studies in a murine hindlimb ischemia model for angiogenesis showed high nanorobe accumulation targeted at $\alpha_V\beta_3$ integrins in angiogenic muscles allowing highly selective imaging (Figure 100).[1570]

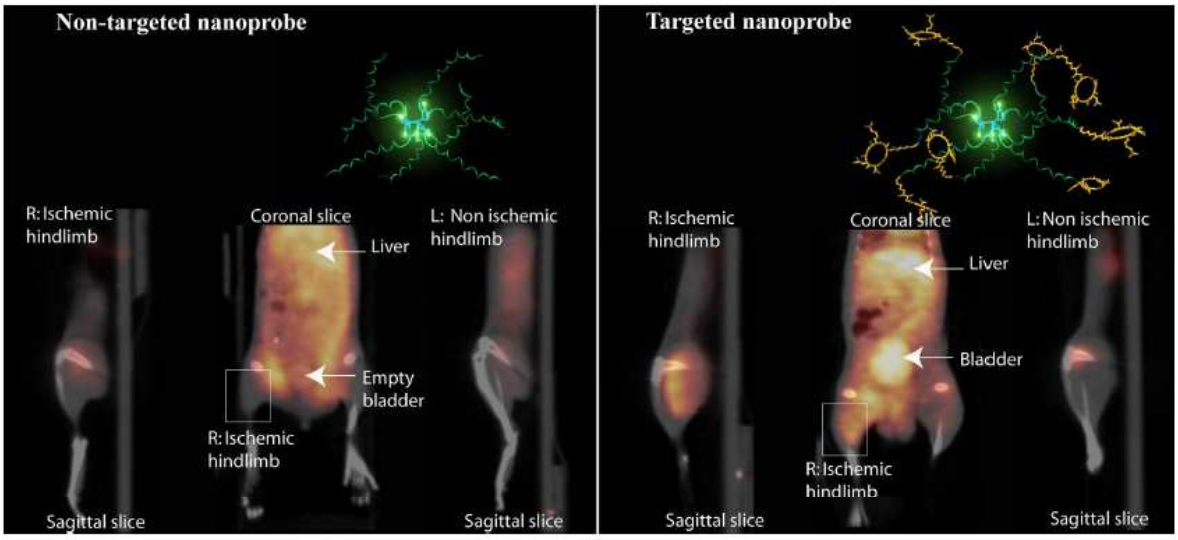

Figure 100. Noninvasive PET/CT images of angiogenesis induced by hindlimb ischemia in a murine model. (A) Nontargeted dendritic nanoprobes (shown bottom center) (B) Uptake of $\alpha_v\beta_3$-targeted dendritic nanoprobes was higher in ischemic hindlimb (left side of image) as compared with control hindlimb (right side of image) Reprinted with permission of the National Academy of Sciences of the USA (ref. 1570, Fréchet's group).

6.8.3. Fluorescence

Fluorescence quantification in tissues using conventional techniques can be difficult due to the absorption and scattering of light in these tissues. One-photon (see also § 3),[1571] and two-photon[255,256] (see § 3.7) fluorescent tumor sensing systems have been developed with the advantage for the latter of high spatial (μM) resolution. Two-photon optical fluorescence fibers use a single-mode fiber to transport femtosecond laser pulses for excitation and to collect emitted tissue fluorescence.[1572,1573] This technique has been used with a G_5-PAMAM dendrimer conjugated to folic acid and the fluorescent probe 6-carboxytetramethylrhodamine succinic ester (6-TAMRA) to target xenograft tumors in mice; it showed accumulation in the tumor up to 673 ± 67 nM at 2h, whereas the analogous conjugate without folic acid reached only 136 ± 28 nM in 2h.[1574-1576] The same fiber probe was used for labeling human squamous KB cell tumors grown *in vivo* in mice and detected a three-fold increased tumor fluorescence in animal that were treated with the targeted dendrimer conjugate compared to the conjugate that did not contain folic acid, which demonstrated the utility of this technique.[1577] Newkome-type dendrimers were found ideal nanovectors of two non-peptidic fluorescent markers that were internalized into mammalian cells with strong subcellular localization (Figure 101).[1578] Antibody-Au quantum dot-PAMAM dendrimer complexes were used as an immunoglobin immunoassay based on linear fluorescence quenching over a micromolar to nanomolar concentration range.[1579] Dendrons containing fluorescent probes with two other usuefully functionalized tethers (carboxylic acid and azido) have been designed for branching to biomedical devices.[1580]

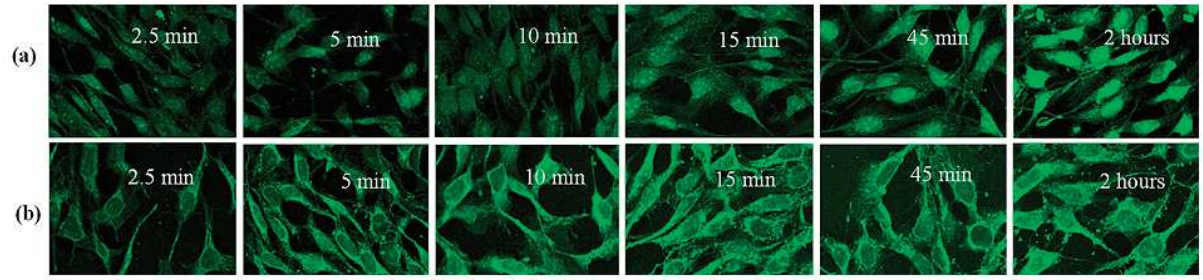

Figure 101. Time course of internalization of (a) FD-1 and (b) FD-2 into NIH-3T3 cells (fixed) at 37 °C. The conjugate concentration was 10 μM. Reprinted with permission of the American Chemical Society (ref. 1578, Harth's group).

The interactions between $G_{4.5}$-PAMAM dendrimers and bovine serum albumin were analyzed using fluorescence and equilibrium dialysis.[1581-1585] Optical fluorescence has been coupled to MRI in a single hybrid probe in dendrimers to localize the sentinel lymph node and other targets.[1586-1588] Dansyl fluorescence in dendrimers (cf. § 3.4) has been used for cellular uptake and intracellular localization by confocal fluorescence microscopy.[1589] Covalent encapsulation of near-IR fluorophores in a biodegradable dendrimer surrounded by a shell of polyethylene oxide conferred enhanced stability to the nanoprobe with additional resistance to enzymatic degradation, prolonged blood residence time, and enabled monitoring fluorescence lifetime changes *in vivo*.[1590] The extracellular cell matrix (ECM) surrounds cells and plays important roles in many aspects of cellular fate, including cell migration, stem cell differentiation, and cancer progression. Therefore the Müllen group has reported a positively charged fluorescent core-shell dendritic macromolecule containing multiple $–NH_2$ groups that binds to highly charged ECM components with aventageous optical properties and biological specificity.[1591]

6.9. Biosensors

6.9.1. Dendritic DNA biosensors

Nucleic acids have been used as dendrimer constituents at the end of the 1990's and beginning of this decade,[1592,1593] and some of them are commercially available (3DNA)[1594]. Physical properties of interest included AFM, dynamic light scattering,[1592] flow cytometry,[1593,1595] fluorescence,[1595] diffusion[1596] and conductivity (Figure 102).[1597-1599]

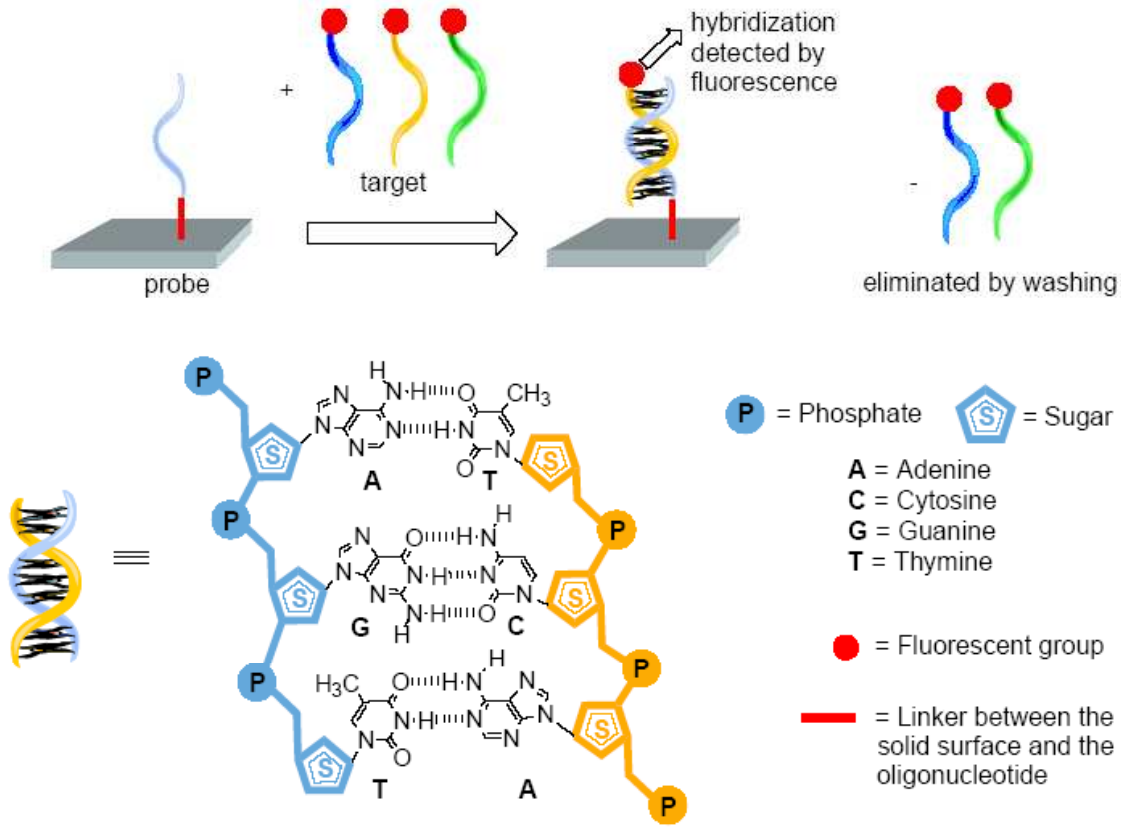

Figure 102. Principle of a DNA chip or DNA array. Only the oligonucleotide complementary to the one immobilized on the surface can hybridize. The hybridization occurs through supramolecular recognition of complementary bases (Adenine with Thymine, and Cytosine with Guanine) linked to the sugar and phosphate backbones, as illustrated by one example. Reprinted with permission of the Molecular Diversity Preservation International (ref. 1598, Majoral's group).

DNA microarrays and biosensors are a broad area, in which dendrimers are involved, and it has been the subject of two special volumes[1600,1601] and a review article by Rosi and Mirkin[1602] published in 2005. The principle consists in immobilizing nucleotides on glass slides by covalent grafting in order to analyze mixtures of fluorescent-labelled nucleic acids, fluorescence serving for quantifying the hybridization. First, dendrons were grown on the slide,[1603] a technique that has been then largely improved.[1604-1606] In 2001, the Niemeyer group pioneered the field with PAMAM dendrimers and obtained stable fluorescence intensity that was considerably increased compared to non-dendritic linkers.[1607-1608] PPI dendrimers have also been used.[1609] Subsequently, larger increases in intensities were obtained,[1610-1614] in particular using high-generation aldehyde-terminated dendrimers and aminated slides that provided high sensitivities.[1610-1613] A G_3-PAMAM dendrimer conjugated to biotin was immobilized on glass slides using avidin complexation and examined using AFM and SEM for low-concentration DNA detection, increasing the sensitivity for fluorescence-labeled target DNA.[1613] An elegant patterning method reported by Reinhoudt's group involved stamps for microprinting providing microarray replication. The stamp, inked with the PPI dendrimer, was incubated with DNA labeled with fluorescein. The dendrimer was then washed out after printing on the slide, allowing fluorescence analysis of the patterned DNA microarray.[1615,1616]

Other recently used techniques in this context involve dendrimer nanotubes,[1617] ZnCdSe quantum dots,[1618,1619] quartz-crystal microbalance, piezoelectric membranes, gold colloids,[1620] plasmon resonance,[1621] and electrochemistry (Figure 103).[1622-1625]

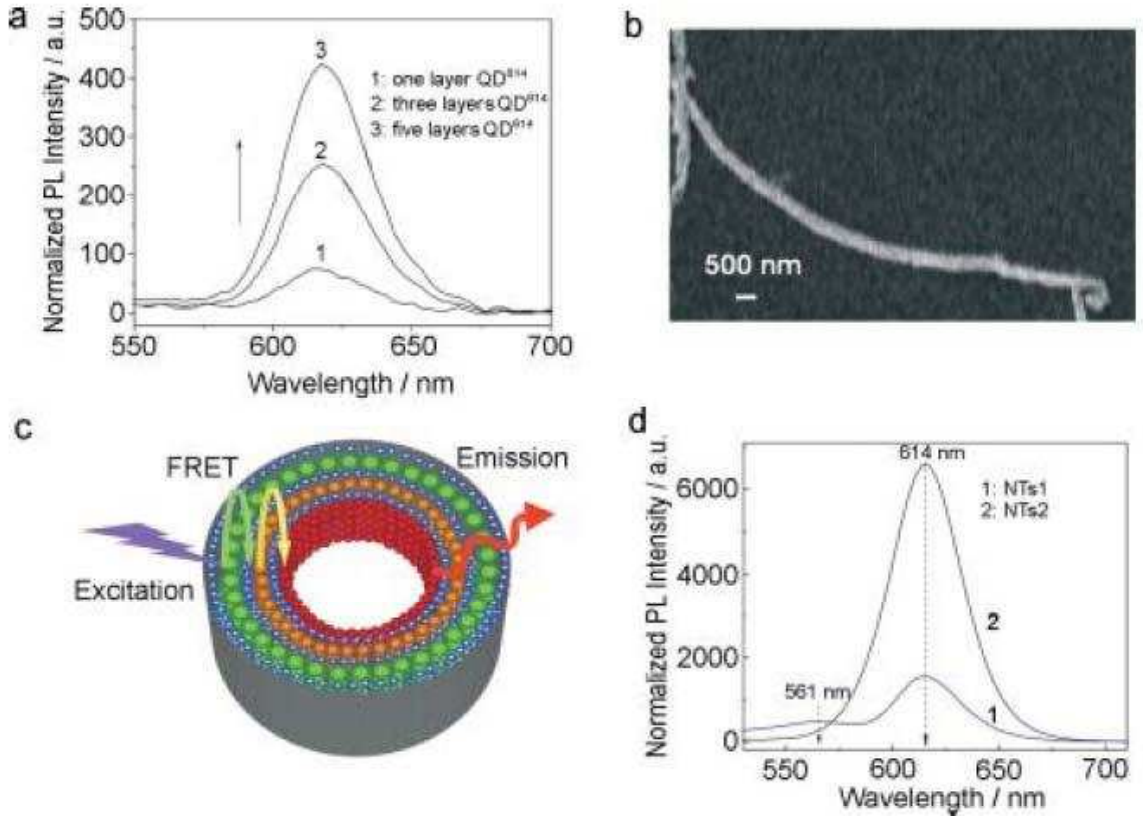

Figure 103. Characterization of QD/dendrimer composite NTs. a) PL spectra of NTs containing 1) one, 2) three, and 3) five QD^{614} layers. b) SEM image of an individual NT containing 15 G_4^+/QD^{614} bilayers; c) schematic diagram of an NT with a graded bandgap structure formed by assembling three different sizes of QDs (QDs^{561},QDs^{594}, QDs^{614}) inside an AAO template; d) PL spectra of two different types of NTs: 1) NTs1 containing five QD^{561}/G_4^+ and five QD^{614}/G_4^+ bilayers. 2) NTs2 containing five QD^{561}/G_4^+, five QDs^{594}/G_4^+ and five QDs^{614}/G_4^+ bilayers. The QDs were excited at λ=460 nm. The PL spectra were normalized to the absorption maximum of the NTs at λ= 460 nm. Reprinted with permission of Wiley Interscience (ref. 1619, Knoll's group).

Electrostatic interactions between positively charged (mostly) PAMAM dendrimers and oligonucleotides involved studies that were essentially directed towards gene transfection (cf. § 6.2.7); they provided information on these interactions through various physical methods,[619,620,1599,1626-1631] and were reviewed in 2005 by Florence.[619,620]

6.9.2. Electrochemical dendritic ATP sensors

Adenosine triphosphate (ATP), a DNA fragment, is a cell energy source and cellular messenger. It can be recognized by electrostatic binding with a synthetic cationic sensor, for instance electrochemically using the redox potential fluctuation of ferrocenyl[490] or cobaltocenyl[526,527] redox systems.

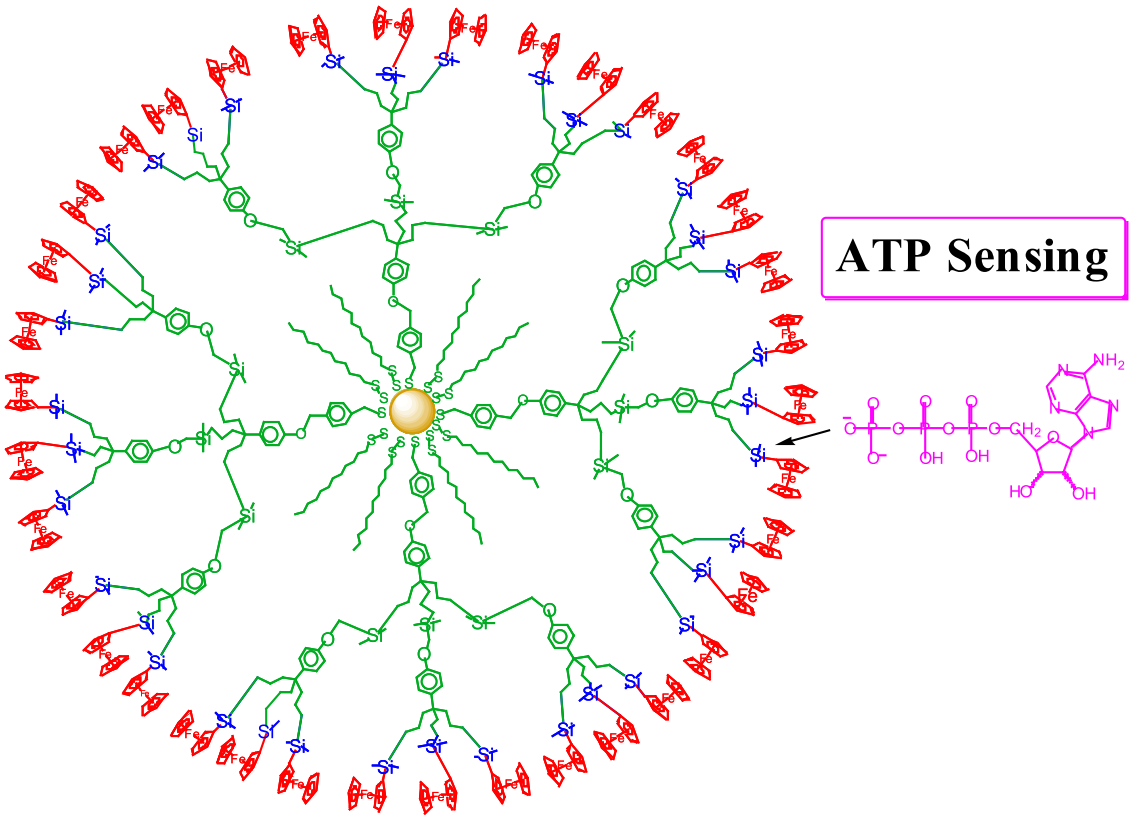

Figure 104. ATP^{2-} sensing and regeneration of the modified electrode for re-use. Reprinted with permission of the American Chemical Society (ref. 1632, Astruc's group).

It is the cationic form of the redox system that forms an ion pair with the anionic groups of ATP. If this sensor is linear, however, this interaction is too weak to provoke a significant change of redox potential. On the other hand, ferrocenyl-terminated dendrimers show a positive dendritic effect, i.e. a new ferrocenyl redox wave at a less positive anodic potential is appearing in the cyclic voltammogram upon addition of ATP to a solution of the ferrocenyl-terminated dendrimer of low or high generation. Thus, ion pairing in the ferrocenyl dendrimers in which the ferrocenyl groups are simply linked to the core by alkyl chains involves dendritic encapsulation of ATP in the dendrimer interior provoking a much stronger interaction than with linear alkylferrocenes. This also allows titration of the ATP solution (Figure 104).[1632] It is possible (although not indispensable) to introduce additional supramolecular interactions that can enhance the ionic interaction between the ATP phosphate groups and the ferricinium moiety. For instance, gold-nanoparticle-cored dendrimers containing silylferrocenyl termini show an increased interaction as indicated by a larger potential difference between the ferrocenyl dendrimer in the presence or absence of ATP.[487,1633-1635] This is probably due to the hypervalency of the silicon atom in the silylferricinium form. Thus, although the silicon atom has no oxygen affinity in tetraalkyl silanes, such an interaction can be envisaged in silylferricinium due to the partial positive charge of silicon resulting from silicon hypervalency.[487-490,1636-1638] Another kind of additional supramolecular interaction is provided in triazolylferrocenyl-[658] or triazolylmethylferrocenyl dendrimers[487] formed by click reactions of azido-terminated dendrimer with ethynylferrocene or alkyne-terminated dendrimers with azidomethylferrocene respectively, providing facile electrochemical recognition and titration of ATP. Supramolecular assistance of dihydrogenophosphate recognition by endoreceptors was pioneered by Beer,[725,726] and the first example of dendritic endoreceptors capable of dihydrogenophosphate recognition was disclosed by our group in 1997.[1639] At this occasion, a dramatic positive dendritic effect was

disclosed using amidoferrocenyl-terminated dendrimers, i.e., recognition was all the easier with a larger difference of redox potential as the dendrimer generation was higher. The amido group is ideal in provoking a large potential difference because of the synergy between the double hydrogen bonding with the dihydrogenophosphate.[1636] Ferrocenylurea termini have also been successfully used by Alonso et al. for hydrogenophoshate sensing,[1637] and inorganic molybdenum cluster-cored silylferrocenyl-terminated dendrimers were also used for ATP sensing.[1638]

An additional advantage of large ferrocenyl dendrimers is that they adsorb on Pt electrodes all the more easily as they are larger, facilitating sensing by dendrimer-derivatized electrodes that allow subsequent ATP washing and re-use of the electrode sensor. This also is an advantage provided by AuNP-cored dendrimers that are very large.[487-490] Dihydrogenophosphate anion is a good ATP model, but sensing is slightly easier with dihydrogenophoshate anion than with ATP using ferrocenyl-terminated dendrimers.[490,1640] With larger $[Fe_4Cp_4(CO)_4]$-cluster termini instead of ferrocenyl termini, however, ATP recogniton is easier and is observed with a larger redox potential variations of the redox system $[Fe_4Cp_4(CO)_4]^{+/0}$ than with ferrocenyl ($Fe^{III/II}$) termini, because the cluster better matches the ATP size than the smaller ferrocenyl group.[1641,1642]

6.9.3. Electrochemical dendritic glucose sensors

Enzyme glucose biosensors for *in vitro* assays have been developed extensively to monitor the glycemia of diabete patients, and therefore glucose oxidase (GOx)-based electrodes are a major application of immobilized enzymes. The reaction involved is the GOx-catalyzed oxidation of β-D-glucose by O_2 to D-glucono-1,5-lactone and H_2O_2.[1643]

Losada et al. used silylferrocenyl dendrimers as mediators in amperometric biosensors. It was shown that these sensors respond rapidly to the addition of glucose by steady-state amperometric response of carbon paste electrodes containing these dendritic mediators and glucose oxidase as a function of the glucose concentration and applied potential.[1644] Subsequent to this seminal work, the Losada group also developed the electrochemical method with other dendrimers such as PPI-cored polymethylferrocenyl dendrimers deposited onto a platinum electrode, including studies of the influence of the layer thickness and concentrations, quantifying hydrogen peroxide produced by the oxidase catalysis during the enzymatic reaction in direct proportion to the available glucose (amperometric titration: $H_2O_2 \rightarrow O_2 + 2H^+ + 2e^-$). Amperometric enzyme electrodes with horseradish peroxidase and lactate oxidase were also used.[1645-1651] The electro-oxidation ability of glucose in alkaline solution was tested using a sensor based on dendritic CuNi alloy.[1652]

Streptokinase, GOx and phosphorylcholine were immobilized on polyglycerol dendrimers in order to obtain a blood compatible bioconjugate possessing glucose-sensing properties. This bioconjugate was entrapped in polyaniline nanotubes through template electrochemical polymerization of aniline. This material was used as a glucose-oxidation mediator and appeared as a good candidate for oxidoreductase-based implantable biosensors.[1653] Other glucose biosensors systems with GOx involve PtNPs on multiwalled carbon nanotubes[1654-1656] or layer-by-layer dendrimer-AuNP membranes (Figure 105).[1657] Other dendritic hydrogen peroxide amperometric sensors are based on horseradish peroxidase.[1658]

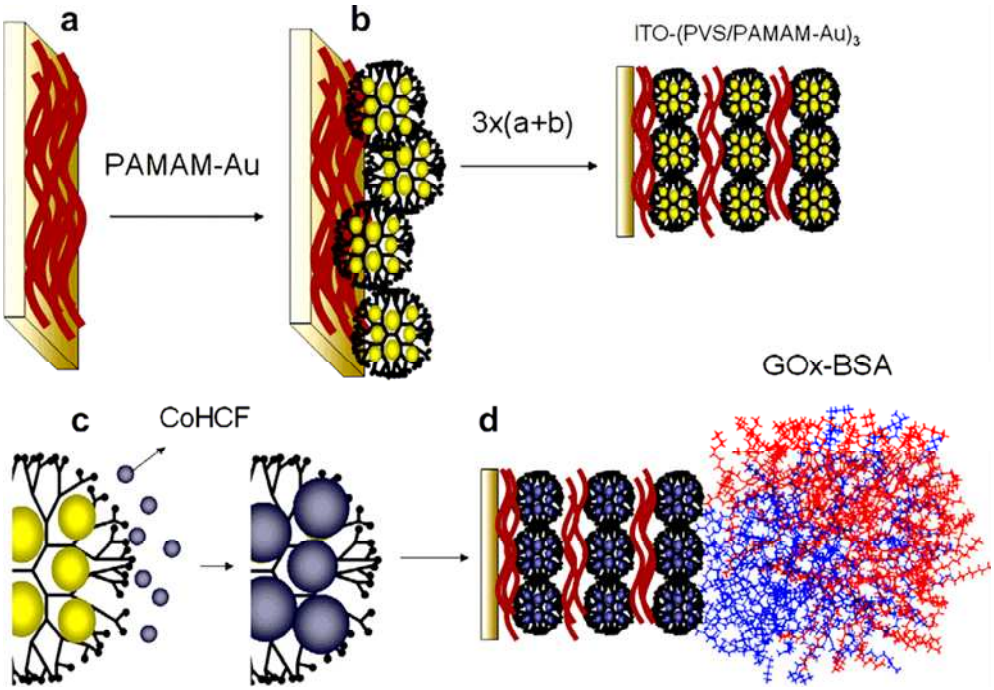

Figure 105. Schematic fabrication of LbL films comprising PVS and PAMAM–Au. The sequential deposition of LbL multilayers was carried out by immersing the substrates alternately into PVS (a) and PAMAM–Au (b) solutions for 5 min per step. After deposition of 3 bilayers, an ITO–(PVS/ PAMAM–Au)$_3$@CoHCF electrode was prepared by potential cycling (c) The enzyme immobilization to produce ITO–(PVS/PAMAM–Au)$_3$@CoHCFGOx (d) was carried out in a solution containing BSA, glutaraldehyde and GOx. Reprinted with permission of Elsevier (ref. 1657, Brett's group).

Non-electrochemical methods for glucose sensing are based on luminescence. Affinity adsorption solid-substrate phosphorimetry allowed the determination of glucose traces, based on labeling Triticum vulgaris lectin on the surface of PAMAM dendrimers.[1659] A flow-through electrochemical immunosensor for monitoring IgG in human serum has been developed using core-shell SiO_2/Au nanocomposites and G_4-PAMAM dendrimer as matrixes. Ferrocenecarbaldehyde-labeled anti-IgG was initially chemisorbed onto the NP surface, then GOx was backfilled onto the modified surface. The selectivity, reproducibility and stability of the immunosensor were acceptable.[1660]

6.9.4. Functionalized antibody and antigen biosensors

The reversible affinity interactions of immunosensing surfaces are based on biospecific association and displacement reactions between functional antigen ligands and antibody molecules. A typical example of antigen/antibody couple is biotin/anti-biotin system. Functionalized monolayers provided a platform for biospecific recognition with monoclonal anti-biotin immunoglobulin G (IgG) using PAMAM dendrimers functionalized with ferrocenyl and biotinyl groups, the ferrocenyl termini serving as mediators for the electrochemical track method with GOx.[1661] Glycoproteins, especially antibodies, were sensed amperometrically based on the content of galactosyl and *N*-acetylgalactosamidyl residues in glycoprotein carbohydrate chains. This method does not require antibody labeling or enzyme-tagged secondary antibodies, and total assay time was about 20 min.[1662]

The antibody IgG were used as dendronic supramolecular structures connected to the antibody IgM that has a pentameric structure of IgG and ten antigen binding sites, which anables to bind tightly to antigens containing multiple identical epitopes. The antibody dendrimer has an advantage in its amplification of detection signals for antigens, with the

characteristics of being composed of proteins with non-covalent bonds and strong specific antigen binding capacity.[1663]
The use of immunoassays in clinical diagnostics has stimulated the development of sensitive and specific techniques to determine the presence of specific antigen in samples. For instance, non-competitive fluoroimmunoassay allows the analysis of cortisol based on the blocking of unbound sites of the capture antibody by a PAMAM dendrimer-cortisol conjugate.[1664]
Dendrimerized cellulose was used as a scaffold for artificial antigens, which provides a tool for developping clinically testable materials to study adverse immunological responses to drugs in human (Figure 106).[1665]

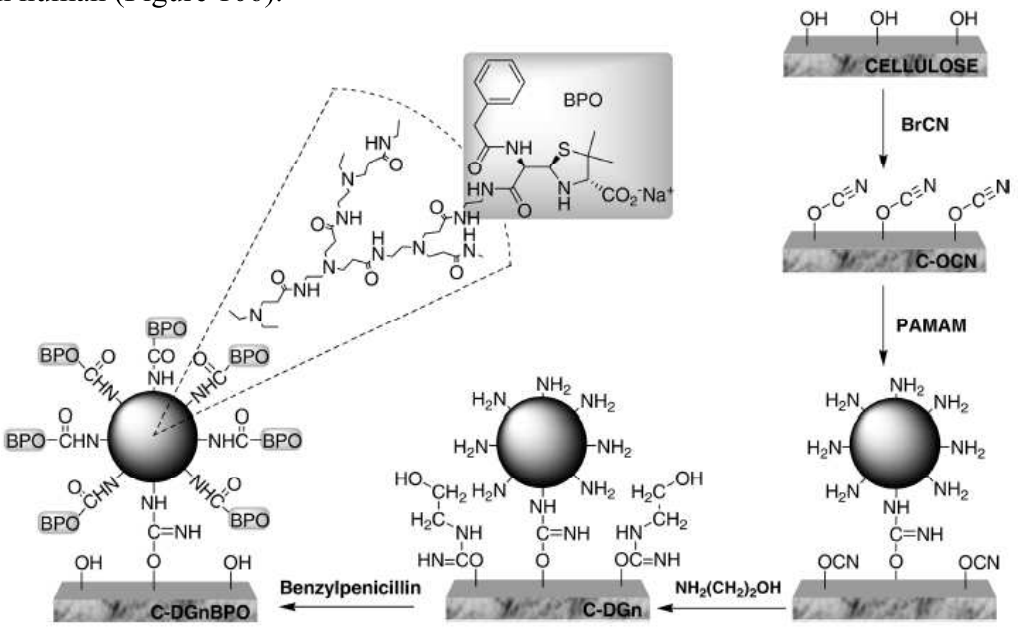

Figure 106. Modification of cellulose surfaces to generate dendritic-linked systems for the preparation of solid surface supported GnBPO conjugates. Reprinted with permission of the American Chemical Society (ref. 1665, Perez-Inestrosa's group).

DNA dendrimers, conjugated with both anti-biotin and up to 350 labeling entities, were adapted to protein microarray and ELISA cytokine detection resulting in up to threefold improvement of the detection limits with no significant increase in the inter- and intra-assay coefficient of variation compared to streptavidin horseradish peroxidase detection.[1666]
Antigen mannolysation has been shown to be an effective approach to enhanced antigen uptake and presentation by APC. Mannose-based antigen delivery system with a PAMAM dendrimer has been used in order to overcome disadvantages associated with conventional methods involving the mannosylation of antigens. Mannosylated dendrimer overalbumin (MDO) was shown to be a potent immune inducer of OVA-specific T cell response *in vitro*. The immunogenicity of MDO was due to both enhanced antigen presentation and induction of DC maturation.[1667]
Immunotherapeutic approaches are investigated for treatment of neurodegenerative Alzheimer disease. The identification of a β-amyloid-plaque specific epitope Ab(4-10) (4FRHDSGY10), recognized by therapeutically active antibodies from transgenic Alzheimer dementia could provide the basis for the development of vaccines. Therefore the design and immuno-analytical properties of antigenic bioconjugates comprising a β-amyloid-plaque specific epitope were reported.[1668]

6.9.5. Miscellaneous dendritic biosensors

Recognition according to the supramolecular lock-and-key principle that is the basis of sensor design is intrinsic to natural processes, specifically with enzymatic catalysis, and has been

applied to many biomolecules as diagnostic tools. Seminal works by Lehn,[3] Whitesides[1669] and Reinhoudt[1670] groups beautifully illustrate this concept. Thus organizations of biocomposite sensing materials based on supramolecular interactions were actively persued *inter alia* by Willner's group[1671]and others.[1672,1673] A single weak-binding event is multiplied into an efficient receptor site for protein surfaces because of the subsequent binding events that take advantage of the pre-organization in biological processes, but also in biomimetic ones with dendritic artificial receptors.[1674] Sophisticated artificial receptors exhibiting nanoscale substrate recognition can be obtained by introducing unsymmetrical patched structures in dendrimers. This strategy has been developed with porphyrin dendrimers; for instance, oligopeptide-patched dendrimers are nanoscale receptors of cytochrome *c* proteins.[1675] Flurophore-cored dendrimers interact with proteins that quench the fluorescence, a generation dependent phenomenon that could provide selective protein sensors (Figure 107).[1676]

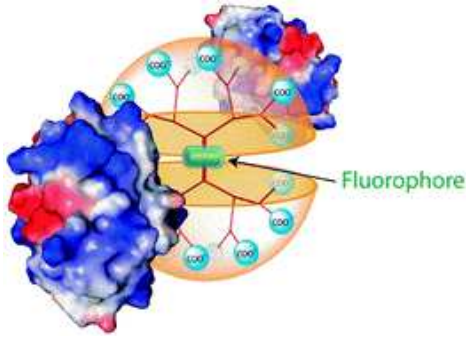

Figure 107. Fluorophore-cored dendrimers for patterns in metalloprotein sensing. Reprinted with permission of the Royal Society of Chemistry (ref. 1676, Thayumanavan's group).

Bile acid dendrons show a remarkable ability to act as normal and inverse micelles owing to the facially amphiphiliic nature of the bile acid backbone. Exploiting Newkome's concept of dendritic molecular micelles,[8,128] it has been possible to show the supramolecular function of these gelating bile acid dendrons in biomimetic molecular recognition.[1677] An ultrasensitive and simple DNA-free method for protein sensing by electrochemical signal amplification was reported with an IgG layer on an indium oxide electrode using ferrocenyl dendrimers and AuNPs as nanocatalysts. The IgG –AuNp conjugate and the immunosensing layer sandwiched the target protein, and the AuP label generates aminophenol from nitrophenol by catalytic reduction. The kinetics is fast, due to the easy access of the small nitrophenol molecules to the AuNP surface through pinholes of IgG-AuNP conjugate and to the large number of catalytic sites per nanocatalyst label (Figure 108).[1678]

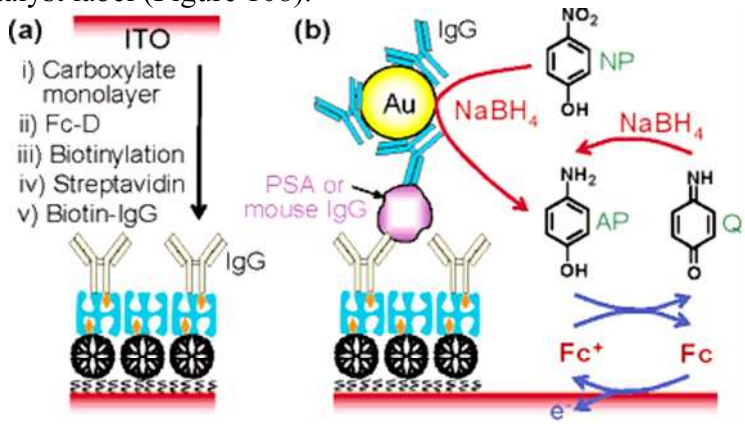

Figure 108. (a) Schematic representation of the preparation of an immunosensing layer. (b) Schematic view of electrochemical detection of mouse IgG or PSA. Reprinted with permission of the American Chemical Society (ref. 1676, Yang's group).

Glutamate, an important neurotransmitter in the mammalian central nervous system and neuronal pathway in the brain, is related to several neurological disorders such as schizophrenia, Parkinson' s disease, epilepsy and stroke. Amperometric glutamate have been developed with glutamate oxidase incorporated into modified electrodes using multiwall carbon nanotubes modified with PAMAM dendrimers loaded with PtNPs as an efficient redox mediator.[1679,1680] Another neurotransmitter, dopamine, also plays an important role in the functioning of the central nervous system as well as in the cardiovascular, renal and hormonal systems. The Unified Parkinson's Disease Rating Scale is currently used to assess Parkinson's disease, although it cannot quantify the extent of disease. Accordingly, the dopamine concentration, which is one of the key factors in determining this disease, needs to be quantified. Compared analytical performances indicated that the electrochemical detection was the method of choice for dopamine determination with PAMAM-OH-dendrimer loaded with RhNPs and immobilized on glassy carbon electrodes.[1681]Forster resonance energy transfer involved in optical sensors has also been used for this purpose.[1682] Sensing of the carbohydrate-binding proteins lectins, important in cell growth, inflammatory response and viral infections, was achieved optically using a Ru^{II}-tris(bipyridine) cored-dendrimer (cf. § 3.2) terminated with carbohydrate groups (mannose) in order to increase avidity.[1683]
The Niemeyer group has reported photomasks for surface patterning using the thiol-ene reaction. This allows the control of biotinylated enzyme immobilization on silica surface upon surface fixation by interaction with silica-PAMAM-dendrimer derivatized with streptavidin.[1684] Recognition by cell surface integrin receptors was provided by transglutaminase enzyme-crosslinked G_2-PAMAM dendrimers that mimic collagen withstanding triple-helical conformation.[1685] *In vitro* targeting efficacy to integrin receptors expressing cells was shown with G_5-PAMAM Au DENs functionalized with fluorescein isothiocyanate and Arg-Gly-sp (RGD) as template.[1686] Amperometric detection of 8-hydroxy-2'-deoxyguanosine was achieved with a low limit of 1.2×10^{-9} M using a Au electrode modified with $G_{3.5}$ and $G_{4.5}$-PAMAM-CO_2H dendrimers-based thin fims. This Au electrode was modified by SAM using aliphatic aminothiols on which the PAMAM-CO_2H dendrimers were attached using peptidic bonds.[1687] The direct electrochemistry of laccase was promoted by 1.7 nm-sized Au DENs, and this was applied to catechin detection with a lower limit of 0.05 ± 0.003 μM. The quasi-reversible peak of the Cu redox center of laccase was observed at -0.03/0.13 V vs. AgCl, and the electron-transfer rate constant was 1.28 s^{-1} (Figure 109).[1688]

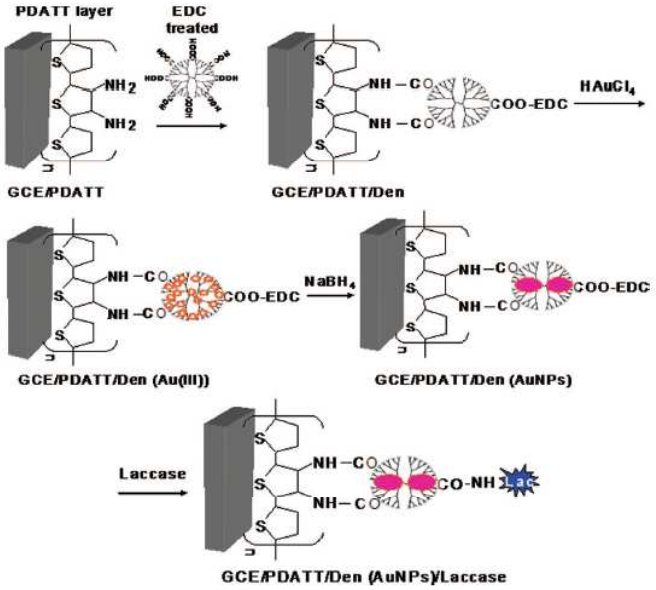

Figure 109. Schematic representation of the fabrication of PDATT/Den(AuNPs)/laccase-modified electrode. Reprinted with permission of the American Chemical Society (ref. 1688, Shim's group).

Poly(dimethylsiloxane) elastomers were surface modified with both polyoethylene oxide and G_3-DAB dendrimers, and these dendrimers were used as linkers for surface grafting of cell adhesion peptides including endothelial cells.[1689]
Although redox cycling of enzymatically amplified electroactive species has been widely employed for signal amplification in electrochemical biosensors, Au electrodes are generally not suitable for redox cycling using a redox reagent because of the high background current due to the redox reaction of the reagent at highly electrocatalytic Au electrodes. Thus, Au electrodes were modified with a mixed-assembly monolayer of mercaptododecanoic acid and mercaptoundecanol and a partially ferrocenyl-tethered dendrimer layer. The SAM of long thiols significantly decreases the background current of the modified Au electrode, and the ferrocenyl modification facilitates easy oxidation of *p*-aminophenol and its redox cycling using NAD (NADH) that enables low detection limit for mouse IgG (1 pg/mL).[1690]

7. Conclusion and prospects

Dendritic macromolecules, pioneered in the 1980's, have been developed in a variety of ways that involve molecular engineering in order to target precise functions and applications. Their physical and photophysical studies have led to the disclosure of supramolecular properties that are the basis of functional use. These properties, reviewed in the first four sections, have shown the crucial role of the generation number and peripheral groups. In particular, when the generation number increases, the dendrimer becomes globular, the periphery becomes bulkier despite backbonding of the terminal groups, and possibilities of encapsulation and dendrimer-substrate interactions (surface, medium, other dendrimer, etc.) also increase. The nature of the peripheral groups governs the solubility and related biological properties such as biocompatibility and, for instance with PEG, the enhanced penetration and retention (EPR) effect. Although properties of dendrimers may vary from one series to the next, these two properties appear to be more important than the nature of the core that is hidden within the dendritic structure. Most of the studies have been carried out using the PAMAM dendrimers, because they were commercialized very early after their discovery in the 1980's and can be functionalized in a variety of ways. The PAMAM dendrimers are also useful for most applications in catalysis, molecular electronics, photonics, sensing and nanomedicine. Several other dendrimer families are equally useful, however, such as the polylysine, PPI, polyether, polyamine, melanine, polyaryl, phenylazomethine, phosphorus, peptide and glycopeptide dendrimer families depending on which property, function, or application is targeted. Biodegradable polyether dendrimers are of prime importance in future biomedical applications. Indeed, encapsulation properties depend on whether the dendrimer frame is rigid or flexible, and in the latter case on the medium (solvent), the nature of which governs tether contraction. Modeling studies are becoming more and more frequent to predict, define and optimize the dendrimer features and properties.

The photophysical applications of dendrimers include light harvesting with the antenna effect to funnel energy from many photosensitive branch termini towards the focal group of the dendron, organic light-emitting diodes (OLEDs, organic field effect transistors (OFETs) and photovoltaic (PV) devices. A crucial point in these photophysical dendrimer devices is that quenching the photoactivity of the core is inhibited by the dendrimer tether framework, which provides a considerable advantage compared to regular polymers. Green phosphorescent dendrimers providing highly efficient OLEDS make an important application. The photophysical properties are a powerful source of sensors, as also are the redox properties using for instance the ferrocenyl groups located at the dendrimer branch termini for anion and glucose sensing. Photochemical, redox, and *pH* switches are useful for such sensing, the

dendrimer behaving then as a molecular machine considerably changing structure upon application of one of these stimuli. Dendrimer effect, i.e. generation-depending properties, are spectacular in this area. The photophysical field is also intimately connected to the biomedical applications, because fluorescence is essential for diagnostics.
Catalysis is another important application of dendrimers, because the location of catalytic sites at the dendritic core or periphery offers unique topological aspects allowing to mimic the enzyme catalytic site when the catalytic center is buried and protected at the core by the dendrimer frame or to multiply the number of catalytic sites within a small place when the catalyst is located at the periphery. The macromolecular size of these dendritic catalysts also allows easy removal from the medium and recycling using a solid support, membrane nanofiltration, precipitation or biphasic systems. Various dendritic effects were observed and are precious mechanistic information's to understand and optimize the catalytic constraints. Here again, encapsulation plays a key role, because small catalytically active transition-metal nanoparticles can be embedded in the dendritic nanoreactor that dictates its specific properties. Another interesting effect is the positive dendritic effect brought about by the polarity gradient in the framework in dendritic organocatalysis. It should be noted that the catalysis by dendrimers is also important for the biomedical applications, because many biosensors involve redox catalysis with electrodes modified with redox active dendrimers.

Last, but not least, the role of dendrimer in biomedical applications i.e. nanomedicine is bursting. Again, the supramolecular properties of dendrimers govern the functions. They are involved in drug encapsulation and solubilization in so-called supramolecular "complexes" for vectorization although "conjugates" resulting from covalent dendrimer-drug binding are often preferred for efficient delivery. They are also governing dendrimer-DNA interaction for gene transfection using ionic bonding between the ammonium groups of the dendrimer termini and the anionic phosphate DNA groups. They are essential in the crucial role of PEG chain termini of dendrimers for the biocompatibility, biodistristribution and EPR effect of these groups. They can also be found in the anti-bacterial "cluster effect" of glycopeptide dendrimers and in the overexpression of folate, glycosides and specific peptide receptors by tumor cells. These supramolecular properties of dendrimers are thus involved in both great domains of dendrimers applications in nanomedicine: diagnostic (with fluorescence) and therapy (with vectorization), targeting functions being needed in both area in which the benefits of dendrimers include the multiplication of active terminal groups in a minimal space. The precise molecular definition of dendrimers including the choice of generation number and terminal groups and the possibility to introduce two or more functional group types at the periphery are enormous advantages of dendrimers over polymers. This is the reason why dendrimers represent a true hope to largely improve diagnostic and therapeutic facilities for major human diseases. Toxicity remains a crucial issue, however, that needs by taken care of. In this review, we have delineated the toxicity issues in many instances, but broad investigations are continuously required in order to bring dendrimers to human drugs. The advent on the market of Vivagel^{TM} (Starpharma), a poly(L-lysyne)-dendrimer based microbiocide against HIV and herpes infections represents a first success that will undoubtedly be followed by others.
To conclude, if in chemistry the XVIIIth century was that of atoms, the XIXth century that of compounds, the XXth century that of reactions, the XXIth century already is and will be that of nanoscience engineering, and dendrimers are therefore a major family of tools in the tool box.

8. Acknowledgement.
Financial support from the Institut Universitaire de France (IUF, DA), the Agence Nationale de la Recherche (ANR, Ph. D. grant to EB), the Fundação para a Ciência e a Technologia

(FCT), Portugal (PhD grant to CO), the Université Bordeaux 1 and the Centre National de la Recherche Scientifique (CNRS, DA) is gratefully acknowledged.

9. List of abbreviations

A	Acceptor chromophore
AFM	Atomic Force Microscopy
AIDS	Acquired Immune Deficiency Syndrome
ALA	5-AminoLevulinic Acid
AM	Air Mass
ANS	8-Aniline-1-Naphtalene Sulfonate
APC	Antigen-Presenting Cell
ATP	Adenosine TriPhosphate
BARF	tetrakis(3,5-bis(trifluoromethyl)phenyl)borate
BINAP	2,2'-bis(diphenylphosphino)-1,1'-BINAPhthyl
BINAL	BINaphthol-modified lithium ALuminum
BNCT	Boron Neutron Capture Therapy
Boc	t-ButOxyCarbonyl
CCRF-CEM	Human T cell lymphoblast-like cell line
CD	CycloDextrin
CFMR	Continuous-Flow Membranes Reactor
CHO	Chinese Hamster Ovary
CID-MS	Collision-Induced Dissociation Mass Spectroscopy
CPK	Corey, Pauling and Koltun
CPP	Cell-Penetrating Peptides
CSA	Chondroitin Sulfate A
CT	Computed Tomography
CV	CycloVoltammetry
D	Donor chromophore
DAB	DiAmino Butane
DC	Dendritic Cell
DEA	DiElectric Analysis
DEN	Dendrimer-Encapsulated Nanoparticle
DFT	Density Functional Theory
DLS	Dynamic Light Scattering
DMAP	4-DiMethylAminoPyridine
DMF	DiMethylFormamide
DNA	DeoxyriboNucleic Acid
DOSY	Diffusion-Ordered SpectroscopY
DOT	Dendritic OligoThiophene
DOTA	N,N',N",N"'-tetracarboxymethyl-1,4,7,10-tetraazacyclododecane
DSC	Differential Scanning Calorimetry
DSR	Dielectric Relaxation Spectroscopy
ECM	Extracellular Cell Matrix
EDS	Energy-Dispersed X-ray Spectrocopy
EGFR	Epidermal Growth Factor Receptor
ELISA	Enzyme Linked ImmunoSorbent Assay
EO	Electro-Optic
EPR	Enhanced Penetration and Retention
ESR	Electron Spin Resonance
EXAFS	Extended X-Ray Absorption Fine Structure

Fmoc	9-FluorenylMethylOxyCarbonyl
FRET	Fluorescence Resonance Energy Transfer
FTIR	Fourier Transform InfraRed
5-FU	Fluorouracile
Gn	number of generations
GFP	Green Fluorescent Protein
GI	GastroIntestinal
GOx	Glucose Oxidase
GSH	Glutathione
HA	HemAgglutinin
HEK	Human Embryonic Kidney
HepG2	Human hepatocellular liver carcinoma cell line
HIV	Human Immunodeficiency Virus
HOMO-LUMO	Highest Occupied Molecular Orbital - Lowest Unoccupied Molecular Orbital
HOPG	Highly Oriented Pyrolytic Graphite
HRTEM	High-Resolution Transmission Electron Microscopy
IC_{50}	Half Maximal Inhibitory Concentration
IgG	Immunoglobulin G
IPEC-J2	Intestinal Pig Epithelial Cell Jejenum
IR	InfraRed
ITO	Indium Tin Oxide
L-DOPA	L-DihydrOxyPhenylAlanine
LED	Light-Emitting Diodes
LH	Luteinizing hormone
MAG	Multiple Antigen Glycopeptide
MAO	MethylAluminOxane
MAP	Multiple Antigen Peptide
MDO	Mannosylated Dendrimer Overalbumin
MNP	Metal NanoParticle
MRI	Magnetic Resonance Imaging
MTX	MethoTreXate
MV^{2+}	MethylViologen
NAD	Nicotinamide Adenine Dinucleotide
NCAFM	Non-Contact Atomic Force Microscopy
NLO	NonLinear Optical
NMR	Nuclear Magnetic Resonance
NP	NanoParticle
NSAID	Non-Steroidal Anti-Inflammatory Drug
OFET	Organic Field-Effect Transistors
OLED	Organic Light-Emitting Diode
OVA	OVAlbumin
PAMAM	PolyAmido Amine
PBMC	Peripheral Blood Mononuclear Cells
PCBM	[6,6]-Phenyl C_{60} Butyric Acid Methyl Ester
PD	PharmacoDynamic
pD	polyDispersity
PDT	PhotoDynamic Therapy
PEG	PolyEthylene Glycol
PEI	Poly(EthyleneImine)
PET	Positron Emitting Tomography

PFM-AFM	Pulse Force Mode Atomic Force Microscopy
PGLSA	Poly(GLycerol Succinic Acid)
PGSE	Pulse Gradient Stimulated Echo
PK	PharmacoKinetics
PL	Photo Luminescence
PLP	ProteoLipid Proteins
PMMA	Dendrimer-Poly(Methyl Metacrylate)
POM	PolyOxo Metallate
PPAR	Peroxisome Proliferator-Activated Receptor
PPI	Poly(Propylene Imine)
PPP	Poly-*p*-Phenylene
PSMA	Prostate Specific Membrane Antigen
PV	PhotoVoltaic
PVP	Poly(VinylPyrrololidone)
RBC	Red Blood Cell
RCM	Ring Closing Metathesis
REDOR	Rotational-Echo-Double-Resonance NMR
R_G	Gyration radius
RGD	Arginine-Glycine-Aspartic Acid
RNA	RiboNucleic Acid
RNAi	RiboNucleic Acid interference
RNase	RiboNuclease
ROM	Ring Opening Metathesis
ROMP	Ring Opening Metathesis Polymerization
ROS	Reactive Oxygen Species
SA	Sialic Acid
SANS	Small Angle Neutron Scattering
SAM	Self Assembled Monolayers
SAXS	Small Angle X-Rays Scattering
SBA	Santa Barbara Amorphous silica
SEC	Size Exclusion Chromatography
SEM	Scanning Electron Microscope
SiRNA	Interfering RiboNucleic Acid
SPIO	SuperParamagnetic Iron Oxide
TADDOL	α,α,α',α'-TetraAryl-1,3-Dioxolane-4,5-DimethanOL
TAMRA	6- 6-carboxytetramethylrhodamine succinic ester
TDD	Transdermal Drug Delivery
TEM	Transmission Electron Microscopy
Tg	Glass transition Temperature
THG	Third Harmonic Generation
TNT	2,4,6-TriNitroToluene
TOF	TurnOver Frequency
TON	TurnOver Number
TPA	Two-Photon Absorption
TPI	Two-Photon Ionization
TTF	TetraThiafulvalene
TU-DTPA	2-(4-isothiocyanatobenzyl)-6-methyldiethylene triaminepentaacetic acid
UV	UltraViolet
UV-vis	UltraViolet-Visible
VEGF	Vascular Endothelial Growth Factor

WAXD	Wide angle X-ray Diffraction
XNOR	Exclusive-NOR
XOR	Exclusive-OR
XPS	X-ray Photoelectron Spectroscopy

10. References

1. Newkome, G. R.; Moorefield, C. N.; Vögtle, F. *Dendrimers and Dendrons. Concepts, Syntheses, Applications*, Wiley-VCH, Weinheim, 2001.
2. *Dendrimers and Other Dendritic Polymers*, Tomalia, D. A.; Fréchet; J. M. J. Eds; Wiley: Amsterdam, 2003.
3. Lehn, J.-M. *Supramolecular Chemistry: Concepts and Perspectives*, VCH, Weinheim, 1995.
4. Buhleir, E.; Wehner, W.; Vögtle, F. *Synthesis*, **1978**, *155*-158.
5. Astruc, D.; Hamon, J.-R.; Althoff, G.; Román, E.; Batail, P.; Michaud, P.; Mariot, J.-P.; Varret, F.; Cozak, D. *J. Am. Chem. Soc.*, **1979**, *101*, 5445-5447.
6. Denkewalter, R. G.; Kolc, J. F.; Lukasavage, W. J. US Patent, **1983**, 4 410688 53; *Chem. Abstr.* **1984**, *100*, 103 907 p.24.
7. Tomalia, D. A., Baker, H, Dewald, J.; Hall, M., Kallos, G.; Martin, S.; Roeck, J., Ryder, J; Smith, P. *Polym. J.* **1985**, *17*, 117-132.
8. Newkome, G. R.; Yao, Z.; Baker, G. R.; Gupta, V. K. *J. Org. Chem.* **1985**, *50*, 2003-2004.
9. Tomalia, D. A.; Naylor, A. M.; Goddard III, W. *Angew. Chem., Int. Ed.* **1990**, *29*, 138-175.
10. Jansen, J. F. G. A., de Brabander-van den Berg, E. M. M.; Meijer, E W. *Science*, **1999**, *266*, 1226-1229.
11. *Advances in Dendritic Molecules*, Newkome, G. R. Ed., JAI Press, Greenwich, Vols 1, 2, 3, 4 and 5, resp. 1994, 1995, 1996, 1999 and 2002.
12. Vögtle, F.; Richardt, G.; Werner, N. *Dendrimer Chemistry: Concepts, Syntheses, Properties, Applications,* Wiley: Weinheim, 2009.
13. *Dendrimer I, II and III*. Vögtle, F. Ed. Springer, Berlin, resp. 1998, 2000, 2001.
14. Newkome, G. R.; Yao, Z.-q.; Baker, J. R., Jr.; Gupta, G. A.; Russo, P. S.; Saunders, M. J. *J. Am. Chem. Soc*. **1986**, *108*, 849-850.
15. Newkome, G. R.; Moorefield, C. N. *Aldrichim. Acta*, **1992**, *25* (2), 31-38.
16. Newkome, G. R. *Pure Appl. Chem.* **1998**, *70*, 2337-2343.
17. Tomalia, D. A.; Dupont Durst, H. *In Topics Curr. Chem., Supramolecular Chemistry, Directed Synthesis and Molecular Recognition*, Weber, E. Ed.; Springer: Berlin, **1993**, *165*, 193-313.
18. Tomalia, D. A. *Materials Today* **2005**, *8*, 34-46.
19. Ardoin, N.; Astruc, D. *Bull Soc Chim. Fr.* **1995**, *132*, 875-909.
20. Matthews, O. A.; Shipway, A. N.; Stoddart, J. F. *Prog. Polym. Sci.* **1998**, *23*, 1-56.
21. Newkome, G. R.; He, E.; Moorefield, C. N. *Chem. Rev.* **1999**, *99*, 1689-1746.
22. Bosman, A. W.; Janssen, H. M.; Meijer, E. W. *Chem. Rev.* **1999**, *99*, 1665-1688.
23. Hawker, C.; Fréchet, J. M. J. *Chem. Commun.* **1990**, 1010-1013.
24. Hawker, C. J.; Frechet, J. M. J. *J. Am. Chem. Soc.* **1990**, *112*, 7638-7647.
25. Miller, T. M.; Neeman, T. X. *Mater. Chem.* **1990**, *2*, 346-349.
26. Fréchet, J. M. J. *Science* **1994**, *263*, 1710-1715.
27. Fréchet, J. M. J. *Science*, **1995**, *269*, 1080-1083.
28. Hecht, S.; Fréchet, J. M. J. *Angew. Chem., Int. Ed. Engl.* **2001**, *40*, 74-91.
29. Grayson, S. M.; Fréchet, J. M. J. *Chem. Rev.* **2001**, *101*, 3819-3867.
30. Fréchet, J. M. J. *Pure Appl. Chem.* **1999**, *A33*, 1399-1425.

31. Issberner, J.; Moors, R.; Vögtle, F. *Angew. Chem., Int. Ed.* **1994**, *33*, 2413-2420.
32. Fischer, M.; Vögtle, *Angew. Chem., Int. Ed.* **1999**, *38*, 884-905.
33. Friedhofen, J.; Vögtle, F. *New J. Chem.* **2006**, *30*, 32-43.
34. Chow, H.-F.; Mong, K.-K.; Nongrum, M. F.; Wan, C.-W. *Tetrahedron* **1998**, *54*, 8543-8660.
35. Bauer R. E.; Grimsdale, A. C.; Müllen, K. *Top. Curr. Chem.* **2005**, *245*, 253-286.
36. Feng, C. L.; Yu, Y.; Zhong, X. H.; Steinhart, M.; Majoral, J.- P.; Knoll, W. *Adv. Sci. Nanotechnol*. **2008**, *55*, 84-90.
37. Gudat, D. *Angew. Chem., Int. Ed. Engl.* **1997**, *36*, 1951.
38. Caminade, A.-M.; Majoral, J.-P. *Chem. Rev.* **1999**, *99*, 845-880.
39. *Dendrimers and Nanoscience*, Astruc, D. Ed., C. R. Chimie, **2003**, *6*.
40. Astruc D. *Pure Appl. Chem*. **2003**, *75*, (4), 461-481.
41. Tomalia, D. A. *Adv. Mat.* **1994**, *6*, 529-539.
42. Dvornic, P. R. *J. Polym. Sci.: A Polym. Chem.* **2006**, *44*, 2755-2773.
43. Tomalia, D. A. *Mater. Today* **2005**, *8*, 34-46.
44. Meltzer, A. D.; Tirrel, D. A.; Jones, A. A.; Inglefield, P. T.; Hedstrand, D. M.; Tomalia, D. A. *Macromolecules* **1992**, *25*, 4541-4548**.**
45. Mijovic, J.; Ristic, S.; Kenny, J. *Macromolecules* **2007**, *40*, 5212-5221.
46. Chase, P. A.; Gebbink, R. J. M. Klein; van Koten, G. *J. Organom. Chem.* **2004**, *689*, 4016-4054.
47. Schlüter, A. D.; Rabe, P. J. *Angew. Chem., Int. Ed. Engl.* **2000**, *39*, 864-883.
48. Flory, P. J. *Principles of Polymer Chemistry*, Cornell University Press: Ithaca, **1953**.
49. Voit, B. I. *C. R. Chimie*, **2003**, *6*, 821-832.
50. De Gennes, P. G.; Hervet, H. *J. Phys. Lett.* **1983**, *44*, 351-360.
51. Zooks, T. C.; Pickett, *G. Phys. Rev. Lett.* **2003**, *90*, 105502.
52. Lescanec, R. L.; Muthucumar, M. *Macromolecules*, **1990**, *23*, 2280-2288.
53. Ballauff, M.; Likos, C. N. *Angew. Chem., Int. Ed.* **2004**, *43*, 2998-3020.
54. Ruiz, J.; Lafuente, G.; Marcen, S.; Ornelas, C.; Lazare, S.; Cloutet, E.; Blais, J.-C.; Astruc, D. *J. Am. Chem. Soc*. **2003**, *125*, 7250-7257.
55. Higgins, J. S., Benoit, H. C. *Polymers and Neutron Scattering*. Clarenden Press: Oxford.
56. Pötschke, D.; Ballauff, M. *In Structure and Dynanics of Polymers and Colloidal Systems,* Borsali R; Pecora, R. Eds.; Kluwer: Dordrecht, **2002**.
57. Pötschke, D.; Ballauff, M.; Lindner, P.; Fischer M.; Vögtle, F. *Macromolecules.* **1999**, *32*, 4079-4087.
58. Ballauff, M. *Top. Curr. Chem.*, **2001**, *212*, 177-194.
59. Likos, C. N.; Ballauff, M. *Top. Curr. Chem.* **2005**, *245*, 239-252.
60. Chen, W. R.; Porcar, L.; Liu, Y.; Butler, P. D.; Magid L. J. *Macromolecules* **2007**, *40*, 5887-5898.
61. Topp, A.; Buer B. J.; Tomalia D. A.; Amis, E. J. *Macromolecules* **1999**, *32*, 7232-7237.
62. Huang, Q. R.; Dubin, P. L.; Lal, J.; Moorefield, C. N.; Newkome, G. R. *Langmuir* **2005**, *21*, 2737-2742.
63. Seyrek E.; Dubin, P. L.; Newkome, G. R. *J. Phys. Chem B* **2004**, *108*, 10168-10171.
64. Naidoo, K. J.; Hugues, S. J.; Moss, J. R. *Macromolecules*, **1999**, *32*, 331-332.
65. Welch, P.; Muthukumar, M. *Macromolecules*, **1998**, *31*, 5892-5897.
66. Chen, W.; Tomalia, D. A.; Thomas, J. L. *Macromolecules* **2000**, *33*, 9169-9172.
67. Lee, I.; Athey, D. B.; Wetzel, A. W.; Meixner, W.; Baker, J. R., Jr. *Macromolecules* **2002**, *35*, 4510-4520.
68. Karatasos, K.; Luylin, A. V. *J. Chem. Phys.* **2006**, *125*, 184907-1 – 184907-9.

69. Karatasos, K. *Macromolecules*, **2006**, *39*, 4619-4626.
70. Cheng, L.; Cao, D. *J. Phys. Chem. B* **2007**, *111*, 9218-9227.
71. Bosko, J. T.; Todd, B. D.; Sadus, R. J. *J. Chem. Phys.* **2006**, *124*, 044910/1-044910/6.
72. Paulo, P. M. R.; Lopes J. N. C.; Costa, S. M. B. *J. Phys. Chem. B* **2007,** *111*, 10651-10664.
73. Suman, B.; Kumar, S. *J. Phys. Chem. B.* **2007**, *111*, 8728-8739.
74. Carbone, P.; Calabretta, A.; Di Stefano, M.; Negri, F.; Müllen, K. *J. Phys. Chem. A* **2006**, *110*, 2214-2224.
75. Brocorens, P.; Lazzaroni, R.; Bredas, J.-L. *J. Phys. Chem. B.* **2007**, *127*, 9218-9227.
76. Harnau, L.; Rosenfeldt, S.; Ballauff, M. *J. Chem. Phys.* **2007**, *127*, 014901-1 – 014901-6.
77. Gorman, C. B.; Smith, J. C. *Polym.* **2000**, *41*, 675-683.
78. Daniel, M.-C.; Sakamoto, A.; Ruiz, J.; Astruc, D.; Nishihara, H. *Chem. Lett*., **2006** *, 35,* 38-39.
79. Murat, M.; Grest, G. S. *Macromolecules*, **1996**, *29*, 1278-1285.
80. Welch, P.; Muthukumar, M. *Macromolecules*, **1998**, *31*, 5892-5897.
81. Mourey, T. H.; Turner, S. R.; Rubinstein, M.; Fréchet, J. M. J.; Hawker, C. J.; Wooley, K. L. Macromolecules, **1992**, *25*, 2401-2406.
82. Wooley, K. L.; Hawker, C. J.; Pochan, J. M.; Fréchet, J. M. J. *Macromolecules*, **1993**, *26*, 1514-1519.
83. Wooley, K. L.; Klug, C. A.; Tasaki, K.; Schaefer, J. *J. Am. Chem. Soc*. **1997**, *119*, 53-58.
84. Gorman, C. B.; Hager, M. W.; Parkhurst, B. L.; Smith, J. C. *Macromolecules* **1998**, *31*, 815-822.
85. De Backer, S.; Prinzie, Y.; Verheijen, W.; Smet, M.; Desmedt, K.; Delahen, W.; De Schryver, F. C. *J. Phys. Chem.* **1998**, *102*, 5451-5459.
86. Percec, V.; Johansson, G.; Ungar, G.; Zhou, J. *J. Am. Chem. Soc.* **1996**, *118*, 9855-9866.
87. Percec, V.; Chu, P., Ungar, G.; Zhou, J. *J. Am. Chem. Soc.* **1995**, *117*, 11441-11454.
88. Balagurusamy, V. S. K.; Ungar, G.; Percec, V.; Johansson, G. *J. Am. Chem. Soc.* **1997**, *119*, 1539-1555.
89. Hudson, S. D.; Jung, H.-T.; Percec, V.; Cho, W.-D.; Johansson, G.; Ungar, G.; Balagurusamy, V. S. K. *Science*, **1997**, *278*, 449-452.
90. Tomalia, D. A.; Hall, V. B.; Hedstrand, D. M. *Macromolecules* **1987**, *20*, 1167-1169.
91. Dubin, P. L.; Edwards, S. L.; Kaplan, J. I.; Mehta, M. S.; Tomalia, D. A.; Xia, J. *Anal. Chem.* **1992**, *64*, 2344-2347.
92. Meltzer, A. D.; Tirrel, D. A.; Jones, A. A. Ingelfield, P. T.; Herstrand, D. M.; Tomalia, D. A. *Macromolecules*, **1992**, *25*, 4541-4546.
93. Uppuluri, S.; Keinath, S. E., Tomalia, D. A.; Dvornic, P. R. *Macromolecules* **1998**, *31*, 4498-4510.
94. Bosman, A. W.; Bruining, M. J.; Koojman, H.; Spek, A. L.; Janssen, R. A. J.; Meijer, E. W. *J. Am. Chem. Soc.* **1998**, *120*, 8547-8548.
95. Pavlov, G. M.; Korneeva, E. V.; Meijer, E. W. *Colloid. Polym. Sci.* **2002**, *280*, 416-423.
96. Cantor, C.; Schimmel, P. *Biophysical Chemistry*. Freeman, San Francisco, **1980**.
97. Hawker, C. J.; Malmström, E. E.; Franck, C. W.; Kamf, J. P. *J. Am. Chem. Soc.* **1997**, *119*, 9903-9904.
98. Giupponi, G.; Buzza, D. M.. A.; Adolf, D. B. *Macromolecules* **2007**, *40*, 5959-5965.
99. Zhuang, W.; Kasemi, E.; Ding, Y.; Kroeger, M.; Schlüter, A. D.; Rabe, J. P. *Adv. Mater*. **2008**, *20*, 3204-3210.

100. Blaak, R.; Lehmann, S.; Likos, C. N. *Macromolecules* **2008**, *41*, 4452-4458.
101. Li, M.; Li, Y.; Zeng, Y.; Chen, J.; Li, Y. *J. Phys. Chem. C* **2009**, *113*, 11554-11559.
102. Newkome, G. R.; Baker, G. R.; Saunders, M. J.; Russo, P. S.; Gupta, V. K.; Yao, Z.-K.; Miller, J. E.; Buillon, K. J. *Chem. Commun.* **1986**, 752-753.
103. Newkome, G. R.; Baker, G. R.; Arai, S.; Russop, P. S.; Theriot, K. J.; Moorefield, C. N.; Rogers, L. E.; Miller, J. E.; Lieux, T. R. Murray, M. E.; Phillips, B.; Pascal, L. *J. Am. Chem. Soc.* **1990**, *112*, 8458-8465.
104. Newkome, G. R.; Moorefield, C. N.; Baker, G. R.; Behera, R. K., Escamillia, G. H.; Saunders, M. J. *Angew. Chem., Int. Ed. Engl.* **1992**, *31*, 917-919.
105. Engelhard, T.-P.; Belkoiura, L.; Woermann, D. *Ber. Bunsenges. Phys. Chem.* **1996**, *100*, 1064-1072.
106. Han Yu, K.; Russo, P. S.; Younger, L.; Henk, W. G.; Hua, D.-W.; Newkome, G. R.; Baker, G. *J. Polym. Sci.: Part B: Polym. Phys.* **1997**, *35*, 2787-2793.
107. Masuo, S.; Yoshikawa, H.; Asahi, T.; Mashara, H..; Sato, T.; Jiang, D.-L.; Aida, T. *J. Phys. Chem.* **2002**, *106*, 905-909.
108. Hirst, A. R.; Smith, D. K. *Top. Curr. Chem.* **2005**, *256*, 237-273.
109. Klok, H.-A.; Hwang, J. J.; Hartgerink, J. D.; Stupp, S. I. *Macromolecules* **2002**, *35*, 6101-6111.
110. Jang, W. D.; Aida, T. *Macromolecules* **2003**, *36*, 8461-8469.
111. Li, W.-S.; Jia, X.-R.; Wang, B.-B.; Ji, Y.; Wei, Y. *Tetrahedron* **2007**, *63*, 8794-8800.
112. Gao, M.; Kuang, G.-C.; Jia, X.-R.; Li, W.-S.; Li, Y.; Wei, Y. *Tetrahedron Lett.* **2008**, *49*, 6182-6187.
113. Percec, V.; Peterca, M.; Yurchenko, M. E.; Rudick, R. G.; Heinzey, P. A. *Chem. Eur. J.* **2008**, *14*, 909-918.
114. Chen, Y.; Lv, Y.; Han, Y.; Zhu, B.; Zhang, F.; Bo, Z.; Liu, C.-Y. *Langmuir* **2009**, 25, 8548-8555.
115. Hawker, C. J.; Malmström, E. E.; Frank, C. W.; Kampf, J. P. *J. Am. Chem. Soc.* **1997**, *119*, 9903-9904.
116. Stewart, G. M.; Fox, M. A. *Chem. Mater.* **1998**, *10*, 860-863.
117. Kim, Y. H.; Webster, O. W. *Macromolecules* **1992**, *25*, 5561-5572.
118. Massa, D. J.; Shriner, K. A.; Turner, S. R.; Voit, B. I. *Macromolecules*, **1995**, *28*, 3214-3220.
119. Emran, S. K.; Liu, Y.; Newkome, G. R.; Harmon, J. P. *J. Polym. Sci.: Part B: Polym. Phys.* **2001**, *39*, 1381-1393.
120. Gitsov, I.; Wooley, K. L.; Fréchet, J. M. J. *Angew. Chem., Int. Ed.* **1992**, *31*, 1200-1202.
121. vanHest, J. C. M.; Delnoye, D. A. P.; Baars, M. W. P. L.; Vangenderen, M. H. P.; Meijer, E. W. *Science* **1995**, *268*, 1592-1595.
122. Zhu, L. Y.; He, Y.; Zhu, G. L.; Li, M. Z.; Wang, E. J.; Zhu, R. P.; Qi, X. *Acta Chim. Sin.* **2001**, *59*, 1484-1489.
123. Zhu, L. Y.; Zhu, G. L.; Li, M. Z.; Wang, E. J.; Zhu, R. P.; Qi, X. *Eur. J. Polym.* **2002**, *38*, 2503-2506.
124. Zubarev, E. R.; Pralle, M. U.; Sone, S. D.; Stupp, S. I. *J. Am. Chem. Soc.* **2001**, *123*, 4105-4106.
125. Zubarev, E. R.; Sone, S. D.; Stupp, S. I. *Chem. Eur. J.* **2006**, *12*, 7313-7327.
126. Messmore, B. W.; Sukerbar, P. A.; Stupp, S. I. *J. Am. Chem. Soc.* **2005**, *127*, 7992-7993.
127. Palmer, L. C.; Stupp, S. I. *Acc. Chem. Res.* **2008**, *41*, 1674-1684.
128. Newkome, G. R.; Moorefield, C. N.; Baker, G. R.; Saunders, M. J.; Grossman, S. H. *Angew. Chem., Int. Ed. Engl.* **1991**, *30*, 1178-1180.

129. Slaney, M.; Bardaji, M.; Casanove, M-J.; Caminade, A.-M.; Majoral, J.-P.; Chaudret, B. *J. Am. Chem. Soc.* **1995**, *117*, 9764-9765.
130. Lorenz, K.; Müllhaupt, R.; Frey, H.; Rapp, U.; Mayer-Posner, F. J. *Macromolecules*, **1995**, *28*, 6657-6661.
131. Buchko, C. J.; Wilson, P. M.; Xu, Z.; Zhang, J.; Moore, J. S.; Martin, D. C. *Polymer*, **1995**, *36*, 1817-1826.
132. Moore, J. S. *Acc. Chem. Res.* **1997**, *30*, 402-413.
133. Kackson, C. L.; Chanzy, H. D.; Booy, F. D.; Drake, B. J.; Tomalia, D. A.; Bauer, B.; Amis, E. J. *Macromolecules* **1998**, *31*, 6259-6265.
134. Tsuruk, V. T. *Adv. Mater.* **1998**, *10*, 253-257.
135. Sheiko, S. S.; Muzafarov, A. M.; Winkler, R. G.; Getmanova, E.; V.; Eckert, G.; Reineker, P. *Langmuir*, **1997**, *13*, 4172-4181.
136. Tan, S.; Su, A.; Ford, W. T. *Soft Matter* **2008**, *27*, 205-211.
137. Saville, P. M.; White, J. W.; Hawker, C. J.; Wooley, K. L.; Fréchet, J. M. J. *J. Phys. Chem.* **1993**, *97*, 293-294.
138. Saville, P. M.; Reynolds, P. A. White, J. W.; Wooley, K. L.; Penfold, J.; Webster, J. R. P. *J. Phys. Chem.* **1995**, *99*, 8283-8289.
139. Sayed-Sweet, Y.; Hedstrand, D. M.; Spinder, R.; Tomalia, D. A. *J. Mater. Chem.* **1997**, *7*, 1199-1205.
140. Schenning, A. P. H.; Elissen-Roman, C.; Weener, J.-W.; Baars, M. W. P. L.; van der Gaast, S. J.; Meijer, E. W. *J. Am. Chem. Soc.* **1998**, *120*, 8199-8208.
141. Percec, V.; Chu, P.; Ungar, G.; Zhou, J. *J. Am. Chem. Soc.* **1995**, *117*,11441-11454.
142. Lorenz, K.; Hölter, D.; Stühn, B.; Müllhaupt, R.; Frey, H. *Adv. Mater.* **1996**, *8*, 414-416.
143. Bottomley, L. *Anal. Chem.* **1998**, *70*, 425R-475R.
144. McCarty, G. S.; Weiss, P. S. *Chem. Rev.* **1999**, *99*, 1983-1990.
145. Takano, H.; Kenseth, J. R.; Wong, S.-S.; O'Brien, J. C.; Porter, M. D. *Chem. Rev.* **1999**, *99*, 2845-2890.
146. Watanabe, S.; Regen, S. L. *J. Am. Chem. Soc.* **1994**, *116*, 8855-8856.
147. Evenson, S. A.; Badyal, J. P. S. *Adv. Mater.* **1997**, *9*, 1097-1099.
148. Li, J.; Piehler, L. T.; Baker, J. R. Jr.; Tomalia, D. A. *Langmuir* **2000**, *16*, 5613-5616.
149. Betley, T. A.; Banaszak Holl, M. M.; Orr, B. G.; Swanson, D. R.; Tomalia, D. A.; Baker, J. R., Jr. *Langmuir* **2001**, *17*, 2768-2773.
150. Li, J.; Qin, D.; Baker, J. R., Jr.; Tomalia, D. A. *Macrosymp.* **2001**, *167*, 257-269.
151. Miller, L. L.; Hashimoto, T.; tabakovic, I.; Swanson, D. S.; Tomalia, D. *Chem. Mart.* **1995**, *7*, 9-11.
152. Müller, T.; Yablon, D. G.; Karchner, R.; Knapp, D.; Kleinman, M. H.; Fang, H.; Durning, C. J.; Tomalia, D. A.; Turro, N. J.; Flynn, G. W. *Langmuir* **2002**, *1*, 7452-7455.
153. Zhang, H.; Grim, P. C. M.; Foubert, P.; Vosch, T.; Vanoppen, P.; Wiesler, U.-M.; Berresheim, A. J.; Müllen, K., De Schryver, F. C. *Langmuir* **2000**, *16*, 9009-9014.
154. Liu, D.; Zhang, H.; Grim, P. C. M.; De Feyter, S.; Wiesler, U.-M.; Berresheim, A. J.; Müllen, K.; De Schryver, F. C. *Langmuir* **2002**, *18*, 2385-2391.
155. Tully, D. C.; Wilder, K.; Fréchet, J. M. J.; Trimble, A. R.; Quate, C. F. *Adv. Mater.* **1999**, *11*, 314-318.
156. Tully, D. C.; Wilder, K.; Fréchet, J. M. J. *Chem. Mater* **1999**, *11*, 2892-2988.
157. Chang, D.; Rozkiewicz, D. I.; Jan Ravoo, B.; Meijer, E. W.; Reinhoudt, D. N. *Nano Lett.* **2007**, *7*, 978-980.
158. Martinovic, J.; Chiorcea-Paquim, A.-M.; Diculescu, V. C.; Van Wyk, J.; Iwuoha, E.; Baker, P.; Mapolie, S.; Oliveira-Brett, A.-M *Electrochem. Acta* **2008**, *53*, 4907-4919.

159. Bosko, J.; Prakash, J. R. *J. Chem. Phys.* **2008**, *128*, 034902.
160. Lehninger, A. L.; Nelson, D. L.; Cox, M. M.; *Principles of Biochemistry*; Worth Publishers: New York, **1993**.
161. Lewis, N. S.; Crabtree, G. W. Eds *Basic Research Needs for Solar Energy Utilization*.; Report of the Basic Energy Sciences Workshop on Solar Energy Utilization, April 18–21, **2005**, US Department of Energy Office of Basic Energy Sciences; **2005**; http://www.sc.doe.gov/bes/reports/abstracts.html#SEU.
162. Balzani, V.; Scandola, F. *Supramolecular Photochemistry*; Horwood: Chichester, **1991**.
163. Balzani, V.; De Cola, L. *Supramolecular Chemistry*, Kluwer: Dordrecht, **1992**.
164. Ahn, T. S.; Thompson, A. L.; Bharati, P.; Müller, A.; Bardeen, C. J. *J. Phys. Chem.* **2006**, *110*, 19810-19819.
165. Goddson III, T. G. *Acc. Chem. Res.* **2005**, *38*, 99-107.
166. Cho, S.; Li, W.-S.; Yoon, M.-C.; Ahn, T. K.; Jang, D.-L.; Kim, J.; Aida, T.; Kim, D. *Chem. Eur. J.* **2006**, *12*, 7576-7584.
167. Cotlet, M.; Masuo, S.; Luo, G.; Hofkens, J.; Van der Auweraer, M.; Verhoeven, J.; Müllen, K.; Xie, X.; De Schryver, F. *Proc. Nat. Ac. Sci.* **2004**, *101*, 14343-14248.
168. Furuta, P.; Brooks, J.; Thompson, M. E.; Fréchet, J. M. J. *J. Am. Chem. Soc.* **2003**, *125*, 13165-13172.
169. Turro, N. J. *Modern Molecular Photochemistry*, University Science Books: Sausalito, **1991**.
170. Campagna, S.; Denti, G.; Serroni, S.; Ciano, M.; Juris, A.; Balzani, V. *Inorg. Chem.* **1992**, *31*, 2982-2984.
171. Campagna, S.; Denti, G.; Serroni, S.; Ciano, M.; Balzani, V. *Inorg. Chem.* **1991**, *30*, 3728-3732.
172. Denti, G.; Campagna, S.; Serroni, S.; Ciano, M.; Balzani, V. *J. Am. Chem. Soc.* **1992**, *114*, 2944-2950.
173. Serroni, S.; Denti, G. *Inorg. Chem.* **1992**, *31*, 4251-4255.
174. Juris, A.; Balzani, V.; Barrigelletti, F.; Campagna, S.; Denti, G.; Juris, A.; Serroni, S.; Venturi, M. *Acc. Chem. Res.* **1998**, *31*, 26-34.
175. Belser, A.; von Zelewski, A.; Frank, M.; Seel, C.; Vögtle, F.; de Cola, L.; Barigelletti, F.; Balzani, V. *J. Am. Chem. Soc.* **1993**, *115*, 4076-3086.
176. Campagna, S.; Denti, G.; Serroni, Juris, A.; Venturi, M.; Ricevuto, V.; Balzani, V. *Chem. Eur. J.* **1995**, *1*, 211-221.
177. Serroni, S.; Juris, A.; Venturi, M.; Campagna, S.; Resino, I. R.; Denti, G.; Credi, A.; Balzani, V. J. *Mater. Chem.* **1997**, *7*, 1227-1236.
178. Balzani, V.; Campagna, S.; Denti, G.; Juris, A.; Serroni, S.; Venturi, M. *Acc. Chem. Res.* **1998**, *31*, 26-34.
179. Ceroni, P.; Vicinelli, V.; Maestri, M.; Balzani, V.; Lee, S.-k; van Heyst, J.; Gorka, M.; Vögtle, F. J. *Organomet. Chem.* **2004**, *689*, 4375-4383.
180. Balzani, V.; Ceroni, P.; Juris, A.; Venturi, M.; Campagna, S.; Puntoriero, F.; Serroni, S. *Coord. Chem. Rev.* **2001**, 219-221, 545-572.
181. Tsukube, H.; Suzuki, Y.; Paul, D.; Kataoka, Y.; Shinoda, S. *Chem. Commun.* **2007**, 2533-2535.
182. Yang, S.-P.; Lin, L.; Yang, L.-Z.; Chen, J.-M.; Chen, Q.-Q.; Cao, D.; Yu, X.-B. *J. Lumin.* **2007**, *126*, 515-530.
183. Lee, D. N.; Soh, B. K.; Kim, S. H.; Jun, Y. M.; Sook, Y.; Lee, W. Y.; Kim, B. H., *J. Organomet. Chem.* **2008**, *693*, 655-666.
184. Ceroni, P.; Bergamini, G.; Marchioni, F.; Balzani, V. *Prog. Polym. Sci.* **2005**, *30*, 453-473.

185. Serroni, S.; Campagna, S.; untoriero, F.; Loiseau, F.; Ricevuto, V.; Passalacqua, R.; Galletta, M. *In Dendrimers and Nanoscience*, Astruc, D. Ed.; Elsevier, Paris, C. R. Chimie, **2003**, *6*, 883-893.
186. D'Ambruoso, G. D.; McGrath, D. V. *Adv. Polym. Sci.* **2008**, *214*, 87-147.
187. Xu, Z.; Moore, J. S. *Angew. Chem., Int. Ed. Engl.* **1993**, *32*, 246-248.
188. Xu, Z.; Moore, J. S. *Angew. Chem., Int. Ed. Engl.* **1993**, *32*, 1354-1357.
189. Devadoss, C.; Bharati, P.; Moore, J. S. *J. Am. Chem.Soc.* **1996**, *118*, 9635-9644.
190. Shortreed, M. R.; Swallen, S. F.; Shi, Z.-Y.; Tan, W.; Xu, Z.; Devadoss, C.; Moore, J. S.; Kopelman, R. *J. Phys. Chem. B* **1997**, *101*, 6318-6322.
191. Bar-Haim, A.; Klafter, J.; Kopelman, R. *J. Am. Chem. Soc.* **1997**, *119*, 6197-6198.
192. Bar-Haim, A.; Klafter, J. *J. Phys. Chem. B* **1998**, *10* (2), 1662-1664.
193. Kawa, M.; Fréchet, J. M. *J. Chem. Mater.* **1998**, *10*, 286-296.
194. Kawa, M.; Fréchet, J. M. J. *Thin Solid Films*, **1998**, *331*, 259-263.
195. Andronov, A.; Fréchet, J. M. J. *Chem. Commun.* **2000**, 1701-1710.
196. Gilat, S. L.; Adronov, A.; Fréchet, J. M. J. *Angew. Chem., Int. Ed.* **1999**, *38*, 1422-1427.
197. Adronov, A.; Gilat, S. L.; Fréchet, J. M. J.; Ohta, K.; Neuwahl, F. V. R.; Fleming, G. R. *J. Am. Chem. Soc.* **2000**, *122*, 1175-1185.
198. Jiang, D.-L.; Aida, T. *J. Am. Chem. Soc.* **1998**, *120*, 10895-10901.
199. Jiang, D.-L.; Aida, T. *J. Am. Chem. Soc*. **1999**, *121*, 1064-10649.
200. Kimura, M.; Shiba, T.; Muto, T.; Shirai, K. *Macromolecules* **1999**, *32*, 8237-8239.
201. Matos, M. S.; Hofkens, J.; Verheijen, W.; De Schryver, F. C.; Hecht, S. K.; Pollak, W.; Fréchet, J. M. J.; Forier, B.; Dehaen, W. *Macromolecules* **2000**, *33*, 2967-2973.
202. Vijayalakshmi, N.; Maitra, U. *Macromol*. **2006**, *29*, 7931-7940.
203. Wang, P.-W.; Liu, Y.-J.; Devadoss, C.; Bharati, P.; Moore, J. S. *Adv. Mater.* **1996**, *8*, 237-241.
204. Put, E. J. H.; Clays, K.; Persoons, A.; Biemans, H. A. M.; Luijkx, C. P. M.; Meijer, E. W. *Chem. Phys. Lett.* **1996**, *260*, 136-141.
205. Bergamini, G.; Ceroni, P.; Maestri, M.; Balzani, V.; Lee, S.-K.; Vögtle, F. *Photochem. Photobiol. Sci.* **2004**, *3*, 898-905.
206. Marcacio, M.; Paolucci, F.; Paradisi, C.; Roffia, S.; Fontanesi, C.; Yellowlees, L. J.; Serroni, S.; Campagna, S.; Denti, G.; Balzani, V. *J. Am. Chem. Soc.* **1999**, *121*, 10081-10091.
207. Issberner, J.; Vögtle, F.; De Cola, L.; Balzani, V. *Chem. Eur. J.* **1997**, *3*, 706-712.
208. Plevoets, M.; Vögtle, F.; De Cola, L.; Balzani, V. *New J. Chem.* **1999**, *23*, 63-69.
209. Balzani, V.; Juris, A. *Coord. Chem. Rev.* **2001**, *211*, 97-115.
210. Flomenbom, O.; Amir, R. J.; Shabat, D.; Klafter, J. *J. Lumin.* **2005**, *111*, 315-325.
211. Balzani, V.; Bergamini, G.; Ceroni, P.; Vögtle, F. *Coord. Chem. Rev.* **2007**, *251*, 525-535.
212. Giansante, C.; Ceroni, P.; Balzani, V.; Vögtle, F. *Angew. Chem., Int. Ed*. **2008**, *47*, 5422-5425.
213. Moreno-Bondi, M. C.; Orellana, Turro, N. J.; Tomalia, D. A. *Macromolecules* **1990**, *23*, 910-912.
214. Glazier, S.; Barron, J. A.; Houston, P. L.; Abruna, H. D. *J. Phys. Chem.* **2002**, *106*, 9993-10003.
215. Gopidas, K. R.; Leheny, A. R.; Caminati, G.; Turro, N. J.; Tomalia, D. A. *J. Am. Chem. Soc.* **1991**, *113*, 7335-7342.
216. Turro, N. J.; Niu, S.; Boomann, S. H.; Tomalia, D. A. *J. Phys. Chem.* **1995**, *99*, 5512-5517.

217. Balzani, V.; Ceroni, P.; Gestermann, S.; Kauffmann, C.; Gorka, M.; Vögtle, F. *Chem. Commun.* **2000**, 853-854.
218. Vögtle, F.; Gestermann, S.; Kauffmann, C.; Ceroni, P.; Vicinelli, V.; De Cola, L.; Balzani, V. *J. Am. Chem. Soc.* **1999**, *121*, 12161-12166.
219. Vögtle, F.; Gestermann, S.; Kauffmann, C.; Ceroni, P.; Vicinelli, V.; Balzani, V. *J. Am. Chem. Soc.* **2000**, *122*, 10398-10404.
220. Prodi, L.; Bolletta, F.; Montalti, M.; Zaccheroni, N. *Eur. J. Chem.* **1999**, *3*, 455-460.
221. Aumanen, J.; Lehtovuori, V.; Werner, N.; Richardt, G.; van Heyst, J.; Vögtle, F.; Tommola-Korppi, J. *Chem. Phys. Lett.* **2006**, *433*, 75-79.
222. Han, U.; Gorka, M.; Vögtle, F.; Vicinelli, V.; Cerooni, P.; Maestri, M.; Balzani, V. *Angew. Chem., Int. Ed.* **2002**, *41*, 3595-3598.
223. Vivinelli, V.; Ceroni, P.; Maestri, M.; Balzani, V.; Gorka, M.; Vögtle, F. *J. Am. Chem. Soc.* **2002**, *124*, 6461-6468.
224. Branchi, B.; Ceroni, P.; Balzani, V.; Bergamii, G.; Klaerner, F. G.; Vögtle, F. *Chem. Eur. J.* **2009**, *15*, 7876-7882.
225. Saudan, C.; Balzani, V.; Ceroni, P.; Gorka, M.; Maestri, M.; Vicinelli, V.; Vögtle, F. *Tetrahedron* **2003**, *59*, 3845-3852.
226. Saudan, C.; Ceroni, P.; Vicinelli, V.; Maestri, M.; Balzani, V.; Gorka, M.; Lee, S.-K.; van Heyst, J.; Vögtle, F. *Dalton Trans.* **2004**, 1597-1600.
227. Saudan, C.; Balzani, V.; Gorka, M.; Lee, S.-K.; Maestri, M.; Vicinelli, V.; Vögtle, F. *J. Am. Chem. Soc.* **2003**, *125*, 4424-4425.
228. Saudan, C.; Balzani, V.; Gorka, M.; Lee, S.-K.; van Heyst, J.; Maestri, M.; Ceroni, P.; Vicinelli, V.; Vögtle, F. *Chem. Eur. J.* **2004**, *10*, 899-905.
229. Saudan, C.; Ceroni, P.; Vicinelli, V.; Maestri, M.; Balzani, V.; Gorka, M.; Lee, S.-K.; van Heyst, J.; Vögtle, F. *Dalton Trans.* **2004**, 1597-1600.
230. Bergamini, G.; Ceroni, P.; Balzani, V.; Cornelissen, L.; S.-K.; van Heyst, J.; Lee, S.-K.; Vögtle, F. J. *Mater. Chem.* **2005**, *15*, 2959-2964.
231. Bergamini, G.; Saudan, P.; Ceroni, P.; Balzani, V.; Maestri, M.; Balzani, V.; Gorka, M.; Lee, S.-K.; Van Heyst, J.; Vögtle, F. *J. Am. Chem. Soc.* **2004**, *126*, 16466-16471.
232. Balzani, V.; Bergamini, G.; Ceroni, Vögtle, F. *Coord. Chem. Rev.* **2007**, *251*, 525-535.
233. Saudan, C.; Balzani, V.; Ceroni, P.; Gorka, M.; Maestri, M.; Vicinelli, V.; Vögtle, F. *Tetrahedron* **2003**, *59*, 3845-3852.
234. Balzani, V.; Venturi, M.; Credi, A. *Molecular Devices and Machines- A Journey into the Nanoworld*; Wiley-VCH: Weinheim, **2001**.
235. Atoni, P.; Malkoch, M.; Vamvounis, G.; Nystroem, D.; Nystroem, A.; Lindgren, M.; Hult, A. *J. Mater. Chem*. **2008**, *18*, 2545-2554.
236. Jin, R.-H.; Aida, T.; Inoue, S. *J. Chem. Soc., Chem. Commun* **1993**, *10*, 1260-1262.
237. Jiang, D.-L.; Aida, T. *J. Am. Chem. Soc.* **1998**, *120*, 10895-10901.
238. Jiang, D.-L.; Aida, T. A. *Chem. Commun.* **1996**, *13*, 1523-1524.
239. Tomoyose, Y.; Jiang, D.-L.; Jin, R.-H.; Aida, T.; Yamashita, T.; Horie, K. *Macromolecules* **1996**, *29*, 5236-5238.
240. Sadamoto, R.; Tomioka, N.; Aida, T. *J. Am. Chem. Soc.* **1996**, *118*, 3978-3979.
241. Tomioka, N.; Takasu, D.; Takahashi, T.; Aida, T. *Angew. Chem., Int. Ed.* **1998**, *37*, 1531-1534.
242. Stapert, H. R.; Nishiyama, N.; Jiang, D.-L.; Aida, T.; Kataoka, K. *Langmuir* **2000**, *16*, 8182-8188.
243. Zhang, G.-D.; Nihiyama, N.; Harada, A.; Jiang, D.-L.; Aida, T.; Kataoka, K. *Macromolecules* **2003**, *36*, 1304-1309.

244. Zhang, G.-D., Harada, A.; Nishiyama, N.; Jiang, D.-L.; Koyaama, H.; Aida, T.; Kataoka, K. *J. Control Release* **2003**, *93*, 141-150.
245. Collman, J.P.; Fu, L.; Zing, A.; Diederich, F. *Chem. Commun.* **1997**, *14*, 193-194.
246. Choi, M. S.; Yamakaki, T.; Yamazaki, I.; Aida, T. *Angew. Chem., Int. Ed.* **2001**, *40*, 3194-3198.
247. Loiseau, F.; Campagna, S.; Hameurlaine,, A.; Dehaen, W. *J. Am. Chem. Soc.* **2005**, *127*, 11352-11363**.**
248. Helms, B.; Fréchet, J. M. J. *Adv. Syn. Catal.* **2006**, *348*, 1125-1148.
249. Kosaki, M.; Akita, K.; Okada, K. *Org. Lett.* **2007**, *9*, 1509-1512.
250. Choi, M. S.; Aida, T.; Yamazaki, T.; Yamazaki, I. *Angew Chem. Int. Ed.* **2001**, *40*, 3194-3198.
251. Matos, M. S.; Hofkens, J.; Gehlen, M. H. *J. Fluoresc*. **2008**, *18*, 821-826.
252. Choi, M. S.; Aida, T.; Yamazaki, T.; Yamazaki, I. *Chem. Eur. J.* **2002**, *8*, 2668-2678.
253. Jiang, D.-L.; Aida, T. *Prog. Polym. Chem.* **2005**, *30*, 403-422.
254. Guo, M.; Yan, X.; Goodsoon, T., III *Adv. Mater*. **2008**, *20*, 4167-4171.
255. Parthenopoulos, D. A.; Rentzepis, P. N. *Science* **1989**, *245*, 843-845.
256. Denk, W.; Stricker, J. H.; Webb, W. W. *Science* **1990**, *248*, 73-76.
257. Chung, S.-J.; Kim, K.-S.; Lin, T. C.; He, G. S.; Swiatkiewicz, P. N.; Prasad, J. *J. Phys. Chem. B* **1999**, *103*, 10741-10745.
258. Hong, M. A.; Jen Alex, K.-Y.; Alex, J. *Adv. Mater.* **2001**, *13*, 1201-1205.
259. Drobizhev, M.; Karotki, A.; Rebane, A.; Spangler, C. W. *Optics Letters* **2001**, *26*, 1081-1083.
260. Cho, B. R.; Son, K. H.; Lee, S. H.; Song, Y.-S.; Lee, Y.-K.; Jeon, S.-J.; Choi, J. H.; Lee, H.; Cho, M. *J. Am. Chem. Soc.* **2001**, *123*, 10039-10045.
261. Fuks-Janczarek, I; Nunzi, J.-M.; Sahraoui, B.; Kityk, I. V.; Berdowski, J.; Caminade, A.-M.; Majoral, J.-P.; Martineau, A C.; Frere, P.; Roncali, J. *Opt. Comm.* **2002**, *209*, 461-466.
262. Mongin, O.; Brunel, J.; Porrès, L.; Blanchard-Desce, M. *Tetrahedron Lett.* **2003**, *44*, 2813-2816.
263. Ren, Y.; Xin, Q.; Tapo, X.-T.; Wang, L.; Yu, X.-Q.; Yang, J.-X.; Jiang, M.-H. *Chem. Phys. Letters* **2005**, *414*, 253-258.
264. Vestberg, R.; Westlund, R.; Eriksson, A.; Lopes, C.; Carlsson, M.; Eliasson, B.; Glimsdal, E.; Lindgren, M.; Malmström, E. *Macromolecules* **2006**, *39*, 2238-2246.
265. Varnavski, O.; Yan, X.; Mongin, O.; Blanchard-Desce, M.; Goodson, T. *J. Phys. Chem. C* **2007**, *111*, 149-162.
266. Guo, M.; Varnavski, O.; Narayanan, A.; Mongin, O.; Majoral, J.-P.; Blanchard-Desce, M.; Goodson, T., III *J. Phys. Chem*. **2009**, *113*, 4763-4771.
267. Dichtel, W. R.; Serin, J. M.; Edder, C.; Fréchet, J. M. J.; Matuszewski, M.; Tan, L. S.; Ohulchanskyy, T. Y.; Prasad, P. N. *J. Am. Chem. Soc.* **2004**, *126*, 5380-5381.
268. Oar, M. A.; Serin, J. M.; Dichtel W. R.; Fréchet, J. M. J. *Chem. Mater.* **2005**, *17*, 2267-2275.
269. Oar, M. A.; Dichtel W. R.; Serin, J. M.; Fréchet, J. M. J. *Chem. Mater.* **2006**, *18*, 3682-3692.
270. Bonnett, R. *Chem. Soc. Rev.* **1995**, *24*, 19-33.
271. De Rosa, M. C.; Crutchley, R. J. *Coord. Chem. Rev.* **2003**, *233/234*, 351-371.
272. Prasad, P. N. *Introduction to Biophotonics*; Wiley: New York, **2003**.
273. Bhawalkar, J. D.; Kumar, N. D.; Zhao, C. F.; Prasad, P. N. *J. Clin. Laser Med. Surg.* **1997**, *15*, 201-204.
274. Frederiksen, P. K.; Jorgensen, M.; Ogilby P. R. *J. Am. Chem. Soc.* **2001**, *123*, 1215-1221.

275. Hara, M.; Samori, S.; Cai, X.; Tojo, S.; Arai, T.; Monotake, A.; Hayakawa, J.; Uda, M.; Kawai, K.; Endo, M.; Fujitsuka, M.; Majima, T. *J. Am. Chem. Soc.* **2004**, *126*, 14217-14223.
276. Mongin, O.; Krishma, T. R.; Werts, M. H. V.; Caminade, A.-M.; Majoral, J.-P.; Blanchard-Desce, M. *Chem. Commun.* **2006**, 915-917.
277. Narayanan, A.; Varnavski, O.; Mongin, O.; Majoral, J.-P.; Blanchad-Desce, M.; Goodson III, T. *Nanotechnol*. **2008**, *19*, 115502/1-115502/6.
278. Tsiminis, G.; Ribierre, J.-C.; Rusekas, A.; Barcena, H. S.; Richards, G. J.; Turnbull, G. A.; Burn, P. L.; Samuel, I. D. W. *Adv. Mater.* **2008**, *20*, 1940-1944.
279. Cloutet, E.; Fillaut, J.-L.; Gnanou, Y.; Astruc, D. *J. Chem. Soc. Chem. Commun.* **1996**, 1565-1566.
280. Cloutet, E.; Fillaut, J.-L.; Astruc, D.; Gnanou, Y. *Macromolecules* **1999**, *32*, 1043-1054.
281. Cardullo, F.; Diederich, F.; Echegoyen, L.; Habicher, T.; Jayaraman, N.; Leblanc, R. M.; Stoddart, J. F.; Wang, S. *Langmuir* **1998**, *14*, 1955-1959.
282. Dardel, B.; Descheneaux, M.; Even, M.; Serrano, E. *Macromolecules* **1999**, *32*, 5193-5198.
283. Nierengarten, J.-F. *Chem. Eur. J.* **2000**, *6*, 3667-3670.
284. Hirsch, A.; Vostrowsky, O. *Top. Curr. Chem.* **2001**, *217*, 51-93.
285. Nierengarten, J.-F.; Eckert, J. F.; Rio, Y.; Carreon, M. P.; Gallani, J.-L.; Guillon, D. *J. Am. Chem. Soc.* **2001**, *123*, 9743-9748.
286. Campidelli, S.; Deschenaux, R.; Eckert, J. F.; Guillon, D.; Nierengarten, J.-F. *Chem. Commun.* **2002**, 656-657.
287. Nierengarten, J.-F. *Top. Curr. Chem.* **2003**, *228*, 87-110.
288. Nierengarten, J.-F.; Armaroli, N.; Accorsi, G.; Rio, Y.; Eckert, J. F. *Chem. Eur. J.* **2003**, *9*, 36-41.
289. Gutierrez-Nava, M.; Accorsi, G.; Masson, P.; Armaroli, N.; Nierengarten, J.-F. *Chem. Eur. J.* **2004**, *10*, 5076-5086.
290. Hahn, U.; Cardinali, F.; Nierengarten, J.-F. *New J. Chem.* **2007**, *31*, 1128-1138.
291. Rio, Y.; Accorsi, G.; Rehspringer, J.-L.; Hönerlage, B.; Kopitkovas, G.; Chugreev, A.; van Dorsselaer, A.; Armaroli, N.; Nierengarten, J.-F. *New J. Chem.* **2002**, *26*, 1146-1154.
292. Rio, Y.; Accorsi, G.; Nierengarten, J.-F.; Bourgogne, C.; Strub, J.-M.; van Dorsselaer, A.; Armaroli, N.; Nierengarten, J.-F. *Tetrahedron* **2003**, *59*, 3833-3844.
293. Nierengarten, J.-F. In *Dendrimers and Nanoscience*, Astruc, D. Ed., C. R. Chimie, **2003**, *6*, 725-733.
294. Scanu, D.; Yevlampieva, N.; Deschenaux, R. *Macromolecules* **2007**, *40*, 1133-1139.
295. Yevlampieva, N.; Beljaev, N.; Deschenaux, R.; *IDS5*, Toulouse, **2007**, Abstract, p. 109.
296. Xie, A.; Pérez-Cordero, E.; Echegoyen, L. *J. Am. Chem. Soc.* **1992**, *114*, 3978-3980.
297. Bossard, C.; Rigaut, S.; Astruc, D.; Delville, M.-H. Félix, G.; Février-Bouvier, A.; Amiell, J.; Flandrois, S.; Delhaès, P. *J. Chem. Soc., Chem. Commun.* **1993**, 333-334.
298. Ruiz, J.; Daniel, M.-C. Astruc, D. *Can. J. Chem.* **2006**, *84*, 288-299.
299. Choi, M. S.; Aida, T.; Luo, H.; Araki, Y.; Ito, O. *Angew. Chem., Int. Ed.* **2003**, *42*, 4060-4063.
300. Pérez, L.; Garcia-Martinez, J. C.; Diaz-Barra, E.; Atienzar, P.; Garcia, H.; Rodriguez-Lopez, J.; Langa, F.; *Chem. Eur. J.* **2006**, *12*, 5149-5157.
301. Ruiz, J.; Pradet, C.; Varret, F.; Astruc, D. *Chem. Commun.* **202**, 1108-1109.
302. Armaroli, N.; Accorsi, J.; Clifford, N.; Eckert, J.-F.; Nierengarten, J.-F. *Chem. Asian J.* **2006**, *1*, 564-574.

303. Hasobe, T.; Kamat, P. V.; Absolum, M. A.; Kashiwagi, Y.; Sly, J.; Crossely, M. J.; Hosomizu, K.; Imahori, H.; Fukuzumi, S. *J. Phys. Chem. B* **2004**, *108*, 12865-12872.
304. Li, W. S.; Kim, K. S.; Jiang, D. L.; Tanaka, H.; Kawai, T.; Kwon, J. H.; Kim, D.; Aida, T. *J. Am. Chem. Soc.* **2006**, *128*, 10527-10532.
305. Kosaki, M.; Akita, K.; Suzuki, S.; Okada, K. *Org. Lett.* **2007**, *9*, 3315-3318.
306. Ahn, U.; Nirengarten, J.-F.; Vögtle, F.; Listorti, A.; Monti, F.; Armaroli, N. *New J. Chem*. **2009**, *33*, 337-344.
307. Sun, Y.-P.; Huang, W.; Lin, Y.; Fu, K.; Kitaygorodskiy, A.; Riddle, L. A.; Joy Yu, Y.; Caroll, D. L. *Chem. Mater.* **2001**, *13*, 2864-2869.
308. Holzinger, M.; Abraham, J.; Whelan, P.; Graupner, R.; Ley, L.; Hennrich, F.; Kappes, M.; Hirsch, A. *J. Am. Chem. Soc.* **2003**, *125*, 8566-8580.
309. Cao, L.; Yang, W.; Yang, J. W.; Wang, C. C.; Fu, S. K. *Chem. Lett.* **2004**, *33*, 490-491.
310. Campidelli, S.; Sooambar, C.; Lozano Diz, E.; Ehli, C.; Guldi, D. M.; Prato, M. *J. Am. Chem. Soc.* **2006**, *128*, 12544-12552.
311. Hofkens, J.; Maus, M.; Gensch, T.; Vosch, T.; Cotlet, M.; Köhn, F.; Herrmann, A.; Müllen, K.; De Schryver, F. *J. Am. Chem. Soc.* **2000**, *122*, 9278-9288.
312. Tinnefeld, P.; Weston, K. D.; Vosch, T.; Cotlet, M.; Weil, T.; Hofkens, J.; Müllen, K. *J. Am. Chem. Soc.* **2002**, *124*, 14310-14311.
313. Maus, M.; De, R.; Lor, M.; Weil, T.; Mitra, S.; Wiesler, U.-M.; Herrmann, A.; Hofkens, J.; Vosch, T.; Müllen, K. *J. Am. Chem. Soc.* **2001**, *123*, 7668-7676.
314. De Schryver, F. C.; Vosch, T.; Cotlet, M.; van der Auweraer, M.; Müllen, K.; Hofkens, J. *Acc. Chem. Res.* **2005**, *38*, 514-522.
315. Lor, M.; Thielemans, J.; Viaene, L.; Cotlet, M.; Hofkens, J.; Wel, T.; Hampel, C.; Müllen, K.; Vehoven, J. W.; Van der Auweraer, M.; De Schryver, F. C. *J. Am. Chem. Soc.* **2002**, *124*, 9918-9925.
316. Peng, Z.; Melinger, J. S.; Kleiman, V. *Photosynth. Res.* **2006**, *87*, 115-131.
317. Carbone, P. Negri, F.; Müller-Plathe, F. *Macromolecules* **2007**, *40*, 7044-7055.
318. Tinnefeld, P.; Weston, K. D.; Vosch, T.; Cotlet, M.; Weil, T.; Hofkens, J.; Müllen, K.; De Schryver, F. C.; Sauer, M. *J. Am. Chem. Soc.* **2002**, *124*, 14310-14311.
319. Klärner, G.; Miller, R. D.; Hawker, C. *J. Polym. Prepr.* **1998**, *39* (2), 1006-1007.
320. Setayesh, S.; Grimsdale, A. C.; Weil, T.; Enkelmann, V.; Müllen, K.; Meghdadi, F.; List, E. J. W.; Leising, G. *J. Am. Chem. Soc.* **2001**, *123*, 946-953.
321. Zhao, Z.; Li, J.-H.; Chen, X.; Lu, P.; Yang, Y. *Org. Lett*. **2008**, *10*, 3041-3044.
322. Ribierre, J. C.; Ruseckas, A.; Samuel, I. D. W.; Bacena, H. S.; Burn, P. L. *J. Chem. Phys*. **2008**, *128*, 204703/1-204703/8.
323. Minard-Basquin, C.; Weil, T.; Hohner, A.; Rädler, J. O.; Müllen, K. *J. Am. Chem. Soc.* **2003**, *125*, 5832-5838.
324. Bernhardt, S.; Kastler, M.; Enkelmann, V.; Baumgarten, M.; Müllen, K. *Chem. Eur. J.* **2006**, *12*, 6117-6128.
325. Bergamini, G.; Ceroni, P.; Balzani, V.; Del, M.; Villavieja, M.; Kandre, R.; Zhun, I.; Lukin, O. *ChemPhysChem* **2006**, *7*, 1980-1984.
326. Clarck Jr., C. G.; Wenzel, R. J.; Andreitchenko, E. V.; Steffen, W.; Zenobi, R.; Müllen, K. *J. Am. Chem. Soc.* **2007**, *129*, 3292-3301.
327. Adhikari, R. M.; Mondal, R.; Shah, B. K.; Neckers, D. C. *J. Org. Chem.* **2007**, *72*, 4727-4732.
328. Akai, I.; Higuchi, M.; Kanemoto, K.; Karasawa, T.; Hashimoto, H.; Kimura, M. *J. Lumin.* **2008**, *128*, 948-951.
329. Qin, T.; Zhou, G.; Scheiber, H.; Bauer, R. E.; Bauggarten, M.; Anson, C. E.; List, E. J. W.; Müllen, K. *Angew. Chem., Int. Ed.* **2008**, *47*, 8292-8296.

330. Rau, H. In *Photochromism, Molecules and Sytems*, Dürr, H.; Bouas-Laurent, H., Eds.; Elsevier, Amsterdam, **1990**.
331. Archut, A.; Azzellini, G. C.; Balzani, V.; De Cola, L.; Vögtle, F. *J. Am. Chem. Soc.* **1998**, *120*, 12187-12191.
332. Puntoriero, F.; Ceroni, P.; Balzani, V.; Bergamini, G.; Vögtle, F *J. Am. Chem. Soc.* **2007**, *129*, 10714-10719.
333. Puntoriero, F.; Bergamini, G.; Ceroni, P.; Balzani, V. *New J. Chem.* **2008**, *32*, 401-406.
334. Archut A.; Vögtle, F.; De Cola, L.; Azzelini, G. C.; Balzani, V.; Ramanujam, P. S.; Berg, R. H. *Chem. Eur. J.* **1998**, *4*, 699-706.
335. Junge, D. M.; McGrath, D. V. *J. Am. Chem. Soc.* **1999**, *121*, 4912–4913.
336. Junge, D.; McGrath, D. V. *Chem. Commun.* **1997**, 857-858.
337. Jiang, D.-L.; Aida, T. *Nature* **1997**, *388*, 454-456.
338. Yokoyama, S.; Nakahama, T.; Otomo, A.: Mashiko, S. *Chem. Lett.* **1997**, 1137-1138.
339. Tsuda, K.; Dol, G. C.; Gensch, T.; Hofkens, J.; Latterini, L.; Weener, J. W.; Meijer, E. W.; De Schryver, F. C. *J. Am. Chem. Soc.* **2000**, *122*, 3445-3452.
340. Liu, J.; Ni, P.; Qiu, D.; Hou, W.; Zhang, Q. *React. Funct. Polym.* **2007**, *67*, 416-421.
341. Ghosh, S.; Banthia, A. K.; Maiya, B. G. *Org. Lett.* **2002**, *4*, 3603-3606.
342. Zhang, W.; Xie, J.; Shi, W.; Deng, X.; Cao, Z.; Shen, Q. *Eur. Polym*. J. **2008**, *44*, 872-880.
343. Weener, J.-W.; Meijer, E. W. *Adv. Mater.* **2000**, *12*, 741-746.
344. Higushi, M.; Shiki, S.; Ariga, S.; Yamamoto, K. *J. Am. Chem. Soc.* **2001**, *123*, 4414-4420.
345. Yamamoto, K.; Higushi, M.; Shiki, S.; Tsuruta, M.; Chiba, H. *Nature* **2002**, *415*, 509-511.
346. Satoh, N.; Cho, J. S.; Higushi, M.; Yamamoto, K. *J. Am. Chem. Soc.* **2003**, *125*, 8104-8105.
347. Higushi, M.; Shiki, S.; Yamamoto, K. *Org. Lett.* **2000**, *2*, 3079-3082.
348. Cho, J.-S.; Takanashi, K.; Higushi, M.; Yamamoto, M. *Syn. Metals* **2005**, *150*, 79-82.
349. Nakashjima, T.; Satoh, N.; Albrecht, K.; Yamamoto, K. *Chem. Mater.* **2008**, *20*, 2538-2543.
350. Satoh N.; Nakashima T.; Kamikura K.; Yamamoto, K. *Nature Nanotechnol.* **2008**, *3*, 106-111.
351. Dalton, L. R. Nonlinear Optical Plymeric Materials: From Chromophore Design to Commercial Applications. *Adv. Polym. Sci.*;Springer-Verlag: Berlin, 2002; Vol. *158*.
352. Fichou, D. *Handbook of Oligo- and Polythiophene*; Wiley-VCH: New York, 2004.
353. Handbook of Conducting Polymers; Skotheim; T. A.; Elsenbaumer, R. L.; Reynolds, *J. R. Eds.*; Dekker, New York, **1998**.
354. Roncali, J. *Chem. Rev.* **1992**, *92*, 711-738.
355. Andrews, D. L.; Shaopeng, L.; Rodriguez, J.; Slota, J. *J. Chem. Phys.* **2007**, *127*, 134902-134907.
356. Schenning, A. P. H.; Meijer, E. W. *Chem. Commun.* (feature article) **2005**, 3245-3258.
357. Green, M. A.; Emery, K.; Hishikawa, Y.; Warta, W. *Prog. Photovolt.: Res. Apl.* **2006**, *14*, 455-461.
358. Li, G.; Shrotriya, V.; Huang, J. S.; Yao, Y.; Moriarty, T.; Emery, K.; Yang, Y. *Nature Mater.* **2005**, *4*, 864-868.
359. Sullivan, P. A.; Akelaitis, A. J. P.; Lee, S. K.; McGrew, G.; Lee, S. K.; Choi, D. H.; Dalton, L. R. *Chem. Mater.* **2006**, *18*, 344-351.

360. Luponosov, Y. N.; Ponomarenko, S. A.; Surin, N. M.; Muzafarov, A. M. *Org. Lett.* **2008**, *10*, 2753-2756.
361. Kopidakis, N.; Mitchell, W. J.; van de Lagemaat, J.; Ginley, D. S.; Rumbles, G.; Shaheen, S. E. *Appl. Phys. Lett.* **2006**, *89*, 103524-1 - 103524-3.
362. Borshchev, O. V.; Ponomarenko, S. A.; Surin, N. M.; Kaptyug, M; M.; Buzin, M. I.; Pleshkova, A. P.; Demchenko, N. V.; Myakushev, V. D.; Muzafarov, A. M. *Organomet.* **2007**, *26*, 5165-5173.
363. Malenfant, P. R. L.; Fréchet, J. M. J. *Macromolecules* **2000**, *33*, 3634-3640.
364. Furuta, P.; Brooks, J.; Thompson, M. E.; Fréchet, J. M. J. *J. Am. Chem. Soc.* **2003**, *125*, 13165-13172.
365. Satoh, N.; Nakashima, T.; Yamamoto, K. *J. Am. Chem. Soc.* **2005**, *127*, 13030-13038.
366. Anthopoulos, T. D.; Markham, J. P. J.; Namdas, E. B.; Samuel, I. D. W.; Lo, S.; Burn, P. L. *Appl. Phys. Lett.* **2003**, *82*, 4824-4826.
367. Ribierre, J. C.; Rusekkas, A.; Samuel, I. D. W.; Staton, S. V.; Burn, P. L. Phys. Rev. B.: *Condensed Matter Mater. Phys.* **2008**, *77*, 085211/1-085211/5.
368. Gambino, S.; Samuel, I. D. W.; Barcena, H.; Burn, P. L. *Org. Electron.* **2008**, *9*, 220-226.
369. Locklin, J.; Patton, D.; Deng, S.; Baba, A.; Millan, M.; Advincula, R. C. *Chem. Mater.* **2004**, *16*, 5187-5193.
370. Deng, S.; Locklin, J.; Patton, D.; Baba, A.; Advincula, R. C. *J. Am. Chem. Soc.* **2005**, *127*, 1744-1751.
371. Xia, C.; Fan, X.; Locklin, J.; Advincula, R. C.; Gies A.; Nonidez, W. *J. Am. Chem. Soc.* **2004**, *126*, 8735-8743.
372. Ma, C.-Q.; Mena-Osteritz, E.; Debaerdemaeker, T.; Wienk, M.M.; Janssen, R. A. J.; Bäerle, P. *Angew. Chem., Int. Ed.* **2007**, *46*, 1679-1683.
373. Pogantsch, A.; Wenzl, F. P.; List, E. J. W.; Leising, G.; Grimsdale, A. C.; Müllen, K. *Adv. Mater.* **2002**, *14*, 1061-1063.
374. Bettignies, R.; Nicholas, Y.; Blanchard, P.; Levillain, E.; Nunzi, J. M.; Roncali, J. *Adv. Mater.* **2003**, *15*, 1939-1943.
375. Hasobe, T.; Kashiwagi, Y.; Absalom, M. A.; Sly, J.; Hozomizu, K. Crossley, M. J.; Imahori, H.; Kamat, P. V.; Fukuzumi, S. *Adv. Mater.* **2004**, *16*, 975-946.
376. Satoh, N.; Nakashima, T.; Yamamoto, K. *J. Am. Chem. Soc.* **2005**, *127*, 13030-13038.
377. Lu, J.; Xia, P. F.; Lo, P. K.; Tao, Y.; Wong, M. S. *Chem. Mater.* **2006**, *18*, 6194-6203.
378. John, H.; Bauer, R.; Espindola, P.; Sonar, P.; Heinze, J.; Müllen K. *Angew. Chem., Int. Ed.* **2005**, *44*, 2447-2451.
379. Ramakrishna, G.; Bhaskar, A.; Bauerle, P.; Goodson, T. III *J. Phys. Chem. A* **2008**, 112, 2018-2026.
380. Suxiang, D.; Locklin, J.; Patton, D.; Baba, A.; Advincula, R. C. *J. Am. Chem. Soc.* **2005**, *127*, 1744-1751.
381. Rupert, B. L.; Mitchell, W., J.; Ferguson, A. J.; Koese, M. E.; Rance, W. L.; Rumbles, G.; Ginley, D. S. Shaheen, S. E.; Kopidakis, N. *J. Mater. Chem*. **2009**, *19*, 5311-5324.
382. Fischer, M. K. R.; Kaiser, T. E.; Wuerthner, F.; Bauerle, P. *J. Mater. Chem*. **2009**, *19*, 1129-1141.
383. Halim, M.; Pillow, J. N. G.; Burn, P. L.; Samuel, D. W. *Adv. Mater.* **1999**, *11*, 371-374.
384. Luptron, J. M.; Samuel, I. D. W.; Burns, P. L.; Mukamel, S. *J. Phys. Chem. B* **2002**, *106*, 7647-7653.
385. Halim, M.; Samuel, I. D. W.; Pillow; J. N. G.; Burn, P. L. *Synth. Met.* **1999**, *102*, 1113-1114.

386. Palson, L.-O.; Beavington, R.; Frampton, M. J.; Lupton, J. M.; Magennis, S. W.; Markham, J. P. J.. Pillow, J. N. G.; Burn, P. L.; Samuel, I. D. W. *Macromolecules* **2002**, *35*, 7891-7901.
387. Lupton, J. M.; Samuel, I. D. F.; Burn, P. L.; Mukamel, S. *J. Phys. Chem.B* **2002**, *106*, 7647-7653.
388. Lupton, J. M.; Samuel, I. D. W.; Beavington, R.; Frampton, M. J.; Burn, P. L.; Bässler, H. *Phys. Rev. B* **2001**, *63*, 155-206.
389. Deb, S. K.; Maddux, T. M.; Yu, L. *J. Am. Chem. Soc.* **1997**, 119, 9079-9080.
390. Meier, H.; Lehmann, M.; Kolb, K. *Chem. Eur. J.* **2000**, *6*, 2462-2469.
391. Precup-Blaga, F. S.; Garcia-Martinez, J. C.; Schenning, A. P. H.; Jonkheijm, P.; Meijer, E. W. *J. Am. Chem. Soc.* **2003**, *125*, 12953-12960.
392. Lehmann, M.; Fishbach, I.; Spiess, H. W.; Meier, H. *J. Am. Chem. Soc.* **2004**, *126*, 772-784.
393. Lo, S.-C.; Burn, P. L. *Chem. Rev.* **2007**, *107*, 1097-1116.
394. Yang; S.-H.; Chen, S.-Y.; Wu, Y.-C.; Hsu, C. S. *J. Polym. Sci. A: Polym. Chem.* **2007**, *45*, 3440-3450.
395. Tang, R.; Cuai, Y.; Cheng, C.; Xi, F.; Zou, D. *J. Polym. Sci. Part A,: Polym. Chem.* **2005**, *43*, 3126-3140.
396. Schulz, A.; Meirer, H. *Tetrahedron* **2007**, *63*, 11429. Schulz, A.; Meier, H. *Tetrahedron* **2007**, *63*, 11429-11435.
397. Choi, D. H.; Han, K. I.; Chang, I.-H.; Choi, S.-H.; Zhang, X.-H.; Ahn, K.-H.; Lee, Y. K.; Jang, J. *Synthetic Metals* **2007**, *157*, 332-335.
398. Schenning, A. P. H. J.; Peeters, E.; Meijer, E. W. *J. Am. Chem. Soc.* **2000**, *122*, 4489-4495.
399. Precup-Blaga, F. S.; Garcia-Martinez, J. C.; Schenning, A. P. H. J.; Meijer, E. W. *J. Am. Chem. Soc.* **2003**, *125*, 12953-12960.
400. Garcia-Martinez, J. C.; Diez-Barra, E.; Rodriguez-Lopez, J. *Curr. Org. Syn*. **2008**, *5*, 267-290.
401. Marham, J. P. J.; Samuel, I. D. W.; Lo, S. C.; Burn, P. L.; Samuel, I. D. W. *Appl. Phys. Lett.* **2002**, *80*, 2645-2647.
402. Lo, S.-C.; Harding, R. E.; Brightman, E.; Burn, P. L.; Samuel, I. D. W. *J. Mater. Chem*. **2009**, *19*, 3213-3227.
403. Adachi, C.; Baldo, M. A.; O'Brien, D. F.; You, Y.; Shoustikov, A.; Sibley, S., Thompson, M. E.; Forrest, S. R. *Nature* **1998**, *395*, 151-154.
404. Lo, S. C.; Nambdas, E. B.; Burn, P. L.; Samuel, I. D. W. *Macromolecules* **2003**, *36*, 9721-9730.
405. Bera, R. N.; Cumpstey, N.; Burn, P. L.; Samuel, I. D. W. *Advan. Funct. Mater.* **2007**, *17*, 1149-1152.
406. Anthopoulos, T. D.; Frampton, M. J.; Namdas, E. B.; Burn, P. L.; Samuel, I. D. W. *J. Mater. Chem.* **2004**, *16*, 557-560.
407. Frampton, M. J.; Namdas, E. B.; Lo, S. C.; Burn, P. L.; Samuel, I. D. W. *J. Mater. Chem.* **2004**, *16*, 2881-2888.
408. Lo, S. C.; Richards, G. J.; Markham, J. P. J.; Namdas, E. B.; Sharma, S.; Burn, P. L.; Samuel, I. D. W. *Adv. Funct. Mater.* **2005**, *15*, 1451-1458.
409. Bera, R. N.; Cumspstey, N.; Burn, P. L.; Samuel, I. D. W. *Adv. Funct. Mater.* **2007**, *17*, 1149-1152.
410. Knights, K. A.; Stevenson, S. G.; Shipley, C. P.; Lo, S.-C.; Olsen, S.; Harding, R. E.; Gambino, S.; Burn, P. L.; Samuel, I. D. W. *J. Mater. Chem*. **2008**, *18*, 2121-2130.
411. Bauer, R. E.; Grimsdale, A. C.; Müllen, K. *Top. Curr. Chem.* **2005**, *245*, 253-286.

412. Huang, C.; Zhen, C.-G.; Su, S. P.; Loh, K. P.; Chen, Z.-K. *Org. Lett.* **2005**, *7*, 391-394.
413. Chen, C.-H.; Lin, J.-T.; Yeh, M.-C. P. *Org. Lett.* **2006**, *8*, 2233-2236.
414. Chien, C.-H.; Kung, L.-R.; Wu, C.-H.; Shu, C.-F.; Chang, S.-Y.; Chi, Y. *J. Mater. Chem*. **2008**, 18, 3461-3466.
415. Cha, S. W.; Choi, S.-H.; Kim, K.; Jin, J.-I. *Mater. Chem.* **2003**, *13*, 1900-1904.
416. Justin, K. R.; Lin, J. T.; Tao, Y.-T.; Ko, C.-W. *Chem. Mater.* **2002**, *14*, 1354-1361.
417. Tsuzuki, T.; Shirasawa, N.; Suzuki, T.; Tokito, S. *Jpn. J. Appl. Phys. Part 1* **2005**, *44*, 4151-4154.
418. Anthopoulos, T. D.; Markham, J. P. J.; Namdas, E. B.; Samuel, I. D. W.; Lo, S.-C.; Burn, P. L. *Org. Electron.* **2006**, *7*, 85-98.
419. Li, S.; Zhong, G.; Zhu, W.; Li, F.; Pan, J.; Huang, W.; Tian, H. *J. Mater. Chem.* **2005**, *15*, 3221-3228.
420. Adachi, C.; Baldo, M. A.; Thomson, M. E.; Forrest, S. R. *J. Appl. Phys.* **2001**, *90*, 5048-5051.
421. Holmes, R. J.; Forrest, S. R.; Tung, Y.-J.; Kwong, R. C.; Brown, J. J.; Garon, S.; Thompson, M. E. *Appl. Phys. Lett.* **2003**, *82*, 2422-2424.
422. Promarak, V.; Ichikawa, M.; Sudyoadsuk, T.; Saengsuwan, S.; Jungsuttiwong, S.; Keawin, T. *Thin Film Solids* **2008**, *516*, 2881-2888.
423. Nambdas, E. B.; Ruseckas, A.; Samuel, I. D. W.; Lo, S. C.; Burn, P. L. *Appl. Phys. Lett.* **2005**, *86*, 091104.
424. Lo, S. C.; Anthopoulos, T. D.; Namdas, E. B.; Burn, P. L.; Samuel, I. D. W. J. *Adv. Mater.* **2005**, *17*, 1945-1948.
425. Burns, P. ML.; S-C. Lo, Samuel, D. W. *Adv. Mater.* **2007**, *19*, 1675-1688.
426. Lo, S.-C.; Bera, R. N.; Harding, R. E.; Burn, P. L.; Samuel, I. D. W. *Adv. Funct. Mater*. **2008**, *18*, 3080-3090.
427. Kwon, T.-H.; Kim, M. K.; Kim, M. K.; Kwon, J.; Shin, D.-Y.; Park, S. J.; Lee, C.-L.; Kim, J.-J.; Hong, J.-I. *Chem. Mater.* **2007**, *19*, 3673-3680.
428. Ribierre, J. C.; Ruseckas, A.; Samuel, I. D. W.; Staton, S. V.; Burn, P. L. *Phys. Rev. B: Condensed Mater. Phys.* **2008**, *77*, 085211/1.
429. Ribiere, J. C.; Ruseckas, A.; Knights, K.; Staton, S. V.; Cumpstey, N.; Burn, P. L.; Samuel, I. D. W. *Phys. Rev. Lett.* **2008**, *100*, 017402/1-017402/4.
430. Liu, Q-D.; Lu, J.; Ding, J.; Tao, Y. *Macromol. Chem. Phys*. **2008**, *209*, 1931-1941.
431. Vicinelli, V.; Ceroni, P.; Maestri, M.; Lazzari, M.; Balzani, V.; Lee, S.-K.; van Heyst, J.; Vögtle, F. *Org. Biol. Chem.* **2004**, *2*, 2297-2213.
432. Albrecht, K.; Kasai, Y.; Kinoto, A.; Yamamoto, K. *Macromolecules* **2008**, *41*, 3793-3800.
433. Hwang, S.-H.; Moorefield, C. N.; Newkome, G. R. *Chem. Soc. Rev*. **2008**, *37*, 2543-2557.
434. Ranasinghe, M. I.; Varnavski, O. P.; Pawlas, J.; Hauck, S. I.; Louie, J.; Hartwig, J. F.; Goodson, II, T. *J. Am. Chem. Soc.* **2002**, *124*, 6520-6521.
435. Aathimanikandan, S. V.; Sandanaraj, B. S.; Arges, C. G.; Bardeen, C. J.; Thayumanavan *Org. Lett.* **2005**, *7*, 2807-2812.
436. Shcharbin, D.; Szedzka, M.; Bryszewska, M. *Bioorg. Chem.* **2007**, *35*, 170-174.
437. Vivinelli, V.; Bergamini, G.; Ceroni, P.; Balzani, V.; Vögtle, F.; Lukin, O. *J. Phys. Chem. B* **2007**, *111*, 6620-6627.
438. Sullivan, P. A.; Rommel, H.; Liao, Y.; Olbricht, B. O.; Akelaitis, A. J. P.; Firestone, K. A.; Kang, J. W.; Luo, J.; Davies, J. A.; Choi, D. H.; Eichinger, B. E.; Reid, P. J.; Chen, A.; Jen, A. K.-Y.; Robinson, B. H.; Dalton, L. R. *J. Am. Chem. Soc.* **2007**, *129*, 7523-7530.

439. Li, C-F.; Jin, F.; Dong, X.-Z.; Cen, W.-Q.; Duan, X.-M. *J. Lumin.* **2007**, *127*, 321-326.
440. Boubou, K. H.; Ghaddar, T. H. *Langmuir* **2005**, *21*, 8844-8851.
441. Ogasawara,S.; Ikeda, A.; Kikuchi, J. *Chem. Mater.* **2006**, *18*, 5982-5987.
442. Li, C.; Mitamura, K.; Imae, T. *Macromolecules* **2003**, *36*, 9957-9965.
443. Hasobe, T.; Kashiwagi, Y.; Absalom, M. A.; Sly, J.; Hosomizu, K.; Crossley, M. J.; Imahori, H.; Kamat, P. V.; Fukuzumi, S. *Adv. Mater.* **2004**, *16*, 975-979.
444. Hasobe, T.; Kamat, P. V.; Absalom, M. A.; Kashiwagi, Y.; Sly, J.; Crossley, M. J.; Hosomizu, K.; Imahori, H.; Fukusumi, S. *J. Phys. Chem. B* **2004**, *108*, 12865-12872.
445. Hosomizu, K.; Imaahori, H.; Hahn, U.; Nierengarten, J.-F.; Listori, A.; Armaroli, N.; Nemoto, T.; Isoda, S. *J. Phys. Chem. C* **2007**, *111*, 2777-2786.
446. Saab, M. A.; Abdel-Malak, R.; Wishart, J. F.; Ghaddar, T. H. *Langmuir* **2007**, *23*, 10807-10815**.**
447. Bertorelle, F.; Lavabre, D.; Fery-Forgues, S. *J. Am. Chem. Soc.* **2003**, *125*; 6244-6253.
448. Bertorelle, F.; Rodrigues, F.; Fery-Forgues, S. *Langmuir* **2006**, *22*, 8523-8531.
449. Justin Thomas, K. R.; Thopso, A. L.; Sivakumar, A. V.; Bardeen, C. J.; Thayumanavan, S. *J. Am. Chem. Soc.* **2005**, *127*, 373-383.
450. Vukmirovic, N.; Wang, L.-W. *J. Chem. Phys.* **2008**, *128*, 121102/1.
451. Puntoriero, F.; Bergamini, G.; Ceroni, P.; Balzani, V.; Vögtle, F. *New J. Chem.* **2008**, *32*, 401-406.
452. Takahashi, M.; Morimoto, H.; Miyake, K. Kawai, H.; Sei, Y.; Yamagushi, K.; Sengoku, T.; Yoda, H. *New J. Chem.* **2008**, *32*, 547-553.
453. Bolink, H. J.; Barea, E.; Costa, R. D.; Coronado, E.; Sudhakar, S.; Zhen, C.; Sellinger, A. *Org. Electronics* **2008**, *9*, 155-163.
454. Grabchev, I.; Dumas, S.; Chovelon, J.-M.; Nedelcheva, A. *Tetrahedron* **2008**, *64*, 2113-2119.
455. Jayamurugan, G.; Umesh, C. P.; Jayaraman, N. *Org. Lett.* **2008**, *10*, 9-12.
456. Kaanumalle, L. S.; Nithyanandhan, J.; Pattabiraman, M.; Jayaraman, N.; Ramanurthy, V. *J. Am. Chem. Soc.* **2004**, *126*, 8999-9006.
457. Kaanumalle, L. S.; Ramesh, R.; Maddipatla, V. S. N. M.; Nithyanandhan, J.; Jayaraman, N.; Ramanurthy, V. *J. Org. Chem.* **2005**, *70*, 5062-5069.
458. Akai, I.; Miyanatri, K.; Shimamoto, T.; Fujii, A.; Nakao, H.; Okada, A.; Kanemoto, K.; Karasawa, T.; Hashimoto, H.; Ishida, A.; Yamada, A.; Katayama, I.; Takeda, J.; Kimura, M. *New J. Phys*. **2008**, *10*, 125024.
459. Shi, D.; Sha, Y.; Wang, F.; Tian, Q. *Macromolecules* **2008**, *41*, 7478-7484.
460. Wang, J.-L.; Yan, J.; Tang, Z.-M.; *J. Am. Chem. Soc*. **2008**, *130*, 9952-9962.
461. Bergamini, G.; Cezroni, P.; Balzani, V.; Kandre, R.; Lukin, O. *ChemPhysChem* **2009**, *10*, 265-269.
462. McDonald, A. R.; Mores, D.; Donega, C.; van Walree, C.; Klein Gebbink, R. J. M.; Lutz, M.; Spek, A. L.; Meijerink, A.; van Klink, G. P. M.; van Koten, G. *Organometallics* **2009**, 28, 1082-1092.
463. Richardson, S.; Barcena, H. S.; Turnbull, G. A.; Burn, P. L.; Samuel, I. D. W. *Appl. Phys. Lett.* **2009**, *95*, 063305/1-063305/3.
464. Singh, P.; Onodera, T.; Mizuta, Y.; Matsumoto, K.; Miura, N.; Oko, K. *Sensors Actuat. B: Chemical* **2009**, 137, 403-409.
465. Yamaji, D.; Takagushi, Y. *Polym. J.* **2009**, *41*, 293-296.
466. Holtmann, J.; Walczuck, E.; Dede, M.; Wittenburg, C.; Heck, J.; Archetti, G.; Wortmann, R.; Kubal, H.-G.; Wang, Y.-H.; Liu, K.; Luo, Y. *J. Phys. Chem. B* **2008**, *112*, 14751-14761.
467. Victorovna-Lijanova, I.; Reyes-Valderrama, M. I.; Maldonado, J.-L.; Ramoz-Ortiz, G.; Taniana, K.; Martinez-Garcia, M. *Tetrahedron* **2008**, *64*, 4460-4467.

468. Roberts, R. L.; Schwichensten, C. T.; Cifuentes, M. P.; Green, K. A.; Farmer, J. D.; Low, P. J.; Marder, T. B.; Samok, M.; Humphrey, M. G. *Advan. Mater.* **2009**, *21*, 2318-2322.
469. Harpham, M. R.; Suzer, O.; Ma, C.-Q.; Bauerle, P.; Goodson, T. *J. Am. Chem. Soc.* **2009**, *131*, 973-979.
470. Naylor, A. M.; Goddart, W. A. I.; Kiefer, G. E.; Tomalia, D. A. *J. Am. Chem. Soc.* **1989**, *111*, 2339-2341.
471. Shao, J.; Tam, J. P. *J. Am. Chem. Soc.* **1995**, *117*, 3893-3899.
472. Roy, R. *Polym. News* **1996**, *21*, 226-232.
473. Zeng, F.; Zimmermann, S. C. *Chem. Rev.* **1997**, *97*, 1681-1712.
474. Kim, Y.-P.; Hong, M.-Y.; Shon, H.-K.; Chegal, W.; Cho, H. M.; Moon, D. W.; Kim, H. S.; Lee, T. G. *Appl. Surf. Sci.* **2008**, *255*, 1110-1112.
475. Escamilla, G. H.; Newkome, G. R. *Angew. Chem., Int. Ed. Engl.* **1994**, *33*, 1937-1940.
476. Chapman, T. M.; Hillyer, G. L.; Mahan, E. J.; Shaffer, K. A. *J. Am. Chem. Soc.* **1994**, *116*, 11195-11196.
477. Vanhest, J. C. M.; Delnoye, D. A. P.; Baars, M. W. P. L.; Elissenroman, C.; Vangenderen, M. H. P.; Meijer, E. W. *Science*, **1995** , *268*, 1592-1595.
478. Gitsov, I.; Fréchet, J. M. J. *J. Am. Chem. Soc.* **1996**, *118*, 3785-3786.
479. Percec, V.; Chu, P. W.; Ungar, G.; Zhou, J. P. *J. Am. Chem. Soc.* **1995**, *117*, 11441-11454.
480. Percec, V. *Pure Appl. Chem.* **1995**, *67*, 2031-2038.
481. Lorentz, K.; Holter, D.; Stuhn, B.; Mülhaupt, R.; Frey, H. *Adv. Mater.* **1996**, *8*, 414-416.
482. Amabiloino, D. B.L; Ashton, P. R.; Balzani, V.; Brown, C. L.; Credi, A.; Fréchet, J. M. J.; Leon, J. W.; Raymo, F. M.; Spencer, M.; Stoddart, J. F.; Venturi, M. *J. Am. Chem. Soc.* **1996**, *118*, 12012-12020.
483. Elizarov, A. M.; Chiu, S.-H.; Glink, P. T.; Stoddart, J. F. *Org. Lett.* **2002**, *4*, 679-682.
484. Elizarov, A. M.; Chang, T.; Chiu, S.-H.; Stoddart, J. F. *Org. Lett.* **2002**, *4*, 3565-3568.
485. Jones, J. W.; Bryant, W. S.; Bosman, A. W.; Jansen, R. A. J.; Meijer, E. W.; Gibson, H. W. *J. Org. Chem.* **2003**, *68*, 2385-2389.
486. Kim, S.-Y.; Ko, Y.-H.; Lee, J. W.; Sakamoto, S.; Yamaguchi, K.; Kim, K. *Chem. Asian J.* **2007**, *2*, 747-754.
487. Daniel, M.-C.; Ruiz, J.; Astruc, D. *J. Am. Chem. Soc*. **2003**, *125*, 1150-1151.
488. Daniel, M.-C.; Ba, F.; Ruiz, J.; Astruc, D. *Inorg. Chem*., **2004**, 43, 8649-8657.
489. Deng, L.; Wang, L.; Yu, H.; Wang, J.; Dong, X.; Li, J.; Tan, Q.; Huo, J. *J. Appl. Polym. Sci.* **2008**, *107*, 1539-1546.
490. Astruc, D.; Daniel, M.-C.; Ruiz, J. *Chem. Commun* **2004**, 2637-2649.
491. Ong, W.; Grindstaff, J.; Sobransingh, D.; Toba, R.; Quintela, J. M.; Peinador, C.; Kaifer, A. E. *J. Am. Chem. Soc.* **2005**, *127*, 3353-3361.
492. Corbin, P. S.; Lawless, L. J.; Li, Z.; Ma, Y.; Witmer, M. J.; Zimmerman, S. C. *Proc. Natl. Acad. Sci. U. S. A.* **2002**, *8*, 5099-5104;
493. Ma, Y. M.; Kolotuchin, S. V.; Zimmerman, S. C. *J. Am. Chem. Soc.* **2002**, *124*, 13757-13769.
494. Gibson, H. W.; Yamagushi, N.; Hamilton, L.; Jones, J. W. *J. Am. Chem. Soc.* **2002**, *124*, 4653-4665.
495. Huang, F.; Nagvekar, D. S.; Slebodnick, C.; Gibson, H. W. *J. Am. Chem. Soc.* **2005**, *127*, 484-485.
496. Franz, A.; Bauer, W.; Hirsch, A. *Angew. Chem., Int. Ed.* **2005**, *44*, 1564-1567.
497. Rudzevitch, Y.; Rudzevitch, V.; Moon, C.; Schnell, I.; Fischer, K.; Böhmer, V. *J. Am. Chem. Soc.* **2005**, *127*, 14168-14169.

498. Versteegen, R. M.; van Beek, D. J. M.; Sijbesma, R. P.; Vlassopoulos, D.; Fytas, G.; Meijer, E. W. *J. Am. Chem. Soc.* **2005**, *127*, 13862-13868.
499. Laliberté, D.; Maris, T.; Sirois, A.; Wuest, J. D. *Org. Letters* **2003**, *5*, 4787-4790.
500. Metrangolo, P.; Meyer, F.; Pilati, T.; Prosperpio, D. M.; Resnati, G. *Cryst. Gowth Design* **2008**, *8*, 654-659.
501. Castro, R.; Cuadrado, I.; Alonso, B.; Casado, C. M.; Moran, M.; Kaifer, A. E. *J. Am. Chem. Soc.* **1997**, *119*, 5760-5761.
502. Alvarez, J.; Ren, T.; Kaifer, A. E. *Organometallics* **2001**, *20*, 3543-3549.
503. Kaifer, A. E. *Eur. J. Inorg. Chem.* **2007**, 5015-5027.
504. Villoslada, R.; Alonso, B.; Casado, C. M.; Garcia-Armada, P.; Losada, J. *Organometallics* **2009**, *28*, 727-733.
505. Vicinelli, V.; Maestri, M.; Balzani, V.; Müller, W. M.; Müller, U.; Hahn, U.; Oswald, F.; Vögtle, F. *New J. Chem.* **2001**, *25*, 989-993.
506. Cameron, C. S.; Mendoza, S.; Kaifer, A. E. *Chem. Soc. Rev.* **2000**, *29*, 37-42.
507. Cameron, C. S.; Gorman, C. B. *Adv. Funct Mater.* **2002**, *12*, 17-20.
508. Braun, S.; Kalinovski, H.-O.; Berger, S. *150 and More Basic NMR Experiments*; VCH: Weinheim, **1988**, 442-444.
509. Abruña, H. D. *Anal. Chem.* **2004**, *76*, 310A-319A.
510. Cardona, C. M.; Mc Carley, T. D.; Kaifer, A. E. *J. Org. Chem.* **2000**, *65*, 1857-1864.
511. Ong, W.; Kaifer, A. E. *Angew. Chem., Int. Ed.* **2003**, *42*, 2164-2167.
512. Krishnamoorthy, K.; Dasari, R. R.; Nantalaksakul, A.; Thayumanavan, S. *Chem. Commun.* **2007**, 739-741.
513. van de Coevering, R.; Bruijnincx, P. C. A.; van Walree, C. A.; Klein Gebbink, J. M.; van Koten, G. *Eur. J. Org. Chem.* **2007**, 2931-2939.
514. van de Coevering, R.; Bruijnincx, P. C. A.; Lutz, M.; Spek, A. L; van Koten, G.; .; Klein Gebbink, J. M. *New J. Chem.* **2007**, *31*, 1337-1348.
515. Balzani, V.; Ceroni, P.; Gestermann, S.; Gorka, M.; Kauffmann, C.; Vögtle, F. *Tetrahedron*, **2002**, *58*, 629-637.
516. Marchioni, F.; Venturi, M.; Credi, A.; Balzani, V.; Belohadsky, M.; Elizarov, A. M.; Tseng, H. R.; Stoddart, J. F. *J. Am. Chem. Soc.* **2004**, *126*, 568 - 573
517. Jokiel, M.; Shcharbin, D.; Janiszewska, J.; Urbanczyk-Lopkowska, Z.; Bryszewska, M. *J. Fluoresc.* **2007**, *17*, 73-79.
518. Jokusch, S.; Turro, N. J.; Tomalia, D. A. *Macromolecules* **1995**, *28*, 7416-7418.
519. Diallo, M.; Falconer, K.; Johnson, Jr; J. H.; Goddart, III, W. A. *Envir. Sci. Technol.* **2007**, *41*, 6521-6527.
520. Dillon, R. E. A.; Shriver, D. F. *Chem. Mater.* **2001**, *13*, 1369-1373.
521. Namazi, H.; Adell, M. *Biomaterials* **2005**, *26*, 1175-1183.
522. Smith, D. K. *Chem. Commun.* **2006**, 34-44.
523. Smith, D. K.; Hirst, A. R.; Love, C. S.; Hardy, J. G.; Brignel, S. V.; Huang, B. Q. *Prog. Polym. Sci.* **2005**, 220-293.
524. Liu, Y.; Bryantsev, V.; Diallo, M. S.; Goddart, W. A., III *J. Am. Chem. Soc.* **2009**, *131*, 2798-2799.
525. Moorefield, C. N.; Jeong, K. U.; Hwang, S. H.; Li, S.; Cheng, S. Z. D.; Newkome, G. R. *Advan. Mater.* **2008**, *20*, 1381-1382.
526. Alonso, E.; Valério, C.; Ruiz, J.; Astruc, D. *New J. Chem.* **1997**, *21*, 1139-1141.
527. Valério, C.; Ruiz, J.; Fillaut, J. L.; Astruc, D. *C. R. Acad. Sci. Paris* **1999**, *2*, Sér. IIc, 79-83.
528. Takada, K.; Diaz, D. J.; Abruña, H.; Cuadrado, I.; Gonzalez, B.; Casado, C. M.; Alonso, B.; Morán, M.; Losada, J. *Chem. Eur. J.* **2001**, *7*, 1109-1117.
529. Astruc, D.; Daniel, M.-C.; Ruiz, J. *Topics Organomet. Chem.* **2006**, *20*, 121-148.

530. Camponovo, J.; Ruiz, J.; Cloutet, E.; Astruc, D. *Chemistry, Eur. J.*, **2009**, *15,* 2990-3002.
531. Boas, U.; Söntjens, S. H. M.; Jensen, K. J.; Christensen, J. B.; Meijer, E. W. *Chem.BioChem* **2002**, *3*, 433-439.
532. Pittelkow, M.; Chistensen, J. B.; Meijer, E. W. *J. Polym. Sci. A* **2004**, *42*, 3792-3799.
533. Pittelkow, M.; Nielsen, C. B.; Broeren, A. C.; van Dongen, J. L. J.; van Genderen, M. H. P.; Meijer, E. W.; Christensen, J. B. *Chem. Eur. J.* **2005**, *11*, 5126-5135.
534. Broeren, M. A. C.; de Waal, B. F. M.; van Genderen, M. H. P.; Sanders, H. M. H. F.; Fytas, G.; Meijer, E. W. *J. Am. Chem. Soc.* **2005**, *127*, 10334-10343.
535. Ornelas, C.; Boisselier, E.; Martinez, V.; Pianet, I.; Ruiz, J.; Astruc, D. *Chem. Commun.* **2007**, 5093-5095.
536. Boisselier, E.; Ornelas, C.; Pianet, I.; Ruiz, J.; Astruc, D. *Chem. Eur. J.* **2008**, *14*, 5577-5587.
537. Méry, D.; Astruc, D. *Coord. Chem. Rev.* **2006**, *250*, 903-914.
538. Reek, J. N. H.; Arevalo, S. van Heerbeeck, R.; Kamer, P. C. J.; van Leeuwen, P. W. N. M. *Advan. Catal.* **2006**, *49*, 71-151.
539. Hwang, S.-H.; Shreiner, C. D.; Moorefield, C. N.; Newkome, C. N. *New J. Chem.* **2007**, *31*, 1192-1217.
540. Andrés, R.; de Jesus, E.; Flores, J. C. *New J. Chem.* **2007**, *31*, 1161-1191
541. de Jesus, E.; Flores, J. C. *Ind. Eng. Chem. Res*. **2008**, *47*, 7968-7981.
542. Martinez-Olid, F.; Benito, J. M.; Flores, J. C.; de Jesus, E. *Isr. J. Chem*. **2009**, *49*, 99-108.
543. Nepomnyashchii, A. B.; Alpuche-Aviles, M. A.; Pan, S.; Zhan, D.; Fan, F.-R. F.; Bard, A. J. *J. Electroanal. Chem*. **2008**, *621*, 286-296.
544. Newkome, G. R.; Wang, P. S.; Moorefield, C. N.; Cho, T. J.; Mohapatra, P. P.; Li, S. N.; Hwang, S. H.; Lukoyanova, O.; Echegoyen, L.; Palagallo, J. A.; Iancu, V.; Hla, S. W. *Science* **2006**, *312*, 1782-1785.
545. Leung, K. C. Arico, F. Cantrill, S. J. Stoddart, J. F. *J. Am. Chem. Soc.* **2005**, *127*, 5808-5810.
546. Nierengarten, J.-F.; Oswald, L.; Eckert, J.-F.; Nicoud, J.-F.; Armaroli, N. *Tetrahedron Lett.* **1999**, *40*, 5681-5684.
547. Eckert, J.-F.; Byrne, D.; Nicoud, J.-F.; Oswald, L.; Nierengarten, J.-F.; Numata, M.; Ikeda, A.; Shinkai, S. Armaroli, N. *New J. Chem.* **2000**, *24*, 749-758.
548. Armaroli, N.; Boudon, C.; Felder, D.; Gisselbrecht, J.-P.; Gross, M.; Marconi, G.; Nicoud, J.-F.; Nierengarten, J.-F.; Vicinelli, V. *Angew. Chem., Int. Ed. Engl.* **1999**, *38*, 3730-3733.
549. Tewari, A. K.; Dubey, R. *Biorg. Medicin. Chem.* **2008**, *16*, 126-143.
550. Liu, M.; Kono, K.; Fréchet, J. M. J. *Controlled Release* **2000**, *85*, 85-90.
551. Beezer, A E.; King, A. S. H.; Martin, I. K.; Mitchel, J. C.; Twyman, L. J.; Wain, C. F. *Tetrahedron* **2003**, *59*, 3873-3880.
552. Morgan, M. T.; Carnahan, M. A.; Immos, C. E.; Ribeiro, A. A.; Finkelstein, S.; Lee, S. J.; Grinstaff, M. W. *J. Am. Chem. Soc.* **2003**, *125*, 15485-15489.
553. Baars, M. W. P. L.; Kleppinger, R.; Koch, M. H. J.; Yeu, S. L.; Meijer, E. W. *Angew. Chem., Int. Ed.* **2000**, *39*, 1285-1288.
554. Chapman, T.; Hillyer, G. L.; Mahan, E. J.; Shaffer, K. A. *J. Am. Chem. Soc.* **1994**, *116*, 11195-11196.
555. Hawker, C. J.; Wooley, K. L.; Fréchet, J. M. J. *J. Chem. Soc., Perkin Trans.* **1993**, *1*, 1287-1297.
556. Yang, H.; Morris, J. J.; Lopina, S. T. J. *Colloid. Inter. Sci.* **2004**, *273*, 145-154.
557. Pistolis, G.; Malliaris, A. *Langmuir* **2002**, *18*, 246-251.

558. Vutukuri, D. R.; Basu, S.; Thayumanavan, S. *J. Am. Chem. Soc.* **2004**, *126*, 15636-15637.
559. Gupta, U.; Agashe, H. B.; Asthana, A.; Jain, N. K. *Biomacromol.* **2006**, *7*, 649-658.
560. Kaanumalle, L. S.; Nithyanandhan, J.; Pattabiraman, M.; Jayaraman, N.; Ramamurthy, V. *J. Am. Chem. Soc.* **2004**, *126*, 8999-9006.
561. Yiyun, C.; Tongwen, X. *Eur. J. Med. Chem.* **2005**, *40*, 1188-1192.
562. Kono, K.; Fukui, T.; Takahiro, T.; Takagishi, T.; Sakurai, S.; Kojima, C. *Polymer* **2008**, *49*, 2832-2838.
563. Xu, S.; Luo, Y.; Haag, R. *Macromol. Rapid Commun*. **2008**, *29*, 171-174.
564. Kojima, C.; Toi, Y.; Harada, A.; Atsushi, K. K. *Bioconj. Chem*. **2008**, *19*, 2280-2284.
565. Ogawa, M.; Momotake, A.; Arai, T. *Tetrahedron Lett.* **2004**, *45*, 8515-8518.
566. Copper, A. I.; Lonodo, J. D.; Wignall, G.; McClain, J. B.; Samulski, E. T.; Lin, J. S.; Dobrynin, A.; Rubinstein, M.; Buke, A. L. C.; Fréchet, J. M. J.; Desimone, J. M. *Nature* **1997**, *389*, 368-371.
567. Kannaiyan, D.; Imae, T. *Langmuir* **2009**, *25*, 5282-5285.
568. Balagurusamy, V. S. K.; Ungar, G.; Percec, V.; Johansson, G. *J. Am. Chem. Soc.* **1997**, *119*, 1539-1555.
569. Zeng, X. B.; Ungar, G.; Liu, Y. S.; Percec, V.; Dulcey, A. E.; Hobbs, J. K. *Nature* **2004**, *428*, 157-160.
570. Percec, V.; Peterca, M.; Dulcey, A. E.; Iman, M. R.; Hudson, S. D.; Nummelin, S.; Adelman, P.; Heiney, P. A. *J. Am. Chem. Soc.* **2008**, *130*, 13079-13094.
571. Rudick, J. G.; Percec, V. *Acc. Chem. Res.* **2008**, *41*, 1641-1652.
572. Percec, Cho, W.-D.; Ungar, G.; Yeardley, D. J. P. J. *J. Am. Chem. Soc.* **2001**, *123*, 1302-1315.
573. Peterca, M.; Percec, V.; Iman, M. R.; Leowanawat, P.; Morimitsu, K.; Heiney, P. A. *J. Am. Chem. Soc.* **2008**, *130*, 14840-14852.
574. Percec, V.; Iman, M. R.; Peterca, M.; Wilson, D. A.; Heiney, P. A. *J. Am. Chem. Soc.* **2009**, *131*, 1294-1304.
575. Percec, V.; Glodde, M.; Johansson, G.; Venkatachalapathy, S. K.; Balagurusamy, V. S. K.; Heiney, P. A. *Angew. Chem., Int. Ed.* **2003**, *42*, 4338-4342.
576. Kim, C.; Kim, K. T.; Chang, Y.; Song, H. H.; Cho, T. Y.; Jeon, H. J. *J. Am. Chem. Soc.* **2001**, *123*, 5586-5587.
577. Percec, V.; Bera, T. K.; Glodde, M.; Fu, Q.; Balagurusamy, V. S. K.; Heiney, P.A *Chem. Eur. J.* **2003**, *9*, 921-935.
578. Percec, V.; Smidrkal, J.; Peterca, M.; Mitchell, C. M.; Nummelin, S.; Dulcey, A. E.; Sienkowska, M. J.; Heiney, P. A. *Chem. Eur. J.* **2007**, *13*, 3989-4007.
579. Percec, V.; Iman, M. R.; Bera, T. K.; Balagurusamy, V. S. K.; Peterca, M.; Heiney, P. A. *Angew. Chem., Int. Ed.* **2005**, *44*, 4739-4745.
580. Percec, V.; Dulcey, A. E.; Peterca, M.; Ilies, M.; Nummelin, S.; Sienkowska, M.; Heiney, P. A. *Proc. Natl. Acad. Sci. U. S. A.* **2006**, *103*, 2518-2523;.
581. Percec, V.; Imam, M. R.; Peterca, M.; Mihai, C.; Cho, W.-D.; Heiney, P. A. *Isr. J. Chem.* **2009**, *49*, 55-70.
582. Cho, B. K.; Jain, A.; Mahajan, S.; Gruner, S. M.; Wiesner, U. *Science* **2004**, *305*, 1598-1601.
583. Cho, B.-K.; Jain, A.; Mahajan, S.; Ow, H.; Gruner, S. M.; Wiesner, U. *J. Am. Chem. Soc.* **2004**, *126*, 4070-4071.
584. Percec, V.; Glodde, M.; Bera, T. K.; Miura, Y.; Shiyanovskaya, I.; Singer, K. D.; Balagurusamy, V. S. K.; Heiney, P. A.; Schnell, I.; Rapp, A.; Spiess, H.-W.; Hudson, S. D.; Duan, H. *Nature* **2002**, *419*, 384-387.

585. Wen, Y. Q.; Song, Y. L.; Jiang, G. Y.; Zhao, D. B.; Ding, K.; Yuan, W. F.; Lin, X.; Gao, H. J.; Jiang, L.; Zhu, D. B. *Adv. Mater.* **2004**, *16*, 2018-2023.
586. O'MNeill, M.; Kelly, S. M. *Adv. Mater.* **2003**, *15*, 1135- 1138.
587. Percec, V.; Bera, T. K. *Biomacromol.* **2002**, *3*, 167-181.
588. Landskron, K.; Ozin, G. A. *Science* **2004**, *306*, 1529-1532.
589. Gopidas, K. R.; Whitesell, J. K.; Fox, M. A. *J. Am. Chem. Soc.* **2003**, *125*, 6491-6502.
590. Yoon, D. K.; Lee, S. R.; Kim, H. O.; Choi, S.-M.; Jung, H.-T. *Advan. Mater.* **2006**, *18*, 509-513.
591. Tomalia, D. A. *News and Views* **2003**, *2*, 711-712
592. Donnio, B.; Buathong, S.; Bury, I.; Guillon, D. *Chem. Soc. Rev.* **2007**, *36*, 1495-1513.
593. Barbera, J.; Donnio, B.; Gerhinger, L.; Guillon, D.; Marcos, M.; Omenat, A.; Serrano, J. L. *Chem. Eur. J.* **2005**, *15*, 4093-4105.
594. Rueff, J. M.; Barbera, J.; Marcos, M.; Omenat, A.; Martin-Rapun, R.; Donnio, B.; Guillon, D.; Serrano, J. L. *Chem. Mater.* **2006**, *18*, 249-254.
595. McKenna, M. D.; Barbera, M.; Marcos, M.; Serrano, J. L. *J. Am. Chem. Soc.* **2005**, *127*, 619-625.
596. Martin-Rapun, R.; Marcos, M.; Omenat, A.; Barbera, J.; Romero,P.; Serrano, J. L. *J. Am. Chem. Soc.* **2005**, *127*, 7397-7403.
597. Ponomarenko, S. A.; Boiko, N. I.; Shibaev, V. P. *Polym. Sci. Ser. C* **2001**, *43*, 1-45.
598. Donnio, B.; Guillon, D *Adv. Polym. Sci.* **2006**, *201*, 45-155.
599. Bioko, N. I.; Lysachkov, A. I.; Ponomarenko, S. A.; Shibaev, V. P.; Richardson, R. M. *Colloid Polym. Sci.* **2005**, *283*, 1155-1162.
600. Han, H.; Keith, C.; Lang, H.; Reddy, R. A.; Tschierke, C. *Adv. Mater.* **2006**, *18*, 2629-2633.
601. Saez, I. M.; Goodby, J. W. J. *Mater. Chem.* **2005**, *15*, 26-40.
602. Felekis, T.; Tsiourvas, D.; Tziveleka, L; Paleos, C. M. *Liq. Cryst.* **2005**, *32*, 39-43.
603. Busson, P.; Örtegren, J.; Ihre, H.; Gedde, U. W.; Hult, A.; Andersen, G.; Eriksson, A.; Lindgren, M. *Macromolecules* **2002**, 35, 1663-1671.
604. Gehringer, L.; Guillon, D.; Donnio, B. *Macromolecules* **2003**, *36*, 5593-5601.
605. Gehringer, L.; Bourgogne, C.; Guillon, D.; Donnio, B. *J. Am. Chem. Soc.* **2004**, *126*, 3856-3867.
606. Kato, T.; Mizishita, N.; Kishimoto, K. *Angew. Chem., Int. Ed.* **2006**, *45*, 38-68.
607. Deschenaux, R.; Serrano, E.; Levelu, A. M. *Chem. Commun.* **1997**, 1577-1578.
608. Dardel, B.; Guillon, D.; Heinrich, B.; Deschenaux, R. J. *Mater. Chem.* **2001**, *11*, 2814-2831.
609. Maringa, N.; Lenoble J.; Donnio, B.; Guillon, D.; Descheneaux, R. *J. Mater. Chem.* **2008**, *18*, 1524-1534.
610. Campidelli, S.; Pérez, L.; Rodriguez-Lopez, J.; Barbera, J.; Langa, F.; Deschenaux, R. *Tetrahedron* **2006**, *62*, 2115-2122.
611. Campidelli, S.; Vasquez, E.; Milic, D.; Lenoble, J.; Castellano, C. A.; Sarova, G.; Guldi, D. M.; Deschenaux, R.; Prato, M. *J. Org. Chem.* **2006**, *71*, 7603-7610.
612. Campidelli, S; Sevenac, M.; Scanu, D.; Descheneaux, R.; Vazquez, E.; Milic, D.; Prato, M.; Carano, M.; Marcaccio, M.; Paolucci, F.; Rahman, G. M. A.; Guldi, D. M. *J. Mater. Chem.* **2008**, *18*, 1504-1509.
613. Deschenaux, R.; Donnio, B.; Guillon, D. *New J. Chem.* **2007**, *31*, 1064-1073.
614. Marcos, M.; Omenat, A.; Barbera, J.; Duran, F.; Serrano, J. L. J. *Mater. Chem.* **2004**, *14*, 3321-327.
615. Terazzi, E.; Bocquet, B.; Campidelli, S.; Donnio, B.; Guillon, D.; Deschenaux, R.; Piguet, C. *Chem. Commun.* **2006**, 2922-2924.
616. Pesak, D. J.; Moore, J. S. *Angew. Chem., Int. Ed.* **1997**, *36*, 1636-1639.

617. Marcos, M.; Alcala R.; Barbera, J.; Romero, P.; Sanchez, C.; Serrano, J. L. *Chem. Mater*. **2008**, *20*, 5209-5217.
618. Antharjanam, P. K.; Sudhadevi, J.; Jaseer, M.; Ragi, K. N.; Prasad, E. J. *Photochem. Photobiol. A: Chem*. **2009**, *203*, 50-55.
619. Al-Jamal, K. T.; Ramaswany, C.; Florence, A. T. *Adv. Drug. Deliv. Rev.* **2005**, *57*, 2238-2270.
620. Shao, H.; Parquelle, J. R. In *Molecular Recognition and Polymers*, Rotello, V. M.; Thayumanavan, S. Eds.; Wiley: Hoboken, **2008**, 259-306.
621. Ramaswany, C.; Florence, A. T. *J. Drug Deliv. Sci. Tech.* **2005**, *15*, 307-311.
622. Al-Jamal, K. T.; Sakthivel, T.; Florence, A. T. *Int. J. Pharm.* **2003**, *254*, 33-36.
623. Al-Jamal, K. T.; Sakthivel, T.; Florence, A. T. *Int. J. Pharm.* **2005**, *94*, 102-113.
624. Singh, B.; Florence, A. T. *Int. J. Pharm.* **2005**, *298*, 348-353.
625. Heyen, A. J. J. V.; Buron, C. C.; Tianshi, Q.; Bauer, R.; Jonas, A. M.; Müllen, K.; De Schryver, F. C.; De Feyter, S. *Small* **2008**, *4*, 1160-1167.
626. Urbani, C. N.; Lonsdale, D. E.; Bell, C. A.; Whittaker, M. R.; Monteiro, M. J. *J. Polym. Sci., Part A: Polym. Chem*. **2008**, *46*, 1533-1547.
627. Giles, M. D.; Liu, S.; Emanuel, R. L.; Gibb, B. C.; Grayson, S. M. *J. Am. Chem. Soc.* **2008**, *130*, 14430-14431.
628. Peterca, M.; Percec, V.; Imam, M. R.; Leowanawat, P.; Morimitsu, K.; Heiney, P. A. *J. Am. Chem. Soc*. **2008**, *130*, 14840-14852.
629. Gomez-Escudero, A.; Azagarsay, M. A.; Theddu, N.; Vachet, R. W.; Thayumanavan, S. *J. Am. Chem. Soc*. **2008**, *130*, 11156-11163.
630. Fernandez, G.; Sanchez, L.; Perez, E. M.; Martin, M. N. *J. Am. Chem. Soc*. **2008**, *130*, 10674-10683.
631. Hamilton, P. D.; Jacobs, D. Z.; Rapp, B.; Ravi, N. *Mater.* **2009**, *2*, 883-902.
632. Caminati, G.; Turro, N. J.; Tomalia, D. A. *J. Am. Chem. Soc.* **1990**, *112*, 8515-8522.
633. Esumi, K.; Chiba, T.; Mizutami, H.; Shoji, K.; Torigoe, K. *Colloids Surf. A* **2000**, *166*, 115-121.
634. Esumi, K.; Chiba, T.; Misutani, H.; Shoji, K.; Torigoe, K. *Colloids Surf., A* **2001**, *179*, 103-109.
635. Yoshimura, T.; Fukai, J.; Mizutani, H.; Esumi, K. J. *Colloid Interf. Sci.* **2002**, *255*, 428-431.
636. Minard-Basquin, C.; Weil, T.; Honer, J. O.; Radler, K.; Müllen, A. *J. Am. Chem. Soc.* **2003**, *125*, 5832-5838.
637. Blanzat, M.; Turrin, C-O.; Perez, E.; Rico-Lattes, I.; Caminade, A.-M.; Majoral, J.-P. *Chem. Commun.* **2002**, 1864-1865.
638. Karukstis K. K.; Thonstad S. C.; Hall M. E. *J. Dispers. Sci. Technol.* **2002**, *23*, 737-746.
639. Rogacheva, V. B.; Novoskol'tseva, O. A.; Zezin, A. B.; Joosten, J.; Brackman, J. *Polym. Sci., A* **2007**, *49*, 1000-1007.
640. Yia, C.; Xua, Z.; Ford, W. T. *China Particuology* **2004**, *2*, 222-225.
641. Yi, C. F.; Shen, Y. H.; Deng, Z. W.; Xu, Z. S.; Ford, W. T. *Acta Polym. Sin.* **2004**, 831-834.
642. Yi, C. F.; Xu, Z. S.; Ford, W. T. *Colloid. Polym. Sci.* **2004**, *282*, 1054-1058.
643. Xu, Z. S.; Ford, W. T. *Macromolecules* **2002**, *35*, 7662-7668.
644. Xu, Z. S.; Ford, W. T. *J. Polym. Sci., A* **2003**, *41*, 597-605.
645. Ford, W. T. *React. Funct. Polym.* **2001**, *48*, 3-13.
646. Donners, J. J. J. M.; Heywood, B. R.; Meijer, E. W.; Nolte, R. J. M.; Sommerdijk, N. A. J. M. *Chemistry Eur. J.* **2002**, *8*, 2561-2567;

647. Rico-Lattes, I.; Blanzat, M; Franceschi-Messant, S; Perez, T.; Lattes, A. *C. R. Chimie* **2005**, *8*, 807-814.
648. Thérien-Aubin, H.; Zhu, X. X.; Moorefield, C. N.; Kotta, K.; Newkome, G. *Macromolecules* **2007**, *40*, 3644-3649.
649. Zhao, M.; Sun, L.; Crooks, R. M. *J. Am. Chem. Soc.* **1998**, *120*, 4877-4878.
650. Balogh, L.; Tomalia, D. A. *J. Am. Chem. Soc.* **1998**, *120*, 7355-7356.
651. Esumi, K.; Suzuki, A.; Aihara, N.; , Usu, K.; Torigoe, K. *Langmuir* **1998**, *14*, 3157-3159.
652. Crooks, R. M.; Zhao, M.; Sun, L.; Chechik, V.; Yeung, L. K. *Acc. Chem. Res.* **2001**, *34*, 181-190.
653. Niu, Y.; Crooks, R. M. *C. R. Chimie* **2003**, *6*, 1049-1060.
654. Scott, R. W. J.; Wilson, O. M.; Crooks, R. M. *J. Phys. Chem B* **2005**, *109*, 692-704.
655. Yeung, L. K.; Crooks, R. M. *Nano Lett.* **2001**, *1*, 14-17.
656. Lemo, J.; Heuzé, K.; Astruc, D. *Inorg. Chim. Acta* **2006**, *359*, 4909-4911.
657. Gomez, M. V.; Guerra, J.; Velders, A. H.; Crooks, R. M. *J. Am. Chem. Soc.* **2008**, *131*, 341-350.
658. Ornelas, C.; Ruiz, J.; Cloutet, E.; Alves, S.; Astruc, D. *Angew. Chem,. Int. Ed.* **2007,** 46, 872-877.
659. Ornelas, C.; Salmon, L.; Ruiz, J.; Astruc, D. *Chem. Eur. J.*, **2008**, *14*, 50-64.
660. Candelon, N.; Lastécouères, D.; Diallo, A. K.; Ruiz, J.; Astruc, D.; Vincent, J.-M. *Chem. Commun.* , **2008**, 741-743.
661. Badèche, S.; Daran, J.-C.; Ruiz, J.; Astruc, D. *Inorg. Chem*., **2008***, 47,* 4903-4908.
662. Camponovo, J.; Hadad, C.; Ruiz, J.; Cloutet, E.; Gatard, S.; Bouquillon, S.; Astruc, D. *J. Org. Chem.* **2009**, *74*, 5071-5074.
663. Boisselier, E.; Salmon, L.; Ruiz, J.; Astruc, D. *Chem. Commun.* **2008**, 5788-5790.
664. Balogh, L.; Swanson, D. R.; Tomalia, D. A.; Hagnauer, G. L.; McManus, A. T. *Nano Lett.* **2001**, *1*, 18-21.
665. Dickson, R. M. *J. Am. Chem. Soc.* **2002**, *124*, 13982-13983.
666. Esumi, K.; Matsumoto, T.; Seto, Y.; Yoshimura J. *Coll. Interf. Sci.* **2005**, *284*, 199-203.
667. Pan, B.; Gao, F.; Ao, L.; Tian, H.; He, R.; Cui, D. *Coll. Surf. A: Physicochem. Eng. Asp.* **2005**, *259*, 89-94.
668. Wu, H.; Liu, Z.; Wang, X.; Zhao, B.; Zhang, J.; Li, C. J. *Coll. Interf. Sci.* **2006**, *302*, 142-148.
669. Lebedeva, O. V.; Kim, B.-S.; Gröhn, F.; Vinogradova, O. I. *Polymer* **2007**, *48*, 5024-5029.
670. Bao, Y.; Zhong, C.; Vu, D. M.; Temirov, J. T.; Dyer, R. B.; Martinez, J. S. *J. Phys. Chem. C* **2007**, *111*, 12194-12198.
671. Bergamini, G.; Ceroni, P.; Balzani, V.; Gingras, M.; Raimundo, J.-M.; Morandi, V.; Merli, P. G. *Chem. Commun.* **2007**, 4167-4169.
672. Fahmi, A.; D'Aléo, A.; Williams, R. M.; De Cola, L.; Gindy, N.; Vögtle, F. *Langmuir* **2007**, *23*, 7831-7835.
673. Tanaka, H.; Koizumi, S.; Hashimoto, T.; Itoh, H.; Satoh, M.; Naka, K.; Chujo, Y. *Macromolecules* **2007**, *40*, 4327-4337.
674. Li, G.; Luo, Y. *Inorg. Chem.* **2008**, *47*, 360-364.
675. Yamamoto, K.; Takanashi, K. *Polymer* **2008**, *49*, 4033-4041.
676. Srivastava, S.; Frankamp, B. L.; Rotello, V. M. *Chem. Mater.* **2005**, *17*, 487-490.
677. Worden, J. G.; Huo, Q. D. *Chem. Commun.* **2006**, 1536-1538.
678. Knecht, M. R.; Weir, M. G.; Frenkel, A. I.; Crooks, R. M. *Chem. Mater.* **2008**, *20*, 1019-1028.

679. Larpent, C.; Cannizzo, C.; Delgado, A.; Gouanve, F.; Sanghvi, P.; Gaillard, C.; Bacquet, G. *Small* **2008**, *4*, 833-840.
680. Atwater, J. E.; Akse, J. R.; Holtsnider, J. T. *Mater. Lett.* **2008**, *62*, 3131-3134.
681. Donners, J. J. J.; Hoogenboom, R.; Schenning, A. P. H. J.; van Hal, P. A.; Nolte, R. J. M.; Meijer, E. W.; Sommerdijk, N. A. J. M. *Langmuir* **2002**, *18*, 2571-2576.
682. Guo, W.; Li, J. J.; Wang, A.; Peng, X. *Chem. Mater.* **2003**, *15*, 3125-3133.
683. Tomalia, B. H.; Tomalia, D. A. *J. Luminesc.* **2005**, *111*, 215-223.
684. Liu., J.; Li, H.; Wang, W.; Xu, H.; Yang, X.; Liang, J.; He, Z. *Small* **2006**, *2*, 999-1002.
685. Li, M.; Wang, J.; Feng, L.; Wang, B.; Jia, X.; Jiang, L.; Song, Y.; Zhu, D. *Coll. Surf. A: Physicochem. Eng. Asp.* **2006**, *290*, 233-238.
686. Donners, J. J. J. M.; Heywood, B. R.; Meijer, E. W.; Nolte, R. J. M.; Sommerdijk, N. A. J. M. *Chem. Eur. J.* **2002**, *8*, 2561-2567.
687. Zhang, F.; Zhou, Z.-H.; Mao, L.-H.; Chen, H.-M.; Yu, X.-B. *Mater. Lett.* **2005**, *59*, 1422-1425.
688. Gladtz, M.; Reinemann, S.; Radusch, H.-J. *Macromol. Mater. Eng.* **2009**, *294*, 178-189.
689. Love, J. CC.; Estroff, L. A.; Kriebel, J. K.; Nuzzo, R. G.; Whitesides, G. M. *Chem. Rev.* **2005**, *105*, 1103-1169.
690. Onclin, S.; Ravoo, B. J.; Reinhoudt, D. N. *Angew. Chem., Int. Ed.* **2005**, *44*, 6282-6304.
691. Nijhuis, C. A.; Yu, F.; Knoll, W.; Huskens, J.; Rheinhout, D. N. *Langmuir* **2005**, *21*, 7866-7876.
692. Nijhuis, C. A.; Boucamp, B. A.; Ravoo, B. J.; Huskens, J.; Reinhoudt, D. N. *J. Phys. Chem. C* **2007**, *111*, 9799-9810, cor. 12872-12872.
693. Nijhuis, C. A.; ter Maat, J.; Bisri, S. Z.; Weusthof, M. H. H.; Salm, C.; Schmitz, J.; Ravoo, B. J.; Huskensa, J.; Reinhoud, D. N. *New J. Chem.* **2008**, *32*, 652-661.
694. Nijhuis, C. A., Dolatowska, K. A., Ravoo, B. J.; Huskens, J.; Reinhoudt, D. N. *Chem. Eur. J.* **2007**, *13*, 69-80.
695. Cieplak, M.; Thompson, D. *J. Chem. Phys.* **2008**, *128*, 234906.
696. Sun, L.; Crooks, R. M. *Langmuir* **2002**, *18*, 8231-8236.
697. Decher, G. *Science* **1997**, *277*, 1232-1237.
698. He, J. A.; Valluzzi, R.; Yang, K.; Dolukhanyan, T..; Sung, C. M.; Kumar, J.; Tripathy, S. K.; Samuelson, L.; Balogh, L.; Tomalia, D. A. *Chem. Mater.* **1999**, *11*, 3268-3274.
699. Esumi, K.; Akiyama, S.; Yoshimura, T. *Langmuir* **2003**, *19*, 7679-7681.
700. Lebedeva, O. V.; Kim, B. S.; Grön, F.; Vinogradova, O. I. *Polymer* **2007**, *48*, 5024-5029.
701. Nijhuis, C. A., Oncel, J., Huskens, J.; Zandvliet, H. J. W.; Ravoo, B. J.; Poelsema, B. Reinhoudt, D. N. *Small*, **2006**, *2*, 1422-1426.
702. Tomita, S.; Sato, K.; Anzai, J.-i. *J. Colloid Interf. Sci.* **2008**, *326*, 35-40.
703. Li, H.; Kang, D.-J.; Blamire, M. G.; Huck, W. T. S. *Nano Lett.* **2002**, *2*, 347-349.
704. de Gans, B. J.; Xue, L.; Agarwal, U. S.; Schubert, U. S. *Macromol. Rapid. Commun.* **2005**, *26*, 310-314.
705. Yamazaki, T.; Imae, T.; Sugimura, H.; Saito, N.; Hayashi, K.; Takai, O. *J. Nanosci. Nanotechnol.* **2005**, *5*, 1792-1800.
706. Thibault, C.; Severac, C.; Trévisol, E.; Vieu, C. *Microelectron. Eng.* **2006**, *83*, 1513-1516; Thompson, D. *Langmuir* **2007**, *23*, 8441-8451
707. Bittner, A. M.; Wu, X. C.; Kern, K. *Adv. Funct. Mater.* **2002**, *12*, 432-436.
708. Wu X. C.; Bittner, A. M.; Kern, K. *Langmuir* **2002**, *18*, 4984-4988.

709. Bruinink, C. M.; Nijhuis, C. A.; Peter, M.; Dordi, B.; Crespo-Biel, O.; Auletta, T.; Mulder, A.; Schönherr, H.; Vancso, G. J.; Huskens, J.; Reinhoudt, D. N. *Chem. Eur. J.* **2005**, *11*, 3988-3996.
710. Nijhuis, C. A.; Kinsha, J.; Wittstock, G.; Ravoo, B. J.; Huskens, J.; Reinhoudt, D. N. *Langmuir* **2006**, *22*, 9770-9775.
711. Nijuis, C. A.; ter Maat, J.; Bisri, S. Z.; Weusthof, M. H. H.; Sam, C.; Schmitz, J.; Ravoo, B. J.; Huskens, J.; Reinhoudt, D. N. *New J. Chem.* **2008**, *32*, 652-661.
712. Amama, P. B.; Mashmann, M. R.; Fischer, T. S.; Sands, T. D. *J. Phys. Chem. B* **2006**, *110*, 10636-10644.
713. Nijhuis, C. A.; ter Maat, J.; Bisri, S. Z.; Weusthof, M. H. H.; Salm, C.; Schmitz, J.; Ravoo, B. J.; Huskens, J.; Reinhoudt, D. N. *New J. Chem.* **2008**, *32*, 652-651.
714. Ling, X. Y.; Reinhoudt, D. N.; Huskens, J. *Chem. Mater*. **2008**, *20*, 3574-3578.
715. Ravoo, B. *J. Dalton Trans.* (Frontiers) **2008**, 1533-1537.
716. Rozkiewicz, D. I.; Brugman, W.; Kerkhoven, R. M.; Ravoo, B. J.; Reinhoudt, D. N. *J. Am. Chem. Soc.* **2007**, *129*, 11593-11599.
717. Latini, G.; Wykes, M.; Schlapak, R.; Horworka, S.; Cacialli, F. *Appl. Phys. Letters* **2008**, *92*, 013511/1-013511/3.
718. Nakashima, T.; Satoh, N.; Abrecht, K.; Yamamoto, K. *Chem. Mater*. **2008**, *20*, 2538-2543.
719. Chen, S.; Yu, Q.; Li, L.; Boozer, C. L.; Homola, J.; Yee, S. S.; Jiang, S. *J. Am. Chem. Soc.* **2002**, *124*, 3395-3401.
720. Finikova, O.; Galkin, A.; Rozhkov, V.; Cordero, M.; Hägerhäll; Vinogradov, S. *J. Am. Chem. Soc.* **2003**, *125*, 4882-4883.
721. Li, W.-S.; Jiang, D.-L.; Suna, Y.; Aida, T. *J. Am. Chem. Soc.* **2005**, *127*, 7700-7702.
722. Brinas, R. P.; Troxler, T.; Hochstrasser, R. M.; Vinogradov, S. A. *J. Am. Chem. Soc.* **2005**, *127*, 11851-11862.
723. Grabchev, I.; Chovelon, J.-M.; Nedelcheva, A. *J. Photochem. Photobiol. A: Chem.* **2006**, *183*, 9-14.
724. Harpham, M. R.; Süzer, M. R. : Ma, C.-Q.; Bäuerle, P.; Goodson III, T. *J. Am. Chem. Soc.* **2009**, *131*, 973-979.
725. Beer, P. D. *Angew. Chem., Int. Ed.* **2001**, *40*, 486-516.
726. Beer, P. D.; Bayly, S. R. *Top. Curr. Chem.* **2005**, *255*, 125-162.
727. Crespilho, F. N.; Zucolotto, V.; Brett, C. M.; Oliveira, O. N., Jr.; Nart, F. C. *J. Phys. Chem. B* **2006**, *110*, 17478-17483.
728. Crespilho, F. N.; Nart, F. C.; Oliveira, O. N. Jr. *Electrochim. Acta* **2007**, *52*, 4649-4653.
729. Crespilho, F. N.; Ghica, M. E.; Zucolotto, V.; Nart, F. C.; Oliveira, O. N. Jr. *Electroanal*. **2007**, *19*, 805-812.
730. Chandra, S.; Buschbeck, R.; Lang, H. *Talanta* **2006**, *70*, 1087-1093.
731. Bustos, E. B.; Chapman, T. W.; Rodriguez-Valadez, F.; Godinez, L. A. *Electroanal.* **2006**, *21*, 2092-2098;
732. Krasteva, N.; Besnard, I.; Guse, B.; Bauer, R. E.; Müllen, K.; Yasuda, A.; Vossmeyer, T. *Nano Lett.* **2002**, *2*, 551-555.
733. Duan, S.; Kouketsu, T.; Kasama, S.; Yamada, K. *J. Membrane Sci.* **2006**, *283*, 2-6.
734. Kouketsu, T.; Duan, S.; Kai, T.; Kasama, S.; Yamada, K. *J. Membrane Sci.* **2007**, *287*, 51-69.
735. Gao, T.; Tillman, E. S.; Lewis, N. S. *Chem. Mater.* **2005**, *17*, 2904-2911.
736. Duan, S.; Chowdhury, F. A.; Kai, T.; Kazama, S.; Fujioka, Y. *Desalinatin* **2008**, *234*, 278-285.
737. Koo, B. W.; Song, C. K.; Kim, C. *Sens. Actuators B* **2001**, *77*, 432-436.

738. Liang, Z.; Fahdel, B.; Schneider, C. J.; Chaffee, A. L. Microprous *Mesoporous Mater.* **2008**, *111*, 536-543.
739. Zimmermann, S. C.; Wendland, M. S.; Rakow, N. A.; Zharov, I.; Suslick, K. S. *Nature* **2002**, *418*, 399-403.
740. Wells, M.; Crooks, R. M. *J. Am. Chem. Soc.* **1996**, *118*, 3988-3989.
741. Zimmerman, S. C.; Zharov, I.; Wendland, M. S.; Rakow, N. A.; Suslick, K. S. *J. Am. Chem. Soc.* **2003**, *125*, 13505-13518.
742. Elmer, S. L.; Lemcoff, N. G.; Zimmerman, S. C. *Macromolecules* **2007**, *40*, 8114-8118.
743. Mertz, E.; Zimmerman, S. C. *J. Am. Chem. Soc.* **2003**, *125*, 3424-3425.
744. Ornelas, C.; Méry, D.; Ruiz, J.; Blais, J.-C.; Cloutet, E.; Astruc, D. *Angew. Chem., Int. Ed.* **2005,** *44***,** 7399-7404.
745. Ornelas, C.; Méry, D.; Cloutet, E.; Ruiz, J.; Astruc D. *J. Am. Chem. Soc*. **2008**, *130*, 1495-1506.
746. Astruc, D. *New J. Chem*., **2005**, *29*, 42-56.
747. Astruc, D. *Oil & Gas Science and Technology* **2007**, *62*, 787-797.
748. Elmer, S. L.; Lemcoff, N. G.; Zimmerman, S. C. *Macromolecules* **2007**, *40*, 8114-8118.
749. Mertz, E.; Zimmerman, S. C. *J. Am. Chem. Soc.* **2003**, *125*, 3424-3425.
750. Zimmerman, S. C.; Lemcoff, N. G. *Chem. Commun.* **2004**, 5-14.
751. Kim, Y.; Mayer, M. F.; Zimmerman, S. C. *Angew. Chem., Int. Ed.* **2003**, *42*, 1121-1126.
752. Beil, J. B.; Zimmerman, S. C. *Chem. Commun.* **2004**, 488-489.
753. Mertz, E.; Elmer, S. L.; Balija, A. L.; Zimmerman, S. C. *Tetrahedron* **2004**, *60*, 11191-11204.
754. Lemcoff, N. G.; Spurlin, T. A.; Gewirth, A. A.; Zimmermann, S. C.; Beil, J. B.; Elmer, S. L.; Vandeveer, H. G. *J. Am. Chem. Soc.* **2004**, *126*, 11420-11421.
755. Beil, J. B.; Lemcoff, N. G.; Zimmerman, S. C. *J. Am. Chem. Soc.* **2004**, *126*, 13576-13577.
756. Adana, J.; Wang, X.; Peng, J. *J. Am. Chem. Soc.* **2001**, *123*, 8844-8845.
757. Wang, Y. A.; Li, J. J.; Chen, H.; Peng, X. *J. Am. Chem. Soc.* **2002**, *124*, 2293-2294.
758. Guo, W.; Li, H. H.; Wang, Y. A.; Peng, X. *J. Am. Chem. Soc.* **2003**, *125*, 3901-3909.
759. Guo, W.; Peng. X. *C. R. Chimie* **2003**, *6*, 989-997.
760. Astruc, D. *Electron-Tranfer and Radical Processes in Transition-Metal Chemistry*, VCH: New York, 1995.
761. Gorman, C. B. *Acc. Chem. Res*. **2001**, *34*, 60-71.
762. Dandliker, P. J.; Diederich, F., Gross, M., Knobler, C. B., Louati, A.; Sanford, E. M. *Angew. Chem., Int. Ed*. **1994**, *33*, 1739-1742.
763. Moulines, F.; Djakovitch, L.; Boese, R.; Gloaguen, B.; Thiel, W.; Fillaut, J.-L.; Delville M.-H.; Astruc, D. *Angew. Chem., Int. Ed. Engl.* **1993**, *32*, 1075-1077.
764. Flanagan, J. B.; Marel, A.; Bard, A. J.; Anson, F. C.; *J. Am. Chem. Soc.* **1978**, 100, 4258-4253.
765. Ronconi, C. M.; Stoddart, J. F.; Balzani, V.; Baroncini M.; Ceroni, P.; Giansante, C.; Venturi, M. *Chem. Eur. J.* **2008**, *14*, 8365-8373 **.**
766. Ornelas, C.; Ruiz, J.; Belin, C.; Astruc, D. *J. Am. Chem. Soc*., **2009**, *131*, 590-601.
767. Ornelas, C.; Astruc, D.; Ruiz, J. *Chem. Eur. J.* **2009**, *15*, 8936-8944.
768. Amatore, C.; Grun, F.; Maisonhaute, E. *Angew. Chem., Int. Ed.* **2003**, 40, 4944-4947.
769. Amatore, C.; Bouret, Y.; Maisonhaute, E.; Goldsmith, J. I.; Abruña, H. D. *Chem. Eur. J.* **2001**, *7*, 2206-2226.

770. Green, S. J.; Pietron, J. J.; Stokes, J. J.; Hostetler, M. J.; Wu, H.; Wuelfing, W. P.; Murray, R. W. *Langmuir* **1998**, *14*, 5612-5619.
771. Wang, A.; Ornelas, C.; Astruc, D.; Hapiot, P. *J. Am. Chem. Soc*. **2009**, *131*, 6652-6653.
772. Wang, A.; Nöel, J.-M.; Zigah, D.; Ornelas, C.; Lagrost, C.; Astruc, D.; Hapiot, P. *J. Electrochem*. **2009**, *11*, 1703-1706.
773. Nlate, S.; Ruiz, J.; Sartor, V.; Navarro, R.; Blais, J.-C.; Astruc, D. *Chemistry, Eur. J.* **2000**, *6*, 2544-2553.
774. Gladysz, J. A. *Chem. Rev*. **2002**, *102*, 3215-3216.
775. Cole-Hamilton, D.; Toose, R.P. *Catalyst Separation, Recovery and Recycling.* Eds. Springer, Heidelberg, **2006**.
776. Kleij, R. A.; van Leeuwen, P. W. N. M., van der Made, A. W.; EP0456317, **1991** [*Chem. Abstr.* **1992**, *116*, 129870].
777. Brunner, H.; Fürst, J.; Ziegler, J. *J. Organomet. Chem*. **1993**, *454*, 87-94.
778. Brunner, H.; Fürst, J. *Tetrahedron* **1994**, *50*, 4303-4310.
779. Brunner, H.; Altmann, S. *Chem. Ber.* **1994**, *127*, 2285-2296.
780. Brunner, H. *J. Organomet. Chem.* **1995**, *500*, 39-46.
781. Miedaner, A.; Curtis, C. J.; Barkley, R. M.; DuBois, D. L. *Inorg. Chem.* **1994**, *33*, 5482-5490.
782. Lee, J.-J.; Ford, W. T.; Moore, J. A.; Li, Y. *Macromolecules* **1994**, *27*, 4632-4634.
783. Knapen, J. W. J.; van der Made, A. W.; de Wilde, J. C.; van Leeuwen, P. W. N. M.; Wijkens, P.; Grove, D. M.; van Koten, G. *Nature* **1994**, *372*, 659-663.
784. Reetz, M.-T; Lohmer, G.; Schwickardi, R. *Angew. Chem., Int. Ed. Engl.* **1997**, *36*, 1526-1529.
785. de Vries, G. J. *Dalton. Trans.* **2006**, 421-429
786. Astruc, D.; Lu, F.; Ruiz, J. *Angew. Chem., Int. Ed.* **2005**, *44*, 7852-7872.
787. Astruc, D. *Inorg. Chem.* **2007**, *46*, 1884-1894.
788. Brinkmann, N.; Giebel, D.; Lohmer, G.; Reetz, M. T.; Kragl, U. *J. Catal.* **1999**, *183*, 163-168.
789. Bourque, S. C.; Maltais, F.; Xiao, W. J.; Tardif, O.; Alper, H.; Manzer, L. E.; Arya, P. *J. Am. Chem. Soc.* **1999**, *121*, 3035-3038.
790. Zhao, M.; Crooks, R. M. *Angew. Chem., Int. Ed.* **1999**, *38*, 364-366.
791. Rigaut, S.; Delville, M.-H.; Astruc, D. *J. Am. Chem. Soc.,* **1997**, *119*, 11132-11133.
792. Valério, C.; Rigaut, S.; Ruiz, J.; Fillaut, J.-L.; Delville, M.-H.; Astruc, D. *Bull. Pol. Acad. Sci*. **1998**, *46*, 309-318.
793. Rigaut, S.; Delville, M.-H.; Losada, J.; Astruc, D. *Inorg. Chim. Acta*, **2002**, *334*, 225-242.
794. Bhyrappa, P.; Young, J. K.; Moore, J. S.; Suslick, K. S. *J. Mol. Catal. A: Chem.* **1996**, *113*, 109-116.
795. Bhyrappa, P.; Young, J. K.; Moore, J. S.; Suslick, K. S. *J. Am. Chem. Soc.* **1996**, *118*, 5708-5711.
796. Liang, C. O.; Helms, B.; Hawker, C. J.; Fréchet, J. M. J. *Chem. Commun.* **2003**, *20*, 2524-2525.
797. Helms, B.; Liang, C. O.; Hawker, C. J.; Fréchet, J. M. J. *Macromolecules* **2005**, *38*, 5411-5415.
798. Oosterom, G. E.; Reek, J. N. H.; Kamer, P. C. J.; van Leeuwen, P. W. N. M. *Angew. Chem., Int. Ed.* **2001**, *40*, 1828-1849.
799. Astruc, D.; Chardac, F. *Chem. Rev.* **2001**, *101*, 2991-3031.
800. Kreiter, R.; Kleij, A. W.; Klein Gebbink, R. J. M.; van Koten, G. *Top. Curr. Chem.* **2001**, *217*, 163-199.

801. van Heerbeek, R.; Kamer, P. C. J.; van Leeuwen, P. W. N. M.; Reek, J. N. H. *Chem. Rev.* **2002**, *102*, 3717-3756.
802. Caminade, A.-M.; Maraval, V.; Laurent, R.; Majoral, J.-P. *Curr. Org. Chem.* **2002**, *6*, 739-774.
803. Dijkstra, H. P.; van Klink G. P. M.; van Koten, G. *Acc. Chem. Res.* **2002**, *35*, 798-810.
804. Reek, R. N. H.; de Groot, D.; Oosterom, E.; Kamer, P. C. J.; van Leeuwen, P. W. N. M. *C. R. Chimie*, **2003**, *6*, 1061-1078.
805. *Dendrimer Catalysis* Gade, L. Ed. Springer: Heidelberg, **2006**.
806. Ribourdouille, Y.; Engel, G. D.; Gade, L. In *Dendrimers and Nanosciences*, Astruc, D. Ed., *C. R. Chimie*, **2003**, *6*, 1087-1096.
807. Soai, K.; Sato, I. In *Dendrimers and Nanosciences*, Astruc, D. Ed. *C. R. Chimie* **2003**, *6*, 1097-1104.
808. Che, C.-M.; Huang, J.-S.; Zhang, J.-L. In *Dendrimers and Nanosciences*, Astruc, D. Ed. *C. R. Chimie*, **2003**, *6*, 1105-1115.
809. van Klink, G. P. M.; Dijstra, H. P.; van Koten, G. In *Dendrimers and Nanosciences*, Astruc, D. Ed. *C. R. Chimie*, **2003**, *6*, 1079-1085.
810. Bourrier, O.; Kakkar, A.K. *Macromol. Symp.* **2004**, *209*, 97-118.
811. Müller, C.; Nijkamp, M. G.; Vögt, D. *Eur. J. Inorg. Chem.* **2005**, 4011-4021.
812. Dahan, A.; Portnoy, M. J. *Polymer Science: Part A: Polymer Chemistry* **2005**, *43*, 235-262.
813. Astruc, D.; Heuzé, K.; Gatard, S.; Méry, D.; Nlate, S.; Plault, L. *Adv. Synth. Catal.* **2005**, *347*, 329-338.
814. Astruc, D. *C. R. Chimie*, **2005**, *8*, 1101-1107.
815. Reek, J. N. H.; Arévalo, S.; van Herrbeck, R.; Kamer, P. C. J.; van Leeuwen, P. W. N. M. In *Advan. Catal. Gates*, B.; Knözinger, H. Eds. Academic Press: San Diego, CA, **2006**, *49*, 71-151;
816. Helms, B.; Fréchet, J. M. J. *Adv. Synth. Catal.* **2006**, *348*, 1125-1148.
817. Méry, D; Astruc, D. *Coord. Chem. Rev.* **2006**, *250*, 1965-1979.
818. Berger, A.; Gebink, R. J. M. K. *Top. Organomet. Chem.* **2006**, *20*, 1-38.
819. de Jesús, E.; Flores, J. C. *Ind. Eng. Chem. Res.* **2008**, *47*, 7968-7981.
820. Wang, Z. J.; Deng, G.-J.; Li, Y.; He, Y.-M.; Tang, W.-J.; Fan, Q.-H. *Org. Lett.* **2007**, *9*, 1243-1246.
821. Liu, W.; Cui, X.; Cun, L.; Zhu, J.; Deng, J. *Tetrahedron Assymmetry* **2005**, *16*, 2525-2530.
822. Jiang, L.; Wu, T.F.; Chen, Y.-C.; Deng, J.-G. *Org. Biomol. Chem.* **2006**, *4*, 3319-3324.
823. Zeng, H.; Newkome, G. R.; Hill, C. L. *Angew. Chem., Int. Ed.* **2000**, *39*, 1772-1774.
824. Plault, L.; Hauseler, A.; Nlate, S.; Astruc, D.; Ruiz, J.; Gatard, S.; Neumann, R. *Angew. Chem., Int. Ed.* **2004**, *43*, 2924-2928.
825. Vasylyev, M. V.; Astruc, D.; Neumann, R. *Adv. Synth. Catal.* **2005**, *347*, 39-43.
826. Nlate, S.; Astruc, D.; Neumann, R. *Adv. Synth. Catal.* **2004**, *346*, 1445-1448.
827. Nlate, S.; Plault, L.; Astruc, D. *Chem. Eur. J.* **2006,** *12*, 903-914.
828. Nlate, S.; Plault, L.; Astruc, D. *New J. Chem*. **2007**, *31*, 1264-1274.
829. Heuzé, K.; Méry, D.; Gauss, D.; Astruc, D. *Chem. Commun.* **2003**, 2274-2275.
830. Méry, D.; Heuzé, K.; Astruc, D. *Chem. Commun.* **2003**, 1934-1935.
831. Heuzé, K.; Méry, D.; Gauss, D.; Blais, J.-C.; D. Astruc *Chem. Eur. J*. **2004**, *10*, 3936-3944.
832. Servin, P.; Laurent, R.; Romerosa, A.; Peruzzini, M.; Majoral, J.-P.; Caminade, A.-M. *Organometallics* **2008**, *27*, 2066-2073.
833. Lemo, J.; Heuzé, K.; Astruc, D. *Org. Letters* **2005**, *7*, 2253-2256.

834. Lemo, J.; Heuzé, K.; Astruc, D. *Chem. Commun*. **2007**, 4351-4353
835. Laurent, R.; Caminade, A.-M.; Majoral, J.-P. *Tetrahedron Lett*. **2005**, *46*, 6503-6506
836. Gissibl, A.; Padié, C.; Hager, M.; Jaroschik, F.; Rasappan, R.; Cuevas-Yanez, E.; Turin, C.-O.; Caminade, A.-M.; Majoral, J.-P.; Reiser, O. *Org. Lett*. **2007**, 2895-2898.
837. Murati, T.; Fujita, K.; Kujime, M. *J. Org. Chem.* **2007**, *72*, 7863-7870.
838. Zweni, P. P.; Alper, H. *Adv. Syn. Catal.* **2004**, *346*, 849-854.
839. Chanthateyanonth, R.; Alper, H. *Adv. Syn. Cat*. **2004**, *346*, 1375-1384.
840. Lu, S.-M.; Alper, H. *J. Org. Chem.* **2004**, *69*, 3558-3561.
841. Lu, S.-M.; Alper, H. *J. Am. Chem. Soc.* **2005**, *127*, 14776-14784.
842. Touzani, R.; Alper, H. *J. Mol. Catal. A* **2005**, *227*, 197-207.
843. Zweni, P. P.; Alper, H. *Adv. Syn. Catal.* **2006**, *348*, 725-731.
844. Lu, S.-M.; Alper, H. *Chem. Eur. J.* **2007**, *13*, 5908-5916.
845. Dahan, A.; Portnoy, M. *J. Am. Chem. Soc.* **2007**, *129*, 5860-5869.
846. Kehat, T.; Goren, K.; Portnoy, M. *New J. Chem.* **2007**, *31*, 1218-1242.
847. Reynardt, J. P. K.; Yang, Y.; Sayari, A.; Alper, H. *Chem. Mater.* **2004**, *16*, 4095-4102.
848. Acosta, E. J.; Carr, C. S.; Simanek, E. E.; Shantz, D. F. *Adv. Mater.* **2004**, *16*, 985-989.
849. Reynhardt, J. P. K.; Yang, Y.; Sayari, A.; Alper, H. *Adv. Funct. Mater.* **2005**, *15*, 1641-1646.
850. Reynhardt, J. P. K.; Yang, Y.; Sayari, A. *Adv. Syn. Catal.* **2005**, *347*, 1379-1388.
851. Kehat, T.; Portnoy, M. *Chem. Commun.* **2007**, 2823-2825.
852. Abu-Rezik, R.; Alper, H.; Wang, D.; Post, M. L. *J. Am. Chem. Soc.* **2006**, *128*, 5279-5282.
853. Chandler, B. D.; Gilbertson, J. D. In *Nanoparticles and Catalysis*, Astruc, D. Ed. Wiley-VCH, Weinheim, **2007**, 129-160.
854. Long, C. G.; Gilbertson, J. D.; Vijayaraghavan, G.; Stevenson, K. J.; Pursell, C. J.; Chandler, B. D. *J. Am. Chem. Soc.* **2008**, *130*, 10103-10115.
855. Chandler, B. D.; Gilbertson, J. D. *Top. Organomet.* **2006**, *20*, 97-120.
856. Auten, B.; Lang, H.; Chandler, B. D. *Appl. Catal. B: Environmental* **2008**, *81*, 225-235.
857. Wang, C. L.; Zhu, G. S.; Li, J.; Cai, X. H.; Wei, Y. H.; Zhang, D. L.; Qiu, S. L. *Chem. Eur. J.* **2005**, *11*, 4975-4982.
858. Jiang, Y. J.; Gao, Q. *J. Am. Chem. Soc.* **2006**, *128*, 716-717.
859. Lang, H.; May, R. A.; Iversen, B. L.; Chandler, B. D. *J. Am. Chem. Soc.* **2003**, *125*, 14832-14836.
860. Scott, R. W. J.; Wilson, O. M.; Crooks, R. M. *Chem. Mater.* **2004**, *16*, 5682-5688.
861. Lang, H.; Maldonado, S.; Stevenson, K. J.; Chandler, B. D. *J. Am. Chem. Soc.* **2004**, *126*, 12949-12956.
862. Singh, A.; Chandler, B. D. *Langmuir* **2005**, *21*, 10776-10782.
863. Hoover, N. N.; Auten, B. J.; Chandler, B. D. *J. Phys. Chem.* **2006**, *110*, 8606- 8612.
864. Reetz, M. T.; Giebel, D. *Angew. Chem., Int. Ed.* **2000**, *39*, 2498-2501.
865. Pittelkow, M.; Moth-Poulsen, K.; Boas, U.; Christensen, J. B. *Langmuir* **2003**, *19*, 7682-7684.
866. Narayanan, R.; El-Sayed, M. A. *J. Phys. Chem. B* **2004**, *108*, 8672-8673.
867. Horvath, I. T. *Acc. Chem. Res.* **1998**, *31*, 641-650.
868. Barthel-Rosa, L. P.; Gladysz, J. A. *Coord. Chem. Rev.* **1999**, *190-192*, 587-605.
869. Ooe, M.; Murata, M.; Mizugaki, T.; Ebitani, K.; Kaneda, K. *J. Am. Chem. Soc.* **2004**, *126*, 1604-1605.
870. Murata, M.; Tanaka, Y.; Mizugaki, Y.; Ebitani, K.; Kaneda, K. *Chem. Lett.* **2005**, *34*, 272-273.

871. Yang, N.-F.; Gong, H.; Tang, W.-J.; Fan, Q.-H.; Cai, C.-Q.; Yang, L.-W. *J. Mol. Catal. A* **2005**, *233*, 55-59.
872. Tang, W.-J.; Yang, N.-F.; Yi, B.; Deng, G.-J.; Huang, Y.-Y.; Fan, Q.-H. *Chem. Commun.* **2004**, 1378-1379.
873. Vandezande, P.; Gevers, L. E. M.; Vankekecom, I. F. J. *Chem. Soc. Rev.* **2008**, *37*, 365-405.
874. Kleij, A. W.; Gossege, R. A.; Klein Gebbink, R. J. M.; Brinkmann, N .; Reijerse, E. J.; Kragl, U.; Lutz, M.; Spek, A. L.; van Koten, G. *J. Am. Chem. Soc.* **2000**, *122*, 12112-12124.
875. van de Coevering, R.; Klein Gebbink, R. J. M.; van Koten, G. *Prog. Polym. Sci.* **2005**, *30*, 474-490.
876. de Groot, D.; de Waal, B. F. M.; Reek, J. N. H.; Schenning, A. P. H. J.; Kamer, P. C. J.; Meijer, E. W.; van Leeuwen, P. W. N. M. *J. Am. Chem. Soc.* **2001**, *123*, 8453-8458.
877. Dijskstra, H. P.; Kruihof, C. A.; Ronde, N.; van de Coevering, R.; Ramon, D. J.; Vogt, D.; van Klink, G. M. P.; van Koten, G. *J. Org. Chem.* **2003**, *68*, 675-685.
878. Dijskstra, H. P.; Ronde, N.; Ramon, D. J.; van Klink, G. M. P.; Vogt, D.; van Koten, G. *Adv. Synth. Catal.* **2003**, *345*, 364-369.
879. Diedrerich, F. *Metal-Catalyzed Cross Coupling Reactions,* Stang, P. Eds.; Wiley-VCH : Weinheim, Germany, **1998**.
880. Beletskaya, I. P. *Chem. Rev.* **2000**, *100*, 3009-3066.
881. Littke, A. F.; Fu, G. C. *Angew. Chem., Int. Ed.* **2002**, *41*, 4176-4211.
882. *Handbook of Organopalladium Chemistry for Organic Synthesis*; Negishi, E. Ed.; Wiley : Hoboken, NJ, 2002.
883. Mejere, A *Metal-Catalyzed Cross Coupling Reactions*, Diederich, F. Eds.; Wiley-VCH : Weinheim, Germany, 2004; Vol. 1 and 2.
884. Phan, N. T. S.; van der Sluis, .M.; Jones, C. J. *Adv. Syn. Catal.* **2006**, *348*, 609-679.
885. Amatore, C.; Jutand, A. *Acc. Chem. Res.* **2000**, *33*, 314-321.
886. Astruc, D. *Organometallic Chemisty and Catalysis*; Wiley-VCH : Heidelberg, 2007, Chap. *21*, p. 489-531.
887. Catsoulacos, D. P.; Steele, B. R.; Heropoumos, G. A.; Micha-Scettas, M.; Scettas, C. G. *Tetrahedron Lett.* **2003**, *44*, 4575-4578.
888. Krishna, T. R.; Jayaraman, N. *Tetrahedron* **2004**, *60*, 10325-10334.
889. Smith, G. S.; Mapolie, S. F. *J. Mol. Catal. A : Chem.* **2004**, *213*, 187-192.
890. Diez-Barra, E.; Guerra, R. I.; Rodriguez-Curiel, R. I.; Merino, S.; Tejeda, J. *J. Organomet. Chem.* **2002**, *660*, 50-54.
891. Beletskaya, I. P.; Chuchuryukin, A. V., van Koten, G.; Dijkstra, H. P.; van Klink, G. M. P.; Kashin, A. N.; Nefedov, S. E.; Eremenko, I. L. Russ. *J. Org. Chem.* **2003**, *39*, 1268-1281.
892. Montilla, F.; Galindo, A.; Andrés, R.; Cordoba, M.; de Jesús, E.; Bo, C. *Organometallics* **2006**, *25*, 4138-4143.
893. Mansour, A.; Kehat, T.; Portnoy, M. *Org. Biorg. Chem.* **2008**, *6*, 3382-3387.
894. Liu, Q. P.; Chen, Y. C.; Wu, Y.; Zhu, J.; Deng, J. G. *Synlett* **2006**, 1503-1506.
895. Meise, M.; Haag, R. *ChemSusChem* **2008**, *1*, 637-642.
896. Fujihara, T.; Yoshida, S.; Ohta, H.; Tsuji, Y. *Angew. Chem., Int. Ed.* **2008**, *47*, 8310-8314.
897. Koprowski, M.; Sebastian, R. M.; Maraval, V.; Zablocka, M.; Cadierno, V.; Donnadieu, B.; Igau, A.; Caminade, A.-M.; Majoral, J.-P. *Organometallics* **2002**, *21*, 4680-4687.
898. Bernechea, M.; de Jesus, E.; Lopez-Mardomingo, C.; Terreros, P. *Inorg. Chem*. **2009**, *48*, 4491-4496.

899. Li, C. F.; Li, D. WX.; Zhang, Z. J.; Feng, S. Y. *Chin. Chem. Lett.* **2005**, *16*, 1389-1392.
900. Eggeling, E. B. Hovestad, N. J.; Jastrzebski, J. T. B. H.; Vogt, D.; van Koten, G. *J. Org. Chem.* **2000**, *65*, 8857-8865.
901. Benito, M.; Rossell, O.; Seco, M.; Muller, G.; Ordinas, J. I.; Font-Bardia, M.; Solans, X. *Eur. J. Inorg. Chem.* **2002**, 2477-2487.
902. Rodriguez, L.-I.; Rossell, O.; Seco, M.; Grabulosa, A.; Muller, G.; Rocamora, M. *Organometallics* **2006**, *25*, 1368-1376.
903. Rodriguez, L.-I.; Rossell, O.; Seco, M.; Muller, G. *Organometallics* **2008**, *27*, 1328-1333.
904. Smith, G.; Chen, R.; Mapolie, S. J. *Organomet. Chem.* **2003**, *673*, 111-115.
905. Benito, J. M.; de Jesús, E.; de la Mata, F. J.; Flores, J. C.; Gómez, R. *Organometallics* **2006**, *25,* 3045-3055.
906. de Groot, D.; Reek, J. N. J.; Kamer, P. C. J.; van Leeuwen, P. W. N. M. *Eur. J. Org. Chem.* **2002**, 1085-1095.
907. Mizugaki, T.; Murata, M.; Ooe, M.; Ebitani, K.; Kaneda, K. *Chem. Commun.* **2002**, 52-53.
908. Köllner, C.; Togni, A. *Can. J. Chem*. **2001**, *79*, 1762-1774.
909. Laurent, R.; Caminade, A. M.; Majoral, J.-P. *Tetrahedron* **2005**, *46*, 6503-6506.
910. Ribourdouille, Y.; Engel, G. D.; Richard-Plouet, M .; Gade, L. H. *Chem. Commun.* **2003**, 1228-1229.
911. Rodriguez, G.; Lutz, M.; Speck, A. L.; van Koten, G. *Chem. Eur. J.* **2002**, *8*, 45-57.
912. Slagt, M. Q.; Jastrzebski, J. T. B. H.; Klein Gebbink, R. J. M.; van Ramesdonk, H. J.; Verhoven, J. W.; Ellis, D. D.; Spek, A. L.; van Koten, G. *Eur. J. Inorg. Chem.* **2003**, 1692-1703.
913. Suijkerbbuijk, B. M. J. M.; Shu, L. J.; Klein Gebbink, R. J. M.; Schlüter, A. D.; van Koten, G. *Organometallics* **2003**, *22*, 4175-4177.
914. Schlenk, C.; Kleij, A. W.; Frey, H.; van Koten, G. *Angew. Chem., Int. Ed.* **2000**, *39*, 3445-3447.
915. Dijkstra, H. P.; Kruithof, C. A.; Ronde, N.; van de Coevering, R.; Ramon, D. J.; Vogt, D.; van Klink, G. P. M.; van Koten, G. *J. Org. Chem.* **2003**, *68*, 675-685.
916. Dijkstra, H. P.; Slagt, M. Q.; McDonald, A.; Kruithof, C. A.; Mills, A. M.; Lutz, M.; Spek, A. L.; Klopper, W.; van Klink, G. P. M.; van Koten, G. *Eur. J. Inorg. Chem.* **2003**, 830-838.
917. Dijkstra, H. P.; Ronde, N.; van Klink, G. P. M.; Vogt, D.; van Koten, G. *Avd. Synth. Catal.* **2003**, *345*, 364-369.
918. Cornils, B. *Applied Homogeneous Catalysis with Organometallic Compounds*, Herrmann, W. A. Eds.; Vols 1 and 2, VCH : Weinheim, **1996**.
919. Trzeciak, A. M.; Ziolkowski, J. *Coord. Chem. Rev.* **1999** , *190-192*, 883-900.
920. Ropartz, L.; Forster, D. F.; Morris, R. E.; Slawin, A. M. Z.; Cole-Hamilton, D. J. *J. Chem. Soc., Dalton Trans.* **2002**, 1997-2008.
921. Busseto, L.; Cassni, M. C.; van Leeuwen, P. W. N. M.; Mazzoni, R. *Dalton Trans.* **2004**, 2767-2770.
922. Li, P.; Kawi, S. *Catal. Today* **2008**, *131*, 61-69.
923. Bourrie, O.; Butlin, J.; Hourani, R.; Kakkar, A. K. *Inorg. Chim. Acta* **2004**, *196*, 145-154.
924. Kakkar, A. K. *Macromol. Symp.* **2003**, *196*, 145-154.
925. Angurell, I.; Muller, G.; Rocamora, M.; Rossell, O.; Seco, M. *Dalton Trans.* **2003**, 1194-1200.

926. Botman, P. N. M.; Amore, R.; van Heerbeek, R.; Back, J. W.; Hiemstra, H.; Reek, J. N. H.; van Maarseveen, J. H. *Tetrahedron Lett.* **2004**, *45*, 5999-6002.
927. van der Berg, M.; Minnaard, A. J.; Haak, R. M.; Leeman, M.; Schudde, E. P.; Meetsma, A.; Feringa, B. L.; de Vries, A. H. M.; Maljaars, C. E. P.; Willans, C. E.; Hyett, D.; Boogers, J. A. F.; Henderickx, H. J. W.; de Vries, J. G. *Adv. Synth. Catal.* **2003**, *345*, 308-323.
928. Yi, B.; Fan, Q.-H.; Deng, G.-J.; Li, Y.-Q.; Chan, A. S. C. *Org. Lett.* **2004**, *6*, 1361-1364.
929. Tang, W.-J.; Huang, Y.-Y.; He, Y.-M.; Fan, Q. H. *Tetrahedron Asymmetry* **2006**, *17*, 536-543.
930. Fujihara, T.; Obora, Y.; Tokunaga, M.; Sato, H.; Tsuji, Y. *Chem. Commun.* **2005** 4526-4528.
931. Garber, S. B.; Kingsbury, J. S.; Gray, B. L.; Hoveyda, A. H. *J. Am. Chem. Soc.* **2000**, *122*, 8168-8179.
932. Wijkens, P.; Jastrzebski, J. T. B. H.; van der Schaaf, P. A.; Kolly, R.; Hafner, A.; van Koten, G. *Org. Lett.* **2000**, *2*, 1621-1624.
933. Gatard, S.; Nlate, S.; Cloutet, E.; Bravic, G.; Blais, J.-C.; Astruc D. *Angew. Chem., Int. Ed*. **2003**, *42*, 452-456.
934. Gatard, S.; Kahlal, S.; Méry, D.; Nlate, S.; Cloutet, E.; Saillard, J.-Y.; D. Astruc *Organometallics* **2004**, *23*, 1313-1324.
935. Malgas-Enus, R.; Mapolie, S. F.; Smith, G. S. *J. Organomet. Chem*. **2008**, *693*, 2279-2286.
936. Deng, G.-J.; Li, G.-R.; Zhu,H.-F.; Zhou, H.-F.; He, Y.-M.; Fan, Q.-H.; Shuai, Z.-G. *J. Mol. Catal. A: Chem.* **2006**, *244*, 118-123.
937. Chen, Y.; Wu, T.; Deng, J.; , Liu, H.; Cui, X.; Zhu, J.; Jiang, Y.; Choi, M. C. K.; Chen, A. S. C. *J. Org. Chem.* **2002**, *67*, 5301-5306.
938. Alonso, E.; Ruiz, J.; Astruc, D. *J. Clust. Sci.* **1998**, *9*, 271-287.
939. Alonso, E.; Astruc, D. *J. Am. Chem. Soc*, **2000**, 122, 3222-3223.
940. Moinet, C.; Román, E.; Astruc, D. *J. Electroanal. Interfac. Chem.*, **1981**, *121*, 241-246.
941. Green, J.C.; Kelly, M.R.; Payne, M. P.; Seddon, E.A.; Astruc, D.; Hamon, J.-R.; Michaud, P. *Organometallics*, **1983**, *2*, 211-218.
942. Desbois, M.-H.; Astruc, D.; Guillin, J.; Varret, F.; Trautwein, A.X.; Villeneuve, G. *J. Am. Chem. Soc.*, **1989**, *111*, 5800-5809.
943. Maraval, V.; Laurent, R.; Caminade, A.-M.; Majoral, J.-P. *Organometallics* **2000**, *19*, 4025-4029.
944. Claeys, M.; Hearshaw, M.; Moss, J. R.; van Steen, E. *Stud. Surf. Sci. Catal B* **2000**, *130*, 1157-1162.
945. Kriesel, J. W.; Tilley, T. D. *Adv. Mater.* **2001**, *13*, 1645-1648.
946. Sellner, H.; Rheiner, P. B.; Seebach, D. *Helv. Chim. Acta* **2002**, *79*, 352-387.
947. Pugh, V. J.; Hu, Q-S.; Pu, L. *Angew. Chem., Int. Ed.* **2000**, *39*, 3638-3641.
948. Andrés, R.; de Jesús, E., de la Mata, F. J.; Flores, J. C.; Gómes, R. *J. Organomet. Chem.* **2005**, *690*, 939-943.
949. Andrés, R.; de Jesús, E., de la Mata, F. J.; Flores, J. C.; Gómes, R. *Eur. J. Inorg. Chem.* **2002**, 2281-2286.
950. Gibson, V. C.; Spitzmesser, S. K. *Chem. Rev.* **2003**, *103*, 283-316.
951. Mager, M.; Becke, S.; Windish, H.; Denninger, U. *Angew. Chem., Int. Ed.* **2001**, *40*, 1898-1902.
952. Zheng, Z. J.; Chen, J.; Li, Y.-S. J. *Organomet. Chem.* **2004**, *689*, 3040-3045.

953. Benito, J. M.; de Jesús, E.; de La Mata, F. J.; Flores, J. C.; Gómez, R. *Chem. Commun.* **2005**, 5217-5219.
954. Malgas, R.; Mapolie, S. F.; Ojwach, S. O.; Smith, G. S.; Darkwa, J. *Catal. Commun*. **2008**, *9*, 1612-1617.
955. Dahan, A.; Portnoy, M. *Chem. Commun.* **2002**, 2700-2701.
956. Bu, J.; Judeh, Z. M. A.; Ching, C. B.; Kawi, S. *Catal. Lett.* **2003**, *85*, 183-187.
957. Kassube, J. K.; Wadepohl, H.; Gade, L. H. *Adv. Syn. Catal*. **2009**, *351*, 607-616.
958. Francavilla, C.; Bright, F. V.; Detty, M. R. *Org. Lett.* **1999**, *1*, 1043-1046.
959. Drake, M. D.; Bight, F. V.; Detty, M. R. *J. Am. Chem. Soc.* **2003**, *125*, 12558-12566.
960. Zubia, A.; Cossio, F. P.. Morao, I.; Rieumont, M.; Lopez, X. *J. Am. Chem. Soc.* **2004**, *126*, 5243-5252.
961. Chow, H.-F.; Mak, C. C. *J. Org. Chem.* **1997**, *62*, 5116-5127.
962. Oosterom, G. E.; van Haaren, R. J.; Reek, J. N. H.; Kamer, P. C. J.; van Leeuwen, P. W. N. M. *Chem. Commun.* **1999**,1119-1120.
963. Rheiner, P. B.; Seebach, D. *Chem. Eur. J.* **1999**, *5*, 3221-3236.
964. Habicher, T.; Diederich, F.; Gramlich, V. *Helv. Chim. Acta*. **1999**, *82*, 1066-1095.
965. Malkoch, M.; Hallman, K.; Lutsenko, S.; Hult, A.; Malmström, E.; Moberg, C. *J. Org. Chem.* **2002**, *67*, 8197-8202.
966. Andrés, R.; de Jesùs, E.; de La Mata, F. J.; Flores, J. C.; Gomez, R. *Eur. J. Inorg. Chem.* **2002**, 2281-2286.
967. Hecht, S.; Fréchet, J. M. J. *Angew. Chem., Int. Ed.* **2001**, *40*, 74-91.
968. Oosterom, G. E.; Steffens, S.; Reek, J. N. H.; Kamer, P. C. J.; van Leeuwen, P. W. N. M. *Top. Catal.* **2002**, *19*, 61-73.
969. Fujihara, T.; Obora, Y.; Tokunaga, M.; Sato, H.; Tsuji, Y. *Chem. Commun.* **2005**, 4526-4528.
970. Müller, C.; Ackerman, L. J.; Reek, J. N. H.; Kamer, P. C. J.; van Leeuwen, P. W. N. M. *J. Am. Chem. Soc.* **2004**, *126*, 14960-14963.
971. Liang, C.; Fréchet, J. M. J. *Prog. Polym. Sci.* **2005**, *30*, 385-402.
972. Zhang, X.; Xu, H.; Dong, Z.; Wang, Y.; Liu, J.; Shen, J. *J. Am. Chem. Soc.* **2004**, *126*, 10556-10557.
973. Gerritz, S. W. *Curr. Opin. Chem. Biol.* **2001**, *5*, 264-268.
974. Piotti, M. E.; Rivera, F.; Bond, R.; Hawker, C. J.; Fréchet, J. M. J. *J. Am. Chem. Soc.* **1999**, *121*, 9471-9472.
975. Hecht, S.; Fréchet, J. M. J. *J. Am. Chem. Soc*. **2001**, *123*, 6959-6960.
976. Mizugaki, T.; Hetrick, C. E.; Murata, M.; Ebitani, K.; Amiridis, M. D.; Kaneda, K. *Chem. Lett.* **2005**, *34*, 420-421.
977. Deng, G.-J.; Fan, Q.-H.; Chen, X.-M.; Liu, G.-H. *J. Mol. Catal. A: Chem.* **2003**, *193*, 21-25.
978. Deng, G.-J.; Yi, B.; Huang, Y.-Y.; Tang, W.-J.; He, Y.-M.; Fan, Q.-H. *Adv. Synth. Catal.* **2004**, *346*, 1440-1444.
979. Liu, L.; Breslow, R. *J. Am. Chem. Soc*. **2003**,*125*, 12110-12111.
980. Kofoed, J.; Reymond, J.-L. *Curr. Opin. Chem. Biol.* **2005**, *9*, 656-664.
981. Douat-Casassus, C.; Darbre, T.; Reymond, J.-L. *J. Am. Chem. Soc*. **2004**, *126*, 7817-7226.
982. Delort, E.; Darbre, T.; Reymond, J.-L. *J. Am. Chem. Soc*. **2004**, *126*, 15642-15643.
983. Sommer, P.; Uhlich, N. A.; Reymond, J.-L.; Darbre, T. *ChemBioChem* **2008**, *9*, 689-693.
984. Krishnan, G. R.; Sreekumar, K. *Eur. J. Org. Chem*. **2008**, 4763-4768.
985. Liu, Y-h.; Shi, M. *Adv. Syn. Catal*. **2008**, *350*, 122-128.

986. Scottt, R. W. J.; Datye, A. K.; Crooks, R. M. *J. Am. Chem. Soc*. **2003**, *125*, 3708-3709.
987. Yeung, L. K.; Lee, C. T.; Johnston, K. P.; Crooks, R. M. *Chem. Commun.* **2001**, 2290-2291.
988. Garcia-Martinez, J. C.; Lezutekong, R.; Crooks, R. M. *J. Am. Chem. Soc.* **2005**, *127*, 5097-5098.
989. Oee, M.; Murata, M.; Mizugaki, T.; Ebitani, K. Kaneda, K. *Nano Lett.* **2002**, *2*, 999-1002.
990. Mizugaki, T.; Muratra, M.; Fukubayashi, S.; Mitsudome, T.; Jitsujkawa, K.; Kaneda, K. *Chem. Commun.* **2008**, 241-243.
991. Marty, J.-D.; Martinez-Aripe, E.; Mingotaud, A.-F.; Mingotaud, C. *J. Colloid Interf. Sci.* **2008**, *326*, 51-54.
992. Sutton, A.; Fran, G.; Kakkar, A. *J. Polym. Sci*. **2009**, *47*, 4482-4493.
993. Esumi, K.; Miyamoto, K.; Yoshimura, T. *J. Jpn. Colour Mater.* **2001**, *75*, 561-566.
994. Endo, T.; Kuno, T.; Yoshimura, T.; Esumi, K. *J. Nanosci. Nanotechnol.* **2005**, *5*, 1875-1882.
995. Nakamula, I.; Yamanoi, Y.; Yonezawa, T.; Imaoka, T.; Yamamoto, K.; Nishihara, H. *Chem. Commun.* **2008**, 5716-5718.
996. Nakamula, I.; Yamanoi, Y.; Yonezawa, T.; Imaoka, T.; Yamamoto, K.; Nishihara, I. *Chem. Commun*. **2008**, 5716-5718.
997. Feng, Z. V.; Lyon, J. L.; Croley, J. S.; Crooks, R. M.; Vanden Bout, D. A.; Stevenson, K. J. *J. Chem. Ed*. **2009**, 86, 368-372.
998. Li, Y.; El-Sayed, M. A. *J. Phys. Chem. B* **2001**, *105*, 8938-8943.
999. Narayanan, R.; El-Sayed, M. A. *J. Phys. Chem. B* **2004**, *108*, 8572-8580.
1000. Rahim, E. H.; Kamounah, F. S.; Fredricksen, J.; Christensen, J. B. *Nano Lett.* **2001**, *1*, 499-501.
1001. Ornelas, C.; Salmon, L.; Ruiz, J.; Astruc, D. *Chem. Commun*. **2007**, 4946-4948.
1002. Diallo, A. K.; Ornelas, C.; Salmon, L.; Ruiz, J.; Astruc, D. *Angew. Chem., Int. Ed. Engl*. **2007**, *46*, 8644-8648.
1003. C. Ornelas, J. Ruiz , L. Salmon, D. Astruc, *Adv. Syn. Catal*. **2008**, *350*, 837-845
1004. Ornelas, C.; Diallo, A. K.; Ruiz , J.; Astruc, D. *Adv. Syn. Catal*. **2009**, DOI: 10.1002/adsc.200900270.
1005. Wu, L.; Li, Z.-W.; Zhang, F.; He, Y.-M.; Fan, Q.-H. *Adv. Syn. Catal*. **2008**, *350*, 846-862.
1006. Peng, X.; Pann, Q.; Rempel, G. L. *Chem. Soc. Rev.* **2008**, *37*, 1619-1628.
1007. Ye, H. *J. Am. Chem. Soc.* **2007**, *129*, 3627-3633.
1008. Chung, Y.-M.; Rhee, H.-K. *Catal. Surv. Asia* **2004**, *8*, 211-223.
1009. Scott, R. W.; Wilson, O. M.; Oh, S.-K.; Kenik, E. A.; Crooks, R. M. *J. Am. Chem. Soc.* **2004**, *126*, 15583-15591.
1010. Wilson, O. M.; Scott, R. W. J.; Garcia-Martinez, J. C.; Crooks, R. M. *J. Am. Chem. Soc.* **2005**, *127*, 1015-1024.
1011. Scott, R. W. J.; Sivadiranarayana, C.; Wilson, O. M.; Yan, Z.; Goodman, D. W.; Crooks, R. M. *J. Am. Chem. Soc.* **2005**, *127*, 1380-1381.
1012. Gu, Y.; Xie, H.; Gao, J.; Liu, D.; Williams, C. T.; Murphy, C. J.; Ploehn, H. J. *Langmuir* **2005**, *21*, 3122-3131.
1013. Qian, L.; Yang, X. *J. Phys. Chem. B* **2006**, *110*, 16672-16678.
1014. Ye, H.; Crooks, R. M. *J. Am. Chem. Soc.* **2007**, *129*, 3627-3633.
1015. Chung, Y.; Rhee, H. K. *J. Mol. Catal. A* **2003**, *206*, 291-298.
1016. Qian, L.; Yang, X. *Talanta* **2008**, *74*, 1649-1653.
1017. Harada, M.; Asakura, K.; Toshima, N. *J. Phys. Chem.* **1993**, *97*, 5103-5114.

1018.Sinfelt, J. H. *Acc. Chem. Res.* **1987**, *20*, 134-139.
1019.Toshima, N.; Yonezawa, T.; Kushihashi, K. *J. Chem. Soc., Faraday Trans.* **1993**, *89*, 2537-2543.
1020.Toshima, N.; Yonezawa, T. *New J. Chem.* **1998**, 1179-1201.
1021.Chung, Y.; Rhee, H. K. *Catal. Lett.* **2003**, *85*, 159-164.
1022.Schmid, G.; Lehnert, A.; Malm, J.-O.; Bovin, J.-O *Angew. Chem., Int. Ed. Engl.* **1991**, *30*, 874-876.
1023.Peng, X.-H.; Pan, Q. M.; Rempel G. L.; Peng, X.-C. *Chem. J. Chin. Univ.-Chin.* **2009**, *30*, 813-817.
1024.Deutsch, D. S.; Siani, A.; Fanson, P. T.; Hirata, H.; Matsumoto, S.; Williams, C. T.; Amiridis, M. D. *J. Phys. Chem. C* **2007**, *111*, 4246-4255.
1025.Ye, H.; Scott, R. W.; Crooks, R. M. *Langmuir* **2004**, *20*, 2915-2920.
1026.Oh, S.-K.; Kim, Y.-G.; Ye, H.; Crooks, R. M. *Langmuir* **2003**, *19*, 10420-10425.
1027.Ye, H.; Crooks *J. Am. Chem. Soc.* **2005**, *127*, 4930-4934.
1028.Alvarez, J.; Sun, L.; Crooks, R. M. *Chem. Mater.* **2002**, *14*, 3995-4001.
1029.Ruckenstein, E.; Yin, W. *J. Poym. Sci. A* **2000**, *38*, 1443-1449.
1030.Velarde-Ortiz, R.; Larsen, G. *Chem. Mater.* **2002**, *14*, 858-866.
1031.Choi, H. C.; Kim, W.; Wang, D.; Dai, H. *J. Phys. Chem. B* **2002**, *106*, 12361-12365.
1032.Boyen, H.-G.; Kästle, G.; Weigl, F.; Koslowski, B.; Dietrich, C.; Ziemann, P.; Spatz, J.-P.; Rietmüller, S.; Hartmann, C.; Möller, M.; Schmid, G.; Garnier, M. G.; Oelhafen, P. *Science* **2002**, *297*, 1533-1536.
1033.Scott, R. W.; Wilson, O. M.; Crooks, R. M. *Chem. Mater* **2004**, *16*, 167-172.
1034.Ledesma-Garcia, J.; Escalanta-Garcia, I. L.; Rodriguez, F. J.; Chapman, T. W.; Thomas, W. G.; Godinez, L. A. *J. Appl. Electrochem*. **2008**, *38*, 515-522.
1035.Zhao, M.; Crooks, R. M. *Adv. Mater.* **1999**, *11*, 217-220.
1036.Ye, H.; Crooks, R. M. *J. Am. Chem. Soc.* **2007**, *129*, 3627-3633.
1037.Yamamo, K.; Imaoka, T.; Chun, W. J.; Enoki, O.; Katoh, H.; Takenaga, M.; Sonoi, A. *Nature Chem*. **2009**, *1*, 397-402.
1038.Quian, L.; Yang, X. *J. Phys. Chem. B* **2006**, *110*, 16672-16678.
1039.Haruta, M.; Tsuboda, S.; Kobayashi, T.; Hagehiama, H.; Genet, M. J.; Demon, B. *J. Catal.* **1993**, *144*, 175-182.
1040.Haruta, M. *Catal Today* **1997**, *36*, 153-166.
1041.Louis, C. In *Nanoparticles and Catalysis*, Astruc, D. Ed.; Wiley-VCH: Weinheim, **2008**, Chap. 15, pp. 475-504.
1042.Crump, C. J.; Gilbertson, J. D.; Chandler, B. D. *Top. Catal.* **2008**, *49*, 233-240.
1043.Huang, W.; Kuhn, J. N.; Tsung, C.-K.; Zhang, Y.; Habas, S. E.; Yang, P.; Somorjai, G. A. *Nano Lett*. **2008**, *8*, 2027-2034.
1044.Kuhn, J. N.; Huang, W.; Tsung, C. K.; Zhang, Y.; Somorjai, G. A. *J. Am. Chem. Soc*. **2008**, *130*, 14026-14027.
1045.Lopez-de Jesus; Yaritsza, M.; Vicente, A.; Lafaye, G.; Marecot, P.; Williams, C. T. *J. Phys. Chem. C* **2008**, *112*, 13837-13845.
1046.Esumi, K.; Miyamoto, K.; Yoshimura, T. J. *Jpn. Colour Mater.* **2001**, *75*, 561-566.
1047.Endo, T.; Kuno, T.; Yoshimura, T.; Esumi, K. J. *Nanosci. Nanotechnol.* **2005**, *5*, 1875-1882.
1048.Siani, A.; Alexeev, O.; Deutsch, D. S.; Monnier, J.; Fanson, P. T.; Hirata, H.; Matsumoto, S.; Williams, C. T.; Amaridis, M. D. *J. Cat.* **2009** *266*, 331-342.
1049.Xie, H.; Howe, J. Y.; Schwartz, V.; Monnier, J. R.; Williams, C. T.; Ploen, H. J. *J. Catal.* **2008**, *259*, 111-122.
1050.Svenson, S.; Tomalia, D. A. *Adv. Drug Deliv. Rev.* **2005**, *57*, 2106-2129.
1051.Tomalia, D. A.; Reyna, L. A.; Svenson, S. *Biochem. Soc. Trans.* **2007**, *35*, 61-67.

1052.Svenson, S. *Eur. J. Pharm. Biopharm.* **2009**, *71*, 445-462.
1053.Esfand, R.; Tomalia, D. A. *Drug. Discov. Today* **2001**, *6*, 427-436.
1054.Fréchet, J. M. J. *Pharm. Sci. Technol. Today* **2000**, *2*, 393-401.
1055.Stiriba, S. E.; Frey, H.; Haag, R. *Angew. Chem., Int. Ed. Engl.* **2002**, *41*, 1329-1334.
1056.Boas, U.; Heegaard, P. M. H. *Chem. Soc. Rev.* **2004**, *33*, 43-63.
1057.Boas, U.; Christensen, J. B. *Dendrimers in medicine and biotechnology.* Royal Chemical Society Publishing: Cambridge, **2006**.
1058.Gillies, E. R.; Fréchet, J. M. J. *Drug Discov. Today* **2005**, *10*, 35-43.
1059.Gillies, E. R.; Fréchet, J. M. J. *Bioconjug. Chem.* **2005**, *16*, 361-368.
1060.Allen, T. M.; Cullis, P. R. *Science* **2004**, *303*, 1818-1822
1061.Lee, C. C.; MacKay, J. A.; Fréchet, J. M. J.; Szoka, F. C. *Nature Biotechnol.* **2005**, *23*, 1517-1526.
1062.Svenson, S.; Chauhan, A. S. *Nanomedicine* **2008**, *3*, 679-702.
1063.Jang, W.-D.; Selim, K. M. K.; Lee, C.-H. Lee; Kang, I. K. *Prog. Polym. Sci.* **2009**, *34*, 1-23.
1064.Choi, Y.; Thomas, T.; Kotlyar, A.; Islam, M. T.; Baker, J. R., Jr. *Chem. Biol.* **2005**, *12*, 35-43.
1065.*Dendrimer based nanomedicine.* Majoros, I. J.; Baker, J. R., Jr. Eds., Pan Stanford Publishing: Stanford, **2008**.
1066.Duncan, R.; Izzo, L. *Adv. Drug. Deliv. Rev.* **2005**, *57*, 2215-2237.
1067.Singh, I.; Rehni, A. K.; Kalra, R.; Joshi, G.; Kumar, M. *Pharmazie* **2008**, *63*, 491-496.
1068.W.-D. Jang, W.-D.; Kamruzzaman, S. K. M.; Lee, C.-H. Kang, I.-K. *Prog. Polym. Sci.* **2009**, *34*, 1-23.
1069.Grinstaff J. *Polym. Sci.: Part A: Polym. Chem.* **2008**, *46*, 383-400.
1070.Wolinsky, J. B.; Grinstaff, M. W. *Adv. Drug. Deliv. Rev.* **2008**, *60*, 1037-1055.
1071.Ely, T. O.; Sharma, M.; Lesniak, W.; Klippenstein, D. L.; Foster, B. A.; Balogh, L. P. *Mater. Res. Soc. Symp. Proc.* **2008**, *1064*, 6-18.
1072.Agarwahl, A.; Saraf, S.; Asthana, A.; Gupta,, U.; Gajbhiye, V.; Jain, N. K. *Int. J. Pharm.* **2008**, *350*, 3-13.
1073.Tekade, R.; Kumar, P. V.; Jain, N. K. *Chem. Rev.* **2009**, *109*, 49-87.
1074.Khan, M. K.; Nigavekar, S. S.; Minc, L. D.; Kariapper, M. S.; Nair, B. M.; Lesniak, W. G.; Balogh, L. P. *Technol. Cancer Treat.* **2005**, *4*, 603-613.
1075.Yellepedi, V.; Nenkata, K.; Palakhurti, S. *Exp. Opin. Drug Deliv.* **2009**, *6*, 835-850.
1076.Jang, W.-D.; Kamruzzaman, S. K. M.; Lee, C.-H.; Kang, I.-K. *Prog. Polym. Sci.* **2009**, *34*, 1-23.
1077.Allen, T. M.; Cullis, P. R. *Science* **2004**, *303*, 1818-1822.
1078.Sosnik, A.; Carcaboso, A. M.; Chiapetta, D. A. *Rec. Pat. Biomed. Eng.* **2008**, *1*, 43-59.
1079.Tyshenko, M. G. *Int. J. Nanotechnol.* **2008**, *5*, 116-123.
1080.Veldhoen, S.; Laufer, S. D.; Restle, T. *Int. J. Mol. Sci.* **2008**, *9*, 1276-1320.
1081.Majoros, I.; Baker, J. R., Jr. *PMSE Preprints* **2008**, *98*, 750-751.
1082.Cheng, Y.; Xu, T. *Eur. J. Med. Chem.* **2008**, *43*, 2291-2297.
1083.Gregoradis, G.; Wills, E. J.; Swain, C. P.; Tavill, A. S. *Lancet* **1974**, *1*, 1313-1316.
1084.Soppimath, K. S.; Aminabhavi, T. M.; Kulkarni, A. R.; Rudzinski, W. E. *J. Control. Rel.* **2001**, *70*, 1-20.
1085.Delie, F.; Blanco-Prieto, M. J. *Molecules* **2005**, *10*, 65-80.
1086.Kataoka, K.; Harada, A.; Nagasaki, Y. *Adv. Drug Deliv. Rev.* **2001**, *47*, 113-131.
1087.Discher, D. E.; Ahmed, F. *Ann. Rev. Biomed. Eng.* **2006**, *8*, 323-341.
1088.Patri, A. K.; Majoros I. J., Baker, J. R., Jr. *Curr. Op. Chem. Biol.* **2002**, *6*, 466-471.
1089.Sadler, K.; Tam, J. P. *Rev. Mol. Biotechnol.* **2002**, *90*, 195-229.

1090.Crespo, L.; Sanclimens, G.; Pons, M.; Giralt, E.; Royo, M.; Alberico, F. *Chem. Rev.* **2005**, *105*, 1663-1681.
1091.Johansson, E. M. V.; Crusz, S. A.; Kolomits, E.; Buts, L.; Lieven, K.; Rameshwar, U.; Carriarini, M.; Bartels, K.-M.; Diggle, S. P.; Camara, M.; Williams, P.; Loris, R.; Nativi, C.; Rosenau, F.; Jaeger, K.-E.; Darbre, T.; Reymond, J.-L. *Chem. Biol*. **2008**, *15*, 1249-1257.
1092.Supattapone, S.; Nguyen, H.-O. B.; Cohen, F. E.; Prusiner, S. B.; Scott, M. R. *Proc. Natl. Acad. Sci. USA* **1999**, *96*, 14529-14534.
1093.Supattapone, S.; Ville, H.; Uyechi, L.; Safar, J.; Tremblay, P.; Szoka, F. C.; Cohen, F. E.; Prusiner, S. B.; Scott, M. R. *J. Virol.* **2001**, *75*, 3453-3461.
1094.Heegaard, P. M. H.; Boas, U.; Otzen, D. E. *Macromol. Biosci.* **2007**, *7*, 1047-1059.
1095.Martin, H.; Kinns, H.; Mitchell, N.; Astier, Y.; Madathil, R.; Howorka, S. *J. Am. Chem. Soc.* **2007**, *129*, 9640-9649.
1096.Kojima, C.; Tsumura, S.; Harada, A.; Kono, K. *J. Am. Chem. Soc.* **2009**, *131*, 6052-6053.
1097.Aguilar, R. M.; Talamantes, F. J.; Bustamante, J. J.; Munoz, J.; Trevino, L. R.; Martinez, A. O.; Haro, L. S. *J. Pept. Sci.* **2009,** *15*, 78-88.
1098.Klajnert, B.; Cangiotti, M.; Calii, S.; Ionov, M.; Majoral, J.-P.; Caminade, A.-M.; Cladera, J.; Bryszewska, M.; Ottaviani, M. F. *New J. Chem.* **2009**, *33*, 1087-1093.
1099.Yiyun, C.; Na, M.; Tongwen, X.; Rongqiang, F.; Xueyuan, W.; Xiaomin, W.; Longping, W. *J. Pharm. Sci.* **2007**, *96*, 595-602.
1100.Chandrasekar, D.; Sistla, R.; Ahmad, F. J.; Khar, R. K.; Diwan, P. V. *J. Biomed. Mater. Res. Part A* **2007**, *82*, 92-103.
1101.Na, M.; Yiyun, C.; Tongwen, X.; Yang, D.; Xiaomin, W.; Zhenwei, L.; Zhichao, C.; Guanyi, H.; Yunyu, S.; Longping, W. *Eur. J. Med. Chem.* **2006**, *41*, 670-674.
1102.Chandrasekar, D.; Sistla, R.; Ahmad, F. J.; Khar, R. K.; Diwan, P. V. *Biomaterials* **2007**, *28*, 504-512.
1103.Yiyun, C.; Tongwen, X. *Eur. J. Med. Chem.* **2005**, *40*, 1188-1192.
1104.Kohhlhe, P.; Khandare, J.; Pillai, O.; Kannan, S.; Lieh-Lai, M.; Kannan, R. M. *Biomaterials* **2006**, *27*, 660-669.
1105.Cloninger, M. *J. Curr. Op. Chem. Biol.* **2002**, *6*, 742-748.
1106.Cheng, Y. Y.; Wang, J.; Rao, T.; He, X.; Xu, T. *Frontiers Biosci.* **2008**, *13*, 1447-1471.
1107.Cheng, Y. Y.; Xu, T. *Eur. J. Med. Chem.* **2008**, *43*, 2291-2297.
1108.Tang, Y.; Ma, L.; Guo, L.; Dai, H.; He, S. *Zhongguo Yaofang* **2009**, *20*, 21-24 (CAN 151: 63617 AN **2009**:298104).
1109.Cheng, Y. Y.; Xu, Z.; Ma, M.; Xu, T. *J. Pharm. Sci.* **2007**, *4*, 246-254.
1110.Man, N.; Cheng. Y. Y.; Xu, T.; Ding, Y.; Wang, X.; Li, Z.; Chen, Z.; Huang, G.; Shi, Y.; Wen, L. *Eur. J. Med.* **2006**, *41*, 670-674.
1111.Cheng, Y. Y.; Qu, H.; Ma, M.; Xu, Z.; Xu, P.; Fang, Y.; Xu, T. *Eur. J. Med. Chem.* **2007**, *42*, 1032-1038.
1112.Ma, M.; Cheng, Y. Y.; Xu, Z.; Xu, P.; Qu, H.; Fang, Y.; Xu, T.; Wen, L. *Eur. J. Med. Chem.* **2007**, *42*, 93-98.
1113.Calabretta, M. K.; Kumar, A.; McDermott, A. M.; Cai, C. *Biomacromolecules* **2007**, *8*, 1807-1811.
1114.Cho, K.; Wang, X.; Nie, S.; Che, Z.; Shin, D. N. *Clin. Cancer Res.* **2008**, *14*, 1310-1316.
1115.Medina, S. H.; El-Sayed, M. E. H. *Chem. Rev.* **2009**, *109*, 3141-3157.
1116.Bharali, D. J.; Khalil, M.; Gurbuz, M.; Simone, T. M.; Mousa, S. A. *Int. J. Nanomed.* **2009**, *4*, 1-7.

1117.Meyers, S. R.; Juhn, F. S.; Griset, A. P.; Luman, N. R.; Grinstaff, M. W. *J. Am. Chem. Soc.* **2008**, *130*, 14444-14445.
1118.Svenson, S. *Eur. J. Pharma. Biopharma.* **2009**, *71*, 445-462.
1119.D'Emanuele, A.; Attwood, D. *Adv. Drug Deliv. Rev.* **2005**, *57*, 2147-2162.
1120.Devarakonka, B.; Hill, R. A.; de Villiers, M. M. *Int. J. Pharm.* **2004**, *284*, 133-140.
1121.Gupta, U.; Agashe, H. B.; Asthana, A.; Jain, N. K. *Biomacromol.* **2006**, *7*, 649-658.
1122.Jain, N. K.; Gupta, U. *Expert Opin. Drug Metab. Toxicol.* **2008**, *4*, 1035-1052.
1123.Agarwal, A.; Asthana, A.; Gupta, U.; Jain, N. J. *J. Pharm. Pharcol.* **2008**, *60*, 671-688.
1124.Bharali, D. J.; Khalil, M.; Gurbuz, M.; Simone, T. M.; Mousa, S. A. *Int. J. Nanomed.* **2009**, *4*, 1-7.
1125.Morgan, M. T.; Grinstaff, M. W. *Cancer Res.* **2006**, *66*, 11913-11921.
1126.Cheng, Y.; Li, M.; Xu, T. *Eur. J. Med. Chem.* **2008**, *43*, 1791-1795.
1127.Venditto, V. J.; Lawani, S. K.; Allred, K.; Allred, C. D.; Clinton, D.; Simanek, E. E. Abstracts of Papers, *237th ACS National Meeting*, Salt Lake City, **2009**, POLY-345.
1128.Cheng, Y. Y.; Xu, T. W. *Eur. J. Med. Chem.* **2005**, *40*, 1188-1192
1129.Cheng, Y. Y.; Xu, T. W. *Eur. J. Med. Chem.* **2005**, *40*, 1384-1389.
1130.Kolhe, P.; Misra, E.; Kannan, R. M.; Kanna, S.; Lieh-Lai, M. *Int. J. Pharm.* **2003**, *259*, 143-160.
1131.Kannan, S.; Kohle, P.; Raykova, V.; Glibatec, M.; Kannan, R. M.; Lieh-Lai, M.; Bassett, D. *J. Biomater. Sci. Polym. Ed.* **2004**, *15*, 311-330.
1132.Morgan, M. T.; Carnahan, M. A.; Finkelstein, S.; Patra, C. A.; Degoricija, L.; Lee, S. J.; Grinstaff, M. W. *Chem. Commun.* **2005**, 4309-4311
1133.Morgan, M. T.; Carnahan, M. A.; Immos, C. E.; Robeiro, A. A.; Finkelstein, S.; Lee, S. J.; Grinstaff, M. W. *J. Am. Chem. Soc.* **2003**, *125*, 15485-15489.
1134.Devarakonda, B.; Hill, R. A.; de Villiers, M. M. *Int. J. Pharm.* **2004**, *284*, 133-140.
1135.Devarakonda, B.; Hill, R. A.; Liebenberg, W.; Brits, M.; de Villiers, M. M. *Int. J. Pharm.* **2005**, *304*, 193-209.
1136.Chauhan, A S.; Sridevi, S.; Chalasani, K. B.; Jain, A. K.; Jain, S. K.; Jain, N. K. *J. Control. Release* **2003**, *90*, 335-343.
1137.Vandamme, T. F.; Brobeck, L. *J. Controlled Release* **2005**, *102*, 23-38.
1138.Kukowska-Latallo, J. F.; Candido, K. A.; Cao, Z.; Nigavekar, S. S.; Majoros, I. J.; Thomas, T. P.; Balogh, L. P.; Khan, M. K.; Baker, J. R., Jr. *Cancer Res.* **2005**, *65*, 5317-5324.
1139.Padila de Jesus, O. L.; Ihre, H. R.; Gagne, L.; Fréchet, J. M. J.; Szoka, F. C. *Bioconjugate Chem.* **2002**, *13*, 453-461.
1140.Crampton, H. L.; Simanek, E. E. *Polym. Int.* **2007**, *56*, 489-496.
1141.Gajbhiye, V.; Kumar, P. V.; Sharma, A.; Jain, N. K. *Curr. Nanosci.* **2008**, *4*, 267-277.
1142.Asthana, A.; Chauhan, A. S.; Diwan, P. V.; Jain, N. K. *AAPS PharmaSciTech.* **2005**, *6*, E535-E542.
1143.Chauhan, A. S.; Jain, N. K.; Diwan, P. V.; Khopade, A. J. *J. Drug* **2004**, *12*, 575-583.
1144.Cheng, Y. Y.; Xu, T. W.; Fu, R. Q. *Eur. J. Med. Chem.* **2005**, *40*, 1390-1393.
1145.Man, N.; Yiyun, C.; Tongwen, X.; Yang, D.; Xiaomin, W.; Zhenwei, L.; Zhichao, C.; Guanyi, H.; Yunyu, S.; Longping, W. *Eur. J. Med. Chem.* **2006**, *41*, 670-674.
1146.Cheng, Y. Y.; Man, N.; Xu, T. W.; Wang, X. Y.; Wang, X. M.; Wen, L. P. *J. Pharm. Sci.* **2007**, *96*, 595-602.
1147.Patri, A. K.; Kukowska-Latallo, J. F.; Baker, J. R., Jr. *Adv. Drug. Deliv. Rev.* **2005**, *57*, 2203-2214.
1148.Shi, X.; Majoros, I. J.; Baker, J. R., Jr. *Mol. Pharm.* **2005**, *2*, 278-294.

1149.Markatou, E.; Gionis, V.; Chryssikos, G. D.; Hatziantoniou, S.; Georgopoulos, A.; Demetzos, C. *Int. J. Pharm.* **2007**, *339*, 231-236.
1150.Papagiannaros, A.; Dimas, K.; Papaiannou, G. T.; Demetzos, C. *Int. J. Pharm.* **2005**, *302*, 29-38.
1151.Wang, F.; Bronich, T. K.; Kabanov, A. V.; Rauh, R. D.; Roovers, J. *Bioconjug. Chem.* **2005**, *16*, 397-405.
1152.Dhanikula, R. S.; Hildgen, P. *Biomater.* **2007**, *28*, 3140-3152.
1153.Potluri, S. K.; Ramulu, A. R.; Pardhasaradhi, M. *Tetrahedron* **2004,** *60*, 10915-10920.
1154.Parrott, M. C.; Marchington, E. B.; Valliant, J. F.; Adronov, A. *J. Am. Chem. Soc.* **2005**,*127*, 12081-12089.
1155.Najlah, M.; Freeman, S.; Attwood, D.; D'Emanuele, A. *Int. J. Pharm.* **2006**, *308*, 175-182.
1156.Najlah, M.; Freeman, S.; Attwood, D.; D'Emanuele, A. *Bioconjug. Chem.* **2007**, *18,* 937-946.
1157.Najlah, M.; Freeman, S.; Attwood, D.; D'Emanuele, A. *Int. J. Pharm.* **2007**, *336*, 183-190.
1158.Kohle, P.; Khandare, J.; Pillai, O.; Kannan, S.; Lieh-Lai, M.; Kannan, R. M. *Biomater.* **2006**, *27*, 660-669.
1159.D'Emanuele, A.; Jevprasesphant, R.; Penny, J.; Attwood, D. *J. Controlled Release* **2004**, *95*, 447-453.
1160.Yang, H.; Lopina, S. T. *J. Biomater. Sci. Polym. Ed.* **2003**, *14*, 1043-1056.
1161.Yang, H.; Kao, W. J. *J. Biomater. Sci. Polymer Ed.* **2006**, *17*, 3-19.
1162.Gurdag, S.; Khandare, J.; Stapels, S.; Matherly, L.H.; Kannan, R. M. *Bioconjug. Chem.* **2006**, *17*, 275-283.
1163.Khandare, J. J.; Jayant, S.; Singh, A.; Chandna, P.; Wang, Y.; Vorsa, N.; Minko, T. *Bioconjugate Chem.* **2006**, *17*, 1464-1472.
1164.Zhou, R. X.; Du, B.; L, Z. R. *J. Controlled Release* **1999**, *57*, 249-257.
1165.Malik, N.; Evagorou, E. G.; Duncan, R. *Anticancer Drugs* **1999**, *10*, 767-767.
1166.Bellis, E.; Hajba, L.; Kovacs, B.; Sandor, K.; Kollar, L.; Kokotos, G. *J. Biochem. Biophys. Met.* **2006**, *69*, 151-161.
1167.Greenfield, R. S.; Kaneko, T.; Daues, A.; Edson, M. A.; Fitzgerald, A.; Olech, L. J.; Grattan, J. A.; Spitalny, G. L.; Braslawsky, G. R. *Cancer Res.* **1990**, *50*, 6600-6607.
1168.Ihre, H. R.; Padilla De Jesus, O. L.; Szoka Jr, F. C.; Fréchet, J. M. J. *Bioconjugate Chem.* **2002**, *13*, 443-452.
1169.Lee, C. C.; Gillies, E. R.; Fox, M. E.; Guillaudeu, S. J.; Fréchet, J. M. J.; Dy, E. E.; Szoka, F. C. *Proc. Natl. Acad. Sci. USA* **2006**, *103*, 16649-16654.
1170.Ke, W.; Zhao, Y.; Huang, R.; Jiang, C.; Pei, Y. *J. Pharma. Sci.* **2008**, *97*, 2208-2216.
1171.Khandare, J.; Kohle, P.; Kannan, S.; Lieh-Lai,M.; Kannan, R. M. *Bioconjugate Chem.* **2005**, *16*, 1049-1049.
1172.Kurtoglu, Y. E.; Navath, R. S.; Wang, B.; Kannan, S.; Romero, R.; Kannan, R. M. *Biomater.* **2009**, *30*, 2112-2121.
1173.Wang, X.; Inapagolla, R.; Kannan, S.; Lieh-Lai, M.; Kannan, R. M. *Bioconjugate Chem.* **2007**, *18*, 791-799.
1174.Kochendoerfer, G. *IDrugs* **2004**, *7*,118-121.
1175.Liu, M.; Kono, K.; Fréchet, J. M. J. *Polym. Sci. A* **1999**, *37*, 3492-3503.
1176.Liu, M.; Kono, K.; Fréchet, J. M. J. *Controlled Release* **2000**, *65*, 121-131.
1177.Bhadra, D.; Bhadra, S.; Jain, N. K. *Pharmazie* **2002**, *57*, 5-29.
1178.Tang, S.; Martinez, L. J.; Sharma, A.; Chai, M. *Org. Lett.* **2006**, *8*, 4421-4424.
1179.Ringsdorf, H. *J. Polym. Sci. Polym. Symp.* **1975**, *51*, 135-153.
1180.Ringsdorf, H.; Schlarb, B.; Venzmer, J. *Angew. Chem., Int. Ed.* **1988**, *27*, 113-158.

1181.Türk, H.; Shukla, A.; Rodrigues, P. C. A.; Rehage, H.; Haag, R. *Chem. Eur. J.* **2007**, *13*, 4187-4196.
1182.Langer, R. *Nature* **1998**, *392*, 5-10.
1183.Uhrich, K. E.; Cannizzaro, S. M.; Langer, R. S.; Shakessheff, K. M. *Chem. Rev.* **1999**, *99*, 3181-3198.
1184.Lasic, D. D.; Martin, F. J.; Gabizon, A.; Huang, S. K.; Papahadjopoulos, D. *Biochim. Biophys. Acta* **1991**, *1070*, 187-192.
1185.Muller, B. G.; Kissel, T. *Pharm. Pharmacol. Lett.* **1993**, *3*, 67-70.
1186.Kataoka, K.; Kwon, G. S.; Yokoyama, M.; Okano, T.; Sakurai, Y. *J. Controlled Release* **1998**, *53*, 25-37.
1187.Duncan, R. *Nat. Rev. Drug. Discovery* **2003**, *2*, 347-360.
1188.Kataoka, K.; Kwon, G. S.; Yokoyama, M.; Okano, T.; Sakurai, Y. *J. Controlled Release* **1993**, *24*, 119-132.
1189.Ambade, A. A.; Savariar, E. N.; Thayumanan, S. *Mol. Pharm.* **2005**, *2*, 264-272.
1190.Pang, S. N. J. *J. Am. Coll. Toxicol.* **1993**, *12*, 429-457.
1191.Gillies, E. R.; Fréchet, J. M. J. *J. Am. Chem. Soc.* **2002**, *124*, 14137-14146.
1192.Kojima, C.; Kono, K.; Maruyama, K.; Takagishi, T. *Bioconjugate Chem.* **2000**, *11*, 910-917.
1193.Kono, K.; Kojima, C.; Hayashi, N.; Nishisaka, E.; Kiura, K.; Watarai, S.; Harada, A. *Biomater.* **2008**, *29*, 1664-1675.
1194.Lai, P.-S.; Lou, P.-J.; Peng, C.-L.; Young, T.-H.; Shieh, M.-J. *J. Controlled Release* **2007**, *122*, 39-46.
1195.Guillaudeau, S. J.; Fox, M. E.; Haider, Y. M.; Dy, E.; Szoka, F. C.; Fréchet, J. M. J. *Bioconj. Chem.* **2008**, *19*, 461-469.
1196.Chen, H. T.; Neerman, M. F.; Parrish, A. R.; Simanek, E. E. *J. Am. Chem. Soc.* **2004**, *126*, 10044-10048.
1197.Neerman, M. F.; Zhang, W.; Parrish, A. R.; Simanek, E. E. *Int. J. Pharmaceutics* **2004**, *281*, 129-132.
1198.Lim, J.; Guo, Y.; Rostollan, C. L.; Stanfield, J. Hsieh, J. T.; Sun, X.; Simanek, E. E. *Mol. Pharma.* **2008**, *5*, 540-547.
1199.Crampton, H. L.; Simanek, E. *Polym. Int.* **2007**, *56*, 489-496.
1200.Neerman, M. F.; Chen, H.-T.; Parrish, A. R.; Simanek, E. E. *Mol. Pharm.* **2004**, *1*, 390-393.
1201.Ooya, T.; Lee, J.; Park, K. *J. Controlled Release* **2003**, *5*, 121-127.
1202.Ooya, T.; Lee, J.; Park, K. *Bioconjugate Chem.* **2004**, *15*, 1221-1229.
1203.Lim, J.; Simanek, E. E. *Org. Lett.* **2008**, *10*, 201-204.
1204.Yang, H.; Morris, J. J.; Lopina, S. T. *J. Colloid Interface Sci.* **2004**, *273*, 148-154.
1205.Wu, G.; Barth, R. F.; Yang, W.; Kawabata, S.; Zhang, L.; Green-Church, K. *Mol. Cancer Ther.* **2006**, *5*, 52-59.
1206.Pan, G.; Lemmouchi, Y.; Akala, E. O.; Bakare, O. J. *Bioact. Compat. Polym.* **2005**, *20*, 113-128.
1207.Dhanikula, R. S.; Argaw, A.; Bouchard, J.-F.; Hilgen, P. *Mol. Pharma.* **2008**, *5*, 105-116.
1208.Shukla, R.; Thomas, T. P.; Desai, A. M.; Kotlyar, A.; Park, S. J.; Baker, J. R., Jr. *Nanotechnol.* **2008**, *19*, 295102/1-295102/7.
1209.Patel, D.; Henry, J.; Good, T. *Biochim. Biophys. Acta* **2006**, *1760*, 1802-1809.
1210.Patel, D. A.; Henry, J. E.; Good, T. A. *Brain Res.* **2007**, *1161*, 95-105.
1211.Zhou, T.; Neubert, H.; Liu, D. Y.; Liu, Z. D.; Ma, Y. M.; Kong, X. L.; Luo, W.; Mark, S.; Hider, R. C. *J. Med. Chem.* **2006**, *49*, 4171-4182.

1212.Fernandes, E. G. R.; Alencar de Queiroz, A. A.; Abraham, G. A.; Roman, J. S. *J. Mater. Sci.: Mater. Med.* **2006**, *17*, 105-111.
1213.Yang, H.; Lopina, S. T. *J. Biomed. Mater. Res.* **2004**, *72A*, 107-114.
1214.Wang, B.; Navath, R. S.; Romero, R.; Kannan, S.; Kannan, R. *Int. J. Pharm.* **2009**, *377*, 159-168.
1215.Kasyanov, V.; Isenburg, J.; Draughn, R. A.; Hazard, S.; Hodde, J.; Ozolanta, I.; Murovska, M.; Halkes, S. B.; Vrasidas, I.; Liskamp, R. M. J.; Pieters, R. J.; Simionescu, D.; Markwald, R. R.; Mironov, V. *Biomater.* **2006**, *27*, 745-751.
1216.Bhadra, D.; Bhadra, S.; Jain, S.; Kain, N. K. *Int. J. Pharm.* **2003**, *257*, 111-124.
1217.Venuganti, V. V. K.; Perumal, O. P. *Int. J. Pharma.* **2008**, *361*, 230-238.
1218.Bhadra, D.; Bhadra, S.; Kain, N. K. *J. Pharm. Sci.* **2005**, *8*, 467-482.
1219.Bhadra, D.; Bhadra, S.; Kain, N. K. *Pharm. Res.* **2006**, *23*, 623-633.
1220.Wang, W.; Xiong, W.; Wan, J.; Sun, X.; Xu, H.; Yang, X. *Nanotechnol.* **2009**, *20*, 105103.
1221.Jevprasesphant, R.; Penny, J.; Jalal, R.; Attwood, D.; McKeonwn, N. B.; D'Emanuele, A. *Int. J. Pharm.* **2003**, *252*, 263-266.
1222.Wegmann, K. W.; Wagner, C. R.; Whitham, R. H.; Hinrichs, D. J. *J. Immunol.* **2008**, *181*, 3301-3309.
1223.Jevprasesphant, R.; Penny, J.; Jalal, R.; Attwood, D.; McKeonwn, N. B.; D'Emanuele, A. *Pharm. Res.* **2003**, *20*, 1543-1550.
1224.Bai, S.; Thomas, C.; Rawat, A.; Ahsan, F. *Crit. Rev. Therapeutic Drug Carrier Syst.* **2006**, *23*, 437-495.
1225.Mishra, V.; Gupta, U.; Jain, N. K. *J. Biomater. Sci.* **2009**, *20*, 141-166.
1226.Okuda, T.; Kawakami, S.; Maeie, T.; Niidome, T.; Yamashita, F.; Hashida, M. *Controlled Release* **2006**, *114*, 69-77.
1227.Okuda, T.; Kawakami, S.; Akimoto, N.; Niidome, T.; Yamashita, F.; Hashida, M. *Controlled Release* **2006**, *116*, 330-336.
1228.Schiavon, O.; Pasut, G.; Moro, S.; Orsolini, P.; Guiotto, A.; Veronese, F. M. *J. Med. Chem.* **2004**, *39*, 123-133.
1229.Passut, G.; Scaramuzza, S.; Sciavon, O.; Mendici, R.; Veronese, F. M. *J. Bioactive Polym.* **2005**, *20*, 213-230.
1230.Gillies, E. R.; Jonsson, T. B.; Fréchet, J. M. J. *J. Am. Chem. Soc.* **2004**, *126*, 11936-11943.
1231.Sideratou, Z.; Tsiourvas, D.; Paleos, C. M. *J. Colloid Interface Sci.* **2001**, *242*, 272-276.
1232.Paleos, C. M.; Tsiourvas, D.; Sideratou, Z; Tziveleka, L.-A. *Biomacromolecules* **2004**, *5*, 524-529.
1233.Tziveleka, L.-A.; Kontoyianni, C.; Sideratou, Z; Tsiourvas, D.; Paleos, C. M. *Macromol. Biosci.* **2006**, *6*, 161-169.
1234.Luo, D.; Harverstick, K.; Belcheva, N.; Han, E.; Saltzman, W. M. *Macromolecules* **2002**, *35*, 3456-3462.
1235.Huang, R. Q.; Qu, Y. H.; Ke, W. L.; Zhu, J. H.; Pei, Y. Y.; Jiang, C.; *FASEB J.* **2007**, *21*, 1117-1125.
1236.Huang, R. Q.; Ke, W. L.; Liu, Y.; Jiang, C.; Pei, Y. Y. *Biomaterials* **2008**, *29*, 228-246.
1237.Bhadra, D.; Bhdra, S.; Jain, N. K. *Pharmaceutical Research* **2006**, *23*, 623-633.
1238.Tang, H.; Lopina, S. T.; Dipersio, L. P.; Schmidt, S. P. *J. Mater. Sci.: Mater. Med.* **2008**, *19*, 1991-1997.
1239.Gajbhiye, V.; Vijayaraj, K. P.; Tekade, R. K.; Jain, N. K. *Eur. J. Med. Chem.* **2009**, *44*, 1155-1166.

1240.Thanou, M.; Duncan, R. *Curr. Opin. Invest. Drugs* **2003**, *4*, 701-709.
1241.Duncan, R. *Nat. Rev. Drug. Discov.* **2003**, *2*, 347-360.
1242.Wu, G.; Barth, R. F.; Yang, W. L.; Chatterjee, M.; Tjarks, W.; Ciesielski, M. J.; Fenstermaker, R. A. *Bioconjugate Chem.* **2004**, *15*, 185-194.
1243.Shukla, S.; Wu, G.; Chatterjee, M.; Yang, W. L.; Sekido, M.; Diop, L. A.; Mulle, R.; Sudimak, J. J.; Lee, R. J.; W. L.; Barth, R. F.; Tjarks, W. *Bioconjug. Chem.* **2003**, *14*, 158-167.
1244.Hosmane, N. S.; Yinghuai, Z.; Maguire, J. A.; Kaim, W.; Tagagaki, M. J. *Organomet. Chem.* **2009**, *694*, 1690-1697.
1245.Leuchtenberger, C.; Lewisohn, R.; Laszlo, D.; Leuchtenberger, R. *Proc. Soc. Exp. Biol. Med.* **1944**, *55*, 204-205.
1246.Elnakat, H.; Ratnam, M. *Adv. Drug Deliv. Rev.* **2004**, *56*, 1067-1084.
1247.Boisselier, E.; Astruc, D. *Chem. Soc. Rev.* **2009**, *38*, 1759-1782.
1248.Kono, K.; Liu, M.; Fréchet, J. M. J. *Bioconjugate Chem.* **1999**, *10*, 1115-1121.
1249.Thomas, T. P.; Majoros, I. J.; Kotlayar, A.; Kukowska-Latallo, J. F.; Bielinska, A.; Myc, A.; Baker, J. R., Jr. *J. Med. Chem.* **2005**, *48*, 3729-3735.
1250.Majoros, I. J.; Myc, A.; Thomas, T. P.; Mehta, C. B.; Baker, J. R., Jr. *Biomacromolecules* **2006**, *7*, 572-579.
1251.Myc, A.; Patri, A. K.; Baker, J. R., Jr. *Biomacrolecules* **2007**, *8*, 2986-2989.
1252.Majoros, I. J.; Williams, C. R.; Baker, J. R., Jr. *Cur. Top. Med. Chem.* **2008**, *8*, 1165-1179.
1253.Myc, A.; Majoros, I. J.; Thomas, T. P.; Baker, J. R., Jr. *Biomacromolecules* **2007**, *8*, 13-18.
1254.Gingras, M.; Raimundo, J.-M.; Chabre, Y. M. *Angew. Chem., Int. Ed.* **2007**, *46*, 1010-1017.
1255.Calvert, H. *Semin. Oncol.* **2002**, *29*, 3-17.
1256.Kukowska-Latallo, J. F.; Candido, K. A.; Cao, Z.; Nigavekar, S. S.; Majoros, I. J.; Thomas, T. P.; Balogh, L. P.; Khan , M. K.; Baker, J. R., Jr. *Cancer Res.* **2005**, *65*, 5317-5324.
1257.Islam, M. T.; Majoros, I. J.; Baker, J. R., Jr. *J. Chromatog. B* **2005**, *822*, 21-26.
1258.Shi, X.; Patri, A. K.; Bi, X.; Islam, M. T.; Desai, A.; Ganser, T. R.; Baker, J. R., Jr. *Analyst* **2006**, *131*, 374-381.
1259.Choi, Y.; Thomas, T.; Kotlyar, A.; Islam, M. T., Baker, J. R., Jr. *Chem. Biol.* **2005**, *12*, 35-43.
1260.Iwamura, M. *Nippon Rinsho.* **2006**, *64*, 231-237.
1261.Choi, Y.S.; Mecke, A.; Orr, B. G.; Holl, M. M. B.; Baker, J. R., Jr. *Nano Lett.* **2004**, *4*, 391-397.
1262.Wiener, E. C.; Brechbiel, M. W.; Brothers, H.; Magin, R. L.; Gansow, O. A.; Tomalia, D. A.; Lauterburg, P. C. *Magn. Res. Med.* **1994**, *31*, 1-8.
1263.Wiener, E. C.; Konda, S.; Shadron, A.; Brechbiel, M.; Gan-sow, O. *Invest. Radiol.* **1997**, *32*, 748-754.
1264.Konda, S. D.; Aref, M.; Brechbiel, M.; Wiener, E. C. *Invest. Radiobiol.* **2000**, *35*, 50-57.
1265.Konda, S. D.; Aref, M.; Wang, S.; Brechbiel, M.; Wiener, E. C. *Biol. Med.* **2001**, *12*, 104-113.
1266.Konda, S. D.; Wang, S.; Brechbiel, M.; Wiener, E. C. *Invest. Radiobiol.* **2002**, *37*, 199-204.
1267.Mantovani, L. T.; Miotti, S. *Eur. J. Cancer* **1994**, *30A*, 363-369.
1268.Tansey, W.; Ke, S.; Cao, X.-Y.; Pasuelo, M. J.; Wallace, S.; Li, C. *J. Controlled Release* **2004**, *94*, 39-51.

1269.Roy, R. *Trends in Glycosci. Glycotechnol.* **2003**, *15*, 291-310.
1270.Roy, R. Zanini, D.; Meuier, S. J.; Romanovska, A. *Chem. Commun.* **1993**, 1869-1872.
1271.Roy, R.; Baek, M. G. *Rev. Mol. Biotechnol.* **2002**, *90*, 291-309.
1272.Roy, R.; Baek, M. G. *J. Biotechnol.* **2002**, *90*, 291-309.
1273.Thoma, G.; Streiff, M. B.; Katopodis, A. G.; Duthaler, R. O.; Voelcker, N. H.; Ehrhardt, C.; Masson, C. *Chem. Eur. J.* **2006**, *12*, 99-117.
1274.Turbull, W. B.; Stoddart, J. F. *Rev. Mol. Biotechnol.* **2002**, *90*, 231-255.
1275.Bezouska, K. *Rev. Mol. Biotechnol.* **2002**, *90*, 269-290.
1276.Lindhorst, T. K. *Top. Curr. Chem.* **2002**, *218*, 201-235.
1277.Roy, R. *Trends Glycosci. Glycotehnol.* **2003**, *15*, 291-310.
1278.Rockendorf, N.; Lindhorst, T. K. *Top. Curr. Chem.* **2001**, *217*, 201-238.
1279.Tsetkov, D. E.; Nifantiev, N. E. *Russ. Chem. Bull. Int. Ed.* **2005**, *54*, 1065-1083.
1280.Niederhafner, P.; Sebestik, J.; Jezek, J. *J. Pept. Sci.* **2005**, *11*, 757-758.
1281.Niederhafner, P.; Sebestik, J.; Jezek, J. *J. Pept. Sci.* **2008**, *14*, 2-43.
1282.Niederhafner, P.; Sebestik, J.; Jezek, J. *J. Pept. Sci.* **2008**, *14*, 44-65.
1283.Niederhafner, P.; Reinis, M. Sebestik, J.; Jezek, J. *J. Pept. Sci.* **2008**, *14*, 556-587.
1284.Badjic, J. D.; Nelson, A.; Cantrill, S. J.; Turnbull, W. B.; Stoddart, J. F. *Acc. Chem. Res.* **2005**, *38*, 723-732.
1285.Ernst, B.; Hart, W.; Sinay, P., Eds. *Carbohydrates in Chemistry and Biology, Part I: Chemistry of Saccharides; Vol 1: Chemical Synthesis of Glycosides and Glycomimetics*; Wiley-VCH: Weinheim, 2000.
1286.Gestwicki, J. E.; Cairo, Ch. W.; Strong, L. E.; Oetjen, K. A.; Kiesling, L. L. *J. Am. Chem. Soc.* **2002**, *124*, 14922-14933.
1287.Matsuura, K.; Kobayashi, K. *Glycoconj. J.* **2004**, *21*, 139-148.
1288.Wolfenden, M. L.; Cloninger, M. J. *J. Am. Chem. Soc.* **2005**, *127*, 12168-12169.
1289.Hayashida, O.; Mizuki, K.; Akagi, K.; Matsuo, A.; Kanamori, T.; Nakai, T.; Sando, S.; Aoyama, Y. *J. Am. Chem. Soc.* **2003**, *125*, 594-601.
1290.Wu, A. M.; Wu, J. H.; Liu, J. H.; Singh, T.; Andre, S.; Kalner, H.; Gabius, H. *J. Biochimie* **2004**, *86*, 317-326.
1291.Arosio, D.; Fontanella, M.; Baldini, L.; Mauri, L.; Bernardi, A.; Casnati, A.; Sansone, F.; Ungaro, R. *J. Am. Chem. Soc.* **2005**, *127*, 3660-3661.
1292.Andre, S.; Pieters, R. J.; Vrasidas, I.; Kllner, H.; Kuwabara, I.; Liu, F. T.; Liskamp, R. M.; Gabius, H. J. *ChemBioChem.* **2001**, *2*, 822-830.
1293.Benito, J. M.; Gomez-Garcia, M.; Ortiz Mellet, C.; Bausanne, I.; Defaye, J.; Garcia Fernandez, J. M. *J. Am. Chem. Soc.* **2004**, *126*, 10355-10363.
1294.Kobayashi, H.; Brechbiel, M. W. *Curr. Pharm. Biotechnol.* **2004**, *5*, 539-549.
1295.Lundquist, J. J.; Toone, E. J. *Chem. Rev.* **2002**, *102*, 555-578.
1296.Reymond, J. L. *Chem. Eur. J.* **2005**, *11*, 3441-3950.
1297.Matsuoka, K.; Terabatake, M.; Esumi, Y.; Hatano, K.; Terunuma, D.; Kuzuhara, H. *Biomacroloecules* **2006**, *7*, 2284-2290.
1298.Gao, Y.; Egushi, A.; Kakehi, K.; Lee, Y. C. *Org. Lett.* **2004**, *6*, 3457-3460.
1299.Sakamoto, J.; Müllen, K. *Org. Lett.* **2004**, *6*, 4277-4280.
1300.Lagnoux, D.; Darbre, T.; Schmitz, M. L.; Reymond, J. L. *Chemistry* **2005**, *11*, 3941-3950.
1301.Bay, S.; Lo-Man, R.; Osinaga, E.; Nakada, H.; Leclerc, C.; Cantacuzène, D. *J. Pep. Res.* **1997**, *49*, 620-625.
1302.Ambrosi, M.; Cameron, N. R.; Davis, B. G. *Org. Biomol. Chem.* **2005**, *3*, 1593-1608.
1303.Houseman, B. T.; Mrksich, M. *Top. Curr. Chem.* **2002**, *218*, 1-44.
1304.Fulton, D. A.; Stoddart, J. F. *Bioconj. Chem.* **2001**, *12*, 655-672.
1305.Zeng, Y.; Yan, Z. T.; Kong, F. Z. *Prog. Chem.* **2005**, *17*, 111-121.

1306.van Ameijde, J.; Liskamp, R. M. *Org. Biomol. Chem.* **2003**, *1*, 2661-2669.
1307.Sansone, F.; Chierici, E.; Casnati, A.; Ungaro, R. *Org. Biomol. Chem.* **2003**, *1*, 1802-1809.
1308.Casnati, A.; Sansone, F.; Ungaro, R. *Acc. Chem. Res.* **2003**, *36*, 246-254.
1309.Baklouti, L.; Cheriaa, N.; Mahouachi, M.; Othman, A. B.; Abidi, R.; Kim, J. S.; Kim, Y.; Vicens, J. *Mini-Rev. Org. Chem.* **2006**, *3*, 219-228.
1310.Baklouti, L.; Cheriaa, N.; Mahouachi, M.; Abidi, R.; Kim, J. S.; Kim, Y.; Vicens, J. *J. Incl. Phenom. Macrocycl. Chem.* **2006**, *54*, 1-7.
1311.Aoyama, Y. *Chem. Eur. J.* **2004**, *10*, 588-593.
1312.Nakai, T.; Sasaki, T.; Aoyama, Y. *J. Am. Chem. Soc.* **2003**, *125*, 8465-8475.
1313.Hayashida, O.; Misuki, K.; Akagi, K.; Matsuo, A.; Kanamori, T.; Nakai, T.; Sando, S.; Aoyama, Y. *J. Am. Chem. Soc.* **2003**, *125*, 594-601.
1314.Thulstrup, P. W.; Brask, J.; Jensen, K. J.; Larsen, E. *Biopolymers* **2005**, *78*, 46-52.
1315.Bubber, M.; Patel, A.; Sadalapure, K.; Aumuller, I.; Lindhorst, T. K. *Eur. J. Org. Chem.* **2006**, 5357-5366.
1316.Ballardini, R.; Colonna, B.; Gandolfi, M. T.; Kalovidouris, S. A.; Orzel, L.; Raymo, F. M.; Stoddart, J. F. *Eur. J. Org. Chem.* **2003**, 288-294.
1317.Isobe, H.; Mashima, H.; Yorimitsu, H.; Nakamura, E. *Org. Lett.* **2003**, *5*, 4461-4463.
1318.Roy, R.; Kim, J. M. *Tetrahedron* **2003**, *59*, 3881-3893.
1319.Renaudet, O.; Dumy, P. *Org. Lett.* **2003**, *5*, 243-246.
1320.Singh, Y.; Renaudet, O.; Defrancq, E.; Dumy, P. *Org. Lett.* **2005**, *7*, 1359-1362.
1321.Grigalevicius, S.; Chierici, S.; Renaudet, O.; Lo-Man, R.; Dériaud, E.Leclerc, C.; Dumy, P. *Bioconj. Chem.* **2005**, *16*, 1149-1159.
1322.Han, S.; Baigude, H.; Hattori, K.; Yoshida, T.; Uryu, T. *Carbohydr. Polym.* **2007**, *68*, 26-34.
1323.Baigude, H.; Katsuraya, K.; Okuyama, K.; Hatanaka, K.; Ikeda, E.; Shibata, N.; Uryu, T. *J. Polym. Sci., Part A: Polym. Chem.* **2004**, *42*, 1400-1414.
1324.Sanclimens, G.; Cresopo, L.; Giralt, E.; Albericio, F.; Royo, M. *J. Org. Chem.* **2005**, *70*, 6274-6281.
1325.Katajisto, J.; Karskela, T.; Heinonen, P.; Lonnberg, H. *J. Org. Chem.* **2002**, *67*, 7995-8001.
1326.Ravi Kumar, M. N. V.; Muzzarelli, R. A. A.; Muzzarelli, C.; Sashiwa, H. *Chem. Rev.* **2004**, *104*, 6017-6084.
1327.Zhang, M.; Muller, A. H. E. *J. Polym. Sci. Part A: Polym. Chem.* **2005**, *43*, 3461-3481.
1328.Zhang, L.; Li, W.; Zhang, A. *Prog. Chem.* **2006**, *18*, 939-949.
1329.Veprek, P.; Hajduch, M.; Dzubach, P. Kuklik, R.; Polakova, J.; Bezouska, K. *J. Med. Chem.* **2006**, *49*, 6400-6407.
1330.Ouerfelli, O.; Warren, J. D.; Wilson, R. M.; Danishefsky, S. J. *Expert Rev. Vaccines* **2005**, *4*, 677-685.
1331.Hang, H. C.; Bertozzi, C. R. *Biorg. Med. Chem.* **2005**, *13*, 5021-5034.
1332.Dziadek, S.; Kunz, H. *Chem. Rec.* **2004**, *3*, 308-321.
1333.Buskas, T.; Ingale, S.; Boons, G. J. *Glycobiology* **2006**, *16*, 113R-136R.
1334.Ragupathi, G.; Gathuru, J.; Livingston, P. *Cancer Treat. Res.* **2005**, *123*, 157-180.
1335.Galonic, D. P.; Gin, D. Y. *Nature* **2007**, *446*, 1000-1007.
1336.Hoos, A.; Parmiani, G.; Hege, K.; Sznol, M.; Loibner, H.; Eggermont, A.; Urba, W.; Blumenstein, B.; Sacks, N.; Keiholz, U.; Nichol, G. *J. Immunother.* **2007**, *30*, 1-15.
1337.Ragupathi, G.; Koide, F.; Livingston, P. O.; Choi, Y. S.; Endo, A.; Wan, Q.; Spassva, M. K.; Kedding, S. J.; Allen, J.; Ouerfelli, O.; Wilson, R. M.; Danishefsky, S. J. *J. Am. Chem. Soc.* **2006**, *128*, 2715-2725.

1338.Popisil, M.; Vannucci, L.; Fiserova, A.; Krausova, K.; Horvath, O.; Bezouska, K.; Mosca, F. *Adv.. Exp. Biol. Med.* **2001**, *495*, 343-347.
1339.Kunz, H. *J. Pept. Sci.* **2003**, *9*, 563-573.
1340.Darbre, T.; Reymond, J. L. *Acc. Chem. Res.* **2006**, *39*, 925-934.
1341.Darbre, T.; Reymond, J. L. *Curr. Top. Med. Chem.* **2008**, *8*, 1286-1293.
1342.Jang, W. D.; Kataoka, K. J. *Drug Deliv. Sci. Tech.* **2005**, *15*, 15, 19-30.
1343.Danishefsky, S. J.; Allen, J. R. *Angew. Chem., Int. Ed. Engl.* **2000**, *39*, 836-863.
1344.Livingston, P. O.; Ragupathi, G. *Hum. Vaccin.* **2006**, *2*, 137-143.
1345.Doores, K. J.; Gamblin, D. P.; Davis, B. G. *Chem. Eur. J.* **2006**, *12*, 656-665.
1346.Brooks, P. C.; Clark, R. A. F.; Cheresh, D. A. *Science* **1994**, *264*, 569-571.
1347.Cleaver, O.; Melton, D. A. *Nat. Med.* **2003**, *9*, 661-668.
1348.Xu, L.; Tang, W. H.; Huang, C. C.; Alexander, W.; Xiang, L. M.; Pirollo, K. F.; Rait, A.; Chang, E. *Mol. Med.* **2001**, *7*, 723-734.
1349.Waengler, C.; Moldenhauer, G.; Eisenhut, M.; Hakenborn, U.; Mier, W. *Bioconj. Chem.* **2008**, *19*, 813-820.
1350.Chang, S. S.; O'Keefe, D. S.; Bacich, D. J.; Reuter, V. E.; Heston, W. D.; Gaudin, P. B. *Clin. Cancer Res.* **1999**, *5*, 2674-2681.
1351.McCarthy, T. D.; Karellas, P.; Henderson, S. A.; Giannis, M.; O'Keefe, D. F.; Heery, G.; Paull, J. R. A.; Matthews, B. R.; Holan, G. *Mol. Pharm.* **2005**, *2*, 312-318.
1352.Wang, L. X. *Curr. Opin. Drug Discov. Devel.* **2006**, *9*, 194-206.
1353.Krauss, J. J.; Joyce, J. G.; Finnefrock, A. C.; Song, H. C.; Dudkin, V. Y.; Geng, X.; Warren, J. D.; Chastain, M.; Shiver, J. W.; Danishefsky, S. J. *J. Am. Chem. Soc.* **2007**, *129*, 11042-11044.
1354.Gomara, M. J.; Haro, I. *Curr. Med. Chem.* **2007**, *14*, 531-546.
1355.Myc, A.; Douce, T. B.; Ahuja, N.; Kotlyar, A.; Kukowska-Latallo, J.; Thomas, T. P.; Baker, J. R., Jr. *Anti-Cancer Drugs* **2008**, *19*, 143-149.
1356.Koyanagi, S.; Tanigawa, N.; Nakagawa, H.; Soeda, S.; Shimeno, H. *Biochem. Pharmacol.* **2003**, *65*, 173-179.
1357.Ohta, T.; Miura, N.; Fujitani, N.; Najajima, F.; Niikura, K.; Sadamoto, R.; Guo, Ch. T.; Suzuki, T.; Suzuki, Y.; Monde, K.; Nishimura, S. I. *Angew. Chem., Int. Ed.* **2003**, *42*, 5186-5189
1358.Sakamoto, J. I.; Koyama, T.; Miyamoto, D.; Yingsakmongkon S.; Hidari, K. I. P. J.; Jampangern, W.; Suzuki, T.; Suzuki, Y.; Esumi, Y.; Hatano, K.; Terunuma, D.; Matsuoka, K. *Bioorg. Med. Chem. Lett.* **2007**, *17*, 717-721.
1359.Caruthers, S. D.; Wickline, S. A.; Lanza, G. M. *Curr. Opin. Biotechnol.* **2007**, *18*, 26-30.
1360.Kolomiets, E.; Swiderska, M; Kadam, R. U.; Johansson, E. M. V.; Jaeger, K.-E.; Darbre, T.; Reymond, J.-L. *ChemMedChem* **2009**, *4*, 562-569.
1361.Maillard, N.; Darbre, T.; Reymond, J.-L. *J. Combinat. Chem.* **2009**, *11*, 667-675.
1362.Kojima, C.; Tsumura, S.; Harada, A.; Kono, K. *J. Am. Chem. Soc.* **2009**, *131*, 6052-6053.
1363.Shukla, R.; Thomas, T. P.; Peters, A.; Kotlyar, A.; Myc, A., Baker, J. R., Jr. *Chem. Commun.* **2005**, 5739-5741.
1364.Boswell, C. A.; Eck, P. K.; Regino, C. A. S.; Bernardo, M.; Wong, K. J.; Milenic, D. E.; Choyke, P. L.; Brechbiel, M. W. *Mol. Pharma.* **2008**, *5*, 527-539.
1365.Pisal, D. S.; Yellepeddi, V. K.; Kumar, A.; Kaushil, R. S.; Radhey, R. S.; Hildreth, M. B.; Guan, X.; Xiangming, P. S. *Int. J. Pharma.* **2008**, *350*, 113-121.
1366.Dijkgraaf, I.; Rijders, A. Y.; Soede, A.; Dechesne, A. C.; van Esse, G. W.; Brouwer, A. J.; Corstens, F. H.; Boerman, O. C.; Rijkers, D. T.; Liskamp, R. M *Biomol. Chem.* **2007**, *5*, 935-944.

1367.Jevprasesphant R.; Penny, J; D'Emanuele, A. D. *Controlled Release* **2004**, *97*, 259-267.
1368.Paleos, C.; Tziveleka, L.-A.; Sideratou, Z. Tsiuotvas, D. *Expert Opin. Drug Deliv.* **2009**, *6*, 27-38.
1369.Gao, Y.; Gao, G.; He, Y.; Liu, T.; Qi, R. *Mini-rev. Med. Chem.* **2008**, *8*, 889-900.
1370.Patil, S. D.; Rhodes, D. G.; Burgess, D. J. *J. Am. Assoc. Pharm. Sci.* **2005**, *7*, E61-E77.
1371.Raper, S. E.; Chirmule, N.; Lee, F. S.; Wivel, N. A.; Bagg, A.; Gao, G. P.; Wilson, J. M.; Batshaw, M. L. *Mol. Gene. Metab.* **2000**, *18*, 33-37.
1372.Luo, D.; Salzman, W. M. *Nat. Biotech.* , *132*, 1078-1084.
1373.Behr, J.-P. *Acc. Chem. Res.* **1993**, *26*, 274-278.
1374.Boussif, O.; Lezoualch, F.; Zanta, M. A.; Mergny, M. D.; Scherman, D.; Demeneix, B.; Behr, J.-P. *Proc. Nat.. Acad. Sci. U. S. A.* **1995**, *92*, 7297-7301.
1375.LeHoux, J. G.; Grondin, F. *Endocrinology* **1993**, *132*, 1078-1084.
1376.Liu, Y. M.; Reineke, T. M. *Bioconjugate Chem.* **2006**, *17*, 101-108.
1377.Paleos, C. M.; Tsiourvas, D.; Sideratou, Z. *Mol. Pharmaceutics* **2007**, *4*, 169-188.
1378.Dufès, C.; Uchegbu, I. F.; Schätslein, A. G. *Adv. Drug Delivery Rev.* **2005**, *57*, 2177-2202.
1379.Dennig, J. *Top. Curr. Chem.* **2003**, *228*, 227-236.
1380.Kitchens, K. M.; El-Sayed, M. E. H.; Ghanderi, H. *Adv. Drug Delivery Rev.* **2005**, *57*, 2163-2176.
1381.Ramaswamy, C.; Skathivel, T.; Wilderspin, A. F.; Florence, A. T. *Int. J. Pharm.* **2003**, *254*, 17-21.
1382.Caminade, A.-M.; Turrin, C.-O.; Majoral, J.-P. *Chem. Eur. J.* **2008**, *14*, 7422-7432.
1383.Seib, F. P.; Jones, A. T.; Duncan, R. *J. Controlled Release* **2007**, *117*, 291-300.
1384.Guillot-Nieckowski, M.; Joester, D.; Stör, M.; Losson, M.; Adrian, M.; Wagner, B.; Kansy, M.; Heizelmann, H.; Pugin, R.; Diederich, F.; Gallani, J.-L. *Langmuir* **2007**, *23*, 737-746.
1385.Dennig, J.; Duncan, E. *Rev. Mol. Biotechnol.* **2002**, *90*, 339-347.
1386.Manunta, M.; Tan, P. H.; Sagoo, P.; Kashefi, K.; George, A. J. T. *Nucleic Acid Res.* **2004**, *32*, 2730-2739.
1387.Hong, S.; Lerouiel, P. R.; Janus, E. K.; Peters, J. L.; Kober, M. M.; Islam, M. T.; Orr, B. G. Jr.; Banaszak Holl, M. M. *Bioconjugate Chem.* **2006**, *17*, 728-734.
1388.Majoros, I.; Williams, C. R.; Becker, A. C.; Baker, J. R., Jr. *J. Comput. Theor. Nanoscience* **2009**, *6*, 1430-1436.
1389.Hong, S.; Rattan, R.; Majoros, I. J.; Mullen, D. G.; Peters, J. L.; Jennifer, L.; Shi, X.; Bielinska, A. U.; Blanco, L.; Orr, B. G.; Bradford, G.; Baker, J. R., Jr.; Banaszak Holl, M. M. *Bioconj. Chem.* **2009**, *20*, 1503-1513.
1390.Dufès, C.; Keith, W. N.; Bilsland, A.; Proutski, I.; Uchegbu, I. F.; Schätzlein, A. G. *Cancer Res.* **2005**, *65*, 8079-8084.
1391.Maszewska, M.; Leclaire, J.; Cieslak, M.; Nawrot, B.; Okruszek, A.; Caminade, A.-M.; Majoral, J.-P. *Oligonucleotides* **2003**, *13*, 193-207.
1392.Bermejo, J. F.; Ortega, P.; Chonco, L.; Eritja, R.; Samaniego, R.; Müllner, M.; de Jesus, E.; de la Mata, F. J.; Flores, J. C.; Gomez, R.; Nunoz-Fernandez, A. *Chem. Eur. J.* **2007**, *13*, 483-495.
1393.Joester, D.; Losson, M.; Pugin, R.; Heinzelmann, H.; Walter, E.; Merkle, H. P.; Diederich, F. *Angew. Chem., Int. Ed.* **2003**, *42*, 1486-1490.
1394.Guillot-Niekowski, M.; Joester, D.; Stör, M.; Losson, M.; Adrian, M.; Wagner, B.; Kansy, M.; Heinzelmann, H.; Pugin, R.; Diederich, F.; Gallani, J. L. *Langmuir* **2007**, *23*, 737-746.

1395.Ewert, K. K.; Evans, H. M.; Zidoska, A.; Bouxsein, N. F.; Ahmad, A.; Safinya, C. R. *J. Am. Chem. Soc.* **2006**, *128*, 3998-4006.
1396.Zinselmeyer, B. H.; Mackay, S. P.; Schatzleibn, A. G.; Uchebu, I. F. *Pharm. Res.* **2002**, *19*, 960-967.
1397.Lee, J. H.; Lim, Y. B.; Choi, J. S.; Lee, Y.; Kim, T. I.; Kim, H. J.; Yoon, J. K.; Kim, K.; Park, J. S. *Bioconjugate Chem.* **2003**, *14*, 1214-1221.
1398.Wood, K. C.; Little, S. R.; Langer, R.; Hammond, P. T. *Angew. Chem., Int. Ed.* **2005**, *44*, 6704-6708.
1399.Pan, B.; Cui, D.; Sheng, Y.; Ozkan, C.; Gao, F.; He, R.; Li, Q.; Xu, P.; Huang, T. *Cancer Res.* **2007**, *67*, 8156-8163.
1400.Shi, X.; Wang, S. H.; Swanson, S. D.; Ge, S.; Cao, Z.; Van Antwerp, M. E.; Landmark, K. J.; Baker, J. R., Jr. *Adv. Mater.* **2008**, *20*, 1671-1678.
1401.Vivès, E.; Brodin, P.; Lebleu, B. *J. Biol. Chem.* **1997**, *272*, 16010-16017.
1402.Kirschberg, T. A.; VanDeusen, C. L.; Rothbard, J. B.; Yang, M.; Wender, P. A. *Org. Lett.* **2003**, *5*, 3459-3462.
1403.Futaki, S. *Adv. Drug Delivery Rev.* **2005**, *57*, 547-558.
1404.Choi, J. S.; Nam, K.; Park, J.; Kim, J. B.; Lee, J. K.; Park, J. S. *J. Controlled Release* **2004**, *99*, 445-456.
1405.Kim, T. I.; Baek, J. U.; Bai, C. Z.; Park, J. S. *Biomaterials* **2007**, *28*, 2061-2067.
1406.Tziveleka, A.; Psarra, A.-M. G.; Tsiouvas, D.; Paleos, C. M. *J. Controlled Release* **2007**, *117*, 137-146.
1407.Kim, J. B.; Choi, J. S.; Nam, K.; Lee, M.; Park, J. S.; Lee, J. K. *J. Controlled Release* **2006**, *114*, 110-117.
1408.Yamagata, M.; Kawano, T.; Shiba, K.; Mori, T.; Katayama, Y.. Niidome, T. *Biorg. Med. Chem.* **2007**, *15*, 526-532.
1409.Kono, K.; Akiyama, H.; Takahashi, T.; Harada, A. *Bioconjugate Chem.* **2005**, *16*, 208-214.
1410.Bi, X.; Shi, X.; Baker, J. R., Jr. *J. Biomater. Sci., Polym. Ed.* **2008**, *19*, 131-142.
1411.Zhong, H.; He, Z.-G.; Li, Z.; Li, G.-Y.; Shen, S.-R.; Li, X.-L. *J. Biomater. Appl.* **2008**, *22*, 527-544.
1412.Fant, K.; Esbjoerner, E. K.; Lincoln, P.; Norden, B. *Biochemistry* **2008**, *47*, 1732-1740.
1413.Prevette, L. E.; Mills, M.; Ramamoorthy, A.; Orr, B. G.; Andricioaei, I.; Holl, M. M. B. *PMSE Preprint* **2008**, *99*, 678-679.
1414.Qamhieh, K.; Nylander, T.; Ainalem, M.-L. *Biomacromol.* **2009**, *10*, 1720-1726.
1415.Santhakumaran, L. M.; Thomas, T.; Thomas, T. *J. Nucleic Acids Res.* **2004**, *32*, 2102-2112.
1416.Russ, V.; Guenther, M.; Halama, A.; Ogris, M.; Wagner, E. *J. Controlled Release* **2008**, *132*, 131-140.
1417.Kim, S. H.; Jeong, J. H.; Cho, K. C.; Kim, S. W.; Park, T. G. *J. Controlled Release* **2005**, *104*, 223-232.
1418.Bayele, H. K.; Ramaswamy, C.; Wilderspin, A. F.; Srai, S. K.; Toth, I.; Florence, A. T. *J. Pharm. Sci.* **2006**, *95*, 1227-1237.
1419.Takahashi, T.; Hirose, J.; Kojima, C.; Harada, A.; Kono, K. *Bioconj. Chem.* **2007**, *18*, 1163-1169.
1420.Ewert, K. K.; Evans, H. M.; Bouxsein, N. F.; Safinya, C. R. *Bioconj. Chem.* **2006**, *17*, 877-888.
1421.Pan, B.; Cui, D.; Xu, P.; Ozkan, C.; Feng, G.; Ozkan, M.; Huang, T.; Chu, B.; Li, Q.; He, R.; Hu, G. *Nanobiotechnol.* **2009**, *20*, DOI:10.1088/0957-4484/20/12/12501.

1422.Arima, H.; Chihara, Y.; Arizono, M.; Yamashita, S.; Wada, K.; Hirayama, F.; Uekama, K. *J. Controlled Release* **2006**, *116*, 64-74.
1423.Wada, K.; Arima, H.; Tsutsumi, T.; Hirayama, F.; Uekama K. *Biol. Pharm. Bull.* **2005**, *28*, 500-505.
1424.Tsutsumi, T.; Hirayama, F.; Uekama, K.; Arima, H. *J. Controlled Release* **2007**, *119*, 349-359.
1425.Fu, H-L.; Cheng, S.-X.; Zhang, X.-Z.; Zhuo, R.-X. *J. Gene Med.* **2008**, *10*, 1334-1342.
1426.Perumal, O. P.; Inamagolla, R.; Kannan, S.; Kannan, R. M. *Biomater.* **2008**, *29*, 3469-3476.
1427.Zhang, W.; Chen, Z.; Song, X.; Si, J.; Tang, G. *Technol. Cancer Res. Treatment* **2008**, *7*, 103-108.
1428.Shieh, M. J.; Peng, C.-L.; Lou, P.-J.; Chiu, C.-H.; Lai, P.-S. *J. Controlled Release* **2008**, *129*, 200-206.
1429.Jones, S. P.; Gabrielson, S. P.; Pack, D. W.; Smith, D. K. *Chem. Commun.* **2008**, 4700-4702.
1430.Hassane, F. S.; Ivanova, G. D.; Bolewska-Pedyczak, E.; Abes, R.; Arzumanov, A. A.; Gait, M. J.; Lebleu, B.; Gariepy, J. *Bioconj. Chem.* **2009**, *20*, 1523-1530.
1431.Pavan, G.; Danani, A.; Pricl, S.; Smith, D. R. *J. Am. Chem. Soc.* **2009**, *131*, 9686-9694.
1432.Su, C.-J.; Chen, H.-L.; Wei, M.-C.; Peng, S.-F.; Sung, H.-W.; Ivanov, V. A. *Biomacromol.* **2009**, *10*, 773-783.
1433.Santos, J. L.; Oramas, E.; Pego, A. P.; Granja, P. L.; Tomas, H. *J. Controlled Release* **2009**, *134*, 141-148.
1434.Padie, C.; Maszewska, M.; Majchrzak, K.; Nawrot, B.; Caminade, A.-M.; Majoral, J.-P. *New J. Chem.* **2009**, *33*, 318-326.
1435.Zhou, J.; Wu, J.; Hafdi, N.; Behr, J.-P.; Erbacher, P.; Peng, L. *Chem. Commun.* **2006**, 2362-2364.
1436.Inoue, Y.; Kurihara, R.; Tsishida, A.; Hasegawa, M.; Nagashima, T.; Mori, T.; Niidome, T.; Katayama, Y.; Okitsu, O. *J. Controlled Release* **2008**, *126*, 59-66.
1437.Weber, N.; Ortega, P.; Clemente, M. I.; Shcharbin, D.; Bryswezska, M.; de la Mata, F. J.; Gomez, R.; Munoz-Fernandez, M. A. *J. Controled Release* **2008**, *132*, 55-64.
1438.Menuel, S.; Fontanay, S.; Clarot, I.; Duval, R. E.; Diez, L.; Marsura, A. *Bioconj. Chem.* **2008**, *19*, 2357-2362.
1439.Patil, M. L.; Zhang, M.; Betigeri, S.; Taratula, O.; He, H.; Minko, T. *Bioconj. Chem.* **2008**, *19*, 1396-1403.
1440.Pati, M.; Zhang, M.; Taratula, O.; Garbuzenko, O. B.; He, H.; Minko, T. *Biomacromol.* **2009**, *10*, 258-266.
1441.Gregoriadis, G. *Liposomes in drug targeting. In Cell Biology: A Laboratory Handbook*, 2nd ed., Academic Press: London, **1998**.
1442.Khuloud, A.; Sakthivel, T.; Florence, A. T. *Int. J. Pharm.* **2003**, *254*, 33-36.
1443.Kelly, C. V.; Liroff, M. G.; Triplett, L. D. Lerouil, P. R.; Mullen, D. G.; Wallace, J. M.; Meshinchi, S.; Baker, J. R., Jr.; Orr, B. G.; Banaszak Holl, M. M. *ACS Nano* **2009**, *3*, 1886-1896.
1444.Purohit, G.; Sakthivel, T.; Florence, A. T. *Int. J. Pharm.* **2001**, *214*, 71-76.
1445.Khopade, A. J.; Caruso, F.; Tripathi, P.; Nagaich, S.; Jain, N. K. *Int. J. Pharm.* **2002**, *232*, 157-162.
1446.Horovic, A.; Barenholtz, Y.; Gabizon, A. *Biochim. Biophys. Acta* **1992**, *1109*, 203-209.
1447.Khopade, A. J.; Caruso, F. *Biomacromolecules* **2002**, *3*, 1154-1162.

1448.Moraes, M. L.; Baptista, M. S.; Itri, R.; Zucolotto, V.; Olivera, O. N., Jr. *Mater. Sci. Eng., C: Biomim. Supramol. Syst.* **2008**, *28*, 467-471.
1449.Pantos, A.; Tsiourvas, D.; Nounesis, G.; Paleos, C. M. *Langmuir*, **2005**, *21*, 7483-7490.
1450.Ohori, R.; Uchida, K.; Saito, A.; Yajima, H. *Chem. Lett.* **2008**, *37*, 324-325.
1451.Hawthorne, M. F. *Pure Appl. Chem.* **1991**, *63*, 327-334.
1452.Barth, R. F.; Coderre, J. A.; Vicente, M. G.; Blue, T. E. *Clin. Cancer Res.* **2005**, *11*, 3987-4002.
1453.Heldt, J. M.; Durand, N. F.; Salmain, M.; Vessieres, A.; Jaouen, G. *J. Organomet. Chem.* **2004**, *689*, 4775-4782.
1454.Tansey, W.; Ke, S.; Cao, X.-Y.; Pasuelo, M. J.; Wallace, S.; Li, C. *J. Controlled Release* **2004**, *94*, 39-51.
1455.Wu, G.; Barth, R. F.; Yang, W.; Lee, R. J.; Tjarks, W.; Backer, M. V.; Backer, J. M. *Anticancer Agents Med. Chem.* **2006**, *6*, 167-184.
1456.Yang, W.; Barth, R. F.; Adams, D. M.; Ciesielski, M. J.; Fenstermaker, R. A.; Shukla, S.; Tjrks, W.; Caligiuri, M. A. *Cancer Res.* **2002**, *62*, 6552-6558.
1457.Wu, G.; Barth, R. F.; Yang, W.; Chatterjee, M.; Jjarks, W.; Ciesielki, M. J.; Fenstermaker, R. A. *Bioconjug. Chem.* **2004**, *15*, 185-194.
1458.Shukla, R.; Thomas, T. P.; Peters, J. L.; Desai, A. M.; Kukowska-Latallo, J.; Patri, A. K.; Kotlyar, A.; Baker, J. R., Jr. *Bioconj. Chem.* **2006**, *17*, 1109-1115.
1459.Wu, G.; Barth, R. F.; Swidall, M.; Bandyopadhyaya, A. K.; Jjarks, W.; Khorsandio, B.; Blue, T. E.; Ferketich, A. K.; Yang, M.; Christoforidis, G. A.; Sferra, T. J.; Binns, P. J.; Riley, K. J.W.; Ciesielki, M. J.; Fenstermaker, R. A. *Clin. Cancer Res.* **2007**, *13*, 1260-1268.
1460.Yang, W.; Barth, R. F.; Wu, G.; Kawabata, S.; Sferra, T. J.; Bandyopadhyaya, A. K.; Jjarks, W.; Ferketich, A. K.; Moeshberger, M. L.; Binn, P. J.; Riley, K. J.; Coderre, J. A.; Ciesielki, M. J.; Fenstermaker, R. A.; Wikstrand, C. J. *Clin. Cancer Res.* **2006**, *12*, 3792-3802.
1461.Backer, M. V.; Gaynutdinov, T. I.; Patel, V.; Bandyopadhyaya, A. K.; Thirumamagal, B. T.; Jjarks, W.; Barth, R. F.; Claffey, K.; Backer, J. M. *Mol. Cancer Ther.* **2005**, *4*, 1423-1429.
1462.Yan, W.; Wu, G.; Barth, R. F.; Schwindall, M. R.; Bandyopadhyaya, A. K.; Tjarks, W.; Tordoff, K.; Moeshberger, M.; Sferra, T. J.; Binns, P. J.; Riley, K. J.; Cisesielski, M. J.; Fenstermaker, R. A.; Wilkstrand, C. *J. Clin. Cancer Res.* **2008**, *14*, 883-891.
1463.Kobayashi, H.; Kawamoto, S.; Bernardo, M.; Brechbiel, M. W.; Knopp, M. V.; Choyke, P. L. *J. Control. Release* **2006**, *111*, 343-351.
1464.Triescheinijn, M.; Bass, P.; Schellens, J. H.; Stewart, F. A. *Oncologist* **2006**, *11*, 1034-1044.
1465.Peng, Q.; Berg, K.; Moan, J.; Kongshaug, M.; Nesland, J. M. *Photochem. Photobiol.* **1997**, *65*, 235-251.
1466.Quiang, Y.; Zhang, X.; Li, J.; Huang, Z. *Chin. Med. J.* **2006**, *119*, 845-857.
1467.Casas, A.; Battah, S.; Di Venosa, G.; Dobbin, P.; Rodriguez, L.; Fukuda, H.; Batlle, A.; McRobert, A. J. *J. Controlled Release* **2009**, *135*, 136-143.
1468.Battah, S.; Balaratnam, S.; Casas, A.; O'Neill, S.; Edwards, C.; Batlle, A.; Dobbin, P.; MacRobert, A. J. *Mol Cancer Ther* **2007**, *6*, 876-885.
1469.Chauhan, A. S.; Sridevi, S.; Chalasani, K. B.; Jain, A. K.; Jain, S. K.; Jain, N. K.; Diwan, P. V. *J. Controlled Release* **2003**, *90*, 335-343.
1470.Di Venosa, G. M.; Casas, A. G.; Battah, S.; Dobbin, P.; Fukuda, H.; Macrobert, A. J.; Batlle, A. *Int. J. Biochem. Cell. Biol.* **2006**, *38*, 82-91.

1471.Battah, S.; O'Neill, S.; Edwards, C.; Balaratnam, S.; Dobbin, P.; MacRobert, A. J. *Int. J. Biochem. Cell Biol.* **2006**, *38*, 1382-1392.
1472.Battah, S.; Balaratnam, S.; Casas, S.; O'Neill, S.; Edwards, C.; Batlle, A.; Dobbin, P.; MacRobert, A. J. *Mol. Cancer Ther.* **2007**, *6*, 876-885.
1473.Ideta, R.; Tasaka F.; Jang, W. D.; Nishiyama, N.; Zhang, G. D.; Harada, A.; Yanagi, Y.; Tamaki, T.; Aida, T.; Kataoka, K. *Nano Lett.* **2005**, *5*, 2426-2431.
1474.Jang, W. D.; Nishiyama, N.; Zhang, G. D.; Harada, A.; Jiang, D. L.; Kawauchi, S.; Morimoto, Y.; Koyama, H.; Aida, T.; Kataoka, K. *Angew. Chem., Int. Ed.* **2005**, *44*, 419-423.
1475.Kubat, P.; Lang, K.; Zelinger, Z. *J. Mol. Liq.* **2007**, *131-132*, 200-205.
1476.Gibbs, S. L.; Chen, B.; O'hara, J. A.; Hoopes, P. J.; Hasan, T.; Pogue, P. W. *Photochem. Photobiol.* **2006**, *82*, 1334-1342.
1477.Larsen, J.; Bruggemann, B.; Sly, J.; Crossley, M. J.; Sundstrom, V.; Akesson, E. *Chem. Phys. Lett.* **2006**, *433*, 159-164.
1478.Juzeviene, A.; Juzenas, P.; Bronshtein, I.; Vorobey, A.; Moan, J. *J. Photochem. Biol.* **2006**, *16*, 84-161.
1479.Gomez, C. J.; Ferrario, A.; Luna, M.; Rucker, N.; Wong, S. *Laser Surg. Med.* **2006**, *38*, 516-521.
1480.Jang, W. D.; Nakagishi, Y.; Nishiyama, N.; Kawaushi, S.; Morimoto, Y.; Kikuchi, M.; Kataoka, K. *J. Controlled Release* **2006**, *113*, 73-79.
1481.Huang, Z.; Quiang, Y. G.; Chen, W. R. *Chin. Med. J.* **2006**, *119*, 845-857.
1482.Solban, N.; Rizvi, I.; Hasan, T. *Laser Surg. Med.* **2006**, *38*, 522-531.
1483.Malatesti, N.; Smith, K.; Savoie, H.; Greenman, J.; Boyle, R. W. *Int. J. Oncol.* **2006**, *28*, 1561-1569.
1484.Kepszynski, M.; Nawalany, K.; Jachimska, B.; Romek, M.; Nowakowska, M. *Colloids Surf. Biointerfaces* **2006**, *15*, 22-30.
1485.Kojima, C.; Toi, Y.; Harada, A.; Kono, K. *Bioconj. Chem.* **2007**, *18*, 663-670.
1486.Karotki, A.; Khurana, M.; Lepock, J. R.; Wilson, B. C. *Photochem. Photobiol.* **2006**, *82*, 443-452.
1487.Nishiyama, N.;Morimoto, Y.; Jang, W.-D.; Kataoka, K. *Adv. Drug Deliv. Rev.* **2009**, *61*, 327-338.
1488.Cabral, M.; Nakanishi, M.; Kumagai, M.; Jang, W.-D.; Nishiyama, N.; Kataoka, A. *Pharm. Res.* **2009**, *26*, 82-92.
1489.Nishiyama, N.; Nakagishi, Y.; Morimoto, Y.; Lai, P.-S.; Miyazaki, K.; Urano, K.; Horie, S.; Kumagai, M.; Fukushima, S.; Cheng, Y.; Jang, W.-D.; Kikuchi, M.; Kataoka, K. *J. Controlled Release* **2009**, *133*, 245-251.
1490.Ideta, R.; Tasaka, F.; Jang, W.-D.; Nishiyama, N.; Zhang, G.-D.; Harada, A.; Yanagi, Y.; Tamaki, Y.; Aida, T.; Kataoka, K. *Nano Lett.* **2005**, *5*, 2426-2431.
1491.Nishiyama, N.; Nakagishi, Y.; Morimoto, Y.; Lai, P.-S.; Miyazaki, K.; Urano, K.; Horie, S.; Souta, K.; Kumagai, M.; Fukushima, S.; Cheng, Y.; Jang, W.-D.; Kikuchi, M.; Kataoka, K. *J. Controlled Release* **2009**, *133*, 245-251.
1492.Shi, X.; Wang, S.; Sun, H.; Baker, J. R., Jr. *Soft Matter* **2007**, *3*, 71-74.
1493.Shi, X.; Wang, S.; Meshinshi, S.; van Antwerp, M. E.; Bi, X.; Lee, I.; Baker, J. R., Jr. *Small* **2007**, *3*, 1245-1252.
1494.Haba, Y.; Kojima, C.; Harada, A.; Ura, T.; Horinaka, H.; Kono, K. *Langmuir* **2007**, *23*, 5343-5246.
1495.Shi, X.; Lee, I.; Baker, J. R., Jr. *J. Mater. Chem.* **2008**, *18*, 586-593.
1496.Shi, X.; Wang, S. H.; Van Anrwerp, Mary, E.; Chen, X.; Baker, J. R., Jr. *Analyst* **2009**, *134*, 1373-1379.

1497. Wiwattanapatapee, R.; Lomlim, L.; Saramunee, K. *J. Controlled Release* **2003**, *88*, 1-9.
1498. Vandamme, Th. F.; Brobeck, L. *J. Controlled Release* **2005**, *102*, 23-38.
1499. Yang, H.; Lopina, S. T. *J. Mater. Sci: Mater. Med.* **2007**, *18*, 2061-2065.
1500. Bai, S.; Thomas, C.; Ahsan, F. *J. Phar. Sci.* **2007**, *96*, 2090-2106.
1501. Bharatam, P.; Sundriyal, S. *J. Nanosci. Nanotechnol.* **2006**, *6*, 3277-3282.
1502. Princz, M. A.; Sheardown, H. *J. Biomater. Sci., Polym. Ed.* **2008**, *19*, 1201-1218.
1503. Helms, B. A.; Reulen, S. W. A.; Nijhuis, S.; de Graaf-Heuvelmans, P. T. H. M.; Meijer, E. W. *J. Am. Chem. Soc.* **2009**, *131*, 11683-11685.
1504. Tekade, R. K.; Dutta, T.; Gajbhiye, V.; Jain, N. K. *J. Microencap.* **2009**, *26*, 287-296.
1505. Rekas, A.; Gadd, G. E.; Cappai, R.; Yun, S. I. *Macromol. Biosci.* **2009**, *9*, 230-238.
1506. Kurtuglu, Y. E.; Navath, R.; Wang, B.; Kannan, S.; Romero, R.; Kannan, R. M. *Biomater.* **2009**, *30*, 2112-2121.
1507. Hamilton, S. K.; Harth, E. *ACS Nano* **2009**, *3*, 402-410.
1508. Williams, D. F. *J. Biomed. Eng.* **1989**, *11*, 185-191.
1509. Xyloyiannis, M.; Padilla de Jesus, O. L.; Fréchet, J. M. J.; Duncan, R. *Proc. Int. Symp. Control. Release Bioact. Mater.* **2003**, *30*, 149-149.
1510. Zuckerman, S. T.; Kao, W. J. In *Nanotechnology in Drug Delivery*, de Villiers, M. M. Ed.; American Association of Pharmaceutical Scientists, 2009; Chap. *7*, pp. 193-228.
1511. Kitchens, K. M.; Ghandehari, H. In *Nanotechnology in Drug Delivery*, de Villiers, M. M. Ed.;American Association of Pharmaceutical Scientists, 2009; Chap. *14*; pp. 423-455.
1512. Kohatkar, K.; Kitchens, K. M.; Swaan, P.; Ghandehari, H. *Bioconjugate Chem.* **2007**, *18*, 2054-2060.
1513. Kitchens, K. M.; Foraker, A. B.; Kolhatkar, R. B.; Swann, P. W.; Ghandehari, H. *Pharm. Res.* **2007**, *24*, 2138-2145.
1514. Malik, N.; Wiwattanapatapee, R.; Klopsch, R.; Lorenz, K.; Frey, H.; Weener, J. W.; Meijer, E. W. *J. Controlled Release* **2000**, *65*, 133-148.
1515. Wiwattanapatapee, R.; Carreno-Gomez, B.; Malik, N.; Duncan, R. *Pharm. Res.* **2000**, *17*, 991-998.
1516. Kuo, J. S.; Jan, M.; Lin, Y. L. *J. Control. Rel.* **2007**, *120*, 51-60.
1517. Tack, F.; Bakker, A.; Maes, S.; Dekeyser, N.; Bruining, M.; Roman, C. E.; Janicot, M.; Brewster, M.; Janssen, H. M.; de Waal, B. F. M.; Fransen, P. M.; Lou, X. W.; Meijer, E. W. *J. Drug Target.* **2006**, *14*, 69-86.
1518. Dutta, T.; Jain, N. K. *Biochim. Biophys. Acta* **2007**, *1770*, 681-686.
1519. Boyd, B. J.; Kaminskas, L. M.; Karellas, P.; Krippner, G.; Lessene, R.; Porter, C. J. H. *Mol. Pharmaceutics* **2006**, *3*, 614-627.
1520. Kainthan, R. K.; Hester, S. R.; Levin, E.; Devine, D. V.; Brooks, D. E. *Biomaterials* **2007**, *28*, 4581-4590.
1521. Criscione, J. M.; Le, B. L.; Brennan, M.; Rahner, C.; Papademetris, X.; Fahmy, T. M. *Biomater.* **2009**, *30*, 3946-3955.
1522. Hama, Y.; Bernardo, M.; Regino, C. A. S.; Koyama, Y.; Brechbiel, M. W.; Krishna, M. C.; Choyke, P. L.; Kobayashi, H. *Magn. Reson. Med.* **2007**, *57*, 431-436.
1523. Chauhan, A. S.; Diwan, P. V.; Jain, N. K.; Tomalia, D. A. *Biomacromol.* **2009**, *10*, 1195-1202.
1524. Saovapakhiran, A.; D'Emanuele, A.; Attwood, D.; Penny, J. *Bioconj. Chem.* **2009**, *20*, 693-701.
1525. Yang, W.; Chen, Y.; Xu, T.; Wang, X.; Wen, L.-P *Eur. J. Med. Chem.* **2009**, *44*, 862-868.
1526. Cheng, Y. Y.; Xu, Z.; Ma, M.; Xu, T. *J. Pharm. Sci.* **2008**, *97*, 123-143.

1527.Tripathi, P. K.; Khopade, A. J.; Nagaich, S.; Shrivastava, S.; Jain, S.; Jain, N. K. *Pharmazie* **2002**, *57*, 261-264.
1528.Kolhatkar, R. B.; Swaan, P.; Ghandehari, H. *Pharma. Res.* **2008**, *25*, 1723-1729.
1529.Pisal, D. S.; Yellepedi, V. KJ.; Kumar, A.; Palakurthi, S. *Drug Deliv.* **2008**, *15*, 515-522.
1530.Ramachandran, C.; Fleisher, D. *Adv. Drug Deliv. Rev.* **2000**, *42*, 197-223.
1531.Thomas, B. J.; Finnin, B. C. *Drug Discov. Today* **2004**, *9*, 697-703.
1532.Myles, M. E.; Neumann, D. M.; Hill, J. M. *Adv. Drug Deliv.* **2005**, *57*, 2063-2079.
1533.Zhu, W.; Okolilie, B.; Bhujwalla, Z. M.; Artemov, D. *Mag. Reson. Med.* **2008**, *59*, 679-685.
1534.Shimpi, S.; Chauhan, B.; Shimpi, P. *Acta Pharm.* **2005**, *55*, 139-156.
1535.Duan, X.; Sheardown, H. *Biomaterials* **2006**, *27*, 4608-4617.
1536.Dan, X.; McLaughlin, C.; Griffith, M.; Sheardown, H. *Biomaterials* **2007**, *28*, 78-88.
1537.Marano, R. J.; Wimmer, N.; Kearns, P. S.; Thomas, B. G.; Toth, I.; Brankov, M.; Rackoczy, P. E. *Exp. Eye Res.* **2004**, *79*, 525-535.
1538.Marano, R. J.; Toth, I.; Wimmer, N.; Brankov, M.; Rakoczy, P. E. *Gene therapy* **2005**, *12*, 1544-1550.
1539.Patton, D. L.; Sweeney, Y. T. C.; McCarthy, T. D.; Hillier, S. L. *Antimicrob. Agents Chemother.* **2006**, *50*, 1696-1700.
1540.Mumper, R.J.; Bell, M. A.; Worthen, D. R.; Cone, R. A.; Lewis, G. R.; Paull, J. R. A. *Drug Dev. Int. Pharm.* **2009**, *35*, 515-524.
1541.Ndesendo, V. M. K.; Pillay, V.; Choonara, Y. E.; Buchmann, E.; Bayever, D. N.; Meyer, L. C. R. *AAPS PharmSciTech* **2008**, *9*, 505-520.
1542.Sweet, D. M.; Kolhatkar, R. B.; Ray, A.; Swaan, P.; Ghandehari, H. *J. Controlled Release* **2009**, *138*, 78-85.
1543.Peters, J. A.; Huskens, J.; Raber, D. J. *Prog. Nucl. Magn. Reson. Spectrosc.* **1996**, *28*, 283-350.
1544.Caravan, P.; Ellison, J. J.; McMurray, T. J.; Lauffer, R. B. *Chem. Rev.* **1999**, *99*, 2293-2352.
1545.Laus, S.; Sour, A.; Ruloff, R.; Toth, E.; Merbach, A. E. *Chem. Eur. J.* **2005**, *11*, 3064-3076.
1546.Toth, E.; Helm, L.; Merbach, A. E. *Top. Curr. Chem.* **2002**, *221*, 61-101.
1547.Pierre, V. C.; Botta, M.; Raymond, K. N. *J. Am. Chem. Soc.* **2005**, *127*, 504-505.
1548.Dijkgraaf, I.; Rijnders, A. Y.; Soede, A.; Dechesne, A. C.; van Esse, G. W.; Brouwer, A. J.; Corstens, F. H. M.; Boerman, O. C.; Rijkers, D. T. S.; Liskamp, R. M. J. *Org. Biomol. Chem.* **2007**, *5*, 935-944.
1549.Swanson, S. D.; Kukowska-Latallo, J.; Patri, A. K.; Chen, C.; Ge, S.; Cao, Z.; Kotlyar, A.; East, A. T.; Baker, J. R., Jr. *Int. J. Nanomed.* **2008**, *3*, 201-210.
1550.Lei, X.-g; Jockusch, S.; Turro, N. J.; Tomalia, D. A. *J. Colloid Interf. Sci.* **2008**, *322*, 457-464.
1551.Wiener, E. C.; Brechbiel, M. W.; Brothers, H.; Magin, R. L.; Gansow, O. A.; Tomalia, D. A.; Lauterbur, P. C. *Magn. Reson. Med.* **1994**, *311*, 1-8.
1552.Longmire, M.; Choyke, P. L.; Kobayashi, H. *Curr. Top. Med. Chem.* **2008**, *8*, 1180-1186.
1553.Venditto, V. J.; Regino, C. A. S.; Brechbiel, M. W. *Mol. Pharm.* **2005**, *2*, 302-311.
1554.Kobayashi, H.; Brechbiel, M. W. *Adv. Drug. Delivery Rev.* **2005**, *57*, 2271-2286.
1555.Langeris, S.; de Lussanet, Q. G.; van Genderen, M. H. P.; Meijer, E. W.; Beets-Tan, R. G. H.; Griffioen, A. W.; van Engelshoven, J. M. A.; Backes, W. H. *NMR Biomed.* **2006**, *19*, 133-141.

1556.Vetterlein, K.; Bergmann, U.; Büche, K.; Walker, M.; Lehmann, J.; Linsheid, M. W.; Criba, G. K. E.; Hildebrand, M. *Electrophoresis* **2007**, *28*, 3088-3099.
1557.Kobayashi, H.; Reijnders, K.; English, S.; Yordanov, A. T.; Milenic, D. E.; Sowers, L.; Citrin, D.; Krishna, M. C.; Waldmann, T. A.; Mitchel, J. B.; Brechbiel, M. W. *Clin. Cancer Res.* **2004**, *10*, 7712-7720.
1558.Nwe, K.; Xu, H.; Regino, C. A. S.; Bernardo, M.; Ileva, L.; Riffle, L.; Wong, K. J.; Becbiel, M. W. *Bioconj. Chem.* **2009**, *20*, 1412-1418.
1559.Kobayashi, H.; Kawamoto, S.; Bernardo, M.; Brechbiel, Bernardo, M.; Sato, N.; Waldmann, A.; Tagaya, Y.; Choyke, P. L. *Neoplasia* **2005**, *7*, 984-991.
1560.Kobayashi, H.; Kawamoto, S.; Bernardo, M.; Brechbiel, Knopp, M. V.; Choyke, P. L. *J. Controlled Release* **2006**, *111*, 343-351.
1561.Langerieis, S.; de Lussanet, Q. G.; van Genderen, M. H.; Meijer, E. W.; Beets-Tan, R. G.; Griffioen, A. W.; van Engelshoven, J. M.; Backes, W. H. *NMR Biomed.* **2006**, *19*, 133-141.
1562.Kobayashi, H.; Kawamoto, S.; Jo, S. K.; Briant, H. L. Jr.; Brechbiel, M. W.; Star, R. A. *Bioconj. Chem.* **2003**, *14*, 388-394.
1563.Kobayashi, H.; Kawamoto, S.; Brechbiel, M. W.; Bernardo, M.; Sato, N.; Waldmann, T. A.; Tagaya, Y.; Choyke, P. L. *Neoplasia* **2005**, *7*, 984-991.
1564.Amirkhanov, N. V.; Wickstrom, E. *Nucleosides Nucleic Acids* **2005**, *24*, 423-426.
1565.Regino, C. A. S.; Waldbridge, S.; Bernardo, M.; Wong, K. J.; Johnson, D.; Lonser, R.; Oldfield, E.H.; Choyke, P L. Brechbiel, M. W. *Contrast Media Mol. Imaging* **2008**, *3*, 2-8.
1566.Martin, A. L.; Bernas, L. M.; Rutt, B. K.; Foster, P. J.; Gillies, E. R. *Bioconj. Chem.* **2008**, *19*, 2375-2384.
1567.Kobayashi, H.; Ogawa, M.; Kosaka, N.; Choyke, P. L.; Urano, Y. *Nanomed.* **2009**, *4*, 411-419.
1568.Fu, Y.; Nitecki, D. E.; Maltby, D.; Simon, G. H.; Berejnoi, K.; Raatschen, H. J.; Yeh, D. M.; Brasch, R. C. *Bioconjug. Chem.* **2006**, *17*, 1043-1056.
1569.Parrot, M. C.; Benhabbour, S. R.; Saab, C.; Lemon, J. A.; Parker, S.; Valliant, J. F.; Andrianoov, A. *J. Am. Chem. Soc.* **2009**, *131*, 2906-2916.
1570.Almutairi, A.; Rossin, R.; Shokeen, M.; Hagooly, A.; Ananth, A.; Capoccia, B.; Guillaudeu, S.; Abendschein, D.; Anderson, C. J.; Welch, M. J.; Fréchet, J. M. J. *Proc. Nat. Acad. Sci. USA* **2009**, *106*, 685-690.
1571.Baker, S. L. R.; Zha, Y.; Marletta, M. A.; Kopelman, R. *Anal. Chem.* **1999**, *71*, 2071-2075.
1572.Ye, J. Y.; Myaing, M. T.; Norris, T. B.; Thomas Jr., T. P. *Opt. Lett.* **2002**, *27*, 1412-1414.
1573.Thomas, T.; Ye, J. Y.; Chang, Y.-C.; Kotlyar, A.; Cao, Z.; Majoros, I.; Norris, T.; Baker, J. R., Jr. *Biomed. Optics* **2008**, *13*, 014024/1-014024/6.
1574.Thomas, T. P.; Ye, J. Y.; Yang, C.; Myaing, M. T.; Majoros, I. J.; Kotlyar, A.; Cao, P.; Norris, T. B. *Proc. SPIE* **2006**, 6095, Q1-Q7.
1575.Majoros, I. J.; Thomas, T. P.; Mehta, C. B. *J. Med. Chem.* **2005**, *48*, 5892-5899.
1576.Thomas, T. P.; Ye, J. Y.; Chang, Y.-C.; Kotlyar, A.; Cao, Z.; Majoros, I.; Borris, T.; Baker, J. R., Jr. *J. Biomed. Optics* **2008**, *13*, 014024.
1577.Thomas, T. P.; Myaing, M. T.; Ye, J. Y.; Candido, K.; Kotlyar, A.; Beal, J.; Cao, P.; Keszler, B.; Patri, A. K.; Norris, T. B.; Baker, J. R., Jr. *Biophys. J.* **2004**, *86*, 3959-3965.
1578.Huang, K.; Bryan, V.; Kumar, D.; Hamm, H. E.; Harth, E. *Bioconjugate Chem.* **2007**, *18*, 403-409.

1579.Triulzi, R. C.; Micic, M.; Orbulescu, J.; Giodani, S.; Mueller, B.; Leblanc, R. M. *Analyst* **2008**, *133*, 667-672.
1580.Ornelas, C.; Weck, M. *Chem. Commun.* **2009**, DOI: 10.1039/b913139f.
1581.Shcharbin, D.; Mazur, J.; Szwedzka, M.; Wasiak, M.; Bartlomiej, P.; Przybyszewska, M.; Zaborsky, M.; Bryszewska, M. *Coll. Surf. Sci. B: Biointerf.* **2007**, *58*, 286-289.
1582.Domanski, D. M.; Klajnert, B.; Bryszewska, M. *Bioelectrochem*. **2004**, *63*, 189-191.
1583.Shcharbin, D.; Janicka, M.; Wasiak, M.; Bartlomiej, P.; Przybyszewska, M.; Zaborsky, M.; Bryszewska, M. *Coll. Surf. Sci. B: Biointerf.* **2007**, *58*, 286-289.
1584.Shcharbin, D.; Janicka, M.; Wasiak, M.; Bartlomiej, P.; Przybyszewska, M.; Zaborsky, M.; Bryszewska, M. *Biochimica et Biophysica Acta* **2007**, *1774*, 946-951.
1585.Pan, B.-F.; Gao, F.; Ao, L.-M. *J. Mag. Mag. Mat.* **2005**, 252-258.
1586.Koyama, Y.; Talanov, V. S.; Bernardo, M.; Hama, Y.; Regino, C. A. S.; Brechbiel, M. W.; Choyke, P. L.; Kobayashi, H. *J. Magn. Reson. Imaging* **2007**, *25*, 866-871.
1587.Talanov, V. S.; Regino, C. A. S.; Kobayashi, H.; Bernardo, M.; Choyke, P. L.; Brechbiel, M. W. *Nano Lett.* **2006**, *6*, 1459-1463.
1588.Xu, H; Regino, C. A. S.; Koyama, Y.; Hama, Y.; Gunn, A. J.; Bernardo, M.; Kobayashi, H.; Choyke, P. L.; Brechbiel, M. W. *Bioconj. Chem.* **2007**, *18*, 1474-1482.
1589.Fuchs, S.; Otto, H.; Jehle, S.; Henklein, P.; Schlüter, A. D. *Chem. Commun.* **2005**, 1830-1832.
1590.Almutairi, A.; Akers, W. J.; Berezin, M. K. Y.; Achilefu, S.; Fréchet, J. M. J. *Mol. Pharma.* **2008**, *5*, 1003-1010.
1591.Yin, M.; Shen, J.; Pfugfeder, G. O.; Müllen, K. *J. Am. Chem. Soc.* **2008**, *130*, 7806-7807.
1592.Choi, Y.; Mecke, A.; Orr, B. G.; Banaszak Holl, Baker, J. R., Jr. *Nano Lett.* **2004**, *4,* 391-397.
1593.Lowe, M.; Spiro, A.; Zhang, Y. Z.; Getts, R. *Cytometry* **2004**, *60A*, 135-144.
1594.Li, Y.; Tseng, Y. D.; Kwon, S. Y.; d'Espaux, L.; Bunch, J. S.; McEuen, P. L.; Luo, D. *Nat. Mater.* **2004**, *3*, 38-42.
1595.Li, Y.; Cu, Y. T. H.; Luo, D. *Nature Biotechnol.* **2005**, *23*, 885-889.
1596.Freedman, K. O.; Lee, J.; Luo, D.; Skobeleva, V. B.; Ke, P. C. *J. Phys. Chem. B* **2005**, *109*, 9839-9842.
1597.Burley, G. A.; Gierlich, J.; Mofid, M. R.; Nir, H.; Tal, S.; Eichen, Y.; Carell, T. *J. Am. Chem. Soc.* **2006**, *128*, 1398-1399.
1598.Caminade, A.-M.; Padié, C.; Laurent, R.; Maraval, A.; Majoral, J.-P. *Sensors* **2006**, *6*, 901-914.
1599.Caminade, A.-M.; Turrin, C.-O.; Majoral, J.-P. *Chem. Eur. J.* **2008**, *14*, 7422-7432.
1600.Wittmann, C. Ed. *Immobilization of DNA on chips I,* Top. Curr. Chem. Springer, Berlin, **2005**, *260*.
1601.Wittmann, C. Ed. *Immobilization of DNA on chips II,* Top. Curr. Chem.; Springer, Berlin, **2005**, *261*.
1602.Rosi, N. L.; Mirkin, C. A. *Chem. Rev.* **2005,** *105*, 1547-1562.
1603.Beier, M.; Hoheisel, J. D. *Nucleic Acids Res.* **1999,** *27*, 1970-1977.
1604.Oh, S. J.; Ju, J.; Kim, B. C.; Ko, E.; Hong, J.; Park, J. G.; Park, J. W.; Choi, K. Y. *Nucleic Acid Res.* **2005**, *33*, e90-1-e90-8.
1605.Hong, B. J.; Sunkara, V.; Park, J. W. *Nucleic Acid Res.* **2005**, *33*, e106-1-e106-8.
1606.Jung, Y. J.; Hong, B. J.; Zhang, W.; Tendler, S. J. B.; Williams, S.; Allen, J. W.; Park, J. W. *J. Am. Chem. Soc.* **2007**, *129*, 9349-9355.
1607.Benters, R.; Niemeyer, C. M.; Wöhrle, D. *ChemBioChem* **2001**, *2*, 686-694.
1608.Benters, R.; Niemeyer, C. M.; Wöhrle, D. *Nucleic Acid Res.* **2003** , *31*, e87-1-e87-19.

1609. Talor, S.; Smith, S.; Windle, B.; Guiseppi-Elie, A. *Nucleic Acids Res.* **2003**, *31*, e87-1-e87-19.
1610. Trévisol, E.; Leberre-Anton, V.; Leclaire, J.; Pratviel, G.; Caminade, A.-M.; Majoral, J.-P.; Meunier, B. *New J. Chem.* **2003**, *27*, 1713-1719.
1611. Le Berre, V.; Trévisol, E.; Dagkessamanskaia, A.; Sokol, S.; Caminade, A.-M.; Majoral, J.-P.; Meunier, B.; François , J. *Nucleic Acid Res.* **2003**, *31*, e88-1-e88-8.
1612. Chaize, B.; Nguyen, N.; Ruysschaert,T.; Le Berre, V.; Trévisol, E.; Caminade, A.-M.; Majoral, J.-P.; Pratviel, G.; Meunier, B.; Winterhalter, M.; Fournier, D. *Bioconjugate Chem.* **2006**, *17*, 245-247.
1613. Lim, S. B.; Kim, K.-W.; Le, C.-W.; Kim, H.-S.; Lee, C.-S.; Oh, M.-K. *Biotechnol. Bioproc. Eng.* **2008**, *13*, 683-689.
1614. Bhatnagar, P.; Mark, S. S.; Kim, I.; Chen, H.; Schmidt, B.; Lipson, M.; Batt, C. A. *Adv. Mater.* **2006**, *18*, 315-319.
1615. Rozkiewicz, D. I.; Brugman, W.; Kerkhoven, R. M.; Ravoo, B. J.; Reinhoudt, D. N. *J. Am. Chem. Soc.* **2007**, *129*, 11593-11599.
1616. Rozkiewicz, D. I.; Gierlich, J.; Burley, G. A.; Gutsmiedl, K.; Carell, T.; Ravoo, B. J.; Reinhoudt, D. N. *ChemBioChem* **2007**, *8*, 1997-2002.
1617. Kim, D. H.; Karan, P.; Göring, P.; Leclaire, J.; Caminade, A.-M.; Majoral, J.-P.; Gösele, U.; Steinhart, M.; Knoll, W. *Small* **2005**, *1*, 99-102.
1618. Feng, C. L.; Zhong, X. H.; Steinhart, M.; Caminade, A.-M.; Majoral, J.-P.; Knoll, W. *Adv. Mater.* **2007**, *19*, 1933-1936.
1619. Feng, C. L.; Zhong, X. H.; Teinhart, M.; Caminade, A.-M.; Majoral, J.-P.; Knoll, W. *Small* **2008**, *4*, 566-571.
1620. Nicu, L.; Guirardel, M.; Chambosse, F.; Rougerie, P.; Hinh, S.; Trévisiol, E.; François, J. M.; Majoral, J.-P.; Cattan, E.; Bergaud, C. *Sens. Actuators B* **2005**, *110*, 125-136.
1621. Mark, S. S.; Sandhyarani, N.; Zhu, C.; Campagnolo, C.; Batt, C. A. *Langmuir* **2004**, *20*, 6808-6817.
1622. Kim, E.; Kim, K.; Yang, H.; Kim, Y. T.; Kwak, J. *Anal. Chem.* **2003**, *75*, 5665-5672.
1623. Zhu, N.; Gu, Y.; Chang, Z.; He, P.; Fang, Y. *Electroanal.* **2006**, *21*, 2107-2114.
1624. Li, A.; Yang, F.; Ma, Y.; Yang, X. *Biosensors Biolelectr.* **2007**, 22, 1716-1722.
1625. Shiddiky, M. J. A.; Rahman, Md. A.; Shim, Y.-B. *Anal. Chem.* **2007**, *79*, 6886-6890.
1626. Kim, B. S.; Lebedeva, O. V.; Koynov, K.; Gong, H.; Caminade, A.-M.; Majoral, J.-P.; Vinogradova, O. I. *Macromolecules* **2006**, *39*, 5479-5483.
1627. Ritort, F.; Mihardja, S.; Smith, S. B.; Bustamante, C. *Phys. Rev. Lett.* **2006**, *96*, 118301-1-118301-4.
1628. Maiti, P. K.; Bagchi, B. *Nano Lett.* **2006**, *6*, 2478-2485.
1629. Kostainen, M. A.; Szilvay, G. R.; Smith, D. K.; Linder, M. B.; Ikkala, O. *Angew. Chem., Int. Ed.* **2006**, *45*, 3538-3542.
1630. Kostainen, M. A.; Smith, D. K.; Ikkala, O. *Angew. Chem., Int. Ed.* **2007**, *46*, 7600-7604.
1631. Su, C. J.; Liu, Y. C.; Chen, H. L.; Li, Y. C.; Lin, H. K.; Liu, W. L.; Hsu, C. S. *Langmuir* **2007**, *38*, 975-978.
1632. Ornelas, C.; Ruiz, J.; Astruc, D. *Organometallics* **2009**, *28,* 4431–4437.
1633. Labande, A.; Astruc, D. *Chem. Commun.* **2000,** 1007-1008.
1634. Daniel, M.-C.; Ruiz, J.; Nlate, S.; Palumbo, J.; Blais, J. C.; Astruc, D. *Chem. Commun.* **2001**, 2000-2001.
1635. Labande, A.; Astruc, D. *J. Am. Chem. Soc.* **2002**, *124*, 1784-1789.
1636. Daniel, M.-C.; Juiz, J.; Blais, J. C.; Daro, N.; Astruc, D. *Chem. Eur. J.* **2003**, *9*, 4371-4379.

1637.Alonso, B., Casado, C. M., Cuadrado, I., Moran, M., Kaifer, A. E. *Chem Commun.* **2002**, 1778-1779.
1638.Méry, D.; Plault, L.; Ornelas, C.; Ruiz, J.; Nlate, S. Astruc, D.: Blais, J.-C.; Rodrigues, J.; Cordier, S.; Kiracki, K.; Perrin, C. *Inorg. Chem*., **2006**, 45, 1156-1167.
1639.Valério, C.; Fillaut, J.-L.; Ruiz, J.; Guittard, J.; Blais, J.-C.; Astruc, D. *J. Am. Chem. Soc.* **1997**, *119*, 2588-2589.
1640.Reynes, O.; Moutet, J. C.; Pecaut, J.; Royal, G.; Saint-Aman, E. *Chem. Eur. J.* **2000**, *6*, 2544-2553.
1641.Ruiz, J.; Belin, C.; Astruc, D. *Angew. Chem., Int. Ed*., **2006,** *45*, 132-136.
1642.Ruiz, J.; Belin, C.; Astruc, D. *Chem. Commun*. **2007**, 3456 -3458.
1643.Newman, J. D.; Turner, A. P. F. *Biosens. Bioelectron.* **2005**, *20*, 2435-2453.
1644.Losada, J.; Cuadrado, I.; Moran, M.; Casado, C. M.; Alonso, B.; Barranco, M. *Anal. Chim. Acta* **1997**, *338*, 191-198.
1645.Armada, M. P. G.; Losada, J.; Zamora, M.; Alonso, B.; Cuadrado, I.; Casado, C. M. *Bioelectrochem.* **2006**, *69*, 65-73.
1646.Losada, J.; Zamora, M.; Armada, P. G.; Cuadrado, I; Alonso, B.; Casado, C. M. *Anal. Bioanal.Chem.* **2006**, *385*, 1209-1217.
1647.Losada, J.; Armada, M. P. G.; Cuadrado, I.; Alonso, B.; Gonzalez, B.; Casado, C. M.; Zhang, J. *J. Organomet. Chem.* **2004**, *689*, 2799-2807.
1648.Armada, M. P. G., Losada, J.; Cuadrado, I.; Alonso, B.; Gonzalez, B.; Casado, C. M.; Zhang, J. B. *Sensors. Actuators B- Chem.* **2004**, *101*, 143-149.
1649.Armada, M. P.G.; Losada, J.; Cuadrado, I.; Alonso, B.; Gonzalez, B.; Casado, C. M. *Electroanal.* **2003**, *15*, 1109-1114.
1650.Martinez, F. J.; Gonzalez, B.; Alonso, B.; Losada, J.; Garcia-Armada, M. P.; Casado, C. M. *J. Inorg. Organomet. Polym. Mater.* **2008**, *18*, 51-58.
1651.Deriu, D.; Favero, G.; D'Annibale, A.; Mazzei, F. *ECS Trans.* **2008**, *16*, 105-113.
1652.Qiu, R.; Zhang, X. L.; Qiao, R.; Li, Y.; Kim, Y. I.; Kag, Y. S. *Chem. Mater.* **2007**, *19*, 0897-4756, 4174-4180.
1653.Fernandes, E. G. R.; De Queiroz, A., A., A. *J. Mater. Sci.: Mater. Med.* **2009**, *20*, 473-479.
1654.Zhu, H.; Zu, Y.; Yang, X.; Li, C. *Chem. Letters* **2006**, *35*, 326-327.
1655.Xu, L.; Tang, L.; Yang, X.; Li, C. *Electroanal.* **2007**, *6*, 717-722.
1656.Zhu, Y.; Zhu, H.; Yang, X.; Xu, L.; Li, C. *Electroanal.* **2007**, *6*, 698-703.
1657.Crespilho, F. N.; Ghica, M. E.; Florescu, M.; Nart, F. C.; Oliveira, Jr., O. N.; Brett, C. M. A. *Electrochem. Commun.* **2006**, *8*, 1665-1670.
1658.Liu, Z.-M.; Yang, Y.; Wang, H.; Liu, Y.-L.; Shen, G.-L.; Yu, R.-Q. *Sensors Actuators B* **2005**, *106*, 394-400.
1659.Liu, J.-M.; Liu, Z-B.; Zhu, G.-H.; Li, X.-L.; Huang, X.-M; Li, F.-M.; Shi, X.-M.; Zeng, L.-Q. *Talanta* **2008**, 74, 625-631.
1660.Tang, D.; Niessmer, R.; Knopp, D *Biosens. Bioelectron.* **2009**, *24*, 2125-2130.
1661.Yoon, H. C.; Lee, D.; Kim, H.-S. *Anal. Chim. Acta* **2002**, *456*, 209-212.
1662.Jeon, S. I.; Hong, J. W.; Yoon, H. C. *Biotechnol. Lett.* **2006**, *28*, 1401-1408.
1663.Yamagushi, H.; Harada, A. *Chem. Letters* **2008**, *37*, 1184-1189.
1664.Rios, L.; Garcia, A. A. *React. Funct. Polym*. **2008**, *68*, 307-314.
1665.Montanez, M. I.; Perez-Inestrosa, E.; Suau, R.; Mayorga, C.; Torres, M. J.; Blanca, M. *Biomacromol*. **2008**, *9*, 1461-1466.
1666.Mora, J. R.; Zielinski, T. L.; Nelson, B. P.; Getts, R. C. *BioTechniques* **2008**, *44*, 815-818.
1667.Sheng, K-C.; Kalkanidis, M.; Pouniotis, D. S.; Esparon, S.; Tang, C. K.; Apostolopoulos, V.; Pietersz, G. A. *Eur. J. Immunol*. **2008**, *38*, 424-436.

1668.Manea, M.; Przybilski, M.; Hudecz, F.; Mezoe, G. *Biopolymers* **2008**, *90*, 94-104.
1669.Kumar, A.; Abbott, N. L.; Kim, E.; Biebuyck, H. A.; Whitesides, G. M. *Acc. Chem. Res.* **1995**, *28*, 219-226.
1670.Antonisse, M. M. G., Reinhoudt, D. N. *Chem. Commun.***1998**, 443-448.
1671.Piperberg, G; Wilner, O. I.; Yehezkeli, O.; Tel-Vered, R.; Willner, I. *J. Am. Chem. Soc.* **2009**, *131*, 8724-8725.
1672.Chen, L.; McBranch, H.-L.; Helgeson, R.; Wudl, F.; Whitten, D. G. *Proc. Nat. Acad. Sci. U. S. A.* **1999**, *96*, 12287-12292.
1673.Dequaire, M.; Degrand, C.; Limoges, B. J. *J. Am. Chem. Soc.* **1999**, *121*, 6946-6947.
1674.Arendt, M.; Sun, W.; Thomann, J.; Xie, X.; Schrader, T. *Chem. Asian J.* **2006**, *1*, 544-554.
1675.Nonappa, Maitra, U. *Org. Biomol. Chem.* **2008**, *6*, 657-669.
1676.Jiwpanitch, S.; Sandanaraj, B. S.; Thayumanavan, S. *Chem. Commun.* **2009**, 806-808.
1677.Shinoda, S. *J. Incl. Phenom. Macrocycl. Chem.* **2007**, *59*, 1-9.
1678.Das, J.; Aziz, A.; Yang, H. *J. Am. Chem. Soc.* **2006**, *128*, 16022-16023.
1679.Tang, L.; Zhu, Y.; Xu, L.; Yang, X.; Li, C. *Talanta* **2007**, *73*, 438-443.
1680.Tang, L.; Zhu, Y.; Xu, L.; Yang, X.; Li, C. *Anal. Chim. Acta* **2007**, *597*, 145-150.
1681.Bustos, E. B.; Jimenez, Ma. G. G.; Diaz-Sanchez, B. R.; Juaristi, E.; Chapman, T. W.; Godinez, L. A. *Talanta* **2007**, *72*, 1586-1592.
1682.Lee, K. R.; Kang, I. J. Ultramicrosc. **2009**, *109*, 894-898.
1683.Kikkeri, R.; Garcia-Rubio, I.; Seeberger, P. H. *Chem. Commun.* **2009**, 235-237.
1684.Jonkheijm, P.; Weinrich, D.; Koehn, M.; Engelkamp, H.; Christianen, P. C. M.; Kuhlman, J.; Maan, J. C.; Nuesse, D.; Schroeder, H.; Wacker, R.; Breinbauer, R.; Niemeyer, C. M.; Waldmann, H. *Angew. Chem., Int. Ed. Engl*. **2008**, *47*, 4421-4424.
1685.Khew, S. T.; Yang, Q. J.; Tong, Y. W. *Biomater*. **2008**, *29*, 3034-3045.
1686.Shukla, R. H. E.; Shi, X.; Kim, J.; Muniz, M. C.; Sun, K.; Baker, J. R., Jr. *Soft Matter* **2008**, *4*, 2160-2163.
1687.Gutierrez, A.; Osegueda, S.; Gutierrez-Granados, S.; Alatorre, A.; Garcia, Ma. G.; Godinez, L. A. *Electroanalysis* **2008**, *20*, 2294-2300.
1688.Rahman, Md. A.; Noh, H.-B.; Shim, Y.-B. *Anal. Chem*. **2008**, *80*, 8020-8027.
1689.Mikhail, A. S.; Jones, K. S.; Sheardown, H. *Biotechnol. Prog*. **2008**, *24*, 938-944.
1690.Kwon, S. J.; Jang, H.; Jo, K.; Kwak, J. *Analyst* **2008**, *133*, 1599-1604.